Propagation Phenomena in Population Dynamics

Quentin Griette

Mémoire d'Habilitation à Diriger des Recherches

Réalisé à l'Institut de Mathématiques de Bordeaux, Université de Bordeaux.
Spécialité: Mathématiques Appliquées et Calcul Scientifique

Phénomènes de propagation en dynamique des populations

par
Quentin GRIETTE

Thèse soutenue publiquement le 27 Janvier 2022 devant un jury composé de

Vincent Calvez	Université Claude Bernard Lyon 1	Examinateur
Jacques Demongeot	Université Joseph Fourier	Président
Laurent Desvillettes	Université de Paris	Examinateur
Pierre Magal	Université de Bordeaux	Examinateur
Alain Miranville	Université de Poitiers	Rapporteur
Glenn Webb	Vanderbilt University	Rapporteur
Xiaoqiang Zhao	Memorial University of Newfoundland	Rapporteur

après avis de **Alain Miranville**, **Glenn Webb** et **Xiaoqiang Zhao**.

université de BORDEAUX

Acknowledgements

I would like to start by expressing my gratitude to the members of the jury. They are leading scientific figures who are an inspiration to the (still) young scientist that I am. In the first place, I thank Alain Miranville, Glenn Webb, and Xiaoqiang Zhao, who have accepted to write a report on this thesis. I am greatly honored that they took the time to discover my work and particularly grateful for their positive comments and feedback. I warmly thank Vincent Calvez, Jacques Demongeot, and Laurent Desvillettes for taking part in the jury. Although we did not collaborate (yet), Vincent Calvez was of particular importance to the development of my career, since he referred me to my Ph.D. advisors in the first place. It is also the second time he agrees to examine my work. I have the pleasure of counting Jacques Demongeot as an examiner of my thesis, who continually impresses me by his culture and scientific spectrum - as well as his cheerful friendliness. I am very grateful to Laurent Desvillettes to bring his expertise to this committee. I deeply regret not being able to welcome all of them because of the COVID situation.

Pierre Magal deserves a special place in this section, not only for his participation in the jury but for his involvement and constant support since I came to Bordeaux in 2018. To me, he has been nothing less than a mentor scientifically and, to some extent, personally, and I continue to learn a lot from our interactions.

My scientific story starts with my Ph.D. and I take the opportunity of this second thesis to thank again my advisors, Matthieu Alfaro, Gaël Raoul, and Sylvain Gandon, who launched me on this amazing (and slightly reckless) adventure, of keeping a strong connection with the biology while doing mathematics. I am deeply indebted and immensely grateful to Hiroshi Matano, who welcomed me many times in Japan including at the occasion of my post-doctorate. I owe him a lot of my understanding of the qualitative behavior of solutions to reaction-diffusion equations. Arnaud Ducrot has a great influence on my view of dynamical systems and he has always been a huge support as well as an inspiration; he has all my gratitude. I also thank Jean-Baptiste Burie for his friendliness and team spirit. I also wish to thank Seb Motsch for his friendliness and warm welcome at ASU.

This work has been built thanks to many collaborations and interactions. This is the place to thank Xiaoming Fu who entrusted me to act as an informal advisor, and who contributed to a substantial part of this thesis. I also want to thank Léo Girardin with whom I share many scientific interests and has proved to be of great help. This is also the place to thank Zhihua Liu, Quentin Richard, Denis Roze, Benoît Sarels, and Robin Thompson for their collaboration. I take this opportunity to thank Grégory Faye who has trusted me to be a part of his group, I'm sure that it will lead to great science! I also want to thank here Olivier Dordan and Mostafa Bendahmane along whom it is a pleasure to teach, as well as the colleagues at IMB for their welcome.

I don't have enough space here to thank all those who should be thanked. But let me end by sending a warm thought to my family and friends. And all my love to Rosmeliz, who has been my α and ω for almost ten years now.

La vida te da sorpresas
Sorpresas te da la vida

Contents

Chapter 1

General presentation

Since the beginning of my Ph.D., my main research interest has been the mathematical study of population dynamics models. In my work, I have tried to diversify as much as possible the type of mathematical problem while keeping the biological applications as a central topic. In particular, my work as a Ph.D. student (2014-2017) has been focused on the qualitative properties of solutions of reaction-diffusion equations modeling the spread of an evolving pathogen. I have pursued this line of investigation in my research as a post-doctoral student and as an associate professor, since 2018. But I have also started to investigate models from other fields, namely, a novel hyperbolic problem (in collaboration with Pierre Magal and Xiaoming Fu, see section 1.2), and different mathematical questions, for instance, the precise description of the stationary solutions of a model with phenotypic structure (see section 1.3). Last but not least, I have recently participated in the development of new methods that bridge the epidemiological models and the real data in the context of the COVID-19 epidemic (see section 1.4).

Except for the articles which I began during my Ph.D. [P1, P2, P3, P4], the works presented in this thesis have been realized between 2017 and 2021. They are summarized in the present chapter and presented in detail later in the thesis.

Section 1.1 and chapter 2 are devoted to my work on the qualitative properties of reaction-diffusion equations and systems. In section 1.1.1, I summarize the core of my Ph.D. on the construction of traveling waves (collaboration with Gael Raoul [P2]) and pulsating fronts (collaboration with Matthieu Alfaro [P3]) for a non-monotone system of reaction-diffusion equations. This section is supplemented with a very recent preprint with Hiroshi Matano [P19]. In this work, we answer similar questions in a more general setting but also deal with spreading speed and several singular limits (homogenization, strong coupling). We also reveal a non-isotropic propagation phenomenon specific to systems. In section 1.1.2, I present a work that began at the end of my Ph.D. [P4] and concerns the construction of a singular measure traveling waves in a model of mixed type (spatial diffusion, non-local dispersion, and competition in phenotype). Section 1.1.3 is concerned with a collaboration with Léo Girardin [P9] in which we proved the convergence to the equilibrium for a family of reaction-diffusion systems and non-local equations thanks to a well-constructed Lyapunov functional. Finally, section 1.1.4 is devoted to a recent preprint in collaboration with Matthieu Alfaro, Denis Roze, and Benoît Sarels [P17], in which we prove the existence and stability of traveling waves (clines) in a model of heterozygote incompatibility which involves a nonlinear gradient term.

Section 1.2 and chapter 3 describe the study of a hyperbolic model of cell-cell repulsion. The works presented in this section are the result of a collaboration with Xiaoming Fu and Pierre Magal. Section 1.2.1 presents the principle of the equation which models the growth and repulsion of cells in a circular two-dimensional model (Petri dish). This study [P8] was motivated by co-culture experiments done by Pasquier and collaborators [318] in the context of breast cancer research. In sections 1.2.2 and 1.2.3, we focused on the qualitative properties of the solutions to a related model in one dimension, to understand the propagation behavior of the solutions to the equation. In section 1.2.2, we establish the well-posedness of the Cauchy problem of this hyperbolic equation on the whole line thanks to the reduction of the problem along the characteristics [P11]. In section 1.2.3, we focused on the qualitative properties of solutions. In particular, we prove that a jump discontinuity is forming at the propagating edge of the solutions. We also prove the existence of discontinuous traveling waves and give bounds on their speed.

Section 1.3 contains two works on the asymptotic behavior and stationary solutions of a nonlocal model for epidemics caused by a spore-producing pathogen. The first is described in section 1.3.1 and corresponds to a collaboration with Arnaud Ducrot, Jean-Baptiste Burie, and Quentin Richard [P6]. We study a non-

local model of pathogen evolution with two hosts and give a precise description of the stationary states when the mutation kernel is sharply concentrated (*i.e.* close to a Dirac mass). Section 1.3.2 is concerned with a recent preprint with Arnaud Ducrot and Jean-Baptiste Burie [P18] in which we focus on the pure competition limit for the same model. We describe the concentration of the time-dependent solutions to singular measures concentrated on the maxima of the fitness function. We give precise examples in which the asymptotic support of the measure depends on the initial condition (and not only on the fitness function).

Finally, Section 1.4 and chapter 5 are concerned with the modeling and parameter identification of the COVID-19 epidemic. In section 1.4.1 we identify the parameters of a mathematical model with unreported cases. We use its output as the input of a stochastic model to predict the last day of the epidemic if a rigorous lockdown is maintained (preprint in collaboration with Zhihua Liu, Pierre Magal, and Robin Thompson 1.4.1). Section 1.4.2 presents a collaboration with Pierre Magal and Ousmane Seydi in which we construct an epidemic model which is structured by age. We developed a method to identify the parameters of this model by using the Japanese age-structured reported cases data. In section 1.4.3, we clarify the predictions made by reported cases data by using a new model which takes into account the daily number of tests. Section 1.4.4 is devoted to the identification of the time-dependent transmission rate of a SIUR model in a single epidemic wave by matching a phenomenological model to the data [P7]. In section 1.4.5, we extend the method to multiple epidemic waves and apply it to the French data [P13]. Finally, in section 1.4.6, we extend the method to model with exposed cases and identify the parameters in eight different regions [P15]. We also reconstruct two notions of reproduction numbers and compare our results to other statistical methods. These last three works are collaborations with Pierre Magal and Jacques Demongeot.

Some of my published works and projects have not been included in this thesis but should be mentioned here briefly. It is the case for the first paper of my Ph.D. (collaboration with Gael Raoul and Sylvain Gandon [P1]) in which we analyzed the biological implications of the model in Griette and Raoul [P2]. On this occasion, I had written (in C++) a simulation code for a stochastic microscopic model corresponding to this system, based on the Gillespie algorithm, in one and two dimensions of space. We explored the effect of stochasticity on the propagation speed. In a collaboration with Sebastien Motsch [P5], we built a numerical finite-difference framework for the simulation of a kinetic model close to the Vicsek model. We observed numerically the formation of self-organized bands. Last but not least, I am the co-author of a book with Arnaud Ducrot, Zhihua Liu, and Pierre Magal, entitled "Differential Equations and Population Dynamics I: Introductory Approaches". It has been accepted in the "Lecture Notes on Mathematical Modelling in the Life Sciences" series at Springer. A second volume is currently in preparation.

1.1 Reaction-diffusion systems as models in population dynamics

Reaction-diffusion equations are popular in the modeling of population dynamics and have a history of almost one hundred years, considering the seminal works of Kolmogorov, Petrovskii, and Piskunov [238], and Fisher [170], in 1937. It so happens that my early work, including my work as a Ph.D. student, was concerned with reaction-diffusion models for evolutionary epidemiology.

Section 1.1.1 summarizes this early work, consisting in the core of my Ph.D. thesis, in collaboration with my advisors Matthieu Alfaro, Gaël Raoul, and Sylvain Gandon [P1, P2, P3]. I also include a later development that began during my post-doctoral fellowship hosted by Hiroshi Matano, and which is currently released in the form of a preprint [P19]. The collaboration with Sylvain Gandon and Gaël Raoul [P1] is mostly concerned with the biological implications and the derivation of a reaction-diffusion system of two equations in evolutionary epidemiology. In [P2], we analyze the same model mathematically to prove the existence of traveling waves traveling at the expected minimal speed. We also describe the shape of those waves. In [P3], we focus on a similar system with a periodic heterogeneity in the coefficients and construct a nontrivial stationary solution and minimal speed pulsating fronts for this system (the fronts are obtained by a vanishing viscosity method). In [P19], we study general reaction-diffusion systems with an arbitrary number of components with periodic coefficients which are monotone in a neighborhood of the boundary of the positive cone of $\mathbb{R}^d$. We prove a spreading property for the solutions of those systems and construct both minimal speed and super-critical pulsating fronts. We also prove some homogenization formulas for the speed. Finally, going back to the two-components system studied in [P2], we prove the global asymptotic stability of the unique equilibrium for a wide range of coefficients and propagate this result to systems with rapidly oscillating coefficients. Finally, we discover an unexpected phenomenon: when the matrix field giving the order-zero term of the system is asymmetric, the propagation speed of the solutions might depend on the direction of propagation, even in the absence of an advection term. This phenomenon cannot occur for

scalar equations and is therefore specific to reaction-diffusion systems. We construct a non-trivial example for this phenomenon.

In section 1.1.2, I summarize the results that I obtained in an independent work [P4] begun at the end of my Ph.D. I study a reaction-diffusion equation with spatial and phenotypic structure; the spatial motion of individuals is modeled by a diffusion and the mutation-selection at every point of space by nonlocal operators. It is known that the non-local operators in the homogeneous case (without spatial structure) have a singular measure as a principal eigenvector and therefore have no regularizing effect. I construct stationary solutions for the homogeneous equation and establish a sufficient condition to observe a singular measure in the constructed stationary solution. Then I focus on the traveling wave problem and construct a traveling wave with the expected minimal speed by the vanishing viscosity method.

Section 1.1.3 presents a collaboration with Léo Girardin [P9], in which we focus on a certain type of reaction-diffusion systems having the constant state 1 as their unique stationary solution. We prove the convergence of the traveling waves to the unique stationary solution at the back of the wave by constructing a Lyapunov functional. We extend this result to reaction-diffusion equations on cylinders with non-local competition in the local part of the cylinder.

Finally, section 1.1.4 is concerned with a collaboration with Matthieu Alfaro, Denis Roze, and Benoît Sarels [P17] (preprint). We derive a reaction-diffusion model for the time evolution of the fractions of haploid individuals carrying certain genes in the presence of a heterozygote incompatibility on two loci and recombination occurring during sexual reproduction. The individuals live and diffuse in a continuous linear habitat. In the symmetric case when the two loci have equal contributions to the fitness, the existence of stationary clines was studied by Barton [36]; we prove rigorously that the stationary cline is stable, *i.e.* that a small perturbation of the stationary cline converges to a possibly shifted stationary cline. We also study the asymmetric case and show that, when there is a small difference in the contribution of the two loci to the fitness, the cline starts to move. We also provide an analytic approximation of the speed.

1.1.1 Reaction-diffusion systems and application in evolutionary epidemiology

A large part of my early work was concerned with reaction-diffusion systems as models of pathogen evolution. The corresponding part of my work was done in collaboration with Matthieu Alfaro, Sylvain Gandon, and Gaël Raoul [P1, P2, P3], and more recently in a preprint with Hiroshi Matano [P19].

The original motivation for this line of works is the following model of pathogen evolution

$$\begin{cases} w_t(t,x) = w_{xx}(t,x) + w(t,x)\big(1-(w(t,x)+m(t,x))\big) + \mu\big(m(t,x)-w(t,x)\big), \\ m_t(t,x) = m_{xx}(t,x) + rm(t,x)\left(1-\dfrac{w(t,x)+m(t,x)}{K}\right) - \mu\big(m(t,x)-w(t,x)\big). \end{cases} \tag{1.1.1}$$

In this model, two types of pathogens coexist in a population of hosts which live on a one-dimensional habitat: *wild-type* pathogens, which are assumed to adopt a moderate strategy with respect to their hosts, and *mutant* pathogens, which are assumed to adopt an aggressive strategy. $w(t,x)$ stands for a density of hosts infected with a wild-type pathogen at time $t>0$ and position $x\in\mathbb{R}$, and $m(t,x)$ stands for the density of hosts infected by a mutant pathogen. There are three parameters involved in this model: the reproduction rate of the mutant $r>1$, its carrying capacity $K<1$, and the mutation rate $\mu>0$; the assumptions that $r>1$ and $K<1$ reflect the difference in strategy of the two types.

In [P2], we constructed minimal speed traveling waves for system (1.1.1) by a topological degree argument and established a formula for the speed of those waves. An example of the fronts is presented in Figure 1.1.1. We also described precisely the shape of the waves and showed the non-monotonicity when the mutation rate $\mu>0$ is sufficiently small and showed the convergence to a super-critical Fisher-KPP wave when $\mu\to 0$. In the companion paper [P1], we studied the biological implication and constructed a related stochastic model, to investigate numerically the dependency of the propagation speed on the local population size.

In [P3], we investigate an extension of (1.1.1) to heterogeneous environments:

$$\begin{cases} u_t(t,x) = u_{xx}(t,x) + u(t,x)\big(r_u(x)-\gamma_u(x)(u(t,x)+v(t,x))\big) + \mu\big(v(t,x)-u(t,x)\big), \\ v_t(t,x) = v_{xx}(t,x) + v(t,x)\big(r_v(x)-\gamma_v(x)(u(t,x)+v(t,x))\big) + \mu\big(u(t,x)-v(t,x)\big), \end{cases} \tag{1.1.2}$$

where $u(t,x)$ and $v(t,x)$ stand for population densities at time $t>0$ and $x\in\mathbb{R}$, $r_u(x)$ and $r_v(x)$ are $L-$periodic functions for some $L>0$, $\gamma_u(x)>0$ and $\gamma_v(x)>0$ are L-periodic functions which characterize

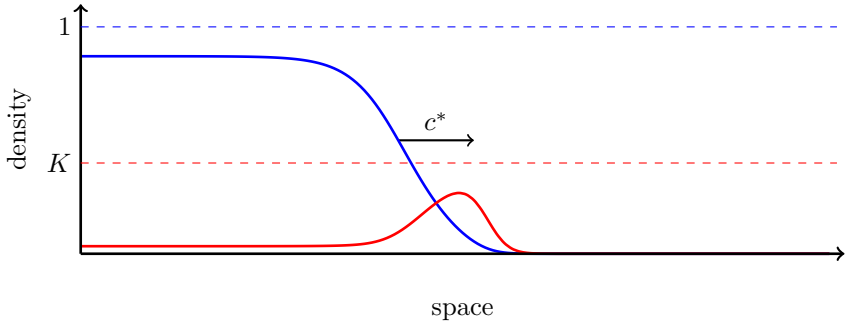

Figure 1.1.1: Traveling wave for the system (1.1.1). The blue curve represents the wild-type component w and the red curve the mutant m.

the strength of the competition between the species, and $\mu > 0$ is a mutation rate. Here, because of the periodic heterogeneity of the environment, the appropriate notion that serves to describe the long-term dynamics of the solutions to the initial value problem is the one of *pulsating waves*, which are special entire solutions satisfying

$$\left(u\left(t+\frac{L}{c},x\right),v\left(t+\frac{L}{c},x\right)\right)=\big(u(t,x-L),v(t,x-L)\big),$$

for some $c>0$, along with conditions at infinity

$$\limsup_{x\to+\infty}\max\big(u(t,x),v(t,x)\big)=0,\qquad \liminf_{x\to+\infty}\min\big(u(t,x),v(t,x)\big)>0.$$

We show the existence of a positive stationary solution to (1.1.2) by a global bifurcation argument adapted from the theory of bifurcation from simple eigenvalues of Crandall and Rabinowitz [123], and related to the work of Krasnosel'skii [244]. Next, we prove the existence of pulsating traveling waves by using the change of variable $(s,x)=(x-ct,x)$ and studying the resulting equation,

$$\begin{cases} -u_{xx}-2u_{xs}-u_{ss}-cu_s &= u(r_u-\gamma_u(u+v))+\mu v-\mu u \quad \text{in } \mathbb{R}^2\\ -v_{xx}-2v_{xs}-v_{ss}-cv_s &= v(r_v-\gamma_v(u+v))+\mu u-\mu v \quad \text{in } \mathbb{R}^2\\ (u,v)(s,\cdot) \quad \text{is } L\text{-periodic.} \end{cases} \tag{1.1.3}$$

Since the differential operator in (1.1.3) is degenerate elliptic, we first regularize it by adding a small viscosity term $-\varepsilon\partial_{ss}$ to the left-hand side, construct the fronts for the regularized problem, and let $\varepsilon\to 0$ to recover a solution to the original problem. The vanishing viscosity argument $\varepsilon\to 0$ requires some regularity to be preserved to make the argument work; this regularity is obtained by a Bernstein-type estimate on the gradient.

The last work in this line of works and probably the most complete is the recent preprint with Hiroshi Matano [P19], in which we study parabolic reaction-diffusion systems with hybrid nonlinearity

$$\begin{cases} u_t(t,x)=\mathcal{L}u(t,x)+f(x,u), & t>0, x\in\mathbb{R},\\ u(t=0,x)=u_0(x), & x\in\mathbb{R}. \end{cases} \tag{1.1.4}$$

Here $u(t,x)\in\mathbb{R}^d$ is a vector representing a population density composed of several genotypes; $\mathcal{L}$ is a differential second-order uniformly elliptic operator (with no zero-order term), and $f(x,u)$ is L-periodic with respect to x and *hybrid* with respect to u, in the sense that it is monotone in a vicinity of the boundary of the positive cone (i.e. the set of $u=(u_1,\dots,u_d)^T$ such that $0\le u_i\le\varepsilon$ for some i), but not necessarily in the whole positive cone. We also assume that f is sublinear in the sense that $f(x,u)\le D_uf(x,0)u$ for all $u\in\mathbb{R}^d$, and that the partial Jacobian matrix of f with respect to u, $D_uf(x,0)$, is cooperative and irreducible. Under these assumptions, we first study the principal eigenvalue problem

$$-e^{\lambda x}\mathcal{L}\big(e^{-\lambda x}\varphi^\lambda(x)\big)=D_uf(x,0)\varphi^\lambda(x)+k(\lambda)\varphi^\lambda(x),$$

where $\lambda > 0$ is a parameter, and $(k(\lambda), \varphi^\lambda(x) > 0)$ is the principal eigenpair of the above problem with L-periodic boundary conditions. We show that $\lambda \mapsto k(\lambda)$ is strictly concave, which gives a meaning to the expected formula for the minimal speed of traveling waves

$$c^* := \inf_{\lambda>0} \frac{-k(\lambda)}{\lambda}. \tag{1.1.5}$$

When the nonlinearity f can be controlled from below by a monotone function f^- which shares the same Jacobian matrix at 0: $D_u f(x,0) = D_u f^-(x,0)$, we show that the spreading speed of solutions starting from front-like initial conditions,

$$u_0(x) > 0 \text{ for } x < 0, \qquad u_0(x) = 0 \text{ for } x > 0,$$

is equal to c^*. We also show the existence of traveling waves for any $c \geq c^*$ by using a fixed-point argument on the map $u_0(x) \mapsto u(\frac{L}{c}, x + L)$.

Surprisingly, the spreading speed for compactly supported initial data might be different in general from the one of front-like initial data given by (1.1.5), even when the differential operator $\mathcal{L}$ has no first-order term. The reason is that the matrix $D_u f(x,0)$ might not be symmetric, and the antisymmetric part of $D_u f(x,0)$ can induce an asymmetry in the map $\lambda \mapsto k(\lambda)$. This, in turn, might induce a different value for the rightward spreading speed (given by (1.1.5)) and the leftward spreading speed

$$c^*_{\text{left}} := \inf_{\lambda>0} \frac{-k(-\lambda)}{\lambda}.$$

We provide an example of a two-component system for which the rightward and leftward spreading speeds are indeed different. It is constructed as a strongly coupled system whose singular limit is a scalar reaction-diffusion equation with a first-order term.

We also investigate the existence of a weak hair-trigger effect for time-dependent solutions to (1.1.4), in the sense that positive non-trivial initial data become eventually locally uniformly positive. There is a sharp criterion for such a weak hair-trigger effect, which is that the Dirichlet principal eigenvalue, defined as $\lambda_1^\infty := \lim_{R\to+\infty} \lambda_1^R$, is negative, where λ_1^R is the principal eigenvalue for the Dirichlet problem on the interval $(-R, R)$,

$$\begin{cases} -\mathcal{L}\varphi(x) = D_u f(x,0)\varphi(x) + \lambda_1^R \varphi(x), & x \in (-R, R), \\ \varphi(-R) = \varphi(R) = 0, \end{cases}$$

and $\varphi(x) > 0$ for all $x \in (-R, R)$. We show that

$$\lambda_1^\infty = \max_{\lambda\in\mathbb{R}} k(\lambda),$$

and since the function $k(\lambda)$ is not necessarily even, there might be a positive gap between the Dirichlet principal eigenvalue λ_1^∞ and the periodic principal eigenvalue $\lambda_1^{per} := k(0)$ even in the absence of a first-order term in $\mathcal{L}$. The strongly coupled system mentioned above, in particular, is an example of a two-components system with such a positive gap.

However, the situation for systems is similar to the scalar case when there is no first-order term (i.e. the leftward and rightward speeds are equal, and the weak hair-trigger effect holds as soon as $k(0) < 0$) provided there is no first-order term in $\mathcal{L}$ and we are in one of the two following cases:

1. both $\mathcal{L}$ and the matrix $D_u f(x,0)$ are self-adjoint, or

2. both $\mathcal{L}$ and $D_u f(x,0)$ are even in x.

Other results are also established in [P19]: a formula for the speed in the case of rapidly oscillating coefficients (by a homogenization argument) and a more precise description of the long-time behavior of (1.1.1) and (1.1.2) in the case of homogeneous coefficients. In particular, we prove the convergence of the time-dependent problem for the spatially homogeneous problem under some assumptions of the coefficient and extend it to the case of rapidly oscillating coefficients. The local asymptotic stability is proved in the homogeneous case without restrictive assumptions.

1.1.2 Singular measure traveling waves

In [P4], I introduced the following equation to model the spatial spread of an evolving species with a continuous phenotypic structure,

$$u_t(t,x,y) = u_{xx}(t,x,y) + \mu\left(\int_\Omega M(y,z)u(t,x,z)\mathrm{d}z - u(t,x,y)\right) + u(t,x,y)\left(a(y) - \int_\Omega K(y,z)u(t,x,z)\mathrm{d}z\right), \tag{1.1.6}$$

where $u(t,x,y)$ stands for the density of population at time $t>0$, position $x\in\mathbb{R}$, and phenotypic value $y\in\Omega$ where $\Omega\subset\mathbb{R}^n$ is a bounded domain; $a(y)\in C^\alpha(\overline{\Omega})$ is a fitness function which depends only on the phenotypic value y, $\mu>0$ is the mutation rate, $M(y,z)\in C^\alpha(\overline{\Omega}^2)$ is a mutation kernel, and $K(y,z)\in C^\alpha(\overline{\Omega}^2)$ is a competition kernel ($\alpha\in(0,1]$). It had been noted previously by Coville [119] that the linearized equation corresponding to (1.1.6),

$$\mu\left(\int_\Omega M(y,z)\varphi(z)\mathrm{d}z - \varphi(y)\right) + \varphi(y)a(y) + \lambda\varphi(y) = 0, \tag{1.1.7}$$

for $\lambda\in\mathbb{R}$ and $\varphi(y)>0$ (in a sense to be precised) might have some singular measure solutions under the condition that

$$\frac{1}{\sup_{z\in\Omega}a(z) - a(y)} \in L^1(\Omega). \tag{1.1.8}$$

The first result in the article [P4] is extending the result of Coville by showing that, when the assumption (1.1.8) holds, there is a unique λ (the *principal eigenvalue*) which is associated with a nonnegative Radon measure solution to (1.1.7) (even if that measure is singular). Next, it is specified under which condition (involving μ, M, and a) the equation (1.1.7) actually has a nonnegative singular measure solution. In addition to (1.1.8), there exists a $\mu_0=\mu_0(M,a)>0$ such that the equation (1.1.7) has a singular measure solution precisely when $\mu<\mu_0$, and μ_0 can be determined by a related principal eigenproblem. When $\mu<\mu_0$, the principal eigenvalue is given by the formula

$$\lambda_1 = -\big(\sup_{z\in\Omega} a(z) - \mu\big),$$

and there exists a nonnegative singular measure $\varphi(\mathrm{d}y)$ solution to (1.1.7); and finally any solution to (1.1.7) has a singularity concentrated on

$$\Omega_0 := \left\{ y\in\Omega \,:\, a(y) = \sup_{z\in\Omega} a(z)\right\}.$$

Once the linearized problem is understood, the nonlinear problem is investigated. In particular, it is shown that there exists a nonnegative stationary solution $p(\mathrm{d}y)$ to (1.1.6) (in the sense of measures) which is independent of x, under the assumption (1.1.8) and $\mu<\mu_0$, provided that the principal eigenvalue has the correct sign: $\lambda_1<0$. This stationary solution is constructed by a vanishing viscosity argument. Under an additional assumption on the competition kernel,

$$K(z_0,z)\le K(y,z) \text{ for some } z_0\in\Omega_0 \text{ and for all } y,z\in\Omega,$$

it can be shown that the stationary measure $p(\mathrm{d}y)$ has a singularity which is concentrated on a subset of Ω_0.

Last but not least, we focus on traveling wave solutions to (1.1.6), which are entire solutions satisfying $u(t,x,y)=u(x-ct,y)$ for all $t\in\mathbb{R}$, $x\in\mathbb{R}$, and $y\in\Omega$ (with a small abuse of notation) and the following conditions at infinity:

$$\liminf_{\bar{x}\to+\infty}\int_{\mathbb{R}\times\overline{\Omega}}\varphi(x+\bar{x},y)u(\mathrm{d}x,\mathrm{d}y) > 0,$$
$$\limsup_{\bar{x}\to-\infty}\int_{\mathbb{R}\times\overline{\Omega}}\varphi(x+\bar{x},y)u(\mathrm{d}x,\mathrm{d}y) = 0,$$

for any compactly supported test function $\varphi \in C_c(\mathbb{R} \times \overline{\Omega})$. It is shown that there exist such traveling waves travelling at a speed

$$c^* := 2\sqrt{-\lambda_1},$$

when the principal eigenproblem has a singular measure solution and the principal eigenvalue is negative $\lambda_1 < 0$. The proof is rather technical and involves the construction of travelling fronts for a regularized problem with small viscosity, and then a vanishing viscosity argument.

1.1.3 Convergence to equilibrium for KPP-type traveling waves on cylinders

In a work in collaboration with Léo Girardin [P9], we investigated elliptic systems of the type

$$-cu_x(x) - Du_{xx}(x) = Mu(x) + u(x) - u(x) \circ Cu(x), \tag{1.1.9}$$

where $c \in \mathbb{R}$, $u(x) \in \mathbb{R}^N$ is a vector-valued function of $x \in \mathbb{R}$, D is a diagonal matrix with positive entries; M is a mutation matrix which is assumed to be cooperative, irreducible, line-sum-symmetric (namely, $M1 = M^T1$) and satisfies $M1 = 0$; C is a normal matrix which is positive and satisfies $C1 = 1$; finally, the symbol $\circ$ denotes the componentwise (sometimes called Hadamard) vector product. Under those assumptions, we show that (1.1.9) satisfies a Liouville property: if $p(x)$ is a solution to (1.1.9) satisfying

$$\inf_{x\in\mathbb{R}} \min_{i=1,\dots,N} p_i(x) > 0,$$

then in fact $p(x) \equiv 1$. As a consequence, if u is a traveling wave solution to (1.1.9), *i.e.* a nonnegative solution satisfying

$$\lim_{x\to+\infty} u(x) = 0 \text{ and } \liminf_{x\to-\infty} u(x) > 0,$$

then in fact we can prove

$$\lim_{x\to-\infty} u(x) = 1.$$

The importance of this result lies in the fact that, if we relax the assumptions made on the matrices M and C, then in general it is difficult to determine the asymptotic behavior of the traveling waves solutions to (1.1.9). Here we have determined a large class of problems for which this behavior can be completely determined.

Similar arguments allow us to extend the Liouville property and the convergence on the back of the waves to equations set on cylinders which can be written as

$$\begin{aligned} -d(y)u_{xx}(x,y) - cu_x(x,y) = \nabla_y\big(\sigma(y)\nabla u(x,y)\big) + \int_\Omega m(y,z)\big(u(x,z) - u(x,y)\big)\mathrm{d}z \\ + u(x,y)\left(1 - \int_\Omega k(y,z)p(x,z)\mathrm{d}z\right), \end{aligned}$$

with homogeneous Neumann boundary conditions on $\mathbb{R} \times \partial\Omega$. Here the function m is continuous on $\overline{\Omega}^2$, positive, and satisfies

$$\int_\Omega m(y,z)\mathrm{d}z = \int_\Omega m(z,y)\mathrm{d}z.$$

The function k is continuous on $\overline{\Omega}^2$, positive, and the induced operator on $L^2(\Omega)$:

$$K[p] := \int_\Omega k(y,z)p(z)\mathrm{d}z$$

is normal. Moreover $K[1] = 1$. If those assumptions are satisfied, it is also possible to state a Liouville property and to determine the asymptotic behavior of travelling waves.

1.1.4 A model of genetic incompatibilities in parapatry

In a recent preprint with Matthieu Alfaro, Denis Roze, and Benoît Sarels [P17], we investigate the interaction between two genetic incompatibilities in a spatial context via a population genetic model. More precisely, we focus on a simple situation involving two coupled underdominant loci, with alleles A and a at the first locus and B and b at the second locus. In other words, at each locus, heterozygotes (say Aa) have lower fitness than homozygotes, while the two homozygotes AA and aa have equal fitness. This form of symmetric selection against heterozygotes can maintain stable clines in allele frequencies [41, 35], separating regions where AA and aa individuals are abundant. When two such clines overlap in space (one separating regions where AA and aa are abundant, and the other separating regions where BB and bb are abundant), they tend to attract each other until they coincide, and then become motionless. This process was studied by Barton [36] in the case of a continuous linear habitat.

Here we study the situation when the fitness of the homozygote $AB|AB$ becomes slightly larger than the one of $ab|ab$. In this asymmetric situation, it is not *a priori* obvious whether the stationary cline stays stationary or begins to move. When the difference in fitness between homozygotes has a low order of magnitude (measured by a parameter $0 < \varepsilon \ll 1$) compared to the fitness cost of heterozygotes, we show that a front traveling at speed $c_\varepsilon > 0$ of stacked clines emerges from the stationary cline of the symmetric case. The proof involves a rather intricate perturbation analysis and allows us to give an explicit approximation of the speed c_ε.

After a series of approximations which are detailed in the article, the equation for the stacked clines in the asymmetric case under the assumption that the clines remain stacked can be written as

$$u_t(t,x) = u_{xx}(t,x) + Sf(u(t,x)) + \varepsilon g(u(t,x)) + \frac{2}{r}\big(S(2u(t,x)-1)+\varepsilon\big)(u_x(t,x))^2. \tag{1.1.10}$$

Here $u(t,x)$ stands for the density of individuals possessing the allele A, $S > 0$ is the penality in fitness of heterozygotes, r is the rate of recombination, and ε measures the difference in fitness between homozygotes $AB|AB$ and $ab|ab$; the functions f and g are given by

$$f(u) = u(2u-1)(1-u), \qquad g(u) = u(1-u).$$

Note that the equation (1.1.10) involves a gradient nonlinearity, which contributes to the difficulty of the study.

In the case when $\varepsilon = 0$, we recover the symmetric case and prove mathematically the existence of and uniqueness of a standing wave for (1.1.10), *i.e.* a function u_0 satisfying

$$\begin{gathered} u_0''(x) + Sf(u_0(x)) + \frac{2}{r}S(2u_0(x)-1)(u_0'(x))^2 = 0, \\ u_0(-\infty) = 1, \qquad u_0(+\infty) = 0. \end{gathered} \tag{1.1.11}$$

By using the ideas of Sattinger [349], we prove the local stability of the standing wave as a solution to the Cauchy problem (1.1.10) (with $\varepsilon = 0$) for the L^∞ topology.

Next, we focus on the full problem (1.1.10) with $\varepsilon > 0$ small. We prove the existence of travelling waves traveling at a positive speed $c_\varepsilon > 0$, *i.e.* positive solutions to the problem

$$\begin{gathered} u''(x) + cu'(x) + Sf(u(x)) + \varepsilon g(u(x)) + \frac{2}{r}\big(S(2u(x)-1)+\varepsilon\big)(u'(x))^2 = 0, \\ u(-\infty) = 1, \qquad u(+\infty) = 0. \end{gathered} \tag{1.1.12}$$

This is done by using the implicit function theorem in the adequate space, and we get an approximation formula for the speed of the traveling wave:

$$c_\varepsilon = -\frac{\displaystyle\int_{\mathbb{R}} \left(g(u_0) + \frac{2}{r}(u_0')^2\right) u_0' e^{\frac{4S}{4}(u_0^2-u_0)}}{\displaystyle\int_{\mathbb{R}} (u_0')^2 e^{\frac{4S}{4}(u_0^2-u_0)}}\varepsilon + o(\varepsilon), \tag{1.1.13}$$

where u_0 is the standing wave solving (1.1.11). While this expression allows In order to apply the implicit functions theorem we had to show the bijectivity of the Fréchet differential of the left-hand side of (1.1.12) with respect to u, which is a uniformly elliptic operator; this part is done by combining *a priori* estimates

on u_0 and the computation of the Fredholm index of elliptic operators described by Volpert, Volpert, and Collet [386] and described in the book of Volpert [384].

While (1.1.13) already permits the computation of c_ε at the order 1 in ε, it still depends on the knowledge of u_0. It turns out that this formula can still be simplified as

$$c_\varepsilon = c_1\varepsilon + o(\varepsilon), \qquad \text{where } c_1 = \frac{\displaystyle\int_0^1 \frac{r}{4S}\left(1 - e^{-\frac{4S}{r}(u-u^2)}\right) \mathrm{d}u}{\displaystyle\int_0^1 \left(\frac{r^2}{8S}e^{\frac{4S}{r}(u-u^2)} - \frac{r}{2}(u-u^2) - \frac{r^2}{8S}\right)^{\frac{1}{2}} e^{-\frac{4S}{r}(u-u^2)}\mathrm{d}u}.$$

Hence we recover an explicit approximation for c_ε (independent of u_0).

1.2 A hyperbolic cell-cell repulsion model

This part of my work was done in collaboration with Xiaoming Fu, and Pierre Magal [P8, P11, P12]. These articles are all part of the Ph.D. thesis of Xiaoming Fu, to which I participated as an informal advisor.

In section 1.2.1, we derive a model for a population of cells living in a Petri dish [P8]. We work on a circular domain of $\mathbb{R}^2$ representing the Petri dish. Since cells do not move by themselves, we do not include a diffusion operator in the equation but only model the cell-cell repulsion forces ("pressure") acting on the cells. The pressure itself is determined by the local density of the cells through a non-local kernel. Thus we obtain a hyperbolic model. We prove mathematically the local well-posedness of the Cauchy problem when a single species exists in the Petri dish. When two species exist in the Petri dish with comparable susceptibility to the pressure, we prove that initially segregated initial data will stay segregated at later times. This preservation of segregation is one of the most important features of the model. Last, we developed a numerical code to simulate the behavior of the cells and tested various scenarios.

Section 1.2.2 and section 1.2.3 contain the continuation of this work, which concerns a refined study of the qualitative properties of the same model set on the line instead of the disk [P11, P12].

1.2.1 A cell-cell repulsion model on a hyperbolic Keller-Segel equation

In [P8], we presented a new mathematical model for cell-cell repulsion in a Petri dish. Our aim was to describe the cell growth in the co-culture experiments of Pasquier et al [318], with a particular focus on the segregation property observed in those experiments. Rather than turning to existing models of nonlinear diffusion or strong competition, we developed a new model in the inviscid case, *i.e.* when the motion of the cells is not subject to random motion. A simulation using our code is presented in Figure 1.2.1.

We first consider the following model for a single cell species,

$$\begin{cases} \partial_t u(t,x) - d\nabla\cdot\big(u(t,x)\nabla P(t,x)\big) = u(t,x)h(u(t,x)), & t\in(0,T], x\in\Omega, \\ u(0,x) = u_0(x), & x\in\Omega, \end{cases} \tag{1.2.1}$$

where the pressure $P(t,x)$ satisfies the following equation

$$\begin{cases} P(t,x) - \chi\Delta P(t,x) = u(t,x), & t\in(0,T], x\in\Omega, \\ \nabla P(t,x)\cdot\nu(x) = 0, & t\in[0,T], x\in\partial\Omega. \end{cases} \tag{1.2.2}$$

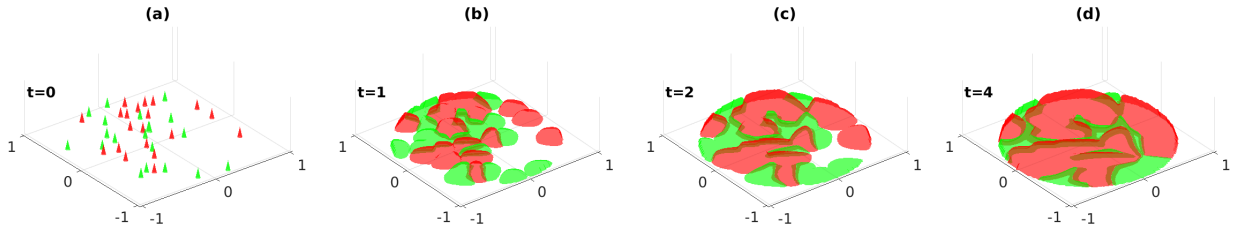

Figure 1.2.1: Solution of the multi-species model (1.2.5) through time. The red and green areas represent different types of cells who live in a circular domain.

Here $\Omega \subset \mathbb{R}^2$ is the disk centered at $x = 0$ and with radius $r = 1$, $\nu(x)$ is the outward normal vector for $x \in \partial\Omega$, $d > 0$ is the dispersion coefficient, and $\chi > 0$ is a sensing coefficient. Note that there is no second-derivative of u in space in the model (1.2.1)–(1.2.2): the motion of the cells is completely determined by the gradient of the pressure $P(t, x)$.

In order to give a precise meaning to the solutions to (1.2.1)–(1.2.2), we introduce the *characteristic flow* associated with (1.2.1),

$$\begin{cases} \dfrac{\partial}{\partial t}\Pi(t, s; x) = -d\nabla P(t, \Pi(t, s; x)), & t, s \geq 0, x \in \Omega \\ \Pi(s, s; x) = x, & x \in \Omega. \end{cases} \tag{1.2.3}$$

If $\nabla P(t, x)$ is sufficiently smooth (i.e. continuous and Lipschitz continuous in the x variable) then (1.2.3) defined a unique characteristic flow. In this case, we can rigorously prove the invariance of Ω for the flow of (1.2.3). This allows us to introduce an auxiliary variable $w(t, x) := u\big(t, \Pi(t, 0; x)\big)$, which satisfies a differential equation in time only:

$$\partial_t w(t, x) = w(t, x)\big(1 + \Delta P(t, \Pi(0, t; x)) - w(t, x)\big). \tag{1.2.4}$$

Therefore the knowledge of $P(t, x)$ allows us to reconstruct $u(t, x)$ by integrating (1.2.3) and the ordinary differential equation (1.2.4). This remark allows us to write $(u(t, x), P(t, x))$ as the solution of a fixed-point problem and prove the existence and uniqueness of the solution to (1.2.1)–(1.2.2) locally in time, provided $u_0(x)$ is sufficiently smooth. The solutions obtained by this method are a new notion of solutions which we call *solution integrated along the characteristics*.

We also consider the multi-species model, which can be written as follows

$$\begin{cases} \partial_t u_1(t, x) - d_1\nabla \cdot \big(u_1(t, x)\nabla P(t, x)\big) = u_1(t, x)h_1(u_1(t, x), u_2(t, x)), & t \in (0, T], x \in \Omega, \\ \partial_t u_2(t, x) - d_2\nabla \cdot \big(u_2(t, x)\nabla P(t, x)\big) = u_2(t, x)h_2(u_1(t, x), u_2(t, x)), & t \in (0, T], x \in \Omega, \\ P(t, x) - \chi\Delta P(t, x) = u_1(t, x) + u_2(t, x), & t \in (0, T], x \in \Omega, \\ \nabla P(t, x) \cdot \nu(x) = 0, & t \in [0, T], x \in \partial\Omega, \\ u_1(0, x) = u_{10}(x), u_2(0, x) = u_{20}(x), & x \in \Omega. \end{cases} \tag{1.2.5}$$

In the important case when $d_1 = d_2 = d$, we can use the characteristic flow to prove that solutions starting from initially segregated initial solutions stay segregated for all positive time $t > 0$. An illustration of this property is presented in Figure 1.2.2. This property has been observed in mono-layered cultured experiments and is one of the reasons why we introduced the inviscid model.

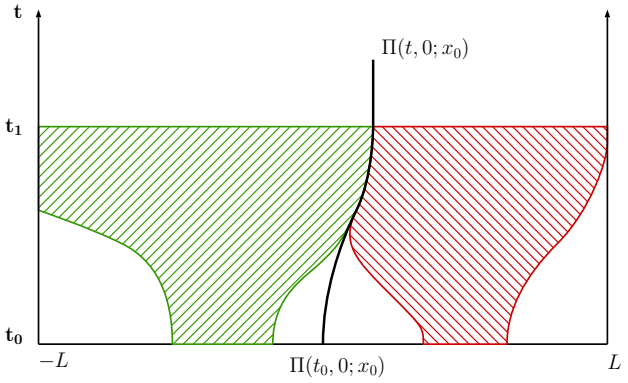

Figure 1.2.2: Illustration of the preservation of the segregation.

Finally, we studied numerical simulations of (1.2.5) to study the influence of the spatial structure imposed by the Petri dish on the population dynamics of the cells. The result of a simulation at different times is shown in Figure 1.2.1. We tested more specifically two factors that may have an influence on the eventual population ratios. The first factor is the initial cell distribution, measured by the initial number of cell clusters and the law of the initial distribution. We found that the most significant factor in the eventual distribution of the cells is the initial number of clusters and that the law of the initial repartition of the

clusters has a limited effect. The second factor is the motility of the cells, measured by the coefficients d_1 and d_2. We found that the influence of the motilities of the cells is most important at the beginning of the simulation when the cells are invading the Petri dish; but the dynamics of the cells $u_i h_i(u_1, u_2)$ become the key factors at larger time scales.

1.2.2 Existence and uniqueness of solutions for a hyperbolic Keller–Segel equation

In [P11, P12], we studied more precisely the mathematical properties and the qualitative behavior of the solutions to a hyperbolic equation similar to (1.2.1)–(1.2.2) but set on a one-dimensional space. We study the equation

$$\begin{cases} u_t(t,x) - \chi \partial_x(u(t,x)\partial_x p(t,x)) = u(t,x)\big(1-u(t,x)\big), & t>0, x\in\mathbb{R}, \\ u(0,x) = u_0(x), & x\in\mathbb{R}, \end{cases} \tag{1.2.6}$$

where $p(t,x)$ solves the equation

$$p(t,x) - \sigma^2 \partial_{xx} p(t,x) = u(t,x). \tag{1.2.7}$$

In [P11], we study the Cauchy problem for the solutions to (1.2.6)–(1.2.7). We take advantage of the spatial derivative in x by introducing the characteristic flow associated with (1.2.6):

$$\begin{cases} \partial_t h(t,s;x) = -\chi(\rho_x \star u)(t, h(t,s;x)), \\ h(s,s;x) = x. \end{cases} \tag{1.2.8}$$

Here ρ is the Green function associated with the equation (1.2.7) on $p(t,x)$, which can be explicitly computed as $\rho(x) = \frac{1}{2\sigma} e^{-\frac{|x|}{\sigma}}$, and $\star$ is the usual convolution. In particular, $p(t,x) = (\rho \star u)(t,x)$ and $p_x(t,x) = (\rho_x \star u)(t,x)$. Note that, thanks to the explicit formula for ρ, the function $(\rho \star u)(t,x) := \int_{\mathbb{R}} \rho_x(x-y)u(t,y)\mathrm{d}y$ is uniformly Lipschitz continuous in x as soon as $u(t,\cdot)$ is in $L^\infty(\mathbb{R})$.

By using the characteristic flow (1.2.8) we can introduce the notion of *solution integrated along the characteristics* as a function $u(t,x)$ such that (1.2.8) has a classical solution for all $x\in\mathbb{R}$ and the rescaled equation

$$\begin{cases} \partial_t u(t, h(t,0;x)) = u(t,h(t,0;x))\big(1 + \hat{\chi} p(t,h(t,0;x)) - (1+\hat{\chi}) u(t,h(t,0;x))\big) \\ u(0,x) = u_0(x), \end{cases}$$

also has a classical solution in t for all $x\in\mathbb{R}$, where $\hat{\chi} := \frac{\chi}{\sigma^2}$ and $p(t,x) = (\rho \star u)(t,x)$. *Importantly, the notion of solution integrated along the characteristics does not require any regularity in x.* We showed that the problem (1.2.6)–(1.2.7) is well-posed for the notions of solutions integrated along the characteristics when $u_0 \in L^\infty(\mathbb{R})$, in the sense that the Cauchy problem admits a unique solution for all $u_0 \in L^\infty$, and the semiflow $t \mapsto u(t,\cdot)$ is continuous for the weighted L^1 topology induced by the norm

$$\|f\|_{L^1_\eta(\mathbb{R})} := \int_{\mathbb{R}} |f(x)| e^{-\eta|x|}\mathrm{d}x, \text{ for some } \eta \in (0,1).$$

Moreover the map $u_0 \in L^\infty(\mathbb{R}) \mapsto u(t,\cdot) \in L^1_\eta(\mathbb{R})$ is also continuous. The maximal time of existence associated with an initial condition $u_0 \in L^\infty$ can then be properly defined, and when $u_0(x) \in [0,1]$ for almost every $x\in\mathbb{R}$, the maximal solution exists for all $t\in(0,+\infty)$ and we have $u(t,\cdot)\in[0,1]$ almost everywhere.

We also show that the map $u_0 \mapsto u(t,\cdot)$ preserves some of the properties of u_0; in particular, the continuity, C^1 and higher regularity, and monotony of the initial condition are all preserved by the semiflow. When the initial data is C^1, we can prove that the solution integrated along the characteristics is a classical solution to the original equation (1.2.6)–(1.2.7).

Finally, when $u_0(x)\in[0,1]$ is uniformly positive in the sense that there exists $\delta>0$ such that $u_0(x)\geq 0$ for almost all $x\in\mathbb{R}$, then we can prove that the solution $u(t,x)$ to (1.2.6)–(1.2.7) converges to 1 uniformly as $t\to+\infty$.

1.2.3 Sharp discontinuous traveling waves in a hyperbolic Keller–Segel equation

In [P12], we focused on the qualitative properties of the time-dependent solutions to (1.2.6) and (1.2.7), as well as on the existence of particular traveling waves for this model. When $u_0(x)$ is compactly supported, it

is possible to show that the solution integrated along the characteristics $u(t,x)$ is also compactly supported for all $t>0$. More precisely, the position of the interfaces between $\{u(t,\cdot)>0\}$ and $\{u(t,\cdot)=0\}$ are given by particular characteristic curves.

Suppose for simplicity that $u_0(x)$ is front-like, *i.e* $u_0(x)>0$ for all $x<0$ and $u_0(x)=0$ for all $x\geq 0$. Then the interface between $\{u(t,\cdot)>0\}$ and $\{u(t,\cdot)=0\}$ is reduced to a single point which position is given by the characteristic curve $t\mapsto h(t,0;0)$ called the *separatrix*. When u_0 does not vanish too fast near the boundary of its support (namely, u_0 is controlled from below by a polynomial), then it is possible to give precise asymptotics on the behavior of the level sets in the vicinity of $u=0$. We show that the level set $\xi(t,\beta)$, defined by $\sup\{\xi\,:\,u(t,\xi)=\beta\}$, satisfies

$$h^*(t)-\left(\frac{\beta}{\gamma}\right)^{\frac{1}{\alpha}}e^{-\frac{\eta}{2\alpha}t}\leq \xi(t,\beta)\leq h^*(t),$$

when $\beta\leq \frac{1}{1+\hat\chi+\alpha\chi}$, where $h^*(t):=h(t,0;0)$ is the separatrix, α,γ are such that $u_0(x)\geq\gamma|x|^\alpha$ for all $x<0$ sufficiently small, and $\eta:=1-\frac{1+\hat\chi+\alpha\chi}{\beta}$. In other words, even if u_0 is continuous (and in this case so is $u(t,\cdot)$ for all $t>0$), a jump discontinuity is forming at the interface in infinite time. A comparison between the behavior of the solutions starting from two different initial conditions is presented in Figure 1.2.3.

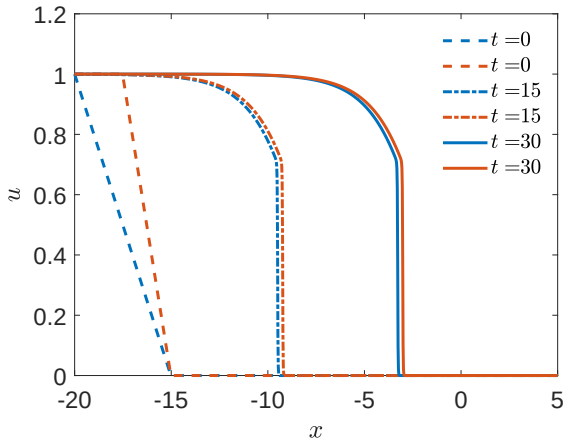

Figure 1.2.3: Comparison of the solutions of equation (1.2.1)–(1.2.2) for two different initial condition. We only plot $u(t,x)$. The solutions look like they approach the same asymptotic shape, which has a steep transision between the level $u\approx 0.73$ and $u=0$.

This suggests that the spatial behavior of the solution to (1.2.6)–(1.2.7) might be described by *sharp discontinuous* traveling wave profiles, *i.e.* particular entire solutions integrated along the characteristics satisfying

$$u(t,x)=U(x-ct)\text{ for all }x\in\mathbb{R}\text{ and }t\in\mathbb{R},$$

for a speed $c\in\mathbb{R}$ and a profile $U\in L^\infty(\mathbb{R})$ such that $U(x)\equiv 0$ for all $x>0$. We show the existence of such a profile for a parameter range $\hat\chi\in(0,\bar\chi)$ for some $\bar\chi>1$. It is obtained as a solution to the following ordinary differential equation

$$-cU'(x)-(U(x)P'(x))'=U(x)\big(1-U(x)\big)\text{ for }x<0,$$

where $P=\rho\star U$. Moreover, the constructed profile is continuous and C^1 except at the singularity, decreasing and we have an estimate of the size of the jump:

$$U(0^-)-U(0^+)=\frac{2}{2+\hat\chi},$$

if the jump is located at 0 (*i.e.* $U(x)>0$ for $x<0$, and $U(x)=0$ for $x>0$). Because of the estimate on the jump size, we can obtain bounds on the speeds for which a profile exists:

$$c\in\left(\frac{\sigma\hat\chi}{2+\hat\chi},\frac{\sigma\hat\chi}{2}\right).$$

Finally, we can show that the discontinuous traveling waves are the only sharp traveling waves (*i.e.* whose profile is equal to zero on the positive half-line) for our system of equations (1.2.6)–(1.2.7). More precisely we show that continuous traveling wave profiles U are necessarily smooth and satisfy

$$-\chi(\rho_x \star U)(x) < c \text{ for all } x \in \mathbb{R}.$$

But if U is sharp then the speed of the traveling wave is precisely given by $c = -\chi(\rho \star U)(0) = \partial_t h(t, 0; 0)$. Thus U cannot be sharp and continuous.

1.3 Long-time dynamics in epidemic models

In this section, I present a collaboration with Jean-Baptiste Burie, Arnaud Ducrot, and Quentin Richard [P6], in which we describe the stationary solutions of an epidemic model caused by a spore-producing pathogen. More precisely we consider a situation in which the population of pathogens is structured by a continuous variable and subject to mutations; the pathogen can potentially infect two different hosts with different fitnesses. We describe precisely the shape of the stationary solutions for this system when the mutation kernel is concentrated and prove the uniqueness by a topological degree method. In a more recent preprint in collaboration with Jean-Baptiste Burie and Arnaud Ducrot [P18], we focus on the mutation-less model for a single host and describe the asymptotic behavior of the solutions in a space of measures. We interpret our findings in the light of the competitive exclusion principle. This study can be considered as the first step towards a refined description of the transient and asymptotic behavior of the time-dependent problem in the presence of a sharply concentrated mutation kernel.

1.3.1 Concentration estimates in a multi-host epidemic model structured by trait

In our work [P6], we focus on the stationary solutions for a multi-host epidemiological model structured by continuous trait, which represents the infection of plants by a fungal disease. We consider two types of host plants, which can be infected by a pathogen whose characteristics depend on a phenotypic trait $x \in \mathbb{R}^N$. We consider that hosts are represented by a density of plant tissue denoted $S_1(t)$ and $S_2(t)$ respectively. In the absence of the pathogen, there is a continuous influx of hosts at rate $\xi_k \Lambda$ ($k = 1, 2$) because the plant constantly renews its tissue, and the cells die at rate θ. The density of tissue of the host k which is infected by a pathogen of trait $x \in \mathbb{R}^N$ at time $t > 0$ is denoted $I_k(t, x)$. The pathogen we consider has to produce spores in order to infect new hosts, and the density of spores is denoted $A(t, x)$. The infectivity of a spore depends on its phenotypic value and on the host, we denote it $\beta_k(x)$; the additional mortality due to infection is denoted $d_k(x)$, and the rate of spore production is denoted $r_k(x)$. Spores become inactive at rate $\delta > 0$. Finally, we take into account mutations occurring during reproduction with a kernel $m_\varepsilon(x) := \frac{1}{\varepsilon^N} m\left(\frac{x}{\varepsilon}\right)$ for $m \in L^1(\mathbb{R}^N)$ and a parameter $\varepsilon > 0$. The equations for our model are as follows.

$$\begin{cases} \dfrac{\mathrm{d}S_k}{\mathrm{d}t} = \xi_k \Lambda - \theta S_k(t) - S_k(t) \displaystyle\int_{\mathbb{R}^N} \beta_k(y) A_k(t, y) \mathrm{d}y, & k = 1, 2, \\ \dfrac{\partial}{\partial t} I_k(t, x) = \beta(x) S(t) A(t, x) - \big(\theta + d_k(x)\big) I_k(t, x), & k = 1, 2, \\ \dfrac{\partial}{\partial t} A(t, x) = -\delta A(t, x) + \displaystyle\int_{\mathbb{R}^N} m_\varepsilon(x - y) \big[r_1(y) I_1(t, y) + r_2(y) I(t, y)\big] \mathrm{d}y. \end{cases} \tag{1.3.1}$$

This model has been proposed in [263] to study the impact of resistant plants on the evolutionary adaptation of a fungal pathogen, and the stationary solutions for the single-host model have been described with precision in [145]. The asymptotic and transient behavior of this single-host model are studied in [85]. A simulation of the stationary solution of this model is presented in Figure 1.3.1.

Here we focus on the stationary solutions to (1.3.1), which we rewrite as the following equation on A only:

$$A^\varepsilon = T^\varepsilon(A^\varepsilon) \tag{1.3.2}$$

where $A^\varepsilon = A^\varepsilon(x) \in L^1_+(\mathbb{R}^N)$ is the stationary density of spores, and the nonlinear operator $T^\varepsilon(\varphi)$ is given by

$$T^\varepsilon(\varphi) := T_1^\varepsilon(\varphi) + T_2^\varepsilon(\varphi) =: \frac{L_1^\varepsilon(\varphi)}{1 + \theta^{-1} \int_{\mathbb{R}^N} \beta_1(z) \varphi(z) \mathrm{d}z} + \frac{L_2^\varepsilon(\varphi)}{1 + \theta^{-1} \int_{\mathbb{R}^N} \beta_2(z) \varphi(z) \mathrm{d}z},$$

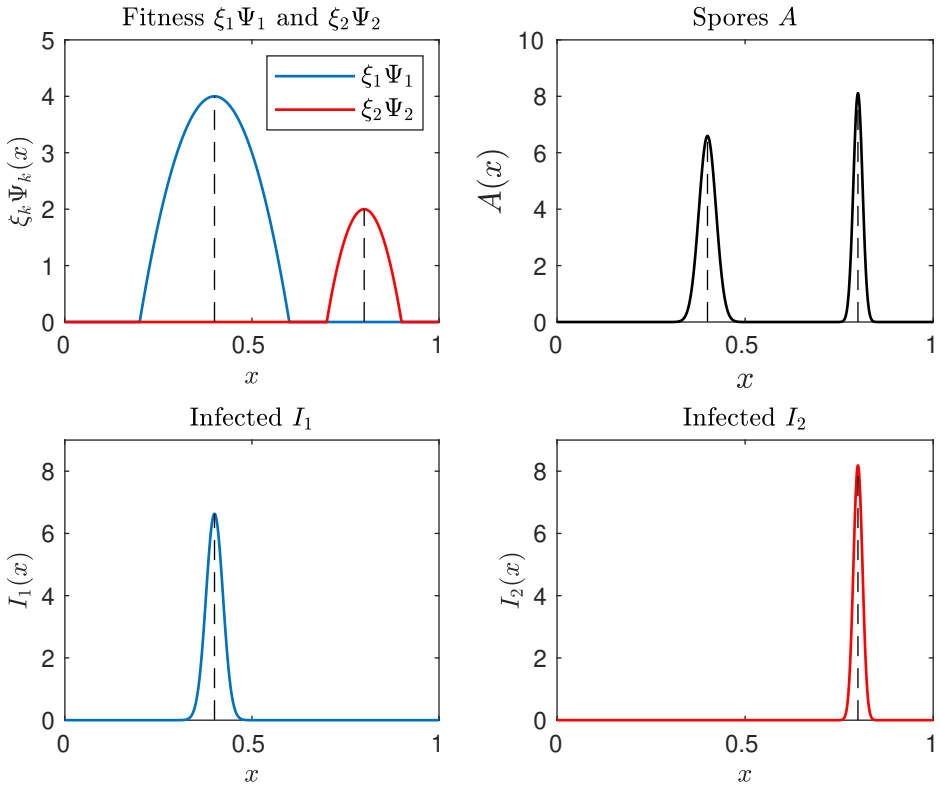

Figure 1.3.1: Stationary solution of system (1.3.1). The pathogen survives in both hosts at different fitness maxima.

wherein L_k^ε is the linear operator given by

$$L_k^\varepsilon(\varphi) = \frac{\Lambda\xi_k}{\theta} m_\varepsilon \star \big(\Psi_k\varphi\big), \qquad \Psi_k(x) := \frac{\beta_k(x) r_k(x)}{(\delta\theta + d_k(x))}$$

and $\star$ stands for the standard convolution. Under some additional assumptions on the coefficients, we first investigate the existence of a positive stationary solution and show that, when the spectral radius $r_\sigma(L^\varepsilon) \leq 1$, the extinct stationary state $A \equiv 0$ is the only solution to (1.3.2), where $L^\varepsilon := L_1^\varepsilon + L_2^\varepsilon$. When $r_\sigma(L^\varepsilon) > 1$, we construct a positive stationary solution by using the uniform persistence theory of Magal and Zhao [276].

Next, we can be more precise about the number and shape of the solutions to (1.3.2) when the spectral gap of the operators L_k^ε $(k = 1, 2)$ is bounded below by a polynomial:

$$\liminf_{\varepsilon\to 0} \frac{\lambda_k^{\varepsilon,1} - \lambda_k^{\varepsilon,2}}{\varepsilon^n} > 0, \tag{1.3.3}$$

for some $n \in \mathbb{N}$, where $\lambda_k^{\varepsilon,1}$ (respectively, $\lambda_k^{\varepsilon,2}$ is the largest (respectively, second largest) eigenvalue of the operator L_k^ε. It is a natural assumption as it can be shown to hold for operators of the type of L_k^ε when the mutation kernel decreases sufficiently fast when $\|x\| \to +\infty$ and function Ψ_k is sufficiently regular, has a finite number of global maxima and a negative definite Hessian matrix at those maxima (among other assumptions on m and Ψ_k, see [145, Proposition 5.1] for a precise statement).

Another crucial assumption in our analysis is that the supports of β_1 and β_2 are compact and separated by a positive distance.

When our assumptions hold, we can show that any solution to (1.3.2) actually looks like the sum of two stationary solutions for the uncoupled problem,

$$T_1^\varepsilon(A_1^\varepsilon) = A_1^\varepsilon, \qquad T_2^\varepsilon(A_2^\varepsilon) = A_2^\varepsilon,$$

in the sense that

$$\|A^\varepsilon - A_1^\varepsilon + A_2^\varepsilon\|_{L^1(\mathbb{R}^N)} = o(\varepsilon^\infty).$$

In other words the distance between a solution A^ε to (1.3.2) and $A_1^\varepsilon + A_2^\varepsilon$ in the space $L^1(\mathbb{R}^n)$ decreases to 0 faster than any polynomial in ε when $\varepsilon \to 0$. In particular, when both Ψ_1 and Ψ_2 have a unique maximum x_k $(k = 1, 2)$, the limit as $\varepsilon \to 0$ is explicit:

$$\lim_{\varepsilon\to 0} A^\varepsilon(x)\mathrm{d}x = \frac{\theta}{\beta(x_1)}(R_{0,1} - 1)\delta_{x_1}(\mathrm{d}x) + \frac{\theta}{\beta(x_2)}(R_{0,2} - 1)\delta_{x_2}(\mathrm{d}x),$$

where the limit holds in the sense of the weak convergence of measures, $\delta_y(\mathrm{d}x)$ is the Dirac mass concentrated at $y \in \mathbb{R}^N$ and the numbers $R_{0,k} := \dfrac{\xi_k}{\theta}\|\Psi_k\|_{L^\infty(\mathbb{R}^N)}$ are supposed to be strictly greater than 1 for $k = 1, 2$.

Finally, under the above assumptions and one additional assumption (which is automatically satisfied when both $R_{0,1} > 1$ and $R_{0,2} > 1$) we prove the uniqueness of the positive solution to (1.3.2) for $\varepsilon > 0$ sufficiently small. The proof is based on a computation of the Leray-Schauder degree in the positive cone of the appropriate space of continuous functions; indeed we can prove that the degree in the positive cone is equal to one, and since any equilibrium is stable (for $\varepsilon > 0$ sufficiently small), the degree in a neighborhood of any stationary solution is also equal to one. Since the degree in the positive cone is equal to the sum of the degrees in the neighborhood of all stationary solutions, the uniqueness of the stationary solution follows.

1.3.2 On the competitive exclusion principle for continuously distributed populations

This section concerns a joint work with Jean-Baptiste Burie and Arnaud Ducrot [P18], which is currently submitted for publication.

We investigate a single-host epidemiological model which can be considered as a limit of the single-host model in (1.3.1) under vanishing mutation and fast spore dynamics,

$$\begin{cases} \dfrac{\mathrm{d}S}{\mathrm{d}t} = \Lambda - \theta S(t) - S(t)\displaystyle\int_{\mathbb{R}^N} \alpha(y)\gamma(y)I(t,y)\mathrm{d}y, \\ \dfrac{\mathrm{d}}{\mathrm{d}t}I(t,x) = \gamma(y)\big(\alpha(x)S(t) - 1\big)I(t,x). \end{cases} \tag{1.3.4}$$

Notice that we changed the names of some parameters of the model ($\alpha(x)$ and $\gamma(x)$), in order to express our results more easily. Our objective was to provide a description of the long-time dynamics of (1.3.4) as a first step towards understanding the behavior of the time-dependent solutions to (1.3.1).

It can be easily seen that the natural candidates for the stationary solutions to (1.3.4) all satisfy $\alpha(x) = \frac{1}{S^\infty}$, where $S^\infty > 0$ is a real number. Therefore if α is regular (for instance, $\alpha(x) = 1 - |x|^2$) the stationary solutions to (1.3.4) cannot be functions (not even measurable functions) but should be looked for in some appropriate space of measure. Indeed it has been proved in many different contexts related to (1.3.4) (see, for instance, [139]) that, when α has a single maximum, the natural candidate for a stationary solution to (1.3.4) is precisely the Dirac mass located at the point that maximizes α.

However, since we aim at characterizing the transient behavior of solutions to (1.3.1) under vanishing mutations among other things, it is not sufficient to restrict the problem to functions α that possess a single maximum. This is particularly true as we want to consider compactly supported initial conditions in (1.3.4): there is no particular reason why the support of I_0 would include the supremum of α. Keeping this situation in mind, we should include in our analysis cases when α has a finite number of maxima which may lie in the boundary of the support of I_0, or even a continuum of maxima. The situation of a fitness function having a maximizing set of positive measure is presented in Figure 1.3.2.

Therefore in our minimal setting, we assume that $\gamma(x) > 0$ is a bounded continuous function, I_0 is a nonnegative Radon measure and $\alpha(x)$ is a bounded continuous function. To avoid losing mass at infinity we assume moreover that the superlevel sets,

$$L_\varepsilon(I_0) := \{y \in \text{supp } I_0 \,:\, \alpha(y) \geq \alpha^* - \varepsilon\}, \qquad \text{with } \alpha^* := \sup_{z\in\text{supp } I_0} \alpha(z),$$

are bounded when $\varepsilon > 0$ is sufficiently small. Letting

$$\mathcal{R}_0(I_0) := \frac{\Lambda}{\theta}\alpha^*,$$

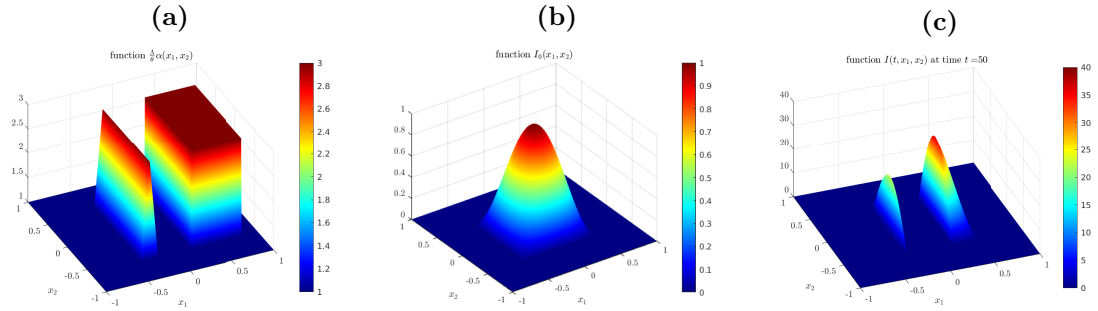

Figure 1.3.2: Numerical solution of the system (1.3.4) when the fitness function attains its maxima on a set of positive measures. **(a)** Fitness function. **(b)** Initial condition. **(c)** Solution at $t = 50$.

we first remark that the solution $(S(t), I(t, \mathrm{d}x))$ to (1.3.4) converges towards the disease-free equilibrium $(\frac{\Lambda}{\theta}, 0)$ when $\mathcal{R}_0(I_0) < 1$. Therefore in what follows we also assume that $\mathcal{R}_0(I_0) > 1$.

When the initial mass on the maximizing set of α is positive, namely,

$$I_0\big(\{\alpha(y) = \alpha^*\}\big) = \int_{\alpha(y)=\alpha^*} I_0(\mathrm{d}y) > 0,$$

we can completely characterize the long-time behavior of the equation. More precisely, we show that

$$S(t) \xrightarrow[t\to+\infty]{} \frac{1}{\alpha^*} \text{ and } I(t, \mathrm{d}x) \xrightarrow[t\to+\infty]{} \mathbb{1}_{\alpha(x)=\alpha^*} e^{\tau\gamma(x)} I_0(\mathrm{d}x),$$

where the convergence of $I(t, \mathrm{d}x)$ holds in total variation and the constant τ can be characterized as the solution of an implicit equation. When $I_0(\{\alpha(y) = \alpha^*\}) = 0$, the situation is more intricate. In all generality we can prove that $S(t)$ converges to $\frac{1}{\alpha^*}$ and that the population of pathogen survives (*i.e.* $\liminf \int I(t, \mathrm{d}x) > 0$) and becomes concentrated on

$$L_0(I_0) = \{y \in \text{supp } I_0 \,:\, \alpha(y) = \alpha^*\},$$

in the sense of the Kantorovitch-Rubinstein metric. We can achieve a slightly more precise description if we assume that the initial measure puts some mass around the maximizing set of $\gamma(x)$. This assumption can be expressed as

$$\int_{\gamma(x)\in[\overline{\gamma},\gamma^*]} I_0(y, \mathrm{d}x) \geq m > 0 \text{ for } A - \text{almost every } y \in (\alpha^* - \delta, \alpha^*), \tag{1.3.5}$$

where $\gamma^* := \sup_{\alpha(y)=\alpha^*} \gamma(y)$, $\overline{\gamma} < \gamma^*$, and $I_0(y, \mathrm{d}x), A(\mathrm{d}y)$ is a *disintegration* of $I_0(\mathrm{d}y)$ with respect to α:

$$\int_{\mathbb{R}^N} f(x) I_0(\mathrm{d}x) = \int_{\mathbb{R}} \int_{\alpha^{-1}(y)} f(x) I_0(y, \mathrm{d}x) A(\mathrm{d}y), \text{ for all } f \in BC(\mathbb{R}^N),$$

with $\int_{\mathbb{R}^N} I_0(y, \mathrm{d}x) = 1$ for almost every y and supp $I_0(y, \mathrm{d}x) \subset \alpha^{-1}(y)$. Under the assumption (1.3.5) we can prove that the mass $I(t, \mathrm{d}x)$ eventually concentrates on the set $\alpha^{-1}(\alpha^*) \cap \gamma^{-1}(\gamma^*)$, and we can determine the asymptotic mass of I:

$$I(t, \mathrm{d}x) \xrightarrow[t\to+\infty]{} \frac{\theta}{\alpha^*\gamma^*}\big(\mathcal{R}_0(I_0) - 1\big).$$

Finally, we focus on the case when α has a finite number of regular maxima $x_1, \dots, x_p$, *i.e.* α is C^2 with a negative definite Hessian matrix around each maximum. If moreover $I_0(x)$ behaves like a polynomial $I_0 \asymp |x - x_i|^{\kappa_i}$ around each maximum x_i for $i = 1, \dots, p$, then we can determine the asymptotic behavior of $I(t, \mathrm{d}x)$ near each maximum as

$$\int_{|x-x_i|\leq\varepsilon} I(t, \mathrm{d}x) \asymp t^{\gamma(x_i)\rho - \frac{N+\kappa_i}{2}}, \qquad i = 1, \dots, p, \text{ where } \rho := \min_{i=1,\dots,p} \frac{N + \kappa_i}{2\gamma(x_i)}.$$

Therefore $I(t, \mathrm{d}x)$ does not necessarily concentrate on $\alpha^{-1}(\alpha^*) \cap \gamma^{-1}(\gamma^*)$ as could have been suspected, but on the set

$$\{x_i, i \in J\} \text{ where } J := \left\{1 \leq i \leq p \, : \, \frac{N + \kappa_i}{2\gamma(x_i)} = \rho\right\}.$$

In particular the asymptotic behavior of $I(t, \mathrm{d}x)$ does not only depend on the support of I_0 but also on the precise behavior of $I_0(\mathrm{d}x)$ close to the maximum of α. To the extent of our knowledge, this kind of behavior has never been observed before in pure competition models.

1.4 Parameter identification in epidemiological models and applications to the COVID-19 epidemic

The works described in this section are collaborations with several co-authors and correspond to several explorations around the links between models and data in the context of the COVID-19 pandemic. The common ancestor of these models is the SIUR model introduced by Liu, Magal, Seydi, and Webb in February 2020 in the context of the COVID-19 outbreak in Wuhan [261]. This model can be written as follows:

$$\begin{cases} S'(t) = -\tau(t)S(t)[I(t) + U(t)], \\ I'(t) = \tau(t)S(t)[I(t) + U(t)] - \nu I(t), \\ R'(t) = \nu f I(t) - \eta R(t), \\ U'(t) = \nu(1-f)I(t) - \eta U(t). \end{cases} \tag{1.4.1}$$

Here $t \geq t_0$ is time in days, t_0 is the beginning date of the model of the epidemic, $S(t)$ is the number of individuals susceptible to infection at time t, $I(t)$ is the number of asymptomatic infectious individuals, $R(t)$ is the number of reported symptomatic infectious individuals and $U(t)$ is the number of unreported symptomatic infectious individuals. The transmission rate at time t is $\tau(t)$, the average infectious period for an asymptomatic individual I is $1/\nu$ days, and the average infectious period for a symptomatic individual R or U is $1/\eta$ days. We assume that reported symptomatic infectious individuals $R(t)$ are reported and isolated immediately and cause no further infections. The asymptomatic individuals $I(t)$ can also be viewed as having a low-level symptomatic state. All infections are acquired from either $I(t)$ or $U(t)$ individuals. The fraction f of asymptomatic infectious become reported symptomatic infectious, and the fraction $1 - f$ become unreported symptomatic infectious. The rate asymptomatic infectious become reported symptomatic is $\nu_1 = f\,\nu$, the rate asymptomatic infectious become unreported symptomatic is $\nu_2 = (1-f)\,\nu$.

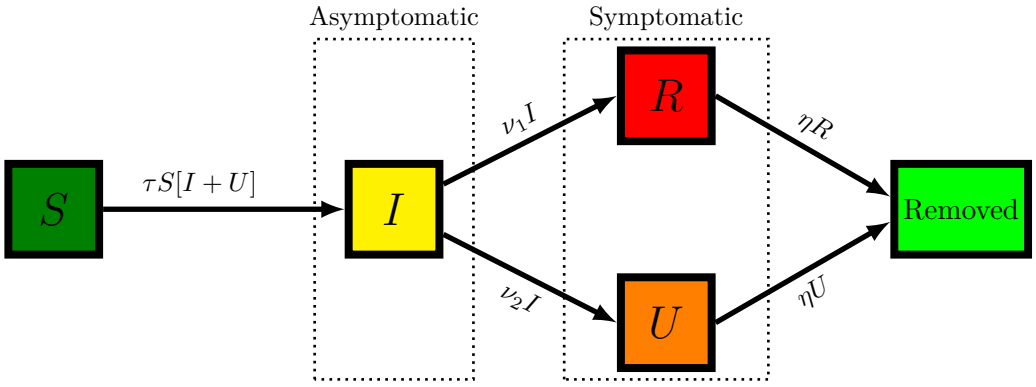

Figure 1.4.1: Flow chart for the SIUR model

A method to identify the initial state and some of the parameters in the equation (1.4.1) from cumulative reported case data and the knowledge of some of the parameters was developed by Liu, Magal, Seydi and Webb [261].

In what follow I summarize my contributions to the mathematical modeling of the COVID-19 epidemic. There are 6 papers in total; the first [P16] presents a bridge between stochastic models and deterministic models to issue a prediction of the last day of the epidemic; two later works [P10] and [P14] present original models to take into account the age structure of the population, and the variability of the daily number of tests, respectively; the last three [P7, P13, P15] present – among other things – an innovative method to

reconstruct the time-dependent transmission rate from the cumulative reported cases data in the context of a single [P7] or multiple [P13] waves for the SIR model, the SIUR model (1.4.1), and the SEIUR model (with an additional exposed state) [P15].

1.4.1 Real-time prediction of the end of an epidemic wave: COVID-19 in China as a case-study

In a joint work with Zhihua Liu, Pierre Magal, and Robin Thompson [P16], which was done during the first COVID-lockdown in France, we developed a mathematical model to estimate the total duration of the COVID-19 outbreak in Wuhan, assuming that the strong lockdown measures imposed by the Chinese government were perfectly effective and maintained until the recovery of the last infected. We first used the method described in [261] to identify the unknown parameters in (1.4.1) under the assumption that the parameters S_0, ν, f, and η were known (the values were taken from the literature). More precisely, we assumed that the transmission rate is given as

$$\tau(t) = \begin{cases} \tau_0 \text{ if } t \leq N, \\ \tau_0 \exp(-\mu(t-N)) \text{ if } t > N. \end{cases}$$

We fitted the initial date of the epidemic t_0, as well as I_0, U_0, R_0, and τ_0 to the exponential phase of the epidemic, and then chose the values of N and μ to obtain the best fit to the data at later times. These parameter values were used to estimate the state of the epidemic at any date t.

Next, we introduced a date t_1 at which strong lockdown measures are taken by the authorities. We assume that the lockdown is perfect, *i.e.* we assume that the flux of newly infected individuals can be effectively neglected. Therefore the period of stay of each infected individual in state I follows an exponential law of rate ν and the length of stay in the state U follows an exponential law of rate η. In particular, the total number of individuals in the states I or U is analytically tractable and it becomes possible to derive an analytic formula for the last date of the epidemic, *i.e.* the date at which the sum of the two quantities $I+U$ reach the number 0,

$$\begin{aligned} &\mathbb{P}(I(s)+U(s)=0 \text{ for } s \geq t \,|\, I(t_1)=I_1, U(t_1)=U_1) \\ &\qquad = \left(1-e^{-\eta(t-t_1)}\right)^{U_1} \times \left(1-e^{-\nu(t-t_1)}-(1-f)\nu(t-t_1)e^{-\eta(t-t_1)}\right)^{I_1}, \end{aligned} \tag{1.4.2}$$

where $I_1 = I(t_1)$ and $U_1 = U(t_1)$ are estimated by the ordinary differential model (1.4.1). This formula allows us to give three estimates of the last date of the epidemic, given a risk level which we chose at 10%, 5% and 1%, respectively. We also tested different value of the parameter f. We estimated that the extinction date between May 19, 2020 (for $f = 0.8$ and a risk level of 10%) and June 24, 2020 (for $f = 0.2$ and a risk level of 1%), when t_1 is set on March 15, 2020. We also simulated an individual-based model (IBM) by the Gillespie direct method [188] to confirm our analytic prediction.

1.4.2 Unreported Cases for Age Dependent COVID-19 Outbreak in Japan

In a joint work with Pierre Magal and Ousmane Seydi [P10], we were interested in the influence of the age structure on the epidemiological dynamics and developed a method to identify the parameters of an age-dependent epidemic model with the age-structured data from Japan. We used a model with 10 age classes (0-9 years old, 10-19, etc.) where each age class interacts with other age classes via a contact matrix ϕ:

$$\begin{cases} S_1'(t) = -\tau_1(t)S_1(t)\left[\phi_{1,1}\dfrac{(I_1(t)+U_1(t))}{N_1} + \ldots + \phi_{1,10}\dfrac{(I_{10}(t)+U_{10}(t))}{N_{10}}\right], \\ \vdots \\ S_{10}'(t) = -\tau_{10}(t)S_{10}(t)\left[\phi_{10,1}\dfrac{(I_1(t)+U_1(t))}{N_1} + \ldots + \phi_{10,10}\dfrac{(I_{10}(t)+U_{10}(t))}{N_{10}}\right], \end{cases} \tag{1.4.3}$$

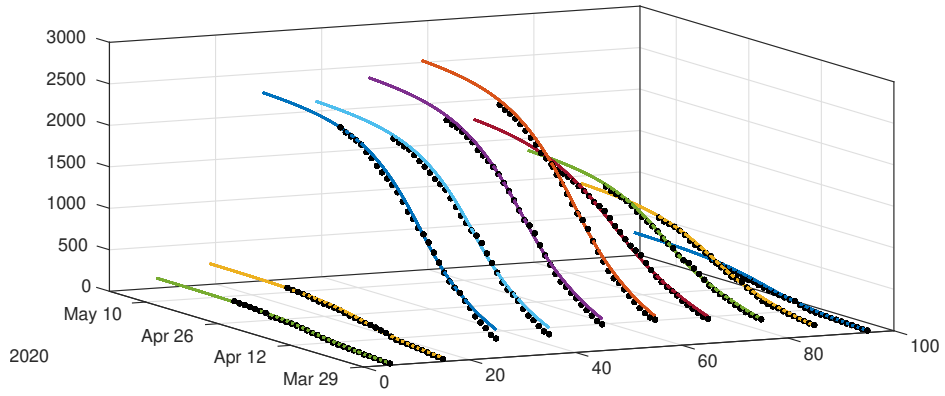

Figure 1.4.2: Age-structured data from Japan (black dots) and the corresponding solution of the mathematical model (colored curves).

and similarly, for $i = 1, \dots, 10$,

$$\begin{cases} I_i'(t) = -\tau_i(t) S_i(t) \left[\phi_{i,1} \dfrac{(I_1(t) + U_1(t))}{N_1} + \dots + \phi_{i,10} \dfrac{(I_{10}(t) + U_{10}(t))}{N_{10}} \right], \\ R_i'(t) = \nu_i f_i I_i(t) - \eta R_i(t), \\ U_i'(t) = \nu_i (1 - f_i) I_i(t) - \eta U_i(t), \end{cases} \tag{1.4.4}$$

where N_i is the number of individuals in each age class. We adapted data from an existing study (POLYMOD, Mossong et al [292], extrapolated to Japan in Prem et al. [325]) to construct a matrix ϕ adapted to our framework. We managed to identify the initial state of (1.4.3)–(1.4.4) by a similar method as in [261, P16]. To obtain the transmission rates τ_1, ..., τ_{10}, we minimized the error between the left-hand side and the right-hand side of the I equation in (1.4.4) during the exponential growth phase of the epidemic. It does not seem possible, however, to estimate directly the coefficients of ϕ from the data, since our procedure can be applied for any ϕ. To match the behavior of the epidemic in later times, we used the following form for the transmission rate $\tau_i(t)$:

$$\tau_i(t) = \tau_i^0 \exp(-\mu_i (t - D_i)_+),$$

where τ_i^0 is the rate identified in the exponential growth phase, D_i is the first day at which the individuals begin to change their behavior in response to the epidemic and μ_i is a shape parameter. Importantly, μ_i and D_i depend on the age class. A plot of the result of the simulation compared with the original data is presented in Figure 1.4.2. We managed to find parameters so that the model stays in good agreement with the age-structured data between the beginning of March 2020 and the end of April 2020 (the date at which we did the investigation).

1.4.3 Clarifying predictions for COVID-19 from testing data: the example of New York State

Last, in collaboration with Pierre Magal [P14], we investigated the inclusion of testing data in epidemiological models. The main idea behind this study is to propose a mechanism to compensate for the bias induced by the daily number of tests in deterministic models. Such a correction is naturally present in Bayesian mechanistic models by the necessity of an observation model, but previous deterministic models did not necessarily acknowledge this bias. It is all the more important to take into account the daily number of tests that, at the beginning of the epidemic, shortages in chemical components have limited the realization of PCR tests and might therefore have induced an underreporting of COVID-19 cases.

Here we use a SEIUR model (an "exposed" class was added compared to (1.4.1)) with an additional compartment to model the COVID-19 epidemic in New York. The model consists of the following ordinary

differential equation

$$\begin{cases} S'(t) = -\tau S(t)[I(t) + U(t) + D(t)], \\ E'(t) = \tau S(t)[I(t) + U(t) + D(t)] - \alpha E(t), \\ I'(t) = \alpha E(t) - \nu I(t), \\ U'(t) = \nu\,(1-f)\,I(t) + n(t)\,(1-\sigma)\,g\,D(t) - \eta U(t), \\ D'(t) = \nu\,f\,I(t) - n(t)\,g\,D(t) - \eta D(t), \\ R'(t) = n(t)\,\sigma\,g\,D(t) - \eta R(t). \end{cases} \tag{1.4.5}$$

A flow chart of the model is presented in Figure 1.4.3. The time t_1 corresponds to the time where the tests started to be used constantly. Therefore the epidemic started before t_1. Here $t \geq t_1$ is the time in days. $S(t)$ is the number of individuals susceptible to infection. $E(t)$ is the number of exposed individuals (*i.e.* who are incubating the disease but not infectious). $I(t)$ is the number of individuals incubating the disease, but already infectious. $U(t)$ is the number of undetected infectious individuals (*i.e.* who are expressing mild or no symptoms), and the infectious that have been tested with a false negative result, are therefore not candidates for testing. $D(t)$ is the number of individuals who express severe symptoms and are candidates for testing ("detectables"). $R(t)$ is the number of individuals who have been tested positive for the disease.

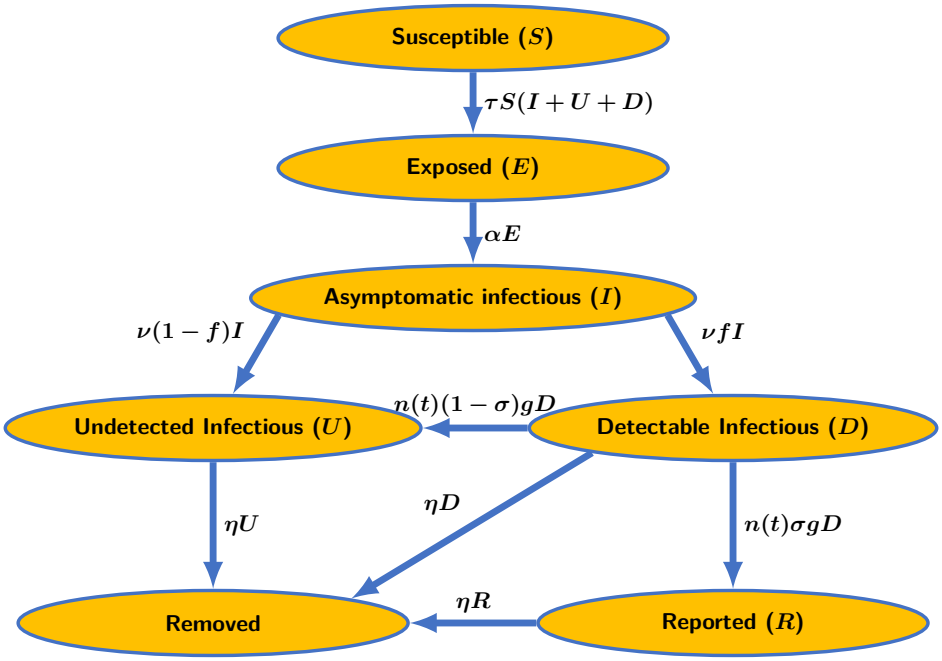

Figure 1.4.3: Flow chart for the model (1.4.5) with partial reporting and variable testing.

The length of the exposed period is $1/\alpha$ days. After the exposure period, individuals are becoming asymptomatic infectious $I(t)$. The average length of the asymptomatic infectious period is $1/\nu$ days. After this period, individuals are becoming either mildly symptomatic individuals $U(t)$ or individuals with severe symptoms $D(t)$. The average length of this infectious period is $1/\eta$ days. Some of the U-individuals may show no symptoms at all.

In our study, we provide a new method for the identification of parameters for our model (1.4.5) based on the identification of a time frame during which the daily number of tests increases linearly. The method was applied to the data corresponding to the State of New York, and provides a good match between the cumulative reported case data and the corresponding curve produced by the model. As an application, we computed the outcome of the epidemic for different scenarios of testing, based on the parameters found from the data. We found that increasing the daily number of tests can have a surprising non-monotone effect on the cumulative reported cases data. When multiplying the daily number of tests by positive constants, we first observe that the cumulative number of cases increases, which might seem natural since it increases our ability to recognize infected individuals. However, there we observe an inversion of the tendency for a

multiplicative factor between 5 and 10 in the case of New York, with the number of reported cases being lower with 10 times more tests than in the case of 5 times more. Therefore there must be a threshold above which the testing policy becomes to significantly impact the epidemiological dynamics, to the point that it actually reduces the number of infections.

1.4.4 SI epidemic model applied to COVID-19 data in mainland China

In the previous works on parameter identification for epidemiological models, the focus was on the modeling of different features to achieve a better description of the COVID-19 epidemic. A recurrent approach to take into account the awareness of the population of the virus, which yields a non-constant transmission rate, is to impose a predefined parameterized shape for the transmission coefficient, and to identify the parameters via a nonlinear least-square minimization method.

In the following works in collaboration with Jacques Demongeot and Pierre Magal [P7, P13, P15], we looked for a more intrinsic relation between the reported case data and the time-dependent transmission coefficient of the models used to reconstruct the epidemic.

In [P7], we focused on the SIR model with time-dependent transmission rate

$$\begin{cases} S'(t) = -\tau(t)S(t)I(t) \\ I'(t) = \tau(t)S(t)I(t) - \nu I(t), \\ S(t_0) = S_0, I(t_0) = I_0, \end{cases} \tag{1.4.6}$$

when the observable data (cumulative reported cases) has the form

$$\mathrm{CR}'(t) = \nu f I(t)$$

for some $f \in (0,1)$ which characterized the probability of observing an infection. Our first result is the identifiability of $\tau(t)$ and the initial state I_0 with respect to CR: given any increasing twice differentiable function $\widehat{\mathrm{CR}}$ and the parameters S_0, ν and f, there is at most one set of parameters $(I_0, \tau(t))$ so that the solution CR to (1.4.4) satisfies $\mathrm{CR}(t) = \widehat{\mathrm{CR}}(t)$ for all $t \geq t_0$, and these parameters are given by

$$\begin{cases} I_0 := \dfrac{\widehat{\mathrm{CR}}(t)}{\nu f} \\ \tau(t) := \dfrac{\nu f \left(\widehat{\mathrm{CR}}''(t)/\widehat{\mathrm{CR}}'(t) + \nu \right)}{\nu f(I_0 + S_0) - \widehat{\mathrm{CR}}'(t) - \nu(\widehat{\mathrm{CR}}(t) - \widehat{\mathrm{CR}}(t_0))}. \end{cases} \tag{1.4.7}$$

Moreover, if the denominator in (1.4.7) is positive for all $t \geq t_0$, then we have in fact $\widehat{\mathrm{CR}}(t) = \mathrm{CR}(t)$ for all $t \geq t_0$. This means that $\tau(t)$ and I_0 are indeed identifiable, provided the data is sufficiently regular.

Real data, on the other hand, is usually very irregular, due to many factors which include the inherent stochasticity of the contamination process and the multiple human errors or delays in the reporting. Therefore it is another challenge to find a proper way to use our formula (1.4.7) in the context of real data. In this work we focused on a single epidemic wave and found that the solutions to the Bernoulli-Verhulst equation,

$$\mathrm{CR}'(t) = \chi \mathrm{CR}(t) \left(1 - \left(\frac{\mathrm{CR}(t)}{\mathrm{CR}_\infty} \right)^\theta \right),$$

where χ, $\mathrm{CR}_0 = \mathrm{CR}(t_0)$, CR_∞ and θ are five parameters, can be matched closely to cumulative reported cases data. The Bernoulli-Verhulst equation has explicit solutions,

$$\mathrm{CR}(t) = \frac{e^{\chi(t-t_0)}\mathrm{CR}_0}{\left[1 + \mathrm{CR}_0^\theta/\mathrm{CR}_\infty^\theta (e^{\chi\theta(t-t_0)} - 1)\right]^{1/\theta}}, \tag{1.4.8}$$

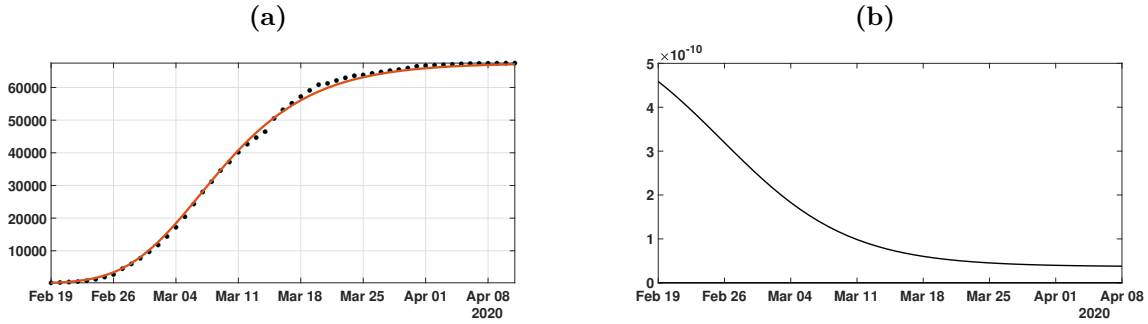

Figure 1.4.4: **(a)** Comparison between reported cases data from Mainland China (black dots) and the best fit Bernoulli-Verhulst curve (orange curve). **(b)** The corresponding transmission rate.

and it makes it possible to write the explicit formula for $\tau(t)$ and I_0 without derivatives:

$$I_0 = \frac{\chi}{\nu f}\mathrm{CR}_0\left(1-\left(\frac{\mathrm{CR}_0}{\mathrm{CR}_\infty}\right)^\theta\right), \tag{1.4.9}$$

$$\tau(t) = \frac{\nu f\left(\chi_2\left(1-(1+\theta)\left(\frac{\mathrm{CR}(t)}{\mathrm{CR}_\infty}\right)^\theta\right)+\nu\right)}{\nu f\left(I_0+S_0\right)+\nu\mathrm{CR}_0-\mathrm{CR}(t)\left(\chi_2\left(1-\left(\frac{\mathrm{CR}(t)}{\mathrm{CR}_\infty}\right)^\theta\right)+\nu\right)}, \tag{1.4.10}$$

where $\mathrm{CR}(t)$ is given by the formula (1.4.8).

This given us a method for reconstructing the instantaneous transmission rate from real data. First, we fit a solution to the Bernoulli-Verhulst equation to the cumulative reported cases data by a standard curve-fitting method, *i.e.* we find the parameters χ, $\mathrm{CR}_0 = \mathrm{CR}(t_0)$, CR_∞ and θ that best match the data. Then we use formula (1.4.9)–(1.4.10) to recover the parameters of the underlying epidemic model. An example of Bernoulli-Verhulst curve matched with real data and the corresponding transmission rate are presented in Figure 1.4.4. This method also provides additional information on non-identifiable parameters, because parameters which induce a negative transmission rate cannot be realistic.

Alternatively, we developed a discrete-time algorithm based on the monotony of the cumulative cases for the solution to (1.4.6) to compute $\tau(t)$ on a daily basis, based on the reported data.

We tested this method on the data of the first wave of COVID-19 in mainland China and compared it with several other regularization of the data. In the end, because of the lack of regularity of the data, weekly average and Gaussian filter applied on the data yield an unrealistic transmission rate, strongly impacted by the noise and which can become negative. The transmission rate obtained by Bernoulli-Verhulst regularization, however, yields a monotonic and smooth transmission rate.

1.4.5 A robust phenomenological approach to investigate COVID-19 data for France

In [P13], we generalized the Bernoulli-Verhulst phenomenological models to multi-wave epidemics. Using the data for France, we found that the Bernoulli-Verhulst phenomenological model works for the successive waves independently, but the transition period between two epidemic curves is somewhat difficult to handle. This is linked to the fact that our phenomenological model works well to match the data corresponding to an epidemic with population awareness of the disease followed possibly by a lockdown; however, the release of a lockdown is accompanied by a sharp transition in the epidemiological dynamics, and the new infections look like a completely random process for a short period of time. Therefore, to match the dynamics of the cases after a lockdown, we use an affine function (straight line) rather than a Bernoulli-Verhulst curve.

Therefore our phenomenological model is defined piecewise on different intervals - a Bernoulli-Verhulst phenomenological model during an epidemic wave, a straight line between epidemic waves. To regularize the model and avoid differentiability issues at the transition, we apply a Gaussian filter with a small variance to get a smooth curve. Then we apply the formula (1.4.7) to recover the initial state and the transmission coefficient.

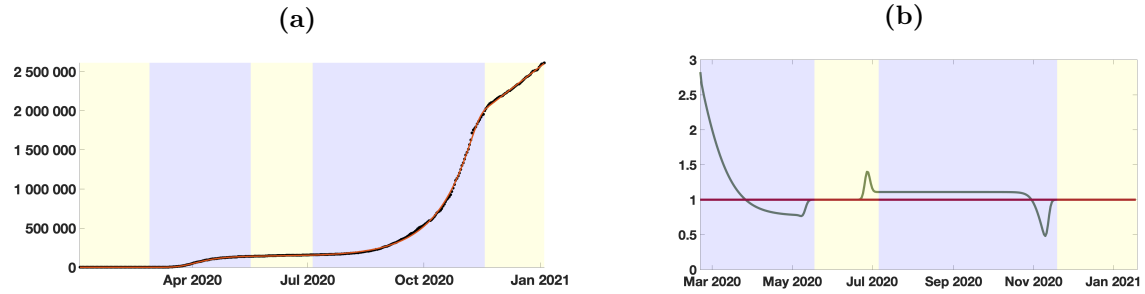

Figure 1.4.5: **(a)** Best fit of the phenomenological model (orange curve) and the reported cases data (black dots) for the French epidemic. The background color indicates the type of phenomenological used for the curve fitting. **(b)** The corresponding effective reproduction number.

In particular, the transmission rate is linked to the instantaneous basic reproduction number by the formula

$$\mathcal{R}_0(t) = \frac{\tau(t)S(t)}{\nu}.$$

Therefore by solving the S-equation in (1.4.6), we can compute the basic reproduction number for our system. The result is a smooth, easily tractable basic reproduction number. In Figure 1.4.5 we plot the comparison between the phenomenological model and the basic reproductive number corresponding to the phenomenological model.

Thanks to our method, we compared the data to a theoretical situation in which the social distancing and mitigation measures would have been better respected during the transition between the first and second wave in France, reducing the rate of increase of the affine phenomenological model in the transition between the waves (without changing the $\tau(t)$ during the second wave). This impacts mostly the starting point for the second wave. We assumed that the infections were reduced by a factor 10 during the transition, and observed that the magnitude of this reduction factor is kept throughout the second wave (reduction by a factor 10). Thus an increased vigilance between the waves would have resulted in a much less severe second wave.

1.4.6 What can we learn from COVID-19 data by using epidemic models with unidentified infectious cases?

In the last collaboration with Pierre Magal and Jacques Demongeot [P15], we generalized the method to the SEIUR model (with an additional "exposed" compartment) and applied it to the data from 8 different geographic areas: California, France, India, Israel, Japan, Peru, Spain, and United Kingdom. More precisely we used the model

$$\begin{cases} S'(t) = -\tau(t)\left[I(t) + \kappa\, U(t)\right] S(t), \\ E'(t) = \tau(t)\left[I(t) + \kappa\, U(t)\right] S(t) - \alpha\, E(t), \\ I'(t) = \alpha\, E(t) - \nu\, I(t), \\ U'(t) = \nu\,(1-f)\, I(t) - \eta\, U(t), \\ R'(t) = \nu\, f\, I(t) - \eta\, R(t), \end{cases} \tag{1.4.11}$$

where E is the added exposed case and $1/\alpha$ is the duration of the exposed state. A flow chart of the model is presented in Figure 1.4.6. Among the difficulties of the paper, the addition of the exposed case complicates the algebra when computing the link between $\mathrm{CR}(t)$ and $\tau(t)$ in (1.4.11). The formula can be written as

$$\tau(t) = \frac{1}{I(t) + \kappa U(t)} \times \frac{\mathrm{CE}''(t) + \alpha \mathrm{CE}'(t)}{E_0 + S_0 - \mathrm{CE}'(t) - \alpha \mathrm{CE}(t)}, \tag{1.4.12}$$

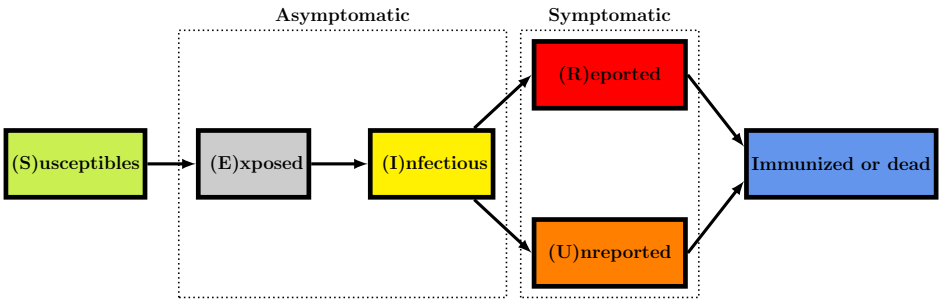

Figure 1.4.6: Flow chart for the model (1.4.11)

where $\mathrm{CE}(t) = \int_{t_0}^{t} E(s)\mathrm{d}s$. Note that, because of the relations

$$I(t) = \frac{\mathrm{CR}'(t)}{\nu\, f}, \tag{1.4.13}$$

$$\mathrm{CE}(t) = \frac{1}{\alpha\,\nu\, f}\left[\mathrm{CR}'(t) - \nu\, f\, I_0 + \nu\,(\mathrm{CR}(t) - \mathrm{CR}_0)\right], \tag{1.4.14}$$

$$U(t) = \mathrm{e}^{-\eta(t-t_0)}U_0 + \int_{t_0}^{t} \mathrm{e}^{-\eta(t-s)}\,\frac{(1-f)}{f}\mathrm{CR}'(s)\mathrm{d}s, \tag{1.4.15}$$

the transmission rate is still identifiable from the data $\mathrm{CR}(t)$. The other identifiable parameters are $I_0 = I(t_0)$ (from (1.4.13)) and $E_0 = E(t_0)$ (from (1.4.14)). Unfortunately (1.4.15) cannot be used to identify U_0, so this parameter has to be assumed.

Finally, as in [P13], our method allows us to compute the so-called *instantaneous reproduction number*,

$$R_e(t) = \frac{\tau(t)S(t)}{\eta\nu}(\eta + \nu(1-f)), \tag{1.4.16}$$

from our reconstruction of $\tau(t)$. For the 8 geographic area considered, we were thus able to provide a real epidemic model with exposed period which matches the data from the beginning to the end of the period considered (which contains several epidemic waves), and provide an alternative method to compute the instantaneous reproduction number. In Figure 1.4.7 we plot the reported cases data and the phenomenological model in four of the eight countries considered, and in Figure 1.4.8 the corresponding effective reproduction numbers compared to other related notions.

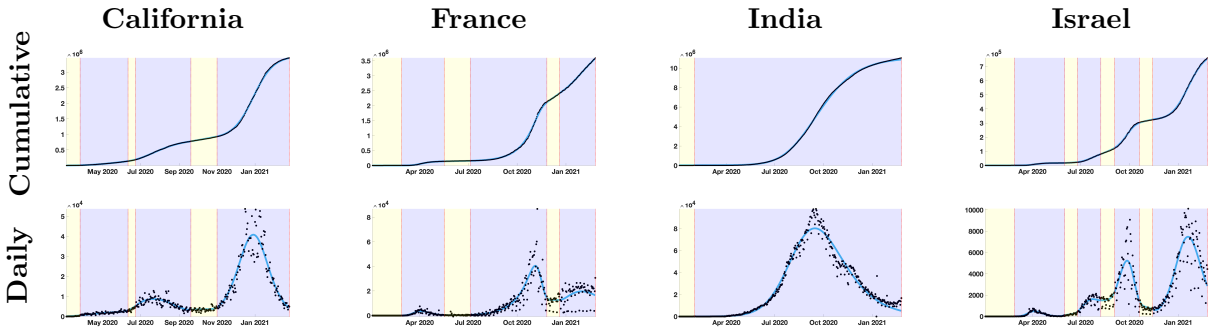

Figure 1.4.7: Phenomenological model applied to the data from California, France, India, and Israel. **Top row:** Cumulative reported cases data (black dots) and the phenomenological model (blue curve). **Bottom row:** Daily reported cases (black dots) and the first derivative of the phenomenological model.

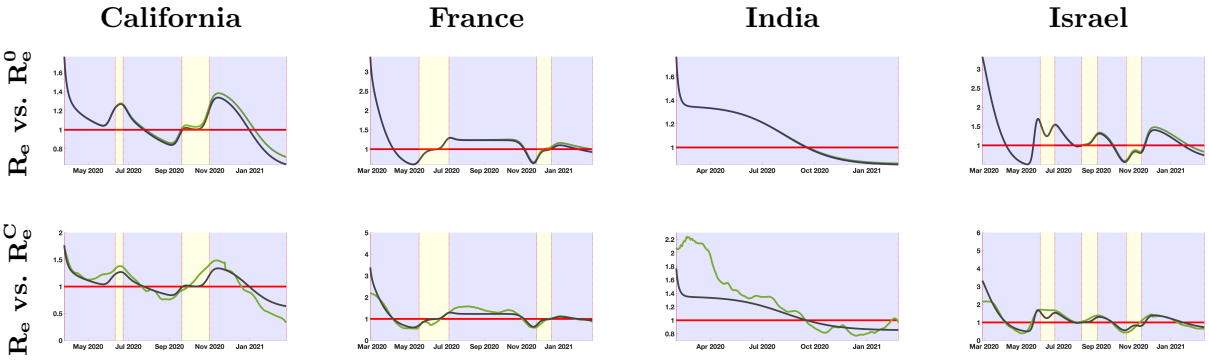

Figure 1.4.8: Effective reproduction number from the phenomenological model for California, France, India, and Israel.
Top row: $R_e(t)$ (grey curve) compared with $R_e^0(t) := \frac{\tau(t)S_0}{\eta\nu}(\eta + \nu(1-f))$ (green curve).
Bottom row: $R_e(t)$ (grey curve) compared with the statistical effective reproduction number described in Cori et al [116] (green curve).

Bibliography of the author's work

Published articles

[P1] Q. Griette, G. Raoul, and S. Gandon. Virulence evolution at the front line of spreading epidemics. *Evolution* **69**.**11** (2015), pp. 2810–2819. DOI: 10.1111/evo.12781.

[P2] Q. Griette and G. Raoul. Existence and qualitative properties of travelling waves for an epidemiological model with mutations. *J. Differential Equations* **260**.**10** (2016), pp. 7115–7151. DOI: 10.1016/j.jde.2016.01.022.

[P3] M. Alfaro and Q. Griette. Pulsating fronts for Fisher-KPP systems with mutations as models in evolutionary epidemiology. *Nonlinear Anal. Real World Appl.* **42** (2018), pp. 255–289. DOI: 10.1016/j.nonrwa.2018.01.004.

[P4] Q. Griette. Singular measure traveling waves in an epidemiological model with continuous phenotypes. *Trans. Amer. Math. Soc.* **371**.**6** (2019), pp. 4411–4458. DOI: 10.1090/tran/7700.

[P5] Q. Griette and S. Motsch. Kinetic equations and self-organized band formations. In: *Active particles, Vol. 2*. Model. Simul. Sci. Eng. Technol. Birkhäuser/Springer, Cham, 2019, pp. 173–199.

[P6] J.-B. Burie, A. Ducrot, Q. Griette, and Q. Richard. Concentration estimates in a multi-host epidemiological model structured by phenotypic traits. *J. Differential Equations* **269**.**12** (2020), pp. 11492–11539. DOI: 10.1016/j.jde.2020.08.029.

[P7] J. Demongeot, Q. Griette, and P. Magal. SI epidemic model applied to COVID-19 data in mainland China. *R. Soc. Open Sci.* **7**.**12** (2020), p. 201878. DOI: 10.1098/rsos.201878.

[P8] X. Fu, Q. Griette, and P. Magal. A cell-cell repulsion model on a hyperbolic Keller-Segel equation. *J. Math. Biol.* **80**.**7** (2020), pp. 2257–2300. DOI: 10.1007/s00285-020-01495-w.

[P9] L. Girardin and Q. Griette. A Liouville-type result for non-cooperative Fisher-KPP systems and nonlocal equations in cylinders. *Acta Appl. Math.* **170** (2020), pp. 123–139. DOI: 10.1007/s10440-020-00327-9.

[P10] Q. Griette, P. Magal, and O. Seydi. Unreported Cases for Age Dependent COVID-19 Outbreak in Japan. *Biology* **9**.**6** (2020), p. 132. DOI: 10.3390/biology9060132.

[P11] X. Fu, Q. Griette, and P. Magal. Existence and uniqueness of solutions for a hyperbolic Keller-Segel equation. *Discrete Contin. Dyn. Syst. Ser. B* **26**.**4** (2021), pp. 1931–1966. DOI: 10.3934/dcdsb.2020326.

[P12] X. Fu, Q. Griette, and P. Magal. Sharp discontinuous traveling waves in a hyperbolic Keller-Segel equation. *Math. Models Methods Appl. Sci.* **31**.**5** (2021), pp. 861–905. DOI: 10.1142/S0218202521500214.

[P13] Q. Griette, J. Demongeot, and P. Magal. A robust phenomenological approach to investigate COVID-19 data for France. *Math. Appl. Sci. Eng.* **2**.**4** (2021), pp. 149–218. DOI: 10.5206/mase/14031.

[P14] Q. Griette and P. Magal. Clarifying predictions for COVID-19 from testing data: The example of New York State. *Infect. Dis. Model.* **6** (2021), pp. 273–283. DOI: https://doi.org/10.1016/j.idm.2020.12.011.

[P15] Q. Griette, J. Demongeot, and P. Magal. What can we learn from COVID-19 data by using epidemic models with unidentified infectious cases? *Math. Biosci. Eng.* **19**.**1** (2022), pp. 539–594. DOI: 10.3934/mbe.2022025.

Articles submitted to a pre-publication archive

[P16] Q. Griette, Z. Liu, P. Magal, and R. Thompson. Real-time prediction of the end of an epidemic wave: COVID-19 in China as a case-study. *medRxiv* (2020). DOI: 10.1101/2020.04.14.20064824.

[P17] M. Alfaro, Q. Griette, D. Roze, and B. Sarels. The spatio-temporal dynamics of interacting genetic incompatibilities. Part I: The case of stacked underdominant clines. *arXiv preprint* (2021).

[P18] J.-B. Burie, A. Ducrot, and Q. Griette. *On the competitive exclusion principle for continuously distributed populations*. 2021.

[P19] Q. Griette and H. Matano. Propagation dynamics of solutions to spatially periodic reaction-diffusion systems with hybrid nonlinearity. *arXiv preprint* (2021).

Chapter 2

Reaction-diffusion systems as models in population dynamics

2.1 Existence and qualitative properties of travelling waves for an epidemiological model with mutations

2.1.1 Introduction

Epidemics of newly emerged pathogen can have catastrophic consequences. Among those who have infected humans, we can name the black plague, the Spanish flu, or more recently SARS, AIDS, bird flu or Ebola. Predicting the propagation of such epidemics is a great concern in public health. Evolutionary phenomena play an important role in the emergence of new epidemics: such epidemics typically start when the pathogen acquires the ability to reproduce in a new host, and to be transmitted within this new hosts population. Another phenotype that can often vary rapidly is the virulence of the pathogen, that is how much the parasite is affecting its host; Field data show that the virulence of newly emerged pathogens changes rapidly, which moreover seems related to unusual spatial dynamics observed in such populations ([204, 324], see also [256, 206]). It is unfortunately difficult to set up experiments with a controlled environment to study evolutionary epidemiology phenomena with a spatial structure, we refer to [43, 235] for current developments in this direction. Developing the theoretical approach for this type of problems is thus especially interesting. Notice finally that many current problems in evolutionary biology and ecology combine evolutionary phenomena and spatial dynamics: the effect of global changes on populations [317, 132], biological invasions [355, 234], cancers or infections [185, 176].

In the framework of evolutionary ecology, the virulence of a pathogen can be seen as a life-history trait of the pathogen [336, 174]. To explain and predict the evolution of virulence in a population of pathogens, many of the recent theories introduce a *trade-off* hypothesis, namely a link between the parasite's virulence and its ability to transmit from one host to another, see e.g. [10]. The basic idea behind this hypothesis is that the more a pathogen reproduces (in order to transmit some descendants to other hosts), the more it "exhausts" its host. A high virulence can indeed even lead to the premature death of the host, which the parasite within this host rarely survives. In other words, by increasing its transmission rate, a pathogen reduces its own life expectancy. There exists then an optimal virulence trade-off, that may depend on the ecological environment. An environment that changes in time (e.g. if the number of susceptible hosts is heterogeneous in time and/or space) can then lead to a Darwinian evolution of the pathogen population. For instance, in [56], an experiment shows how the composition of a viral population (composed of the phage λ and its virulent mutant λcl857, which differs from λ by a single locus mutation only) evolves in the early stages of the infection of an *E. Coli* culture.

The Fisher-KPP equation is a classical model for epidemics, and more generally for biological invasions, when no evolutionary phenomenon is considered. It describes the time evolution of the density $n = n(t, x)$ of a population, where $t \geqslant 0$ is the time variable, and $x \in \mathbb{R}$ is a space variable. The model writes as follows:

$$\partial_t n(t,x) - \sigma \Delta n(t,x) = r n(t,x) \left(1 - \frac{n(t,x)}{K}\right). \tag{2.1.1}$$

It this model, the term $\sigma \Delta n(t,x) = \sigma \Delta_x n(t,x)$ models the random motion of the individuals in space, while the right part of the equation models the logistic growth of the population (see [381]): when the density

of the population is low, there is little competition between individuals and the number of offsprings is then roughly proportional to the number of individuals, with a growth rate r ; when the density of the population increases, the individuals compete for e.g. food, or in our case for susceptible hosts, and the growth rate of the population decreases, and becomes negative once the population's density exceeds the so-called carrying capacity K. The model (2.1.1) was introduced in [170, 238], and the existence of travelling waves for this model, that is special solutions that describe the spatial propagation of the population, was proven in [238]. Since then, travelling waves have had important implications in biology and physics, and raise many challenging problems. We refer to [406] for an overview of this field of research.

In this study, we want to model an epidemics, but also take into account the possible diversity of the pathogen population. It has been recently noticed that models based on (2.1.1) can be used to study this type of problems (see [72, 7, 71]). Following the experiment [56] described above, we will consider two populations: a wild type population w, and a mutant population m. For each time $t \geqslant 0$, $w(t,\cdot)$ and $m(t,\cdot)$ are the densities of the respective populations over a one dimensional habitat $x \in \mathbb{R}$. The two populations differ by their growth rate in the absence of competition (denoted by r in (2.1.1)) and their carrying capacity (denoted by K in (2.1.1)). We will assume that the mutant type is more virulent than the wild type, in the sense that it will have an increased growth rate in the absence of competition (larger r), at the expense of a reduced carrying capacity (smaller K). We assume that the dispersal rate of the pathogen (denoted by σ in (2.1.1)) is not affected by the mutations, and is then the same for the two types. Finally, when a parent gives birth to an offspring, a mutation occurs with a rate μ, and the offspring will then be of a different type. Up to a rescaling, the model is then:

$$\begin{cases} \partial_t w(t,x) - \Delta_x w(t,x) = w(t,x)\left(1 - (w(t,x) + m(t,x))\right) + \mu(m(t,x) - w(t,x)), \\ \partial_t m(t,x) - \Delta_x m(t,x) = r m(t,x)\left(1 - \left(\frac{w(t,x)+m(t,x)}{K}\right)\right) + \mu(w(t,x) - m(t,x)), \end{cases} \tag{2.1.2}$$

where $t \geq 0$ is the time variable, $x \in \mathbb{R}$ is a spatial variable, $r > 1$, $K < 1$ and $\mu > 0$ are constant coefficients. In (2.1.2), $r > 1$ represents the fact that the mutant population reproduces faster than the wild type population if many susceptible hosts are available, while $K < 1$ represents the fact that the wild type tends to out-compete the mutant if many hosts are infected. Our goal is to study the travelling wave solutions of (2.1.2), that is solutions with the following form :

$$w(t,x) = w(x - ct), \quad m(t,x) = m(x - ct),$$

with $c \in \mathbb{R}$. (2.1.2) can then be re-written as follows, with $x \in \mathbb{R}$:

$$\begin{cases} -cw'(x) - w''(x) = w(x)\left(1 - (w(x) + m(x))\right) + \mu(m(x) - w(x)), \\ -cm'(x) - m''(x) = r m(x)\left(1 - \left(\frac{w(x)+m(x)}{K}\right)\right) + \mu(w(x) - m(x)). \end{cases} \tag{2.1.3}$$

The existence of planar fronts in higher dimension ($x \in \mathbb{R}^N$) is actually equivalent to the $1D$ case ($x \in \mathbb{R}$), our analysis would then also be the first step towards the understanding of propagation phenomena for (2.1.2) in higher dimension.

There exists a large literature on travelling waves for systems of several interacting species. In some cases, the systems are monotonic (or can be transformed into a monotonic system). Then, sliding methods and comparison principles can be used, leading to methods close to the scalar case [383, 385, 338]. The combination of the inter-specific competition and the mutations prevents the use of this type of methods here. Other methods that have been used to study systems of interacting populations include phase plane methods (see e.g. [369, 167]) and singular perturbations (see [181, 180]). More recently, a different approach, based on a topological degree argument, has been developed for reaction-diffusion equations with non-local terms [46, 7]. The method we use here to prove the existence of travelling wave for (2.1.3) will indeed be derived from these methods. Notice finally that we consider here that dispersion, mutations and reproduction occur on the same time scale. This is an assumption that is important from a biological point of view (and which is satisfied in the particular λ phage epidemics that guides our study, see [56]). In particular, we will not use the Hamilton-Jacobi methods that have proven useful to study this kind of phenomena when different time scales are considered (see [286, 72, 71]).

This mathematical study has been done jointly with a biology work, see [P1]. We refer to this article for a deeper analysis on the biological aspects of this work, as well as a discussion of the impact of stochasticity for a related individual-based model (based on simulations and formal arguments).

We will make the following assumption,

Assumption 2.1.1. We assume that

$$r \in (1,\infty),\ \mu \in \left(0, \min\left(\frac{r}{2}, 1-\frac{1}{r}, 1-K, K\right)\right) \text{ and } K \in \left(0, \min\left(1, \frac{r}{r-1}\left(1-\frac{\mu}{1-\mu}\right)\right)\right).$$

This assumption ensures the existence of a unique stationary solution of (2.1.2) of the form $(w,m)(t,x) \equiv (w^*,m^*) \in (0,1)\times(0,K)$ (see [P2, Appendix]). It does not seem very restrictive for biological applications, and we believe the first result of this study (Existence of travelling waves, Theorem 2.1.2) could be obtained under a weaker assumption, namely:

$$r \in (1,\infty), \quad K \in (0,1), \quad \mu \in (0,K).$$

Throughout this document we will denote by f_w and f_m the terms on the left hand side of (2.1.3):

$$\begin{aligned} f_w(w,m) &:= w(1-(w+m)) + \mu(m-w), \\ f_m(w,m) &:= rm\left(1-\left(\tfrac{w+m}{K}\right)\right) + \mu(w-m). \end{aligned} \tag{2.1.4}$$

The structure of section 2.1 is as follows: in section 2.1.2, we will present the main results of this section 2.1, which are three fold: Theorem 2.1.2 shows the existence of travelling waves for (2.1.3), Theorem 2.1.3 describes the profile of the fronts previously constructed, and Theorem 2.1.4 relates the travelling waves for (2.1.3) to travelling waves of (2.1.1), when μ and K are small. Sections 2.1.3, 2.1.4 and 2.1.5 are devoted to the proof of the three theorems stated in section 2.1.2.

2.1.2 Main results

The first result is the existence of travelling waves of minimal speed for the model (2.1.2), and an explicit formula for this minimal speed. We recall that the minimal speed travelling waves are often the biologically relevant propagation fronts, for a population initially present in a bounded region only ([74]), and it seems to be the one that is relevant when small stochastic perturbations are added to the model ([294]). Although we expect the existence of travelling waves for any speed higher than the minimal speed, we will not investigate this problem here - we refer to [46, 7] for the construction of such higher speed travelling waves for related models. Notice also that the convergence of the solutions to the parabolic model (2.1.2) towards travelling waves, and even the uniqueness of the travelling waves, remain open problems.

Theorem 2.1.2. *Let r, K, μ satisfy Assumption 2.1.1. There exists a solution $(c,w,m) \in \mathbb{R}\times C^\infty(\mathbb{R})^2$ of (2.1.3), such that*

$$\forall x \in \mathbb{R}, \quad w(x) \in (0,1),\ m(x) \in (0,K),$$

$$\liminf_{x\to-\infty}(w(x)+m(x)) > 0, \quad \lim_{x\to\infty}(w(x)+m(x)) = 0,$$

$$c = c_*,$$

where

$$c_* := \sqrt{2\left(1+r-2\mu+\sqrt{(r-1)^2+4\mu^2}\right)} \tag{2.1.5}$$

is the minimal speed $c>0$ for which such a travelling wave exists.

The difficulty of the proof of Theorem 2.1.2 has several origins:

- The system cannot be modified into a monotone system (see [369, 66]), which prevents the use of sliding methods to show the existence of traveling waves.
- The competition term has a negative sign, which means that comparison principles often cannot be used directly.

As mentioned in the introduction, new methods have been developed recently to show the existence of travelling wave in models with negative nonlocal terms (see [46, 7]). To prove Theorem 2.1.2, we take advantage of those recent progress by considering the competition term as a nonlocal term (over a set composed of only two elements : the wild and the virulent type viruses). The method of [46, 7] are however based on the Harnack inequality (or related arguments), that are not as simple for systems of equations (see [87]). We have thus introduced a different localized problem, which allowed us to prove our result without any Harnack-type argument.

Our second result describes the shape of the travelling waves that we have constructed above. We show that three different shapes at most are possible, depending on the parameters. In the most biologically relevant case, where the mutation rate is small, we show that the travelling wave we have constructed in Theorem 2.1.2 is as follows: the wild type density w is decreasing, while the mutant type density m has a unique global maximum, and is monotone away from this maximum. In numerical simulations of (2.1.2), we have always observed this situation (represented in Figure 2.1.1), even for large μ. This result also allows us to show that behind the epidemic front, the densities $w(x)$ and $m(x)$ of the two pathogens stabilize to w^*, m^*, which is the long-term equilibrium of the system if no spatial structure is considered. For some results on the monotony of solutions of the non-local Fisher-KPP equation, we refer to [163, 6]. For models closer to (2.1.2) (see e.g. [7, 72]), we do not believe any qualitative result describing the shape of the travelling waves exists.

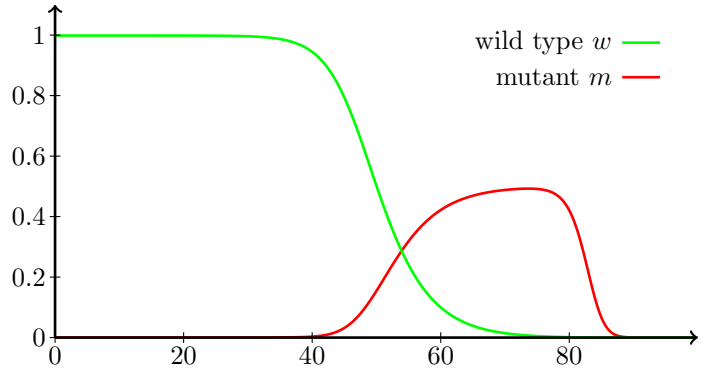

Figure 2.1.1: Numerical simulation of (2.1.2) with $r = 2$, $K = 0.5$, $\mu = 0.01$, with a heaviside initial condition for w and null initial condition for m. The numerical code is based on an implicit Euler scheme. For large times, the solution seems to converge to a travelling wave, that we represent here, propagating towards large x. In the initial phase of the epidemics, the mutant (m, red line) population is dominant, but this mutant population is then quickly replaced by a population almost exclusively composed of wild types (w, green line).

Theorem 2.1.3. *Let r, K, μ satisfy Assumption 2.1.1. There exists a solution $(c, w, m) \in \mathbb{R}_+ \times C^\infty(\mathbb{R})^2$ of* (2.1.3) *such that*

$$\lim_{x\to-\infty}(w(x), m(x)) = (w^*, m^*), \quad \lim_{x\to\infty}(w(x), m(x)) = (0, 0),$$

where (w^*, m^*) is the only solution $(w^*, m^*) \in (0, 1] \times (0, K]$ of $f_w(w, m) = f_m(w, m) = 0$.

The solution $(c, w, m) \in \mathbb{R}_+ \times C^\infty(\mathbb{R})^2$ satisfies one of the three following properties:

(a) *w is decreasing on $\mathbb{R}$, while m is increasing on $(-\infty, \bar{x}]$ and decreasing on $[\bar{x}, \infty)$ for some $\bar{x} < 0$,*

(b) *m is decreasing on $\mathbb{R}$, while w is increasing on $(-\infty, \bar{x}]$ and decreasing on $[\bar{x}, \infty)$ for some $\bar{x} < 0$,*

(c) *w and m are decreasing on $\mathbb{R}$.*

Moreover, there exists $\mu_0 = \mu_0(r, K) > 0$ such that if $\mu < \mu_0$, then there exists a solution as above which satisfies (a).

Finally, we consider the special case where the mutant population is small (due to a small carrying capacity $K > 0$ of the mutant, and a mutation rate satisfying $0 < \mu < K$). If we neglect the mutants

completely, the dynamics of the wild type would be described by the Fisher-KPP equation (2.1.1) (with $\sigma = r = K = 1$), and they would then propagate at the minimal propagation speed of the Fisher-KPP equation, that is $c = 2$. Thanks to Theorem 2.1.2, we know already that the mutant population will indeed have a major impact on the minimal speed of the population which becomes $c_* = 2\sqrt{r} + \mathcal{O}(\mu) > 2$, and thus shouldn't be neglected. In the next theorem, we show that the profile of w is indeed close to the travelling wave of the Fisher-KPP equation with the non-minimal speed $2\sqrt{r}$, provided the conditions mentioned above are satisfied (see Figure 2.1.2). The effect of the mutant is then essentially to speed up the epidemics.

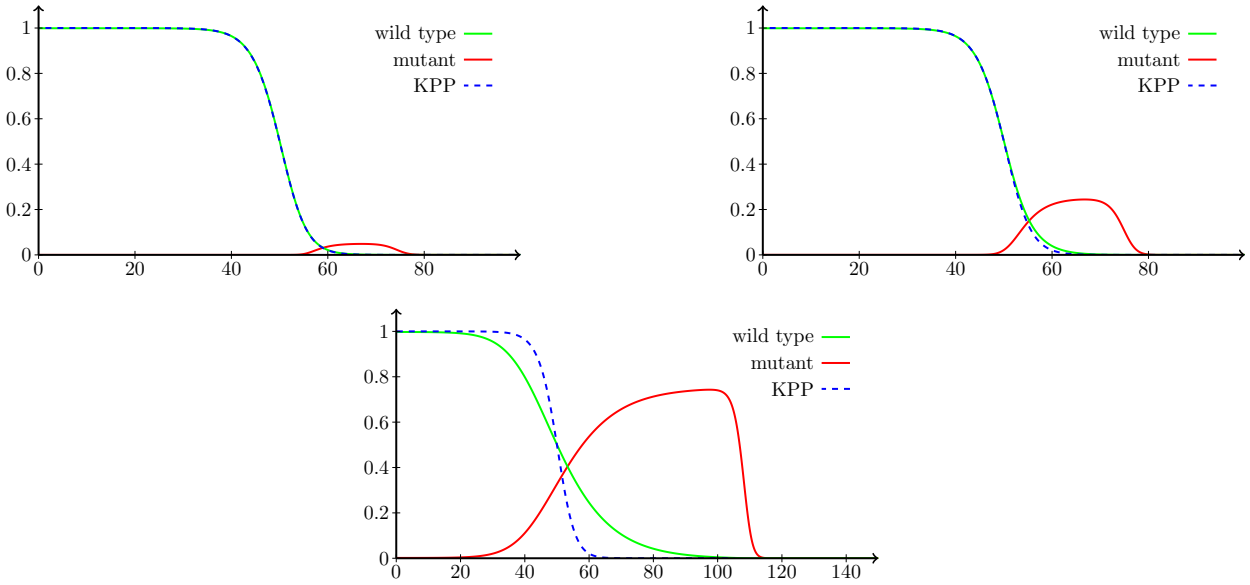

Figure 2.1.2: Comparison of the travelling wave solutions of (2.1.2) and the travelling wave solution of the Fisher-KPP equation of (non-minimal) speed $2\sqrt{r}$. These figures are obtained for $r = 2$, $\mu = 0.001$, and three values of K: $K = 0.05, 0.25, 0.75$. We see that the agreement between the density of the wild type (w, green line) and the corresponding solution of the Fisher-KPP equation (u, dashed blue line) is good as soon as $K \leq 0.25$. The travelling waves solutions of (2.1.2) are obtained numerically as long-time solutions of (2.1.2) (based on an explicit Euler scheme), while the travelling waves solutions of the Fisher-KPP equations (for a the given speed $2\sqrt{r}$ that is not the minimal travelling speed for the Fisher-KPP model) is obtained thanks to a phase-plane approach, with a classical ODE numerical solver.

Theorem 2.1.4. *Let $r \in (1, \infty)$, $K \in (0, 1)$, $\mu \in (0, K)$ and $(c_*, w, m) \in \mathbb{R} \times C^0(\mathbb{R})^2$ (see Theorem 2.1.2 for the definition of c_*), w, $m > 0$, a solution of (2.1.3) such that*

$$\liminf_{x \to -\infty} (w(x) + m(x)) > 0, \quad \lim_{x \to \infty} (w(x) + m(x)) = 0.$$

There exists $C = C(r) > 0$, $\beta \in \left(0, \frac{1}{2}\right)$ and $\varepsilon > 0$ such that if $0 < \mu < K < \varepsilon$, then

$$\|w - u\|_{L^\infty} \leqslant C K^\beta,$$

where $u \in C^0(\mathbb{R})$ is a traveling wave of the Fisher-KPP equation, that is a solution (unique up to a translation) of

$$\begin{cases} -cu' - u'' = u(1-u), \\ \lim\limits_{x \to -\infty} u(x) = 1, \ \lim\limits_{x \to \infty} u(x) = 0, \end{cases} \tag{2.1.6}$$

with speed $c = c_0 = 2\sqrt{r}$.

The Theorem 2.1.4 is interesting from an epidemiological point of view: it describes a situation where the spatial dynamics of a population would be driven by the characteristics of the mutants, even though the population of these mutants pathogens is very small, and thus difficult to sample in the field.

2.1.3 Proof of Theorem 2.1.2

We will prove Theorem 2.1.2 in several steps. We refer to Remark 2.1.19 for the conclusion of the proof.

2.1.3.1 A priori estimates on a localized problem

We consider first a restriction of the problem (2.1.3) to a compact interval $[-a,a]$, for $a>0$. More precisely, we consider, for $c\in\mathbb{R}$,

$$\begin{cases} w,\, m\in C^0([-a,a]),\\ -cw'-w''=f_w(w,m)\chi_{w\geq 0}\chi_{m\geq 0},\\ -cm'-m''=f_m(w,m)\chi_{w\geq 0}\chi_{m\geq 0},\\ w(-a)=w^*,\, m(-a)=m^*,\, w(a)=m(a)=0, \end{cases} \tag{2.1.7}$$

where we have used the notation (2.1.4), and (w^*,m^*) are defined in the Appendix, see section 2.1.6.2.

Regularity estimates on solutions of (2.1.7) The following result shows the regularity of the solutions of (2.1.7).

Proposition 2.1.5. *Let r, K, μ satisfy Assumption 2.1.1 and $a>0$. If $(w,m)\in L^\infty([-a,a])$ satisfies*

$$\begin{cases} -cw'-w''=f_w(w,m),\\ -cm'-m''=f_m(w,m), \end{cases} \tag{2.1.8}$$

on $[-a,a]$, where f_w, f_m are defined by (2.1.4), and $c\in\mathbb{R}$, then $w,m\in C^\infty([-a,a])$.

Proof of Proposition 2.1.5. Since $f_w(w,m)$, $f_m(w,m)\in L^\infty([-a,a])\subset L^p([-a,a])$ for any $p>1$, the classical theory ([187], theorem 9.15) predicts that the solutions of the Dirichlet problem associated with (2.1.8) lies in $W^{2,p}$. This shows that $w,m\in W^{2,p}((-a,a))$ for any $p>1$. But then $w,m\in C^{1,\alpha}((-a,a))$ for any $0\leqslant\alpha<1$ (thanks to Sobolev embeddings). It follows that $f(w,m)$ is a $C^{1,\alpha}((-a,a))$ function of the variable $x\in(-a,a)$ (see (2.1.4) for the definition of f). Let us choose one such $\alpha\in(0,1)$. Now we can apply classical theory ([187], theorem 6.14) to deduce that $w,m\in C^{2,\alpha}((-a,a))$. But then w'' and m'' verify some uniformly elliptic equation of the type

$$-c(w'')'-(w'')''=g,$$
$$-c(m'')'-(m'')''=h,$$

with $g,h\in C^{0,\alpha}((-a,a))$, and we can apply again ([187], theorem 6.14). This argument can be used recursively to show that $w,m\in C^{2n,\alpha}((-a,a))$ for any $n\in\mathbb{N}$, so that finally, $w,m\in C^\infty((-a,a))$. □

Positivity and L^∞ bounds for solutions of (2.1.7) In this section, we prove the positivity of the solutions of (2.1.7), as well as some L^∞ bounds.

Proposition 2.1.6. *Let r, K, μ satisfy Assumption 2.1.1, $a>0$, and $c\in\mathbb{R}$. If $(w,m)\in C^0([-a,a])^2$ is a solution of (2.1.7), then w and m satisfy are positive, that is $w(x)>0$ and $m(x)>0$ for all $x\in[-a,a)$.*

Proof of Proposition 2.1.6. We observe that

$$f_w(w,m)=w(1-(w+m))+\mu(m-w)=w(1-\mu-w)+m(\mu-w),$$

so that if $w\leqslant\min(\mu,1-\mu)$, then $f_w(w,m)\chi_{w\geqslant 0}\chi_{m\geqslant 0}\geqslant 0$. Let $x_0\in[-a,a]$ such that $w(x_0)\leqslant 0$, and $[\alpha,\beta]$ the connex compound of the set $\{w\leqslant\min(\mu,1-\mu)\}$ that contains x_0. Since $-cw'-w''\geqslant 0$ over (α,β) and $w(\alpha),w(\beta)\geqslant 0$, the weak minimum principle imposes $\inf_{(\alpha,\beta)} w\geqslant 0$, and thus $w(x_0)=0$. But then w reaches its global minimum at x_0, so the strong maximum principle imposes that $x_0\in\{\alpha,\beta\}$, or else w would be constant. We deduce then from our hypothesis $(w(-a)>0, w(a)=0)$ that $x_0=\beta=a$. That shows that $w>0$ in $[-a,a)$.

To show that $m > 0$, we notice that

$$\begin{aligned} f_m(w,m) &= rm\left(1-\frac{w+m}{K}\right)+\mu(w-m) \\ &= m\left(r-\mu-\frac{r}{K}m\right)+w\left(\mu-\frac{r}{K}m\right), \end{aligned}$$

so that if $m \leqslant \min\left(\frac{K}{r}\mu, K\left(1-\frac{\mu}{r}\right)\right)$, then $f_m(w,m)\chi_{w\geqslant 0}\chi_{m\geqslant 0} \geqslant 0$. The end of the argument to show the positivity of w can the n be reproduced to show that $m > 0$.

□

Proposition 2.1.7. *Let r, K, μ satisfy Assumption 2.1.1, $a > 0$, and $c \in \mathbb{R}$. If $(w,m) \in C^0([-a,a])^2$ is a positive solution of* (2.1.7)*, then w and m satisfy*

$$\forall x \in (-a,a), \quad w(x) < 1,$$

$$\forall x \in (-a,a), \quad m(x) < K.$$

Proof of Proposition 2.1.7. Let (w,m) a positive solution of (2.1.7).

- We assume that there exists $x_0 \in (-a,a)$ such that $w(x_0) > 1$. Let then $[a_1,a_2]$ the connex compound of the set $\{w \geqslant 1\}$ that contains x_0. Then in (a_1,a_2) we have

$$\begin{aligned} -cw'-w'' &= w(1-\mu-w-m)+\mu m \leqslant w(-\mu-m)+\mu m \\ &= m(\mu-w)-\mu w \leqslant 0, \end{aligned}$$

  along with $w(a_1) = w(a_2) = 1$, so that the weak maximum principle states $w \leqslant 1$ in (a_1,a_2), which is absurd because $w(x_0) > 1$. Therefore, $w(x) \leqslant 1$ for all $x \in (-a,a)$

- We assume that there exists $x_0 \in (-a,a)$ such that $m(x_0) > K$. Let then $[a_1,a_2]$ the connex compound of the set $\{m \geqslant K\}$ that contains x_0. Then in (a_1,a_2) we have

$$\begin{aligned} -cm'-m'' &= m\left(r-\mu-\frac{r}{K}(w+m)\right)+\mu w \leqslant m\left(-\mu-\frac{rw}{K}\right)+\mu w \\ &= w\left(\mu-\frac{r}{K}m\right)-\mu m \leqslant 0, \end{aligned}$$

  Thanks to Assumption 2.1.1. Since $m(a_1) = m(a_2) = K$, the weak maximum principle states $m \leqslant K$ in (a_1,a_2), which is absurd because $m(x_0) > K$. Therefore, $m(x) \leqslant K$ for all $x \in (-a,a)$.

- Now if $w(x) \in (\max(\mu, 1-\mu), 1]$, we still have the estimate

$$-cw'(x)-w''(x) \leqslant m(x)(\mu-w(x))+w(x)(1-\mu-w(x)) \leqslant 0,$$

  so that if there exists $x_0 \in (-a,a)$ such that $w(x_0) = 1$, then w is locally equal to 1 thanks to the strong maximum principle. But in that case

$$0 = (-cw'-w'')(x_0) = -m(x_0)+\mu(m(x_0)-1) < 0,$$

  which is absurd. Hence, $w < 1$. Similarly, if $m(x_0) = K$, we get

$$0 = (-cm'-m'')(x_0) = -K\mu+w(x_0)(\mu-r) < 0,$$

  which is absurd, and thus $m < K$.

□

Estimates on solutions of (2.1.7) **when** $c \geq c^*$ **or** $c = 0$ The next result shows that the solutions of (2.1.7) degenerate when $a \to +\infty$ if the speed c is larger than a minimal speed c^* (see Theorem 2.1.2 for the definition of c^*).

Proposition 2.1.8 (Upper bound on c)**.** *Let r, K, μ satisfy Assumption 2.1.1. There exists $C > 0$ such that for $a > 0$ and $c \geqslant c_*$, any solution $(w, m) \in C^0([-a, a])^2$ of* (2.1.7) *satisfies*

$$\forall x \in [-a, a], \quad \max(w(x), m(x)) \leq Ce^{\frac{-c-\sqrt{c^2-c_*^2}}{2}(x+a)}.$$

Proof of Proposition 2.1.8. Let $c \geqslant c_*$, and

$$M := \begin{pmatrix} 1-\mu & \mu \\ \mu & r-\mu \end{pmatrix}.$$

Since $M + \mu\, Id$ is a positive matrix, the Perron-Frobenius theorem implies that M has a principal eigenvalue h^+ and a positive principal eigenvector X (that is $X_i > 0$ for $i = 1, 2$), given by

$$h_+ = \frac{1+r-2\mu+\sqrt{(1-r)^2+4\mu^2}}{2}, \quad X = \begin{pmatrix} 1-r+\sqrt{(1-r)^2+4\mu^2} \\ 2\mu \end{pmatrix}. \tag{2.1.9}$$

The function $\psi_\eta(x) := \eta X e^{\lambda_- x}$ with $\lambda_- := \frac{-c-\sqrt{c^2-c_*^2}}{2}$ and $\eta > 0$ is then a solution of the equation

$$-c\psi_\eta' - \psi_\eta'' = M\psi_\eta = h_+\psi_\eta.$$

We can define $\mathcal{A} = \{\eta, (\psi_\eta)_1 \geqslant w \text{ on } [-a, a]\} \cap \{\eta, (\psi_\eta)_2 \geqslant m \text{ on } [-a, a]\}$, which is a closed subset of $\mathbb{R}^+$. $\mathcal{A}$ is non-empty since w and m are bounded while $\left(Xe^{\lambda_- x}\right)_i \geq X_i e^{\lambda_- a} > 0$ for $i = 1, 2$.

Consider now $\eta_0 := \inf \mathcal{A}$. Then $(\psi_\eta)_1 \geq w$, $(\psi_\eta)_2 \geq m$, and there exists $x_0 \in [-a, a]$ such that either $(\psi_\eta)_1(x_0) = w(x_0)$ or $(\psi_\eta)_2(x_0) = m(x_0)$. We first consider the case where $(\psi_\eta)_1(x_0) = w(x_0)$. Then

$$-c(w - (\psi_\eta)_1)'(x_0) - (w - (\psi_\eta)_1)''(x_0) \leqslant -w(x_0)\,(w(x_0) + m(x_0)) \leqslant 0$$

over $[-a, a]$. The weak maximum principle ([187], theorem 8.1) implies that

$$\sup_{[-a,a]} (w - (\psi_\eta)_1) = \max((w - (\psi_\eta)_1)(-a), (w - (\psi_\eta)_1)(a)),$$

and then, thanks to the definition of η_0, $\sup_{[-a,a]} (w - (\psi_\eta)_1) = 0$. Since $w(a) = 0 < (\psi_\eta)_1(a)$, this means that $(\psi_\eta)_1(-a) = w(-a)$, and thus

$$\eta_0 = \frac{b_w^-}{1-r+\sqrt{(1-r)^2+4\mu^2}} e^{\lambda_- a}.$$

The argument is similar if $(\psi_\eta)_2(x_0) = m(x_0)$, which concludes the proof. □

The following Proposition will be used to show that $c \neq 0$.

Proposition 2.1.9. *Let r, K, μ satisfy Assumption 2.1.1, and $a > a_0 := \frac{\pi}{\sqrt{2(1-\mu)}}$. Every positive solution $(w, m) \in C^0([-a, a])^2$ of* (2.1.7) *with $c = 0$ satisfies the estimate*

$$\max_{[-a_0,a_0]} (w + m) \geqslant \frac{K}{2}(1 - \mu). \tag{2.1.10}$$

Proof of Proposition 2.1.9. We assume that $c = 0$, $a > a_0$, and that (2.1.10) does not hold. We want to show that those assumptions lead to a contradiction. For $A \geqslant 0$, the function defined by

$$\psi_A(x) = A\cos\left(\sqrt{\frac{1-\mu}{2}}x\right),$$

is a solution of the equation $-\psi_A'' = \frac{1-\mu}{2}\psi_A$ over $[-a_0, a_0]$. Since $w, m > 0$ over $[-a_0, a_0]$ and are bounded, the set $\mathcal{A} := \{A, \forall x \in [-a_0, a_0], \psi_A(x) \leqslant \min(w(x), m(x))\}$ is a closed bounded nonempty set in $(0, +\infty)$. Let now $A_0 := \max \mathcal{A}$. We still have $\psi_{A_0} \leqslant \min(w, m)$ over $[-a_0, a_0]$, and then, since (2.1.10) does not hold and $K < 1$,

$$\begin{aligned} -(w - \psi_{A_0})'' &\geqslant (1 - \max_{[-a_0,a_0]}(w+m) - \mu)w - \frac{1-\mu}{2}\psi_{A_0} \\ &\geqslant \frac{1-\mu}{2}(w - \psi_{A_0}) \geqslant 0. \end{aligned} \tag{2.1.11}$$

Similarly, using additionally that $r > 1$,

$$-(m - \psi_{A_0})'' \geqslant \frac{1-\mu}{2}(m - \psi_{A_0}) \geqslant 0.$$

The weak minimum principle ([187], theorem 8.1) then imposes

$$\begin{aligned} &\min\left(\inf_{[-a_0,a_0]}(w - \psi_{A_0}), \inf_{[-a_0,a_0]}(m - \psi_{A_0})\right) \\ &\quad = \min((w - \psi_{A_0})(-a_0), (w - \psi_{A_0})(a_0), (m - \psi_{A_0})(-a_0), (m - \psi_{A_0})(a_0)). \end{aligned}$$

But the left side of the equation is 0 by definition of A_0, while the right side is strictly positive since $\psi_{A_0}(-a_0) = \psi_{A_0}(a_0) = 0$. This contradiction shows the result. □

Remark 2.1.10. Notice that Propositions 2.1.5, 2.1.6,2.1.7, 2.1.8 and 2.1.9 also holds if $(c, w, m) \in \mathbb{R} \times C^0([-a, a])$ is a solution of

$$\begin{cases} w,\, m \in C^0([-a,a]), \\ -cw' - w'' = \left(w(1 - (w + \sigma m)) + \mu(\sigma m - w)\right)\chi_{w\geq 0}\chi_{m\geq 0}, \\ -cm' - m'' = \left(rm\left(1 - \left(\frac{\sigma w + m}{K}\right)\right) + \mu(\sigma w - m)\right)\chi_{w\geq 0}\chi_{m\geq 0}, \\ w(-a) = w^*,\, m(-a) = m^*,\, w(a) = m(a) = 0, \end{cases} \tag{2.1.12}$$

where $\sigma \in [0, 1]$.

2.1.3.2 Existence of solutions to a localized problem

To show the existence of travelling waves solutions of (2.1.3), we will follow the approach of [7]. The first step is to show the existence of solutions of (2.1.7) satisfying the additional normalization property $\max_{[-a_0,a_0]}(w + m) = \nu_0$, that is the existence of a solution (c, w, m) to

$$\begin{cases} (c, w, m) \in \mathbb{R} \times C^0([-a,a])^2, \\ -cw' - w'' = f_w(w, m)\chi_{w\geqslant 0}\chi_{m\geqslant 0}, \\ -cm' - m'' = f_m(w, m)\chi_{w\geqslant 0}\chi_{m\geqslant 0}, \\ w(-a) = w^*,\, m(-a) = m^*,\, w(a) = m(a) = 0, \\ \max_{[-a_0,a_0]}(w + m) = \nu_0, \end{cases} \tag{2.1.13}$$

where f_w, f_m are defined by (2.1.4), $\nu_0 = \min\left(\frac{K}{4}(1-\mu), \frac{w^*+m^*}{2}\right)$ and w^*, m^* are defined in Appendix 2.1.6.2.

We introduce next the Banach space $(X, \|\cdot\|_X)$, with $X := \mathbb{R} \times C^0([-a,a])^2$ and $\|(c,w,m)\|_X := \max(|c|, \sup_{[-a,a]} |w|, \sup_{[-a,a]} |m|)$. We also define the operator

$$\begin{array}{rccc} K^\sigma : & X & \longrightarrow & X, \\ & (c,w,m) & \longmapsto & (c + \max_{[-a_0,a_0]}(\tilde{w}+\tilde{m}) - \nu_0, \tilde{w}, \tilde{m}) \end{array} \tag{2.1.14}$$

where $(\tilde{w}, \tilde{m}) \in C^0([-a,a])^2$ is the unique solution of

$$\begin{cases} -c\tilde{w}' - \tilde{w}'' = [w(1-(w+\sigma m)) + \mu(\sigma m - w)]\,\chi_{w\geqslant 0}\chi_{m\geqslant 0} \text{ on } (-a,a), \\ -c\tilde{m}' - \tilde{m}'' = \left[rm\left(1-\left(\frac{\sigma w+m}{K}\right)\right) + \mu(\sigma w - m)\right]\chi_{w\geqslant 0}\chi_{m\geqslant 0} \text{ on } (-a,a), \\ \tilde{w}(-a) = w^*,\ \tilde{m}(-a) = m^*,\ \tilde{w}(a) = \tilde{m}(a) = 0. \end{cases}$$

The solutions of (2.1.13) with $c \geqslant 0$ are then the fixed points of K^1 in the domain $\{(c,w,m), 0 \leqslant w \leqslant 1, 0 \leqslant m \leqslant K, c \geqslant 0\}$.

We define

$$\Omega := \Big\{(c,w,m) \in \mathbb{R}_+ \times C^0([-a,a])^2;\ c \in (0,c_*),\ \forall x \in [-a,a], \\ -1 < w(x) < 1,\ -K < m(x) < K\Big\},$$

where c_* is defined by (2.1.5).

Lemma 2.1.11. *Let r, K, μ satisfy Assumption 2.1.1, and $a > 0$. Then, $(K^\sigma)_{\sigma\in[0,1]}$, defined by (2.1.14), is a family of compact operators on $(X, \|\cdot\|_X)$, that is continuous with respect to $\sigma \in [0,1]$.*

Proof of Lemma 2.1.11. We can write $K^\sigma = (\mathcal{L}_D)^{-1} \circ \mathcal{F}^\sigma$ where $(\mathcal{L}_D)^{-1}$ is defined by

$$(\mathcal{L}_D)^{-1}(c,g,h) = (\tilde{c}, \tilde{w}, \tilde{m}),$$

where $(\tilde{c}, \tilde{w}, \tilde{m})$ is the unique solution of

$$\begin{cases} -c\tilde{w}' - \tilde{w}'' = g \text{ on } (-a,a), \\ -c\tilde{m}' - \tilde{m}'' = h \text{ on } (-a,a), \\ \tilde{w}(-a) = w^*,\ \tilde{m}(-a) = m^*,\ \tilde{w}(a) = \tilde{m}(a) = 0, \\ \tilde{c} = c + \max_{[-a_0,a_0]}(\tilde{w}+\tilde{m}) - \nu_0, \end{cases}$$

and $\mathcal{F}^\sigma$ is the mapping

$$\mathcal{F}^\sigma(c,w,m) = \left(c, w(1-(w+\sigma m)) + \mu(\sigma m - w), rm\left(1-\frac{\sigma w+m}{K}\right) + \mu(\sigma w - m)\right).$$

$\sigma \mapsto \mathcal{F}^\sigma$ is a continuous mapping from $[0,1]$ to $C^0(\Omega, X)$, and $(\mathcal{L}_D)^{-1}$ is a continuous application from $(X, \|\cdot\|_X)$ into itself (see Lemma 2.1.28), it then follows that $\sigma \mapsto K^\sigma = (\mathcal{L}_D)^{-1} \circ \mathcal{F}^\sigma$ is a continuous mapping from $[0,1]$ to $C^0(\Omega, X)$. Finally, the operator $(\mathcal{L}_D)^{-1}$ is compact (see Lemma 2.1.28), which implies that K^σ is compact for any fixed $\sigma \in [0,1]$. □

We now introduce the following operator, for $\sigma \in [0,1]$:

$$F^\sigma := Id - K^\sigma. \tag{2.1.15}$$

Similarly, we introduce the operator

$$\begin{array}{rccc} K_\tau : & X & \longrightarrow & X, \\ & (c,w,m) & \longmapsto & (c + \max_{[-a_0,a_0]}(\tilde{w}+\tilde{m}) - \nu_0, \tilde{w}, \tilde{m}) \end{array} \tag{2.1.16}$$

where $(\tilde{w}, \tilde{m}) \in C^0([-a,a])^2$ is the unique solution of

$$\begin{cases} -c\tilde{w}' - \tilde{w}'' = \tau w(1-\mu-w)\chi_{w\geqslant 0}\chi_{m\geqslant 0} \text{ on } (-a,a), \\ -c\tilde{m}' - \tilde{m}'' = \tau r m\left(1-\frac{\mu}{r}-\frac{m}{K}\right)\chi_{w\geqslant 0}\chi_{m\geqslant 0} \text{ on } (-a,a), \\ \tilde{w}(-a) = w^*,\ \tilde{m}(-a) = m^*,\ \tilde{w}(a) = \tilde{m}(a) = 0. \end{cases} \tag{2.1.17}$$

The argument of Lemma 2.1.11 can be be reproduced to prove that $(K_\tau)_{\tau\in[0,1]}$ is also a continuous family of compact operators on $(X, \|\cdot\|_X)$, and we can define, for $\tau \in [0,1]$, the operator

$$F_\tau := Id - K_\tau. \tag{2.1.18}$$

Finally, we introduce, for some $\bar{c} < 0$ that we will define later on,

$$\tilde{\Omega} := \Big\{(c,w,m) \in \mathbb{R}_+ \times C^0([-a,a])^2;\ c \in (\bar{c}, c_*),\ \forall x \in [-a,a], \\ -1 < w(x) < 1,\ -K < m(x) < K\Big\}.$$

In the next Lemma, we will show that the Leray-Schauder degree of F_0 in the domain $\tilde{\Omega}$ is non-zero as soon as $a > 0$ is large enough. We refer to chapter 12 of [364] or to chapter 10-11 of [82] for more on the Leray-Schauder degree.

Lemma 2.1.12. *Let r, K, μ satisfy Assumption 2.1.1. There exists $\bar{a} > 0$ such that the Leray-Schauder degree of F_0 in the domain $\tilde{\Omega}$ is non-zero as soon as $a \geqslant \bar{a}$.*

Proof of Lemma 2.1.12. We first notice that for $\tau = 0$, the solution $(\tilde{w}, \tilde{m})$ of (2.1.17) is independent of (w,m), and then,

$$F_0(c,w,m) = \left(\nu_0 - \max_{[-a_0,a_0]}(w_c + m_c), w - w_c, m - m_c\right),$$

where (w_c, m_c) is the solution of (2.1.17) with $\tau = 0$, that is

$$(w_c, m_c)(x) := \left(w^*\left(\frac{e^{-cx}-e^{-ca}}{e^{ca}-e^{-ca}}\right), m^*\left(\frac{e^{-cx}-e^{-ca}}{e^{ca}-e^{-ca}}\right)\right),$$

for $c \neq 0$, and $(w_c, m_c)(x) = (\frac{a-x}{2a}w^*, \frac{a-x}{2a}m^*)$ for $c = 0$. The solutions of $F_0(c,w,m) = 0$ then satisfy $w = w_c$ and $m = m_c$. In particular, the solutions of $F_0(c,w,m) = 0$ satisfy $0 < w < 1$ and $0 < m < K$ on $[-a,a)$, and then,

$$(c,w,m) \notin \big\{(\tilde{c},\tilde{w},\tilde{m}) \in \mathbb{R}\times C^0([-a,a])^2;\ \exists x \in [-a,a],\ \tilde{w}(x) \in \{-1,1\}\big\} \\ \cup \big\{(\tilde{c},\tilde{w},\tilde{m}) \in \mathbb{R}\times C^0([-a,a])^2;\ \exists x \in [-a,a],\ \tilde{m}(x) \in \{-K,K\}\big\}\Big).$$

The solutions of $F_0(c_*,w,m) = 0$ also satisfy

$$\max_{[-a_0,a_0]}(w_{c_*} + m_{c_*}) \leq 2\frac{e^{c_* a_0}}{e^{c_* a} - 1},$$

so that $\max_{[-a_0,a_0]}(w_{c_*} + m_{c_*}) < \nu_0$ if $a > \bar{a}$ for some $\bar{a} > 0$. It follows that $F_0 = 0$ has no solution in $\overline{\tilde{\Omega}} \cap \big(\{c^*\} \times C^0([-a,a])^2\big)$, provided $a > \bar{a}$. Finally, for $c \leq 0$, the solutions of $F_0(c,w,m) = 0$ satisfy $(w_c, m_c)(x) \geq (w_0, m_0)(x) = \left(-\frac{w^*}{2a}x + \frac{w^*}{2}, -\frac{m^*}{2a}x + \frac{m^*}{2}\right)$, so that

$$\max_{[-a_0,a_0]}(w_c + m_c) > \max_{[-a_0,a_0]}(w_0 + m_0) = \frac{w^*+m^*}{2}\left(1 + \frac{a_0}{a}\right) > \frac{w^*+m^*}{2} \geq \nu_0,$$

and $F_0 = 0$ has no solution in $\overline{\tilde{\Omega}} \cap \big(\mathbb{R}_- \times C^0([-a,a])^2\big)$.

We notice next that since $c \mapsto \max_{[-a_0,a_0]}(w_c + m_c)$ is decreasing, there exists a unique $c_0 \in (0, c_*)$ such that $\max_{[-a_0,a_0]}(w_{c_0} + m_{c_0}) = \nu_0$. We can then define

$$\Phi_\tau(c,w,m) = \left(\nu_0 - \max_{[-a_0,a_0]}(w_c + m_c), w - ((1-\tau)w_c + \tau w_{c_0}), m - ((1-\tau)m_c + \tau m_{c_0})\right),$$

which connects continuously $F_0 = \Phi_0$ to

$$\Phi_1(c,w,m) = \left(\nu_0 - \max_{[-a_0,a_0]}(w_c + m_c), w - w_{c_0}, m - m_{c_0}\right).$$

Notice that $\Phi_\tau(c,w,m) = 0$ implies $\max_{[-a_0,a_0]}(w_c + m_c) = \nu_0$, which in turn implies that $c = c_0$. For any $\tau \in [0,1]$, the only solution of $\Phi_\tau(c,w,m) = 0$ is then $(c_0, w_{c_0}, m_{c_0}) \notin \partial\tilde{\Omega}$, which implies that the Leray-Schauder degree $\deg(F_0, \tilde{\Omega})$ of F_0 is equal to $\deg(\Phi_1, \tilde{\Omega})$, which can easily be computed since its variables are separated :

$$\begin{aligned}\deg(\Phi_1, \Omega) &= \deg\left(\nu_0 - \max_{[-a_0,a_0]}(w_c + m_c), (\bar{c}, c_*)\right)\\ &\quad \deg\left(w - w_{c_0}, \left\{\tilde{w} \in C^0([-a,a]);\ -1 < \tilde{w}(x) < 1\right\}\right)\\ &\quad \deg\left(m - m_{c_0}, \left\{\tilde{m} \in C^0([-a,a]);\ -K < \tilde{m}(x) < K\right\}\right) = 1.\end{aligned}$$

□

Next, we show that the Leray-Schauder degree of F^0 in the domain Ω is also non-zero, as soon as $a > 0$ is large enough.

Lemma 2.1.13. *Let r, K, μ satisfy Assumption 2.1.1. There exists $\bar{a} > 0$ such that the Leray-Schauder degree of F^0 in the domain Ω is non-zero as soon as $a \geqslant \bar{a}$.*

Proof of Lemma 2.1.13. Thanks to Proposition 2.1.9 and Remark 2.1.10, any triplet solution $(c,w,m) \in \tilde{\Omega}$ of (2.1.12), and thus any solution $(c,w,m) \in \tilde{\Omega}$ of $F^0(c,w,m) = 0$ satisfies $c > 0$, that is $(c,w,m) \in \Omega$. Then,

$$\deg(F^0, \Omega) = \deg(F^0, \tilde{\Omega}) = \deg(F_1, \tilde{\Omega}). \tag{2.1.19}$$

For $\tau \in [0,1]$, any solution $(c,w,m) \in \tilde{\Omega}$ of $F_\tau(c,w,m) = 0$ satisfies

$$-cw' - w'' \geq -\mu w, \quad -cm' - m'' \geq -\mu m,$$

and then $w, m \geq \phi_c$, where ϕ_c is the solution of $-c\phi_c' - \phi_c'' = -\mu\phi_c$ with $\phi_c(-a) = K$, $\phi_c(a) = 0$. This solution can easily be computed explicitly, and satisfies (for any fixed $a > 0$)

$$\lim_{c \to -\infty} \phi_c(0) = K.$$

we can then choose $-\bar{c} > 0$ large enough for $\phi_{\bar{c}}(0) \geq \nu_0$ to hold (note that the constant $\bar{c} \in \mathbb{R}$ is not independent of a). Then, $F_\tau(\bar{c},w,m) = 0$ implies $\max_{[-a_0,a_0]}(w + m) \geq 2\phi_{\bar{c}}(0) > \nu_0$, which implies in turn that $F_\tau(c,w,m) = 0$ has no solution on $\left(\{\bar{c}\} \times C^0([-a,a])^2\right) \cap \overline{\tilde{\Omega}}$, for any $\tau \in [0,1]$. If $F_\tau(c,w,m) = 0$ with $(c,w,m) \in \overline{\tilde{\Omega}}$, a classical application of the strong maximum principle shows that $0 < w < 1$ and $0 < m < K$ on $(-a,a)$ (notice that w and m are indeed solutions of two uncoupled Fisher-KPP equations on $[-a,a]$). Moreover, the proof of Proposition 2.1.8 applies to solutions of $F_\tau(c_*,w,m) = 0$, which implies that (for any $\tau \in [0,1]$),

$$\max_{[-a_0,a_0]}(w + m) \leq Ce^{-c_* \frac{a-a_0}{2}},$$

and thus, $F_\tau(c,w,m) = 0$ has no solution on $\left(\{c_*\} \times C^0([-a,a])^2\right) \cap \overline{\tilde{\Omega}}$ as soon as $a > 0$ is large enough (uniformly in $\tau \in [0,1]$).

We have shown that $F_\tau(c,w,m) = 0$ has no solution on $\partial\tilde{\Omega}$ for $\tau \in [0,1]$. Since $\tau \mapsto F_\tau$ is a continuous familly of compact operators on $\tilde{\Omega}$, this implies that

$$\deg(F_1, \tilde{\Omega}) = \deg(F_0, \tilde{\Omega}),$$

which, combined to (2.1.19) and Proposition 2.1.12, concludes the proof.

□

Proposition 2.1.14. *Let r, K, μ satisfy Assumption 2.1.1. There exists $\bar{a} > 0$ such that for $a \geqslant \bar{a}$, there exists a solution $(c, w, m) \in \mathbb{R} \times C^0([-a, a])^2$ of (2.1.13) with $c \in (0, c_*)$.*

Proof of Proposition 2.1.14. The first step of the proof is to show that there exists no solution $(c, w, m) \in \partial\Omega$ of $F^\sigma(c, w, m) = 0$ with $\sigma \in [0, 1]$.

If such a solution exists, then Proposition 2.1.9 (see also Remark 2.1.10) implies that $c \neq 0$, and if $c = c_*$, then Proposition 2.1.8 (see also Remark 2.1.10) implies that

$$\max_{[-a_0,a_0]}(w + m) \leqslant Ce^{-c_* \frac{a-a_0}{2}}, \tag{2.1.20}$$

where $C > 0$ is a positive constant independent from $\sigma \in [0, 1]$. If a is large enough (more precisely if $a \geq a_0 + \frac{2}{c_*} \ln\left(\frac{2C}{\nu_0}\right)$), then $\max_{[-a_0,a_0]}(w + m) \leq \frac{\nu_0}{2}$, which is a contradiction. Any solution $(c, w, m) \in \overline{\Omega}$ of $F^\sigma(c, w, m) = 0$ then satisfies $c \in (0, c_*)$, as soon as $a > 0$ is large enough.

Any solution $(c, w, m) \in \overline{\Omega}$ of $F^\sigma(c, w, m) = 0$ is a solution of (2.1.12), Proposition 2.1.6 and Proposition 2.1.7 (see also Remark 2.1.10) then imply that for any $x \in (-a, a)$, $0 < w(x) < 1$ and $0 < m(x) < K$.

We have shown that $F^\sigma(c, w, m) = 0$ had no solution $(c, w, m) \in \partial\Omega$, for $\sigma \in [0, 1]$. Since moreover $(F_\sigma)_{\sigma\in[0,1]}$ is a continuous family of compact operators (see Lemma 2.1.11) this is enough to show that $\deg(F^\sigma, \Omega)$ is independent of $\sigma \in [0, 1]$, and then, thanks to Lemma 2.1.13, as soon as $a > 0$ is large enough,

$$\deg(F^1, \Omega) = \deg(F^0, \Omega) \neq 0.$$

which implies in particular that there exists at least one solution $(c, w, m) \in \Omega$ of $F^1(c, w, m) = 0$, that is a solution (c, w, m) of (2.1.13) in Ω. □

2.1.3.3 Construction of a travelling wave

Proposition 2.1.15. *Let r, K, μ satisfy Assumption 2.1.1. There exists a solution $(c, w, m) \in (0, c_*] \times C^0(\mathbb{R})^2$ of problem (2.1.3) that satisfies $0 < w(x) < 1$ and $0 < m(x) < K$ for $x \in \mathbb{R}$, as well as $(w+m)(0) = \nu_0$.*

Proof of Proposition 2.1.15. For $n \geq 0$, let $a_n := \bar{a} + n$ (where $\bar{a} > 0$ is defined in Proposition 2.1.14), and (c_n, w_n, m_n) a solution of (2.1.13) provided by Proposition 2.1.14. We denote by (w_n^k, m_n^k) the restriction of (w_n, m_n) to $[-a_k, a_k]$ $(k < n)$. From interior elliptic estimates (see e.g. Theorem 8.32 in [187]), we know that there exists a constant $C > 0$ independent of $k > 0$, such that for any $n \geq k + 1$,

$$\max\left(\left\|w_n|_{[-a_k,a_k]}\right\|_{C^1([-a_k,a_k])}, \left\|m_n|_{[-a_k,a_k]}\right\|_{C^1([-a_k,a_k])}\right) \leqslant C,$$

Since $c_n \in [0, c^*]$ for all $n \in \mathbb{N}$, we can extract from (c_n, w_n, m_n) a subsequence (that we also denote by (c_n, w_n, m_n)), such that $c_n \to c_0$ for some $c_0 \in [0, c^*]$. Since $c_n \in (0, c_*)$ for all $n \geq 3$, the limit speed satisfies $c_0 \in [0, c_*]$. Thanks to Ascoli's Theorem, $C^1([-a_k, a_k])$ is compactly embedded in $C^0([-a_k, a_k])$. We can then use a diagonal extraction, to get a subsequence such that w_n and m_n both converge uniformly on every compact interval of $\mathbb{R}$. Let w_0, $m_0 \in C^0(\mathbb{R})$ the limits of $(w_n)_n$ and $(m_n)_n$ respectively. Then, thanks to the uniform convergence, we get that

$$\forall x \in \mathbb{R}, \quad 0 \leqslant w_0(x) \leqslant 1, \quad 0 \leqslant m_0(x) \leqslant K,$$

$$-c_0 w_0' - w_0'' = f_w(w_0, m_0) \text{ on } \mathbb{R},$$
$$-c_0 m_0' - m_0'' = f_m(w_0, m_0) \text{ on } \mathbb{R},$$

in the sense of distributions. Thanks to Proposition 2.1.5, these two functions are smooth and are thus classical solutions of (2.1.3). Moreover, $\max_{[-a_0,a_0]}(w_0 + m_0) = \nu_0$, and Lemma 2.1.9 implies that $c_0 \neq 0$. Finally, up to a shift, $w_0(0) + m_0(0) = \nu_0$.

□

In the next proposition, we show that the solution of (2.1.3) obtained in Proposition 2.1.15 are indeed propagation fronts.

Proposition 2.1.16. *Let r, K, μ satisfy Assumption 2.1.1 and $(c, w, m) \in \mathbb{R} \times C^0(\mathbb{R})^2$ a solution of* (2.1.3) *such that $(w+m)(0) = \nu_0$. Then $w+m$ is decreasing on $(0, +\infty)$,*

$$\lim_{x\to\infty} w(x) = \lim_{x\to\infty} m(x) = 0,$$

and $w(x) + m(x) \geq \nu_0$ on $(-\infty, 0]$.

Proof of Proposition 2.1.16. Assume that $w(x) + m(x) < K$, and $w'(x) + m'(x) \geq 0$. Then,

$$-c(w+m)'(x) - (w+m)''(x) = w(x)(1 - (w(x) + m(x))) + rm(x)\left(1 - \frac{w(x)+m(x)}{K}\right), \tag{2.1.21}$$

with the right side positive, and then $(w+m)''(x) < 0$. If there exists $x_0 \in \mathbb{R}$ satisfying $w(x_0)+m(x_0) < K$, and $w'(x_0) + m'(x_0) \geq 0$, then we can define $\mathcal{C} = \{x \leqslant x_0, \forall y \in [x, x_0], (w+m)''(y) \leqslant 0\}$. Then $\mathcal{C} \neq \varnothing$ and $\mathcal{C}$ is closed since $(w+m)''$ is continuous. Let $x_1 \in \mathcal{C}$. Then $(w+m)'$ is decreasing on $[x_1, x_0]$, so that $(w+m)'(x_1) \geqslant (w+m)'(x_0) > 0$ and $(w+m)(x_1) \leqslant (w+m)(x_0)$. (2.1.21) then implies that $(w+m)''(x_1) < 0$, which proves that $\mathcal{C}$ is open, and thus $\mathcal{C} = (-\infty, 0)$. This implies in particular that $w(x) + m(x) < 0$ for some $x < x_0$, which is a contradiction. We have then proven that $x \mapsto w(x) + m(x)$ is decreasing on $[x_0, \infty)$ as soon as $w(x_0) + m(x_0) \leq K$. It implies that $w(x) + m(x) \geq \nu_0$ for $x \leq 0$, and that $x \mapsto w(x) + m(x)$ is decreasing on $[0, \infty)$.

Then, $\lim_{x\to\infty} w(x)+m(x) = l \in [0, K)$ exists, which implies that $\lim_{x\to\infty} w'(x)+m'(x) = \lim_{x\to\infty} w''(x)+m''(x) = 0$, since w and m are regular. Then,

$$\lim_{x\to\infty} \left(-c(w+m)'(x) - (w+m)''(x)\right) = 0,$$

which, combined to (2.1.21), proves that $\lim_{x\to\infty} w(x) + m(x) = 0$. □

2.1.3.4 Characterization of the speed of the constructed travelling wave

Lemma 2.1.17. *Let r, K, μ satisfy Assumption 2.1.1 and $(c, w, m) \in \mathbb{R} \times C^0(\mathbb{R})^2$ a solution of* (2.1.3) *such that $(w+m)(0) = \nu_0$. Then there exists $x_0 \in \mathbb{R}$ and $C > 0$ such that*

$$\forall x \geqslant x_0, \quad w(x) + m(x) \leqslant C \min(w(x), m(x)).$$

Proof of Lemma 2.1.17. Let $S(x) := w(x) + m(x)$, and $\alpha > 0$. Then

$$-c(S - \alpha w)' - (S - \alpha w)'' = ((1 - S) - (1 - S - \mu)\alpha)w + (S - w)\left(r\left(1 - \frac{S}{K}\right) - \alpha\mu\right).$$

Let $x_1 \in \mathbb{R}$ such that $S(x) \leqslant \frac{1-\mu}{2}$ for all $x \geq x_1$ (x_1 exists thanks to Proposition 2.1.16). Then, for $\alpha \geqslant \alpha_0 := \max\left(\frac{2}{1-\mu}, \frac{r}{\mu}\right)$ and $x \geqslant x_1$,

$$-c(S - \alpha w)'(x) - (S - \alpha w)''(x) \leqslant 0.$$

Let $\alpha_1 := \max\left(\frac{S(x_1)}{w(x_1)}, \alpha_0\right) + 1$. Then $-c(S - \alpha_1 w)' - (S - \alpha_1 w)'' \leqslant 0$ over $(x_1, +\infty)$. We can then apply the weak maximum principle to show that for any $x_2 > x_1$,

$$\max_{[x_1, x_2]} (S - \alpha_1 w)(x) = \max\left((S - \alpha_1 w)(x_1), (S - \alpha_1 w)(x_2)\right).$$

Since $(S - \alpha_1 w)(x_1) \leqslant 0$ and $\lim_{x_2\to+\infty} (S - \alpha_1 w)(x_2) = 0$, we have indeed shown that $\sup_{[x_1,\infty)} (S - \alpha_1 w)(x) = 0$, and then,

$$\forall x \geq x_1, \quad w(x) + m(x) \leq \alpha_1 w(x).$$

A similar argument can be used to show that there exists $x_2 \in \mathbb{R}$ and $\alpha_2 > 0$ such that $w(x)+m(x) \leqslant \alpha_2 m(x)$ for $x \geqslant x_2$, which concludes the proof of the Lemma. □

Proposition 2.1.18. *Let r, K, μ satisfy Assumption 2.1.1 and $(c, w, m) \in \mathbb{R}_+ \times C^0(\mathbb{R})^2$ a solution of* (2.1.3) *such that $(w+m)(0) = \nu_0$ and $c \leq c_*$. Then, $c = c_*$.*

Remark 2.1.19. Combined to Proposition 2.1.15 and Proposition 2.1.16, this proposition completes the proof of Theorem 2.1.2.

Proof of Proposition 2.1.18. Let $(c, w, m) \in [0, c_*] \times C^0(\mathbb{R})^2$ a solution of (2.1.3) such that $(w+m)(0) = \nu_0$. Thanks to Lemma 2.1.17, there exists $x_0 > 0$ and $C > 0$ such that

$$\begin{cases} -cw' - w'' \geq w(1 - \mu - Cw) + \mu m, \\ -cm' - m'' \geq m(r - \mu - Cm) + \mu w. \end{cases}$$

Let now $\varphi_\eta(x + x_1) := \eta e^{-\frac{c}{2}x} \sin\left(\frac{\sqrt{4h-c^2}}{2}x\right)$, where $\eta > 0$, $h \geq c^2/4$ and $x_1 > x_0$. φ_η then satisfies $\varphi_\eta(x_1) = \varphi_\eta\left(x_1 + 2\pi/\sqrt{4h-c^2}\right) = 0$, and $-c\varphi_\eta' - \varphi_\eta'' = h\varphi_\eta$ on $\left[x_1, x_1 + 2\pi/\sqrt{4h-c^2}\right]$. $\psi_\eta := \varphi_\eta X$ (X is defined by (2.1.9)) is then a solution of

$$-c\psi_\eta' - \psi_\eta'' = (M + (h - h_+)Id)\psi_\eta,$$

where h_+ is defined by (2.1.9), and we can also write this equality as follows

$$\begin{cases} -c(\psi_\eta)_1' - (\psi_\eta)_1'' = (\psi_\eta)_1 \left(1 - \mu + (h - h_+)\right) + \mu(\psi_\eta)_2, \\ -c(\psi_\eta)_2' - (\psi_\eta)_2'' = (\psi_\eta)_2 \left(r - \mu + (h - h_+)\right) + \mu(\psi_\eta)_1. \end{cases}$$

Assume now that $c < c_*$. Then, we can choose $c^2/4 < h < c_*^2/4 = h_+$, and define

$$\bar\eta = \max\left\{\eta > 0;\, \forall x \in \left[x_1, x_1 + 2\pi/\sqrt{4h-c^2}\right],\, (\psi_\eta)_1(x) \leq w(x),\, (\psi_\eta)_2(x) \leq m(x)\right\}.$$

Since w and m are positive bounded function, $\bar\eta > 0$ exists, and since

$$(\psi_\eta)_i(x_1) = (\psi_\eta)_i\left(x_1 + 2\pi/\sqrt{4h-c^2}\right) = 0,$$

there exists $\bar x \in \left(x_1, x_1 + 2\pi/\sqrt{4h-c^2}\right)$ such that either $(\psi_\eta)_1(\bar x) = w(\bar x)$ or $(\psi_\eta)_2(\bar x) = m(\bar x)$. Assume w.l.o.g. that $(\psi_\eta)_1(\bar x) = w(\bar x)$. Then $w - (\psi_\eta)_1$ has a local minimum in $\bar x$, which implies that

$$\begin{aligned} 0 &\geq -c(w - (\psi_{\bar\eta})_1)'(\bar x) - (w - (\psi_{\bar\eta})_1)''(\bar x) \\ &\geq [w(\bar x)(1 - \mu - Cw(\bar x)) + \mu m(\bar x)] - [(\psi_{\bar\eta})_1(\bar x)\left(1 - \mu + (h - h_+)\right) + \mu(\psi_{\bar\eta})_2(\bar x)] \\ &\geq (\psi_{\bar\eta})_1(\bar x)\left[(h_+ - h) - C(\psi_{\bar\eta})_1(\bar x)\right], \end{aligned}$$

and then $\bar\eta \geq (h_+ - h)/(CX_1)$. A similar argument holds if $(\psi_\eta)_2(\bar x) = m(\bar x)$, so that in any case, $\bar\eta \geq (h_+ - h)/(C\max(X_1, X_2))$, and $\psi_{\bar\eta}(x_1 + \cdot) \leq m$, $\psi_{\bar\eta}(x_1 + \cdot) \leq m$ on $\left[x_1, x_1 + 2\pi/\sqrt{4h-c^2}\right]$, as soon as $x_1 \geq x_0$. In particular, for any $x_1 \geq x_0$,

$$w\left(x_1 + \pi/\sqrt{4h-c^2}\right) \geq \frac{h_+ - h}{C\max(X_1, X_2)} e^{-\frac{c\pi}{2\sqrt{4h-c^2}}} X_1 > 0,$$

which is a contradiction, since $w(x) \to_{x\to\infty} 0$ thanks to Proposition 2.1.16. □

2.1.4 Proof of Theorem 2.1.3

2.1.4.1 General case

The proof of the next lemma is based on a phase-plane-type analysis, see Figure 2.1.3

Lemma 2.1.20. *Let r, K, μ satisfy Assumption 2.1.1. Let $(c, w, m) \in \mathbb{R}_+ \times C^0([-a, a])^2$ be a solution of (2.1.7). Then there exists $\bar x \in [-a, 0)$ such that one of the following properties is satisfied:*

- *w is decreasing on $[-a, a]$, while m is increasing on $[-a, \bar x]$ and decreasing on $[\bar x, a]$,*
- *m is decreasing on $[-a, a]$, while w is increasing on $[-a, \bar x]$ and decreasing on $[\bar x, a]$.*

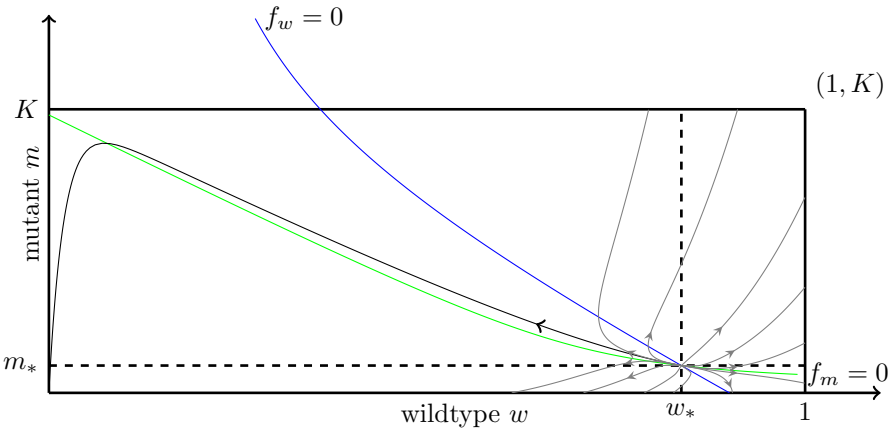

Figure 2.1.3: Phase-plane-type representation of a solution of (2.1.7): we represent (dark line) $x \mapsto (w(x), m(x)) \in [0,1] \times [0,K]$. Note that the usual phase-plane for (2.1.7) is of dimension 4. The blue line represents the set of (w,m) such that $f_w(w,m) = 0$ (see (2.1.4)), $f_w(w,m) > 0$ for (m,w) on the left of the blue curve. The green line represent the set of (w,m) such that $f_m(w,m) = 0$ (see (2.1.4)), $f_m(w,m) > 0$ for (m,w) under the green curve. the gray lines represent several other solutions of (2.1.3) such $(w(-a), m(-a)) = (w^*, m^*)$. The dashed dark lines separate this phase plane into four compartiments that will be used in the third step of the proof of Lemma 2.1.20. Finally, the solid black line corresponds to the travelling wave.

Proof of Lemma 2.1.20. Step 1: sign of f_w and f_m.

We recall the definition (2.1.4) of f_w, f_m. The inequality $f_w(w,m) \geq 0$ is equivalent, for $w \in [0,1]$ and $m \in [0,K]$, to

$$w \leq \phi_w(m) := \frac{1}{2}\left[1 - \mu - m + \sqrt{(1-\mu-m)^2 + 4\mu m}\right]. \tag{2.1.22}$$

Notice that $m \in [0,K] \mapsto \phi_w(m)$ is a decreasing function (see Lemma 2.1.29), that divides the square $\{(w,m) \in [0,1] \times [0,K]\}$ into two parts.

Similarly, $f_m(w,m) \geq 0$ is equivalent, for $w \in [0,1]$ and $m \in [0,K]$, to

$$m \leq \phi_m(w) := \frac{1}{2}\left[K - \frac{\mu K}{r} - w + \sqrt{\left(K - \frac{\mu K}{r} - w\right)^2 + 4\frac{\mu K}{r} w}\right]. \tag{2.1.23}$$

Here also, $w \in [0,1] \mapsto \phi_m(w)$ is a decreasing function (see Lemma 2.1.29), since $\mu \leq 1/2$ (see Assumption 2.1.1), that divides the square $\{(w,m) \in [0,1] \times [0,K]\}$ into two parts.

Step 2: possible monotony changes of $w(x)$, $m(x)$. Let $(c,w,m) \in \mathbb{R}_+ \times C^0([-a,a])^2$ be a solution of (2.1.7). If $w'(x) \geq 0$ for some $x > -a$, we can define $\bar{x} := \inf\{y \geq x;\, w'(y) < 0\}$. Then $w'(\bar{x}) = 0$, and $w''(\bar{x}) \leq 0$, which implies

$$f_w(w(\bar{x}), m(\bar{x})) = -cw'(\bar{x}) - w''(\bar{x}) \geq 0,$$

that is $w(\bar{x}) \leq \phi_w(m(\bar{x}))$. The symmetric property also holds: if $w'(x) \leq 0$ for some $x > -a$, we can define $\bar{x} := \inf\{y \geq x;\, w'(y) > 0\}$, and then, $w(\bar{x}) \geq \phi_w(m(\bar{x}))$.

We repeat the argument for the function m: let $(c,w,m) \in \mathbb{R}_+ \times C^0([-a,a])^2$ be a solution of (2.1.7). If $m'(x) \geq 0$ for some $x > -a$, we can define $\bar{x} := \inf\{y \geq x;\, m'(y) < 0\}$, and then, $m(\bar{x}) \leq \phi_m(w(\bar{x}))$. Finally, if $m'(x) \leq 0$ for some $x > -a$, we can define $\bar{x} := \inf\{y \geq x;\, m'(y) > 0\}$, and then, $m(\bar{x}) \geq \phi_m(w(\bar{x}))$.

Step 3: phase plane analysis Notice that $(w(-a), m(-a)) = (w^*, m^*)$, and then,

$$m(-a) = \phi_m(w(-a)), \quad w(-a) = \phi_w(m(-a)). \tag{2.1.24}$$

We will consider now consider individually the four possible signs of $w'(-a)$, $m'(-a)$ (the cases where $w'(-a) = 0$ or $m'(-a) = 0$ will be considered further in the proof):

(i) Assume that $w'(-a) > 0$ and $m'(-a) > 0$. We define $\bar{x} := \inf\{y \geq -a;\ w'(y) < 0 \text{ or } m'(y) < 0\}$. Since w and m are increasing on $[-a, \bar{x}]$, (2.1.24) holds and $w \mapsto \phi_m(w)$, $m \mapsto \phi_w(m)$ are decreasing functions, we have

$$w(\bar{x}) > w(-a) = \phi_w(m(-a)) \geq \phi_w(m(\bar{x})),$$
$$m(\bar{x}) > m(-a) = \phi_m(w(-a)) \geq \phi_m(w(\bar{x})).$$

Then, $f_w(w(\bar{x}), m(\bar{x})) < 0$ and $f_m(w(\bar{x}), m(\bar{x})) < 0$. It then follows from Step 2 that $\bar{x} = a$, which means that w and m are increasing on $[-a, a]$. It is a contradiction, since $0 = w(a) < w(-a) = \bar{w}$.

Notice that the same argument would also work on $[x, a]$, for any $(w(x), m(x))$ that satisfies $w(x) > \Phi_w(m(x))$, $m(x) > \Phi_m(w(x))$, $w'(x) > 0$ and $m'(x) > 0$.

(ii) Assume that $w'(-a) < 0$ and $m'(-a) < 0$. Let $\bar{x} := \inf\{y \geq -a;\ w'(y) > 0 \text{ or } m'(y) > 0\}$. Since w and m are decreasing on $[-a, \bar{x}]$, (2.1.24) holds and $w \mapsto \phi_m(w)$, $m \mapsto \phi_w(m)$ are decreasing functions, we have

$$w(\bar{x}) < w(-a) = \phi_w(m(-a)) \leq \phi_w(m(\bar{x})),$$
$$m(\bar{x}) < m(-a) = \phi_m(w(-a)) \leq \phi_m(w(\bar{x})).$$

It then follows from Step 2 that $\bar{x} = a$, which means that w and m are non-increasing on $[-a, a]$. Notice that this is not a contradiction, since $w(a) = 0 < w^* = w(-a)$, $m(a) = 0 < m^* = m(-a)$.

Notice that the same argument would work on $[x, a]$, for any $(w(x), m(x))$ that satisfies $\Phi_w(m(x)) > w(x)$, $m(x) < \Phi_m(w(x))$, $w'(x) < 0$ and $m'(x) < 0$.

(iii) Assume that $w'(-a) < 0$ and $m'(-a) > 0$. We define $\bar{x} := \inf\{y \geq -a;\ w'(y) > 0 \text{ or } m'(y) < 0\}$. The argument used in the two previous cases cannot be employed here. We know however that $w(\bar{x}) < w^*$, $m(\bar{x}) > m^*$. Since $m(a) = 0 < m^*$, it implies in particular that $\bar{x} < a$, and, with the notations of Lemma 2.1.33, $(w(\bar{x}), m(\bar{x})) \in \mathcal{D}_l$.

If w' changes sign in $\bar{x}$, then Step 2 implies that $w(\bar{x}) \geq \phi_w(m(\bar{x}))$, that is, with the notations of Lemma 2.1.33, $(w(\bar{x}), m(\bar{x})) \in Z_w^-$. Thanks to Lemma 2.1.33, it follows that $(w(\bar{x}), m(\bar{x})) \in Z_w^- \cap \mathcal{D}_l \subset Z_m^-$, and then $m(\bar{x}) > \phi_m(w(\bar{x}))$, which implies $-cm'(\bar{x}) - m''(\bar{x}) = f_m(w(\bar{x}), m(\bar{x})) < 0$. If $m'(\bar{x}) = 0$, then $m''(\bar{x}) > 0$, which is incompatible with the fact that $m' \geq 0$ on $[-a, \bar{x})$ and $m'(\bar{x}) = 0$. We have thus shown that $m'(\bar{x}) > 0$. Thanks to the definition of $\bar{x}$, either w is locally increasing near $\bar{x}^+$, or there exists a sequence $(x_n) \to \bar{x}^+$ such that $w'(x_{2n}) > 0$ and $w'(x_{2n+1}) < 0$. In the first case, for $\varepsilon > 0$ small enough, $w(\bar{x} + \varepsilon) > w(\bar{x}) \geq \Phi_w(m(\bar{x})) \geq \Phi_w(m(\bar{x} + \varepsilon))$ along with $w'(\bar{x} + \varepsilon) > 0$. In the second case, $w''(\bar{x}) = 0$, then $f_w(w, m)(\bar{x}) = 0$, and a simple computation shows that for $\varepsilon > 0$ small enough,

$$f_w\left(w(\bar{x} + \varepsilon), m(\bar{x} + \varepsilon)\right) = (\mu - w(\bar{x}))\varepsilon m'(\bar{x}) + o(\varepsilon) < 0,$$

where we have used the fact that $\mu - w(\bar{x}) < 0$ (since $w(\bar{x}) \geq \phi_w(m(\bar{x})) \subset \phi_w([0, K]) \subset (\mu, \infty)$, see Lemma 2.1.29). In any case, for some $\varepsilon > 0$ arbitrarily small, $w(\bar{x} + \varepsilon) > \phi_w(m(\bar{x} + \varepsilon))$, $m(\bar{x} + \varepsilon) > \phi_m(w(\bar{x} + \varepsilon))$, along with $w'(\bar{x} + \varepsilon) > 0$ and $m'(\bar{x} + \varepsilon) > 0$. argument (i) can now be applied to $(w, m)|_{[\bar{x}+\varepsilon, a]}$, leading to a contradiction.

If m' changes sign in $\bar{x}$, then Step 2 implies that $m(\bar{x}) \leq \phi_m(w(\bar{x}))$, that is, with the notations of Remark 2.1.34, $(w(\bar{x}), m(\bar{x})) \in Z_m^+$. Thanks to Remark 2.1.34, it follows that $(w(\bar{x}), m(\bar{x})) \in Z_m^+ \cap \mathcal{D}_l \subset Z_w^+$, and then $w(\bar{x}) < \phi_w(m(\bar{x}))$, which implies $-cw'(\bar{x}) - w''(\bar{x}) = f_w(w(\bar{x}), m(\bar{x})) > 0$. If $w'(\bar{x}) = 0$, then $w''(\bar{x}) < 0$, which is incompatible with the fact that $w' \leq 0$ on $[-a, \bar{x})$ and $w'(\bar{x}) = 0$. We have thus shown that $w'(\bar{x}) < 0$. Thanks to the definition of $\bar{x}$, either m is locally decreasing near $\bar{x}^+$, or there exists a sequence $(x_n) \to \bar{x}^+$ such that $m'(x_{2n}) > 0$ and $m'(x_{2n+1}) < 0$. In the first case, for $\varepsilon > 0$ small enough, $m(\bar{x} + \varepsilon) < m(\bar{x}) \leq \Phi_m(w(\bar{x})) \leq \Phi_m(w(\bar{x} + \varepsilon))$ along with $m'(\bar{x} + \varepsilon) > 0$. In the second case, $m''(\bar{x}) = 0$, then $f_m(w, m)(\bar{x}) = 0$, and a simple computation shows that for $\varepsilon > 0$ small enough,

$$f_m\left(w(\bar{x} + \varepsilon), m(\bar{x} + \varepsilon)\right) = \left(\mu - \frac{r}{K} m(\bar{x})\right) \varepsilon w'(\bar{x})) + o(\varepsilon) > 0,$$

where we have used the fact that $\mu - \frac{r}{K} m(\bar{x}) < 0$ (since $m(\bar{x}) > m^* = \phi_m(w^*) \subset \phi_m([0, 1]) \subset (\mu K/r, \infty)$, see Lemma 2.1.29). In both cases, argument (ii) can now be applied to $(w, m)|_{[\bar{x}+\varepsilon, a]}$, which is not a contradiction, since $w(a) = 0 < w(\bar{x})$, $m(a) = 0 < m(\bar{x})$.

(iv) Assume that $w'(-a) > 0$ and $m'(-a) < 0$. We define $\bar{x} := \inf\{y \geq -a;\ w'(y) < 0 \text{ or } m'(y) > 0\}$. Then $w(\bar{x}) > w^*$, $m(\bar{x}) < m^*$. Since $m(a) = 0 < m^*$, it implies in particular that $\bar{x} < a$, and, with the notations of Lemma 2.1.33, $(w(\bar{x}), m(\bar{x})) \in \mathcal{D}_r$.

If w' changes sign in $\bar{x}$, then Step 2 implies that $w(\bar{x}) \leq \phi_w(m(\bar{x}))$, that is, with the notations of Remark 2.1.34, $(w(\bar{x}), m(\bar{x})) \in Z_w^+$. Thanks to Remark 2.1.34, it follows that $(w(\bar{x}), m(\bar{x})) \in Z_w^+ \cap \mathcal{D}_r \subset Z_m^+$,

and then $m(\bar{x}) < \phi_m(w(\bar{x}))$, which implies $-cm'(\bar{x}) - m''(\bar{x}) = f_m(w(\bar{x}), m(\bar{x})) > 0$. If $m'(\bar{x}) = 0$, then $m''(\bar{x}) < 0$, which is incompatible with the fact that $m' \leq 0$ on $[-a, \bar{x}]$ and $m'(\bar{x}) = 0$. We have thus shown that $m'(\bar{x}) < 0$. Thanks to the definition of $\bar{x}$, either w is locally decreasing near $\bar{x}^+$, or there exists a sequence $(x_n) \to \bar{x}^+$ such that $w'(x_{2n}) > 0$ and $w'(x_{2n+1}) < 0$. In the first case, for $\varepsilon > 0$ small enough, $w(\bar{x} + \varepsilon) < w(\bar{x}) \leq \Phi_w(m(\bar{x})) \leq \Phi_w(m(\bar{x} + \varepsilon))$ along with $w'(\bar{x} + \varepsilon) < 0$. In the second case, $w''(\bar{x}) = 0$, then $f_w(w, m)(\bar{x}) = 0$, and a simple computation shows that for $\varepsilon > 0$ small enough,

$$f_w(w, m)(\bar{x} + \varepsilon) = (\mu - w(\bar{x}))\varepsilon m'(\bar{x}) + o(\varepsilon) > 0,$$

where we have used the fact that $\mu - w(\bar{x}) < 0$ (since $w(\bar{x}) > w^* = \phi_w(m^*) \subset \phi_w([0, 1]) \subset (\mu, \infty)$, see Lemma 2.1.29). In both cases, argument (ii) can now be applied to $(w, m)|_{[\bar{x}+\varepsilon, a]}$, which is not a contradiction, since $w(a) = 0 < w(\bar{x})$, $m(a) = 0 < m(\bar{x})$.

If m' changes sign in $\bar{x}$, then Step 2 implies that $m(\bar{x}) \geq \phi_m(w(\bar{x}))$, that is, with the notations of Lemma 2.1.33, $(w(\bar{x}), m(\bar{x})) \in Z_m^-$. Thanks to Lemma 2.1.33, it follows that $(w(\bar{x}), m(\bar{x})) \in Z_m^- \cap \mathcal{D}_r \subset Z_w^-$, and then $w(\bar{x}) > \phi_w(m(\bar{x}))$, which implies $-cw'(\bar{x}) - w''(\bar{x}) = f_w(w(\bar{x}), m(\bar{x})) < 0$. If $w'(\bar{x}) = 0$, then $w''(\bar{x}) > 0$, which is incompatible with the fact that $w' \geq 0$ on $[-a, \bar{x}]$ and $w'(\bar{x}) = 0$. We have thus shown that $w'(\bar{x}) > 0$. Thanks to the definition of $\bar{x}$, either m is locally increasing near $\bar{x}^+$, or there exists a sequence $(x_n) \to \bar{x}^+$ such that $m'(x_{2n}) > 0$ and $m'(x_{2n+1}) < 0$. In the first case, for $\varepsilon > 0$ small enough, $m(\bar{x} + \varepsilon) > m(\bar{x}) \geq \Phi_m(w(\bar{x})) \geq \Phi_m(w(\bar{x} + \varepsilon))$ along with $m'(\bar{x} + \varepsilon) > 0$. In the second case, $m''(\bar{x}) = 0$, then $f_m(w, m)(\bar{x}) = 0$, and a simple computation shows that for $\varepsilon > 0$ small enough,

$$f_m(w, m)(\bar{x} + \varepsilon) = \left(\mu - \frac{r}{K} m(\bar{x})\right) \varepsilon w'(\bar{x}) + o(\varepsilon) < 0,$$

where we have used the fact that $\mu - \frac{r}{K} m(\bar{x}) < 0$ (since $m(\bar{x}) \geq \phi_m(w(\bar{x})) \subset \phi_m([0, 1]) \subset (\mu K/r, \infty)$, see Lemma 2.1.29). In both cases, argument (i) can now be applied to $(w, m)|_{[\bar{x}+\varepsilon, a]}$, leading to a contradiction.

Let consider now the case where $w'(-a) = 0$ or $m'(-a) = 0$. If $w'(-a) = m'(-a) = 0$, then $w \equiv w^*$, $m \equiv m^*$, which is a contradiction. Assume w.l.o.g. that $w'(-a) \neq 0$. If there exists $\varepsilon > 0$ such that for any $x \in [-a, -a + \varepsilon]$, $m'(x) = 0$, then m is constant on the interval $[-a, -a + \varepsilon]$, and then $f_m(w(x), m(x)) = 0$ for $x \in [-a, -a + \varepsilon]$. This implies in turn that $m(x) = \phi_m(w(x))$, and then w is constant on $[-a, -a + \varepsilon]$, since ϕ_m is a decreasing function, which is a contradiction. There exists thus a sequence $x_n \to -a$, $x_n > -a$, such that $w(x_n) \neq w^*$, and $\operatorname{sgn}(m(x_n) - m^*) = \operatorname{sgn}(m'(x_n)) \neq 0$, while $\operatorname{sgn}(w(x_n) - w^*) = \operatorname{sgn}(w'(0)) \neq 0$. The above argument (i-iv) can therefore be reproduced for $(w, m)|_{[x_n, a]}$.

Finally, the fact that $\bar{x} \leq 0$ is a consequence of $w(0) + m(0) < \min(w^*, m^*)$. □

Proposition 2.1.21. *Let r, K, μ satisfy Assumption 2.1.1. Let $(c, w, m) \in \mathbb{R}_+ \times C^0(\mathbb{R})^2$ be a solution of (2.1.3) constructed in Theorem 2.1.2. Then, there exists $\bar{x} \in [-\infty, 0)$ such that*

- *either w is decreasing on $\mathbb{R}$, while m is increasing on $(-\infty, \bar{x}]$ and decreasing on $[\bar{x}, \infty)$,*
- *or m is decreasing on $\mathbb{R}$, while w is increasing on $(-\infty, \bar{x}]$ and decreasing on $[\bar{x}, \infty)$,*

Moreover,

$$w(x) \to w^*, \quad m(x) \to m^* \text{ as } x \to -\infty.$$

Proof of Proposition 2.1.21. The travelling wave (c, w, m) constructed in Theorem 2.1.2 is obtained as a limit (in $L^\infty_{loc}(\mathbb{R})$) of solutions $(w_n, m_n, c_n) \in \mathbb{R}_+ \times C^0([-a_n, a_n])^2$ of (2.1.7) on $[-a_n, a_n]$, with $a_n \underset{n\to\infty}{\longrightarrow} \infty$. Each of those solutions then satisfy one of the two the monotonicity properties of Lemma 2.1.20. In particular, there is at least one of those properties that is satisfied by an infinite sequence of solutions (w_n, m_n, c_n). We may then assume w.l.o.g. that all the solutions (w_n, m_n, c_n) satisfy the first monotonicity property in Lemma 2.1.20. We assume therefore that for all $n \in \mathbb{N}$, there exists $\bar{x}_n \in [-a_n, 0)$ such that w_n is decreasing on $[-a_n, a_n]$, while m_n is increasing on $[-a_n, \bar{x}_n]$ and decreasing on $[\bar{x}_n, a_n]$. Up to an extraction, we can define $\bar{x} := \lim_{n\to\infty} a_n \in [-\infty, 0]$. Then, w is a uniform limit of decreasing function on any bounded interval, and is thus decreasing. Let now $\tilde{x} > \bar{x}$. m_n is then a decreasing function on $[\tilde{x}, \infty) \cap [-a_n, a_n]$ for n large enough, and $m|_{[\tilde{x}, \infty)}$ is thus a uniform limit of decreasing functions on any bouded interval of $[\tilde{x}, \infty)$. This implies that m is decreasing on $[\bar{x}, \infty)$. A similar argument shows that m is increasing on $(-\infty, \bar{x}]$, if $\bar{x} > -\infty$. the case where all the solutions (w_n, m_n, c_n) satisfy the second monotonicity property in Lemma 2.1.20 can be treated similarly.

We have shown in particular that w, m are monotonic on $(-\infty, \tilde{x})$, for some $\tilde{x} < 0$ ($\tilde{x} = \bar{x}$ if $\bar{x} > -\infty$, $\tilde{x} = 0$ otherwise). Since w and m are regular bounded functions, it implies that

$$f_w(w(x), m(x)) = -cw'(x) - w''(x) \to 0,$$

$$f_m(w(x), m(x)) = -cm'(x) - m''(x) \to 0,$$

as $x \to -\infty$. This combined to $\liminf_{x\to-\infty} w(x) + m(x) > 0$ and $(w, m) \in [0, 1] \times [0, K]$ implies that $w(x) \to w^*$ and $m(x) \to m^*$ as $x \to -\infty$. □

2.1.4.2 Case of a small mutation rate

The result of this section shows that if $\mu > 0$ is small, then only the first situation described in Lemma 2.1.20, with $\bar{x} > -\infty$, is possible.

Proposition 2.1.22. *Let r, K, μ satisfy Assumption 2.1.1. Let $(c, w, m) \in \mathbb{R}_+ \times C^0(\mathbb{R})$ be a solution of (2.1.3) constructed in Theorem 2.1.2. There exists $\bar{\mu} = \bar{\mu}(r, K) > 0$ such that $\mu < \bar{\mu}$ implies that w is decreasing on $\mathbb{R}$, while m is increasing on $(-\infty, \bar{x}]$ and decreasing on $[\bar{x}, \infty)$, for some $\bar{x} \in \mathbb{R}_-$.*

Proof of Proposition 2.1.22. Notice that the solution (c, w, m) satisfies the assumptions of Proposition 2.1.21.

Let us assume that $\|m\|_\infty \le m^*$. We will show that this assumption leads to a contradiction if $\mu > 0$ is small. Let $\bar{x} = \max\{x > -\infty;\, w(x) \ge m^*\}$. Then w satisfies $-cw' - w'' \le (1-\mu)w + \mu m^*$ on $(-\infty, \bar{x}]$. Since (c, w, m) satisfies the assumptions of Proposition 2.1.21 and $w(\bar{x}) = m^* < w^*$, we have that $w(x) \ge m^*$ for all $x \le \bar{x}$. w thus satisfies $-cw' - w'' \le w$ on $(-\infty, \bar{x}]$. We define now

$$\bar{w}(x) = m^*\, e^{\frac{c-\sqrt{c^2-4}}{2}(\bar{x}-x)},$$

which satisfies $-c\bar{w}' - \bar{w}'' = \bar{w}$ on $(-\infty, \bar{x}]$, $\bar{w}(\bar{x}) = w(\bar{x})$, and $\bar{w}(y) \ge 1 \ge w(y)$ for $y << 0$. Since w is bounded, $\alpha\bar{w} > w$ for $\alpha > 0$ large enough. We can then define $\alpha^* := \min\{\alpha > 0;\, \alpha\bar{w} > w \text{ on } (-\infty, \bar{x})\}$. If $\alpha^* > 1$, there exists $x^* \in (-\infty, \bar{x})$ such that $\alpha^*\bar{w}(x^*) = w(x^*)$, and then, $-c(\alpha^*\bar{w} - w)'(x^*) - (\alpha^*\bar{w} - w)''(x^*) > \alpha^*\bar{w}(x^*) - w(x^*) = 0$, which is a contradiction, since $\alpha^*\bar{w} > w$ implies that $-c(\alpha^*\bar{w} - w)'(x^*) - (\alpha^*\bar{w} - w)''(x^*) \le 0$. Thus,

$$w(x) \le \bar{w}(x), \text{ for } x \in (-\infty, \bar{x}]. \tag{2.1.25}$$

In particular, if we define

$$\tilde{x} := \bar{x} - \frac{2}{c - \sqrt{c^2-4}} \ln\left(\frac{K}{m^*}\left(\frac{1}{2} - \frac{\mu}{r} - \frac{1}{2r}\right) - 1\right), \tag{2.1.26}$$

then $w(x) \le K\left(\frac{1}{2} - \frac{\mu}{r} - \frac{1}{2r}\right) - m^*$ on $[\tilde{x}, \bar{x}]$. Notice that $m^* \to 0$ as $\mu \to 0$ (see Lemma 2.1.35), and then $\frac{K}{m^*}\left(\frac{1}{2} - \frac{\mu}{r} - \frac{1}{2r}\right) \to \infty$ as $\mu \to 0$; $\tilde{x}$ is then well defined as soon as $\mu > 0$ is small enough, and $\tilde{x} - \bar{x} \to -\infty$ as $\mu \to 0$. This estimate applied to the equation on m (see (2.1.3)), implies, for $x \in [\tilde{x}, \bar{x}]$, that

$$-cm'(x) - m''(x) \ge r\left(1 - \frac{\mu}{r} - \frac{m^* + w(x)}{K}\right) m(x) + \mu\, w \ge \frac{1+r}{2} m + \mu\, m^*, \text{ for } x \in (\tilde{x}, \bar{x}],$$

where we have also used the fact that $w \ge m^*$ on $(-\infty, \bar{x}]$.

We define next

$$\bar{m}_1 := -\frac{\mu\, m^*}{c+2}(x - \bar{x})\,(x - (\bar{x} - 1))\,,$$

which satisfies $-c\bar{m}_1' - \bar{m}_1'' \le \mu m^*$ as well as $\bar{m}_1(\bar{x} - 1) = 0 \le m(\bar{x} - 1)$ and $\bar{m}_1(\bar{x}) = 0 \le m(\bar{x})$. The weak maximum principle ([187], Theorem 8.1) then implies that $m(x) \ge \bar{m}_1(x)$ for all $x \in [\bar{x} - 1, \bar{x}]$, and in particular,

$$m(\bar{x} - 1/2) \ge \frac{\mu\, m^*}{4(c+2)}.$$

We define (we recall the definition (2.1.26) of $\tilde{x}$)

$$\bar{m}_2 := \frac{\mu\, m^*}{4(c+2)} e^{\frac{c-\sqrt{c^2-2(1+r)}}{2}(\bar{x}-1/2-x)} - Ae^{\frac{c}{2}(\bar{x}-1/2-x)},$$

with $A = \frac{\mu\, m^*}{4(c+2)} e^{-\frac{\sqrt{c^2-2(r+1)}}{2}(\bar{x}-1/2-\tilde{x})}$, so that $\bar{m}_2(\tilde{x}) = 0$. $\bar{m}_2$ then satisfies $-c\bar{m}_2' - \bar{m}_2'' < \frac{(1+r)}{2}\bar{m}_2$, since $c(c/2) - (c/2)^2 > \frac{1+r}{2}$ (see (2.1.5)). Let now

$$\alpha^* := \max\{\alpha; m(x) \geq \alpha \bar{m}_2(x),\ \forall x \in [\tilde{x}, \bar{x} - 1/2]\}.$$

$\alpha^* > 0$, since $\min_{[\tilde{x},\bar{x}-1/2]} m > 0$. If $\alpha^* < 1$, then $\alpha^* \bar{m}_2(\bar{x} - 1/2) < \frac{\mu\, m^*}{4(c+2)} \leq m(\bar{x} - 1/2)$, while $\alpha^* \bar{m}_2(\tilde{x}) = 0 < m(\tilde{x})$. Then $\alpha^* \bar{m}_2 \leq m$ on $[\tilde{x}, \bar{x} - 1/2]$, and there exists $x^* \in [\tilde{x}, \bar{x} - 1/2]$ such that $\alpha^* \bar{m}_2(x^*) = m(x^*)$, and

$$0 \leq -c(\bar{m}_2 - m)'(x^*) - (\bar{m}_2 - m)''(x^*) < \frac{(1+r)}{2}(\bar{m}_2 - m)(x^*) = 0,$$

which is a contradiction. We have thus proven that $m \geq \bar{m}_2$ on $[\tilde{x}, \bar{x} - 1/2]$, and in particular, for $\mu > 0$ small enough,

$$\|m\|_\infty \geq \bar{m}_2\left(\tilde{x} + \frac{2\ln(2)}{\sqrt{c^2 - 2(1+r)}}\right) = \frac{\mu\, m^*}{4(c+2)} e^{\frac{c \ln 2}{\sqrt{c^2-2(1+r)}}} e^{\frac{c-\sqrt{c^2-2(1+r)}}{2}(\bar{x}-1/2-\tilde{x})}.$$

We recall indeed that $\tilde{x} - \bar{x} \to -\infty$ as $\mu \to 0$, and then $\tilde{x} + \frac{2\ln(2)}{\sqrt{c^2-2(1+r)}} \in [\tilde{x}, \bar{x} - 1/2]$ if $\mu > 0$ is small enough. Thanks to the definition of $\tilde{x}$, this inequality can be written

$$\begin{aligned}
&\ln\left(\frac{4(c+2)\|m\|_\infty}{\mu\, m^*}\right) - \frac{c \ln 2}{\sqrt{c^2 - 2(1+r)}} \\
&\quad \geq \frac{c - \sqrt{c^2 - 2(1+r)}}{2}\left(-1/2 + \frac{2}{c - \sqrt{c^2-4}} \ln\left(\frac{K}{m^*}\left(\frac{1}{2} - \frac{\mu}{r} - \frac{1}{2r}\right) - 1\right)\right).
\end{aligned}$$

We have assumed that $\|m\|_\infty = m^*$, thus, if we denote by $\mathcal{O}_{\mu\sim 0^+}(1)$ a function of $\mu > 0$ that is bounded for μ small enough, we get

$$\ln\left(\frac{1}{\mu}\right) + \mathcal{O}_{\mu\sim 0^+}(1) \geq \frac{c - \sqrt{c^2 - 2(1+r)}}{c - \sqrt{c^2-4}} \ln\left(\frac{1}{m^*}\right).$$

Moreover, we know that $m^* \leq C\mu$ for some $C > 0$, see Lemma 2.1.35. Then,

$$\ln\left(\frac{1}{\mu}\right) + \mathcal{O}_{\mu\sim 0^+}(1) \geq \frac{c - \sqrt{c^2 - 2(1+r)}}{c - \sqrt{c^2-4}} \ln\left(\frac{1}{\mu}\right),$$

which is a contradiction as soon as $\mu > 0$ is small, since $r > 1$.

We have thus proved that for $\mu > 0$ small enough, we have $\|m\|_\infty > m^*$. This estimate combined to Proposition 2.1.21 proves Proposition 2.1.22. □

2.1.5 Proof of Theorem 2.1.4

Notice first that if we chose $\varepsilon > 0$ small enough, then $0 < \mu < K < \varepsilon$ implies that Assumption 2.1.1 is satisfied.

We will need the following estimate on the behavior of travelling waves of (2.1.3):

Proposition 2.1.23. *Let r, K, μ satisfy Assumption 2.1.1. Let (c, w, m) be a smooth solution of* (2.1.3)*, such that $c \geq 0$ and $\liminf_{x\to-\infty}(w(x) + m(x)) > 0$. Then,*

$$\liminf_{x\to-\infty} w(x) \geq 1 - \mu - K.$$

Moreover, if $w(\bar{x}) < 1 - K - \mu$ for some $\bar{x} \in \mathbb{R}$, then w is decreasing on $[\bar{x}, \infty)$.

Proof of Proposition 2.1.23. Since $m(x) < K$ for all $x \in \mathbb{R}$, any local minimum $\bar{x}$ of w satisfies

$$\begin{aligned}
0 &\geq -cw'(\bar{x}) - w''(\bar{x}) = (1 - \mu - w(\bar{x}) - m(\bar{x}))w(\bar{x}) + \mu m(\bar{x}) \\
&> (1 - \mu - K - w(\bar{x}))w(\bar{x}),
\end{aligned} \tag{2.1.27}$$

and then $w(\bar{x}) \geq 1-\mu-K$.

Assume that $\liminf_{x\to-\infty} w(x) < 1-\mu-K$. Then, $x \mapsto w(x)$ can not have a minimum for $x << 0$, and is thus monotonic for $x << 0$. Then $l := \lim_{x\to-\infty} w(x) \in [0, 1-\mu-K]$ exists and $w'(x) \to_{x\to-\infty} 0$, $w''(x) \to_{x\to-\infty} 0$. This implies $-cw'(x) - w''(x) \to_{x\to\infty} 0$, which, coupled to (2.1.27) implies that $l = 0$ or $l = 1-\mu-K$. $l = 0$ leads to a contradiction, since $\liminf_{x\to-\infty}(w(x)+m(x)) > 0$, which proves the first assertion.

To prove the second assertion, we notice that since w cannot have a minimum $\tilde{x} \in \mathbb{R}$ such that $w(\tilde{x}) < 1-K-\mu$, w is monotonic on $\{x \in \mathbb{R};\ w(x) < 1-K-\mu\}$. This monotony combined to $\liminf_{x\to-\infty} w(x) \geq 1-\mu-K > w(\bar{x})$ implies that w is decreasing on $[\bar{x}, \infty)$. □

The main idea of the proof of theorem 2.1.4 is to compare w to solutions of modified Fisher-KPP equations, which we introduce in the following lemma:

Lemma 2.1.24. *Let r, K, μ satisfy Assumptions 2.1.1. Let $(c, w, m) \in \mathbb{R}_+ \times C^\infty(\mathbb{R}) \times C^\infty(\mathbb{R})$ be a solution of (2.1.3), with $c \geq 2+K$. Let also $\overline{w} \in C^\infty(\mathbb{R})$, $\underline{w} \in C^\infty(\mathbb{R})$ solutions of*

$$\begin{cases} -c\overline{w}' - \overline{w}'' = \overline{w}(1-\overline{w}) + K, \\ \overline{w}(x) \to_{x\to-\infty} \frac{1+\sqrt{1+4K}}{2},\ \overline{w}(x) \to_{x\to+\infty} -\frac{\sqrt{1+4K}-1}{2}, \end{cases} \tag{2.1.28}$$

$$\begin{cases} -c\underline{w}' - \underline{w}'' = \underline{w}(1-2K-\underline{w}), \\ \underline{w}(x) \to_{x\to-\infty} 1-2K,\ \underline{w}(x) \to_{x\to+\infty} 0. \end{cases} \tag{2.1.29}$$

Assume $\underline{w}(0) \leqslant w(0) \leqslant \overline{w}(0)$. Then

$$\forall x \leqslant 0, \qquad \underline{w}(x) \leqslant w(x) \leqslant \overline{w}(x).$$

Remark 2.1.25. Notice that $\overline{w} + \frac{\sqrt{1+4K}-1}{2}$ and $\underline{w}$ are solution of a classical Fisher-KPP equation $-cu' - u'' = u(a-bu)$ with $a \in (0, 1+2K)$, $b > 0$, and a speed $c \geq 2\sqrt{a}$. The existence, uniqueness (up to a translation) and monotony of $\overline{w}$ and $\underline{w}$ are thus classical results (see e.g. [238]). Thanks to those relations, the argument developed in this section can indeed be seen as a precise analysis on the profile of $x \mapsto u(x)$ for $x > 0$ large.

Proof of Lemma 2.1.24. To prove this lemma, we use a sliding method.

- Let $\underline{w}_\eta(x) := \underline{w}(x+\eta)$. Thanks to Proposition 2.1.23, there exists $x_0 \in \mathbb{R}$ such that $w(x) > 1-2K = \sup_{\mathbb{R}} \underline{w}_\eta$ for all $x \leq x_0$ (we recall that $\mu < K$). Since $\lim_{x\to\infty} \underline{w}(x) = 0$, there exists $x^0 > 0$ such that $\underline{w}(x) < \min_{[x_0,0]} w$ for all $x > x^0$. Then, for $\eta \geq x_0 + x^0$,

  $$\underline{w}_\eta(x) < w(x), \quad \forall x \leqslant 0.$$

  We can then define $\overline{\eta} := \inf\{\eta, \forall x \leqslant 0, \underline{w}_\eta(x) \leqslant w(x)\}$. We have then $\underline{w}_{\overline{\eta}}(x) \leqslant w(x)$ for all $x \leq 0$. If $\overline{\eta} > 0$, since $\inf_{(-\infty,x_0]} w > 1-2K = \sup_{\mathbb{R}} \underline{w}_\eta$ and $\underline{w}_{\overline{\eta}}(0) = \overline{w}(\eta) < \overline{w}(0) \leq w(0)$ (we recall that $\underline{w}$ is decreasing, see Remark 2.1.25), there exists $\underline{x} \in (x_0, 0)$ such that $\underline{w}_{\overline{\eta}}(\underline{x}) = w(\underline{x})$. $\underline{x}$ is then a minimum of $w - \underline{w}_{\overline{\eta}}$, and thus

  $$\begin{aligned} 0 &\geq -c(w-\underline{w}_{\overline{\eta}})'(\underline{x}) - (w-\underline{w}_{\overline{\eta}})''(\underline{x}) \\ &= w(\underline{x})(1-\mu-m(\underline{x})-w(\underline{x})) + \mu m(\underline{x}) - \underline{w}_{\overline{\eta}}(\underline{x})(1-2K-\underline{w}_{\overline{\eta}}(\underline{x})) \\ &> w(\underline{x})(1-2K-w(\underline{x})) - \underline{w}_{\overline{\eta}}(\underline{x})(1-2K-\underline{w}_{\overline{\eta}}(\underline{x})) = 0, \end{aligned} \tag{2.1.30}$$

  where we have used the estimate $\|m\|_\infty \leq K$ obtained in Proposition 2.1.7. (2.1.30) is a contradiction, we have then shown that $\overline{\eta} \leq 0$, and thus, for all $x \leq 0$, $\underline{w}(x) \leq w(x)$.

- Similarly, let $\overline{w}_\eta(x) := \overline{w}(x-\eta)$. Since $\lim_{x\to-\infty} \overline{w}(x) > 1$ and w satisfies the estimate of Proposition 2.1.7, we have, for $\eta \in \mathbb{R}$ large enough,

  $$\forall x \leqslant 0, \quad w(x) < 1 < \overline{w}_\eta(x).$$

We can then define $\overline{\eta} := \inf\{\eta, \forall x \leqslant 0, w(x) \leqslant \overline{w}_\eta(x)\}$. We have then $w(x) \leqslant \overline{w}_{\overline{\eta}}$ for all $x \leq 0$. If $\overline{\eta} > 0$, since $\sup_{\mathbb{R}} w < 1 < \lim_{x\to-\infty} \overline{w}(x)$ and $w(0) \leq \overline{w}(0) < \overline{w}(-\overline{\eta}) = \overline{w}_{\overline{\eta}}(0)$ (we recall that $\overline{w}$ is decreasing, see Remark 2.1.25), there exists $\bar{x} < 0$ such that $w(\underline{x}) = \overline{w}_{\overline{\eta}}(\underline{x})$. $\bar{x}$ is then a minimum of $\overline{w}_{\overline{\eta}} - w$, and thus

$$\begin{aligned} 0 &\geq -c(\overline{w}_{\overline{\eta}} - w)'(\bar{x}) - (\overline{w}_{\overline{\eta}} - w)''(\bar{x}) \\ &= \overline{w}_{\overline{\eta}}(\bar{x})(1 - \overline{w}_{\overline{\eta}}(\bar{x})) + K - w(\bar{x})(1 - \mu - w(\bar{x}) - m(\bar{x})) - \mu m(\bar{x}) \\ &> \overline{w}_{\overline{\eta}}(\bar{x})(1 - \overline{w}_{\overline{\eta}}(\bar{x})) - w(\bar{x})(1 - w(\bar{x})) = 0, \end{aligned}$$

which is a contradiction. We have then shown that $\bar{\eta} \leq 0$, and thus, for all $x \leq 0$, $w(x) \leq \overline{w}(x)$.

□

We also need to compare the solution of the Fisher-KPP equation with speed c to the solutions of the modified Fisher-KPP equations introduced in Lemma 2.1.24.

Lemma 2.1.26. *Let r, K, μ satisfy Assumption 2.1.1, and $c \geq 2 + K$. Let (c, u), with $u \in C^\infty(\mathbb{R})$, be a travelling wave of the Fisher-KPP equation, see* (2.1.6)*. Let also $\overline{w}$, $\underline{w}$ solutions of* (2.1.28) *and* (2.1.29) *respectively. Assume $\underline{w}(0) \leqslant u(0) \leqslant \overline{w}(0)$. Then*

$$\forall x \leqslant 0, \qquad \underline{w}(x) \leqslant u(x) \leqslant \overline{w}(x).$$

classical

The arguments of the proof of Lemma 2.1.24 can be used to prove Lemma 2.1.26. We omit the details.

We can now prove theorem 2.1.4.

Proof of Theorem 2.1.4. Notice first that $c_* > 2 + K$, provided $K, \mu > 0$ are small enough. Let $\overline{w} \in C^\infty(\mathbb{R})$ and $\underline{w} \in C^\infty(\mathbb{R})$ satisfying (2.1.28) and (2.1.29) respectively. $\overline{w}$ and $\underline{w}$ are then decreasing (see Remark 2.1.25), and we may assume (up to a translation) that they satisfy $\underline{w}(0) = w(0) = u(0) = \overline{w}(0)$. Then Lemma 2.1.24 and 2.1.26 imply that $\underline{w}(x) \leqslant w(x), u(x) \leqslant \overline{w}(x)$ for $x \leq 0$, and then, $\|w - u\|_{L^\infty(-\infty,0]} \leqslant \|\overline{w} - \underline{w}\|_{L^\infty(-\infty,0]}$.

Let $\tilde{w} = \overline{w} - \underline{w} \geqslant 0$, which satisfies

$$-c\tilde{w}' - \tilde{w}'' = \tilde{w}(1 - (\overline{w} + \underline{w})) + K + 2K\underline{w}.$$

We estimate first the maximum of $\tilde{w}$ over $\{x \in \mathbb{R};\ \underline{w}(x) \leqslant 3/4 - K\}$ to prove the estimate on $\|\tilde{w}\|_{L^\infty(-\infty,0]}$ stated in Theorem 2.1.4. If $\underline{w} \leqslant 3/4 - K$, then

$$-c\underline{w}' - \underline{w}'' \geqslant \underline{w}(1/4 - K). \tag{2.1.31}$$

Let

$$\lambda_+ := \frac{c + \sqrt{c^2 - 4(1/4 - K)}}{2}, \qquad \lambda_- := \frac{c - \sqrt{c^2 - 4(1/4 - K)}}{2},$$

and $\varphi(x) := e^{-\lambda_- x} - e^{-\lambda_+ x}$. Then φ satisfies $-c\varphi' - \varphi'' = (1/4 - K)\varphi$, $\varphi(-\infty) = -\infty$ and $\varphi(+\infty) = 0$. Moreover, φ is positive when $x > 0$ and negative when $x < 0$. Finally, the maximum of φ is attained at $\overline{x} := \frac{\ln \lambda_+ - \ln \lambda_-}{\lambda_+ - \lambda_-} > 0$. One can show that $\varphi(\bar{x})$ is a continuous and positive function of c and K, which is uniformly bounded away from 0 for $K \in (0, 1/8)$ and $c \in [2, \infty)$. There exists thus a universal constant $C > 0$ such that $\varphi(\bar{x}) > C > 0$, for any $K \in (0, 1/8)$, $c \in [2, \infty)$. Let $\gamma \in (0, 3/4 - K)$ and φ^γ defined by

$$\varphi^\gamma(x) := \gamma \frac{\varphi(x)}{\varphi(\bar{x})},$$

and $\varphi^\gamma_\eta(x) := \varphi^\gamma(x + \eta)$ for $\eta \in \mathbb{R}$. Since (for $K > 0$ small) $\max_{\mathbb{R}} \varphi^\gamma \leq 3/4 - K < 1 - 2K = \lim_{x\to-\infty} \underline{w}(x)$ and $\lim_{\eta\to\infty} \varphi^\gamma_\eta(0) = \lim_{x\to\infty} \varphi^\gamma(x) = 0 < \underline{w}(0)$, we have that for $\eta > 0$ large enough,

$$\forall x \leqslant 0, \quad \varphi^\gamma_\eta(x) \leqslant \underline{w}(x).$$

Let $\tilde\eta := \inf\{\eta \in \mathbb{R};\ \forall x \leqslant 0,\ \varphi^\gamma_\eta(x) \leqslant \underline{w}(x)\}$. Then $\varphi^\gamma_{\tilde\eta} \leq \underline{w}$ on $(-\infty, 0]$, and since $\varphi^\gamma_{\tilde\eta}(x) < 0$ for $x << 0$, either $\underline{w}(0) = \varphi^\gamma_{\tilde\eta}(0)$, or there exists $\tilde x \in (-\infty, 0)$ such that $\underline{w}(\tilde x) = \varphi^\gamma_{\tilde\eta}(\tilde x)$. In the latter case, $\tilde x$ is the minimum of $\underline{w} - \varphi^\gamma_{\tilde\eta}$, and then

$$\begin{aligned} 0 &\geq -c(\underline{w} - \varphi^\gamma_{\tilde\eta})'(\tilde x) - (\underline{w} - \varphi^\gamma_{\tilde\eta})''(\tilde x) \\ &= (1 - 2K - \underline{w}(\tilde x))\underline{w}(\tilde x) - (1/4 - K)\varphi^\gamma_{\tilde\eta}(\tilde x) \\ &\geq (3/4 - K - \underline{w}(\tilde x))\,\underline{w}(\tilde x) > 0, \end{aligned}$$

since $\underline{w}(\tilde x) = \varphi^\gamma_{\tilde\eta}(\tilde x) \leq \gamma < 3/4 - K$. The above estimate is a contradiction, which implies $\underline{w}(0) = \varphi^\gamma_{\tilde\eta}(0)$. Then

$$(e^{-\lambda_-\tilde\eta} - e^{-\lambda_+\tilde\eta}) = \frac{w(0)}{\gamma}\left(e^{-\lambda_-\overline{x}} - e^{-\lambda_+\overline{x}}\right),$$

and then

$$-\lambda_-\tilde\eta \geq \ln\left(\frac{w(0)}{\gamma}\left(e^{-\lambda_-\overline{x}} - e^{-\lambda_+\overline{x}}\right)\right),$$

which implies $\varphi^\gamma_\eta(x) \leq \underline{w}(x)$ for all $x \in (-\infty, 0]$, where the constants γ and η satisfy $\gamma \in (0, 3/4 - K)$ and $\eta = -\frac{1}{\lambda_-}\ln\left(\frac{w(0)}{\gamma}(e^{-\lambda_-\overline{x}} - e^{-\lambda_+\overline{x}})\right)$. Passing to the limit $\gamma \to 3/4 - K$, we then get that $\varphi^{3/4-K}_\eta(x) \leq \underline{w}(x)$ for all $x \in (-\infty, 0]$, with

$$\bar\eta := -\frac{1}{\lambda_-}\ln\left(\frac{w(0)}{3/4 - K}\left(e^{-\lambda_-\overline{x}} - e^{-\lambda_+\overline{x}}\right)\right).$$

In particular, $\varphi^{3/4-K}_{\bar\eta} \leq \underline{w}$ implies that $\{x \in (-\infty, 0];\ \underline{w}(x) \leqslant 3/4 - K\} \subset [\min(0, \overline{x} - \bar\eta), 0] \subset [\min(0, -\bar\eta), 0]$ (indeed, $-\bar\eta < 0$ if $w(0)$ is small enough).

Since $\sup_{\mathbb{R}} \underline{w} = 1 - 2K$, we have

$$-c\tilde w' - \tilde w'' = \tilde w(1 - (\underline{w} + \overline{w})) + K + 2K\underline{w} < \tilde w + K(3 - 4K),$$

and $\tilde w(0) = 0$. We can then introduce $\psi(x) = K(3 - 4K)\,(e^{-\alpha x} - 1)$, with $\alpha = \frac{c - \sqrt{c^2 - 4}}{2}$ which satisfies $-c\psi' - \psi'' = \psi + K(3 - 4K)$. A sliding argument (that we skip here) shows that

$$\forall x \leq 0, \quad \tilde w(x) \leqslant \psi(x) = K(3 - 4K)\left(e^{-\alpha x} - 1\right).$$

This estimate implies that

$$\max_{[-\bar\eta, 0]} \tilde w \leqslant K(3 - 4K)\exp\left(-\frac{\alpha}{\lambda_-}\ln\left(\frac{w(0)}{3/4 - K}\left(e^{-\lambda_-\overline{x}} - e^{-\lambda_+\overline{x}}\right)\right)\right) \leqslant C\,K w(0)^{-\frac{\alpha}{\lambda_-}},$$

where $C > 0$ is a universal constant.

We consider now the case where the maximum of $\tilde w$ is reached on $[-\infty, 0) \setminus \{x \in \mathbb{R};\ \underline{w}(x) \leqslant 3/4 - K\}$. If this supremum is a maximum attained in $\bar x$, then $\overline{w}(\bar x) + \underline{w}(\bar x) \geq \frac{3}{2} - 2K > 1$ (this last inequality holds if K is small enough), and $-c\tilde w'(\bar x) - \tilde w''(\bar x) \geqslant 0$, which implies

$$(\overline{w} + \underline{w} - 1)\tilde w(\overline{x}) \leqslant K + 2K\underline{w} \leqslant K(3 - 4K),$$

that is $\tilde w(\overline{x}) \leqslant \frac{K(3-4K)}{1/2-2K} \leq CK$ for some constant $C > 0$, provided $K > 0$ is small enough. If the supremum is not a maximum, it is possible to obtain a similar estimate, we skip here the additional technical details.

We have shown that

$$\sup_{[-\infty, 0]} \tilde w \leq \max\left(CK, CKw(0)^{-\frac{\alpha}{\lambda_-}}\right),$$

We choose now $\beta = (1 + \alpha/\lambda_-)^{-1} \in (0, 1/2)$ and $w(0) = K^\beta$ (we recall that the solution (c, w, m) is still a solution when w and m are translated). Then, $\sup_{[-\infty,0]} \tilde w \leqslant CK^\beta$, and thus

$$\|w - u\|_{L^\infty((-\infty,0])} \leqslant \|\tilde w\|_{L^\infty((-\infty,0])} \leqslant CK^\beta.$$

Furthermore, w and u are decreasing for $x \geqslant 0$ thanks to Proposition 2.1.23, which implies that

$$\forall x \geqslant 0, |w - u|(x) \leqslant w(x) + u(x) \leqslant w(0) + u(0) \leqslant 2K^\beta.$$

From [187], theorem 8.33, there exists a universal constant that we denote $C > 0$ such that

$$\|v\|_{C^{1,\alpha}} \leqslant C, \tag{2.1.32}$$

where v is a solution of (2.1.6), and this constant C is uniform in the speed c in the neighbourhood of $c_0 = 2\sqrt{r}$. In particular, u satisfies

$$-c_0 u' - u'' = (c_* - c_0)u' + u(1-u) = u(1-u) + \mathcal{O}(K). \tag{2.1.33}$$

Let v the solution of (2.1.6) with speed c_0 and $v(0) = u(0)$, the above argument can then be reproduced to show that

$$\|u - v\|_{L^\infty} \leq CK^\beta, \tag{2.1.34}$$

where C is a universal constant and β depend only on r, which finishes the proof. □

2.1.6 Appendix

2.1.6.1 Compactness results

We provide here two results that are used in the proof of Theorem 2.1.2.

Lemma 2.1.27 (Elliptic estimates)**.** *Let a, b^-, $b^+ \in \mathbb{R}_+^*$, $g \in L^\infty(-a,a)$, and $\gamma > 0$. For any $b^+, b^- \in \mathbb{R}$ and $c \in [-\gamma, \gamma]$, the Dirichlet problem*

$$\begin{cases} -cw' - w'' = g, \quad (-a,a), \\ w(-a) = b^-,\ w(a) = b^+, \end{cases}$$

has a unique weak solution w. In addition we have $w \in C^{1,\alpha}([-a,a])$ for all $\alpha \in [0,1)$, and there is a constant $C > 0$ depending only on a and γ such that

$$\|w\|_{C^{1,\alpha}([-a,a])} \leqslant C(\max(|b^+|, |b^-|) + \|g\|_{L^\infty}),$$

Proof of Lemma 2.1.27. As the domain lies in $\mathbb{R}$, we are not concerned with the regularity problem near the boundary. Since

$$L^\infty(-a,a) \subset \bigcap_{p>1} L^p(-a,a),$$

theorem 9.16 [187] gives us existence and uniqueness of a solution $w \in W^{2,p}$, for all $p > 1$. We deduce from Sobolev imbedding that $w \in C^{1,\alpha}([-a,a])$ for all $\alpha < 1$.

The classical theory ([187], theorem 3.7) gives us a constant $C' > 0$ depending only on a and γ such that

$$\|w\|_{L^\infty} \leqslant \max(b^+, b^-) + C'\|g\|_{L^\infty}.$$

The estimate on the Hölder norm of the first derivative comes now from [187], theorem 8.33, which states that whenever w is a $C^{1,\alpha}$ solution of $-cw' - w'' = g$ with $g \in L^\infty$, then

$$\|w\|_{C^{1,\alpha}([-a,a])} \leqslant C''(\|w\|_{C^0([-a,a])} + \|g\|_{L^\infty}),$$

with a constant $C'' = C''(a,\gamma)$ depending only on a and γ. That proves the theorem. □

Lemma 2.1.28. *Let a, b^-, $b^+ \in \mathbb{R}_+^*$. The operator $(L)_D^{-1} : \mathbb{R} \times C^0([-a,a]) \longrightarrow C^0([-a,a])$ defined by*

$$L_D^{-1}(c,g) = w,$$

where w is the unique solution of

$$\begin{cases} -cw' - w'' = g, \quad (-a,a), \\ w(-a) = b^+, w(a) = b^-, \end{cases}$$

is continuous and compact.

Proof of Lemma 2.1.28. Let $(c,g),(\tilde{c},\tilde{g}) \in \mathbb{R}\times C^0([-a,a])$, $\gamma>0$ and $w,\tilde{w}\in C^0([-a,a])$ such that $c,\tilde{c}\leqslant\gamma$ and

$$\begin{cases} -cw' - w'' = g \text{ on } (-a,a), \\ w(-a)=b^+, w(a)=b^-, \end{cases}$$

$$\begin{cases} -\tilde{c}\tilde{w}' - \tilde{w}'' = \tilde{g} \text{ on } (-a,a), \\ \tilde{w}(-a)=b^+, \tilde{w}(a)=b^-. \end{cases}$$

Then $w-\tilde{w}$ satisfies

$$\begin{cases} -c(w-\tilde{w})' - (w-\tilde{w})'' = g-\tilde{g}+(c-\tilde{c})\tilde{w}' \text{ on } (-a,a), \\ (w-\tilde{w})(-a)=0, (w-\tilde{w})(a)=0. \end{cases}$$

We deduce from Lemma 2.1.27 that there exists a constant C depending only on $a>0$ such that

$$\|w-\tilde{w}\|_{C^0} \leqslant C(\|g-\tilde{g}\|_{C^0} + |c-\tilde{c}|(\|\tilde{g}\|_{C^0} + \max(b^+,b^-))),$$

which shows the pointwise continuity of L_D^{-1}.

Now let (c_n,g_n) a bounded sequence in $\mathbb{R}\times C^0$. Let $\gamma = \limsup |c_n|$. From Lemma 2.1.27 we deduce the existence of a constant $C>0$ depending only on a and γ such that

$$\|u_n\|_{C^1} \leqslant C(\max(b^+,b^-) + \|g_n\|_{C^0}),$$

where $u_n = L_D^{-1}(c_n,g_n)$, which shows that (g_n) is bounded in C^1. Since C^1 is compactly embedded in C^0, there exists a $w\in C^0$ such that $\|u_n-w\|_{C^0}\to 0$. This shows the compactness of L_D^{-1}. □

2.1.6.2 Properties of the reaction terms

The proofs of Theorem 2.1.3 requires precise estimates on the reaction terms f_w and f_m. Here we prove a number of technical lemmas that are necessary for our study.

Lemma 2.1.29. *Let r, K, μ satisfy Assumption 2.1.1, and ϕ_w, ϕ_m defined by* (2.1.22) *and* (2.1.23) *respectively. Then, ϕ_w, $\phi_m : \mathbb{R}_+ \to \mathbb{R}$ are decreasing functions such that*

$$\phi_w([0,K]) \subset (\mu,\infty), \quad \phi_m([0,1]) \subset (\mu K/r,\infty).$$

Proof of Lemma 2.1.29. We prove the lemma for ϕ_m. The results on ϕ_w follow since both functions coincide when $r=K=1$. The fact that ϕ_m is decreasing simply comes from the computation of its derivative:

$$\phi_m'(w) = \frac{1}{2}\left[-1 + \frac{-2\left(K-\frac{\mu K}{r}-w\right)+4\frac{\mu K}{r}}{2\sqrt{\left(K-\frac{\mu K}{r}-w\right)^2+4\frac{\mu K}{r}w}}\right],$$

one can check that $\phi_m'(w)<0$ for all $w\geq 0$ as soon as $\mu<\frac{r}{2}$. Next, we can estimate $\phi_m(w)$ for $w>0$ large:

$$\begin{aligned} \phi_m(w) &= \frac{w+\frac{\mu K}{r}-K}{2}\left(-1+\sqrt{1+\frac{4\mu K w}{r\left(w+\frac{\mu K}{r}-K\right)^2}}\right) \\ &= \frac{w+\frac{\mu K}{r}-K}{2}\left(\frac{2\mu K w}{r\left(w+\frac{\mu K}{r}-K\right)^2}+o(1/w)\right) \\ &= \frac{\mu K}{r}+o(1), \end{aligned}$$

that is $\lim_{w\to\infty}\phi_m(w)=\frac{\mu K}{r}$, which, combined to the variation of ϕ_w, shows that $\phi_m([0,1])\subset(\mu K/r,\infty)$. □

Lemma 2.1.30. *Let r, K, μ satisfy Assumption 2.1.1, ϕ_w, ϕ_m defined by* (2.1.22) *and* (2.1.23) *respectively.*

$$Z_w = \{(w,m) \in (0,1) \times (0,K) / f_w(w,m) = 0\},$$

$$Z_m = \{(w,m) \in (0,1) \times (0,K) / f_m(w,m) = 0\},$$

and denote

$$\mathcal{D} = (0,1) \times (0,K). \tag{2.1.35}$$

Then:

1. *Z_w can be described in two ways:*

$$Z_w = \{(\phi_w(m), m), m \in (0,K)\}, \tag{2.1.36}$$

and

$$Z_w = \{(w, \varphi_w(w)), w \in (\mu,1)\} \cap \mathcal{D}, \tag{2.1.37}$$

where $\varphi_w(w) = \frac{w(1-\mu-w)}{w-\mu}$.

2. *Similarly, Z_m can be described as:*

$$Z_m = \{(w, \phi_m(w)), w \in (0,1)\}, \tag{2.1.38}$$

and

$$Z_m = \left\{(\varphi_m(m), m), m \in \left(\frac{\mu K}{r}, K\right)\right\} \cap \mathcal{D}, \tag{2.1.39}$$

where $\varphi_m(m) := \frac{m(K-\frac{\mu K}{r}-m)}{m-\frac{\mu K}{r}}$.

Proof of Lemma 2.1.30. Notice that point 1 can be obtained from point 2 by setting $r = K = 1$. Thus, we are only going to prove point 2. We write

$$f_m(w,m) = rm\left(1 - \frac{w+m}{K}\right) + \mu(w-m) = -\frac{r}{K}m^2 + \left(r - \mu - \frac{r}{K}w\right)m + \mu w.$$

Since $\Delta = \left(r - \mu - \frac{r}{K}w\right)^2 + 4\frac{\mu r}{K}w > 0$ for any $w \geq 0$, $f_m(w,m) = 0$ admits only two solutions for $w \geq 0$ fixed. Those write:

$$\frac{1}{2}\left((K - \frac{\mu K}{r} - w) \pm \sqrt{(K - \frac{\mu K}{r} - w)^2 + 4\frac{\mu K}{r}w}\right),$$

one of those two solutions is negative for all $w \neq 0$, so that $f_m(w,m) = 0$ with $(w,m) \in \mathcal{D}$ implies that $m = \phi_m(w)$, which leads to (2.1.38).

Thanks to Lemma 2.1.29, $m > \mu K/r$ on Z_m, $f(w,m) = 0$ with $(w,m) \in \mathcal{D}$ then implies $w = \varphi_m(m)$. For $m \in \left(0, \frac{\mu K}{r}\right)$, $\varphi_m(m)$ is decreasing and

$$\begin{cases} \varphi_m(0) = 0, \\ \lim\limits_{m \to (\frac{\mu K}{r})^-} \varphi_m(m) = -\infty, \end{cases}$$

so that $\varphi_m(m) < 0$ for $m \in \left(0, \frac{\mu K}{r}\right)$. That proves (2.1.39). □

The next lemma proves that f admits only one zero in $\mathcal{D}$, and proves some inclusions between $f_m > 0$ and $f_w > 0$.

Lemma 2.1.31. *Let r, K, μ satisfy Assumption 2.1.1, ϕ_w, ϕ_m, φ_w, φ_m defined by* (2.1.22), (2.1.23), (2.1.37) *and* (2.1.39) *respectively. Then ϕ_w and φ_m are convex, strictly decreasing functions over $(0,K)$ and $\left(\frac{\mu K}{r}, K\right)$ respectively.*

Proof of Lemma 2.1.31. We have already shown that ϕ_w is decreasing on $(0, K)$. We compute:

$$\phi'_w(m) = -\frac{1}{2}\left(1 + \frac{1-3\mu-m}{\sqrt{(1-\mu-m)^2+4\mu m}}\right).$$

Computing the second derivative, we find:

$$\begin{aligned}\phi''_w(m) &= \frac{(1-\mu-m)^2+4\mu m-(1-3\mu-m)^2}{2\left((1-\mu-m)^2+4\mu m\right)^{\frac{3}{2}}}\\ &= \frac{2\mu(1-2\mu)}{\left((1-\mu-m)^2+4\mu m\right)^{\frac{3}{2}}} > 0,\end{aligned}$$

so that ϕ_w is convex over $\mathbb{R}_+$. Thanks to polynomial arithmetics, we compute:

$$\varphi_m(m) = \frac{m\left(K\left(1-\frac{\mu}{r}\right)-m\right)}{m-\frac{\mu K}{r}} = K\left(1-\frac{2\mu}{r}\right) - m + \frac{\frac{\mu K^2}{r}\left(1-\frac{2\mu}{r}\right)}{m-\frac{\mu K}{r}},$$

which makes φ_m obviously convex and strictly decreasing on $\left(\frac{\mu K}{r}, K\right)$. □

Lemma 2.1.32. *There exists a unique solution to the problem:*

$$f_w(w,m) = f_m(w,m) = 0, \tag{2.1.40}$$

with $(w,m) \in (0,1)\times(0,K)$.

Proof of Lemma 2.1.32. We write:

$$f_w = w(1-\mu-w) + m(\mu-w).$$

Since $\mu < \frac{1}{2}$, we have

$$f_w(\mu, m) = \mu(1-2\mu) > 0,$$

so that there cannot be a solution of $f_w(w,m) = 0$ with $w = \mu$. Thus, $f_w(w,m) = 0$ if and only if

$$m = \frac{w(1-\mu-w)}{w-\mu}. \tag{2.1.41}$$

Substituting (2.1.41) in $f_m(w,m) = 0$, we get:

$$(2.1.40) \Rightarrow \underbrace{r\frac{w(1-\mu-w)}{w-\mu}\left(1-\frac{\frac{w(1-\mu-w)}{w-\mu}+w}{K}\right)}_{A} + \underbrace{\mu\left(w-\frac{w(1-\mu-w)}{w-\mu}\right)}_{B} = 0.$$

We compute:

$$A = \frac{rw(1-\mu-w)}{K(w-\mu)^2}\left(w(K+2\mu-1)-\mu K\right),$$

$$B = \mu\frac{w(2w-1)}{w-\mu}.$$

From now on we assume $w \neq 0$. Then:

$$(2.1.40) \Rightarrow C(w) := \frac{r}{K}(1-\mu-w)(w(K+2\mu-1)-\mu K) + \mu(2w-1)(w-\mu) = 0.$$

Now C is a polynomial function of degree at most 2. We compute:

$$C(0) = \mu(1-r(1-\mu)) < 0,$$

$$C(1) = \mu\left(1-\mu+\frac{r}{K}((1-\mu)(1-K)-\mu)\right) > 0,$$

under the following assumptions:

$$\mu < 1 - \frac{1}{r},$$

$$K < \frac{r}{r-1}\left(1 - \frac{\mu}{1-\mu}\right).$$

That proves the uniqueness of a solution of (2.1.40) with $w \in (0,1)$.

Now recall the notations of lemmas 2.1.30 and 2.1.31. The existence of a solution to problem (2.1.40) is equivalent to showing $Z_m \cap Z_w \neq \varnothing$. Since:

$$\Phi_w\left(\frac{\mu K}{r}\right) \in \mathbb{R},$$

$$\lim_{m \to \left(\frac{\mu K}{r}\right)^+} \varphi_m(m) = +\infty,$$

$$\Phi_w(K) = \frac{1}{2}\left(1 - \mu - K + \sqrt{(1-\mu-K)^2 + 4\mu K}\right) > 0,$$

$$\varphi_m(K) = -\frac{\mu}{r-\mu} < 0,$$

and since Φ_w and φ_m are continuous over $\left(\frac{\mu K}{r}, K\right)$, there exists a solution to $\varphi_m(m) = \Phi_w(m)$ with $m \in \left(\frac{\mu K}{r}, K\right)$.

Since $\forall m \in (0,K), 0 < \Phi_w(m) < 1$, that gives us a solution to (2.1.40), and proves Lemma 2.1.32. □

Lemma 2.1.33. *Let* $\mathcal{D} = (0,1) \times (0,K)$,

$$Z_w = \{f_w = 0\} \cap \mathcal{D} = \{w = \phi_w(m)\} \cap \mathcal{D}, \quad Z_w^- = \{f_w < 0\} \cap \mathcal{D} = \{w > \phi_w(m)\} \cap \mathcal{D},$$

$$Z_m = \{f_m = 0\} \cap \mathcal{D} = \{m = \phi_m(w) = 0\} \cap \mathcal{D}, \quad Z_m^- = \{f_m < 0\} \cap \mathcal{D} = \{m > \phi_m(w) < 0\} \cap \mathcal{D},$$

and

$$\mathcal{D}_l = \{(w,m) \in \mathcal{D}, w \leq w^*, m \geq m^*\},$$

$$\mathcal{D}_r = \{(w,m) \in \mathcal{D}, w \geq w^*, m \leq m^*\},$$

where (w^*, m^*) *is the only solution of* $f_m = f_w = 0$ *in* $\mathcal{D}$. *Then*

$$Z_m \cup Z_w \subset \mathcal{D}_l \cup \mathcal{D}_r. \tag{2.1.42}$$

Moreover,

$$Z_w^- \cap \mathcal{D}_l \subset Z_m^-, \tag{2.1.43}$$

$$Z_m^- \cap \mathcal{D}_r \subset Z_w^-. \tag{2.1.44}$$

Remark 2.1.34. Let

$$Z_w^+ = \{f_w > 0\} \cap \mathcal{D} = \{w < \phi_w(m)\} \cap \mathcal{D}, \quad Z_m^+ = \{f_m > 0\} \cap \mathcal{D} = \{m < \phi_m(w)\} \cap \mathcal{D}.$$

Lemma 2.1.33 implies that

$$Z_m^+ \cap \mathcal{D}_l \subset Z_w^+, \quad Z_w^+ \cap \mathcal{D}_r \subset Z_m^+.$$

Proof of Lemma 2.1.33. Assertion (2.1.42) comes from the fact that Φ_w and φ_m are decreasing.

Assertion (2.1.43) comes from the fact that $\Phi_w - \varphi_m$ is negative for m close to $\left(\frac{\mu K}{r}\right)^+$ and does not change sign in $\left(\frac{\mu K}{r}, m^*\right)$ since (w^*, m^*) is the only solution of (2.1.40). A similar argument proves assertion (2.1.44) □

The last thing we need here is an estimate of the behaviour of $m^*(\mu, r, K)$ when $\mu \to 0$:

Lemma 2.1.35. *For* $\mu < 1 - K$, *we have*

$$m^*(\mu, r, K) \leq \frac{\frac{\mu K}{r}(1-\mu)}{1 - \mu - K\left(1 - \frac{2\mu}{r}\right)}. \tag{2.1.45}$$

Proof of Lemma 2.1.35. Recall the notations of Lemma 2.1.31. From Lemma 2.1.32 we know that m^* is the only solution of $\Phi_w = \varphi_m$ that lies in $(0, K)$. Since $m \mapsto \sqrt{m}$ is increasing and $1 - \mu - K > 0$, we have:

$$\Phi_w(m) \geq 1 - \mu - m. \tag{2.1.46}$$

We deduce then:

$$\varphi_m(m) - \Phi_w(m) \leq \varphi_m(m) - (1 - \mu - m).$$

Now $\varphi_m - \Phi_w$ is positive near $\left(\frac{\mu K}{r}\right)^+$, and for $w \in \left(\frac{\mu K}{r}, m^*\right)$,

$$0 < \varphi_m(w) - \Phi_w(w) \leq \varphi_m(w) - (1 - \mu - m),$$

which means that if $\bar{m}$ satisfies

$$\varphi_m(\bar{m}) = 1 - \mu - \bar{m}. \tag{2.1.47}$$

then $\bar{m} \geq m^*$. A simple computation shows that the only solution of (2.1.47) is:

$$\bar{m} = \frac{\frac{\mu K}{r}(1 - \mu)}{1 - \mu - K\left(1 - \frac{2\mu}{r}\right)},$$

which finishes to prove Lemma 2.1.35 □

2.2 Pulsating fronts for Fisher-KPP systems with mutations as models in evolutionary epidemiology

2.2.1 Introduction

This work is concerned with the heterogeneous reaction diffusion system

$$\begin{cases} \partial_t u = \partial_{xx} u + u\left[r_u(x) - \gamma_u(x)(u+v)\right] + \mu(x)v - \mu(x)u, & t>0,\ x\in\mathbb{R}, \\ \partial_t v = \partial_{xx} v + v\left[r_v(x) - \gamma_v(x)(u+v)\right] + \mu(x)u - \mu(x)v, & t>0,\ x\in\mathbb{R}, \end{cases} \tag{2.2.1}$$

where r_u, r_v are periodic functions and γ_u, γ_v, μ are periodic positive functions. After discussing the existence of nontrivial steady states via bifurcation technics, we construct pulsating fronts, despite the lack of comparison principle for (2.2.1). Before going into mathematical details, let us describe the relevance of the the above system in evolutionary epidemiology.

System (2.2.1) describes a theoretical population divided into two genotypes with respective densities $u(t,x)$ and $v(t,x)$, and living in a one-dimensional habitat $x\in\mathbb{R}$. We assume that each genotype yields a different phenotype which also undergoes the influence of the environment. The difference in phenotype is expressed in terms of growth rate, mortality and competition, but we assume that the diffusion of the individuals is the same for each genotype. Finally, we take into account mutations occuring between the two genotypes.

The reaction coefficients r_u and r_v represent the intrinsic growth rates, which depend on the environment and take into account both birth and death rates. Notice that r_u and r_v may take some negative values, in deleterious areas where the death rate is greater than the birth rate. Function μ corresponds to the mutation rate between the two species. It imposes a truly *cooperative* dynamics in the small populations regime, and couples the dynamics of the two species. In particular, one expects that, at least for small mutation rates, *mutation aids survival and coexistence*. We also make the assumption that the mutation process is symmetric. From the mathematical point of view, this simplifies some of the arguments we use and improves the readability of section 2.2. We have no doubt that similar results hold in the non-symmetric case, though the proofs may be more involved.

In this context, the ability of the species to survive *globally in space* depends on the sign of the principal eigenvalue of the linearized operator around extinction $(0,0)$, as we will show further, which involves the coefficients r_u, r_v, μ.

Finally, γ_u and γ_v represent the strength of the competition (for e.g. a finite resource) between the two strains. The associated dynamics arises when populations begin to grow. It has no influence on the survival of the two species, but regulates the equilibrium densities of the two populations.

Such a framework is particularly suited to model the propagation of a pathogenic species within a population of hosts. Indeed system (2.2.1) can easily be derived from a host-pathogen microscopic model [P1] in which we neglect the influence of the pathogen on the host's diffusion.

In a homogeneous environment the role of mutations, allowing survival for both u and v, has recently been studied by Griette and Raoul [P2], through the system

$$\begin{cases} \partial_t u = \partial_{xx} u + u(1-(u+v)) + \mu(v-u) \\ \partial_t v = \partial_{xx} v + rv\left(1 - \dfrac{u+v}{K}\right) + \mu(u-v). \end{cases}$$

On the other hand, it is known that the spatial structure has a great influence on host-parasites systems, both at the epidemiological and evolutionary levels [62], [22], [257]. In order to understand the influence of heterogeneities, we aim at studying steady states and propagating solutions, or *fronts*, of system (2.2.1).

Traveling fronts in homogeneous environments. In a homogeneous environment, propagation in reaction diffusion equations is typically described by *traveling waves*, namely solutions to the parabolic equation consisting of a constant profile shifting at a constant speed. This goes back to the seminal works [170], [238] on the Fisher-KPP equation

$$\partial_t u = \Delta u + u(1-u),$$

a model for the spreading of advantageous genetic features in a population. The literature on traveling fronts for such homogeneous reaction diffusion equations is very large, see [170], [238], [19, 20], [169], [181],

[53] among others. In such situations, many techniques based on the comparison principle — such as some monotone iterative schemes or the sliding method [47]— can be used to get *a priori* bounds, existence and monotonicity properties of the solution.

Nevertheless, when considering nonlocal effects or systems, the comparison principle may no longer be available so that the above techniques do not apply and the situation is more involved. One usually uses topological degree arguments to construct traveling wave solutions: see [46], [163], [6], [200] for the nonlocal Fisher-KPP equation, [8] for a bistable nonlocal equation, [7] for a nonlocal equation in an evolutionary context, [P2] for a homogeneous system in an evolutionary context... Notice also that the boundary conditions are then typically understood in a weak sense, meaning that the wave connects 0 to "something positive" that cannot easily be identified: for example, in the nonlocal Fisher-KPP equation the positive steady state $u \equiv 1$ may present a Turing instability.

In a heterogeneous environment, however, it is unreasonable to expect the existence of such a solution. The particular type of propagating solution we aim at constructing in our periodic case is the so called *pulsating front*, first introduced by [354] in a biological context, and by Xin [408, 407, 405] in the framework of flame propagation.

Pulsating fronts in heterogeneous environments. The definition of a pulsating front is the natural extension, in the periodic framework, of the aforementioned traveling waves. We introduce a speed c and shift the origin with this speed to catch the asymptotic dynamics. Technically, a *pulsating front* (with speed c) is then a profile $(U(s,x), V(s,x))$ that is periodic in the space variable x, and that connects $(0,0)$ to a non-trivial state, such that $(u(t,x), v(t,x)) := (U(x-ct,x), V(x-ct,x))$ solves (2.2.1). Equivalently, a pulsating front is a solution of (2.2.1) connecting $(0,0)$ to a non-trivial state, and that satisfies the constraint

$$\left(u\left(t+\frac{L}{c},x\right), v\left(t+\frac{L}{c},x\right)\right) = (u(t,x-L), v(t,x-L)), \quad \forall (t,x) \in \mathbb{R}^2.$$

As far as monostable pulsating fronts are concerned, we refer among others to the seminal works of Weinberger [398], Berestycki and Hamel [48]. Let us also mention [221], [50], [197], [199] for related results.

One of the main difficulties we encounter when studying system (2.2.1) is that two main dynamics coexist. On the one hand, when the population is small, (2.2.1) behaves like a cooperative system which enjoys a comparison principle. On the other hand, when the population is near a non-trivial equilibrium, (2.2.1) is closer to a competitive system. Since those dynamics cannot be separated, our system does not admit any comparison principle, and standard techniques such as monotone iterations cannot be applied. As far as we know, the present work is the first construction of pulsating fronts in a KPP situation (see [113], [207] for an ignition type nonlinearity and a different setting) where comparison arguments are not available.

2.2.2 Main results and comments

2.2.2.1 Assumptions, linear material and notations

Periodic coefficients. Throughout this work, and even if not recalled, we always make the folllowing assumptions. Functions $r_u, r_v, \gamma_u, \gamma_v, \mu : \mathbb{R} \to \mathbb{R}$ are smooth and periodic with period $L > 0$. We assume further that γ_u, γ_v and μ are positive. We denote their bounds

$$\begin{array}{rccl} 0 < & \gamma^0 \leq & \gamma_u(x), \gamma_v(x) & \leq \gamma^\infty \\ 0 < & \mu^0 \leq & \mu(x) & \leq \mu^\infty \\ & r^0 \leq & r_u(x), r_v(x) & \leq r^\infty, \end{array}$$

for all $x \in \mathbb{R}$. Notice that r_u and r_v are allowed to take negative values, which is an additional difficulty, in particular in the proofs of Lemma 2.2.13 and Lemma 2.2.21. The fact that r_u, r_v do not have a positive lower bound is the main reason why we need to introduce several types of eigenvalue problems, see (2.2.19) and (2.2.34), to construct subsolutions of related problems.

On the linearized system around $(0,0)$**.** We denote by A the symmetric matrix field arising after linearizing system (2.2.1) near the trivial solution $(0,0)$, namely

$$A(x) := \begin{pmatrix} r_u(x) - \mu(x) & \mu(x) \\ \mu(x) & r_v(x) - \mu(x) \end{pmatrix}. \tag{2.2.2}$$

Since $A(x)$ has positive off-diagonal coefficients, the elliptic system associated with the linear operator $-\Delta - A(x)$ is cooperative, *fully coupled* and therefore satisfies the strong maximum principle as well as other convenient properties [87].

Remark 2.2.1 (Cooperative elliptic systems and comparison principle)**.** Cooperative systems enjoy similar comparison properties as scalar elliptic operators. In particular, [87] and [127] show that the maximum principle holds for cooperative systems if the principal eigenvalue is positive. Moreover, Section 13 (see also the beginning of Section 14) of [87] shows that, for so-called *fully coupled systems* (which is the case of all the operators we will encounter since $\mu(x) \geq \mu^0 > 0$), the converse holds. These facts will be used for instance in the proof of Lemma 2.2.12.

Let us now introduce a principal eigenvalue problem that is necessary to enunciate our main results.

Definition 2.2.2 (Principal eigenvalue)**.** We denote by ł the principal eigenvalue of the stationary operator $-\Delta - A(x)$ with periodic conditions, where A is defined in (2.2.2).

In particular, we are equipped through this work with a principal eigenfunction $\Phi := \begin{pmatrix} \varphi \\ \psi \end{pmatrix}$ satisfying

$$\begin{cases} -\Phi_{xx} - A(x)\Phi = \text{ł}\Phi \\ \Phi \text{ is } L\text{-periodic}, \quad \Phi \text{ is positive}, \quad \|\Phi\|_{\mathbf{L}^\infty} = 1. \end{cases} \tag{2.2.3}$$

For more details on principal eigenvalue for systems, we refer the reader to [87], in particular to Theorem 13.1 (Dirichlet boundary condition) which provides the principal eigenfunction. Furthermore, in the case of symmetric (self-adjoint) systems as the one we consider, the equivalent definition [127, (2.14)] provides some additional properties, in particular that the eigenfunction minimizes the Rayleigh quotient.

Function spaces. To avoid confusion with the usual function spaces, we denote the function spaces on a couple of functions with a bold font. Hence $\mathbf{L}^p(\Omega) := L^p(\Omega) \times L^p(\Omega)$ for $p \in [1, \infty]$ and $\mathbf{H}^q(\Omega) := H^q(\Omega) \times H^q(\Omega)$ for $q \in \mathbb{N}$ are equipped with the norms

$$\left\| \begin{pmatrix} u \\ v \end{pmatrix} \right\|_{\mathbf{L}^p} := \left\| \begin{pmatrix} \|u\|_{L^p} \\ \|v\|_{L^p} \end{pmatrix} \right\|_p, \quad \left\| \begin{pmatrix} u \\ v \end{pmatrix} \right\|_{\mathbf{H}^q} := \left\| \begin{pmatrix} \|u\|_{H^q} \\ \|v\|_{H^q} \end{pmatrix} \right\|_2.$$

Similarly, $\mathbf{C}^{\alpha,\beta} := C^{\alpha,\beta} \times C^{\alpha,\beta}$ for $\alpha \in \mathbb{N}$ and $\beta \in [0,1]$ is equipped with $\left\| \begin{pmatrix} u \\ v \end{pmatrix} \right\|_{\mathbf{C}^{\alpha,\beta}} := \max\left(\|u\|_{C^{\alpha,\beta}}, \|v\|_{C^{\alpha,\beta}}\right)$ and $\mathbf{C}^\alpha := \mathbf{C}^{\alpha,0}$. The subscript of those spaces denotes a restriction to a subspace : $\mathbf{L}^p_{per}$, $\mathbf{H}^q_{per}$, $\mathbf{C}^0_{per}$, $\mathbf{C}^{0,1}_{per}$, $\mathbf{C}^1_{per}$ for L-periodic functions, $\mathbf{H}^1_0$ for functions that vanish on the boundary, etc. Those function spaces are Banach spaces, and $\mathbf{H}^1$, $\mathbf{H}^1_{per}$, $\mathbf{H}^1_0$, $\mathbf{L}^2$ and $\mathbf{L}^2_{per}$ have a canonical Hilbert structure.

2.2.2.2 Main results

As well-known in KPP situations, the sign of the principal eigenvalue ł is of crucial importance for the fate of the population: we expect extinction when $\text{ł} > 0$ and propagation (hence survival) when $\text{ł} < 0$. To confirm this scenario, we first study the existence of a nontrivial nonnegative steady state of problem (2.2.1), that is a nontrivial nonnegative L-periodic solution to the system

$$\begin{cases} -p'' = (r_u(x) - \gamma_u(x)(p+q))p + \mu(x)q - \mu(x)p \\ -q'' = (r_v(x) - \gamma_v(x)(p+q))q + \mu(x)p - \mu(x)q. \end{cases} \tag{2.2.4}$$

Theorem 2.2.3 (On nonnegative steady states)**.** *If $\text{ł} > 0$ then $(0,0)$ is the only nonnegative steady state of problem* (2.2.1)*.*

On the other hand, if $\text{ł} < 0$ then there exists a nontrivial positive steady state $(p(x) > 0, q(x) > 0)$ of problem (2.2.1)*.*

Next we turn to the long time behavior of the Cauchy problem associated with (2.2.1). First, we prove extinction when the principal eigenvalue is positive.

Proposition 2.2.4 (Extinction)**.** *Assume* $\lambda > 0$*. Let a nonnegative and bounded initial condition* $(u^0(x), v^0(x))$ *be given. Then, any nonnegative solution* $(u(t,x), v(t,x))$ *of* (2.2.1) *starting from* $(u^0(x), v^0(x))$ *goes extinct exponentially fast as* $t \to \infty$*, namely*

$$\max\left(\|u(t,\cdot)\|_{L^\infty(\mathbb{R})}, \|v(t,\cdot)\|_{L^\infty(\mathbb{R})}\right) = O(e^{-\lambda t}).$$

The proof of Proposition 2.2.4 is rather simple so we now present it. The cooperative parabolic system

$$\begin{cases} \partial_t \bar{u} = \partial_{xx}\bar{u} + (r_u(x) - \mu(x))\bar{u} + \mu(x)\bar{v} \\ \partial_t \bar{v} = \partial_{xx}\bar{v} + (r_v(x) - \mu(x))\bar{v} + \mu(x)\bar{u}, \end{cases} \tag{2.2.5}$$

enjoys the comparison principle, see [171, Theorem 3.2]. On the one hand, any nonnegative $(u(t,x), v(t,x))$ solution of (2.2.1) is a subsolution of (2.2.5). On the other hand one can check that $(M\varphi(x)e^{-\lambda t}, M\psi(x)e^{-\lambda t})$ — with (φ, ψ) the principal eigenfunction satisfying (2.2.3)— is a solution of (2.2.5) which is initially larger than (u^0, v^0), if $M > 0$ is sufficiently large. Conclusion then follows from the comparison principle.

The reverse situation $\lambda < 0$ is much more involved. Since in this case we aim at controlling the solution from below, the nonlinear term in (2.2.1) has to be carefully estimated. When $\lambda < 0$, as a strong indication that the species does invade the whole line, we are going to construct pulsating fronts for (2.2.1).

Definition 2.2.5 (Pulsating front)**.** A pulsating front for (2.2.1) is a speed $c > 0$ and a classical positive solution $(u(t,x), v(t,x))$ to (2.2.1), which satisfy the constraint

$$\begin{pmatrix} u(t + \frac{L}{c}, x) \\ v(t + \frac{L}{c}, x) \end{pmatrix} = \begin{pmatrix} u(t, x - L) \\ v(t, x - L) \end{pmatrix}, \quad \forall (t,x) \in \mathbb{R}^2, \tag{2.2.6}$$

and supplemented with the boundary conditions

$$\liminf_{t \to +\infty} \begin{pmatrix} u(t,x) \\ v(t,x) \end{pmatrix} > \begin{pmatrix} 0 \\ 0 \end{pmatrix}, \quad \lim_{t \to -\infty} \begin{pmatrix} u(t,x) \\ v(t,x) \end{pmatrix} = \begin{pmatrix} 0 \\ 0 \end{pmatrix}, \tag{2.2.7}$$

locally uniformly w.r.t. x.

Following [50], we introduce a new set of variables that correspond to the frame of reference that follows the front propagation, that is $(s,x) := (x - ct, x)$. In these new variables, system (2.2.1) transfers into

$$\begin{cases} -(u_{xx} + 2u_{xs} + u_{ss}) - cu_s = (r_u(x) - \gamma_u(x)(u+v))u + \mu(x)v - \mu(x)u \\ -(v_{xx} + 2v_{xs} + v_{ss}) - cv_s = (r_v(x) - \gamma_v(x)(u+v))v + \mu(x)u - \mu(x)v, \end{cases} \tag{2.2.8}$$

and the constraint (2.2.6) is equivalent to the L-periodicity in x of the solutions to (2.2.8). An inherent difficulty to this approach is that the underlying elliptic operator, see the left-hand side member of system (2.2.8), is degenerate. This requires to consider a regularization of the operator and to derive a series of *a priori* estimates that do not depend on the regularization, see [48] or [50]. In addition to this inherent difficulty, the problem under consideration (2.2.1) does not admit a comparison principle, in contrast with the previous results on pulsating fronts. Nevertheless, as in the traveling wave case, if we only require boundary conditions in a weak sense — see (2.2.7) in Definition 2.2.5— then we can construct a pulsating front for (2.2.1) when the underlying principal eigenvalue is negative. This is the main result of section 2.2 since, as far as we know, this is the first construction of a pulsating front in a KPP situation without comparison principle.

Theorem 2.2.6 (Construction of a pulsating front)**.** *Assume* $\lambda < 0$*. Then there exists a pulsating front solution to* (2.2.1)*.*

As clear in our construction through the section 2.2, the speed $c^* > 0$ of the pulsating front of Theorem 2.2.6 satisfies the bound

$$0 < c^* \leq \bar{c}^0 := \inf\{c \geq 0 : \exists \lambda > 0, \mu_{c,0}(\lambda) = 0\},$$

where $\mu_{c,0}(\lambda)$ is the first eigenvalue of the operator

$$S_{c,\lambda,0}\Psi := -\Psi_{xx} + 2\lambda\Psi_x + [\lambda(c-\lambda)Id - A(x)]\,\Psi$$

with L-periodic boundary conditions. In previous works on pulsating fronts [398], [48], [50], it is typically proved that $\bar{c}^0$ is actually the minimal speed of pulsating fronts (and that faster pulsating fronts $c > \bar{c}^0$ also exist). Nevertheless, those proofs seem to rely deeply on the fact that pulsating fronts, as in Definition 2.2.5, are increasing in time, which is far from obvious in our context without comparison. We conjecture that this remains true but, for the sake of conciseness, we leave it as an open question.

The section 2.2 is organized as follows. Section 2.2.3 is concerned with the proof of Theorem 2.2.3 on steady states. In particular the construction of nontrivial steady states requires an adaptation of some bifurcations results [329, 330], [123] that are recalled in Appendix, Section 2.2.6.1. The rest of the section 2.2 is devoted to the proof of Theorem 2.2.6, that is the construction of a pulsating front. We first consider in Section 2.2.4 an ε-regularization of the degenerate problem (2.2.8) in a strip, where existence of a solution is proved by a Leray-Schauder topological degree argument. Then, in Section 2.2.5 we let the strip tend to $\mathbb{R}^2$ and finally let the regularization ε tend to zero to complete the proof of Theorem 2.2.6. This requires, among others, a generalization to elliptic systems of a Bernstein-type gradient estimate performed in [49], which is proved in Appendix, Section 2.2.6.2.

2.2.3 Steady states

This section 2.2.3 is devoted to the proof of Theorem 2.2.3. The main difficulty is to prove the existence of a positive steady state to (2.2.1) when $\mathfrak{l} < 0$. To do so, we shall use the bifurcation theory introduced in the context of Sturm-Liouville problems by Crandall and Rabinowitz [123], [329, 330]. Though an equivalent result may be obtained using a topological degree argument, this efficient theory shows clearly the relationship between the existence of solutions to the nonlinear problem and the sign of the principal eigenvalue of the linearized operator near zero.

We shall first state and prove an independent theorem that takes advantage of the Krein-Rutman theorem in the context of a bifurcation originating from the principal eigenvalue of an operator. We will then use this theorem to show the link between the existence of a non-trivial positive steady state for (2.2.1), and the sign of the principal eigenvalue defined in (2.2.3).

2.2.3.1 Bifurcation result, a topological preliminary

We first prove a general bifurcation theorem, interesting by itself, which will be used as an end-point of the proof of Theorem 2.2.3. It consists in a refinement of the results in [123], [330, 329], under the additional assumption that the linearized operator satisfies the hypotheses of the Krein-Rutman Theorem. Our contribution is to show that the set of nontrivial fixed points only "meets" $\mathbb{R} \times \{0\}$ at point $(\frac{1}{\mathfrak{l}(T)}, 0)$, with $\mathfrak{l}(T)$ the principal eigenvalue of the linearized operator T: as shown in the proof of Theorem 2.2.7, the only trivial solution (in $\mathbb{R} \times \{0\}$) which is also in the closure of the set of positive solutions is $(\frac{1}{\lambda_1(T)}, 0)$.

This theorem is independent from the rest of the section 2.2 and we will thus use a different set of notations.

Theorem 2.2.7 (Bifurcation under Krein-Rutman assumption)**.** *Let E be a Banach space. Let $C \subset E$ be a closed convex cone with nonempty interior $Int\, C \neq \varnothing$ and of vertex 0, i.e. such that $C \cap -C = \{0\}$. Let*

$$\begin{array}{rccc} F: & \mathbb{R} \times E & \to & E \\ & (\alpha, x) & \mapsto & F(\alpha, x) \end{array}$$

be a continuous and compact operator, i.e. F maps bounded sets into relatively compact ones. Let us define

$$\mathcal{S} := \overline{\{(\alpha, x) \in \mathbb{R} \times E \backslash \{0\} : F(\alpha, x) = x\}}$$

the closure of the set of nontrivial fixed points of F, and

$$\mathbb{P}_{\mathbb{R}}\mathcal{S} := \{\alpha \in \mathbb{R} : \exists x \in C\backslash\{0\}, (\alpha, x) \in \mathcal{S}\}$$

the set of nontrivial solutions in C.

Let us assume the following.

1. $\forall \alpha \in \mathbb{R}$, $F(\alpha, 0) = 0$.
2. *F is Fréchet differentiable near $\mathbb{R} \times \{0\}$ with derivative αT locally uniformly w.r.t. α, i.e. for any $\alpha_1 < \alpha_2$ and $\epsilon > 0$ there exists $\delta > 0$ such that*

$$\forall \alpha \in (\alpha_1, \alpha_2),\ \|x\| \leq \delta \Rightarrow \|F(\alpha, x) - \alpha T x\| \leq \epsilon \|x\|.$$

3. *T satisfies the hypotheses of Theorem 2.2.23 (Krein-Rutman), i.e. $T(C\backslash\{0\}) \subset \operatorname{Int} C$. We denote by $\mathfrak{l}(T) > 0$ its principal eigenvalue.*
4. *$\mathcal{S} \cap (\{\alpha\} \times C)$ is bounded locally uniformly w.r.t. $\alpha \in \mathbb{R}$.*
5. *There is no fixed point on the boundary of C, i.e. $\mathcal{S} \cap (\mathbb{R} \times (\partial C\backslash\{0\})) = \varnothing$.*

Then, either $\left(-\infty, \frac{1}{\lambda_1(T)}\right) \subset \mathbb{P}_{\mathbb{R}}\mathcal{S}$ or $\left(\frac{1}{\lambda_1(T)}, +\infty\right) \subset \mathbb{P}_{\mathbb{R}}\mathcal{S}$.

Proof. Let us first give a short overview of the proof. Since $\mathfrak{l}$ is a simple eigenvalue, we know from Theorem 2.2.24 that there exists a branch of nontrivial solutions originating from $\left(\frac{1}{\mathfrak{l}}, 0\right)$. We will show that this branch is actually contained in $\mathbb{R} \times C$, thanks to Theorem 2.2.25. Since it cannot meet $\mathbb{R} \times \{0\}$ except at $\left(\frac{1}{\mathfrak{l}}, 0\right)$, it has to be unbounded, which proves our result.

Let us define

$$\mathcal{S}_C := \overline{\{(\alpha, x) \in \mathbb{R} \times (C\backslash\{0\}) : F(\alpha, x) = x\}}$$

which is a subset of $\mathcal{S}$, and $\alpha_1 := \frac{1}{\lambda_1(T)}$. We may call $(\alpha, x) \in \mathcal{S}_C$ a *degenerate* solution if $x \in \partial C$, and a *proper* solution otherwise.

Our first task is to show that the only degenerate solution is $\{(\alpha_1, 0)\}$. We first show $\mathcal{S}_C \cap (\mathbb{R} \times \partial C) \subset \{(\alpha_1, 0)\}$. Let $(\alpha, x) \in \mathcal{S}_C \cap (\mathbb{R} \times \partial C)$ be given. By item 5 we must have $x = 0$. Let $(\alpha_n, x_n) \to (\alpha, 0)$ such that $x_n \in C \setminus \{0\}$ and $F(\alpha_n, x_n) = x_n$. Let us define $y_n = \frac{x_n}{\|x_n\|} \in C \setminus \{0\}$. On the one hand since y_n is a bounded sequence and T is a compact operator, up to an extraction the sequence (Ty_n) converges to some z which, by item 3, must belong to C. On the other hand

$$y_n = \frac{x_n}{\|x_n\|} = \alpha_n T y_n + \frac{F(\alpha_n, x_n) - \alpha_n T x_n}{\|x_n\|} = \alpha z + o(1)$$

in virtue of items 1 and 2, so that in particular $z \neq 0$ and $\alpha \neq 0$. Since $y_n \to \alpha z$ and $Ty_n \to z$ we have $z = \alpha T z$. Hence $z \in C \setminus \{0\}$ is an eigenvector for T associated with the eigenvalue $\frac{1}{\alpha}$ so that Theorem 2.2.23 (Krein-Rutman) enforces $\alpha = \frac{1}{\mathfrak{l}(T)} = \alpha_1$.

Next we aim at showing the reverse inclusion, that is $\{(\alpha_1, 0)\} \subset \mathcal{S}_C \cap (\mathbb{R} \times \partial C)$. We shall use the topological results of Appendix 2.2.6.1, namely Theorem 2.2.24 and Theorem 2.2.25. Let $z \in C$ be the eigenvector of T associated with $\lambda_1(T)$ such that $\|z\| = 1$, T^* the dual of T, and $l \in E'$ the eigenvector[1] of T^* associated with $\lambda_1(T)$ such that $\langle l, z\rangle = 1$, where $\langle \cdot, \cdot \rangle$ denotes the duality between E and its dual E'.

Now, for $\xi > 0$ and $\eta \in (0, 1)$, let us define

$$K^+_{\xi,\eta} := \{(\alpha, x) \in \mathbb{R} \times E : |\alpha - \alpha_1| < \xi, \langle l, x\rangle > \eta \|x\|\}.$$

The above sets are used to study the local properties of $\mathcal{S}$ near the branching point $(\alpha_1, 0)$. More precisely, it follows from Theorem 2.2.25 that $\mathcal{S}\backslash\{(\alpha_1, 0)\}$ contains a nontrivial connected component $\mathcal{C}^+_{\alpha_1}$ which is included in $K^+_{\xi,\eta}$ and near $(\alpha_1, 0)$:

$$\forall \xi > 0, \forall \eta \in (0, 1), \exists \zeta_0 > 0, \forall \zeta \in (0, \zeta_0),\ (\mathcal{C}^+_{\alpha_1} \cap B_\zeta) \subset K^+_{\xi,\eta},$$

[1] Let us recall that according to the Fredholm alternative, we have $\dim\ker(I - \lambda T) = \dim\ker(I - \lambda T^*) < \infty$ so that each eigenvalue of T is an eigenvalue of T^* with the same multiplicity.

where

$$B_\zeta = \{(\alpha, x) \in \mathbb{R} \times E : |\alpha - \alpha_1| < \zeta, \|x\| < \zeta\}.$$

Moreover, $\mathcal{C}^+_{\alpha_1}$ satisfies either item 1 or 2 in Theorem 2.2.24. Let us show that $(\mathcal{C}^+_{\alpha_1} \cap B_\zeta) \subset \mathbb{R} \times C$ for $\zeta > 0$ small enough, i.e.

$$\exists \zeta > 0, (\mathcal{C}^+_{\alpha_1} \cap B_\zeta) \subset \mathbb{R} \times C. \tag{2.2.9}$$

To do so, assume by contradiction that there exists a sequence $(\alpha^n, x_n) \to (\alpha_1, 0)$ such that

$$\forall n \in \mathbb{N}, (\alpha^n, x_n) \in \mathcal{C}^+_{\alpha_1} \text{ and } x_n \notin C.$$

Writing $\frac{x_n}{\|x_n\|} = \alpha^n T \frac{x_n}{\|x_n\|} + \frac{F(\alpha^n, x_n) - \alpha^n T x_n}{\|x_n\|}$ and reasoning as above, we see that (up to extraction) the sequence $\left(\frac{x_n}{\|x_n\|}\right)$ converges to some w such that $Tw = \frac{1}{\alpha_1} w = \mathfrak{l}(T)w$. As a result $w = z$ or $w = -z$ (recall that z is the unique eigenvector of T such that $z \in C$ and $\|z\| = 1$). But the property $\langle l, x_n \rangle \geq \eta \|x_n\|$ enforces $\frac{x_n}{\|x_n\|} \to z$. Since $\frac{x_n}{\|x_n\|} \notin C$ and $z \in Int\, C$, this is a contradiction. Hence (2.2.9) is proved.

Since $\mathcal{C}^+_{\alpha_1}$ is connected and $\mathcal{C}^+_{\alpha_1} \cap (\mathbb{R} \times \partial C) = \varnothing$ by item 5, we deduce from (2.2.9) that $\mathcal{C}^+_{\alpha_1} \subset \mathcal{S}_C$. Moreover, since by definition $\{(\alpha_1, 0)\} \in \overline{\mathcal{C}^+_{\alpha_1}}$ and $\mathcal{S}_C$ is closed, we have

$$\{(\alpha_1, 0)\} \subset \mathcal{S}_C \cap (\mathbb{R} \times \partial C).$$

We have then established that $\{(\alpha_1, 0)\}$ is the only degenerate solution in C i.e. $\mathcal{S}_C \cap (\mathbb{R} \times \partial C) = \{(\alpha_1, 0)\}$. As stated above, there exists a branch $\mathcal{C}^+_{\alpha_1}$ of solutions such that $\{(\alpha_1, 0)\} \subset \overline{\mathcal{C}^+_{\alpha_1}}$, and such that $\mathcal{C}^+_{\alpha_1} \subset \mathcal{S}_C$. Since $\mathcal{C}^+_{\alpha_1}$ cannot meet $\mathbb{R} \times \{0\}$ at $(\alpha, 0) \neq (\alpha_1, 0)$, it follows from Theorem 2.2.25 that $\mathcal{C}^+_{\alpha_1}$ is unbounded. It therefore follows from item 4 that there exists a sequence $(\alpha^n, x^n) \in \mathcal{C}^+_{\alpha_1}$ with $|\alpha^n| \to \infty$. Since $\mathcal{C}^+_{\alpha_1}$ contains only proper solutions (i.e. $\mathcal{C}^+_{\alpha_1} \cap (\mathbb{R} \times \partial C) = \varnothing$), the projection $P_{\mathbb{R}}(\mathcal{C}^+_{\alpha_1})$ of $\mathcal{C}^+_{\alpha_1}$ on $\mathbb{R}$ is included in $\mathbb{P}_{\mathbb{R}}\mathcal{S}$. Finally, the continuity of the projection $P_{\mathbb{R}}$ and the fact that $\mathcal{C}^+_{\alpha_1}$ is connected show that either $(\alpha_1, \alpha^n) \subset P_{\mathbb{R}}(\mathcal{C}^+_{\alpha_1})$ or $(\alpha^n, \alpha_1) \subset P_{\mathbb{R}}(\mathcal{C}^+_{\alpha_1})$, depending on $\alpha_1 \leq \alpha^n$ or $\alpha^n \leq \alpha_1$. Letting $n \to \infty$ proves Theorem 2.2.7. □

2.2.3.2 A priori estimates on steady states

In order to meet the hypotheses of Theorem 2.2.7 in section 2.2.3.3, we prove some *a priori* estimates on stationary solutions. We have in mind to apply Theorem 2.2.7 in the cone of nonnegativity of $\mathbf{L}^\infty_{per}(\mathbb{R})$. Specifically, Lemma 2.2.8 will be used to meet item 4 (the solutions are locally bounded), and Lemma 2.2.9 will be used to meet item 5 (there is no solution on the boundary of the cone).

Lemma 2.2.8 (Uniform upper bound)**.** *There exists a constant $C = C(r^\infty, \mu^\infty, \gamma^0) > 0$ such that any nonnegative periodic solution (p, q) to (2.2.4) satisfies $p(x) \leq C$ and $q(x) \leq C$, for all $x \in \mathbb{R}$.*

Proof. Let $\begin{pmatrix} p \\ q \end{pmatrix}$ be a solution to system (2.2.4), so that

$$\left\{ \begin{array}{rcl} -p'' & \leq & p(r_u - \gamma_u p) + q(\mu - \gamma_u p) \\ -q'' & \leq & q(r_v - \gamma_v q) + p(\mu - \gamma_v q). \end{array} \right. \tag{2.2.10}$$

Let us define $C := \max\left(\frac{r^\infty}{\gamma^0}, \frac{\mu^\infty}{\gamma^0}\right) > 0$. Denote by x_0 a point where p reaches its maximum, so that $-p''(x_0) \geq 0$. Assume by contradiction that $p(x_0) > C$. Then, in virtue of (2.2.10), one has $-p''(x_0) \leq p(x_0)(r_u(x_0) - \gamma_u(x_0)C) < 0$, which is a contradiction. Thus $p \leq C$. Inequality $q \leq C$ is proved the same way. □

Lemma 2.2.9 (Positivity of solutions)**.** *Any nonnegative periodic solution (p, q) to (2.2.4) such that $(p, q) \not\equiv (0, 0)$ actually satisfies $p(x) > 0$ and $q(x) > 0$, for all $x \in \mathbb{R}$.*

Proof. Write

$$\left\{ \begin{array}{rcl} -p'' & \geq & p(r_u - \mu - \gamma_u(p + q)) \\ -q'' & \geq & q(r_v - \mu - \gamma_v(p + q)), \end{array} \right.$$

and the result is a direct application of the strong maximum principle. □

2.2.3.3 Proof of the result on steady states

We are now in the position to prove Theorem 2.2.3.

The $\mathfrak{l} > 0$ case is an immediate consequence of the extinction result, namely Proposition 2.2.4.

The reverse situation $\mathfrak{l} < 0$, where we need to prove the existence of a nontrivial steady state, is more involved. We shall combine our *a priori* estimates of section 2.2.3.2 with our bifurcation result, namely Theorem 2.2.7. We will also use the $\mathfrak{l} > 0$ case. We want to stress eventually that we will use the notations introduced in section 2.2.2.1, in particular for functional spaces.

Before starting the proof itself, we would like to present briefly the core of the argument we use. We introduce a new parameter $\beta \in \mathbb{R}$ and look at the modified system

$$\left\{ \begin{array}{rcl} -p'' & = & p(r_u + \beta - \gamma_u(p+q)) + \mu(q-p) \\ -q'' & = & q(r_v + \beta - \gamma_v(p+q)) + \mu(p-q) \end{array} \right. \tag{2.2.11}$$

which is system (2.2.4) with r_u (resp. r_v) replaced by $r_u + \beta$ (resp. $r_v + \beta$). We apply Theorem 2.2.7 to system (2.2.11) with the bifurcation parameter β. There exists then a branch of solutions originating from $\beta = \mathfrak{l}$, and which spans to $\beta \to +\infty$ since the eigenvalue of the linearization of system (2.2.11) is *positive* for $\beta < \mathfrak{l}$ (i.e. no solution exists for $\beta \in (-\infty, \mathfrak{l})$). In particular there exists a solution for $\beta = 0$ since $\mathfrak{l} < 0$. Let us make this argument rigorous.

The $\mathfrak{l} < 0$ case. We start with the following lemma.

Lemma 2.2.10 (Fréchet differentiability)**.** *Let*

$$f\begin{pmatrix} p \\ q \end{pmatrix} := \begin{pmatrix} -\gamma_u(p+q)p \\ -\gamma_v(p+q)q \end{pmatrix}.$$

Then, the induced operator $\mathbf{L}^\infty_{per}(\mathbb{R}) \longrightarrow \mathbf{L}^\infty_{per}(\mathbb{R})$ is Fréchet differentiable at $\begin{pmatrix} 0 \\ 0 \end{pmatrix}$ with derivative $0_{\mathbf{L}^\infty}$.

Proof. We need to show that

$$\left\| f\begin{pmatrix} p \\ q \end{pmatrix} \right\|_{\mathbf{L}^\infty_{per}(\mathbb{R})} = o\left(\left\| \begin{pmatrix} p \\ q \end{pmatrix} \right\|_{\mathbf{L}^\infty_{per}(\mathbb{R})} \right)$$

as $\left\| \begin{pmatrix} p \\ q \end{pmatrix} \right\|_{\mathbf{L}^\infty_{per}(\mathbb{R})} \to 0$. We have

$$\left\| f\begin{pmatrix} p \\ q \end{pmatrix} \right\|_{\mathbf{L}^\infty_{per}(\mathbb{R})} \leq \gamma^\infty \left\| \begin{pmatrix} p \\ q \end{pmatrix} \right\|_{\mathbf{L}^\infty_{per}(\mathbb{R})} \|p+q\|_{L^\infty_{per}(\mathbb{R})} \leq 2\gamma^\infty \left\| \begin{pmatrix} p \\ q \end{pmatrix} \right\|^2_{\mathbf{L}^\infty_{per}(\mathbb{R})}$$

which proves the lemma. □

We are now in the position to complete the proof of Theorem 2.2.3. It follows from classical theory that, for $M > 0$ large enough, the problem

$$\left\{ \begin{array}{l} -\begin{pmatrix} \tilde{p} \\ \tilde{q} \end{pmatrix}'' - A(x)\begin{pmatrix} \tilde{p} \\ \tilde{q} \end{pmatrix} + M\begin{pmatrix} \tilde{p} \\ \tilde{q} \end{pmatrix} = \begin{pmatrix} p \\ q \end{pmatrix} \\ \begin{pmatrix} \tilde{p} \\ \tilde{q} \end{pmatrix} \in \mathbf{H}^1_{per} \end{array} \right. \tag{2.2.12}$$

has a unique weak solution $\begin{pmatrix}\tilde{p}\\ \tilde{q}\end{pmatrix}$, for each $\begin{pmatrix}p\\ q\end{pmatrix} \in \mathbf{L}^2_{per}$. Let us call L_M^{-1} the associated operator, namely

$$\begin{array}{rccc} L_M^{-1}: & \mathbf{L}^2_{per} & \to & \mathbf{H}^1_{per} \\ & \begin{pmatrix}p\\ q\end{pmatrix} & \mapsto & \begin{pmatrix}\tilde{p}\\ \tilde{q}\end{pmatrix}. \end{array}$$

Notice that, assuming $M > -\lambda_1$, the principal eigenvalue associated with problem (2.2.12) is $\mathfrak{l}' := \mathfrak{l} + M > 0$, and recall that the actual algebraic eigenvalue $\mathfrak{l}(L_M^{-1})$ of the operator L_M^{-1} is given by

$$\lambda_1(L_M^{-1}) = \frac{1}{\mathfrak{l}'} > 0.$$

From elliptic regularity, the restriction of L_M^{-1} to $\mathbf{L}^\infty_{per}(\mathbb{R})$ maps $\mathbf{L}^\infty_{per}(\mathbb{R})$ into $\mathbf{C}^{0,\theta}_{per}(\mathbb{R})$, $0 < \theta < 1$, and L_M^{-1} is therefore a compact operator on $\mathbf{L}^\infty_{per}(\mathbb{R})$. Hence,

$$\begin{array}{rccc} F: & \mathbb{R} \times \mathbf{L}^\infty_{per}(\mathbb{R}) & \to & \mathbf{L}^\infty_{per}(\mathbb{R}) \\ & \left(\alpha, \begin{pmatrix}p\\ q\end{pmatrix}\right) & \mapsto & L_M^{-1}\left(f\begin{pmatrix}p\\ q\end{pmatrix} + \alpha\begin{pmatrix}p\\ q\end{pmatrix}\right) \end{array}$$

is a continuous and compact map, to which we aim at applying Theorem 2.2.7. Let us recall that the cone of nonegativity

$$C := \left\{ \begin{pmatrix}p\\ q\end{pmatrix} \in \mathbf{L}^\infty_{per}(\mathbb{R}) : \begin{pmatrix}p\\ q\end{pmatrix} \geq \begin{pmatrix}0\\ 0\end{pmatrix} \right\}$$

is, as required by Theorem 2.2.7, a closed convex cone of vertex 0 and nonempty interior in $\mathbf{L}^\infty_{per}$. Finally, we want to stress that solutions to $F\left(\alpha, \begin{pmatrix}p\\ q\end{pmatrix}\right) = \begin{pmatrix}p\\ q\end{pmatrix}$ are classical solutions to the system

$$-\begin{pmatrix}p\\ q\end{pmatrix}'' - A(x)\begin{pmatrix}p\\ q\end{pmatrix} = f\begin{pmatrix}p\\ q\end{pmatrix} + (\alpha - M)\begin{pmatrix}p\\ q\end{pmatrix} \tag{2.2.13}$$

which is equivalent to system (2.2.11) with $\beta = \alpha - M$, where α is the bifurcation parameter. Let us check that all assumptions of Theorem 2.2.7 are satisfied.

1. Clearly we have $\forall \alpha \in \mathbb{R}, F\left(\alpha, \begin{pmatrix}0\\ 0\end{pmatrix}\right) = \begin{pmatrix}0\\ 0\end{pmatrix}$.

2. From Lemma 2.2.10 and the composition rule for derivatives, F is Fréchet differentiable near $\mathbb{R} \times \left\{\begin{pmatrix}0\\ 0\end{pmatrix}\right\}$ with derivative αL_M^{-1} locally uniformly w.r.t. α.

3. From the comparison principle (available for L_M^{-1} since $\mathfrak{l}' > 0$, see [87]), L_M^{-1} satisfies the hypotheses of the Krein-Rutman Theorem, namely $L_M^{-1}(C \setminus \{0\}) \subset Int\, C$.

4. Lemma 2.2.8 shows that, for any $\alpha_* < \alpha^*$, $\mathcal{S} \cap (\alpha_*, \alpha^*) \times C$ is bounded (in view of system (2.2.11), the constant C defined in the proof of Lemma 2.2.8 is locally bounded w.r.t. α).

5. From Lemma 2.2.9, any nonnegative fixed point is positive, i.e. $\mathcal{S} \cap (\mathbb{R} \times (\partial C \setminus \{0\})) = \varnothing$.

We may now apply Theorem 2.2.7 which states that either $\mathcal{S}\cap(\{\alpha\}\times(C\setminus\{0\}))\neq\varnothing$ for any $\alpha\in(\mathfrak{l}',+\infty)$ or $\mathcal{S}\cap(\{\alpha\}\times(C\setminus\{0\}))\neq\varnothing$ for any $\alpha\in(-\infty,\mathfrak{l}')$. Invoking the case of positive principal eigenvalue (see the begininning of the present section), we see that there is no nonnegative nontrivial fixed points when $\alpha<\mathfrak{l}'$. As a result we have

$$\forall\alpha\in(\mathfrak{l}',+\infty),\mathcal{S}\cap(\{\alpha\}\times(C\setminus\{0\}))\neq\varnothing.$$

In particular, since $\mathfrak{l}'=M+\mathfrak{l}<M$, there exists a positive fixed point for $\alpha=M$, which is a classical solution of (2.2.13). This completes the proof of Theorem 2.2.3. □

2.2.4 Towards pulsating fronts: the problem in a strip

We have established above the existence of a nontrivial periodic steady state $(p(x)>0,q(x)>0)$ when the first eigenvalue of the linearized stationary problem $\mathfrak{l}$ is negative. The rest of the section 2.2 is devoted to the construction of a pulsating front, see Definition 2.2.5, when $\mathfrak{l}<0$[2].

In order to circumvent the degeneracy of the elliptic operator in (2.2.8) we need to introduce a regularization via a small positive parameter ε. Also, in order to gain compactness, the system (2.2.8) posed in $(s,x)\in\mathbb{R}^2$ (recall that $s=x-ct$) is first reduced to a strip $(s,x)\in(-a,a)\times\mathbb{R}$ (recall the periodicity in the x variable).

More precisely, let us first define the constants $a_0^*>0$ (minimal size of the strip in the s variable on which we impose a normalization), $\nu_0>0$ (maximal normalization), and $K_0>0$ by

$$a_0^*:=2\sqrt{\frac{5}{-\mathfrak{l}}},\qquad \nu_0:=\min\left(1,\frac{-\mathfrak{l}}{4\gamma^\infty},\min_{x\in\mathbb{R}}(p(x),q(x))\right),$$

$$K_0:=\max\left(\frac{8\gamma^\infty\max_{x\in\mathbb{R}}(p(x)+q(x))}{-\mathfrak{l}},1+\max_{x\in\mathbb{R}}\left(\frac{p(x)}{q(x)},\frac{q(x)}{p(x)}\right)\right).$$

Also we define the strip $\Omega_0:=(-a_0,a_0)\times\mathbb{R}$ for $a_0\geq a_0^*$. We keep a_0 as a degree of freedom since it is crucial in the proof of Theorem 2.2.18 to impose a normalization on a wide enough set.

Theorem 2.2.11 (A solution of the regularized problem in a strip)**.** *Assume $\mathfrak{l}<0$. Let $a_0>a_0^*$, $0<\nu<\nu_0$ and $K>K_0$ be given. Then there is $C>0$ such that, for any $\varepsilon\in(0,1)$, there is $\bar a=\bar a^\varepsilon>0$ (whose definition can be found in Lemma 2.2.13 item 4) such that: for any $a\geq a_0+\bar a$, there exist a L-periodic in x and positive $(u(s,x),v(s,x))$, bounded by C, and a speed $c\in(0,\bar c^\varepsilon+\varepsilon)$, solving the following mixed Dirichlet-periodic problem on the domain $\Omega:=(-a,a)\times\mathbb{R}$*

$$\begin{cases} L_\varepsilon u-cu_s &= u(r_u-\gamma_u(u+v))+\mu v-\mu u \quad \text{in } \Omega\\ L_\varepsilon v-cv_s &= v(r_v-\gamma_v(u+v))+\mu u-\mu v \quad \text{in } \Omega\\ (u,v)(-a,x)=(Kp(x),Kq(x)),\quad \forall x\in\mathbb{R}\\ (u,v)(a,x)=(0,0),\quad \forall x\in\mathbb{R}\\ \sup\limits_{\Omega_0}(u+v)=\nu, \end{cases}\tag{2.2.14}$$

where $L_\varepsilon:=-\partial_{xx}-2\partial_{xs}-(1+\varepsilon)\partial_{ss}$ and the speed $\bar c^\varepsilon\geq 0$ is defined in Lemma 2.2.12.

This whole section 2.2.4 is concerned with the proof of Theorem 2.2.11. In order to use a topological degree argument, we transform continuously our problem until we get a simpler problem for which we know how to compute the degree explicitely.

Our first homotopy allows us to get rid of the competitive behaviour of the system. Technically we interpolate the nonlinear terms $-\gamma_u uv$, $-\gamma_v uv$ with the linear terms $-\gamma_u u\frac{q}{K}$, $-\gamma_v v\frac{p}{K}$ respectively, to obtain system (2.2.20) which is truly cooperative. In particular, since the boundary condition at $s=-a$ is a supersolution to (2.2.20), we can prove the existence of a unique solution to (2.2.20) for each $c\in\mathbb{R}$ via a monotone iteration technique, the monotonicity of the constructed solutions and further properties. Nevertheless we still need to compute the degree explicitely, to which end we use a second homotopy that interpolates the right-hand side of (2.2.20) with a linear term, and then a third homotopy to get rid of the coupling between

[2]In Section 2.2.4 and Section 2.2.5 even if not stated we always assume $\mathfrak{l}<0$.

the speed c and the profiles u and v. At this point we are equipped to compute the degree. For related arguments in a traveling wave context, we refer the reader to [46], [7, 8], [P2].

The role of the a priori estimates in sections 2.2.4.1, 2.2.4.2 and 2.2.4.3 is to ensure that there is no solution on the boundary of the open sets that we choose to contain our problem, and thus that the degree is a constant along our path. In section 2.2.4.4, we complete the proof of Theorem 2.2.11.

Before that, we need to establish some properties on the upper bound $\bar{c}^\varepsilon$ for the speed in Theorem 2.2.11.

Lemma 2.2.12 (On the upper bound for the speed)**.** *Let*

$$S_{c,\lambda,\varepsilon}\Psi := -\Psi_{xx} + 2\lambda\Psi_x + \left[\lambda(c-(1+\varepsilon)\lambda)Id - A(x)\right]\Psi,$$

and define

$$\bar{c}^\varepsilon = \inf\left\{c \geq 0, \exists \lambda > 0, \mu_{c,\varepsilon}(\lambda) = 0\right\}, \tag{2.2.15}$$

where $\mu_{c,\varepsilon}(\lambda)$ is the first eigenvalue of the operator $S_{c,\lambda,\varepsilon}$ with L-periodic boundary conditions. Then the following holds.

1. *For any $\varepsilon \in (0,1)$, we have $\bar{c}^\varepsilon < +\infty$.*
2. *We have $\bar{c}^\varepsilon = \min\left\{c \geq 0, \exists \lambda > 0, \mu_{c,\varepsilon}(\lambda) = 0\right\}$.*
3. *$\varepsilon \mapsto \bar{c}^\varepsilon$ is nondecreasing.*

Proof. 1. We need to prove that the set in the right-hand side of (2.2.15) is non-empty. We first notice that $\mu_{c,\varepsilon}(0) = ł < 0$ for any $c > 0$. Next, for the eigenfunction $\Phi := \begin{pmatrix}\varphi\\ \psi\end{pmatrix}$ solving (2.2.3), we have $S_{c,\lambda,\varepsilon}\Phi = ł\Phi + 2\lambda\Phi_x + \lambda(c-(1+\varepsilon)\lambda)\Phi$. In particular for $\lambda = \frac{c}{2}$, we have

$$S_{c,\frac{c}{2},\varepsilon}\Phi \geq (ł + \frac{c^2}{4}(1-\varepsilon))\Phi + c\Phi_x \geq \begin{pmatrix}0\\0\end{pmatrix}$$

as soon as $c \geq c_*$ where $c_* > 0$ depends only on the quantities $\min(\varphi,\psi)$, $\|\Phi_x\|_{\mathbf{L}^\infty}$ and $-ł$. Recalling, see [87], that the eigenvalue is given by

$$\mu_{c_*,\varepsilon}\left(\frac{c_*}{2}\right) = \sup\left\{\rho \in \mathbb{R} : \exists \Psi \in \mathbf{C}^2_{per}, \Psi > 0, S_{c,\frac{c}{2},\varepsilon}\Psi - \rho\Psi \geq 0\right\},$$

it follows from the above that $\mu_{c_*,\varepsilon}\left(\frac{c_*}{2}\right) \geq 0$. Since the principal eigenvalue of $S_{c,\lambda,\varepsilon}$ is continuous[3] with respect to λ (and c), there exists $\lambda \in (0, \frac{c_*}{2}]$ such that $\mu_{c_*,\varepsilon}(\lambda) = 0$, which proves that (2.2.15) is well-posed.

2. For the eigenfunction Φ solving (2.2.3), we have

$$S_{c,\lambda,\varepsilon}\Phi \leq 2\lambda\Phi_x - \lambda^2\left(1+\varepsilon-\frac{c}{\lambda}\right)\Phi < \begin{pmatrix}0\\0\end{pmatrix}$$

as soon as $\lambda \geq \lambda_*$ where $\lambda_* > 0$ depends only on $\min(\varphi,\psi)$, $\|\Phi_x\|_{\mathbf{L}^\infty}$, and an upper bound for c. Hence the maximum principle does not hold for $S_{c,\lambda,\varepsilon}$, and it follows from [87, Theorem 14.1] that $\mu_{c,\varepsilon}(\lambda) \leq 0$.

Now, we consider sequences $c_n \searrow \bar{c}^\varepsilon$, and $\lambda_n \geq 0$ such that $\mu_{c_n,\varepsilon}(\lambda_n) = 0$. From the above, we have $\lambda_n \leq \lambda_*$ so that, up to extraction, $\lambda_n \to \lambda_\infty$. From the continuity of the principal eigenvalue, we deduce that $\mu_{\bar{c}^\varepsilon,\varepsilon}(\lambda_\infty) = 0$, and the infimum in (2.2.15) is attained.

[3]This property is potentially false in general but has a simple proof in our setting. Take a sequence of operators $T_n \to T$ that send a proper cone C into $K \subset \mathrm{Int}\, C$ with K compact, i.e. $T_n(C) \subset K$ and $T(C) \subset K$. Assume that the series of normalized eigenvectors $x_n \in C$ s.t. $T_n x_n = \lambda_n x_n$ diverges, then we can extract to sequences $x_n^1 \to y \in C$ and $x_n^2 \to z \in C$ with $y \neq z$. Extracting further, there exists μ and ν s.t. $Ty = \mu y$ and $Tz = \nu z$ which is a contradiction since $y \neq z$. Hence the continuity of the eigenvalue.

3. Let $\varepsilon' \leq \varepsilon$ and $c > 0$ such that there is a positive solution Θ to $S_{c,\lambda,\varepsilon}\Theta = \begin{pmatrix} 0 \\ 0 \end{pmatrix}$. Then $S_{c,\lambda,\varepsilon'}\Theta = (\varepsilon - \varepsilon')\lambda^2\Theta \geq \begin{pmatrix} 0 \\ 0 \end{pmatrix}$ so that, as in the proof of item 1, there exists $0 < \lambda' \leq \lambda$ such that $\mu_{c,\varepsilon'}(\lambda') = 0$.

   Thus
$$\{c \geq 0, \exists \lambda > 0, \mu_{c,\varepsilon}(\lambda) = 0\} \subset \{c \geq 0, \exists \lambda > 0, \mu_{c,\varepsilon'}(\lambda) = 0\}.$$

   Taking the infimum on c yields $\bar{c}^{\varepsilon'} \leq \bar{c}^{\varepsilon}$.

Lemma 2.2.12 is proved. □

2.2.4.1 Estimates along the first homotopy

Let us recall that the role of the first homotopy is to get rid of the competition of our original problem ($\tau = 1$), so that the classical comparison methods become available for $\tau = 0$. Notice that it is crucial that the Dirichlet condition at $s = -a$ is a supersolution for the $\tau = 0$ problem, in order to apply a sliding method in the following section. Hence, for $0 \leq \tau \leq 1$, we consider the problem

$$\begin{cases} L_\varepsilon u - cu_s &= u[r_u - \gamma_u(u + (\tau v + (1-\tau)\frac{q}{K}))] + \mu v - \mu u \\ L_\varepsilon v - cv_s &= v[r_v - \gamma_v((\tau u + (1-\tau)\frac{p}{K}) + v)] + \mu u - \mu v \\ (u,v)(-a,x) = (Kp(x), Kq(x)), &\quad \forall x \in \mathbb{R} \\ (u,v)(a,x) = (0,0), &\quad \forall x \in \mathbb{R}, \end{cases} \tag{2.2.16}$$

complemented with the normalization condition

$$\sup_{\Omega_0} (u+v) = \nu, \tag{2.2.17}$$

whose role is to bound the admissible speeds (see for instance item 4 below).

Lemma 2.2.13 (A priori estimates along the first homotopy)**.** *Let a nonnegative $(u,v) \in \mathbf{C}^1_{per}(\Omega)$ (where $\Omega = (-a,a) \times \mathbb{R}$ and the periodicity is understood only w.r.t. the $x \in \mathbb{R}$ variable) and $c \in \mathbb{R}$ solve* (2.2.16)*, with $0 \leq \tau \leq 1$. Then*

1. *(u,v) is a classical solution to* (2.2.16)*, i.e. $(u,v) \in \mathbf{C}^2(\overline{\Omega})$.*
2. *The positive constant $C := \max(\frac{2r^\infty}{\gamma^0}, K\max(p+q))$ is such that*
$$u(s,x) + v(s,x) \leq C, \quad \forall (s,x) \in \overline{\Omega} = [-a,a] \times \mathbb{R}.$$
3. *(u,v) is positive in Ω.*
4. *Let $\lambda_0 > 0$ and $\Phi_0(x) = \begin{pmatrix} \Phi_u(x) \\ \Phi_v(x) \end{pmatrix} > \begin{pmatrix} 0 \\ 0 \end{pmatrix}$ be such that $S_{\bar{c}^\varepsilon,\lambda_0,\varepsilon}\Phi_0 = 0$ and $\|\Phi_0\|_{\mathbf{L}^\infty_{per}(\mathbb{R})} = 1$. Define $\bar{a} = \bar{a}^\varepsilon := \max(-\frac{1}{\lambda_0}\ln\left(\frac{\nu\min(\Phi_u,\Phi_v)}{4K\max(p,q)}\right), 1)$. Then if $a \geq a_0 + \bar{a}$ and $c \geq \bar{c}^\varepsilon$, we have $\sup_{\Omega_0}(u+v) < \frac{\nu}{2}$.*
5. *If $c = 0$ and $a \geq a_0 + 1$ then*
$$\sup_{\Omega_0} (u+v) \geq \frac{-\lambda_1^\varepsilon}{\gamma^\infty} - \frac{\max(p+q)}{K}, \tag{2.2.18}$$
   where λ_1^ε is the principal eigenvalue of the operator $L_\varepsilon - A(x)$ defined in (2.2.19)*.*

Proof. 1. This is true from classical elliptic regularity. We omit the details.

2. In view of (2.2.16), the sum $S := u + v$ satisfies

$$\begin{aligned} L_\varepsilon S - cS_s &= r_u u + r_v v - \gamma_u u(u + (1-\tau)\tfrac{q}{K} + \tau v) - \gamma_v v(v + (1-\tau)\tfrac{p}{K} + \tau u) \\ &\leq r^\infty S - \gamma^0(u^2 + v^2). \end{aligned}$$

Since $S^2 = u^2 + 2uv + v^2 \leq 2(u^2 + v^2)$, we have

$$L_\varepsilon S - cS_s \leq \frac{\gamma^0}{2} S\left(\frac{2r^\infty}{\gamma^0} - S\right).$$

Since the maximum principle holds for the operator $L_\varepsilon - c\partial_s$ independently of c and $\varepsilon > 0$, S cannot have an interior local maximum which is greater than $\frac{2r^\infty}{\gamma^0}$. This along with the boundary conditions $S(-a, x) = K(p(x) + q(x))$, $S(a, x) = 0$ proves item 2.

3. Assume that there exists $(s_0, x_0) \in (-a, a) \times \mathbb{R}$ such that $u(s_0, x_0) = 0$. Since

$$L_\varepsilon u - cu_s \geq u\left[r_u(x) - \gamma_u(x)\left(u + \left(\tau v + (1-\tau)\frac{q}{K}\right)\right) - \mu(x)\right],$$

the strong maximum principle enforces $u \equiv 0$ which contradicts the boundary condition at $s = -a$. The same argument applies to v.

4. Let $\zeta(s, x) := Be^{-\lambda_0 s}\Phi_0(x)$, $B > 0$. Then we have

$$L_\varepsilon \zeta - c\zeta_s = Be^{-\lambda_0 s}\left(S_{\bar{c}^\varepsilon, \lambda_0, \varepsilon}\Phi_0 + A(x)\Phi_0 + \lambda_0(c - \bar{c}^\varepsilon)\Phi_0\right) = A(x)\zeta + \lambda_0(c - \bar{c}^\varepsilon)\zeta \geq A(x)\zeta$$

so that ζ is a strict supersolution to problem (2.2.16). By item 2, one can define

$$B_0 := \inf\left\{B > 0, \forall (s, x) \in [-a, a] \times \mathbb{R}, \begin{pmatrix} u(s, x) \\ v(s, x) \end{pmatrix} \leq \zeta(s, x)\right\} > 0$$

and $\zeta_0(s, x) = \begin{pmatrix} \zeta_u(s, x) \\ \zeta_v(s, x) \end{pmatrix} := B0e^{-\lambda_0 s}\Phi_0(x)$. From the strong maximum principle in $(-a, a) \times \mathbb{R}$, and the $s = a$ boundary condition, the touching point — between $\begin{pmatrix} u \\ v \end{pmatrix}$ and $\begin{pmatrix} \zeta_u \\ \zeta_v \end{pmatrix}$ — has to lie on $s = -a$. Thus there exists x_0 such that either $\zeta_u(-a, x_0) = u(-a, x_0)$ or $\zeta_v(-a, x_0) = v(-a, x_0)$. In any case one has $B_0 \leq Ke^{-\lambda_0 a}\frac{\max(p,q)}{\min(\Phi_u, \Phi_v)}$, which in in turn implies

$$\sup_{\Omega_0}(u + v) \leq 2B_0 e^{\lambda_0 a_0} \leq 2K\frac{\max(p, q)}{\min(\Phi_u, \Phi_v)}e^{-\lambda_0(a - a_0)} \leq 2K\frac{\max(p, q)}{\min(\Phi_u, \Phi_v)}e^{-\lambda_0 \bar{a}} \leq \frac{\nu}{2},$$

in view of the definition of $\bar{a}$. This proves item 4.

5. Assume by contradiction that $\sup_{\Omega_0}(u + v) < \frac{-\lambda_1^\varepsilon}{\gamma^\infty} - \frac{\max(p+q)}{K}$ (which in particular enforces $\lambda_1^\varepsilon < 0$). Then, in $(-a_0, a_0) \times \mathbb{R}$, we have

$$\begin{cases} L_\varepsilon u &= (r_u - \mu - \gamma_u(u + \tau v + (1-\tau)\frac{q}{K}))u + \mu v \geq (r_u - \mu + \lambda_1^\varepsilon)u + \mu v \\ L_\varepsilon v &= (r_v - \mu - \gamma_v(v + \tau u + (1-\tau)\frac{p}{K}))v + \mu u \geq (r_v - \mu + \lambda_1^\varepsilon)v + \mu u. \end{cases}$$

Denote by $\Phi^\varepsilon(s, x) := \begin{pmatrix} \bar{\varphi}(s, x) \\ \bar{\psi}(s, x) \end{pmatrix}$ the principal eigenvector associated with λ_1^ε (vanishing at $s = \pm a_0$, L periodic in x) normalized by $\|\bar{\Phi}^\varepsilon\|_{\mathbf{L}^\infty_{per}(\mathbb{R})} = 1$, see problem (2.2.19). Define

$$A_0 := \max\{A > 0 : A\bar{\varphi}(s, x) \leq u(s, x) \text{ and } A\bar{\psi}(s, x) \leq v(s, x), \forall (s, x) \in [-a_0, a_0] \times \mathbb{R}\}.$$

Then we have $A_0\bar\varphi \le u$, $A_0\bar\psi \le v$, with equality at at least one point for at least one equation, say $A_0\bar\varphi(s_0,x_0) = u(s_0,x_0)$ for some $-a_0 < s_0 < a_0$ and $x_0 \in \mathbb{R}$. But

$$L_\varepsilon(u - A_0\bar\varphi) - (r_u - \mu + \lambda_1^\varepsilon)(u - A_0\bar\varphi) \ge \mu(v - A_0\bar\psi) \ge 0,$$

so that the strong maximum principle enforces $u \equiv A_0\bar\varphi$, which is a contradiction since u is positive on $(-a,a)\times\mathbb{R}$ and $\bar\varphi$ vanishes on $\{\pm a_0\}\times\mathbb{R}$. A similar argument leads to a contradiction in the case $v(s_0,x_0) = A_0\bar\psi(s_0,x_0)$. This proves item 5.

Lemma 2.2.13 is proved. □

Item 5 of the above lemma is relevant only when $\lambda_1^\varepsilon < 0$, which is actually true if $a_0 > 0$ is large enough, as proved below. Let us denote by λ_1^ε, $\Phi^\varepsilon(s,x)$ the principal eigenvalue, eigenfunction solving the mixed Dirichlet-periodic eigenproblem

$$\begin{cases} L_\varepsilon\Phi^\varepsilon = A(x)\Phi^\varepsilon + \lambda_1^\varepsilon\Phi^\varepsilon \quad \text{ in } \Omega_0 = (-a_0,a_0)\times\mathbb{R} \\ \Phi^\varepsilon(-a_0,x) = \Phi^\varepsilon(a_0,x) = 0 \quad \forall x \in \mathbb{R} \\ \Phi^\varepsilon(s,x) \quad \text{ is periodic w.r.t. } x \\ \Phi^\varepsilon > \begin{pmatrix} 0 \\ 0 \end{pmatrix} \text{ in } \Omega_0 = (-a_0,a_0)\times\mathbb{R}. \end{cases} \tag{2.2.19}$$

Lemma 2.2.14 (An estimate for λ_1^ε)**.** *We have* $\lambda_1^\varepsilon \le ł + \frac{5}{2a_0^2}(1+\varepsilon)$.

Proof. Since the matrix $A(x)$ is symmetric, we are equipped with the Rayleigh quotient

$$\lambda_1^\varepsilon = \inf_{w\in H^1_{0,per}\times H^1_{0,per}} \frac{\int_{(-a_0,a_0)\times(0,L)} ({}^t w_x w_x + 2\,{}^t w_x w_s + (1+\varepsilon)\,{}^t w_s w_s - {}^t w A(x) w)\,\mathrm{d}s\mathrm{d}x}{\int_{(-a_0,a_0)\times(0,L)} {}^t w w\,\mathrm{d}s\mathrm{d}x}.$$

Let us denote $\Phi(x) = \begin{pmatrix} \varphi(x) \\ \psi(x) \end{pmatrix}$ the principal eigenvector solving (2.2.3), and define

$$\bar\Phi := \|\Phi\|^{-1}_{\mathbf{L}^2_{per}}\Phi.$$

We define the test function $w(s,x) := \eta(s)\bar\Phi(x)$, with $\eta(s) := \sqrt{\frac{15}{16a_0^5}}(a_0-s)(a_0+s)$, so that $\int_{(-a_0,a_0)}\eta^2(s)ds = 1$. Noticing that $\int {}^t w_x w_s \mathrm{d}x\mathrm{d}s = 0$, we get

$$\lambda_1^\varepsilon \le \int_{(0,L)} ({}^t\bar\Phi_x\bar\Phi_x - {}^t\bar\Phi A(x)\bar\Phi)(x)\mathrm{d}x + \int_{(-a_0,a_0)}(1+\varepsilon)\eta_s^2(s)\mathrm{d}s = ł + \frac{5}{2a_0^2}(1+\varepsilon),$$

which shows the result. □

Remark 2.2.15 (Consistency of the choice of parameters in Theorem 2.2.11)**.** Let us say a word on the choice of the positive parameters (a_0^*, ν_0, K_0) in Theorem 2.2.11. First, the choice of a_0^* and Lemma 2.2.14 imply that $\lambda_1^\varepsilon \le \frac{3ł}{4}$ for any $\varepsilon \in (0,1)$ and $a_0 \ge a_0^*$. Then, (2.2.18) and the choices of K_0, ν_0 imply that, for $c = 0$,

$$\sup_{\Omega_0}(u+v) \ge \frac{-ł}{2\gamma^\infty} \ge 2\nu_0.$$

In particular, item 5 in Lemma 2.2.13 gives a true lower bound for $\sup_{\Omega_0}(u+v)$ in the case $c = 0$.

2.2.4.2 Estimates for the end-point $\tau = 0$ of the first homotopy

We introduce the problem

$$\begin{cases} L_\varepsilon u - cu_s &= u(r_u - \gamma_u(u + \frac{q}{K})) + \mu v - \mu u \\ L_\varepsilon v - cv_s &= v(r_v - \gamma_v(\frac{p}{K} + v)) + \mu u - \mu v \\ (u,v)(-a,x) = (Kp(x), Kq(x)), \quad \forall x \in \mathbb{R} \\ (u,v)(a,x) = (0,0), \quad \forall x \in \mathbb{R}, \end{cases} \tag{2.2.20}$$

which corresponds to (2.2.16) with $\tau = 0$ and for which comparison methods are available. In this section we derive refined estimates for (2.2.20) that will allow us to enlarge the domain on which the degree is computed, which is necessary for the second homotopy that we will perform.

Lemma 2.2.16 (On problem (2.2.20))**.** *1. For each $c \in \mathbb{R}$, there exists a unique nonnegative solution (u,v) to* (2.2.20)*, which satisfies*

$$\forall (s,x) \in \Omega, \quad 0 < u(s,x) < Kp(x) \ \text{ and } \ 0 < v(s,x) < Kq(x). \tag{2.2.21}$$

2. Let $c \in \mathbb{R}$ and (u,v) the nonnegative solution to (2.2.20)*. Then u and v are nonincreasing in s.*

3. The mapping $c \mapsto \begin{pmatrix} u \\ v \end{pmatrix}$ is decreasing, where (u,v) is the unique nonnegative solution to (2.2.20)*.*

Proof. In this proof we denote

$$f : \left(x, \begin{pmatrix} u \\ v \end{pmatrix} \right) \mapsto \begin{pmatrix} u(r_u(x) - \gamma_u(x)(u + \frac{q}{K})) + \mu(x)v - \mu(x)u \\ v(r_v(x) - \gamma_v(x)(\frac{p}{K} + v)) + \mu(x)u - \mu(x)v \end{pmatrix} \tag{2.2.22}$$

so that (2.2.20) is recast $L_\varepsilon \begin{pmatrix} u \\ v \end{pmatrix} - c \begin{pmatrix} u \\ v \end{pmatrix}_s = f\left(x, \begin{pmatrix} u \\ v \end{pmatrix}\right)$. We select $M > 0$ large enough so that $f(x,\cdot) + MId$ is uniformly nondecreasing on $[0,C]^2$, with C the constant from Lemma 2.2.13, that is

$$\begin{pmatrix} 0 \\ 0 \end{pmatrix} \le \begin{pmatrix} u_1 \\ v_1 \end{pmatrix} \le \begin{pmatrix} u_2 \\ v_2 \end{pmatrix} \le \begin{pmatrix} C \\ C \end{pmatrix} \Rightarrow f\left(x, \begin{pmatrix} u_2 \\ v_2 \end{pmatrix}\right) - f\left(x, \begin{pmatrix} u_1 \\ v_1 \end{pmatrix}\right) \ge -M \begin{pmatrix} u_2 - u_1 \\ v_2 - v_1 \end{pmatrix},$$

for all $x \in \mathbb{R}$.

1. We first claim that $(s,x) \mapsto (Kp(x), Kq(x))$ is a strict supersolution to problem (2.2.20). Since $K \ge K_0$, we have $p + q < Kp \le Kp + \frac{q}{K}$ so that

$$\begin{aligned} L_\varepsilon(Kp) - c(Kp)_s &= -(Kp)'' \\ &= (Kp)(r_u(x) - \gamma_u(x)(p+q)) + \mu(x)Kq - \mu(x)Kp \\ &> (Kp)(r_u(x) - \gamma_u(x)(Kp + \tfrac{q}{K})) + \mu(x)(Kq) - \mu(x)(Kp), \end{aligned}$$

and similarly

$$L_\varepsilon(Kq) - c(Kq)_s > (Kq)(r_v(x) - \gamma_v(x)(\tfrac{p}{K} + Kq)) + \mu(x)(Kp) - \mu(x)(Kq),$$

which proves the claim. Obviously, $(s,x) \mapsto \begin{pmatrix} 0 \\ 0 \end{pmatrix}$ is a strict subsolution to problem (2.2.20) because of the boundary condition at $s = -a$. Since system (2.2.20) is cooperative, the classical monotone

iteration method shows that, for any $c \in \mathbb{R}$, there exists at least a solution (u, v) to problem (2.2.20) which satisfies (2.2.21).

Next, in order to prove uniqueness, let (u, v) and $(\tilde{u}, \tilde{v})$ be two nonnegative solutions to (2.2.20), such that $(u, v) \neq (\tilde{u}, \tilde{v})$. Then, for any $0 < \zeta < 1$, $(U^\zeta, V^\zeta) := (\zeta u, \zeta v)$ satisfies

$$\begin{cases} L_\varepsilon U^\zeta - cU^\zeta_s &= U^\zeta(r_u - \gamma_u \frac{q}{K} - \mu - \frac{\gamma_u(x)}{\zeta} U^\zeta) + \mu(x) V^\zeta \\ &< U^\zeta(r_u - \gamma_u \frac{q}{K} - \mu - \gamma_u(x) U^\zeta) + \mu(x) V^\zeta \\ L_\varepsilon V^\zeta - cV^\zeta_s &= V^\zeta(r_v - \gamma_v \frac{p}{K} - \mu - \frac{\gamma_v(x)}{\zeta} V^\zeta) + \mu(x) U^\zeta \\ &< V^\zeta(r_v - \gamma_v \frac{p}{K} - \mu - \gamma_v(x) V^\zeta) + \mu(x) U^\zeta \\ (U^\zeta, V^\zeta)(-a, x) = (\zeta K p(x), \zeta K q(x)) \leq (K p(x), K q(x)) \\ (U^\zeta, V^\zeta)(a, x) = (0, 0), \end{cases}$$

and is therefore a strict subsolution to problem (2.2.20). From Hopf lemma we know that $(\tilde{u}_s, \tilde{v}_s)(a, x) < (0, 0)$ so that we can define

$$\zeta_0 := \sup\{\zeta > 0 : (U^\zeta, V^\zeta)(s, x) < (\tilde{u}, \tilde{v})(s, x), \forall (s, x) \in \Omega\} > 0.$$

Then we have $(0, 0) \leq (U^{\zeta_0}, V^{\zeta_0}) \leq (\tilde{u}, \tilde{v}) \leq (C, C)$. Assume by contradiction that $\zeta_0 < 1$. Then we have

$$\begin{cases} L_\varepsilon(\tilde{u} - U^{\zeta_0}) - c(\tilde{u} - U^{\zeta_0})_s + M(\tilde{u} - U^{\zeta_0}) &\geq 0 \\ L_\varepsilon(\tilde{v} - V^{\zeta_0}) - c(\tilde{v} - V^{\zeta_0})_s + M(\tilde{v} - V^{\zeta_0}) &\geq 0 \\ (\tilde{u} - U^{\zeta_0}, \tilde{v} - V^{\zeta_0})(-a, x) \geq (0, 0) \\ (\tilde{u} - U^{\zeta_0}, \tilde{v} - V^{\zeta_0})(a, x) = (0, 0). \end{cases}$$

From Hopf lemma we deduce

$$((\tilde{u} - U^{\zeta_0})_s, (\tilde{v} - V^{\zeta_0})_s)(a, x) < (0, 0)$$

so that there exists $(s_0, x_0) \in (-a, a) \times \mathbb{R}$ such that, say, $\tilde{u}(s_0, x_0) = U^{\zeta_0}(s_0, x_0)$. From the strong maximum principle we deduce $\tilde{u} \equiv U^{\zeta_0}$, which is a contradiction in view of the boundary condition at $s = -a$. We conclude that $\zeta_0 \geq 1$ and thus $(u, v) \leq (\tilde{u}, \tilde{v})$. Then exchanging the roles of (u, v) and $(\tilde{u}, \tilde{v})$ in the above argument, we get that $(\tilde{u}, \tilde{v}) \leq (u, v)$ so that finally $(\tilde{u}, \tilde{v}) = (u, v)$. This is in contradiction with our initial hypothesis. We conclude that the nonnegative solution to equation (2.2.20) is unique.

2. For given $c \in \mathbb{R}$, let (u, v) be the solution to (2.2.20). In order to use a sliding technique, we define

$$(u^t(s, x), v^t(s, x)) := (u(s + t, x), v(s + t, x))$$

for $t > 0$ and $(s, x) \in [-a, a - t] \times \mathbb{R}$. From the boundary conditions, there is $\delta > 0$ such that

$$\forall t \in (2a - \delta, 2a), \forall (s, x) \in (-a, a - t) \times \mathbb{R}, \quad u^t(s, x) < u(s, x) \text{ and } v^t(s, x) < v(s, x).$$

In particular, one can define

$$t_0 := \inf\{t > 0, \forall (s, x) \in [-a, a - t],\ u^t(s, x) \leq u(s, x) \text{ and } v^t(s, x) \leq v(s, x)\}.$$

Assume by contradiction that $t_0 > 0$. Then there exists $(s_0, x_0) \in (-a, a - t_0) \times \mathbb{R}$ such that, say, $u^{t_0}(s_0, x_0) = u(s_0, x_0)$ (notice that $s_0 = -a$ and $s_0 = a - t_0$ are prevented by (2.2.21)). Since we have

$$L_\varepsilon \begin{pmatrix} u^{t_0} - u \\ v^{t_0} - v \end{pmatrix} - c \begin{pmatrix} u^{t_0} - u \\ v^{t_0} - v \end{pmatrix}_s + M \begin{pmatrix} u^{t_0} - u \\ v^{t_0} - v \end{pmatrix} = (f + M) \begin{pmatrix} u^{t_0} \\ v^{t_0} \end{pmatrix} - (f + M) \begin{pmatrix} u \\ v \end{pmatrix} \leq 0$$

and $\begin{pmatrix} u^{t_0} - u \\ v^{t_0} - v \end{pmatrix} \leq 0$, the strong maximum principle implies $u^{t_0} \equiv u$, which contradicts $0 < u < Kp$. We conclude that $t_0 = 0$, which means that u and v are nonincreasing in s.

3. Let (c,u,v) and $(\tilde{c},\tilde{u},\tilde{v})$ two solutions of equation (2.2.20) with $c<\tilde{c}$. As above, we define

$$(\tilde{u}^t(s,x),\tilde{v}^t(s,x)):=(\tilde{u}(s+t,x),\tilde{v}(s+t,x)),$$

and

$$t_0:=\inf\{t>0,\forall(s,x)\in[-a,a-t],\ \tilde{u}^t(s,x)\leq u(s,x) \text{ and } \tilde{v}^t(s,x)\leq v(s,x)\}.$$

Assume by contradiction that $t_0>0$. Then there again exists $(s_0,x_0)\in(-a,a-t_0)\times\mathbb{R}$ such that, say, $\tilde{u}^{t_0}(s_0,x_0)=u(s_0,x_0)$. Moreover we have

$$\begin{aligned}
&L_\varepsilon\begin{pmatrix}\tilde{u}^{t_0}-u\\ \tilde{v}^{t_0}-v\end{pmatrix}-c\begin{pmatrix}\tilde{u}^{t_0}-u\\ \tilde{v}^{t_0}-v\end{pmatrix}_s+M\begin{pmatrix}\tilde{u}^{t_0}-u\\ \tilde{v}^{t_0}-v\end{pmatrix}\\
&=(f+M)\begin{pmatrix}\tilde{u}^{t_0}\\ \tilde{v}^{t_0}\end{pmatrix}-(f+M)\begin{pmatrix}u\\ v\end{pmatrix}+(\tilde{c}-c)\begin{pmatrix}\tilde{u}^{t_0}\\ \tilde{v}^{t_0}\end{pmatrix}_s\\
&\leq\begin{pmatrix}0\\ 0\end{pmatrix},
\end{aligned}$$

since $\tilde{u}_s\leq 0$ and $\tilde{v}_s\leq 0$ (recall that $\tilde{u}$ and $\tilde{v}$ are decreasing), so that we again derive a contradiction. As a result $t_0=0$, that is $\begin{pmatrix}\tilde{u}\\ \tilde{v}\end{pmatrix}\leq\begin{pmatrix}u\\ v\end{pmatrix}$ and then $\begin{pmatrix}\tilde{u}\\ \tilde{v}\end{pmatrix}<\begin{pmatrix}u\\ v\end{pmatrix}$ from the strong maximum principle.

The lemma is proved. □

2.2.4.3 Estimates along the second homotopy

The second homotopy allows us to get rid of the nonlinearity and the coupling in u and v at the expense of an increased linear part. For $0\leq\tau\leq 1$, we consider

$$\begin{cases}
L_\varepsilon u-cu_s &= \tau\left(u\left(r_u-\gamma_u\frac{q}{K}-\mu-\gamma_u u\right)+\mu v\right)-(1-\tau)\mathcal{C}u\\
L_\varepsilon v-cv_s &= \tau\left(v\left(r_v-\gamma_v\frac{p}{K}-\mu-\gamma_v v\right)+\mu u\right)-(1-\tau)\mathcal{C}v\\
(u,v)(-a,x)=(Kp(x),Kq(x)),\quad \forall x\in\mathbb{R}\\
(u,v)(a,x)=(0,0),\quad \forall x\in\mathbb{R},
\end{cases}\tag{2.2.23}$$

with

$$\mathcal{C}:=-\min_{x\in\mathbb{R}}\left(r_u(x)-\gamma_u(x)\left(\frac{q(x)}{K}+C\right)-\mu(x),r_v(x)-\gamma_v(x)\left(\frac{p(x)}{K}+C\right)-\mu(x),0\right)\tag{2.2.24}$$

where C is as in Lemma 2.2.13 item 2.

Lemma 2.2.17 (A priori estimates along the second homotopy)**.** *Let a nonnegative $(u,v)\in\mathbf{C}^1_{per}(\Omega)$ (where $\Omega=(-a,a)\times\mathbb{R}$ and the periodicity is understood only w.r.t. the $x\in\mathbb{R}$ variable) and $c\in\mathbb{R}$ solve* (2.2.23)*, with $0\leq\tau\leq 1$. Then*

1. *(u,v) is a classical solution to* (2.2.23)*, i.e. $(u,v)\in\mathbf{C}^2(\overline{\Omega})$.*
2. *We have*
$$u(s,x)+v(s,x)\leq C,\quad\forall(s,x)\in\bar{\Omega}=[-a,a]\times\mathbb{R}.$$
3. *(u,v) is positive in Ω.*
4. *If $a\geq a_0+\bar{a}$ and $c\geq\bar{c}^\varepsilon$, we have $\sup_{\Omega_0}(u+v)<\frac{\nu}{2}$, where $\bar{a}$ is as in Lemma 2.2.13 item 4.*
5. *There exists $\underline{c}=\underline{c}(a)\geq 0$ such that if $c\leq-\underline{c}(a)$ then $\sup_{\Omega_0}(u+v)>\nu$.*

Proof. Items 1, 2, 3 and 4 can be proved as in Lemma 2.2.13. We therefore omit the details, and only focus on item 5.

From item 2 and the choice of $\mathcal{C}$ we see that, for any $0 \leq \tau \leq 1$,

$$L_\varepsilon u - cu_s + \mathcal{C}u \geq 0, \quad u(-a,x) = Kp(x), \quad u(a,x) = 0.$$

Now, let $\alpha_\pm := \frac{-c \pm \sqrt{c^2+4(1+\varepsilon)\mathcal{C}}}{2(1+\varepsilon)}$ and $m := K \min_{x\in\mathbb{R}} (p(x), q(x)) > 0$. Then the function $\theta(s,x) = \theta(s) := m\frac{e^{\alpha_- s+\alpha_+ a} - e^{\alpha_+ s+\alpha_- a}}{e^{(\alpha_+-\alpha_-)a} - e^{(\alpha_- -\alpha_+)a}}$ solves

$$L_\varepsilon \theta - c\theta_s + \mathcal{C}\theta = 0, \quad \theta(-a) = m, \quad \theta(a) = 0.$$

From the comparison principle, we infer that $u(s,x) \geq \theta(s)$, and similarly $v(s,x) \geq \theta(s)$, for all $(s,x) \in (-a,a)\times\mathbb{R}$. As a result $\sup_{\Omega_0} (u+v) \geq 2\sup_{(-a_0,a_0)} \theta \geq 2\theta(0)$.

Next, for $c \leq -c^1(a) := -\frac{1+\varepsilon}{a} \ln 4$ one has $e^{(\alpha_- -\alpha_+)a} \leq \frac{1}{4}$ so that

$$\theta(0) \geq m\frac{e^{\alpha_+ a} - e^{\alpha_- a}}{e^{(\alpha_+-\alpha_-)a}} = me^{\alpha_- a}\left(1 - e^{(\alpha_- -\alpha_+)a}\right) \geq m\frac{3e^{\alpha_- a}}{4}.$$

Next, thanks to a Taylor expansion, we have

$$\alpha_- = \frac{-c}{2(1+\varepsilon)}\left(1 - \sqrt{1 + \frac{4(1+\varepsilon)\mathcal{C}}{c^2}}\right) = \frac{-c}{2(1+\varepsilon)}\left(-\frac{2(1+\varepsilon)\mathcal{C}}{c^2} + o\left(\frac{1}{c^2}\right)\right) = \frac{\mathcal{C}}{c} + o\left(\frac{1}{|c|}\right)$$

so that there exists $c^2 = c^2(a) > 0$ such that for any $c \leq -c^2(a)$ we have $e^{\alpha_- a} > \frac{2}{3}$. As a result when $c \leq -\underline{c}(a) := -\max(c^1(a), c^2(a))$, we have

$$\sup_{\Omega_0} (u+v) \geq m \geq \nu_0 > \nu,$$

which proves item 5. □

2.2.4.4 Proof of Theorem 2.2.11

Equipped with the above estimates, we are now in the position to prove Theorem 2.2.11 using three homotopies and the Leray Schauder topological degree. To do so, let us define the following open subset of $\mathbb{R}\times\mathbf{C}^1_{per}(\Omega)$

$$\Gamma := \left\{ \left(c, \begin{pmatrix} u \\ v \end{pmatrix}\right) \in \mathbb{R}\times\mathbf{C}^1_{per}(\Omega) : c \in (0, \overline{c}^\varepsilon + \varepsilon), \begin{pmatrix} 0 \\ 0 \end{pmatrix} < \begin{pmatrix} u \\ v \end{pmatrix} < \begin{pmatrix} C \\ C \end{pmatrix} \text{ in } \Omega \right\}$$

where $\Omega = (-a,a)\times\mathbb{R}$, and $C > 0$ is the constant defined in Lemma 2.2.13 item 2.

• We develop the first homotopy argument. For $0 \leq \tau \leq 1$, let us define the operator

$$F_\tau : \quad \mathbb{R}\times\mathbf{C}^1_{per}(\Omega) \quad \to \quad \mathbb{R}\times\mathbf{C}^1_{per}(\Omega)$$

where $F_\tau\left(c, \begin{pmatrix} u \\ v \end{pmatrix}\right) = \left(\tilde{c}, \begin{pmatrix} \tilde{u} \\ \tilde{v} \end{pmatrix}\right)$, with

$$\tilde{c} = c + \sup_{\Omega_0} (\tilde{u} + \tilde{v}) - \nu$$

and $\begin{pmatrix} \tilde{u} \\ \tilde{v} \end{pmatrix}$ is the unique solution in $\mathbf{C}^1_{per}(\Omega)$ of the linear problem

$$\begin{cases} L_\varepsilon \tilde{u} - c\tilde{u}_s &= u(r_u - \gamma_u(u + (\tau v + (1-\tau)\frac{q}{K}))) + \mu v - \mu u \\ L_\varepsilon \tilde{v} - c\tilde{v}_s &= v(r_v - \gamma_v((\tau u + (1-\tau)\frac{p}{K}) + v)) + \mu u - \mu v \\ (u,v)(-a,x) = (Kp(x), Kq(x)), \quad \forall x \in \mathbb{R} \\ (u,v)(a,x) = (0,0), \quad \forall x \in \mathbb{R}. \end{cases}$$

From standard elliptic estimates, for any $0 \leq \tau \leq 1$, F_τ maps $\mathbf{C}^1_{per}(\Omega)$ into $\mathbf{C}^2_{per}(\overline{\Omega})$, which shows that F_τ is a compact operator in $\mathbf{C}^1_{per}(\Omega)$. Moreover F_τ depends continuously on the parameter $0 \leq \tau \leq 1$. The Leray-Schauder topological argument can thus be applied: in order to prove that the degree is independent of the parameter τ, it suffices to show that there is no fixed point of F_τ on the boundary $\partial\Gamma$, which will be a consequence of estimates in section 2.2.4.1. Indeed, let $\left(c, \begin{pmatrix} u \\ v \end{pmatrix}\right) = (c, u, v)$ be a fixed point of F_τ in $\overline{\Gamma}$.

1. From Lemma 2.2.13, Lemma 2.2.14 and Remark 2.2.15 we know that if $c = 0$ then $\sup_{\Omega_0} (u + v) > \nu$ so that $\tilde{c} > c$, which is absurd. That shows $c \neq 0$.
2. From Lemma 2.2.13 we know that if $c \geq \bar{c}^\varepsilon$ then $\sup_{\Omega_0} (u + v) < \nu$ so that $\tilde{c} < c$, which is absurd. That shows $c < \bar{c}^\varepsilon + \varepsilon$.
3. From Lemma 2.2.13 we know that $u < C$ and $v < C$.
4. From Lemma 2.2.13 and the boundary condition at $s = -a$, we know that $u > 0$ and $v > 0$ in $[-a, a) \times \mathbb{R}$. Moreover, we know from Hopf lemma that $\forall x \in \mathbb{R}$, $u_s(a, x) < 0$ and $v_s(a, x) < 0$.

As a result, $(c, u, v) \notin \partial\Gamma$ so that

$$\deg(Id - F_1, \Gamma, 0) = \deg(Id - F_0, \Gamma, 0). \tag{2.2.25}$$

• We now consider the second homotopy. For $0 \leq \tau \leq 1$, let us define the operator

$$\begin{array}{rccc} G_\tau : & \mathbb{R} \times \mathbf{C}^1_{per}(\Omega) & \to & \mathbb{R} \times \mathbf{C}^1_{per}(\Omega) \\ & \left(c, \begin{pmatrix} u \\ v \end{pmatrix}\right) & \mapsto & \left(\tilde{c}, \begin{pmatrix} \tilde{u} \\ \tilde{v} \end{pmatrix}\right) \end{array}$$

with again

$$\tilde{c} = c + \sup_{\Omega_0} (\tilde{u} + \tilde{v}) - \nu$$

and $\begin{pmatrix} \tilde{u} \\ \tilde{v} \end{pmatrix}$ is the unique solutions in $\mathbf{C}^1_{per}(\Omega)$ of the linear problem

$$\begin{cases} L_\varepsilon \tilde{u} - c\tilde{u}_s + (1-\tau)\mathcal{C}\tilde{u} &= \tau\left(u\left(r_u - \gamma_u \frac{q}{K} - \mu - \gamma_u u\right) + \mu v\right) \\ L_\varepsilon \tilde{v} - c\tilde{v}_s + (1-\tau)\mathcal{C}\tilde{v} &= \tau\left(v\left(r_v - \gamma_v \frac{p}{K} - \mu - \gamma_v v\right) + \mu u\right) \\ (u, v)(-a, x) = (Kp(x), Kq(x)), \quad \forall x \in \mathbb{R} \\ (u, v)(a, x) = (0, 0), \quad \forall x \in \mathbb{R}, \end{cases}$$

and $\mathcal{C}$ is defined by (2.2.24). Notice that G_τ is a continuous family of compact operators and that $G_1 = F_0$. From Lemma 2.2.13 and Lemma 2.2.16, we see that there is no fixed point of F_0 such that $c \leq 0$ since $c \mapsto \begin{pmatrix} u \\ v \end{pmatrix}$ is nonincreasing. As a result enlarging Γ into

$$\tilde{\Gamma} := \left\{ \left(c, \begin{pmatrix} u \\ v \end{pmatrix}\right) \in \mathbb{R} \times \mathbf{C}^1_{per}(\Omega) : c \in (-\underline{c}(a), \bar{c}^\varepsilon + \varepsilon), \begin{pmatrix} 0 \\ 0 \end{pmatrix} < \begin{pmatrix} u \\ v \end{pmatrix} < \begin{pmatrix} C \\ C \end{pmatrix} \text{ in } \Omega \right\},$$

with $\underline{c}(a) \geq 0$ as in Lemma 2.2.17, does not alter the degree, that is

$$\deg(Id - F_0, \Gamma, 0) = \deg(Id - F_0, \tilde{\Gamma}, 0) = \deg(Id - G_1, \tilde{\Gamma}, 0). \tag{2.2.26}$$

Next, using the estimates of Lemma 2.2.17 and Hopf lemma as above, we see that there is no fixed point of G_τ on the boundary $\partial\tilde{\Gamma}$. We have then

$$\deg(Id - G_1, \tilde{\Gamma}, 0) = \deg(Id - G_0, \tilde{\Gamma}, 0). \tag{2.2.27}$$

Now G_0 is independent of (u, v). Since $L_\varepsilon - c\partial_s + \mathcal{C}Id$ is invertible for each $c \in \mathbb{R}$, there exists exactly one solution of (2.2.23) with $\tau = 0$ for each $c \in \mathbb{R}$, which we denote (u_c, v_c). Thanks to a sliding argument, which we omit here, the solutions to (2.2.23) with $\tau = 0$ are nonincreasing in s and $c \mapsto (u_c, v_c)$ is decreasing, so that there exists a unique $c \in (-\underline{c}(a), \bar{c}^\varepsilon + \varepsilon)$, which we denote c_0, such that (c_0, u_{c_0}, v_{c_0}) is a fixed point to G_0.

• Finally a third homotopy allows us to compute the degree. For $0 \le \tau \le 1$, let us define the operator $H_\tau : \mathbb{R} \times \mathbf{C}^1_{per}(\Omega) \to \mathbb{R} \times \mathbf{C}^1_{per}(\Omega)$ by

$$H_\tau(c, u, v) = \left(c + \sup_{\Omega_0} (u_c + v_c) - \nu, \tau u_c + (1-\tau)u_{c_0}, \tau v_c + (1-\tau)v_{c_0} \right).$$

Noticing that $H_1 = G_0$ and that, again, H_τ has no fixed point on the boundary $\partial\tilde{\Gamma}$, we obtain

$$\deg(Id - G_0, \tilde{\Gamma}, 0) = \deg(Id - H_1, \tilde{\Gamma}, 0) = \deg(Id - H_0, \tilde{\Gamma}, 0). \tag{2.2.28}$$

Then since H_0 has separated variables and $c \mapsto \sup_{\Omega_0} (u_c + v_c)$ is decreasing, we see that

$$\deg(Id - H_0, \tilde{\Gamma}, 0) = 1. \tag{2.2.29}$$

• Combining (2.2.25), (2.2.26), (2.2.27), (2.2.28) and (2.2.29), we get $\deg(Id - F_1, \Gamma, 0) = 1$, which shows the existence of a solution to (2.2.14) in $\mathbf{C}^1_{per}(\Omega)$. Theorem 2.2.11 is proved. □

2.2.5 Pulsating fronts

From the previous section 2.2.4.4, we are equipped with a solution to (2.2.14) in the strip $(-a, a) \times \mathbb{R}$. From the estimates of Theorem 2.2.11 and standard elliptic estimates, we can — up to a subsequence— let $a \to \infty$ and then recover, for any $0 < \varepsilon < 1$, a speed $0 \le c = c^\varepsilon < \bar{c}^\varepsilon + \varepsilon$ and smooth profiles $(0, 0) < (u(s, x), v(s, x)) = (u^\varepsilon(s, x), v^\varepsilon(s, x)) < (C, C)$ solving

$$\begin{cases} -u_{xx} - 2u_{xs} - (1+\varepsilon)u_{ss} - cu_s &= u(r_u - \gamma_u(u+v)) + \mu v - \mu u \quad \text{in } \mathbb{R}^2 \\ -v_{xx} - 2v_{xs} - (1+\varepsilon)v_{ss} - cv_s &= v(r_v - \gamma_v(u+v)) + \mu u - \mu v \quad \text{in } \mathbb{R}^2 \\ (u, v)(s, \cdot) \quad \text{is } L\text{-periodic} \\ \sup_{\Omega_0} (u + v) = \nu. \end{cases} \tag{2.2.30}$$

Notice that, by reproducing the proof of item 5 in Lemma 2.2.13, it is immediately seen that $0 < c = c^\varepsilon$. Let us mention again that, because of the lack of comparison, we do not know that the above solution is decreasing in s, in sharp contrast with the previous results on pulsating fronts [398], [48], [221], [50], [197], [199]. To overcome this lack of monotony, further estimates will be required.

Now, the main difficulty is to show that, letting $\varepsilon \to 0$, we recover a nonzero speed and thus a pulsating front. To do so, it is not convenient to use the (s, x) variables, and we therefore switch to functions

$$\tilde{u}(t, x) := u(x - ct, x), \quad \tilde{v}(t, x) := v(x - ct, x), \quad (t, x) \in \mathbb{R}^2,$$

which are consistent with Definition 2.2.5 of a pulsating front. Hence, after dropping the tildes, (2.2.30) is recast

$$\begin{cases} -\frac{\varepsilon}{c^2} u_{tt} - u_{xx} + u_t &= u(r_u - \gamma_u(u+v)) + \mu v - \mu u \quad \text{in } \mathbb{R}^2 \\ -\frac{\varepsilon}{c^2} v_{tt} - v_{xx} + v_t &= v(r_v - \gamma_v(u+v)) + \mu u - \mu v \quad \text{in } \mathbb{R}^2 \\ \sup_{x - ct \in (-a_0, a_0)} u(t, x) + v(t, x) = \nu. \end{cases} \tag{2.2.31}$$

Also the L periodicity for (2.2.30) is transferred into the constraint (2.2.6) for (2.2.31). Moreover, up to a translation, we can assume w.l.o.g. that the solution to (2.2.31) satisfies

$$\sup_{x\in(-a_0,a_0)} (u(0,x)+v(0,x)) = \nu. \tag{2.2.32}$$

Also, though t can be interpreted as a time, we would like to stress out that (2.2.31) is not a Cauchy problem.

Our first goal in this section 2.2.5 is to let $\varepsilon \to 0$ in (2.2.31) and get the following.

Theorem 2.2.18 (Letting the regularization tend to zero)**.** *There exist a speed $0 < c \le \bar{c}^0 := \lim_{\varepsilon\to 0} \bar{c}^\varepsilon$ (see Lemma 2.2.12) and positive profiles (u,v) solving, in the classical sense,*

$$\begin{cases} u_t - u_{xx} &= u(r_u - \gamma_u(u+v)) + \mu(v-u) \quad \text{in } \mathbb{R}^2 \\ v_t - v_{xx} &= v(r_v - \gamma_v(u+v)) + \mu(u-v) \quad \text{in } \mathbb{R}^2, \end{cases} \tag{2.2.33}$$

satisfying the constraint (2.2.6) *and, for some $a_0 > 0$, the normalization*

$$\sup_{x-ct\in(-a_0,a_0)} (u+v) = \nu.$$

The present section 2.2.5 is organized as follows. After proving further estimates on solutions to (2.2.31) in section 2.2.5.1, we prove Theorem 2.2.18 in section 2.2.5.2, the main difficulty being to exclude the possibility of a standing wave. Finally, in section 2.2.5.3 we conclude the construction of a pulsating front, thus proving our main result Theorem 2.2.6.

2.2.5.1 Lower estimates on solutions to (2.2.31)

We start by showing a uniform lower bound on the solutions to (2.2.31) that have a positive lower bound. The argument relies on the sign of the eigenvalue ł, or more precisely that of the first eigenvalue to the stationary Dirichlet problem in large bounded domains. For $b > 0$, we denote (λ_1^b, Φ^b) with $\Phi^b(x) := \begin{pmatrix} \varphi^b(x) \\ \psi^b(x) \end{pmatrix}$ the unique eigenpair solving

$$\begin{cases} -\Phi^b_{xx} - A(x)\Phi^b = \lambda_1^b \Phi^b \\ \varphi^b(x) > 0,\ \psi^b(x) > 0, \quad x \in (-b,b) \\ \varphi^b(\pm b) = \psi^b(\pm b) = 0, \end{cases} \tag{2.2.34}$$

and $\|\Phi^b\|_{\mathbf{L}^\infty(-b,b)} = 1$. From Lemma 2.2.27, we know that $\lambda_1^b \to ł < 0$ when $b \to \infty$. We can thus select $a_1 > a_0^*$, with a_0^* as in Theorem 2.2.11, large enough so that

$$b \ge a_1 \Rightarrow \lambda_1^b \le \frac{3ł}{4}. \tag{2.2.35}$$

Also, from Hopf lemma we have $C^b := \sup_{x\in(-b,b)} \left(\frac{\varphi^b(x)}{\psi^b(x)}, \frac{\psi^b(x)}{\varphi^b(x)} \right) < +\infty$.

Lemma 2.2.19 (A uniform lower estimate)**.** *Let $(u(t,x), v(t,x))$ be a classical positive solution to*

$$\begin{cases} \beta u_t - \kappa u_{tt} - u_{xx} &= u(r_u - \gamma_u(u+v)) + \mu v - \mu u \quad \text{in } \mathbb{R}^2 \\ \beta v_t - \kappa v_{tt} - v_{xx} &= v(r_v - \gamma_v(u+v)) + \mu u - \mu v \quad \text{in } \mathbb{R}^2, \end{cases} \tag{2.2.36}$$

with $\kappa \ge 0$ and $\beta \in \mathbb{R}$. Let also $b \ge a_1$ and Φ^b the solution to (2.2.34)*.*

Then there exists a constant $\alpha_0 = \alpha_0(\mu^0, \gamma^\infty, \lambda_1^b, C^b) > 0$ such that if

$$\inf_{(t,x)\in\mathbb{R}\times(-b,b)} \min(u(t,x), v(t,x)) > 0$$

then

$$\forall (t,x) \in \mathbb{R}\times(-b,b),\ \begin{pmatrix} u(t,x) \\ v(t,x) \end{pmatrix} \ge \alpha_0 \Phi^b(x).$$

Proof. Let $0 < \eta \leq 1$ be given. For $\alpha > 0$, we define

$$\begin{pmatrix} U^{\alpha,\eta}(t,x) \\ V^{\alpha,\eta}(t,x) \end{pmatrix} := \alpha(1-\eta t^2) \begin{pmatrix} \varphi^b(x) \\ \psi^b(x) \end{pmatrix}.$$

Then for small $\alpha < \min\left(\inf_{(t,x)\in\mathbb{R}\times(-b,b)} u, \inf_{(t,x)\in\mathbb{R}\times(-b,b)} v \right)$ we have $\begin{pmatrix} U^{\alpha,\eta}(t,x) \\ V^{\alpha,\eta}(t,x) \end{pmatrix} \leq \begin{pmatrix} u(t,x) \\ v(t,x) \end{pmatrix}$ for all $(t,x) \in \mathbb{R}\times(-b,b)$, whereas for large $\alpha > \frac{\max(u(0,0),v(0,0))}{\min(\varphi^b(0),\psi^b(0))}$ one has $\begin{pmatrix} U^{\alpha,\eta}(0,0) \\ V^{\alpha,\eta}(0,0) \end{pmatrix} > \begin{pmatrix} u(0,0) \\ v(0,0) \end{pmatrix}$. Thus we can define

$$\alpha_0^\eta = \alpha_0 := \sup\left\{ \alpha > 0, \forall (t,x) \in \mathbb{R}\times(-b,b), \begin{pmatrix} U^{\alpha,\eta}(t,x) \\ V^{\alpha,\eta}(t,x) \end{pmatrix} \leq \begin{pmatrix} u(t,x) \\ v(t,x) \end{pmatrix} \right\} > 0.$$

Assume by contradiction that

$$\alpha_0 \leq \alpha_0^* := \min\left(1, \frac{\mu^0}{2\gamma^\infty}, \frac{-\lambda_1^b}{2(1+2C^b)\gamma^\infty}\right).$$

There exists a touching point $(t_0,x_0) \in (-\sqrt{\eta},\sqrt{\eta})\times(-b,b)$ such that either $u(t_0,x_0) = U^{\alpha_0,\eta}(t_0,x_0)$ or $v(t_0,x_0) = V^{\alpha_0,\eta}(t_0,x_0)$. Assume $u(t_0,x_0) = U^{\alpha_0,\eta}(t_0,x_0)$ for instance. Then $u - U^{\alpha_0,\eta}$ reaches a zero minimum at (t_0,x_0) so that

$$\begin{aligned} 0 &\geq \beta\left(u-U^{\alpha_0,\eta}\right)_t - \kappa\left(u-U^{\alpha_0,\eta}\right)_{tt} - \left(u-U^{\alpha_0,\eta}\right)_{xx} \\ &= (\beta u_t - \kappa u_{tt} - u_{xx}) + \alpha_0(1-\eta t_0^2)\varphi^b_{xx} + 2\alpha_0\beta\eta t_0\varphi^b - 2\alpha_0\kappa\eta\varphi^b \end{aligned}$$

at point (t_0,x_0). Using (2.2.34) and (2.2.36) yields

$$0 \geq u(r_u - \mu - \gamma_u(u+v)) + \mu v - \alpha_0(1-\eta t_0^2)(\varphi^b(r_u - \mu + \lambda_1^b) + \mu\psi^b) + 2\alpha_0\eta\varphi^b(\beta t_0 - \kappa)$$

at point (t_0,x_0), and since $u(t_0,x_0) = \alpha_0(1-\eta t_0^2)\varphi^b(x_0)$ we end up with

$$0 \geq u_0[-\lambda_1^b - \gamma_u(x_0)(u_0+v_0)] + \mu(x_0)[v_0 - \alpha_0(1-\eta t_0^2)\psi^b(x_0)] + 2\alpha_0\eta\varphi^b(x_0)(\beta t_0 - \kappa), \tag{2.2.37}$$

with the notations $u_0 = u(t_0,x_0)$, $v_0 = v(t_0,x_0)$. Now two cases may occur.

• Assume first that $v_0 \leq 2\alpha_0(1-\eta t_0^2)\psi^b(x_0)$. Then we have

$$v_0 \leq 2\alpha_0(1-\eta t_0^2)\frac{\psi^b(x_0)}{\varphi^b(x_0)}\varphi^b(x_0) \leq 2C^b u_0,$$

and since $v_0 - \alpha_0(1-\eta t_0^2)\psi^b(x_0) \geq 0$, we deduce from (2.2.37) that

$$\gamma_u(x_0)(1+2C^b)u_0^2 \geq -\lambda_1^b u_0 + 2\alpha_0\eta\varphi^b(x_0)(\beta t_0 - \kappa),$$

which in turn implies

$$\gamma^\infty(1+2C^b)\alpha_0 \geq \gamma_u(x_0)(1+2C^b)u_0 \geq -\lambda_1^b + \frac{2\alpha_0\eta\varphi^b(x_0)(\beta t_0-\kappa)}{u_0} \geq -\lambda_1^b - \frac{2\eta}{\inf u}(|\beta||t_0| + \kappa),$$

since $\alpha_0 \leq 1$ and $\varphi^b \leq 1$. Since $|t_0| \leq \frac{1}{\sqrt{\eta}}$, one then has

$$\alpha_0 \geq \frac{-\lambda_1^b}{(1+2C^b)\gamma^\infty} - 2\sqrt{\eta}\frac{|\beta|+\kappa}{(1+2C^b)\gamma^\infty \inf u}. \tag{2.2.38}$$

• On the other hand, assume $v_0 \geq 2\alpha_0(1-\eta t_0^2)\psi^b(x_0)$. Then we deduce from (2.2.37) that

$$\begin{aligned} \gamma_u(x_0)u_0^2 &\geq -\lambda_1^b u_0 + \frac{\mu(x_0)}{2}(v_0 - 2\alpha_0(1-\eta t_0^2)\psi^b(x_0)) + v_0\left(\frac{\mu(x_0)}{2} - \gamma_u(x_0)u_0\right) \\ &\quad + 2\alpha_0\eta\varphi^b(x_0)(\beta t_0 - \kappa) \\ &\geq -\lambda_1^b u_0 + 2\alpha_0\eta\varphi^b(x_0)(\beta t_0 - \kappa), \end{aligned}$$

since $\gamma_u u \leq \gamma_u \alpha_0^* \leq \frac{\mu^0}{2}$. Arguing as in the first case, we end up with

$$\alpha_0 \geq \frac{-\lambda_1^b}{\gamma^\infty} - 2\sqrt{\eta}\frac{|\beta|+\kappa}{\gamma^\infty \inf u}. \tag{2.2.39}$$

From (2.2.38) , (2.2.39) and the symmetric situation where $v(t_0,x_0) = V^{\alpha_0,\eta}(t_0,x_0)$, we deduce that, in any case,

$$\alpha_0 \geq \frac{-\lambda_1^b}{(1+2C^b)\gamma^\infty} - 2\sqrt{\eta}\frac{|\beta|+\kappa}{\gamma^\infty \inf(u,v)}. \tag{2.2.40}$$

One sees that for

$$0 < \eta < \eta^* := \min\left(1, \left(\frac{-\lambda_1^b \inf(u,v)}{4(|\beta|+\kappa)(1+2C^b)}\right)^2\right),$$

inequality (2.2.40) is a contradiction since it implies $\alpha_0 > \alpha_0^*$. Hence we have shown that for any $0 < \eta < \eta^*$ one has $\alpha_0 = \alpha_0^\eta > \alpha_0^*$. In particular

$$\forall \eta \in (0,\eta^*), \forall (t,x) \in \mathbb{R}\times(-b,b), \begin{pmatrix} u(t,x) \\ v(t,x)\end{pmatrix} \geq \alpha_0^*(1-\eta t^2)\begin{pmatrix}\varphi^b(x)\\ \psi^b(x)\end{pmatrix}.$$

Taking the limit $\eta \to 0$, we then obtain

$$\forall (t,x) \in \mathbb{R}\times(-b,b), \begin{pmatrix} u(t,x) \\ v(t,x)\end{pmatrix} \geq \alpha_0^*\Phi^b(x),$$

which concludes the proof of Lemma 2.2.19. □

Next we establish a forward-in-time lower estimate for solutions of the (possibly degenerate) problem (2.2.41). The proof is based on the same idea as in Lemma 2.2.19, but it is here critical that the coefficient β of the time-derivative has the right sign. Roughly speaking, the following lemma asserts that once a population has reached a certain threshold on a large enough set, it cannot fall under that threshold at a later time.

Lemma 2.2.20 (A forward-in-time lower estimate)**.** *Let $(u(t,x),v(t,x))$ be a classical positive solution to*

$$\left\{\begin{array}{rcll} \beta u_t - \kappa u_{tt} - u_{xx} &=& u(r_u - \gamma_u(u+v)) + \mu v - \mu u & \text{in } \mathbb{R}^2 \\ \beta v_t - \kappa v_{tt} - v_{xx} &=& v(r_v - \gamma_v(u+v)) + \mu u - \mu v & \text{in } \mathbb{R}^2, \end{array}\right. \tag{2.2.41}$$

with $\kappa \geq 0$ and $\beta \geq 0$. Let also $b \geq a_1$ and Φ^b the solution to (2.2.34).

Then there exists a constant $\alpha_0 = \alpha_0(\mu^0,\gamma^\infty,\lambda_1^b,C^b) > 0$ such that if $0 < \alpha < \alpha_0$ and

$$\forall x \in (-b,b),\ \alpha\Phi^b(x) < \begin{pmatrix} u(0,x) \\ v(0,x)\end{pmatrix}, \tag{2.2.42}$$

then

$$\forall t > 0, \forall x \in (-b,b),\ \alpha\Phi^b(x) \leq \begin{pmatrix} u(t,x) \\ v(t,x)\end{pmatrix}.$$

Proof. Let

$$0 < \alpha < \alpha_0 := \min\left(1, \frac{-\lambda_1^b}{2(1+2C^b)\gamma^\infty}, \frac{\mu^0}{2\gamma^\infty}\right)$$

and assume (2.2.42). For $\eta > 0$ we define

$$\zeta(t,x) = \begin{pmatrix}\zeta_u(t,x)\\ \zeta_v(t,x)\end{pmatrix} := \alpha(1-\eta t)\begin{pmatrix}\varphi^b(x)\\ \psi^b(x)\end{pmatrix}.$$

From (2.2.42), we can define

$$\eta_0 := \inf \left\{ \eta \in \mathbb{R} : \forall t \geq 0, \forall x \in [-b,b], \begin{pmatrix} u(t,x) \\ v(t,x) \end{pmatrix} \geq \zeta(t,x) \right\}.$$

Assume by contradiction that $\eta_0 > 0$. Then there exists $t_0 > 0$ and $x_0 \in (-b,b)$ such that, say, $u(t_0,x_0) = \zeta_u(t_0,x_0)$. Then at point (t_0,x_0) we have

$$0 \geq \beta(u-\zeta_u)_t - \kappa(u-\zeta_u)_{tt} - (u-\zeta_u)_{xx} = u(r_u - \gamma_u(u+v)) + \mu(v-u) + \zeta_{u_{xx}} + \beta\alpha\eta\varphi^b.$$

Using (2.2.34) and $u(t_0,x_0) = \alpha(1-\eta_0 t_0)\varphi^b(x_0)$, we end up with

$$0 \geq u_0(-\lambda_1^b - \gamma_u(x_0)(u_0+v_0)) + \mu(x_0)(v_0 - \zeta_v(t_0,x_0)), \tag{2.2.43}$$

with the notations $u_0 = u(t_0,x_0)$, $v_0 = v(t_0,x_0)$ and thanks to $\beta \geq 0$. Now two cases may occur.

• Assume first that $v_0 \leq 2\zeta_v(t_0,x_0)$. Then $v_0 \leq 2\frac{\zeta_v(t_0,x_0)}{\zeta_u(t_0,x_0)}\zeta_u(t_0,x_0) \leq 2C^b\zeta_u(t_0,x_0) = 2C^b u_0$, so that (2.2.43) yields (recall that $v_0 \geq \zeta_v(t_0,x_0)$)

$$\gamma_u(x_0)(1+2C^b)u_0^2 \geq \gamma_u(x_0)(u_0+v_0)u_0 \geq -\lambda_1^b u_0.$$

As a result $u_0 > \alpha_0$, which is a contradiction.

• Assume now that $v_0 \geq 2\zeta_v(t_0,x_0)$. Then we deduce from (2.2.43) that

$$\begin{aligned} \gamma_u(x_0)u_0^2 &\geq -\lambda_1^b u_0 + v_0\left(\frac{\mu(x_0)}{2} - \gamma_u(x_0)u_0\right) + \frac{\mu(x_0)}{2}(v_0 - 2\zeta_v(t_0,x_0)) \\ &\geq -\lambda_1^b u_0 + \frac{1}{2}\mu(x_0)(v_0 - 2\zeta_v(t_0,x_0)), \end{aligned}$$

since $u_0 \leq \alpha_0 \leq \frac{\mu^0}{2\gamma^\infty}$. As a result $u_0 \geq \frac{-\lambda_1^b}{\gamma^\infty} > \alpha_0$, which is also a contradiction.

Thus $\eta_0 \leq 0$ and in particular

$$\forall t > 0, \forall x \in (-b,b), \ \begin{pmatrix} u(t,x) \\ v(t,x) \end{pmatrix} \geq \alpha \begin{pmatrix} \varphi^b(x) \\ \psi^b(x) \end{pmatrix},$$

which concludes the proof of Lemma 2.2.20. □

2.2.5.2 Proof of Theorem 2.2.18

In this section 2.2.5.2, we prove that a well-chosen series of solutions to equation (2.2.31) cannot converge, as $\varepsilon \to 0$, to a standing wave ($c = 0$). In other words, we prove Theorem 2.2.18, making a straightforward use of the crucial Lemma 2.2.21. The rough idea of the proof of Lemma 2.2.21 is that a standing wave cannot stay in the neighborhood of 0 for a long time. Hence the normalization allows us to prevent a sequence of solutions from converging to a standing wave, provided ν is chosen small enough. Notice also that the interior gradient estimate for elliptic systems of Lemma 2.2.26 will be used.

In the sequel we select $a_1 > a_0^*$ as in (2.2.35), recall that $\lambda_1^{a_1}$ denotes the eigenvalue of problem (2.2.34) in the domain $(-a_1,a_1)$, and define

$$\nu^* := \frac{1}{2}\min(\nu_0, \underline{\nu}) > 0,$$

where $\underline{\nu} := \alpha_0 \inf_{x \in (-a_0^*, a_0^*)} \min(\varphi^{a_1}(x), \psi^{a_1}(x))$, with $\alpha_0 > 0$ the constant in Lemma 2.2.19 in the domain $(-a_1,a_1)$.

Lemma 2.2.21 (Nonzero limit speed)**.** *Let $(\varepsilon_n, c_n, u^n(t,x), v^n(t,x))$ be a sequence such that $\varepsilon_n > 0$, $\varepsilon_n \to 0$, $c_n \neq 0$, (u^n, v^n) is a positive solution to problem (2.2.31) with $\varepsilon = \varepsilon_n$, $c = c_n$, $0 < \nu < \nu^*$ and $a_0 > a_1$. Then*

$$\liminf_{n\to\infty} c_n > 0. \tag{2.2.44}$$

Proof. Assume by contradiction that there is a sequence as in Lemma 2.2.21 with $\lim c_n = 0$. Define the sequence $\kappa_n := \frac{\varepsilon_n}{c_n^2} > 0$ which, up to an extraction, tends to $+\infty$, or to some $\kappa \in (0, +\infty)$ or to 0. In each case we are going to construct a couple of functions (u, v) that shows a contradiction. We refer to [48] or to [50] for a similar trichotomy.

Case 1: $\kappa_n \to +\infty$. Defining $(\tilde{u}^n, \tilde{v}^n)(t, x) := (u^n, v^n)(\sqrt{\kappa_n} t, x)$, problem (2.2.31) is recast

$$\left\{ \begin{array}{rcl} -u^n_{tt} - u^n_{xx} + \frac{1}{\sqrt{\kappa_n}} u^n_t &=& u^n(r_u - \gamma_u(u^n + v^n)) + \mu v^n - \mu u^n \\ -v^n_{tt} - v^n_{xx} + \frac{1}{\sqrt{\kappa_n}} v^n_t &=& v^n(r_v - \gamma_v(u^n + v^n)) + \mu u^n - \mu v^n \\ \sup\limits_{x - \sqrt{\varepsilon_n} t \in (-a_0, a_0)} u^n(t, x) + v^n(t, x) = \nu, \end{array} \right. \tag{2.2.45}$$

where we have dropped the tildes. From standard elliptic estimates, this sequence converges, up to an extraction, to a classical nonnegative solution (u, v) of

$$\left\{ \begin{array}{rcl} -u_{tt} - u_{xx} &=& u(r_u - \gamma_u(u + v)) + \mu v - \mu u \\ -v_{tt} - v_{xx} &=& v(r_v - \gamma_v(u + v)) + \mu u - \mu v, \end{array} \right. \tag{2.2.46}$$

and since (u^n, v^n) satisfies the third equality in (2.2.45) together with (2.2.32), (u, v) satisfies $\sup\limits_{(t,x) \in \mathbb{R} \times (-a_0, a_0)} (u + v) = \nu$. In particular, (u, v) is nontrivial and thus positive by the strong maximum principle.

Now, applying Lemma 2.2.20 to (u, v) with $\alpha := \frac{1}{2} \min \left(\inf\limits_{x \in (-a_0, a_0)} (u(0, x), v(0, x)), \alpha_0 \right) > 0$, we get

$$\forall t > 0, \forall x \in (-a_0, a_0), \begin{pmatrix} u(t, x) \\ v(t, x) \end{pmatrix} \geq \alpha \Phi^{a_0}(x).$$

Next, thanks to standard elliptic estimates, the sequence

$$(\bar{u}^n(t, x), \bar{v}^n(t, x)) := (u(t + n, x), v(t + n, x))$$

converges, up to an extraction, to a solution of (2.2.46) — that we denote again by (u, v)— which satisfies

$$\sup_{(t,x) \in \mathbb{R} \times (-a_0, a_0)} (u + v) \leq \nu, \tag{2.2.47}$$

and

$$\forall (t, x) \in \mathbb{R} \times (-a_0, a_0), \begin{pmatrix} u(t, x) \\ v(t, x) \end{pmatrix} \geq \alpha \Phi^{a_0}(x).$$

In particular, since $a_0 > a_1$, the latter implies

$$\inf_{(t,x) \in \mathbb{R} \times (-a_1, a_1)} \min(u, v) > 0. \tag{2.2.48}$$

Case 2: $\kappa_n \to \kappa \in (0, +\infty)$. Thanks to standard elliptic estimates, the sequence (u^n, v^n) converges, up to an extraction, to a solution (u, v) of

$$\left\{ \begin{array}{rcl} -\kappa u_{tt} - u_{xx} + u_t &=& u(r_u - \gamma_u(u + v)) + \mu v - \mu u \\ -\kappa v_{tt} - v_{xx} + v_t &=& v(r_v - \gamma_v(u + v)) + \mu u - \mu v, \end{array} \right. \tag{2.2.49}$$

and since (u^n, v^n) satisfies the third equality in (2.2.31) together with (2.2.32), (u, v) satisfies $\sup\limits_{(t,x) \in \mathbb{R} \times (-a_0, a_0)} (u + v) = \nu$. In particular, (u, v) is nontrivial and thus positive by the strong maximum principle.

Now, using Lemma 2.2.20 and a positive large shift in time exactly as in Case 1, we end up with a solution (u, v) to (2.2.49) which satisfies (2.2.47) and (2.2.48).

Case 3: $\kappa_n \to 0$**.** In this case, the elliptic operator becomes degenerate as $n \to \infty$, so that we cannot use the standard elliptic theory. The idea is then to use a Bernstein interior gradient estimate for elliptic systems that we present and prove in Appendix 2.2.6.2.

Applying Lemma 2.2.26 to the series (u^n, v^n) solving (2.2.31), we get a uniform L^∞ bound for (u^n_x, v^n_x). Furthermore by differentiating (2.2.31) with respect to x, we see that (u^n_x, v^n_x) solves a system for which Lemma 2.2.26 still applies. As a result, we get a uniform L^∞ bound for (u^n_{xx}, v^n_{xx}).

Let us show that there is also a uniform L^∞ bound for (u^n_t, v^n_t). From the uniform bounds found above, we can write

$$u^n_t - \kappa_n u^n_{tt} = F^n(t,x).$$

Let $F := \max(1, \sup_n \|F^n\|_{L^\infty(\mathbb{R}^2)}) < +\infty$. Assume by contradiction that there is a point (t_0, x_0) where $u^n_t(t_0, x_0) > 2F$. From the above equation we deduce that $u^n_t(t, x_0) > 2F$ remains valid for $t \geq t_0$, and thus

$$\kappa_n u^n_{tt}(t, x_0) > F, \quad \forall t \geq t_0.$$

Integrating twice, we get

$$u^n(t, x_0) \geq F(2(t - t_0) + \frac{1}{2\kappa_n}(t - t_0)^2) - \|u^n\|_{L^\infty}, \quad \forall t \geq t_0.$$

Letting $t \to \infty$ we get that u^n is unbounded, a contradiction. Thus, $u^n_t(t,x) \leq 2F$ for any $(t,x) \in \mathbb{R}^2$ and, in a straightforward way, $|u^n_t(t,x)|, |v^n_t(t,x)| \leq 2F$ for any $(t,x) \in \mathbb{R}^2$.

Since we have uniform L^∞ bounds for (u^n, v^n), (u^n_x, v^n_x) and (u^n_t, v^n_t), there are u and v in $H^1_{loc}(\mathbb{R}^2)$ such that, up to a subsequence,

$$(u^n, v^n) \to (u, v) \text{ in } L^\infty_{loc}(\mathbb{R}^2), \quad (u^n_x, v^n_x, u^n_t, v^n_t) \rightharpoonup (u_x, v_x, u_t, v_t) \text{ in } L^2_{loc}(\mathbb{R}^2) \text{ weak.}$$

As a result, letting $n \to \infty$ into (2.2.31) yields

$$\left\{ \begin{array}{rcl} u_t - u_{xx} & = & u(r_u - \gamma_u(u+v)) + \mu v - \mu u \\ v_t - v_{xx} & = & v(r_v - \gamma_v(u+v)) + \mu u - \mu v \end{array} \right. \tag{2.2.50}$$

in a weak sense. From parabolic regularity, (u, v) is actually a classical solution to (2.2.50). Since the convergence occurs locally uniformly and since (u^n, v^n) satisfies the third equality in (2.2.31) together with (2.2.32), (u, v) satisfies $\sup_{(t,x) \in \mathbb{R} \times (-a_0, a_0)} (u + v) = \nu$. In particular, (u, v) is nontrivial and thus positive by the strong maximum principle.

Now, using Lemma 2.2.20 and a positive large shift in time as in Case 1 (parabolic estimates replacing elliptic estimates), we end up with a solution (u, v) to (2.2.50) which satisfies (2.2.47) and (2.2.48).

Conclusion. In any of the three above cases, we have constructed a classical solution (u, v) to ($\beta \geq 0$, $\kappa \geq 0$)

$$\left\{ \begin{array}{rcl} \beta u_t - \kappa u_{tt} - u_{xx} & = & u(r_u - \gamma_u(u+v)) + \mu v - \mu u \\ \beta v_t - \kappa v_{tt} - v_{xx} & = & v(r_v - \gamma_v(u+v)) + \mu u - \mu v, \end{array} \right.$$

which satisfies (2.2.47) and (2.2.48). Applying Lemma 2.2.19, we find that (recall that $a_1 > a^*_0$)

$$\inf_{\mathbb{R} \times (-a^*_0, a^*_0)} (u, v) \geq \alpha_0 \inf_{(-a^*_0, a^*_0)} (\varphi^{a_1}, \psi^{a_1}) = \underline{\nu}.$$

But, since $a_0 > a^*_0$ the above implies

$$\sup_{\mathbb{R} \times (-a_0, a_0)} (u + v) \geq 2 \inf_{\mathbb{R} \times (-a^*_0, a^*_0)} (u, v) \geq 2\underline{\nu} > \nu^* > \nu,$$

which contradicts (2.2.47). Lemma 2.2.21 is proved. □

We are now in the position to prove Theorem 2.2.18.

Proof of Theorem 2.2.18. From the beginning of Section 2.2.5 and Lemma 2.2.21 we can consider a sequence $(\varepsilon_n, c_n, u^n(t,x), v^n(t,x))$ such that $\varepsilon_n > 0$, $\varepsilon_n \to 0$, $0 < c_n \leq \bar{c}^{\varepsilon_n} + \varepsilon_n$, (u^n, v^n) is a positive solution to problem (2.2.31) with $\varepsilon = \varepsilon_n$, $c = c_n$, $\nu < \nu^*$ and $a_0 > a_1$, satisfying the constraint (2.2.6), and the crucial fact

$$\lim_{n\to\infty} c_n > 0. \tag{2.2.51}$$

Notice that, as a by-product, this shows that $\bar{c}^0 := \lim_{\varepsilon\to 0} \bar{c}^\varepsilon > 0$ (see Lemma 2.2.12). We can now repeat the argument in the proof of Lemma 2.2.21 Case 3 and extract a sequence (u^n, v^n) which converges to a classical solution (u, v) of equation (2.2.33), satisfying the normalization

$$\sup_{x-ct\in(-a_0,a_0)} (u+v) = \nu$$

as well as the constraint (2.2.6). Theorem 2.2.18 is proved. □

2.2.5.3 Proof of Theorem 2.2.6

We are now close to conclude the proof of our main result of construction of a pulsating front, Theorem 2.2.6. From Theorem 2.2.18, it only remains to prove the boundary conditions (2.2.7), namely

$$\liminf_{t\to+\infty} \begin{pmatrix} u(t,x) \\ v(t,x) \end{pmatrix} > \begin{pmatrix} 0 \\ 0 \end{pmatrix}, \quad \lim_{t\to-\infty} \begin{pmatrix} u(t,x) \\ v(t,x) \end{pmatrix} = \begin{pmatrix} 0 \\ 0 \end{pmatrix}, \quad \text{locally uniformly w.r.t. } x,$$

to match Definition 2.2.5 of a pulsating front. The former is derived by another straighforward application of Lemma 2.2.20, while the latter is proved below. Hence, Theorem 2.2.6 is proved. □

Lemma 2.2.22 (Zero limit behavior)**.** *For $a_1 > a_0^*$ and $\nu^* > 0$ as in section 2.2.5.2, let $c > 0$ and (u, v) be as in Theorem 2.2.18, satisfying in particular the normalization $\sup_{x-ct\in(-a_0,a_0)} (u+v) = \nu$ with $\nu < \nu^*$ and $a_0 > a_1$. Then*

$$\lim_{t\to-\infty} \max(u,v)(t,x) \to 0, \quad \textit{locally uniformly w.r.t. } x.$$

Proof. We first claim that $\inf_{\mathbb{R}\times(-a_0,a_0)} \min(u,v) = 0$. Indeed if this is not the case then, in particular, $\inf_{\mathbb{R}\times(-a_1,a_1)} \min(u,v) > 0$, and we derive a contradiction via Lemma 2.2.19 by a straightforward adaptation of the Conclusion of the proof of Lemma 2.2.21, because $\mathbb{R}\times(-a_1,a_1)$ intersects $\{(t,x) : x - ct \in (-a_0,a_0)\}$.

Now let $a > a_0$ be given and assume by contradiction that there is $m > 0$ and a sequence $t_n \to -\infty$ such that $\sup_{x\in(-a,a)} \max(u,v)(t_n,x) \geq m$. Thanks to the Harnack inequality for parabolic systems, see [171, Theorem 3.9], there is $C > 0$ such that

$$\forall n \in \mathbb{N}, \quad \inf_{x\in(-a,a)} \min(u,v)(t_n+1,x) \geq \frac{1}{C} \sup_{x\in(-a,a)} \max(u+v)(t_n,x) \geq \frac{m}{C}.$$

We now use our forward-in-time lower estimate, see Lemma 2.2.20, in $(-a,a)$ and with $\alpha := \frac{1}{2}\min(\alpha_0, \frac{m}{C}) > 0$ to get

$$\forall n \in \mathbb{N},\ \forall t > t_n + 1,\ \forall x \in (-a,a),\ \begin{pmatrix} u(t,x) \\ v(t,x) \end{pmatrix} \geq \alpha \begin{pmatrix} \varphi^a(x) \\ \psi^a(x) \end{pmatrix}.$$

Since $t_n \to -\infty$ and $a > a_0$, the above implies

$$\inf_{(t,x)\in\mathbb{R}\times(-a_0,a_0)} \min(u,v)(t,x) \geq \alpha \inf_{x\in(-a_0,a_0)} (\varphi^a, \psi^a)(x) > 0.$$

This is a contradiction and the lemma is proved. □

2.2.6 Appendix

2.2.6.1 Topological theorems

Let us first recall the classical Krein-Rutman theorem.

Theorem 2.2.23 (Krein-Rutman theorem)**.** *Let E be a Banach space. Let $C \subset E$ be a closed convex cone of vertex 0, such that $C \cap -C = \{0\}$ and $Int\, C \neq \varnothing$. Let $T : E \to E$ be a linear compact operator such that $T(C\backslash\{0\}) \subset Int\, C$.*

Then, there exists $u \in Int\, C$ and $\l > 0$ such that $Tu = \l u$. Moreover, if $Tv = \mu v$ for some $v \in C\backslash\{0\}$, then $\mu = \l$. Finally, we have

$$\l = \max\{|\mu|, \mu \in \sigma(T)\},$$

and the algebraic and geometric multiplicity of $\l$ are both equal to 1.

We now quote some results on the structure of the solution set for nonlinear eigenvalue problems in a Banach space, more specifically when bifurcation occurs. For more details and proofs, we refer the reader to the works of Rabinowitz [329, 330], Crandall and Rabinowitz [123]. See also earlier related results of Krasnosel'skii [244] and the book of Brown [82].

Theorem 2.2.24 (Bifurcation from eigenvalues of odd multiplicity)**.** *Let E be a Banach space. Let $F : \mathbb{R} \times E \to E$ be a (possibly nonlinear) compact operator such that*

$$\forall \lambda \in \mathbb{R},\ F(\lambda, 0) = 0.$$

Assume that F is Fréchet differentiable near $(\lambda, 0)$ with derivative λT. Let us define

$$\mathcal{S} := \overline{\{(\lambda, x) \in \mathbb{R} \times E\backslash\{0\} : F(\lambda, x) = x\}}.$$

Let us assume that $\frac{1}{\mu} \in \sigma(T)$ is of odd multiplicity.

Then there exists a maximal connected component $\mathcal{C}_\mu \subset \mathcal{S}$ such that $(\mu, 0) \in \mathcal{C}_\mu$ and either

1. *$\mathcal{C}_\mu$ is not bounded in $\mathbb{R} \times E$, or*
2. *there exists $\mu^* \neq \mu$ with $\frac{1}{\mu^*} \in \sigma(T)$ and $(\mu^*, 0) \in \mathcal{C}_\mu$.*

When the eigenvalue is simple, one can actually refine the above result as follows.

Theorem 2.2.25 (Bifurcation from simple eigenvalues)**.** *Let the assumptions of Theorem 2.2.24 hold. Assume further that $\frac{1}{\mu} \in \sigma(T)$ is simple. Let T^* be the dual of T, and $l \in E'$ an eigenvector of T^* associated with $\frac{1}{\mu}$ with $\|l\| = 1$ (recall that $\frac{1}{\mu}$ is of multiplicity 1 for both T and T^*). Let us define*

$$K^+_{\xi,\eta} := \{(\lambda, u) \in \mathbb{R} \times E, |\lambda - \mu| < \xi, \langle l, u\rangle > \eta\|u\|\}, \quad K^-_{\xi,\eta} := -K^+_{\xi,\eta}.$$

Then $\mathcal{C}_\mu\backslash\{(\mu, 0)\}$ contains two connected components $\mathcal{C}^+_\mu$ and $\mathcal{C}^-_\mu$ which satisfy

$$\forall \nu \in \{+, -\}, \forall \xi > 0, \forall \eta \in (0, 1), \exists \zeta_0 > 0, \forall \zeta \in (0, \zeta_0),\ (\mathcal{C}^\nu_\mu \cap B_\zeta) \subset K^\nu_{\xi,\eta},$$

where $B_\zeta := \{(\lambda, u) \in \mathbb{R} \times E, |\lambda - \mu| < \zeta, \|u\| < \zeta\}$ is the ball of center $(\mu, 0)$ and radius ζ. Moreover, $\mathcal{C}^+_\mu$ and $\mathcal{C}^-_\mu$ satisfy either item 1 or 2 in Theorem 2.2.24.

2.2.6.2 A Bernstein-type interior gradient estimate for elliptic systems

We present here some L^∞ gradient estimates for regularizations of degenerate elliptic systems, which are uniform with respect to the regularization parameter $\kappa \geq 0$. The result below generalizes the result of Berestycki and Hamel [49], which is concerned with scalar equations.

Lemma 2.2.26 (Interior gradient estimates)**.** *Let Ω be an open subset of $\mathbb{R}^2$. Let $f, g : \Omega \times \mathbb{R}^2 \to \mathbb{R}$ be two C^1 functions with bounded derivatives. Let $0 \leq \kappa \leq 1$ and $(u(y, x), v(y, x))$ be a solution of the class C^3 of the system*

$$\left\{ \begin{array}{rcll} -\kappa u_{yy} - u_{xx} + u_y & = & f(y, x, u, v) & \text{in } \Omega, \\ -\kappa v_{yy} - v_{xx} + v_y & = & g(y, x, u, v) & \text{in } \Omega. \end{array} \right. \tag{2.2.52}$$

Then, for all $(y,x) \in \Omega$,

$$|u_x(y,x)|^2 + |v_x(y,x)|^2 + \kappa|u_y(y,x)|^2 + \kappa|v_y(y,x)|^2 \leq C\left(1 + \frac{1}{(dist((y,x),\partial\Omega))^2}\right)$$

where

$$C = C(\|u\|_{L^\infty(B)} + \|v\|_{L^\infty(B)}, osc_B u, osc_B v, \|f\|_{C^{0,1}(B\times[\underline{u},\overline{u}]\times[\underline{v},\overline{v}])}, \|g\|_{C^{0,1}(B\times[\underline{u},\overline{u}]\times[\underline{v},\overline{v}])}),$$

with B *the ball of center* (y,x) *and radius* $\frac{dist((y,x),\partial\Omega)}{2}$ *in* $\mathbb{R}^2$, $\underline{u} := \inf_B u$, $\overline{u} := \sup_B u$, $\underline{v} := \inf_B v$, $\overline{v} := \sup_B v$. *In particular, this estimate is independent on the regularization parameter* $0 \leq \kappa \leq 1$.

Proof. Let h be the smooth function defined on $\mathbb{R}$ by

$$h(z) := \begin{cases} \exp\left(\frac{z^2}{z^2-1}\right) & |z| < 1 \\ 0 & |z| \geq 1. \end{cases}$$

Let us then define $C_0 := \max(\|h\|_{L^\infty}, \|h'\|_{L^\infty}, \|h''\|_{L^\infty})$ and $\zeta(Y,X) := h\left(\frac{\sqrt{Y^2+X^2}}{2}\right)$.

Let $(y_0,x_0) \in \Omega$ be a given point, $d_0 := dist((y_0,x_0),\partial\Omega)$, $d := \min\left(\frac{d_0}{2},1\right)$, B_0 the ball of center (y_0,x_0) and radius d. Let χ be the function defined by

$$\forall (y,x) \in \mathbb{R}^2, \quad \chi(y,x) := \zeta\left(\frac{y-y_0}{d}, \frac{x-x_0}{d}\right).$$

Finally, let P^u and P^v be defined in Ω by

$$\begin{aligned} P^u(y,x) &:= \chi^2(y,x)(u_x^2(y,x) + \kappa u_y^2(y,x)) + \lambda u^2(y,x) + \rho e^{x-x_0} \\ P^v(y,x) &:= \chi^2(y,x)(v_x^2(y,x) + \kappa v_y^2(y,x)) + \lambda v^2(y,x) + \rho e^{x-x_0}, \end{aligned}$$

where $\lambda > 0$ and $\rho > 0$ are constants to be fixed later. Our goal is to apply the maximum principle to the function $P := P^u + P^v$ for convenient values of λ and ρ. We present below the computations on P^u only and reflect them on P^v.

We first compute the partial derivatives of P^u and get

$$\begin{aligned} P^u_y &= 2\chi_y\chi u_x^2 + 2\chi^2 u_{xy}u_x + 2\kappa(\chi_y\chi u_y^2 + \chi^2 u_{yy}u_y) + 2\lambda u_y u \\ P^u_{yy} &= 2(\chi_{yy}\chi + \chi_y^2)u_x^2 + 8\chi_y\chi u_{xy}u_x + 2\chi^2(u_{xyy}u_x + u_{xy}^2) \\ &\quad +\kappa[2(\chi_{yy}\chi + \chi_y^2)u_y^2 + 8\chi_y\chi u_{yy}u_y + 2\chi^2(u_{yyy}u_y + u_{yy}^2)] \\ &\quad +2\lambda(u_{yy}u + u_y^2) \\ P^u_{xx} &= 2(\chi_{xx}\chi + \chi_x^2)u_x^2 + 8\chi_x\chi u_{xx}u_x + 2\chi^2(u_{xxx}u_x + u_{xx}^2) \\ &\quad \kappa[2(\chi_{xx}\chi + \chi_x^2)u_y^2 + 8\chi_x\chi u_{xy}u_y + 2\chi^2(u_{yxx}u_y + u_{yx}^2)] \\ &\quad +2\lambda(u_{xx}u + u_x^2) + \rho e^{x-x_0}. \end{aligned}$$

Let $M := \partial_y - \kappa\partial_{yy} - \partial_{xx}$. Then we have

$$\begin{aligned} MP^u &= 2\left[\chi_y\chi - \kappa(\chi_{yy}\chi + \chi_y^2) - (\chi_{xx}\chi + \chi_x^2)\right]u_x^2 \\ &\quad +2\kappa\left[\chi_y\chi - \kappa(\chi_{yy}\chi + \chi_y^2) - (\chi_{xx}\chi + \chi_x^2)\right]u_y^2 \\ &\quad +2\chi^2\left[u_{xy} - \kappa u_{xyy} - u_{xxx}\right]u_x \\ &\quad +2\kappa\chi^2\left[u_{yy} - \kappa u_{yyy} - u_{yxx}\right]u_y \\ &\quad -2\left[\kappa(\chi^2 u_{xy}^2 + 4\chi_y\chi u_{xy}u_x) + (\chi^2 u_{xx}^2 + 4\chi_x\chi u_{xx}u_x)\right] \\ &\quad -2\kappa[\kappa(4\chi_y\chi u_y u_{yy} + \chi^2 u_{yy}^2) + (4\chi_x\chi u_y u_{xy} + \chi^2 u_{xy}^2)] \\ &\quad +2\lambda\left[(u_y - \kappa u_{yy} - u_{xx})u - \kappa u_y^2 - u_x^2\right] \\ &\quad -\rho e^{x-x_0}. \end{aligned}$$

We now reformulate some of the lines of the above equality, starting with lines three and four. We differentiate the first equation of system (2.2.52) with respect to x to obtain

$$\begin{aligned} 2\chi^2\left[u_{xy}-\kappa u_{xyy}-u_{xxx}\right]u_x &= 2\chi^2(f_x+u_xf_u+v_xf_v)u_x \\ &\leq \chi^2(u_x^2+f_x^2)+2\chi^2u_x^2|f_u|+\chi^2(u_x^2+v_x^2)|f_v|, \end{aligned}$$

and then with respect to y to get

$$\begin{aligned} 2\chi^2\left[u_{yy}-\kappa u_{yyy}-u_{yxx}\right]u_y &= 2\chi^2(f_y+u_yf_u+v_yf_v)u_y \\ &\leq \chi^2(u_y^2+f_y^2)+2\chi^2u_y^2|f_u|+\chi^2(u_y^2+v_y^2)|f_v|. \end{aligned}$$

As far as lines five and six are concerned, we use the factorizations

$$\begin{aligned} \chi^2u_{xy}^2+4\chi_y\chi u_{xy}u_x &= (\chi u_{xy}+2\chi_yu_x)^2-4\chi_y^2u_x^2 \\ \chi^2u_{xx}^2+4\chi_x\chi u_{xx}u_x &= (\chi u_{xx}+2\chi_xu_x)^2-4\chi_x^2u_x^2 \\ \chi^2u_{yy}^2+4\chi_y\chi u_{yy}u_y &= (\chi u_{yy}+2\chi_yu_y)^2-4\chi_y^2u_y^2 \\ \chi^2u_{xy}^2+4\chi_x\chi u_{xy}u_y &= (\chi u_{xy}+2\chi_xu_y)^2-4\chi_x^2u_y^2. \end{aligned}$$

For line seven, we use the first equation in (2.2.52) to write $(u_y-\kappa u_{yy}-u_{xx})u=fu$. As a result, we collect

$$\begin{aligned} MP^u \leq\ & 2\left[\chi_y\chi-\kappa\chi_{yy}\chi-\chi_{xx}\chi+3\chi_x^2+3\kappa\chi_y^2+\chi^2\left(|f_u|+\tfrac{1+|f_v|}{2}\right)-\lambda\right](u_x^2+\kappa u_y^2) \\ & +2\lambda fu+\chi^2(v_x^2+\kappa v_y^2)|f_v|+\chi^2(f_x^2+\kappa f_y^2)-\rho e^{x-x_0}, \end{aligned}$$

and, similarly,

$$\begin{aligned} MP^v \leq\ & 2\left[\chi_y\chi-\kappa\chi_{yy}\chi-\chi_{xx}\chi+3\chi_x^2+3\kappa\chi_y^2+\chi^2\left(|g_v|+\tfrac{1+|g_u|}{2}\right)-\lambda\right](v_x^2+\kappa v_y^2) \\ & +2\lambda gv+\chi^2(u_x^2+\kappa u_y^2)|g_u|+\chi^2(g_x^2+\kappa g_y^2)-\rho e^{x-x_0}. \end{aligned}$$

Notice that $|\chi|\leq C_0$, $|\chi_x|,|\chi_y|\leq\frac{C_0}{d}$, $|\chi_{xx}|,|\chi_{yy}|\leq\frac{C_0}{d^2}$ and recall that $\kappa,d\leq 1$. Hence, putting everything together, we arrive at

$$\begin{aligned} MP \leq\ & \left(20\tfrac{C_0^2}{d^2}+4C_0^2(\|f\|_{C^{0,1}}+\|g\|_{C^{0,1}})+C_0^2-\lambda\right)(u_x^2+v_x^2+\kappa u_y^2+\kappa v_y^2) \\ & +2\lambda(\|f\|_{L^\infty}+\|g\|_{L^\infty})(\|u\|_{L^\infty}+\|v\|_{L^\infty})+2C_0^2(\|f\|_{C^{0,1}}^2+\|g\|_{C^{0,1}}^2)-2\rho e^{x-x_0}. \end{aligned}$$

It is now time to specify

$$\begin{cases} \lambda &= 20\frac{C_0^2}{d^2}+4C_0^2(\|f\|_{C^{0,1}}+\|g\|_{C^{0,1}})+C_0^2>0 \\ \rho &= \frac{e}{2}\left[2\lambda(\|f\|_{L^\infty}+\|g\|_{L^\infty})(\|u\|_{L^\infty}+\|v\|_{L^\infty})+2C_0^2(\|f\|_{C^{0,1}}^2+\|g\|_{C^{0,1}}^2)+1\right]>0. \end{cases}$$

As a result we have $MP(y,x)<0$ for all $(y,x)\in B_0$ (since then $x-x_0\geq -1$). The maximum principle then implies

$$P(y_0,x_0)\leq\max_{(y,x)\in\partial B_0}P(y,x).$$

Since $\chi(y_0,x_0)=1$ and $\chi(y,x)=0$ when $(y,x)\in\partial B_0$, the above inequality implies

$$\begin{aligned} (u_x^2+v_x^2+\kappa u_y^2+\kappa v_y^2)(y_0,x_0) &\leq \lambda(\|u\|_{L^\infty}^2+\|v\|_{L^\infty}^2)-\lambda(u^2+v^2)(y_0,x_0)+2\rho e \\ &\leq 2\lambda(\|u\|_{L^\infty}osc_{B_0}(u)+\|v\|_{L^\infty}osc_{B_0}(v))+2\rho e \\ &\leq K\{(\|u\|_{L^\infty}+\|v\|_{L^\infty})(osc_{B_0}(u)+osc_{B_0}(v) \\ &\quad +\|f\|_{C^{0,1}}+\|g\|_{C^{0,1}})+\|f\|_{C^{0,1}}^2+\|g\|_{C^{0,1}}^2+1\}\left(1+\frac{1}{d^2}\right) \end{aligned}$$

using the expressions of λ and ρ above, for a universal positive constant $K>0$ and where the $C^{0,1}$ norms of f, g are taken on $B_0\times[\inf_{B_0}u,\sup_{B_0}u]\times[\inf_{B_0}v,\sup_{B_0}v]$. This proves the lemma. □

2.2.6.3 Dirichlet and periodic principal eigenvalues

We prove here that the principal eigenvalue with Dirichlet boundary conditions in a ball converges to the principal eigenvalue with periodic boundary conditions, when the radius tends to $+\infty$.

Lemma 2.2.27 (Dirichlet and periodic principal eigenvalues)**.** *Let $A \in L^\infty(\mathbb{R}; \mathcal{S}_2(\mathbb{R}))$ be a symmetric cooperative matrix field that is periodic with period $L > 0$. Let $\mathfrak{l}$ be the principal eigenvalue of the operator $-\partial_{xx} - A(x)$ with periodic boundary conditions, that is*

$$-\begin{pmatrix}\varphi\\ \psi\end{pmatrix}'' - A(x)\begin{pmatrix}\varphi\\ \psi\end{pmatrix} = \mathfrak{l}\begin{pmatrix}\varphi\\ \psi\end{pmatrix}, \tag{2.2.53}$$

with $\varphi, \psi \in H^1_{per}$ and $\varphi > 0, \psi > 0$. For $R > 0$, let λ_1^R be the principal eigenvalue of the operator $-\partial_{xx} - A(x)$ with Dirichlet boundary conditions on $(-R, R)$, that is

$$-\begin{pmatrix}\varphi^R\\ \psi^R\end{pmatrix}'' - A(x)\begin{pmatrix}\varphi^R\\ \psi^R\end{pmatrix} = \lambda_1^R\begin{pmatrix}\varphi^R\\ \psi^R\end{pmatrix}, \tag{2.2.54}$$

with $\varphi^R, \psi^R \in H^1_0(-R, R)$ and $\varphi^R > 0, \psi^R > 0$. Then, there exists $C > 0$ depending only on A such that, for all $R > 0$,

$$\mathfrak{l} \le \lambda_1^R \le \mathfrak{l} + \frac{C}{R}.$$

Proof. Without loss of generality we assume $L = 1$. Inequality $\mathfrak{l} \le \lambda_1^R$ is very classical, see [51, Proposition 4.2] or [4, Proposition 3.3] for instance, and we omit the details. Also, the same classical argument yields that $R \mapsto \lambda_1^R$ is nonincreasing so it is enough to prove $\lambda_1^R \le \mathfrak{l} + \frac{C}{R}$ when $R = 2, 3, ...$

We consider a smooth auxiliary function $\eta : \mathbb{R} \to \mathbb{R}$ satisfying

$$\eta \equiv 1 \text{ on } (-\infty, 0],\ 0 < \eta < 1 \text{ on } (0, 1),\ \eta \equiv 0 \text{ on } [1, \infty).$$

Since the operator in (2.2.54) is self-adjoint in the domain $(-R, R)$, the principal eigenvalue λ_1^R is given by the Rayleigh quotient

$$\lambda_1^R = \inf_{\Psi \in \mathbf{H}^1_0(-R,R), \Psi \neq 0} Q(\Psi, \Psi), \quad Q(\Psi, \Psi) := \frac{\int_{-R}^R ({}^t\Psi_x \Psi_x - {}^t\Psi A(x)\Psi)\mathrm{d}x}{\int_{-R}^R {}^t\Psi\Psi \mathrm{d}x}.$$

In particular we have $\lambda_1^R \le Q(\Theta, \Theta)$, with Θ the $\mathbf{H}^1_0(-R, R)$ test function defined by

$$\Theta(x) := \eta(-R + 1 - x)\eta(-R + 1 + x)\Phi(x), \quad \Phi(x) := \begin{pmatrix}\varphi(x)\\ \psi(x)\end{pmatrix},$$

where φ, ψ are as in (2.2.53), with the normalization $\int_0^1 {}^t\Phi\Phi \mathrm{d}x = 1$. We then have $Q(\Theta, \Theta) = Q^1(\Theta) + Q^2(\Theta)$, where

$$Q^1(\Theta) := \frac{\int_{|x| \le R-1} ({}^t\Theta_x\Theta_x - {}^t\Theta A(x)\Theta)\mathrm{d}x}{\int_{-R}^R {}^t\Theta\Theta \mathrm{d}x}, \quad Q^2(\Theta) := \frac{\int_{R-1 \le |x| \le R} ({}^t\Theta_x\Theta_x - {}^t\Theta A(x)\Theta)\mathrm{d}x}{\int_{-R}^R {}^t\Theta\Theta \mathrm{d}x}.$$

We write

$$Q^1(\Theta) = \frac{\int_{|x| \le R-1} ({}^t\Theta_x\Theta_x - {}^t\Theta A(x)\Theta)\mathrm{d}x}{\int_{|x| \le R-1} {}^t\Theta\Theta \mathrm{d}x} \frac{\int_{-(R-1)}^{R-1} {}^t\Theta\Theta \mathrm{d}x}{\int_{-R}^R {}^t\Theta\Theta \mathrm{d}x} = \lambda_1 \frac{\int_{-(R-1)}^{R-1} {}^t\Theta\Theta \mathrm{d}x}{\int_{-R}^R {}^t\Theta\Theta \mathrm{d}x},$$

thanks to $\Theta \equiv \Phi \equiv \begin{pmatrix}\varphi\\ \psi\end{pmatrix}$ on $(-(R-1), R-1)$ and the 1-periodicity of φ, ψ (recall that $R-1$ is an integer).

As a result

$$|Q^1(\Theta) - \lambda_1| = |\lambda_1| \frac{\int_{R-1<|x|<R} {}^t\Theta\Theta \mathrm{d}x}{\int_{-R}^R {}^t\Theta\Theta \mathrm{d}x} \le |\lambda_1| \frac{\int_{R-1<|x|<R} {}^t\Phi\Phi \mathrm{d}x}{\int_{-(R-1)}^{R-1} {}^t\Phi\Phi \mathrm{d}x} = |\lambda_1| \frac{1}{R-1},$$

since $0 \leq \eta \leq 1$. On the other hand one can see that, for a constant $C_2 > 0$ depending only on $\|\eta'\|_{L^\infty(\mathbb{R})}$ and $\|A\|_{L^\infty(\mathbb{R};\mathcal{S}_2(\mathbb{R}))}$,

$$\begin{aligned}\left|\int_{R-1<|x|<R} ({}^t\Theta_x\Theta_x - {}^t\Theta A(x)\Theta)\mathrm{d}x\right| &\leq C_2\int_{R-1<|x|<R}({}^t\Phi\Phi + {}^t\Phi_x\Phi_x)\mathrm{d}x \\ &= 2C_2\int_{0<|x|<1}({}^t\Phi\Phi + {}^t\Phi_x\Phi_x)\mathrm{d}x =: C_2'\end{aligned}$$

so that

$$|Q^2(\Theta)| \leq \frac{C_2'}{\int_{-R}^{R} {}^t\Theta\Theta\mathrm{d}x} \leq \frac{C_2'}{\int_{-(R-1)}^{R-1} {}^t\Phi\Phi\mathrm{d}x} = \frac{C_2'}{(2R-2)\int_0^1 {}^t\Phi\Phi\mathrm{d}x} = \frac{C_2'}{(2R-2)}.$$

This concludes the proof of the lemma. □

2.3 Propagation dynamics of solutions to spatially periodic reaction-diffusion systems with hybrid nonlinearity.

2.3.1 Introduction

In this section 2.3 we are interested in the following reaction-diffusion system:

$$\begin{cases} u_t = \mathcal{L}u + f(x,u), & t>0, x\in\mathbb{R}, \\ u(t=0,x) = u_0(x), & x\in\mathbb{R}, \end{cases} \tag{2.3.1}$$

where $u(t,x)\in\mathbb{R}^d$ is a nonnegative vector-valued function of a space variable $x\in\mathbb{R}$ and a time variable $t\geq 0$; $\mathcal{L}$ is a diagonal matrix of second-order elliptic differential operators with spatially L-periodic coefficients and $f(x,u)$ is a reaction term that is L-periodic in $x\in\mathbb{R}$. We will assume throughout the section 2.3 that $f(x,u)$ is cooperative when u lies in the vicinity of the boundary of the positive cone of $\mathbb{R}^d$. An important example, which has motivated the current study, is the following two-components system

$$\begin{cases} u_t = \sigma_u(x)u_{xx} + (r_u(x) - \kappa_u(x)(u+v))u + \mu_v(x)v - \mu_u(x)u, & t>0, x\in\mathbb{R}, \\ v_t = \sigma_v(x)v_{xx} + (r_v(x) - \kappa_v(x)(u+v))v + \mu_u(x)u - \mu_v(x)v, & t>0, x\in\mathbb{R}. \end{cases} \tag{2.3.2}$$

Here $u(t,x)$, $v(t,x)$ stand for the density of a population of individuals living in a periodically heterogeneous environment. We assume that the reproduction rates $r_u(x)$ and $r_v(x)$ are L-periodic functions, and that the competition coefficients $\kappa_u(x)$ and $\kappa_v(x)$ are L-periodic and positive. Finally, the coefficients $\mu_u(x)>0$, $\mu_v(x)>0$ (also L-periodic) denote the mutation rates between the two populations, which creates an effect of cooperative coupling in the region where both u and v are small.

In the context of epidemiology, System (2.3.2) describes the propagation of a genetically unstable pathogen in a population of hosts which exhibits heterogeneity in space. This heterogeneity may simply come from a heterogeneous repartition of the host population [348]. Spatial heterogeneity in the use of antibiotics, fungicides or insecticides affects the transmission of pathogens and pests and is explored as a way to minimize the risk of emergence of drug resistance [134]. Beaumont et al [42] study a related model of propagation of salmonella in an industrial hen house. In their study the heterogeneity comes from the alignment of cages separated by free space that allow farmers to take care of the animals.

System (2.3.2) has some similarity with Fisher-KPP equations. In their seminal work of 1937, Fisher [170] and Kolmogorov, Petrovsky, and Piskunov [238] introduced the following model, later called Fisher-KPP equation,

$$u_t - du_{xx} = ru(1-u). \tag{2.3.3}$$

They observed that there exists traveling wave solutions of speed c for $c\geq c^* := 2\sqrt{dr}$. They claimed that the spreading speed from localized initial data should coincide with c^*, the minimal speed of traveling waves. The spreading property starting from localized initial data was analysed more rigorously by Aronson and Weinberger [19, 20] and Weinberger [397]. Not long after, people started to consider equations in periodically heterogeneous environments; among others, the paper of Shigesada, Kawasaki and Teramoto [354] was a pioneer. A more systematic mathematical theory was developed later (see Xin [405], Berestycki and Hamel [48] and Weinberger [398]).

It is sometimes possible to compute the propagation speed of initially localized solutions to a reaction-diffusion equation by analyzing the one of the linearized equation in a neighborhood of zero. When this happens, the equation is said to be *linearly deteminate*, or we say that *linear determinacy* holds. This property has been studied for scalar equations (see, for instance, [397]) but also in the context of homogeneous systems (see Lui [269] and Weinberger, Lewis and Li [399]). In the case of systems, it is required that both the nonlinear and the linear equations be order-preserving in time. An important example equations that are monotone in time are reaction-diffusion systems which are coupled only in their zero-order term, and which coupling is *cooperative*. In the case of matrices, this means that all off-diagonal entries are nonnegative. Traveling wave for cooperative systems have also been studied, by Volpert, Volpert and Volpert [383] and Ogiwara and Matano [309, 310], among others. Spreading speeds and linear determinacy have been generalized to Banach lattices in the work of Liang and Zhao [254].

In the case of System (2.3.2) with homogeneous coefficients, it can be seen that it is cooperative near 0 because the quadratic term can be neglected. However, far away from the unstable equilibrium 0, the nonlinearity becomes competitive in general (that is, if μ_u and μ_v are not too big). This means that equation (2.3.2) is of hybrid nature, so that the theory developed in [269, 399] cannot be used directly. In

fact, solutions to System (2.3.2) actually reach a non-monotone regime (see, in particular, [P2] in which non-monotone waves are constructed). Several other models consider traveling waves in a non-monotone setting. Hsu and Zhao [219], for instance, considered a non-monotone integro-difference equation that is different from ours and proved the existence of traveling waves of speed c for any c greater than a minimal speed c^* — as is the case in many KPP situations. Their idea is to construct super and sub-solutions by replacing the nonlinearity by its monotone envelope from above and from below. Such a method cannot be applied directly to our system, unfortunately, since our equation is vector-valued.

In a spatially homogeneous setting, several results exist already for systems of reaction-diffusion equations for which the monotone theory does not apply directly. Let us mention the work of Wang [388], who studied spreading speeds and traveling waves for non-monotone systems in a case where the nonlinearity can be framed by two cooperative functions. Morris, Börger and Crooks [291] studied a two-component system quite similar to (2.3.2) and gave precise estimates on the tails of the fronts. Girardin [190, 189] proved the existence of traveling waves and studied their asymptotic behavior in a quite general setting of homogeneous KPP-type systems similar to (2.3.1). Our approach here is different, since we want our argument to work for periodic coefficients and the canonical equation for traveling waves is not elliptic in this context. We use the Poincaré map of the time-dependent problem and a fixed-point theorem to construct the traveling waves. In the process we use a monotone subsystem to obtain a lower estimate on the solution.

In the case of a system with spatially homogeneous coefficients, we can further prove the convergence of the traveling waves and time-dependent problem to the unique constant stationary solution in many cases (Theorem 2.3.33). Previously there were results on the existence of traveling waves [P2, 190] and their qualitative behavior [189, 291] but the long-time convergence to a stationary solution was only studied in a bounded domain [100].

In the case of periodically heterogeneous equations, pulsating traveling waves for (2.3.2) traveling at the candidate minimal speed were constructed in [P3] by a vanishing viscosity method applied to the equation in the moving frame, but the minimality of the speed was not known. Here we not only show that this speed is indeed minimal, but also prove that it corresponds to the spreading speed of front-like initial data and construct traveling waves for larger speeds. The crucial remark which allows such a construction is that one can identify a cooperative system to which any solution of (2.3.2) is a supersolution, which provides a way to estimate the solutions to (2.3.2) from below.

Before stating our results, let us discuss some technical notions. One of the first natural questions that one might ask when investigating models like (2.3.1) is whether a population can survive in time. Indeed, in equation (2.3.2) for instance, taking $r_u(x) \leq -\delta < 0$ and $r_v(x) \leq -\delta$ leads to the global extinction of any solution starting from a bounded initial data. It turns out that, for our class of problems, the answer to this question only depends on the linearization of (2.3.1) and, more precisely, on the *generalized principal eigenvalue* λ_1^∞ defined as the limit, as $R \to \infty$, of the principal eigenvalue in the bounded domain $(-R, R)$,

$$\begin{cases} -\mathcal{L}\varphi^R = Df(x,0)\varphi^R + \lambda_1^R \varphi^R, \\ \varphi^R(-R) = \varphi(R) = 0, \end{cases} \tag{2.3.4}$$

where $Df(x,u)$ is the Jacobian matrix of f in the variable u only, under the requirement that $\varphi^R(x) > 0$ componentwise on $(-R, R)$. That λ_1^R is unique and that it admits a limit when $R \to +\infty$ is classical but will be recalled in the present section 2.3 (Proposition 2.3.4). To distinguish it from other notions of principal eigenvalues (see Berestycki and Rossi [54, 55] and Nadin [298] for an overview of these notions) we will often call λ_1^∞ the *generalized Dirichlet principal eigenvalue*.

The generalized Dirichlet principal eigenvalue characterizes the survival of *compactly supported initial data*. More precisely, any solution starting from nontrivial compactly supported initial data becomes uniformly positive as $t \to +\infty$ when $\lambda_1^\infty < 0$, and some solution gets extinct when $\lambda_1^\infty > 0$. Another important notion of principal eigenvalue that will be used in the present section 2.3 is the *periodic principal eigenvalue*, defined as the solution to

$$\begin{cases} -\mathcal{L}\varphi^{per} = Df(x,0)\varphi^{per} + \lambda_1^{per}\varphi^{per}, \\ \varphi^{per} \text{ is } L\text{-periodic}, \end{cases} \tag{2.3.5}$$

under the requirement that $\varphi^{per}(x) > 0$ componentwise on $\mathbb{R}$. This notion characterizes the survival of *periodic initial data*. More precisely, any solution starting from nontrivial periodic initial data becomes uniformly positive as $t \to +\infty$ when $\lambda_1^{per} < 0$, and any bounded solution gets extinct when $\lambda_1^{per} > 0$. In a way, λ_1^∞ characterizes the *survival of the species in an initially empty space* (compactly supported initial data) and λ_1^{per} characterizes the *survival of the species in an already invaded space* (periodic initial data).

There is no necessity in general that these two notions be equal; the most that can be said is that

$$\lambda_1^{per} \leq \lambda_1^{\infty}.$$

An interpretation of this inequality is that *it is more difficult to survive in an empty space than in an already invaded space*. It turns out that, for scalar reaction-diffusions without a first-order (advection) term, the equality $\lambda_1^{per} = \lambda_1^{\infty}$ is always true. This fact was remarked by Nadin [298, Proposition 3.2]. As we will see in the present section 2.3 (Proposition 2.3.43), the situation for systems is in sharp contrast with what happens for scalar equations, as it is possible to construct a system with no advection and $\lambda_1^{per} < \lambda_1^{\infty}$. We recover the equality $\lambda_1^{per} = \lambda_1^{\infty}$ between the two notions under some symmetry assumption on the coefficients of the equation, detailed in Assumption 2.3.5 (in particular, it is true for constant coefficients).

Next we turn to the formula for the propagation speed. It involves again spectral notions related to the linearized problem, this time the function $k(\lambda)$ defined as

$$\begin{cases} -e^{\lambda x}\mathcal{L}\big(\varphi^\lambda e^{-\lambda x}\big) = Df(x,0)\varphi^\lambda + k(\lambda)\varphi^\lambda, \\ \varphi^\lambda \text{ is } L\text{-periodic}, \end{cases} \tag{2.3.6}$$

under the requirement that $\varphi^\lambda(x) > 0$ componentwise on $\mathbb{R}$. This function will be extensively studied in Proposition 2.3.6. The propagation speed towards $+\infty$ of solutions starting from front-like initial data supported in $(-\infty, 0)$ to (2.3.1) can then be expressed as

$$c^* = \inf_{\lambda>0} \frac{-k(\lambda)}{\lambda}, \tag{2.3.7}$$

which is a well-known formula in the scalar case [405, 398, 48, 50]. However, once again, systems do not behave exactly like scalar equations. When investigating the speed of towards $-\infty$ of solutions starting from front-like initial data supported in $(+\infty, 0)$ to (2.3.1), we naturally arrive at the formula

$$c^*_{\text{left}} = \inf_{\lambda>0} \frac{-k(-\lambda)}{\lambda}, \tag{2.3.8}$$

which is not necessarily equal to c^*_{right} defined by (2.3.7). For scalar equations without advection, it turns our that the equality $c^*_{\text{left}} = c^*_{\text{right}}$ is always true, because the function $k(\lambda)$ is even (this can be seen from [298, proof of Proposition 3.2]). In the context of systems it is possible to construct counterexamples in which $c^*_{\text{left}} \neq c^*_{\text{right}}$ even though there is no advection (Remark 2.3.44). Thus the situation for systems is, once again, in sharp contrast with the one of scalar equations. We recover the equality $c^*_{\text{left}} = c^*_{\text{right}}$ (Proposition 2.3.10) under an additional symmetry assumption on the coefficients of the equation (Assumption 2.3.5).

Among other main results of the section 2.3, we show the linear determinacy (Theorem 2.3.19) and existence of traveling waves (Theorem 2.3.21) for solutions to (2.3.1) with sublinear nonlinearity, under some additional requirements. We require in particular that the Jacobian matrix be cooperative and irreducible. We also study the case of rapidly oscillating coefficients and show that the qualitative properties of such systems are very close to the ones of homogeneous systems. Regarding the general system (2.3.1), we prove a homogenization formula for the speed (Theorem 2.3.11). The homogenization limit allows us to study the particular case of (2.3.2) in more details. In particular, we prove the existence, uniqueness and global stability of the equilibrium for rapidly oscillating coefficients under some conditions, by using dynamical system arguments (see Theorem 2.3.34). This gives a non-trivial example of non-homogeneous systems for which the global behavior can be determined. This part of the study is based on the homogenization theory for elliptic and parabolic operators, see *e.g.* [45] for an introduction to the theory. In the case of scalar equations, the homogenization limits of spreading speeds and pulsating traveling waves have been studied by El Smaily [159, 160] and El Smaily, Hamel and Roques [161].

The structure of the section 2.3 is as follows. In section 2.3.2 we state our main results, concerning the original system (2.3.1) with sub-linear nonlinearity and the particular case (2.3.2). In section 2.3.3 we prove the results in the general framework of KPP-type nonlinearities for d-dimensional systems. In section 2.3.4 we propose two singular limits of our systems. In section 2.3.5, we prove the results which are specific to the model (2.3.2), including the local stability of the constant equilibrium, global stability under more restrictive assumptions and the homogenization limit.

2.3.2 Main results

In this section 2.3.2 we state the main results presented in the section 2.3. We first state the results we obtain on the specific equation (2.3.2), then present the more general results on generic one-dimensional systems.

Our interest lies in systems of the form

$$u_t = \mathcal{L}u + f(x,u), \tag{2.3.9}$$

set on the real line, where $\mathcal{L}$ is an elliptic differential operator written either in divergence form

$$\mathcal{L}u = \mathcal{L}^d u := (\sigma(x)u_x)_x + q(x)u_x, \tag{2.3.10}$$

or in nondivergence form

$$\mathcal{L}u = \mathcal{L}^{nd} u := \sigma(x)u_{xx} + q(x)u_x, \tag{2.3.11}$$

where $\sigma \in C^{1,\alpha}_{per}(\mathbb{R}, M_d(\mathbb{R}))$ is a positive diagonal matrix field, $q \in C^{\alpha}_{per}(\mathbb{R}, M_d(\mathbb{R}))$ is a diagonal matrix field, and $f \in Lip(\mathbb{R}\times\mathbb{R}^d, \mathbb{R}^d)$ are L-periodic in the variable x. First we introduce some definitions and notations.

Order on $\mathbb{R}^d$ Let $u = (u_1, \dots, u_d)^T \in \mathbb{R}^d$ and $v = (v_1, \dots, v_d)^T \in \mathbb{R}^d$. We denote by $u \le v$ the component-wise order of $\mathbb{R}^d$, that is to say

$$u \le v \quad \Longleftrightarrow \quad (u_i \le v_i \text{ for all } i \in \{1, \dots, d\}).$$

Recall that $(\mathbb{R}^d, \le)$ is a Banach lattice which positive cone is $\mathbb{R}^d_+ := \{u \in \mathbb{R}^d \,|\, u \ge 0\}$. We will use the notation $u \ll v$ to denote the component-wise strict order

$$u \ll v \quad \Longleftrightarrow \quad (u_i < v_i \text{ for all } i \in \{1, \dots, d\}).$$

When u and v are two vectors, then $\min(u,v)$ and $\max(u,v)$ are the usual component-wise minimum and maximum of u and v:

$$\min(u,v) = \big(\min(u_1,v_1), \dots, \min(u_d,v_d)\big)^T, \quad \max(u,v) = \big(\max(u_1,v_1), \dots, \max(u_d,v_d)\big)^T.$$

Finally we denote $\mathbf{1} := (1,1,\dots,1)^T \in \mathbb{R}^d$ the d-dimensional vector with all components equal to 1.

2.3.2.1 The linear problem. Principal eigenvalues and spreading speeds.

We first focus on the linear part of System (2.3.9), that is when $f(x,u)$ is a linear function of u. Our interest lies in systems which preserve the canonical partial order on $\mathbb{R}^d$.

Definition 2.3.1 (Cooperative matrix)**.** Let $A(x) = (a_{ij}(x))_{1\le i,j\le d}$ be a matrix-valued function (from $\mathbb{R}$ to $M_d(\mathbb{R})$). $A(x)$ is *cooperative* if $a_{ij}(x) \ge 0$ for all $i \ne j$ and $x \in \mathbb{R}$.

Next we introduce the notion of fully coupled system. This corresponds, in a way, to systems that cannot be split into two independent subsystems.

Definition 2.3.2 (Fully coupled matrix.)**.** Let $A(x) = (a_{ij}(x))_{1\le i,j\le d}$ be a matrix-valued function (from $\mathbb{R}$ to $M_d(\mathbb{R})$). We say that $A(x)$ *fully coupled* if there exists $\nu > 0$ and $r > 0$ such that for any non-trivial partition $I, J \subset \{1, \dots, d\}$ (i.e. $I \cup J = \{1, \dots, d\}$ and $I \cap J = \varnothing$), there exists $i \in I$, $j \in J$, and a ball $B(x_{ij}, r)$ for some $x_{ij} \in \mathbb{R}$, such that

$$\inf_{x \in B(x_{ij}, r)} a_{ij}(x) \ge \nu > 0. \tag{2.3.12}$$

Note that, if $A(x)$ is a constant matrix, then it is fully coupled in the sense introduced above if and only if it is cooperative and irreducible.

We suspect that the ball $B(x_0, r)$ above could be replaced by a measurable set of positive Lebesgue measure, as is done in [87], but we will not pursue such generality as it would add unnecessary complexity to the proofs; moreover it is not essential in our analysis.

As usual in sublinear situations, the principal eigenvalue of the system under consideration plays a crucial role in the survival of the population. We define the notion of *periodic principal eigenvalue* in the case of systems with d components

Definition 2.3.3 (Principal eigenpairs)**.** Let $A(x)$ be a fully coupled cooperative matrix function and $\mathcal{L}$ be a diagonal uniformly elliptic operator.

By a *periodic principal eigenpair* associated with system (2.3.9), we refer to a solution pair $(\lambda_1^{per}, \varphi^{per}(x))$ to the system

$$-\mathcal{L}\varphi^{per} = A(x)\varphi^{per}(x) + \lambda_1^{per}\varphi^{per}(x) \tag{2.3.13}$$

under the L-periodic boundary conditions, satisfying $\varphi^{per}(x) \gg 0$. Here λ_1^{per} is called the *periodic principal eigenvalue* and $\varphi^{per}(x)$ a *periodic principal eigenfunction* or *periodic principal eigenvector*.

Similarly, by *Dirichlet principal eigenpair* associated with system (2.3.9) in the interval of radius $R > 0$ we refer to a solution pair $(\lambda_1^R, \varphi^R(x))$ to the system

$$-\mathcal{L}\varphi^R = A(x)\varphi^R(x) + \lambda_1^R\varphi^R(x) \quad \text{in } (-R, R), \tag{2.3.14}$$

satisfying the Dirichlet boundary conditions $\varphi^R(-R) = \varphi^R(R) = 0$ and $\varphi^R(x) \gg 0$ in $(-R, R)$. Here λ_1^R is called the *Dirichlet principal eigenvalue* and $\varphi^R(x)$ a *Dirichlet principal eigenfunction* or *Dirichlet principal eigenvector*. We denote

$$\lambda_1^\infty := \lim_{R\to\infty} \lambda_1^R. \tag{2.3.15}$$

The existence of the principal eigenpairs $(\lambda_1^{per}, \varphi^{per})$ and (λ_1^R, φ^R) and the uniqueness of λ_1^{per} and λ_1^R follow immediately from the Krein-Rutman Theorem. Moreover there always holds $\lambda_1^{R'} > \lambda_1^R > \lambda_1^{per}$ for $0 < R' < R$. Consequently, we have

$$\lambda_1^\infty \geq \lambda_1^{per}. \tag{2.3.16}$$

The above two notions of principal eigenvalue correspond to very different qualitative properties of the solutions to (2.3.9). The Dirichlet eigenvalue λ_1^R gives a criterion for the survival in the bounded domain $(-R, R)$ under the Dirichlet boundary conditions, and $\lambda_1^\infty = \lim_{R\to\infty} \lambda_1^R$ characterizes, in a sense, the survival of solutions with compactly supported initial conditions on the real line. More precisely, the species does not get extinct if $\lambda_1^\infty < 0$ (see Theorem 2.3.17 below), while it converges to 0 (extinction) as $t \to \infty$ if $\lambda_1^\infty > 0$. On the other hand, λ_1^{per} characterises the survival of solutions starting from positive periodic initial conditions or, more generally, the sustainability of an already invaded space. We will state a condition under which both eigenvalues have the same sign in Proposition 2.3.9.

Whether or not equality holds in (2.3.16) depends on the situation. Proposition 2.3.43 provides a counterexample to the equality in (2.3.16) in the case of a system of two equations with no advection term and strong coupling. These properties, along with some other properties of those eigenpairs, will be proved in section 2.3.3.2 and in Appendix B. Here we collect some useful properties of the principal eigenvalues.

Proposition 2.3.4 (On the Dirichlet principal eigenvalue for cooperative systems)**.** *Let $A(x)$ be a cooperative and fully coupled d-dimensional L-periodic matrix field, $\mathcal{L}$ be a L-periodic diagonal uniformly elliptic operator. Then:*

(i) For any $R \in (0, +\infty)$, there exists a principal eigenfunction $\varphi^R > 0$ associated with λ_1^R, which is unique up to the multiplication by a positive scalar.

(ii) For any $R \in (0, +\infty)$, we have

$$\lambda_1^R := \sup\{\lambda \in \mathbb{R} \,|\, \exists \phi \in C^2((-R, R), \mathbb{R}^d) \cap C^1([-R, R], \mathbb{R}^d), \phi > 0, -\mathcal{L}\phi - A(x)\phi - \lambda\phi \geq 0\}. \tag{2.3.17}$$

(iii) The mapping $R \mapsto \lambda_1^R$ is decreasing.

(iv) There exists a positive eigenfunction associated with λ_1^∞.

(v) For $R \in (0, +\infty]$, we have

$$\lambda_1^R = \max_{\phi>0} \inf_{x\in(-R,R)} \min_{1\leq i\leq d} \frac{(-\mathcal{L}\phi - A(x)\phi)_i}{\phi_i} \tag{2.3.18}$$

Next we introduce an important object for the study of the spatial behavior of the solutions to (2.3.9). Given $\lambda \in \mathbb{R}$, we let $L_\lambda\phi(x) := e^{\lambda x}\mathcal{L}(e^{-\lambda x}\phi(x))$ and $k(\lambda)$ be the principal eigenvalue of the operator $-L_\lambda - A(x)$ restricted on L-periodic functions. Equivalently, we have

$$L_\lambda\phi = (\sigma(x)\phi_x)_x + (-2\lambda\sigma(x) + q(x))\phi_x + (-\lambda\sigma_x(x) - \lambda q(x) + \lambda^2\sigma(x))\phi,$$

if $\mathcal{L}$ is written in divergence form, or

$$L_\lambda \phi = \sigma(x)\phi_{xx} + (-2\lambda\sigma(x) + q(x))\phi_x + (-\lambda q(x) + \lambda^2\sigma(x))\phi,$$

if $\mathcal{L}$ is written in nondivergence form, and $k(\lambda)$ is the unique real number for which there exists a solution $\phi > 0$ to

$$\begin{cases} -L_\lambda\phi(x) - A(x)\phi(x) = k(\lambda)\phi(x), & x \in \mathbb{R}, \\ \phi > 0, \qquad \phi \text{ is } L\text{-periodic}. \end{cases} \tag{2.3.19}$$

The map $k(\lambda)$ plays a crucial role regarding the spatial properties of (2.3.9) as it the center of a formula for the spreading speed associated with (2.3.9). It also provides a connection between the generalized Dirichlet an periodic principal eigenvalue, as will be stated in the next Proposition. However, in order to state our results, we first need to introduce an assumption which ensures that the dynamics of the model is the same in both directions of $\mathbb{R}$.

Assumption 2.3.5 (Isotropic behavior)**.** We assume that the operator $\mathcal{L}$ has no advection: $q(x) \equiv 0$. Furthermore, we assume that either of the following conditions is satisfied.

a) Both $\sigma(x)$ and $A(x)$ are even in x,

b) $\mathcal{L} = \mathcal{L}^d$ is written in divergence form (2.3.10) and $A(x)$ is a symmetric matrix.

Proposition 2.3.6 (On $k(\lambda)$)**.** *Let $\mathcal{L}$ be a L-periodic diagonal uniformly elliptic operator, $A(x)$ be a cooperative and fully coupled L-periodic matrix field. Then:*

(i) For each $\lambda \in \mathbb{R}$, there exists a principal eigenpair $(k(\lambda), \phi^\lambda(x))$ with $\phi^\lambda \gg 0$ which solves (2.3.19)*, and ϕ^λ is unique up to the multiplication by a positive scalar.*

(ii) The following characterization of $k(\lambda)$ is valid:

$$k(\lambda) = \max_{\substack{\phi > 0 \\ \phi \in C^2_{per}(\mathbb{R}), \mathbb{R}^d}} \inf_{x \in \mathbb{R}} \min_{1 \le i \le d} \frac{(-L_\lambda\phi - A(x)\phi)_i}{\phi_i} \tag{2.3.20}$$

(iii) The map $\lambda \mapsto k(\lambda)$ is analytic and strictly concave. Furthermore, there exist constants $\alpha > 0$ and $\beta > 0$ such that

$$k(\lambda) \le \alpha - \beta\lambda^2 \text{ for all } \lambda \in \mathbb{R}. \tag{2.3.21}$$

(iv) The following equality holds:

$$\lambda_1^\infty = \max_{\lambda \in \mathbb{R}} k(\lambda).$$

(v) If $\mathcal{L}$ satisfies Assumption 2.3.5, then the mapping $\lambda \mapsto k(\lambda)$ is even.

Finally, we introduce a formula which gives the minimal speed of traveling waves to (2.3.9), and show some related properties.

Proposition 2.3.7 (On the formula for the minimal speed)**.** *Let $\mathcal{L}$ be a L-periodic diagonal uniformly elliptic operator, $A(x)$ be a cooperative and fully coupled L-periodic matrix field. Suppose that $\lambda_1^{per} < 0$ and let*

$$c^* := \inf_{\lambda > 0} \frac{-k(\lambda)}{\lambda}. \tag{2.3.22}$$

Then:

(i) if $c < c^*$, then for any $\lambda > 0$, we have $c\lambda < -k(\lambda)$,

(ii) if $c = c^*$, then there exists a unique $\lambda^* > 0$ such that $\lambda^* c^* = k(\lambda^*)$, and for any $\lambda > 0$ with $\lambda \neq \lambda^*$ we have $\lambda c^* < -k(\lambda)$,

(iii) if $c > c^*$, there exists $\lambda_1^* < \lambda_2^*$ such that $\lambda_1^* c = -k(\lambda_1^*)$ and $\lambda_2^* c = -k(\lambda_2^*)$. For $\lambda \in (\lambda_1^*, \lambda_2^*)$ we have $\lambda c > -k(\lambda)$, while for $\lambda \notin [\lambda_1^*, \lambda_2^*]$ we have $\lambda c < -k(\lambda)$.

(iv) c^* is continuous in A with respect to the supremum norm.

As we will discuss in Theorem 2.3.19, the speed c^* defined by (2.3.22) is the natural speed of propagation of solutions to (2.3.9) starting from front-like initial data u_0 supported in $(-\infty, 0]$ and with $\liminf_{x\to-\infty} u_0(x) > 0$. In order to catch the propagation speed of solutions starting from initial data supported in $[0, +\infty)$ and with $\liminf_{x\to+\infty} u_0(x) > 0$, it suffices to introduce the quantity

$$c^*_{\text{left}} := \inf_{\lambda<0} \frac{k(\lambda)}{\lambda} = \inf_{\lambda>0} \frac{-k(-\lambda)}{\lambda}. \tag{2.3.23}$$

Whether the rightward speed c^* and the leftward speed c^*_{left} are equal depends, again, on the situation. In many cases, including the case of constant coefficients, such a property is true. A sufficient condition for this property to hold is given in Assumption 2.3.5. However it is false in general as can be seen as a straightforward consequence of Proposition 2.3.43; see Remark 2.3.44.

A consequence of the above results is the following Proposition.

Proposition 2.3.8. *Suppose that $\lambda_1^{per} < 0$ and that the rightward speed $c^* =: c^*_{right}$ (defined by (2.3.22)) and the leftward speed (defined by (2.3.23)) are both positive. Then*

$$\lambda_1^{\infty} < 0.$$

The proof is immediate so we sketch it here. When $c^*_{\text{right}} > 0$, it follows from the definition of c^*_{right} that $0 > -\lambda c^* \geq k(\lambda)$ for all $\lambda > 0$. Similarly since $c^*_{\text{left}} > 0$ there holds that $0 > \lambda c^* \geq k(\lambda)$ for all $\lambda < 0$. Finally since $k(0) = \lambda_1^{per} < 0$, we have that $k(\lambda) < 0$ for all $\lambda \in \mathbb{R}$ and it follows from (2.3.21) that

$$\lambda_1^{\infty} = \max_{\lambda\in\mathbb{R}} k(\lambda) < 0.$$

Proposition 2.3.8 is proved.

When $\lambda_1^{per} = 0$, it is known that the hair-trigger property may fail for nonlinear problems even in the case of a scalar equation. This can be shown by considering the following Fisher-KPP equation :

$$u_t(t,x) = u_{xx}(t,x) + u(t,x)\big(r - u(t,x)\big).$$

When $r = 0$, any bounded nonnegative solution to the above equation converges to 0 as $t \to \infty$. The proof results from a comparison with the ODE $u_t = -u^2$.

Next we derive a condition under which there is equality between the periodic principal eigenvalue and the generalized Dirichlet principal eigenvalue. As in the scalar case (see [298, 299]), it may happen that the two principal eigenvalues λ_1^{per} and λ_1^{∞} are different, for instance in the presence of a first-order term. Similarly, because of the dependency in x in the diffusion coefficient, the speed of propagation may differ when looking at solutions spreading to the right or to the left.

Proposition 2.3.9 (Dirichlet and periodic principal eigenvalues)**.** *Let Assumption 2.3.5 hold. Then*

$$\lambda_1^{\infty} := \lim_{R\to\infty} \lambda_1^R = \lambda_1^{per}. \tag{2.3.24}$$

Since λ_1^{per} is sometimes easier to estimate than λ_1^{∞}, the above proposition gives a useful criterion for the survival of solutions whose initial data is compactly supported in view of Theorem 2.3.17.

Proposition 2.3.10. *Under Assumption 2.3.5, the rightward and leftward spreading speeds are the same.*

If Assumption 2.3.5 fails to hold, the rightward speed and the leftward speed may not be the same, even if there is no advection, i.e. $q(x) \equiv 0$. As explained in Remark 2.3.44, Proposition 2.3.43 provides a counterexample in the case of strong coupling. This is in sharp contrast with the scalar case, where it is known that the two speeds are always the same in the absence of an advection.

Last we turn our interest to systems with rapidly oscillating coefficients and give a description of the asymptotic behavior of the spreading speed.

Theorem 2.3.11 (The speed of rapidly oscillating systems)**.** *Let $\sigma(x) > 0$, $q(x)$ and $A(x)$ be 1-periodic. For each $\varepsilon \in (0,1)$, let*

$$\mathcal{L}^{\varepsilon} u := (\sigma^{\epsilon}(x)u_x)_x + q^{\varepsilon}(x)u = \left(\sigma\left(\frac{x}{\varepsilon}\right)u_x\right)_x + q\left(\frac{x}{\varepsilon}\right)u$$

be a uniformly elliptic operator and $A^\varepsilon(x) := A\left(\frac{x}{\varepsilon}\right)$ *be a cooperative fully coupled matrix field. We let* c^*_ε *be the spreading speed associated with* $\mathcal{L}^\varepsilon$ *and* $A^\varepsilon(x)$*. Then, we have*

$$\lim_{\varepsilon\to 0} c^*_\varepsilon = c^*(\overline{\mathcal{L}}^H + \overline{A}), \tag{2.3.25}$$

where:

$$\overline{\mathcal{L}}^H u := \overline{\sigma}^H u_{xx} + \overline{q}^H u_x,$$

$$\overline{\sigma}^H_i := \left(\int_0^1 \frac{1}{\sigma_i(z)}\mathrm{d}z\right)^{-1}, \qquad \overline{q}^H_i := \overline{\sigma}^H_i \int_0^1 \frac{q_i(z)}{\sigma_i(z)}\mathrm{d}z, \qquad \overline{A} := \int_0^1 A(z)\mathrm{d}z,$$

and $c^*(\overline{\mathcal{L}}^H + \overline{A})$ *is given by:*

$$c^*(\overline{\mathcal{L}}^H + \overline{A}) = \inf_{\lambda>0} \frac{\lambda_{PF}\left(\lambda^2\overline{\sigma}^H - \lambda\overline{q}^H + \overline{A}\right)}{\lambda}$$

where $\lambda_{PF}(X)$ *is the Perron-Frobenius eigenvalue of an constant irreducible cooperative matrix* X*.*

2.3.2.2 Spreading in equations of hybrid nature and traveling waves.

In this section 2.3.2.2 we derive some proerties of the solutions to the nonlinear equation (2.3.9). We first recall some notions that we will use in the statement of our results.

Lipschitz continuity Let $U \subset \mathbb{R}^d$ be given. We say that $f(x,u) = (f_1(x,u),\dots,f_d(x,u)) : \mathbb{R}\times U \to \mathbb{R}^d$ is locally Lipschitz continuous with respect to u if, for all $M > 0$, there is a constant $K > 0$ such that

$$\|f(x,u) - f(x,v)\| \le K\|u - v\| \text{ for all } x \in \mathbb{R} \text{ and } u, v \in U \text{ with } \|u\| \le M \text{ and } \|v\| \le M.$$

Definition 2.3.12 (Cooperative function)**.** Let $U \subset \mathbb{R}^d$ and $f : \mathbb{R}\times U \to \mathbb{R}^d$. The function $f = (f_1,\dots,f_d)$ is *cooperative* (or equivalently, *quasi-monotone*) on U if there is a real number $\gamma > 0$ such that $f(x,u) + \gamma u$ is monotone non-decreasing with respect to u for the usual component-wise order.

Remark 2.3.13. The notion of cooperative function is equivalent to the notion of quasi-monotonicity, which is more commonly used in the dynamical systems community.

Alternatively, a function f is cooperative if, and only if, for any $x \in \mathbb{R}$, $u = (u_1,\dots,u_d) \in U$, $1 \le i, j \le d$ such that $i \ne j$, the function $v \mapsto f_i(x,u_1,\dots,u_{j-1},v,u_{j+1},\dots,u_d)$ is nondecreasing.

Next we define the notion of sublinear nonlinearity that we will use throughout the section 2.3:

Definition 2.3.14 (Sublinear nonlinearity)**.** We say the nonlinearity $f(x,u) = (f_1(x,u),\dots,f_d(x,u))$ is sublinear provided it is continuous in both variables, Lipschitz continuous with respect to u and

(i) for all $x \in \mathbb{R}$, $f(x,0) = 0$.

(ii) $f(x,u)$ is differentiable at $u = 0$ uniformly in x.

(iii) for each $x \in \mathbb{R}$ and each $u \ge 0$, we have

$$f(x,u) \le Df(x,0)u.$$

Finally, in order to compute the spreading speed, we need an additional regularity assumption on the properties of the nonlinearity in a vicinity of 0.

Assumption 2.3.15 (Regularity in a neighborhood of 0)**.** We assume that f is a sublinear nonlinearity and that the differential matrix field $Df(x,0)$ is cooperative and fully coupled. Moreover, we assume that there exists a family of cooperative and fully coupled matrix fields $(A^\delta(x))_{\delta\in(0,1)}$ satisfying

$$\sup_{x\in\mathbb{R}} \|A^\delta(x) - Df(x,0)\|_{M_d(\mathbb{R})} \to 0 \text{ as } \delta \to 0,$$

and for each $\delta \in (0,1)$ there exists $\eta > 0$ such that whenever $\|u\| \le \eta$ and $u > 0$, we have

$$f(x,u) \ge A^\delta(x)u.$$

As an example of nonlinearity satisfying Assumption 2.3.15, one can remark that if the Jacobian matrix $Df(x,0)$ has only positive coefficients, then f satisfies Assumption 2.3.15 with $A^\delta(x) = (1-\delta)Df(x,0)$.

Definition 2.3.16 (Monotone lower barrier)**.** Let $f = (f_1, \dots, f_d) \in Lip(\mathbb{R} \times \mathbb{R}^d, \mathbb{R}^d)$ be a L-periodic function. We say that $f^- \in Lip(\mathbb{R} \times \mathbb{R}^d, \mathbb{R}^d)$ is a *monotone lower barrier* of f if there exists a constant $\eta > 0$ such that

1. $f(x,u) \geq f^-(x,u)$ for all $u = (u_1, \dots, u_d) \geq 0$ with $u_i \leq \eta$ for some $i \in \{1, \dots, d\}$.
2. $Df^-(x,0)u = Df(x,0)u$ for all $(x,u) \in \mathbb{R} \times \mathbb{R}^d$.
3. for all $i, j \in \{1, \dots, d\}$ with $j \neq i$, the function $u_j \mapsto f_i^-(x, u_1, \dots, u_d)$ is non-decreasing whenever $|u_i| \leq \eta$.

Note that the above assumptions imply, in particular, that f^- is cooperative (or equivalently, quasi-monotone) in a neighborhood of 0, more precisely on the domain $\mathbb{R} \times B_\infty^+(0,\eta)$ (where $B_\infty(0,\eta) := \{u \geq 0 \,|\, \|u\|_\infty \leq \eta\}$).

Equipped with these notions, we now state the first result on nonlinear equations of this section 2.3. Theorem 2.3.17 showed that there is a hair-trigger effect when the Dirichlet principal eigenvalue λ_1^∞ is negative. More precisely, any solution starting from a non-trivial initial data becomes locally uniformly positive when $t \to +\infty$.

Theorem 2.3.17 (Hair-Trigger effect)**.** *Let $\mathcal{L}$ be a diagonal uniformly elliptic operator and f be a sublinear function. Assume that f admits a monotone lower barrier in the sense of Definition 2.3.16 and suppose finally that $\lambda_1^\infty < 0$. Then there exists $\delta > 0$ with such that whenever $u(t,x)$ is a solution of* (2.3.9) *with an initial condition $u(0,x) := u_0(x)$ which is non-negative and non-trivial, then*

$$\liminf_{t \to +\infty} u(t,x) \geq \delta \mathbf{1},$$

uniformly in bounded sets of $\mathbb{R}$.

Next we introduce our notion of spreading speed.

Definition 2.3.18 (Spreading speed)**.** The real number c^* is the *spreading speed* associated with system (2.3.9) if all non-negative solutions $u(t,x)$ of (2.3.9) satisfy

(i) if $\liminf_{x \to -\infty} u \gg 0$, then for each $c < c^*$ we have

$$\liminf_{t \to +\infty} \inf_{x \leq ct} u(t,x) \gg 0.$$

(ii) if there is $K \in \mathbb{R}$ such that $u(0,x) \equiv 0$ for all $x \geq K$, then for all $c > c^*$ we have

$$\limsup_{t \to +\infty} \left[\sup_{x \geq ct} \|u(t,x)\| \right] = 0.$$

Note the we impose by convention that the propagation happens towards the right. It may happen that the rightward and leftward spreading speeds differ, as remarked in the previous section 2.3.2.1.

Next we prove the linear determinacy of sublinear systems which have a monotone lower barrier. Such systems need not possess a comparison principle (system (2.3.2), in particular, does not), therefore the classical theory cannot be applied directly.

Theorem 2.3.19 (Linear determinacy)**.** *Let $\mathcal{L}$ be a L-periodic elliptic operator, and $f \in Lip(\mathbb{R} \times \mathbb{R}^d, \mathbb{R}^d)$ is L-periodic in x, admits a monotone lower barrier as defined in Definition 2.3.16 and satisfies Assumption 2.3.15. We denote $A(x) := Df(x,0)$ and assume that the periodic principal eigenvalue λ_1^{per} is negative. Then:*

(i) System (2.3.9) *has a spreading speed c^* as in Definition 2.3.18.*

(ii) We have

$$c^* = \inf_{\lambda>0} -\frac{k(\lambda)}{\lambda}, \tag{2.3.26}$$

where $(k(\lambda), \varphi_\lambda(x) \gg 0)$ *is defined by* (2.3.19).

We finally specify what we mean by *traveling wave*:

Definition 2.3.20 (Traveling wave)**.** A *traveling wave* u with speed $c > 0$ and period L for equation (2.3.9) is a nonnegative entire solution to (2.3.9) which satisfies the following condition:

$$\forall x \in \mathbb{R}, \forall t \in \mathbb{R}, u\left(t + \frac{L}{c}, x\right) = u(t, x - L),$$

as well as the boundary conditions at $\pm\infty$ for all $t \in \mathbb{R}$:

$$\lim_{x\to+\infty} u(t,x) = 0,$$
$$\liminf_{x\to-\infty} u(t,x) \gg 0.$$

With a little more regularity on f we get the existence of traveling waves for $c \geq c^*$.

Theorem 2.3.21 (Existence of traveling waves)**.** *In addition to the assumptions of Theorem 2.3.19, suppose that there exist constants* $M > 0$ *and* $\beta > 0$ *such that*

$$\|f^-(x,u) - A(x)u\|_\infty \leq M\|u\|_\infty^{1+\beta} \text{ for all } x \in \mathbb{R} \text{ and } \|u\|_\infty \leq \eta. \tag{2.3.27}$$

Then, there exists a traveling wave for (2.3.9) *for all* $c \geq c^*$.

Remark 2.3.22 (On monotone sub-solutions of (2.3.2))**.** Theorem 2.3.19 allows us to compute the spreading speed and construct traveling waves for system (2.3.2). Indeed the modified system

$$\begin{cases} u_t = \sigma_u(x)u_{xx} + \big(r_u(x) - \mu_u(x) - \kappa_u(x)u - \beta u\big)u + v\big(\mu_v(x) - \kappa_u(x)u\big), \\ v_t = \sigma_v(x)v_{xx} + \big(r_v(x) - \mu_v(x) - \kappa_v(x)v - \beta v\big)v + u\big(\mu_u(x) - \kappa_v(x)\big), \end{cases} \tag{2.3.28}$$

is a monotone lower barrier for the original system (which corresponds to $\beta = 0$). The original system itself is a monotone lower barrier in the region

$$\left\{0 \leq u \leq \inf_{x\in\mathbb{R}} \left(\frac{\mu_v(x)}{\kappa_u(x)}\right)\right\} \times \left\{0 \leq v \leq \inf_{x\in\mathbb{R}} \left(\frac{\mu_u(x)}{\kappa_v(x)}\right)\right\}.$$

However, in order to estimate solutions to (2.3.28) when t becomes large, we need to construct a monotone lower barrier which leaves the interval $[0, \eta\mathbf{1}] := \{u \,|\, 0 \leq u \leq \eta\mathbf{1}\}$ invariant. This is precisely achieved for $\beta > 0$ sufficiently large.

In particular, Theorem 2.3.24 below is a direct consequence of Theorem 2.3.19.

2.3.2.3 On System (2.3.2)

Our first result concerns the formula for the spreading speed of (2.3.2), which provides a way to compute the speed of traveling waves for (2.3.2). The framework in which we prove this linear determinacy property is the following.

Assumption 2.3.23 (Cooperative-competitive system)**.** We let $\sigma_u(x) > 0$, $\sigma_v(x) > 0$, $\kappa_u(x) > 0$, $\kappa_v(x) > 0$, $\mu_v(x) > 0$, $\mu_u(x) > 0$, be L-periodic positive continuous functions and $r_u(x)$, $r_v(x)$ be L-periodic continuous functions of arbitrary sign.

Our first result concerns the propagation of solutions to the parabolic equations (2.3.2).

Theorem 2.3.24 (Spreading speed for (2.3.2))**.** *Let Assumption 2.3.23 be satisfied. Assume that the principal eigenvalue of the linearised system is negative. Then, there exists a real number* c^* *such that for any nonnegative initial condition* $(u_0(x) \geq 0, v_0(x) \geq 0)$,

(i) if $\inf_{x\le K}\min(u_0(x),v_0(x))>0$ *for some* $K\in\mathbb{R}$*, then*

$$\liminf_{t\to\infty}\left[\inf_{K\le x\le ct}\min(u(t,x),v(t,x))\right]>0, \qquad \text{for all } 0<c<c^*,$$

(ii) if there is $K>0$ *such that* $u_0(x)\equiv 0$ *and* $v_0(x)\equiv 0$ *for all* $x\ge K$*, then*

$$\limsup_{t\to\infty}\left[\sup_{x\ge ct}\max(u(t,x),v(t,x))\right]=0, \qquad \text{for all } c>c^*,$$

where $(u(t,x),v(t,x))$ *is the solution to the Cauchy problem* (2.3.2) *starting from the initial condition* $(u_0(x),v_0(x))$*.*

Moreover, we have the formula

$$c^*=\inf_{\lambda>0}\frac{-k(\lambda)}{\lambda},$$

where $k(\lambda)$ *is defined in* (2.3.19)*.*

Remark 2.3.25. As shown in Remark 2.3.44, with some particular choice of the parameters, the spatial behavior of System (2.3.2) approaches the one of a scalar KPP-type equation with an arbitrary first-order advection term. In particular, we expect that the spreading speed to the right is different than the spreading speed to the left. One may even reach a situation in which the speed to the right is positive, but the speed to the left is negative. In such a situation, compactly supported initial data would propagate to the right but also regress in the same direction, causing a pulse-like behavior with variable width that doesn't achieve a positive infimum in any bounded interval in the long run, even when the periodic principal eigenvalue is positive. Therefore we have no hope to have a hair-trigger effect in general for our kind of system when $\lambda_1^{per}<0$. The correct notion of principal eigenvalue for a hair-trigger effect is the *generalized Dirichlet principal eigenvalue* λ_1^{∞}, which will be introduced in Definition 2.3.3 in the section 2.3.2.1. We refer to Theorem 2.3.17 for a precise statement of the hair-trigger effect.

Next we introduce the notion of traveling wave solutions, which are entire solutions propagating at a fixed speed c.

Definition 2.3.26 (Traveling wave solutions)**.** Let $(u(t,x),v(t,x))$ be an entire solution to (2.3.2), *i.e.* a solution that is defined for all $t\in\mathbb{R}$ and $x\in\mathbb{R}$. We say that $(u(t,x),v(t,x))$ is a *traveling wave solution* traveling at speed c if it satisfies

$$u\left(t+\frac{L}{c},x\right)=u(t,x-l),\ v\left(t+\frac{L}{c},x\right)=v(t,x-l),\ \text{for all } (t,x)\in\mathbb{R}^2, \tag{2.3.29}$$

as well as the boundary conditions

$$\begin{aligned}&\lim_{x\to+\infty}u(t,x)=0,\ \lim_{x\to+\infty}v(t,x)=0,\ \text{ for all } t\in\mathbb{R},\\ &\liminf_{x\to-\infty}u(t,x)>0,\ \liminf_{x\to-\infty}v(t,x)>0,\ \text{ for all } t\in\mathbb{R}.\end{aligned}$$

Theorem 2.3.27 (Existence of traveling waves)**.** *Let Assumption 2.3.23 hold. There exists a traveling wave for* (2.3.2) *with speed* c *if, and only if,* $c\ge c^*$*.*

Remark 2.3.28. Just as in the case with the spreading speed, the above theorem implies that the minimal speed of the traveling wave propagating to the right direction coincides with the spreading speed. The speed to the left may not be the same (see Remark 2.3.44) and might even be negative.

As we will see, Theorems 2.3.24 and 2.3.27 are direct consequences of results on more general cooperative-competitive systems, namely Theorems 2.3.19 and 2.3.21.

Next we turn to the long-time behavior of the solutions to the Cauchy problem (2.3.2), starting from a bounded nonnegative nontrivial initial condition. In the case where the coefficients are independent of x, we were able to show convergence to a unique stationary state. More precisely, we consider the homogeneous problem

$$\begin{cases}u_t-\sigma_u u_{xx}=(r_u-\kappa_u(u+v))u+\mu_v v-\mu_u u\\ v_t-\sigma_v v_{xx}=(r_v-\kappa_v(u+v))v+\mu_u u-\mu_v v,\end{cases} \tag{2.3.30}$$

where $r_u \in \mathbb{R}$, $r_v \in \mathbb{R}$, $\kappa_u > 0$, $\kappa_v > 0$, $\mu_u > 0$, $\mu_v > 0$. The linearization of the right-hand side of (2.3.30) around $(u, v) = (0, 0)$ is given by the matrix

$$A := \begin{pmatrix} r_u - \mu_u & \mu_v \\ \mu_u & r_u - \mu_v \end{pmatrix}. \tag{2.3.31}$$

Since the off-diagonal entries of A are positive, we easily see that A has real eigenvalues. Let λ_A denote the largest eigenvalue of A

$$\lambda_A := \max\{\lambda \in \mathbb{R} \,|\, \lambda \text{ is an eigenvalue of A}\}. \tag{2.3.32}$$

Then by the Perron-Frobenius theory, the eigenvector corresponding to λ_A is positive: $(\varphi_A^u, \varphi_A^v)^T$, $\varphi_A^u > 0$, $\varphi_A^v > 0$.

Assumption 2.3.29. We assume that $(0, 0)$ is linearly unstable for the ODE problem (2.3.33),

$$\begin{cases} u_t = (r_u - \kappa_u(u + v))u + \mu_v v - \mu_u u \\ v_t = (r_v - \kappa_v(u + v))v + \mu_u u - \mu_v v. \end{cases} \tag{2.3.33}$$

i.e. $\lambda_A > 0$.

It can be seen that the condition $\lambda_A > 0$ is always satisfied when $r_u > 0$ and $r_v > 0$, and always fails when $r_u < 0$ and $r_v < 0$. The situation when r_u and r_v do not have the same sign is more intricate. In this case, there may exist a threshold depending on the values of μ_u, μ_v, such that $(0, 0)$ is stable for small values of μ_u, μ_v, and unstable for larger values. We discuss this threshold later in the section 2.3, in Lemma 2.3.47.

Since system (2.3.30) has a sublinear nonlinearity, the sign of the eigenvalue λ_A is a sharp condition for the existence of a non-trivial non-negative stationary solution. Indeed, the matrix A is cooperative and therefore admits a unique eigenpair with a positive eigenvector (λ_A, φ_A); if $\lambda_A < 0$, then for all $M > 0$ $(\bar{u}(t), \bar{v}(t)) := Me^{\lambda_A t}(\varphi_A^u, \varphi_A^v)$ is a super-solution to (2.3.30) which converges to 0, and a direct application of the maximum principle shows that the solution (u, v) satisfies $(u(t, x), v(t, x)) \leq (\bar{u}(t), \bar{v}(t))$ if $M > \max(\|u(0, \cdot)\|_{L^\infty}, \|v(0, \cdot)\|_{L^\infty})$. The non-existence of a stationary solution when $\lambda_A = 0$ was treated in [190, Theorem 1.4 (ii)] and can also be seen as a direct consequence of [87, Theorem 13.1 (c)].

Before turning to the PDE problem (2.3.30), we first describe the long-time behavior of the associated ODE system (2.3.33). Note that elements of the proof of the next Proposition can be found in the work of Cantrell, Cosner and Yu [100].

Proposition 2.3.30 (Long-time behavior of the ODE system)**.** *Let $(u(t), v(t))$ be the solution of* (2.3.33) *starting from a non-negative non-trivial initial condition (u_0, v_0).*

(i) If $\lambda_A > 0$, there is a unique positive equilibrium (u^*, v^*) for (2.3.33)*, and $(u(t), v(t))$ converges to (u^*, v^*) as $t \to \infty$.*

(ii) If $\lambda_A \leq 0$, then $(u(t), v(t))$ converges to $(0, 0)$ as $t \to +\infty$.

Next we turn to the local asymptotic stability of the PDE, *i.e.* the long-time convergence of the solution to the parabolic equation (2.3.30) starting from an initial condition in a vicinity of the constant stationary solution.

Theorem 2.3.31 (Local stability of the constant stationary solution)**.** *Assume that $\lambda_A > 0$ and let (u^*, v^*) be the unique stationary solution for the ODE* (2.3.33)*. Then (u^*, v^*) is locally asymptotically stable as a stationary solution to* (2.3.30) *in the space $BUC(\mathbb{R})^2$. More precisely, (u^*, v^*) is stable and there exists $\delta > 0$ such that for any $(u_0(x), v_0(x)) \in BUC(\mathbb{R})^2$ satisfying $\|u_0 - u^*\|_{BUC(\mathbb{R})} \leq \delta$ and $\|v_0 - v^*\|_{BUC(\mathbb{R})} \leq \delta$, then*

$$\lim_{t \to +\infty} \sup_{x \in \mathbb{R}} |u(t, x) - u^*| = 0 \text{ and } \lim_{t \to +\infty} \sup_{x \in \mathbb{R}} |v(t, x) - v^*| = 0,$$

and the convergence is exponential in time.

Note that the difficulty in this result is to overcome the absence of a comparison principle, even asymptotically (in the case where $\sigma_1 \neq \sigma_2$ and Assumption 2.3.32 does not hold). To this end we had to introduce an argument coming from semigroup theory [274, 107].

While Assumption 2.3.29 is sufficient to describe the long-time behavior of the ODE problem, we require a little more for the study of the PDE problem (2.3.30). We extend the Lyapunov argument which was used for the ODE system in the non-cooperative case, though only when $\sigma_u = \sigma_v$, and in the remaining cases the long-time behavior may be determined by using the comparison principle for either cooperative or two-component competitive systems. The cases under which global stability can be shown are summarized in Assumption 2.3.32.

Assumption 2.3.32. We assume that either $\max(r_u - \mu_u, r_v - \mu_v) \leq 0$, $\min(r_u - \mu_u - \mu_v, r_v - \mu_v - \mu_u) > 0$, or $\sigma_u = \sigma_v$.

Under this assumption, we can prove that the solutions to the Cauchy problem associated with (2.3.30) converge in long time to the unique nonnegative nontrivial stationary solution.

Theorem 2.3.33 (Long-time behavior of the homogeneous problem)**.** *Let Assumptions 2.3.29 and 2.3.32 be satisfied. Let $(u_0(x) \geq 0, v_0(x) \geq 0)$ be bounded continuous nontrivial functions, and c^* be the spreading speed associated with* (2.3.30)*. Then, the solution $(u(t,x), v(t,x))$ to the Cauchy problem* (2.3.30) *converges as $t \to \infty$ to the unique stationary solution (u^*, v^*) to* (2.3.30)*, uniformly in the sense that for each $0 < c < c^*$ we have:*

$$\lim_{t \to +\infty} \sup_{|x| \leq ct} \max(|u(t,x) - u^*|, |v(t,x) - v^*|) = 0.$$

Finally, we were able to extend this result to the case of rapidly oscillating coefficients by using arguments from the theory of dynamical systems and the homogenization of solutions to parabolic equations with rapidly oscillating coefficients. To this end it is more convenient to write the heterogeneous system (2.3.2) in divergence form (2.3.35).

In order to state our results for the homogenization limit of parabolic systems, we restrict ourselves to the case $L = 1$, without loss of generality. For each 1-periodic function $\sigma_u(x)$, $\sigma_v(x)$, $r_u(x)$, $r_v(x)$, $\kappa_u(x)$, $\kappa_v(x)$, $\mu_u(x)$, $\mu_v(x)$, we denote:

$$\begin{aligned} \overline{r_u} &:= \int_0^1 r_u(x)\mathrm{d}x, & \overline{\kappa_u} &:= \int_0^1 \kappa_u(x)\mathrm{d}x, & \overline{\mu_u} &:= \int_0^1 \mu_u(x)\mathrm{d}x, \\ \overline{r_v} &:= \int_0^1 r_v(x)\mathrm{d}x, & \overline{\kappa_v} &:= \int_0^1 \kappa_v(x)\mathrm{d}x, & \overline{\mu_v} &:= \int_0^1 \mu_v(x)\mathrm{d}x, \end{aligned} \tag{2.3.34}$$

and finally:

$$\overline{\sigma_u}^H := \left(\int_0^1 \frac{1}{\sigma_u(x)} \mathrm{d}x \right)^{-1}, \qquad \overline{\sigma_v}^H := \left(\int_0^1 \frac{1}{\sigma_v(x)} \mathrm{d}x \right)^{-1}.$$

Theorem 2.3.34 (Homogenisation)**.** *Let $\sigma_u(x)$, $\sigma_v(x)$, $r_u(x)$, $r_v(x)$, $\kappa_u(x)$, $\kappa_v(x)$, $\mu_u(x)$ and $\mu_v(x)$ be 1-periodic functions such that $\overline{\sigma_u}^H$, $\overline{\sigma_v}^H$, $\overline{r_u}$, $\overline{r_v}$, $\overline{\kappa_u}$, $\overline{\kappa_v}$, $\overline{\mu_u}$ and $\overline{\mu_v}$ satisfy Assumption 2.3.29 and Assumption 2.3.32. Consider*

$$\begin{cases} u_t = (\sigma_u^\varepsilon(x) u_x)_x + (r_u^\varepsilon(x) - \kappa_u^\varepsilon(x)(u+v))u + \mu_v^\varepsilon(x) v - \mu_u^\varepsilon(x) u \\ v_t = (\sigma_v^\varepsilon(x) v_x)_x + (r_v^\varepsilon(x) - \kappa_v^\varepsilon(x)(u+v))v + \mu_u^\varepsilon(x) u - \mu_v^\varepsilon(x) v. \end{cases} \tag{2.3.35}$$

Then, there is $\bar{\varepsilon} > 0$ such that for each $0 < \varepsilon < \bar{\varepsilon}$,

(i) there exists a unique positive nontrivial stationary solution $(u_\varepsilon^*(x), v_\varepsilon^*(x))$ to (2.3.35)*,*

(ii) the ω-limit set of any $(u^\varepsilon(t,x), v^\varepsilon(t,x))$ solution to (2.3.35) *starting from a nonnegative nontrivial bounded initial condition is $\{(u_\varepsilon^*(x), v_\varepsilon^*(x))\}$.*

(iii) any solution to the Cauchy problem (2.3.35) *starting from a nonnegative bounded initial condition converges as $t \to +\infty$ to $(u_\varepsilon^*(x), v_\varepsilon^*(x))$, uniformly in the sense that for any $0 < c < c_\varepsilon^*$ we have*

$$\lim_{t \to +\infty} \sup_{|x| \leq ct} \max(|u(t,x) - u_\varepsilon^*(x)|, |v(t,x) - v_\varepsilon^*(x)|) = 0,$$

where c_ε^* is the minimal speed defined in (2.3.7)*.*

2.3.3 Proofs of the results on general cooperative-competitive systems

In section 2.3.3.1, we show that solutions to equations can be estimated from below by a monotone lower barrier. In section 2.3.3.2 we prove some properties on principal eigenproblems for periodic system, including the equivalence between the various notions of principal eigenvalue on the real line for operators satisfying Assumption 2.3.5. In section 2.3.3.3 we prove the linear determinacy for sublinear functions satisfying Assumption 2.3.15 (Theorem 2.3.19) by adapting an argument of Weinberger [398]. In section 2.3.3.4 we prove and the existence of traveling waves, Theorem 2.3.21. Finally in section 2.3.4.1 we prove Theorem 2.3.11.

Before resuming the proofs, let us mention two important conventions. The constant $d > 0$ stands for the dimension of the system being investigated. Also, whenever u is a vector, we denote $(u)_i$ the i-th component of u, or simply u_i if the context is clear.

2.3.3.1 A comparison principle for systems with a monotone lower barrier.

In this section 2.3.3.1 we prove that a function that admits a monotone lower barrier generates a semiflow that remains above the one generated by the lower barrier. More precisely, we show that as long as the solution $u(t,x)$ of the equation corresponding to the lower monotone barrier stays in the quasi-monotone area, then the solution $v(t,x)$ is componentwise greater than $u(t,x)$ (even if it leaves the quasi-monotone domain).

Theorem 2.3.35 (Comparison principle)**.** *Let f be a given sublinear function and $\mathcal{L}$ be a d-dimensional diagonal uniformly elliptic operator. We assume that $Df(x,0)$ is cooperative and fully coupled and that f admits a monotone lower barrier f^- in the sense of Definition 2.3.16.*

Let $T \in (0, +\infty]$ and $u(t,x)$ and $v(t,x)$ solve

$$\begin{cases} u_t(t,x) - \mathcal{L}u(t,x) = f(x,u(t,x)) \\ u(0,x) = u_0(x), \end{cases} \text{ and } \begin{cases} v_t(t,x) - \mathcal{L}v(t,x) = f^-(x,v(t,x)) \\ v(0,x) = v_0(x), \end{cases}$$

for $t \in [0,T]$ and $x \in \mathbb{R}$, $u_0, v_0 \in BUC(\mathbb{R})$.

Suppose that $\|v(t,x)\|_\infty < \eta$ for all $t \in [0,T]$. Then $u(t,x)$ satisfies

$$v(t,x) \le u(t,x) \text{ for any } t \in [0,T] \text{ and } x \in \mathbb{R}.$$

Proof. We show the result under the assumption that $u_0(x) \ge v_0(x) + \delta \mathbf{1}$ and $\|v(t,x)\| \le \eta - \delta$ for some $\delta \in (0,\eta)$. The general result is obtained by taking the limit $\delta \to 0$. Since $t \mapsto u(t,x)$ is continuous at $t = 0$, there exists $t_0 > 0$ such that $v(t,x) \le u(t,x)$ for all $t \in [0,t_0]$ and $x \in \mathbb{R}$.

We define

$$t^* := \sup\{t > 0 \,|\, v(t,x) \le u(t,x) \text{ for all } x \in \mathbb{R}\}.$$

Then by definition $t^* \ge t_0$. Assume by contradiction that $t^* < T$. Then, because of the definition of t^*, there exists a sequence $(t_n, x_n) \in [0,T] \times U$ and $i \in \{1,\dots,d\}$ such that $t_n \to t^*$, $t_n \ge t^*$ and

$$v_i(t_n,x_n) \to u_i(t_n,x_n) \text{ and } v_j(t_n,x_n) \le u_j(t_n,x_n) \text{ for all } j \ne i.$$

If x_n is bounded, then we may extract a subsequence such that $x_n \to x$. By the continuity of v_i and u_i we have then $v_i(t^*,x) = u_i(t^*,x)$. Since moreover $v_i(t,x) \le \|v(t,x)\|_\infty \le \eta$ we have $f^-\big(x,v(t,x)\big) \le f^-\big(x,u(t,x)\big) \le f(x,u(t,x))$. Testing the i-th equation we get

$$(v_i)_t(t,x) - \mathcal{L}v_i(t,x) = (f^-)_i(x,v(t,x)) \le f_i(x,u(t,x)) = (u_i)_t - \mathcal{L}u_i(t,x),$$

and there is a contradiction by the strong maximum principle. If (t_n,x_n) is unbounded we get a similar contradiction by extracting a converging subsequence from the sequence of functions $u(t+t_n,x+x_n)$ and $v(t+t_n,x+x_n)$. This proves that $t^* = T$, therefore the result holds. □

Proposition 2.3.36. *Let $f = (f_1,\dots,f_d)^T$ be a given sublinear function and $\mathcal{L}$ be a d-dimensional diagonal uniformly elliptic operator. We assume that $Df(x,0)$ is cooperative and fully coupled, that $\lambda_1^{per} < 0$ and that f admits a monotone lower barrier f^- in the sense of Definition 2.3.16. Let $\eta > 0$ be as in Definition 2.3.16.*

There exists a monotone lower barrier $f^{*-}(x,u)$ for f with the properties that

1. *we have*
$$f^{*-}(x,u) \le f^-(x,u) \text{ for all } x \in \mathbb{R} \text{ and } u \ge 0.$$

2. *there exists a L-periodic equilibrium* $p(x) = (p_1(x), \dots, p_d(x))$ *such that* $0 \le p(x) \le \eta \mathbf{1}$,
$$-\mathcal{L}p(x) = f^{*-}\big(x, p(x)\big),$$
and p *attracts every nontrivial periodic initial condition* $u_0(x)$ *satisfying* $0 \le u_0(x) \le p(x)$ *for all* $x \in \mathbb{R}$.

Proof. Let $\beta > 0$ be given and define
$$f^-_\beta(x,u) := f^-(x,u) - \beta u^2 = (f^-_1(x,u) - \beta u_1^2, \dots, f^-_d(x,u) - \beta u_d^2)^T.$$
It is clear that $f^-_\beta(x,u) \le f^-(x,u)$ for all $x \in \mathbb{R}$ and $u \in \mathbb{R}^d$, and that $f^-(x,u)$ and $f^-_\beta(x,u)$ have the same Jacobian matrix near $u = 0$, $Df^-(x,0) = Df^-_\beta(x,0) =: A(x)$.

We investigate the equation
$$u_t - \mathcal{L}u = f^-_\beta(x,u). \tag{2.3.36}$$
If
$$\beta \ge \beta^* := \frac{\sup_{x\in\mathbb{R}} \max_{i\in\{1,\dots,d\}} \sum_{j=1}^d a_{ij}(x)}{\eta},$$
where $\eta > 0$ is the constant from Definition 2.3.16, then the constant vector $\eta\mathbf{1}$ satisfies
$$f^-_\beta(x, \eta\mathbf{1}) \le A(x)\eta\mathbf{1} - \beta\eta^2\mathbf{1} \le \eta\left(\sup_{x\in\mathbb{R}} \max_{i\in\{1,\dots,d\}} \sum_{i=1}^d a_{ij}(x) - \beta\eta\right),$$
therefore $\eta\mathbf{1}$ is a super-solution to (2.3.36).

Next we look for a sub-solution to (2.3.36). Recall that we denote $(\lambda_1^{per}, \varphi^{per}(x) > 0)$ the periodic principal eigenpair as in Definition 2.3.3, with $\|\varphi^{per}\|_{L^\infty(\mathbb{R})^d} = 1$, and recall that $\lambda_1^{per} < 0$. Define
$$\kappa := \inf_{x\in\mathbb{R}} \min_{1\le i\le d} \frac{\varphi_i^{per}(x)}{\|\varphi^{per}(x)\|_\infty},$$
which is finite and positive by the elliptic strong maximum principle. Because of the differentiability of $u \mapsto f^-_\beta(x,u)$, there exists $\varepsilon_0 > 0$ such that for each $u \ge 0$ with $\|u\| \le \varepsilon_0$, we have
$$\|f^-_\beta(x,u) - A(x)u\|_\infty \le -\lambda_1^{per}\kappa\|u\|_\infty.$$
Reducing ε_0 if necessary, we may assume that $\varepsilon_0 < \eta$. Then for $0 < \varepsilon \le \varepsilon_0$, $\varepsilon\varphi^{per}(x)$ is a sub-solution to (2.3.36). Indeed,
$$\begin{aligned} -\mathcal{L}\varepsilon\varphi^{per}(x) &= A(x)\varepsilon\varphi^{per}(x) + \lambda_1^{per}\varepsilon\varphi^{per}(x) \le A(x)\varphi^{per}(x) + \lambda_1^{per}\kappa\|\varepsilon\varphi^{per}\|_\infty \\ &\le A(x)\varepsilon\varphi^{per} + f^-_\beta\big(x, \varepsilon\varphi^{per}(x)\big) - A(x)\varepsilon\varphi^{per}(x) = f^-_\beta\big(x, \varepsilon\varphi^{per}(x)\big). \end{aligned}$$

Let $\varepsilon > 0$ be fixed and $\underline{u}^\varepsilon(t,x)$ be the solution to the initial-value problem (2.3.36) with $\underline{u}^\varepsilon(0,x) = \varepsilon\varphi^{per}(x)$. It follows from the parabolic comparison principle and the strong maximum principle that $\underline{u}^\varepsilon(t,x) \gg \varepsilon\varphi^{per}(x)$ for all $t > 0$ and $x \in \mathbb{R}$. Next, fix $\tau > 0$. Then $\underline{u}^\varepsilon(\tau,x) > \varepsilon\varphi^R(x) = \underline{u}_0^\varepsilon(x)$ and therefore
$$\underline{u}^\varepsilon(t+\tau,x) > \underline{u}^\varepsilon(t,x),$$
in other words, $\underline{u}^\varepsilon(t,x)$ is strictly increasing in time. Thus the limit
$$V^\varepsilon := \lim_{t\to+\infty} \underline{u}^\varepsilon(t,x)$$
exists and is an equilibrium of (2.3.36). It is not difficult to show, by using Serrin's sweeping method, that
$$V^\varepsilon(x) \ge \varepsilon_0\varphi^{per}(x).$$

Indeed, define

$$\varepsilon_1 := \sup\{\varepsilon' \geq 0 \,|\, \varepsilon' \varphi^{per}(x) \leq V^{\varepsilon}(x)\}.$$

Then clearly $\varepsilon_1 \geq \varepsilon$ (by the parabolic comparison principle). If $\varepsilon_1 < \varepsilon_0$, then there exists a contact point x_0 such that $\varepsilon_1 \varphi^{per}(x_0) \leq V^{\varepsilon}(x_0)$ and $\varepsilon_1 \varphi_i^{per}(x_0) = V_i^{\varepsilon}(x_0)$ for some $i \in \{1, \dots, d\}$. We find a contradiction by applying the elliptic strong maximum principle in the i-th equation of the system. Since $V^{\varepsilon}(x)$ is an equilibrium and $V^{\varepsilon}(x) \geq \varepsilon_0 \varphi^{per}(x)$, we conclude that

$$V^{\varepsilon}(x) \geq V^{\varepsilon_0}(x).$$

Define $p^{\beta}(x) := V^{\varepsilon_0}(x)$ and let $u_0(x) \leq p^{\beta}(x)$ be a nontrivial L-periodic initial data. Let $u(t,x)$ be the solution of (2.3.36) satisfying $u(0,x) = u_0(x)$. Fix some $t_0 > 0$. Then $u(t_0, x) > 0$ for all $x \in \mathbb{R}$. Since $u(t_0, x)$ is periodic in x, there exists $\varepsilon > 0$ sufficiently small, so that $\varepsilon \varphi^{per}(x) \leq u(t_0, x)$. It follows from the comparison principle that

$$p^{\beta}(x) = V^{\varepsilon_0}(x) \leq V^{\varepsilon}(t,x) \leq \lim_{t \to +\infty} u(t,x) \leq p^{\beta}(x).$$

Therefore we have found $f^{*-}(x,u) := f_{\beta}^{-}(x,u)$ satisfying the requirements of Proposition 2.3.36. □

2.3.3.2 The principal eigenvalue of cooperative systems with periodic coefficients

In this section 2.3.3.2 we focus on the principal eigenvalue problem for general cooperative elliptic systems with periodic coefficients. For $1 \leq i \leq d$ and $\alpha > 0$, let $\sigma(x) \in C_{per}^{1+\alpha}(\mathbb{R}, \mathbb{R}^d)$ be positive, and $q(x) \in C_{per}^{\alpha}(\mathbb{R}, \mathbb{R}^d)$ be given. We recall that:

$$\mathcal{L}_i u := (\sigma_i(x) u_x)_x + q_i(x) u_x, 1 \leq i \leq d; \qquad \mathcal{L}u = \big(\mathcal{L}_i u_i\big)_{1 \leq i \leq d},$$

if $\mathcal{L}$ is written in divergence form, and

$$\mathcal{L}_i u := \sigma_i(x) u_{xx} + q_i(x) u_x, 1 \leq i \leq d; \qquad \mathcal{L}u = \big(\mathcal{L}_i u_i\big)_{1 \leq i \leq d}$$

if $\mathcal{L}$ is written in non-divergence form. The particular choice of writing the operator in divergence form or non-divergence form makes little difference for the principal eigenproblem, except when a symmetry property is involved; non-divergence form systems are better suited for systems which are composed of even functions, and systems in divergence form are most convenient when a symmetry for the canonical H^1 scalar product is needed.

We start with some elementary properties of the Dirichlet principal eigenvalue.

Proof of Proposition 2.3.4. We prove each statement separately.

Step 1: Existence of a principal eigenfunction.

The existence and uniqueness of a principal eigenfunction associated with λ_1^R in the case $R < +\infty$ is an immediate consequence of the Krein-Rutman Theorem.

Step 2: Proof of (2.3.17).

Assume by contradiction that there exists $\lambda \in \mathbb{R}$ and $\phi \in C^2((-R,R), \mathbb{R}^d) \cap C^1([-R,R], \mathbb{R}^d)$, $\phi > 0$, such that

$$-\mathcal{L}\phi - A(x)\phi - \lambda \phi \geq 0,$$

and $\lambda > \lambda_1^R$. On the one hand, it follows from Hopf's Lemma that, for each $i \in \{1, \dots, d\}$, we have $\frac{\mathrm{d}\varphi_i^R}{\mathrm{d}x}(-R) > 0$ and $\frac{\mathrm{d}\varphi_i^R}{\mathrm{d}x}(R) < 0$. On the other hand, for each $i \in \{1, \dots, d\}$, either $\phi_i(\pm R) > 0$ or $\pm \phi_i(\pm R) < 0$ by Hopf's Lemma. Therefore, the set $\{\zeta > 0 \,|\, \zeta \varphi^R \leq \phi\}$ is nonempty and admits a supremum $\eta > 0$. We remark that, by definition of η, the inequality in $\zeta \varphi^R \leq \phi$ is an equality for a $x_0 \in [-R, R]$. Moreover, we have:

$$-\mathcal{L}(\phi - \eta\varphi^R) - A(x)(\phi - \eta\varphi^R) - \lambda(\phi - \eta\varphi^R) \geq (\lambda - \lambda_1)\eta\varphi^R \geq 0,$$

thus for $1 \leq i \leq d$, either $\phi_i(\pm R) - \eta\varphi_i^R(\pm R) > 0$ or, by Hopf's Lemma, $\pm \frac{\mathrm{d}(\phi_i - \eta\varphi_i^R)}{\mathrm{d}x}(\pm R) < 0$. In particular, we have $x_0 \in (-R, R)$ and there exists $j \in \{1, \dots, d\}$ such that $\phi_j(x_0) = \eta\varphi_j^R(x_0)$. At this point, we have

$$\begin{aligned} 0 &\geq -\mathcal{L}(\phi_j - \eta\varphi_j^R)(x_0) - (A(x_0)(\phi - \eta\varphi^R)(x_0))_j \\ &= \lambda\phi_j(x_0) - \lambda_1^R \varphi_j^R(x_0) = \phi_j(x_0)(\lambda - \lambda_1^R), \end{aligned}$$

which shows $\lambda \leq \lambda_1^R$. This is a contradiction. We conclude that $\lambda \leq \lambda_1^R$. Since λ and ϕ are arbitrary, we have shown

$$\lambda_1^R \geq \sup\{\lambda \in \mathbb{R} \,|\, \exists \phi \in C^2((-R,R),\mathbb{R}^d) \cap C^1([-R,R],\mathbb{R}^d), \phi > 0, -\mathcal{L}\phi - A(x)\phi - \lambda\phi \geq 0\}.$$

Finally, the equality in (2.3.14) shows the reverse inequality. Statement (ii) is proved.

Step 3: $R \mapsto \lambda_R$ is decreasing.

Let $R < R'$. Then, the function $\varphi^{R'}$ is a valid test function in the characterization (2.3.17) of λ_1^R. Therefore $\lambda_1^{R'} \leq \lambda_1^R$. Since the equalities $\lambda_1(R') = \lambda_1^{R'}$ and $\lambda_1^R = \lambda_1^R$ hold, we have $\lambda_1^R \geq \lambda_1^{R'}$. A direct application of the strong maximum principle shows that equality cannot be achieved. Statement (iii) is proved.

Step 4: Existence of a principal eigenfunction for λ_1^∞ and limit of λ_1^R.

Let $R_n \to +\infty$, then $\lambda_1^{R_n}$ is a nonincreasing sequence and thus converges to λ_1^∞. Let φ^n be the associated principal eigenfunction satisfying $\varphi_1^n(0) = 1$. Then, by the classical Schauder estimates and the Harnack inequality for fully coupled elliptic systems [87, Theorem 8.2], the sequence $(\varphi^n)_{n>0}$ converges locally uniformly to a limit φ^∞ which satisfies $-\mathcal{L}\varphi^\infty - A(x)\varphi^\infty = \lambda_1^\infty \varphi^\infty$ (up to the extraction of a subsequence).

Let us show that $\lambda_1^\infty = \lambda_1(+\infty)$. Let (λ, ϕ) be such that $-\mathcal{L}\phi - A(x)\phi - \lambda\phi \geq 0$. Then by (2.3.17), for any $n \in \mathbb{N}$ we have $\lambda \leq \lambda_1^{R_n}$. Taking the limit in the inequality, we find $\lambda_1(+\infty) \leq \lambda_1^\infty$. Since $(\lambda_1^\infty, \varphi^\infty)$ satisfies the equality $-\mathcal{L}\varphi^\infty - A(x)\varphi^\infty = \lambda_1^\infty \varphi^\infty$, we have $\lambda_1^\infty \leq \lambda_1(+\infty)$. Statement (iv) is proved.

Step 5: We prove the minimax formula (2.3.18).

Using φ^R as a test function in (2.3.18), we find that

$$\lambda_1^R \leq \lambda^* := \sup_{\phi > 0} \inf_{x \in (-R,R)} \min_{1 \leq i \leq d} \frac{(-\mathcal{L}\phi - A(x)\phi)_i}{\phi_i}.$$

Let us show the converse inequality. Let $\epsilon > 0$ be given, then by definition of λ^* there exists $\phi > 0$ such that

$$\forall x \in (-R,R), \forall i \in \{1,\dots,d\}, \frac{(-\mathcal{L}\phi(x) - A(x)\phi(x))_i}{\phi_i(x)} \geq \lambda^* - \epsilon,$$

and thus for all $x \in \mathbb{R}$ we have $-\mathcal{L}\phi(x) - A(x)\phi(x) - (\lambda^* - \epsilon)\phi(x) \geq 0$. By (2.3.17), we have $\lambda^* - \epsilon \leq \lambda_1^R$. Since $\epsilon > 0$ is arbitrary, $\lambda^* \leq \lambda_1^R$. Finally, since $\lambda^* = \lambda_1^R$, the supremum is attained for the principal eigenfunction. Statement (v) is proved. □

Proof of Lemma 2.3.6. Statement (i) is a direct consequence of the Krein-Rutman Theorem, and statement (ii) is a consequence of Lemma 2.3.4 statement (v) (by modifying the elliptic operator $\mathcal{L}$). Therefore we concentrate on the remaining statements.

Proof of Statement (iii). We first note that the analyticity of $k(\lambda)$ is classical. In the terminology of Kato [228], the family L_λ is a holomorphic family of type (A) [228, Paragraph 2.1 on page 375] and the principal eigenvalue is isolated in the spectrum by the Krein-Rutman Theorem; therefore the spectral projection and the principal eigenvalue are analytic (see [228, Remark 2.9 on page 379]. The analyticity of $k(\lambda)$ and a well-chosen parameterization of the principal eigenvector ϕ^λ with respect to λ follow.

Let us prove (2.3.21). Let $(k(\lambda), \phi^\lambda)$ be a solution to (2.3.19). Because ϕ^λ is periodic, there exists a point $x \in \mathbb{R}$ and an index $i \in \{1,\dots,d\}$ such that $\phi_i^\lambda(x)$ minimizes $(y,j) \mapsto \phi_j^\lambda(y)$ with $y \in \mathbb{R}$ and $j \in \{1,\dots,d\}$. Therefore

$$\begin{aligned} k(\lambda)\phi_i^\lambda(x) &= -\big(L_\lambda \phi^\lambda\big)_i - \big(A(x)\phi^\lambda(x)\big)_i \leq +\lambda q_i(x)\phi_i^\lambda(x) - \lambda^2 \sigma_i(x)\phi_i^\lambda(x) - \sum_{j=1}^d a_{ij}(x)\phi_j^\lambda(x) \\ &\leq \lambda q^\infty \phi_i^\lambda(x) - \lambda^2 \sigma_0 \phi_i^\lambda(x) - a_0 \phi_i^\lambda(x), \end{aligned}$$

where $q^\infty := \sup_{y \in \mathbb{R}, j \in \{1,\dots,d\}} |q_j(y)|$, $\sigma_0 := \inf_{y \in \mathbb{R}, j \in \{1,\dots,d\}} \sigma_j(x)$ and $a_0 := \inf_{y \in \mathbb{R}, j \in \{1,\dots,d\}} a_j(y)$. This proves (2.3.21).

Next we follow [298, Proposition 2.10] to prove the concavity of $\lambda \mapsto k(\lambda)$. By the assumption that $\sigma \in C^{1,\alpha}(\mathbb{R}, M_d(\mathbb{R}))$, we need only consider the non-divergence case.

We first remark that (2.3.20) can be rewritten as:

$$k(\lambda) = \max_{\substack{\psi>0 \\ e^{\lambda x}\psi(x) \text{ is } L-\text{periodic}}} \inf_{x\in\mathbb{R}} \min_{1\le i\le d} \frac{(-\mathcal{L}\psi(x) - A(x)\psi(x))_i}{\psi_i(x)}.$$

Let $\lambda_1 < \lambda_2$ and $r \in (0,1)$. Let ψ^1 and ψ^2 be such that $e^{\lambda_1 x}\psi^1(x)$ and $e^{\lambda_2 x}\psi^2(x)$ are L-periodic in x. Define further $z^1 = (\ln(\psi_i^1))_{1\le i\le d}$, $z^2 = (\ln(\psi_i^2))_{1\le i\le d}$, $z(x) = rz^1 + (1-r)z^2(x)$, and finally $\lambda = r\lambda_1 + (1-r)\lambda_2$. Elementary computations then show that $\psi(x) := e^{z(x)} := (e^{z_i(x)})_{1\le i\le d}$ is a valid test function for $k(\lambda)$ since $e^{\lambda x}\psi(x)$ is L-periodic. Thus:

$$k(\lambda) \ge \inf_{x\in\mathbb{R}} \min_{1\le i\le d} \frac{(-\mathcal{L}\psi - A(x)\psi)_i}{\psi_i(x)}.$$

We compute:

$$\begin{aligned}
\frac{-\mathcal{L}_i\psi_i(x)}{\psi_i(x)} &= \frac{1}{\psi_i(x)}\left[\sigma_i(x)\left(-r\frac{\psi^1_{i,xx}(x)}{\psi^1_i(x)} - (1-r)\frac{\psi^2_{i,xx}(x)}{\psi^2_i(x)} + r(1-r)\left(\frac{\psi^1_x(x)}{\psi^1(x)} - \frac{\psi^2_x(x)}{\psi^2(x)}\right)^2\right)\right. \\
&\quad \left. -q_i(x)\left(r\frac{\psi^1_{i,x}(x)}{\psi^1_i(x)} + (1-r)\frac{\psi^2_{i,x}(x)}{\psi^2_i(x)}\right)\right] e^{z_i(x)} \\
&\ge \left[r\frac{-\mathcal{L}_i\psi^1_i(x)}{\psi^1_i(x)} + (1-r)\frac{-\mathcal{L}_i\psi^2_i(x)}{\psi^2_i(x)} + \sigma_i(x)r(1-r)\left(\frac{\psi^1_x(x)}{\psi^1(x)} - \frac{\psi^2_x(x)}{\psi^2(x)}\right)^2\right]\frac{e^{z_i(x)}}{\psi_i(x)}. \qquad (2.3.37)
\end{aligned}$$

Then, we remark that

$$\begin{aligned}
\sum_{j=1}^d a_{ij}(x)\frac{\psi_j(x)}{\psi_i(x)} &= \sum_{j=1}^d a_{ij}(x)\frac{\exp\left(r\ln(\psi^1_j(x)) + (1-r)\ln(\psi^2_j(x))\right)}{\exp\left(r\ln(\psi^1_i(x)) + (1-r)\ln(\psi^2_i(x))\right)} \\
&= \sum_{j=1}^d a_{ij}(x)\exp\left(r\ln\left(\frac{\psi^1_j(x)}{\psi^1_i(x)}\right) + (1-r)\ln\left(\frac{\psi^2_j(x)}{\psi^2_i(x)}\right)\right) \\
&\le \sum_{j=1}^d a_{ij}(x)\left[r\left(\frac{\psi^1_j(x)}{\psi^1_i(x)}\right) + (1-r)\left(\frac{\psi^2_j(x)}{\psi^2_i(x)}\right)\right] \qquad (2.3.38) \\
&= r\frac{\sum_{j=1}^d a_{ij}(x)\psi^1_j(x)}{\psi^1_i(x)} + (1-r)\frac{\sum_{j=1}^d a_{ij}(x)\psi^2_j(x)}{\psi^2_i(x)},
\end{aligned}$$

where the last inequality holds by the convexity of $x \mapsto e^x$. The inequality (2.3.38), together with (2.3.37), implies

$$\frac{(-\mathcal{L}\psi - A(x)\psi)_i}{\psi_i(x)} \ge r\frac{(-\mathcal{L}\psi^1 - A(x)\psi^1)_i}{\psi^1_i(x)} + (1-r)\frac{(-\mathcal{L}\psi^2 - A(x)\psi^2)_i}{\psi^2_i(x)}.$$

Taking the infimum over x and the supremum over all admissible ψ^1 and ψ^2 leads to the concavity of $k(\lambda)$, as in [298, Proposition 2.10].

To get the strict concavity, we observe that the particular choice $\psi^1(x) = \phi^{\lambda_1}(x)e^{-\lambda_1 x}$, $\psi^2(x) = \phi^{\lambda_2}(x)e^{-\lambda_2 x}$ and consequently $\psi(x) = \phi(x)e^{\lambda x}$, where ϕ^1 and ϕ^2 are the corresponding solutions to (2.3.19) and $\phi(x) = \exp(r\ln(\phi^1(x)) + (1-r)\ln(\phi^2(x)))$, also leads to

$$k(\lambda) \ge \inf_{x\in\mathbb{R}} \min_{1\le i\le d} \frac{-L_\lambda\phi(x) - A(x)\phi(x)}{\phi_i(x)} = \inf_{x\in\mathbb{R}} \min_{1\le i\le d} \frac{(-\mathcal{L}\psi - A(x)\psi)_i}{\psi_i(x)} \ge rk(\lambda_1) + (1-r)k(\lambda_2),$$

and the first inequality is strict unless $\phi = \phi^\lambda$ is the periodic principal eigenfunction associated with $k(\lambda)$. In this case, recalling (2.3.37) and (2.3.38), one must have $\frac{(\psi^1_i)_x}{\psi^1_i} \equiv \frac{(\psi^2_i)_x}{\psi^2_i}$ for all $1 \le i \le d$, which (after integration) results in $\psi^1 \equiv \psi^2$ (up to a multiplicative factor). This is a contradiction.

Statement (iii) is proved.

Proof of Statement (iv). The proof is inspired by [298, Theorem 2.11]. Again, since we allow q to be non-zero, we need only prove the result in the non-divergence case.

We first remark that for any $\lambda \in \mathbb{R}$, the function $e^{-\lambda x}\varphi^\lambda(x)$, where φ^λ solves (2.3.19), satisfies

$$-\mathcal{L}(\varphi(x)e^{-\lambda x}) - A(x)e^{-\lambda x}\varphi^\lambda(x) - k(\lambda)e^{-\lambda x}\varphi^\lambda(x) = 0,$$

hence $\lambda_1^\infty \geq k(\lambda)$ for all $\lambda \in \mathbb{R}$. Therefore $\lambda_1^\infty \geq \sup_{\lambda\in\mathbb{R}} k(\lambda)$.

Let $\varphi > 0$ be a principal eigenfunction associated with λ_1^∞. We let

$$\psi(x) := \left(\frac{\varphi_i(x+L)}{\varphi_i(x)}\right)_{1\leq i\leq d}.$$

Then, applying the Harnack inequality for fully coupled elliptic systems [87, Theorem 8.2] to φ, the function $\psi(x)$ is uniformly bounded. We let

$$m := \sup_{x\in\mathbb{R}} \max_{1\leq i\leq d} \psi_i(x) < +\infty.$$

Let $k \in \{1, \dots, d\}$ be such that $\sup_{x\in\mathbb{R}} \psi_k(x) = m$ and x_n be a sequence such that $\lim_{n\to\infty} \psi_k(x_n) = m$. Define $\psi^n(x) := \psi(x + x_n)$, and $\varphi^n(x) := \frac{1}{\varphi_k(x_n)}\varphi(x + x_n)$.

We remark that ψ satisfies the equation:

$$\begin{aligned}\mathcal{L}_i\psi_i(x) &= \frac{\mathcal{L}_i\varphi_i(x+L)}{\varphi_i(x)} - \psi_i(x)\frac{\mathcal{L}_i\varphi_i(x)}{\varphi_i(x)} - 2\sigma_i(x)\frac{\varphi_{i,x}(x)}{\varphi_i(x)}\psi_{i,x}(x)\\ &= -2\sigma_i(x)\frac{\varphi_{i,x}(x)}{\varphi_i(x)}\psi_{i,x}(x) + \sum_{j=1}^d a_{ij}(x)\frac{\varphi_j(x)}{\varphi_i(x)}(\psi_j(x) - \psi_i(x)).\end{aligned}$$

Using the classical elliptic estimates, and up to the extraction of a subsequence, the sequence ψ_n converges locally uniformly to a limit function ψ^∞, and φ^n converges to φ^∞. Extracting further, there exists $x \in [0, L]$ such that $x_n \to x^\infty \mod L$. Then, the function ψ^∞ satisfies the equation:

$$-\mathcal{L}_i\psi_i^\infty(x) + 2\sigma_i(x + x^\infty)\frac{\varphi_{i,x}^\infty(x)}{\varphi_i^\infty(x)}\psi_{i,x}^\infty(x) - \sum_{j=1}^d a_{ij}(x + x^\infty)\frac{\varphi_j^\infty(x)}{\varphi_i^\infty(x)}(\psi_j^\infty(x) - \psi_i^\infty(x)) = 0.$$

Then, defining $\tilde{\mathcal{L}}_i\phi(x) := \mathcal{L}_i\phi(x) + 2\sigma(x+x^\infty)\frac{\varphi_{i,x}^\infty(x)}{\varphi_i^\infty(x)}\phi$ and the cooperative matrix field $\tilde{A}(x) := \left(a_{ij}(x + x^\infty)\frac{\varphi_j^\infty(x)}{\varphi_i^\infty(x)}\right)_{1\leq i,j\leq d}$, we have

$$-\tilde{\mathcal{L}}\psi(x) - \tilde{A}(x)\tilde{\psi}(x) \leq 0.$$

Since $\tilde{A}(x)$ is fully coupled, and the global maximum of ψ is attained at $x = 0$, the strong maximum principle [87, Proposition 12.1] implies $\psi^\infty(x) \equiv \psi(0) \equiv m$. Then, define $\lambda = -\ln m$. Since $\frac{\varphi_i^\infty(x+L)}{\varphi_i^\infty(x)} = \psi_i^\infty(x) \equiv m$ for $x \in \mathbb{R}$, the function $\varphi^\infty(x)e^{\lambda x}$ is L-periodic. Since $-\mathcal{L}\varphi^\infty - A(x)\varphi^\infty = \lambda_1^\infty\varphi^\infty$, we have

$$-L_\lambda(e^{\lambda x}\varphi^\infty(x)) - A(x)e^{\lambda x}\varphi^\infty(x) = e^{\lambda x}\left(-\mathcal{L}\varphi^\infty - A(x)\varphi^\infty\right) = \lambda_1^\infty e^{\lambda x}\varphi^\infty,$$

hence $\varphi^\infty(x)e^{-\lambda x}$ is the periodic principal eigenfunction of $-L_\lambda - A(x)$. By the uniqueness of the periodic principal eigenvalue, $\lambda_1^\infty = k(\lambda)$. This shows $\lambda_1 = \max_{\lambda\in\mathbb{R}} k(\lambda)$, which finishes the proof of Statement (iv)

Proof of Statement (v): We first deal with Assumption 2.3.5 case a), *i.e.* the case where both σ and A are even. We write the proof for $\mathcal{L}$ written in nondivergence form, however the computations are similar in the case $\mathcal{L}$ is written in divergence form. Recalling the formula (2.3.20),

$$k(\lambda) = \max_{\substack{\phi>0\\ \phi\in C^2_{per}(\mathbb{R},\mathbb{R}^d)}} \inf_{x\in\mathbb{R}} \min_{1\leq i\leq d} \frac{(-L_\lambda\phi - A(x)\phi)_i}{\phi_i},$$

we notice that the set of admissible test functions is invariant by the change of variables $x \leftarrow -x$. More precisely, for any $\phi \in C^2_{per}(\mathbb{R}, \mathbb{R}^d)$ with $\phi > 0$, there exists $\check{\phi}(x) := \phi(-x)$ satisfying $\check{\phi} \in C^2_{per}(\mathbb{R}, \mathbb{R}^d)$, $\check{\phi} > 0$ and $L_\lambda\phi(x) = (\check{L_{-\lambda}\check{\phi}})(-x) = L_{-\lambda}\check{\phi}(-x)$, so that:

$$\inf_{x\in\mathbb{R}} \min_{1\leq i\leq d} \frac{(-L_\lambda\phi(x) - A(x)\phi(x))_i}{\phi_i(x)} = \inf_{x\in\mathbb{R}} \min_{1\leq i\leq d} \frac{(-L_{-\lambda}\check{\phi}(-x) - A(x)\check{\phi}(-x))_i}{\check{\phi}_i(-x)}.$$

Hence, for all $\phi \in C^2_{per}(\mathbb{R}, \mathbb{R}^d)$ satisfying $\phi > 0$:

$$\inf_{x\in\mathbb{R}} \min_{1\le i\le d} \frac{(-L_\lambda \phi(x) - A(x)\phi(x))_i}{\phi_i(x)} \le \max_{\substack{\phi'>0 \\ \phi'\in C^2_{per}(\mathbb{R}),\mathbb{R}^d}} \inf_{x\in\mathbb{R}} \min_{1\le i\le d} \frac{(-L_{-\lambda}\phi' - A(x)\phi')_i}{\phi'_i} = k(-\lambda).$$

Taking the supremum on ϕ, we get $k(\lambda) \le k(-\lambda)$. Changing λ into $-\lambda$, we similarly get $k(-\lambda) \le k(\lambda)$, which shows that the equality $k(-\lambda) = k(\lambda)$ holds.

Next we consider that Assumption 2.3.5 case b) holds, *i.e.*, $\mathcal{L} = \mathcal{L}^d$ is in divergence form (2.3.10) and A is a symmetric matrix (i.e. equals its transpose for all $x \in \mathbb{R}$), then the operator $L_{-\lambda}$ is the adjoint of the operator L_λ for the canonical scalar product in $L^2_{per}(\mathbb{R})^d$:

$$\langle \varphi, \psi \rangle := \langle \varphi, \psi \rangle_{L^2_{per}(\mathbb{R})^d} = \sum_{i=1}^{d} \int_0^1 \varphi_i(x)\psi_i(x)\mathrm{d}x,$$

and it follows easily from the Krein-Rutman Theorem [413, Theorem 7.C] that $k(-\lambda) = k(\lambda)$.

This finishes the proof of Statement (v). □

We are now in a position to prove Proposition 2.3.9.

Proof of Proposition 2.3.9. We first notice that $\lambda_1^{per} = k(0)$. Since the operator $\mathcal{L}$ in Proposition 2.3.9 satisfies Assumption 2.3.5, Lemma 2.3.6 statement (v) implies that $k(\lambda)$ is even, and Lemma 2.3.6 statement (iii) implies that it is concave and continuous. Hence,

$$\lambda_1^{per} = k(0) = \max_{\lambda\in\mathbb{R}} k(\lambda).$$

Finally, by Lemma 2.3.6 statement (iv) we have $\lambda_1 = \max_{\lambda\in\mathbb{R}} k(\lambda)$, and by Lemma 2.3.4 statement (iv) we have $\lambda_1 = \lim_{R\to+\infty} \lambda_1^R$. This ends the chain of equalities:

$$\lambda_1^{per} = k(0) = \max_{\lambda\in\mathbb{R}} k(\lambda) = \lambda_1 = \lim_{R\to+\infty} \lambda_1^R,$$

which proves Proposition 2.3.9. □

Last, we prove our statements on the formula for the minimal speed.

Proof of Proposition 2.3.7. Statement (i) is a direct consquence of the definition of c^* in (2.3.22). Next, by the fact that $k(0) = \lambda_1^{per} < 0$ and (2.3.21), the infimum on the right-hand side of (2.3.22) is attained by some $\lambda^* > 0$. Furthermore, since $k(\lambda)$ is strictly concave, λ^* is the only solution of the equation $\lambda c^* = k(\lambda)$. This proves (ii). Statements (ii) and (iii) follow directly from the strict concavity of $\lambda \mapsto k(\lambda)$. The continuity with respect to A follows easily from the sequential characterisation of continuity and the regularising properties of elliptic operators. □

2.3.3.3 Speed of sublinear systems

Our main goal is to prove Theorem 2.3.19. This theorem follows as a direct consequence of Lemma 2.3.37 and Lemma 2.3.38 below.

Lemma 2.3.37 (Lower spreading speed)**.** *Let $\mathcal{L}$ be a diagonal uniformly elliptic L-periodic operator, and $f = (f_1, \dots, f_d)$ be a cooperative sublinear nonlinearity satisfying Assumption 2.3.15. Assume that there is a periodic function $p(x) \gg 0$ solution to the equation*

$$p_t - \mathcal{L}p = f(x, p(x))$$

which attracts every nontrivial periodic initial condition $p(x) \ge u_0(x) \ge \delta \mathbf{1} \gg 0$.

Let $u(t,x)$ be a solution of (2.3.9) *associated with an initial condition which is positive on a half-line*

$$\inf_{x\le -K} \min_{1\le i\le d} u_i(0,x) > 0$$

for some $K > 0$. Then for any $c < c^*$, we have

$$\limsup_{t\to+\infty} \sup_{x\le ct} \|u(t,x) - p(x)\| = 0,$$

where $c^* = \inf_{\lambda>0} -\frac{k(\lambda)}{\lambda}$ is defined by (2.3.22) *in Proposition 2.3.7.*

Proof. Let $\mathcal{H} := \bigcup_{1\le i\le d} \mathbb{R}\times\{i\} \subset \mathbb{R}^2$. We remark that any continuous function $u : \mathbb{R}\times\mathbb{R} \to \mathbb{R}^d$ can be represented as a function $u : \mathbb{R}\times\mathcal{H} \to \mathbb{R}$ by letting $u(t,x,i) = u_i(t,x)$. Hence a vector function can be represented by a scalar function on the habitat $\mathcal{H}$. In particular, system (2.3.9) makes sense as an equation on $u \in BUC(\mathcal{H})$.

Let $\delta > 0$, $\tau > 0$ be given and let $Q : BUC(\mathcal{H}) \to BUC(\mathcal{H})$ be defined by

$$Q[v_0](x) := v(\tau, x).$$

where $v(t,x)$ is the solution to (2.3.9) satisfying $v(0,x) = v_0(x)$. It follows from standa rd arguments that Q is monotone.

Let us now check that the Hypothesis 2.1 in [398] are satisfied for $\mathcal{H}$ and Q^δ. L et us mention at this point that our setting is a little different from the one of the paper of Weinberger [398], since $\mathcal{H}$ is not left invariant by a 2-dimensional lattice, as it is bounded in one direction. In our case, $\mathcal{H}$ is periodic with respect to the 1-dimensional lattice $L\mathbb{Z}\times\{0\}$ (for which Q^δ is periodic). However, as stated in section 8 of [398] (Partially bounded habitats), all the results in [398] can be adapted in directions ξ which are not orthogonal to all members of our lattice $L\mathbb{Z}\times\{0\}$ (which are the directions in which the spreading happens). In the rest of the proof we will use those results.

Let us now check point by point that Hypothesis 2.1 is satisfied:

i. $\mathcal{H}$ is not contained in any 1-dimensional subset of $\mathbb{R}^2$.

ii. Q is monotone because f is quasi-monotone.

iii. $\mathcal{H}$ is invariant under translation by elements of $L\mathbb{Z}\times\{0\}$, and Q^δ is periodic with respect to $L\mathbb{Z}\times\{0\}$. Moreover there is a bounded subset $P := [0,1)\times\{1,\dots.d\} \subset \mathcal{H}$, such that any $x \in \mathcal{H}$ has a unique representation of the form $x = l + p$ with $l \in L\mathbb{Z}\times\{0\}$ and $p \in P$.

iv. $Q(0) = \pi_0 :\equiv 0$, and there exists $\pi_1 := p(x) > 0$ which is the unique nonnegative nontrivial fixed point of Q^δ.

v. Q is continuous.

vi. Due to the classical parabolic estimates, Q is sequentially compact for the topology of th e local uniform convergence on $BUC(\mathcal{H})$.

In particular, [398, Theorem 2.1] applies to Q and there exists a spreading speed c^* associated with Q^δ. Moreover, because of Assumption 2.3.15, [398, Theorem 2.4] implies

$$c^*(Q) \ge \inf_{\lambda>0} \frac{-k^\delta(\lambda)}{\lambda} =: c^*_\delta,$$

where $(k^\delta(\lambda), \varphi^{\delta,\lambda}(x))$ is the periodic principal eigenvalue solution to

$$-e^{\lambda x}\mathcal{L}(\varphi^{\delta,\lambda}(x)e^{-\lambda x}) - A^\delta(x)\varphi^{\delta,\lambda}(x) = k^\delta(\lambda)\varphi^{\delta,\lambda}(x).$$

Since $A^\delta(x) \to A(x)$ as $\delta \to 0$, it follows from classical arguments that $c^*_\delta \to c^*$ as $\delta \to 0$.
This completes the proof of Lemma 2.3.37. □

Let us turn to the upper estimates of the spreading speed:

Lemma 2.3.38 (Upper spreading speed)**.** *Let $\mathcal{L}$ be a uniformly elliptic L-periodic operator, and f be a L-periodic sublinear nonlinearity. Assume that $Df(x,0) =: A(x)$ is cooperative and fully coupled. Then, for any $c > c^*(\mathcal{L} + A(x))$, we have:*

$$\limsup_{t\to+\infty} \sup_{x\ge ct} \max_{1\le i\le d} u_i(t,x) = 0,$$

for any $u(t,x)$ solution to (2.3.9)*, provided there is $K > 0$ such that $u(0,x) \equiv 0$ for all $x \ge K$.*

Proof. The result is an immediate consequence of the comparison principle applied to $u(t,x)$ and the function $M\varphi^{\lambda_*}(x)e^{-\lambda_*(x-ct)}$, where $\lambda_* > 0$ is a minimizer for $-\frac{k(\lambda)}{\lambda}$, φ^{λ_*} is the associated 1-periodic principal eigenfunction, and $M > 0$ is a large constant satisfying

$$u_0(x) \le M\varphi^{\lambda_*}(x)e^{-\lambda_* x}.$$

□

Proof of Theorem 2.3.19. Let c^* be the number defined as

$$c^* := \inf_{\lambda>0} \frac{-k(\lambda)}{\lambda},$$

where $k(\lambda)$ is defined in Lemma 2.3.6 Statement (i) with $A(x) = Df(x,0)$. Recall that c^* is well-defined by Proposition 2.3.7.

Let $u_0 \in BUC(\mathbb{R}, \mathbb{R}^d_+)$ be given and $u(t,x)$ be the solution to (2.3.9) satisfying $u(0,x) = u_0(x)$. We assume that $u_0(x) = 0$ for all $x \geq 0$ and that

$$\liminf_{x\to-\infty} \|u_0(x)\| > 0.$$

It has been shown in Lemma 2.3.38 that

$$\limsup_{t\to+\infty} \sup_{x\geq ct} \|u(t,x)\|_\infty = \limsup_{t\to+\infty} \sup_{x\geq ct} \max_{1\leq i\leq d} u_i(t,x) = 0,$$

therefore Statement (ii) in Definition 2.3.18 holds.

Let $\eta > 0$ and f^- be as in Definition 2.3.16. Recall that, by Proposition 2.3.36, f^- can be chosen so that the equation $-\mathcal{L}p = f^-(x,p)$ admits a positive periodic fixed point $p(x)$ which attracts any periodic initial condition $0 \leq u_0(x) \leq p(x)$, and $\|p\|_{L^\infty(\mathbb{R})^d} \leq \eta$.

We define $\underline{u}(t,x)$ as the unique solution to

$$\begin{cases} \underline{u}_t(t,x) - \mathcal{L}\underline{u}(t,x) = f^-(x, \underline{u}(t,x)), \\ \underline{u}(0,x) = \min\big(u_0(x), p(x)\big). \end{cases} \tag{2.3.39}$$

By Proposition 2.3.36, the interval

$$[0, p(x)] := \{v(x) \in BUC(\mathbb{R})^d \,|\, 0 \leq v(x) \leq p(x)\},$$

is positively invariant by the semiflow generated by (2.3.39). Therefore $\underline{u}(t,x) \leq p(x)$ for all $t \geq 0$ and $x \in \mathbb{R}$. By Theorem 2.3.35, we have then

$$u(t,x) \geq \underline{u}(t,x) \text{ for all } t \geq 0 \text{ and } x \in \mathbb{R}.$$

Applying Lemma 2.3.37 to u and $\underline{u}$, we find that

$$\lim_{t\to+\infty} \inf_{x\leq ct} u(t,x) \geq \lim_{t\to+\infty} \inf_{x\leq ct} \underline{u}(t,x) \geq p(x) \geq \delta\mathbf{1} \gg 0,$$

for all $c < c^*$ and $\delta > 0$ sufficiently small, hence we have shown Item (i) in Definition 2.3.18. □

2.3.3.4 Traveling waves: proof of Theorem 2.3.21

We now prove Theorem 2.3.21 and the existence of traveling waves. The proof is done by constructing an upper barrier and a lower barrier. The construction of the upper barrier is rather simple as the following Lemma shows:

Lemma 2.3.39 (Upper barrier)**.** *Let $\lambda > 0$ and $c > 0$ be such that $\lambda c + k(\lambda) \geq 0$. Define*

$$\overline{u}(t,x) := e^{-\lambda(x-ct)}\varphi_\lambda(x) \tag{2.3.40}$$

where φ_λ is the solution to (2.3.19) *associated with λ, and satisfies $\|\varphi_\lambda\|_{L^\infty} = 1$. Any solution $u(t,x)$ of* (2.3.9) *starting from below $\overline{u}(t,x)$ at $t = 0$ stays below $\overline{u}(t,x)$ at later times. More precisely, if the inequality*

$$0 \leq u(0,x) \leq \overline{u}(0,x)$$

holds componentwise for all $x \in \mathbb{R}$, then for all $t > 0$ the inequality

$$0 \leq u(t,x) \leq \overline{u}(t,x)$$

holds componentwise for all $x \in \mathbb{R}$.

Proof. We remark that

$$\overline{u}_t(t,x) - \mathcal{L}\overline{u}(t,x) = \big(\lambda c + A(x) + k(\lambda)\big)\overline{u}(t,x) \tag{2.3.41}$$

Since $\lambda c + k(\lambda) \geq 0$, we have

$$u_t(t,x) - \mathcal{L}u(t,x) = f(x,u(t,x)) \leq A(x)u(t,x) \leq \big(\lambda c + k(\lambda) + A(x)\big)u(t,x).$$

Therefore $u(t,x)$ is a subsolution to (2.3.41). By the comparison principle for cooperative parabolic systems, we have

$$u(t,x) \leq \overline{u}(t,x)$$

for all $t > 0$ whenever $u(0,x) \leq \overline{u}(0,x)$. □

Next we construct a lower barrier. The function ξ in the following Lemma will play an important role in this construction for the case $c > c^*$.

Lemma 2.3.40. *Under the assumptions of Theorem 2.3.21, let $c > c^*$ and $\lambda > 0$ be such that $\frac{-k(\lambda)}{\lambda} = c$. Define*

$$\xi(t,x) = e^{-\lambda(x-ct)}\varphi_\lambda(x) - \omega e^{-\mu(x-ct)}\varphi_\mu(x), \tag{2.3.42}$$

where $\mu > 0$ satisfies $k(\mu) + \mu c > 0$ and $\lambda < \mu < \lambda(1+\beta)$ where $\beta > 0$ is the constant defined in the assumptions of Theorem 2.3.21. There exists $\omega^* > 0$ such that, for all $\omega \geq \omega^*$, the function $\xi(t,x)$ satisfies the differential inequality

$$(\xi_i)_t(t,x) - \mathcal{L}_i\xi_i(t,x) \leq f_i^-(x,\xi(t,x)) \tag{2.3.43}$$

as well as $\|\xi(t,x)\|_\infty \leq \eta$, whenever there is $i \in \{1,\dots,d\}$ such that $\xi_i(t,x) > 0$, where f^- and η are as in Definition 2.3.16.

In particular, if $\omega > \omega^*$, any solution $u(t,x)$ of (2.3.9) satisfying the inequality $u(0,x) \geq \max\big(\xi(0,x),0\big)$ also satisfies

$$u(t,x) \geq \max\big(\xi(t,x),0\big) \text{ for all } t > 0 \text{ and } x \in \mathbb{R}. \tag{2.3.44}$$

Proof. The existence of μ as defined in the statement of the Lemma is a consequence of $c > c^*$ and the properties of the principal eigenvalue k, see Proposition 2.3.7. Our goal is to find $\omega > 0$ such that

$$\xi_t(t,x) - \mathcal{L}\xi(t,x) \leq f^-(x,\xi(t,x)) \text{ whenever } \xi(t,x) > 0. \tag{2.3.45}$$

Let us select (t,x) such that $\xi(t,x) > 0$. Recall that, for all $\nu > 0$, we have the equation $-\mathcal{L}(\varphi_\nu(x)e^{-\nu x}) = (A(x) + k(\nu))e^{-\nu x}\varphi_\nu(x)$ by definition of $k(\nu)$. We compute

$$\begin{aligned}\xi_t - \mathcal{L}\xi &= \big(A(x) + k(\lambda) + \lambda c\big)\, e^{-\lambda(x-ct)}\varphi_\lambda(x) - \big(A(x) + k(\mu) + \mu c\big)e^{-\mu(x-ct)}\omega\varphi_\mu(x)\\ &= A(x)\xi(t,x) - (k(\mu) + \mu c)\omega e^{-\mu(x-ct)}\varphi_\mu(x).\end{aligned}$$

It follows from our assumption in the statement of Theorem 2.3.21 that

$$\|f^-(x,u) - A(x)u\|_\infty \leq M\|u\|_\infty^{1+\beta},$$

for some constant $M > 0$.

$$\begin{aligned}\|f^-(x,\xi(t,x)) - A(x)\xi(t,x)\|_\infty &\leq M\|\xi(t,x)\|_\infty^{1+\beta}\\ &\leq M\left(\sup_{y\in\mathbb{R}}\max_{1\leq i\leq d}(\varphi_\lambda)_i(y)\right)^{1+\beta} e^{-(1+\beta)\lambda(x-ct)},\end{aligned}$$

and it follows that

$$(k(\mu) + \mu c)\omega e^{-\mu(x-ct)}\varphi_\mu(x) \geq A(x)\xi(t,x) - f^-(x,\xi(t,x))$$

for all $x - ct \geq \frac{1}{(1+\beta)\lambda - \mu}\left[\ln\left(\frac{M\sup_{y\in\mathbb{R}}\max_{1\leq i\leq d}(\varphi_\lambda)_i^{1+\beta}(y)}{(k(\mu)+\mu c)\inf_{y\in\mathbb{R}}\min_{1\leq i\leq d}(\varphi_\mu)_i(y)}\right) - \ln\omega\right]$. On the other hand, because of the specific form of ξ, we have $\xi(t,x) \ll 0$ for all $x - ct \leq \frac{-1}{\mu-\lambda}\ln\left(\frac{\sup_{y\in\mathbb{R}}\max_{1\leq i\leq d}(\varphi_\lambda)_i(y)}{\inf_{y\in\mathbb{R}}\min_{1\leq i\leq d}(\varphi_\mu)_i(y)}\right) + \frac{1}{\mu-\lambda}\ln\omega$. Therefore if ω is sufficiently large, namely

$$\ln\omega > \frac{\mu-\lambda}{\beta\lambda}\ln\left(\frac{M\sup_{y\in\mathbb{R}}\max_{1\leq i\leq d}(\varphi_\lambda)_i^{1+\beta}(y)}{(k(\mu)+\mu c)\inf_{y\in\mathbb{R}}\min_{1\leq i\leq d}(\varphi_\mu)_i(y)}\right) - \frac{(1+\beta)\lambda - \mu}{\beta\lambda}\ln\left(\frac{\sup_{y\in\mathbb{R}}\max_{1\leq i\leq d}(\varphi_\lambda)_i(y)}{\inf_{y\in\mathbb{R}}\min_{1\leq i\leq d}(\varphi_\mu)_i(y)}\right),$$

then $\xi(t,x) > 0$ implies that $(k(\mu)+\mu c)\omega e^{-\mu(x-ct)}\varphi_\mu(x) \geq A(x)\xi(t,x) - f^-(x,\xi(t,x))$ and therefore

$$\begin{aligned}\xi_t - \mathcal{L}\xi(t,x) &\leq A(x)\xi(t,x) - (k(\mu)+\mu c)\omega e^{-\mu(x-ct)}\varphi_\mu(x)\\ &\leq A(x)\xi(t,x) - \big(A(x)\xi(t,x) - f^-(x,\xi(t,x))\big)\\ &= f^-(x,\xi(t,x)).\end{aligned}$$

We have shown that (2.3.45) holds for $\omega > 0$ sufficiently large. Finally

$$\begin{aligned}\sup_{x\in\mathbb{R}}\xi(t,x) &\leq \sup_{x\in\mathbb{R}}\left(e^{-\lambda x}\sup_{y\in\mathbb{R}}\varphi_\lambda(y) - \omega e^{-\mu x}\inf_{y\in\mathbb{R}}\varphi_\mu(y)\right)\\ &\leq \sup_{y\in\mathbb{R}}\varphi_\lambda(y)\left(\frac{\lambda\sup_{y\in\mathbb{R}}\varphi_\lambda(y)}{\mu\inf_{y\in\mathbb{R}}\varphi_\mu(y)}\right)^{\frac{\lambda}{\mu-\lambda}}\omega^{-\frac{\lambda}{\mu-\lambda}},\end{aligned}$$

therefore the supremum of $\xi(t,x)$ is arbitrarily small for ω sufficiently large.

To finish our argument we remark that (if $\omega \geq \omega^*$) $\xi(t,x)$ and $u(t,x)$ are respectively a sub-solution and a super-solution to the cooperative system

$$v_t(t,x) - \mathcal{L}v(t,x) = f^-(x,v(t,x)),$$

which admits a comparison principle. Therefore if $u(0,x) \geq \xi(0,x)$ for all $x \in \mathbb{R}$, then $u(t,x) \geq \xi(t,x)$ for all $t > 0$ and $x \in \mathbb{R}$. The Lemma is proved. □

In the critical case $c = c^*$, we need to define ξ differently. Recall that, by Proposition 2.3.7, there exists a unique λ^* such that $c^* = \frac{k(\lambda^*)}{\lambda^*}$. By lemma 2.3.6, $k(\lambda)$ is strictly concave and analytic, therefore there exists a nonnegative integer $m \geq 0$ such that the multiplicity of $k(\lambda) + c^*\lambda$ is $2m+2$, in the sense that

$$\lambda^* c^* + k(\lambda^*) = 0,\ c^* + k'(\lambda^*) = 0,\ k^{(i)}(\lambda^*) = 0 \text{ for } 2 \leq i \leq 2m+1, \text{ and } k^{(2m+2)}(\lambda^*) < 0.$$

Lemma 2.3.41. *Let the assumptions of Theorem 2.3.21 hold. Define*

$$\xi(t,x) = \begin{cases}\max\left(\frac{\partial^{2m+2}}{\partial\lambda^{2m+2}}\left(e^{-\lambda(x-c^*t)}\varphi_\lambda(x)\right)\big|_{\lambda=\lambda^*} - \omega e^{-\lambda^*(x-c^*t)}\varphi_{\lambda^*}(x), 0\right) & \text{if } x - c^*t \geq \left(\frac{\omega}{2}\right)^{\frac{1}{2m+2}},\\ 0 & \text{if } x - c^*t < \left(\frac{\omega}{2}\right)^{\frac{1}{2m+2}}\end{cases} \tag{2.3.46}$$

where the maximum is taken componentwise, then there exists $\omega^* > 0$ such that, for all $\omega \geq \omega^*$, the function $\xi(t,x)$ satisfies the differential inequality

$$(\xi_i)_t(t,x) - \mathcal{L}_i\xi_i(t,x) \leq f_i^-(x,\xi(t,x)) \tag{2.3.47}$$

as well as $\|\xi(t,x)\|_\infty \leq \eta$ whenever $\xi_i(t,x) > 0$ for some $i \in \{1,\dots,d\}$, where f^- and η are as in Definition 2.3.16. In particular, if $\omega \geq \omega^*$, any solution $u(t,x)$ of (2.3.9) satisfying the inequality $u(0,x) \geq \max\big(\xi(0,x),0\big)$ also satisfies

$$u(t,x) \geq \max(\xi(t,x),0) \ \text{ for all } t > 0 \text{ and } x \in \mathbb{R}. \tag{2.3.48}$$

Proof. Let us define the function $\Xi(t,x) := e^{-\lambda(x-c^*t)}\varphi_\lambda(x)$ for $\lambda > 0$, $\omega > 0$ and $(t,x) \in \mathbb{R}$. We have

$$\Xi_t(t,x) - \mathcal{L}\,\Xi(t,x) = A(x)\Xi(t,x) + \big(\lambda c^* + k(\lambda)\big)\Xi(t,x), \tag{2.3.49}$$

then by the analyticity of $k(\lambda)$ and φ_λ with respect to λ we have, taking $(2m+2)$ times the derivative in the above expression:

$$\begin{aligned}\partial_t\left(\frac{\partial^{2m+2}}{\partial\lambda^{2m+2}}\Xi(t,x)\right) - \mathcal{L}\left(\frac{\partial^{2m+2}}{\partial\lambda^{2m+2}}\Xi(t,x)\right) &= A(x)\left(\frac{\partial^{2m+2}}{\partial\lambda^{2m+2}}\Xi(t,x)\right)\\ &\quad + \sum_{j=0}^{2m+2}\binom{2m+2}{j}(\lambda c^* + k(\lambda))^{(j)}(\lambda)(e^{-\lambda(x-c^*t)}\varphi_\lambda(x))^{(2m+2-j)}.\end{aligned}$$

If $\lambda = \lambda^*$ we have

$$\partial_t\left(\Xi^{(2m+2)}(t,x)\right) - \mathcal{L}\left(\Xi^{(2m+2)}(t,x)\right) = A(x)\left(\Xi^{(2m+2)}(t,x)\right) + k^{(2m+2)}(\lambda^*)e^{-\lambda(x-c^*t)}\varphi_\lambda(x), \tag{2.3.50}$$

where $k^{(2m+2)}(\lambda^*) < 0$ (because of the concavity of k) and $\Xi^{(2m+2)}(t,x) := \frac{\partial^{2m+2}}{\partial\lambda^{2m+2}}\Xi(t,x)$. Next the leading term in $\Xi^{(2m+2)}(t,x)$ when $x - c^*t \to +\infty$ is $(x-c^*t)^{2m+2}e^{-\lambda(x-c^*t)}\varphi_\lambda(x)$, therefore

$$\Xi^{(2m+2)}(t,x) \sim (x-c^*t)^{2m+2}e^{-\lambda(x-c^*t)}\varphi_\lambda(x) \text{ when } x - c^*t \to +\infty,$$

and there is $s_0 \in \mathbb{R}$ such that

$$\frac{1}{2}(x-c^*t)^{2m+2}e^{-\lambda(x-c^*t)}\varphi_\lambda(x) \le \Xi^{(2m+2)}(t,x) \le 2(x-c^*t)^{2m+2}e^{-\lambda(x-c^*t)}\varphi_\lambda(x) \le \eta \quad \text{if } x - c^*t \ge s_0. \tag{2.3.51}$$

Now, we define $\xi(t,x) := \Xi^{(2m+2)}(t,x) - \omega e^{-\lambda^*(x-c^*t)}\varphi_{\lambda^*}(x)$. Since $e^{-\lambda^*(x-c^*t)}\varphi_{\lambda^*}(x)$ is a solution of (2.3.49) with $\lambda = \lambda^*$, (2.3.50) implies the following:

$$\partial_t\left(\xi(t,x)\right) - \mathcal{L}\left(\xi(t,x)\right) = A(x)\left(\xi(t,x)\right) + k^{(2m+2)}(\lambda^*)e^{-\lambda(x-c^*t)}\varphi_\lambda(x). \tag{2.3.52}$$

Next, since $\varphi_{\lambda^*}(x)$ is uniformly positive on $\mathbb{R}$, for ω sufficiently large, we have $\xi(t,x) < 0$ for all $x - c^*t \in \big(0, s_0\big]$, and (2.3.51) implies

$$\left[\frac{1}{2}(x-c^*t)^{2m+2} - \omega\right] e^{-\lambda^*(x-c^*t)}\varphi_{\lambda^*}(x) \le \xi(t,x) \le \left[2(x-c^*t)^{2m+2} - \omega\right] e^{-\lambda^*(x-c^*t)}\varphi_{\lambda^*}(x)$$

if $x - c^*t > s_0$. In particular, if $x - c^*t \le \max\left(\left(\frac{\omega}{2}\right)^{\frac{1}{2m+2}}, s_0\right)$, then $\xi(t,x) \le 0$. If $x - c^*t \ge \max\left(\left(\frac{\omega}{2}\right)^{\frac{1}{2m+2}}, s_0\right)$, we have

$$\|\xi(t,x)\| \le \max\left[\omega - \frac{(x-c^*t)^{2m+2}}{2}, 2(x-c^*t)^{2m+2} - \omega\right] e^{-\lambda^*(x-c^*t)}\|\varphi_{\lambda^*}(x)\|$$

In order to estimate the right-hand side of the above inequality, we first consider the case when $\left(\frac{\omega}{2}\right)^{\frac{1}{2m+2}} \le (x-c^*t) \le (2\omega)^{\frac{1}{2m+2}}$. Then we have

$$\begin{aligned}
\|\xi(t,x)\| &\le 3\omega e^{-\lambda^*(x-c^*t)}\|\varphi_{\lambda^*}(x)\| \\
&\le 3\omega e^{-\frac{\beta}{1+\beta}\lambda^*(x-c^*t)}\|\varphi_{\lambda^*}(x)\|^{\frac{\beta}{1+\beta}} \times e^{-\frac{1}{1+\beta}\lambda^*(x-c^*t)}\|\varphi_{\lambda^*}(x)\|^{\frac{1}{1+\beta}} \\
&\le 3\omega e^{-\lambda^*\frac{\beta}{1+\beta}\left(\frac{\omega}{2}\right)^{\frac{1}{2m+2}}}\|\varphi_{\lambda^*}(x)\|^{\frac{\beta}{1+\beta}} \times e^{-\frac{1}{1+\beta}\lambda^*(x-c^*t)}\|\varphi_{\lambda^*}(x)\|^{\frac{1}{1+\beta}} \\
&\le K_1(\omega)e^{-\frac{1}{1+\beta}\lambda^*(x-c^*t)}\|\varphi_{\lambda^*}(x)\|^{\frac{1}{1+\beta}},
\end{aligned}$$

where

$$K_1(\omega) := 3\omega e^{-\lambda^*\frac{\beta}{1+\beta}\left(\frac{\omega}{2}\right)^{\frac{1}{2m+2}}} \max_{x\in\mathbb{R}}\|\varphi_{\lambda^*}(x)\|^{\frac{\beta}{1+\beta}}$$

and $\beta > 0$ is the constant from (2.3.27). Next we consider the case when $(x-c^*t) \ge (2\omega)^{\frac{1}{2m+2}}$. We have

$$\begin{aligned}
\|\xi(t,x)\| &\le 2(x-c^*t)^{2m+2}e^{-\lambda^*(x-c^*t)}\|\varphi_{\lambda^*}(x)\| \\
&\le 2(x-c^*t)^{2m+2}e^{-\frac{\beta}{1+\beta}\lambda^*(x-c^*t)}\|\varphi_{\lambda^*}(x)\|^{\frac{\beta}{1+\beta}} \times e^{-\frac{1}{1+\beta}\lambda^*(x-c^*t)}\|\varphi_{\lambda^*}(x)\|^{\frac{1}{1+\beta}} \\
&\le 2(x-c^*t)^{2m+2}e^{-\frac{\beta}{1+\beta}\lambda^*(x-c^*t)}\|\varphi_{\lambda^*}(x)\|^{\frac{\beta}{1+\beta}} \times e^{-\frac{1}{1+\beta}\lambda^*(x-c^*t)}\|\varphi_{\lambda^*}(x)\|^{\frac{1}{1+\beta}} \\
&\le K_2(\omega)e^{-\frac{1}{1+\beta}\lambda^*(x-c^*t)}\|\varphi_{\lambda^*}(x)\|^{\frac{1}{1+\beta}},
\end{aligned}$$

where

$$K_2(\omega) := 2 \sup_{s \ge (2\omega)^{\frac{1}{2m+2}}} s^{2m+2}e^{-\frac{\beta}{1+\beta}\lambda^* s} \max_{x\in\mathbb{R}}\|\varphi_{\lambda^*}(x)\|^{\frac{\beta}{1+\beta}}.$$

Let $\kappa > 0$ be a constant such that $\varphi_{\lambda^*}(x) \ge \kappa\|\varphi_{\lambda^*}(x)\|_\infty \mathbf{1}$ for any $x \in \mathbb{R}$ and let $M > 0$ be the constant that appears in (2.3.27). Since $K_1(\omega)$ and $K_2(\omega)$ converge to 0 as $\omega \to +\infty$, the following holds if ω is chosen sufficiently large:

$$\|\xi(t,x)\| \le \left(\frac{\kappa\big(-k^{(2m+2)}(\lambda^*)\big)}{M}\right)^{\frac{1}{1+\beta}} e^{-\frac{\lambda^*}{1+\beta}(x-c^*t)}\|\varphi_{\lambda^*}(x)\|^{\frac{1}{1+\beta}}$$

for all $x - c^*t \geq \left(\frac{\omega}{2}\right)^{\frac{1}{2m+2}}$. Combining this inequality with $\varphi_{\lambda^*}(x) \geq \kappa \|\varphi_{\lambda^*}(x)\|_\infty \mathbf{1}$ and (2.3.27), we obtain

$$\begin{aligned} -k^{(2m+2)}(\lambda^*)e^{-\lambda^*(x-c^*t)}(\varphi_{\lambda^*})_i(x) &\geq \kappa\big(-k^{(2m+2)}(\lambda^*)\big)e^{-\lambda^*(x-c^*t)}\|\varphi_{\lambda^*}(x)\| \\ &\geq M\|\xi(t,x)\|^{1+\beta} \geq \|f^-(t,\xi(t,x)) - A(x)\xi(t,x)\|_\infty \geq \big(A(x)\xi(t,x)\big)_i - f_i^-(x,\xi(t,x)) \end{aligned}$$

for all $i \in \{1,\dots,d\}$ whenever $\xi_j(t,x) > 0$ for some $j \in \{1,\dots,d\}$. Recalling (2.3.52), we have shown that

$$\xi_t(t,x) - \mathcal{L}\xi(t,x) \leq f^-(t,\xi(t,x))$$

whenever $\xi_i(t,x) > 0$ for some $i \in \{1,\dots,d\}$. This completes the proof of Lemma 2.3.41. □

Now we are ready to construct a lower barrier. If $c > c^*$, we define $\underline{u}(t,x)$ as

$$\underline{u}(t,x) = \max_{n\in\mathbb{N}} \xi(t, x+nL),$$

where ξ is defined by (2.3.42), $\omega > \omega^*$, and the maximum is taken componentwise. It follows immediately from the periodicity of the equation (2.3.9) that the functions $(t,x) \mapsto \xi(t,x+nL)$ for $n \in \mathbb{N}$ are lower barriers for (2.3.9); therefore $\underline{u}(t,x)$ is also a lower barrier. Since $\xi(t,x) > 0$ for $x > 0$ sufficiently large, $\underline{u}$ is uniformly positive when $x \to -\infty$. Moreover, $\xi(t,x) < \overline{u}(t,x)$ and

$$\xi(t,x+nL) \leq \overline{u}(t,x+nL) = e^{-\lambda(x+nL-ct)}\varphi_\lambda(x+nL) = e^{-\lambda nL}\overline{u}(t,x) \leq e^{-\lambda L}\overline{u}(t,x) < \overline{u}(t,x),$$

for all $n \in \mathbb{N}$ and $n \geq 1$, therefore

$$\underline{u}(t,x) < \overline{u}(t,x) \text{ for all } (t,x) \in \mathbb{R}^2. \tag{2.3.53}$$

If $c = c^*$ we need to modify the process slightly. We let $\xi(t,x)$ be defined by (2.3.46) and pick $\lambda < \lambda^*$, so that $\lambda c^* + k(\lambda) > 0$. Since the leading term in (2.3.46) is controlled by $(x-c^*t)^{2m+2}e^{-\lambda^*(x-c^*t)}$, there is $s^* \geq 0$ such that

$$\xi(t,x+s^*) < \overline{u}(t,x) := e^{-\lambda(x-c^*t)}\varphi_{\lambda^*}(x) \text{ for all } x \in \mathbb{R} \text{ and } t \geq 0,$$

therefore we define

$$\underline{u}(t,x) = \max_{n\in\mathbb{N}} \xi(t, x+s^*+nL). \tag{2.3.54}$$

Reasoning as above, we obtain that $\underline{u}(t,x)$ is a lower barrier and satisfies (2.3.53).

We are now in a position to prove Theorem 2.3.21.

Proof of Theorem 2.3.21. The fact that there exists no traveling wave for $c < c^*$ is a direct consequence of the spreading property (Theorem 2.3.19). In order to construct a traveling wave for $c \geq c^*$, we first deal with the case $c > c^*$ and apply the Schauder fixed-point Theorem to construct the traveling wave. We finally send c to c^* the minimal speed in order to construct the minimal speed traveling wave.

Let us select $c > c^*$, and let λ be the smallest positive solution to $\lambda c = -k(\lambda)$ (which exists by Proposition 2.3.7). We let $\overline{u}(t,x)$ be the function defined in Lemma 2.3.39 and $\underline{u}(t,x)$ be the function defined in equation (2.3.53).

For $M > 0$, we define the (convex) space

$$E_M := \left\{ v \in BUC([-M,+\infty),\mathbb{R}^d) \,|\, \underline{u}(0,x) \leq v(x) \leq \overline{u}(0,x) \right\},$$

and the operator $Q^M : E_M \to BUC([-M,+\infty),\mathbb{R}^d)$ by $Q^M(v)(x) = \tilde{v}(x+L)$, where $\tilde{v}$ is the solution at time $t = \frac{L}{c}$ to

$$\begin{cases} \tilde{v}_t - \mathcal{L}\tilde{v} = f(x,\tilde{v}), & x \in \mathbb{R}, \\ \tilde{v}(t=0,x) = \begin{cases} v(x) & \text{if } x \geq -M \\ \max\Big(\min\big(v(-M), \overline{u}(t,x)\big), \underline{u}(t,x)\Big) & \text{if } x \leq -M. \end{cases} \end{cases}$$

Then, it follows from Lemma 2.3.39 that $Q^M(v) \leq \overline{u}(t+\frac{L}{c}, x+L) = \overline{u}(t,x)$ for each $v \in E_M$, and from Lemma 2.3.40 and Theorem 2.3.35 (recall that $\underline{u}(t,x) \leq \eta$) that $Q^M(v) \geq \underline{u}$ for each $v \in E_M$. Thus E_M is left stable by Q^M. Moreover, by the regularizing properties of parabolic operators, Q^M is compact. Thus, the Schauder fixed-point Theorem implies the existence of a fixed-point $u^M \in E_M$ such that $Q^M(u^M) = u^M$. By

the classical elliptic regularity, there exists a sequence $M_n \to +\infty$ such that u^{M_n} converges locally uniformly to a solution u^∞ to $Q^\infty(u^\infty) = u^\infty$, and which belongs to

$$E_\infty := \left\{ v \in BUC((-\infty, +\infty), \mathbb{R}^d) \,|\, \underline{u}(0,x) \le v(x) \le \overline{u}(0,x) \right\}.$$

$u_c := u^\infty$ is the expected traveling wave.

If $c = c^*$ we can repeat the same procedure, but by replacing the above $\overline{u}(t,x)$ by $\overline{u}(t,x) := e^{-\lambda(x-c^*t)}\varphi_\lambda(x)$ for some $\lambda \in (0, \lambda^*)$ (where λ^* is the unique solution of $\lambda^* c^* + k(\lambda^*) = 0$) and $\underline{u}(t,x)$ by (2.3.54). This leads to the existence of the minimal speed traveling wave $u_{c^*}(t,x)$, which then satisfies

$$\underline{u}(t,x) \le u_{c^*}(t,x) \le \overline{u}(t,x).$$

The theorem is proved. □

Remark 2.3.42 (Exponential behavior of traveling waves)**.** Since the function $\omega e^{-\mu(x-ct)}\varphi_\mu(x)$ in the definition of $\xi(t,x)$ above is dominated by the term $e^{-\lambda(x-ct)}\varphi_\lambda(x)$ as $x \to +\infty$, we have $\overline{u}(t,x) \approx \underline{u}(t,x)$ for large x, in the sense that $\underline{u}_i/\overline{u}_i \to 1$ as $x \to +\infty$. Consequently, for each $c > c^*$, the traveling wave u_c which we constructed above satisfies $u_c(t,x) \approx \overline{u}(t,x)$ for large x. This implies, in particular,

$$0 < \liminf_{x\to+\infty} \min_{1\le i\le d} \frac{u_i(t,x)}{e^{-\lambda_c x}} \le \limsup_{x\to+\infty} \max_{1\le i\le d} \frac{u_i(t,x)}{e^{-\lambda_c x}} < +\infty,$$

where $\lambda_c > 0$ is the minimal root of $\lambda c + k(\lambda) = 0$. Thus the asymptotic profile of the traveling wave u_c along the leading edge is well approximated by that of $\overline{u}$, which is a solution of the linearized equation around $u = 0$. However, from the analogy of the scalar KPP type equations (see, e.g., [197]) it is likely that the minimal speed traveling wave u_{c^*} does not have the same asymptotics; more precisely we suspect that $u_{c^*}(t,x) \ne \mathcal{O}(e^{-\lambda_c x})$ as $x \to +\infty$ because of the degeneracy of the characteristic equation $\lambda c + k(\lambda) = 0$ for $c = c^*$.

2.3.3.5 Hair-Trigger effect

In this section 2.3.3.5 we prove the hair-trigger effect (Theorem 2.3.17) when the Dirichlet principal eigenvalue is negative, $\lambda_1^\infty < 0$.

Proof of Theorem 2.3.17. First we note that, by Proposition 2.3.36, we may assume without loss of generality that the constant function $x \mapsto \eta\mathbf{1}$ is a super-solution of the equation $-\mathcal{L}u \ge f^-(x,u)$. In the following proof we will work under this assumption.

Let $R > 0$ be sufficiently large, so that the Dirichlet principal eigenvalue λ_1^R is negative (recall the definition of $(\lambda_1^R, \varphi^R(x))$ in Definition 2.3.3) and let φ^R be the associated principal eigenfunction, normalized with $\|\varphi^R\|_{L^\infty(-R,R)^d} = 1$. Define

$$\kappa := \inf_{x\in(-R,R)} \min_{1\le i\le d} \frac{\varphi_i^R(x)}{\|\varphi(x)\|_\infty},$$

which is finite and positive by the elliptic strong maximum principle and Hopf's Lemma. Then, because of the differentiability of $u \mapsto f^-(x,u)$, there exists $\varepsilon_0 > 0$ such that for each $u \ge 0$ with $\|u\| \le \varepsilon_0$, we have

$$\|f^-(x,u) - A(x)u\|_\infty \le -\lambda_1^R \kappa \|u\|_\infty.$$

Reducing ε_0 if necessary so that $\varepsilon_0 \le \eta$ (where η is as in Definition 2.3.16), this shows that, for $0 < \varepsilon \le \varepsilon_0$, $\varepsilon\varphi^R(x)$ is a lower barrier for (2.3.9). Indeed,

$$\begin{aligned} -\mathcal{L}\varepsilon\varphi^R(x) &= A(x)\varepsilon\varphi^R(x) + \lambda_1^R \varepsilon\varphi^R(x) \le A(x)\varphi^R(x) + \lambda_1^R\kappa\|\varepsilon\varphi^R\|_\infty \\ &\le A(x)\varepsilon\varphi^R + f^-\big(x, \varepsilon\varphi^R(x)\big) - A(x)\varepsilon\varphi^R(x) = f^-\big(x, \varepsilon\varphi^R(x)\big). \end{aligned}$$

Let $\underline{u}^{R,\varepsilon}(t,x)$ be the solution to the initial-value problem

$$\begin{cases} \underline{u}_t^{R,\varepsilon} - \mathcal{L}\underline{u}^{R,\varepsilon} = f^-(x, \underline{u}^{R,\varepsilon}), \\ \underline{u}^{R,\varepsilon}(0,x) = \underline{u}_0^{R,\varepsilon}(x), \end{cases}$$

where $\underline{u}_0^{R,\varepsilon}(x) = \varepsilon\varphi^R(x)$ if $x \in (-R, R)$, and $\underline{u}_0^{R,\varepsilon}(x) = 0$ otherwise. It follows from the parabolic strong maximum principle that $\underline{u}^{R,\varepsilon}(t,x) > 0$ for all $t > 0$ and $x \in \mathbb{R}$, so that in particular $\underline{u}^{R,\varepsilon}(t, \pm R) > 0$. Then, we deduce from the parabolic comparison principle that

$$\underline{u}^{R,\varepsilon}(t,x) > \varepsilon\varphi^R(x), \text{ for all } t > 0 \text{ and } x \in \mathbb{R}. \tag{2.3.55}$$

Next, fix $\tau > 0$. Then it follows from (2.3.55) that $\underline{u}^{R,\varepsilon}(\tau, x) > \varepsilon\varphi^R(x) = \underline{u}_0^{R,\varepsilon}(x)$. We deduce from the parabolic comparison principle that

$$\underline{u}^{R,\varepsilon}(t+\tau, x) > \underline{u}^{R,\varepsilon}(t,x),$$

in other words, $\underline{u}^{R,\varepsilon}(t,x)$ is strictly increasing in time. Thus the limit

$$V^{R,\varepsilon} := \lim_{t\to+\infty} \underline{u}^{R,\varepsilon}(t,x)$$

exists and is an equilibrium of the equation involving f^-. It is not difficult to show, by using Serrin's sweeping method, that

$$V^{R,\varepsilon}(x) \geq \varepsilon_0\varphi^R(x).$$

Indeed, define

$$\varepsilon_1 := \sup\{\varepsilon' \geq 0 \,|\, \varepsilon'\varphi^R(x) \leq V^R(x)\}.$$

Then clearly $\varepsilon_1 \geq \varepsilon$ (by the parabolic comparison principle). If $\varepsilon_1 < \varepsilon_0$, then there exists a contact point x_0 such that $\varepsilon_1\varphi^R(x_0) \leq V^{R,\varepsilon}(x_0)$ and $\varepsilon_1\varphi_i^R(x_0) = V_i^{R,\varepsilon}(x_0)$ for some $i \in \{1, \dots, d\}$. We find a contradiction by applying the elliptic strong maximum principle in the i-th equation of the system.

Let u_0 be any nontrivial initial data and fix $t_0 > 0$ and $u(t,x)$ be the solution to (2.3.9) satisfying $u(0,x) = u_0(x)$. Then $u(t_0, x) > 0$ for all $x \in \mathbb{R}$. Therefore, for any $k \in \mathbb{Z}$, we can find $\varepsilon_k \in (0, \varepsilon_0]$ such that

$$u(t_0, x) \geq \varepsilon_k\varphi^R(x + kL).$$

Now we compare $u(t,x)$ and the solution $\underline{u}(t,x)$ with initial data $\underline{u}_0(x) := \varepsilon_k\varphi^R(x+kL)$ inside $(-kL - R, -kL + R)$ and 0 outside. Then by the result (4), we see that

$$\liminf_{t\to\infty} u(t,x) \geq \varepsilon_0\varphi^R(x+kL) \text{ in } (-kL - R, -kL + R)$$

for any $k \in \mathbb{Z}$. This implies that there exists $\delta > 0$ (independent of u_0) such that

$$\liminf_{t\to\infty} u(t,x) \geq \delta\mathbf{1}$$

for all $x \in \mathbb{R}$. □

2.3.4 Singular limits

2.3.4.1 Spreading speed for rapidly oscillating coefficients

In this section 2.3.4.1 we prove Theorem 2.3.11.

Formal computations to get the formula for the speed. Here we present the classical computations that allow to retrieve the correct result, though without the correct mathematical justification. The basic idea is to apply known results from homogenization theory to the eigenvalue problem involved in the definition of the minimal speed (2.3.19), i.e.

$$-L_\lambda^\varepsilon\varphi = -(\sigma^\varepsilon(x)\varphi_x)_x + (2\lambda\sigma^\varepsilon(x) - q^\varepsilon(x))\varphi_x + (\lambda\sigma_x^\varepsilon(x) + \lambda q^\varepsilon(x) - \lambda^2\sigma^\varepsilon(x) - A^\varepsilon(x))\varphi = k^\varepsilon(\lambda)\varphi. \tag{2.3.56}$$

We follow the approach of Bensoussan, Lions and Papanicolaou [45] and introduce an asymptotic expansion in ε:

$$\varphi(x) = \phi\left(x, \frac{x}{\varepsilon}\right) = \phi^0\left(x, \frac{x}{\varepsilon}\right) + \varepsilon\phi^1\left(x, \frac{x}{\varepsilon}\right) + \varepsilon^2\phi^2\left(x, \frac{x}{\varepsilon}\right) + \cdots \tag{2.3.57}$$

where the functions $\phi(x,y)$, $\phi^0(xy)$, $\phi^1(x,y)$ and $\phi^2(x,y)$ and are 1-periodic in y. We substitute (2.3.57) into (2.3.56) and rewrite it in terms of the variables x and y.

$$\begin{aligned}
&\varepsilon^{-2}\left[-(\sigma(y)\phi_y)_y\right]+\varepsilon^{-1}\left[-(\sigma(y)\phi_x)_y-(\sigma(y)\phi_y)_x+(2\lambda\sigma(y)-q(y))\phi_y+\lambda\sigma_y(y)\phi\right]\\
&\qquad+\varepsilon^{0}\left[-(\sigma(y)\phi_x)_x+(2\lambda\sigma(y)-q(y))\phi_x+(\lambda q(y)-\lambda^2\sigma(y)-A(y)-k^\varepsilon(\lambda)I)\phi\right]\\
&\qquad\quad=\varepsilon^{-2}\left[-(\sigma(y)\phi^0_y)_y\right]\\
&\qquad\qquad+\varepsilon^{-1}\left[-(\sigma(y)\phi^1_y)_y-(\sigma(y)\phi^0_y)_x-(\sigma(y)\phi^0_x)_y+(2\lambda\sigma(y)-q(y))\phi^0_y+\lambda\sigma_y(y)\phi^0\right]\\
&\qquad\qquad+\varepsilon^{0}\left[-(\sigma(y)\phi^2_y)_y-(\sigma(y)\phi^1_y)_x-(\sigma(y)\phi^1_x)_y+(2\lambda\sigma(y)-q(y))\phi^1_y+\lambda\sigma_y(y)\phi^1\right.\\
&\qquad\qquad\quad\left.-(\sigma(y)\phi^0_x)_x+(2\lambda\sigma(y)-q(y))\phi^0_x+(\lambda q(y)-\lambda^2\sigma(y)-A(y)-k^\varepsilon(\lambda)I)\phi^0\right]\\
&\qquad\qquad+\mathcal{O}(\varepsilon)\\
&\qquad\quad=0.
\end{aligned}\tag{2.3.58}$$

In (2.3.58), the coefficients of ε^{-2} and ε^{-1} must be zero. In particular, we have:

$$-(\sigma(y)\phi^0_y(x,y))_y=0,$$

which yields $\phi^0_y(x,y)=\sigma^{-1}(y)\tilde{\phi}^0(x)$, however since ϕ is 1-periodic in y we have $\int_0^1\phi^0_y(x,y)\mathrm{d}y=\int_0^1\sigma^{-1}(y)\mathrm{d}y\tilde{\phi}^0(x)=0$ and therefore $\tilde{\phi}^0(x)=0$ for all $x\in\mathbb{R}$. Thus, integrating again, we get:

$$\phi^0(x,y)=\varphi(x),\ \text{for all } x\in\mathbb{R}.\tag{2.3.59}$$

Next we focus on the coefficient in ε^{-1} term in (2.3.58). Using (2.3.59), we rewrite the ε^{-1} coefficient as:

$$-(\sigma(y)\phi^1_y)_y=\sigma_y(y)(\varphi_x(x)-\lambda\varphi(x)).$$

We remark that $\chi(y):=\int_0^y\left(\int_0^1\sigma^{-1}(z')\mathrm{d}z'\right)^{-1}\sigma^{-1}(z)-1\mathrm{d}z$ is a particular solution to:

$$-(\sigma(y)\chi_y(y))_y=-\sigma_y(y).$$

Therefore we can write:

$$\phi^1(x,y)=\chi(y)(\varphi_x(x)-\lambda\varphi(x))+\tilde{\phi}^1(x).\tag{2.3.60}$$

Last, integrating the coefficient in ε^0 in (2.3.58) gives us the homogenization limit for (2.3.56). We get:

$$\begin{aligned}
&0-\overline{\sigma\chi_y}(\varphi_{xx}-\lambda\varphi_x)-0+(2\lambda\overline{\sigma\chi_y}-\overline{q\chi_y})(\varphi_x-\lambda\varphi)+\lambda\overline{\sigma_y\chi}(\varphi_x-\lambda\varphi)\\
&-(\overline{\sigma}\varphi_x)_x+(2\lambda\overline{\sigma}-\overline{q})\varphi_x+(\lambda\overline{q}-\lambda^2\overline{\sigma}-\overline{A}-k^\varepsilon(\lambda)I)\varphi=0,
\end{aligned}$$

where $\overline{u}$ denotes the average of a function u over one period. Using the fact that

$$\chi_y(y)=\left(\int_0^1\sigma^{-1}(z)\mathrm{d}z\right)^{-1}\sigma^{-1}(y)-1$$

and integrating by parts, we get:

$$-\overline{\sigma^{-1}}^{-1}\varphi_{xx}+\left(2\lambda\overline{\sigma^{-1}}^{-1}-\overline{\sigma^{-1}}^{-1}\overline{\sigma^{-1}q}\right)\varphi_x+\left(\lambda\overline{\sigma^{-1}}^{-1}\overline{\sigma^{-1}q}-\lambda^2\overline{\sigma^{-1}}^{-1}-\overline{A}-k^0(\lambda)I\right)\varphi=0.$$

By the uniqueness of the periodic principal eigenvalue, φ is equal to the Perron-Frobenius eigenvector of the matrix $\lambda\overline{\sigma^{-1}}^{-1}\overline{\sigma^{-1}q}-\lambda^2\overline{\sigma^{-1}}^{-1}-\overline{A}-k^0(\lambda)I$. We retrieve (2.3.25) indeed.

Proof of Theorem 2.3.11. We divide the proof in two steps.

Step 1: We show that $k^\varepsilon(\lambda)$ converges locally uniformly to

$$k^0(\lambda):=\lambda_{PF}\left(\lambda\overline{q}^H-\lambda^2\overline{\sigma}^H-\overline{A}\right)$$

in $(0,+\infty)$, where we recall that $\overline{\sigma}^H:=\overline{\sigma^{-1}}^{-1}$, $\overline{q}^H:=\overline{\sigma^{-1}}^{-1}\overline{\sigma^{-1}q}$,

$$L^\varepsilon_\lambda\phi^\varepsilon_\lambda-A^\varepsilon(x)\phi^\varepsilon_\lambda=k^\varepsilon(\lambda)\phi^\varepsilon_\lambda\tag{2.3.61}$$

and $L^\varepsilon_\lambda \varphi := e^{\lambda x}\mathcal{L}^\varepsilon(e^{-\lambda x}\varphi)$ for all φ.

We argue by contradiction and assume that there exists a bounded interval $\left[\frac{1}{R}, R\right]$, $\delta > 0$ and $\varepsilon_n > 0$ such that $\sup_{\frac{1}{R}\le\lambda\le R} |k^{\varepsilon_n}(\lambda) - k^0(\lambda)| \ge \delta$. Since $\left[\frac{1}{R}, R\right]$ is bounded, for each $n \in \mathbb{N}$ there exists $\lambda^{\varepsilon_n} \in \left[\frac{1}{R}, R\right]$ such that $\sup_{\frac{1}{R}\le\lambda\le R} |k^{\varepsilon_n}(\lambda) - k^0(\lambda)| = |k^{\varepsilon_n}(\lambda^{\varepsilon_n}) - k^0(\lambda^{\varepsilon_n})|$. Up to the extraction of a subsequence we assume that $\lambda^\varepsilon \to \lambda_0 \in \left[\frac{1}{R}, R\right]$. For simplicity in the rest of the proof we will omit the subscript n and write ε instead of ε_n.

Let $\phi^\varepsilon := \phi^\varepsilon_{\lambda^\varepsilon}(x) > 0$ be a sequence of solutions to $L^\varepsilon_{\lambda^\varepsilon}\phi^\varepsilon = k^\varepsilon(\lambda)\phi^\varepsilon$ with $\varepsilon \to 0$ and $\lambda^\varepsilon \to \lambda_0$, which satisfies $\|\phi^\varepsilon\|^2_{L^2(0,1)^d} = \int_0^1 \sum_{i=1}^d (\phi^\varepsilon_i)^2(x)dx = 1$. Testing (2.3.61) at a maximum and minimum point of ϕ^ε, respectively, we find that

$$-(\lambda^\varepsilon)^2 - \sup_{\substack{1\le i\le d\\ x\in\mathbb{R}}} \sum_{j=1}^d a_{ij}(x) \le k^\varepsilon(\lambda^\varepsilon) \le -(\lambda^\varepsilon)^2 - \inf_{\substack{1\le i\le d\\ x\in\mathbb{R}}} \sum_{j=1}^d a_{ij}(x).$$

In particular, $k^\varepsilon(\lambda^\varepsilon)$ is uniformly bounded in n and we may extract a subsequence such that $k^\varepsilon(\lambda^\varepsilon) \to k^0$.

Let us show that ϕ^ε is uniformly bounded in $H^1(0,1)^d$. Indeed, we have

$$\begin{aligned}
\underline{\sigma}\|\phi^\varepsilon_x\|^2_{L^2(0,\varepsilon)^d} &\le \sum_{i=1}^d \int_0^\varepsilon \sigma_i\left(\varepsilon^{-1}x\right)(\partial_x\phi^\varepsilon_i(x))^2 \mathrm{d}x \\
&= \sum_{i=1}^d \int_0^\varepsilon q^\varepsilon_i(x)(\partial_x\phi^\varepsilon_i(x))\phi^\varepsilon_i(x)\mathrm{d}x + \int_0^\varepsilon (\lambda^\varepsilon q^\varepsilon_i(x) + (\lambda^\varepsilon)^2\sigma^\varepsilon_i(x) + k^\varepsilon(\lambda_\varepsilon))\phi^\varepsilon_i(x)^2\mathrm{d}x \\
&\quad + \sum_{i=1}^d\sum_{j=1}^d \int_0^\varepsilon a^\varepsilon_{ij}(x)\phi^\varepsilon_i(x)\phi^\varepsilon_j(x)\mathrm{d}x \\
&\le \|q\|_{L^\infty}\|\phi^\varepsilon_x\|_{L^2(0,\varepsilon)^d}\|\phi^\varepsilon\|_{L^2(0,\varepsilon)^d} \\
&\quad + C\left(\lambda^\varepsilon\|q\|_{L^\infty} + (\lambda^\varepsilon)^2\|\sigma\|_{L^\infty} + k^\varepsilon(\lambda^\varepsilon) + \|A\|_{L^\infty}\right)\|\phi^\varepsilon\|^2_{L^2(0,\varepsilon)^d},
\end{aligned}$$

and by periodicity

$$\lfloor\varepsilon^{-1}\rfloor\|\phi^\varepsilon_x\|_{L^2(0,\varepsilon)^d} \le \|\phi^\varepsilon_x\|_{L^2(0,1)^d} \le (\lfloor\varepsilon^{-1}\rfloor + 1)\|\phi^\varepsilon_x\|_{L^2(0,\varepsilon)^d},$$

where $\lfloor\varepsilon^{-1}\rfloor$ is the lower integer part of ε^{-1}, and therefore

$$\underline{\sigma}\|\phi^\varepsilon_x\|^2_{L^2(0,1)^d} \le \frac{\lfloor\varepsilon^{-1}\rfloor + 1}{\lfloor\varepsilon^{-1}\rfloor} C\|\phi^\varepsilon\|^2_{L^2(0,1)^d}$$

where C is independent of ε and $\|\phi^\varepsilon\|_{L^2(0,1)^d} = 1$. Therefore, (up to the extraction of a subsequence) there is $\phi \in H^1(0,1)^d$ such that $\phi^\varepsilon \to \phi$ *strongly* in $L^2(0,1)^d$ and $\phi^\varepsilon \rightharpoonup \phi$ *weakly* in $H^1(0,1)^d$. Next we remark that, rewriting (2.3.56) as:

$$-(\sigma^\varepsilon(\phi^\varepsilon_x - \lambda^\varepsilon\phi^\varepsilon))_x + (\lambda^\varepsilon\sigma^\varepsilon - q^\varepsilon)(\phi^\varepsilon_x - \lambda^\varepsilon\phi^\varepsilon) = A^\varepsilon\phi^\varepsilon + k^\varepsilon(\lambda^\varepsilon)\phi^\varepsilon, \tag{2.3.62}$$

the function $\xi^\varepsilon := \sigma^\varepsilon\phi^\varepsilon_x - \lambda^\varepsilon\phi^\varepsilon$ is uniformly bounded in $H^1(0,1)^d$. Indeed multiplying (2.3.62) by ξ^ε_x and integrating, we get

$$\begin{aligned}
&\int_0^\varepsilon \sigma^\varepsilon\left|\xi^\varepsilon_x\right|^2 = \int_0^\varepsilon \left[(q^\varepsilon - \lambda^\varepsilon\sigma^\varepsilon)(\phi^\varepsilon_x - \lambda^\varepsilon\phi^\varepsilon)\right]\cdot\xi^\varepsilon_x + \int_0^\varepsilon \left[\left(A^\varepsilon + k^\varepsilon(\lambda^\varepsilon)I\right)\phi^\varepsilon\right]\cdot\xi^\varepsilon_x \\
&\le \|q^\varepsilon - \lambda^\varepsilon\sigma^\varepsilon\|_{L^\infty(0,\varepsilon)^d}\|\phi^\varepsilon_x - \lambda^\varepsilon\phi^\varepsilon\|_{L^2(0,\varepsilon)^d}\|\xi^\varepsilon_x\|_{L^2(0,\varepsilon)^d} + \|A^\varepsilon + k^\varepsilon(\lambda^\varepsilon)I\|_{L^\infty(0,\varepsilon)^d}\|\phi^\varepsilon\|_{L^2(0,\varepsilon)^d}\|\xi_x\|_{L^2(0,\varepsilon)^d}.
\end{aligned}$$

By the periodicity of ξ^ε we easily conclude that ξ^ε_x is uniformly bounded in $L^2(0,1)^d$. Therefore (up to the extraction of a subsequence), there is $\xi \in H^1(0,1)^d$ such that $\xi^\varepsilon \to \xi$ strongly in $L^2(0,1)^d$ and $\xi^\varepsilon \rightharpoonup \xi$ weakly in $H^1(0,1)^d$. In particular $\phi^\varepsilon_x - \lambda^\varepsilon\phi^\varepsilon = \sigma^{-1}\xi^\varepsilon \rightharpoonup \overline{\sigma^{-1}}\xi$ in $L^2(0,1)^d$ weakly and therefore $\xi = \overline{\sigma}^H(\phi_x - \lambda_0\phi)$. This allows us to determine the limits of each term in (2.3.62) by using the convergence of ξ^ε:

$$\begin{aligned}
\sigma^\varepsilon(\phi^\varepsilon_x - \lambda^\varepsilon\phi^\varepsilon) = \xi^\varepsilon \to \xi = \overline{\sigma}^H(\phi_x - \lambda_0\phi), &\qquad \text{in } L^2(0,1)^d \text{ strong}, \\
(\sigma^\varepsilon(\phi^\varepsilon_x - \lambda^\varepsilon\phi^\varepsilon))_x \rightharpoonup (\overline{\sigma}^H(\phi_x - \lambda_0\phi))_x, &\qquad \text{in } H^1(0,1)^d \text{ weak}, \\
q^\varepsilon(\phi^\varepsilon_x - \lambda^\varepsilon\phi^\varepsilon) = (\sigma^\varepsilon)^{-1}q^\varepsilon\xi^\varepsilon \rightharpoonup \overline{\sigma^{-1}q}\xi = \overline{q}^H(\phi_x - \lambda_0\phi), &\qquad \text{in } L^2(0,1)^d \text{ weak},
\end{aligned}$$

and (2.3.62) becomes:

$$-\overline{\sigma}^H((\phi_x-\lambda_0\phi))_x+(\lambda_0\overline{\sigma}^H-\overline{q}^H)(\phi_x-\lambda_0\phi)=\overline{A}\phi+k^0\phi.$$

Note that because of the periodicity of ϕ^ε, the convergence in $L^2(0,1)^d$ or $H^1(0,1)^d$, weak or strong, implies the same convergence for the L^2 or H^1 local uniform topology on $\mathbb{R}$. Thus ϕ satisfies (2.3.56) with σ^ε replaced by $\overline{\sigma}^H$ and q^ε replaced by $\overline{q}^H$. By the uniqueness of the principal eigenvector, we find that ϕ is a positive constant vector satisfying:

$$(-\lambda_0^2\overline{\sigma}^H+\lambda_0\overline{q}^H-\overline{A})\phi=k^0\phi,$$

therefore $k^0=\lambda_{PF}(-\lambda_0^2\overline{\sigma}^H+\lambda_0\overline{q}^H-\overline{A})=k^0(\lambda_0)$. This is a contradiction.

Step 2: We show that the minimum of $\frac{k^\varepsilon(\lambda)}{\lambda}$ converges to the one of $\frac{k^0(\lambda)}{\lambda}$.

It is well-known, in the scalar matrix case, that $\lambda\mapsto\lambda_{PF}\big(\lambda^2\langle\sigma\rangle_A+\langle A\rangle_A\big)=k^0(\lambda)$ is a strictly concave function, and that $\frac{-k^0(\lambda)}{\lambda}$ has a unique minimum for $\lambda>0$. We have extended this property to the case of systems in Proposition 2.3.7. From the local uniform convergence of $k^\varepsilon(\lambda)$ to $k^0(\lambda)$, we conclude the local uniform convergence of $-\frac{k^\varepsilon(\lambda)}{\lambda}$ to $\frac{k^0(\lambda)}{\lambda}$ and $\lambda_\varepsilon^*:=\arg\min\left(-\frac{k^\varepsilon(\lambda)}{\lambda}\right)$ to $\lambda_0^*:=\arg\min\left(-\frac{k^0(\lambda)}{\lambda}\right)$. This finishes the proof of Theorem 2.3.11. □

2.3.4.2 Strong coupling

In this section 2.3.4.2 we study the singular limit of the following system, which is a modified version of system (2.3.2) with strong coupling

$$\begin{cases}u_t=(\sigma_u(x)u_x)_x+\big(r_u(x)-\kappa_u(x)(u+v)\big)u-\dfrac{1}{\varepsilon}\big(p(x)u-\big(1-p(x)\big)v\big),\\ v_t=(\sigma_v(x)v_x)_x+\big(r_v(x)-\kappa_v(x)(u+v)\big)v+\dfrac{1}{\varepsilon}\big(p(x)u-\big(1-p(x)\big)v\big),\end{cases}\tag{2.3.63}$$

where $p(x)\in(0,1)$ is smooth (at leat C^2) and $\varepsilon>0$, with a particular interest in the limit $\varepsilon\to0$. A formal way to compute the limit is to consider asymptotic expansions of u and v

$$\begin{aligned}u(t,x)&=u^0(t,x)+\varepsilon u^1(t,x)+\varepsilon^2u^2(t,x)+\cdots,\\ v(t,x)&=v^0(t,x)+\varepsilon v^1(t,x)+\varepsilon^2v^2(t,x)+\cdots,\end{aligned}$$

and this method has the advantage of allowing an arbitrary degree of precision in the asymptotic behavior of the solution when $\varepsilon\to0$. However, since we are presently concerned with the zero-order term only, we present an easier way to compute the limit. We let $P(t,x):=p(x)u(t,x)-\big(1-p(x)\big)v(t,x)$ and remark that, for a limit to exist, one must have $P(t,x)\to0$ as $\varepsilon\to0$. Therefore the limit (u^0,v^0) satisfies

$$p(x)u^0=\big(1-p(x)\big)v^0$$

and the sum $S:=u^0+v^0$ is the solution of a closed scalar reaction-diffusion equation which can be determined explicitly by the relations $u^0=\big(1-p(x)\big)S$, $v^0=p(x)S$,

$$\begin{aligned}u_x&=-p_xS+(1-p)S_x,\\ v_x&=p_xS+pS_x,\end{aligned}$$

and therefore

$$\begin{aligned}S_t&=\big((1-p(x))\sigma_u(x)+p(x)\sigma_v(x)S_x\big)_x+((\sigma_v(x)-\sigma_u(x))p_xS)_x+\big(r(x)-\kappa(x)S\big)S\\ &=\big(\sigma(x)S_x\big)_x+q(x)S_x+\big(r(x)+q_x(x)-\kappa(x)S\big)S,\end{aligned}$$

where

$$\begin{aligned}\sigma(x)&=(1-p(x))\sigma_u(x)+p(x)\sigma_v(x),\\ r(x)&=(1-p(x))r_u(x)+p(x)r_v(x),\\ \kappa(x)&=(1-p(x))\kappa_u(x)+p(x)\kappa_v(x),\\ q(x)&=(\sigma_v(x)-\sigma_u(x))p_x.\end{aligned}$$

In particular, $\sigma_u(x)$, $\sigma_v(x)$ and $p(x)$ can be chosen so that the sign of $\sigma_v(x)-\sigma_u(x)$ is the same as the sign of $p_x(x)$, in which case $q(x)>0$ and

$$\int_0^L \frac{q(x)}{2\sigma(x)}\mathrm{d}x>0.$$

In this case it is known (see (2.3.75) in Appendix 2.3.6) that the leftward and rightward speeds are different. Since there is a strict sign between c^*_{left} and c^*_{right}, the same holds for the original system (2.3.63) with $\varepsilon>0$ sufficiently small.

For the sake of concision, we will not make this entire argument rigorous but focus on the limit of the principal eigenproblem, which implies the convergence of the minimal speed.

Proposition 2.3.43. *Let $\lambda\in\mathbb{R}$ and $\varepsilon>0$ be given. Denote $k^\varepsilon(\lambda)$, $\varphi^\varepsilon_\lambda(x)$, $\psi^\varepsilon_\lambda(x)$ the principal eigenpair associated with the problem*

$$\begin{cases} -\big(\sigma_u(x)(\varphi^\varepsilon_\lambda)_x\big)_x+2\lambda\sigma_u(x)(\varphi^\varepsilon_\lambda)_x+\big(\lambda(\sigma_u)_x(x)-\lambda^2\sigma_u(x)-r_u(x)\big)\varphi^\varepsilon_\lambda+\dfrac{1}{\varepsilon}\big(p(x)\varphi^\varepsilon_\lambda-\big(1-p(x)\big)\psi^\varepsilon_\lambda\big)=k^\varepsilon(\lambda)\varphi^\varepsilon_\lambda,\\ -\big(\sigma_v(x)(\psi^\varepsilon_\lambda)_x\big)_x+2\lambda\sigma_v(x)(\psi^\varepsilon_\lambda)_x+\big(\lambda(\sigma_v)_x(x)-\lambda^2\sigma_v(x)-r_v(x)\big)\psi^\varepsilon_\lambda-\dfrac{1}{\varepsilon}\big(p(x)\varphi^\varepsilon_\lambda-\big(1-p(x)\big)\psi^\varepsilon_\lambda\big)=k^\varepsilon(\lambda)\psi^\varepsilon_\lambda, \end{cases} \tag{2.3.64}$$

with L-periodic boundary conditions and $\|\varphi^\varepsilon_\lambda\|_{L^2_{per}}=\|\psi^\varepsilon_\lambda\|_{L^2_{per}}=1$. Then, as $\varepsilon\to0$, the function $k^\varepsilon(\lambda)$ converges locally uniformly to $k^0(\lambda)$, the principal eigenvalue of the problem

$$-\big(\sigma(x)(\varphi)_x\big)_x+\big(2\lambda\sigma(x)-q(x)\big)\varphi_x+\big(\lambda\sigma_x(x)+\lambda q(x)-\lambda^2\sigma(x)-r(x)-q_x(x)\big)\varphi=k^0(\lambda)\varphi,$$

for a L-periodic positive scalar function φ, where

$$\sigma(x)=(1-p(x))\sigma_u(x)+p(x)\sigma_v(x),\quad r(x)=(1-p(x))r_u(x)+p(x)r_v(x),\quad q(x)=(\sigma_v(x)-\sigma_u(x))p_x.$$

Proof. We argue by contradiction and assume that there exists a bounded interval $[-R,R]$, $\delta>0$ and $\varepsilon_n>0$ such that $\sup_{-R\le\lambda\le R}|k^{\varepsilon_n}(\lambda)-k^0(\lambda)|\ge\delta$. Since $[-R,R]$ is bounded, for each $n\in\mathbb{N}$ there exists $\lambda^{\varepsilon_n}\in[-R,R]$ such that $\sup_{-R\le\lambda\le R}|k^{\varepsilon_n}(\lambda)-k^0(\lambda)|=|k^{\varepsilon_n}(\lambda^{\varepsilon_n})-k^0(\lambda^{\varepsilon_n})|$. Up to the extraction of a subsequence we assume that $\lambda^\varepsilon\to\lambda_0\in[-R,R]$. For simplicity in the rest of the proof we will omit the subscript n and write ε instead of ε_n. We will also omit the subscripts and superscripts, when there is no ambiguity, for the solutions (φ,ψ) of (2.3.64).

Let us show that φ and ψ are bounded in H^1_{per} when $\varepsilon\to0$. Indeed, multiplying the first line of (2.3.64) by $p(x)\varphi(x)$, we get

$$\begin{aligned}\int\sigma_u(x)p(x)\varphi_x^2+\int\sigma_u(x)p_x(x)\varphi_x\varphi+2\lambda\int\sigma_u(x)p(x)\varphi\varphi_x=&\int\big(-\lambda(\sigma_u)_x(x)+\lambda^2\sigma_u(x)+r_u(x)+k^\varepsilon(\lambda)\big)p(x)\varphi^2\\&-\frac{1}{\varepsilon}\left(\int p(x)^2\varphi^2-\int p(x)\big(1-p(x)\big)\varphi\psi\right),\end{aligned}$$

and multiplying the second line by $\big(1-p(x)\big)\psi(x)$ we get

$$\begin{aligned}&\int\sigma_v(x)\big(1-p(x)\big)\psi_x^2-\int\sigma_v(x)p_x(x)\psi\psi_x+2\lambda\int\sigma_v(x)\big(1-p(x)\big)\psi\psi_x\\&\qquad=\int\big(-\lambda(\sigma_v)_x(x)+\lambda^2\sigma_v(x)+r_v(x)+k^\varepsilon(\lambda)\big)\big(1-p(x)\big)\psi^2\\&\qquad\qquad+\frac{1}{\varepsilon}\left(\int p(x)\big(1-p(x)\big)\varphi\psi-\int\big(1-p(x)\big)^2\psi^2\right),\end{aligned}$$

and finally the sum of the two equations above yields

$$\int p(x)\varphi_x^2+\int\big(1-p(x)\big)\psi_x^2\le C_1\left(\|\varphi\|^2_{L^2_{per}}+\|\psi\|^2_{L^2_{per}}\right),$$

where C_1 is independent of ε. Since $p(x)$ and $(1-p(x))$ are bounded below, we conclude that φ and ψ are indeed bounded in H^1_{per} uniformly when $\varepsilon\to0$.

Therefore, up to the extraction of a subsequence, φ and ψ converge respectively to $\bar\varphi$ and $\bar\psi$ as $\varepsilon \to 0$, weakly in H^1_{per} and strongly in L^2_{per}. Let $f \in C^2_{per}$ be a smooth test function, then multiplying the first line of (2.3.64) by f leads to

$$\begin{aligned}\int f(x)\big(p(x)\psi - \big(1-p(x)\big)\psi\big) = \varepsilon\Big[&- \int \sigma_u(x)\varphi_x f_x(x) - 2\lambda\int \varphi_x f(x) \\ &+ \int \big(-\lambda(\sigma_u)_x(x) + \lambda^2\sigma_u(x) + r_u(x) + k^\varepsilon(\lambda)\big)\varphi f(x)\Big] \\ &\xrightarrow[\varepsilon\to 0]{} 0,\end{aligned}$$

which shows that, since $f(x)$ is arbitrary,

$$p(x)\bar\varphi(x) = \big(1-p(x)\big)\bar\psi(x).$$

By elementary computations, we find that $S(x) := \varphi(x) + \psi(x)$ converges weakly to a function $\bar S \in H^1_{per}$ which solves

$$-\big(\sigma(x)(\bar S)_x\big)_x + \big(2\lambda_0 - q(x)\big)(\bar S)_x + \big(\lambda_0\sigma_x(x) + \lambda_0 q(x) - \lambda_0^2\sigma(x) - r(x) - q_x(x)\big)\bar S = \bar k\bar S,$$

where $\bar k = \lim k^\varepsilon(\lambda)$ and $\sigma(x)$, $q(x)$, $r(x)$ are as in the statement of the proposition. Note that $\bar S$ is non-trivial because $\|\bar\varphi\|_{L^2_{per}} = \|\bar\psi\|_{L^2_{per}} = 1$, and is non-negative as a consequence of Morrey's inequality. Therefore $\bar k = k^0(\lambda_0)$, which is a contradiction. Proposition 2.3.43 is proved. □

Remark 2.3.44. In particular, with the notations of Proposition 2.3.43, assume that

$$0 > \lambda_1^\infty = \max_{\lambda\in\mathbb{R}} k(\lambda).$$

Then the left- and rightward propagation speeds for the limit problem and the corresponding notions for the approximating problem,

$$c^0_{\text{left}} := \inf_{\lambda>0}\frac{-k^0(-\lambda)}{\lambda}, \qquad c^0_{\text{right}} := \inf_{\lambda>0}\frac{-k^0(\lambda)}{\lambda},$$
$$c^\varepsilon_{\text{left}} := \inf_{\lambda>0}\frac{-k^\varepsilon(-\lambda)}{\lambda}, \qquad c^\varepsilon_{\text{right}} := \inf_{\lambda>0}\frac{-k^\varepsilon(\lambda)}{\lambda},$$

are well-defined for $\varepsilon > 0$ and

$$\lim_{\varepsilon\to 0} c^\varepsilon_{\text{left}} = c^0_{\text{left}}, \qquad \lim_{\varepsilon\to 0} c^\varepsilon_{\text{right}} = c^0_{\text{right}}.$$

In particular, under the framework described at the beginning of the section 2.3.4.2 (see also the Appendix 2.3.6), it is not difficult achieve $c^0_{\text{left}} \neq c^0_{\text{right}}$ by a careful selection of the coefficients of the problem.

2.3.5 Long-time behavior of the original model

In this section 2.3.5 we focus on the original problem (2.3.2). In section 2.3.5.1 we study a related ODE problem and show local asymptotic stability and the uniqueness of stationary solutions. We then extend those results to problems with homogeneous coefficients, in section 2.3.5.2, provided Assumption 2.3.29 is satisfied. In the same section we show Theorem 2.3.33. Finally we prove Theorem 2.3.34 in section 2.3.5.3.

2.3.5.1 A complete study of the ODE problem

Let us look into the stationary states for the ODE system (2.3.33):

$$\begin{cases} u_t = (r_u - \kappa_u(u+v))u + \mu_v v - \mu_u u =: f^u(u,v), \\ v_t = (r_v - \kappa_v(u+v))v + \mu_u u - \mu_v v =: f^v(u,v). \end{cases}$$

In this section 2.3.5.1 we work under the assumption that every coefficient in the above equation is positive. Surprisingly, it is possible to show that the solution converges to a unique equilibrium in all cases. To achieve

this goal, two different methods are to be employed, depending on the sign of $r_u - \mu_u$ and $r_v - \mu_v$. If one is positive, the system admits a Lyapunov functional, which will be our main tool to study the long-time behavior of the system; whereas in the case where both are nonpositive, the system is ultimately cooperative and the long-time behavior can be determined by monotonicity arguments (here the method of super- and subsolutions). Note that both arguments were inspired by the paper of Cantrell, Cosner and Yu [100]. We still include the proofs for the sake of completeness.

Lemma 2.3.45 (Stability of stationary states)**.** *Let $r_u, r_v \in \mathbb{R}$, $\kappa_u > 0$, $\kappa_v > 0$, and $\mu > 0$. Let $(u^* \geq 0, v^* \geq 0)$ be a nontrivial stationary state for* (2.3.33)*. Then (u^*, v^*) is locally asymptotically stable.*

More precisely, the Jacobian matrix of the nonlinearity at (u^*, v^*) is

$$D_{(u^*,v^*)}f = \begin{pmatrix} r_u - \mu_u - \kappa_u(2u+v) & \mu_v - \kappa_u u \\ \mu_u - \kappa_v v & r_v - \mu_v - \kappa_v(u+2v) \end{pmatrix} =: \begin{pmatrix} a & b \\ c & d \end{pmatrix} \tag{2.3.65}$$

and we have $a = -\left(\kappa_u u^* + \mu_v \frac{v^*}{u^*}\right) < 0$, $d = -\left(\kappa_v v^* + \mu_u \frac{u^*}{v^*}\right) < 0$ and

$$\begin{aligned} \operatorname{tr}(D_{(u^*,v^*)}f) &= a + d < 0, \\ \det(D_{(u^*,v^*)}f) &= ad - bc > 0. \end{aligned}$$

Proof. We divide the proof in three steps.

Step 1: We show that $u^* > 0$ and $v^* > 0$.

Assume by contradiction that $u^* = 0$. Then, by our assumption that (u^*, v^*) is non-trivial, we have $v^* > 0$. Evaluating the first line of (2.3.33), we find $0 = \mu v^* > 0$, which is a contradiction.

The assumption that $v^* > 0$ leads to a similar contradiction. We conclude that $u^* > 0$ and $v^* > 0$.

Before resuming the proof, let us remark the following formula, which is a consequence of (2.3.33):

$$\begin{cases} r_u - \mu_u - \kappa_u(u^* + v^*) = -\mu_v \dfrac{v^*}{u^*}, \\ r_v - \mu_v - \kappa_v(u^* + v^*) = -\mu_u \dfrac{u^*}{v^*}. \end{cases}$$

Step 2: We show that $\operatorname{tr}(D_{(u^*,v^*)}f) < 0$.

Using the fact that (u^*, v^*) is a stationary state for (2.3.33), we have

$$\operatorname{tr}(D_{(u^*,v^*)}f) = r_u - \mu_u - \kappa_u(2u^* + v^*) + r_v - \mu_v - \kappa_v(u^* + 2v^*) = -\mu_v \frac{v^*}{u^*} - \mu_u \frac{u^*}{v^*} - \kappa_u u^* - \kappa_v v^* < 0.$$

Step 3: We show that $\det(D_{(u^*,v^*)}f) > 0$.

We compute:

$$\begin{aligned} \det(D_{(u^*,v^*)}f) &= (r_u - \mu_u - \kappa_u(2u^* + v^*))(r_v - \mu_v - \kappa_v(u^* + 2v^*)) - (\mu_v - \kappa_u u^*)(\mu_u - \kappa_v v^*) \\ &= \left(\mu_v \frac{v^*}{u^*} + \kappa_u u^*\right)\left(\mu_u \frac{u^*}{v^*} + \kappa_v v^*\right) - (\mu_v - \kappa_u u^*)(\mu_u - \kappa_v v^*) \\ &= \mu_u\mu_v + \mu_v\kappa_v \frac{(v^*)^2}{u^*} + \mu_u\kappa_u \frac{(u^*)^2}{v^*} + \kappa_u\kappa_v u^* v^* - \mu_u\mu_v + \mu_v\kappa_v v^* + \mu_u\kappa_u u^* - \kappa_u\kappa_v u^* v^* \\ &= \mu_v\kappa_v \frac{(v^*)^2}{u^*} + \mu_u\kappa_u \frac{(u^*)^2}{v^*} + \mu_v\kappa_u u^* + \mu_u\kappa_v v^* > 0. \end{aligned}$$

This finishes the proof of Lemma 2.3.45 □

Lemma 2.3.46 (Existence and uniqueness of stationary state)**.** *Let $r_u, r_v \in \mathbb{R}$, $\kappa_u > 0$, $\kappa_v > 0$, and $\mu_u, \mu_v > 0$. Then, there exists at most one nonnegative nontrivial stationary state for* (2.3.33)*. If Assumption 2.3.29 is met, then there is a positive stationary state (u^*, v^*), which satisfies:*

(i) if $r_u - \mu_u > 0$ (resp. $r_v - \mu_v > 0$), then

$$\begin{aligned} \frac{\min(\mu_v, r_u - \mu_u)}{\kappa_u} \leq u^* \leq \frac{\max(\mu_v, r_u - \mu_u)}{\kappa_u} \\ \textit{resp. } \frac{\min(\mu_u, r_v - \mu_v)}{\kappa_v} \leq v^* \leq \frac{\max(\mu_u, r_v - \mu_v)}{\kappa_v}. \end{aligned}$$

Moreover, equality happens in the above inequalities if, and only if $\mu_v = r_u - \mu_u$ (resp. $r_v - \mu_v = \mu_u$).

(ii) if $r_u - \mu_u \le 0$ *(resp.* $r_v - \mu_v \le 0$*), then* $0 < u^* < \frac{\mu_v}{\kappa_u}$ *(resp.* $0 < v^* < \frac{\mu_u}{\kappa_v}$*)*

Proof. Let (u, v) be a nonnegative nontrivial stationary state for (2.3.33). Then (u, v) satisfies

$$\begin{cases} u(r_u - \kappa_u(u+v)) + \mu_v v - \mu_u u = 0, \\ v(r_v - \kappa_v(u+v)) + \mu_u u - \mu_v v = 0. \end{cases}$$

As remarked in the proof of Lemma 2.3.45, since (u, v) is nonegative and nontrivial, we have in fact $u > 0$ and $v > 0$. Let us change the variables:

$$\begin{cases} S = u + v, \\ Q = \dfrac{u}{v}. \end{cases}$$

Then the new variables (S, Q) satisfy the system:

$$\begin{aligned} &\begin{cases} Q(r_u - \kappa_u S) + \mu_v - \mu_u Q = 0, \\ r_v - \kappa_v S + \mu_u Q - \mu_v = 0, \end{cases} \\ \Leftrightarrow &\begin{cases} Q(r_u - \kappa_u S) + \mu_v - \mu_u Q = 0, \\ S = \dfrac{r_v + \mu_u Q - \mu_v}{\kappa_v}, \end{cases} \\ \Leftrightarrow &\begin{cases} -\mu_u \dfrac{\kappa_u}{\kappa_v} Q^2 + \left(r_u - \mu_u \dfrac{\kappa_u}{\kappa_v}(r_v - \mu_v) \right) Q + \mu_v = 0, \\ S = \dfrac{r_v + \mu_u Q - \mu_v}{\kappa_v}. \end{cases} \end{aligned}$$

The first line of the latter system has a unique positive solution:

$$Q = \frac{\kappa_v}{2\mu_u \kappa_u} \left(r_u - \mu_u - \frac{\kappa_u}{\kappa_v}(r_v - \mu_v) + \sqrt{\left(r_u - \mu_u - \frac{\kappa_u}{\kappa_v}(r_v - \mu_v) \right)^2 + 4\frac{\kappa_u}{\kappa_v}\mu_u \mu_v} \right).$$

Since the change of variables is reversible, there cannot exist two nonnegative nontrivial solutions for the original system.

The proof of existence of a stationary solution is quite straightforward by using a global bifurcation argument; we refer to an earlier work [P3, Theorem 2.3] for a proof in a periodic setting.

Next we focus on the estimates on nontrivial stationary states. Since the statement is symmetric with respect to the variable u or v, we only prove the result for u^*. Assume first that $r_u - \mu_u > \mu_v > 0$. Then u^* satisfies:

$$0 = u^*(r_u - \mu_u - \kappa_u u^*) + v^*(\mu_v - \kappa_u u^*). \tag{2.3.66}$$

If $u^* < \frac{\mu_v}{\kappa_u}$, then both terms in the right-hand side of (2.3.66) are positive, which is a contradiction. Similarly, if $u^* > \frac{r_u - \mu_u}{\kappa_u}$, then both terms are negative, which is also a contradiction. We conclude that $\frac{\mu_v}{\kappa_u} \le u^* \le \frac{r_u - \mu_u}{\kappa_u}$. Finally, if equality is achieved in the latter inequality, then one of the terms in (2.3.66) is 0 and the other is positive, which is a contradiction. Thus

$$\frac{\mu_v}{\kappa_u} < u^* < \frac{r_u - \mu_u}{\kappa_u}.$$

In the case $0 < r_u - \mu_u < \mu_v$, a similar argument shows that

$$\frac{r_u - \mu_u}{\kappa_u} < u^* < \frac{\mu_v}{\kappa_u}.$$

Finally, if $r_u - \mu_u = \mu_v$, then both terms in the right-hand side of (2.3.66) have the same sign independently of u^*, hence the only possibility is

$$u^* = \frac{r_u - \mu_u}{\kappa_u} = \frac{\mu_v}{\kappa_u}.$$

Statement (i) is proved. To show Statement (ii), since $r_u - \mu_u \le 0$, we simply rewrite (2.3.66) as:

$$u^* = \frac{\mu_v}{\kappa_u} + \frac{u^*}{\kappa_u v^*}(r_u - \mu_u - \kappa_u u^*) < \frac{\mu_v}{\kappa_u}.$$

Lemma 2.3.46 is proved. □

Next we study the stability of the trivial steady state:

Lemma 2.3.47 (Stability of 0)**.** *Let $r_u, r_v \in \mathbb{R}$ and $\mu_u > 0$, $\mu_v > 0$. Define*

$$A := \begin{pmatrix} r_u - \mu_u & \mu_v \\ \mu_u & r_v - \mu_v \end{pmatrix}.$$

Then, the matrix A has two simple real eigenvalues:

$$\lambda_1 = \frac{r_u - \mu_u + r_v - \mu_v + \sqrt{(r_u - \mu_u - r_v + \mu_v)^2 + 4\mu_u\mu_v}}{2},$$
$$\lambda_2 = \frac{r_u - \mu_u + r_v - \mu_v - \sqrt{(r_u - \mu_u - r_v + \mu_v)^2 + 4\mu_u\mu_v}}{2}.$$

Moreover the eigenvector associated with λ_1 lies in the first quadrant:

$$\varphi_1 := \begin{pmatrix} r_u - \mu_u - (r_v - \mu_v) + \sqrt{(r_u - \mu_u - (r_v - \mu_v))^2 + 4\mu_u\mu_v} \\ 2\mu_u \end{pmatrix}.$$

Finally, if $\frac{\mu_v}{\mu_u+\mu_v} r_u + \frac{\mu_u}{\mu_u+\mu_v} r_v > 0$, then $\lambda_1 > 0$.

Proof. The characteristic polynomial associated with A is:

$$\chi_A(X) = X^2 - (r_u - \mu_u + r_v - \mu_v)X + r_u r_v - \mu_u r_v - \mu_v r_u.$$

The roots of this second-order polynomial can be computed thanks to its discriminant Δ:

$$\begin{aligned}
\Delta &= (r_u + r_v - \mu_u - \mu_v)^2 - 4(r_u r_v - \mu_v r_u - \mu_u r_v) \\
&= r_u^2 + r_v^2 + \mu_u^2 + \mu_v^2 + 2r_u r_v - 2r_u\mu_u - 2r_u\mu_v - 2r_v\mu_u - 2r_v\mu_v + 2\mu_u\mu_v \\
&\quad - 4r_u r_v + 4\mu_v r_u + 4\mu_u r_v \\
&= r_u^2 + r_v^2 + \mu_u^2 + \mu_v^2 - 2r_u r_v - 2r_u\mu_u + 2r_u\mu_v + 2r_v\mu_u - 2r_v\mu_v + 2\mu_u\mu_v \\
&= \big(r_u - \mu_u - (r_v - \mu_v)\big)^2 + 4\mu_u\mu_v.
\end{aligned}$$

In particular, $\Delta > 0$ and thus χ_A always has two real roots:

$$\lambda_1 := \frac{r_u - \mu_u + r_v - \mu_v + \sqrt{\big(r_u - \mu_u - (r_v - \mu_v)\big)^2 + 4\mu_u\mu_v}}{2},$$
$$\lambda_2 := \frac{r_u - \mu_u + r_v - \mu_v - \sqrt{\big(r_u - \mu_u - (r_v - \mu_v)\big)^2 + 4\mu_u\mu_v}}{2}.$$

The eigenvector associated with λ_1 can be easily computed and is always positive:

$$\varphi_1 := \begin{pmatrix} r_u - \mu_u - (r_v - \mu_v) + \sqrt{(r_u - \mu_u - (r_v - \mu_v))^2 + 4\mu_u\mu_v} \\ 2\mu_u \end{pmatrix}.$$

It follows easily from the Perron-Frobenius Theorem that φ_1 is the unique positive eigenvector of the matrix A.

Next we investigate the sign of λ_1. To this end we introduce for $\alpha \geq 0$:

$$\lambda_1(\alpha) := \frac{r_u - \alpha\mu_u + r_v - \alpha\mu_v + \sqrt{\big(r_u - \alpha\mu_u - (r_v - \alpha\mu_v)\big)^2 + 4\alpha^2\mu_u\mu_v}}{2}.$$

Notice that $\lambda_1 = \lambda_1(\alpha = 1)$, the mapping $\alpha \mapsto \lambda_1(\alpha)$ is convex (as we will show below) and $\lambda_1(0) = \max(r_u, r_v) > 0$. To catch the behavior of the function as $\alpha \to +\infty$, we rewrite $\lambda_1(\alpha)$ as

$$\begin{aligned}
\lambda_1(\alpha) &= \frac{1}{2}\Big(r_u - \alpha\mu_u + r_v - \alpha\mu_v \\
&\quad + \sqrt{r_u^2 + r_v^2 - 2r_u r_v + 2\alpha(-r_u\mu_r + r_u\mu_v + r_v\mu_u - r_v\mu_v) + \alpha^2(\mu_u^2 + \mu_v^2 + 2\mu_u\mu_v)}\Big) \\
&= \frac{1}{2}\left(r_u - \alpha\mu_u + r_v - \alpha\mu_v + \sqrt{(r_u - r_v)^2 + 2\alpha(r_v - r_u)(\mu_u - \mu_v) + \alpha^2(\mu_u + \mu_v)^2}\right) \\
&= \frac{1}{2}\left(r_u + r_v - \alpha(\mu_u + \mu_v) + \alpha(\mu_u + \mu_v)\sqrt{1 + \frac{2(r_v - r_u)(\mu_u - \mu_v)}{\alpha(\mu_u + \mu_v)^2} + o_{\alpha\to+\infty}\left(\frac{1}{\alpha}\right)}\right) \\
&= \frac{1}{2}\left(r_u + r_v + \frac{(r_v - r_u)(\mu_u - \mu_v)}{\mu_u + \mu_v} + o_{\alpha\to+\infty}(1)\right) \\
&= \frac{\mu_v}{\mu_u + \mu_v} r_u + \frac{\mu_u}{\mu_u + \mu_v} r_v + o_{\alpha\to+\infty}(1).
\end{aligned}$$

Thus, $\lambda_1(\alpha) > 0$ for all $\alpha > 0$, and in particular $\lambda_1 = \lambda_1(\alpha = 1) > 0$.

To show the convexity of $\alpha \mapsto \lambda_1(\alpha)$, we simply notice that

$$\frac{\mathrm{d}^2}{\mathrm{d}x^2}\lambda_1(\alpha) = \frac{4A^2\alpha^2 + 4AB\alpha + 8AC - B^2}{16\left(A\alpha^2 + B\alpha + C\right)^{\frac{3}{2}}},$$

with

$$\begin{aligned}
A &:= (\mu_u + \mu_v)^2, \\
B &:= 2(r_v - r_u)(\mu_u - \mu_v), \\
C &:= (r_u - r_v)^2.
\end{aligned}$$

Hence the roots of $\dfrac{\mathrm{d}^2}{\mathrm{d}x^2}\lambda_1(\alpha)$ are determined by the quantity

$$\Delta := 32A^2B^2 - 128A^3C = 32A^2(B^2 - 4AC).$$

Since:

$$\begin{aligned}
B^2 - 4AC &= 4(r_u - r_v)^2(\mu_u - \mu_v)^2 - 4(r_u - r_v)(\mu_u + \mu_v) \\
&= 4(r_u - r_v)^2\left((\mu_u - \mu_v)^2 - (\mu_u + \mu_v)^2\right) \\
&= -16(r_u - r_v)^2\mu_u\mu_v \leq 0,
\end{aligned}$$

then for all $\alpha > 0$ we have $\dfrac{\mathrm{d}^2}{\mathrm{d}x^2}\lambda_1(\alpha) \geq 0$, hence $\lambda_1(\alpha)$ is convex. This finishes the proof of Lemma 2.3.47. □

Remark 2.3.48 (Stability of 0)**.** The previous computation can be carried out the same way independently of the sign of r_u and r_v. This gives a criterion for the instability of 0 in the case $\min(r_u, r_v) < 0$: if $\frac{\mu_v}{\mu_u+\mu_v} r_u + \frac{\mu_u}{\mu_u+\mu_v} r_v \geq 0$ then 0 is always unstable, whereas if $\frac{\mu_v}{\mu_u+\mu_v} r_u + \frac{\mu_u}{\mu_u+\mu_v} r_v < 0$ the stability of 0 depends on the size of the mutation rate. In the latter case, the ratio $\frac{\mu_u}{\mu_v}$ being fixed, 0 is always unstable if μ_u, μ_v are sufficiently small, and always stable if μ_u, μ_v are sufficiently large.

We are now in a position to give our arguments for the long-time behavior of the ODE problem. We begin with the case where there exists a Lyapunov functional for the system. We introduce the functionals:

$$\mathcal{F}_u(u) := u - u^* - u^* \ln\left(\frac{u}{u^*}\right), \qquad \mathcal{F}_v(v) := v - v^* - v^* \ln\left(\frac{v}{v^*}\right). \tag{2.3.67}$$

Note that this Lyapunov functional is rather classical and has been used for instance by Hsu [217] in a competitive context. The present argument was inspired by the more recent article of Cantrell, Cosner and Yu [100].

Lemma 2.3.49 (Lyapunov functional)**.** *Let Assumption 2.3.29 hold and assume* $\max(r_u - \mu_u, r_v - \mu_v) > 0$*. Then, there is* $K > 0$ *such that the functional* $\mathcal{F}^K(u,v) := \mathcal{F}_u(u) + K\mathcal{F}_v(v)$ *is a Lyapunov functional for* (2.3.33)*, i.e.*

$$\frac{\mathrm{d}}{\mathrm{d}t}\mathcal{F}^K(u(t),v(t)) \leq 0,$$

along any positive trajectory $(u(t),v(t))$*. Moreover, the inequality is strict unless* $(u(t),v(t)) = (u^*,v^*)$*.*

Proof. Since it is clear that $\mathcal{F}(u^*,v^*) = 0$, we will focus on the case of an orbit starting from a positive initial condition (u_0,v_0). We first compute:

$$\begin{aligned}
\frac{\mathrm{d}}{\mathrm{d}t}\mathcal{F}_u(u(t)) &= u_t\left(1 - \frac{u^*}{u}\right) = (u-u^*)\frac{u_t}{u} \\
&= (u-u^*)\left(r_u - \mu_u - \kappa_u(u+v) + \mu_v\frac{v}{u}\right) \\
&= (u-u^*)\left(\kappa_u(u^*+v^*) - \mu_v\frac{v^*}{u^*} - \kappa_u(u+v) + \mu_v\frac{v}{u}\right) \\
&= -\kappa_u(u-u^*)^2 - \kappa_u(u-u^*)(v-v^*) + \mu_v(u-u^*)\left(\frac{u^*v - uv^*}{uu^*}\right) \\
&= -\left(\kappa_u + \mu_v\frac{v^*}{uu^*}\right)(u-u^*)^2 - \left(\kappa_u - \frac{\mu_v}{u^*}\right)(u-u^*)(v-v^*) \\
&\leq -\kappa_u(u-u^*)^2 - \left(\kappa_u - \frac{\mu_v}{u^*}\right)(u-u^*)(v-v^*),
\end{aligned}$$

and the inequality is strict unless $u = u^*$. Similarly,

$$\frac{\mathrm{d}}{\mathrm{d}t}\mathcal{F}_v(y) \leq -\kappa_v(v-v^*)^2 - \left(\kappa_v - \frac{\mu_u}{v^*}\right)(u-u^*)(v-v^*),$$

and the inequality is strict unless $v = v^*$. Since $(u,v) \neq (u^*,v^*)$, we have for all $K > 0$:

$$\frac{\mathrm{d}}{\mathrm{d}t}\mathcal{F}^K(u,v) \;<\; -\kappa_u(u-u^*)^2 - \left(\kappa_u - \frac{\mu_v}{u^*} + K\left(\kappa_v - \frac{\mu_u}{u^*}\right)\right)(u-u^*)(v-v^*) - K\kappa_v(v-v^*)^2.$$

Next we prove that the right-hand side can be made nonpositive for all $(u,v) > (0,0)$ for a well-chosen value of K. We remark that the right-hand side is a quadratic form in $(U := u-u^*, V := v-v^*)$, which can be written as $-Q(U,V)$ where:

$$Q(U,V) := AU^2 + (B+KC)UV + KDV^2,$$

and $U = u-u^*$, $V = v-v^*$, $A = \kappa_u$, $B = \kappa_u - \frac{\mu_v}{u^*}$, $C = \kappa_v - \frac{\mu_u}{v^*}$ and $D = \kappa_v$. We claim that $Q(U,V)$ can be made positive definite by a proper choice of $K > 0$. Indeed, algebraic computations lead to

$$Q(U,V) = A\left(U + \frac{B+KC}{2A}V\right)^2 + \left(KD - \frac{(B+KC)^2}{4A}\right)V^2,$$

and therefore it suffices to find $K > 0$ such that

$$0 < KD - \frac{(B+KC)^2}{4A} = \frac{-C^2K^2 + (4AD - 2BC)K - B^2}{4A} =: -\frac{P(K)}{4A}.$$

Now $P(K)$ is a second-order polynomial and its number of roots is determined by the sign of the quantity

$$\Delta = (4AD - 2BC)^2 - 4B^2C^2 = 16AD(AD - BC) > 0.$$

If $BC < AD$, the polynomial P has two roots, and those roots have to be nonnegative since $P(K) < 0$ for all $K < 0$. This shows that there exists $K > 0$ with $P(K) < 0$, which proves our claim and consequently finishes the proof of Lemma 2.3.49.

Our last task is therefore to check that $BC < AD$. Assume first that $r_u - \mu_u > 0$ and $r_v - \mu_v > 0$, then $B = \kappa_u - \frac{\mu_v}{u^*} > 0$ and $C = \kappa_v - \frac{\mu_u}{v^*} > 0$ are both positive by Lemma 2.3.46. Thus,

$$BC = \left(\kappa_u - \frac{\mu_v}{u^*}\right)\left(\kappa_v - \frac{\mu_u}{v^*}\right) \leq \kappa_u\kappa_v = AD.$$

Next assume that $r_u - \mu_u \leq 0$ and $r_v - \mu_v > 0$ (the case $r_v - \mu_v \leq 0$ and $r_u - \mu_u > 0$ can be treated similarly). In this case, $\kappa_u - \frac{\mu_v}{u^*} \leq 0$ and $\kappa_v - \frac{\mu_u}{v^*} > 0$ and thus

$$BC = \left(\kappa_u - \frac{\mu_v}{u^*}\right)\left(\kappa_v - \frac{\mu_u}{v^*}\right) \leq 0 < \kappa_u\kappa_v = AD.$$

Hence $BC < AD$ always holds under our hypotheses. Lemma 2.3.49 is proved. □

Notice in particular that Proposition 2.3.30 follows directly from Lemma 2.3.49 in the case $\max(r_u - \mu_u, r_v - \mu_v) > 0$. Next we consider the case $\max(r_u - \mu_u, r_v - \mu_v) \leq 0$. In this case, we show that the dynamics is eventually cooperative and we use the method of monotone iteration to conclude.

Lemma 2.3.50 (Ultimately cooperative dynamics)**.** *Let Assumption 2.3.29 hold and assume* $\max(r_u - \mu_u, r_v - \mu_v) \leq 0$. *Then, we have*

$$\lim_{t\to+\infty}(u(t), v(t)) = (u^*, v^*).$$

Proof. Let $(u(t), v(t))$ be a positive solution to (2.3.33). Then $(u(t), v(t))$ is a subsolution to the cooperative system:

$$\begin{cases} \bar{u}_t = \bar{u}(r_u - \mu_u - \kappa_u\bar{u}) + \bar{v}\max(\mu_v - \kappa_u\bar{u}, 0), \\ \bar{v}_t = \bar{v}(r_v - \mu_v - \kappa_v\bar{v}) + \bar{u}\max(\mu_u - \kappa_v\bar{v}, 0), \end{cases}$$

and in particular $u(t) \leq \bar{u}(t)$ and $v(t) \leq \bar{v}(t)$. Since $\bar{u}, \bar{v}$ eventually enters the cooperative region $0 < \bar{u} < \frac{\mu_v}{\kappa_u}$ and $0 < \bar{v} < \frac{\mu_u}{\kappa_v}$, so does (u, v). Next we use the method of sub- and supersolutions to show the convergence of $(u(t), v(t))$ starting from $(u_0, v_0) \in \left(0, \frac{\mu_v}{\kappa_u}\right) \times \left(0, \frac{\mu_u}{\kappa_v}\right)$. We remark that $(\bar{u}, \bar{v}) := (\frac{\mu_v}{\kappa_u}, \frac{\mu_u}{\kappa_v})$ is a strict supersolution:

$$\begin{cases} \bar{u}(r_u - \mu_u - \kappa_u\bar{u}) + \bar{v}(\mu_v - \kappa_u\bar{u}) < 0, \\ \bar{v}(r_v - \mu_v - \kappa_v\bar{v}) + \bar{u}(\mu_u - \kappa_v\bar{v}) < 0, \end{cases}$$

while for $\alpha > 0$ sufficiently small the vector $(\underline{u}, \underline{v}) := \alpha\varphi_1$ (where φ_1 is defined in Lemma 2.3.47) is a strict subsolution:

$$\begin{cases} \underline{u}(r_u - \mu_u - \kappa_u\underline{u}) + \underline{v}(\mu_v - \kappa_u\underline{u}) = \lambda_1\underline{u} + o(\alpha) > 0, \\ \underline{v}(r_v - \mu_v - \kappa_v\underline{v}) + \underline{u}(\mu_u - \kappa_v\underline{v}) = \lambda_1\underline{v} + o(\alpha) > 0. \end{cases}$$

Then, the technique of monotone iterations gives us a maximal stationary solution $(\overline{u}^*, \overline{v}^*) < (\bar{u}, \bar{v})$ and a minimal stationary solution $(\underline{u}^*, \underline{v}^*) > (\underline{u}, \underline{v})$ such that:

$$(\underline{u}^*, \underline{v}^*) \leq \liminf_{t\to+\infty}(u(t), v(t)) \leq \limsup_{t\to+\infty}(u(t), v(t)) \leq (\overline{u}^*, \overline{v}^*).$$

Finally since (u^*, v^*) is the unique stationary solution to (2.3.33), we have indeed:

$$(u^*, v^*) \leq \liminf_{t\to+\infty}(u(t), v(t)) \leq \limsup_{t\to+\infty}(u(t), v(t)) \leq (u^*, v^*),$$

hence $(u(t), v(t))$ converges to the stationary solution as $t \to +\infty$. Lemma 2.3.50 is proved. □

We are now in a position to prove Proposition 2.3.30 and conclude this section 2.3.5.1:

Proof of Proposition 2.3.30. If $\lambda_A > 0$, the existence and uniqueness of a stationary solution (u^*, v^*) has been shown in Lemma 2.3.46. The convergence of $(u(t), v(t))$ when $t \to +\infty$ has been shown in Lemma 2.3.49 if $\max(r_u - \mu_u, r_v - \mu_v) > 0$ by the means of a Lyapunov argument, and in Lemma 2.3.50 if $\max(r_u - \mu_u, r_v - \mu_v) \leq 0$ by the means of a monotone iteration sequence. This covers all the possibilities and hence finishes the proof of the statement in Proposition 2.3.30 when $\lambda_A > 0$.

Let $\lambda_A < 0$, and let $(u(t), v(t))$ be a solution to (2.3.33). Then $(u(t), v(t))$ is a sub-solution for the cooperative system

$$\begin{cases} \bar{u}_t = (r_u - \mu_u)\bar{u} + \mu_v\bar{v}, \\ \bar{v}_t = \mu_u\bar{u} + (r_v - \mu_v)\bar{v}, \end{cases}$$

hence for $M > \max(u(0), v(0))$ and $(\bar{u}(t), \bar{v}(t)) := Me^{\lambda_A t}(\varphi_A^u, \varphi_A^v)$ we have

$$(u(t), v(t)) \leq (\bar{u}(t), \bar{v}(t))$$

for all $t > 0$, and in particular $\lim_{t\to\infty} \max(u(t), v(t)) \le \lim_{t\to\infty} \max(\bar{u}(t), \bar{v}(t)) = 0$.

Let $\lambda_A = 0$, and let $(u(t), v(t))$ be a solution to (2.3.33). Then $(u(t), v(t))$ is a sub-solution for the cooperative system

$$\begin{cases} \bar{u}_t = (r_u - \mu_u - \min(\kappa_u, \kappa_v)\bar{u})\bar{u} + \mu_v \bar{v}, \\ \bar{v}_t = \mu_u \bar{u} + (r_v - \mu_v - \min(\kappa_u, \kappa_v)\bar{v})\bar{v}. \end{cases}$$

Let $(\bar{u}(0), \bar{v}(0)) := M_0(\varphi_A^u, \varphi_A^v)$ where $(\varphi_A^u, \varphi_A^v)$ is the principal eigenvector of the matrix A as defined in Assumption 2.3.29. Then $(\bar{u}(t), \bar{v}(t)) = M(t)(\varphi_A^u, \varphi_A^v)$ and the function $M(t)$ satisfies

$$\frac{\mathrm{d}}{\mathrm{d}t} M(t) = -\min(\kappa_u, \kappa_v) M(t)^2.$$

In particular, $\lim_{t\to\infty} M(t) = 0$. Since M_0 can be chosen so that $(u(0), v(0)) \le (\bar{u}(0), \bar{v}(0))$, we deduce that $\lim_{t\to\infty}(u(t), v(t)) = (0, 0)$. Proposition 2.3.30 is proved. □

2.3.5.2 Long-time behavior for the solutions to the homogeneous problem

We aim at showing that the ω-limit set of a positively bounded from below initial condition is reduced to a single element $\{(u^*, v^*)\}$, where (u^*, v^*) is the unique stationary state for (2.3.33). As shown below, we can prove such a result only for a subset of the set of parameters.

Theorem 2.3.51 (Entire solutions)**.** *Let Assumption 2.3.29 and 2.3.32 hold. Let $(u(t,x), v(t,x))$ be an nonnegative bounded entire solution to* (2.3.30)*. Assume that (u, v) is bounded from below, i.e. that there exists $\delta > 0$ such that for all $t \in \mathbb{R}$ and $x \in \mathbb{R}$ we have:*

$$u(t,x) \ge \delta > 0 \text{ and } v(t,x) \ge \delta > 0,$$

then $(u, v) \equiv (u^*, v^*)$.

Proof. We divide the proof in three steps.

Step 1: The ultimately cooperative case: $\max(r_u - \mu_u, r_v - \mu_v) \le 0$, with $(\sigma_1, \sigma_2) > (0, 0)$.

In this case, our argument is very similar to the one in Lemma 2.3.50. We first notice that $(u(t,x), v(t,x))$ is a sub-solution to the cooperative ODE system:

$$\begin{cases} \bar{u}_t = (r_u - \mu_u - \kappa_u \bar{u})\bar{u} + \bar{v}\max(\mu_v - \kappa_u \bar{u}, 0), \\ \bar{v}_t = (r_v - \mu_v - \kappa_v \bar{v})\bar{v} + \bar{u}\max(\mu_u - \kappa_v \bar{v}, 0), \end{cases} \tag{2.3.68}$$

and in particular $u(t,x) \le \bar{u}(t)$ and $v(t,x) \le \bar{v}(t)$. Since $\bar{u}, \bar{v}$ eventually enters the cooperative region $0 < \bar{u} < \frac{\mu_v}{\kappa_u}$ and $0 < \bar{v} < \frac{\mu_u}{\kappa_v}$, so does (u, v). Moreover, since $(u(t,x), v(t,x))$ is defined for all $t \in \mathbb{R}$, we deduce that

$$\sup_{(t,x)\in\mathbb{R}^2} u(t,x) < \frac{\mu_v}{\kappa_u},$$
$$\sup_{(t,x)\in\mathbb{R}^2} v(t,x) < \frac{\mu_u}{\kappa_v}.$$

Hence, the entire solution $(u(t,x), v(t,x))$ of the reaction-diffusion system (2.3.30) stays in the cooperative region and can thus be compared with the solution to the ODE system (2.3.33). More precisely, for all $t \in \mathbb{R}$ and $x \in \mathbb{R}$, we have:

$$\underline{u}(t_0, t) \le u(t,x) \le \bar{u}(t_0, t),$$
$$\underline{v}(t_0, t) \le v(t,x) \le \bar{v}(t_0, t),$$

where $(\underline{u}(t_0,t), \underline{v}(t_0,t))$ is the solution to (2.3.33) at time t starting from the initial condition $(\underline{u}(t_0), \underline{v}(t_0)) = (\delta, \delta)$, and $(\bar{u}(t_0,t)\bar{v}(t_0,t))$ is the solution to (2.3.33) at time t starting from the initial condition $(\bar{u}(t_0), \bar{v}(t_0)) = \left(\frac{\mu_v}{\kappa_u}, \frac{\mu_u}{\kappa_v}\right)$. Since:

$$\lim_{t_0\to-\infty}(\underline{u}(t_0,t), \underline{v}(t_0,t)) = \lim_{t_0\to-\infty}(\bar{u}(t_0,t), v(t_0,t)) = (u^*, v^*),$$

we have indeed $(u(t,x), v(t,x)) \equiv (u^*, v^*)$ and Theorem 2.3.51 is proved in this case.

Step 2: The ultimately competitive case: $\min(r_u - \mu_u - \mu_v, r_v - \mu_v - \mu_u) > 0$, with $(\sigma_1, \sigma_2) > (0, 0)$.

First notice that, as in Step 1, the solution $(u(t,x), v(t,x))$ can be controlled from above by the solution to the ODE (2.3.68), and hence we have the upper estimate:

$$u(t,x) < \frac{r_u - \mu_u}{\kappa_u}, \qquad v(t,x) < \frac{r_v - \mu}{\kappa_v}.$$

Next we remark that $(u(t,x), v(t,x))$ is a supersolution to the cooperative system:

$$\begin{cases} \underline{u}_t = \underline{u}\left(r_u - \mu_u - \kappa_u\left(\dfrac{r_u - \mu_u}{\mu_v}\right)\underline{u}\right) + \delta(\mu_v - \kappa_u \underline{u}), \\ \underline{v}_t = \underline{v}\left(r_v - \mu_v - \kappa_v\left(\dfrac{r_v - \mu_v}{\mu_u}\right)\underline{v}\right) + \delta(\mu_u - \kappa_v \underline{v}). \end{cases}$$

In particular, we have for all $t \in \mathbb{R}$ and $x \in \mathbb{R}$:

$$\frac{\mu_v}{\kappa_u} \leq u(t,x), \qquad \frac{\mu_u}{\kappa_v} \leq v(t,x).$$

Hence $(u(t,x), v(t,x))$ stays in the invariant rectangle $\left[\frac{\mu_v}{\kappa_u}, \frac{r_u - \mu_u}{\kappa_u}\right] \times \left[\frac{\mu_u}{\kappa_v}, \frac{r_v - \mu_v}{\kappa_v}\right]$, where system (2.3.30) is competitive. In particular, system (2.3.30) is order-preserving for the non-classical order $\leq_c$ on $\mathbb{R}^2$ (see e.g. [361, Proposition 5.1]):

$$(u, v) \leq_c (\tilde{u}, \tilde{v}) \Longleftrightarrow u \leq \tilde{u} \text{ and } v \geq \tilde{v},$$

in this rectangle. Thus,

$$\begin{aligned} \underline{u}(t_0, t) \leq_c u(t,x) \leq_c \bar{u}(t_0, t), \\ \underline{v}(t_0, t) \leq_c v(t,x) \leq_c \bar{v}(t_0, t), \end{aligned}$$

where $(\underline{u}(t_0,t), \underline{v}(t_0,t))$ is the solution to (2.3.33) at time t starting from the initial condition $(\underline{u}(t_0), \underline{v}(t_0)) = \left(\frac{\mu_u}{\kappa_u}, \frac{r_v - \mu_v}{\kappa_v}\right)$, and $(\bar{u}(t_0,t)\bar{v}(t_0,t))$ is the solution to (2.3.33) at time t starting from the initial condition $(\bar{u}(t_0), \bar{v}(t_0)) = \left(\frac{r_u - \mu}{\kappa_u}, \frac{\mu_u}{\kappa_v}\right)$. Since:

$$\lim_{t_0 \to -\infty} (\underline{u}(t_0,t), \underline{v}(t_0,t)) = \lim_{t_0 \to -\infty} (\bar{u}(t_0,t), v(t_0,t)) = (u^*, v^*),$$

we have indeed $(u(t,x), v(t,x)) \equiv (u^*, v^*)$ and Theorem 2.3.51 is proved in this case.

Step 3: The Lyapunov case: $\sigma_u = \sigma_v =: \sigma$ and $\max(r_u - \mu_u, r_v - \mu_v) \geq 0$.

In this case the system is mixed quasimonotone and, to the extent of our knowledge, monotonicity arguments cannot be employed. We therefore turn to a generalisation of the Lyapunov argument which was used in Lemma 2.3.49. Let $\mathcal{F}_u$, $\mathcal{F}_v$ be the functions defined in (2.3.67) and K be the constant given by Lemma 2.3.49, so that $\mathcal{F}^K(u,v) := \mathcal{F}_u(u) + K\mathcal{F}_v(v)$ is a Lyapunov functional for the flow of the ODE (2.3.33). Define $w(t,x) = \mathcal{F}^K(u(t,x), v(t,x))$. Then w satisfies:

$$\begin{aligned} w_t - \sigma w_{xx} &= (u_t - \sigma u_{xx})\mathcal{F}_u'(u) + K(v_t - \sigma v_{xx})\mathcal{F}_v'(v) - \sigma(u_x^2 \mathcal{F}_u''(u) + K v_x^2 \mathcal{F}_v''(v)) \\ &\leq -\kappa_u(u - u^*)^2 - \left(\kappa_u - \frac{\mu_v}{u^*} + K\left(\kappa_v - \frac{\mu_u}{v^*}\right)\right) - K\kappa_v(v - v^*)^2 =: Q(u,v). \end{aligned}$$

Indeed $\mathcal{F}_u$ and $\mathcal{F}_v$ are convex functions, hence $\mathcal{F}_u''(u) \geq 0$ and $\mathcal{F}_v''(v) \geq 0$ for all u, v. Since $Q(u,v) \leq 0$, w is a bounded entire subsolution to the heat equation, therefore has to be a constant. Since $Q(u,v) < 0$ whenever $(u,v) \neq (u^*, v^*)$, the only possibility is $w(t,x) \equiv 0$ and therefore $(u(t,x), v(t,x)) \equiv (u^*, v^*)$. This finishes the proof of Theorem 2.3.51 in the case $\max(r_u - \mu_u, r_v - \mu_v) \geq 0$ and $\sigma_u = \sigma_v$.

Since all the possible cases have been covered, Theorem 2.3.51 is proved. □

Proof of Theorem 2.3.33. Let $(u_0(x) \geq 0, v_0(x) \geq 0)$ be a nontrivial initial condition and $(u(t,x), v(t,x))$ be the corresponding solution to (2.3.2). We argue by contradiction and assume that there exists $\varepsilon > 0$ and a sequences $t_n \to +\infty$ and $x_n \in \mathbb{R}$ such that $|x_n| \leq ct_n$ and

$$|u(t_n, x_n) - u^*| \geq \varepsilon > 0.$$

Then, due to the classical parabolic estimates, the sequence $(u(t+t_n,x), v(t+t_n,x)$ converges locally uniformly and up to an extraction to an entire solution $(u^\infty(t,x), v^\infty(t,x))$ which satisfies $|u^\infty(0,0) - u^*| \geq \varepsilon$. By Theorem 2.3.24, there exists $\delta > 0$ such that $(u^\infty(t,x), v^\infty(t,x)) \geq (\delta, \delta)$. Hence Theorem 2.3.51 applies and we have $(u^\infty(t,x), v^\infty(t,x)) \equiv (u^*, v^*)$. This is a contradiction. If $|v(t_n, x_n) - v^*| \geq \varepsilon$, we easily derive a similar contradiction. Therefore, we have

$$\lim_{t\to\infty} \sup_{|x|\leq ct} \max(|u(t,x) - u^*|, |v(t,x) - v^*|) = 0,$$

and Theorem 2.3.33 holds. □

In the case when Assumption 2.3.32 fails to hold, we can no longer prove the *global* stability of the stationary solution, however, since the spectrum of the linearized operator is included in the nonpositive complex plane, we can still prove *local* stability by studying the semigroup associated with the system (in particular, no Turing bifurcation is occurring with our system). This is the content of Theorem 2.3.31.

Proof of Theorem 2.3.31. We divide the proof in two steps. Our strategy is as follows: in the first step we show that the constant stationary solution is linearly stable for the elliptic PDE, meaning that the spectrum of the linearized operator lies in the complex half-plane of negative real parts. In the second step we show how this linear stability leads to nonlinear stability, by using semigroup theory.

Step 1: We show that the spectrum of the linearized operator is included in the negative complex plane. In this Step we investigate the operator:

$$\mathcal{A}\begin{pmatrix} g \\ h \end{pmatrix} := \begin{pmatrix} \sigma_u g_{xx} \\ \sigma_v h_{xx} \end{pmatrix} + \begin{pmatrix} (r_u - \mu_u - 2\kappa_u u^* - \kappa_u v^*)g + (\mu_v - \kappa_u v^*)h \\ (\mu_u - \kappa_v u^*)h + (r_v - \mu_v - \kappa_v u^* - 2\kappa_v v^*)g \end{pmatrix},$$

considered as an unbounded operator acting on $(g,h) \in BUC(\mathbb{R})^2$, $BUC(\mathbb{R})$ being the space of bounded and uniformly continuous functions on $\mathbb{R}$ equipped with the supremum norm (this is classically a Banach space), with domain $D(\mathcal{A}) = C_b^2(\mathbb{R})^2$.

Let $\lambda \in \mathbb{C}$ and $(\varphi, \psi) \in BUC(\mathbb{R})^2$ be given and consider the resolvent equation

$$(\lambda I - \mathcal{A})\begin{pmatrix} g \\ h \end{pmatrix} = \begin{pmatrix} \varphi \\ \psi \end{pmatrix}. \tag{2.3.69}$$

The set of solutions of the latter equation can be computed explicitly by the variation of constants formula. More precisely, we let $Y(x) = (g, g_x, h, h_x)^T$ and rewrite (2.3.69) as an ODE on $\mathbb{R}^4$:

$$\begin{aligned} \frac{\mathrm{d}}{\mathrm{d}x}Y(x) &= \begin{pmatrix} 0 & 1 & 0 & 0 \\ \sigma_u^{-1}(\lambda - (r_u - \mu_u - 2\kappa_u u^* - \kappa_u v^*)) & 0 & -\sigma_u^{-1}(\mu_v - \kappa_u u^*) & 0 \\ 0 & 0 & 0 & 1 \\ -\sigma_v^{-1}(\mu_u - \kappa_v v^*) & 0 & \sigma_v^{-1}(\lambda - (r_v - \mu_v - \kappa_v u^* - 2\kappa_v v^*)) & 0 \end{pmatrix} Y - \begin{pmatrix} 0 \\ \varphi \\ 0 \\ \psi \end{pmatrix} \\ &=: B_\lambda Y(x) + Z(x). \end{aligned}$$

We first investigate the bounded eigenvectors of the ODE $Y' = B_\lambda Y$. These correspond to the imaginary eigenvalues of the matrix B_λ, *i.e.* the imaginary roots of the polynomial

$$\chi_\lambda(X) := X^4 + \big(\sigma_u^{-1}a + \sigma_v^{-1}d - \lambda(\sigma_u^{-1} + \sigma_v^{-1})\big)X^2 + \sigma_u^{-1}\sigma_v^{-1}\big(\lambda^2 - (a+d)\lambda + ad - bc\big),$$

where it is convenient to use the notation a, b, c, d introduced to denote the coefficients of the Jacobian matrix of the nonlinearity at the equilibrium point:

$$\begin{aligned} a &:= r_u - \mu_u - 2\kappa_u u^* - \kappa_u v^* = -\left(\kappa_u u^* + \mu_v \frac{v^*}{u^*}\right), & b &:= \mu_v - \kappa_u u^*, \\ d &:= r_v - \mu_v - \kappa_v u^* - 2\kappa_v v^* = -\left(\kappa_v v^* + \mu_u \frac{u^*}{v^*}\right), & c &:= \mu_u - \kappa_v v^*. \end{aligned}$$

We show that there exists a curve $\mathcal{C} \subset \mathbb{C}$, which is contained in the half-plane $\Re(z) \leq -\omega$ for $z \in \mathbb{C}$, where

$$\omega := \min\left(-\frac{a+d}{2}, -\frac{\sigma_u^{-1}a + \sigma_v^{-1}d}{\sigma_u^{-1}+\sigma_v^{-1}}\right), \tag{2.3.70}$$

and such that B_λ has no imaginary eigenvalue if λ is in the connected compound $\mathcal{C}^+$ of $\mathbb{C}\backslash\mathcal{C}$ which contains the positive real axis. Moreover $\mathcal{C}$ asymptotically looks like straight lines:

$$\Im(z) \sim \pm\left|2\frac{\sigma_u^{-1}\sigma_v^{-1}}{\sigma_u^{-1}+\sigma_v^{-1}} - \sqrt{\sigma_u^{-1}\sigma_v^{-1}}\right|\Re(z), \text{ for } z \in \mathcal{C} \text{ with } \Re(z) \to -\infty.$$

Indeed, investigating the values taken by $\chi_\lambda(iX)$ for real values of X, we find that

$$\chi_\lambda(iX) = X^4 + \big(-(\sigma_u^{-1}a + \sigma_v^{-1}d) + \lambda(\sigma_u^{-1}+\sigma_v^{-1})\big)X^2 + \sigma_u^{-1}\sigma_v^{-1}\big(\lambda^2 - (a+d)\lambda + ad - bc\big).$$

Since $a<0$, $d<0$ and $ad-bc>0$ (see Lemma 2.3.45 and note that our notation coincides with (2.3.65)), we immediately see that $\chi_\lambda(iX) > 0$ if λ is real and $\lambda \geq \max\left(a+d, \frac{\sigma_u^{-1}a+\sigma_v^{-1}d}{\sigma_u^{-1}+\sigma_v^{-1}}\right)$. If $\Im(\lambda) \neq 0$, we remark that

$$\Im(\chi_\lambda(iX)) = \Im(\lambda)\left[(\sigma_u^{-1}+\sigma_v^{-1})X^2 + \sigma_u^{-1}\sigma_v^{-1}(2\Re(\lambda) - (a+d))\right],$$

therefore if $\Re(\lambda) > \frac{a+d}{2}$ the polynomial $\chi_\lambda(iX)$ cannot have a real root. If $\Re(\lambda) \leq \frac{a+d}{2}$ there are two candidates

$$X_\pm := \pm\sqrt{\frac{\sigma_u^{-1}\sigma_v^{-1}}{\sigma_u^{-1}+\sigma_v^{-1}}(a+d-2\Re(\lambda))},$$

and for those values of X we have

$$\begin{aligned}\Re(\chi_\lambda(X)) = &\left(\frac{\sigma_u^{-1}\sigma_v^{-1}}{\sigma_u^{-1}+\sigma_v^{-1}}(a+d-2\Re(\lambda))\right)^2 - (\sigma_u^{-1}a+\sigma_v^{-1}d)\frac{\sigma_u^{-1}\sigma_v^{-1}}{\sigma_u^{-1}+\sigma_v^{-1}}(a+d-2\Re(\lambda))\\ &+ ad - bc + \Re(\lambda)\sigma_u^{-1}\sigma_v^{-1}(a+d-2\Re(\lambda)) + \sigma_u^{-1}\sigma_v^{-1}\big(\Re(\lambda)^2 - \Im(\lambda)^2 - (a+d)\Re(\lambda)\big).\end{aligned}$$

We conclude that $\chi_\lambda(iX)$ cannot have a real root in this case either, provided $\Im(\lambda)^2$ is bounded from below by a polynomial of degree two in $\Re(\lambda)$. Hence we have found our curve $\mathcal{C}$.

When $\lambda \in \mathcal{C}^+$ (*i.e.* lies in the connected component of $\mathbb{C}\backslash\mathcal{C}$ containing $\mathbb{R}^+$) we show that Y is uniquely determined and depends continuously on Z. Indeed, the set of solutions to the equation $Y' = B_\lambda Y + Z$ can be determined by the *variation of constants formula*

$$Y(x) = e^{xB_\lambda}Y_0 + \int_0^x e^{(x-s)B_\lambda}Z(s)\mathrm{d}z, \tag{2.3.71}$$

for arbitrary $Y_0 \in \mathbb{R}^4$. We show that there exists a unique choice of Y_0 such that $Y(x)$ remains bounded on $\mathbb{R}$. Indeed, because of the specific form of $\chi_\lambda(X)$, the matrix B_λ has either four or two distinct eigenvalue. The latter case occurs exactly when the discriminant of the characteristic polynomial $\chi_\lambda(X)$ is null, namely

$$\big(\sigma_u^{-1}a + \sigma_v^{-1}d - \lambda(\sigma_u^{-1}+\sigma_v^{-1})\big)^2 - 4\sigma_u^{-1}\sigma_v^{-1}\big(\lambda^2 - (a+d)\lambda + ad - bc\big) = 0.$$

The left-hand polynomial $D(\lambda)$ of the former equation can be written as

$$\begin{aligned}D(\lambda) &= \sigma_u^{-2}a^2 + \sigma_v^{-2}d^2 + \lambda^2(\sigma_u^{-1}+\sigma_v^{-1})^2 + 2\sigma_u^{-1}\sigma_v^{-1}ad - 2\sigma_u^{-1}a\lambda(\sigma_u^{-1}+\sigma_v^{-1}) - 2\sigma_v^{-1}d\lambda(\sigma_u^{-1}+\sigma_v^{-1})\\ &\quad - 4\sigma_u^{-1}\sigma_v^{-1}\lambda^2 + 4\sigma_u^{-1}\sigma_v^{-1}(a+d)\lambda - 4\sigma_u^{-1}\sigma_v^{-1}(ad-bc)\\ &= \lambda^2\big(\sigma_u^{-1}-\sigma_v^{-1}\big)^2 + \lambda\big(-2(\sigma_u^{-1}a+\sigma_v^{-1}d)(\sigma_u^{-1}+\sigma_v^{-1}) + 4\sigma_u^{-1}\sigma_v^{-1}(a+d)\big) + (\sigma_u^{-1}a - \sigma_v^{-1}d)^2 + 4bc\\ &= \lambda^2\big(\sigma_u^{-1}-\sigma_v^{-1}\big)^2 + \lambda\big(2\sigma_u^{-1}\sigma_v^{-1}(a+d) - 2(\sigma_u^{-2}a + \sigma_v^{-2}d)\big) + (\sigma_u^{-1}a - \sigma_v^{-1}d)^2 + 4bc\\ &= \lambda^2\big(\sigma_u^{-1}-\sigma_v^{-1}\big)^2 + 2\lambda(\sigma_v^{-1}-\sigma_u^{-1})(\sigma_u^{-1}a - \sigma_v^{-1}d) + (\sigma_u^{-1}a - \sigma_v^{-1}d)^2 + 4bc\\ &= \big(\lambda(\sigma_u^{-1}-\sigma_v^{-1}) + \sigma_u^{-1}a - \sigma_v^{-1}d\big)^2 + 4bc.\end{aligned}$$

The roots are determined by the sign of bc:

$$\lambda^\pm = \frac{\sigma_v^{-1}d - \sigma_u^{-1}a \pm 2\sqrt{-bc}}{\sigma_u^{-1}-\sigma_v^{-1}} \quad \text{if } bc<0, \quad \lambda^\pm = \frac{\sigma_v^{-1}d - \sigma_u^{-1}a \pm 2i\sqrt{bc}}{\sigma_u^{-1}-\sigma_v^{-1}} \quad \text{if } bc>0. \tag{2.3.72}$$

Note that, since

$$B_\lambda^2 = \begin{pmatrix} \sigma_u^{-1}(\lambda - a) & 0 & -\sigma_u^{-1}b & 0 \\ 0 & \sigma_u^{-1}(\lambda - a) & 0 & -\sigma_u^{-1}b \\ -\sigma_v^{-1}c & 0 & \sigma_v^{-1}(\lambda - d) & 0 \\ 0 & -\sigma_v^{-1}c & 0 & \sigma_v^{-1}(\lambda - d) \end{pmatrix},$$

there is no hope that the matrix B_λ is diagonalizable when the characteristic polynomial has only two roots (because the minimal polynomial has degree > 2; see also the Motzkin-Taussky Theorem [228, Theorem 2.6 p.85]).

Therefore we distinguish two cases.

Case 1. The matrix B_λ is diagonalizable.

In this case there exists $\lambda_0, \lambda_1 \in \mathbb{C}$ such that $0 < \Re(\lambda_0) \leq \Re(\lambda_1)$ and an invertible matrix $P \in M_4(\mathbb{R})$ such that

$$B_\lambda = P \operatorname{diag}(\lambda_1, \lambda_0, -\lambda_0, -\lambda_1) P^{-1}.$$

In this case solving equation (2.3.71) on each eigenspace yields

$$Y_0 = P \begin{pmatrix} -\int_0^{+\infty} e^{-\lambda_1 s} \tilde{Z}_+^1(s) \mathrm{d}s \\ -\int_0^{+\infty} e^{-\lambda_0 s} \tilde{Z}_+^0(s) \mathrm{d}s \\ \int_{-\infty}^0 e^{\lambda_0 s} \tilde{Z}_-^0(s) \mathrm{d}s \\ \int_{-\infty}^0 e^{\lambda_1 s} \tilde{Z}_-^1(s) \mathrm{d}s \end{pmatrix}, \text{ where } \tilde{Z}(x) := \begin{pmatrix} \tilde{Z}_+^1(x) \\ \tilde{Z}_+^0(x) \\ \tilde{Z}_-^0(x) \\ \tilde{Z}_-^1(x) \end{pmatrix} = P^{-1} Z(x).$$

Therefore Y_0 is a continuous function of Z and (2.3.71) is recast

$$Y(x) = P \begin{pmatrix} -\int_x^{+\infty} e^{\lambda_1 (x-s)} \tilde{Z}_+^1(s) \mathrm{d}s \\ -\int_x^{+\infty} e^{\lambda_0 (x-s)} \tilde{Z}_+^0(s) \mathrm{d}s \\ \int_{-\infty}^x e^{-\lambda_0 (x-s)} \tilde{Z}_-^0(s) \mathrm{d}s \\ \int_{-\infty}^x e^{-\lambda_1 (x-s)} \tilde{Z}_-^1(s) \mathrm{d}s \end{pmatrix}.$$

We have found that $\lambda - \mathcal{A}$ admits a bounded inverse in $BUC(\mathbb{R})^2$.

Case 2. The matrix B_λ is not diagonalizable (i.e. $\lambda = \lambda^\pm$ given by (2.3.72)).

In this case, there is $\lambda_0 \in \mathbb{C}$ with $\Re(\lambda_0) > 0$ and an invertible matrix $P \in M_4(\mathbb{R})$ such that B_λ is equivalent to its Jordan normal form:

$$B_\lambda = P \begin{pmatrix} \lambda_0 & 1 & 0 & 0 \\ 0 & \lambda_0 & 0 & 0 \\ 0 & 0 & -\lambda_0 & 1 \\ 0 & 0 & 0 & -\lambda_0 \end{pmatrix} P^{-1},$$

and therefore

$$e^{xB_\lambda} = P \begin{pmatrix} e^{\lambda_0 x} & x e^{\lambda_0 x} & 0 & 0 \\ 0 & e^{\lambda_0 x} & 0 & 0 \\ 0 & 0 & e^{-\lambda_0 x} & x e^{-\lambda_0 x} \\ 0 & 0 & 0 & e^{-\lambda_0 x} \end{pmatrix} P^{-1}.$$

In this case solving equation (2.3.71) on each eigenspace yields

$$Y_0 = P \begin{pmatrix} -\int_0^{+\infty} e^{-\lambda_0 s} \big(\tilde{Z}_+^1(s) - s \tilde{Z}_+^0(s) \big) \mathrm{d}s \\ -\int_0^{+\infty} e^{-\lambda_0 s} \tilde{Z}_+^0(s) \mathrm{d}s \\ \int_{-\infty}^0 e^{\lambda_0 s} \big(\tilde{Z}_-^0(s) - s \tilde{Z}_-^1(s) \big) \mathrm{d}s \\ \int_{-\infty}^0 e^{\lambda_1 s} \tilde{Z}_-^1(s) \mathrm{d}s \end{pmatrix}, \text{ where } \tilde{Z}(x) := \begin{pmatrix} \tilde{Z}_+^1(x) \\ \tilde{Z}_+^0(x) \\ \tilde{Z}_-^0(x) \\ \tilde{Z}_-^1(x) \end{pmatrix} = P^{-1} Z(x).$$

Once again we have found that Y_0 depends continuously on Z and therefore $\lambda - \mathcal{A}$ admits a continuous inverse on $BUC(\mathbb{R})^2$ given by the formula

$$Y(x) = P \begin{pmatrix} -\int_x^{+\infty} e^{\lambda_0(x-s)}\big(\tilde{Z}_+^1(s) + (x-s)\tilde{Z}_+^0(s)\big)\mathrm{d}s \\ -\int_x^{+\infty} e^{\lambda_0(x-s)}\tilde{Z}_+^0(s)\mathrm{d}s \\ \int_{-\infty}^x e^{-\lambda_0(x-s)}\big(\tilde{Z}_-^0(s) + (x-s)\tilde{Z}_-^1(s)\big)\mathrm{d}s \\ \int_{-\infty}^x e^{-\lambda_0(x-s)}\tilde{Z}_-^1(s)\mathrm{d}s \end{pmatrix}.$$

To finish our first Step we remark that the operator $\mathcal{A}$ is sectorial and generates an analytic semigroup on $BUC(\mathbb{R})^2$. Indeed, $\mathcal{A}$ is a bounded perturbation of the unbounded operator $(\sigma_u\partial_{xx}, \sigma_v\partial_{xx})^T$ (acting on $D(A) = C_{UC}^2(\mathbb{R})^2$ in $BUC(\mathbb{R})^2$), which is sectorial and generates an analytic semigroup on $BUC(\mathbb{R})^2$ [270, Corollary 3.1.9 p. 81]. In particular, $e^{t\mathcal{A}}$ can be computed by the Dunford-Taylor integral

$$e^{t\mathcal{A}} = \frac{1}{2i\pi}\int_\Gamma e^{\lambda t}(\lambda I - \mathcal{A})^{-1}\mathrm{d}\lambda,$$

where Γ is a curve in $\mathcal{C}^+$ joining a straight line $\{\rho e^{-i\theta}, \rho > 0\}$ for some $\theta \in \left[\frac{\pi}{2}, \pi\right)$ to the straight line $\{\rho e^{-i\theta} : \rho > 0\}$ and oriented so that $\Im(\lambda)$ increases on Γ. From the above computations it is clear that Γ can be chosen so that $\Re(\lambda) \leq -\frac{\omega}{2}$ (where ω is given by (2.3.70)) for all $\lambda \in \Gamma$, in which case

$$e^{t\mathcal{A}} = e^{-\frac{\omega}{2}t}\cdot\frac{1}{2i\pi}\int_\Gamma e^{\left(\lambda+\frac{\omega}{2}\right)t}(\lambda - \mathcal{A})^{-1}\mathrm{d}\lambda$$

therefore

$$\begin{aligned}\|e^{t\mathcal{A}}\|_{BUC(\mathbb{R})^2} &\leq e^{-\frac{\omega}{2}t}\cdot\frac{1}{2\pi}\int_\Gamma e^{-(\Re(\lambda)+\frac{\omega}{2})t}\|(\lambda-\mathcal{A})^{-1}\|_{\mathcal{L}(BUC(\mathbb{R})^2)}\mathrm{d}\lambda \\ &\leq Ce^{-\frac{\omega}{2}t},\end{aligned}$$

for all $t > 0$, where C depends only on $\mathcal{A}$ and ω.

Step 2: We show the nonlinear stability.

Let $(u(t,x), v(t,x))$ be the solution of (2.3.30) starting from $(u_0, v_0) \in BUC(\mathbb{R})^2$. We remark that

$$\begin{pmatrix} u-u^* \\ v-v^* \end{pmatrix}_t - \mathcal{A}\begin{pmatrix} u-u^* \\ v-v^* \end{pmatrix} = o\left(\left\|\begin{pmatrix} u-u^* \\ v-v^* \end{pmatrix}\right\|_{BUC(\mathbb{R})^2}\right),$$

that our original equation (2.3.30) is a Lipschitz perturbation of the semigroup $T(t)$ generated by $\mathcal{A}$, and that it has been shown in Step 1 that $e^{\frac{\omega}{2}t}T(t)$ is bounded, with $\omega > 0$ defined by (2.3.70). In this context, it has been shown in [107, Theorem 10.2.2 p.157] (as a consequence of Gronwall's inequality) that there exists a $\varepsilon_0 > 0$ and a constant $M > 0$ such that

$$\left\|\begin{pmatrix} u(t,\cdot) \\ v(t,\cdot) \end{pmatrix} - \begin{pmatrix} u^* \\ v^* \end{pmatrix}\right\|_{BUC(\mathbb{R})^2} \leq M\left\|\begin{pmatrix} u_0 \\ v_0 \end{pmatrix} - \begin{pmatrix} u^* \\ v^* \end{pmatrix}\right\|_{BUC(\mathbb{R})^2} e^{-\frac{\omega}{2}t}, \text{ if } \left\|\begin{pmatrix} u_0-u^* \\ v_0-v^* \end{pmatrix}\right\|_{BUC(\mathbb{R})^2} \leq \varepsilon_0.$$

This finishes the proof of Theorem 2.3.31. □

2.3.5.3 Homogenization

In this section 2.3.5.3 we extend the results obtained for the homogeneous systems to the class of systems with rapidly oscillating coefficients.

Recall that we are concerned with system (2.3.35):

$$\begin{cases} u_t = (\sigma_u^\varepsilon(x)u_x)_x + (r_u^\varepsilon(x) - \kappa_u^\varepsilon(x)(u+v))u + \mu_v^\varepsilon(x)v - \mu_u^\varepsilon(x)u \\ v_t = (\sigma_v^\varepsilon(x)v_x)_x + (r_v^\varepsilon(x) - \kappa_v^\varepsilon(x)(u+v))v + \mu_u^\varepsilon(x)u - \mu_v^\varepsilon(x)v, \end{cases}$$

where $\sigma_u^\varepsilon(x) := \sigma_u\left(\frac{x}{\varepsilon}\right)$, $\sigma_v^\varepsilon(x) := \sigma_v\left(\frac{x}{\varepsilon}\right)$, $r_u^\varepsilon(x) := r_u\left(\frac{x}{\varepsilon}\right)$, $r_v^\varepsilon(x) := r_v\left(\frac{x}{\varepsilon}\right)$, $\kappa_u^\varepsilon(x) := \kappa_u\left(\frac{x}{\varepsilon}\right)$, $\kappa_v^\varepsilon(x) := \kappa_v\left(\frac{x}{\varepsilon}\right)$, $\mu_u^\varepsilon(x) := \mu_u\left(\frac{x}{\varepsilon}\right)$, $\mu_v^\varepsilon(x) := \mu_v\left(\frac{x}{\varepsilon}\right)$ and r_u, r_v, κ_u, κ_v are periodic with period 1. We also recall the definitions of the mean coefficients as in (2.3.34):

$$\overline{r_u} := \int_0^1 r_u(x)\mathrm{d}x, \qquad \overline{\kappa_u} := \int_0^1 \kappa_u(x)\mathrm{d}x, \qquad \overline{\mu_u} := \int_0^1 \mu_u(x)\mathrm{d}x,$$
$$\overline{r_v} := \int_0^1 r_v(x)\mathrm{d}x, \qquad \overline{\kappa_v} := \int_0^1 \kappa_v(x)\mathrm{d}x, \qquad \overline{\mu_v} := \int_0^1 \mu_v(x)\mathrm{d}x,$$

and finally:

$$\overline{\sigma_u}^H := \left(\int_0^1 \frac{1}{\sigma_u(x)}\mathrm{d}x\right)^{-1}, \qquad \overline{\sigma_v}^H := \left(\int_0^1 \frac{1}{\sigma_v(x)}\mathrm{d}x\right)^{-1}.$$

Lemma 2.3.52 (The homogenisation limit of entire solutions)**.** *Let $\overline{\sigma_u}^H$, $\overline{\sigma_v}^H$, $\overline{r_u}$, $\overline{r_v}$, $\overline{\kappa_u}$, $\overline{\kappa_v}$, $\overline{\mu_u}$ and $\overline{\mu_v}$ satisfy Assumption 2.3.29 and 2.3.32. Let $\varepsilon > 0$ and $(u^\varepsilon(t,x), v^\varepsilon(t,x))$ be a nonnegative nontrivial entire solution to* (2.3.35) *which is bounded from above and from below by positive constants. Then, as $\varepsilon \to 0$, the functions $(u^\varepsilon(t,x), v^\varepsilon(t,x))$ converge locally uniformly to the unique nonnegative nontrivial stationary state (u^*, v^*) of the homogenised problem* (2.3.30) *with σ_u, σ_v, r_u, r_v, κ_u, κ_v, μ_u, μ_v replaced by $\overline{\sigma_u}^H$, $\overline{\sigma_v}^H$, $\overline{r_u}$, $\overline{r_v}$, $\overline{\kappa_u}$, $\overline{\kappa_v}$, $\overline{\mu_u}$, $\overline{\mu_v}$.*

Proof. We divide the proof in three steps.

Step 1: We show that $(u^\varepsilon(t,x), v^\varepsilon(t,x))$ does not vanish.

Let $\left(\lambda_1^\varepsilon, (\varphi^\varepsilon(x) > 0, \psi^\varepsilon(x) > 0)\right)$ be the principal eigenpair associated with the eigenproblem:

$$\begin{cases} -(\sigma_u^\varepsilon(x)\varphi_x^\varepsilon)_x = (r_u^\varepsilon(x) - \mu_u^\varepsilon(x))\varphi^\varepsilon(x) + \mu_v^\varepsilon(x)\psi^\varepsilon(x) + \lambda_1^\varepsilon\varphi^\varepsilon(x) \\ -(\sigma_v^\varepsilon(x)\psi_x^\varepsilon)_x = \mu_u^\varepsilon(x)\varphi^\varepsilon(x) + (r_v^\varepsilon(x) - \mu_v^\varepsilon(x))\psi^\varepsilon(x) + \lambda_1^\varepsilon\psi^\varepsilon(x), \end{cases}$$

with ε-periodic boundary conditions, and normalised with $\max_{x\in\mathbb{R}} \sup \max(\varphi^\varepsilon(x), \psi^\varepsilon(x)) = 1$. Since $(u^\varepsilon, v^\varepsilon)$ is bounded from below, there exists $\alpha > 0$ such that $\alpha(\varphi^\varepsilon(x), \psi^\varepsilon(x)) \le (u^\varepsilon(t,x), v^\varepsilon(t,x))$. Let us define

$$A := \sup\left\{\alpha > 0, \forall x \in \mathbb{R}, \alpha(\varphi^\varepsilon(x), \psi^\varepsilon(x)) \le (u^\varepsilon(t,x), v^\varepsilon(t,x))\right\}.$$

Then by definition of $A > 0$ (and up to a shift and limiting process), there exists $t, x \in \mathbb{R}$ such that either $u^\varepsilon(t,x) = A\varphi^\varepsilon(x)$ or $v^\varepsilon(t,x) = A\psi^\varepsilon(x)$. Let us assume that the former holds. Then, we have

$$\begin{aligned} 0 &\ge -\kappa_u^\varepsilon(x)u(t,x)(u(t,x) + v(t,x)) - \lambda_1^\varepsilon A\varphi^\varepsilon(x) = -A^2\kappa_u^\varepsilon(x)\varphi(x)(\varphi(x) + \psi(x)) - \lambda_1^\varepsilon A\varphi^\varepsilon(x) \\ &\ge A\varphi^\varepsilon(x)(-2A\sup_{y\in\mathbb{R}}\kappa_u(y) - \lambda_1^\varepsilon), \end{aligned}$$

which implies that $A \ge \frac{-\lambda_1^\varepsilon}{2\sup_{y\in\mathbb{R}}\kappa_u(y)}$. We get a similar estimate in the case $v^\varepsilon(x) = A\psi^\varepsilon(x)$, which shows the inequality

$$A \ge \frac{-\lambda_1^\varepsilon}{2\max_{x\in\mathbb{R}}\left(\max(\kappa_u(x), \kappa_v(x))\right)}.$$

Then, it is classical (and has been proved in the proof of Theorem 2.3.11) that $(\lambda_1^\varepsilon, (\varphi^\varepsilon(x), \psi^\varepsilon(x))) \to (\lambda_1^0 < 0, (\varphi^0, \psi^0))$ uniformly as $\varepsilon \to 0$, where $(\lambda_1^0, (\varphi^0, \psi^0))$ is the principal eigenpair of the homogenised problem.

Note that in particular, there exists $\overline{\varepsilon} > 0$ such that for $0 < \varepsilon \le \overline{\varepsilon}$, we have a true uniform lower bound on $(u^\varepsilon(x), v^\varepsilon(x))$:

$$\inf_{(t,x)\in\mathbb{R}^2} \min(u(t,x), v(t,x)) \ge \frac{1}{2} \cdot \frac{-\lambda_1^0}{2\max_{x\in\mathbb{R}}\left(\max(\kappa_u(x), \kappa_v(x))\right)} \min(\varphi^0, \psi^0) > 0.$$

Step 2: We show that $u^\varepsilon(t,x)$ and $v^\varepsilon(t,x)$ are uniformly bounded.

Indeed, since $(u^\varepsilon, v^\varepsilon)$ is bounded, it follows directly from the maximum principle that

$$\sup_{(t,x)\in\mathbb{R}^2} \max(u(t,x), v(t,x)) \le \max\left(\frac{\max_{x\in\mathbb{R}} r_u(x)}{\min_{x\in\mathbb{R}} \kappa_u(x)}, \frac{\max_{x\in\mathbb{R}} r_v(x)}{\min_{x\in\mathbb{R}} \kappa_v(x)}\right).$$

Step 3: We derive the limit of $(u^\varepsilon, v^\varepsilon)$.

We first remark that, since $(u^\varepsilon, v^\varepsilon)$ is uniformly bounded, the classical estimates for parabolic equations in divergence form with discontinuous coefficients (see *e.g.* [246, Chapter II Theorem 10.1]) imply that $(U^\varepsilon, v^\varepsilon)$ is locally uniformly bounded in $C^\alpha(\mathbb{R}\times\mathbb{R})$, *i.e.* for any $T>0$ an $R>0$ there exists $C>0$ (independent of ε) such that

$$\max\left(\|u^\varepsilon\|_{C^\alpha([-T,T]\times[-R,R])}, \|v^\varepsilon\|_{C^\alpha([-T,T]\times[-R,R])}\right) \leq C.$$

Then, a classical diagonal extraction process allows us to extract a subsequence along which $(u^\varepsilon, v^\varepsilon)$ converges locally uniformly in $C^{\alpha/2}(\mathbb{R}^2)$ to a limit (u,v). It is then classical (see *e.g.* Remark 1.3 in Chapter 2 of [45]) that (u,v) satisfies weakly:

$$\begin{cases} u_t = \overline{\sigma_u}^H u_{xx} + (\overline{r_u} - \overline{\kappa_u}(u+v))u + \overline{\mu_v}v - \overline{\mu_u}u \\ v_t = \overline{\sigma_v}^H v_{xx} + (\overline{r_v} - \overline{\kappa_v}(u+v))v + \overline{\mu_u}u - \overline{\mu_v}v. \end{cases}$$

Then the Schauder estimates imply that $(u(x), v(x))$ is in fact a classical solution to (2.3.30). Since $(u(x), v(x))$ is nontrivial and bounded from below (by Step 1), Theorem 2.3.51 shows that $u(t,x) \equiv u^*$ and $v(t,x) \equiv v^*$. □

Lemma 2.3.53 (Uniqueness of rapidly oscillating entire solution)**.** *Let $\overline{r_u}$, $\overline{r_v}$, $\overline{\kappa_u}$, $\overline{\kappa_v}$, $\overline{\mu_u}$ and $\overline{\mu_v}$ satisfy Assumption 2.3.29. There exists $\bar\varepsilon$ such that if $0<\varepsilon\leq\bar\varepsilon$, there exists a unique nonnegative nontrivial entire solution $(u^\varepsilon(x), v^\varepsilon(x))$ associated with* (2.3.35)*, which is bounded from above and from below.*

Proof. We argue by contradiction and assume there exists a sequence $\varepsilon_n>0$ and two sequences $(u_1^{\varepsilon_n}(t,x), v_1^{\varepsilon_n}(t,x)) \not\equiv (u_2^{\varepsilon_n}(t,x), v_2^{\varepsilon_n}(t,x))$ of bounded nonnegative nontrivial stationary solutions to (2.3.35). We define $\delta_n := \max\left(\|u_2^{\varepsilon_n}(t,x) - u_1^{\varepsilon_n}(t,x)\|_{BUC(\mathbb{R})^2}, \|v_2^{\varepsilon_n}(t,x) - v_1^{\varepsilon_n}(t,x)\|_{BUC(\mathbb{R})^2}\right)$ and:

$$\varphi^{\varepsilon_n}(t,x) := \frac{1}{\delta_n}(u_2^{\varepsilon_n}(t,x) - u_1^{\varepsilon_n}(t,x))$$
$$\psi^{\varepsilon_n}(t,x) := \frac{1}{\delta_n}(v_2^{\varepsilon_n}(t,x) - v_1^{\varepsilon_n}(t,x)).$$

Up to a shift in time and space we assume that

$$\frac{\delta_n}{2} \leq \sup_{x\in(0,L)}\left(\max(|u_2^{\varepsilon_n}(0,x) - u_1^{\varepsilon_n}(0,x)|, |v_2^{\varepsilon_n}(0,x) - v_1^{\varepsilon_n}(0,x)|)\right) \leq \delta_n. \tag{2.3.73}$$

Then $(\varphi^{\varepsilon_n}(t,x), \psi^{\varepsilon_n}(t,x))$ satisfy:

$$\begin{cases} \varphi_t - \sigma_u^{\varepsilon_n}(x)\varphi_{xx}^{\varepsilon_n} = (r_u^{\varepsilon_n}(x) - \mu^{\varepsilon_n}(x))\varphi^{\varepsilon_n} + \mu_v^{\varepsilon_n}(x)\psi^{\varepsilon_n} - \kappa_u^{\varepsilon_n}(x)(2u_2^{\varepsilon_n} + v_2^{\varepsilon_n})\varphi^{\varepsilon_n} - \kappa_u^{\varepsilon_n}(x)u_2^{\varepsilon_n}\psi^{\varepsilon_n} + o(1) \\ \psi_t - \sigma_v^{\varepsilon_n}(x)\psi_{xx}^{\varepsilon_n} = \mu_u^{\varepsilon_n}(x)\varphi^{\varepsilon_n} + (r_v^{\varepsilon_n}(x) - \mu_v^{\varepsilon_n}(x))\psi^{\varepsilon_n} - \kappa_v^{\varepsilon_n}(x)v_2^{\varepsilon_n}\varphi^{\varepsilon_n} - \kappa_v^{\varepsilon_n}(x)(u_2^{\varepsilon_n} + 2v_2^{\varepsilon_n})\psi^{\varepsilon_n} + o(1) \end{cases}$$

Indeed, owing to Lemma 2.3.52, there holds

$$(u_1^{\varepsilon_n}, v_1^{\varepsilon_n}) \to (u^*, v^*) \text{ and } (u_2^{\varepsilon_n}, v_2^{\varepsilon_n}) \to (u^*, v^*) \text{ in } BUC(\mathbb{R}).$$

Since $\varphi^{\varepsilon_n}(t,x)$ and $\psi^{\varepsilon_n}(t,x)$ are bounded, classical homogenisation theory (see the proof of Theorem 2.3.11 where a similar argument is sketched) then leads to the convergence (up to an extraction) of $(\varphi^{\varepsilon_n}(t,x), \psi^{\varepsilon_n}(t,x))$ to $(\varphi(t,x), \psi(t,x))$ solving

$$\begin{cases} \varphi_t - \overline{\sigma_u}^H\varphi_{xx} = (\overline{r_u} - \overline{\mu_u})\varphi + \overline{\mu_v}\psi - \overline{\kappa_u}(2u^* + v^*)\varphi - \overline{\kappa_u}u^*\psi \\ \psi_t - \overline{\sigma_v}^H\psi_{xx} = \overline{\mu_u}\varphi + (\overline{r_v} - \overline{\mu_v})\psi - \overline{\kappa_v}v^*\varphi - \overline{\kappa_v}(u^* + 2v^*)\psi, \end{cases}$$

and the convergence holds (at least) locally uniformly. Because of our normalisation (2.3.73), the limit is non-trivial. Moreover, $(\varphi(t,x), \psi(t,x))$ is bounded, which not possible since (u^*, v^*) is locally asymptotically stable by Theorem 2.3.31. The Lemma is proved. □

Proof of Theorem 2.3.34. Theorem 2.3.34 is a direct consequence of the two previous Lemma. Statements (i) and (ii) are a direct consequence of Lemma 2.3.53. As for Statement (iii), it is also a consequence of Lemma 2.3.53.

Indeed, let $\varepsilon > 0$ be sufficiently small, so that there exists a unique entire solution to (2.3.35) which is uniformly bounded from below. Let $(u_0(x) \geq 0, v_0(x) \geq 0)$ be a nontrivial initial condition and $(u(t,x), v(t,x))$ be the corresponding solution to (2.3.35). We argue by contradiction and assume that there exists $\varepsilon > 0$, $0 < c < c^*_\varepsilon$ and a sequences $t_n \to +\infty$ and $x_n \in \mathbb{R}$ such that $|x_n| \leq ct_n$ and

$$|u(t_n, x_n) - u^*| \geq \varepsilon > 0.$$

Then, due to the classical parabolic estimates, the sequence $(u(t + t_n, x), v(t + t_n, x)$ converges locally uniformly and up to an extraction to an entire solution $(u^\infty(t,x), v^\infty(t,x))$ which satisfies $|u^\infty(0,0) - u^*| \geq \varepsilon$. By Theorem 2.3.24, there exists $\delta > 0$ such that $(u^\infty(t,x), v^\infty(t,x)) \geq (\delta, \delta)$. Hence Theorem 2.3.51 applies and we have $(u^\infty(t,x), v^\infty(t,x)) \equiv (u^*, v^*)$. This is a contradiction. If $|v(t_n, x_n) - v^*| \geq \varepsilon$, we easily derive a similar contradiction. Therefore, we have

$$\lim_{t\to\infty} \sup_{|x|\leq ct} \max(|u(t,x) - u^*|, |v(t,x) - v^*|) = 0.$$

This shows Statement (iii) and finishes the proof of Theorem 2.3.34. □

2.3.6 Appendix: On the spreading speed in the presence of a drift

Let us consider the equation:

$$\begin{aligned} u_t &= \mathcal{L}u - \kappa(x)u^2 \\ \mathcal{L}u &:= (\sigma(x)u_x)_x + q(x)u_x + r(x)u, \end{aligned} \tag{2.3.74}$$

where $\sigma(x) > 0$, $\kappa(x) > 0$, $r(x)$ and $q(x)$ are 1-periodic functions. It is known (see Nadin [298, 398] that the rightward and leftward spreading speeds associated with (2.3.74) are given by the following minimization formula

$$c^*_{\text{right}} := \inf_{\lambda>0} \frac{-k(\lambda)}{\lambda} \text{ and } c^*_{\text{left}} := \inf_{\lambda>0} \frac{-k(-\lambda)}{\lambda}.$$

If $q \equiv 0$ then, as a consequence of the Fredholm alternative, the function $k(\lambda)$ is even and $c^*_{\text{right}} = c^*_{\text{left}}$, but this is also the case if $\int_0^1 \frac{q(x)}{2\sigma(x)}\mathrm{d}x = 0$ [298, Proposition 2.14], because the advection term can then be "absorbed" by a change of function. Further dependencies of the speed on the various coefficients involved in (2.3.74) are studied in [300]. Here we are interested in a sufficient condition for the speeds c^*_{right} and c^*_{left} to be different, $c^*_{\text{right}} \neq c^*_{\text{left}}$.

It turns out that this can be achieved by considering the function

$$\mathcal{Q}(x) := \int_0^x \frac{q(y)}{2\sigma(y)}\mathrm{d}y - x\int_0^1 \frac{q(y)}{2\sigma(y)}\mathrm{d}y \text{ for all } x \in \mathbb{R}.$$

Indeed, writing

$$\mathcal{L}u = e^{-\mathcal{Q}(x)-x\int_0^1 \frac{q(y)}{2\sigma(y)}\mathrm{d}y}\left(\sigma(x)\left(e^{\mathcal{Q}(x)+x\int_0^1 \frac{q(y)}{2\sigma(y)}\mathrm{d}y}u\right)_x\right)_x + \left[-\frac{q_x(x)}{2} - \frac{q(x)^2}{4\sigma(x)} + r(x)\right]u,$$

and computing the principal periodic eigenvalue of the operator $u \mapsto e^{\lambda x}\mathcal{L}(e^{-\lambda x}u)$, we find that

$$k(\lambda) = \tilde{k}\left(\lambda - \int_0^1 \frac{q(y)}{2\sigma(y)}\mathrm{d}y\right),$$

where $\tilde{k}(\lambda)$ is associated with the operator

$$\tilde{\mathcal{L}}u = e^{-\mathcal{Q}(x)}\left(\sigma(x)\left(e^{\mathcal{Q}(x)}u\right)_x\right)_x + \left[-\frac{q_x(x)}{2} - \frac{q(x)^2}{4\sigma(x)} + r(x)\right]u,$$

which is self-adjoint for the weighted scalar product $\langle u, v\rangle_{\mathcal{Q}} = \int_0^1 u(x)v(x)e^{Q(x)}\mathrm{d}x$, and satisfies therefore $\tilde{k}(\lambda) = \tilde{k}(-\lambda)$.

In particular, it is not difficult to see that

$$c^*_{\text{right}} > c^*_{\text{left}} \text{ if } \int_0^1 \frac{q(x)}{2\sigma(x)}\mathrm{d}x < 0 \text{ and } c^*_{\text{right}} < c^*_{\text{left}} \text{ if } \int_0^1 \frac{q(x)}{2\sigma(x)}\mathrm{d}x > 0. \tag{2.3.75}$$

2.4 Singular measure traveling waves in an epidemiological model with continuous phenotypes

2.4.1 Introduction

In this work we consider the reaction-diffusion equation:

$$u_t = u_{xx} + \mu(M \star u - u) + u(a(y) - K \star u), \tag{2.4.1}$$

where $t > 0$, $x \in \mathbb{R}$, $y \in \Omega$ for a bounded domain $\Omega \subset \mathbb{R}^n$, $u = u(t, x, y)$, $\mu > 0$ is a positive constant, $a = a(y)$ is a continuous function, $M = M(y, z)$ and $K = K(y, z)$ are integration kernels, and the $\star$ operation is defined by (2.4.7). After discussing the existence of stationary states for (2.4.1), we construct measure-valued traveling waves and show the existence of a singularity for a subclass of parameters.

Equation (2.4.1) describes an asexual population living on a linear space, represented by the variable x. Several genotypes exist in the population, yielding a continuum of phenotypes, represented by the y variable. We denote $\Omega \subset \mathbb{R}^n$ the set of all reachable phenotypes. Our basic assumption is that the fitness (or intrinsic growth rate) of each individual is a function $a(y)$ of its phenotype. We also assume the existence of an underlying mutation process, by which an individual of phenotype $z \in \Omega$ may give birth to an individual of phenotype $y \in \Omega$, with probability $M(y, z)$. Such mutations are expected to occur at rate $\mu > 0$. Finally, the individuals are in competition for e.g. a finite resource, and we denote $K(y, z)$ the cost on the fitness of y caused by the presence of z.

In the context of epidemiology, $u(t, x, y)$ can be thought as a density of hosts at point x, infected with a pathogen of trait y. Equation (2.4.1) is particularly relevant in this context, since evidences suggest that pathogens (like e.g. viruses [211]) can be subject to rapid evolution, which may then occur at the same time scale as the propagation of the epidemic [322, 324]. Moreover, equation (2.4.1) can easily be derived from a host-pathogen microscopic model [P1] in which we neglect the influence of the pathogen on the hosts' motility.

The study of asymptotic propagation in biological models can be traced back to the seminal works of Fisher [170] and Kolmogorov, Petrovsky, and Piskunov [238], who investigated simultaneously the equation:

$$u_t = u_{xx} + u(1 - u), \tag{2.4.2}$$

where $u = u(t, x)$ stands for the density of a spatially structured theoretical population. They have shown, in particular, that for any compactly supported initial condition, the solution $u(t, x)$ invades the whole space with constant speed $c = 2$ (such a result is often called *spreading*); and that there exists a particular solution to (2.4.2), which consists of a fixed profile shifting along the axis at speed c, $u(t, x) = \tilde{u}(x - ct)$, and connecting the unstable state 0 near $+\infty$ to the stable state 1 near $-\infty$ (such a particular solution is called *traveling wave*). Since then, these results have been generalized to a variety of related models: see e.g. [405, 48, 398], and the references therein.

In the last decades, there has been an increasing interest in propagation models that take into account a multiplicity of different species. The main problems in the field include the replacement of a species by competitive interaction (see e.g. [181]), predation [255], adaptation to climate change [7], or cooperation [269, 399]. This last class of *cooperative* reaction-diffusion system has lead to particularly strong results, since its properties are somewhat comparable to those of scalar equations.

In a recent work [P2], the authors investigated the existence of traveling waves in the spatially homogeneous epidemiological model:

$$\begin{cases} rclw_t = & w_{xx} + w(1 - (w + m)) + \mu(m - w) \\ m_t = & m_{xx} + rm\left(1 - \dfrac{w + m}{K}\right) + \mu(w - m), \end{cases} \tag{2.4.3}$$

where w and m stand for a density of hosts infected by a wild type and mutant pathogen, respectively. Though this system is not globally cooperative, the authors managed to prove the existence and to compute the minimal speed of traveling waves as a function of the principal eigenvalue λ of the associated *principal eigenvalue problem*:

$$\begin{pmatrix} 1 - \mu & \mu \\ \mu & r - \mu \end{pmatrix} \begin{pmatrix} w \\ m \end{pmatrix} + \lambda \begin{pmatrix} w \\ m \end{pmatrix} = 0,$$

via the formula $c = 2\sqrt{-\lambda}$. Intuitively, the spatial dynamics is then guided by the linearized system far away from the front (such a traveling wave is sometimes called a *pulled front* [182, 366]). Since then, these results have been extended to a more general class of systems in [190].

Equation (2.4.1) can be seen as the continuous limit of system (2.4.3) with a large number of equations. Since we aim at computing the propagation speed for this equation, we turn to the associated principal eigenvalue problem:

$$\mu(M \star u - u) + u(a(y) + \lambda) = 0. \tag{2.4.4}$$

This problem has been investigated in [118] and [119], where the author shows an unexpected *concentration phenomenon* occurring for very natural fitness functions: if

$$\frac{1}{\sup_{z\in\Omega} a(z) - a(y)} \in L^1(\Omega), \tag{2.4.5}$$

and μ is small enough, there exists no continuous eigenfunction associated to (2.4.4), but rather *singular measure eigenvectors* with a singularity concentrated on the maximum of fitness $\Omega_0 := \{y \in \overline{\Omega} \,|\, a(y) = \sup_{z\in\Omega} a(z)\}$. According to (2.4.5), this phenomenon happens when $a(y)$ is sufficiently steep near its global maximum, and is highly dependant on the Euclidean dimension of Ω. For instance, if $n = 1$, a concentration may appear at the optimum $y = 0$ for the particular fitness function $a(y) = 1 - \sqrt{|y|}$, when $a(y) = 1 - |y|$ always yields continuous eigenfunctions; if $n = 2$, $a(y) = 1-|y|$ may induce concentration, but $a(y) = 1-|y|^2$ cannot. In dimension $n = 3$ or higher, smooth fitness functions such as $a(y) = 1 - |y|^2$ may induce concentration. A similar phenomenon, and in particular the critical mutation rate under which concentration appears for a sufficiently steep fitness function, has been discussed by Waxman and Peck [394, 395].

The nonlocal competition term $-K \star u(y)$ in (2.4.1) is quite standard in models involving competition between different phenotypes. Many models focus on the case where the competition is simply the integral of the distribution — this corresponds to $K(y, z) = 1$. As an example, the nonlocal Fisher-KPP equation

$$u_t - \Delta u = \mu u(1 - \Phi * u), \tag{2.4.6}$$

where $\Phi(y)$ is usually in $L^1(\mathbb{R}^n)$ with possibly additional restrictions, has attracted a lot of attention in the past [193, 184, 46, 200, 165, 203]. Nonlocal competition also appears in numerous other studies in population genetics and population dynamics [4, 186, 5, 72, 52]. In general, the qualitative behavior of traveling waves, and the long-time behavior of the solutions to the parabolic equation, are still difficult to handle. Recent advances have been made towards a better understanding of the asymptotic location of the front for the solutions to the parabolic equations, see [200, 70, 321, 3] for the nonlocal Fisher-KPP equation; [69] for the cane toads equation. In the case of the nonlocal Fisher-KPP equation (2.4.6), the existence of traveling waves has been established and the associated minimal speed characterized in [46, 200]. The convergence towards a stationary state on the back of the wave, has been shown in [46] for small μ or when the Fourier transform of the competition kernel is positive (in which cases one can prove the stability of the constant steady state $u \equiv 1$); and more recently, in a perturbative case [3], the convergence in long time has been shown for solutions to the parabolic equation. In the general case, the convergence towards a stationary solution on the back of the wave is far from being clear. The situation is similar in the case of many other models involving nonlocal competition.

As an indication that spreading happens, in the present section 2.4 we construct traveling waves for equation (2.4.1) which travel at the expected spreading speed. One of the main difficulties we encountered studying equation (2.4.1) is the lack of a regularizing effect in the mutation operator $M\star u$. This phenomenon is confirmed by the existence of traveling waves having a nontrivial singular part — in particular, there is no hope for asymptotic regularity. This lack of regularity also makes it more difficult to apply some of the techniques commonly used in the study of reaction-diffusion equations (in particular, taking the limit of a subsequence of large shifts of a solution). Finally, the non-compactness of the time-1 map prevents an application of the spreading results of Weinberger [398]. One other challenging issue is the absence of a comparison principle for equation (2.4.1), because of the nonlocal competition term. As in many other studies involving a nonlocal competition, this prevents a precise study of the long-time behavior of the solutions to the Cauchy problem and the behavior at the back of the waves (see also the above paragraph). To show that the traveling waves stay away from 0 on the back, we introduce a secondary problem, constructed by increasing self-competition in equation (2.4.1), which satisfies a comparison principle and serves as a sub-solution factory. To overcome the lack of regularity, we approximate the solutions of (2.4.1) by a vanishing viscosity method. We choose the zero Neumann boundary conditions for the approximating problem because

they behave well with respect to the integration across the domain. Finally, we introduce a weak notion of traveling waves which admit singularities. As we will see below, there is little hope to obtain more regularity in general, since there exist traveling waves for equation (2.4.1) which present an actual singularity. As far as we know, the present work constitutes the first construction of a measure-valued traveling wave in a reaction-diffusion equation.

2.4.2 Main results and comments

2.4.2.1 Function spaces and basic notions

Throughout this document we use a number of function spaces that we make precise here to avoid any confusion. Whenever X is a subset of a Euclidean space, we will denote $C(X)$, $C_b(X)$, $C_0(X)$, $C_c(X)$ the space of continuous functions, bounded continuous functions, continuous functions vanishing at ∞ and continuous functions with compact support over X, respectively. Notice that if X is compact, then those four function spaces coincide. Whenever $X \subset \mathbb{R}^d$ is a Borel set, we define $M^1(X)$ as the set of all Borel-regular measures over X. Let us recall that $M^1(X)$ is the topological dual of $C_0(X)$, by Riesz's representation theorem [343]. In our context, $M^1(X)$ coincides with the set of Borel measures that are inner and outer regular [343, 63]. We will thus call *Radon measure* an element of $M^1(X)$.

When $p \in M^1(X)$, we say that the equality $p = 0$ holds *in the sense of measures* if

$$\forall \psi \in C_c(X), \int_X \psi(x) p(dx) = 0.$$

We now define the notion of *transition kernel* (see [63, Definition 10.7.1]), which is crucial for our notion of traveling wave:

Definition 2.4.1 (Transition kernel)**.** We say that $u \in M^1(\mathbb{R} \times X)$ has a *transition kernel* if there exists a function $k(x, dy)$ such that

1. for any Borel set $A \subset X$, $k(\cdot, A)$ is a measurable function, and
2. for almost every $x \in \mathbb{R}$ (with respect to the Lebesgue measure on $\mathbb{R}$), $k(x, \cdot) \in M^1(X)$

and $u(dx, dy) = k(x, dy)dx$ in the sense of measures, i.e. for any $\varphi \in C_c(\mathbb{R} \times X)$, the following equality holds

$$\int_{\mathbb{R}\times X} \varphi(x, y) u(dx, dy) = \int_{\mathbb{R}} \int_X \varphi(x, y) k(x, dy) dx.$$

For simplicity, if the measure u has a transition kernel, we will often say that u *is* a transition kernel and use directly the notation $u(dx, dy) = u(x, dy)dx$.

We denote $f \star g$ the function:

$$f \star g(y) := \int_{\overline{\Omega}} f(y, z) g(dz) \tag{2.4.7}$$

whenever $f : \overline{\Omega}^2 \to \mathbb{R}$ and g is a measure on $\overline{\Omega}$. If g is continuous or $L^1(\Omega)$ we use the convention $g(dz) := g(z)dz$ in the above formula. Remark that the operation $\star$ is not the standard convolution, though both notions share many properties.

Finally, for $y \in \partial\Omega$ we will call $\nu(y)$ or simply ν the outward normal unit vector of Ω.

2.4.2.2 Main results

Our main result is the existence of a measure traveling wave, possibly singular, for equation (2.4.1). Before stating the result, let us give our assumptions, as well as subsidiary results.

Assumption 2.4.2 (Minimal assumptions)**.**

1. $\Omega \subset \mathbb{R}^n$ is a bounded connected open set with C^3 boundary. For simplicity we assume $0 \in \Omega$.
2. $M = M(y, z)$ is a C^α positive function $\overline{\Omega} \times \overline{\Omega} \to \mathbb{R}$ satisfying

$$\forall z \in \overline{\Omega}, \int_{\overline{\Omega}} M(y, z) dy = 1.$$

In particular, $0 < m_0 \leq M(y, z) \leq m_\infty < +\infty$ for any $(y, z) \in \overline{\Omega} \times \overline{\Omega}$.

3. $K = K(y,z)$ is a C^α positive function $\overline{\Omega}\times\overline{\Omega} \to \mathbb{R}$. In particular, we have $0 < k_0 \leq K(y,z) \leq k_\infty < +\infty$ for any $(y,z) \in \overline{\Omega} \times \overline{\Omega}$.

4. $a = a(y) \in C^\alpha(\overline{\Omega})$ is a non-constant function with $\sup_{y\in\overline{\Omega}} a(y) > 0$. We assume that $a(0) = \sup a$. In particular, $-\infty < \inf a < \sup a < +\infty$ holds.

5. We let $\Omega_0 := \left\{ y \in \overline{\Omega} \,|\, a(y) = a(0) = \sup_{z\in\overline{\Omega}} a(z) \right\}$ be the set of maximal value for a and assume $\Omega_0 \subset\subset \Omega$.

6. $0 < \mu < \sup a - \sup\limits_{z\in\partial\Omega} a^+(z)$.

We are particularly interested in a more restrictive set of assumptions, under which we hope to see a concentration phenomenon in (2.4.1):

Assumption 2.4.3 (Concentration hypothesis)**.** In addition to Assumption 2.4.2, we suppose

$$y \mapsto \frac{1}{\sup_{z\in\Omega} a(z) - a(y)} \in L^1(\Omega).$$

Let us introduce the principal eigenvalue problem that guides our analysis:

Definition 2.4.4 (Principal eigenvalue)**.** We call *principal eigenvalue* associated with (2.4.1) the real number:

$$\lambda_1 := \sup\{\lambda \,|\, \exists \varphi \in C(\overline{\Omega}), \varphi > 0 \text{ s.t. } \mu(M \star \varphi - \varphi) + (a(y) + \lambda)\varphi \leq 0\}. \tag{2.4.8}$$

Clearly, λ_1 is well-defined and we have $\lambda_1 \leq -(\sup a - \mu)$ by evaluating (2.4.8) at $y = 0$. Though we call λ_1 the principal eigenvalue, we stress that λ_1 is not always associated with a usual eigenfunction. In particular, Coville, in his work [119, 118], gives conditions on the coefficients of (2.4.1) under which there exists no associated eigenfunction. We will recall and extend these results in section 2.4.3.1.

Proposition 2.4.5 (On the principal eigenvalue)**.** *Under Assumption 2.4.2, there exists a unique $\lambda \in \mathbb{R}$ such that the equation*

$$\mu(M \star \varphi - \varphi) + (a(y) + \lambda)\varphi = 0 \tag{2.4.9}$$

has a nonnegative nontrivial solution in the sense of measures, and $\lambda = \lambda_1$.

Moreover, under Assumption 2.4.3, there exists $\mu_0 > 0$ such that if $\mu < \mu_0$, we have

$$\lambda_1 = -(\sup a - \mu)$$

and, in this case, there exists a nonnegative measure φ solution to (2.4.9) *with a non-trivial singular part concentrated in Ω_0.*

The most part of Proposition 2.4.5 comes from the work of Coville [118, 119]. Our contribution to the result is the uniqueness of the real number λ such that there exists a nonnegative nontrivial measure solution to (2.4.9). We use this uniqueness result several times in the section 2.4.2.2, in particular, in many of the arguments involving a vanishing viscosity; for instance in the proofs of Theorem 2.4.15 and Theorem 2.4.6.

As well-known in KPP situations, we expect the sign of λ_1 to dictate the long-time persistence of solutions to equation (2.4.1). In particular, when $\lambda_1 > 0$, we expect that any nonnegative solution to the Cauchy problem (2.4.1) starting from a positive bounded initial condition goes to 0 as $t \to \infty$. Indeed, in this case there exists a positive continuous function $\psi > 0$ such that

$$\mu(M \star \psi - \psi) + \left(a + \frac{\lambda_1}{2}\right)\psi \leq 0.$$

One can check that $Ce^{-\frac{\lambda_1}{4}t}\psi(y)$ and $u(t,x,y)$ are respectively a super- and subsolution of the equation

$$u_t = u_{xx} + \mu(M \star u - u) + a(y)u.$$

with ordered initial data (for C large enough). The result is then a consequence of the comparison principle satisfied by the (linear) above equation.

In the $\lambda_1 = 0$ case, we expect extinction as in the $\lambda_1 > 0$ case. This is generally the case for scalar reaction-diffusion equations, as well as in the case of some systems (see in particular [190, Proposition 5.2]).

However, the usual strategy, which consists in establishing a contradiction by studying the least multiple of the principal eigenfunction which lies above the ω-limit set of a solution to (2.4.1), seems difficult to apply here. Indeed we lack three of the main ingredients for this argument: a Harnack inequality, compactness, and a L^∞ bound on the orbit which would allow us to place a multiple of the principal eigenvector above the ω-limit set. Thus, in the present section 2.4, we leave this particular point open. Note however that, in the case where M is symmetric ($M(y,z) = M(z,y)$), an argument similar to the one employed in [67, Section 5] may lead to an actual proof, by working directly on the parabolic problem.

In the present section 2.4 we focus on the $\lambda_1 < 0$ case, in which we expect survival of the population. To confirm this scenario, we first prove the existence of a nonnegative nontrivial stationary state for equation (2.4.1).

Theorem 2.4.6 (Survival of the population)**.** *Let Assumption 2.4.2 hold and assume further $\lambda_1 < 0$. Then, there exists a nonnegative nontrivial stationary state for equation* (2.4.1)*, i.e. a nonnegative nontrivial measure $p \in M^1(\overline{\Omega})$ which satisfies*

$$\mu(M \star p - p) + p(a(y) - K \star p) = 0 \tag{2.4.10}$$

in the sense of measures.

Under the hypothesis for concentration (Assumption 2.4.3) and in the special case where the competition kernel $K(y,z)$ is independent of the trait y, Bonnefon, Coville and Legendre [64] have shown that the solution to (2.4.10) has a singularity concentrated in Ω_0 when μ is small. A key argument was a separation of variables method, allowed by the assumption $K(y,z) = K(z)$. Here we show that the concentration phenomenon occurs under a more general hypothesis on K, namely that the trait $y \in \Omega_0$ suffers less from the competition than any other trait. Since Ω_0 also maximizes the basic reproductive ratio $a(y)$, it seems natural to expect concentration in Ω_0 in this case.

Assumption 2.4.7 (Nonlinear concentration)**.** In addition to Assumption 2.4.3, we suppose that

$$\forall (y,z) \in \overline{\Omega} \times \overline{\Omega}, \quad K(0,z) \leq K(y,z).$$

Theorem 2.4.8 (Concentration on dominant trait)**.** *Let Assumption 2.4.7 hold, and assume $\lambda_1 < 0$. Then, there exists $\mu_0 > 0$ such that, for any $\mu < \mu_0$, the measure p, constructed in Theorem 2.4.6, has a singular part concentrated in Ω_0.*

To better characterize the spatial dynamics of solutions to (2.4.1), we are going to construct traveling waves for (2.4.1).

Definition 2.4.9 (Traveling wave)**.** A *traveling wave* for equation (2.4.1) is a couple (c,u) where $c \in \mathbb{R}$ and u is a locally finite transition kernel (see Definition 2.4.1) defined on $\mathbb{R} \times \overline{\Omega}$. We require that (c,u) satisfies:

$$-cu_x - u_{xx} = \mu(M \star u - u) + u(a - K \star u) \tag{2.4.11}$$

in the sense of distributions, and that the measure u satisfies the limit conditions:

$$\liminf_{\bar{x} \to +\infty} \int_{\mathbb{R} \times \overline{\Omega}} \psi(x + \bar{x}, y) u(dx, dy) > 0, \tag{2.4.12}$$

$$\limsup_{\bar{x} \to -\infty} \int_{\mathbb{R} \times \overline{\Omega}} \psi(x + \bar{x}, y) u(dx, dy) = 0 \tag{2.4.13}$$

for any positive test function $\psi \in C_c(\mathbb{R} \times \overline{\Omega})$.

Condition (2.4.12) differs from the usual behavior of traveling waves as defined, for instance, in [397, 48, 309], in which the convergence to a stationary state is required. Because of the nonlocal competition, indeed, it is very difficult to prove that a solution to equation (2.4.1) converges to a stationary state when $t \to \infty$. Imposing a weak condition like (2.4.12) on the back of the wave is the usual way to go around this issue. One can refer for instance to [46, 7, 65, 190], where a similar condition is imposed on the back of traveling waves.

We are now in the position to state our main result, which concerns the existence of a traveling wave for (2.4.1).

Theorem 2.4.10 (Existence of a traveling wave)**.** *Under Assumption 2.4.2 and if $\lambda_1 < 0$, there exists a traveling wave (c, u) for* (2.4.1) *with $c = c^* := 2\sqrt{-\lambda_1}$.*

As it is the case in many nonlocal problem, the uniqueness and stability of the traveling waves are unknown. In this section 2.4, we focus on the construction of a traveling wave for $c = c^*$. Altough this is expected, we leave the construction of traveling waves for $c > c^*$ for future work, as well as a proof of the non-existence of traveling waves for $c < c^*$. In the general case, it seems very involved to determine whether u has a singular part or not. Nevertheless, there are some particular cases where singular traveling waves do exist.

Remark 2.4.11 (Traveling waves with a singular part)**.** In the special case where K is independent from y ($K(y, z) = K(z)$), a separation of variables argument — see [52] for a related argument— allows us to construct traveling waves that actually have a singular part in $\overline{\Omega}$. From Proposition 2.4.5, under Assumption 2.4.3, there is $\mu_0 > 0$ such that, for any $\mu < \mu_0$, there exists a measure eigenvector $\varphi \in M^1(\overline{\Omega})$ with a singular part concentrated in Ω_0. We choose such a φ with normalization $\int_{\overline{\Omega}} K(z)\varphi(dz) = 1$. If moreover $\lambda_1 < 0$, then there exists a positive front ρ, connecting $-\lambda_1$ to 0, for the Fisher-KPP equation

$$-\rho_{xx} - c\rho_x = \rho(-\lambda_1 - \rho) \tag{2.4.14}$$

for any $c \geq 2\sqrt{-\lambda_1}$. If we define $u(x, dy) := \rho(x)\varphi(dy)$, we see that u matches the definition of a traveling wave. Hence for any $x \in \mathbb{R}$, $u(x, \cdot)$ possesses a singular part concentrated in Ω_0.

The organization of the section 2.4 is as follows. In Section 2.4.3 we study related eigenvalue problems for which concentration may occur. Section 2.4.4 is devoted to the construction of stationary states through a bifurcation method. Last, we construct a (possibly singular) measure traveling wave in Section 2.4.5.

2.4.3 On the principal eigenvalue problem

In this section 2.4.3, we prove Proposition 2.4.5, which allows an approximation by an elliptic Neumann eigenvalue problem in Theorem 2.4.15 of crucial importance for the construction of steady states in Section 2.4.4.

2.4.3.1 The principal eigenvalue of nonlocal operators

Under Assumption 2.4.2, Coville *et al.* [118, 119, 120] have extensively studied the principal eigenvalue problem associated with (2.4.1). We summarize and extend the results in [119]. Our contribution is to show the uniqueness of the principal eigenvalue as a solution to (2.4.9) in the sense of measures.

Theorem 2.4.12 (On the principal eigenproblem (2.4.9))**.** *1. Let Assumption 2.4.2 be satisfied. Then, there exists a unique $\lambda \in \mathbb{R}$ such that* (2.4.9) *admits a nonnegative nontrivial Radon measure solution, and $\lambda = \lambda_1$.*

2. Let Assumption 2.4.3 hold, and let $-\gamma_1$ be the principal eigenvalue[4] of the operator

$$\mathcal{M}[\psi] := \int_\Omega \mu M(y, z) \frac{\psi(z)}{\sup a - a(z)} dz,$$

acting on $\psi \in C_b(\Omega)$. Then the following holds:

(i) $\gamma_1 > 1$ if, and only if, $\lambda_1 < -(\sup a - \mu)$. In this case, any solution to (2.4.9) *in the sense of measures is a pointwise solution.*

(ii) $\gamma_1 = 1$ if, and only if, $\lambda_1 = -(\sup a - \mu)$ and there exists a nonnegative nontrivial function $\varphi \in L^1(\Omega)$ solution to (2.4.9) *almost everywhere. In this case, φ is unique (up to multiplication by a positive constant).*

(iii) $\gamma_1 < 1$ if, and only if, $\lambda_1 = -(\sup a - \mu)$ and there exists a nonnegative singular measure $\varphi \in M^1(\overline{\Omega})$ solution to (2.4.9)*. In this case, any nonnegative nontrivial solution to* (2.4.9) *has a singularity concentrated in Ω_0.*

[4] We use the "minus" sign for consistency between Definition 2.4.4 and the algebraic notion generally used in the Krein-Rutman Theorem : $\mathcal{M}[\Phi] = \gamma_1^1 \Phi$.

Proof. The existence of a measure-valued solution to (2.4.9) has been shown in [119, Theorem 1.2]. Here we focus on the uniqueness of λ. We first prove the uniqueness of λ when the complement of Assumption 2.4.3 holds, by showing that any eigenvector is in fact a continuous eigenfunction. Then, we show that uniqueness holds under Assumption 2.4.3. Finally we prove the trichotomy in item 2.

Step 1: Let the complement of Assumption 2.4.3 hold, i.e. $\frac{1}{\sup a - a(y)} \notin L^1(\Omega)$. Let $\varphi \in M^1(\overline{\Omega})$ be a nonnegative nontrivial Radon measure solution to (2.4.9). Then by the Lebesgue-Radon-Nikodym Theorem [343, Theorem 6.10], there exists a nonnegative $\varphi_{ac} \in L^1(\Omega)$ and a nonnegative measure $\varphi_s \in M^1(\overline{\Omega})$, which is singular with respect to the Lebesgue measure on Ω, such that:

$$\varphi = \varphi_{ac} dy + \varphi_s.$$

Equation (2.4.9) is then equivalent to the following system:

$$\begin{cases} lr\mu M \star \varphi + (a(y) - \mu + \lambda)\varphi_{ac} = 0 \quad a.e.(dy) \\ a(y) - \mu + \lambda = 0 \quad a.e.(\varphi_s). \end{cases} \tag{2.4.15}$$

This readily shows that $(a(y) - \mu + \lambda)\varphi_{ac} = -\mu M \star \varphi$ is a continuous negative function and in particular $\lambda \leq -(\sup a - \mu)$.

We distinguish two cases:

Case 1: Assume first that $\lambda < -(\sup a - \mu)$. Then the second line of (2.4.15) implies $\operatorname{supp} \varphi_s = \varnothing$, i.e. $\varphi_s \equiv 0$. In this case we have $\varphi_{ac}(y) = \frac{\mu M \star \varphi_{ac}(y)}{-\lambda - (a(y) - \mu)}$, which is a positive continuous function since the kernel $M(y, z)$ is itself continuous. A classical comparison argument (such as the one presented below on Step 2 case 1) then shows $\lambda = \lambda_1$.

Case 2: Assume $\lambda = -(\sup a - \mu)$. Then

$$\varphi_{ac}(y) = \frac{\mu M \star \varphi}{\sup a - a(y)},$$

and since $\mu(M \star \varphi)(y) \geq \mu m_0 \int_\Omega \varphi(dz) > 0$, this implies $\varphi_{ac} \notin L^1(\Omega)$, which contradicts the definition of φ_{ac}.

We have thus shown the uniqueness of the real number λ such that there exists a solution (λ, φ) to (2.4.9).

Step 2: Let Assumption 2.4.3 hold. We first establish that γ_1 is well-defined, then resume the proof.

The operator $\mathcal{M}$ defined above is compact by virtue of the Arzelà-Ascoli Theorem [79, Theorem 4.25]. Since for any $\psi \geq 0$, $\psi \not\equiv 0$, we have

$$\begin{aligned} \forall y \in \overline{\Omega}, \quad \mathcal{M}[\psi](y) &= \int_\Omega \mu M(y, z) \frac{\psi(z)}{\sup a - a(z)} dz \\ &\geq \mu m_0 \int_\Omega \frac{\psi(z)}{\sup a - a(z)} dz > 0, \end{aligned}$$

$\mathcal{M}$ satisfies the hypotheses of the Krein-Rutman Theorem [79, Theorem 6.13], which ensures that the real number γ_1, defined by $\mathcal{M}[\Psi] = \gamma_1 \Psi$ for a positive $\Psi \in C_b(\Omega)$, is well-defined and positive.

Let us resume the proof. Let (λ, φ) be a solution to (2.4.9) in the sense of measures. Then, as above, by Lebesgue-Radon-Nikodym Theorem [343, Theorem 6.10], there exists a nonnegative $\varphi_{ac} \in L^1(\Omega)$ and a nonnegative measure $\varphi_s \perp dy$, such that $\varphi = \varphi_{ac} dy + \varphi_s$. In this context, equation (2.4.9) is equivalent to system (2.4.15), and in particular we have $\lambda \leq -(\sup a - \mu)$. We subdivide the rest of the proof in two cases.

1. Let us first assume $\lambda < -(\sup a - \mu)$. Then it follows from equation (2.4.15) that $\varphi_s \equiv 0$. Moreover, $\varphi_{ac}(y) = \frac{\mu(M \star \varphi)(y)}{-\lambda - (a(y) - \mu)}$ is then a positive bounded continuous function and satisfies:

$$\mu(M \star \varphi_{ac} - \varphi_{ac}) + (a(y) + \lambda)\varphi_{ac} = 0$$

in the classical sense.

Let us show that $\lambda = \lambda_1$. Let $(\overline{\lambda}, \overline{\varphi}) \in \mathbb{R} \times C(\Omega)$ be a supersolution to (2.4.9), i.e. $\overline{\varphi} > 0$ and

$$\mu M \star \overline{\varphi} + \overline{\varphi}(a(y) - \mu + \overline{\lambda}) \leq 0.$$

Then $\overline{\varphi}(0)(-a(0)+\mu-\overline{\lambda}) \geq \mu M \star \overline{\varphi} > 0$ and thus $\overline{\lambda} < -(a(0)-\mu) = -(\sup a - \mu)$. Moreover $\overline{\varphi}(y) \geq \frac{\mu M \star \overline{\varphi}(y)}{\mu - a(y) - \overline{\lambda}} \geq \frac{\mu m_0 \int \varphi}{-(\inf a + \overline{\lambda} - \mu)} > 0$ and thus $\overline{\varphi}$ is uniformly bounded from below. In particular, $\alpha := \sup\{\zeta > 0 \,|\, \forall y \in \overline{\Omega}, \zeta\varphi_{ac}(y) \leq \overline{\varphi}(y)\}$ is well-defined and positive. By definition of α we have $\alpha\varphi_{ac}(y) \leq \overline{\varphi}(y)$ for any $y \in \overline{\Omega}$, and there exists a converging sequence $\Omega \ni y_n \to y \in \overline{\Omega}$ such that $\alpha\varphi_{ac}(y_n) - \overline{\varphi}(y_n) \to 0$. Up to further extraction $\varphi_{ac}(y_n)$ converges to a positive limit that we denote $\varphi_{ac}(y)$. We have then

$$\begin{aligned}
0 &\geq \mu \int_{\overline{\Omega}} M(y_n, z)\big(\overline{\varphi}(z) - \alpha\varphi_{ac}(z)\big)dz \\
&\quad + \big(\overline{\varphi}(y_n) - \alpha\varphi_{ac}(y_n)\big)(a(y_n) - \mu) + \overline{\lambda}\overline{\varphi}(y_n) - \lambda\alpha\varphi_{ac}(y_n) \\
&\geq 0 + \big(\overline{\varphi}(y_n) - \alpha\varphi_{ac}(y_n)\big)(a(y_n) - \mu) + \overline{\lambda}\overline{\varphi}(y_n) - \lambda\alpha\varphi_{ac}(y_n) \\
&= (\overline{\lambda} - \lambda)\alpha\varphi_{ac}(y) + o_{n\to\infty}(1).
\end{aligned}$$

Taking the limit $n \to \infty$, we have shown $\overline{\lambda} \leq \lambda$. Hence,

$$\lambda \geq \sup\{\overline{\lambda} \,|\, \exists \psi \in C(\Omega), \psi > 0 \text{ s.t. } \mu(M \star \psi - \psi) + \psi(a(y) + \overline{\lambda}) \leq 0\} = \lambda_1.$$

The reverse inequality $\lambda \leq \lambda_1$ is clear since φ_{ac} is a supersolution to (2.4.9). Thus $\lambda = \lambda_1$.

In this case, we notice that

$$\mathcal{M}[(\sup a - a(y))\varphi_{ac}] = \mu M \star \varphi_{ac} > (\sup a - a(y))\varphi_{ac}.$$

Hence, by a classical comparison argument, $\gamma_1 > 1$.

2. Let us assume now $\lambda = -(\sup a - \mu)$.

We define the auxiliary function $\Psi(y) := \varphi_{ac}(y)(\sup a - a(y)) = \mu(M \star \varphi)$. Then Ψ is a nontrivial positive bounded continuous function which satisfies:

$$\mathcal{M}[\Psi] - \Psi = \mu(M \star \varphi_{ac} - \varphi_{ac}) + (a(y) + \lambda)\varphi_{ac} = -\mu M \star \varphi_s \leq 0.$$

Thus, by a classical comparison argument, $\gamma_1 \leq 1$.

We claim that $\lambda_1 = \lambda$. As above, φ_{ac} is a supersolution to (2.4.9), and thus $\lambda \leq \lambda_1$. Assume by contradiction that $\lambda_1 < \lambda$. By the existence property [119, Theorem 1.1], there exists a continuous function $\varphi_1 > 0$ associated with λ_1. Since $\lambda_1 < \lambda = -(\sup a - \mu)$, point 1 above then applies to (λ_1, φ_1) and we have $\gamma_1 > 1$. This is a contradiction. Hence $\lambda = \lambda_1$.

Step 3: We show (i), (ii), and (iii).

Assume $\lambda_1 < -(\sup a - \mu)$. Then, $\gamma_1 > 1$, and the fact that any measure eigenvector is a continuous eigenfunction has been shown in Step 2.

Assume $\lambda_1 = -(\sup a - \mu)$ and $\varphi_s \equiv 0$. Let $\Psi(y) := (\sup a - a(y))\varphi_{ac}(y)$. Then, by a straightforward computation, Ψ satisfies $\Psi(y) = \mu M \star \varphi(y)$, which shows that Ψ is bounded and continuous. We remark that:

$$\mathcal{M}[\Psi] - \Psi = \mu M \star \varphi_{ac} - (\sup a - a)\varphi_{ac} = -\mu M \star \varphi_s = 0.$$

By the Krein-Rutman Theorem, we have $\gamma_1 = 1$ and $\varphi \equiv \varphi_{ac}$ is unique up to multiplication by a scalar.

Assume that $\lambda_1 = -(\sup a - \mu)$ and $\varphi_s \not\equiv 0$. Let $\Psi(y) := (\sup a - a(y))\varphi_{ac}(y)$, then

$$\mathcal{M}[\Psi] - \Psi = -\mu M \star \varphi_s < 0$$

and thus $\gamma_1 < 1$. Notice that in this case, the second line in equation (2.4.15) implies by definition $\varphi_s\big(\{y \in \overline{\Omega} \,|\, a(y) \neq \sup a\}\big) = 0$, hence supp $\varphi_s \subset \Omega_0$.

Since we have investigated all the possibilities (recall $\lambda \leq -(\sup a - \mu)$), the equivalence holds in each case. This finishes the proof of Theorem 2.4.12. □

2.4.3.2 The critical mutation rate

In this section 2.4.3.2 we investigate further the linear eigenvalue problem (2.4.9), with $\lambda = \lambda_1$ as compelled by Theorem 2.4.12, under Assumption 2.4.3.

We introduce the notion of *critical mutation rate*, which distinguishes between the existence of a bounded continuous eigenfunction for equation (2.4.9) and the existence of a singular measure.

Theorem 2.4.13 (Critical mutation rate)**.** *Let Assumption 2.4.3 hold. Then, there exists a threshold* $\mu_0 = \mu_0(\Omega, M, \sup a - a)$ *such that for any* $0 < \mu < \mu_0$*, problem* (2.4.9) *has only singular measures solutions with a singularity concentrated in* Ω_0 *(in which case* $\lambda_1 = -(\sup a - \mu)$ *from Theorem 2.4.12), whereas for* $\mu > \mu_0$ *equation* (2.4.9) *has only bounded continuous eigenfunctions.*

Finally, $\mu_0 = \frac{1}{\gamma_1^1}$ *where* $-\gamma_1^1$ *is the principal eigenvalue of the operator*

$$\mathcal{M}^1[\psi] = \int_\Omega M(y,z)\frac{\psi(z)}{\sup a - a(z)}dz,$$

acting on bounded continuous functions.

Proof. Let us define, for $\psi \in C_b(\Omega)$, $\mathcal{M}^\mu[\psi] = \mu \int_\Omega M(y,z)\frac{\psi(z)}{\sup a - a(z)}dz$. Then by the Krein-Rutman Theorem there exists a unique principal eigenpair $(-\gamma_1^\mu, \Phi^\mu)$ satisfying $\gamma_1^\mu > 0$, $\Phi^\mu(y) > 0$, $\sup \Phi^\mu = 1$ and $\mathcal{M}^\mu[\Phi^\mu] = \gamma_1^\mu \Phi^\mu$. Since $\mathcal{M}^\mu = \mu\mathcal{M}^1$, we deduce from the uniqueness of $(-\gamma_1^\mu, \Phi^\mu)$ that the equalities $\gamma_1^\mu = \mu\gamma_1^1$ and $\Phi^\mu = \Phi^1$ hold for any $\mu > 0$. The result then follows from the trichotomy in Theorem 2.4.12 □

We can now summarize our findings and prove Proposition 2.4.5.

Proof of Proposition 2.4.5. The first part, under Assumption 2.4.2, follows from Proposition 2.4.12, while the second part, under Assumption 2.4.3, follows from Theorem 2.4.13. □

We prove below that μ_0 is linked to the steepness of the fitness function a near its maximum. This property will be used in the proof of Theorem 2.4.8.

Corollary 2.4.14 (Monotony of μ_0)**.** *Let Assumption 2.4.3 hold and* b *be a continuous function on* $\overline{\Omega}$*, satisfying*

$$\forall y \in \overline{\Omega}, \quad \sup a - a(y) \leq \sup b - b(y).$$

Then we have

$$\mu_0(\Omega, M, \sup a - a) \leq \mu_0(\Omega, M, \sup b - b),$$

where μ_0 *is defined in Theorem 2.4.13.*

Proof. It follows from our assumptions that, for $y \in \overline{\Omega}$:

$$0 < \frac{1}{\sup b - b(y)} \leq \frac{1}{\sup a - a(y)}. \tag{2.4.16}$$

In particular $y \mapsto \frac{1}{\sup b - b(y)} \in L^1(\Omega)$. Thus Theorem 2.4.13 can be applied with both a and b.

We claim that $\gamma_1^b \leq \gamma_1^a$, where γ_1^b, γ_1^a denote the first eigenvalue of the nonlocal operator $\mathcal{M}_b[\psi] = \int_\Omega M(y,z)\frac{\psi(z)}{\sup b - b(z)}dz$ and $\mathcal{M}_a[\psi] = \int_\Omega M(y,z)\frac{\psi(z)}{\sup a - a(z)}dz$ acting on the function $\psi \in C_b(\Omega)$, respectively. Indeed, let $\varphi^a \in C_b(\Omega)$, $\varphi^a > 0$ satisfy $\int_\Omega M(y,z)\frac{\varphi^a(z)}{\sup a - a(z)}dz = \gamma_1^a\varphi^a(y)$ and $\varphi^b \in C_b(\Omega)$, $\varphi^b > 0$ respectively satisfy $\int_\Omega M(y,z)\frac{\varphi^b(z)}{\sup b - b(z)}dz = \gamma_1^b\varphi^b(y)$. Up to multiplication by a positive constant, we assume without loss of generality that $\varphi^b \leq \varphi^a$ and that there exists $y \in \overline{\Omega}$ satisfying $\varphi^b(y) = \varphi^a(y) = 1$. At this point, we have

$$\gamma_1^b = \int_\Omega M(y,z)\frac{\varphi^b(z)}{\sup b - b(z)}dz \leq \int_\Omega M(y,z)\frac{\varphi^a(z)}{\sup a - a(z)}dz = \gamma_1^a.$$

We conclude that

$$\mu_0(\Omega, M, \sup a - a) = \frac{1}{\gamma_1^a} \leq \frac{1}{\gamma_1^b} = \mu_0(\Omega, M, \sup b - b)$$

which finishes the proof of Corollary 2.4.14. □

2.4.3.3 Approximation by a degenerating elliptic eigenvalue problem

Here we show that the previously introduced principal eigenvalue can be approximated by an elliptic Neumann eigenvalue.

Theorem 2.4.15 (Approximating λ_1 by vanishing viscosity)**.** *Let Assumption 2.4.2 hold, and* $(\lambda_1^\varepsilon, \varphi^\varepsilon(y) > 0)$ *be the solution to the principal eigenproblem:*

$$\begin{cases} lr - \varepsilon\Delta\varphi^\varepsilon - \mu(M \star \varphi^\varepsilon - \varphi^\varepsilon) = a(y)\varphi^\varepsilon + \lambda_1^\varepsilon\varphi^\varepsilon \ \text{ in } \Omega \\ \qquad\qquad\qquad\qquad\qquad\qquad \dfrac{\partial\varphi^\varepsilon}{\partial\nu} = 0 \ \text{ on } \partial\Omega, \end{cases} \tag{2.4.17}$$

with $\int_\Omega \varphi^\varepsilon(z)dz = 1$*, where* ν *is the unit normal vector.*

Then $\lim_{\varepsilon\to 0}\lambda_1^\varepsilon = \lambda_1$*, where* λ_1 *is the principal eigenvalue defined by* (2.4.8)*.*

Proof. We divide the proof into three steps.

Step 1: We show that λ_1^ε is bounded when $\varepsilon \to 0$.

Integrating equation (2.4.17) by parts, we have $0 = \int_\Omega(\lambda_1^\varepsilon + a(y))\varphi^\varepsilon dy$. In particular, the function $a(y) + \lambda_1^\varepsilon$ takes both nonnegative and nonpositive values. Hence, we have $-\sup a \le \lambda_1^\varepsilon \le -\inf a$, and $(\lambda_1^\varepsilon)_{\varepsilon>0}$ is bounded.

Step 2: We identify the limit of converging subsequences.

Let $\lambda_1^{\varepsilon_n}$ be a converging sequence and $\lambda_1^0 := \lim\lambda_1^{\varepsilon_n}$. Then φ^{ε_n} satisfies, for any $\psi \in C^2(\overline{\Omega})$,

$$\int_\Omega -\varepsilon_n\varphi^{\varepsilon_n}\Delta\psi dy - \varepsilon_n\int_{\partial\Omega}\varphi^{\varepsilon_n}\frac{\partial\psi}{\partial\nu}dS - \int\mu(M\star\varphi^{\varepsilon_n} - \varphi^{\varepsilon_n})\psi - a(y)\varphi^{\varepsilon_n}\psi = \lambda_1^{\varepsilon_n}\int\varphi^{\varepsilon_n}\psi.$$

Let

$$F_0 := \left\{\psi \in C^2(\overline{\Omega}) \,|\, \forall y \in \partial\Omega, \frac{\partial\psi}{\partial\nu}(y) = 0\right\} \tag{2.4.18}$$

denote the space of functions in $C^2(\Omega)$ with zero boundary flux as in Lemma 2.4.35 item (i). For $\psi \in F_0$, this equation becomes:

$$\int_\Omega -\varepsilon_n\varphi^{\varepsilon_n}\Delta\psi dy - \int\mu(M\star\varphi^{\varepsilon_n} - \varphi^{\varepsilon_n})\psi - a(y)\varphi^{\varepsilon_n}\psi = \lambda_1^{\varepsilon_n}\int\varphi^{\varepsilon_n}\psi.$$

Since $\int_\Omega\varphi^{\varepsilon_n}(y)dy = 1$ and $\overline{\Omega}$ is compact and by Prokhorov's Theorem [63, Theorem 8.6.2], the sequence $(\varphi^{\varepsilon_n})$ is precompact for the weak topology in $M^1(\overline{\Omega})$, and there exists a weakly convergent subsequence $\varphi^{\varepsilon_n'}$, which converges to a nonnegative Radon measure φ. Since $1 \in C_c(\overline{\Omega})$, we have $\lim\int_{\overline{\Omega}}\varphi^{\varepsilon_n'} = \int_{\overline{\Omega}}\varphi(dy) = 1$. Hence φ is non-trivial. Moreover, we have

$$\mu\int_\Omega\int_\Omega M(y,z)d\varphi(z)\psi(y)dy + \int_\Omega(a(y)-\mu)\psi(y)d\varphi(y) + \lambda_1^0\int_\Omega\psi(y)d\varphi(y) = 0 \tag{2.4.19}$$

for any test function $\psi \in F_0$. Since F_0 is densely embedded in $C_b(\overline{\Omega})$ by Lemma 2.4.35, (2.4.19) holds for any $\psi \in C_b(\overline{\Omega})$. Applying Proposition 2.4.5, we have then $\lambda_1^0 = \lambda_1$.

Step 3: Conclusion.

We have shown that for any sequence $\varepsilon_n \to 0$, there exists a subsequence $\varepsilon_n' \to 0$ such that $\lambda_1^{\varepsilon_n'} \to \lambda_1$. Thus $\lambda_1^\varepsilon \to \lambda_1$ when $\varepsilon \to 0$. □

2.4.4 Stationary states in trait

This section 2.4.4 deals with stationary states for (2.4.1). In particular, we prove Theorem 2.4.6 and Theorem 2.4.8 via a bifurcation argument.

2.4.4.1 Regularized solutions

We investigate the existence of positive solutions $p = p(y)$ to the following problem

$$\begin{cases} ll - \varepsilon\Delta p - \mu(M \star p - p) = p(a(y) - K \star p - \beta p) \text{ in } \Omega \\ \qquad\qquad\qquad\qquad\qquad\qquad \dfrac{\partial p}{\partial \nu} = 0 \text{ on } \partial\Omega, \end{cases} \tag{2.4.20}$$

for any $\beta \geq 0$. We prove the existence of positive solutions for (2.4.20) when $\lambda_1^\varepsilon < 0$. We plan to let $\varepsilon \to 0$ with $\beta = 0$ in Section 2.4.4.2, in order to prove the existence of stationary solutions to (2.4.1). The reason why we include a weight $\beta \geq 0$ on the competition term in equation (2.4.20) is that solutions to the latter will be used as subsolutions in the construction of traveling waves in Section 2.4.5.

Throughout this section 2.4.4.1 we denote $(\lambda_1^\varepsilon, \varphi^\varepsilon)$ the eigenpair of the regularized problem, solving (2.4.17). Notice that $(\lambda_1^\varepsilon, \varphi^\varepsilon)$ is independent from β. Our main result is the following:

Theorem 2.4.16 (Regularized steady states)**.** *Let Assumption 2.4.2 hold, $\varepsilon > 0$, $(\lambda_1^\varepsilon, \varphi^\varepsilon)$ be defined by* (2.4.17)*, and $\beta \geq 0$.*

(i) Assume $\lambda_1^\varepsilon > 0$. Then 0 is the only nonnegative solution to (2.4.20)*.*

(ii) Assume $\lambda_1^\varepsilon < 0$. Then there exists a positive solution to (2.4.20) *for any $\beta \geq 0$.*

Item (i) is rather trivial and we will discuss it later in the proof of Theorem 2.4.16. The actual construction in the case $\lambda_1^\varepsilon < 0$ is more involved. Our method is inspired by the similar situation in [P3]. We start by establishing *a priori* estimates on the solutions p to (2.4.20).

Lemma 2.4.17 (*A priori* estimates on p)**.** *Let Assumption 2.4.2 hold, let $\varepsilon > 0$, $\beta \geq 0$ and p be a nonnegative nontrivial solution to* (2.4.20)*. Then:*

(i) p is positive.

(ii) If $\beta = 0$, there exists a positive constant $C = C(\Omega, \varepsilon, \mu, \|a\|_{L^\infty}, m_\infty, k_0, k_\infty)$ such that $\|p\|_{L^\infty} \leq C$. If $\beta > 0$ then we have $\sup p \leq \frac{\sup a}{\beta}$.

Proof. Point (i) follows from the strong maximum principle. We turn our attention to point (ii).

Assume first $\beta > 0$. Let $y \in \overline{\Omega}$ such that $p(y) = \sup_{z\in\Omega} p(z)$ and assume by contradiction that $p(y) > \frac{\sup a}{\beta}$. If $y \in \Omega$, then we have

$$0 \leq -\varepsilon\Delta_y p(y) - \mu(M \star p - p) = p(a(y) - K \star p - \beta p) < 0$$

which is a contradiction. If $y \in \partial\Omega$, then $\mu(M \star p - p) \leq 0$ and $a - K \star p - \beta p \leq 0$ in a neighbourhood of y, and thus $-\varepsilon\Delta p - (a(y) - K \star p - \beta p)p \leq 0$ in a neighbourhood of y. It follows from Hopf's Lemma that $\frac{\partial p}{\partial \nu}(y) > 0$, which contradicts the Neumann boundary conditions satisfied by p. Hence $\sup p \leq \frac{\sup a}{\beta}$.

We turn our attention to the case $\beta = 0$, which is more involved. We divide the proof in four steps.

Step 1: We establish a bound on $\int_\Omega p(y)dy$.

Integrating over Ω, we have

$$\int_\Omega a(y)p(y)\mathrm{d}y - \int_\Omega\int_\Omega p(y)K(y,z)p(z)\mathrm{d}y\mathrm{d}z = \beta\int_\Omega p^2(y)dy \geq 0.$$

Thus $\int a(y)p(y)dy \geq k_0\left(\int_\Omega p(y)dy\right)^2$ and

$$\int_\Omega p(y)dy \leq \frac{\sup a}{k_0}. \tag{2.4.21}$$

Step 2: We reduce the problem to a boundary estimate.

By a direct application of the local maximum principle [187, Theorem 9.20], for any ball $B_R(y) \subset \Omega$, there exists a constant $C = C(R, \varepsilon, \|a\|_{L^\infty}, k_0, k_\infty, \mu, m_\infty) > 0$ such that $\sup_{B_{R/2}(y)} p \leq C$. This shows an interior bound for any point at distance R from $\partial\Omega$.

To show that this estimate does not degenerate near the boundary, we use a coronation argument. Let $d(y, \partial\Omega) := \inf_{z\in\partial\Omega} |y - z|$, and

$$\Omega_R := \{y \in \Omega \,|\, d(y, \partial\Omega) < R\}$$

for any $R > 0$. As noted in [172], the function $y \mapsto d(y, \partial\Omega)$ has C^3 regularity on a tubular neighbourhood of $\partial\Omega$. In particular, $\partial\Omega_R\backslash\partial\Omega$ is C^3 for R small enough, since $\nabla d \neq 0$ in this neighbourhood. Moreover, by the comparison principle in narrow domains [47, Proposition 1.1], the maximum principle holds for the operator $-\varepsilon\Delta v - (a(y) - \mu)v$ in Ω_R provided $|\Omega_R|$ is small enough, meaning that if v satisfies $-\varepsilon\Delta v - (a(y) - \mu)v \geq 0$ in Ω_R and $v \geq 0$ on $\partial\Omega_R$, then $v \geq 0$. In particular, we choose R small enough for this property to hold.

At this point, $p \leq C$ in $\Omega\backslash\Omega_R$ and comparison holds in Ω_R.

Step 3: We construct a supersolution.

Notice that, in contrast with [7] where Dirichlet boundary conditions are used, we need an additional argument to deal with the Neumann boundary conditions. Since the comparison principle holds in the narrow domain Ω_R, the Fredholm alternative implies that, for any $\delta \in (0, 1]$, there exists a unique (classical) solution to the system:

$$\begin{cases} ll - \varepsilon\Delta v^\delta - (a(y) - \mu)v^\delta = \mu m_\infty \dfrac{\sup a}{k_0} \text{ in } \Omega_R \\ \qquad\qquad\qquad\qquad\qquad\qquad v^\delta = C \text{ on } \partial\Omega_R\backslash\partial\Omega \\ \qquad\qquad\qquad\qquad \delta v^\delta + (1 - \delta)\dfrac{\partial v^\delta}{\partial\nu} = \delta \text{ on } \partial\Omega. \end{cases}$$

As a result of the classical Schauder interior and boundary estimates, the mapping $\delta \mapsto v^\delta$ is continuous from $(0, 1]$ to $C_b(\Omega_R)$. Moreover, v^δ is positive for $\delta \in (0, 1]$ by virtue of the maximum principle.

Next, still by a direct application of the Schauder estimates, $(v^\delta)_{0<\delta\leq 1}$ is precompact and there exists a sequence $\delta_n \to 0$ and $v \in C^2$ such that $v^{\delta_n} \to v$ in $C^2_{loc}(\Omega_R) \cap C^1(\overline{\Omega}_R)$. Then $v \geq 0$ satisfies:

$$\begin{cases} ll - \varepsilon\Delta v - (a(y) - \mu)v = \mu m_\infty \dfrac{\sup a}{k_0} \text{ in } \Omega_R \\ \qquad\qquad\qquad\qquad\qquad\qquad v = C \text{ on } \partial\Omega_R\backslash\partial\Omega \\ \qquad\qquad\qquad\qquad\qquad\qquad \dfrac{\partial v}{\partial\nu} = 0 \text{ on } \partial\Omega. \end{cases}$$

By a direct application of the strong maximum principle and Hopf's Lemma, we have $v > 0$ on $\overline{\Omega}_R$.

Step 4: We show that $p \leq v$ on Ω_R.

Let p be a solution to (2.4.20) and select $\alpha := \inf\{\zeta > 0 \,|\, \zeta v \geq p \text{ in } \Omega_R\}$.

Assume by contradiction that $\alpha > 1$. Then there exists $y_0 \in \overline{\Omega}_R$ such that the equality $p(y_0) = \alpha v(y_0)$ holds, and $\alpha v - p \geq 0$. In particular y_0 is a zero minimum for the function $\alpha v - p$. Because of the boundary conditions satisfied by p and v, y_0 cannot be in $\partial\Omega_R$. y_0 is then an interior local minimum to $\alpha v - p$ and thus

$$\begin{aligned} 0 \geq -\varepsilon\Delta(\alpha v - p)(y_0) &= (a(y_0) - \mu)(\alpha v - p)(y_0) + \alpha\mu m_\infty \frac{\sup a}{k_0} \\ &\quad - \mu(M \star p)(y_0) + p(y_0)(K \star p)(y_0) \\ &> \alpha\mu m_\infty \frac{\sup a}{k_0} - \mu(M \star p)(y_0) \geq 0, \end{aligned}$$

using estimate (2.4.21), which is a contradiction. Thus $\alpha \leq 1$.

This shows that $p \leq v$. Since v is a bounded function, we have our uniform bound for p in Ω_R. In $\Omega\backslash\Omega_R$, we have $p \leq C$. This ends the proof of Lemma 2.4.17. □

In order to proceed to the proof of Theorem 2.4.16, we yet need an additional technical remark.

Lemma 2.4.18 (Fréchet differentiability at 0)**.** *Let Assumption 2.4.2 hold, $\beta \geq 0$ and*

$$\begin{array}{rccc} G: & C_b(\Omega) & \to & C_b(\Omega) \\ & p(y) & \mapsto & p(y)(K \star p)(y) + \beta p^2(y), \end{array}$$

then G is Fréchet differentiable at $p = 0$ and its derivative is $DG(p) = 0$.

Proof. This comes from the remark

$$\left|\int_\Omega K(y,z)p(z)dzp(y)+p^2(y)\right| \le \int_\Omega K(y,z)|p(z)|dz|p(y)| + \beta p^2(y)$$
$$\le k_\infty|\Omega|\|p\|^2_{C_b(\Omega)} + \beta\|p\|^2_{C_b(\Omega)} \qquad \square$$

Proof of Theorem 2.4.16. **Step 1:** We prove item (i).

We assume $\lambda_1^\varepsilon > 0$. We recall that $(\lambda_1^\varepsilon, \varphi^\varepsilon)$ is the solution to (2.4.17) with the normalization $\int_\Omega \varphi^\varepsilon(y)dy = 1$. Let $p > 0$ be a nonnegative solution to (2.4.20) in Ω. Since p is bounded and φ^ε is positive on $\overline{\Omega}$, the quantity $\alpha := \inf\{\zeta > 0 \,|\, \zeta\varphi^\varepsilon > p\}$ is well-defined and finite. Then, there exists $y_0 \in \overline{\Omega}$ such that $p(y_0) = \alpha\varphi^\varepsilon(y_0)$. Remark that y_0 is a minimum to the nonnegative function $\alpha\varphi^\varepsilon - p$. If $y_0 \in \partial\Omega$, then Hopf's Lemma implies $\frac{\partial(\alpha\varphi^\varepsilon - p)}{\partial\nu}(y_0) < 0$, which contradicts the Neumann boundary conditions satisfied by p and φ^ε. Thus $y_0 \in \Omega$. Evaluating equation (2.4.20), we have:

$$\begin{aligned} 0 \ge -\varepsilon\Delta(\alpha\varphi^\varepsilon - p)(y_0) &= \mu\big(M\star(\alpha\varphi^\varepsilon - p) - (\alpha\varphi^\varepsilon - p)\big) \\ &\quad + a(y_0)\big(\alpha\varphi^\varepsilon(y_0) - p(y_0)\big) + p(y_0)(K\star p)(y_0) + \beta p^2(y_0) + \lambda_1^\varepsilon\alpha\varphi^\varepsilon \\ &\ge p(y_0)(K\star p)(y_0) + \beta p^2(y_0) + \lambda_1^\varepsilon\alpha\varphi^\varepsilon > 0 \end{aligned}$$

which is a contradiction.

Step 2 : We prove item (ii).

We assume $\lambda_1^\varepsilon < 0$. We argue as in [P3]: if the nonlinearity is negligible near 0 and we can prove local boundedness of the solutions in L^∞, then we can prove existence through a bifurcation argument. This requires a topological result stated in Appendix 2.4.5.6.

More precisely, for $\alpha \in \mathbb{R}$ and $p \in C_b(\Omega)$, we let $F(\alpha, p) = \tilde{p}$ where $\tilde{p}$ is the unique solution to:

$$\begin{cases} ll - \varepsilon\Delta\tilde{p} + (\sup a - a(y))\tilde{p} - \mu(M\star\tilde{p} - \tilde{p}) = \alpha p - G(p) \text{ in } \Omega \\ \qquad\qquad\qquad\qquad\qquad\qquad\qquad\qquad \dfrac{\partial\tilde{p}}{\partial\nu} = 0 \text{ on } \partial\Omega \end{cases}$$

where G is as in Lemma 2.4.18. Notice that $\sup a - a(y) \ge 0$, so comparison applies and the operator F is well-defined due to the Fredholm alternative. In particular, for each $\alpha \in \mathbb{R}$, $F(\alpha, \cdot)$ is Fréchet differentiable near 0 and its derivative is the linear operator αT, where $Tp = \tilde{p}$ and $\tilde{p}$ is defined by:

$$\begin{cases} ll - \varepsilon\Delta\tilde{p} + (\sup a - a(y))\tilde{p} - \mu(M\star\tilde{p} - \tilde{p}) = p \text{ in } \Omega \\ \qquad\qquad\qquad\qquad\qquad\qquad\qquad\qquad \dfrac{\partial\tilde{p}}{\partial\nu} = 0 \text{ on } \partial\Omega. \end{cases}$$

Let $C := \{p \in C_b(\Omega) \,|\, p \ge 0\}$. By a classical comparison argument, T maps the cone $C\backslash\{0\}$ into $Int\ C = \{p \in C_b(\Omega) \,|\, p > 0\}$. By virtue of the Krein-Rutman Theorem [79, Theorem 6.13], T has a *first*[5] eigenvalue $\lambda(T)$ (satisfying $T\psi = \lambda(T)\psi$ for a $\psi > 0$) and we have the formula $\lambda(T) = \frac{1}{\lambda_1^\varepsilon + \sup a}$.

We now check one by one the hypotheses of Theorem 2.4.36:

1. Clearly we have $F(\alpha, 0) = 0$ for any $\alpha \in \mathbb{R}$.

2. It follows from Lemma 2.4.18 that G is Fréchet differentiable near 0 with derivative 0. As a consequence, $F(\alpha, \cdot)$ is Fréchet differentiable near 0 with derivative αT.

3. T satisfies the hypotheses of the Krein-Rutman Theorem.

4. It follows from Lemma 2.4.17 that the solutions to $F(\alpha, p) = p$ are locally uniformly bounded in α.

5. Since any nontrivial nonnegative fixed point p is positive, there is no nontrivial fixed point in the boundary of C.

Thus, applying Theorem 2.4.36, there exists a branch of solutions $\mathcal{C}$ connecting $\alpha = \frac{1}{\lambda(T)}$ to either $\alpha \to +\infty$ or $\alpha \to -\infty$.

By the uniqueness in the Krein-Rutman Theorem, if λ^α denotes the principal eigenvalue associated with $F(\alpha, p) = p$, we have $\lambda^\alpha = \lambda_1^\varepsilon + \sup a - \alpha = \frac{1}{\lambda(T)} - \alpha$. In particular, for $\alpha < -\sup a - \lambda_1^\varepsilon$, we deduce from Step 1 that there cannot exist a solution to $F(\alpha, p) = p$ in C. Thus $\mathcal{C}$ connects $\frac{1}{\lambda(T)}$ to $+\infty$. In particular, there exists a positive solution for $\alpha = \sup a = \frac{1}{\lambda(T)} - \lambda_1^\varepsilon > \frac{1}{\lambda(T)}$, which solves (2.4.20). This ends the proof of Theorem 2.4.16. $\square$

[5] We stress that this *first* eigenvalue is *not* the *principal* eigenvalue of the problem $F(\alpha, p) = p$, but the algebraic eigenvalue.

We now prove a lower estimate for solutions to (2.4.20), which is crucial for the construction of traveling waves, but will not be used in the meantime. We stress that in the lemma below, the constant ρ_β is independent from ε.

Lemma 2.4.19 ($p^{\varepsilon,\beta}$ does not vanish)**.** *Let Assumption 2.4.2 be satisfied, let $\beta > 0$ and $\lambda_1 < 0$. Let finally $p^{\varepsilon,\beta}$ be a solution to* (2.4.20)*. Then, there exists constants $\varepsilon_0 = \varepsilon_0(\Omega, \mu, M, a) > 0$ and $\rho_\beta = \rho_\beta(\Omega, M, a, \beta) > 0$ such that if $\varepsilon \leq \varepsilon_0$, then*

$$\inf_\Omega p^{\varepsilon,\beta} \geq \rho_\beta.$$

Proof. This proof is inspired by the one of [120, Lemma 5.2].

Step 1: Setting of an approximating eigenvalue problem.

Here we introduce an approximating eigenvalue problem, that will be used to estimate from below the solutions to (2.4.20).

Let $\delta > 0$, $\varepsilon > 0$, $a^\delta(y) := \min(a(y), \sup a - \delta)$ and $(\lambda^{\delta,\varepsilon}, \varphi^{\delta,\varepsilon})$ be the principal eigenpair solving the problem

$$\begin{cases} ll\varepsilon\Delta\varphi^{\delta,\varepsilon} + \mu(M \star \varphi^{\delta,\varepsilon} - \varphi^{\delta,\varepsilon}) + (a^\delta(y) + \lambda^{\delta,\varepsilon})\varphi^{\delta,\varepsilon} = 0 \text{ in } \Omega \\ \dfrac{\partial \varphi^{\delta,\varepsilon}}{\partial \nu} = 0 \text{ on } \partial\Omega, \end{cases} \tag{2.4.22}$$

with $\int_\Omega \varphi^{\delta,\varepsilon}(y)dy = 1$. It follows from Theorem 2.4.15 that $\lambda^{\delta,\varepsilon}$ converges to the principal eigenvalue $\lambda^{\delta,0}$ of the operator $\psi \mapsto \mu(M \star \psi - \psi) + a^\delta(y)\psi$ when $\varepsilon \to 0$. $\lambda^{\delta,0}$, in turn, converges to λ_1 when $\delta \to 0$ by Lipschitz continuity [118, Proposition 1.1]. Thus we may approximate λ_1 by $\lambda^{\delta,\varepsilon}$ for $\delta > 0$ and $\varepsilon > 0$ small enough.

Since $y \mapsto \frac{1}{\sup a^\delta - a^\delta(y)} \notin L^1(\Omega)$, it follows from [118, Theorem 1.1] (which can be adapted in our context; see [119]) that there exists a continuous eigenfunction associated with $\lambda^{\delta,0}$. In this case [119, Theorem 1.1] shows the strict upper bound $\lambda^{\delta,0} < -\sup a^\delta + \mu = -\sup a + \delta + \mu$.

In what follows we fix the real number $\delta > 0$ small enough so that the inequality

$$\delta < \frac{1}{2}\min\left(\mu, \sup a - \inf a, \sup a - \sup_{\partial\Omega} a^+ - \mu\right)$$

holds, together with $\lambda^{\delta,0} \leq \frac{3\lambda_1}{4}$. We define $\eta := -\lambda^{\delta,0} - \sup a + \delta + \mu > 0$. Since $\lambda^{\delta,\varepsilon} \to \lambda^{\delta,0}$ as $\varepsilon \to 0$, we fix $\varepsilon_0 > 0$ such that for any $0 < \varepsilon < \varepsilon_0$, $|\lambda^{\delta,\varepsilon} - \lambda^{\delta,0}| \leq \frac{-\lambda_1}{4}$, and $\lambda^{\delta,\varepsilon} \leq \lambda^{\delta,0} + \frac{\eta}{2}$.

Finally, integrating equation (2.4.22), we have $0 = \int_\Omega (a^\delta(y) + \lambda^{\delta,\varepsilon})\varphi^{\delta,\varepsilon}(y)dy$, thus the function $a^\delta(y) + \lambda^{\delta,\varepsilon}$ takes nonpositive and nonnegative values. This shows

$$\inf a = \inf a^\delta \leq -\lambda^{\delta,\varepsilon} \leq \sup a^\delta = \sup a - \delta.$$

Step 2: Estimates from above and from below of $\varphi^{\delta,\varepsilon}$.

Let us establish some upper and lower bounds for $\varphi^{\delta,\varepsilon}$. Since $\varphi^{\delta,\varepsilon}$ is continuous on $\overline{\Omega}$, there exists $y_0 \in \overline{\Omega}$ such that $\varphi^{\delta,\varepsilon}(y_0) = \inf_{z\in\overline{\Omega}} \varphi^{\delta,\varepsilon}(z)$. If $y_0 \in \partial\Omega$, then it follows from Hopf's Lemma that $\frac{\partial\varphi^{\delta,\varepsilon}}{\partial\nu}(y_0) < 0$, which contradicts the Neumann boundary conditions satisfied by $\varphi^{\delta,\varepsilon}$ (recall that $a(y_0) + \lambda^{\delta,\varepsilon} < 0$ for $y_0 \in \partial\Omega$). We conclude that $y_0 \in \Omega$. Thus we can evaluate equation (2.4.22):

$$\begin{aligned} 0 \geq -\varepsilon\Delta\varphi^{\delta,\varepsilon}(y_0) &= \mu\left(M \star \varphi^{\delta,\varepsilon} - \varphi^{\delta,\varepsilon}\right) + \left(a^\delta(y_0) + \lambda^{\delta,\varepsilon}\right)\varphi^{\delta,\varepsilon}, \\ (\sup a - \inf a + \mu)\varphi^{\delta,\varepsilon}(y_0) &\geq \left(-\lambda^{\delta,\varepsilon} - a^\delta(y_0) + \mu\right)\varphi^{\delta,\varepsilon}(y_0) \geq \mu m_0 \int_\Omega \varphi^{\delta,\varepsilon}, \\ \min_{z\in\Omega} \varphi^{\delta,\varepsilon}(z) &\geq \frac{\mu m_0}{\sup a - \inf a + \mu}. \end{aligned}$$

Similarly, there exists $y_0 \in \Omega$ such that $\varphi^{\delta,\varepsilon}(y_0) = \max_{z\in\Omega} \varphi^{\delta,\varepsilon}(z)$. Evaluating equation (2.4.22), we get (recalling $a^\delta(y_0) - \mu + \lambda^{\delta,\varepsilon} \leq -\frac{\eta}{2} < 0$):

$$\begin{aligned} 0 \leq -\varepsilon\Delta\varphi^{\delta,\varepsilon} &= \mu M \star \varphi^{\delta,\varepsilon} + \left(a^\delta(y_0) - \mu + \lambda^{\delta,\varepsilon}\right)\varphi^{\delta,\varepsilon}(y_0), \\ \frac{\eta}{2}\varphi^{\delta,\varepsilon} &\leq \mu m_\infty \int_\Omega \varphi^{\delta,\varepsilon} = \mu m_\infty, \\ \max_{z\in\Omega} \varphi^{\delta,\varepsilon}(z) &\leq 2\frac{\mu m_\infty}{\eta}. \end{aligned}$$

Hence, for $0 < \varepsilon \leq \varepsilon_0$ and $y_0 \in \Omega$, we have shown that

$$\frac{\mu m_0}{\sup a - \inf a + \mu} \leq \varphi^{\delta,\varepsilon}(y_0) \leq 2\frac{\mu m_\infty}{\eta}.$$

Step 3: Lower estimate for $p^{\varepsilon,\beta}$.

We are now in a position to derive a lower bound for $p^{\varepsilon,\beta}$. Since $p^{\varepsilon,\beta} > 0$ in $\overline{\Omega}$, we can define $\alpha := \sup\left\{\zeta > 0 \,|\, \forall y \in \Omega, \zeta\varphi^{\delta,\varepsilon}(y) \leq p^{\varepsilon,\beta}(y)\right\}$.

Assume by contradiction that $\alpha < \alpha_0 := \min\left(\frac{m_0\eta}{2k_\infty m_\infty}, \frac{-\lambda^{\delta,\varepsilon}\eta}{2\beta\mu m_\infty + \eta k_\infty}\right)$. By definition of α there exists $y_0 \in \overline{\Omega}$ such that $\alpha\varphi^{\delta,\varepsilon}(y_0) = p(y_0)$. Assume $y_0 \in \partial\Omega$, then it follows from Hopf's Lemma that $\frac{\partial(p^{\varepsilon,\beta} - \alpha\varphi^{\delta,\varepsilon})}{\partial\nu}(y_0) < 0$, which contradicts the Neumann boundary conditions satisfied by $p^{\varepsilon,\beta}$ and $\varphi^{\delta,\varepsilon}$. Thus $y_0 \in \Omega$. We have:

$$\begin{aligned}
0 \geq -\varepsilon\Delta(p^{\varepsilon,\beta} - \alpha\varphi^{\delta,\varepsilon})(y_0) &= \mu\left(M \star (p^{\varepsilon,\beta} - \alpha\varphi^{\delta,\varepsilon}) - (p^{\varepsilon,\beta} - \varphi^{\delta,\varepsilon})\right) \\
&\quad + p^{\varepsilon,\beta}\big(a(y_0) - K \star p^{\varepsilon,\beta} - \beta p^{\varepsilon,\beta}\big) - \big(\lambda^{\delta,\varepsilon} + a^\delta(y_0)\big)\alpha\varphi^{\delta,\varepsilon} \\
&= \int_\Omega \big(\mu M(y_0,z) - \alpha\varphi^{\delta,\varepsilon}(y_0)K(y_0,z)\big)\big(p^{\varepsilon,\beta}(z) - \alpha\varphi^{\delta,\varepsilon}(z)\big)dz \\
&\quad - \alpha\varphi^{\delta,\varepsilon}(y_0)\int_\Omega K(y_0,z)\big(\alpha\varphi^{\delta,\varepsilon}(z)\big)dz \\
&\quad + \alpha\varphi^{\delta,\varepsilon}\big(a(y_0) - a^\delta(y_0)\big) - \beta\left(p^{\varepsilon,\beta}\right)^2 - \lambda^{\delta,\varepsilon}\alpha\varphi^{\delta,\varepsilon}(y_0).
\end{aligned}$$

By definition, $\mu M(y_0,z) - \alpha\varphi^{\delta,\varepsilon}(y_0)K(y_0,z) \geq \mu m_0 - k_\infty\frac{m_0\eta}{2k_\infty m_\infty}\frac{2\mu m_\infty}{\eta} = 0$ for any $z \in \Omega$, and thus, recalling $a(y_0) \geq a^\delta(y_0)$,

$$0 \geq -\alpha\lambda^{\delta,\varepsilon}\varphi^{\delta,\varepsilon}(y_0) - \alpha^2\varphi^{\delta,\varepsilon}(y_0)\left(\beta\varphi^{\delta,\varepsilon} + \int_\Omega K(y_0,z)\varphi^{\delta,\varepsilon}(z)dz\right),$$

$$\left(2\beta\frac{\mu m_\infty}{\eta} + k_\infty\right)\alpha \geq \alpha\left(\beta\varphi^{\delta,\varepsilon}(y_0) + \int_\Omega K(y_0,z)\varphi^{\delta,\varepsilon}(z)dz\right) \geq -\lambda^{\delta,\varepsilon},$$

which is a contradiction since $\alpha < \alpha_0 = \min\left(\frac{m_0\eta}{2k_\infty m_\infty}, \frac{-\lambda^{\delta,\varepsilon}\eta}{2\beta\mu m_\infty + \eta k_\infty}\right)$.

We conclude that $\alpha \geq \alpha_0$ and thus (recalling $\lambda^{\delta,\varepsilon} \leq \frac{\lambda_1}{2}$)

$$\begin{aligned}
\min_{y\in\Omega} p^{\varepsilon,\beta}(y) &\geq \alpha_0 \min_{y\in\Omega}\varphi^{\delta,\varepsilon}(y) \\
&\geq \min\left(\frac{m_0\eta}{2k_\infty m_\infty}, \frac{(-\lambda_1)\eta}{4\beta\mu m_\infty + 2\eta k_\infty}\right)\frac{\mu m_0}{\sup a - \inf a + \mu} > 0.
\end{aligned}$$

Since this lower bound is independent from ε, this ends the proof of Lemma 2.4.19. □

2.4.4.2 Construction of a stationary solution at $\varepsilon = 0$

In this section 2.4.4.2 we assume $\lambda_1 < 0$. Then, Theorem 2.4.16 guarantees the existence of a positive solution to (2.4.20) for ε small enough, since $\lambda_1^\varepsilon \to \lambda_1$ as $\varepsilon \to 0$ (recall Theorem 2.4.15). In this context, we expect the solution constructed in Theorem 2.4.16 with $\beta = 0$ to converge weakly to a (possibly singular) Radon measure, solution to (2.4.10). Here we prove this result, and complete the proof of Theorem 2.4.6. In particular, in this section 2.4.4.2 we assume $\beta = 0$.

Before we can prove Theorem 2.4.6, we need a series of estimates on the previously constructed solutions $p^\varepsilon := p^{\varepsilon,0}$.

Lemma 2.4.20 (Estimates on the mass)**.** *Let Assumption 2.4.2 hold, let $\varepsilon > 0$, $\lambda_1^\varepsilon < 0$, and p^ε be a solution to equation* (2.4.20) *with $\beta = 0$. Then*

$$\frac{-\lambda_1^\varepsilon}{k_\infty} \leq \int_\Omega p^\varepsilon(y)dy \leq \frac{\sup a}{k_0}. \tag{2.4.23}$$

Proof. The upper bound in equation (2.4.23) has been established in Lemma 2.4.17. We turn our attention to the lower estimate.

We assume by contradiction that $\lambda_1^\varepsilon + k_\infty \int_\Omega p^\varepsilon(y)dy < 0$. Let $(\lambda_1^\varepsilon, \varphi^\varepsilon > 0)$ be the solution to the eigenproblem (2.4.17), normalized with $\int \varphi^\varepsilon = 1$. Then, we define the real number $\alpha := \sup\{\zeta > 0 \,|\, \forall y \in \Omega, \zeta\varphi^\varepsilon \le p^\varepsilon\} > 0$, which is then well-defined since $p^\varepsilon > 0$ and φ^ε is bounded.

By definition of α we have $\alpha\varphi^\varepsilon \le p^\varepsilon$ and there exists a point $y_0 \in \overline{\Omega}$ such that $p^\varepsilon(y_0) = \alpha\varphi^\varepsilon(y_0)$. If $y_0 \in \partial\Omega$, since y_0 is a maximum point for the function $\alpha\varphi^\varepsilon - p^\varepsilon$, then it follows from Hopf's Lemma that $\frac{\partial \alpha\varphi^\varepsilon - p^\varepsilon}{\partial \nu}(y_0) > 0$, which contradicts the Neumann boundary conditions satisfied by p^ε and φ^ε. Thus $y_0 \in \Omega$ and we compute

$$\begin{aligned} 0 &\le -\mu\big(M \star (\alpha\varphi^\varepsilon - p^\varepsilon) - (\alpha\varphi^\varepsilon - p^\varepsilon)\big) - \varepsilon\Delta(\alpha\varphi^\varepsilon - p^\varepsilon) \\ &= \lambda_1^\varepsilon \alpha\varphi^\varepsilon + (K \star p^\varepsilon)p^\varepsilon + a(y_0)(\alpha\varphi^\varepsilon - p^\varepsilon) = \big(\lambda_1^\varepsilon + (K \star p^\varepsilon)(y_0)\big)p^\varepsilon(y_0), \end{aligned}$$

which is a contradiction since $\lambda_1 + (K \star p)(y_0) \le \lambda_1 + k_\infty \int_\Omega p^\varepsilon(y)dy < 0$. This finishes the proof of Lemma 2.4.20. □

Proof of Theorem 2.4.6. It follows from Lemma 2.4.20 that the family $(p^\varepsilon)_{0<\varepsilon\le 1}$ of solutions to (2.4.20) with $\varepsilon > 0$ and $\beta = 0$ is uniformly bounded in $M^1(\overline{\Omega})$. Hence, applying Prokhorov's Theorem [63, Theorem 8.6.2], $(p^\varepsilon)_{0<\varepsilon<1}$ is precompact for the weak topology in $M^1(\overline{\Omega})$, and there exists a sequence p^{ε_n} (with $\varepsilon_n \to 0$) and a measure p such that $p^{\varepsilon_n} \rightharpoonup p$ in the sense of measures. In particular, taking $\psi = 1$, we recover the estimate of Lemma 2.4.20: $0 < \frac{-\lambda_1}{k_\infty} \le \int_{\overline{\Omega}} p(dy) \le \frac{\sup a}{k_0}$. Hence p is non-trivial.

Let us show that p is indeed a solution to (2.4.10). Multiplying equation (2.4.20) by $\psi \in F_0$, where F_0 is the set of functions with zero boundary flux as defined in (2.4.18), and integrating by parts, we get

$$\begin{aligned} -\varepsilon_n \int_\Omega p^{\varepsilon_n}\Delta\psi dy = &\int_\Omega \mu(M \star p^{\varepsilon_n} - p^{\varepsilon_n})\psi + a(y)p^{\varepsilon_n}\psi dy \\ &- \int_\Omega (K \star p^{\varepsilon_n})(y)\psi(y)p^{\varepsilon_n}(y)dy. \end{aligned} \tag{2.4.24}$$

Since $\Delta\psi \in C_b(\overline{\Omega})$ and $\int_\Omega p^{\varepsilon_n}$ is bounded uniformly in n, the left-hand side of (2.4.24) goes to 0 when $n \to \infty$. Moreover since $\psi(y)(a(y)-\mu) \in C(\overline{\Omega})$, then by definition the convergence $\int_\Omega \psi(y)(a(y)-\mu)p^{\varepsilon_n}(y)dy \to_{n\to\infty} \int_{\overline{\Omega}} \psi(y)(a(y)-\mu)p(dy)$ holds.

We turn our attention to the term $\int_\Omega M \star p^{\varepsilon_n}(y)\psi(y)dy$. We notice that

$$\int_\Omega \int_\Omega M(y,z)p^{\varepsilon_n}(z)dz\psi(y)dy = \int_\Omega p^{\varepsilon_n}(z)\int_\Omega M(y,z)\psi(y)dy = \int_\Omega p^{\varepsilon_n}(z)\check{M} \star \psi(z)dz,$$

where $\check{M}(y,z) = M(z,y)$. Since $\check{M} \star \psi(z)$ is a valid test function, we have indeed $\int_\Omega M \star p^{\varepsilon_n}(y)\psi(y)dy \to \int_\Omega M \star p(y)\psi(y)dy$.

We turn to the convergence of the nonlinearity $\int_\Omega (K \star p^{\varepsilon_n})(y)\psi(y)p^{\varepsilon_n}(y)dy$. Since the sequence p^{ε_n} appears twice in this term, the above argument cannot be used directly. Therefore, we first show a stronger convergence for $K \star p^{\varepsilon_n}$, namely that it converges uniformly to a continuous limit. We notice that

$$\begin{aligned} |(K \star p^{\varepsilon_n})(y) - (K \star p^{\varepsilon_n})(y')| = &\left|\int_\Omega \big(K(y,z) - K(y',z)\big)p^{\varepsilon_n}(z)dz\right| \\ \le &2\|K(y,\cdot) - K(y',\cdot)\|_{C_b(\overline{\Omega})}\frac{\sup a}{k_0}. \end{aligned}$$

Thus, the modulus of continuity of $K \star p^{\varepsilon_n}$ is uniformly bounded. Up to the extraction of a subsequence, $K \star p^{\varepsilon_n}$ converges in $C_b(\overline{\Omega})$ to a limit which we identify as $K \star p$ (by using another test function and the weak convergence $p^{\varepsilon_n} \rightharpoonup p$). Along this subsequence, we have then

$$\lim_{n\to\infty} \int_\Omega (K \star p^{\varepsilon_n})(y)\psi(y)p^{\varepsilon_n}(y)dy = \int_\Omega (K \star p)\psi(y)p(dy).$$

We have shown that equation (2.4.24) is satisfied for any $\psi \in F_0$. Applying Lemma 2.4.35, F_0 is densely embedded in $C_b(\overline{\Omega})$. Equation (2.4.24) is thus satisfied for any $\psi \in C_b(\overline{\Omega})$. This ends the proof of Theorem 2.4.6. □

2.4.4.3 Proof of Theorem 2.4.8

Under Assumption 2.4.7 and if μ is small enough according to Theorem 2.4.13, we can actually prove that the measure solution to (2.4.10) is concentrated in Ω_0 (Theorem 2.4.8). To do so, we write a solution p to (2.4.10) as an eigenvector for a problem similar to (2.4.9), and make use of Theorem 2.4.12.

Proof of Theorem 2.4.8. Let $p \in M^1(\overline{\Omega})$, $p \not\equiv 0$ be a nonnegative solution to (2.4.10). Define $b(y) := a(y) - (K \star p)(y)$. Then b is a continuous function and we have

$$\forall y \in \overline{\Omega}, b(y) = a(y) - \int_{\overline{\Omega}} K(y,z)p(dz) \leq a(0) - \int_{\overline{\Omega}} K(0,z)p(dz) = b(0),$$

as a result of Assumption 2.4.7. This shows that $\sup b = b(0)$. Next we compute:

$$b(0) - b(y) = a(0) - a(y) + \int_{\overline{\Omega}} \big(K(y,z) - K(0,z)\big)p(dz) \geq a(0) - a(y).$$

Thus, b satisfies Assumption 2.4.3.

We remark that p solves

$$\mu(M \star p - p) + b(y)p = 0 \tag{2.4.25}$$

in the sense of measures. Thus p is a solution to (2.4.9) with a replaced by b. Applying Corollary 2.4.14, since $\mu < \mu_0(\Omega, M, \sup a - a)$, then $\mu < \mu_0(\Omega, M, \sup b - b)$ and thus the only solutions to (2.4.25) are singular measures which singular part is concentrated in $\{y \in \Omega \,|\, b(y) = \sup b\}$. Let us show that $\{y \,|\, b(y) = \sup b\} \subset \Omega_0$. Let $y \in \overline{\Omega}$ such that $y \notin \Omega_0$. Then $a(y) < a(0)$ and

$$b(y) = a(y) - (K \star p)(y) < a(0) - (K \star p)(y) \leq a(0) - (K \star p)(0) = \sup b,$$

which shows that $y \notin \{y \,|\, b(y) = \sup b\}$. This ends the proof of Theorem 2.4.8. □

2.4.5 Construction of traveling waves

In this section 2.4.5, we prove our main result Theorem 2.4.10. To construct the desired measure traveling wave, we first consider a regularized problem in a box $-l \leq x \leq l$, $y \in \Omega$.

2.4.5.1 Construction of a solution in a box

Here we aim at constructing solutions $(c, u = u(x,y))$ to

$$\begin{cases} ll - \varepsilon\Delta_y u - u_{xx} - cu_x = \mu(M \star u - u) \\ \qquad\qquad +u(a(y) - K \star u - \beta u) \text{ in } (-l,l) \times \Omega \\ \qquad\qquad \nabla_y u(x,y) \cdot \nu = 0 \text{ on } (-l,l) \times \partial\Omega \\ \qquad\qquad u(l,y) = 0 \text{ in } \Omega \\ \qquad\qquad u(-l,y) = p(y) \text{ in } \Omega, \end{cases} \tag{2.4.26}$$

for $\beta \geq 0$ and p solving (2.4.20). Notice that any solution to (2.4.26) with $\beta > 0$ is a subsolution to (2.4.26) with $\beta = 0$. In particular, we will use some solutions to (2.4.26) with $\beta > 0$ to get lower estimates on solutions to (2.4.26) with $\beta = 0$.

In contrast with [53, 46, 7, P2], we use a global continuation theorem (in the proof of Theorem 2.4.21 below) instead of a topological degree to construct solutions to the local problem (2.4.26). Though both arguments have the same topological basis, we believe that this is an improvement of the usual method, since it spares the need to explicitly compute the topological degree associated with (2.4.26).

Let us also introduce the following quantity, which is the minimal speed for traveling waves (as we will show later):

$$c^*_\varepsilon := 2\sqrt{-\lambda^\varepsilon_1}. \tag{2.4.27}$$

Our result is the following:

Theorem 2.4.21 (Existence of solutions in the box)**.** *Let Assumption 2.4.2 hold, $\varepsilon > 0$ be such that $\lambda_1^\varepsilon < 0$, and $\beta \geq 0$. Then, there exists a nonnegative solution to* (2.4.26)*. Moreover, let $l_0 := \frac{\pi}{\sqrt{-\lambda_1^\varepsilon}} > 0$, $\tau_0 := \frac{-\lambda_1^\varepsilon}{2} > 0$. Then, for any $0 < \tau < \tau_0$, there exists $\bar{l}(\tau) \geq l_0 + 1$ such that if $l > \bar{l}(\tau)$, there exists a nonnegative solution (c, u) to* (2.4.26) *with $0 < c \leq c_\varepsilon^*$, which also satisfies the normalization condition*

$$\sup_{(x,y)\in(-l_0,l_0)\times\Omega} \left(\int_\Omega K(y,z)u(x,z)\mathrm{d}z + \beta u(x,y) \right) = \tau. \tag{2.4.28}$$

Before we prove Theorem 2.4.21, we need to establish some *a priori* estimates on the solutions to (2.4.26). For technical reasons, we actually study the solutions to

$$\begin{cases} ll - \varepsilon\Delta_y u - u_{xx} - cu_x = \sigma\big(\mu(M \star u - u) \\ \qquad\qquad +u\chi_{u\geq 0}(a(y) - K \star u - \beta u)\big) \text{ in } (-l,l)\times\Omega \\ \qquad\qquad \nabla_y u(x,y)\cdot\nu = 0 \text{ on } (-l,l)\times\partial\Omega \\ \qquad\qquad u(l,y) = 0 \text{ in } \Omega \\ \qquad\qquad u(-l,y) = p(y) \text{ in } \Omega, \end{cases} \tag{2.4.29}$$

where $\chi_{u\geq 0} = 0$ if $u \leq 0$, $\chi_{u\geq 0} = 1$ if $u > 0$, and $\sigma \in (0,1]$. We introduce the positive-part cutoff involving χ in Problem (2.4.29) in order to ensure that the nontrivial solutions to this problem are positive.

Lemma 2.4.22 (A priori estimates on the solutions to (2.4.29))**.** *Let Assumption 2.4.2 hold, $\varepsilon > 0$ such that $\lambda_1^\varepsilon < 0$, $\beta \geq 0$, and $|c| \leq c_\varepsilon^*$. We define $l_0 := \frac{\pi}{\sqrt{-\lambda_1^\varepsilon}}$. Let u be a solution to* (2.4.29)*, then*

(i) $u \in C^2_{loc}\big((-l,l)\times\Omega\big) \cap C^1_{loc}\big((-l,l)\times\overline{\Omega}\big) \cap C_b\big([-l,l]\times\overline{\Omega}\big)$.

(ii) u is positive in $(-l,l)\times\overline{\Omega}$.

(iii) For any $x \in [-l,l]$, we have $\int_\Omega u(x,y)dy \leq \frac{\sup a}{k_0}$.

(iv) There exists a positive constant C^ε, independent from c, l and σ, such that we have $\|u\|_{C_b((-l,l)\times\Omega)} \leq C^\varepsilon$. If $\beta > 0$, then we have the estimate $\|u\|_{C_b((-l,l)\times\Omega)} \leq \frac{\sup a}{\beta}$.

(v) If $\sigma = 1$, $c = 0$, and $l > l_0$, then

$$\sup_{(x,y)\in(-l_0,l_0)\times\Omega} \left(\int_\Omega K(y,z)u(x,z)\mathrm{d}z + \beta u(x,y) \right) > \frac{-\lambda_1^\varepsilon}{2}.$$

Remark that for this result to hold, u needs only be defined on $(-l_0,l_0)\times\Omega$.

(vi) If $\sigma = 1$ and $c = c_\varepsilon^*$, then there exists a constant A (independent from l) and $\lambda := \frac{c_\varepsilon^*}{2} > 0$ such that $\forall (x,y) \in (-l,l)\times\Omega, u \leq Ae^{-\lambda(x+l)}$.

In particular for any $l \geq \bar{l}(\tau) := \frac{1}{\lambda}\ln\left(\frac{\tau}{2A(k_\infty\int_\Omega\varphi^\varepsilon + \beta\sup_\Omega\varphi^\varepsilon)}\right) - l_0$ and $0 < \tau \leq \tau_0 = \frac{-\lambda_1^\varepsilon}{2}$, we have

$$\sup_{(x,y)\in(-l_0,l_0)\times\Omega} \left(\int_\Omega K(y,z)u(x,z)\mathrm{d}z + \beta u(x,y) \right) < \tau.$$

Proof. Item (i) holds by a direct application of [47, Lemma 7.1], and item (ii) by a classical comparison argument. Let us resume to the remaining items.

Item *(iii)*: By the estimate in Lemma 2.4.20, we have $\int_\Omega p(y)dy \leq \frac{\sup a}{k_0}$. Assume that the function $x \mapsto \int_\Omega u(x,y)dy$ has a maximal value at $x_0 \in (-l,l)$, then integrating (2.4.29) over Ω we have

$$\begin{aligned} 0 &\leq -\frac{d^2\int_\Omega u(x_0,y)dy}{dx^2} - c\frac{d\int_\Omega u(x_0,y)dy}{dx} \\ &= \sigma\int_\Omega a(y)u(x_0,y) - (K\star u)(x_0,y)u(x_0,y)dy, \end{aligned}$$

and thus:

$$k_0\left(\int_\Omega u(x_0,y)dy\right)^2 \le \int_\Omega\int_\Omega K(y,z)u(x_0,z)u(x_0,y)dydz$$
$$= \int_\Omega a(y)u(x_0,y)dy \le \sup a\int_\Omega u(x_0,y)dy.$$

This shows item (*iii*).

Item (*iv*): Assume first $\beta>0$ and let $u(x_0,y_0)=\sup u$ at $(x_0,y_0)\in[-l,l]\times\overline{\Omega}$. Assume by contradiction that $u(x_0,y_0)>\frac{\sup a}{\beta}$. If $x_0=-l$, since p satisfies the upper bound $\sup p\le\frac{\sup a}{\beta}$ by the estimate in Lemma 2.4.17 item (*ii*), we have a contradiction. If $x_0=+l$, since $u(x_0,y_0)=0$, we have a contradiction. Assume $x_0\in(-l,l)$. If $y_0\in\partial\Omega$, then it follows from Hopf's Lemma that $\frac{\partial u}{\partial\nu}(x_0,y_0)>0$, which is a contradiction. Thus $y_0\in\Omega$. Now, testing (2.4.29) at (x_0,y_0), we have

$$0\le -\varepsilon\Delta_y u(x_0,y_0)-u_{xx}(x_0,y_0)-cu_x(x_0,y_0)-\sigma\mu\big((M\star u)-u\big)(x_0,y_0)$$
$$=\sigma u(x_0,y_0)\big(a(y_0)-(K\star u)(x_0,y_0)-\beta u(x_0,y_0)\big)<0$$

which is a contradiction. Thus $u\le\frac{\sup a}{\beta}$.

We turn our attention to the case $\beta=0$. In this case, we construct a supersolution as in Lemma 2.4.17. Recalling that u satisfies Dirichlet boundary conditions at $x=\pm l$, the local maximum principle up to the boundary [187, Theorem 9.26] shows the existence of $C=C(\Omega,R,\varepsilon,\|a\|_{L^\infty},k_0,k_\infty,\mu,c_\varepsilon^*)$ such that for any $x\in[-l,l]$, $y\in\Omega$ with $d(y,\partial\Omega)\ge R$, we have the estimate $\sup\limits_{B_{R/2}(x,y)} u\le C$.

To show that this estimate does not degenerate near the boundary, we use the same kind of supersolution as in Lemma 2.4.17. Let

$$\Omega_R:=\{y\in\Omega\,|\,d(y,\partial\Omega)<R\}$$

for any $R>0$. We select R small enough so that Ω_R has a C^3 boundary and the comparison principle [47, Proposition 1.1] holds in the narrow domain Ω_R. Let us stress that since $\sigma\in(0,1)$, R can be chosen uniformly in σ.

This allows us to construct a positive solution to

$$\begin{cases} ll-\varepsilon\Delta v-\sigma(a(y)-\mu)v=\mu m_0\dfrac{m_\infty\sup a}{k_0} \text{ in } \Omega\\ \qquad\qquad\qquad\qquad\qquad\qquad v=C \text{ on } \partial\Omega_R\backslash\partial\Omega\\ \qquad\qquad\qquad\qquad\qquad\qquad \dfrac{\partial v}{\partial\nu}=0 \text{ on } \partial\Omega, \end{cases}$$

which is bounded uniformly in σ, as we did in the proof of Lemma 2.4.17. Now we select $\alpha:=\inf\{\zeta>0\,|\,\forall x\in(-l,l),\forall y\in\Omega,\zeta v(y)\ge u(x,y)\}$. Assume by contradiction that $\alpha>1$. Then there exists $(x_0,y_0)\in[-l,l]\times\overline{\Omega}$ such that $u(x_0,y_0)=\alpha v(y_0)$. If $x_0=l$ then $u=0$, which is a contradiction. If $x_0=-l$, since $u(-l,y_0)=p(y_0)$ solves (2.4.20), we argue as in Lemma 2.4.17 and get a contradiction. We are left to investigate the case $x_0\in(-l,l)$. If $y_0\in\partial\Omega$, since (x_0,y_0) is a minimum to the function $\alpha v-u$, then by Hopf's Lemma we have $\frac{\partial(\alpha v-u)}{\partial\nu}(x_0,y_0)<0$ which is a contradiction. Thus $y_0\notin\partial\Omega$. Since $\alpha>1$ and $u\le C$ on $\partial\Omega_R\backslash\partial\Omega$, then $y_0\in\Omega_R$. Now (x_0,y_0) is a local minimum to $\alpha v-u$ and thus

$$0\ge-\varepsilon\Delta(\alpha v-u)(x_0,y_0)=\sigma(a(y_0)-\mu)(\alpha v-u)(x_0,y_0)+\alpha\mu m_0\frac{m_\infty\sup a}{k_0}$$
$$-\sigma\mu(M\star u)(x_0,y_0)+u(x_0,y_0)(K\star u)(x_0,y_0)$$
$$>\alpha\mu m_0\frac{m_\infty\sup a}{k_0}-\sigma\mu(M\star u)(x_0,y_0)\ge 0$$

which is a contradiction. Thus $\alpha\le 1$.

This shows that $u(x,y)\le v(y)$ in $(-l,l)\times\Omega_R$. Since v is bounded uniformly in σ, we have our uniform bound for u in $[-l,l]\times\Omega_R$. In the rest of the domain $(-l,l)\times\Omega\backslash\Omega_R$, we have $u\le C$.

This proves item (*iv*), with $C^\varepsilon:=\max(\sup_{y\in\Omega_R}v(y),C)$.

Item (*v*): This proof is similar to the one in [7]. Assume by contradiction that $\sup_{(x,y)\in(-l_0,l_0)\times\Omega}\left(\int_\Omega K(y,z)u(x,z)\mathrm{d}z+\beta u\right.$ τ_0. Then u satisfies:

$$-u_{xx}-\varepsilon\Delta_y u-\mu(M\star u-u)-a(y)u\ge-\tau_0 u \qquad \text{in } (-l_0,l_0). \tag{2.4.30}$$

Define $\psi(x,y) := \cos\left(\frac{\pi}{2l_0}x\right)\varphi^\varepsilon(y)$, where φ^ε is the principal eigenfunction solution to (2.4.17) satisfying $\sup_{y\in\Omega}\varphi^\varepsilon = 1$. Since u is positive in $[-l_0,l_0]\times\overline{\Omega}$, we can define the real number $\alpha := \sup\{\zeta>0\,|\,\forall(x,y)\in(-l_0,l_0)\times\Omega, \zeta\psi(x,y)\le u(x,y)\}$, and we have $\alpha>0$.

Then, there exists $(x_0,y_0)\in[-l_0,l_0]\times\overline{\Omega}$ such that $\alpha\psi(x_0,y_0)=u(x_0,y_0)$. Because of the boundary conditions satisfied by u and ψ, (x_0,y_0) has to be in $(-l_0,l_0)\times\Omega$. Since (x_0,y_0) is the minimum of $u-\alpha\psi$, we have

$$\begin{aligned}
0 \ge & -\varepsilon\Delta_y(u-\alpha\psi)(x_0,y_0) - (u-\alpha\psi)_{xx}(x_0,y_0)\\
& - \mu\big(M\star(u-\alpha\psi)-(u-\alpha\psi)\big)(x_0,y_0) - a(y_0)(u-\alpha\psi)(x_0,y_0)\\
\ge & -\tau_0 u(x_0,y_0) + \alpha\left(-\lambda_1^\varepsilon - \left(\frac{\pi}{2l_0}\right)^2\right)\psi(x_0,y_0)\\
= & \left(\frac{-3\lambda_1^\varepsilon}{4} - \tau_0\right)u(x_0,y_0) > 0,
\end{aligned}$$

since $-\tau_0 = \frac{\lambda_1^\varepsilon}{2}$. This is a contradiction.

This proves item (v).

Item (vi): Let $\psi(x,y) := e^{-\frac{c_\varepsilon^*}{2}x}\varphi^\varepsilon(y)$ with $(\lambda_1^\varepsilon,\varphi^\varepsilon)$ solution to (2.4.17). Then ψ satisfies:

$$-c_\varepsilon^*\psi_x - \psi_{xx} - \varepsilon\Delta_y\psi - \mu(M\star\psi-\psi) = a(y)\psi.$$

Since $\psi>0$ on $[-l,l]\times\overline{\Omega}$, there exists $\zeta>0$ such that $\zeta\psi\ge u$ on $(-l,l)\times\Omega$. Let us select $\alpha := \inf\{\zeta>0\,|\,\forall(x,y)\in(-l_0,l_0)\times\Omega, \zeta\psi(x,y)\ge u(x,y)\}$. By definition of α we have $\alpha\psi\ge u$ and there exists $(x_0,y_0)\in[-l,l]\times\overline{\Omega}$ such that $\alpha\psi(x_0,y_0)=u(x_0,y_0)$. Because of the boundary conditions satisfied by u and ψ, (x_0,y_0) has to be in $[-l,l)\times\Omega$. If $x_0\in(-l,l)$, we have:

$$\begin{aligned}
0 \le & -\varepsilon\Delta_y(u-\alpha\psi)(x_0,y_0) - (u-\alpha\psi)_{xx}(x_0,y_0)\\
& - \mu\big(M\star(u-\alpha\psi)-(u-\alpha\psi)\big)(x_0,y_0) - a(y_0)(u-\alpha\psi)(x_0,y_0)\\
< & \ 0
\end{aligned}$$

which is a contradiction. We conclude that $x_0=-l_0$ and thus $\alpha\le\frac{\sup_\Omega p}{\inf_\Omega\varphi^\varepsilon}e^{-\frac{c_\varepsilon^*}{2}l}$. By definition of α, we can then write:

$$u(x,y)\le\alpha e^{-\frac{c_\varepsilon^*}{2}x}\varphi^\varepsilon(y)\le\frac{\sup_\Omega p}{\inf_\Omega\varphi^\varepsilon}e^{-\frac{c_\varepsilon^*}{2}(x+l)}\varphi^\varepsilon(y)$$

which concludes the proof of item (vi). □

We are now in the position to prove Theorem 2.4.21, by using the global continuation principle [413, Theorem 14 C].

Proof of Theorem 2.4.21. For $c\in\mathbb{R}$ and $u\in C_b\big((-l,l)\times\Omega\big)$. We define $F(c,u)=\tilde{u}$ where $\tilde{u}$ solves:

$$\begin{cases}
ll - \tilde{u}_{xx} - c\tilde{u}_x - \varepsilon\Delta_y\tilde{u} = \mu M\star u\\
\qquad\qquad +u\chi_{u\ge0}(a(y)-\mu-K\star u-\beta u) \text{ in } (-l,l)\times\Omega\\
\qquad\qquad\qquad \dfrac{\partial\tilde{u}}{\partial\nu}(x,y)=0 \text{ on } (-l,l)\times\partial\Omega\\
\qquad\qquad\qquad\quad \tilde{u}(l,y)=0 \text{ in } \Omega\\
\qquad\qquad\qquad \tilde{u}(-l,y)=p(y). \text{ in } \Omega.
\end{cases}\tag{2.4.31}$$

It follows from [47, Lemma 7.1] that for any u the function $\tilde{u}$ is well-defined and belongs to the space $C_b([-l,l]\times\overline{\Omega})\cap W^{2,p}_{loc}([-l,l]\times\overline{\Omega}\backslash\{-l,l\}\times\partial\Omega)$ for any $p>0$.

Step 1: Let us briefly show that F is in fact a compact operator. Since the right-hand side of the first equation in (2.4.31) is bounded, it is easily seen that the function $(x,y)\mapsto\big(1+\gamma(x+l)^\alpha\big)p(y)$ is a local supersolution to equation (2.4.31) near $x=l$ for $0\le\alpha<\alpha_0$, $\gamma\ge\gamma_0>0$, where α_0 and γ_0 depend only on $\|u\|_{C_b((-l,l)\times\Omega)}$, a bound for c and the data and coefficients of the problem. Similarly, $\big(1-\gamma(x+l)^\alpha\big)p(y)$ is a local subsolution, provided α is chosen small enough. Thus the inequality $\big(1-\gamma(x+l)^\alpha\big)p(y)\le\tilde{u}(x,y)\le$

$\big(1+\gamma(x+l)^\alpha\big)p(y)$ holds for $\alpha > 0$ small enough. In particular, the function $x \in [-l, 0] \mapsto \tilde{u}(x, y)$ is uniformly in C^α for $y \in \overline{\Omega}$. It then follows from [187, Corollary 9.28] (and the classical interior Sobolev embeddings) that $\tilde{u} \in C^\alpha([-l, 0] \times \overline{\Omega})$. Regularity near $x = l$ can be shown the same way. Thus $\tilde{u} \in C^\alpha([-l, l] \times \overline{\Omega})$ where α depends only on a bound for $\|u\|_{C_b((-l,l)\times\Omega)}$ and c, and the data and coefficients of problem (2.4.31). In particular, F maps bounded sets of $\mathbb{R} \times C_b((-l, l) \times \Omega)$ into relatively compact sets in $C_b((-l, l) \times \Omega)$.

Step 2: We aim at applying the Leray-Schauder fixed-point theorem [413, Corollary 13.1 item (iii)] to $F(0, \cdot)$. We remark that the solutions to $u = \sigma F(0, u)$ for $\sigma \in (0, 1]$ are in fact the solutions to (2.4.29). In particular, Lemma 2.4.22 gives us a positive constant $C > 0$ such that any solution to (2.4.29) satisfies the inequality $\|u\|_{C_b(-l,l)\times\Omega} \leq C$. Let $G := \{u \in C_b((-l, l) \times \Omega) \,|\, \|u\|_{C_b((-l,l)\times\Omega)} \leq 2C\}$, then

1. G is a bounded open subset of the Banach space $C_b((-l, l) \times \Omega)$,
2. $0 \in G$,
3. $F(0, \cdot) : G \to C_b((-l, l) \times \Omega)$ is a compact mapping, and
4. applying Lemma 2.4.22, there is no solution to $u = \sigma F(0, u)$ with $u \in \partial G$ and $\sigma \in (0, 1]$.

Thus the Leray-Schauder fixed-point Theorem [413, Corollary 13.1 item (iii)] applies and we have $ind(F(0, \cdot), G) = 1$, where ind is the Leray-Schauder fixed-point index.

Step 3: Let us now check that the hypotheses of the global continuation principle [413, Theorem 14 C] are satisfied. We have:

1. F is a compact mapping from $(0, c^*_\varepsilon) \times \overline{G}$ into $C_b((-l, l) \times \Omega)$,
2. applying Lemma 2.4.22, there is no solution to $u = F(c, u)$ with $u \in \partial G$ and $c \in [0, c^*_\varepsilon]$, and
3. $ind(F(0, \cdot), G) = 1$.

Thus, the global continuation principle applies and there exists a connected set of solutions $\mathcal{C}$ to $u = F(c, u)$ connecting $\{0\} \times G$ to $\{c^*_\varepsilon\} \times G$. In particular, there exists a solution to (2.4.26) for any $c \in [0, c^*_\varepsilon]$.

Step 4: Now let us assume $l \geq \overline{l}(\tau)$ (where $\overline{l}(\tau)$ is given by Lemma 2.4.22, item 5). Since the mapping

$$u \in C_b((-l, l) \times \Omega) \overset{N}{\longmapsto} \sup_{(x,y)\in(-l_0,l_0)\times\Omega} \int_\Omega K(y, z)u(x, z)dz + \beta u(x, y)$$

is continuous, then $N(\mathcal{C})$ is a connected subset of $\mathbb{R}$, i.e. an interval. Applying Lemma 2.4.22, we have:

– From point (v), if $(c, u) \in \mathcal{C}$ and $c = 0$, then $N(u) > \tau$.

– From point (vi), if $(c, u) \in \mathcal{C}$ and $c = c^*_\varepsilon$ then $N(u) < \tau$.

Thus there exists $c \in (0, c^*_\varepsilon)$ and u such that $(c, u) \in \mathcal{C}$ and $N(u) = \tau$. This finishes the proof of Theorem 2.4.21. □

An immediate consequence is the following:

Corollary 2.4.23 (Existence of a solution on the line)**.** *Let Assumption 2.4.2 hold, $\varepsilon > 0$ be such that $\lambda^\varepsilon_1 < 0$, $\beta \geq 0$ and $0 < \tau \leq \frac{-\lambda^\varepsilon_1}{2}$. Then there exists a classical positive solution to*

$$\begin{cases} ll - u_{xx} - cu_x = \varepsilon\Delta_y u + \mu(M \star u - u) \\ \qquad\qquad\qquad\qquad +u(a(y) - K \star u - \beta u) \text{ on } \mathbb{R} \times \Omega \\ \qquad\qquad\qquad\qquad\qquad \dfrac{\partial u}{\partial \nu} = 0 \text{ on } \mathbb{R} \times \partial\Omega, \end{cases} \tag{2.4.32}$$

with $0 < c \leq c^*_\varepsilon$. Moreover $u \in C_b(\mathbb{R} \times \Omega) \cap C^2(\mathbb{R} \times \overline{\Omega})$, satisfies (2.4.28) *and*

$$\forall x \in \mathbb{R}, \quad \int_\Omega u(x, y)dy \leq \frac{\sup a}{k_0}.$$

Proof. Let $0 < \tau \leq \tau_0$ and $\bar{l} = \bar{l}(\tau)$ as in Theorem 2.4.21. Then it follows from the existence theorem (Theorem 2.4.21), that for any $n \in \mathbb{N}$, there exists a positive classical solution $(c_n, u_n) \in (0, c^*_\varepsilon) \times C^2((-l_n, l_n) \times \Omega) \cap C^1((-l_n, l_n) \times \overline{\Omega})$ to (2.4.26) which satisfies (2.4.28), where $l_n := \bar{l} + n$. By the uniform bound satisfied by $\sup u_n$ (Lemma 2.4.22 point (iv)), the classical Schauder interior estimates [187, Theorem 6.2] and the boundary Schauder estimates [187, Theorem 6.29], there exists a constant $C_k > 0$, independent from n such that $\|u_n\|_{C^{2,\alpha}((-l_k,l_k)\times\overline{\Omega})} \leq C_k$ for any $k < n$. Using a classical diagonal extraction process, there exists u, c^0 and a subsequence such that $c_n \to c^0$, and $\|u_n - u\|_{C^2((-l_k,l_k)\times\overline{\Omega})} \to 0$ for any $k \in \mathbb{N}$. Since u solves (2.4.28) with $\tau > 0$, it is a nontrivial solution to (2.4.32). Then, by a direct application of Lemma 2.4.22 point (v), $c^0 > 0$ (indeed Lemma 2.4.22 point (v) also applies to solutions defined on the whole line).

Finally we have $\forall x \in \mathbb{R}, \int_\Omega u(x,y)dy \leq \frac{\sup a}{k_0}$ by the estimate in Lemma 2.4.22 point (iii). This finishes the proof of Corollary 2.4.23. □

2.4.5.2 Proof of minimality for $\beta \geq \beta_0$

In the case $\beta \geq \beta_0 := \frac{k_\infty \sup a}{\mu m_0}$, we recover the comparison principle. Indeed, the increased self-competition (via large β) enforces the solution to remain in the region "u small" where the system is cooperative (see Lemma 2.4.25). We can then retrieve many of the classical properties satisfied by traveling waves in a KPP situation.

Theorem 2.4.24 (Minimal speed traveling waves for $\beta \geq \beta_0$)**.** *Let Assumption 2.4.2 hold, $0 < \varepsilon \leq \varepsilon_0$ — where ε_0 is as in Lemma 2.4.19— be such that $\lambda_1^\varepsilon < 0$, and $\beta \geq \beta_0 = \frac{k_\infty \sup a}{\mu m_0}$. Then, there exists a solution (c, u) to* (2.4.32) *satisfying $c = c^*_\varepsilon$ and the limit conditions*

$$\liminf_{x\to-\infty} \inf_{y\in\Omega} u(x,y) > 0, \qquad \lim_{x\to+\infty} \sup_{y\in\Omega} u(x,y) = 0. \tag{2.4.33}$$

Moreover, u is nonincreasing in x, and there exists no positive solution to (2.4.32) *satisfying* (2.4.33) *and $0 \leq c < c^*_\varepsilon$.*

Finally, we have

$$\lim_{x\to-\infty} \inf_{y\in\Omega} u(x,y) \geq \rho_\beta$$

where ρ_β is the constant defined in Lemma 2.4.19.

Our main tool is the following *comparison principle* for small densities.

Lemma 2.4.25 (Comparison principle)**.** *Let Assumption 2.4.2 hold and $\beta \geq 0$. Let $u \in C^2$ be a supersolution to*

$$-cu_x - u_{xx} - \varepsilon\Delta_y u - \mu(M \star u - u) - u(a(y) - K \star u - \beta u) \geq 0 \tag{2.4.34}$$

and $v \in C^2$ be a subsolution to

$$-cv_x - v_{xx} - \varepsilon\Delta_y v - \mu(M \star v - v) - v(a(y) - K \star v - \beta v) \leq 0. \tag{2.4.35}$$

If there exists $(x_0, y_0) \in \mathbb{R} \times \Omega$ such that $0 < u(x_0, y_0) \leq \frac{\mu m_0}{k_\infty}$, $u \geq v$ in a neighbourhood of $\{x_0\} \times \Omega$, and $u(x_0, y_0) = v(x_0, y_0)$, then $u \equiv v$.

Proof. Let (x_0, y_0) as in Lemma 2.4.25. Then (x_0, y_0) is a local zero minimum to $u - v$. We have:

$$-c(u-v)_x(x_0,y_0) - (u-v)_{xx}(x_0,y_0) - \varepsilon\Delta_y(u-v)(x_0,y_0) \leq 0$$

and thus:

$$\mu\big(M \star (u-v) - (u-v)\big) + a(y)(u-v) - uK \star u + vK \star v - \beta u^2 + \beta v^2 \leq 0. \tag{2.4.36}$$

Using the fact that $u(x_0, y_0) = v(x_0, y_0)$, we rewrite (2.4.36) as

$$\int_\Omega \big(\mu M(y_0,z) - u(x_0,y_0)K(y_0,z)\big)\Big(\big(u(x_0,z) - v(x_0,z)\big) - \big(u(x_0,y_0) - v(x_0,y_0)\big)\Big)dz \leq 0.$$

Since $\mu M(y_0, z) - u(x_0, y_0)K(y_0, z) > 0$ for any $z \in \Omega$ and $u(x_0, y) - v(x_0, y)$ is nonnegative for any $y \in \Omega$, we conclude that $u(x_0, y) = v(x_0, y)$ for any $y \in \Omega$. Applying the strong maximum principle, we have then $u - v \equiv 0$. This ends the proof of Lemma 2.4.25. □

Lemma 2.4.26 (Estimates for $\beta \geq \frac{k_\infty \sup a}{\mu m_0}$)**.** *Assume $\beta \geq \beta_0 = \frac{k_\infty \sup a}{\mu m_0}$. Then there exists a unique solution to* (2.4.26)*. Moreover, the solution to* (2.4.26) *is decreasing in x, and the mapping $c \mapsto u$ is decreasing.*

Proof. We divide the proof in four steps. Recall that, due to Theorem 2.4.21, there exists a solution to (2.4.26).

Step 1: We show that any solution satisfies $u(x,y) < p(y)$ at any interior point.

Let us define $\alpha := \sup\{\zeta > 0 \,|\, \zeta u \leq p\}$. Since u is bounded and p is positive on $\overline{\Omega}$, α is well-defined and positive. Assume by contradiction that $\alpha < 1$. By definition of α, there exists $(x_0, y_0) \in [-l, l] \times \overline{\Omega}$ such that $p(y_0) = \alpha u(x_0, y_0)$. Testing at $x = \pm l$, we have $\alpha u(-l, y_0) = \alpha p(y_0) < p(y_0)$ and $\alpha u(l, y_0) = 0 < p(y_0)$; thus $x_0 \in (-l, l)$. If $y_0 \in \partial\Omega$, then it follows from Hopf's Lemma that $\frac{\partial p - \alpha u}{\partial \nu}(x_0, y_0) < 0$, which contradicts the Neumann boundary conditions satisfied by u and p. Thus $y_0 \in \Omega$. Next we remark that

$$\begin{aligned} -c(\alpha u)_x - (\alpha u)_{xx} - \varepsilon \Delta_y (\alpha u) - \mu\big(M \star (\alpha u) - (\alpha u)\big) - a(y_0)(\alpha u) \\ = (\alpha u)(-K \star u - \beta u) < \alpha u\big(- K \star (\alpha u) - \beta(\alpha u)\big), \end{aligned}$$

since $\alpha < 1$. Hence αu is a subsolution to (2.4.35). Moreover p is a supersolution to (2.4.34). Finally, by the estimate in Lemma 2.4.22 point (iv) and the condition $\beta \geq \beta_0$, we have the inequality $\|u\|_{L^\infty} \leq \frac{\sup a}{\beta} \leq \frac{\mu m_0}{k_\infty}$, and by definition (x_0, y_0) is the global minimum of $(p - \alpha u)$. Thus Lemma 2.4.25 applies and $\alpha u = p$, which is a contradiction.

Thus $\alpha \geq 1$, which shows that $u \leq p$. Assume now that $u(x,y) = p(y)$ for some $(x,y) \in (-l,l) \times \Omega$, then Lemma 2.4.25 applies and we have $u = p$ in $(-l,l) \times \Omega$, which is again a contradiction. We conclude that the strict inequality holds:

$$\forall (x,y) \in (-l,l) \times \Omega, \qquad u(x,y) < p(y).$$

Step 2: We show that the solution u is unique. Here we use a sliding argument. Let u, v be two solutions to (2.4.26), and define:

$$\bar{x} := \inf\{\gamma > 0 \,|\, \forall (x,y) \in (-l,l) \times \Omega, u(x+\gamma, y) \leq v(x,y)\}.$$

Because of the boundary conditions satisfied by u and v, we have $0 \leq \bar{x} < 2l$. Assume by contradiction that $\bar{x} > 0$. We remark that $(x,y) \mapsto u(x + \bar{x}, y)$ is a subsolution to (2.4.35). By definition of $\bar{x}$, there exists $(x_0, y_0) \in (-l, l - \bar{x}) \times \Omega$ such that the equality $u(x_0 + \bar{x}, y_0) = v(x_0, y_0)$ holds. In view Lemma 2.4.25, this leads to a contradiction. Thus $\bar{x} \leq 0$ and $u \leq v$. Exchanging the roles of u and v, we have in turn $v \leq u$. This shows the uniqueness of u.

Step 3: We show that $x \mapsto u(x,y)$ is decreasing. Repeating the sliding argument in Step 2 with $u = v$, we have $u(x + \bar{x}, y) \leq u(x,y)$ for any $\bar{x} > 0$, which shows that u is nonincreasing. Moreover, equality cannot hold at an interior point in the above inequality, for Lemma 2.4.25 would lead to a contradiction. This shows that $x \mapsto u(x, \cdot)$ is decreasing.

Step 4: We show that $c \mapsto u$ is decreasing. Let $\bar{c} \leq c$, u (resp. v) be the solution to (2.4.26) associated with the speed c (resp. $\bar{c}$). Let also:

$$\bar{x} := \inf\{\gamma > 0 \,|\, \forall y \in \Omega, u(x+\gamma, y) \leq v(x,y)\}$$

and assume by contradiction that $\bar{x} > 0$. Then

$$\begin{aligned} -cv_x - v_{xx} - \varepsilon \Delta_y v &= \mu(M \star v - v) + v(a - K \star u - \beta u) + (\bar{c} - c) v_x \\ &\geq \mu(M \star v - v) + v(a - K \star u - \beta u), \end{aligned}$$

since, as shown above, $v_x \leq 0$. Then, v is a supersolution to (2.4.34) and Lemma 2.4.25 leads to a contradiction. Thus $c \mapsto u$ is nonincreasing. Moreover if $\bar{c} < c$, then we deduce from the above argument that $v > u$. Hence $c \mapsto u$ is in fact decreasing.

This ends the proof of Lemma 2.4.26. □

In particular, we notice that:

Corollary 2.4.27 (Existence of monotone fronts)**.** *Let $\beta \geq \beta_0 = \frac{k_\infty \sup a}{\mu m_0}$. Then the solution constructed in Corollary 2.4.23 is decreasing in x.*

The next results shows that if u is a traveling wave, then $c \geq c^*_\varepsilon$.

Lemma 2.4.28 (c_ε^* is the minimal speed)**.** *Let Assumption 2.4.2 hold, $\varepsilon > 0$ be such that $\lambda_1^\varepsilon < 0$, and u be a positive solution to* (2.4.32) *with $0 \le c \le c_\varepsilon^*$ and either*

(i) $\beta > 0$ and $\lim_{x\to+\infty} \sup_{y\in\Omega} u(x,y) = 0$, or

(ii) $\beta = 0$ and $\lim_{x\to+\infty} \int_\Omega u(x,y)dy = 0$.

Then $c = c_\varepsilon^*$.

Proof. It follows from our hypothesis (i) or (ii) that we can find arbitrary large intervals $[\bar{x} - L, \bar{x} + L]$ on which

$$\sup_{(x,y)\in(\bar{x}-L,\bar{x}+L)\times\Omega} \left(\int_\Omega K(y,z)u(x,z)dz + \beta u(x,y) \right) \le \delta, \tag{2.4.37}$$

for arbitrarily small $\delta > 0$. Since equation (2.4.32) is invariant by translation in x, we may assume without loss of generality that $\bar{x} = 0$.

Assume by contradiction that $c < c_\varepsilon^*$. Let $\theta := \sqrt{\frac{(c_\varepsilon^*)^2 - c^2}{8}}$, $L := \frac{\pi}{2\theta}$, $\delta := \frac{-\lambda_1^\varepsilon}{4} > 0$, and $\psi(x,y) := e^{-\frac{c}{2}x}\cos(\theta x)\varphi^\varepsilon(y)$, where φ^ε is the principal eigenfunction solution to (2.4.17) satisfying $\sup_{y\in\Omega} \varphi^\varepsilon = 1$. ψ satisfies

$$-c\psi_x - \psi_{xx} - \varepsilon\Delta_y\psi - \mu(M \star \psi - \psi) = a(y)\psi + \left(\frac{c^2}{4} + \theta^2 + \lambda_1^\varepsilon \right)\psi.$$

Since u is positive in $[-L, L] \times \overline{\Omega}$, we can define $\alpha := \sup\{\zeta > 0 \,|\, \zeta\psi \le u\}$. By definition of α there exists $(x_0, y_0) \in [-L, L] \times \overline{\Omega}$ such that $\alpha\psi(x_0, y_0) = u(x_0, y_0)$. Because of the boundary conditions satisfied by u and ψ, (x_0, y_0) cannot lie on the boundary of $[-L, L] \times \Omega$. Thus (x_0, y_0) belongs to $(-L, L) \times \Omega$ and, since u satisfies (2.4.37) we have

$$\begin{aligned}
0 &\ge -\varepsilon\Delta_y(u - \alpha\psi)(x_0, y_0) - (u - \alpha\psi)_{xx}(x_0, y_0) \\
&\quad - \mu\big(M \star (u - \alpha\psi) - (u - \alpha\psi)\big)(x_0, y_0) - a(y_0)(u - \alpha\psi)(x_0, y_0) \\
&\ge -\delta u(x_0, y_0) - \alpha \left(\frac{c^2}{4} + \theta^2 + \lambda_1^\varepsilon \right)\psi(x_0, y_0) \\
&= \left(-\delta - \frac{c^2}{8} - \frac{3\lambda_1^\varepsilon}{4} \right) u(x_0, y_0) \ge \left(-\delta - \frac{\lambda_1^\varepsilon}{2} \right) > 0,
\end{aligned}$$

since $\delta = \frac{-\lambda_1^\varepsilon}{4}$. This is a contradiction. □

Lemma 2.4.29 (Lower estimate on positive infima)**.** *Let Assumption 2.4.2 be satisfied, let $0 < \varepsilon \le \varepsilon_0$ and $\beta \ge 0$, where ε_0 is as in Lemma 2.4.19. Assume $\lambda_1^\varepsilon < 0$. Let u be a solution to* (2.4.32) *which satisfies $\inf_{(x,y)\in\mathbb{R}\times\Omega} u(x,y) > 0$. Then*

$$\inf_{(x,y)\in\mathbb{R}\times\Omega} u(x,y) \ge \rho_{\max(\beta,\beta_0)}$$

where ρ_β is the constant from Lemma 2.4.19.

Proof. For any $B \ge 0$, let p^B be a nonnegative nontrivial solution to (2.4.20) (substituting β with B). Since $\inf u > 0$ and $\sup p^B \le \frac{\sup a}{B}$ (by the estimate in Lemma 2.4.17 item (ii)), there exists a constant $\beta' > 0$ such that

$$\beta' = \inf\{B > 0 \,|\, p^B \le u\}.$$

Assume by contradiction that $\beta' > \max(\beta, \beta_0)$. Then two cases may occur:

Case 1: Assume there exists $(x_0, y_0) \in \mathbb{R}\times\overline{\Omega}$ such that $u(x_0, y_0) = p^{\beta'}(y_0)$. Assume by contradiction that $y_0 \in \partial\Omega$. Then y_0 is the minimum of $u - p^{\beta'}$ and, by applying Hopf's Lemma, we have $\frac{\partial(u-p^{\beta'})}{\partial\nu}(x_0, y_0) < 0$, which contradicts the Neumann boundary conditions satisfied by u and $p^{\beta'}$. Thus $y_0 \in \Omega$.

Then, since $\beta' > \beta$, $p^{\beta'}$ is a subsolution to (2.4.32), $u \ge p^{\beta'}$ and since $\beta' > \beta_0$ we have $\|p^{\beta'}\|_{C_b(\Omega)} < \frac{\mu m_0}{k_\infty}$. Thus Lemma 2.4.25 applies and $u = p^{\beta'}$. Since $\beta' \ne \beta$, this is a contradiction.

Case 2: If the latter does not hold, then by definition of β' there exists a sequence (x_n, y_n) such that $u(x_n, y_n) - p^{\beta'}(y_n) \to 0$. Since Ω is bounded, up to an extraction we have $y_n \to y_0 \in \overline{\Omega}$. Then $u(x_n, y_n) \to_{n\to\infty} p^{\beta'}(y_0)$.

Since equation (2.4.32) is invariant by translation in x, we consider the shifted functions $u^n(x,y) := u(x+x^n,y)$ which also satisfy (2.4.32). Then from the standard elliptic estimates and up to an extraction, u^n converges locally uniformly to u^∞, which is a classical solution to (2.4.32) and also satisfies $u^\infty(0,y_0) = p^{\beta'}(y_0)$ and $\forall x,y, u^\infty(x,y) \geq p^{\beta'}(y)$. Applying Case 1 to $(u^\infty, p^{\beta'})$ leads to a contradiction.

We have shown that either case leads to a contradiction if $\beta' > \max(\beta,\beta_0)$. Hence $\beta' \leq \max(\beta,\beta_0)$ and we conclude by the estimate in Lemma 2.4.19 that the inequality $u \geq \rho_{\max(\beta,\beta_0)}$ holds. □

Proof of Theorem 2.4.24. Let $\tau := \frac{1}{2}\min\left((k_0|\Omega|+\beta)\rho_\beta, -\lambda_1^\varepsilon\right)$, where ρ_β is the constant from Lemma 2.4.19, and u be the corresponding solution to (2.4.32), i.e. a solution to (2.4.32) constructed in Corollary 2.4.23, which satisfies

$$\sup_{(x,y)\in(-l_0,l_0)\times\Omega}\left(\int_\Omega K(y,z)u(x,z)dz + \beta u(x,y)\right) = \tau \leq \frac{1}{2}(k_0|\Omega|+\beta)\rho_\beta. \tag{2.4.38}$$

Recall that, as stated in Corollary 2.4.27, $x \mapsto u(x,y)$ is decreasing.

We divide the proof in three steps.

Step 1: We show that $\inf_{(x,y)\in\mathbb{R}\times\Omega} u(x,y) = 0$.

Indeed, recalling (2.4.38), we have

$$\begin{aligned}(k_0|\Omega|+\beta)u(0,0) &\leq \sup_{(x,y)\in(-l_0,l_0)\times\Omega}\int_\Omega K(y,z)u(x,z)dz + \beta u(x,y)\\ &\leq \frac{1}{2}(k_0|\Omega|+\beta)\rho_\beta,\end{aligned}$$

and thus $u(0,0) \leq \frac{1}{2}\rho_\beta < \rho_\beta$. The contrapositive of Lemma 2.4.29 concludes.

Step 2: We show that $\lim_{x\to+\infty}\sup_{y\in\Omega} u(x,y) = 0$.

We proved in Step 1 that $\inf u = 0$. Since $u(x,y) > 0$ for $(x,y) \in \mathbb{R}\times\overline{\Omega}$ and u is decreasing in x, we must then have $\lim_{x\to+\infty}\inf_{y\in\Omega} u(x,y) = 0$.

Let $u^n(x,y) := u(x-n,y)$ and y_n such that $u^n(0,y_n) = \inf_{y\in\Omega} u^n(0,y)$. Since Ω is bounded, up to the extraction of a subsequence there exists $y \in \overline{\Omega}$ such that $y_n \to y_0$. It follows from the classical elliptic estimates that we then extract from (u^n) a subsequence which converges locally uniformly on $\mathbb{R}\times\Omega$ to a limit function u^0, which is still a classical solution to (2.4.32).

Since u is decreasing, the equalities

$$\lim_{x\to+\infty}\sup_{y\in\Omega} u(x,y) = \sup_{y\in\Omega} u^0(0,y) \text{ and } 0 = \lim_{x\to+\infty}\inf_{y\in\Omega} u(x,y) = \inf_{y\in\Omega} u^0(0,y) = u(0,y_0)$$

hold. If $y_0 \in \partial\Omega$ and $u^0 \not\equiv 0$, then it follows from Hopf's Lemma that $\frac{\partial u^0}{\partial\nu}(y_0) < 0$, which contradicts the Neumann boundary conditions satisfied by u^0. If $y \in \Omega$ then the strong maximum principle imposes $u^0 \equiv 0$. In either case, we have $u^0 \equiv 0$ and thus $\lim_{x\to+\infty}\sup_{y\in\Omega} u(x,y) = 0$.

Step 3: We show that $\lim_{x\to-\infty}\inf_{y\in\Omega} u(x,y) \geq \rho_\beta$.

Let $u^n(x,y) := u(x+n,y)$. Using the classical elliptic estimates, we extract from (u^n) a subsequence that converges locally uniformly on $\mathbb{R}\times\Omega$ to a limit function u^0, which is still a classical solution to (2.4.32).

Since u is decreasing, we have $\lim_{x\to-\infty}\inf_{y\in\Omega} u(x,y) = \inf_{y\in\Omega,x\in\mathbb{R}} u^0(x,y)$. In particular, we have $\inf_{(x,y)\in\mathbb{R}\times\Omega} u^0(x,y) > 0$. Applying Lemma 2.4.29, we conclude that

$$\lim_{x\to-\infty}\inf_{y\in\Omega} u(x,y) = \inf_{(x,y)\in\mathbb{R}\times\Omega} u^0(x,y) \geq \rho_\beta.$$

To conclude the proof of Theorem 2.4.24, we remark that Lemma 2.4.28 states that $0 \leq c < c_\varepsilon^*$ is incompatible with $\lim_{x\to+\infty}\sup_{y\in\Omega} u(x,y) = 0$. This shows that $c = c_\varepsilon^*$. This finishes the proof of Theorem 2.4.24. □

2.4.5.3 Minimal speed traveling wave for $\beta = 0$

Here we construct traveling waves for our initial regularized problem

$$\begin{cases} ll - \varepsilon\Delta_y u - u_{xx} - cu_x = \mu(M\star u - u) + u(a(y) - K\star u) \text{ in } \mathbb{R}\times\Omega \\ \qquad\qquad\qquad\qquad\qquad\qquad \dfrac{\partial u}{\partial\nu} = 0 \text{ on } \mathbb{R}\times\partial\Omega. \end{cases} \tag{2.4.39}$$

Notice that (2.4.39) is exactly the equation (2.4.32) in the special case $\beta = 0$. In particular, our results obtained in Corollary 2.4.23 and Lemmas 2.4.25, 2.4.28 and 2.4.29 still apply to the solutions of (2.4.39).

Our result is the following:

Theorem 2.4.30 (Regularized minimal speed traveling waves)**.** *Let Assumption 2.4.2 hold, $0 < \varepsilon \leq \varepsilon_0$ (where ε_0 is as in Lemma 2.4.19) and assume $\lambda_1^\varepsilon < 0$. Then, there exists a nonnegative nontrivial traveling wave (c, u) for (2.4.39) with $c = c_\varepsilon^*$, i.e. a bounded classical solution which satisfies:*

$$\liminf_{x\to-\infty} \inf_{y\in\Omega} u(x,y) > 0, \qquad \limsup_{x\to+\infty} \int_\Omega u(x,y)dy = 0. \tag{2.4.40}$$

Moreover, c_ε^* is the minimal speed for traveling waves in the sense that there exists no traveling wave for equation (2.4.39) with $0 \leq c < c_\varepsilon^*$.

Finally, u can be chosen so that $\sup_{x\in\mathbb{R}} \int_\Omega u(x,y)dy \leq \frac{\sup a}{k_0}$ and

$$\liminf_{x\to-\infty} \inf_{y\in\Omega} u(x,y) \geq \rho_{\beta_0},$$

where $\beta_0 = \frac{k_\infty \sup a}{\mu m_0}$ and ρ_{β_0} is given by Lemma 2.4.19.

Two key elements for the proof of Theorem 2.4.30 are the following Harnack-type inequality, and the following Lemma 2.4.32, which states that $\inf_{y\in\Omega} u(x,y)$ and $\int_\Omega u(x,y)dy$ are locally comparable.

Lemma 2.4.31 (Harnack inequality for the mass)**.** *Let Assumption 2.4.2 hold and $\varepsilon > 0$. Let $\bar{c} > 0$, $R > 0$ and $W > 0$ be given. Let (c, u) be a solution to (2.4.39) with $|c| \leq \bar{c}$, $u \geq 0$ and $\int_\Omega u(x,y)dy \leq W$ for $x \in (-R, R)$. Then, there exists a constant $\mathcal{H} > 0$ depending only on R, $\|a\|_{L^\infty}$, W, k_∞ and $\bar{c}$ such that*

$$\sup_{|x|\leq R} \int_\Omega u(x,z)dz \leq \mathcal{H} \inf_{|x|\leq R} \int_\Omega u(x,z)dz.$$

Proof. Let $I(x) := \int_\Omega u(x,y)dy$, then I solves

$$\begin{aligned} -cI_x - I_{xx} &= \int_\Omega a(y)u(x,y)dy - \int_\Omega (K \star u)(y)u(x,y)dy \\ &= \left(\int_\Omega a(y) \frac{u(x,y)}{\int_\Omega u(x,z)dz} dy - \int_\Omega K \star u(x,y) \frac{u(x,y)}{\int_\Omega u(x,z)dz} dy \right) I. \end{aligned}$$

Now we remark that $\left| \int_\Omega a(y) \frac{u(x,y)}{\int_\Omega u(x,z)dz} dy \right| \leq \|a\|_{L^\infty}$ and

$$0 \leq \int_\Omega K \star u(x,y) \frac{u(x,y)}{\int_\Omega u(x,z)dz} dy \leq \|K \star u\|_{L^\infty} \leq k_\infty \int_\Omega u(x,y)dy \leq k_\infty W,$$

for any $x \in \mathbb{R}$, so that the classical Harnack inequality [187, Corollary 9.25] applies. □

Lemma 2.4.32 (Integral-infimum comparison)**.** *Let Assumption 2.4.2 hold and $\varepsilon > 0$. Let $\bar{c} > 0$, $x_0 \in \mathbb{R}$, $\kappa > 0$ and $W > 0$ be given. Let (c, u) be a solution to (2.4.39) with $|c| \leq \bar{c}$, $u \geq 0$ and $\int_\Omega u(x,y)dy \leq W$ for $|x - x_0| \leq 1$. Assume*

$$\int_\Omega u(x_0,y)dy \geq \kappa.$$

Then, there exists a positive constant $\bar{\kappa}$ depending only on $\|a\|_{L^\infty}$, μ, m_0, k_∞, $\bar{c}$, W and κ such that

$$\inf_{y\in\Omega} u(x_0,y) \geq \bar{\kappa}.$$

Proof. Since (2.4.39) is translation-invariant in x, we will assume without loss of generality that $x_0 = 0$.

Step 1: We construct a local subsolution.

From Lemma 2.4.31 there exists a constant $\mathcal{H} > 0$ such that

$$\kappa \leq \sup_{x\in(-1,1)} \int_\Omega u(x,z)dz \leq \mathcal{H} \inf_{x\in(-1,1)} \int_\Omega u(x,z)dz \leq \mathcal{H}\kappa.$$

Thus u satisfies:

$$-cu_x - u_{xx} - \varepsilon\Delta_y u \geq \mu m_0 \frac{\kappa}{\mathcal{H}} + \left(\inf_\Omega a - \mu - k_\infty W\right) u.$$

In particular there exists constants $\gamma > 0$ and $\alpha > 0$ depending only on $\|a\|_{L^\infty}$, μ, m_0, k_∞, W and κ such that

$$-cu_x - u_{xx} - \varepsilon\Delta_y u \geq \gamma - \alpha u \tag{2.4.41}$$

We define, for $\theta := \frac{2}{\sqrt{c^2+4\alpha}}\operatorname{atanh}\left(\frac{c}{\sqrt{c^2+4\alpha}}\right)$,

$$f^\delta(x) := \frac{\gamma}{\alpha} - \delta e^{-\frac{c}{2}(x-\theta)}\cosh\left(\frac{x-\theta}{2}\sqrt{c^2+4\alpha}\right).$$

Then f^δ satisfies

$$-cf^\delta_x - f^\delta_{xx} = \gamma - \alpha f^\delta.$$

In particular, f^δ satisfies the equality in (2.4.41). Moreover for any $\delta > 0$, f^δ has a unique maximum located at 0 and $f^\delta \to -\infty$ as $x \to \pm\infty$. Finally, the mapping $\delta \mapsto f^\delta$ is decreasing.

Step 2: We identify δ_0 such that $u \geq f^{\delta_0}$.

Let $\delta_0 := \inf\{\delta > 0 \,|\, \forall x \in (-1,1), f^\delta \leq u\}$. We claim that we have either $f^{\delta_0}(1) \geq 0$ or $f^{\delta_0}(-1) \geq 0$. Indeed, assume by contradiction that the inequalities $f^{\delta_0}(-1) < 0$ and $f^{\delta_0}(1) < 0$ hold. Then there exists $x_0 \in (-1,1)$, $y_0 \in \overline{\Omega}$ such that $u(x_0,y_0) = f^{\delta_0}(x_0)$. If $y_0 \in \partial\Omega$, then it follows from Hopf's Lemma that $\frac{\partial(u-f^{\delta_0})}{\partial\nu}(x_0,y_0) < 0$ since 0 is a minimum for the function $u - f^{\delta_0}$. This contradicts the Neumann boundary condition satisfied by u since $\frac{\partial f^{\delta_0}}{\partial\nu}(x_0,y_0) = 0$. If $y_0 \in \Omega$, we have

$$\begin{aligned}-c(u-f^{\delta_0})_x(x_0,y_0) - (u-f^{\delta_0})_{xx}(x_0,y_0) - \varepsilon\Delta_y(u-f^{\delta_0})(x_0,y_0)& \\ \geq \big(\gamma - \alpha u(x_0,y_0)\big) - \big(\gamma - \alpha f^{\delta_0}(x_0,y_0)\big) = 0.&\end{aligned}$$

By a direct application of the strong maximum principle, we have then $u = f^{\delta_0}$ in $(-1,1)\times\overline{\Omega}$, which is a contradiction since f^{δ_0} is not positive in $(-1,1)$.

Step 3: We show that δ_0 is bounded by a constant depending only on $\bar{c}$, α and γ.

Let us define $\delta_1^c := \inf\{\delta > 0 \,|\, f^\delta(-1) < 0 \text{ and } f^\delta(1) < 0\}$. δ_1^c is well-defined since $\lim_{\delta\to+\infty} f^\delta(\pm 1) = -\infty$ and $\lim_{\delta\to 0} f^\delta(\pm 1) = \frac{\gamma}{\alpha} > 0$. Moreover, we have either $f^{\delta_1^c}(1) = 0$ or $f^{\delta_1^c}(-1) = 0$. Thus

$$\delta_1^c = \frac{\gamma}{\alpha}\max\left(\frac{e^{\frac{c}{2}(1-\theta)}}{\cosh\left(\frac{1-\theta}{2}\sqrt{c^2+2\alpha}\right)}, \frac{e^{\frac{c}{2}(-1-\theta)}}{\cosh\left(\frac{-1-\theta}{2}\sqrt{c^2+2\alpha}\right)}\right).$$

Since θ depends continuously on c, the mapping $c \mapsto f^{\delta_1^c}(0)$ is continuous. Moreover for any $|c| \leq \bar{c}$, $f^{\delta_1^c}(0) > 0$ since $x = 0$ is the strict maximum of $f^{\delta_1^c}$. Finally $\delta_0 \leq \delta_1^c$ since the mapping $\delta \mapsto f^\delta$ is decreasing. We have then

$$\inf_{y\in\Omega} u(0,y) \geq \inf_{|c|\leq\bar{c}} f^{\delta_1^c}(0) > 0$$

where the right-hand side depends only on $\bar{c}$, α and γ. This finishes the proof of Lemma 2.4.32. □

Lemma 2.4.33 (Infimum estimate on the left)**.** *Let Assumption 2.4.2 be satisfied, let $0 < \varepsilon \leq \varepsilon_0$ be such that $\lambda_1^\varepsilon < 0$ (where ε_0 is given by Lemma 2.4.19), let finally $\beta' \geq \beta_0 = \frac{k_\infty \sup a}{\mu m_0}$ and u be a solution to (2.4.39) with $0 \leq c \leq c_\varepsilon^*$ and $\beta = 0$. Suppose*

$$\forall y \in \Omega, \quad u(0,y) \geq 2\frac{\sup a}{\beta'}.$$

Then,

$$\forall x \leq 0, y \in \Omega, \quad u(x,y) \geq \rho_{\beta'}$$

where $\rho_{\beta'}$ is given by Lemma 2.4.19.

Proof. We divide the proof in two step.

Step 1: We show that $\inf_{x\leq 0, y\in\Omega} u(x,y) > 0$.

Let φ^ε be a positive solution to (2.4.17), normalized so that

$$\sup_{y\in\Omega} \varphi^\varepsilon(y) = \frac{1}{2}\min\left(\inf_{y\in\Omega} u(0,y), \frac{-\lambda_1^\varepsilon}{|\Omega| k_\infty}, \frac{\mu m_0}{k_\infty}\right) > 0.$$

We define $\alpha := \inf\{\zeta > 0 \,|\, \forall x \in (-\infty, 0), y \in \Omega, (1+\zeta x)\varphi^\varepsilon(y) \leq u(x,y)\}$. Remark that, since u is positive and $\varphi^\varepsilon(y) < u(0,y)$ for any $y \in \mathbb{R}$, α is well-defined.

Assume by contradiction that $\alpha > 0$. Then by definition of α there exists a point $(x_0, y_0) \in \left(-\frac{1}{\alpha}, 0\right) \times \overline{\Omega}$ such that $u(x_0,y_0) = (1+\alpha x_0)\varphi^\varepsilon(y_0)$. Because of the boundary conditions satisfied by u and $(1+\alpha x)\varphi$, (x_0, y_0) cannot be in the boundary of $\left[\frac{-1}{\alpha}, 0\right] \times \Omega$. Letting $v(x,y) := (1+\alpha x)\varphi^\varepsilon(y)$, we remark that, since $x_0 < 0$, we have

$$\begin{aligned} -cv_x(x_0,y_0) - v_{xx}(x_0,y_0) - \varepsilon\Delta_y v(x_0,y_0) - \mu(M\star v - v)(x_0,y_0) & \\ -v\big(a(y_0) - K\star v\big)(x_0,y_0) &= -c\alpha\varphi(y_0) + \lambda_1^\varepsilon v(x_0,y_0) \\ &\quad + v(x_0,y_0)(K\star v)(x_0,y_0) \\ &\leq \frac{\lambda_1^\varepsilon}{2} < 0, \end{aligned}$$

since $v(x_0,y_0) \leq \frac{-\lambda_1^\varepsilon}{2|\Omega|k_\infty}$ (recall that v is increasing in x). Hence v is a local subsolution to (2.4.35) near (x_0,y_0), and Lemma 2.4.25 leads to $u \equiv v$, which is a contradiction.

Thus $\alpha = 0$ and we have shown that $\forall x < 0$, $\varphi^\varepsilon(y) \leq u(x,y)$. In particular we have the lower estimate $\inf_{x<0, y\in\Omega} u(x,y) \geq \inf_{y\in\Omega}\varphi^\varepsilon(y) > 0$.

Step 2: We remove the dependency in ε.

Let v be a decreasing solution to (2.4.32) with $c = c_\varepsilon^*$ constructed in Theorem 2.4.24. Define $\tilde{v}(x,y) = v(-x,y)$. Then $\tilde{v}$ satisfies:

$$c_\varepsilon^*\tilde{v}_x - \tilde{v}_{xx} - \varepsilon\Delta_y\tilde{v} - \mu(M\star\tilde{v} - \tilde{v}) = \tilde{v}(a(y) - K\star\tilde{v} - \beta'\tilde{v}).$$

In particular,

$$\begin{aligned} -c\tilde{v}_x - \tilde{v}_{xx} - \varepsilon\Delta_y\tilde{v} - \mu(M\star\tilde{v} - \tilde{v}) &= \tilde{v}(a(y) - K\star\tilde{v} - \beta'\tilde{v}) - (c + c_\varepsilon^*)\tilde{v}_x \\ &\leq \tilde{v}(a(y) - K\star\tilde{v}), \end{aligned}$$

since $\tilde{v}_x \geq 0$. Moreover, $\sup v \leq \frac{\sup a}{\beta'}$ by the estimate in Theorem 2.4.24. Using Lemma 2.4.25 will then allow us to compare $\tilde{v}$ with u.

Since $\tilde{v} \to 0$ when $x \to -\infty$ and as a result of Step 1 above, there exists a positive shift $\zeta > 0$ such that $\tilde{v}(x+\zeta, y) \leq \frac{1}{2}\inf_{\bar{x}<0, \bar{y}\in\Omega} u(\bar{x},\bar{y})$ for any $(x,y) \in (-\infty, 0) \times \Omega$. Using a sliding argument simliar to the one in Step 2 of Lemma 2.4.26, then for any $\zeta \in \mathbb{R}$, $x < 0$ and $y \in \Omega$, we have $u(x,y) \geq \tilde{v}(x+\zeta, y)$. Taking the limit $\zeta \to +\infty$, we get that $\inf_{x<0, y\in\Omega} u(x,y) \geq \lim_{x\to+\infty}\inf_{y\in\mathbb{R}}\tilde{v}(x,y) \geq \rho_{\beta'}$, by the estimate in Theorem 2.4.24.

This finishes the proof of Lemma 2.4.33. □

We are now in a position to prove Theorem 2.4.30.

Proof of Theorem 2.4.30. We divide the proof in two steps.

Step 1: We construct a solution with $\limsup_{x\to+\infty}\int_\Omega u(x,y)dy = 0$.

Let (c,u) be the solution constructed in Corollary 2.4.23 with $\beta = 0$ and the normalization $\tau = \frac{1}{2}\min\left(\rho_{\beta_0}k_0|\Omega|, \frac{-\lambda_1^\varepsilon}{2}\right)$, where $\beta_0 = \frac{k_\infty \sup a}{\mu m_0}$ and ρ_{β_0} is given by Lemma 2.4.19. Assume by contradiction that $\limsup_{x\to+\infty}\int_\Omega u(x,y)dy > 0$. Then by definition there exists a positive number $\kappa > 0$ and a sequence $x_n \to +\infty$ such that $\int_\Omega u(x_n,y)dy \geq \kappa$. By the estimate in Lemma 2.4.32, there exists $\bar{\kappa} > 0$ such that for any $n \in \mathbb{N}$, $\inf_{y\in\Omega} u(x_n,y) \geq \bar{\kappa}$. Let $\beta := \max\left(2\frac{\sup a}{\kappa}, \beta_0\right)$, then a direct application of Lemma 2.4.33 shows that for any $n \in \mathbb{N}$, we have $\inf_{x<x_n, y\in\Omega} u(x,y) > \rho_\beta > 0$. In particular, taking the limit $n \to \infty$, we

get $\inf_{(x,y)\in\mathbb{R}\times\Omega} u(x,y) \geq \rho_\beta > 0$. By the estimate in Lemma 2.4.29, this shows $\inf_{(x,y)\in\mathbb{R}\times\Omega} u(x,y) \geq \rho_{\beta_0}$. However, due to the normalization satisfied by u (2.4.28), we have

$$k_0|\Omega|\rho_{\beta_0} \leq (K \star u)(x,0) \leq \frac{1}{2}k_0|\Omega|\rho_{\beta_0},$$

which is a contradiction. We conclude that $\limsup_{x\to+\infty} \int_\Omega u(x,y)dy = 0$.

Step 2: We show that u satisfies the other properties required by Theorem 2.4.30.

Since u is given by Corollary 2.4.23, u naturally satisfies $\int_\Omega u(x,y)dy \leq \frac{\sup a}{k_0}$.

Let us show briefly that $\liminf_{x\to-\infty} \inf_{y\in\Omega} u(x,y) \geq \rho_{\beta_0}$. Applying the previously proved Lemma 2.4.33 we have $\liminf_{x\to-\infty} \inf_{y\in\Omega} u(x,y) > 0$. Let (x_n, y_n) be a minimizing sequence. By the classical elliptic estimates, $u(x+x_n,\cdot)$ converges locally uniformly to a solution $\bar{u}$ of (2.4.39) with $\inf_{(x,y)\in\mathbb{R}\times\Omega} \bar{u}(x,y) > 0$. Then by the estimate in Lemma 2.4.29, $\inf_{(x,y)\in\mathbb{R}\times\Omega} \bar{u}(x,y) \geq \rho_{\beta_0}$. We conclude by remarking that $\liminf_{x\to-\infty} \inf_{y\in\Omega} u(x,y) = \inf_{(x,y)\in\mathbb{R}} \bar{u}(x,y) \geq \rho_{\beta_0}$.

We finally remark that Lemma 2.4.28 item (ii) gives the minimality property of the speed c^*_ε. In particular $c = c^*_\varepsilon$ for the solution (c,u) constructed here.

This ends the proof of Theorem 2.4.30. □

Next we prove an upper estimate on the limit of $\int_\Omega u(x,y)dy$ when x is in the vicinity of $+\infty$, which is independent of ε.

Lemma 2.4.34 ($\int_\Omega u(x,y)dy \to 0$ when $x \to +\infty$)**.** *Let Assumption 2.4.2 hold, and suppose $\lambda_1 < 0$. There exists $\bar{\varepsilon} > 0$, $\tau > 0$ and a sequence $(x_n)_{n\in\mathbb{N}}$ independent from ε, such that if u solves* (2.4.39) *with $0 < \varepsilon \leq \bar{\varepsilon}$, $c = c^*_\varepsilon$ and satisfies $\int_\Omega u(x,z)dz \leq \tau$ for any $x \geq 0$, then*

$$\forall n \in \mathbb{N}, \forall x \geq x_n, \int_\Omega u(x,z)dz \leq \frac{\tau}{2^n}.$$

Proof. We divide the proof into three steps.

Step 1: Definition of auxiliary parameters.

Since $a(0) = \sup a$, by the continuity of a and Assumption 2.4.2 item 6, there exists $r > 0$ such that for any $|y| \leq r$, $a(y) - \mu \geq \frac{3}{4}(\sup a - \mu)$. In the rest of the proof we fix $r > 0$ such that this property holds and $B_r(y) \subset \Omega$. Notice that for $|y| \leq r$, we have $a(y) - \mu \geq \frac{3}{4}(\sup a - \mu) > 0$.

We define $\bar{\varepsilon} := \min\left(\varepsilon_0, \frac{r^2(\sup a - \mu)}{2n\pi^2}\right)$, where $\varepsilon_0 > 0$ is given by Lemma 2.4.19. We let

$$\tau := \min\left(\frac{1}{2}\rho_{\beta_0}k_0|\Omega|, \frac{\sup a - \mu}{4k_\infty}\right),$$

where $\beta_0 = \frac{k_\infty \sup a}{\mu m_0}$ and ρ_{β_0} is given by Lemma 2.4.19. In particular, arguing as in the proof of Theorem 2.4.30, any solution u to (2.4.39) with $0 < \varepsilon \leq \bar{\varepsilon}$ which satisfies $\int_\Omega u(0,y)dy \leq \tau$ has limit 0 near $+\infty$, i.e. $\int_\Omega u(x,y)dy \to_{x\to+\infty} 0$.

By Lemma 2.4.32 and 2.4.33, there exists $\rho > 0$ such that if $\int_\Omega u(x,y)dy \geq \frac{\tau}{2}$ holds, then for any $x' \leq x$ we have the estimate $\inf_{y\in\Omega} u(x',y) \geq \rho$.

We let $\alpha_0 := \max\left(\frac{\tau}{\int_{|y|\leq r}\cos\left(\frac{\pi|y|}{2r}\right)dy}, 2\rho\right)$, $\gamma := \min\left(1, \left(\frac{\sup a-\mu}{8(c^*_\varepsilon\sqrt{\alpha_0}+1)}\rho\right)^2\right)$. Notice in particular that $2c^*_\varepsilon\sqrt{\gamma}\alpha_0 + 2\gamma - \frac{\sup a-\mu}{4}\rho \leq 0$. Finally we define $\bar{x} := \sqrt{\frac{\alpha_0}{\gamma}}$. Remark that, since $c^*_\varepsilon \to 2\sqrt{-\lambda_1} > 0$ when $\varepsilon \to 0$ (by Theorem 2.4.15), $\bar{x}$ is uniformly bounded when $\varepsilon \to 0$.

Since (2.4.39) is invariant by translation in x we will assume without loss of generality that $\int_\Omega u(x,y)dy \leq \tau$ for $x \geq -\bar{x}$ instead of $x \geq 0$.

Step 2: We show that if $\int_\Omega u(x,y)dy \leq \tau$ for $x \geq -\bar{x}$ then $\int_\Omega u(\bar{x},y)dy \leq \frac{\tau}{2}$.

Here we let u be a solution to (2.4.39) with $0 < \varepsilon \leq \bar{\varepsilon}$, $c = c^*_\varepsilon$ and the upper estimate $\int_\Omega u(x,y) \leq \tau$ for $x \geq -\bar{x}$. We assume by contradiction that $\int_\Omega u(\bar{x},y)dy > \frac{\tau}{2}$. We will first use another proof by contradiction to show that, in that case, the mass of u can be controlled from below.

Since $u > 0$ on $(-\bar{x},\bar{x}) \times \Omega$, we define:

$$\alpha := \sup\left\{\zeta > 0 \,|\, \forall x \in (-\bar{x},\bar{x}), \forall |y| \leq r, \quad (\zeta - \gamma x^2)\cos\left(\frac{\pi|y|}{2r}\right) \leq u(x,y)\right\}.$$

Assume by contradiction that $\alpha < \alpha_0$. Then for any $(x,y) \in [-\bar{x},\bar{x}]\times\Omega$ we have $(\alpha-\gamma x^2)\cos\left(\frac{\pi|y|}{2r}\right) \le u(x,y)$, and there exists a point $x_0 \in [-\bar{x},\bar{x}]$ and y_0 with $|y_0| \le r$ such that $u(x_0,y_0) = (\alpha-\gamma x_0^2)\cos\left(\frac{\pi|y_0|}{2r}\right)$. Let $v := (\alpha-\gamma x^2)\cos\left(\frac{\pi|y|}{2r}\right)$. We have:

$$\begin{aligned}
0 &\le -c_\varepsilon^*(v-u)_x(x_0,y_0) - (v-u)_{xx}(x_0,y_0) - \varepsilon\Delta_y(v-u)(x_0,y_0)\\
&= 2c_\varepsilon^*\gamma x_0 + 2\gamma + n\varepsilon\left(\frac{\pi}{2r}\right)^2 v(x_0,y_0) - \mu(M\star u)(x_0,y_0)\\
&\quad - u(x_0,y_0)\big(a(y_0) - \mu - (K\star u)(x_0,y_0)\big)\\
&< 2\left(c_\varepsilon^*\sqrt{\alpha_0} + \sqrt{\gamma}\right)\sqrt{\gamma} + n\varepsilon\left(\frac{\pi}{2r}\right)^2 + 0\\
&\quad - \left(\frac{3(\sup a - \mu)}{4} - k_\infty\int_\Omega u(x_0,z)dz\right)u(x_0,y_0)\\
&= \left[2\left(c_\varepsilon^*\sqrt{\alpha_0} + \sqrt{\gamma}\right)\sqrt{\gamma} - \frac{\sup a-\mu}{4}\rho\right] + \left(\varepsilon\left(\frac{\pi}{2r}\right)^2 - \frac{\sup a-\mu}{4}\right)u(x_0,y_0)\\
&\le 0,
\end{aligned}$$

recalling that $\inf_y u(x_0,y) \ge \rho$ since $x_0 \le \bar{x}$.

Hence, we have a contradiction and $\alpha \ge \alpha_0 \ge \frac{\tau}{\int_{|y|\le r}\cos\left(\frac{\pi|y|}{2r}\right)dy}$. In particular, we have $(\alpha_0-\gamma x^2)\cos\left(\frac{\pi|y|}{2r}\right) \le u(x,y)$ and

$$\tau \le \alpha_0\int_{|y|\le r}\cos\left(\frac{\pi|y|}{2r}\right)dy < \int_\Omega u(0,y)dy,$$

where the strict inequality holds because $u(0,y) > 0$ on $\Omega\backslash B(0,r)$. This contradicts our hypothesis $\int_\Omega u(x,y)dy \le \tau$ when $x \ge -\bar{x}$. We conclude that $\int_\Omega u(\bar{x},y)dy \le \frac{\tau}{2}$.

Step 3: Bootstrapping

In Step 2 we have shown that for a $\bar{x}$ which is uniformly bounded in ε, we have

$$\left(\forall x \ge -\bar{x}, \int_\Omega u(x,y)dy \le \tau\right) \Rightarrow \left(\int_\Omega u(\bar{x},y)dy \le \frac{\tau}{2}\right).$$

Since (2.4.39) is invariant by translation, this implication still holds for $u(x,y)$ replaced by $u(x+\delta,y)$ for any $\delta > 0$. In particular,

$$\left(\forall x \ge -\bar{x}, \int_\Omega u(x,y)dy \le \tau\right) \Rightarrow \left(\forall x \ge \bar{x}, \int_\Omega u(x,y)dy \le \frac{\tau}{2}\right).$$

Thus we can reproduce Step 1 and 2 replacing τ by $\frac{\tau}{2}$ and $u(x,y)$ by its shift $u(x+\bar{x},y)$. We thus find by an elementary recursion a sequence of points x_n such that for $x \ge x_n$, $\int_\Omega u(x,y)dy \le \frac{\tau}{2^n}$.

This ends the proof of Lemma 2.4.34. □

2.4.5.4 Proof of Theorem 2.4.10

We are now in a position to let $\varepsilon \to 0$ and construct a traveling wave for equation (2.4.1), thus proving our main result Theorem 2.4.10.

Proof of Theorem 2.4.10. We divide the proof in three steps.

Step 1: Construction of a converging sequence to a transition kernel.

Let ε_n be a decreasing sequence with $\lim\varepsilon_n = 0$ and $\varepsilon_0 \le \bar{\varepsilon}$ (where $\bar{\varepsilon}$ is given by Lemma 2.4.34) such that for any $0 < \varepsilon \le \varepsilon_0$, $\lambda_1^\varepsilon < 0$ (such a ε_0 exists by Theorem 2.4.15). Since (2.4.39) is invariant by translations in x, for each ε_n we can choose u^n given by Theorem 2.4.30 (with $\varepsilon = \varepsilon_n$), which satisfies moreover

$$\int_\Omega u^n(0,y)dy = \min\left(\frac{\rho_{\beta_0}}{2},\tau\right), \qquad \forall x \ge 0, \int_\Omega u^n(x,y)dy \le \tau, \tag{2.4.42}$$

where τ is given by Lemma 2.4.34, $\beta_0 = \frac{k_\infty \sup a}{\mu m_0}$ and ρ_{β_0} is given by Lemma 2.4.19.

For any $k \leq n$, let u_k^n be the restriction of u^n to the set $[-k,k]\times\Omega$. Then u_k^n belongs to $M^1([-k,k]\times\overline{\Omega}) = (C_b([-k,k]\times\overline{\Omega}))^*$. Since $\int_\Omega u^n(x,y)dy \leq \frac{\sup a}{k_0}$ for $x\in\mathbb{R}$, we have $\int_{-k}^k\int_\Omega u^n(x,y)dydx \leq 2k\frac{\sup a}{k_0}$, and thus the sequence $(u_k^n)_{n>k}$ is uniformly bounded in variation norm. Moreover $[-k,k]\times\overline{\Omega}$ is compact, and thus $(u_k^n)_{n>k}$ is uniformly tight. Applying Prokhorov's Theorem [63, Theorem 8.6.2], the sequence $(u_k^n)_{n>k}$ is relatively compact in $(C_b([-k,k]\times\overline{\Omega}))^*$. Then, by a classical diagonal extraction process, there exists a subsequence, still denoted u^n, and a measure $u\in M^1(\mathbb{R}\times\overline{\Omega})$ such that $u^n \rightharpoonup u$, in the sense that

$$\forall\psi\in C_c(\mathbb{R}\times\overline{\Omega}), \int_{\mathbb{R}\times\Omega}\psi(x,y)u^n(x,y)dydx \to \int_{\mathbb{R}\times\overline{\Omega}}\psi(x,y)u(dx,dy). \tag{2.4.43}$$

Finally, for $a<b$, by a classical result [63, Theorem 8.2.3], for any Borel set $\omega\subset\overline{\Omega}$ we have

$$u\big((a,b)\times\omega\big) \leq u\big((a,b)\times\overline{\Omega}\big) \leq \liminf_{n\to\infty}\int_a^b\int_\Omega u^n(x,y)dydx \leq |b-a|\frac{\sup a}{k_0}.$$

Hence, Lemma 2.4.37 applies and u is a transition kernel, satisfying the equation $u(dx,dy)=u(x,dy)dx$.

Let us stress at this point that the possibility to think of u as a transition kernel, i.e. a function which takes values in a measure space, is important for the rest of the proof, as it allows us to consider $M\star u(x,y)=\int_{\overline{\Omega}}M(y,z)u(x,dz)$ and $K\star u(x,y)=\int_{\overline{\Omega}}K(y,z)u(x,dz)$ as real functions of x and y, even for singular traveling waves. Handling a term like $\int_{\overline{\Omega}}M(y,z)u(dx,dy)$ would indeed be quite difficult, if ever possible – let aside $(K\star u)u$, which would involve the product of two measures. Also, it is the only regularity that we can get on the solution at the present time.

Step 2: We show that u satisfies the limit conditions (2.4.12) and (2.4.13) of Definition 2.4.9.

By construction, the function u^n satisfies $\int_\Omega u^n(0,y)dy = \min\big(\tau,\frac{\rho_{\beta_0}}{2}\big)$. Applying Lemma 2.4.32 and Lemma 2.4.33, there exists a positive constant $\rho>0$ (independent from n) such that $\inf_{y\in\Omega}u^n(x,y)\geq\rho$ for any $x\leq 0$. In particular, taking the limit $n\to\infty$, we have for any positive $\psi\in C_c\big((-\infty,0)\times\overline{\Omega}\big)$

$$\begin{aligned}\int_{\mathbb{R}\times\overline{\Omega}}\psi(x,y)u(x,dy)dx &= \lim_{n\to\infty}\int_{\mathbb{R}\times\Omega}\psi(x,y)u^n(x,y)dxdy\\ &\geq \rho\int_{\mathbb{R}\times\Omega}\psi(x,y)dxdy>0.\end{aligned}$$

Hence $\liminf_{\bar{x}\to+\infty}\int_{\mathbb{R}\times\overline{\Omega}}\psi(x+\bar{x},y)u(x,dy)dx \geq \rho\int_{\mathbb{R}\times\Omega}\psi(x,y)dxdy>0$, and u satisfies (2.4.12).

Let us show that u satisfies (2.4.13), i.e. vanishes near $+\infty$. Applying Lemma 2.4.34, there exists a sequence x_k independent from n such that we have $\int_\Omega u^n(x,y)dy\leq\frac{\tau}{2^k}$ for any $x\geq x_k$. In particular for any positive $\psi\in C_c\big((x_k,+\infty)\times\overline{\Omega}\big)$, we have

$$\begin{aligned}\int_{\mathbb{R}\times\overline{\Omega}}\psi(x-x_k,y)u(x,dy)dx &= \lim_{n\to\infty}\int_{\mathbb{R}\times\Omega}\psi(x-x_k,y)u^n(x,y)dxdy\\ &\leq \frac{\tau}{2^k}\ \text{diam supp}\ \psi\sup_{(x,y)\in\mathbb{R}\times\Omega}\psi(x,y),\end{aligned}$$

where diam supp $\psi = \sup\big\{d\big((x,y),(x',y')\big)\,|\,\psi(x,y)>0 \text{ and } \psi(x',y')>0\big\}$ is the diameter of the support of ψ. Thus

$$\limsup_{\bar{x}\to+\infty}\int_{\mathbb{R}\times\overline{\Omega}}\psi(x-\bar{x},y)u(x,dy)dx = \limsup_{k\to+\infty}\int_{\mathbb{R}\times\overline{\Omega}}\psi(x-x_k,y)u(x,dy)dx=0,$$

and u satisfies indeed (2.4.13).

Let us stress that, since u satisfies (2.4.12) and (2.4.13), u is neither 0 nor a nontrivial stationary state to (2.4.1).

Step 3: We show that u satisfies (2.4.11) in the sense of distributions.

Let $F_0^y := \left\{\psi \in C_c^2(\mathbb{R}\times\overline{\Omega}) \,|\, \forall x\in\mathbb{R}, \forall y\in\partial\Omega, \frac{\partial\psi}{\partial\nu}(x,y)=0\right\}$ as in Lemma 2.4.35. We fix $\psi \in F_0^y$. Our goal here is to show that

$$\begin{aligned} & c^*\int_{\mathbb{R}\times\overline{\Omega}} \psi_x u(x,dy)dx - \int_{\mathbb{R}\times\overline{\Omega}} \psi_{xx} u(x,dy)dx \\ =& \int_{\mathbb{R}\times\overline{\Omega}}\int_{\overline{\Omega}} M(y,z)u(x,dz)\psi(x,y)dxdy + \int_{\mathbb{R}\times\overline{\Omega}} (a(y)-\mu)\psi(x,y)u(x,dy)dx \\ & - \int_{\mathbb{R}\times\overline{\Omega}}\int_{\overline{\Omega}} \psi(x,y)K(y,z)u(x,dz)u(x,dy)dx, \end{aligned} \tag{2.4.44}$$

where $c^* = 2\sqrt{-\lambda_1}$. Multiplying (2.4.39) by ψ and integrating by parts, we have

$$\begin{aligned} & c^*_{\varepsilon_n}\int_{\mathbb{R}\times\Omega} \psi_x(x,y)u^n(x,y)dxdy - \int_{\mathbb{R}\times\Omega} \psi_{xx}(x,y)u^n(x,y)dxdy \\ =& \varepsilon_n\int_{\mathbb{R}\times\overline{\Omega}} \Delta_y\psi(x,y)u^n(x,y)dxdy + \int_{\mathbb{R}\times\Omega}(a(y)-\mu)\psi(x,y)u^n(x,y)dxdy \\ & + \int_{\mathbb{R}\times\Omega}\psi(x,y)\int_\Omega M(y,z)u^n(x,z)dzdxdy \\ & - \int_{\mathbb{R}\times\Omega}\psi(x,y)\int_\Omega K(y,z)u^n(x,z)dzu^n(x,y)dxdy. \end{aligned} \tag{2.4.45}$$

Clearly, the difficulty here resides in the last two lines of equation (2.4.45) (recall the formula $c^*_\varepsilon = 2\sqrt{-\lambda_1^\varepsilon} \underset{\varepsilon\to 0}{\to} 2\sqrt{-\lambda_1} = c^*$). Let us focus on those.

We first remark that

$$\begin{aligned} \int_{\mathbb{R}\times\overline{\Omega}} \psi(x,y)(M\star u^n)(x,y)dxdy &= \int_{\mathbb{R}\times\overline{\Omega}} \check{M}\star\psi(x,z)u^n(x,z)dxdz \\ &\underset{n\to\infty}{\longrightarrow} \int_{\mathbb{R}\times\overline{\Omega}} \check{M}\star\psi(x,z)u(x,dz)dx = \int_{\mathbb{R}\times\overline{\Omega}}\psi(x,y)\int_{\overline{\Omega}} M(y,z)u(x,dz)dxdy, \end{aligned}$$

where $\check{M}(y,z) = M(z,y)$, since $\check{M}\star\psi(x,y)$ is a valid test function.

The convergence of the nonlinear term requires more work. For $i\in\mathbb{N}$, let $K^i(y,z)\in F_0^2$ be such that $\|K-K^i\|_{C_b(\overline{\Omega}\times\overline{\Omega})} \le \frac{1}{i}$ and $\|K^i\|_{C^\alpha(\overline{\Omega}\times\overline{\Omega})}\le C$, where F_0^2 is the set of smooth kernels with null boundary flux in z, and C is independent from i (see Lemma 2.4.35 item (*iii*)). We want to complete, up to extractions, the informal diagram

$$\begin{array}{ccc} v_i^n(x,y) := \int_\Omega K^i(y,z)u^n(x,z)dz & \underset{n\to+\infty}{\overset{?}{\longrightarrow}} & v_i(x,y) := \int_{\overline{\Omega}} K^i(y,z)u(x,z)dz \\ \downarrow\ i\to\infty & & \downarrow\ i\to\infty \\ v^n(x,y) := \int_\Omega K(y,z)u^n(x,z)dz & \underset{n\to+\infty}{\overset{?}{\longrightarrow}} & v(x,y) := \int_{\overline{\Omega}} K(y,z)u(x,z)dz. \end{array}$$

We first show that $v_i^n(x,y)\to v_i(x,y)$ when $n\to\infty$ in $C_b\big([-R,R]\times\overline{\Omega}\big)$ for arbitrary $R>0$. We fix R so that $\operatorname{supp}\psi\subset[-R,R]\times\overline{\Omega}$. Substituting z to y, multiplying equation (2.4.39) by K^i and integrating in z, we have

$$-c^*_{\varepsilon_n}(v_i^n)_x - (v_i^n)_{xx} = R^n(x,y)$$

where $R^n(x,y)$ is bounded in L^∞ uniformly in n:

$$\begin{aligned} |R^n(x,y)| = \Big| & \varepsilon_n\int_\Omega \Delta_z K^i(y,z)u^n(x,z)dz + \mu\int_\Omega K^i(y,z)(M\star u^n)(x,z)dz \\ & + \int_\Omega K^i(y,z)(a(z)-\mu-K\star u^n)u^n(x,z)dz\Big| \\ \le\ & \varepsilon_n\|K^i\|_{C_b(\overline{\Omega},C^2(\overline{\Omega}))}\frac{\sup a}{k_0} + \mu m_\infty|\Omega|\frac{\sup a}{k_0}\|K^i\|_{C_b(\overline{\Omega}\times\overline{\Omega})} \\ & + \left(\sup a + \mu + k_\infty\frac{\sup a}{k_0}\right)\frac{\sup a}{k_0}\|K^i\|_{C_b(\overline{\Omega}\times\overline{\Omega})}. \end{aligned}$$

For n large enough so that $\varepsilon_n \leq \frac{1}{\|K^i\|_{C_b(\overline{\Omega},C^2(\overline{\Omega}))}}$, by the estimate in [187, Theorem 9.11] and the classical Sobolev embeddings, $\|v_i^n(\cdot,y)\|_{C^\alpha([-R,R])}$ is uniformly bounded by a constant independent from n, i and $y \in \overline{\Omega}$. Since we have $K^i \in C^\alpha(\overline{\Omega}\times\overline{\Omega})$ uniformly in i, v_i^n is then uniformly Hölder in x and y and we have $\|v_i^n\|_{C^\alpha([-R,R]\times\overline{\Omega})} \leq C_R$ with C_R independent from n and i. In particular, there exists an extraction $\varphi^i(n)$ such that

– $\|v_i^{\varphi^i(n)}\|_{C^\alpha([-R,R]\times\overline{\Omega})} \leq C_R$, and

–$\|v_i^{\varphi^i(n)} - \tilde{v}_i\|_{C^{\alpha/2}([-R,R]\times\overline{\Omega})} \to_{n\to\infty} 0$,

for a function $\tilde{v}_i(x,z) \in C^{\alpha/2}\big([-R,R]\times\overline{\Omega}\big)$. Notice that we can assume without loss of generality that $\varphi^i(n)$ is extracted from $\varphi^{i-1}(n)$. Finally, for any test function $\xi(x) \in C_c\big([-R,R]\big)$, we have

$$\int_{-R}^R \xi(x) v_i^{\varphi^i(n)}(x,y)dx = \int_{-R}^R \int_\Omega \xi(x) K^i(y,z) u^{\varphi^i(n)}(x,z)dzdx$$
$$\to_{n\to\infty} \int_{-R}^R \int_{\overline{\Omega}} \xi(x) K^i(y,z) u(x,dz)dx = \int_{-R}^R \xi(x) v_i(x,z)dx,$$

since u^n converges to u in the sense of measures. This shows $\tilde{v}^i(x,y) = v_i(x,y)$ for almost every $x \in [-R,R]$.

Moreover since $\|v_i\|_{C^{\alpha/2}([-R,R]\times\overline{\Omega})} \leq C'_R$, there exists an extraction ζ such that $v_{\zeta(i)}$ converges in $C_b\big([-R,R]\times\overline{\Omega}\big)$ to $v(x,y) = \int_{\overline{\Omega}} K(y,z)u(x,dy)$, which shows a C^0 regularity on v.

We can then construct an extraction $\varphi(i)$ such that

– $\|v_{\zeta(i)}^{\varphi(i)} - v_{\zeta(i)}\|_{C_b([-R,R]\times\overline{\Omega})} \to_{i\to\infty} 0$, and

– $\|v_{\zeta(i)} - v\|_{C_b([-R,R]\times\overline{\Omega})} \to_{i\to\infty} 0$.

Along this subsequence, we have then:

$$\begin{aligned}
&\left|\int_\Omega K(y,z)u^{\varphi(i)}(x,y)dxdy - \int_{\overline{\Omega}} K(y,z)u(x,dy)\right| \\
&\leq \left|\int_\Omega \big(K(y,z) - K^{\zeta(n)}(y,z)\big)u^{\varphi(i)}(x,y)dxdy\right| + \left\|v_{\zeta(i)}^{\varphi(i)} - v_{\zeta(i)}\right\|_{C_b([-R,R]\times\overline{\Omega})} \\
&\quad + \|v_{\zeta(i)} - v\|_{C_b([-R,R]\times\overline{\Omega})} \\
&\leq \|K - K^{\zeta(i)}\|_{C_b(\overline{\Omega}\times\overline{\Omega})} \frac{\sup a}{k_0} + o_{i\to\infty}(1)
\end{aligned}$$

which shows that $\int_\Omega K(y,z)u^{\varphi(i)}(x,y)dy \to \int_{\overline{\Omega}} K(y,z)u(x,dy)$ in $C_b([-R,R]\times\overline{\Omega})$.

We are now in a position to handle the nonlinear term, by using the previously constructed subsequence. We write

$$\begin{aligned}
&\int_{\mathbb{R}\times\Omega\times\Omega} \psi(x,y)K(y,z)u^{\varphi(n)}(x,z)u^{\varphi(n)}(x,y)dxdydz \\
&= \int_{\mathbb{R}\times\Omega} \psi(x,y) \int_{\overline{\Omega}} K(y,z)u(x,dz)u^{\varphi(n)}(x,y)dxdy \\
&\quad + \int_{\mathbb{R}\times\Omega} \psi(x,y)\left(\int_\Omega K(y,z)u^{\varphi(n)}(x,z)dz - \int_{\overline{\Omega}} K(y,z)u(x,dz)\right) \\
&\quad \times u^{\varphi(n)}(x,y)dxdy \\
&= \int_{\mathbb{R}\times\Omega} \psi(x,y) \int_{\overline{\Omega}} K(y,z)u(x,dz)u^{\varphi(n)}(x,y)dxdy \\
&\quad + O\left(\|v^{\varphi(n)}(x,y) - v(x,y)\|_{C_b([-R,R]\times\overline{\Omega})}\right),
\end{aligned}$$

where $v^{\varphi(n)}(x,y) = \int_\Omega K(y,z)u^{\varphi(n)}(x,z)dz$ and $v(x,y) = \int_{\overline{\Omega}} K(y,z)u(x,dz)$. Since $\psi(x,y)\int_{\overline{\Omega}} K(y,z)u(x,dz)$ is a continuous, compactly supported function, we have shown that

$$\int_{\mathbb{R}\times\Omega\times\Omega} \psi(x,y)K(y,z)u^{\varphi(n)}(x,z)u^{\varphi(n)}(x,y)dxdydz \;\to_{n\to\infty}\; \int_{\mathbb{R}\times\overline{\Omega}\times\overline{\Omega}} \psi(x,y)K(y,z)u(x,dz)u(x,dy)dx.$$

Finally we can take the limit in (2.4.45) along the subsequence $\varphi(n)$. This shows that u satisfies (2.4.11) in a weak sense, where the test functions are taken in F_0^y. Since F_0^y is dense in $C_c^2\big(\mathbb{R}, C_b(\overline{\Omega})\big)$, equation (2.4.44) holds for test functions ψ taken in $C_c^2(\mathbb{R}, C_b(\overline{\Omega}))$. In particular, u satisfies (2.4.11) in the sense of distributions.

This ends the proof of Theorem 2.4.10. □

2.4.5.5 Density of the space of functions with null boundary flux

Here we prove elementary results that are crucial to our proofs of Theorem 2.4.15, Theorem 2.4.6 and Theorem 2.4.10.

Lemma 2.4.35 (Density of spaces of functions with null boundary flux)**.** *Let $\Omega \subset \mathbb{R}^n$ be a bounded open set with C^3 boundary.*

(i) The function space

$$F_0 := \left\{ \psi \in C^2(\overline{\Omega}) \,|\, \forall y \in \partial\Omega, \frac{\partial \psi}{\partial \nu}(y) = 0 \right\}$$

is dense in $C_b(\overline{\Omega})$.

(ii) The function space

$$F_0^y := \left\{ \psi \in C_c^2(\mathbb{R} \times \overline{\Omega}) \,|\, \forall x \in \mathbb{R}, \forall y \in \partial\Omega, \frac{\partial \psi}{\partial \nu}(x,y) = 0 \right\}$$

is dense in $C_c^2(\mathbb{R}, C_b(\overline{\Omega}))$.

(iii) The function space

$$F_0^2 := \left\{ \psi \in C^2(\overline{\Omega} \times \overline{\Omega}) \,|\, \forall (y,z) \in \overline{\Omega} \times \partial\Omega, \frac{\partial \psi}{\partial \nu_z}(y,z) = 0 \right\}$$

is dense in $C_b(\overline{\Omega} \times \overline{\Omega})$. Moreover for any $\alpha \in (0,1)$ and any function $\psi \in C^2(\overline{\Omega} \times \overline{\Omega})$ there exists a constant C and a sequence $\psi^r \to \psi$ such that we have $\|\psi^r\|_{C^\alpha(\overline{\Omega}\times\overline{\Omega})} \leq C\|\psi\|_{C^\alpha(\overline{\Omega}\times\overline{\Omega})}$.

Proof. Let us denote $d(y) := \inf_{z\in\partial\Omega} |y - z|$ the distance function. We recall that there exists $R > 0$ such that $y \mapsto d(y, \partial\Omega)$ is C^3 in the tubular neighbourhood $\Omega_R := \{y \in \Omega \,|\, d(y, \partial\Omega) < R\}$ [172]. We fix a smooth function $\theta : \mathbb{R} \to \mathbb{R}$ such that $\theta(x) = 0$ for $x \leq 0$, $\theta(1) = 1$ for $x \geq 1$, and $\forall k > 0$, $\theta^{(k)}(0) = \theta^{(k)}(1) = 0$. Finally for $y \in \Omega$, we let $P(y)$ be the projection of y on $\partial\Omega$, which is well-defined and C^2 on Ω_R.

With these notations, establishing Item (i) and (ii) is elementary by considering (for $0 < r < R$) $\psi^r(y) := \Big(1 - \theta\left(\frac{d(y)}{r}\right)\Big)\psi(P(y)) + \theta\left(\frac{d(y)}{r}\right)\psi(y)$ and similarly $\psi^r(x,y) := \Big(1 - \theta\left(\frac{d(y)}{r}\right)\Big)\psi\big(x, P(y)\big) + \theta\left(\frac{d(y)}{r}\right)\psi(x,y)$ for a function $\psi \in C^2(\overline{\Omega})$ and $\psi \in C^2(\mathbb{R} \times \overline{\Omega})$, respectively. We turn to the proof of Item (iii)

Let $\psi \in C^2(\overline{\Omega} \times \overline{\Omega})$. Let $\psi^r(y,z) := \Big(1 - \theta\left(\frac{d(z)}{r}\right)\Big)\psi\big(y, P(z)\big) + \theta\left(\frac{d(z)}{r}\right)\psi(y,z)$ for $0 < r < \frac{R}{2}$. Clearly, $\psi^r \in F_0^2$ and $\psi^r \to \psi$ in $C_b(\Omega)$. Moreover, for each $(y,z) \in \overline{\Omega} \times \overline{\Omega}$ we have

$$\begin{aligned}
&\frac{\Big|\big(\psi^r(y,z) - \psi(y,z)\big) - \big(\psi^r(y,z') - \psi(y,z')\big)\Big|}{|z - z'|^\alpha} \\
&\leq \frac{\Big|\theta\left(\frac{d(z)}{r}\right) - \theta\left(\frac{d(z')}{r}\right)\Big|}{|z - z'|^\alpha}\big(\psi(y, P(z)) - \psi(y,z)\big) \\
&\quad + \left|1 - \theta\left(\frac{d(z')}{r}\right)\right|\left(\frac{|\psi(y,P(z)) - \psi(y,P(z'))|}{|z - z'|^\alpha} + \frac{|\psi(y,z) - \psi(y,z')|}{|z - z'|^\alpha}\right) \\
&\leq \|\theta\|_{C^\alpha([0,1])}\|d\|^\alpha_{C^{0,1}(\Omega_{R/2})}\|\psi\|_{C^\alpha(\overline{\Omega}\times\overline{\Omega})} + 2\|\psi\|_{C^\alpha(\overline{\Omega}\times\overline{\Omega})},
\end{aligned}$$

since $|\psi(y, P(z)) - \psi(y,z)| \leq r^\alpha \|\psi\|_{C^\alpha(\overline{\Omega}\times\overline{\Omega})}$. This shows item (iii). □

2.4.5.6 A topological theorem

For the sake of completeness, let us recall a result that we proved in a joint work with M. Alfaro [P3], and that we use in the construction of stationary states.

Theorem 2.4.36 (Bifurcation under Krein-Rutman assumption)**.** *Let E be a Banach space. Let $C \subset E$ be a closed convex cone with nonempty interior $Int\, C \neq \varnothing$ and of vertex 0, i.e. such that $C \cap -C = \{0\}$. Let F be a continuous and compact operator $\mathbb{R} \times E \longrightarrow E$. Let us define*

$$\mathcal{S} := \overline{\{(\alpha, x) \in \mathbb{R} \times E \backslash \{0\} \,|\, F(\alpha, x) = x\}}$$

the closure of the set of nontrivial fixed points of F, and

$$\mathbb{P}_{\mathbb{R}}\mathcal{S} := \{\alpha \in \mathbb{R} \,|\, \exists x \in C \backslash \{0\}, (\alpha, x) \in \mathcal{S}\}$$

the set of nontrivial solutions in C.

Let us assume the following.

1. *$\forall \alpha \in \mathbb{R},\ F(\alpha, 0) = 0$.*
2. *F is Fréchet differentiable near $\mathbb{R} \times \{0\}$ with derivative αT locally uniformly with respect to α, i.e. for any $\alpha_1 < \alpha_2$ and $\epsilon > 0$ there exists $\delta > 0$ such that*

$$\forall \alpha \in (\alpha_1, \alpha_2),\ \|x\| \leq \delta \Rightarrow \|F(\alpha, x) - \alpha T x\| \leq \epsilon \|x\|.$$

3. *T satisfies the hypotheses of the Krein-Rutman Theorem. We denote by $\lambda_1(T) > 0$ its principal eigenvalue.*
4. *$\mathcal{S} \cap (\{\alpha\} \times C)$ is bounded locally uniformly with respect to $\alpha \in \mathbb{R}$.*
5. *$\mathcal{S} \cap (\mathbb{R} \times (\partial C \backslash \{0\})) = \varnothing$, i.e. there is no fixed point on the boundary of C.*

Then, either $\left(-\infty, \frac{1}{\lambda_1(T)}\right) \subset \mathbb{P}_{\mathbb{R}}\mathcal{S}$ or $\left(\frac{1}{\lambda_1(T)}, +\infty\right) \subset \mathbb{P}_{\mathbb{R}}\mathcal{S}$.

The proof can be found in [P3].

2.4.5.7 Existence of a transition kernel

Our final lemma is crucial for the construction of traveling waves.

Lemma 2.4.37 (Existence of a transition kernel)**.** *Let Ω be an open domain $\Omega \subset \mathbb{R}^d$, and let μ be a nonnegative measure defined on $\mathcal{B}(\mathbb{R} \times \overline{\Omega})$. Assume there exists a constant $C \geq 0$ such that*

$$\forall a < b, \forall \omega \in \mathcal{B}(\overline{\Omega}), \mu([a, b] \times \omega) \leq C|b - a|.$$

Then there exists a function $\nu : \mathbb{R} \times \mathcal{B}(\overline{\Omega}) \longrightarrow \mathbb{R}^+$ such that

1. *for almost every $x \in \mathbb{R}$, $\omega \mapsto \nu(x, \omega)$ is a nonnegative finite measure on $\mathcal{B}(\overline{\Omega})$*
2. *for every $\omega \in \mathcal{B}(\overline{\Omega})$, $x \mapsto \nu(x, \omega)$ is a Lebesgue-measurable function in $L^1_{loc}(\mathbb{R})$*
3. *$\mu(dx, dy) = \nu(x, dy)dx$, in the sense that*

$$\forall \varphi \in C_c(\mathbb{R} \times \overline{\Omega}), \int_{\mathbb{R} \times \overline{\Omega}} \varphi(x, y)\mu(dx, dy) = \int_{\mathbb{R} \times \overline{\Omega}} \varphi(x, y)\nu(x, dy)dx.$$

Finally ν is unique up to a Lebesgue negligible set, and satisfies

$$\nu(x, \overline{\Omega}) \leq C \qquad a.e.$$

Proof. We divide the proof in four steps.

Step 1: We construct a density for $\mu(A \times \omega)$, $\omega \in \mathcal{B}(\overline{\Omega})$.

Let us take $\omega \in \mathcal{B}(\overline{\Omega})$, and define $A \in \mathcal{B}(\mathbb{R}) \overset{\mu_\omega}{\mapsto} \mu(A \times \omega)$. Then μ_ω is a nonnegative Borel-regular measure on $\mathcal{B}(\mathbb{R})$. Indeed μ_ω is clearly well-defined on $\mathcal{B}(\mathbb{R})$, satisfies the σ-additivity property and is finite on any compact set. Then, for any open set $U \subset \mathbb{R}$, we have $\mu_\omega(U) \leq C\mathcal{L}(U)$. Indeed we can write $U = \bigcup_{n \in \mathbb{N}} K_n$

where K_n is an increasing sequence of compact sets of the form $K_n = \bigsqcup_{i=0}^{m_n} [a_i^n, b_i^n]$ (with $a_i^n < b_i^n < a_{i+1}^n ...$), for which the property holds by assumption. Thus

$$\mu_\omega(U) = \lim_{n\to+\infty} \mu_\omega(K_n) \leq C \lim_{n\to+\infty} \mathcal{L}(K_n) = C\mathcal{L}(U)$$

Finally, $\mu_\omega \ll \mathcal{L}$, where $\mathcal{L}$ is the Lebesgue measure on $\mathbb{R}$. Indeed, let us take $E \subset \mathbb{R}$ bounded such that $\mathcal{L}(E) = 0$. Then by the regularity of μ_ω [343, Theorem 2.18], we have

$$\mu_\omega(E) = \inf_{U \text{ open}, U\supset E} \mu_\omega(U) \leq C \inf_{U \text{ open}, U\supset E} \mathcal{L}(E) = 0.$$

Applying the Radon-Nikodym Theorem [343, Theorem 6.10], there exists then a unique measurable function $h_\omega \in L^1_{loc}(\mathbb{R})$ such that

$$\mu_\omega = h_\omega \mathcal{L} = h_\omega dx.$$

Step 2: We show that the density h_ω is well-defined up to a negligible set independent from ω.

Let ω_n be an enumeration of the sets of the form

$$\overline{\Omega} \cap \prod_{i=1}^{d} [a_i, b_i]$$

where $a_i, b_i \in \mathbb{Q}$. Clearly, ω_n is stable by finite intersections, and the associated monotone class is $\mathcal{B}(\overline{\Omega})$. We let $h_n := h_{\omega_n} \in L^1_{loc}(\mathbb{R})$ be the previously constructed density associated with μ_{ω_n}. Then h_n is well-defined on a set $\mathcal{D}_n$ satisfying $\mathcal{L}(\mathbb{R}\backslash\mathcal{D}_n) = 0$. We let $\mathcal{D} = \bigcap_{n\in\mathbb{N}} \mathcal{D}_n$, then $\mathcal{L}(\mathbb{R}\backslash\mathcal{D}) = 0$ and by construction, every h_n is well-defined on $\mathcal{D}$.

We take $\omega \in \mathcal{B}(\overline{\Omega})$ and show that, up to a redefinition on a negligible set, the function h_ω is well-defined on $\mathcal{D}$. If ω is open, then we can write $\omega = \bigsqcup_{n\in\mathbb{N}} \omega'_n$ for a well-chosen extraction ω'_n of ω_n. Thus for any $A \in \mathcal{B}(\mathbb{R})$, we have the formula $\mu_\omega(A) = \mu(A \times \omega) = \sum_{n\in\mathbb{N}} \mu(A \times \omega'_n)$ and by the uniqueness in the Radon-Nikodym Theorem, we have:

$$h_\omega = \sum_{n\in\mathbb{N}} h_{\omega'_n} \qquad \mathcal{L} - a.e.$$

In the general case we have $\mu(A\times\omega) = \inf_{U \text{ open}, U\supset\omega} \mu(A\times U)$ for $A \in \mathcal{B}(\mathbb{R})$ because of the Borel regularity of μ, which shows that h_ω is well-defined on $\mathcal{D}$.

Step 3: We verify that the constructed family of functions form a nonnegative measure on $\overline{\Omega}$ for $\mathcal{L}$-a.e. $x \in \mathbb{R}$.

Let $w_n \in \mathcal{B}(\overline{\Omega})$ be a countable collection of Borel sets with $w_i \cap w_j = \varnothing$ if $i \neq j$. Then

$$\mu(A \times \bigsqcup_{n\in\mathbb{N}} w_n) = \sum_{n\in\mathbb{N}} \mu(A \times w_n)$$

for any $A \in \mathcal{B}(\mathbb{R})$, and by the uniqueness in the Radon-Nikodym theorem we have

$$h_{\bigsqcup_{n\in\mathbb{N}} w_n} = \sum_{n\in\mathbb{N}} h_{w_n} \qquad \mathcal{L} - a.e.$$

Thus, for any $x \in \mathcal{D}$, the function $\omega \mapsto h_\omega(x)$ is σ-additive. Since h_ω is nonnegative by construction, $\omega \mapsto h_\omega(x)$ is a nonnegative measure on $\mathcal{B}(\overline{\Omega})$.

We define $\nu(x, \omega) := h_\omega(x)$. Then ν matches the definition of a transition kernel (Definition 2.4.1).

Step 4: Conclusion.

Since $\nu(x, dy)dx$ coincides with μ on the monotone class $A \times \omega_n$, where $A \in \mathcal{B}(\mathbb{R})$, we have $\mu(dx, dy) = \nu(x, dy)dx$ on $\mathcal{B}(\mathbb{R} \times \overline{\Omega})$.

Finally, since $x \mapsto \nu(x, \overline{\Omega})$ is in $L^1_{loc}(\mathbb{R})$, then almost every point of $\nu(x, \overline{\Omega})$ is a Lebesgue point (see Rudin [343, Theorem 7.7]) and thus:

$$\nu(x_0, \overline{\Omega}) = \lim_{r\to 0} \frac{1}{2r} \int_{x_0-r}^{x_0+r} \nu(x_0 + s, \overline{\Omega}) ds \leq \frac{1}{2r}(2rC) = C$$

for $\mathcal{L}$-a.e. $x_0 \in \mathbb{R}$.

This finishes the proof of Lemma 2.4.37 □

2.5 A Liouville-type result for some non-cooperative Fisher–KPP systems and nonlocal equations on cylinders

2.5.1 Introduction

We investigate the reaction–diffusion system

$$\partial_t u - D\partial_{xx} u = Mu + u - u \circ (Cu), \tag{2.5.1}$$

where $t \in \mathbb{R}$ is a time variable, $x \in \mathbb{R}$ is a space variable, $u(t,x)$ is a nonnegative column vector [6] collecting $N \geq 2$ phenotype densities among a species, D is a diagonal matrix collecting positive diffusion rates, $\circ$ is the Hadamard product between two vectors and M and C are square matrices collecting respectively mutation rates and competition rates and satisfying the following standing assumptions (below and in the whole section, $\mathbb{1} = (1, 1, \dots, 1)^{\mathrm{T}} \in \mathbb{R}^N$).

(A_1) The matrix $M \in \mathcal{M}_{N,N}(\mathbb{R})$ is essentially nonnegative (namely, with nonnegative off-diagonal coefficients), irreducible, line-sum-symmetric (namely, $M1 = M^{\mathrm{T}}1$) and admits $(0, 1)$ as Perron–Frobenius eigenpair (namely, $M\mathbb{1} = 0$).

(A_2) The matrix $C \in \mathcal{M}_{N,N}(\mathbb{R})$ is positive, normal and admits $(1, \mathbb{1})$ as Perron-Frobenius eigenpair (namely, $C\mathbb{1} = \mathbb{1}$). We denote $U \in \mathcal{M}_{N,N}(\mathbb{C})$ the unitary matrix such that $UCU^{-1} = UC\overline{U}^{\mathrm{T}}$ is diagonal.

(A_3) The spectrum of C is contained in the complex closed right-half plane.

We are interested more specifically in the associated traveling wave equation

$$-Dp'' - cp' = Mp + p - p \circ (Cp), \tag{2.5.2}$$

satisfied by solutions of the system (2.5.1) of the form $u : (t,x) \mapsto p(x - ct)$. This equation might be supplemented with asymptotic conditions for the profile p. The asymptotic conditions of classical traveling waves (p, c) [190] are

$$\lim_{+\infty} p = 0, \quad \min_{i\in[N]} \liminf_{-\infty} p_i \geq 0, \quad \max_{i\in[N]} \liminf_{-\infty} p_i > 0, \tag{2.5.3}$$

where $[N]$ denotes (here and in the rest of the section) the set $\{1, 2, \dots, N\}$.

By (A_1) and (A_2), $\mathbb{1}$ is a constant steady state of the system (2.5.1).

2.5.2 Main results

Our main result is the following theorem.

Theorem 2.5.1 (Liouville-type result)**.** *Assume* (A_1), (A_2) *and* (A_3). *Then, for any* $c \in \mathbb{R}$, $\mathbb{1}$ *is the unique bounded solution* p *of* (2.5.2) *such that* $\min_{i\in[N]} \inf_{\mathbb{R}} p_i > 0$.

The main consequences of this theorem are the two following corollaries, deduced from standard elliptic estimates and limiting procedures [187] as well as a strong positivity property [190, Theorem 1.1].

Corollary 2.5.2 (Uniqueness of the nonzero steady state)**.** *Assume* (A_1), (A_2) *and* (A_3). *Then* $\mathbb{1}$ *is the unique bounded nonnegative nonzero stationary solution of* (2.5.1)*, namely the unique bounded nonnegative nonzero solution* p *of* (2.5.2) *with* $c = 0$.

Corollary 2.5.3 (Limit behavior of the traveling waves)**.** *Assume* (A_1), (A_2) *and* (A_3). *Then all solutions* (p, c) *of* (2.5.2)-(2.5.3) *actually satisfy* $\lim_{-\infty} p = \mathbb{1}$.

[6] In the whole section, nonnegativity and positivity of vectors and matrices are understood component-wise.

2.5.2.1 Extension to nonlocal equations

Those results extend to continuous limits $N \to +\infty$, provided the limit equation has a similar structure. Below we illustrate this principle by focusing on an equation supplemented with Neumann boundary conditions, though it would also be possible to adapt our arguments in the periodic framework with no additional difficulty.

We consider

$$-d(y)\partial_{\xi\xi}p - c\partial_\xi p = \nabla_y \cdot (\sigma(y)\nabla_y p) + M[p(\xi)](y) + p(\xi,y)\,(1 - K[p(\xi)](y)) \tag{2.5.4}$$

set on $(\xi, y) \in \mathbb{R}\times\Omega$ for a smooth domain $\Omega \subset \mathbb{R}^Q$ ($Q \geq 1$ and $\partial\Omega$ is $\mathcal{C}^2$) and supplemented with homogeneous Neumann boundary conditions at $y \in \partial\Omega$. Above, $d \in \mathcal{C}\left(\overline{\Omega}, (0,+\infty)\right)$, $\sigma \in \mathcal{C}^1\left(\overline{\Omega}, (0,+\infty)\right)$,

$$M[p(\xi)] = \int_\Omega m(\cdot,\tilde{y})(p(\xi,\tilde{y}) - p(\xi,\cdot))\mathrm{d}\tilde{y}, \quad K[p(\xi)] = \int_\Omega k(\cdot,\tilde{y})p(\xi,\tilde{y})\mathrm{d}\tilde{y},$$

for some $m, k \in \mathcal{C}(\Omega^2, (0,+\infty))$. Defining naturally the adjoint operators $M^\star$ and $K^\star$, the assumptions (A_1), (A_2) and (A_3) extend to the continuous equation as follows:

- (A_1') The function $\sigma(y) \in \mathcal{C}^1\left(\overline{\Omega}\right)$ is positive and the function $m \in \mathcal{C}(\Omega^2)$ is nonnegative, bounded and satisfies $\int_\Omega m(\cdot,z)\mathrm{d}z = \int_\Omega m(z,\cdot)\mathrm{d}z$.

- (A_2') The function $k \in \mathcal{C}(\overline{\Omega}^2)$ is positive and the induced operator $K[p] = \int_\Omega k(\cdot,z)p(z)\mathrm{d}z$ acting on the Hilbert space $L^2(\Omega)$ is normal. Moreover, the constant function $y \in \Omega \mapsto 1$ is an eigenvector of K associated with the eigenvalue 1 (namely, $K[1] = 1$).

- (A_3') The spectrum of K (considered as an operator acting on $L^2(\Omega)$) is contained in the complex closed right-half plane.

The continuous version of Theorem 2.5.1 reads as follows.

Theorem 2.5.4. *Assume (A_1'), (A_2') and (A_3'). Then, for any $c \in \mathbb{R}$, 1 is the unique bounded solution p of (2.5.4) such that $\inf_{\mathbb{R}\times\Omega} p > 0$.*

We deduce just as before the uniqueness of the stationary states and the uniform convergence to the unique stationary state in the wake of the waves for (2.5.4), provided a uniform estimate from below can be shown.

Corollary 2.5.5. *Assume (A_1'), (A_2') and (A_3'). Then 1 is the unique bounded solution of (2.5.4) with positive infimum in $\mathbb{R}\times\Omega$ and with $c = 0$.*

Corollary 2.5.6. *Assume (A_1'), (A_2') and (A_3'). Then any bounded classical solution (p,c) of (2.5.4) such that*

$$\lim_{\xi\to+\infty} \sup_{y\in\Omega} p(\xi,y) = 0 \text{ and } \liminf_{\xi\to-\infty} \inf_{y\in\Omega} p(\xi,y) > 0$$

actually satisfy

$$\lim_{\xi\to-\infty} \sup_{y\in\Omega} |p(\xi,y) - 1| = 0.$$

2.5.2.2 Organization of the section

In Section 2, we discuss the assumptions, the results and the literature. In Section 3, we prove Theorem 2.5.1. In Section 4, we prove Theorem 2.5.4.

2.5.3 Discussion

2.5.3.1 The conditions on M

By definition, a matrix is line-sum-symmetric if the sum of coefficients in each of its rows equals the sum of coefficients in the corresponding column. Cleary, symmetric matrices are line-sum-symmetric (and line-sum-symmetric matrices in dimension 2 are exactly symmetric matrices), but in general the converse statement

is false. For instance, the following 3×3 matrix is line-sum-symmetric but not symmetric:

$$\begin{pmatrix} a & 2b & 0 \\ b & c & b \\ b & 0 & d \end{pmatrix} \quad \text{with } a, b, c, d \in \mathbb{R}.$$

The study of line-sum-symmetric matrices was initiated by Eaves, Hoffman, Rothblum and Schneider [157]. Roughly speaking, these matrices conveniently generalize symmetric matrices when what we have in mind is summation of lines or rows of linear systems [157, Corollary 3], which is the case in this section 2.5 and more generally whenever we want to "integrate by parts" in a discrete variable. As such, they recently appeared in the literature on reaction–diffusion systems [98, 99].

2.5.3.2 The symmetric case

In the symmetric case, which arises in many applications, our assumption (A_1) on M comes down to assuming that M has an "integration by parts" formula:

$$\langle Mu, v\rangle = \frac{1}{2} \sum_{i,j\in[N]} m_{i,j}\,(u_i - u_j)(v_j - v_i)\,.$$

where $\langle\cdot,\cdot\rangle$ is the canonical (Hermitian) scalar product on $\mathbb{C}^N$. A particularly natural example is the explicit Euler scheme for the one-dimensional heat equation with periodic boundary conditions: $M = -{\boldsymbol{\nabla}_{\mathrm{D}}}^{\mathrm{T}}\Sigma\boldsymbol{\nabla}_{\mathrm{D}}$, $\Sigma = \mathrm{diag}(\sigma_1, \sigma_2, \ldots, \sigma_N)$ $(\sigma_i > 0)$ and

$$\boldsymbol{\nabla}_{\mathrm{D}} = \begin{pmatrix} -1 & 0 & 0 & \cdots & & & 1 \\ 1 & -1 & 0 & 0 & \cdots & \cdots & 0 \\ 0 & 1 & -1 & 0 & 0 & \cdots & \vdots \\ \vdots & \vdots & \vdots & \vdots & \vdots & & \vdots \\ 0 & 0 & \cdots & 0 & & 1 & -1 \end{pmatrix}.$$

The expanded form of M is

$$\begin{pmatrix} -\sigma_1 - \sigma_2 & \sigma_2 & 0 & \ldots & 0 & \sigma_1 \\ \sigma_2 & -\sigma_2 - \sigma_3 & \sigma_3 & 0 & \ldots & 0 \\ 0 & \sigma_3 & -\sigma_3 - \sigma_4 & \sigma_4 & 0 & \ldots \\ \vdots & \vdots & \vdots & \vdots & \vdots & \vdots \\ \sigma_1 & 0 & \ldots & 0 & \sigma_N & -\sigma_N - \sigma_1 \end{pmatrix} \quad \text{if } N \geq 3,$$

$$(\sigma_1 + \sigma_2)\begin{pmatrix} -1 & 1 \\ 1 & -1 \end{pmatrix} \quad \text{if } N = 2.$$

Neumann boundary conditions can be obtained by replacing the first line in $\boldsymbol{\nabla}_{\mathrm{D}}$ by zero and also satisfy (A_1). On the contrary, Dirichlet boundary conditions are qualitatively different (in particular, $\mathbb{1}$ cannot be a solution anymore) and are therefore outside the scope of this section. Note that non-tridiagonal matrices can also be obtained in the form $-\boldsymbol{\nabla}_{\mathrm{D}}^{\mathrm{T}}\Sigma\boldsymbol{\nabla}_{\mathrm{D}}$ by allowing $\boldsymbol{\nabla}_{\mathrm{D}}$ to be non-square: as an example, discretization of divergence-form operators in two-dimensional domain such as

$$M = \begin{pmatrix} -\sigma_1 - \sigma_5 & 0 & \sigma_1 & 0 & \sigma_5 \\ 0 & -\sigma_2 - \sigma_6 & \sigma_2 & \sigma_6 & 0 \\ \sigma_1 & \sigma_2 & -\sigma_1 - \sigma_2 - \sigma_3 - \sigma_4 & \sigma_3 & \sigma_4 \\ 0 & \sigma_6 & \sigma_3 & -\sigma_3 - \sigma_6 & 0 \\ \sigma_5 & 0 & \sigma_4 & 0 & -\sigma_4 - \sigma_5 \end{pmatrix}$$

are not always tridiagonal. In this case $\boldsymbol{\nabla}_{\mathrm{D}} \in \mathcal{M}_{10,5}(\mathbb{R})$ corresponds to a discrete gradient operator on a cell with four boundary points and one interior point, and $\Sigma \in \mathcal{M}_{10,10}(\mathbb{R})$ encodes the diffusion rates.

In addition to the divergence-form differential part presented above, M might also contain the discretization of a nonlocal integral operator, as hinted by (2.5.4).

2.5.3.3 The conditions on C

The assumption that the Perron–Frobenius eigenvalue of C is unitary ($\lambda_{\mathrm{PF}}(C) = 1$) is done without loss of generality (up to replacing (p, C) by $(\lambda_{\mathrm{PF}}(C)p, \lambda_{\mathrm{PF}}(C)^{-1}C)$). However the assumption that $\mathbb{1}$ is a Perron–Frobenius eigenvector is a true assumption, not satisfied in general.

The set of real positive normal matrices contains as particular subsets the set of real positive circulant matrices and the set of real positive symmetric matrices (skew-symmetric and orthogonal matrices are normal but cannot be positive). The following counter-example shows that there are matrices satisfying (A_2) and (A_3) that are neither symmetric nor circulant:

$$\begin{pmatrix} a & b & c & d \\ b & a & d & c \\ d & c & a & b \\ c & d & b & a \end{pmatrix} \quad \text{with } a, b, c, d > 0,\ a + b + c + d = 1.$$

(The eigenvalues of this matrix are 1, $a + b - c - d$, $a - b \pm \mathrm{i}|c - d|$ and therefore (A_3) is satisfied as soon as $a \geq b$ and $a + b \geq c + d$.)

In fact, a polynomial in any permutation matrix is normal. It is therefore possible to construct such counterexamples in any dimension $N \geq 4$, by selecting a permutation matrix associated with a cycle of maximal length which is not a power of the circular permutation.

2.5.3.4 The circulant case

In the circulant case, which is of particular interest to us, there exists a positive vector $\phi \in \mathbb{R}^N$ such that the matrix C is written as $C = (\phi_{i-j})_{i,j\in[N]}$, ϕ being periodically extended by

$$\phi_{i-j} = \begin{cases} \phi_{i-j}, & \text{if } i - j \geq 1, \\ \phi_{N+i-j}, & \text{if } i - j \leq 0. \end{cases}$$

The expanded form of C is then

$$\begin{pmatrix} \phi_N & \phi_{N-1} & \cdots & \phi_1 \\ \phi_1 & \phi_N & \cdots & \phi_2 \\ \vdots & \vdots & \vdots & \vdots \\ \phi_{N-1} & \phi_{N-2} & \cdots & \phi_N \end{pmatrix}$$

and the product Cu can be rewritten as $\phi \star u$, where $\star$ is the discrete circular convolution operator:

$$(\phi \star u)_i = \sum_{j=1}^{N} \phi_{i-j} u_j.$$

Defining the normalized discrete Fourier transform matrix as

$$U_{\mathrm{DFT}} = \frac{1}{\sqrt{N}} \left(\exp\left(-\frac{2\mathrm{i}\pi}{N}(j-1)(k-1) \right) \right)_{j,k\in[N]},$$

we find that $U_{\mathrm{DFT}} = U$ for any circulant matrix C. In particular, $\mathbb{1}$ is automatically a Perron–Frobenius eigenvector (and the normalization $\lambda_{\mathrm{PF}}(C) = 1$ reads $\sum_{i=1}^{N} \phi_i = 1$). Moreover, the following equalities hold true:

$$UCU^{-1}Uu = UCu = U(\phi \star u) = \sqrt{N}(U\phi) \circ (Uu).$$

It follows easily that the spectrum of C is contained in the closed right-half plane if and only if $U\phi$, namely the discrete Fourier transform of ϕ, is valued in the closed right-half plane.

Last, we point out additional alternative writings of the reaction term:

$$u - (Cu) \circ u = u \circ (\mathbb{1} - \phi \star u) = -u \circ (\phi \star (u - \mathbb{1}))\,,$$

2.5.3.5 The case $N = 2$

In the case $N = 2$, the matrix M and C can be rewritten as depending on two parameters only:

$$M = \begin{pmatrix} -\sigma & \sigma \\ \sigma & -\sigma \end{pmatrix}, \qquad C = \begin{pmatrix} 1-\gamma & \gamma \\ \gamma & 1-\gamma \end{pmatrix},$$

where $\sigma > 0$ and $\gamma \in (0, 1)$. The linear stability of $\mathbb{1}$ can be decided by computing the eigenvalues $\lambda_\pm^{M-C}$ of the matrix $M - C$,

$$\lambda_\pm^{M-C} = -1 - (\gamma - \sigma) \pm |\gamma - \sigma|,$$

while the eigenvalues of C are $\lambda_1^C = 1$ and $\lambda_-^C = 1-2\gamma$. Therefore, $M-C$ has always one negative eigenvalue $\lambda_-^{M-C} < 0$ and the behavior of λ_+^{M-C} depends on the value of γ:

a) if $\gamma \in (0, 1/2)$ (in which case (A_3) holds), λ_1^{M-C} always stays negative,

b) if $\gamma \in (1/2, 1)$ (in which case (A_3) does not hold),

$$\lambda_+^{M-C} > 0 \text{ if } 0 < \sigma < \sigma^* := \gamma - \frac{1}{2},$$
$$\lambda_+^{M-C} < 0 \text{ if } \sigma > \sigma^*.$$

In the latter case, using σ as a bifurcation parameter, a local bifurcation is occurring when decreasing σ below σ^* and two stable equilibria emerge when $\mathbb{1}$ loses stability. In particular, in this case there are solutions to (2.5.2) other that the constant $\mathbb{1}$ which are bounded from below. This is confirmed by the result in [100, Proposition 3.4].

2.5.3.6 KPP systems

The system (2.5.1) is a particular example of non-cooperative KPP systems. The first author studied these systems in [190, 189, 192, 191]. The second author studied them with collaborators in [P2, P3] and gave an epidemiological interpretation in [P2]. Other important mathematical references are [147, 32, 291, 100, 101]. For a detailed overview of the literature, we refer to [190].

These nonlinear, non-cooperative and non-variational reaction–diffusion systems are referred to as "KPP systems" due to their structural similarity with the scalar Fisher–KPP equation,

$$\partial_t u - \partial_{xx} u = u(1 - u).$$

(This scalar equation can actually be understood as a KPP system of dimension 1.) This similarity mainly concerns the behavior close to $u = 0$ and it leads to several classical results: a sharp persistence–extinction criterion [190, 191], the existence of traveling waves for all speeds larger than or equal to a linearly determined minimal wave speed $c^\star$ [190, P2, 291], the equality between this minimal wave speed and the asymptotic speed of spreading for initially compactly supported solutions of the Cauchy problem [32, 190] and an exponential equivalent of the profile at the leading edge [189, 291].

However, away from $u = 0$ and in particular in the wake of a traveling wave solution $p\,(x - ct)$, the picture is more complicated. For two-component systems, locally uniform convergence of the solutions of the Cauchy problem to a unique constant steady state can be proved in many cases (and directly implies the convergence in the wake of the traveling waves) [192, Appendix B], [P2], but bistable cases (corresponding to strongly competitive systems with weak mutations) still exist [100, 189] and remain elusive – in particular, traveling waves connecting 0 to an unstable constant steady state exist in some particular bistable cases [189]. For systems of any size but where $d = \mathbb{1}$ and $C = \mathbb{1}a^{\mathrm{T}}$, locally uniform convergence of the solutions of the Cauchy problem to a unique constant steady state can be established [189], but these assumptions are

in fact so strong that the system is basically reduced to a scalar Fisher–KPP equation projected along the Perron–Frobenius eigenvector of the linear part of the reaction term. More recent results confirm that, as soon as there is at least three components, convergence fails in general. In particular, for circulant matrices M and C, Hopf bifurcations can occur and these typically lead to the formation of limit cycles, periodic wave trains, pulsating traveling waves and propagating terraces [192].

In this regard, the main result of this section 2.5 provides some sufficient conditions to prevent the formation of these oscillations in the elliptic and traveling wave problems. In the class of pairs (M, C) satisfying (A_1) and (A_2), the sharpness of (A_3) (the spectrum of C is in the right-half plane) can be discussed as follows:

- in view of the Hopf-bifurcating case in [192], the system can be oscillatory if C admits an eigenvalue with negative real part and nonzero imaginary part;
- in view of the two-component case discussed in Section 2.5.3.5 (see also [100, Proposition 3.4]), there can be a multiplicity of positive constant equilibria when at least one eigenvalue of C is real and negative.

In the class of pairs (M, C) satisfying (A_2), (A_3) and the mere irreducibility of M, the sharpness of (A_1) is unclear. The proof presented here heavily relies on the line-sum-symmetry of M and cannot be extended to more general matrices M (see Remark 2.5.9 below).

Let us point out that the convergence result here is strikingly new in the sense that it does not require the equality between all diffusion rates ($d = \mathbb{1}$), which was required in [189, P2]. The convergence results for two-component systems presented in [100] do not require such an assumption but use the boundedness of the domain to overcome this lack of structure; when extending these results to the unbounded setting, the equality $d_1 = d_2$ is useful [192, Appendix B].

2.5.3.7 The nonlocal KPP equation

The spatially homogeneous system

$$\dot{u} = Mu + u \circ (\mathbb{1} - \phi \star u)$$

is, in a way, a discretized version of the nonlocal Fisher–KPP equation:

$$\partial_t u = \partial_{xx} u + u(1 - \phi \star u).$$

This nonlocal equation has attracted a lot of attention in the last few years. The existing literature (*e.g.*, [46, 6, 165, 70, and references therein]) develops new techniques to overcome the default of comparison principle and these techniques proved to be fruitful when applied to non-cooperative KPP systems [P2, 190]. In the present section 2.5 we will once again import such a technique from [46].

2.5.3.8 The nonlocal cane-toad equation

The diffusive system (2.5.1) is, in a similar way, a discretized version of the nonlocal cane-toad equation:

$$\begin{cases} \partial_t u = d(\theta)\partial_{xx} u + \alpha \partial_{\theta\theta} u + u(t,x,\theta)(1 - \frac{1}{\overline{\theta} - \underline{\theta}} \int_{\theta=\underline{\theta}}^{\overline{\theta}} u(t,x,\theta')\mathrm{d}\theta'), \\ \partial_\theta u(t,x,\underline{\theta}) = \partial_\theta u(t,x,\overline{\theta}) = 0, \end{cases}$$

where $u(t,x,\theta)$ is a population density structured with respect to a phenotypic trait $\theta \in [\underline{\theta}, \overline{\theta}] \subset [0, +\infty]$. This eco-evolutionary model has also attracted attention recently (*e.g.*, [72, 68, 72, 68, 96, 379, 7, 18, 52, P4]), especially due to an acceleration phenomenon when $d(\theta) = \theta$ and $\overline{\theta} = +\infty$ but also because, just like the nonlocal KPP equation, it does not satisfy the comparison principle and requires new techniques.

It turns out that the similarity between our system and this equation is so strong that our proof can be readily adapted and our result extends to this continuous-trait model (see Theorem 2.5.4 and its two corollaries).

2.5.3.9 More general reaction terms

In the system (2.5.1), the reaction term has the form $(I + M)\, u - u \circ (Cu)$. It is natural to try to extend the results to reaction terms of the form $(\mathrm{diag}\,(r) + M)\, u - u \circ (Cu)$, where $\mathrm{diag}\,(r) + M$ has a positive Perron–Frobenius eigenvalue, or $(\mathrm{diag}\,(r) + M)\, u - (\mathrm{diag}\,(r)\, u) \circ (Cu)$, where r is positive. However our proof does not easily extend to such cases. These remain as an open problem.

2.5.3.10 The Cauchy problem

It would be natural to try to prove that, with the same assumptions (A_1)–(A_3) or (A_1')–(A_3'), the solutions of the parabolic Cauchy problem converge locally uniformly to $\mathbb{1}$. However our proof does not easily extend to this problem. This also remains as an open problem.

2.5.4 Proof of Theorem 2.5.1

Our strategy is to mimic the proof of [46, Theorem 4.1] by taking into account the discrete integration by parts formula for M. More precisely, we rely upon

$$\sum_{i=1}^{N} \frac{(Mp)_i}{p_i} \geq 0 \quad \text{with equality iff } p \in \operatorname{span}(\mathbb{1}), \tag{2.5.5}$$

and upon

$$\sum_{i=1}^{N} (p_i - 1)(C(p-\mathbb{1}))_i \geq 0. \tag{2.5.6}$$

The inequality (2.5.5) is a standard property of irreducible line-sum-symmetric matrices (recalled in the forthcoming Lemma 2.5.7); the inequality (2.5.6) is a direct consequence of (a generalized version of) Plancherel's theorem:

$$\begin{aligned}
\sum_{i=1}^{N} q_i (Cq)_i &= \mathsf{Re}\left(\sum_{i=1}^{N} q_i (Cq)_i \right) \\
&= \mathsf{Re}\left(\langle q, Cq \rangle \right) \\
&= \mathsf{Re}\left(\langle q, \overline{U}^{\mathrm{T}} U C \overline{U}^{\mathrm{T}} U q \rangle \right) \\
&= \mathsf{Re}\left(\langle Uq, UC\overline{U}^{\mathrm{T}} Uq \rangle \right) \\
&\geq \min_{\lambda \in \mathrm{sp}(C)} (\mathsf{Re}(\lambda)) \sum_{i=1}^{N} |(Uq)_i|^2 ,
\end{aligned}$$

where $\langle \cdot, \cdot \rangle$ is the canonical (Hermitian) scalar product on $\mathbb{C}^N$.

Lemma 2.5.7 (Classification of line-sum-symmetric matrices [157, Corollary 3])**.** *Let $A \in \mathcal{M}_{N,N}(\mathbb{R})$ be a nonnegative matrix. Then A is line-sum-symmetric if and only if*

$$\sum_{i,j \in [N]} \frac{a_{i,j} u_j}{u_i} \geq \sum_{i,j \in [N]} a_{i,j} \quad \textit{for all } u \in (0, +\infty)^N .$$

Furthermore, if A is irreducible and line-sum-symmetric, equality above holds if and only if $u \in \operatorname{span}(\mathbb{1})$.

The inequality (2.5.5) follows then from Lemma 2.5.7 applied to the nonnegative, line-sum-symmetric and irreducible matrix $A = M - \min_{i \in [N]}(m_{i,i}) I$.

Lemma 2.5.8 (Uniqueness of the nonzero constant solution)**.** *The unique nonnegative nonzero solution of $Mu + u = (Cu) \circ u$ is $\mathbb{1}$.*

Proof. Let u be any nonnegative nonzero solution. Recall that u is in fact positive. Denoting $u^{\circ -1} = (1/u_i)_{i \in [N]}$ and taking the scalar product

$$\langle -Mu - u \circ (\mathbb{1} - Cu), u^{\circ -1} \circ (u - \mathbb{1}) \rangle = 0,$$

we get

$$-\langle Mu, u^{\circ -1} \rangle = \langle C(u - \mathbb{1}), u - \mathbb{1} \rangle.$$

On one hand, by (2.5.5), the left-hand side is nonpositive. On the other hand, by (2.5.6), the right-hand side is nonnegative. Therefore both sides are zero. Using now the case of equality in (2.5.5), we deduce $u \in \operatorname{span}(\mathbb{1})$. We deduce subsequently from the right-hand side that $u = \mathbb{1}$. □

We are now in a position to prove Theorem 2.5.1.

Proof of Theorem 2.5.1. Let (p, c) be a bounded solution of the system (2.5.2) satisfying $\inf_{\mathbb{R}} p_i > 0$ for any $i \in [N]$.

Step 1: We show that

$$\lim_{\xi \to \pm\infty} p(\xi) = \mathbb{1}.$$

At any $\xi \in \mathbb{R}$, denoting $p^{\circ -1}(\xi) = (1/p_i(\xi))_{i\in[N]}$ and taking the scalar product (in $\mathbb{R}^N$)

$$\langle -Dp'' - cp' - Mp - p \circ (\mathbb{1} - Cp), p^{\circ -1} \circ (p - \mathbb{1}) \rangle = 0,$$

we get

$$\sum_{i=1}^{N} \left[-(d_i p_i'' + cp_i') \left(\frac{p_i - 1}{p_i} \right) \right] = -\sum_{i=1}^{N} \frac{(Mp)_i}{p_i} - \sum_{i=1}^{N} (p_i - 1) \left(C(p - \mathbb{1}) \right)_i .$$

By (2.5.5) and (2.5.6), the right-hand side is nonpositive and therefore

$$\sum_{i=1}^{N} \left[-(d_i p_i'' + cp_i') \left(\frac{p_i - 1}{p_i} \right) \right] \leq 0.$$

Since this holds true at any $\xi \in \mathbb{R}$, we fix $R > 0$ and integrate by parts in $[-R, R]$. We get, as in [46, Proof of Lemma 4.1],

$$\sum_{i=1}^{N} d_i \int_{-R}^{R} \left(\frac{p_i'}{p_i} \right)^2 \leq \sum_{i=1}^{N} \left[d_i \frac{p_i'(p_i - 1)}{p_i} + c \ln(p_i) - cp_i \right]_{-R}^{R}, \tag{2.5.7}$$

By the classical elliptic estimates, $|p_i'(\pm R)|$ is bounded by $\|p(\pm R)\|$ up to a multiplicative constant independent of R. Recalling that p_i is uniformly bounded from below by $\min_{i\in[N]} \inf_{\xi\in\mathbb{R}} p_i(\xi) > 0$, the right-hand side is bounded by a constant independent of R. We deduce that $p_i' \in L^2(\mathbb{R})$ for all $i \in [N]$.

Let now ξ_n be any sequence such that $\xi_n \to -\infty$ and define $p^n : \xi \mapsto p(\xi + \xi_n)$. We remark that, for all $i \in [N]$, we have

$$\int_{-\infty}^{-\frac{\xi_n}{2}} [(p_i^n)']^2(\xi) \mathrm{d}\xi = \int_{-\infty}^{\frac{\xi_n}{2}} (p_i')^2(\xi) \mathrm{d}\xi \xrightarrow[n\to+\infty]{} 0 \text{ for all } i \in [N],$$

and therefore $(p^n)'$ converges to 0 locally uniformly in L^2. Next, using the classical elliptic estimates, we extract from $(p^n)_{n\in\mathbb{N}}$ a subsequence which converges in $\mathcal{C}^2_{\mathrm{loc}}$ to a limit $p^\infty \in \mathcal{C}^2(\mathbb{R})$. Note that p^∞ is still a solution to (2.5.2). Since $(p^n)' \to 0$ in L^2_{loc}, we conclude that p^∞ has to be a constant function of the variable ξ, *i.e.* a constant solution of $Mp + p = (Cp) \circ p$. By Lemma 2.5.8, $p^\infty = \mathbb{1}$ identically.

Since the sequence ξ_n is arbitrary, we have shown that

$$\lim_{\xi \to -\infty} p(\xi) = \mathbb{1}.$$

The limit at $+\infty$ can be established by a similar argument.

Step 2: We show that p is identically equal to $\mathbf{1}$. Since p converges to $\mathbb{1}$ on both sides of the real line, the brackets on the right-hand side of (2.5.7) converge to 0 as $R \to +\infty$. Therefore,

$$\begin{aligned}
0 \leq \sum_{i=1}^{N} \int_{-\infty}^{+\infty} (p_i')^2 &= \lim_{R\to+\infty} \sum_{i=1}^{N} \int_{-R}^{R} (p_i')^2 \\
&\leq \lim_{R\to+\infty} \frac{\min_{i\in[N]} \inf p_i}{\max_{i\in[N] d_i}} \sum_{i=1}^{N} d_i \int_{-R}^{R} \left(\frac{p_i'}{p_i} \right)^2 \\
&\leq C \lim_{R\to+\infty} \sum_{i=1}^{N} \left[d_i \frac{p_i'(p_i - 1)}{p_i} + c \ln(p_i) - cp_i \right]_{-R}^{R} = 0,
\end{aligned}$$

where C is a constant independent of R. We conclude that p has to be a constant function of ξ, and the only possibility is $p = \mathbb{1}$. □

Remark 2.5.9. From the proofs of Lemma 2.5.8 and Theorem 2.5.1 above, it is clear that the estimate $\langle u^{\circ -1}, Mu\rangle \geq 0$, together with the equality case, is crucial. Since this estimate fails if M is not line-sum-symmetric (by Lemma 2.5.7), (A_1) is sharp regarding the proof presented here. Note that [157, Theorem 2] proved that every nonnegative irreducible matrix A has a line-sum-symmetric similarity-scaling $\operatorname{diag}(x) A \operatorname{diag}(x)^{-1}$, where x is a positive vector, but it seems to us that this property cannot be used to generalize the above proof to non-line-sum-symmetric matrices M.

Finally we recall briefly the arguments leading to the proof of Corollary 2.5.2 and 2.5.3.

Sketch of the proof of Corollary 2.5.2. Take a standing wave p for equation (2.5.2), *i.e.* a travelling wave with speed $c = 0$. It is known from [190, Theorem 1.3 *(ii)*] that, if p is nonnegative and nonzero, then p is bounded uniformly away from 0. Theorem 2.5.1 concludes. □

Sketch of the proof of Corollary 2.5.3. Let (p, c) be a traveling wave for (2.5.2) satisfying the boundary conditions (2.5.3). By [190, Theorem 1.5 *(iii)*], condition (2.5.3) near $-\infty$ immediately transfers to

$$\min_{i\in[N]} \liminf_{\xi\to-\infty} p_i(\xi) > 0,$$

therefore Theorem 2.5.1 can be applied to any local uniform limit of a converging sequence $p(\xi + \xi_n)$ for some $\xi_n \to -\infty$. Since the limit is uniquely identified, the claim is proved. □

2.5.5 Proof of Theorem 2.5.4

We follow the same steps as for the proof of Theorem 2.5.1, but have to adapt each argument in the correct functional setting.

Lemma 2.5.10 (Positivity of K)**.** *Assume (A_2') and (A_3'). Then for all nonzero $u \in L^2(\Omega)$,*

$$\langle K[u], u\rangle_{L^2(\Omega)} = \int_{\Omega^2} u(y)k(y,z)u(z)\mathrm{d}y\mathrm{d}z \geq 0.$$

Proof. To prove the result, we take advantage of the spectral decomposition of K considered as an operator acting on the complex Hilbert space $L^2_{\mathbb{C}}(\Omega)$ equipped with the canonical hermitian product $\langle f, g\rangle_{L^2_{\mathbb{C}}} = \int_\Omega f\overline{g}$. Clearly K is still normal when considered as an operator on $L^2_{\mathbb{C}}(\Omega)$. Moreover, by Lemma 2.5.13, K is compact (and the compactness classically transfers to the complex extension of K). Since $L^2_{\mathbb{C}}(\Omega)$ is separable, by the spectral decomposition theorem (see e.g. [79, Proposition 11.36 p.369]), there exists a Hilbert basis of $L^2_{\mathbb{C}}(\Omega)$ composed of eigenvectors of K. Let us denote $(e_n)_{n\in\mathbb{N}}$ such a Hilbert basis and $(\lambda_n)_{n\in\mathbb{N}}$ the corresponding sequence of eigenvalues. This decomposition yields

$$\langle K[u], u\rangle_{L^2_{\mathbb{C}}} = \sum_{n=0}^{+\infty} \lambda_n |\langle u, e_n\rangle_{L^2_{\mathbb{C}}}|^2,$$

but since $\langle K[u], u\rangle_{L^2_{\mathbb{C}}}$ is real,

$$\langle K[u], u\rangle_{L^2_{\mathbb{C}}} = \operatorname{Re}\left(\sum_{n=0}^{+\infty} \lambda_n |\langle u, e_n\rangle_{L^2_{\mathbb{C}}}|^2\right) = \sum_{n=0}^{+\infty} \operatorname{Re}(\lambda_n) |\langle u, e_n\rangle_{L^2_{\mathbb{C}}}|^2 \geq 0. \qquad \square$$

Lemma 2.5.11 (Characterization of continuous line-sum-symmetric operators [99, Theorem 4])**.** *Let $a \in \mathcal{C}(\Omega \times \Omega, [0, +\infty))$ be Riemann integrable. Then the following two properties are equivalent:*

1. $\int_\Omega a(x,y)\mathrm{d}y = \int_\Omega a(y,x)\mathrm{d}y$ *for all* $x \in \Omega$*;*
2. $\int_{\Omega\times\Omega} \frac{a(x,y)u(y)}{u(x)}\mathrm{d}y\mathrm{d}x \geq \int_{\Omega\times\Omega} a$ *for all* $u \in \mathcal{C}\left(\overline{\Omega}, (0, +\infty)\right)$.

We point out that the equality case of the second property is not presented in the above lemma but was studied in [99, Theorem 5] under the irreducibility-type assumption that $(x, y) \mapsto a(x, y) + a(y, x)$ does not vanish. Here, we need in any case to include in the mutation operator a nontrivial divergence part ($\sigma > 0$), and this suffices for the irreducibility-type properties we need, so that we do not make any irreducibility-type assumption on the nonlocal part.

Lemma 2.5.12 (Uniqueness of the constant solution)**.** *Assume* (A_1'), (A_2') *and* (A_3'). *The constant 1 is the unique nonnegative nonzero classical solution to the equation*

$$\nabla_y \cdot (\sigma(y)\nabla_y p) + M[p](y) + p(y)\,(1 - K[p](y)) = 0, \tag{2.5.8}$$

supplemented with homogeneous Neumann boundary conditions on $\partial\Omega$.

Proof. We first remark that, by a direct application of the strong maximum principle and Hopf's lemma, the fact that p is nonzero can be reinforced as $p(y) > 0$ on $\overline{\Omega}$. Since moreover p is continuous on $\overline{\Omega}$, p is bounded from below. In particular, the test function $\frac{p(y)-1}{p(y)}$ is well-defined and (at least) in $\mathcal{C}^1(\overline{\Omega})$.

As in the discrete case, we multiply (2.5.8) by $\frac{p(y)-1}{p(y)}$ and integrate over Ω. Integrating by parts the gradient term, we get:

$$\begin{aligned} 0 = &- \int_\Omega \sigma(y)\nabla_y p(y)\nabla_y \left(1 - \frac{1}{p(y)}\right) \mathrm{d}y + \int_{\Omega\times\Omega} m(y,z)(p(z) - p(y))\mathrm{d}z\mathrm{d}y \\ &- \int_{\Omega\times\Omega} m(y,z)(p(z) - p(y))\frac{1}{p(y)}\mathrm{d}z\mathrm{d}y + \int_\Omega (1 - K[p](y))\,(p(y) - 1)\mathrm{d}y. \end{aligned}$$

Let us show that each of those terms is nonpositive. We first remark that

$$- \int_\Omega \sigma(y)\nabla_y p(y)\nabla_y \left(1 - \frac{1}{p(y)}\right) \mathrm{d}y = - \int_\Omega \sigma(y)\frac{|\nabla p|^2}{p(y)^2}\mathrm{d}y \le 0,$$

$$\begin{aligned} \int_{\Omega\times\Omega} m(y,z)(p(z) - p(y))\mathrm{d}z\mathrm{d}y &= \int_\Omega \left(\int_\Omega m(y,z)p(z)\mathrm{d}z - \int_\Omega m(y,z)\mathrm{d}z p(y)\right)\mathrm{d}y \\ &= \int_\Omega \left(\int_\Omega m(y,z)p(z)\mathrm{d}z - \int_\Omega m(z,y)\mathrm{d}z p(y)\right)\mathrm{d}y \\ &= \int_{\Omega\times\Omega} m(y,z)p(z)\mathrm{d}z\mathrm{d}y - \int_{\Omega\times\Omega} m(z,y)p(y)\mathrm{d}z\mathrm{d}y \\ &= 0. \end{aligned}$$

Next, by Lemma 2.5.11,

$$\int_{\Omega\times\Omega} m(y,z)(p(z) - p(y))\frac{1}{p(y)}\mathrm{d}y\mathrm{d}z = \int_{\Omega\times\Omega} \frac{m(y,z)p(z)}{p(y)}\mathrm{d}y\mathrm{d}z - \int_{\Omega\times\Omega} m \ge 0.$$

Finally, since $K[1] = 1$, we have $1 - K[p] = K[1 - p]$ and thus, by Lemma 2.5.10,

$$\int_\Omega (1 - K[p](y))\,(p(y) - 1)\mathrm{d}y = - \int_\Omega K[1-p](y)(1 - p(y))\mathrm{d}y \le 0.$$

Therefore each of those four terms is in fact equal to 0. From $\int_\Omega \sigma(y)\frac{|\nabla p(y)|^2}{p(y)^2}\mathrm{d}y = 0$ we deduce that $p(y)$ is a constant on $\overline{\Omega}$. Since then

$$0 = \int_\Omega K[1-p](1-p)\mathrm{d}y = (1-p)^2 \int_{\Omega^2} k(y,z)\mathrm{d}y\mathrm{d}z$$

and $\int_{\Omega^2} k(y,z)\mathrm{d}y\mathrm{d}z > 0$, we conclude that $p = 1$. □

We are now in a position to prove Theorem 2.5.4.

Proof of Theorem 2.5.4. As in the discrete case (proof of Theorem 2.5.1), we multiply the equation (2.5.4) by the test function $\frac{p(\xi,y)-1}{p(\xi,y)}$ and integrate on the cylinder $\Omega_R = [-R, R] \times \Omega$ for some $R > 0$. With the exact same computations as in the proof of Lemma 2.5.12, we get

$$- \int_{\Omega_R} (d(y)\partial_{\xi\xi} p(\xi,y) + c\partial_\xi p(\xi,y))\frac{p(\xi,y) - 1}{p(\xi,y)}\mathrm{d}\xi\mathrm{d}y \le 0.$$

After integrations by parts in the ξ variable, we find

$$\int_{\Omega_R} d(y)\frac{|\partial_\xi p(\xi,y)|^2}{p(\xi,y)^2}\mathrm{d}\xi\mathrm{d}y \leq \left[\int_\Omega d(y)\frac{\partial_\xi p(\xi,y)(p(\xi,y)-1)}{p(\xi,y)} + c\left(\ln(p(\xi,y)) - p(\xi,y)\right)\mathrm{d}y\right]_{-R}^{R} \quad (2.5.9)$$

where, by the classical elliptic estimates, $|\partial_\xi p(\pm R, y)|$ is controlled from above by $\sup_{y\in\Omega,\xi\in[\pm R-\varepsilon,\pm R+\varepsilon]} p(\xi,y)$, independently of R. Taking the limit $R\to+\infty$, we see that $\partial_\xi p(\xi,y)\in L^2(\mathbb{R}\times\Omega)$. Using elliptic regularity, a translation argument (which is similar to the one developed in the proof of Theorem 2.5.1) and Lemma 2.5.12, we conclude that

$$\lim_{\xi\to\pm\infty}\sup_{y\in\Omega}|p(\xi,y)-1| = 0.$$

Going back to (2.5.9), we easily see that the right-hand side converges to zero as $R\to+\infty$ and therefore

$$\int_{\mathbb{R}\times\Omega} d(y)\frac{|\partial_\xi p(\xi,y)|^2}{p(\xi,y)^2}\mathrm{d}\xi\mathrm{d}y = 0,$$

thus p is constant in ξ. We conclude by the limit conditions that in fact $p=1$ identically. □

Corollary 2.5.5 is a direct application of Theorem 2.5.4. As for Corollary 2.5.6, it is proven by an argument similar to the one that yields the limit of the solution near $\pm\infty$ in the proof of Theorem 2.5.4. Since it is rather classical to adapt this argument for traveling waves, we omit the details.

We end by a technical but necessary Lemma.

Lemma 2.5.13 (Compactness of K)**.** *Assume (A_2'). Then the operator $K: L^2(\Omega)\to L^2(\Omega)$ is compact.*

Proof. We aim at applying the Kolmogorov-Riesz-Fréchet Theorem (see e.g. [79, Theorem 4.26 p.111]) to our operator K. We extend the function $k(y,z)$ to $\mathbb{R}^Q\times\mathbb{R}^Q$ by setting $k(y,z)=0$ for $y,z\notin\Omega$. For $f\in L^2(\mathbb{R}^Q)$ we define:

$$K[f](y) = \int_{\mathbb{R}^Q} k(y,z)f(z)\mathrm{d}z.$$

Let $\varepsilon>0$ and $f\in L^2(\Omega)$, $\|f\|_{L^2(\Omega)}=1$ be given. We extend f to $L^2(\mathbb{R}^Q)$ by setting $f(z)=0$, $z\notin\Omega$. We first remark that, for any $h\in\mathbb{R}$,

$$\begin{aligned}
\|\tau_h K[f]-K[f]\|_{L^2}^2 &= \int_{\mathbb{R}^Q}\left(\int_{\mathbb{R}^Q} k(y+h,z)f(z)\mathrm{d}z - \int_{\mathbb{R}^Q} k(y,z)f(z)\mathrm{d}z\right)^2\mathrm{d}y\\
&= \int_{\mathbb{R}^Q}\left(\int_{\mathbb{R}^Q}(k(y+h,z)-k(y,z))f(z)\mathrm{d}z\right)^2\mathrm{d}y\\
&\leq \int_{\mathbb{R}^Q}\int_{\mathbb{R}^Q}(k(y+h,z)-k(y,z))^2\mathrm{d}z\mathrm{d}y\|f\|_{L^2}\\
&= \int_{\mathbb{R}^Q}\int_{\mathbb{R}^Q}(k(y+h,z)-k(y,z))^2\mathrm{d}z\mathrm{d}y,
\end{aligned}$$

where we have used the classical Cauchy–Schwarz inequality in $L^2(\mathbb{R}^Q)$ and $\tau_h g(z) := g(z+h)$. Therefore there remains only to control the L^2 norm of $k(y+h,\cdot)-k(y,\cdot)$ when h is small. To this aim we fix $\delta_1>0$ be such that

$$|\{d(y,\partial\Omega)\leq\delta_1\}| \leq \frac{\varepsilon}{8\|k\|^2_{L^\infty(\Omega^2)}|\Omega|},$$

where $d(\cdot,\partial\Omega)$ is the Euclidean distance between $y\in\mathbb{R}^Q$ and the set $\partial\Omega$ and $|\{d(y,\partial\Omega)\leq\delta_1\}|$ is the Lebesgue measure of the set of points $y\in\mathbb{R}^Q$ satisfying $d(y,\partial\Omega)\leq\delta_1$. Since k is continuous on the compact set $\overline{\Omega}^2$, there exists $\delta_2>0$ such that $|k(y+h,z)-k(y,z)|\leq\frac{\varepsilon}{\sqrt{2}|\Omega|}$ if $y,y+h,z\in\overline{\Omega}$ and $|h|\leq\delta_2$.

Therefore, if $|h| \leq \min(\delta_1, \delta_2)$, we have:

$$\begin{aligned}
\|\tau_h K[f] - K[f]\|_{L^2}^2 &= \int_{d(y,\partial\Omega)\leq\delta_1} \int_{\mathbb{R}^Q} (k(y+h,z) - k(y,z))^2 \mathrm{d}z\mathrm{d}y \\
&\quad + \int_{d(y,\partial\Omega)>\delta_1} \int_{\mathbb{R}^Q} (k(y+h,z) - k(y,z))^2 \mathrm{d}z\mathrm{d}y \\
&\leq 4|\Omega|\|k\|_{L^\infty}^2 |\{d(y,\partial\Omega) \leq \delta_1\}| + |\Omega|^2 \frac{\varepsilon^2}{2|\Omega|^2} \\
&\leq \varepsilon^2.
\end{aligned}$$

We conclude that K is indeed compact on $L^2(\Omega)$. □

2.6 The spatio-temporal dynamics of interacting genetic incompatibilities

2.6.1 Introduction

Genetic incompatibilities correspond to deleterious interactions between alleles (at the same locus or at different loci) within the same genome, and are the cause of the reduced fitness of hybrids between species [122], [183]. Such incompatibilities may be revealed by crosses between divergent populations or species, which may be performed experimentally [173], but may also occur naturally in hybrid zones resulting from secondary contacts between genetically divergent populations [39, 40]. Indeed, the offspring of such crosses carry a mix of alleles from the two parental populations, which may not function well together. Genetic incompatibilities may also be widespread within the same species, as suggested by recent data from *Drosophila* [115].

How several incompatibilities segregating within the same population interfere with each other has important consequences for the evolution of reproductive isolation, and the maintenance of distinct genetic entities after a secondary contact. Barton & de Cara [37] showed that, in the case of a single population (sympatry), incompatibilities are expected to couple through the buildup of linkage disequilibrium among them, which may eventually lead to strong reproductive isolation between two distinct genetic backgrounds. In spatially structured populations with limited dispersal (parapatry), clines in allele frequencies may form between regions containing different sets of incompatible alleles [35]. In this case, linkage disequilibria generated by dispersal generally tend to pull clines together [358], again leading to the *coupling* of genetic incompatibilities which then tend to reinforce each other. This process was explored by Barton [36] in the case of a continuous, linear habitat, and when genetic incompatibilities are generated by an arbitrary number of underdominant loci: at each locus, heterozygotes (say Aa) have a lower fitness than homozygotes, while the two homozygotes (AA and aa) have equal fitness. This form of *symmetric* selection (against heterozygotes) can maintain stable clines in allele frequencies [41], [35], separating regions where AA and aa individuals are abundant (Aa hybrids being generated between these regions). When two such clines overlap in space (one separating regions where AA and aa are abundant, and the other separating regions where BB and bb are abundant), they tend to attract each other until they coincide, as illustrated by the numerical simulations in Figure 2.6.1, and then become motionless.

In the *asymmetric* situation where one allele has a selective advantage over the other (*i.e.*, one homozygous genotype, say AA, has a higher fitness than the other, aa), the cline will move in the direction of the less fit genotype [35]. The interaction between several such asymmetric incompatibilities raises several questions that remain little explored to date, such as: when clines moving at different speeds come into contact, will they remain *stacked* (increasing the degree of reproductive isolation between the two sides of the clines) or not? If they do remain stacked, what will be the speed of the resulting front? Under which conditions may an asymmetric incompatibility escape from a hybrid zone in which several incompatibilities are segregating?

The article [P17] corresponding to the present section constitutes a first step in the exploration of the spatio-temporal dynamics of interacting asymmetric incompatibilities, focusing on a simple situation involving two coupled underdominant loci (with alleles A, a at the first locus, B, b at the second) with identical fitness effects. Notice that Barton [36] has considered the situation where heterozygotes present a cost in fitness and where the fitness of the homozygotes $AB|AB$ and the one of $ab|ab$ are the same, that is the symmetric case. In Section 2.6.3, we give a mathematical proof of the existence (and uniqueness up to a shift) of such a cline in this symmetric situation, see Proposition 2.6.2. Such a cline is a solution to the equation (2.6.12) involving nonlinear gradient terms. We also prove in Proposition 2.6.3 that this stationary cline is stable, *i.e.* that small perturbations of the profile may shift its spatial position but essentially do not alter its shape. In other words, a perturbed stationary cline comes back to a possibly shifted stationary cline.

When the fitness of the homozygote $AB|AB$ becomes slightly larger than the one of $ab|ab$, it is not *a priori* obvious whether the stationary cline stays stationary or begins to move. Here we answer this question by showing that invasion does occur even if the difference in fitness between homozygotes has a lower order of magnitude (measured by $0 < \varepsilon \ll 1$) compared to the fitness cost of heterozygotes. By using a rather involved perturbation analysis, we show in Theorem 2.6.4 that a front traveling at a constant speed $c_\varepsilon > 0$ emerges from the stationary cline u_0 solving (2.6.12) when ε becomes positive. Such a traveling front is a solution to the reaction-diffusion equation (2.6.11) involving nonlinear gradient terms. We give an explicit approximation of the speed c_ε which is, from the modelling point of view, the main contribution of the present work. Among other implications, it reveals not only that recombination between the two loci tends to slow down the propagation of the front but also that the stacked clines always travel faster than one cline

alone.

The organization of the section 2.6 is as follows. In Section 2.6.2 we derive the mathematical model, a PDE system involving nonlinear gradient terms. Through a phase plane analysis, we construct stationary solutions in Section 2.6.3. Then, in Section 2.6.4, we construct traveling fronts thanks to a perturbation argument. In Section 2.6.5, a trick enables us to derive an explicit approximation of the speed c_ε which sheds light on the original model. We conclude and present some perspectives in Section 2.6.6.

2.6.2 Derivation of the mathematical model

2.6.2.1 Biological assumptions

The population occupies a one-dimensional space, along which density is supposed uniform and large. We focus on the variations of the genetic composition of the population. We consider that the fitness of a (diploid) individual is affected by two loci: a first locus with two alleles A and a and a second locus with two alleles B and b. We assume that heterozygotes have the lowest fitness (underdominance), the fitness of the different genotypes at each locus being given in Table 2.6.1.

genotype	fitness
AA	$1+2s_A$
Aa	$1+s_A-S_A$
aa	1

genotype	fitness
BB	$1+2s_B$
Bb	$1+s_B-S_B$
bb	1

Table 2.6.1: Fitness of the different genotypes at each locus.

Here the constants s_A, s_B, S_A, S_B satisfy $0 \leq s_A < S_A$, $0 \leq s_B < S_B$. We then assume multiplicative effects among loci, so that the fitnesses $\mathcal{W}$ of two-locus genotypes are given in Table 2.6.2.

	AA	Aa	aa
BB	$(1+2s_B)(1+2s_A)$	$(1+2s_B)(1+s_A-S_A)$	$1+2s_B$
Bb	$(1+s_B-S_B)(1+2s_A)$	$(1+s_B-S_B)(1+s_A-S_A)$	$1+s_B-S_B$
bb	$1+2s_A$	$1+s_A-S_A$	1

Table 2.6.2: Fitness of diploid individuals.

Note that, because we will derive expressions to the first order in s_A, s_B, S_A and S_B, assuming additive effects among loci would lead to the same results.

We assume that recombination occurs with probability r, so that $AB|ab$ individuals may produce Ab and aB gametes. Throughout the section 2.6.2, the population occupying the left-hand side of the linear habitat will consist mostly of $AB|AB$ individuals, while the right-hand side will be mostly composed of $ab|ab$ individuals. In the symmetric situation ($s_A = s_B = 0$), if the clines of A and B are shifted in space, linkage disequilibrium will develop between the two loci and will pull both fronts together until they are stacked [358], [36], as illustrated in Figure 2.6.1. This section 2.6.2 is concerned with the established regime where the fronts are stacked (this situation may also result from a secondary contact between two divergent populations, as considered by [36]). Note that in the general case (s_A, $s_B \neq 0$), shifted clines may not necessarily become stacked; however, we postpone the analysis of the conditions for stacking to future works.

The PDEs describing the dynamics of two underdominant loci in a 1-dimensional continuous habitat can be obtained by combining the works [35] and [36]. For the self-containedness of the present work, we present here a derivation of these equations, obtained by approximating a discrete-time model by a continuous-time model. In Section 2.6.2.2 we present the genetic model that drives the genetic dynamics. In Section 2.6.2.3 we introduce the spatial structure and the corresponding equations. Finally in Section 2.6.2.4, we make precise our assumptions on the parameters and their respective magnitudes, as well as our precise objectives.

2.6.2.2 Recursions on gamete frequencies in a discrete in time setting

We start by considering a single population of diploid, hermaphroditic individuals with nonoverlapping generations. At the end of a generation (at time t), individuals release gametes and immediately die. The next generation, at time $t+1$, is formed by the random fusion of gametes. Under these hypotheses, it is sufficient to follow the frequencies of gametes produced at each generation, which completely determine the next generation of individuals (by the law of large numbers). Denote by $y_{\substack{A\\B}}$, $y_{\substack{A\\b}}$, $y_{\substack{a\\B}}$, $y_{\substack{a\\b}}$ the frequencies of the different types of gametes at generation t. The fusion at random of these four combinations gives birth to sixteen types of individuals ("ordered" in the sense that $z_{i|j} \neq z_{j|i}$ for $i \neq j$)

$$z_{i|j}, \quad i,j \in \{\tfrac{A}{B}, \tfrac{A}{b}, \tfrac{a}{B}, \tfrac{a}{b}\},$$

with proportions $p_{i|j}$. Notice that, for $i \neq j$, the fusion can be male-female or female-male so that we have $p_{i|j} = 2 \times \frac{1}{2} y_i y_j$, thus

$$p_{i|j} = y_i y_j.$$

Each one of these individuals then produces gametes according to its fitness, providing the generation of gametes $y'_{\substack{A\\B}}$, $y'_{\substack{A\\b}}$, $y'_{\substack{a\\B}}$, $y'_{\substack{a\\b}}$ at time $t+1$. Here we assume that there is a probability of recombination $0 \leq r \leq \frac{1}{2}$ between the two loci. For each of the sixteen diploid genotypes, the process is as one of the three following examples:

- the individuals $z_{\substack{A\\B}|\substack{A\\B}}$, whose proportion is $y^2_{\substack{A\\B}}$, release gametes $\frac{A}{B}$ in proportion 1.
- the individuals $z_{\substack{A\\B}|\substack{A\\b}}$, whose proportion is $y_{\substack{A\\B}} y_{\substack{A\\b}}$, release gametes $\frac{A}{B}$ in proportion $\frac{1}{2}$ and gametes $\frac{A}{b}$ in proportion $\frac{1}{2}$.
- the individuals $z_{\substack{A\\B}|\substack{a\\b}}$, whose proportion is $y_{\substack{A\\B}} y_{\substack{a\\b}}$, release gametes $\frac{A}{B}$ and $\frac{a}{b}$ both in proportion $\frac{1-r}{2}$ (no recombination), and gametes $\frac{A}{b}$ and $\frac{a}{B}$ both in proportion $\frac{r}{2}$ (recombination).

All these processes are weighted by the fitness of each type of individual, as in the above table. After a tedious but straightforward analysis, one obtains:

$$\begin{aligned}
y'_{\substack{A\\B}} &= \frac{1}{\overline{\mathcal{W}}}\Big[(1+2s_A)(1+2s_B)y^2_{\substack{A\\B}} + (1+2s_A)(1+s_B-S_B)y_{\substack{A\\B}}y_{\substack{A\\b}} + (1+s_A-S_A)(1+2s_B)y_{\substack{A\\B}}y_{\substack{a\\B}} \\
&\qquad + (1-r)(1+s_A-S_A)(1+s_B-S_B)y_{\substack{A\\B}}y_{\substack{a\\b}} + r(1+s_A-S_A)(1+s_B-S_B)y_{\substack{a\\B}}y_{\substack{A\\b}}\Big] \\
y'_{\substack{A\\b}} &= \frac{1}{\overline{\mathcal{W}}}\Big[(1+2s_A)y^2_{\substack{A\\b}} + (1+2s_A)(1+s_B-S_B)y_{\substack{A\\b}}y_{\substack{A\\B}} + (1+s_A-S_A)y_{\substack{A\\b}}y_{\substack{a\\b}} \\
&\qquad + (1-r)(1+s_A-S_A)(1+s_B-S_B)y_{\substack{A\\b}}y_{\substack{a\\B}} + r(1+s_A-S_A)(1+s_B-S_B)y_{\substack{A\\B}}y_{\substack{a\\b}}\Big] \\
y'_{\substack{a\\B}} &= \frac{1}{\overline{\mathcal{W}}}\Big[(1+2s_B)y^2_{\substack{a\\B}} + (1+s_B-S_B)y_{\substack{a\\B}}y_{\substack{a\\b}} + (1+s_A-S_A)(1+2s_B)y_{\substack{a\\B}}y_{\substack{A\\B}} \\
&\qquad (1-r)(1+s_A-S_A)(1+s_B-S_B)y_{\substack{a\\B}}y_{\substack{A\\b}} + r(1+s_A-S_A)(1+s_B-S_B)y_{\substack{A\\B}}y_{\substack{a\\b}}\Big] \\
y'_{\substack{a\\b}} &= \frac{1}{\overline{\mathcal{W}}}\Big[y^2_{\substack{a\\b}} + (1+s_A-S_A)y_{\substack{a\\b}}y_{\substack{A\\b}} + (1+s_B-S_B)y_{\substack{a\\b}}y_{\substack{a\\B}} \\
&\qquad + (1-r)(1+s_A-S_A)(1+s_B-S_B)y_{\substack{a\\b}}y_{\substack{A\\B}} + r(1+s_A-S_A)(1+s_B-S_B)y_{\substack{a\\B}}y_{\substack{A\\b}}\Big],
\end{aligned}$$

where $\overline{\mathcal{W}}$ is the average fitness:

$$\begin{aligned}
\overline{\mathcal{W}} &= \sum_{i,j\in\{\frac{A}{B},\frac{A}{b},\frac{a}{B},\frac{a}{B}\}} p_{i|j}\mathcal{W}_{i|j} \\
&= (1+2s_A)(1+2s_B)y^2_{\substack{A\\B}} + (1+2s_A)y^2_{\substack{A\\b}} + (1+2s_B)y^2_{\substack{a\\B}} + y^2_{\substack{a\\b}} \\
&+ 2(1+2s_A)(1+s_B-S_B)y_{\substack{A\\B}}y_{\substack{A\\b}} + 2(1+s_A-S_A)(1+2s_B)y_{\substack{A\\B}}y_{\substack{a\\B}} \\
&+ 2(1+s_A-S_A)(1+s_B-S_B)y_{\substack{A\\B}}y_{\substack{a\\b}} + 2(1+s_A-S_A)(1+s_B-S_B)y_{\substack{A\\b}}y_{\substack{a\\B}} \\
&+ 2(1+s_A-S_A)y_{\substack{A\\b}}y_{\substack{a\\b}} + 2(1+s_B-S_B)y_{\substack{a\\B}}y_{\substack{a\\b}}.
\end{aligned}$$

Notice that adding the four above equations, one can check $y'_{\substack{A\\B}} + y'_{\substack{A\\b}} + y'_{\substack{a\\B}} + y'_{\substack{a\\b}} = \frac{\overline{\mathcal{W}}}{\overline{\mathcal{W}}} = 1$.

For ease of notation, we now let

$$u := y_{\substack{A\\B}}, \quad v := y_{\substack{A\\b}}, \quad w := y_{\substack{a\\B}}, \quad z := y_{\substack{a\\b}}, \tag{2.6.1}$$

so that

$$u + v + w + z = 1. \tag{2.6.2}$$

As in [36], we shall rather work on the three components system satisfied by

$$p := u + v, \quad q := u + w, \quad D := uz - vw, \tag{2.6.3}$$

where

- p measures the frequency of allele A,
- q measures the frequency of allele B,
- D stands for the linkage disequilibrium, measuring the association between alleles A and B within gametes (notice that, equivalently, $D = u - pq$).

Notice that

$$u = pq + D, \quad v = p\,(1-q) - D, \quad w = (1-p)\,q - D, \quad z = (1-p)(1-q) + D. \tag{2.6.4}$$

Next, we assume that s_A, s_B, S_A, S_B, r are small and of the same order of magnitude, that is

$$s_A \leftarrow s_A\alpha, \quad s_B \leftarrow s_B\alpha, \quad S_A \leftarrow S_A\alpha, \quad S_B \leftarrow S_B\alpha, \quad r \leftarrow r\alpha, \tag{2.6.5}$$

for $0 < \alpha \ll 1$. Taking into account (2.6.1), (2.6.2), (2.6.3), (2.6.4), (2.6.5), one can perform straightforward (but tedious) computations and obtain to the first order in α:

$$\begin{cases} p' &= p + \alpha\Big[\,(S_A(2p-1) + s_A)\,p(1-p) + (S_B(2q-1) + s_B)\,D\Big] \\ q' &= q + \alpha\Big[\,(S_B(2q-1) + s_B)\,q(1-q) + (S_A(2p-1) + s_A)\,D\Big] \\ D' &= D - \alpha\Big[r + (2p-1)\,(S_A(2p-1) + s_A) + (2q-1)\,(S_B(2q-1) + s_B)\,\Big]D. \end{cases} \tag{2.6.6}$$

2.6.2.3 Inserting a spatial structure and switching to continuous time

Finally we consider the associated problem with a spatial structure $x \in \mathbb{R}$ (corresponding to the position of individuals along space) and continuous time $t \geq 0$. More precisely, we assume that gametes migrate according to a dispersal kernel centered on 0 and with variance σ^2. In the diffusion limit, and from (2.6.6), the equations for the frequencies $p = p(t,x)$, $q = q(t,x)$ are

$$\begin{cases} p_t &= \frac{\sigma^2}{2}p_{xx} + (S_A(2p-1) + s_A)\,p(1-p) + (S_B(2q-1) + s_B)\,D \\ q_t &= \frac{\sigma^2}{2}q_{xx} + (S_B(2q-1) + s_B)\,q(1-q) + (S_A(2p-1) + s_A)\,D, \end{cases}$$

where $\sigma > 0$. Notice that, since we assumed that the density of individuals is uniform and large, no advection term appears in the above system. As for the equation for the disequilibrium $D = uz - vw$, we have additional gradient terms (e.g. [38], [36]) since

$$\begin{aligned} D_t &= \left(\frac{\sigma^2}{2}u_{xx} + \cdots\right)z + u\left(\frac{\sigma^2}{2}z_{xx} + \cdots\right) - \left(\frac{\sigma^2}{2}v_{xx} + \cdots\right)w - v\left(\frac{\sigma^2}{2}w_{xx} + \cdots\right) \\ &= \frac{\sigma^2}{2}\left(D_{xx} + 2(-u_xz_x + v_xw_x)\right) + \cdots \\ &= \frac{\sigma^2}{2}\left(D_{xx} + 2(p_xq_x)\right) + \cdots \end{aligned}$$

where we have used the identity

$$p_xq_x = (u+v)_x(u+w)_x = u_x(u_x + v_x + w_x) + v_xw_x = -u_xz_x + v_xw_x.$$

Hence, from (2.6.6), the equation for $D = D(t,x)$ is

$$D_t = \frac{\sigma^2}{2}D_{xx} + \sigma^2p_xq_x - \left[r + (2p-1)\,(S_A(2p-1) + s_A) + (2q-1)\,(S_B(2q-1) + s_B)\right]D.$$

2.6.2.4 Conclusion and goals

Hence the system for the allele frequencies $p = p(t,x)$, $q = q(t,x)$ and the linkage disequilibrium $D = D(t,x)$ is written

$$\begin{cases} p_t &= \frac{\sigma^2}{2} p_{xx} + (S_A(2p-1) + s_A)\, p(1-p) + (S_B(2q-1) + s_B) D \\ q_t &= \frac{\sigma^2}{2} q_{xx} + (S_B(2q-1) + s_B)\, q(1-q) + (S_A(2p-1) + s_A) D \\ D_t &= \frac{\sigma^2}{2} D_{xx} + \sigma^2 p_x q_x - [r + (2p-1)\,(S_A(2p-1) + s_A) + (2q-1)\,(S_B(2q-1) + s_B)]\, D, \end{cases} \tag{2.6.7}$$

where $\sigma > 0$, $r > 0$, $s_A > 0$, $s_B > 0$, $s_A > 0$ and $S_B > 0$ are given parameters. Observe that, starting from $D \equiv 0$ (no disequilibrium) the dynamics of p and q are decoupled but the gradient terms p_x and q_x in the D-equation cause disequilibrium and thus interaction [36], see Figure 2.6.1.

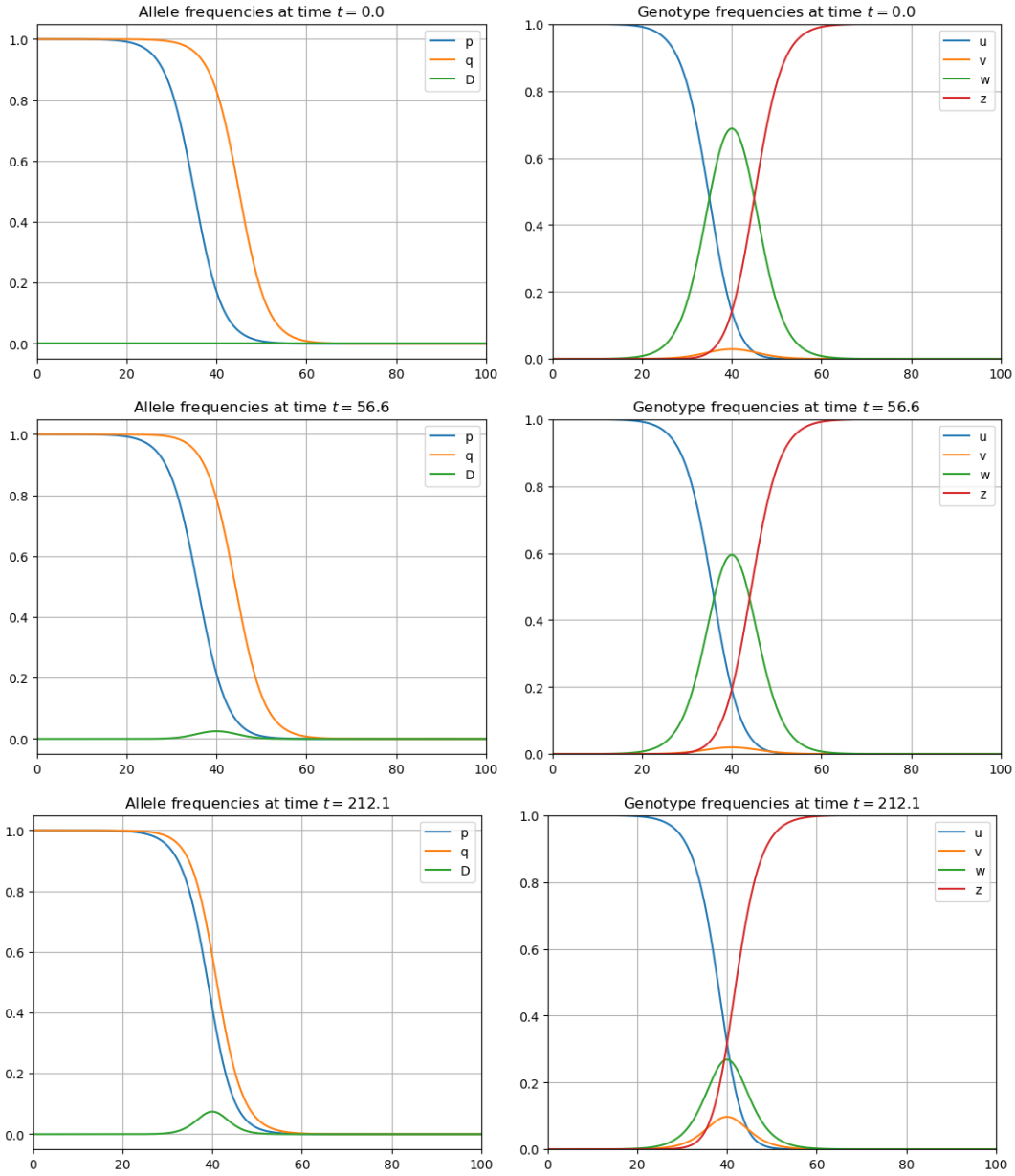

Figure 2.6.1: Numerical solutions with parameters $s_A = s_B = 0$ (symmetric case), $S_A = S_B = r = 0.1$ and $\frac{\sigma^2}{2} = 1$. Left column: p, q and D; the clines are initially uncoupled; next, in a transitory regime, they are driven closer to each other, and eventually become stacked. Right column: the original unknowns, that is the frequencies of gametes u, v, w, z. Remark: the partial differential system in (u, v, w, z) is a reaction-diffusion system for which a standard Strang splitting method was used; numerical simulations were done in python 3.9.2 with the NumPy package version 1.20.1. The code for the simulations and figures is available on the GitHub repository `https://github.com/benoit-sbr/reac-diff-Strang-splitting`.

Assuming that recombination r is sufficiently large relative to the strength of selection against heterozygotes (S_A, S_B, determining the gradients in allele frequencies, e.g. [35]) and homozygotes (s_A, s_B), one expects that D approximately follows

$$D_t \approx \frac{\sigma^2}{2} D_{xx} + \sigma^2 p_x q_x - rD.$$

In the sequel, we use a *quasi-linkage equilibrium* approximation [36], meaning that the dynamics on D is

much faster than the one of p and q. As a result,

$$\frac{\sigma^2}{2}D_{xx} + \sigma^2 p_x q_x - rD \approx 0,$$

whose solution is given by (one may use the Fourier transform to see it)

$$D(t,x) \approx \frac{\sigma^2}{r}\rho_\sigma * (p_x q_x(t,\cdot))(x), \quad \rho_\alpha(x) := \frac{1}{2}\sqrt{\frac{2r}{\sigma^2}}e^{-\sqrt{\frac{2r}{\sigma^2}}|x|}.$$

For σ sufficiently small, the kernel ρ_α "approaches" the Dirac delta function, and thus

$$D \approx \frac{\sigma^2}{r}p_x q_x. \tag{2.6.8}$$

As a result, using (2.6.8) and writing $(p,q)(t,x) = (\tilde{p},\tilde{q})\left(t, \frac{\sqrt{2}}{\sigma}x\right)$, we reach a simplified version of system (2.6.7), namely

$$\begin{cases} \tilde{p}_t &= \tilde{p}_{xx} + S_A f(\tilde{p}) + s_A g(\tilde{p}) + \frac{2}{r}(S_B(2\tilde{q}-1) + s_B)\tilde{p}_x\tilde{q}_x, \\ \tilde{q}_t &= \tilde{q}_{xx} + S_B f(\tilde{q}) + s_B g(\tilde{q}) + \frac{2}{r}(S_A(2\tilde{p}-1) + s_A)\tilde{p}_x\tilde{q}_x, \end{cases}$$

where

$$f(u) := u(2u-1)(1-u), \quad g(u) := u(1-u).$$

For ease of notation in the mathematical analysis, we now drop the tildes but keep in mind that, when returning to the original model, the traveling waves speeds we will find have to be multiplied by the factor $\frac{\sigma}{\sqrt{2}}$. Last, we assume that

$$S_A = S_B = S, \quad s_A = s_B = s =: \varepsilon, \tag{2.6.9}$$

and thus focus on the system

$$\begin{cases} p_t &= p_{xx} + Sf(p) + \varepsilon g(p) + \frac{2}{r}(S(2q-1) + \varepsilon)p_x q_x, \\ q_t &= q_{xx} + Sf(q) + \varepsilon g(q) + \frac{2}{r}(S(2p-1) + \varepsilon)p_x q_x. \end{cases} \tag{2.6.10}$$

Notice that f is a balanced bistable nonlinearity, which is slightly unbalanced by the term εg.

In the sequel, our goal is to inquire on the situation where the A cline, measured by p, and the B cline, measured by q, remain stacked together. To do so we look at $u = p = q$ solving the nonlinear equation

$$u_t = u_{xx} + Sf(u) + \varepsilon g(u) + \frac{2}{r}(S(2u-1) + \varepsilon)u_x^2. \tag{2.6.11}$$

We suspect the existence of a stationary solution connecting 1 to 0 for $\varepsilon = 0$ and that of a front connecting 1 to 0 and traveling at a speed $c_\varepsilon \sim c_1\varepsilon$ for some $c_1 > 0$ and $0 < \varepsilon \ll 1$. These facts are proved in Section 2.6.3 and 2.6.4, while c_1 is explicitly identified in Section 2.6.5.

2.6.3 Standing together ($\varepsilon = 0$)

In this section 2.6.3, we construct a stationary solution connecting 1 to 0 in (2.6.11) when $\varepsilon = 0$, and then prove its stability.

2.6.3.1 Construction of the standing wave

We are here looking after a $u_0 : \mathbb{R} \to \mathbb{R}$ solving

$$\begin{cases} u_0'' + Sf(u_0) + \frac{2}{r}S(2u_0 - 1)(u_0')^2 = 0 \quad \text{on } \mathbb{R}, \\ u_0(-\infty) = 1, \quad u_0(+\infty) = 0. \end{cases} \tag{2.6.12}$$

Lemma 2.6.1 (A priori estimates)**.** *Any standing wave solution of* (2.6.12) *has to satisfy* $0 < u_0 < 1$ *and* $u_0'(\pm\infty) = 0$.

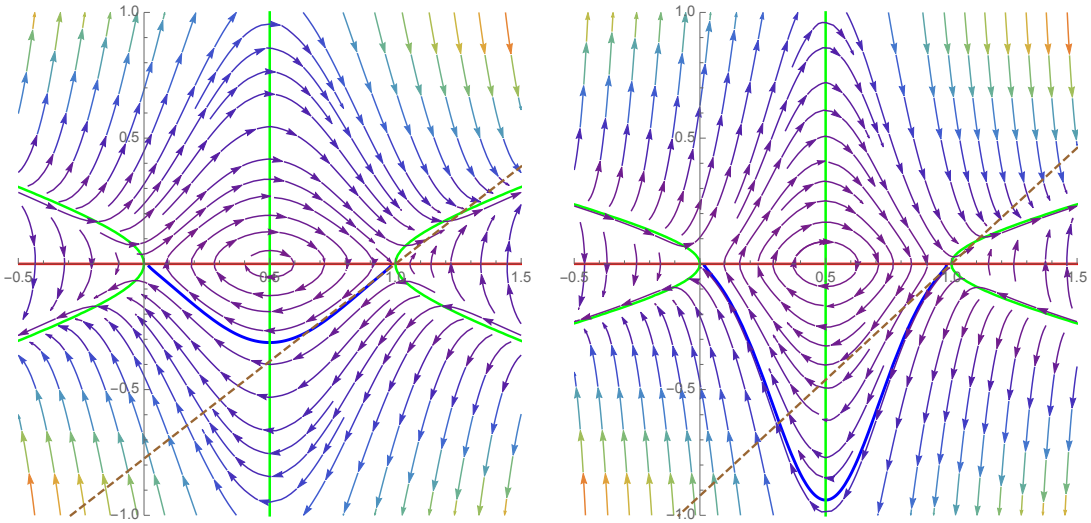

Figure 2.6.2: Phase plane analysis for (2.6.13). In red, the nullcline $x' = 0$, in green the nullcline $y' = 0$, in brown dashed the linear unstable manifold at $(1, 0)$, in blue (an approximation of) the heteroclinic orbit from $(1, 0)$ to $(0, 0)$. Left: the parameters are $S = 0.6$, $r = 0.25$ so that (2.6.14) holds. Right: the parameters are $S = 0.85$, $r = 0.15$ so that (2.6.14) does not hold.

Proof. If $u_0 \leq 1$ is not true then, from the boundary conditions, u_0 has to reach a maximum value strictly larger than 1 at some point but, testing the equation at this point, this cannot hold. Hence $u_0 \leq 1$ and, from the strong maximum principle, $u_0 < 1$. Similarly $u_0 > 0$.

From the equation and the boundary condition, $u_0'' > 0$ in some $(A, +\infty)$, so that u_0' is increasing on $(A, +\infty)$. As a result u_0' has a limit in $+\infty$, which has to be zero since u_0 is bounded. Similarly $u_0'(-\infty) = 0$. □

Using a phase plane analysis $(x, y) = (u_0, u_0')$, the equation in (2.6.12) is recast

$$\begin{cases} x' = y \\ y' = -Sf(x) - \frac{2}{r}S(2x-1)y^2. \end{cases} \tag{2.6.13}$$

The phase plane analysis is depicted in Figure 2.6.2. The equilibria $(0, 0)$ and $(1, 0)$ are saddle points, the eigenvalues of the Jacobian matrix at these points being $\pm\sqrt{S}$, whereas the equilibrium $(\frac{1}{2}, 0)$ is a center, the eigenvalues of the Jacobian matrix at this point being $\pm i\sqrt{\frac{S}{2}}$. At equilibrium $(1, 0)$ the linear unstable manifold is the line $y = \sqrt{S}(x-1)$. To prove the existence of a heteroclinic orbit from $(1, 0)$ to $(0, 0)$, we consider the orbit leaving $(1, 0)$ along the unstable manifold. As long as it has not reached $x = \frac{1}{2}$ this trajectory satisfies $x' < 0$ and $y' < 0$ (south west trajectory). In order to prove that the trajectory does cross the vertical line $x = \frac{1}{2}$, we need to construct a barrier, from below, preventing the situation $x \to l \geq \frac{1}{2}$, $y \to -\infty$. We choose the line $y = \alpha(x-1)$ with $\alpha > 0$ to be selected large enough. Choosing $\alpha > \sqrt{S}$ ensures that the trajectory is above the barrier in a neighborhood of $(1, 0)$. We thus need to show that

$$\frac{|y'|}{|x'|} < \alpha \quad \text{on the points } (x, y) \text{ such that } y = \alpha(x-1),\ \frac{1}{2} \leq x < 1.$$

After some straightforward computations, this is recast

$$\varphi(x) := (2x-1)\left|\left(1 - \frac{2\alpha^2}{r}\right)x + \frac{2\alpha^2}{r}\right| < \frac{\alpha^2}{S}, \quad \text{for all } \frac{1}{2} \leq x < 1.$$

Assuming $1 - \frac{2\alpha^2}{r} < 0$, and evaluating the maximum of φ on $[\frac{1}{2}, 1]$, we reach

$$\frac{\left(\frac{2\alpha^2}{r} + 1\right)^2}{8\left(\frac{2\alpha^2}{r} - 1\right)} < \frac{\alpha^2}{S},$$

which can be obtained with α sufficiently large provided

$$S < 4r. \tag{2.6.14}$$

Notice that, from the modelling point of view, assumption (2.6.14) is consistent with the asymptotics "S small" performed in Section 2.6.2 (quasi-linkage equilibrium approximation). On the other hand, even if (2.6.14) does not hold, the (right) phase plane analysis of Figure 2.6.2 suggests that the heteroclinic orbit joining $(1,0)$ to $(0,0)$ still exists, but the above argument does not apply.

As a result, under assumption (2.6.14), the orbit touches the line $x = \frac{1}{2}$ at some point $(\frac{1}{2}, -\beta)$ for some $\beta > 0$. Since the problem is symmetric with respect to $x = \frac{1}{2}$, we conclude that the orbit then converges to the equilibrium $(0,0)$ along the stable manifold, the linear stable manifold being given by $y = -\sqrt{S}x$. This trajectory provides a positive and decreasing solution u_0 to (2.6.12).

In other words, we have (nearly) proved the following.

Proposition 2.6.2 (Stationary solution for $\varepsilon = 0$)**.** *Let us assume* (2.6.14)*. Then there is a unique* $u_0 : \mathbb{R} \to \mathbb{R}$ *solving* (2.6.12) *and satisfying the normalization condition* $u_0(0) = \frac{1}{2}$.

Moreover, u_0 *is positive, decreasing, symmetric in the sense that*

$$u_0(-x) = 1 - u_0(x) \quad \text{for all } x \in \mathbb{R},$$

and has the asymptotics

$$1 - u_0(x) \sim Ce^{\sqrt{S}x} \text{ as } x \to -\infty, \quad u_0(x) \sim Ce^{-\sqrt{S}x} \text{ as } x \to +\infty, \tag{2.6.15}$$

for some $C > 0$.

Proof. From the above phase plane analysis, we are already equipped with a positive, decreasing and symmetric u_0 solving (2.6.12). The asymptotics (2.6.15) is rather classical but, for the convenience of the reader, we sketch a short and direct proof. We work as $x \to +\infty$. We know from the phase plane analysis that $u_0'(x) \sim -\sqrt{S}u_0(x)$ so that

$$u_0(x) = e^{-\sqrt{S}x + o(x)}. \tag{2.6.16}$$

Now, from the nonlinear ODE, we have, for some $K > 0$,

$$-Ku_0^2(x) \le u_0''(x) - Su_0(x) \le Ku_0^2(x).$$

Multiplying this by $u_0'(x) < 0$ and integrating from x to $+\infty$, we have,

$$-\frac{K}{3}u_0^3(x) \le -\frac{1}{2}(u_0')^2(x) + \frac{S}{2}u_0^2(x) \le \frac{K}{3}u_0^3(x).$$

As a result,

$$|u_0'(x) + \sqrt{S}u_0(x)| = \left|\frac{-(u_0')^2(x) + Su_0^2(x)}{-u_0'(x) + \sqrt{S}u_0(x)}\right| \le \frac{\frac{2K}{3}u_0^2(x)}{\left|-\frac{u_0'(x)}{u_0(x)} + \sqrt{S}\right|} \le Mu_0^2(x), \tag{2.6.17}$$

where $M := \frac{2K}{3\sqrt{S}} > 0$. From this and (2.6.16) we deduce that $e^{\sqrt{S}x}(u_0'(x) + \sqrt{S}u_0(x)) = \frac{d}{dx}\left(e^{\sqrt{S}x}u_0(x)\right)$ must be integrable in $+\infty$. As a result there is $C \ge 0$ such that $e^{\sqrt{S}x}u_0(x) \to C$ as $x \to +\infty$. Now the left inequality in (2.6.17) implies

$$-\sqrt{S} \le \frac{u_0'}{u_0 + \frac{M}{\sqrt{S}}u_0^2} = \frac{u_0'}{u_0} - \frac{\frac{M}{\sqrt{S}}u_0'}{1 + \frac{M}{\sqrt{S}}u_0}.$$

Integrating this from 0 to x, we obtain

$$-\sqrt{S}x \le \ln\left(\frac{u_0(x)}{1 + \frac{M}{\sqrt{S}}u_0(x)} \times \frac{1 + \frac{M}{\sqrt{S}}u_0(0)}{u_0(0)}\right),$$

and thus

$$e^{\sqrt{S}x} \ge \left(1 + \frac{M}{\sqrt{S}}u_0(x)\right)\frac{u_0(0)}{1 + \frac{M}{\sqrt{S}}u_0(0)} \ge \frac{u_0(0)}{1 + \frac{M}{\sqrt{S}}u_0(0)},$$

so that $C > 0$ and we are done with (2.6.15).

It remains to prove uniqueness. We use a sliding method argument. Let v_0 be "another" solution such that $v_0(0) = \frac{1}{2}$. For $K \geq 0$, define the shifted function $v_K(x) := v_0(x - K)$. Since v_0 must also have some asymptotics of the form (2.6.15), say with some constant $C' > 0$ instead of C, we see that $u_0 \leq v_K$ on $\mathbb{R}$ for $K > 0$ sufficiently large. As a result the real number

$$K_0 := \inf \{K \in \mathbb{R} : u_0(x) \leq v_K(x), \forall x \in \mathbb{R}\}$$

is well defined and nonnegative. Assume by contradiction that $K_0 > 0$. Then there is a point $x_0 \in \mathbb{R}$ where $u_0(x_0) = v_{K_0}(x_0)$ and $u_0'(x_0) = v_{K_0}'(x_0)$ so that, from Cauchy-Lipschitz theorem, $u_0 \equiv v_{K_0}$ on $\mathbb{R}$, which is excluded by the normalization conditions. As a result $K_0 = 0$ and thus $u_0 \leq v_0$. Similarly $v_0 \leq u_0$ and we are done. □

2.6.3.2 Stability of the standing wave

We prove here that the standing wave constructed in Proposition 2.6.2 is linearly stable in the L^∞ norm. More precisely the following holds.

Proposition 2.6.3 (Stability of standing waves)**.** *Let u_0 be the standing wave constructed in Proposition 2.6.2. Let $h \in C_b^1(\mathbb{R})$ be given. Let v solve the parabolic Cauchy problem*

$$\begin{cases} v_t(t,x) = v_{xx}(t,x) + Sf(v(t,x)) + \dfrac{2}{r}S(2v(t,x)-1)(v_x(t,x))^2, & t > 0, x \in \mathbb{R}, \\ v(0,x) = u_0(x) + \varepsilon h(x), & x \in \mathbb{R}. \end{cases}$$

Then there is $\lambda_0 > 0$ such that, for any $0 < \lambda < \lambda_0$, the following holds: for sufficiently small ε, there is a continuous function $\gamma(\varepsilon)$ satisfying

$$\gamma(0) = \int_{\mathbb{R}} h(x)u_0'(x)e^{\frac{4S}{r}(u_0^2(x)-u_0(x))}\mathrm{d}x,$$

and a constant $K > 0$ such that, for all $t > 0$,

$$\|v(t,\cdot) - u_0(\cdot + \varepsilon\gamma(\varepsilon))\|_{C_b^1(\mathbb{R})} \leq Ke^{-\lambda t}.$$

Proof. We aim at applying a result of Sattinger, namely [349, Theorem 4.1]. To do so, we need to show that the linear operator (obtained by linearizing (2.6.12) around the solution u_0)

$$Lh := h'' + \frac{4S}{r}(2u_0 - 1)u_0'h' + S\left(f'(u_0) + \frac{4}{r}(u_0')^2\right)h,$$

satisfies the assumptions (i) and (ii) of [349, Lemma 3.4]. Since equation (2.6.12) is a scalar quasilinear second-order differential equation set on $\mathbb{R}$ and with a smooth nonlinearity, the assumption (ii) of [349, Lemma 3.4] can be readily checked thanks to [349, Lemma 5.4]. As for the assumption (i) of [349, Lemma 3.4], we point out that [349, Corollary 5.7] does not apply to our situation. Indeed, because of the u_0' factor, the coefficient of the first-order term in L vanishes when $x \to \pm\infty$. We thus need to determine the spectrum of L.

The liner operator L admits u_0' as principal eigenvector with eigenvalue 0. We remark that L can be written as

$$Lh = e^{-\frac{2S}{r}(u_0^2-u_0)}M\left(he^{\frac{2S}{r}(u_0^2-u_0)}\right),$$

where

$$Mk := k'' + \left(\frac{2S^2}{r}(2u_0 - 1)f(u_0) + Sf'(u_0)\right)k =: k'' + c(x)k.$$

Since the weight function $e^{\frac{4S}{r}(u_0^2-u_0)}$ is bounded and uniformly positive, the operators L and M can be considered as acting on the same space $C_b^0(\mathbb{R})$. In particular, $\lambda I - L$ admits a bounded inverse if and only if $\lambda I - M$ does (where I is the identity mapping on $C_b^0(\mathbb{R})$), and we have

$$(\lambda I - L)^{-1} = e^{-\frac{2S}{r}(u_0^2-u_0)}(\lambda I - M)^{-1}e^{\frac{2S}{r}(u_0^2-u_0)}.$$

Below, by following ideas of [349], we analyze, for $g \in C_b^0(\mathbb{R})$, the set of solutions to the resolvent equation

$$(\lambda I - M)k = -k'' + (\lambda - c(x))k = g(x), \tag{2.6.18}$$

and then determine the spectrum of M.

1. System of fundamental solutions to the homogeneous equation: we first look for a system of fundamental solutions to

$$-k'' + (\lambda - c(x))k = 0, \tag{2.6.19}$$

whose behaviour near $\pm\infty$ can be determined (see [349, Lemma 5.1] for related arguments) for $\lambda \in \mathbb{C}$ such that $\lambda + S \notin \mathbb{R}^-$.

Near $+\infty$, this is performed by substituting $\varphi_1(x) = z_1(x)e^{-\gamma_+ x}$ in (2.6.19), where $\gamma_+ \in \mathbb{C}$ solves $\gamma_+^2 = \lambda + S$ and $\operatorname{Re}\gamma_+ > 0$. We obtain

$$-z_1'' + 2\gamma_+ z_1' - (S + c(x))z_1 = 0, \tag{2.6.20}$$

which is recast

$$-(z_1' e^{-2\gamma_+ x})' - (S + c(x))z_1 e^{-2\gamma_+ x} = 0,$$

so that, assuming $z_1'(+\infty) = 0$,

$$z_1'(x) = \int_x^{+\infty} e^{-2\gamma_+(y-x)}(S + c(y))z_1(y)\mathrm{d}y, \tag{2.6.21}$$

and thus, assuming $z_1(+\infty) = 1$,

$$z_1(x) = 1 + \int_x^{+\infty} \frac{e^{2\gamma_+(x-y)} - 1}{2\gamma_+}(S + c(y))z_1(y)\mathrm{d}y. \tag{2.6.22}$$

Hence z_1 is written as the solution of a fixed-point problem (2.6.22) set on $C_b^0(\mathbb{R}^+)$. Notice that the asymptotic behaviour (2.6.15) of u_0 implies $y \mapsto S + c(y) \in L^1(\mathbb{R}^+)$. As a result, for a given $x_0 > 0$, the right-hand side operator appearing in (2.6.22) is globally Lipschitz continuous on $C_b^0([x_0, +\infty))$ with Lipschitz constant $\frac{1}{2|\gamma_+|}\int_{x_0}^{+\infty} |S + c(y)|\mathrm{d}y$. Hence, equation (2.6.22) has a unique solution z_1 on $C_b^0([x_0, +\infty))$ for x_0 sufficiently large, and this z_1 can be extended to $(-\infty, x_0)$ by solving the adequate Cauchy problem associated with (2.6.20). We have therefore constructed a solution $\varphi_1(x) = z_1(x)e^{-\gamma_+ x}$ to (2.6.19) with $z_1 \in C_b^0(\mathbb{R}^+)$, $z_1(+\infty) = 1$.

By the same procedure, but integrating on $[x_0, x]$ instead of $[x, +\infty)$ in (2.6.21), we can construct a solution $\varphi_2(x) = z_2(x)e^{\gamma_+ x}$ to (2.6.19) with $z_2 \in C_b^0(\mathbb{R}^+)$ provided by the fixed-point problem

$$z_2(x) = 1 + \int_{x_0}^{x} \frac{1 - e^{-2\gamma_+(x-y)}}{2\gamma_+}(S + c(y))z_2(y)\mathrm{d}y.$$

By the continuous dependence of the fixed-point with respect to the parameter x_0 [413, Proposition 1.2], and by selecting x_0 sufficiently large, $z_2(x)$ can be made arbitrarily close to 1. Indeed $z_2(x + x_0)$ is the unique fixed point of the operator

$$T_{x_0} z(x) := 1 + \int_0^{x} \frac{1 - e^{-2\gamma_+(x-y)}}{2\gamma_+}(S + c(x_0 + y))z(y)\mathrm{d}y,$$

and T_{x_0} converges uniformly to the constant operator $T_{+\infty} z \equiv 1$ as $x_0 \to +\infty$:

$$\|T_{x_0} z - 1\|_{C_b^0([0,+\infty))} \leq \left(\frac{1}{2|\gamma_+|}\int_{x_0}^{+\infty} |S + c(y)|\mathrm{d}y\right)\|z\|_{C_b^0([0,+\infty))} \xrightarrow[x_0 \to \infty]{} 0.$$

Therefore we have found a system of fundamental solutions (φ_1, φ_2) to (2.6.19) whose behaviour near $+\infty$ is known. We can proceed similarly near $-\infty$ and find another system of fundamental solutions (ψ_1, ψ_2) whose behaviour near $-\infty$ is known.

Summarizing, for each $\lambda \in \mathbb{C} \setminus (-\infty, -S]$, we have

$$\varphi_1(x) \approx_{+\infty} e^{-\gamma_+ x}, \qquad \varphi_2(x) \approx_{+\infty} e^{\gamma_+ x}, \qquad \psi_1(x) \approx_{-\infty} e^{\gamma_+ x}, \qquad \psi_2(x) \approx_{-\infty} e^{-\gamma_+ x}, \tag{2.6.23}$$

$$\varphi_1'(x) \approx_{+\infty} e^{-\gamma_+ x}, \qquad \varphi_2'(x) \approx_{+\infty} e^{\gamma_+ x}, \qquad \psi_1'(x) \approx_{-\infty} e^{\gamma_+ x}, \qquad \psi_2'(x) \approx_{-\infty} e^{-\gamma_+ x}, \tag{2.6.24}$$

where $A(x) \approx_{+\infty} B(x)$ means $0 < \liminf_{x\to+\infty} \frac{|A(x)|}{B(x)} \le \limsup_{x\to+\infty} \frac{|A(x)|}{B(x)} < +\infty$. Notice that, if λ is not an eigenvalue of M, we further know that φ_1 is unbounded as $x \to -\infty$ (or else it would be an eigenvector), and ψ_1 is unbounded as $x \to +\infty$. Notice also that the constants involved in the above estimates are locally uniform in λ.

2. Solving equation (2.6.18) **if** $\lambda \in \mathbb{C} \setminus (-\infty, -S]$ **is not an eigenvalue of** M: from the behaviours near $-\infty$, the functions φ_1 and ψ_1 are linearly independent. Therefore, up to redefining $\varphi_2 = \psi_1$, we may consider that (φ_1, φ_2) is a system of fundamental solutions satisfying

$$\begin{array}{llll} \varphi_1(x) \approx_{+\infty} e^{-\gamma_+ x}, & \varphi_2(x) \approx_{+\infty} e^{\gamma_+ x}, & \varphi_1(x) \approx_{-\infty} e^{-\gamma_+ x}, & \varphi_2(x) \approx_{-\infty} e^{\gamma_+ x}, \\ \varphi_1'(x) \approx_{+\infty} e^{-\gamma_+ x}, & \varphi_2'(x) \approx_{+\infty} e^{\gamma_+ x}, & \varphi_1'(x) \approx_{-\infty} e^{-\gamma_+ x}, & \varphi_2'(x) \approx_{-\infty} e^{\gamma_+ x}. \end{array}$$

We use the method of variation of constants to solve (2.6.18) and straightforwardly reach

$$k(x) = \left(C_1 - \frac{1}{W}\int_{-\infty}^{x} \varphi_2(y)g(y)\mathrm{d}y\right)\varphi_1(x) + \left(C_2 - \frac{1}{W}\int_{x}^{+\infty} \varphi_1(y)g(y)\mathrm{d}y\right)\varphi_2(x),$$

where C_1 and C_2 are arbitrary constants and W is the constant Wronskian $W = W(x) = \varphi_1(x)\varphi_2'(x) - \varphi_1'(x)\varphi_2(x)$. Therefore, there is a unique bounded solution $k(x)$, which corresponds to $C_1 = C_2 = 0$.

Hence, for each $g \in C_b^0(\mathbb{R})$ there exists a unique $k \in C_b^2(\mathbb{R})$ such that $(\lambda I - M)k = g$. By the open mapping theorem, the operator $\lambda I - M$ has a bounded inverse $(\lambda I - M)^{-1} : C_b^0(\mathbb{R}) \to C_b^2(\mathbb{R}) \hookrightarrow C_b^0(\mathbb{R})$. In particular,

$$\text{if } \lambda \in \mathbb{C} \setminus (-\infty, -S] \text{ is not an eigenvalue of } M, \text{ then } \lambda \text{ is in the resolvent set of } M.$$

3. The eigenvalues in $\mathbb{C} \setminus (-\infty, -S]$ **of** M: if $\lambda \in \mathbb{C} \setminus (-\infty, -S]$ is an eigenvalue of M then, from (2.6.23), the eigenvector must be proportional to both φ_1 and ψ_1, hence φ_1 and ψ_1 are not linearly independent. Hence the Wronskian $\varphi_1\psi_1' - \varphi_1'\psi_1$ must vanish. Since the Wronskian is analytic in λ (see [349, Lemma 5.2]) and not identically zero, the eigenvalues of M in $\mathbb{C} \setminus (-\infty, -S]$ are isolated.

Let $\lambda \in \mathbb{C} \setminus (-\infty, -S]$ be an eigenvalue of M. Then the associated eigenvector φ is a solution to (2.6.18) and the former analysis applies. In particular, φ and φ' converge exponentially fast to 0 near $\pm\infty$ (at rate $\mp\gamma_+$, $\mathrm{Re}\,\gamma_+ > 0$) and therefore $\varphi \in H^1(\mathbb{R})$. Since M is symmetric on $H^1(\mathbb{R})$, we have in fact $\lambda \in \mathbb{R}$. Reproducing the argument of [349, Theorem 5.5], we see that there are no positive eigenvalues of M.

We conclude from the above analysis that the eigenvalues of M in $\mathbb{C} \setminus (-\infty, -S]$ form a sequence $(\lambda_n)_{n\in\mathbb{N}}$ (with $\lambda_0 = 0$) of isolated values in $(-S, 0]$. As a result the spectrum of M satisfies

$$\sigma(L, C_b^0(\mathbb{R})) = \sigma(M, C_b^0(\mathbb{R})) \subset (-\infty, -S] \cup \{\lambda_n, n \ge 0\}.$$

This shows that the assumption (i) of [349, Lemma 3.4] holds in our case and concludes the proof of Proposition 2.6.3. □

2.6.4 Traveling together ($0 < \varepsilon \ll 1$)

In this section 2.6.4, we construct a traveling front connecting 1 to 0 in (2.6.11), when $0 < \varepsilon \ll 1$, through a perturbation argument from the case $\varepsilon = 0$ studied above.

We are here looking after a nonnegative profile $u : \mathbb{R} \to \mathbb{R}$ and a speed $c \in \mathbb{R}$ solving

$$\begin{cases} u'' + cu' + Sf(u) + \varepsilon g(u) + \frac{2}{r}(S(2u-1) + \varepsilon)(u')^2 = 0 \quad \text{on } \mathbb{R}, \\ u(-\infty) = 1, \quad u(+\infty) = 0. \end{cases} \tag{2.6.25}$$

Observe that, from the strong maximum principle we have $u > 0$. Also, as in the proof of Lemma 2.6.1, we have $u < 1$. Hence, we *a priori* know $0 < u < 1$.

We use a perturbation technique and look for u in the form

$$u = u_0 + h,$$

where u_0 is provided by Proposition 2.6.2 and with, typically, $h(\pm\infty) = h'(\pm\infty) = 0$. Plugging this ansatz into the equation, we see that we need $\mathcal{F}(\varepsilon, c, h) = 0$, where

$$\mathcal{F} : \mathbb{R} \times \mathbb{R} \times E \to \widetilde{E}$$

is defined by

$$\begin{aligned}\mathcal{F}(\varepsilon, c, h) := h'' + cu_0' + ch' + S(f(u_0 + h) - f(u_0)) + \varepsilon g(u_0 + h) \\ + \frac{2}{r}\left(S(2u_0 + 2h - 1) + \varepsilon\right)(u_0' + h')^2 - \frac{2}{r}S(2u_0 - 1)(u_0')^2. \end{aligned} \tag{2.6.26}$$

As for the function spaces, we choose the weighted Hölder spaces

$$E := C^{2,\alpha}_\mu(\mathbb{R}), \quad \widetilde{E} := C^{0,\alpha}_\mu(\mathbb{R}), \quad 0 < \alpha < 1, \tag{2.6.27}$$

where, for $k \in \mathbb{N}$,

$$C^{k,\alpha}_\mu(\mathbb{R}) := \left\{ f \in C^k(\mathbb{R}) : \|f\|_{C^{k,\alpha}_\mu(\mathbb{R})} < +\infty \right\}, \quad \|f\|_{C^{k,\alpha}_\mu(\mathbb{R})} := \left\| x \mapsto e^{\mu\sqrt{1+x^2}} f(x) \right\|_{C^{k,\alpha}(\mathbb{R})},$$

for well-chosen $\mu \geq 0$. Here, $C^{k,\alpha}(\mathbb{R})$ denotes the Hölder space consisting of functions of the class C^k, which are continuous and bounded on the real axis $\mathbb{R}$ together with their derivatives of order k, and such that the derivatives of order k satisfy the Hölder condition with the exponent $0 < \alpha < 1$. The norm in this space is the usual Hölder norm.

Our main result in this section 2.6.4 then reads as follows.

Theorem 2.6.4 (Traveling waves for $0 < \varepsilon \ll 1$)**.** *Let $0 \leq \mu < \sqrt{S}$ be given. Let $\mathcal{F} : \mathbb{R} \times \mathbb{R} \times C^{2,\alpha}_\mu(\mathbb{R}) \to C^{0,\alpha}_\mu(\mathbb{R})$ be defined as in* (2.6.26)*.*

Then there is $\varepsilon_0 > 0$ such that, for any $0 \leq \varepsilon \leq \varepsilon_0$, there exists $(c_\varepsilon, h_\varepsilon) \in \mathbb{R} \times E$ such that $\mathcal{F}(\varepsilon, c_\varepsilon, h_\varepsilon) = 0$. Moreover the map $\varepsilon \mapsto (c_\varepsilon, h_\varepsilon)$ is continuous, the speed c_ε satisfies

$$c_\varepsilon = \frac{-\displaystyle\int_{\mathbb{R}} \left(g(u_0) + \frac{2}{r}(u_0')^2 \right) u_0' e^{\frac{4S}{r}(u_0^2 - u_0)}}{\displaystyle\int_{\mathbb{R}} (u_0')^2 e^{\frac{4S}{r}(u_0^2 - u_0)}} \varepsilon + o(\varepsilon), \qquad \text{as } \varepsilon \to 0, \tag{2.6.28}$$

whereas the perturbation profile h_ε satisfies

$$\int_{\mathbb{R}} h_\varepsilon u_0' = 0, \qquad \text{for all } 0 \leq \varepsilon \leq \varepsilon_0. \tag{2.6.29}$$

In what follows we aim at applying the Implicit Function Theorem 2.6.10 to the operator $\mathcal{F}$ defined in (2.6.26), see [14] for a related argument. We straightforwardly compute the derivatives with respect to c and h at the origin $(0, 0, 0)$:

$$\partial_c \mathcal{F}(0, 0, 0)(c) = cu_0',$$

and

$$Lh := \partial_h \mathcal{F}(0, 0, 0)(h) = h'' + \frac{4S}{r} u_0'(2u_0 - 1)h' + S\left(f'(u_0) + \frac{4}{r}(u_0')^2 \right) h. \tag{2.6.30}$$

We need to show that $\partial_{c,h}\mathcal{F}(0, 0, 0)$ given by

$$(c, h) \mapsto Lh + cu_0'$$

is bijective from and to a well-chosen pair of function spaces. Our strategy is as follows. In section 2.6.4.1, thanks to some results of [386], [384] (recalled in Appendix), we show that L is a Fredholm operator and compute its index (which depends on the choice of μ). Next, in section 2.6.4.2, we determine the kernel of L. In particular u_0' is the only bounded solution. We also determine the kernel of L^* thanks to an algebraic symmetric formulation in a well-chosen weighted L^2 space, from which we deduce the surjectivity of $\partial_{c,h}\mathcal{F}(0, 0, 0)$. Then we conclude the proof of Theorem 2.6.4 in section 2.6.4.3.

2.6.4.1 Fredholm property

Lemma 2.6.5 (Fredholm property)**.** *The operator $L : C^{2,\alpha}_\mu(\mathbb{R}) \to C^\alpha_\mu(\mathbb{R})$, defined in* (2.6.30)*, is Fredholm if $\mu \neq \sqrt{S}$ and we have*

$$\text{ind } L = \begin{cases} 0 & \text{if } 0 \leq \mu < \sqrt{S}, \\ -2 & \text{if } \mu > \sqrt{S}. \end{cases}$$

Proof. In view of Remark 2.6.13 it suffices to study the limiting operators $(L^\mu)^\pm$ associated with L^μ defined as in (2.6.41), namely

$$(L^\mu)^\pm h = h'' \mp 2\mu h' + (\mu^2 - S)h,$$

thanks to Theorem 2.6.12. First since $-\xi^2 \mp 2\mu i\xi + \mu^2 - S = 0$, corresponding to (2.6.39), has no real solution, L is Fredholm. Next, the associated characteristic equation, corresponding to (2.6.40), writes

$$X^2 \pm 2\mu X + (\mu^2 - S) = 0,$$

and has the following roots:

$$X^+_{1,2} = -\mu \pm \sqrt{S},$$
$$X^-_{1,2} = +\mu \pm \sqrt{S}.$$

If $0 \leq \mu < \sqrt{S}$ we deduce that $\kappa^+ = 1$ and $\kappa^- = 1$ (in the notations of Theorem 2.6.12), hence ind $L = 0$; if $\sqrt{S} < \mu$ we have $\kappa^+ = 0$ and $\kappa^- = 2$, hence ind $L = -2$. This completes the proof of Lemma 2.6.5. □

2.6.4.2 Kernels of L, L^* and surjectivity of $\partial_{c,h}\mathcal{F}(0,0,0)$

Lemma 2.6.6 (The kernel of L)**.** *Two linearly independent solutions to the linear homogeneous ordinary differential equation*

$$Lh := h'' + \frac{4S}{r}u_0'(2u_0 - 1)h' + S\left(f'(u_0) + \frac{4}{r}(u_0')^2\right)h = 0 \tag{2.6.31}$$

are given by

$$u_0' \quad \text{and} \quad v_0 : x \mapsto u_0'(x)\int_0^x \frac{1}{(u_0')^2(z)} e^{-\frac{4S}{r}\left(u_0^2(z) - u_0(z)\right)} \mathrm{d}z.$$

Among the two, u_0' is the only bounded solution.

As a result, for $0 \leq \mu < \sqrt{S}$, the kernel of the operator L acting on the space $C^{2,\alpha}_\mu(\mathbb{R})$ into $C^{0,\alpha}_\mu(\mathbb{R})$ is given by

$$\ker L = \text{span } u_0'.$$

Proof. We investigate the solutions h to (2.6.31). This is a second-order linear homogeneous ordinary differential equation, and we already know a solution u_0' (as seen by differentiating (2.6.12)). In this case a second solution v_0 can be sought in the form $v_0(x) = z(x)u_0'(x)$. Indeed plugging this ansatz into (2.6.31) yields the following first order linear ordinary differential equation for z':

$$z'' + \left(2\frac{u_0''}{u_0'} + \frac{4S}{r}(2u_0 - 1)u_0'\right)z' = 0,$$

or, equivalently,

$$z'' + \left(\ln((u_0')^2) + \frac{4S}{r}(u_0^2 - u_0)\right)' z' = 0.$$

As a result, we can select the solution

$$z'(x) = \frac{1}{(u_0')^2(x)} e^{-\frac{4S}{r}\left(u_0^2(x) - u_0(x)\right)},$$

which we integrate to reach $z(x)$, and thus

$$v_0(x) = u_0'(x)\int_0^x \frac{1}{(u_0')^2(z)} e^{-\frac{4S}{r}\left(u_0^2(z) - u_0(z)\right)} \mathrm{d}z. \tag{2.6.32}$$

Now, from the analysis in Section 2.6.3, we know that, for some $C > 0$,

$$u_0'(z) \sim Ce^{-\sqrt{S}z}, \quad \text{as } z \to +\infty. \tag{2.6.33}$$

Since $u_0(+\infty) = 0$, the integrand in (2.6.32) is equivalent to $\frac{1}{C^2}e^{2\sqrt{S}z}$ as $z \to +\infty$, and thus

$$v_0(x) \sim \frac{1}{C2\sqrt{S}}e^{\sqrt{S}x}, \quad \text{as } x \to +\infty. \tag{2.6.34}$$

Thus v_0 is unbounded and, in particular, $v_0 \notin C^{2,\alpha}_\mu(\mathbb{R})$. Since solutions to (2.6.31) are the linear combinations of $u_0' \in C^{2,\alpha}_\mu(\mathbb{R})$ when $0 \le \mu < \sqrt{S}$, $v_0 \notin C^{2,\alpha}_\mu(\mathbb{R})$, and since $L : C^{2,\alpha}_\mu(\mathbb{R}) \to C^\alpha_\mu(\mathbb{R})$, we conclude that $\ker L = \text{span } u_0'$ when $0 \le \mu < \sqrt{S}$. □

Lemma 2.6.7 (The kernel of L^*)**.** *If $0 \le \mu < \sqrt{S}$ then the kernel of the adjoint operator L^* is*

$$\ker L^* = \text{span } \left(u_0' e^{\frac{4S}{r}(u_0^2 - u_0)}\right).$$

On the other hand, if $\mu > \sqrt{S}$ then

$$\ker L^* = \text{span } \left(u_0' e^{\frac{4S}{r}(u_0^2 - u_0)}, v_0 e^{\frac{4S}{r}(u_0^2 - u_0)}\right),$$

where $v_0(x) := u_0'(x) \displaystyle\int_0^x \frac{1}{(u_0')^2(z)} e^{-\frac{4S}{r}\left(u_0^2(z) - u_0(z)\right)} \mathrm{d}z$ is as in Lemma 2.6.6.

Proof. Our starting point is to notice that the coefficient of the first-order term in the definition of L, that is $u_0'(2u_0 - 1)$, is the derivative of $u_0^2 - u_0$ so that

$$Lh = h'' + \frac{4S}{r}(u_0^2 - u_0)'h' + S\left(f'(u_0) + \frac{4}{r}(u_0')^2\right)h,$$

from which we deduce the formulation

$$Lh = \left(h' e^{\frac{4S}{r}(u_0^2 - u_0)}\right)' e^{-\frac{4S}{r}(u_0^2 - u_0)} + S\left(f'(u_0) + \frac{4}{r}(u_0')^2\right)h,$$

which is symmetric in the adequate weighted L^2 space:

$$\begin{aligned}\int_{\mathbb{R}} k(Lh) e^{\frac{4S}{r}(u_0^2 - u_0)} &= -\int_{\mathbb{R}} k'h' e^{\frac{4S}{r}(u_0^2 - u_0)} + \int_{\mathbb{R}} S\left(f'(u_0) + \frac{4}{r}(u_0')^2\right) hk e^{\frac{4S}{r}(u_0^2 - u_0)} \\ &= \int_{\mathbb{R}} (Lk) h e^{\frac{4s}{r}(u_0^2 - u_0)}.\end{aligned}$$

In particular, for any $k \in C^{2,\alpha}_\mu(\mathbb{R})$, we have

$$\begin{aligned}\int_{\mathbb{R}} k(Lh) &= \int_{\mathbb{R}} k\left(h' e^{\frac{4S}{r}(u_0^2 - u_0)}\right)' e^{-\frac{4S}{r}(u_0^2 - u_0)} + S\left(f'(u_0) + \frac{4}{r}(u_0')^2\right) hk \\ &= \int_{\mathbb{R}} -\left(k e^{-\frac{4S}{r}(u_0^2 - u_0)}\right)' h' e^{\frac{4S}{r}(u_0^2 - u_0)} \\ &\qquad + \int_{\mathbb{R}} S\left(f'(u_0) + \frac{4}{r}(u_0')^2\right) h \left(k e^{-\frac{4S}{r}(u_0^2 - u_0)}\right) e^{\frac{4S}{r}(u_0^2 - u_0)} \\ &= \int_{\mathbb{R}} h\left(L(k e^{-\frac{4S}{r}(u_0^2 - u_0)})\right) e^{\frac{4S}{r}(u_0^2 - u_0)}.\end{aligned}$$

Therefore, if $v e^{-\frac{4S}{r}(u_0^2 - u_0)} = k \in \ker L$, then we have

$$\begin{aligned}\int_{\mathbb{R}} (L^* v) h &= \int_{\mathbb{R}} v(Lh) \\ &= \int_{\mathbb{R}} h\left(L(v e^{-\frac{4S}{r}(u_0^2 - u_0)})\right) e^{\frac{4S}{r}(u_0^2 - u_0)} = 0,\end{aligned}$$

provided each integral is finite. In particular, since $C^{2,\alpha}_\mu(\mathbb{R})$ is dense in $C^{0,\alpha}_\mu(\mathbb{R})$, this shows that

$$\text{span } \left(u_0' e^{\frac{4S}{r}(u_0^2-u_0)}\right) \subset \ker L^*.$$

Assume $0 \leq \mu < \sqrt{S}$. Then we deduce from Lemma 2.6.5 and Lemma 2.6.6 that $\dim\ker L^* = -\text{ ind } L + \dim\ker L = 0+1 = 1$, and therefore we do have $\ker L^* = \text{span } \left(u_0' e^{\frac{4S}{r}(u_0^2-u_0)}\right)$.

Assume $\mu > \sqrt{S}$. This time, the asymptotics for v_0 being given in (2.6.34), terms $\int_{\mathbb{R}} v_0 h e^{\frac{4S}{r}(u_0^2-u_0)}$ are finite as soon as $h \in C^{0,\alpha}_\mu(\mathbb{R})$, and therefore

$$\text{span } \left(v_0 e^{\frac{4S}{r}(u_0^2-u_0)}\right) \subset \ker L^*,$$

by a density argument. Then we deduce from Lemma 2.6.5 and Lemma 2.6.6 that $\dim\ker L^* = -\text{ ind } L + \dim\ker L = -(-2)+0 = 2$. Since $u_0' e^{\frac{4S}{r}(u_0^2-u_0)}$ and $v_0 e^{\frac{4S}{r}(u_0^2-u_0)}$ are linearly independent, we do have $\ker L^* = \text{span } \left(u_0' e^{\frac{4S}{r}(u_0^2-u_0)}, v_0 e^{\frac{4S}{r}(u_0^2-u_0)}\right)$. □

Lemma 2.6.8 (Surjectivity of $\partial_{c,h}\mathcal{F}(0,0,0)$)**.** *Let $0 \leq \mu < \sqrt{S}$ be given. Then, the application*

$$\begin{array}{rccc} \partial_{c,h}\mathcal{F}(0,0,0): & \mathbb{R}\times C^{2,\alpha}_\mu(\mathbb{R}) & \to & C^{0,\alpha}_\mu(\mathbb{R}) \\ & (c,h) & \mapsto & Lh + cu_0' \end{array}$$

is surjective.

Proof. We check that u_0' is not in the range of L. Since L has closed range we have $\text{Rg } L = (\ker L^*)^\perp$, and thus $\text{Rg } L = \left(\text{span } \left(u_0' e^{\frac{4S}{4}(u_0^2-u_0)}\right)\right)^\perp$ from Lemma 2.6.7. But

$$\left\langle u_0' e^{\frac{4S}{4}(u_0^2-u_0)}, u_0' \right\rangle_{(C^{0,\alpha}_\mu(\mathbb{R}))^*, C^{0,\alpha}_\mu(\mathbb{R})} = \int_{\mathbb{R}} (u_0')^2 e^{\frac{4S}{4}(u_0^2-u_0)} > 0$$

so that $u_0' \notin \text{Rg } L$. Since $\text{Rg } L$ has codimension 1 by Lemma 2.6.5 and 2.6.6, we have $C^{0,\alpha}_\mu(\mathbb{R}) = \text{Rg } L \oplus \text{span } u_0'$. This shows that $\partial_{c,h}\mathcal{F}(0,0,0)$ is surjective. □

Remark 2.6.9. We present here an alternate way to prove that $u_0' \notin \text{Rg } L$ remains true when $\mu \geq \sqrt{S}$. To do so, let us solve the second-order linear ordinary differential equation

$$w'' + \frac{4S}{r} u_0'(2u_0-1)w' + S\left(f'(u_0) + \frac{4}{r}(u_0')^2\right) w = u_0'. \tag{2.6.35}$$

Recall that the solutions of the associated homogeneous equation are spanned by u_0' and v_0 provided by Lemma 2.6.6. To find a particular solution to (2.6.35), we use the method of variation of constants. We see that $\varphi(x) := \lambda_1(x)u_0'(x) + \lambda_2(x)v_0(x)$ solves (2.6.35) as soon as

$$\begin{cases} u_0'\lambda_1' + v_0\lambda_2' &= 0 \\ u_0''\lambda_1' + v_0'\lambda_2' &= u_0', \end{cases}$$

which yields

$$\lambda_2' \frac{u_0'v_0' - u_0''v_0}{u_0'} = u_0', \quad \lambda_1' = -\frac{v_0}{u_0'}\lambda_2'.$$

Since $u_0'v_0' - u_0''v_0$ is nothing else than the Wronskian, it is equal to $\theta^{-1}e^{-\frac{4S}{r}(u_0^2-u_0)}$ for some $\theta \neq 0$, and thus

$$\begin{cases} \lambda_2'(x) = \theta(u_0')^2(x) e^{\frac{4S}{r}(u_0^2(x)-u_0(x))} \sim \theta C^2 e^{-2\sqrt{S}x} \\ \lambda_1'(x) = -\theta v_0(x)u_0'(x) e^{\frac{4S}{r}(u_0^2(x)-u_0(x))} \sim -\frac{\theta}{2\sqrt{S}}, \end{cases}$$

where the equivalents are taken as $x \to +\infty$ and where we have used (2.6.33) and (2.6.34). Hence, we can select

$$\begin{cases} \lambda_2(x) = -\int_x^{+\infty} \theta(u_0')^2(z) e^{\frac{4S}{r}(u_0^2(z)-u_0(z))} \mathrm{d}z \sim \frac{\theta C^2}{2\sqrt{S}} e^{-2\sqrt{S}x} \\ \lambda_1(x) = -\int_0^x \theta v_0(z)u_0'(z) e^{\frac{4S}{r}(u_0^2(z)-u_0(z))} \mathrm{d}z \sim -\frac{\theta}{2\sqrt{S}} x. \end{cases}$$

Hence the solutions to (2.6.35) are

$$w(x) = (C_1 + \lambda_1(x))u_0'(x) + (C_2 + \lambda_2(x))v_0(x)$$

for any $C_1 \in \mathbb{R}$, $C_2 \in \mathbb{R}$. If $C_2 \neq 0$ then, from all the above asymptotic, w is unbounded. If $C_2 = 0$ then, from all the above asymptotics,

$$w(x) \sim -\frac{\theta C}{2\sqrt{S}} x e^{-\sqrt{S}x}, \quad \text{as } x \to +\infty.$$

This shows that $w \notin C^{2,\alpha}_\mu(\mathbb{R})$ when $\mu \geq \sqrt{S}$, and thus $u_0' \notin \text{Rg } L$.

2.6.4.3 Construction of traveling waves

We are now in the position to complete the proof of Theorem 2.6.4, that is the construction of traveling waves for (2.6.25) when $0 < \varepsilon \ll 1$.

Proof of Theorem 2.6.4. Assume $0 \leq \mu < \sqrt{S}$. Let us recall that $\mathcal{F} : \mathbb{R} \times \mathbb{R} \times C^{2,\alpha}_\mu(\mathbb{R}) \to C^{0,\alpha}_\mu(\mathbb{R})$ is given by (2.6.26). It is of the class C^1 and the Fréchet derivatives are

$$\begin{aligned} \partial_\varepsilon \mathcal{F}(0,0,0) &= g(u_0) + \frac{2}{r}(u_0')^2, \\ \partial_c \mathcal{F}(0,0,0) &= u_0', \\ L = \partial_h \mathcal{F}(0,0,0) &: h \mapsto Lh = h'' + \frac{4S}{r} u_0'(2u_0 - 1)h' + S\left(f'(u_0) + \frac{4}{r}(u_0')^2\right) h. \end{aligned}$$

We have shown, in Lemma 2.6.5, that L is a Fredholm operator with indice 0 and, in Lemma 2.6.6, that the kernel of L is span u_0' in the considered weighted Hölder space.

Our concern is the derivative $\partial_{c,h}\mathcal{F}(0,0,0) : (c,h) \mapsto Lh + cu_0'$. It has been shown in Lemma 2.6.8 that it is surjective. It is not difficult to show that

$$\ker \partial_{c,h}\mathcal{F}(0,0,0) = \{0\} \times \text{span } u_0',$$

and that the restriction of $\partial_{c,h}\mathcal{F}(0,0,0)$ to $\mathbb{R} \times N$, where

$$N := \left\{ f \in C^{2,\alpha}_\mu(\mathbb{R}) : \int_{\mathbb{R}} f u_0' = 0 \right\}$$

is a topological complement of $\ker L$, is injective and still surjective. Therefore we can apply the Implicit Function Theorem 2.6.10 to the restriction of $\mathcal{F}$ to $\mathbb{R} \times \mathbb{R} \times N$. We deduce the existence of a branch $(c_\varepsilon, h_\varepsilon)$, $0 \leq \varepsilon \ll 1$, of solutions with $\varepsilon \mapsto (c_\varepsilon, h_\varepsilon)$ continuous and h_ε satisfying (2.6.29).

It remains to prove (2.6.28). Since $\mathcal{F}$ is C^1 in all its variables we deduce from $\mathcal{F}(\varepsilon, c_\varepsilon, h_\varepsilon) = 0$ and the chain rule that

$$\partial_\varepsilon \mathcal{F}(\varepsilon, c_\varepsilon, h_\varepsilon) + \frac{dc_\varepsilon}{d\varepsilon} \partial_c \mathcal{F}(\varepsilon, c_\varepsilon, h_\varepsilon) + \partial_h \mathcal{F}(\varepsilon, c_\varepsilon, h_\varepsilon)\left(\frac{dh_\varepsilon}{d\varepsilon}\right) = 0,$$

which we evaluate at $\varepsilon = 0$ to get

$$g(u_0) + \frac{2}{r}(u_0')^2 + \left.\frac{dc_\varepsilon}{d\varepsilon}\right|_{\varepsilon=0} u_0' + L\left(\left.\frac{dh_\varepsilon}{d\varepsilon}\right|_{\varepsilon=0}\right) = 0.$$

Since $\text{Rg } L = (\ker L^*)^\perp = \left(\text{span } \left(u_0' e^{\frac{4S}{r}(u_0^2 - u_0)}\right)\right)^\perp$, multiplying the above by $u_0' e^{\frac{4S}{r}(u_0^2-u_0)}$ and integrating over $\mathbb{R}$, we reach

$$\left.\frac{dc_\varepsilon}{d\varepsilon}\right|_{\varepsilon=0} = \frac{-\displaystyle\int_{\mathbb{R}} \left(g(u_0) + \frac{2}{r}(u_0')^2\right) u_0' e^{\frac{4S}{r}(u_0^2-u_0)}}{\displaystyle\int_{\mathbb{R}} (u_0')^2 e^{\frac{4S}{r}(u_0^2-u_0)}} > 0,$$

which yields (2.6.28) and concludes the proof of Theorem 2.6.4. □

2.6.5 The speed of the traveling stacked clines

In this section 2.6.5, we obtain an explicit form for $c_1 = c_1(r, S)$ appearing in the asymptotic formula for the speed $c_\varepsilon = c_1\varepsilon + o(\varepsilon)$ as given in (2.6.28). This in turn provides valuable insights on the model for coupled underdominant clines.

For convenience let us temporarily denote $u = u_0$ the standing wave solution constructed in Proposition 2.6.2. From (2.6.12), we see that $v := u'^2$ solves the linear first order ODE

$$v' + \frac{4S}{r}(u^2 - u)'v = -2Su'(2u-1)u(1-u),$$

which is solved as

$$u'^2(x) = e^{-\frac{4S}{r}(u^2-u)(x)}\left(C - 2S\int_0^x (u^2-u)'(t)e^{\frac{4S}{r}(u^2-u)(t)}(u-u^2)(t)dt\right),$$

for some constant C. We integrate by parts and, up to changing the value of the constant C, reach

$$\begin{aligned} u'^2(x) &= e^{-\frac{4S}{r}(u^2-u)(x)}\left(C - \frac{r}{2}\left(e^{\frac{4S}{r}(u^2-u)(x)}(u-u^2)(x) + \int_0^x e^{\frac{4S}{r}(u^2-u)(t)}(u^2-u)'(t)dt\right)\right) \\ &= e^{-\frac{4S}{r}(u^2-u)(x)}\left(C - \frac{r}{2}\left(e^{\frac{4S}{r}(u^2-u)(x)}(u-u^2)(x) + \frac{r}{4S}e^{\frac{4S}{r}(u^2-u)(x)}\right)\right). \end{aligned}$$

Letting for instance $x \to +\infty$ enforces $C = \frac{r^2}{8S}$ and, returning to the notation u_0, we finally obtain

$$u_0'^2(x) = \frac{r^2}{8S}e^{\frac{4S}{r}(u_0-u_0^2)(x)} - \frac{r}{2}(u_0-u_0^2)(x) - \frac{r^2}{8S}. \tag{2.6.36}$$

The fact that u_0' can be expressed in terms of u_0, already observed in [36], enables to obtain an explicit form $c_1 = c_1(r, S)$ appearing in $c_\varepsilon = c_1\varepsilon + o(\varepsilon)$ as given in (2.6.28). Indeed, using (2.6.36) and recalling that $u_0' < 0$, we obtain

$$c_1 = \frac{-\int_{\mathbb{R}} \frac{r}{4S}u_0'(x)\left(1 - e^{-\frac{4S}{r}(u_0-u_0^2)(x)}\right)dx}{-\int_{\mathbb{R}} u_0'(x)\left(\frac{r^2}{8S}e^{\frac{4S}{r}(u_0-u_0^2)(x)} - \frac{r}{2}(u_0-u_0^2)(x) - \frac{r^2}{8S}\right)^{\frac{1}{2}} e^{-\frac{4S}{r}(u_0-u_0^2)(x)}dx}.$$

Performing the change of variable $u = u_0(x)$ this is recast

$$c_1 = \frac{\int_0^1 \frac{r}{4S}\left(1 - e^{-\frac{4S}{r}(u-u^2)}\right)du}{\int_0^1 \left(\frac{r^2}{8S}e^{\frac{4S}{r}(u-u^2)} - \frac{r}{2}(u-u^2) - \frac{r^2}{8S}\right)^{\frac{1}{2}} e^{-\frac{4S}{r}(u-u^2)}du}.$$

Expanding with respect to $\frac{S}{r} \ll 1$, we reach, after a straightforward computation,

$$c_1 = \frac{1}{\sqrt{S}}\left(1 + \frac{4}{15}\frac{S}{r} + \frac{2}{45}\frac{S^2}{r^2} + \cdots\right). \tag{2.6.37}$$

In the sequel we denote

$$c_1^* := \frac{1}{\sqrt{S}}\left(1 + \frac{4}{15}\frac{S}{r}\right), \tag{2.6.38}$$

the first order term of expansion (2.6.37).

To verify the accuracy of our previsions, we ran simulations of the full system (2.6.7), the one established before simplification thanks to the quasi-linkage equilibrium approximation. We numerically estimate the instantaneous speed by following the movement of the center of the fronts. The comparison with the theoretical speed $\varepsilon c_1^* = sc_1^*$ (let us recall that s appearing in the original model is nothing else than ε, see (2.6.9)) is shown in Figure 2.6.3. Let us recall that, to go from the full system (2.6.7) to the equation (2.6.11) under consideration, we used successive approximations, the first one being that "recombination r

is sufficiently large relative to the strength of selection against heterozygotes". Indeed, as seen in Figure 2.6.3, the numerics and the theory we developed do not match when r is too small. On the other hand, we observe that formula (2.6.38) gives a very good approximation of the instantaneous speed when r is not too small. This validates *a posteriori* the quasi-linkage equilibrium approximation.

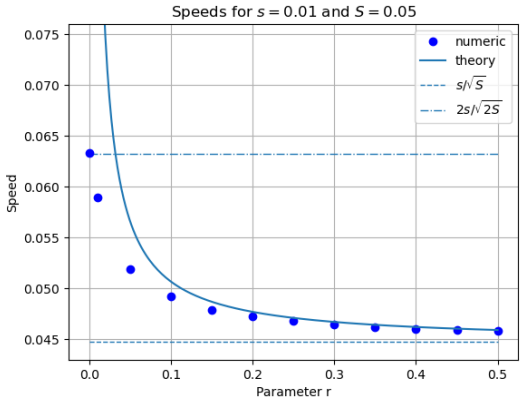

Figure 2.6.3: Comparison of the theoretical speed sc_1^* and of the numerically estimated speed of the stacked fronts.

When $r = 0.5$ (free recombination), the linkage disequilibrium stays small and the coupled clines move at a speed which is close to the one each cline would have if travelling alone, that is $s/\sqrt{S}$ (or $s\sigma/\sqrt{2S}$ in the original spatial scale, as obtained by Barton [35] in a single-locus model). Indeed, without interaction, we are left with $u_t = u_{xx} + Sf(u) + sg(u)$, which is nothing else than the bistable equation ($0 < \frac{s}{S} < 1$)

$$u_t = u_{xx} + Su(1-u)\left(2u - 1 + \frac{s}{S}\right),$$

whose traveling wave, explicitly computed as $\frac{1}{2} - \frac{1}{2}\tanh\left(\frac{\sqrt{S}}{2}(x - \frac{s}{\sqrt{S}}t)\right)$, has speed $s/\sqrt{S}$.

At the other extreme, when $r = 0$ (no recombination) the system becomes equivalent to a single locus where one allele has a fitness advantage $2s$ and with a cost for heterozygotes $2S$, leading to a bistable wave speed of $2s/\sqrt{2S}$.

When $r \in (0, 0.5)$, the speed of the coupled clines decreases monotonously as recombination r increases.

Our concluding remark is as follows: whatever the values of the parameters, interacting and eventually stacked clines travel faster than one cline alone.

2.6.6 Conclusion and perspectives

In this section 2.6 we have investigated the solutions of equation (2.6.11), describing the dynamics of two coupled, asymmetric genetic incompatibilities (underdominant loci) with identical fitness effects, in a population whose density is supposed uniform and large, in a quasi-linkage equilibrium regime. Assuming multiplicative fitness effects among loci and recalling that ε measures the difference in fitness between homozygotes, the two main results are as follows: first, we have shown that when $\varepsilon = 0$, there is a unique standing wave u_0 under a normalization condition; then, in Section 2.6.4, we have shown that when $\varepsilon > 0$ is small enough, there exists a traveling wave u_ε defined as a perturbation of u_0, and we obtained a simple approximation for its speed.

Those results were obtained under a series of assumptions that we recall here for discussion:

$$s_A, s_B < S \tag{H1}$$

$$s_A, s_B, S \ll r \tag{H2}$$

$$S_A = S_B, \quad s_A = s_B \tag{H3}$$

$$p = q. \tag{H4}$$

Assumption (H1) is the frame of this work which was devoted to the heterozygote inferior case. It is therefore not a hypothesis we want to discuss *per se*.

Assumption (H2) expresses that we are in the case of small selective advantages. When it does not hold, D may not be small, in which case the quasi-linkage equilibrium approximation (that allowed us to reduce the number of variables) is no longer valid. It can easily be seen that $-\frac{1}{4} \leq D \leq \frac{1}{4}$ always holds, and that, as shown by the D equation in (2.6.7), positive D is generated whenever p and q travel in the same direction (that is $p_x q_x > 0$), while negative D is generated otherwise. These facts help to understand the kind of contribution D makes to the coupling between p and q in (2.6.7).

Assumption (H3) is basically a hypothesis of exchangeability between loci. Although this allowed us to simplify the algebra, different loci should have different fitness effects, and it would thus be of interest to relax this hypothesis.

Last but not least, assumption (H4) conveys the strong argument that the A cline and the B cline were stacked in the past and will remain stacked forever in the future. This is indeed a good starting point from a mathematical perspective. Nevertheless, in the context of population genetics, more interesting questions arise when (H4) does not hold. In such a situation, the coupling in (2.6.7) can give rise to non-standard behaviours, such as *adaptation of the speed*. The questions that arise are such as: can a traveling front be pinned by a standing front? Will a front traveling at a large speed crossing a slower traveling front adapt its speed so as to remain stacked with the slower one? A preliminary numerical exploration has confirmed that convergence to stacked fronts occurs in some situations but has also shown that there can be a vast zoology of situations. We hope to present them in a future work.

2.6.7 Some useful results and tools

We recall the *Implicit Function Theorem*, see [413, Theorem 4.B] for instance.

Theorem 2.6.10 (Implicit Function Theorem)**.** *Let X, Y and Z be three Banach spaces. Suppose that:*

(i) The mapping $\mathcal{F} : U \subset X \times Y \to Z$ is defined on an open neighbourhood U of $(x_0, y_0) \in X \times Y$ and $\mathcal{F}(x_0, y_0) = 0$.

(ii) The partial Fréchet derivative of $\mathcal{F}$ with respect to y exists on U and

$$\mathcal{F}_y(x_0, y_0) : Y \to Z \text{ is bijective.}$$

(iii) $\mathcal{F}$ and $\mathcal{F}_y$ are continuous at (x_0, y_0).

Then, the following properties hold:

(a) Existence and uniqueness. There exist $r_0 > 0$ and $r > 0$ such that, for every $x \in X$ satisfying $\|x - x_0\| \leq r_0$, there exists a unique $y(x) \in Y$ such that $\|y - y_0\| \leq r$ and $\mathcal{F}(x, y(x)) = 0$.

(b) Continuity. If $\mathcal{F}$ is continuous in a neighbourhood of (x_0, y_0), then the mapping $x \mapsto y(x)$ is continuous in a neighbourhood of x_0.

(c) Higher regularity. If $\mathcal{F}$ is of the class C^m, $1 \leq m \leq \infty$, on a neighbourhood of (x_0, y_0), then $x \mapsto y(x)$ is also of the class C^m in a neighbourhood of x_0.

In Section 2.6.4 we apply Theorem 2.6.10 to the operator $\mathcal{F}$ defined in (2.6.26), with $X = \mathbb{R}$, $x = \varepsilon$, $x_0 = 0$, $Y = \mathbb{R} \times C^{2,\alpha}_\mu(\mathbb{R})$, $y = (c, h)$, $y_0 = (0, 0)$, and $Z = C^{0,\alpha}_\mu(\mathbb{R})$.

Next, we quote some results on Fredholm operators. Let us recall that the operator L has the Fredholm property with index 0 if $\ker L$ has a finite dimension, Rg L is closed and has finite codimension and

$$\text{ind } L := \dim \ker L - \text{codim Rg} L = 0.$$

In particular, since its range is closed, such an operator is *normally solvable*:

$$\exists u \neq 0, Lu = f \quad \Leftrightarrow \quad \forall \phi \in (\text{Rg } L)^\perp, \phi(f) = 0,$$

and remark that $(\text{Rg } L)^\perp = \ker L^*$.

We recall below a theorem from Volpert, Volpert and Collet [386, Theorem 2.1 and Remark p787].

Theorem 2.6.11 (Fredholm property on the line)**.** *For $0 < \alpha < 1$, consider the operator $L : C^{2,\alpha}(\mathbb{R}) \to C^{\alpha}(\mathbb{R})$ defined by*

$$Lu := a(x)u'' + b(x)u' + c(x)u,$$

where the coefficients $a(x)$, $b(x)$, $c(x)$ are smooth, and $a(x) \geq a_0$ for some $a_0 > 0$. Assume further that the coefficients $a(x)$, $b(x)$, and $c(x)$ have finite limits as $x \to \pm\infty$ and denote

$$a^{\pm} := \lim_{x\to\pm\infty} a(x), \qquad b^{\pm} := \lim_{x\to\pm\infty} b(x), \qquad c^{\pm} := \lim_{x\to\pm\infty} c(x).$$

Finally, let us define the limiting operators

$$L^{\pm}u := a^{\pm}u'' + b^{\pm}u' + c^{\pm}u,$$

and assume that for any $\lambda \geq 0$, the equation

$$L^{\pm}u - \lambda u = 0$$

has no nontrivial solution in $C^{2,\alpha}(\mathbb{R})$.

Then L is Fredholm with index 0.

Let us also recall a Fredholm property result for second-order ordinary differential equations, see the monograph of Volpert [384, Chapter 9, Theorem 2.4 p. 366].

Theorem 2.6.12 (Fredholm property for second-order ODEs)**.** *With the notations of Theorem 2.6.11, the operator L is Fredholm provided the two equations*

$$-a^{\pm}\xi^2 + b^{\pm}i\xi + c^{\pm} = 0 \tag{2.6.39}$$

has no real solution $\xi \in \mathbb{R}$. In this case the index of L is given by the formula

$$\text{ind } L = \kappa^{+} - \kappa^{-},$$

where $\kappa^{\pm}$ is the number of complex solutions to the characteristic equation

$$a^{\pm}X^2 - b^{\pm}X + c^{\pm} = 0 \tag{2.6.40}$$

which have a positive real part.

Remark 2.6.13 (Fredholm property in weighted Hölder spaces)**.** We cannot directly apply Theorem 2.6.11 and Theorem 2.6.12 to our situation since we consider the operator L acting from $C^{2,\alpha}_{\mu}(\mathbb{R})$ into $C^{\alpha}_{\mu}(\mathbb{R})$, and not from $C^{2,\alpha}(\mathbb{R})$ into $C^{0,\alpha}(\mathbb{R})$. To circumvent this, we consider the operator $L^{\mu} : C^{2,\alpha}(\mathbb{R}) \to C^{\alpha}(\mathbb{R})$ defined by:

$$\begin{aligned} L^{\mu}(u) &:= e^{\mu\sqrt{1+x^2}} L\left(ue^{-\mu\sqrt{1+x^2}}\right) \\ &= a(x)u'' + \left[\frac{-2\mu x}{\sqrt{1+x^2}}a(x) + b(x)\right]u' \\ &\quad + \left[\left(\frac{\mu^2 x^2}{1+x^2} + \frac{\mu x^2}{(1+x^2)^{\frac{3}{2}}} - \frac{\mu}{\sqrt{1+x^2}}\right)a(x) - \frac{\mu x}{\sqrt{1+x^2}}b(x) + c(x)\right]u. \end{aligned} \tag{2.6.41}$$

Since $T_{\mu} : u \in C^{2,\alpha}_{\mu}(\mathbb{R}) \mapsto e^{\mu\sqrt{1+x^2}}u \in C^{2,\alpha}(\mathbb{R})$ is continuously invertible, and $T_{\mu}^{-1} : u \in C^{0,\alpha}(\mathbb{R}) \mapsto e^{-\mu\sqrt{1+x^2}}u \in C^{0,\alpha}_{\mu}(\mathbb{R})$ is continuously invertible, the map $L = T_{\mu}^{-1}L^{\mu}T_{\mu}$ shares the same Fredholm property and index as L^{μ}. As a result, if L^{μ} satisfies the assumptions of Theorem 2.6.11, or Theorem 2.6.12, then L is a Fredholm operator with the same index as that of L^{μ}.

Chapter 3

A hyperbolic cell-cell repulsion model

3.1 A cell-cell repulsion model on a hyperbolic Keller-Segel equation

3.1.1 Introduction

In many recent biological experiments, the co-culture of multiple types of cells has been used to improve our understanding of cell-cell interactions. Typical examples of such co-culture experiment include the study of the interaction between cancer cells and normal cells, which plays a crucial role in tumor development, and comparative studies of the resistance of different types of cancer cells to a chemotherapeutic drugs. The goal of this work is to introduce a mathematical model taking into account the growth of the cell population and the physical motion of cells induced by the competition for space in a Petri dish, in order to better understand the spatial segregation between two types of cells and its potential impact on the outcome of co-culture experiments. Such a segregation phenomenon was observed by Pasquier et al. [319] in a study of protein transfer between two types of human breast cancer cell. Over a 7-day cell co-culture, a spatial competitive exclusion was observed between these two types of cells and a clear boundary was formed between them on day 7 (see Figure 3.1.1). A segregation property in cell co-culture was also studied recently by Taylor et al. [370], who compared their experimental results with an individual-based model. They found that heterotypic repulsion and homotypic cohesion can account for cell segregation and border formation. A similar segregation property is also found in the mosaic pattern between nections and cadherins in the experiments of Katsunuma et al. [229].

Early attempts to explain the segregation property by continuum equations date back to 1970s. Shigesada, Kawasaki and Teramoto [353] studied segregation with a nonlinear diffusion model and they found that the spatial segregation acts to stabilize the coexistence of two similar species by relaxing the interspecific competition. Lou and Ni [267] generalized the model of Shigesada *et al* and studied the steady state problem for the self/cross-diffusion model. For the nonlinear diffusion model, Bertsch et al. [61] proved the existence of segregated solutions when the reaction term is of Lotka-Volterra type. Other mechanisms such as nonlocal competition in the framework of the Lotka-Volterra model leading to the segregation are considered in [282, 283, 302]. Crooks et al. [124, 128] considered a competition-diffusion system where two populations spatially segregate as the interspecific competition becomes large. Conti, Terracini and Verzini [114] considered a reaction–diffusion system in which asymptotic segregation occurs (the steady states are segregated). One of the main points in the present model is that segregation is achieved directly and not in the asymptotic limit, contrary to [128, 124] and [114].

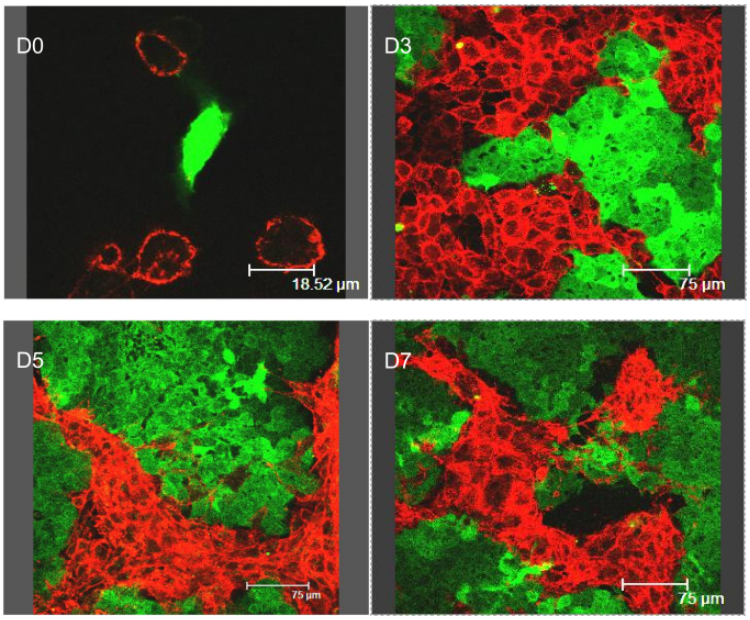

Figure 3.1.1: *Direct immunodetection of P-gp transfers in co-cultures of sensitive (MCF-7) and resistant (MCF-7/Doxo) variants of the human breast cancer cell line.*

Here instead of using nonlinear diffusion models, we focus on a (hyperbolic) Keller-Segel model. Such models have been used to describe the attraction and repulsion of cell populations when the motion of the cells is driven by the concentration gradient of a chemical substance, a phenomenon known as chemotaxis. Theoretical and mathematical modeling of chemotaxis can be traced back to the pioneering works of Patlak [320] in the 1950s and Keller and Segel [232] in the 1970s. It has become an important model in the description of tumor growth or embryonic development. We refer to the review papers of Horstmann [213] and Hillen and Painter [209] for a detailed introduction about the Keller–Segel model.

As explained in this work, our model can also be regarded as a nonlocal advection model. Recently, implementing nonlocal advection models for the study of cell-cell adhesion and repulsion has attracted a lot of attention. As pointed out by many biologists, cell-cell interactions do not only exist in a local scope, but long-range interactions should also be taken into account to guide the mathematical modeling. Armstrong, Painter and Sherratt [16] in their early work proposed a model (the APS model) in which cells undergo a local diffusion process and a nonlocal advection driven by the adhesion forces, in order to describe cell aggregation and sorting. Based on the APS model, Murakawa and Togashi [296] thought that the population pressure should come from the cell volume size instead of the linear diffusion, and changed the linear diffusion term into a nonlinear diffusion in order to capture the sharp fronts and the segregation in cell co-culture. Carrillo et al. [105] recently proposed a new assumption on the adhesion velocity field and their model showed a good agreement with the experiments in the work of Katsunuma et al. [229]. The idea of the long-range attraction and short-range repulsion can also be found in the work of Leverentz, Topaz and Bernoff [250]. They considered a nonlocal advection model to study the asymptotic behavior of swarms. By choosing a Morse-type kernel which encodes both attractive and repulsive interactions, they found that the solution can asymptotically spread, contract (blow-up), or reach a steady-state. Burger, Fetecau and Huang [83] considered a similar nonlocal adhesion model with nonlinear diffusion. They studied the well-posedness of the model and proved the existence of a compactly supported, non-constant steady state. Dyson et al. [156] established the local existence of a classical solution for a nonlocal cell-cell adhesion model in spaces of uniformly continuous functions. For the diffusive model with time delay effect, we refer to Shi et al. [351, 352] where the authors considered the spatial patterns due to bifurcations. For further Turing and Turing-Hopf bifurcations due to the nonlocal effect, we refer to Ducrot et al. [151] and Song et al. [365]. We also refer the readers to Mogliner et al. [288], Eftimie et al. [158], Ducrot and Magal [152], Fu and Magal [178] for more topics about nonlocal advection equations. The derivation of such models as been done in Bellomo et al. [44] and Morale, Capasso and Oelschläger [290].

In this work, we consider a two-dimensional bounded domain which represents a flat circular Petri

dish. We introduce the notion of solution integrated along the characteristics. Thanks to the appropriate boundary condition of the pressure equation (see Equation (3.1.2)), we deduce that the characteristics stay in the domain for any positive time. The positivity of solutions, the segregation property and a conservation law follow from the notion of solutions as well. By using numerical simulations, we investigate the impact of the seeding condition (as well as the law of initial distributions) on the proportion of each species in the final population. In the above-mentioned literature, the numerical simulations are restricted to a rectangular domain with periodic boundary conditions. It is worth mentioning that here the domain is circular and the pressure satisfies a no-flux boundary condition (see Appendix 3.1.5.4 for numerical scheme).

Section 3.1 is organized as follows. In Section 2, we present the model for the single-species case and we prove the local existence and uniqueness of solutions as well as the conservation law by considering the solution integrated along the characteristics. In Section 3, we apply our nonlocal advection model established in Section 2 to study the cell co-culture. The main goal in this work is to investigate the complexity of the short-term (6 days) co-cultured cell distribution depending on the initial distribution of each species. In Section 3.1, we investigate the competitive exclusion principle in our model and compare our spatial model to an ODE model which is homogeneous in space and has been previously studied by Zeeman [412]. In Section 3.2, we investigated the impact of the initial distribution on the proportion of each species in the final population. The spatial competition due to the dispersion coefficients and cell kinetics is considered in Section 3.3. Section 4 is devoted to discussion and conclusion. We also discuss the case of overlapping (non-segregated) initial conditions for the two species, and how numerical simulations suggest that asymptotic segregation occurs.

3.1.2 Mathematical modeling

3.1.2.1 Single species model

Let us consider the following model with one species

$$\begin{cases} \partial_t u(t,x) - d\,\mathrm{div}\,\big(u(t,x)\nabla P(t,x)\big) = u(t,x)h(u(t,x)) & \text{in } (0,T]\times\Omega, \\ u(0,x) = u_0(x) & \text{on } \overline{\Omega}, \end{cases} \tag{3.1.1}$$

where P satisfies the following elliptic equation

$$\begin{cases} \big(I-\chi\Delta\big)P(t,x) = u(t,x) & \text{in } (0,T]\times\Omega \\ \nabla P(t,x)\cdot\nu(x) = 0 & \text{on } [0,T]\times\partial\Omega, \end{cases} \tag{3.1.2}$$

We let $\Omega\subset\mathbb{R}^2$ be the unit open disk centered at $\mathbf{0}=(0,0)$ with radius $r=1$, i.e., $\Omega = B_{\mathbb{R}^2}(\mathbf{0},1)$. Here ν is the outward normal unit vector, d is the dispersion coefficient, χ is the sensing coefficient. The divergence, gradient and Laplacian are taken with respect to x. System (3.1.1)-(3.1.2) can be regarded as a hyperbolic Keller-Segel equation (with chemotactic repulsion) on a bounded domain.

Remark 3.1.1. Equation (3.1.2) can be derived from the following parabolic equation (which is the classical case in the Keller-Segel equation [213]) as ε goes to 0:

$$\varepsilon\partial_t P(t,x) = \chi\Delta P(t,x) + u(t,x) - P(t,x). \tag{3.1.3}$$

The process of letting $\varepsilon\to 0$ corresponds to the assumption that the dynamics of the chemorepellent is fast compared to the evolution of the cell density. In the case of chemoattractant a variant of such a model was considered by Perthame and Dalibard [323], Calvez and Dolak-Struß[95].

Remark 3.1.2. As we mentioned in the introduction, Equation (3.1.2) can be regarded as a nonlocal integral equation by using the following representation

$$P(t,x) = \int_\Omega \kappa(x,y)u(t,y)dy,$$

where κ is the Green function of the operator $(I-\chi\Delta)^{-1}$ with Neumann boundary conditions.

The invariance of domain Ω and the well-posedness of the model Note that in System (3.1.1)-(3.1.2) we do not impose any boundary condition directly on u. Instead, the boundary condition here is induced by $\nabla P \cdot \nu = 0$. If we consider the associated characteristics flow of (3.1.1)-(3.1.2)

$$\begin{cases} \frac{\partial}{\partial t}\Pi(t,s;x) = -d\,\nabla P(t,\Pi(t,s;x)) \\ \Pi(s,s;x) = x \in \Omega, \end{cases} \tag{3.1.4}$$

where $\Pi(t,s;x)$ is the solution of the non-autonomous ODE, t represents the time variable, s is the initial time and x is the initial position. $\Pi(s,s;x) = x$ is our initial condition. We can prove (see Appendix 3.1.5.1) that the characteristics can not leave the domain Ω (see Figure 3.1.2 for an illustration). In fact, we can prove that for any $t > 0$, the mapping $x \mapsto \Pi(t,0;x)$ is a bijection from Ω to itself (see Lemma 3.1.10). We consider the solution along the characteristics

$$w(t,x) := u(t,\Pi(t,0;x)) \quad x \in \Omega, t > 0.$$

Taking any $x \in \Omega$, there exists $y \in \Omega$ such that $x = \Pi(t,0;y)$, and since

$$w(t,y) = w(t,\Pi(0,t;x)) = u(t,x),$$

we can reconstruct the solution $u(t,\cdot)$ from the knowledge of $w(t,\cdot)$ and $\{\Pi(t,s,\cdot)\}_{t,s\in[0,T]}$ on Ω.

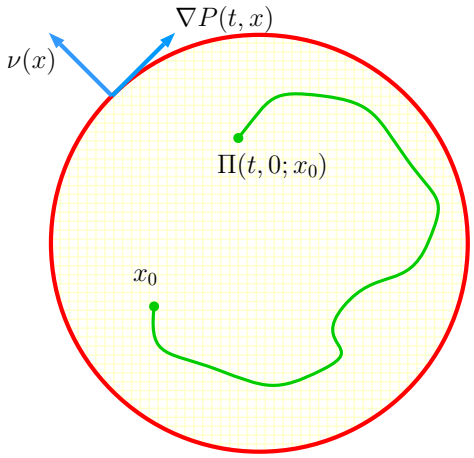

Figure 3.1.2: *An illustration of the invariance of the domain Ω. The green curve represents the trajectory of a characteristic.*

Assumption 3.1.3. The vector field $(t,x) \mapsto \nabla P(t,x)$ is continuous in $[0,T] \times \overline{\Omega}$ and Lipschitz continuous with respect to $x \in \overline{\Omega}$ for each fixed $t \in [0,T]$.

Remark 3.1.4. Assumption 3.1.3 is a sufficient condition for the existence and uniqueness of the characteristic flow $\{\Pi(t,s;\cdot)\}_{t,s\in[0,T]}$ in (3.1.4).

Definition 3.1.5. [162, Section 5.1] Let $\Omega \subset \mathbb{R}^2$ be a bounded domain. If $u : \Omega \to \mathbb{R}$ is bounded and continuous, we write

$$\|u\|_{C(\overline{\Omega})} := \sup_{x\in\Omega} |u(x)|.$$

For any $\gamma \in (0,1]$, the γ^{th}–Hölder norm of $u : \Omega \to \mathbb{R}$ is

$$\|u\|_{C^{0,\gamma}(\overline{\Omega})} := \|u\|_{C(\overline{\Omega})} + [u]_{C^{0,\gamma}(\overline{\Omega})},$$

where

$$[u]_{C^{0,\gamma}(\overline{\Omega})} := \sup_{\substack{x,y\in\Omega \\ x\neq y}} \left\{ \frac{|u(x)-u(y)|}{|x-y|^\gamma} \right\}.$$

The Hölder space $C^{k,\gamma}(\overline{\Omega})$ consists of all functions $u \in C^k(\overline{\Omega})$ having a finite norm

$$\|u\|_{C^{k,\gamma}(\overline{\Omega})} := \sum_{|\alpha|\leq k} \|D^\alpha u\|_{C(\overline{\Omega})} + \sum_{|\alpha|=k} [D^\alpha u]_{C^{0,\gamma}(\overline{\Omega})}$$

where $\alpha = (\alpha_1, \ldots, \alpha_n) \in \mathbb{N}^n$ and $|\alpha| = \alpha_1 + \ldots + \alpha_n$ in the sum above.

Lemma 3.1.6. *[187, Theorem 6.30 and 6.31] Let $\Omega \subset \mathbb{R}^2$ be the unit open disk. Consider the following elliptic equation*

$$\begin{cases} (I - \chi\Delta)P(x) = u(x) & x \in \Omega, \\ \nabla P(x) \cdot \nu(x) = 0 & x \in \partial\Omega, \end{cases} \tag{3.1.5}$$

where ν is the outward unit normal vector on $\partial\Omega$. Then for all $u \in C^{0,\alpha}(\overline{\Omega})$, the elliptic problem (3.1.5) *has a unique solution $P \in C^{2,\alpha}(\overline{\Omega})$. Moreover,*

$$\|P\|_{C^{2,\alpha}(\overline{\Omega})} \leq C\|u\|_{C^{0,\alpha}(\overline{\Omega})},$$

where $C = C(\alpha, \chi, \Omega)$.

The following theorem tells us if we choose our initial value u_0 sufficiently smooth, then Assumption 3.1.3 is automatically satisfied and the existence and uniqueness of solutions follow.

Theorem 3.1.7 (**Existence and uniqueness of solutions**). *Let $u_0 \in W^{1,\infty}(\Omega) \cap C^0_+(\overline{\Omega})$. There exists $T > 0$ such that problem* (3.1.1)-(3.1.2) *has a unique solution $u \in C\left([0,T]; C^0_+(\overline{\Omega})\right)$ which satisfies $u(0,x) = u_0(x)$. Moreover u is non-negative and for any $t \in [0,T]$, we have $u(t,\cdot) \in W^{1,\infty}(\Omega)$ and $\sup_{t\in[0,T]} \|u(t,\cdot)\|_{W^{1,\infty}(\Omega)} < \infty$.*

The proof of Theorem 3.1.7 will be detailed in Appendix 3.1.5.2.

Remark 3.1.8. Since for any $t \in [0,T]$ and for any $\alpha \in (0,1)$, we have $u(t,\cdot) \in W^{1,\infty}(\Omega) \hookrightarrow C^{0,\alpha}(\overline{\Omega})$, we deduce from Lemma 3.1.6 that $P(t,\cdot) \in C^{2,\alpha}(\overline{\Omega})$. Therefore, $(t,x) \to \nabla P(t,x)$ is continuous (since $P \in C([0,T]; C^1(\overline{\Omega}))$) and Lipschitz continuous with respect to x which implies that Assumption 3.1.3 is satisfied.

Conservation law on a volume If the reaction term $h \equiv 0$ is null in System (3.1.1)-(3.1.2), we have a conservation law for u. This can be seen by integrating the solution along the characteristics. In fact, we have the following conservation law.

Theorem 3.1.9. *For each volume $A \subset \Omega$ and each $0 \leq s \leq t$ we have*

$$\int_{\Pi(t,s;A)} u(t,x)\mathrm{d}x = \int_A \exp\left(\int_s^t h\left(u\left(l, \Pi(l,s;z)\right)\right)\mathrm{d}l\right) u(s,z)\mathrm{d}z.$$

In particular, if there is no reaction $h = 0$, then for any $0 \leq s \leq t$

$$\int_{\Pi(t,s;A)} u(t,x)\mathrm{d}x = \int_A u(s,z)\mathrm{d}z.$$

This means that the total number of cells in the volume A is constant along the volumes $\Pi(t,s;A)$.

Before proving Theorem 3.1.9, we need the following lemma.

Lemma 3.1.10. *Let $T > 0$ and $\{\Pi(t,s;x)\}_{t,s\in[0,T]}$ be the characteristic flow generated by* (3.1.4). *Then the map $x \mapsto \Pi(t,s;x)$ is continuously differentiable and the determinant of the Jacobian matrix is given by*

$$\det J_\Pi(t,s;x) = \exp\left(\int_s^t \frac{d}{\chi}\left(u(l,\Pi(l,s;x)) - P(l,\Pi(l,s;x))\right)\mathrm{d}l\right), \tag{3.1.6}$$

where $J_\Pi(t,s;x)$ is the Jacobian matrix of $\Pi(t,s;x)$ with respect to x at $(t,s;x)$.

Proof. From Theorem 3.1.7 and Remark 3.1.8, the mapping $(t,x) \to P(t,x)$ is $C([0,T];C^1(\overline{\Omega}))$ and $P(t,\cdot) \in C^{2,\alpha}(\overline{\Omega})$ for any $\alpha \in (0,1)$ if $u_0 \in W^{1,\infty}(\Omega)$. This ensures that the characteristics $x \to \Pi(t,s;x)$ is continuously differentiable. Taking the partial derivative of Equation (3.1.4) with respect to x yields

$$\begin{cases} \partial_t J_\Pi(t,s;x) = -d\, J_{\nabla P}(t,\Pi(t,s;x)) J_\Pi(t,s;x) \\ J_\Pi(s,s;x) = \mathrm{Id}, \end{cases}$$

where $J_{\nabla P}(t,\Pi(t,s;x))$ is the Jacobian matrix of $\nabla P(t,x)$ with respect to x at point $(t,\Pi(t,s;x))$. For any matrix-valued C^1 function $A : t \mapsto A(t)$, the Jacobian formula reads as follows

$$\frac{\mathrm{d}}{\mathrm{d}t} \det A(t) = \det A(t) \times \mathrm{Trace}\left(A^{-1}(t) \frac{d}{dt} A(t) \right).$$

Hence, we obtain

$$\begin{aligned} \frac{\mathrm{d}}{\mathrm{d}t} \det J_\Pi(t,s;x) &= \det J_\Pi(t,s;x) \times \mathrm{Trace}\left(J_\Pi(t,s;x)^{-1} J_{\nabla P}(t,\Pi(t,s;x)) J_\Pi(t,s;x) \right) \\ &= \det J_\Pi(t,s;x) \times \mathrm{Trace}\left(J_{\nabla P}(t,\Pi(t,s;x)) \right) \end{aligned}$$

and since $\mathrm{Trace}\left(J_{\nabla P}(t,\Pi(t,s;x)) \right) = (\Delta P)(t,\Pi(t,s;x)) = -\frac{1}{\chi}\left(u(t,\Pi(t,s;x)) - P(t,\Pi(t,s;x)) \right)$, we conclude

$$\begin{cases} \dfrac{\mathrm{d}}{\mathrm{d}t} \det J_\Pi(t,s;x) = \det J_\Pi(t,s;x) \times \dfrac{d}{\chi} \left[u(t,\Pi(t,s;x)) - P(t,\Pi(t,s;x)) \right] \\ \det J_\Pi(s,s;x) = 1. \end{cases}$$

The result follows. □

Proof of Theorem 3.1.9. Let $\{\Pi(t,s;x)\}_{t,s\in[0,T]}$ to be the characteristic flow generated by (3.1.4). Given any measurable set $A \subset \Omega$ and any $0 \le s \le t$, we integrate $u(t,x)$ over the volume $\Pi(t,s;A)$ with respect to x

$$\int_\Omega \mathbb{1}_{\Pi(t,s;A)}(x) u(t,x) \mathrm{d}x = \int_\Omega \mathbb{1}_A(z) u(t,\Pi(t,s;z)) \det J_\Pi(t,s;z) \mathrm{d}z, \tag{3.1.7}$$

where we have changed the variable x to $\Pi(t,s;z)$ on the right-hand-side.

We will prove in (3.1.30) in Appendix 3.1.5.2 that

$$u(t,\Pi(t,s;z)) = u(s,z) \exp\left(\int_s^t h(u(l,\Pi(l,s;z))) + \frac{d}{\chi}\left(P(l,\Pi(l,s;z)) - u(l,\Pi(l,s;z)) \right) \mathrm{d}l \right).$$

Combined with (3.1.6), this equality yields

$$u(t,\Pi(t,s;z)) \det J_\Pi(t,s;z) = u(s,z) \exp\left(\int_s^t h(u(l,\Pi(l,s;z))) \mathrm{d}l \right),$$

and substituting into (3.1.7) we get

$$\int_\Omega \mathbb{1}_{\Pi(t,s;A)}(x) u(t,x) \mathrm{d}x = \int_\Omega \mathbb{1}_A(z) u(s,z) \exp\left(\int_s^t h(u(l,\Pi(l,s;z))) \mathrm{d}l \right) \mathrm{d}z,$$

which is equivalent to

$$\int_{\Pi(t,s;A)} u(t,x) \mathrm{d}x = \int_A \exp\left(\int_s^t h\left(u\left(l,\Pi(l,s;z) \right) \right) \mathrm{d}l \right) u(s,z) \mathrm{d}z.$$

The result follows. □

Remark 3.1.11. For the PDE with logistic source, the nonlocal advection term $\mathrm{div}(u(t,x)\nabla P(t,x))$ makes the uniqueness of the equilibrium non-trivial. In our case, the semiflow associated to the solution is not monotone. Therefore, comparison arguments fail and more complex dynamical behaviors may occur. However, from numerical simulations for the single species model with logistic source $uh(u) = u(b-au)$, we

observe that the solution converges to the constant equilibrium of the corresponding ODE case. Let us consider a single species one-dimensional model

$$\begin{aligned} \partial_t u(t,x) - \operatorname{div}(u(t,x)\nabla P(t,x)) &= u(t,x)(1-u(t,x)) \\ (I-\Delta)P(t,x) &= u(t,x), \end{aligned} \qquad [0,T]\times[-1,1]$$

with Neumann boundary conditions $\nabla P \cdot \nu = 0$ for $(t,x) \in [0,T] \times \{-1,1\}$. The behavior of the solution is illustrated in Figure 3.1.3 by using a compactly supported initial condition.

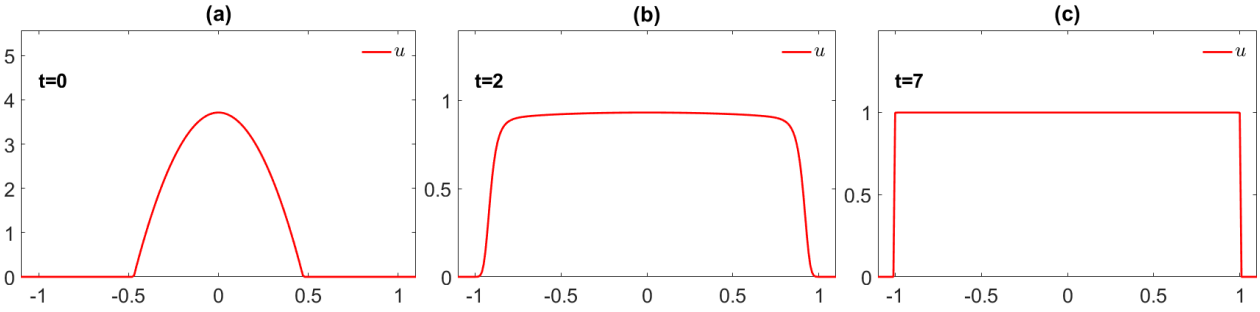

Figure 3.1.3: *In this simulation we show that the solution converges numerically to the constant positive steady state.*

3.1.2.2 Multi-species model

Multi-species ODE model Let us consider the corresponding two species model without the spatial variable x that is $u_i = u_i(t)$ for $i = 1, 2$.

$$\begin{cases} \dfrac{\mathrm{d}u_i}{\mathrm{d}t} = u_i h_i(u_1,u_2) \quad i=1,2, \\ u_i(0) = u_{i,0} \in \mathbb{R}_+. \end{cases} \tag{3.1.8}$$

We adopt the Lotka-Volterra model by setting

$$h_i(u_1,u_2) = b_i - \delta_i - \sum_{j=1}^{2} a_{ij}u_j, \quad i=1,2, \tag{3.1.9}$$

where $b_i > 0$, $i = 1, 2$ are the growth rates, $a_{ij} \geq 0$, $i \neq j$ represent the interspecific competition between the species, a_{ii} is the intraspecific competition (the competition of individuals from the same species) and δ_i is the additional mortality rate caused by drug treatment. In Section 2.2.1 we will always assume $\delta_i = 0$ for $i = 1, 2$ without loss of generality (replacing $b_i - \delta_i$ by b_i if $\delta_i > 0$). If we consider (3.1.8) in the absence of the other species, we can rewrite (3.1.9) as

$$h_i(u_1,u_2) = b_i - a_{ii}u_i, \quad i=1,2.$$

We always assume that for each i, $a_{ii} > 0$ meaning that each species alone exhibits logistic growth. This model has been considered by many authors (for example, see [297, 412]). Here we give a short summary of some qualitative properties of the solution to (3.1.8) in order to compare it with the PDE model.

Equilibrium and stability for (3.1.8)-(3.1.9)

The system has the following equilibria

$$E_0 = (0,0), \quad E_1 = (P_1,0)\,, \quad E_2 = (0,P_2)\,, \quad E^* = (u_1^*,u_2^*),$$

where

$$P_1 := \frac{b_1}{a_{11}}, \quad P_2 := \frac{b_2}{a_{22}}, \quad E^* = \left(\frac{a_{22}b_1 - a_{12}b_2}{a_{11}a_{22}-a_{12}a_{21}}, \frac{a_{21}b_1 - a_{11}b_2}{a_{12}a_{21}-a_{11}a_{22}}\right). \tag{3.1.10}$$

The solution E^* is only of relevance when $a_{12}a_{21} \neq a_{11}a_{22}$ and (u_1^*, u_2^*) is strictly positive, which is equivalent to either condition

$$\begin{cases} \dfrac{a_{12}}{a_{11}} > \dfrac{P_1}{P_2} \\ \dfrac{a_{21}}{a_{22}} > \dfrac{P_2}{P_1} \end{cases} \quad \text{or} \quad \begin{cases} \dfrac{a_{12}}{a_{11}} < \dfrac{P_1}{P_2} \\ \dfrac{a_{21}}{a_{22}} < \dfrac{P_2}{P_1}. \end{cases}$$

We adapt the main stability results from Zeeman [412] where the author considered a general n–species extinction case, Murray [297, Chapter 3.5] and Hirsch [210, Chapter 11] to system (3.1.8)-(3.1.9) for the following fours cases (i)-(iv) and discuss their biological implications.

Proposition 3.1.12. *For system* (3.1.8)-(3.1.9)*, suppose for each* $i = 1, 2$*,* $b_i > 0, a_{ii} > 0$ *and* $a_{ij} \geq 0$ *for any* $i \neq j$*. Let* $P_1 = b_1/a_{11}, P_2 = b_2/a_{22}$ *be the equilibrium for each species alone and assume the initial value* $(u_{1,0}, u_{2,0})$ *lies strictly in the first quadrant that is* $u_{1,0} > 0$ *and* $u_{2,0} > 0$*. Then for the following four cases we have*

(i). $a_{12}/a_{11} < P_1/P_2$*,* $a_{21}/a_{22} < P_2/P_1$*. This case corresponds to Figure 3.1.4 (a). The system* (3.1.8) *has four positive equilibrium, namely* E_0, E_1, E_2 *and* E^**. In such case, only* E^* *is globally asymptotically stable in the region* $\{(u_1, u_2) \in \mathbb{R}^2 \,|\, u_1 > 0, u_2 > 0\}$*.*

(ii). $a_{12}/a_{11} > P_1/P_2, a_{21}/a_{22} < P_2/P_1$*. This case corresponds to Figure 3.1.4 (b). The system* (3.1.8) *has three positive equilibrium, namely* E_0, E_1 *and* E_2*. Only* E_2 *is globally stable in the positive quadrant excepted for the axis* $u_1 = 0$*.*

(iii). $a_{12}/a_{11} < P_1/P_2, a_{21}/a_{22} > P_2/P_1$*. This case corresponds to Figure 3.1.4 (c). The analysis of the stability is similar to the case (ii). Only* E_1 *is globally stable in the positive quadrant excepted for the axis* $u_2 = 0$*.*

(iv). $a_{12}/a_{11} > P_1/P_2, a_{21}/a_{22} > P_2/P_1$*. This case corresponds to Figure 3.1.4 (d). In this case, system* (3.1.8) *has four equilibrium, where* E_1 *and* E_2 *are stable while* E^* *is a saddle point. The steady states* E_1 *and* E_2 *have two non-overlapping domains of attraction, separated by the stable manifold* $\boldsymbol{S}$ *of the equilibrium* E^**.*

Remark 3.1.13. Although among the four cases, (ii) and (iii) always lead to a competitive exclusion principle and so do (iv) due to the natural perturbation in population levels, case (i) leads to the stable coexistence of the two species in the long term. As we further develop our PDE model for (3.1.8), we can show numerically that the competitive exclusion principle occurs even in the case (i). This situation is a major difference between the PDE and the ODE model (3.1.8).

A scheme of the qualitative behavior of the phase trajectory is given in Figure 3.1.4 by numerical simulations.

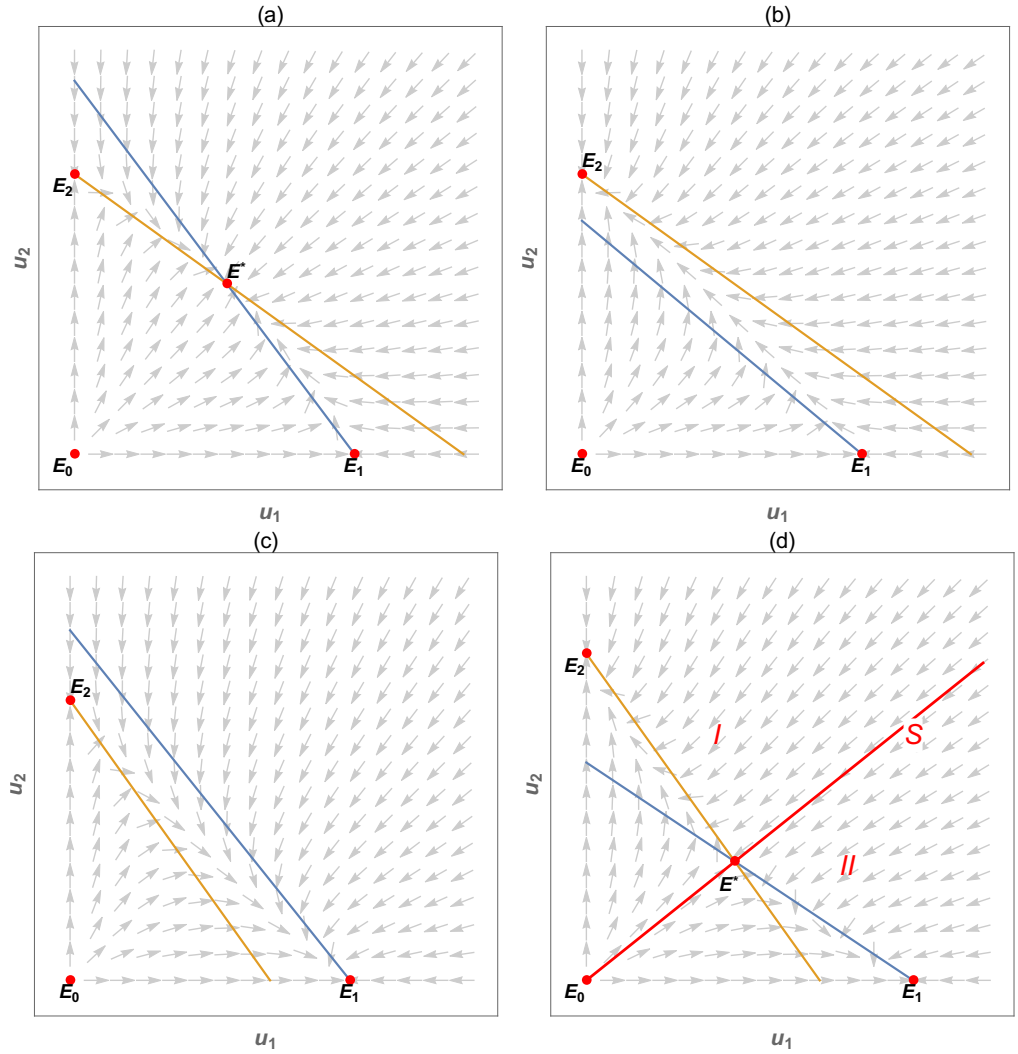

Figure 3.1.4: *A scheme of the qualitative behavior of the phase trajectory for various cases.* ***(a)*** $a_{12}/a_{11} < P_1/P_2$, $a_{21}/a_{22} < P_2/P_1$. *Only the positive steady state* E^* *is stable and all trajectories tend to it.* ***(b)*** $a_{12}/a_{11} > P_1/P_2, a_{21}/a_{22} < P_2/P_1$. *Only one stable steady state* E_2 *exists with the whole positive quadrant its domain of attraction.* ***(c)*** $a_{12}/a_{11} < P_1/P_2, a_{21}/a_{22} > P_2/P_1$. *Only one stable steady state* E_1 *exists with the whole positive quadrant its domain of attraction.* ***(d)*** $a_{12}/a_{11} > P_1/P_2, a_{21}/a_{22} > P_2/P_1$. E_1 *and* E_2 *are stable steady states, each of which has a domain of attraction namely* ***I*** *and* ***II****, separated by a separatrix* ***S*** *which is the stable manifold of equilibria* E^*.

Multi-species PDE model We study a two species population dynamics model on the unit open disk $\Omega \subset \mathbb{R}^2$ given as follows

$$\begin{cases} \partial_t u_1(t,x) - d_1 \operatorname{div}\big(u_1(t,x)\nabla P(t,x)\big) = u_1(t,x)h_1((u_1,u_2)(t,x)) \\ \partial_t u_2(t,x) - d_2 \operatorname{div}\big(u_2(t,x)\nabla P(t,x)\big) = u_2(t,x)h_2((u_1,u_2)(t,x)) \quad \text{in } [0,T]\times\Omega, \\ \big(I-\chi\Delta\big)P(t,x) = u_1(t,x)+u_2(t,x) \\ \nabla P(t,x)\cdot\nu(x) = 0 \qquad\qquad\qquad\qquad\qquad\qquad\qquad\quad \text{on } [0,T)\times\partial\Omega, \end{cases} \tag{3.1.11}$$

where ν is the outward normal vector, d_i is the dispersion coefficient, χ is the sensing coefficient. Recall that the function h_i is given by

$$h_i(u_1,u_2) = b_i - \delta_i - \sum_{j=1}^{2} a_{ij}u_j, \quad i=1,2.$$

System (3.1.11) is supplemented with the initial condition

$$\mathbf{u}_0(\cdot) := (u_1(0,\cdot), u_2(0,\cdot)) \in C^1(\overline{\Omega})^2. \tag{3.1.12}$$

Segregation property It has been observed in mono-layer co-culture experiments that once the two cell populations confront each other, they will stop growing, thus, forming separated islets. We can prove that our model (3.1.11) preserves such segregation property.

Theorem 3.1.14. *Suppose* $\mathbf{u} = (u_1, u_2)(t,x)$ *is the solution of* (3.1.11)-(3.1.12) *and assume* $d_1 = d_2 = d$ *in* (3.1.11). *Then for any initial distribution with* $u_1(0,x)u_2(0,x) = 0$ *for all* $x \in \Omega$, *we have* $u_1(t,x)u_2(t,x) = 0$ *for any* $t > 0$ *and* $x \in \Omega$.

Proof. We argue by contradiction and assume that there exist $t^* > 0, x^* \in \Omega$ such that

$$u_1(t^*,x^*)u_2(t^*,x^*) > 0.$$

Recall that the characteristic flow satisfies the following equation

$$\begin{cases} \frac{\partial}{\partial t}\Pi(t,s;x) = -d\,\nabla P(t,\Pi(t,s;x)) \\ \Pi(s,s;x) = x \in \Omega. \end{cases}$$

Since $x \to \Pi(t,s;x)$ is invertible from Ω to itself, there exists some $x_0 \in \Omega$ such that $\Pi(t^*,0;x_0) = x^*$. Then for any $i = 1,2$, we have

$$u_i(t^*,\Pi(t^*,0;x_0)) = u_i(0,x_0)\, e^{\int_0^{t^*} h_i((u_1,u_2)(l,\Pi(l,0;x_0))) + \frac{d}{\chi}(P(l,\Pi(l,0;x_0)) - (u_1+u_2)(l,\Pi(l,0;x_0)))\mathrm{d}l} > 0, \tag{3.1.13}$$

which implies

$$u_i(0,x_0) > 0, \quad i = 1,2.$$

This is a contradiction. □

For the one dimensional case $N = 1$, suppose u_1, u_2 are solutions to (3.1.11)-(3.1.12), we give an illustration (see Figure 3.1.5) of the segregation for the solutions integrated along the characteristics $u_i(t,\Pi(t,0;x))$ for $i = 1,2$. In fact, if there exists for some x_0 such that $u_i(0,x_0) = 0$ for $i = 1,2$, then from Equation (3.1.13) we obtain

$$u_1(t,\Pi(t,0;x_0)) = u_2(t,\Pi(t,0;x_0)) = 0,\ \forall t > 0.$$

Therefore, the characteristics $t \mapsto \Pi(t,0;x_0)$ forms a segregation barrier for the two cell populations.

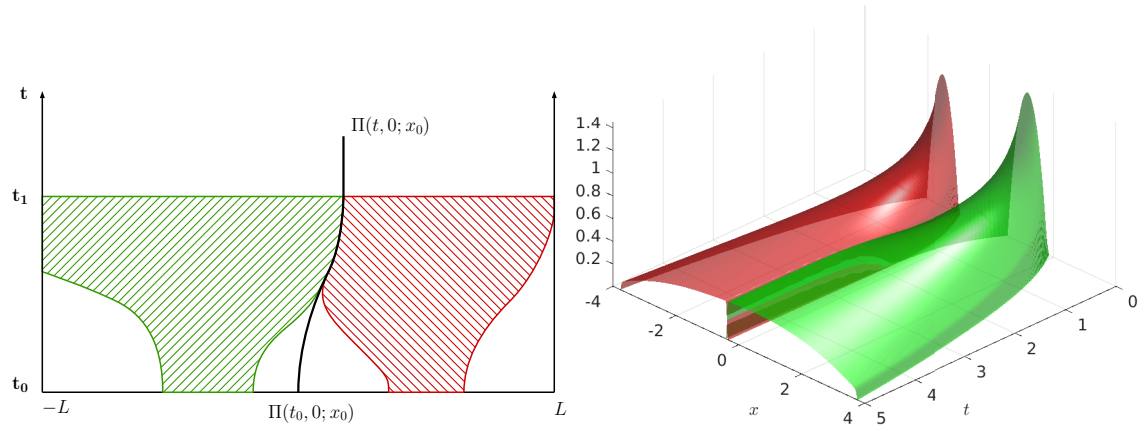

Figure 3.1.5: *In this Figure we illustrate the notion of segregation with a one dimensional bounded domain. Figure (a) shows that the characteristic* $t \mapsto \Pi(t,0;x_0)$ *forms a segregation "wall". Figure (b) shows the temporal-spatial evolution of the two species.*

Remark 3.1.15. Our model can be regarded as an alternative to nonlinear diffusion models which also implements the finite speed propagation property. The local existence and uniqueness of solutions is proved rigorously in Appendix 5.2. The notion of solution integrated along the characteristics also leads to the segregation property.

Note that solutions starting from compactly supported initial value stay compactly supported for the single and multi-species models. This is a consequence of the notion of solution integrated along the characteristics together with the fact that the characteristics cannot blow up in finite time as long as the $W^{1,\infty}$ norm of the solution $u(t,\cdot)$ is finite for time t. Therefore, in our case, the finite speed propagation holds, which is similar to the models with nonlinear diffusion.

Conservation law on a volume If we assume that $d_1 = d_2 = d$ in system (3.1.11), we have the following similar conservation law for two species case. Suppose volume $A \subset \Omega$ and each $0 \leq s \leq t$:

$$\int_{\Pi(t,s;A)} u_i(t,x)\mathrm{d}x = \int_A \exp\left[\int_s^t h_i\left((u_1,u_2)\left(l,\Pi(l,s;z)\right)\right)\mathrm{d}l\right] u_i(s,z)\mathrm{d}z, i = 1,2.$$

Therefore, if we assume in addition that $h_i = 0$ for any $0 \leq s \leq t$

$$\int_{\Pi(t,s;A)} u_i(t,x)\mathrm{d}x = \int_A u_i(s,z)\mathrm{d}z, i = 1,2.$$

This means the total number of cells for each species u_i remains constant along the volume $\Pi(t,s;A)$.

3.1.3 Numerical simulations

In Section 2, we established a PDE model for two species and we also proved that the solution satisfies some basic properties such as local existence and uniqueness, positivity, segregation and conservation law. These properties are ideal to explain the monolayer cell co-culture in the experiments. Based on the data from experiments in [318], we will fit some parameters in our model. By varying certain parameters such as the extra mortality rate caused by drug treatment (see [318] for details), we will simulate the evolution of two populations in the Petri dish and the variation of population number of cells.

3.1.3.1 Impact of the segregation on the competitive exclusion principle

In this section 3.1.3.1, the goal of our simulations is to compare the various cases discussed in Proposition 3.1.12 (ODE case) with our PDE model with segregation. As we will see in the numerical simulations, the model with spatial structure presents completely different results compared to the ODE model. To that aim, we consider the case where the drug (doxorubicine) concentration is low in the cell co-culture for MCF-7 and MCF-7/Doxo (see Figure 3.1.1). The drug treatment causes an additional mortality to the sensitive population MCF-7 represented by u_1 but no extra mortality to the resistant population MCF-7/Doxo represented by u_2 (MCF-7/Doxo is resistant to a small quantity of drug treatment, see Table 3.1.4 in Appendix 3.1.5.3).

We let U_i be the total number of cells in the u_i-population at time $t = 0$,

$$U_i = \int_\Omega u_i(0,x)\mathrm{d}x, \quad i = 1,2. \tag{3.1.14}$$

The parameter values used in the simulations and their interpretations are listed in Table 3.1.1. The growth rate b_i and the intraspecific competition a_{ii} are fitted to the data (see Appendix 3.1.5.3 for details).

Symbol	Interpretation	Value	Unit	Method	Dimensionless value
t	time	1	day	-	1
r	inner radius of the Petri dish	2.62	cm	[318]	1
U_i	total number of cells at $t = 0$	10^5	–	[318]	0.01
b_1	growth rate of cell u_1	0.6420	day^{-1}	fitted	0.6420
b_2	growth rate of cell u_2	0.6359	day^{-1}	fitted	0.6359
a_{11}	intraspecific competition of u_1	1.07×10^{-6}	cm^2/day	fitted	1.5588
a_{22}	intraspecific competition of u_2	1.06×10^{-6}	cm^2/day	fitted	1.5415
d_1	dispersion coefficient of u_1	13.73	cm^4/day	fitted	2
d_2	dispersion coefficient of u_2	13.73	cm^4/day	fitted	2
χ	sensing coefficient	6.86×10^{-2}	cm^2	fitted	0.01

Table 3.1.1: *List of parameters, their interpretations, values and symbols. Here u_1 represents MCF-7 (sensitive cell) and u_2 represents MCF-7/Doxo (resistant cell). From [318], the surface of the Petri dish is $21.5\,cm^2$. Thus the inner radius of the Petri dish r is calculated by $r^2\pi = 21.5\,cm^2$.*

In the presence of the drug, the equilibrium (3.1.10) of the ODE should be rewritten as

$$\bar{P}_1 = \frac{b_1 - \delta_1}{a_{11}}, \quad \bar{P}_2 = \frac{b_2 - \delta_2}{a_{22}}. \tag{3.1.15}$$

Moreover, we assume the drug concentration is low, so that $b_1 - \delta_1 > 0$ and $\delta_2 = 0$, therefore we have

$$\bar{P}_1 < \bar{P}_2.$$

The case when $\bar{P}_1 > \bar{P}_2$ is similar and will be discussed in the end of this section 3.1.3.1. We choose our parameters to satisfy

$$\frac{a_{12}}{a_{11}} < \frac{\bar{P}_1}{\bar{P}_2}, \quad \frac{a_{21}}{a_{22}} < \frac{\bar{P}_2}{\bar{P}_1}, \tag{3.1.16}$$

which corresponds to Case (i) in Proposition 3.1.12 for the ODE system. By using (3.1.15), the condition in (3.1.16) can be interpreted as

$$\frac{a_{12}}{a_{22}} < \frac{b_1 - \delta_1}{b_2 - \delta_2}, \quad \frac{a_{21}}{a_{11}} < \frac{b_2 - \delta_2}{b_1 - \delta_1}.$$

Since we have $b_1 - \delta_1 > 0$ and $\delta_2 = 0$, if the coefficients a_{12} and a_{21} are small, then (3.1.16) holds. We give a possible set of parameters satisfying (3.1.16) :

$$\delta_1 = 0.4,\ \delta_2 = 0,\ a_{12} = 0.2,\ a_{21} = 1. \tag{3.1.17}$$

We assume the initial condition of each species u_i is composed of 20 circular cell clusters (represented by the red/green dots in Figure 3.1.6 (a)), uniformly distributed over the Petri dish Ω. The total number of cells is initially $U_i = 0.01$ (recall (3.1.14)) for each species and we assume that each cluster contains the same quantity of cells. We present the numerical simulation in Figure 3.1.6 from day 0 to day 6. We also plot the proportions of cells in Figure 3.1.6 (f), which are defined as

$$\frac{U_i(t)}{U_1(t) + U_2(t)}, \quad \text{where } U_i(t) := \int_\Omega u_i(t, x)\mathrm{d}x,\ i = 1, 2,$$

for species i.

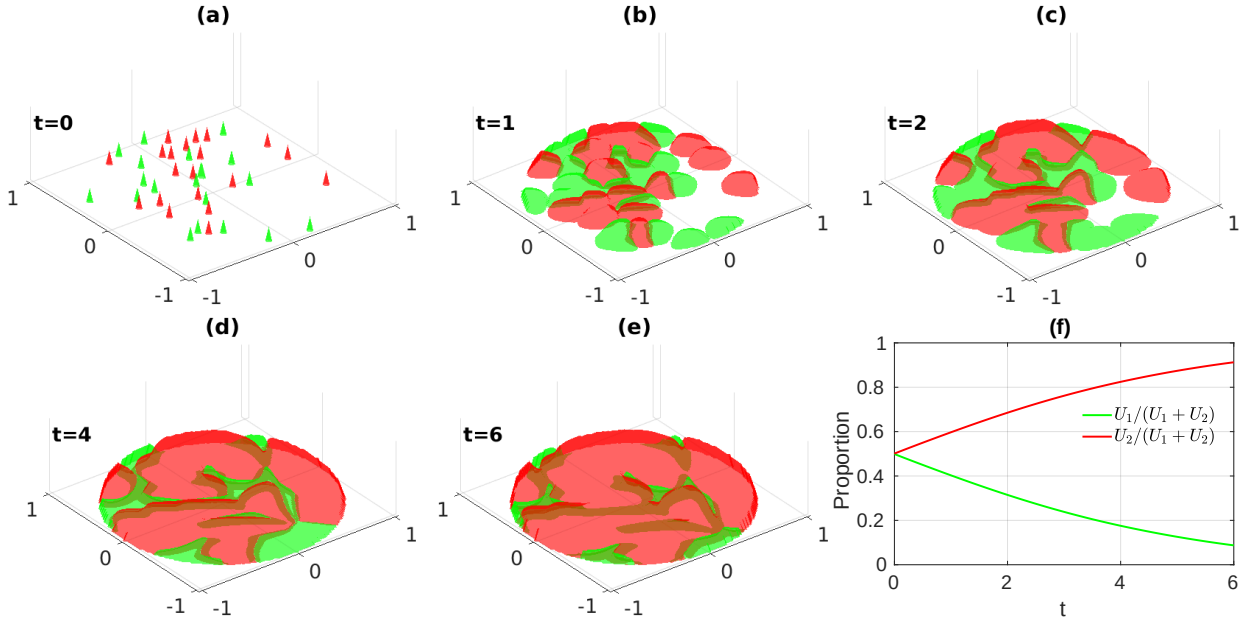

Figure 3.1.6: *Spatial-temporal evolution of the two species u_1 and u_2 and their proportions. Figures (a)-(e) correspond to the evolution of cell growth form day 0 to day 6 and Figure (f) is the plot of the proportion of each species in the total population from day 0 to day 6. We fix the parameters $\delta_1 = 0.4$, $\delta_2 = 0$, $a_{12} = 0.2$, $a_{21} = 1$ in (3.1.17). The initial condition is composed of 20 cell clusters which are uniformly distributed over the Petri dish. The initial total number of cells is $U_1 = U_2 = 0.01$ for each species and cells are equally distributed in each cluster. Other parameter values are listed in Table 3.1.1.*

If the parameters are set as in (3.1.17) for the ODE system, Proposition 3.1.12 indicates that the two species are in the stable coexistence regime and the solution converges to the equilibrium

$$\bar{E}^* := \left(\frac{a_{22}(b_1-\delta_1) - a_{12}(b_2-\delta_2)}{a_{11}a_{22} - a_{12}a_{21}}, \frac{a_{21}(b_1-\delta_1) - a_{11}(b_2-\delta_2)}{a_{12}a_{21} - a_{11}a_{22}} \right) \approx (0.11, 0.34).$$

However, as shown in Figure 3.1.6, we can see the population density u_1 tends to 0 and u_2 tends to 1. In particular, we observe the competitive exclusion principle for the PDE even though the solutions to the ODE are in the stable coexistence regime.

One can notice that unlike the ODE system (3.1.8), the segregation property for the PDE model implies that it is impossible for the two species to coexist at the same position $x \in \Omega$. Thus the coefficients a_{12}, a_{21} do not play any role in the competition because of the segregation principle. This is verified by numerical simulations: when we vary the coefficient coefficients a_{12}, a_{21}, we obtain identical plots for cell evolution and cell population ratio. Since the simulations are identical, we omitted them here.

Through the numerical simulations, we observed that the PDE model (3.1.11) undergoes a competitive exclusion principle. Our numerical simulations strongly indicate that the stable steady states only depend on the relation between $\bar{P}_1$ and $\bar{P}_2$ (see (3.1.15) for definition). If $\bar{P}_1 < \bar{P}_2$ (resp. $\bar{P}_1 > \bar{P}_2$), the population u_2 (resp. u_1) will dominate and the other species will die out. We also simulated the case when $\bar{P}_1 > \bar{P}_2$, the results showed that $\bar{E}_1$ is the only stable steady state, which verifies our conjecture. As Proposition 3.1.12 shows, the stability of the equilibrium of the ODE system depends on the coefficients a_{12}, a_{21} which measure the interspecies competition. However, the stability of the steady states of the PDE system only depends on $\bar{P}_1$ and $\bar{P}_2$, which do not depend on a_{12}, a_{21}. This is a major difference between the ODE and PDE models.

3.1.3.2 Impact of the initial distribution on the final proportion of each species

In the previous section 3.1.3.2, we investigated the competitive exclusion principle for two species. By investigating Figure 3.1.6 (f), we can see that the speed of increase in proportion of the dominant population u_2 (red curve) is varying with time. We remark that the increase of the dominant population u_2 is faster

from day 0 to day 2 than from day 4 to day 6. If we further study the spatial-temporal evolution of the cell co-culture presented in Figure 3.1.6 (a)-(e), we can observe that from day 0 to day 2 the competition between the two groups is mainly expressed in terms of competition for spatial resources. However, from day 4 to day 6, when the surface of the Petri dish is almost fully occupied by cells of either type, the reaction term $u_i h_i(u_1, u_2)$ in the equation begins to play a major role in the change of the number of cells. In order to explore the major factors in cell competition, we investigate the impact on the initial distribution of cells on the proportion of each species on day 6. We will mainly focus on two factors, namely the initial number of cell clusters and the law of initial distribution of those clusters in space, which might influence the proportions for u_1 and u_2. To that aim, we set the following parameters

$$\delta_1 = 0.15,\ \delta_2 = 0,\ a_{12} = 0,\ a_{21} = 0, \tag{3.1.18}$$

and fix the other parameters as in Table 3.1.1.

Dependency on the initial number of cell clusters In cell culture, the initial number of cell clusters is an important factor. Bailey et al. [28] study the sphere-forming efficiency of MCF-7 human breast cancer cell by comparing the cell culture with different initial numbers of cell clusters. Here we consider the impact of the initial number of cell clusters on the final proportion of each species. To that aim, we assume that the initial distribution follows the uniform distribution on a disk.

We consider two sets of initial condition, that is

$$U_1 = U_2 = 0.005, \quad N_{u_1} = N_{u_2} = 10, \tag{3.1.19}$$
$$U_1 = U_2 = 0.1, \quad N_{u_1} = N_{u_2} = 200, \tag{3.1.20}$$

where U_1 and U_2 are defined in (3.1.14) and N_{u_1} (respectively N_{u_2}) is the initial number of cell clusters of species u_1 (respectively, of species u_2).

The above initial conditions correspond to different types of seeding in the experiment, namely cells are sparsely seeded or densely seeded. We assume that the total number of cells is proportional to the initial number of cell clusters, meaning the dilution procedure adopted in the experiment is the same, thus the number of cells in each cell cluster is a constant. In Figure 3.1.7, we first give a numerical simulation for the cell growth with parameters in (3.1.19). In Figure 3.1.8, we present the simulation with parameters in (3.1.20), tracking from day 0 to day 6.

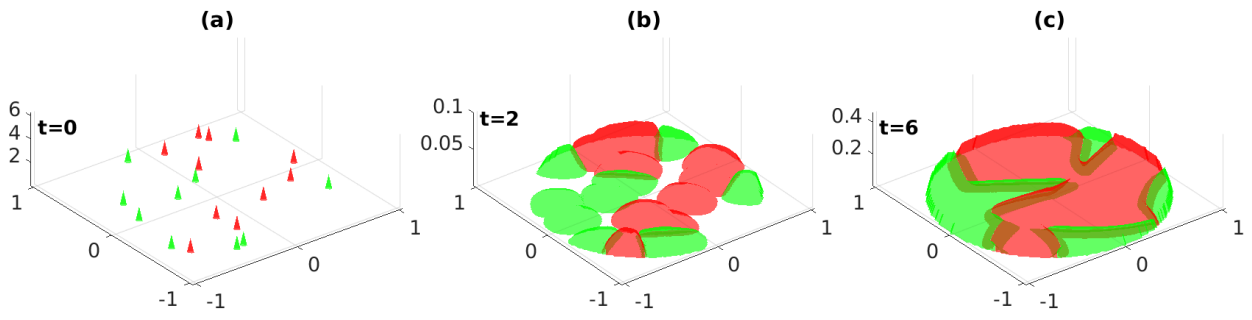

Figure 3.1.7: *Cell co-culture for species u_1 and u_2 over 6 days in the sparsely seeded case, i.e., $U_1 = U_2 = 0.005$, $N_{u_1} = N_{u_2} = 10$, for day $0, 2$ and 6. Parameter values are listed in* (3.1.18) *and Table 3.1.1.*

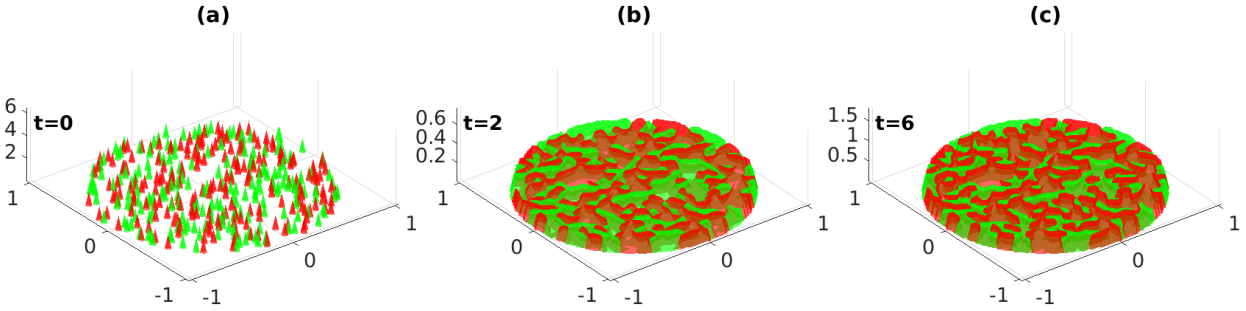

Figure 3.1.8: *Cell co-culture for species u_1 and u_2 over 6 days in the densely seeded case, i.e., $U_1 = U_2 = 0.1$, $N_{u_1} = N_{u_2} = 200$, for day $0, 2$ and 6. Parameter values are listed in* (3.1.18) *and Table 3.1.1.*

In Figure 3.1.9 we plot the evolution of the total number of cells and the proportion of each species over 6 days.

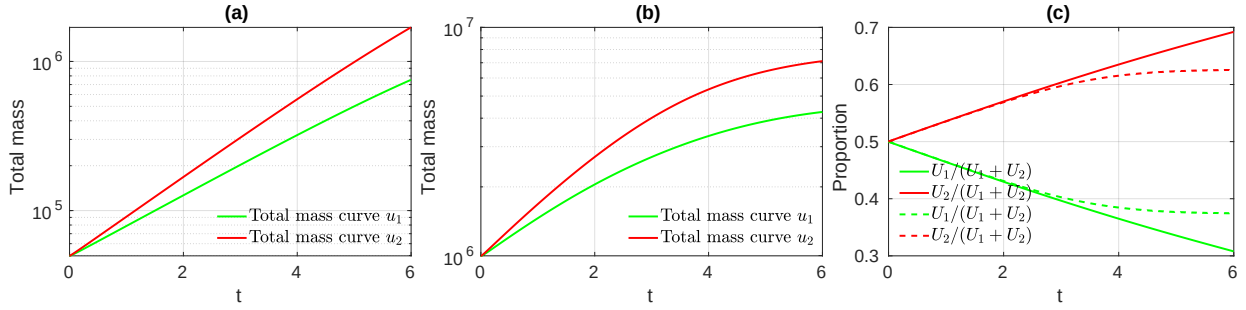

Figure 3.1.9: *Evolution of the total number of cells (in log scale) and their proportion for species u_1 and u_2 over 6 days. Figure (a) corresponds to the sparsely seeded case (with parameter values as in* (3.1.19)*), Figure (b) to the densely seeded case (with parameter values as in* (3.1.20)*) . In Figure (c), the solid lines represent the proportions of each species when we start with $N_{u_1} = N_{u_2} = 10$ and the dashed lines represent the proportions of each species when we start with $N_{u_1} = N_{u_2} = 200$. Parameters are listed in Table 3.1.1 and in* (3.1.18).

From Figure 3.1.9 (a)-(b), we can also observe a difference in the growth of each cell population. In Figure (a) we can see that both cell populations are in the regime of exponential growth from day 0 to day 6 (a base-10 log scale is used for the y-axis). Conversely, in Figure (b) the growth of each population is slowing down from day 4 to day 6, meaning that the cell co-culture is reaching the carrying capacity. More importantly, in Figure (c), we observe a significant difference in the development of proportion of each species. In fact, since the spatial competition is still the dominant factor in the first two days, we can hardly see any difference between the dashed lines and solid lines. The proportion of the dominant population grows almost linearly. However, the variation of the proportion of each species in the densely seeded case changes much slower after day 4, while the sparsely seeded group still varies linearly.

In the above numerical simulations, we considered the case where the total number of cells is proportional to the number of cell clusters. In the following numerical experiments, we fix the total number of cells, and vary only the number of cell clusters. By doing so, we intend to show the influence uniquely due to the number of cell clusters.

We consider two sets of initial condition, that is

$$U_1 = U_2 = 0.075, \quad N_{u_1} = N_{u_2} = 10, \tag{3.1.21}$$

$$U_1 = U_2 = 0.075, \quad N_{u_1} = N_{u_2} = 100, \tag{3.1.22}$$

where U_1 and U_2 are defined in (3.1.14) and N_{u_1} (respectively N_{u_2}) is the initial number of cell clusters of species u_1 (respectively species u_2).

The above initial conditions correspond to different types of seeding in the experiment, namely cells are sparsely seeded or densely seeded. We assume that the total number of cells is not proportional to the initial number of cell clusters, meaning that the dilution procedures adopted in the experiment are different, thus the number of cells in each cell cluster can be different.

In Figure 3.1.10, we first give a numerical simulation for the cell growth with parameters in (3.1.21). In Figure 3.1.11, we present the simulation with parameters in (3.1.22).

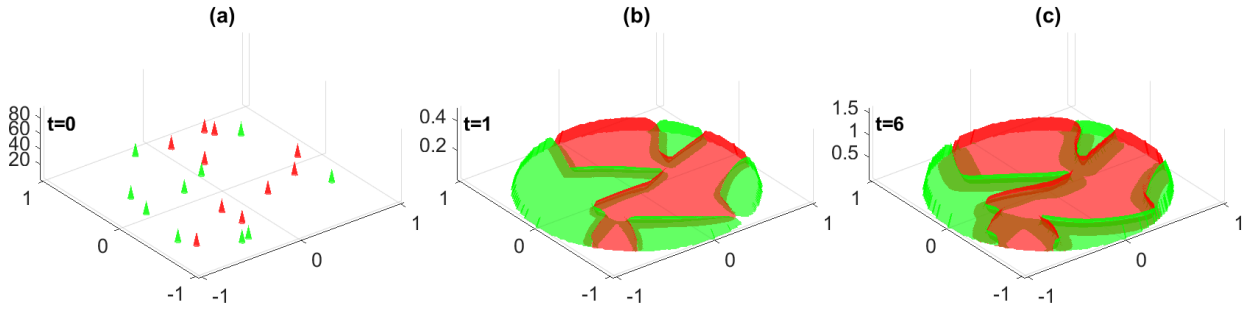

Figure 3.1.10: *Cell co-culture for species* u_1 *and* u_2 *over 6 days in the sparsely seeded case, i.e.,* $U_1 = U_2 = 0.075$, $N_{u_1} = N_{u_2} = 10$, *for day* $0, 1$ *and* 6. *Parameter values are listed in* (3.1.18) *and Table 3.1.1.*

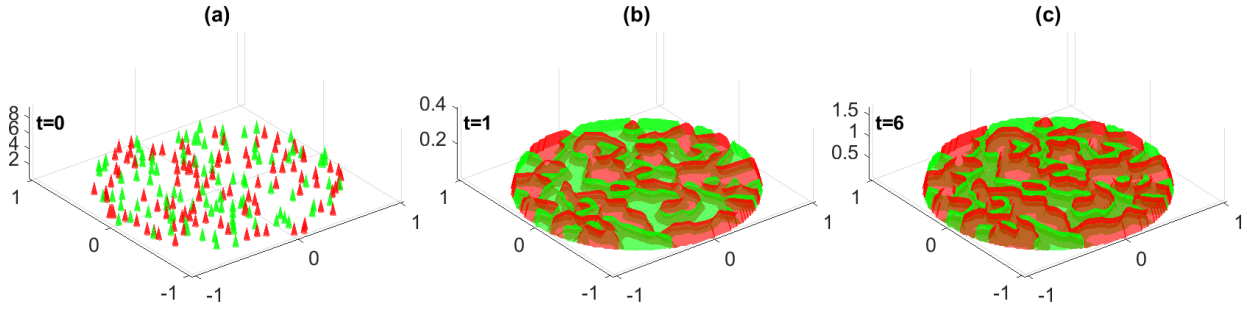

Figure 3.1.11: *Cell co-culture for species* u_1 *and* u_2 *over 6 days in the densely seeded case, i.e.,* $U_1 = U_2 = 0.075$, $N_{u_1} = N_{u_2} = 100$, *for day* $0, 1$ *and* 6. *Parameter values are listed in* (3.1.18) *and Table 3.1.1.*

In Figure 3.1.12 we plot the evolution of the total number of cells and the proportion of each species u_1 and u_2 over 6 days of the simulation.

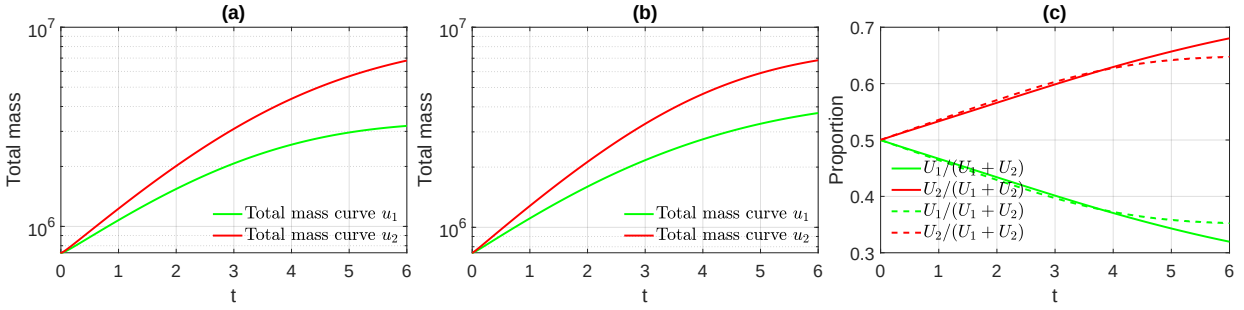

Figure 3.1.12: *Evolution of the total number (in log scale) and the proportion of each species u_1 and u_2 over 6 days. In Figure (a) we plot the total number of each cell population corresponding to the simulations with parameters in* (3.1.21) *while Figure (b) corresponds to the simulations with parameters in* (3.1.22). *In Figure (c), the solid lines represent the proportion of each species in the sparsely seeded case $N_{u_1} = N_{u_2} = 10$ and the dashed lines represent the proportion in the densely seeded case $N_{u_1} = N_{u_2} = 100$. Parameters are listed in Table 3.1.1 and* (3.1.18).

The curves of the growth of the two cell populations in Figure 3.1.12 (a) and (b) are very similar. Both of them are reaching the carrying capacity (a base-10 log scale is used for the y-axis). However, as Figure 3.1.12 (c) shows, there is still a clear difference in the proportion of each species in the total population (dashed lines and solid lines) and this difference persists when we change the random seed for the uniform distribution at $t = 0$. In fact, as the total number of cells for the two scenarios is the same, the transition from the first expansion phase (from day 0 to day 1 in Figure 3.1.10 and 3.1.11) to the second phase of the interspecies competition is very short for both two scenarios. During the first four days, we can hardly see any difference between the dashed lines and solid lines in Figure 3.1.12 (c). The proportion of the dominant population grows almost linearly. However, the proportion of the densely seeded group slows down after day 4, while the sparsely seeded group still grows almost linearly. This difference can be more significant if we increase the difference of the initial number of clusters (See [177, page.119 Figure 3.7 and 3.8]).

Figure 3.1.10 and Figure 3.1.11 show that when we start with the sparsely seeded condition, the species quickly expand to some large and connected clusters. On the contrary, for the densely seeded case, cells form small and scattered islets. Thus, even though the curves for the two scenarios are similar in Figure 3.1.12-(a) and Figure 3.1.12-(b), the interactions of large clusters and small islets are different. This discrepancy can affect the competition between the two populations and eventually be expressed in the population ratio. As for the densely seeded case, though the competitive exclusion principle holds in this case, the time for the extinction of u_1 can be very long.

Dependency on the law of the initial distribution In the experiment, the size of the Petri dish can be a factor to determine the law of the initial distribution for the cell. In general, under the same total number of cells, a small size Petri dish will lead to a biased initial distribution and cells are more likely to aggregate at the border. While a big Petri dish will make the cell distribution more homogeneous, closer to a uniform distribution. Therefore, in this paragraph, we study whether the proportion of each species can be affected by the law of initial distribution.

We will assume that the center of each cluster in the initial distribution is given by its polar coordinates (r, θ), that the radius r follows the Beta distribution with parameters α and β, and that the angle θ is uniformly distributed in $[0, 2\pi]$. More precisely,

$$\{r_n\}_{n=1,\dots,N} \sim \text{Beta}(\alpha, \beta), \quad \{\theta_n\}_{n=1,\dots,N} \sim \text{U}(0, 2\pi).$$

Hence the Cartesian coordinates of the center of each cluster are given by

$$\begin{cases} x_n = \sqrt{r_n}\cos(\theta_n) \\ y_n = \sqrt{r_n}\sin(\theta_n) \end{cases} \quad n = 1, 2, \dots, N. \tag{3.1.23}$$

In Figure 3.1.13, we plot the density function of the Beta distribution for different α, β

$$f_{\alpha,\beta}(r) = 1/B(\alpha, \beta)\, r^{\alpha-1}(1-r)^{\beta-1},$$

where $B(\alpha, \beta)$ is a normalization constant to ensure that the total mass is 1.

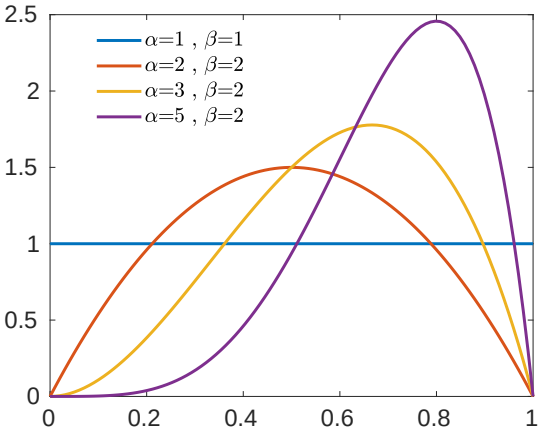

Figure 3.1.13: *Density function of the initial distribution* $f_{\alpha,\beta}(r) = 1/B(\alpha, \beta)\, r^{\alpha-1}(1-r)^{\beta-1}$ *for different* α *and* β*, where* $B(\alpha, \beta)$ *is a normalization constant to ensure that the total integral is* 1*.*

Our simulation will mainly compare the following two cases

$$(\alpha_1, \beta_1) = (1, 1), \quad (\alpha_2, \beta_2) = (3, 2).$$

We plot the initial distributions of the two different cases in Figure 3.1.14 where we choose 40 cell clusters (i.e., $N_{u_1} = 40$ and $N_{u_2} = 40$ in (3.1.23)) for species u_1 and species u_2.

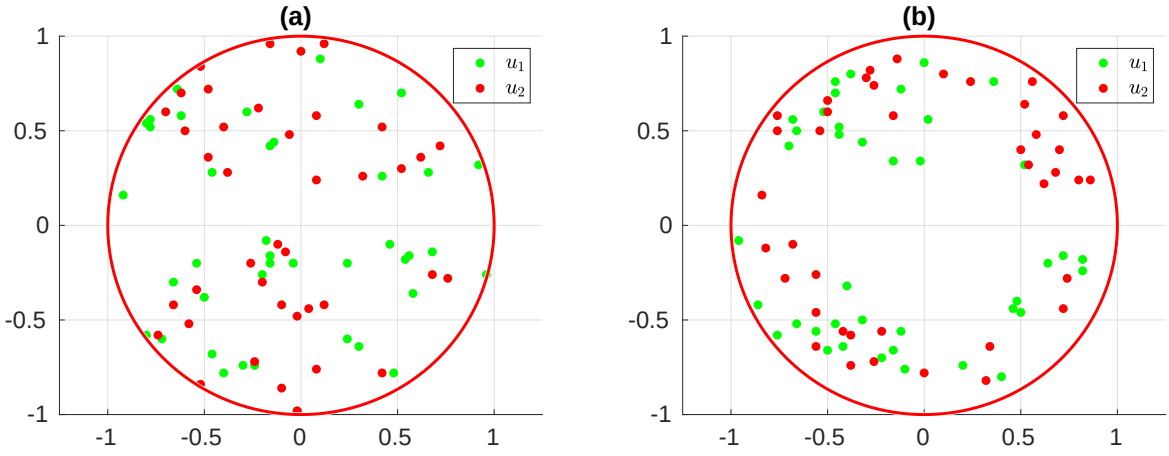

Figure 3.1.14: *Spatial distribution of the initial condition when* $(\alpha, \beta) = (1, 1)$ *(Figure (a)) and* $(\alpha, \beta) = (3, 2)$ *(Figure (b)). Here red dots and green dots represent cell clusters. The initial condition is composed of* $N_{u_1} = 40$ *and* $N_{u_2} = 40$ *cell clusters, in both cases.*

Suppose that the total number of cells $U_1 = U_2 = 0.02$ is equally distributed in each cell cluster. A typical numerical solution is shown in Figure 3.1.15 when $(\alpha_1, \beta_1) = (1, 1)$ and in Figure 3.1.16 when $(\alpha_2, \beta_2) = (3, 2)$.

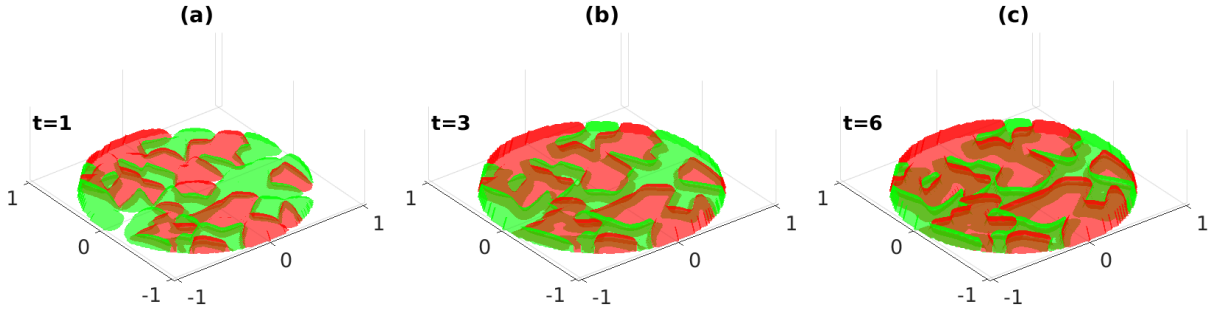

Figure 3.1.15: *Cell co-culture for species u_1 and u_2 over 6 days. We plot the case where the initial distribution follows beta distribution with parameters $(\alpha, \beta) = (1, 1)$. Parameters are listed in Table 3.1.1 and* (3.1.18).

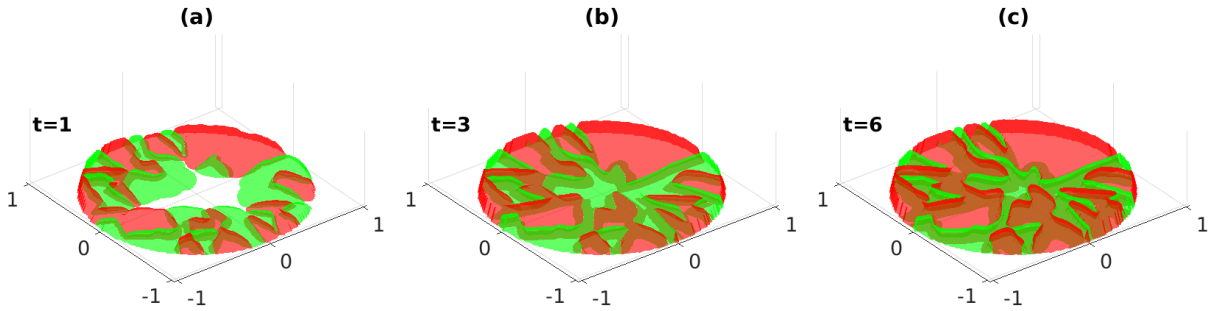

Figure 3.1.16: *Cell co-culture for species u_1 and u_2 over 6 days. We plot the case where the initial distribution follows beta distribution with parameters $(\alpha, \beta) = (3, 2)$. Parameters are listed in Table 3.1.1 and* (3.1.18).

Now we plot the evolution of the total number of cells for each species u_1 and u_2 over 6 days.

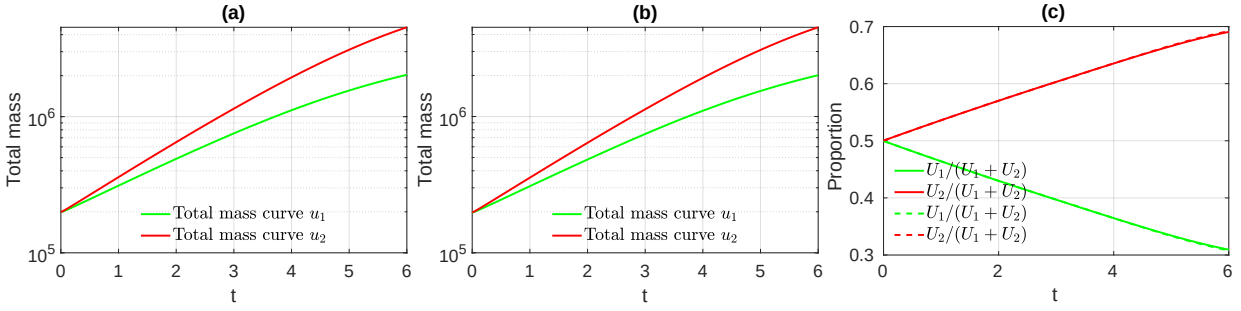

Figure 3.1.17: *Evolution of the total number of cells (in log scale) for species u_1 and u_2 and their proportions over 6 days. In Figure (a) we plot the total number of cells corresponding to the uniform initial distribution in Figure 3.1.15. In Figure (b) we plot the number of cells corresponding to the initial distribution as in Figure 3.1.16. In Figure (c), the solid lines represent the proportion when $(\alpha, \beta) = (1, 1)$ and the dashed lines represent the proportion in the case $(\alpha, \beta) = (3, 2)$. From Figure (c), we can see that they overlap. Parameters are listed in Table 3.1.1 and* (3.1.18).

From Figure 3.1.17 we can see that the law of initial distribution has almost no influence on the final proportion of species. We also tried different scenarios when the total number of cell clusters are 20, 50 and 100 or with different extra mortality rate $\delta_1 = 0, 0.2$ and 0.5, and the results are similar. Thus we can deduce that the final relative proportion is stable under the variation of the law of the initial distribution.

Combining the above numerical experiments in Section 3.2.1 and Section 3.2.2, we can see that under the competitive exclusion principle, the difference in the initial number of cell clusters can have an influence

on the interspecific competition. To be more precise, with the same initial number of cells, the interspecific competition of the densely seeded group is different from the one in the sparsely seeded group.

3.1.3.3 Impact of the dispersion coefficient on the population ratio

In Section 3.2, when the parameters of the model are the same, the competition induced by the cell dynamics can be reflected by the difference in the spatial resource. Now we assume the spatial resource is the same and we investigate the role of the dispersion coefficient in the evolution of the species.

To that aim, we let the initial distribution of the two species follow the same uniform distribution and they are sparsely seeded on the Petri dish. Furthermore, we let the cell dynamics for the two population be almost the same, the only variable we control here is the dispersion coefficient for the population. We take the same uniform initial distribution at day 0, with the same initial number of cell clusters and the same number of cells, i.e.,

$$U_1 = U_2 = 0.005, \quad N_{u_1} = N_{u_2} = 10, \quad a_{12} = a_{21} = 0. \tag{3.1.24}$$

We compare the following two scenarios in Table 3.1.2 where the only difference is the dispersion parameters.

Parameters	d_1	d_2	δ_1	δ_2
scenario 1:	2	2	0	0
scenario 2:	2	0.2	0	0

Table 3.1.2: *Two sets of dispersion coefficients for u_1 and u_2.*

In scenario 1, the dispersion coefficients of the two species are the same, while in scenario 2 we suppose the species u_1 has an advantage in the spatial competition over its competitor u_2.

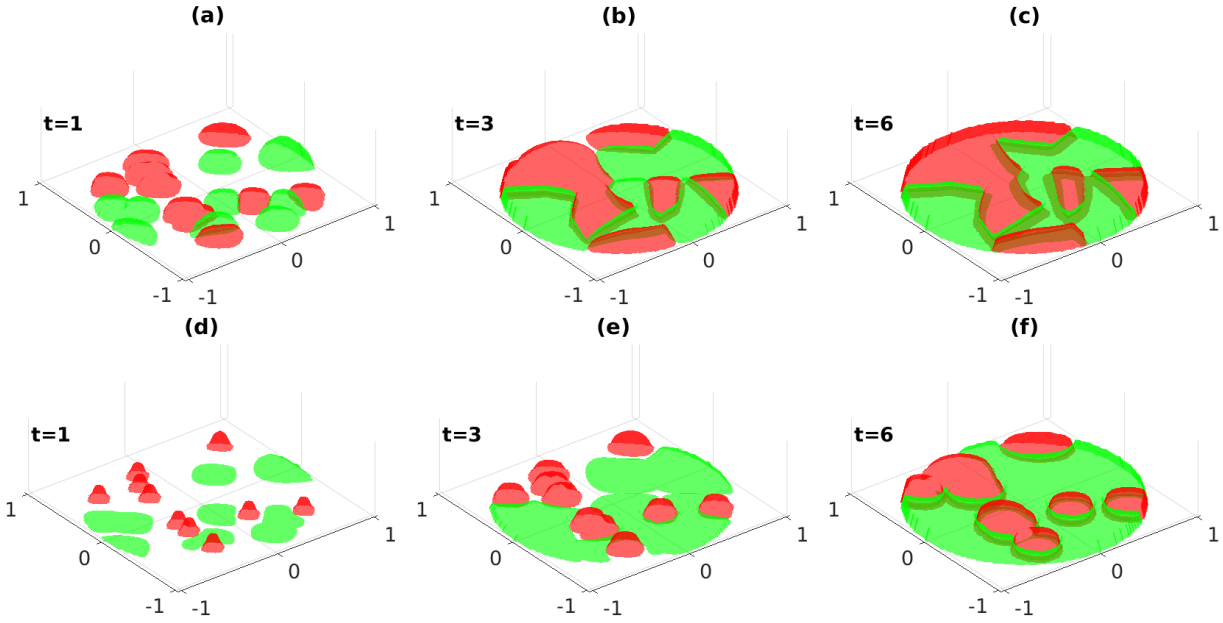

Figure 3.1.18: *Cell co-culture for species u_1 and u_2 over 6 days. Figures(a)-(c) correspond to scenario 1 (i.e. with the parameters $d_1 = 2, d_2 = 2, \delta_1 = \delta_2 = 0$) while Figures (d)-(f) correspond to scenario 2 (i.e. with $d_1 = 2, d_2 = 0.2, \delta_1 = \delta_2 = 0$). In both scenarios, the initial number of cell clusters and the total number of cells are the same and follow* (3.1.24) *and the same uniform distribution. We plot the simulations for day $1, 3$ and day 6. Other parameters are listed in Table 3.1.1.*

Now we plot the evolution of the total number of cells and the proportion of each species for species u_1 and u_2 over 6 days.

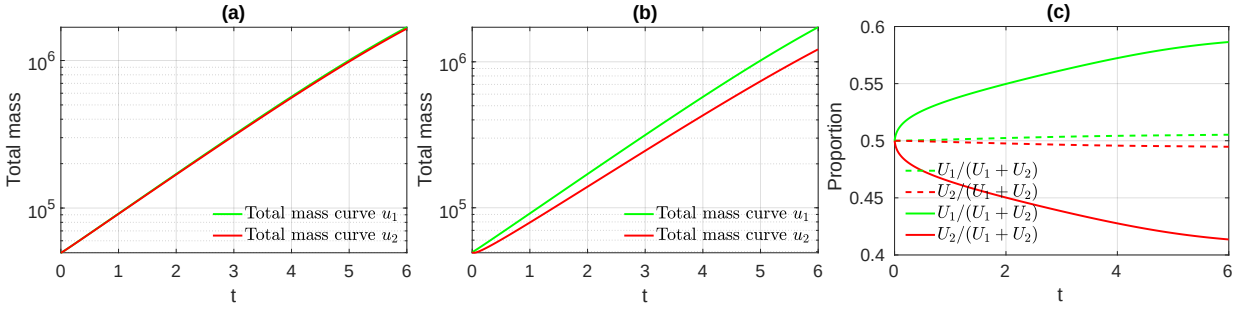

Figure 3.1.19: *Evolution of the total number of cells (in log scale) and the proportion in the total population for species u_1 and u_2 over 6 days. In Figure (a) we plot the total number of cells corresponding to the scenario 1. In Figure (b) we plot the total number of cells corresponding to the scenario 2. In Figure (c) we plot the proportion of each species and the dashed lines corresponds to scenario 1 while the solid lines corresponds to scenario 2 in 3.1.2. Other parameters are listed in Table 3.1.1 and* (3.1.24).

The main result from Figure 3.1.19 is that the dispersion coefficient can have a great impact on the proportion of each species after 6 days. Next, we consider the following scenario where u_1 has the advantage in dispersion coefficient but is at a disadvantage induced by drug treatment. Therefore

Parameters	d_1	d_2	δ_1	δ_2
scenario 3:	2	0.2	**0.1**	0

Table 3.1.3: *This scenario corresponds to the case where the species u_1 spreads faster than the species u_2. Moreover, due to a drug treatment, the mortality of the species u_1 is strictly positive while the mortality of the species u_2 is zero (i.e. the drug treatment does not affect the second species). In the context of cancer cell, the species u_1 would correspond to cells which are sensitive to the drug while u_2 would correspond to the cell resistant to the drug treatment.*

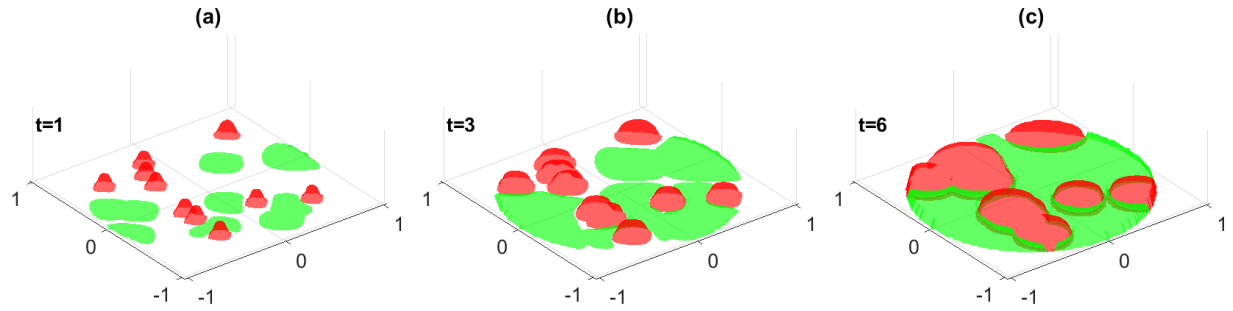

Figure 3.1.20: *Cell co-culture for species u_1 and u_2 over 6 days. Figure (a)-(c) corresponds to the scenario 3 with $d_1 = 2, d_2 = 0.2, \delta_1 = 0.1, \delta_2 = 0$ in Table 3.1.3. The initial number of cell clusters and the total number of cells follow* (3.1.24). *Other parameters are listed in Table 3.1.1.*

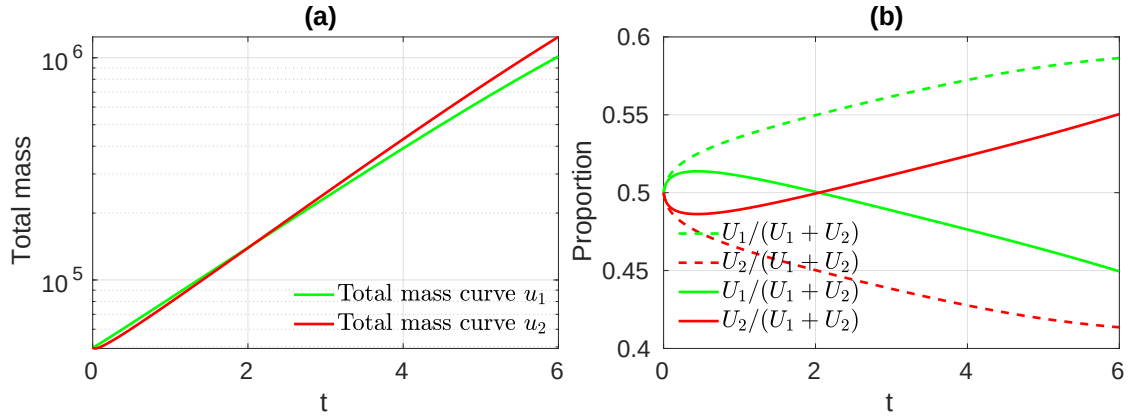

Figure 3.1.21: *Evolution of the total number of cells (in log scale) and the proportion of each species for species u_1 and u_2 over 6 days. In Figure (a) we plot the total number of cells in scenario 3 (see Figure 3.1.20). In Figure (b), the dashed lines correspond to the proportion of each species in the total population in scenario 2 with $d_1 = 2, d_2 = 0.2, \delta_1 = 0, \delta_2 = 0$ in Table 3.1.2 while the solid lines correspond to scenario 3 with $d_1 = 2, d_2 = 0.2, \delta_1 = 0.1, \delta_2 = 0$ in Table 3.1.3. Other parameters are listed in Table 3.1.1 and* (3.1.24).

By including now a drug treatment, we can see from Figure 3.1.20 and Figure 3.1.21 that between day 0 and day 2, the population u_1 dominates u_2 thanks to a larger dispersion rate. After day 2, since the drug is killing the cell for species u_1 while the drug has no effect on the species u_2, the species u_2 finally takes over the species u_1. It leads to a gradual increase in the proportion of the species u_2.

In the numerical simulations for the scenarios 1 and 2 in Table 3.1.2, we let the cell dynamics of the two species be almost equal. Thus the competition due to the cell dynamics is almost negligible. We have shown the dispersion coefficient of populations can have a great impact on the population ratio after 6 days.

In the simulation for scenario 3 in Table 3.1.3, we can observe that despite the competitive exclusion principle, a larger dispersion coefficient can lead to a short-term advantage in the population. In the long term, the competitive exclusion principle still dominates.

3.1.4 Conclusion and discussion

From the experimental data in the work of Pasquier et al. [318], we modeled the mono-layer cell co-culture by a hyperbolic Keller-Segel equation (3.1.11). We proved the local existence and uniqueness of solutions by using the notion of the solution integrated along the characteristics in Theorem 3.1.7 and proved the conservation law in Theorem 3.1.9. For the asymptotic behavior, we analyzed the problem numerically in Section 3.

In Section 3.1 we discussed the competitive exclusion principle, indicating that the asymptotic behavior of the population depends only on the relationship between the steady states $\bar{P}_1$ and $\bar{P}_2$ (see (3.1.15) for definition) which is different from the ODE case. We found that except for the case $P_1 = P_2$, the model with spatial segregation always exhibits a competitive exclusion principle.

Even though the long term dynamics of cell density is decided by the relative values of the equilibrium, the short term behavior needs a more delicate description. We studied two factors which may influence the population ratios. The first factor is the initial cell distribution, as measured by the initial number of cell clusters and the law of initial distribution. We found that the impact of the initial distribution on the proportion of each species lies in the initial number of cell clusters but not in the law of initial distribution.

The second factor influencing the population ratio is the cell movement in space, as measured by the dispersion coefficient d_i. In the first stage (i.e. before the Petri dish is saturated), the dispersion rate d_i is the dominant factor. Once the surface of the Petri dish is saturated by cells, cell dynamics $u_i\, h(u_1, u_2)$ becomes the key factor. Note that the coefficients a_{12}, a_{21} do not play any role in the competition because of the segregation principle.

We briefly summarize the main factors that can influence the population ratio in cell culture for model (3.1.11):

(a). The difference of cell dynamics in the two species (internal factor): if the equilibrium $\bar{P}_1 > \bar{P}_2$ (see (3.1.15) for definition), then u_1 will dominate, u_2 will die out (and vice-versa when $\bar{P}_1 < \bar{P}_2$) (see Figures 3.1.6);

(b). If the initial number of cells is similar, the interspecific competition of the densely seeded group is different than the one of the sparsely seeded group (see Figures 3.1.12). We also concluded that the law of initial distribution has almost no influence on the population ratio (see Figures 3.1.15-3.1.16);

(c). If cells are sparsely seeded at the beginning, the cell competition consists of two stages: the first stage, where the dispersion rate plays a major role, is for cells to occupy the surface of the Petri dish and the second stage, where the cell dynamics becomes the key factor, is for each species to reach a saturation stage (see Figure 3.1.19 and Figure 3.1.21).

3.1.4.1 Mixed initial condition

In this section 3.1, we are mainly focused on applying the model to the monolayer cell co-culture experiments in [318] where the initial condition is always segregated. However, when the dispersion coefficients are the same $d_1 = d_2$ and the initial condition is mixed in the domain, the two population stay mixed even for large time, this can be proved by an argument similar to the one in Theorem 3.1.14. By equation (3.1.13),

$$u_i(t, \Pi(t,0;x)) = u_i(0,x) \exp\left(\int_0^t h_i\left((u_1,u_2)(l,\Pi(l,0;x))\right) + \frac{d}{\chi}\left(P(l,\Pi(l,0;x)) - (u_1+u_2)(l,\Pi(l,0;x))\right) \mathrm{d}l\right).$$

Therefore, if $u_1(0,x_0)u_2(0,x_0) > 0$, we can deduce $u_1(t,\Pi(t,0;x))u_2(t,\Pi(t,0;x)) > 0$ for any $t > 0$. To be more precise, if we take the time derivate of (2.13), we obtain

$$\frac{\mathrm{d}}{\mathrm{d}t}u_i(t,\Pi(t,0;x)) = u_i(t,\Pi(t,0;x))\Big(h_i((u_1,u_2)(t,\Pi(t,0;x))) + \frac{d}{\chi}\big(P(t,\Pi(t,0;x)) - (u_1+u_2)(t,\Pi(t,0;x))\big)\Big).$$

Note that both solutions $u_i(t,\Pi(t,0;x)), i = 1,2$ have a common term $\frac{d}{\chi}(P(t,\Pi(t,0;x)) - (u_1+u_2)(t,\Pi(t,0;x)))$. Therefore, for those mixed (non-segregated) initial condition, it is the term $h_i((u_1,u_2)(t,\Pi(t,0;x)))$ that determines the competition between these two species.

When $d_1 \neq d_2$, it is interesting to show some further numerical simulations with mixed initial condition. Our numerical simulations suggest that segregation occurs asymptotically. We present numerical results of asymptotic segregation in Figure 3.1.22, which were obtain by simulating the following toy model

$$\begin{cases} \partial_t u_1(t,x) - d_1 \operatorname{div}\big(u_1(t,x)\nabla P(t,x)\big) = u_1(t,x)\left(1 - u_1(t,x) - 2u_2(t,x)\right) \\ \partial_t u_2(t,x) - d_2 \operatorname{div}\big(u_2(t,x)\nabla P(t,x)\big) = u_2(t,x)\left(1 - 2u_1(t,x) - u_2(t,x)\right) & \text{in } [0,T]\times[-2,2] \\ \big(I-\Delta\big)P(t,x) = u_1(t,x) + u_2(t,x) \\ \nabla P(t,x)\cdot\nu(x) = 0 & \text{on } [0,T]\times\{-2,2\}, \end{cases} \tag{3.1.25}$$

where we set $T = 15$ and $d_1 = 2$ and $d_2 = 1$.

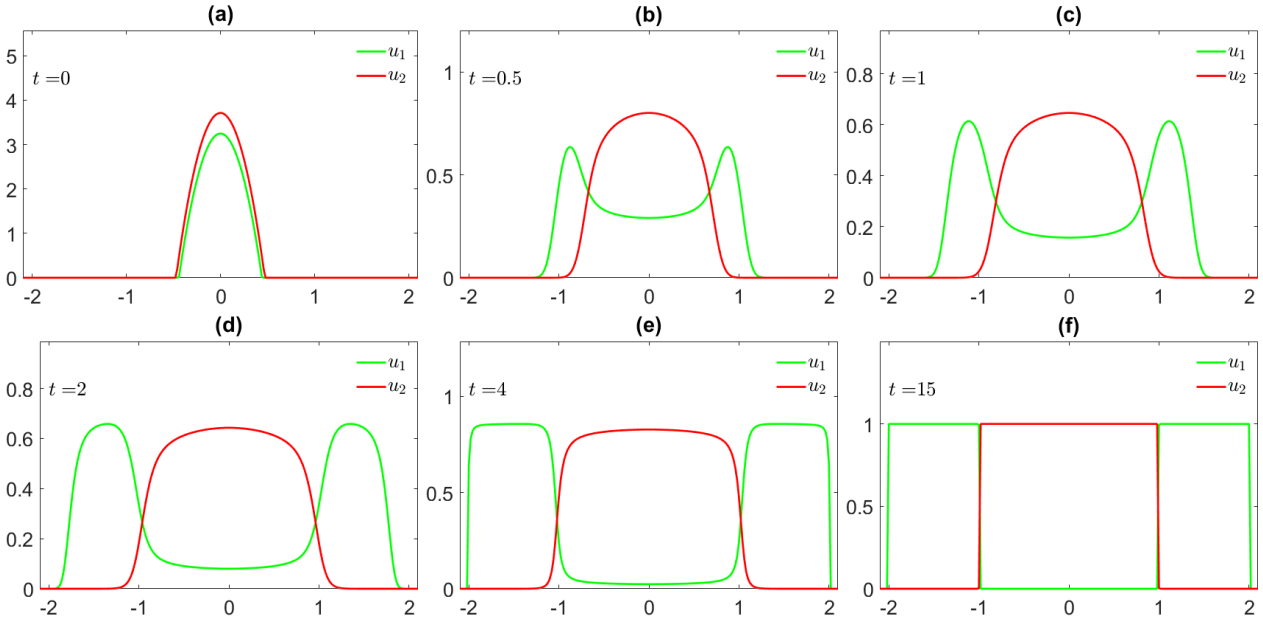

Figure 3.1.22: *Evolution of two species under a toy model* (3.1.25) *with mixed initial condition. The dispersion rate* $d_1 = 2$ *while* $d_2 = 1$. *For* $t > 15$, *the distributions* $u_1(t,.)$ *and* $u_2(t,.)$ *are almost independent of* t. *The numerical results suggest that asymptotic segregation occurs.*

Acknowledgement

The authors would like to thank the referees for their valuable comments and suggestions.

3.1.5 Appendix

3.1.5.1 Invariance of domain Ω

In this section 3.1.5.1, we prove the invariance of domain Ω for the characteristic equation.

Assumption 3.1.16. Let $\Omega \subset \mathbb{R}^2$ be an open bounded subset with $\partial\Omega$ of class C^2.

Since Ω is a bounded domain of class C^2, there exists U a neighborhood of the boundary $\partial\Omega$ such that the distance function $x \to \text{dist}(x, \partial\Omega) := \inf_{y\in\partial\Omega} \|x - y\|$ restricted to U has the regularity C^2 (see Foote [172, Theorem 1]). Furthermore, by Foote [172, Theorem 1] and Ambrosio [11, Theorem 1 p.11], we have the following properties for Ω.

Lemma 3.1.17. *Let Assumption 3.1.16 be satisfied. Then*

(i). There exists a small neighborhood U *of* $\partial\Omega$ *with* $U \subset \overline{\Omega}$ *such that, for every* $x \in U$ *there is a unique projection* $P(x) \in \partial\Omega$ *satisfying* $dist(x, P(x)) = dist(x, \partial\Omega)$.

(ii). The distance function $x \mapsto \delta(x) := dist(x, \partial\Omega)$ *is* C^2 *on* $U\backslash\partial\Omega$.

(iii). For any $x \in U$, $\nabla\delta(x) = -\nu(P(x))$ *where* $\nu(x)$ *is the outward normal vector.*

We consider the following non-autonomous differential equation on Ω

$$\begin{cases} x'(t) = f(t, x(t)) & t > 0 \\ x(0) = x_0 \in \Omega. \end{cases} \tag{3.1.26}$$

Assumption 3.1.18. The vector field $f : [0, \infty) \times \overline{\Omega} \to \mathbb{R}^2$ is continuous and satisfies

$$\nu(x) \cdot f(t, x) \leq 0, \quad \forall t > 0, \forall x \in \partial\Omega. \tag{3.1.27}$$

Moreover, for any $T > 0$, there exists a constant $K = K(T)$ such that vector field f satisfies

$$|f(t,x) - f(t,y)| \le K|x-y|, \quad \forall x, y \in \overline{\Omega},\, t \in [0,T]. \tag{3.1.28}$$

By (3.1.28), we have the existence and uniqueness of the solutions of (3.1.26) and the solutions may eventually reach the boundary $\partial\Omega$ in finite time. We will prove that (3.1.27) implies that the solutions of (3.1.26) actually stay in Ω and can not attain boundary $\partial\Omega$ in finite time under Assumption 3.1.16.

Theorem 3.1.19. *Let Assumption 3.1.16 and 3.1.18 be satisfied. For any $T > 0$, let $x(t)$ be the solution of (3.1.26) on $[0,T]$. Then $x(t) \in \Omega$ for any $t \in [0,T]$.*

Proof. We prove this theorem by contradiction. Let $t^* \in (0,T]$ be the first time when $x(t)$ reaches boundary $\partial\Omega$, i.e.,

$$t^* = \inf\{0 < t \le T : \delta(x(t)) = 0\}.$$

We can find a $\theta > 0$ such that, $x(t) \in U \cap \overline{\Omega}$ for any $t \in [t^* - \theta, t^*]$. Since $t \to x(t)$ is C^1, the mapping $t \mapsto \delta(x(t))$ is C^1 on $[t^* - \theta, t^*]$. By Lemma 3.1.17 (iii), we have

$$\frac{d}{dt}\delta(x(t)) = x'(t) \cdot \nabla\delta(x(t)) = -f(t,x(t)) \cdot \nu(y(t)), \tag{3.1.29}$$

where ν is the outward normal vector and $y(t) := P_{\partial\Omega}(x(t))$ is the unique projection of $x(t)$ onto $\partial\Omega$. By assumption (3.1.27), we have

$$-f(t,x(t)) \cdot \nu(y(t)) = \big(f(t,y(t)) - f(t,x(t))\big) \cdot \nu(y(t)) - f(t,y(t)) \cdot \nu(y(t)) \ge \big(f(t,y(t)) - f(t,x(t))\big) \cdot \nu(y(t)).$$

Hence (3.1.29) becomes

$$\begin{aligned}
\frac{d}{dt}\delta(x(t)) =& - f(t,x(t)) \cdot \nu(y(t)) \\
\ge& \big(f(t,y(t)) - f(t,x(t))\big) \cdot \nu(y(t)) \\
\ge& - |f(t,y(t)) - f(t,x(t))|\, |\nu(y(t))| \\
\ge& - K|y(t) - x(t)| = -K\delta(x(t)), \quad t \in [t^* - \theta, t^*],
\end{aligned}$$

which yields

$$\delta(x(t)) \ge \delta(x(t^* - \theta))e^{-K(t - t^* + \theta)}, \quad \forall t \in [t^* - \theta, t^*],$$

and $\delta(x(t^* - \theta)) > 0$ implies $\delta(x(t^*)) > 0$ which contradicts our assumption $\delta(x(t^*)) = 0$. □

3.1.5.2 Proof of Theorem 3.1.7

The objective of Appendix 5.2 is to give a clear notion of solutions and to prove the local existence and uniqueness of solution.

Solution integrated along the characteristics. Let us temporarily suppose $u \in C^1([0,T] \times \Omega)$, we can rewrite the first equation in (3.1.1) as

$$\begin{aligned}
\partial_t u(t,x) - d\,\nabla u(t,x) \cdot \nabla P(t,x) &= u(t,x)h(u(t,x)) + d\,u(t,x)\Delta P(t,x) \\
&= u(t,x)\left(h(u(t,x)) + \frac{d}{\chi}(P(t,x) - u(t,x))\right).
\end{aligned}$$

Moreover, if we differentiate the solution along the characteristic with respect to t then

$$\begin{aligned}
&\frac{\mathrm{d}}{\mathrm{d}t}u(t,\Pi(t,0;x)) \\
&= \partial_t u(t,\Pi(t,0;x)) + \nabla u(t,\Pi(t,0;x)) \cdot \partial_t \Pi(t,0;x) \\
&= \partial_t u(t,\Pi(t,0;x)) - d\,\nabla u(t,\Pi(t,0;x)) \cdot \nabla P(t,\Pi(t,0;x)) \\
&= u(t,\Pi(t,0;x))\left(h(u(t,\Pi(t,0;x))) + \frac{d}{\chi}\left(P(t,\Pi(t,0;x)) - u(t,\Pi(t,0;x))\right)\right).
\end{aligned}$$

The solution along the characteristics can be written as

$$
\begin{aligned}
&u(t,\Pi(t,0;x))\\
&=u_0(x)\exp\left(\int_0^t h(u(l,\Pi(l,0;x)))+\frac{d}{\chi}\big(P(l,\Pi(l,0;x))-u(l,\Pi(l,0;x))\big)\mathrm{d}l\right).
\end{aligned}
$$

Similarly, we can deduce for any $0\le s\le t$

$$
\begin{aligned}
&u(t,\Pi(t,s;x))\\
&=u(s,x)\exp\left(\int_s^t h(u(l,\Pi(l,s;x)))+\frac{d}{\chi}\big(P(l,\Pi(l,s;x))-u(l,\Pi(l,s;x))\big)\mathrm{d}l\right).
\end{aligned}
\tag{3.1.30}
$$

For the simplicity of notation, we let $d=\chi=1$ in our following discussion and define $w(t,x):=u(t,\Pi(t,0;x))$. We construct the following Banach fixed point problem for the pair (w,P). For each (w,P), we let

$$
w^1(t,x)=u_0(x)\exp\Big(\int_0^t F(w(l,x))+P(l,\Pi(l,0;x))\mathrm{d}l\Big).
\tag{3.1.31}
$$

where we set $F(u)=h(u)-u$ for any $u\ge 0$ and we define

$$
\mathcal{T}\begin{pmatrix}w(t,x)\\P(t,x)\end{pmatrix}:=\begin{pmatrix}w^1(t,x)\\(I-\Delta)^{-1}w^1(t,\Pi(0,t;x))\end{pmatrix}=\begin{pmatrix}w^1(t,x)\\P^1(t,x)\end{pmatrix},
\tag{3.1.32}
$$

where $(I-\Delta)^{-1}$ is the resolvent of the Laplacian operator with Neumann boundary condition.

We define

$$
\begin{aligned}
&X^\tau:=C^0\big([0,\tau],C^0(\overline{\Omega})\big),\quad Y^\tau:=C^0\big([0,\tau],C^1(\overline{\Omega})\big),\\
&\tilde{X}^\tau:=\left\{w\in C^0\big([0,\tau],C^0(\overline{\Omega})\big)\;\middle|\;w\ge 0,\ \sup_{t\in[0,\tau]}\|w(t,\cdot)\|_{W^{1,\infty}(\Omega)}\le C_1\right\},\\
&\tilde{Y}^\tau:=\left\{P\in C^0\big([0,\tau],C^1(\overline{\Omega})\big)\;\middle|\;\sup_{t\in[0,\tau]}\big\|P(t,\cdot)\big\|_{W^{2,\infty}(\Omega)}\le C_2\right\},
\end{aligned}
\tag{3.1.33}
$$

where $C_i, i=1,2$ are two constants to be fixed later. We also set

$$
Z^\tau:=X^\tau\times Y^\tau,\quad \tilde{Z}^\tau:=\tilde{X}^\tau\times\tilde{Y}^\tau.
$$

Notice $\tilde{Z}^\tau$ is a complete metric space for the distance induced by the norm $(\|\cdot\|_{X^\tau},\|\cdot\|_{Y^\tau})$. For simplicity, we denote $\|\cdot\|_{C^{\alpha,k}}:=\|\cdot\|_{C^{\alpha,k}(\Omega)}$ and $\|\cdot\|_{W^{k,\infty}}:=\|\cdot\|_{W^{k,\infty}(\Omega)}$ for $\alpha\in(0,1], k\in\mathbb{N}_+$.

Theorem 3.1.20 (Existence and uniqueness of solutions)**.** *For any initial value $u_0\in W^{1,\infty}(\Omega)$ and $u_0\ge 0$, for any C_1, C_2 large enough in* (3.1.33)*, there exists $\tau=\tau(C_1,C_2)>0$ such that the mapping $\mathcal{T}$ has a unique fixed point in $\tilde{Z}^\tau$.*

Proof. For any positive initial value $u_0\in W^{1,\infty}(\Omega)$ and $r>0$, we fix C_1 to be a constant such that $4\|u_0\|_{W^{1,\infty}}\le C_1$ and C_2 is a constant defined in (3.1.44) later in the proof.

We also denote

$$
\begin{pmatrix}w^0\\P^0\end{pmatrix}=\begin{pmatrix}u_0\\(I-\Delta)_{\mathcal{N}}^{-1}u_0\end{pmatrix}
$$

and let $\overline{B_{\tilde{Z}^\tau}}\left(\begin{pmatrix}w^0\\P^0\end{pmatrix},r\right)$ be the closed ball centered at $\begin{pmatrix}w^0\\P^0\end{pmatrix}$ with radius r in $\tilde{Z}^\tau=\tilde{X}^\tau\times\tilde{Y}^\tau$ with usual product norm

$$
\left\|\begin{pmatrix}w\\P\end{pmatrix}\right\|_{\tilde{Z}^\tau}:=\|w\|_{X^\tau}+\|P\|_{Y^\tau}
$$

and we set

$$
\kappa:=\left\|\begin{pmatrix}w^0\\P^0\end{pmatrix}\right\|_{\tilde{Z}^\tau}+r.
$$

Suppose $\begin{pmatrix} w \\ P \end{pmatrix} \in \overline{B_{Z^\tau}}\left(\begin{pmatrix} w^0 \\ P^0 \end{pmatrix}, r\right)$, we need to prove that there exits a τ small enough such that the following properties hold

(a). For any $t \in [0,\tau]$, $\big(w^1(t,\cdot), P^1(t,\cdot)\big)$ in (3.1.31) and (3.1.32) belong to $W^{1,\infty}(\Omega) \times W^{2,\infty}(\Omega)$ and their norms satisfy

$$\sup_{t\in[0,\tau]} \|w^1(t,\cdot)\|_{W^{1,\infty}} \le C_1, \tag{3.1.34}$$

$$\sup_{t\in[0,\tau]} \|P^1(t,\cdot)\|_{W^{2,\infty}} \le C_2. \tag{3.1.35}$$

(b). Moreover, we have

$$\|w^1 - w^0\|_{X^\tau} \le \frac{r}{2}, \tag{3.1.36}$$

$$\|P^1 - P^0\|_{Y^\tau} \le \frac{r}{2}. \tag{3.1.37}$$

Moreover, we plan to show that the mapping is a contraction: there exists a $\theta \in (0,1)$ such that for any $\begin{pmatrix} \tilde{w} \\ \tilde{P} \end{pmatrix}, \begin{pmatrix} w \\ P \end{pmatrix} \in \overline{B_{\tilde{Z}^\tau}}\left(\begin{pmatrix} w^0 \\ P^0 \end{pmatrix}, r\right)$ we have

$$\left\| \mathcal{T}\begin{pmatrix} \tilde{w} \\ \tilde{P} \end{pmatrix} - \mathcal{T}\begin{pmatrix} w \\ P \end{pmatrix} \right\|_{\tilde{Z}^\tau} \le \theta \left\| \begin{pmatrix} \tilde{w} \\ \tilde{P} \end{pmatrix} - \begin{pmatrix} w \\ P \end{pmatrix} \right\|_{\tilde{Z}^\tau}. \tag{3.1.38}$$

Step 1. We show that there exists a τ small enough such that for any $(w,P) \in \tilde{X}^\tau \times \tilde{Y}^\tau$ then

$$\sup_{t\in[0,\tau]} \|w^1(t,\cdot)\|_{W^{1,\infty}} \le C_1,$$

where w^1 is defined in (3.1.31).

Indeed, since $\nabla P(t,\cdot)$ is Lipschitz continuous, then $x \to \Pi(t,0,x)$ is also Lipschitz continuous. Since $\Pi(t,0;\cdot)$ maps Ω into Ω, we have

$$\begin{aligned} \|P(t,\Pi(t,0;\cdot))\|_{W^{1,\infty}} &\le \|P(t,\Pi(t,0;\cdot))\|_{L^\infty} + \|\nabla P(t,\cdot)\|_{L^\infty}\|\Pi(t,0;\cdot)\|_{W^{1,\infty}} \\ &\le \|P(t,\cdot)\|_{W^{1,\infty}} \max\{\|\Pi(t,0;\cdot)\|_{W^{1,\infty}}, 1\}. \end{aligned}$$

For any $t \in [0,\tau]$, we let $\tilde{F} := \sup_{u\in[0,\kappa]} \{|F(u)| + |F'(u)|\}$. By the definition of w^1 in (3.1.31), we have

$$\begin{aligned} &\|w^1(t,\cdot)\|_{W^{1,\infty}} \\ &\quad\le \|u_0\|_{W^{1,\infty}} \left\| \exp\left\{ \int_0^t F(w(l,\cdot)) + P(l,\Pi(l,0,\cdot))\mathrm{d}l \right\} \right\|_{W^{1,\infty}} \\ &\quad\le \|u_0\|_{W^{1,\infty}} \left\| \exp\left\{ \int_0^t F(w(l,\cdot)) + P(l,\Pi(l,0,\cdot))\mathrm{d}l \right\} \right\|_{L^\infty} \\ &\qquad\times \left(1 + \int_0^t \|F(w(l,\cdot))\|_{W^{1,\infty}} + \|P(l,\Pi(l,0,\cdot))\|_{W^{1,\infty}}\mathrm{d}l\right) \\ &\quad\le \|u_0\|_{W^{1,\infty}} \exp\left\{ \int_0^t \|F(w(l,\cdot))\|_{L^\infty} + \|P(l,\Pi(l,0,\cdot))\|_{L^\infty}\mathrm{d}l \right\} \\ &\qquad\times \Big(1 + \tau\tilde{F}\max\{\sup_{l\in[0,\tau]} \|w(l,\cdot)\|_{W^{1,\infty}}, 1\} + \tau\|P(l,\cdot)\|_{W^{1,\infty}} \max\{\|\Pi(l,0,\cdot)\|_{W^{1,\infty}}, 1\}\Big) \\ &\quad\le \|u_0\|_{W^{1,\infty}} e^{\tau\left(\tilde{F}+\kappa\right)}\Big(1 + \tau\tilde{F}\max\{C_1,1\} + \tau\kappa\max\{\|\Pi(l,0,\cdot)\|_{W^{1,\infty}}, 1\}\Big). \end{aligned} \tag{3.1.39}$$

Next we estimate $\max\left\{\sup_{l\in[0,\tau]}\|\Pi(l,0,\cdot)\|_{W^{1,\infty}},1\right\}$. We have for any $t,s\in[0,\tau]$

$$\Pi(t,s;x)=x-\int_s^t\nabla P(l,\Pi(l,s;x))\mathrm{d}l.$$

Since Ω is the unit open disk, $\|x\|_{W^{1,\infty}(\Omega)}=2$. We can obtain the following estimate

$$\begin{aligned}\|\Pi(t,s;\cdot)\|_{W^{1,\infty}}&\leq 2+\int_s^t\|\nabla P(l,\Pi(l,s;\cdot))\|_{W^{1,\infty}}\mathrm{d}l\\&\leq 2+\sup_{l\in[s,t]}\|\nabla P(l,\cdot)\|_{W^{1,\infty}}\int_s^t\max\left\{\|\Pi(l,s;\cdot)\|_{W^{1,\infty}},1\right\}\mathrm{d}l\\&\leq 2+C_2\int_s^t\max\{\|\Pi(l,s;\cdot)\|_{W^{1,\infty}},1\}\mathrm{d}l.\end{aligned}$$

Thanks to Grönwall's inequality, we have

$$\sup_{t,s\in[0,\tau]}\|\Pi(t,s;\cdot)\|_{W^{1,\infty}}\leq 2e^{\tau C_2}. \tag{3.1.40}$$

Substituting the (3.1.40) into (3.1.39) yields

$$\|w^1(t,\cdot)\|_{W^{1,\infty}}\leq\|u_0\|_{W^{1,\infty}}e^{\tau\left(\tilde{F}+\kappa\right)}\left(1+\tau\tilde{F}\max\{C_1,1\}+2\tau\kappa e^{\tau C_2}\right).$$

Since $C_1\geq 4\|u_0\|_{W^{1,\infty}}$, we can choose $\tau\leq\min\left\{\frac{\ln 2}{\tilde{F}+\kappa},\frac{1}{\tilde{F}\max\{C_1,1\}+2\kappa e^{C_2}},1\right\}$ and we obtain

$$\sup_{t\in[0,\tau]}\|w^1(t,\cdot)\|_{W^{1,\infty}}\leq C_1. \tag{3.1.41}$$

Thus, Equation (3.1.34) holds.

Let us now check that w^1 satisfies (3.1.36). Let $\chi[u]:=ue^u$, we remark that $|e^u-1|\leq ue^u=\chi[u]$ for all $u\geq 0$. We have

$$\begin{aligned}|w^1(t,x)-u_0(x)|&\leq|u_0(x)|\left|\exp\left\{\int_0^t F(w(l,x))+P(l,\Pi(l,0,x))\mathrm{d}l\right\}-1\right|\\&\leq\|u_0\|_{C^0}\chi\left[\int_0^t\|F(w(l,\cdot))\|_{C^0}+\|P(l,\Pi(l,0,\cdot))\|_{C^0}\mathrm{d}l\right]\\&\leq\|u_0\|_{C^0}\chi\left[\tau\tilde{F}+\tau\sup_{l\in[0,\tau]}\|P(l,\cdot)\|_{C^0}\right]\\&\leq\|u_0\|_{C^0}\chi\left[\tau\tilde{F}+\tau\kappa\right],\end{aligned} \tag{3.1.42}$$

where $\tilde{F}=\sup_{u\in[0,\kappa]}\{|F(u)|+|F'(u)|\}$. From (3.1.42) we have

$$\sup_{t\in[0,\tau]}\|w^1(t,\cdot)-u_0(\cdot)\|_{C^0}\leq\|u_0\|_{C^0}\chi\left[\tau\tilde{F}+\tau\kappa\right]. \tag{3.1.43}$$

Since $\lim_{u\to 0}\chi[u]=0$, it suffice to take τ small enough to ensure (3.1.36).

Step 2. Next we verify (3.1.35) and (3.1.37) for P^1 where P^1 is defined as the second component of (3.1.32). We show that there exists τ small enough such that for any $(w,P)\in\tilde{X}^\tau\times\tilde{Y}^\tau$

$$\sup_{t\in[0,\tau]}\|P^1(t,\cdot)\|_{W^{2,\infty}}\leq C_2.$$

Thanks to the Schauder estimate [187, Theorem 6.30], there exists a constant C depending only on Ω such that

$$\|P^1(t,\cdot)\|_{C^{2,\frac{1}{2}}}\leq C\|w^1(t,\Pi(0,t;\cdot))\|_{C^{0,\frac{1}{2}}}.$$

Recalling $\sup_{t\in[0,\tau]}\|\Pi(0,t;\cdot)\|_{W^{1,\infty}} \le 2e^{\tau C_2}$ as a consequence of (3.1.40), we have

$$\begin{aligned}\|P^1(t,\cdot)\|_{W^{2,\infty}} &\le \|P^1(t,\cdot)\|_{C^{2,\frac{1}{2}}}\\ &\le C\|w^1(t,\Pi(0,t;\cdot))\|_{C^{0,\frac{1}{2}}}\\ &\le C\|w^1(t,\Pi(0,t;\cdot))\|_{W^{1,\infty}}\\ &\le C\|w^1(t,\cdot)\|_{W^{1,\infty}}\max\{\|\Pi(0,t;\cdot)\|_{W^{1,\infty}},1\}\\ &\le 2\,C\,C_1e^{\tau C_2}.\end{aligned}$$

We can now define

$$C_2 = 4\,C\,C_1, \tag{3.1.44}$$

which only depends on Ω and $\|u_0\|_{W^{1,\infty}}$. Finally, we let $\tau \le (\ln 2)/C_2$ and we have

$$\|P^1(t,\cdot)\|_{W^{2,\infty}} \le 4\,C\,C_1 = C_2.$$

In particular, we have shown (3.1.35).

Next we prove (3.1.37). Since Ω is a two-dimensional unit disk, using Morrey's inequality [162, Chapter 5. Theorem 6], we have

$$\|P^1(t,\cdot)-P_0(\cdot)\|_{C^{1,\frac{1}{2}}} \le C\|P^1(t,\cdot)-P_0(\cdot)\|_{W^{2,4}},$$

where C is a constant depending only on Ω. For the sake of simplicity, we use the same notation C for a universal constant depending only on Ω in the following estimates. Moreover, by the classical elliptic estimates we have

$$\|P^1(t,\cdot)-P_0(\cdot)\|_{W^{2,4}} \le C\|w^1(t,\Pi(0,t;\cdot))-u_0(\cdot)\|_{L^4}.$$

This implies that

$$\begin{aligned}\|P^1(t,\cdot)-P_0(\cdot)\|_{C^1} &\le C\|w^1(t,\Pi(0,t;\cdot))-u_0(\cdot)\|_{L^4}\\ &\le C\|w^1(t,\Pi(0,t;\cdot))-u_0(\cdot)\|_{C^0}\\ &\le C\|w^1(t,\Pi(0,t;\cdot))-w^1(t,\cdot)\|_{C^0}+C\|w^1(t,\cdot)-u_0(\cdot)\|_{C^0}\\ &\le C\|w^1\|_{W^{1,\infty}}\|\Pi(0,t;\cdot)-\cdot\|_{C^0}+C\|w^1(t,\cdot)-u_0(\cdot)\|_{C^0}\\ &\le C\,C_1\|\Pi(0,t;\cdot)-\cdot\|_{C^0}+C\|w^1(t,\cdot)-u_0(\cdot)\|_{C^0}\\ &\le C\,C_1\,\tau\sup_{t\in[0,\tau]}\|\nabla P(t,\cdot)\|_{C^0}+C\|w^1(t,\cdot)-u_0(\cdot)\|_{C^0}\\ &\le C\,C_1\,\tau\,\kappa+C\|w^1(t,\cdot)-u_0(\cdot)\|_{C^0}\\ &\le C\,C_1\,\tau\,\kappa+C\|u_0\|_{C^0}\chi\left[\tau\tilde{F}+\tau\kappa\right],\end{aligned}$$

where we have used (3.1.43) for the last inequality . We can conclude

$$\sup_{t\in[0,\tau]}\|P^1(t,\cdot)-P_0(\cdot)\|_{C^1}\to 0,\quad \tau\to 0.$$

Thus, it suffice to take τ small enough to ensure the neighborhood condition (3.1.37).

Step 3. Contraction mapping In order to verify (3.1.38), we let $\begin{pmatrix}\tilde{w}\\ \tilde{P}\end{pmatrix},\begin{pmatrix}w\\ P\end{pmatrix}\in\overline{B_{\tilde{Z}^\tau}}\left(\begin{pmatrix}w^0\\ P^0\end{pmatrix},r\right)$. We observe that

$$\begin{aligned}\left|\tilde{w}^1(t,x)-w^1(t,x)\right| = \Big|&u_0(x)\exp\Big(\int_0^t F(w(l,x))+P(l,\Pi(l,0;x))\mathrm{d}l\Big)\\ &-u_0(x)\exp\Big(\int_0^t F(\tilde{w}(l,x))+\tilde{P}(l,\tilde{\Pi}(l,0;x))\mathrm{d}l\Big)\Big|.\end{aligned}$$

Due to the classical inequality $|e^x - e^y| \le e^{x+y}|x-y|$ which holds for any $x, y \in \mathbb{R}$, we deduce

$$\begin{aligned}
&\big|\tilde{w}^1(t,x) - w^1(t,x)\big| \\
&\quad\le \|u_0\|_{C^0} e^{2\tau(\tilde{F}+\kappa)}\Big[\int_0^t \|F(\tilde{w}(l,\cdot)) - F(w(l,\cdot))\|_{C^0}\mathrm{d}l \\
&\qquad + \int_0^t \|\tilde{P}(l,\tilde{\Pi}(l,0;\cdot)) - P(l,\Pi(l,0;\cdot))\|_{C^0}\mathrm{d}l\Big] \\
&\quad\le \|u_0\|_{C^0} e^{2\tau(\tilde{F}+\kappa)}\Big[\tau\tilde{F}\sup_{l\in[0,\tau]}\|\tilde{w}(l,\cdot) - w(l,\cdot)\|_{C^0} \\
&\qquad + \tau\sup_{l\in[0,\tau]}\|\tilde{P}(l,\tilde{\Pi}(l,0;\cdot)) - P(l,\tilde{\Pi}(l,0;\cdot))\|_{C^0} \\
&\qquad + \tau\sup_{l\in[0,\tau]}\|P(l,\tilde{\Pi}(l,0;\cdot)) - P(l,\Pi(l,0;\cdot))\|_{C^0}\Big] \\
&\quad\le \|u_0\|_{C^0} e^{2\tau(\tilde{F}+\kappa)}\Big[\tau\tilde{F}\sup_{l\in[0,\tau]}\|\tilde{w}(l,\cdot) - w(l,\cdot)\|_{C^0} + \tau\sup_{l\in[0,\tau]}\|\tilde{P}(l,\cdot) - P(l,\cdot)\|_{C^0} \\
&\qquad + \tau\sup_{l\in[0,\tau]}\|P(l,\cdot)\|_{W^{1,\infty}}\sup_{l\in[0,\tau]}\|\tilde{\Pi}(l,0;\cdot) - \Pi(l,0;\cdot)\|_{C^0}\Big] \\
&\quad\le \tau\|u_0\|_{C^0} e^{2\tau(\tilde{F}+\kappa)}\Big[\tilde{F}\|\tilde{w} - w\|_{X^\tau} + \|\tilde{P} - P\|_{Y^\tau} \\
&\qquad + C_2\sup_{l\in[0,\tau]}\|\tilde{\Pi}(l,0;\cdot) - \Pi(l,0;\cdot)\|_{C^0}\Big].
\end{aligned} \tag{3.1.45}$$

To estimate $\sup_{l\in[0,\tau]}\|\tilde{\Pi}(l,0;\cdot) - \Pi(l,0;\cdot)\|_{C^0}$ in (3.1.45), we claim that

$$\sup_{t,s\in[0,\tau]}\|\tilde{\Pi}(t,s;\cdot) - \Pi(t,s;\cdot)\|_{C^0} \le \tau e^{\tau C_2}\sup_{t\in[0,\tau]}\|\tilde{P}(l,\cdot) - P(l,\cdot)\|_{C^1} \tag{3.1.46}$$

Indeed, we can obtain that

$$\begin{aligned}
\big|\tilde{\Pi}(t,s;x) - \Pi(t,s;x)\big| &= \Big|\int_s^t \nabla\tilde{P}(l,\tilde{\Pi}(l,s;x)) - \nabla P(l,\Pi(l,s;x))\mathrm{d}l\Big| \\
&\le \int_s^t \|\nabla\tilde{P}(l,\tilde{\Pi}(l,s;\cdot)) - \nabla P(l,\tilde{\Pi}(l,s;\cdot))\|_{C^0}\mathrm{d}l \\
&\quad + \int_s^t \|\nabla P(l,\tilde{\Pi}(l,s;\cdot)) - \nabla P(l,\Pi(l,s;\cdot))\|_{C^0}\mathrm{d}l \\
&\le \tau\sup_{l\in[0,\tau]}\|\nabla\tilde{P}(l,\tilde{\Pi}(l,s;\cdot)) - \nabla P(l,\tilde{\Pi}(l,s;\cdot))\|_{C^0} \\
&\quad + \sup_{l\in[0,\tau]}\|\nabla P(l,\cdot)\|_{W^{1,\infty}}\int_s^t \|\tilde{\Pi}(l,s;\cdot) - \Pi(l,s;\cdot)\|_{C^0}\mathrm{d}l.
\end{aligned}$$

This leads to

$$\begin{aligned}
\sup_{t,s\in[0,\tau]}\|\tilde{\Pi}(t,s;\cdot) - \Pi(t,s;\cdot)\|_{C^0} &\le \tau\sup_{l\in[0,\tau]}\|\tilde{P}(l,\cdot) - P(l,\cdot)\|_{C^1} \\
&\quad + C_2\int_s^t \|\tilde{\Pi}(l,s;\cdot) - \Pi(l,s;\cdot)\|_{C^0}\mathrm{d}l.
\end{aligned}$$

Again due to Grönwall's inequality, we conclude that (3.1.46) holds.

Inserting (3.1.46) into (3.1.45) we have

$$\begin{aligned}
&\sup_{t\in[0,\tau]}\big\|\tilde{w}^1(t,\cdot) - w^1(t,\cdot)\big\|_{C^0} \\
&\quad\le \|u_0\|_{C^0} e^{2\tau(\tilde{F}+\kappa)}\Big[\tau\tilde{F}\|\tilde{w} - w\|_{X^\tau} + \tau\|\tilde{P} - P\|_{Y^\tau} + \tau^2\, C_2\, e^{\tau C_2}\|\tilde{P} - P\|_{Y^\tau}\Big] \\
&\quad\le \tau\|u_0\|_{C^0} e^{2\tau(\tilde{F}+\kappa)}\Big[\tilde{F}\|\tilde{w} - w\|_{X^\tau} + \big(1 + \tau\, C_2\, e^{\tau C_2}\big)\|\tilde{P} - P\|_{Y^\tau}\Big] \\
&\quad\le L_1(\tau)\Big[\|\tilde{w} - w\|_{X^\tau} + \|\tilde{P} - P\|_{Y^\tau}\Big],
\end{aligned} \tag{3.1.47}$$

where we set

$$L_1(\tau) := \tau \|u_0\|_{C^0} e^{2\tau(\tilde{F}+\kappa)} \left(\tilde{F} + \left(1 + \tau\, C_2\, e^{\tau C_2}\right)\right)$$

and $L_1(\tau) \to 0$ as $\tau \to 0$.

Next we prove the contraction property for $\|\tilde{P}^1 - P^1\|_{Y^\tau}$. As before, applying the same argument of Morrey's inequality and the classical elliptic estimates, we can deduce

$$\begin{aligned}
\|\tilde{P}^1(t,\cdot) - P^1(t,\cdot)\|_{C^1} &\leq C\|\tilde{w}^1(t,\tilde{\Pi}(0,t;\cdot)) - w^1(t,\Pi(0,t;\cdot))\|_{L^4} \\
&\leq C\|\tilde{w}^1(t,\tilde{\Pi}(0,t;\cdot)) - w^1(t,\Pi(0,t;\cdot))\|_{C^0} \\
&\leq C\|\tilde{w}^1(t,\tilde{\Pi}(0,t;\cdot)) - w^1(t,\tilde{\Pi}(0,t;\cdot))\|_{C^0} \\
&\quad + C\|w^1(t,\tilde{\Pi}(0,t;\cdot)) - w^1(t,\Pi(0,t;\cdot))\|_{C^0} \\
&\leq C\|\tilde{w}^1(t,\cdot) - w^1(t,\cdot)\|_{C^0} + C\|w^1\|_{W^{1,\infty}}\|\tilde{\Pi}(0,t;\cdot) - \Pi(0,t;\cdot)\|_{C^0} \\
&\leq C\|\tilde{w}^1(t,\cdot) - w^1(t,\cdot)\|_{C^0} + C\, C_1\|\tilde{\Pi}(0,t;\cdot) - \Pi(0,t;\cdot)\|_{C^0} \\
&\leq C\|\tilde{w}^1(t,\cdot) - w^1(t,\cdot)\|_{C^0} + C\, C_1\, \tau\, e^{\tau C_2} \sup_{t\in[0,\tau]} \|\tilde{P}(t,\cdot) - P(t,\cdot)\|_{C^1},
\end{aligned}$$

where we used (3.1.46) in the last inequality and C is a constant depending only on Ω. Defining $L_2(\tau) := C\, C_1\, \tau\, e^{\tau C_2}$ and together with (3.1.47) we obtain

$$\sup_{t\in[0,\tau]} \|\tilde{P}^1(t,\cdot) - P^1(t,\cdot)\|_{C^1} \leq C\, L_1(\tau)\left[\|\tilde{w} - w\|_{X^\tau} + \|\tilde{P} - P\|_{Y^\tau}\right] + L_2(\tau)\|\tilde{P} - P\|_{Y^\tau}. \tag{3.1.48}$$

Combing with (3.1.47) and (3.1.48) we deduce

$$\|\tilde{w}^1 - w^1\|_{X^\tau} + \|\tilde{P}^1 - P^1\|_{Y^\tau} \leq \left(C\, L_1(\tau) + L_2(\tau)\right)\left[\|\tilde{w} - w\|_{X^\tau} + \|\tilde{P} - P\|_{Y^\tau}\right], \tag{3.1.49}$$

where $L_i(\tau) \to 0,\ i = 1, 2$ as $\tau \to 0$. If τ is small enough, this implies (3.1.38) for some $\theta \in (0,1)$. Since $\tilde{Z}^\tau$ is complete metric space for the distance induced by the norm $(\|\cdot\|_{X^\tau}, \|\cdot\|_{Y^\tau})$ in Z_τ, the result follows by the classical Banach fixed point theorem. □

Remark 3.1.21. Let us mention that we can derive a maximal time of solutions as long as the $W^{1,\infty}(\Omega)$ norm of $u(t,.)$ stays bounded. This can be seen by using our local existence result together with the following observations. Let $t_0 > 0$ and assume that the solution exists until $t = t_0$. We define for all $t, s \geq t_0$

$$\begin{cases} \frac{\partial}{\partial t}\Pi_{t_0}(t,s;x) = -d\,\nabla P(t+t_0, \Pi_{t_0}(t,s;x)), \\ \Pi_{t_0}(s,s;x) = x \in \Omega. \end{cases} \tag{3.1.50}$$

Then by the uniqueness of solutions we deduce that

$$\Pi_{t_0}(t,s;x) = \Pi(t+t_0, s+t_0; x)$$

where Π is the solution of (3.1.4). Moreover

$$w(t+t_0,x) := u(t+t_0, \Pi(t+t_0,0;x)) = u(t+t_0, \Pi(t+t_0,t_0;\Pi(t_0,0;x)).$$

Choose $x = \Pi(t_0,0;\widehat{x})$ then in order to deal the fixed point problem starting t_0 it is natural to introduce

$$w_{t_0}(t,\widehat{x}) := w(t+t_0, \Pi(0,t_0;x)) = u(t+t_0, \Pi_{t_0}(t,0;\widehat{x})). \tag{3.1.51}$$

By combining equations (3.1.50)-(3.1.51), we can deduce the existence and uniqueness of solutions as long as the $W^{1,\infty}(\Omega)$ norm of $u(t,.)$ is bounded. This idea can be used to derive a maximal semiflow in the sense [274, Chapter 5].

3.1.5.3 Parameter fitting

From the work in [318], MCF-7 and MCF-7/Doxo cells are cultured at 10^5 initial number of cells separately in 60×15 mm cell Petri dish with or without doxorubicine. We use the cell proliferation data followed every 12 hours during six days to fit the parameters of the following ordinary differential equation

$$\begin{cases} \dfrac{du_i}{dt} = u_i(b_i - a_{ii}u_i) - \delta_i u_i \quad i = 1, 2. \\ u_i(0) = u_{i,0}. \end{cases} \tag{3.1.52}$$

Here we use u_1 to represent the MCF-7 (sensitive to drug) and u_2 to represent the MCF-7/Doxo (resistant to drug) and $b_i > 0$ is the growth rate δ_i is the extra mortality rate caused by drug (doxorubicine) treatment and $a_{ii} > 0$ is a coefficient which controls the carrying capacity.

In the work [367] cell proliferation kinetics for MCF-7 is studied over 11 days in 150 cm^2 flask. Following an inoculation of 3×10^5 cells at day 0, a maximum cell density of 8 to 9×10^7 cells/flask was reached at day 11. Therefore, we assume the carrying capacity for each species in 60×15 mm (surface of $21.5\, cm^2$) Petri dish satisfies

$$\frac{b_i}{a_{ii}} \approx 9 \times 10^7 \times \frac{21.5\, cm^2}{150\, cm^2} = 1.29 \times 10^7, \quad i = 1, 2.$$

By fixing the carrying capacity, we first estimate the growth rate b_i of each species under zero drug concentration, namely $\delta_i = 0$. We divide the number of cells by $u_{i,0} = 10^5$ (the initial number of cells) and rescale the parameters as follows

$$\tilde{u}_i = \frac{u_i}{10^5}, \quad \tilde{a}_i = a_{ii} \times 10^5, \quad \tilde{b}_i = b_i. \tag{3.1.53}$$

As seen in Figure 3.1.23, without treatment, MCF-7 and MCF-7/Doxo displayed very similar growth rates, 0.6420 and 0.6359 per day, respectively.

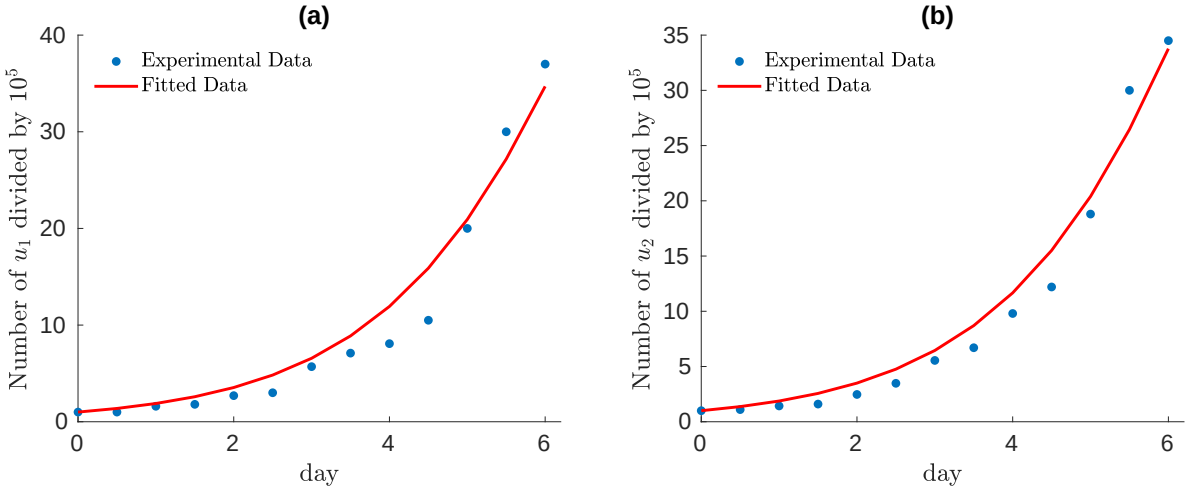

Figure 3.1.23: *Fitting for the parameters (under rescaling* (3.1.53)*) in model* (3.1.52)*. We plot the experimental data (dots in (a)) of MCF-7 (sensitive to drug) and (dots in (b)) MCF-7/Doxo (resistant to drug) with no drug concentration over 6 days. We obtain an estimation of the growth rates* $b_1 = 0.6420, b_2 = 0.6359$ *and* $a_{11} = 0.0050, a_{22} = 0.0049$.

By fixing the parameters

$$b_1 = 0.6420,\ a_{11} = 0.0050, \quad b_2 = 0.6359,\ a_{22} = 0.0049, \tag{3.1.54}$$

we consider different scenarios with the drug concentration varies from $0.1\,\mu M$ to $10\,\mu M$ (see Figure 3.1.24) and we estimate the extra mortality rate δ_i for each population due to doxorubicine (see Table 3.1.4).

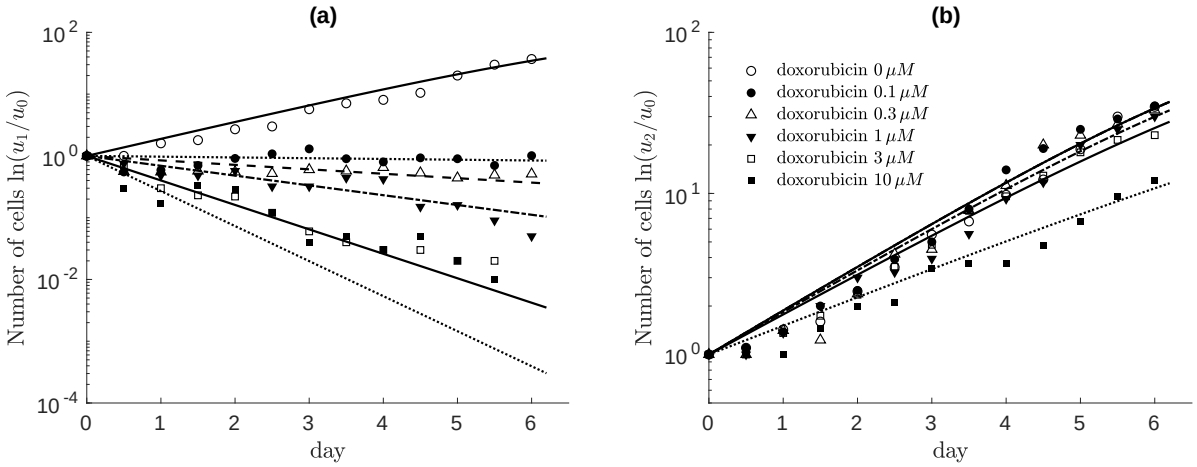

Figure 3.1.24: *Fitting for the growth curves of MCF-7 (a) and MCF-7/Doxo (b) under different drug concentrations in model* (3.1.52) *over 6 days. Cells were grown in the absence or presence of doxorubicine (0.1 to 10 μM, corresponding symbols given in the legend in (b)) and counted every 12 hours in a Malassez chamber. Cell counts are expressed as the logarithm of the numbers of cells (u_i) divided by the number of cells at day 0 ($u_{i,0}$). We fix the growth rate b_i and a_{ii}, $i = 1, 2$ as in* (3.1.54).

Drug concentration (μM)	0	0.1	0.3	1	3	10
Extra mortality δ_1 (day^{-1})	0	0.6619	0.8109	1.0118	1.5585	1.9545
Extra mortality δ_2 (day^{-1})	0	0	0	0.0246	0.0569	0.2192

Table 3.1.4: *List of the estimation of extra mortality rate δ_1 for the sensitive cell and δ_2 for the resistant cell under different concentrations of doxorubicine.*

3.1.5.4 Numerical Scheme

For simplicity, we give the numerical scheme for the following one species and one dimensional model

$$\begin{cases} \partial_t u + d\,\partial_x\left(u\partial_x P\right) = f(u) & \\ (I - \chi\Delta)P(t,x) = u(t,x) & \text{in } (0,T]\times[-L,L] \\ \partial_x P(t,\pm L) = 0 & \text{on } [0,T]. \end{cases} \tag{3.1.55}$$

The numerical method used is based on finite volume method. We refer to [249, 376] for more results about this subject. Our numerical scheme reads as follows

$$\begin{aligned} & u_i^{n+1} = u_i^n - d\,\frac{\Delta t}{\Delta x}\Big(\phi(u_{i+1}^n, u_i^n) - \phi(u_i^n, u_{i-1}^n)\Big) + \Delta t\, f(u_i^n), \\ & i = 1, 2, ..., M,\ \ n = 0, 1, 2, ..., N, \end{aligned} \tag{3.1.56}$$

with the flux $\phi(u_{i+1}^n, u_i^n)$ defined as

$$\phi(u_{i+1}^n, u_i^n) = (v_{i+\frac{1}{2}}^n)^+ u_i^n - (v_{i+\frac{1}{2}}^n)^- u_{i+1}^n = \begin{cases} v_{i+\frac{1}{2}}^n u_i^n, & v_{i+\frac{1}{2}}^n \geq 0, \\ v_{i+\frac{1}{2}}^n u_{i+1}^n, & v_{i+\frac{1}{2}}^n < 0. \end{cases} \tag{3.1.57}$$

and

$$v_{i+\frac{1}{2}}^n = -\frac{l_{i+1}^n - l_i^n}{\Delta x},\ i = 0, 1, 2, \cdots, M, \tag{3.1.58}$$

where we define

$$L^n := (I - \chi A)^{-1} U^n, \quad n = 0, 1, 2, ..., N, \quad L_i^n = \left(l_i^n\right)_{M\times 1} \quad U^n = \left(u_i^n\right)_{M\times 1}.$$

where χ is a constant and $A = (a_{i,j})_{M\times M}$ is the usual linear diffusion matrix with Neumann boundary condition. Therefore, since the Neumann boundary condition corresponds to a no flux boundary condition, we impose

$$\begin{aligned} \phi(u_1^n, u_0^n) &= 0, \\ \phi(u_{M+1}^n, u_M^n) &= 0. \end{aligned} \tag{3.1.59}$$

which corresponds to $l_0 = l_1$ and $l_{M+1} = l_M$.

The numerical scheme at the boundary becomes

$$\begin{aligned} u_1^{n+1} &= u_1^n - d\,\frac{\Delta t}{\Delta x}\phi(u_2^n, u_1^n) + \Delta t\, f(u_1^n), \\ u_M^{n+1} &= u_M^n + d\,\frac{\Delta t}{\Delta x}\phi(u_M^n, u_{M-1}^n) + \Delta t\, f(u_M^n). \end{aligned}$$

By this boundary condition, we have the conservation of mass for Equation (3.1.55) when the reaction term $f \equiv 0$.

3.2 Existence and uniqueness of solutions for a hyperbolic Keller–Segel equation

3.2.1 Introduction

In this section 3.2 we are concerned with the following diffusion equation with logistic source:

$$\begin{cases} \partial_t u(t,x) - \chi \partial_x \big(u(t,x)\partial_x p(t,x)\big) = u(t,x)(1-u(t,x)), \quad t>0,\ x\in\mathbb{R}, \\ u(t=0,x) = u_0(x), \end{cases} \tag{3.2.1}$$

where $\chi > 0$ is a *sensing coefficient* and $p(t,x)$ is an external pressure. Model (3.2.1) describes the behavior of a population of cells $u(t,x)$ living in a one-dimensional habitat $x \in \mathbb{R}$, which undergo a logistic birth and death population dynamics, and in which individual cells follow the gradient of a field p. The constant χ characterizes the response of the cells to the effective gradient p_x. In this work we will consider the case where p is itself determined by the state of the population $u(t,x)$ as

$$-\sigma^2 \partial_{xx} p(t,x) + p(t,x) = u(t,x), \quad t>0, x\in\mathbb{R}. \tag{3.2.2}$$

This corresponds to a scenario in which the field $p(t,x)$ is produced by the cells, diffuses to the whole space with diffusivity σ^2 (for $\sigma > 0$), and vanishes at rate one. As a result cells are pushed away from crowded area to emptier region.

A similar model has been successfully used in our recent work [P8] to describe the motion of cancer cells in a Petri dish in the context of cell co-culture experiments of Pasquier et al. [318]. Pasquier et al. [318] cultivated two types of breast cancer cells to study the transfer of proteins between them in a study of multi-drug resistance. It was observed that the two types of cancer cells form segregated clusters of cells of each kind after a 7-day co-culture experiment. In [P8], the authors studied the segregation property of a model similar to (3.2.1)–(3.2.2), set in a circular domain in two spatial dimensions $x \in \mathbb{R}^2$ representing a Petri dish. The study aims at describing the cancer cells motion in a Petri dish [P8, 318] in the context of a batch culture. The cell population should be regarded as a mono-layer attached to the bottom of the Petri dish covered a large quantity of nutritional liquid (used in the cell culture), which is constantly renewed.

Our model can be included in the family of non-local advection models for cell-cell adhesion and repulsion. As pointed out by many biologists, cell-cell interactions do not only exist in a local scope, but a long-range interaction should be taken into account to guide the mathematical modeling. Armstrong, Painter and Sherratt [16] in their early work proposed a model (APS model) in which a local diffusion is added to the non-local attraction driven by the adhesion forces to describe the phenomenon of cell mixing, full/partial engulfment and complete sorting in the cell sorting problem. Based on the APS model, Murakawa and Togashi [296] thought that the population pressure should come from the cell volume size instead of the linear diffusion. Therefore, the linear diffusion was changed into a nonlinear diffusion in order to capture the sharp fronts and the segregation in cell co-culture. Carrillo et al. [105] recently proposed a new assumption on the adhesion velocity field and their model showed a good agreement in the experiments in the work of Katsunuma et al. [229]. The idea of the long-range attraction and short-range repulsion can also be seen in the work of Leverentz, Topaz and Bernoff [250]. They considered a non-local advection model to study the asymptotic behavior of the solution. By choosing a Morse-type kernel which follows the attractive-repulsive interactions, they found that the solution can asymptotically spread, contract (blow-up), or reach a steady-state. Burger, Fetecau and Huang [83] considered a similar non-local adhesion model with nonlinear diffusion, for which they investigated the well-posedness and proved the existence of a compactly supported, non-constant steady state. Dyson et al. [156] established the local existence of a classical solution for a non-local cell-cell adhesion model in spaces of uniformly continuous functions. For Turing and Turing-Hopf bifurcation due to the non-local effect, we refer to Ducrot et al. [151] and Song et al. [365]. We also refer to Mogliner et al. [288], Eftimie et al. [158], Ducrot and Magal [152], Ducrot and Manceau [153] for more topics on non-local advection equations. For the derivation of such models, we refer to the work of Bellomo et al. [44] and Morale, Capasso and Oelschläger [290].

It can be noticed that, in the limit of slow diffusivity $\sigma \to 0$ (and under the simplifying assumption that $\chi = 1$), we get $u(t,x) \equiv p(t,x)$ and (3.2.1) is equivalent to an equation with *porous medium-type diffusion* and logistic reaction

$$u_t - \frac{1}{2}(u^2)_{xx} = u(1-u). \tag{3.2.3}$$

The propagation dynamics for this kind of equation was first studied, to the extent of our knowledge, by Aronson [21], Atkinson, Reuter and Ridler-Rowe [23], and later by de Pablo and Vázquez [313], in the more general context of nonlinear diffusion

$$u_t = (u^m)_{xx} + u(1-u), \text{ with } m > 1. \tag{3.2.4}$$

We refer to the monograph of Vázquez [380] for a detailed study of solutions to porous medium equations.

The particular relation between the pressure $p(t,x)$ and the density $u(t,x)$ in (3.2.2) strongly reminds the celebrated model of chemotaxis studied by Patlak (1953) and Keller and Segel (1970) [320, 233, 232] (parabolic-parabolic Keller-Segel model) and, more specifically, the parabolic-elliptic Keller-Segel model which is derived from the former by a quasi-stationary assumption on the diffusion of the chemical [226]. Indeed Equation (3.2.2) can be formally obtained as the quasistatic approximation of the following parabolic equation

$$\varepsilon \partial_t p(t,x) = \chi p_{xx}(t,x) + u(t,x) - p(t,x),$$

when $\varepsilon \to 0$.

A rigorous derivation of the limit has been achieved in the case of the Keller-Segel model by Carrapatoso and Mischler [103]. We refer to [94, 209, 323] and the references therein for a mathematical introduction and biological applications. In these models, the field $p(t,x)$ is interpreted as the concentration of a chemical produced by the cells rather than a physical pressure. One of the difficulties in attractive chemotaxis models is that two opposite forces compete to drive the behavior of the equations: the *diffusion* due to the random motion of cells, on the one hand, and on the other hand the *non-local advection* due to the attractive chemotaxis; the former tends to regularize and homogenize the solution, while the latter promotes cell aggregation and may lead to the blow-up of the solution in finite time [109, 226].

Since the pressure $p(t,x)$ is a non-local function of the density $u(t,x)$ in (3.2.2), the spatial derivative appears as a *non-local advection* term in (3.2.1). In fact, our problem (3.2.1)–(3.2.2) can be rewritten as a transport equation in which the speed of particles is non-local in the density,

$$\begin{cases} \partial_t u(t,x) - \chi \partial_x (u(t,x) \partial_x (\rho \star u)(t,x)) = u(t,x)(1-u(t,x)) \\ u(t=0,x) = u_0(x), \end{cases} \tag{3.2.5}$$

where

$$(\rho \star u)(x) = \int_{\mathbb{R}} \rho(x-y) u(t,y) dy, \quad \rho(x) = \frac{1}{2\sigma} e^{-\frac{|x|}{\sigma}}. \tag{3.2.6}$$

Traveling waves for a similar diffusive equation with logistic reaction have been investigated for quite general non-local kernels by Hamel and Henderson [198], who considered the model

$$u_t + (u\,(K \star u))_x = u_{xx} + u(1-u), \tag{3.2.7}$$

where $K \in L^p(\mathbb{R})$ is odd and $p \in [1, \infty]$. Notice that the attractive parabolic-elliptic Keller-Segel model is included in this framework by the particular choice

$$K(x) = -\chi \operatorname{sign}(x) e^{-|x|/\sqrt{d}} / \left(2\sqrt{d}\right).$$

They proved a spreading result for this equation (initially compactly supported solutions to the Cauchy problem propagate to the whole space with constant speed) and explicit bounds on the speed of propagation. Diffusive non-local advection also appears in the context of swarm formation [289]. Pattern formation for a model similar to (3.2.7) by Ducrot, Fu and Magal [151]. Let us mention that the inviscid equation (3.2.5) has been studied in a periodic cell by Ducrot and Magal [152]. A substantial literature has been produced for conservative systems of interacting particles and their kinetic limit (Balagué et al. [30], Carrillo et al. [104], Bernoff and Topaz [57], Bertozzi, Laurent and Rosado [60], among others).

This section 3.2 is a part of a set of two. Here we study the well-posed character of the Cauchy problem (3.2.1)–(3.2.2). In a the next section 3.3, we will build on these results to study the propagation dynamics of compactly supported initial conditions and the existence of sharp discontinuous traveling waves for the model (3.2.1)–(3.2.2).

In this section 3.2 we focus on the particular case of (3.2.1)–(3.2.2) with $\sigma > 0$ and $\chi > 0$. The section 3.2 is organized as follows. In Section 2, we present our main results. Section 3 is devoted to the well-posedness of the Cauchy problem for system (3.2.1)–(3.2.2).

3.2.2 Main results

We begin by defining our notion of solution to equation (3.2.1).

Definition 3.2.1 (Integrated solutions)**.** Let $u_0 \in L^\infty(\mathbb{R})$. A measurable function $u(t,x) \in L^\infty([0,T]\times\mathbb{R})$ is an *integrated solution* to (3.2.1) if the characteristic equation

$$\begin{cases} \dfrac{\mathrm{d}}{\mathrm{d}t}h(t,x) = -\chi(\rho_x \star u)(t,h(t,x)) \\ h(t=0,x) = x. \end{cases} \tag{3.2.8}$$

has a classical solution $h(t,x)$ (*i.e.* for each $x\in\mathbb{R}$ fixed, the function $t\mapsto h(t,x)$ is in $C^1([0,T],\mathbb{R})$ and satisfies (3.2.8)), and for a.e. $x\in\mathbb{R}$, the function $t\mapsto u(t,h(t,x))$ is in $C^1([0,T],\mathbb{R})$ and satisfies

$$\begin{cases} \dfrac{\mathrm{d}}{\mathrm{d}t}u(t,h(t,x)) = u(t,h(t,x))\big(1+\hat{\chi}(\rho\star u)(t,h(t,x)) - (1+\hat{\chi})u(t,h(t,x))\big), \\ u(t=0,x) = u_0(x), \end{cases} \tag{3.2.9}$$

where $\hat{\chi} := \frac{\chi}{\sigma^2}$.

We define weighted space $L^1_\eta(\mathbb{R})$ as follows

$$L^1_\eta(\mathbb{R}) := \left\{ f:\mathbb{R}\to\mathbb{R} \text{ measurable} \,\middle|\, \int_{\mathbb{R}} |f(x)|e^{-\eta|x|}\mathrm{d}x < \infty \right\}.$$

$L^1_\eta(\mathbb{R})$ is a Banach space endowed with the norm

$$\|f\|_{L^1_\eta} := \frac{\eta}{2}\int_{\mathbb{R}} |f(y)|e^{-\eta|y|}\mathrm{d}y.$$

Our first result concerns the existence of integrated solutions to (3.2.1).

Theorem 3.2.2 (Well-posedness)**.** *Let $u_0 \in L^\infty_+(\mathbb{R})$ and fix $\eta>0$. There exists $\tau^*(u_0)\in(0,+\infty]$ such that for all $\tau\in(0,\tau^*(u_0))$, there exists a unique integrated solution $u\in C^0([0,\tau],L^1_\eta(\mathbb{R}))$ to (3.2.1) which satisfies $u(t=0,x)=u_0(x)$. Moreover $u(t,\cdot)\in L^\infty(\mathbb{R})$ for each $t\in[0,\tau^*(u_0))$ and the map $t\in[0,\tau^*(u_0))\mapsto T_t u_0 := u(t,\cdot)$ is a semigroup which is continuous for the $L^1_\eta(\mathbb{R})$-topology. The map $u_0\in L^\infty(\mathbb{R})\mapsto T_t u_0\in L^1_\eta(\mathbb{R})$ is continuous.*

Finally, if $0\le u_0(x)\le 1$, then $\tau^*(u_0)=+\infty$ and $0\le u(t,\cdot)\le 1$ for all $t>0$.

Next we show that the semiflow preserves some properties satisfied by the initial condition, namely the monotony, continuity and continuous differentiability. In the case of a $C^1(\mathbb{R})$ initial condition, we show that the solution integrated along the characteristics is actually a classical pointwise solution to the original problem (3.2.1)–(3.2.2).

Proposition 3.2.3 (Regularity of solutions)**.** *Let $u(t,x)$ be an integrated solution to (3.2.1).*

1. *if $u_0(x)$ is continuous, then $u(t,x)$ is continuous for each $t>0$.*
2. *if $u_0(x)$ is monotone, then $u(t,x)$ has the same monotony for each $t>0$.*
3. *if $u_0(x)\in C^1(\mathbb{R})$, then $u\in C^1([0,T]\times\mathbb{R})$ and u is then a classical solution to (3.2.1)–(3.2.2).*

Next we show the long-time behavior of the solutions to (3.2.1).

Theorem 3.2.4 (Long-time behavior)**.** *Let $0\le u_0(x)\le 1$ be a nontrivial non-negative initial condition and $u(t,x)$ be the corresponding integrated solution. Then $0\le u(t,x)\le 1$ for all $t>0$ and $x\in\mathbb{R}$. If moreover there exists $\delta>0$ such that $\delta\le u_0(x)\le 1$ then*

$$u(t,x)\to 1, \text{ as } t\to\infty$$

and the convergence holds uniformly in $x\in\mathbb{R}$.

The case of bounded initial conditions which are not positively bounded from below is more complex. In the case of initial conditions which are compactly supported, we expect that the support will expand to the whole space with constant speed and that the profile of the solution reaches an asymptotic shape (traveling wave). This situation will be investigated in section 3.3.

3.2.3 Well-posedness of the Cauchy problem

In this section 3.2.3 we investigate the existence and uniqueness of solutions for the system (3.2.8)-(3.2.9). The idea to construct a fixed point problem is to consider the two variables

$$w(t,x) = u(t,h(t,x)) \text{ and } p(t,x) = (\rho \star u)(t,x).$$

Before we state the theorem, let us introduce some functional spaces and definitions. We introduce the following weighted L^1 space for any $\eta > 0$, as

$$L^1_\eta(\mathbb{R}) := \left\{ f : \mathbb{R} \to \mathbb{R} \text{ measurable} \,\middle|\, \int_{\mathbb{R}} |f(x)| e^{-\eta|x|} \mathrm{d}x < \infty \right\},$$

endowed with the norm $\|f\|_{L^1_\eta} := \frac{\eta}{2} \int_{\mathbb{R}} |f(y)| e^{-\eta|y|} \mathrm{d}y$. Then for any $\eta > 0$ the space $L^1_\eta(\mathbb{R})$ is a Banach space and for any $0 < \eta < \eta' < +\infty$ we have

$$L^\infty(\mathbb{R}) \subset L^1_\eta(\mathbb{R}) \subset L^1_{\eta'}(\mathbb{R}) \subset L^1_{loc}(\mathbb{R}).$$

We will say that a measurable set $\mathcal{U} \subset \mathbb{R}$ is *conull* if $|\mathbb{R} \backslash \mathcal{U}| = 0$, where $|A|$ is the Lebesgue measure of the set A. In what follows we need to work in the space of regular bounded functions on a measurable set $\mathcal{U} \subset \mathbb{R}$. Let us recall that the space

$$\mathcal{L}^\infty(\mathcal{U}) := \left\{ f : \mathcal{U} \to \mathbb{R} \,\middle|\, \sup_{x \in \mathcal{U}} |f(x)| < +\infty \right\},$$

endowed with the norm $\|f\|_{\mathcal{L}^\infty(\mathcal{U})} := \sup_{x \in \mathcal{U}} |f(x)|$, is a Banach space. If $\mathcal{U}$ is conull then $\mathcal{L}^\infty(\mathcal{U})$ is continuously embedded in $L^\infty(\mathbb{R})$ since

$$\|f\|_{L^\infty(\mathbb{R})} \leq \|f\|_{\mathcal{L}^\infty(\mathcal{U})}.$$

Finally we introduce the fixed point problem which is the key element of our proof of Theorem 3.2.2. Let $\tau > 0$ and $\mathcal{U} \subset \mathbb{R}$ be a conull set, we introduce the function spaces:

$$\begin{gathered} X^\tau_{\mathcal{U}} := C^0\big([0,\tau], \mathcal{L}^\infty(\mathcal{U})\big), \quad \tilde{X}^\tau_{\mathcal{U}} := C^0\big([0,\tau], \mathcal{L}^\infty_+(\mathcal{U})\big), \\ Y^\tau := C^0\big([0,\tau], W^{1,\infty}(\mathbb{R})\big), \\ \tilde{Y}^\tau := \{p \in Y^\tau \,|\, p(t,\cdot) \in W^{2,\infty}(\mathbb{R}) \text{ for all } t \in [0,\tau] \\ \text{and } \sup_{t \in [0,\tau]} \|p_{xx}(t,\cdot)\|_{L^\infty(\mathbb{R})} < +\infty\}, \\ Z^\tau_{\mathcal{U}} := X^\tau_{\mathcal{U}} \times Y^\tau, \quad \tilde{Z}^\tau_{\mathcal{U}} := \tilde{X}^\tau_{\mathcal{U}} \times \tilde{Y}^\tau. \end{gathered} \tag{3.2.10}$$

Clearly, $\tilde{X}^\tau_{\mathcal{U}}$ is closed in the Banach space $C^0\big([0,\tau], \mathcal{L}^\infty(\mathcal{U})\big)$. $\tilde{Y}^\tau$ is not closed in $C^0\big([0,\tau], W^{1,\infty}(\mathbb{R})\big)$, however for each $K > 0$, the set

$$\tilde{Y}^\tau_K := \{p \in \tilde{Y}^\tau \,|\, \sup_{t \in [0,\tau]} \|p_{xx}(t,\cdot)\|_{L^\infty(\mathbb{R})} \leq K\} \tag{3.2.11}$$

is closed in Y^τ. Indeed, let $p^n(t,x) \to p(t,x)$ be a converging sequence in Y^τ. Since $C^0\big([0,\tau], W^{1,\infty}(\mathbb{R})\big)$ is a Banach space we have $p \in C^0\big([0,\tau], W^{1,\infty}(\mathbb{R})\big)$. Moreover for each $t \in [0,\tau]$ there exists a measurable set $E_t \subset \mathbb{R}$ such that $\int_{\mathbb{R} \backslash E_t} 1 \mathrm{d}x = 0$, $p^n_x(t,x)$ and $p_x(t,x)$ are well-defined for any $x \in E_t$ and $\lim_{n \to +\infty} p^n_x(t,x) = p_x(t,x)$ for each $x \in E$. Let $x, y \in E_t$, we have:

$$\begin{aligned} |p_x(t,x) - p_x(t,y)| &\leq |p_x(t,x) - p^n_x(t,x)| + |p^n_x(t,x) - p^n_x(t,y)| + |p^n_x(t,y) - p^n_x(t,y)| \\ &\leq |p_x(t,x) - p^n_x(t,x)| + K|x-y| + |p^n_x(t,y) - p^n_x(t,y)|. \end{aligned}$$

Taking the limit $n \to \infty$, we obtain

$$|p_x(t,x) - p_x(t,y)| \leq K|x-y|$$

hence $\|p_{xx}\|_{L^\infty} \leq K$ and $p \in \tilde{Y}^\tau_K$.

Given $p \in \tilde{Y}^\tau$, let h be the solution of the following equation

$$\begin{cases} \frac{\partial}{\partial t} h(t,s;x) = -\chi p_x(t, h(t,s;x)), \\ h(s,s;x) = x. \end{cases} \tag{3.2.12}$$

The existence of the solution h is ensured by $p \in \tilde{Y}^\tau$. Moreover,

(i) for any x, the mapping $t \mapsto p_x(t,x)$ is continuous;

(ii) the vector field $p_x(t,x)$ is Lipschitz continuous with respect to x and the Lipschitz coefficient is uniform with respect to t on $[0,\tau]$. *In particular the image of* $\mathcal{U}$ *by* $h(t,s;\cdot)$ *is still conull for any* $t,s \in [0,\tau]$.

We are now in the position to define the mapping $\mathcal{T}^\tau_{\mathcal{U}}[u_0]$ to which we aim at applying a fixed-point theorem:

$$\mathcal{T}^\tau_{\mathcal{U}}[u_0](w,p)(t,x) = \begin{pmatrix} u_0(x)\exp\Big(\int_0^t 1+\hat{\chi}p(l,h(l,0;x)) - (1+\hat{\chi})w(l,x)\mathrm{d}l\Big) \\ \int_{\mathbb{R}} \rho(x-h(t,0;z))u_0(z)e^{\int_0^t 1-w(l,z)\mathrm{d}l}\mathrm{d}z \end{pmatrix}^T, \tag{3.2.13}$$

where

$$(w,p) \in Z^\tau_{\mathcal{U}} := X^\tau_{\mathcal{U}} \times Y^\tau.$$

Remark 3.2.5. In formula (3.2.13), the function h must be understood as the solution of (3.2.12) where p the argument of the function $\mathcal{T}^\tau_{\mathcal{U}}[u_0](w,p)$.

Remark 3.2.6. Since we only impose u_0 to be in L^∞ the time of local existence will depend on each value $u_0(x)$. That is why we are not considering the class of functions L^∞ for $w(t,\cdot)$. Instead we work in the space $\mathcal{L}^\infty(\mathcal{U})$ for $w(t,\cdot)$.

Our first result is the well-definition of $\mathcal{T}^\tau_{\mathcal{U}}[u_0]$. We start with a series technical Lemma.

Lemma 3.2.7 (Lipschitz continuity of the characteristic flow)**.** *Let* $\tau > 0$, $K > 0$ *and* $p \in \tilde{Y}^\tau_K$ *be given (recall that by definition of* $\tilde{Y}^\tau_K$, p_{xx} *is uniformly bounded:* $\sup_{t\in[0,\tau]} \|p_{xx}(t,\cdot)\|_{L^\infty(\mathbb{R})} \leq K < +\infty$*). Then, the solution* $h(t,s;x)$ *to* (3.2.12) *satisfies*

$$|h(t,s;x) - h(t,s;y)| \leq e^{K\chi|t-s|}|x-y|. \tag{3.2.14}$$

Proof. The integrated form of (3.2.12) is

$$h(t,s;x) = x + \int_s^t -\chi p_x(l,h(l,x;x))\mathrm{d}l,$$

therefore

$$\begin{aligned} |h(t,s;x) - h(t,s;y)| &\leq |x-y| + \chi\int_s^t |p_x(t,h(t,s;x)) - p_x(t,h(t,s;y))|\mathrm{d}y \\ &\leq |x-y| + \chi \sup_{t\in[0,\tau]} \|p_{xx}(t,\cdot)\|_{L^\infty(\mathbb{R})} \int_s^t |h(l,s;x) - h(l,s;y)|\mathrm{d}y \\ &\leq |x-y| + K\chi\int_s^t |h(l,s;x) - h(l,s;y)|\mathrm{d}y, \end{aligned}$$

since $p \in \tilde{Y}^\tau_K$. Grönwall's inequality [107, Lemma 4.2.1] implies:

$$|h(t,s;x) - h(t,s;y)| \leq e^{K\chi|t-s|}|x-y|.$$

Lemma 3.2.7 is proved. □

Lemma 3.2.8. *Let* $\tilde{p}, p \in \tilde{Y}^\tau_K$ *(where* $\tilde{Y}^\tau_K$ *is defined as in* (3.2.11)*) and* $\tilde{h}, h$ *be the corresponding characteristic flows defined in* (3.2.12) *with* p *and* $\tilde{p}$ *respectively. Then for any* $\tau > 0$ *and* $t,s \in [0,\tau]$ *we have*

$$\|\tilde{h}(t,s;\cdot) - h(t,s;\cdot)\|_{L^\infty(\mathbb{R})} \leq |t-s|\chi \sup_{l\in[0,\tau]} \|\tilde{p}_x(l,\cdot) - p_x(l,\cdot)\|_{L^\infty(\mathbb{R})} e^{K\chi|t-s|}$$

Proof. Without loss of generality we suppose $t \geq s$, then

$$\begin{aligned} \partial_t\big(\tilde{h}(t,s;x) - h(t,s;x)\big) &= -\chi\tilde{p}_x(t,\tilde{h}(t,s;x)) + \chi p_x(t,h(t,s;x)) \\ &= -\chi\tilde{p}_x(t,\tilde{h}(t,s;x)) + \chi p_x(t,\tilde{h}(t,s;x)) - \chi p_x(t,\tilde{h}(t,s;x)) \\ &\quad + \chi p_x(t,h(t,s;x)). \end{aligned}$$

Therefore, we have

$$\begin{aligned}\|\tilde{h}(t,s;\cdot)-h(t,s;\cdot)\|_{L^\infty(\mathbb{R})}&\\ &\leq |t-s|\chi \sup_{l\in[s,t]}\|p_x(l,\cdot)-\tilde{p}_x(l,\cdot)\|_{L^\infty(\mathbb{R})}\\ &\quad+\chi\sup_{l\in[0,\tau]}\|p_{xx}(l,\cdot)\|_{L^\infty(\mathbb{R})}\int_s^t\|\tilde{h}(l,s;\cdot)-h(l,s;\cdot)\|_{L^\infty(\mathbb{R})}\mathrm{d}l.\end{aligned}$$

The result follows from Grönwall's inequality and the definition of $\tilde{Y}_K^\tau$. □

Lemma 3.2.9 (Continuity properties)**.** *Let $(w,p)\in\tilde{Z}_{\mathcal{U}}^\tau$ be given. Then, the function $u(t,x):=w(t,h(0,t;x))$, defined for each $t\in[0,\tau]$ and a.e. $x\in\mathbb{R}$, is a continuous function of time for the $L^1_\eta(\mathbb{R})$ topology (i.e., the map $t\mapsto u(t,\cdot)$ is continuous in $L^1_\eta(\mathbb{R})$). The maps $t\mapsto(\rho\star u)(t,\cdot)$ and $t\mapsto(\rho_x\star u)(t,\cdot)$ are continuous for the $C^0_b(\mathbb{R})$ topology and moreover $(\rho\star u)(t,\cdot)\in W^{2,\infty}(\mathbb{R})$ for all $t\in[0,\tau]$.*

Proof. Let $(w,p)\in\tilde{Z}_{\mathcal{U}}^\tau$ be given. We first remark that, since p_x is Lipschitz continuous, the function $h(t,s;\cdot)$ is locally Lipschitz continuous for all $t,s\in[0,\tau]$ and therefore $h(t,0;\mathcal{U})$ is conull. In particular, $u(t,x)$ is well-defined for every $x\in h(t,0;\mathcal{U})$, therefore almost everywhere, for each $t\in[0,\tau]$.

We divide the rest of the proof in two steps.

Step 1. We show the continuity of $t\mapsto u(t,\cdot)$.

Let $t\in[0,\tau]$ and $\varepsilon>0$ be given. For $s\in[0,\tau]$, we have:

$$\begin{aligned}\|u(t,\cdot)-u(s,\cdot)\|_{L^1_\eta}&=\frac{\eta}{2}\int_{\mathbb{R}}|w(t,h(0,t;x))-w(s,h(0,s;x))|e^{-\eta|x|}\mathrm{d}x\\ &\leq\frac{\eta}{2}\int_{\mathbb{R}}|w(t,h(0,t;x))-w(t,h(0,s;x))|e^{-\eta|x|}\mathrm{d}x\\ &\quad+\frac{\eta}{2}\int_{\mathbb{R}}|w(t,h(0,s;x))-w(s,h(0,s;x))|e^{-\eta|x|}\mathrm{d}x.\end{aligned}$$

By the continuity of $t\mapsto w(t,\cdot)$ in $\mathcal{L}^\infty(\mathcal{U})$, there is $\delta_0>0$ such that if $|t-s|\leq\delta_0$, then $\|w(t,\cdot)-w(s,\cdot)\|_{\mathcal{L}^\infty(\mathcal{U})}\leq\frac{\varepsilon}{2}$. Therefore if $|t-s|\leq\delta_0$,

$$\begin{aligned}\|u(t,\cdot)-u(s,\cdot)\|_{L^1_\eta}&\\ &\leq\frac{\eta}{2}\int_{\mathbb{R}}|w(t,h(0,t;x))-w(t,h(0,s;x))|e^{-\eta|x|}\mathrm{d}x+\|w(t,\cdot)-w(s,\cdot)\|_{\mathcal{L}^\infty(\mathcal{U})}\\ &\leq\frac{\eta}{2}\int_{\mathbb{R}}|w(t,h(0,t;x))-w(t,h(0,s;x))|e^{-\eta|x|}\mathrm{d}x+\frac{\varepsilon}{2}.\end{aligned}$$

Next we select $R>0$ sufficiently large, so that

$$\begin{aligned}\min(h(s,0;R),-h(s,0;-R))&\\ &\geq\frac{-1}{\eta}\ln\left(\frac{\varepsilon}{18\sup_{t\in[0,\tau]}\|w\|_{\mathcal{L}^\infty(\mathcal{U})}}\right)\text{ for all }s\in[t-\delta_0,t+\delta_0].\end{aligned}$$

By the density of compactly supported smooth function in $L^1(-R,R)$, there is $\varphi\in C^1_c([-R,R])$ such that

$$\|w-\varphi\|_{L^1(-R,R)}\leq\frac{\varepsilon}{18\eta}e^{-K\chi(t+\delta_0)}.$$

Then, we have:

$$\begin{aligned}\|u(t,\cdot)-u(s,\cdot)\|_{L^1_\eta}&\leq\frac{\varepsilon}{2}+\frac{\eta}{2}\int_{\mathbb{R}}|w(t,h(0,t;x))-w(t,h(0,s;x))|e^{-\eta|x|}\mathrm{d}x\\ &\leq\frac{\varepsilon}{2}+\frac{\eta}{2}\int_{\mathbb{R}}|w(t,h(0,t;x))-\varphi(h(0,t;x))|e^{-\eta|x|}\mathrm{d}x &(3.2.15)\\ &\quad+\frac{\eta}{2}\int_{\mathbb{R}}|\varphi(h(0,t;x))-\varphi(h(0,s;x))|e^{-\eta|x|}\mathrm{d}x &(3.2.16)\\ &\quad+\frac{\eta}{2}\int_{\mathbb{R}}|\varphi(h(0,s;x))-w(t,h(0,s;x))|e^{-\eta|x|}\mathrm{d}x. &(3.2.17)\end{aligned}$$

Next we estimate (3.2.16) and (3.2.17) (remark that (3.2.15) is a particular case of (3.2.17), for $s = t$), starting with (3.2.17). We have

$$\begin{aligned}\frac{\eta}{2}\int_{\mathbb{R}} |\varphi(h(0,s;x)) - w(t,h(0,s;x))|e^{-\eta|x|}\mathrm{d}x \\ &= \frac{\eta}{2}\int_{-\infty}^{h(s,0;-R)} |w(t,h(0,s;x))|e^{-\eta|x|}\mathrm{d}x \\ &\quad + \frac{\eta}{2}\int_{h(s,0;-R)}^{h(s,0;R)} |w(t,h(0,s;x)) - \varphi(h(0,s;x))|e^{-\eta|x|}\mathrm{d}x \\ &\quad + \frac{\eta}{2}\int_{h(s,0;R)}^{+\infty} |w(t,h(0,s;x))|e^{-\eta|x|}\mathrm{d}x,\end{aligned}$$

then:

$$\begin{aligned}\frac{\eta}{2}\int_{h(s,0;R)}^{+\infty} |w(t,h(0,s;x))|e^{-\eta|x|}\mathrm{d}x &\le \sup_{t\in[0,\tau]}\|w\|_{\mathcal{L}^\infty}\frac{\eta}{2}\left[\frac{e^{-\eta x}}{-\eta}\right]_{h(s,0;R)}^{+\infty} \\ &= \sup_{t\in[0,\tau]}\|w\|_{\mathcal{L}^\infty}\frac{e^{-\eta h(s,0;R)}}{2} \le \frac{\varepsilon}{36}.\end{aligned}$$

Similarly, we have

$$\frac{\eta}{2}\int_{-\infty}^{h(s,0;-R)} |w(t,h(0,s;x))|e^{-\eta|x|}\mathrm{d}x \le \frac{\varepsilon}{36}.$$

Moreover, changing the variable in the integral, we have

$$\begin{aligned}\frac{\eta}{2}\int_{h(s,0;-R)}^{h(s,0;R)} |w(t,h(0,s;x)) - \varphi(h(0,s;x))|e^{-\eta|x|}\mathrm{d}x \\ &= \frac{\eta}{2}\int_{-R}^{R} |w(t,y) - \varphi(y)|e^{-\eta|h(s,0;y)|}|h_x(s,0;y)|\mathrm{d}y \\ &\le \frac{\eta}{2}e^{K\chi s}\|w-\varphi\|_{L^1(-R,R)} \le \frac{\eta}{2}e^{K\chi(s-t-\delta_0)}\frac{\varepsilon}{18\eta} \le \frac{\varepsilon}{36},\end{aligned}$$

where we recall that $|h_x| \le e^{K\chi|t-s|}$ by (3.2.14) and $s \le t+\delta_0$. We have shown that

$$\frac{\eta}{2}\int_{\mathbb{R}} |\varphi(h(0,s;x)) - w(t,h(0,s;x))|e^{-\eta|x|}\mathrm{d}x \le \frac{\varepsilon}{12},$$

for each $s \in (t-\delta_0, t+\delta_0)$, which is our desired estimate for (3.2.17) (and therefore for (3.2.15)).

Next we estimate (3.2.16). Let

$$R' := \sup_{s\in(t-\delta_0,t+\delta_0)} \max\big(h(s,0;R), -h(s,0;-R)\big),$$

which is well-defined by the continuity of $s \mapsto h(s,0;\pm R)$ on $[t-\delta_0, t+\delta_0]$. Then the functions $x \mapsto \varphi(h(0,s;x))$ have their support in $(-R', R')$ for any $s \in (t-\delta_0, t+\delta_0)$. In particular,

$$\begin{aligned}\frac{\eta}{2}\int_{\mathbb{R}} |\varphi(h(0,t;x)) - \varphi(h(0,s;x))|e^{-\eta|x|}\mathrm{d}x \\ &\le \frac{\eta}{2}\|\varphi'\|_{C^0(-R',R')}\int_{-R'}^{R'} |h(0,t;x) - h(0,s;x)|e^{-\eta|x|}\mathrm{d}x \\ &\le \|\varphi'\|_{C^0(-R',R')}\sup_{x\in[-R,R]} |h(t,0;x) - h(s,0;x)|.\end{aligned}$$

Since $(s,x) \mapsto h(s,0;x)$ is continuous on the compact set $[t-\delta_0, t+\delta_0]\times[-R', R']$, it is uniformly continuous on this set and there exists $\delta_1 > 0$ such that

$$\sup_{x\in[-R,R]} |h(t,0;x) - h(s,0;x)| \le \frac{\varepsilon}{6\|\varphi'\|_{C^0(-R',R')}}$$

whenever $|t-s| \leq \delta_1$. This finishes our estimate of (3.2.16).

Summarizing, we have found $\delta_1 > 0$ such that for all $s \in [t-\delta_1, t+\delta_1]$, the inequality

$$\|u(t,\cdot) - u(s,\cdot)\|_{L^1_\eta(\mathbb{R})} \leq \varepsilon$$

holds. This finishes the proof of the continuity of $u(t,\cdot)$ in $L^1_\eta(\mathbb{R})$.

Step 2. Define $p(t,x) := (\rho \star u)(t,x) = \int_{\mathbb{R}} \rho(x-y)u(t,y)\mathrm{d}y$ in the scope of this Step. We first show that for any $t \in [0,T]$ we have $p(t,\cdot) \in W^{2,\infty}(\mathbb{R})$. Indeed, since $\rho \in W^{1,\infty}(\mathbb{R})$ it is classical that $p_x(t,x)$ exists for each $t \in [0,T]$ and $x \in \mathbb{R}$ and

$$p_x(t,x) = \int_{\mathbb{R}} \rho_x(x-y)u(t,y)\mathrm{d}y.$$

Next we remark that for $x \leq y$ we have

$$\begin{aligned}
|p_x(t,x) - p_x(t,y)| &= \left| \int_{\mathbb{R}} \big(\rho_x(x-z) - \rho_x(y-z)\big)u(t,z)\mathrm{d}z \right| \\
&\leq \int_{\mathbb{R}} |\rho_x(x-z) - \rho_x(y-z)|\mathrm{d}z \|u(t,\cdot)\|_{L^\infty(\mathbb{R})} \\
&\leq \int_{\mathbb{R}} |\rho_x(z) - \rho_x(y-x+z)|\mathrm{d}z \|u(t,\cdot)\|_{L^\infty(\mathbb{R})} \\
&= \|u(t,\cdot)\|_{L^\infty(\mathbb{R})} \times \frac{1}{2\sigma^2} \left[\int_{-\infty}^{x-y} -e^{z/\sigma} + e^{(y-x+z)/\sigma}\mathrm{d}z \right. \\
&\quad + \int_{x-y}^{0} e^{z/\sigma} + e^{(x-y-z)/\sigma}\mathrm{d}z \\
&\quad \left. + \int_0^{+\infty} e^{-z/\sigma} - e^{(x-y-z)/\sigma}\mathrm{d}z \right] \\
&= \frac{\|u(t,\cdot)\|_{L^\infty(\mathbb{R})}}{2} \times 4\left(1 - e^{-\frac{|x-y|}{\sigma}}\right) \leq \frac{2}{\sigma}\|u(t,\cdot)\|_{L^\infty(\mathbb{R})}|x-y|. \qquad (3.2.18)
\end{aligned}$$

We deduce that

$$|p_x(t,x) - p_x(t,y)| \leq \frac{2}{\sigma}\|u(t,\cdot)\|_{L^\infty(\mathbb{R})}|x-y|, \text{ for all } t \in [0,T].$$

In particular $p_x(t,\cdot)$ is globally Lipschitz continuous and thus $p(t,\cdot) \in W^{2,\infty}(\mathbb{R})$.

Next we prove that $p_x(t,x) = (\rho_x \star u)(t,x) \in C^0([0,T]\times\mathbb{R})$. Let $\varepsilon > 0$ and $R := \ln\left(\frac{6\|u\|_{L^\infty([0,T]\times\mathbb{R})}}{\varepsilon}\right)$, then we have $\|\rho_x\|_{L^1(\mathbb{R}\setminus(-R,R))} = \varepsilon/\big(6\|u\|_{L^\infty([0,T]\times\mathbb{R})}\big)$. Let $0 < s < t$, we have

$$\begin{aligned}
|p_x(t,x) - p_x(s,y)| &\leq |p_x(t,x) - p_x(t,y)| + |p_x(t,y) - p_x(s,y)| \\
&\leq \frac{2}{\sigma}\|u\|_{L^\infty([0,T]\times\mathbb{R})}|x-y| + \int_{(-R,R)} |\rho_x(y-z)|\big|u(t,z) - u(s,z)\big|\mathrm{d}z \\
&\quad + \int_{\mathbb{R}\setminus(-R,R)} \big|\rho_x(y-z)u(t,z) - \rho_x(y-z)u(s,z)\big|\mathrm{d}z \\
&\leq \frac{2}{\sigma}\|u\|_{L^\infty([0,T]\times\mathbb{R})}|x-y| + \|\rho\|_{L^\infty}\|u(t,\cdot) - u(s,\cdot)\|_{L^1\left((-R,R)\right)} \\
&\quad + \|\rho_x\|_{L^1(\mathbb{R}\setminus(-R,R))} \times 2\|u\|_{L^\infty([0,T]\times\mathbb{R})} \\
&\leq \frac{2}{\sigma}\|u\|_{L^\infty([0,T]\times\mathbb{R})}|x-y| + \|\rho\|_{L^\infty}\|u(t,\cdot) - u(s,\cdot)\|_{L^1\left((-R,R)\right)} + \frac{\varepsilon}{3}.
\end{aligned}$$

Hence, choosing $|x-y| \leq \frac{\sigma\varepsilon}{6\|u\|_{L^\infty([0,T]\times\mathbb{R})}}$ and $|t-s|$ sufficiently small so that the norm $\|u(t,.)-u(s,.)\|_{L^1\left((-R,R)\right)}$ is controlled by $\frac{\varepsilon}{3\|\rho\|_{L^\infty}}$ we have

$$|p_x(t,x) - p_x(s,y)| \leq \varepsilon.$$

Hence p_x is continuous. The continuity of $t \mapsto p(t,\cdot)$ in $L^\infty(\mathbb{R})$ can be shown similarly. □

Theorem 3.2.10 (Local existence and uniqueness of solutions)**.** *Let $\mathcal{U}$ be conull and $u_0 \in \mathcal{L}^\infty(\mathcal{U})$ be given. There exists $\tau > 0$ such that $\mathcal{T}^\tau_{\mathcal{U}}[u_0]$ has a unique fixed point in $\tilde{Z}^\tau$. Moreover τ can be chosen as a continuous function $\tau\left(\|u_0\|_{\mathcal{L}^\infty(\mathcal{U})}\right)$ of $\|u_0\|_{\mathcal{L}^\infty(\mathcal{U})}$ and the mapping $u_0 \in \mathcal{L}^\infty(\mathcal{U}) \mapsto (w(t,x), p(t,x)) \in \tilde{Z}^\tau$ is continuous in a neighborhood of u_0.*

Proof. We divide the proof in three steps.

Step 1. Stability of $\tilde{Z}^\tau_{\mathcal{U}}$ by $T^\tau_{\mathcal{U}}[u_0]$. We show that $\mathcal{T}^\tau_{\mathcal{U}}[u_0](\tilde{Z}^\tau_{\mathcal{U}}) \subset \tilde{Z}^\tau_{\mathcal{U}}$. Define $(w^1, p^1) := \mathcal{T}^\tau_{\mathcal{U}}[u_0](w,p)$. We first prove $w^1 \in X^\tau = C([0,\tau], \mathcal{L}^\infty(\mathcal{U}))$. By definition we have

$$\begin{aligned} w^1(t,\cdot) - w^1(s,\cdot) = u_0(\cdot)\exp\left(\int_0^t 1 + \hat{\chi}p(l,h(l,0;\cdot)) - (1+\hat{\chi})w(l,\cdot)\mathrm{d}l\right) \\ - u_0(\cdot)\exp\left(\int_0^s 1 + \hat{\chi}p(l,h(l,0;\cdot)) - (1+\hat{\chi})w(l,\cdot)\mathrm{d}l\right). \end{aligned}$$

Let us denote $\Theta[u] := |u|e^{|u|}$, $u \in \mathbb{R}$ and recall the inequality $e^u - 1 \le |u|e^{|u|} = \Theta[u]$ for all $u \in \mathbb{R}$. We have

$$\begin{aligned} &\left\| u_0(\cdot)\exp\left(\int_0^t 1 + \hat{\chi}p(l,h(l,0;\cdot)) - (1+\hat{\chi})w(l,\cdot)\mathrm{d}l\right)\right. \\ &\qquad \left. - u_0(\cdot)\exp\left(\int_0^s 1 + \hat{\chi}p(l,h(l,0;\cdot)) - (1+\hat{\chi})w(l,\cdot)\mathrm{d}l\right)\right\|_{\mathcal{L}^\infty(\mathcal{U})} \\ &\qquad = \|u_0\|_{\mathcal{L}^\infty(\mathcal{U})} e^{s\left(1+\hat{\chi}\|p\|_{L^\infty((0,\tau)\times\mathbb{R})}\right)} \\ &\qquad \times \left\| \exp\left(\int_s^t 1 + \hat{\chi}p(l,h(l,0;\cdot)) - (1+\hat{\chi})w(l,\cdot)\mathrm{d}l\right) - 1\right\|_{\mathcal{L}^\infty(\mathcal{U})} \\ &\qquad \le \|u_0\|_{\mathcal{L}^\infty(\mathcal{U})} e^{s\left(1+\hat{\chi}\|p\|_{L^\infty((0,\tau)\times\mathbb{R})}\right)} \\ &\qquad\quad \times \Theta\Big[(t-s)\big(1+\hat{\chi}\|p\|_{L^\infty((0,\tau)\times\mathbb{R})} + (1+\hat{\chi})\sup_{l\in[0,\tau]}\|w(l,\cdot)\|_{\mathcal{L}^\infty(\mathcal{U})}\big)\Big]. \end{aligned}$$

This implies

$$\begin{aligned} &\|w^1(t,\cdot) - w^1(s,\cdot)\|_{\mathcal{L}^\infty(\mathcal{U})} \\ &\qquad \le \|u_0\|_{\mathcal{L}^\infty(\mathcal{U})} e^{s\left(1+\hat{\chi}\|p\|_{Y^\tau}\right)} \Theta\Big[(t-s)\big(1+\hat{\chi}\|p\|_{Y^\tau} + (1+\hat{\chi})\|w\|_{X^\tau}\big)\Big]. \end{aligned} \tag{3.2.19}$$

Since $\chi[u] \to 0$ as $u \to 0$, the continuity of w^1 is proved.

Next we prove $p^1 \in \tilde{Y}^\tau$. Recall that, by definition of $\tilde{Y}^\tau$ (see (3.2.10)), the second derivative of p is uniformly bounded: $\sup_{t\in[0,\tau]}\|p_{xx}(t,\cdot)\|_{L^\infty(\mathbb{R})} =: K < +\infty$. For any $t, s \in [0,\tau]$ and $x \in \mathbb{R}$, we have

$$\begin{aligned} &\left|p^1(t,x) - p^1(s,x)\right| \\ &\qquad = \left|\int_{\mathbb{R}}\left(\rho(x - h(t,0;z))e^{\int_0^t 1-w(l,z)\mathrm{d}l} - \rho(x-h(s,0;z))e^{\int_0^s 1-w(l,z)\mathrm{d}l}\right)u_0(z)\right| \\ &\qquad \le \|u_0\|_{L^\infty(\mathbb{R})}\left(\left\|e^{\int_0^t 1-w(l,\cdot)\mathrm{d}l} - e^{\int_0^s 1-w(l,\cdot)\mathrm{d}l}\right\|_{L^\infty(\mathbb{R})}\int_{\mathbb{R}}|\rho(x-h(t,0;z))|\mathrm{d}z\right. \\ &\qquad\quad \left. + \left\|e^{\int_0^s 1-w(l,\cdot)\mathrm{d}l}\right\|_{L^\infty(\mathbb{R})}\int_{\mathbb{R}}|\rho(x-h(t,0;z)) - \rho(x-h(s,0;z))|\mathrm{d}z\right). \end{aligned} \tag{3.2.20}$$

Since $p \in \tilde{Y}^\tau$ we have $\|p_{xx}\|_{L^\infty((0,\tau)\times\mathbb{R})} \le K$ and thus, recalling the Lipschitz property of h (3.2.14),

$$\begin{aligned} \left\|e^{\int_0^t 1-w(l,\cdot)\mathrm{d}l} - e^{\int_0^s 1-w(l,\cdot)\mathrm{d}l}\right\|_{L^\infty} &\le |t-s|(e^t + e^s)\left(1 + \sup_{t\in[0,\tau]}\|w(t,\cdot)\|_{\mathcal{L}^\infty(\mathcal{U})}\right) \\ &\le |t-s|2e^\tau\left(1 + \|w\|_{X^\tau_{\mathcal{U}}}\right), \\ \int_{\mathbb{R}}|\rho(x-h(t,0;z))|\mathrm{d}z = \int_{\mathbb{R}}\rho(x-y)\partial_x h(0,t;y)\mathrm{d}y &\le e^{K\chi t}. \end{aligned} \tag{3.2.21}$$

where we have used the classical inequality

$$|e^x - e^y| \leq (e^x + e^y)|x - y| \text{ for all } x, y \in \mathbb{R}. \tag{3.2.22}$$

There remains to estimate the second term in the right-hand side of (3.2.20). Using (3.2.22) we have

$$\begin{aligned}
&\int_{\mathbb{R}} |\rho(x - h(t,0;z)) - \rho(x - h(s,0;z))| \mathrm{d}z \\
&\qquad = \frac{1}{2\sigma} \int_{\mathbb{R}} \left| e^{-\frac{|x-h(t,0;z)|}{\sigma}} - e^{-\frac{|x-h(s,0;z)|}{\sigma}} \right| \mathrm{d}z \\
&\qquad \leq \frac{1}{2\sigma} \int_{\mathbb{R}} \left(e^{-\frac{|x-h(t,0;z)|}{\sigma}} + e^{-\frac{|x-h(s,0;z)|}{\sigma}} \right) \sigma^{-1} |h(t,0;z) - h(s,0;z)| \mathrm{d}z \\
&\qquad \leq \frac{1}{2\sigma^2} \|h(t,0;\cdot) - h(s,0;\cdot)\|_{L^\infty(\mathbb{R})} \\
&\qquad\quad \times \left(\int_{\mathbb{R}} e^{-\frac{|x-y|}{\sigma}} h_x(0,t;y) \mathrm{d}y + \int_{\mathbb{R}} e^{-\frac{|x-y|}{\sigma}} h_x(0,s;y) \mathrm{d}y \right) \\
&\qquad \leq \sigma^{-1} \|h(t,0;\cdot) - h(s,0;\cdot)\|_{L^\infty(\mathbb{R})} (e^{K\chi t} + e^{K\chi s}) \\
&\qquad \leq 2\sigma^{-1} e^{K\chi\tau} \|h(t,0;\cdot) - h(s,0;\cdot)\|_{L^\infty(\mathbb{R})}.
\end{aligned} \tag{3.2.23}$$

Moreover, since

$$h(t,0;x) - h(s,0;x) = -\int_s^t \chi p_x(l, h(l,0;x)) \mathrm{d}l, \tag{3.2.24}$$

we have $\|h(t,0;\cdot) - h(s,0;\cdot)\|_{L^\infty(\mathbb{R})} \leq |t-s|\chi \sup_{l\in[0,\tau]} \|p_x(t,\cdot)\|_{L^\infty(\mathbb{R})}$. Combining (3.2.20) and (3.2.23) we have

$$\left\| p^1(t,\cdot) - p^1(s,\cdot) \right\|_{L^\infty(\mathbb{R})} \leq |t-s| \times 2e^{(K\chi+1)\tau} \|u_0\|_{\mathcal{L}^\infty(\mathcal{U})} \left(1 + \|w\|_{X_{\mathcal{U}}^\tau} + \sigma^{-1}\chi \|p\|_{Y^\tau}\right). \tag{3.2.25}$$

This proves $p^1 \in C([0,\tau], L^\infty(\mathbb{R}))$.

Similarly, we compute for any $t, s \in [0,\tau]$ and $x \in \mathbb{R}$:

$$\begin{aligned}
\left| p_x^1(t,x) - p_x^1(s,x) \right| &\leq |t-s| \times 2\sigma^{-1} e^{(K\chi+1)\tau} \|u\|_{L^\infty(\mathbb{R})} \left(1 + \|w\|_{X_{\mathcal{U}}^\tau}\right) \\
&\quad + \|u\|_{L^\infty(\mathbb{R})} e^s \int_{\mathbb{R}} |\rho_x(x - h(t,0;z)) - \rho_x(x - h(s,0;z))| \mathrm{d}z.
\end{aligned} \tag{3.2.26}$$

In order to estimate the last term in (3.2.26), suppose first that $h(0,t;x) \leq h(0,s;x)$. We have

$$\begin{aligned}
&\int_{\mathbb{R}} |\rho_x(x - h(t,0;z)) - \rho_x(x - h(s,0;z))| \mathrm{d}z \\
&\qquad = \frac{1}{2\sigma^2} \int_{-\infty}^{h(0,t;x)} \left| -e^{-\frac{x-h(t,0;z)}{\sigma}} + e^{-\frac{x-h(s,0;z)}{\sigma}} \right| \mathrm{d}z \\
&\qquad + \frac{1}{2\sigma^2} \int_{h(0,s;x)}^{\infty} \left| e^{\frac{x-h(t,0;z)}{\sigma}} - e^{\frac{x-h(s,0;z)}{\sigma}} \right| \mathrm{d}z \\
&\qquad + \frac{1}{2\sigma^2} \int_{h(0,t;x)}^{h(0,s;x)} \left| e^{\frac{x-h(t,0;z)}{\sigma}} + e^{-\frac{x-h(s,0;z)}{\sigma}} \right| \mathrm{d}z.
\end{aligned}$$

Using (3.2.22) and (3.2.21) we have

$$\begin{aligned}
&\int_{\mathbb{R}} |\rho_x(x-h(t,0;z))-\rho_x(x-h(s,0;z))|\mathrm{d}z \\
&\qquad\le \frac{1}{2\sigma^2}\int_{-\infty}^{h(0,t;x)} \big(e^{-\frac{|x-h(t,0;z)|}{\sigma}}+e^{-\frac{|x-h(s,0;z)|}{\sigma}}\big)|h(t,0;z)-h(s,0;z)|\mathrm{d}z \\
&\qquad\quad+\frac{1}{2\sigma^2}\int_{h(0,s;x)}^{\infty} \big(e^{-\frac{|x-h(t,0;z)|}{\sigma}}+e^{-\frac{|x-h(s,0;z)|}{\sigma}}\big)|h(t,0;z)-h(s,0;z)|\mathrm{d}z \\
&\qquad\quad+\frac{1}{2\sigma^2}\int_{h(0,t;x)}^{h(0,s;x)} \big|e^{\frac{x-h(t,0;z)}{\sigma}}+e^{-\frac{x-h(s,0;z)}{\sigma}}\big|\mathrm{d}z \\
&\qquad\le \frac{1}{2\sigma^2}\|h(t,0;\cdot)-h(s,0;\cdot)\|_{L^\infty}\int_{\mathbb{R}}\big(e^{-\frac{|x-h(t,0;z)|}{\sigma}}+e^{-\frac{|x-h(s,0;z)|}{\sigma}}\big)\mathrm{d}z \\
&\qquad\quad+\frac{1}{2\sigma^2}\int_{h(0,t;x)}^{h(0,s;x)} 2\mathrm{d}z \\
&\qquad\le 2\sigma^{-1}e^{K\chi\tau}\|h(t,0;\cdot)-h(s,0;\cdot)\|_{L^\infty(\mathbb{R})}+\sigma^{-2}\|h(0,t;\cdot)-h(0,s;\cdot)\|_{L^\infty(\mathbb{R})}.
\end{aligned} \tag{3.2.27}$$

Moreover by (3.2.24) we have $\|h(0,t;\cdot)-h(0,s;\cdot)\|_{L^\infty(\mathbb{R})}\le |t-s|\chi\|p\|_{Y^\tau}$. Combining (3.2.26) and (3.2.27) we have

$$\begin{aligned}
&\big\|p_x^1(t,\cdot)-p_x^1(s,\cdot)\big\|_{L^\infty(\mathbb{R})} \\
&\qquad\le |t-s|\times\|u_0\|_{\mathcal{L}^\infty(\mathcal{U})}\sigma^{-1}\big(2e^{(K\chi+1)\tau}(1+\|w\|_{X^\tau})+\chi e^{\tau}(2e^{K\chi\tau}+\sigma^{-1})\|p\|_{Y^\tau}\big).
\end{aligned} \tag{3.2.28}$$

This proves $p_x^1\in C([0,\tau],L^\infty(\mathbb{R}))$. According to (3.2.25) and (3.2.28) we have

$$\big\|p^1(t,\cdot)-p^1(s,\cdot)\big\|_{W^{1,\infty}(\mathbb{R})}\le C|t-s|\times\|u_0\|_{\mathcal{L}^\infty(\mathcal{U})}e^{(K\chi+1)\tau}, \tag{3.2.29}$$

where C is a constant depending on σ, χ, $\|w\|_{X^\tau}$ and $\|p\|_{Y^\tau}$. Therefore $p^1\in Y^\tau$.

There remains to show that $\sup_{t\in[0,\tau]}\|p_{xx}^1(t,\cdot)\|_{L^\infty(\mathbb{R})}<+\infty$. Let $t,s\in[0,\tau]$ and $x\in\mathbb{R}$. We have

$$\begin{aligned}
|p_x^1(t,x)-p_x^1(t,y)| &= \left|\int_{\mathbb{R}}\big(\rho_x(x-h(t,0;z))-\rho_x(y-h(t,0;z))\big)u_0(z)e^{\int_0^t 1-w(l,z)\mathrm{d}l}\mathrm{d}z\right| \\
&\le \|u_0\|_{L^\infty(\mathbb{R})}e^t\int_{\mathbb{R}}|\rho_x(x-z)-\rho_x(y-z)|h_x(0,t;z)\mathrm{d}z \\
&\le 2\sigma^{-1}e^{(K\chi+1)\tau}\|u_0\|_{L^\infty(\mathbb{R})}|x-y|.
\end{aligned}$$

Therefore

$$\sup_{t\in[0,\tau]}\|p_{xx}^1(t,\cdot)\|_{L^\infty(\mathbb{R})}\le 2\sigma^{-1}e^{(K\chi+1)\tau}\|u_0\|_{\mathcal{L}^\infty(\mathcal{U})}<+\infty. \tag{3.2.30}$$

We have shown the stability of $\tilde{Z}_{\mathcal{U}}^\tau$.

Step 2. Local stability of a vicinity. We show the stability of the set

$$\begin{aligned}
\overline{B}_r := \{(w,p)\in\tilde{Z}_{\mathcal{U}}^\tau \,|\, &\sup_{t\in[0,\tau]}\|u_0-w(t,\cdot)\|_{\mathcal{L}^\infty(\mathcal{U})}\le r \text{ and } p\in\tilde{Y}_K^\tau \\
&\text{and } \|p-(\rho\star u_0)\|_{Y^\tau}\le r\},
\end{aligned} \tag{3.2.31}$$

for any $r>0$ and $\tau>0$ sufficiently small, where $K:=4\sigma^{-1}\|u_0\|_{\mathcal{L}^\infty(\mathcal{U})}$. Note that $\overline{B}_r$ is closed in $Z_{\mathcal{U}}^\tau$ for any $r>0$.

Let $(w,p)\in\overline{B}_r$, and define $\kappa:=\|(u_0,\rho\star u_0)\|_{Z^\tau}+r$. By definition, we have

$$\|(w,p)\|_{\tilde{Z}^\tau}\le\|u_0,\rho\star u_0\|_{\tilde{Z}^\tau}+r=\kappa.$$

On the one hand by (3.2.19) (with $s=0$) we find that

$$\begin{aligned}
\sup_{t\in[0,\tau]}\|w^1(t,\cdot)-u_0(\cdot)\|_{\mathcal{L}^\infty(\mathcal{U})} &= \sup_{t\in[0,\tau]}\big\|w^1(t,\cdot)-w^1(0,\cdot)\big\|_{\mathcal{L}^\infty(\mathcal{U})} \\
&\le \|u_0\|_{\mathcal{L}^\infty(\mathcal{U})}\Theta\Big[\tau\big(1+\hat{\chi}\|p\|_{Y^\tau}+(1+\hat{\chi})\|w\|_{X^\tau}\big)\Big] \\
&\le \kappa\chi\Big[\tau(1+(1+2\hat{\chi})\kappa)\Big]\xrightarrow[\tau\to 0]{} 0<r,
\end{aligned}$$

where $\Theta[u] = |u|e^{|u|}$. On the other hand, by (3.2.29) (with $s = 0$), for all $t \in [0, \tau]$,

$$\begin{aligned}\|p^1(t,x) - (\rho \star u_0)(x)\|_{Y^\tau} &= \sup_{t\in[0,\tau]} \|p^1(t,\cdot) - p^1(0,\cdot)\|_{W^{1,\infty}(\mathbb{R})} \\ &\le C\tau \times \|u_0\|_{\mathcal{L}^\infty(\mathcal{U})} e^{(K\chi+1)\tau}. \\ &\le C\tau\kappa e^{(K\chi+1)\tau} \xrightarrow[\tau\to 0]{} 0 < r.\end{aligned}$$

Finally by (3.2.30),

$$\begin{aligned}\sup_{t\in[0,\tau]} \|p^1_{xx}(t,\cdot)\|_{L^\infty(\mathbb{R})} &\le 2\sigma^{-1} e^{(K\chi+1)\tau} \|u_0\|_{\mathcal{L}^\infty(\mathcal{U})} \\ &\xrightarrow[\tau\to 0]{} 2\sigma^{-1}\|u_0\|_{\mathcal{L}^\infty(\mathcal{U})} < 4\sigma^{-1}\|u_0\|_{\mathcal{L}^\infty(\mathcal{U})} = K.\end{aligned}$$

We conclude that for any $r > 0$ there is $\tau > 0$ sufficiently small so that the inclusion $\mathcal{T}^\tau_{\mathcal{U}}[u_0](\overline{B}_r) \subset \overline{B}_r$ holds.

Step 3. $\mathcal{T}^\tau_{\mathcal{U}}[u_0]$ is a contraction. More precisely, we show that $\mathcal{T}^\tau_{\mathcal{U}}[u_0]$ is contracting for τ sufficiently small.

Let $r > 0$ be given and $\tau > 0$ be sufficiently small so that $\overline{B}_r$ is left stable by $\mathcal{T}^\tau_{\mathcal{U}}[u_0]$, and define $\kappa := \|(u_0, \rho \star u_0)\|_{Z^\tau} + r$ as in Step 2. Let $(w,p) \in \overline{B}_r$ and $(\tilde{w},\tilde{p}) \in \overline{B_r}$ be given, we observe that for any $t, s \in [0,\tau]$ and $x \in \mathcal{U}$,

$$\begin{aligned}&|\tilde{w}^1(t,x) - w^1(t,x)| \\ &\qquad \le \|u_0\|_{\mathcal{L}^\infty(\mathcal{U})} \Big| e^{\int_0^t 1+\hat{\chi}p(l,h(l,0;x))-(1+\hat{\chi})w(l,x)\mathrm{d}l} - e^{\int_0^t 1+\tilde{p}(l,\tilde{h}(l,0;x))-(1+\hat{\chi})\tilde{w}(l,x)\mathrm{d}l}\Big| \\ &\qquad \le \|u_0\|_{\mathcal{L}^\infty(\mathcal{U})} e^{t(1+\hat{\chi}\|p\|_{Y^\tau})} \Big| 1 - e^{\int_0^t \hat{\chi}\tilde{p}(l,\tilde{h}(l,0;x))-\hat{\chi}p(l,h(l,0;x))-(1+\hat{\chi})(\tilde{w}(l,x)-w(l,x))\mathrm{d}l}\Big| \\ &\qquad \le \kappa e^{\tau(1+\kappa\chi)} \Big| 1 - e^{\int_0^t \hat{\chi}\tilde{p}(l,\tilde{h}(l,0;x))-\hat{\chi}p(l,h(l,0;x))-(1+\hat{\chi})(\tilde{w}(l,x)-w(l,x))\mathrm{d}l}\Big| \\ &\qquad \le \kappa e^{\tau(1+\kappa\chi)} \Theta\Big[\tau\Big(\hat{\chi} \sup_{l\in[0,\tau]} |\tilde{p}(l,\tilde{h}(l,0;x)) - p(l,h(l,0;x))| + (1+\hat{\chi})\|\tilde{w} - w\|_{X^\tau}\Big)\Big],\end{aligned}$$

where we have used the inequality $|e^u - 1| \le |u|e^{|u|} =: \Theta[u]$, $\forall u \in \mathbb{R}$. Moreover, we have

$$\begin{aligned}&\sup_{l\in[0,\tau]} |\tilde{p}(l,\tilde{h}(l,0;x)) - p(l,h(l,0;x))| \\ &\qquad \le \sup_{l\in[0,\tau]} \|\tilde{p}(l,\cdot) - p(l,\cdot)\|_{L^\infty(\mathbb{R})} + \sup_{l\in[0,\tau]} |p(l,\tilde{h}(l,0;x)) - p(l,h(l,0;x))| \\ &\qquad \le \|\tilde{p} - p\|_{Y^\tau} + \sup_{l\in[0,\tau]} \|p_x(l,\cdot)\|_{L^\infty(\mathbb{R})} \sup_{l\in[0,\tau]} \|\tilde{h}(l,0;\cdot) - h(l,0;\cdot)\|_{L^\infty(\mathbb{R})} \\ &\qquad \le \|\tilde{p} - p\|_{Y^\tau} + \kappa \sup_{l\in[0,\tau]} \|\tilde{h}(l,0;\cdot) - h(l,0;\cdot)\|_{L^\infty(\mathbb{R})}.\end{aligned}$$

According to Lemma 3.2.8 we have

$$\|\tilde{h}(t,0;\cdot) - h(t,0;\cdot)\|_{L^\infty(\mathbb{R})} \le \tau\chi \sup_{l\in[0,\tau]} \|\tilde{p}_x(l,\cdot) - p_x(l,\cdot)\|_{L^\infty(\mathbb{R})} e^{K\chi\tau},$$

which yields

$$\sup_{l\in[0,\tau]} |\tilde{p}(l,\tilde{h}(l,0;x)) - p(l,h(l,0;x))| \le \|\tilde{p} - p\|_{\tilde{Y}^\tau}(1 + \kappa\chi\tau e^{K\chi\tau}).$$

This implies

$$\|\tilde{w}^1 - w^1\|_{\tilde{X}^\tau} \le e^{\tau(1+\kappa\chi)} \Theta\Big[\tau\Big(\hat{\chi}\|\tilde{p} - p\|_{\tilde{Y}^\tau}(1 + \kappa\chi\tau e^{K\chi\tau}) + (1+\hat{\chi})\|\tilde{w} - w\|_{\tilde{X}^\tau}\Big)\Big]. \tag{3.2.32}$$

On the other hand, we have

$$\begin{aligned}
&\left|\tilde{p}^1(t,x)-p^1(t,x)\right| \\
&\qquad=\left|\int_{\mathbb{R}}\left(\rho(x-\tilde{h}(t,0;z))e^{\int_0^t 1-\tilde{w}(l,z)\mathrm{d}l}-\rho(x-h(t,0;z))e^{\int_0^t 1-w(l,z)\mathrm{d}l}\right)u_0(z)\mathrm{d}z\right| \\
&\qquad=\left|\int_{\mathbb{R}}\left(\rho(x-\tilde{h}(t,0;z))\left(e^{\int_0^t 1-\tilde{w}(l,z)\mathrm{d}l}-e^{\int_0^t 1-w(l,z)\mathrm{d}l}\right)\right.\right. \\
&\qquad\quad\left.\left.-\left(\rho(x-\tilde{h}(t,0;z))-\rho(x-h(t,0;z))\right)e^{\int_0^t 1-w(l,z)\mathrm{d}l}\right)u_0(z)\mathrm{d}z\right| \\
&\qquad\le\|u_0\|_{L^\infty(\mathbb{R})}\left(\left\|e^{\int_0^t 1-\tilde{w}(l,\cdot)\mathrm{d}l}-e^{\int_0^t 1-w(l,\cdot)\mathrm{d}l}\right\|_{L^\infty(\mathbb{R})}\int_{\mathbb{R}}|\rho(x-\tilde{h}(t,0;z))|\mathrm{d}z\right. \\
&\qquad\quad\left.+\left\|e^{\int_0^t 1-w(l,\cdot)\mathrm{d}l}\right\|_{L^\infty(\mathbb{R})}\int_{\mathbb{R}}|\rho(x-\tilde{h}(t,0;z))-\rho(x-h(t,0;z))|\mathrm{d}z\right).
\end{aligned}$$

In order to estimate the term $\left\|e^{\int_0^t 1-\tilde{w}(l,\cdot)\mathrm{d}l}-e^{\int_0^t 1-w(l,\cdot)\mathrm{d}l}\right\|_{L^\infty(\mathbb{R})}$, we write

$$\begin{aligned}
\left\|e^{\int_0^t 1-\tilde{w}(l,\cdot)\mathrm{d}l}-e^{\int_0^t 1-w(l,\cdot)\mathrm{d}l}\right\|_{L^\infty(\mathbb{R})}&\le 2e^\tau\left\|\int_0^t\tilde{w}(l,\cdot)-w(l,\cdot)\mathrm{d}l\right\|_{\mathcal{L}^\infty(\mathcal{U})} \\
&\le 2\tau e^\tau\left\|\tilde{w}-w\right\|_{X^\tau},
\end{aligned}$$

where we have used (3.2.22). Next we notice that that $\tilde{p}\in\tilde{Y}^\tau$ implies the inequality $\|\tilde{p}_{xx}\|_{L^\infty((0,\tau)\times\mathbb{R})}\le K$, thus we obtain by a change of variable (recall the Lipschitz continuity of $\tilde{h}$ by Lemma 3.2.7)

$$\int_{\mathbb{R}}|\rho(x-\tilde{h}(t,0;z))|\mathrm{d}z=\int_{\mathbb{R}}\rho(x-z)\partial_x\tilde{h}(0,t;z)\mathrm{d}z\le e^{K\chi\tau}.$$

Finally we have

$$\begin{aligned}
&\int_{\mathbb{R}}|\rho(x-\tilde{h}(t,0;z))-\rho(x-h(t,0;z))|\mathrm{d}z \\
&\qquad=\frac{1}{2\sigma}\int_{\mathbb{R}}\left|e^{-\frac{|x-\tilde{h}(t,0;z)|}{\sigma}}-e^{-\frac{|x-h(t,0;z)|}{\sigma}}\right|\mathrm{d}z \\
&\qquad\le\frac{1}{2\sigma}\int_{\mathbb{R}}\left(e^{-\frac{|x-\tilde{h}(t,0;z)|}{\sigma}}+e^{-\frac{|x-h(t,0;z)|}{\sigma}}\right)|\tilde{h}(t,0;z)-h(t,0;z)|\mathrm{d}z \\
&\qquad\le\|\tilde{h}(t,0;\cdot)-h(t,0;\cdot)\|_{L^\infty(\mathbb{R})}\frac{1}{2\sigma}\int_{\mathbb{R}}e^{-\frac{|x-\tilde{h}(t,0;z)|}{\sigma}}+e^{-\frac{|x-h(t,0;z)|}{\sigma}}\mathrm{d}z \\
&\qquad\le\|\tilde{h}(t,0;\cdot)-h(t,0;\cdot)\|_{L^\infty(\mathbb{R})}(e^{K\chi t}+e^{K\chi t}) \\
&\qquad\le 2e^{K\chi\tau}\|\tilde{h}(t,0;\cdot)-h(t,0;\cdot)\|_{L^\infty(\mathbb{R})}.
\end{aligned}$$

Applying Lemma 3.2.8 yields

$$\begin{aligned}
\int_{\mathbb{R}}|\rho(x-\tilde{h}(t,0;z))-\rho(x-h(t,0;z))|\mathrm{d}z&\le 2e^{K\tau}\|\tilde{h}(t,0;\cdot)-h(t,0;\cdot)\|_{L^\infty(\mathbb{R})} \\
&\le 2\chi\tau e^{2K\chi\tau}\|\tilde{p}-p\|_{\tilde{Y}^\tau}.
\end{aligned}$$

We have shown the following estimate on p:

$$\sup_{t\in[0,\tau]}\left\|\tilde{p}^1(t,\cdot)-p^1(t,\cdot)\right\|_{L^\infty(\mathbb{R})}\le 2\kappa\tau e^{(K\chi+1)\tau}\left\|\tilde{w}-w\right\|_{\tilde{X}^\tau}+2\kappa\chi\tau e^{(2K\chi+1)\tau}\|\tilde{p}-p\|_{\tilde{Y}^\tau}. \quad (3.2.33)$$

Next we estimate the gradient of p. We have:

$$\begin{aligned}
&\left|\tilde{p}_x^1(t,x)-p_x^1(t,x)\right| \\
&\qquad=\left|\int_{\mathbb{R}}\left(\rho_x(x-\tilde{h}(t,0;z))e^{\int_0^t 1-\tilde{w}(l,z)\mathrm{d}l}-\rho_x(x-h(t,0;z))e^{\int_0^t 1-w(l,z)\mathrm{d}l}\right)u_0(z)\right| \\
&\qquad\leq \|u_0\|_{L^\infty(\mathbb{R})}\left(\left\|e^{\int_0^t 1-\tilde{w}(l,\cdot)\mathrm{d}l}-e^{\int_0^t 1-w(l,\cdot)\mathrm{d}l}\right\|_{L^\infty(\mathbb{R})}\int_{\mathbb{R}}|\rho_x(x-\tilde{h}(t,0;z))|\mathrm{d}z\right. \\
&\qquad\quad\left.+\left\|e^{\int_0^t 1-w(l,\cdot)\mathrm{d}l}\right\|_{L^\infty(\mathbb{R})}\int_{\mathbb{R}}|\rho_x(x-\tilde{h}(t,0;z))-\rho_x(x-h(t,0;z))|\mathrm{d}z\right) \\
&\qquad\leq 2\sigma^{-1}\kappa\tau e^{(K\chi+1)\tau}\left\|\tilde{w}-w\right\|_{X^\tau}+\kappa e^{\tau}\int_{\mathbb{R}}|\rho_x(x-\tilde{h}(t,0;z))-\rho_x(x-h(t,0;z))|\mathrm{d}z.
\end{aligned}$$

For the need of this computation, let us introduce $h^-:=\min\big(\tilde{h}(0,t;x),h(0,t;x)\big)$ and $h^+:=\max\big(\tilde{h}(0,t;x),h(0,t;x)\big)$. We have:

$$\begin{aligned}
&\int_{\mathbb{R}}|\rho_x(x-\tilde{h}(t,0;z))-\rho_x(x-h(t,0;z))|\mathrm{d}z \\
&\qquad\leq\frac{1}{2\sigma^2}\int_{-\infty}^{h^-}\big(e^{-\frac{|x-\tilde{h}(t,0;z)|}{\sigma}}+e^{-\frac{|x-h(t,0;z)|}{\sigma}}\big)|\tilde{h}(t,0;z)-h(t,0;z)|\mathrm{d}z \\
&\qquad\quad+\frac{1}{2\sigma^2}\int_{h^+}^{\infty}\big(e^{-\frac{|x-\tilde{h}(t,0;z)|}{\sigma}}+e^{-\frac{|x-h(t,0;z)|}{\sigma}}\big)|\tilde{h}(t,0;z)-h(t,0;z)|\mathrm{d}z \\
&\qquad\quad+\frac{1}{2\sigma^2}\int_{h^-}^{h^+}\big|e^{-\frac{|x-\tilde{h}(t,0;z)|}{\sigma}}+e^{-\frac{|x-h(t,0;z)|}{\sigma}}\big|\mathrm{d}z \\
&\qquad\leq\frac{1}{2\sigma^2}\|\tilde{h}(t,0;\cdot)-h(t,0;\cdot)\|_{L^\infty(\mathbb{R})}\int_{\mathbb{R}}\big(e^{-\frac{|x-\tilde{h}(t,0;z)|}{\sigma}}+e^{-\frac{|x-h(t,0;z)|}{\sigma}}\big)\mathrm{d}z \\
&\qquad\quad+\frac{1}{2\sigma^2}\int_{h^-}^{h^+}2\mathrm{d}z \\
&\qquad\leq 2\sigma^{-1}e^{K\chi\tau}\|\tilde{h}(t,0;\cdot)-h(t,0;\cdot)\|_{L^\infty(\mathbb{R})}+\sigma^{-2}\|\tilde{h}(0,t;\cdot)-h(0,t;\cdot)\|_{L^\infty(\mathbb{R})}.
\end{aligned}$$

According to Lemma 3.2.8 we have then

$$\begin{aligned}
&\int_{\mathbb{R}}|\rho_x(x-\tilde{h}(t,0;z))-\rho_x(x-h(t,0;z))|\mathrm{d}z \\
&\qquad\leq 2\sigma^{-1}e^{K\chi\tau}\|\tilde{h}(t,0;\cdot)-h(t,0;\cdot)\|_{L^\infty(\mathbb{R})}+\sigma^{-2}\|\tilde{h}(0,t;\cdot)-h(0,t;\cdot)\|_{L^\infty(\mathbb{R})} \\
&\qquad\leq\big(2\tau\sigma^{-1}\chi e^{2K\chi\tau}+\sigma^{-2}\chi\tau e^{K\chi\tau}\big)\|\tilde{p}-p\|_{Y^\tau}.
\end{aligned}$$

This implies

$$\begin{aligned}
\sup_{t\in[0,\tau]}\left\|\tilde{p}_x^1(t,\cdot)-p_x^1(t,\cdot)\right\|_{L^\infty(\mathbb{R})}&\leq 2\sigma^{-1}\kappa\tau e^{(K\chi+1)\tau}\left\|\tilde{w}-w\right\|_{X^\tau} \\
&\quad+\big(2\kappa\chi\sigma^{-1}\tau e^{(2K\chi+1)\tau}+\kappa\chi\sigma^{-2}\tau e^{(K\chi+1)\tau}\big)\|\tilde{p}-p\|_{Y^\tau}. \quad (3.2.34)
\end{aligned}$$

Combining (3.2.32), (3.2.33) and (3.2.34), there exists a mapping $\tau\mapsto L(\tau)$ with $L(\tau)\to 0$ as $\tau\to 0$ such that

$$\|\mathcal{T}_{\mathcal{U}}^\tau[u_0](\tilde{w},\tilde{p})-\mathcal{T}_{\mathcal{U}}^\tau[u_0](w,p)\|_{Z^\tau}\leq L(\tau)\left\|(\tilde{w},\tilde{p})-(w,p)\right\|_{Z^\tau}. \quad (3.2.35)$$

Thus for $\tau>0$ sufficiently small we have $L(\tau)<1$ in which case $\mathcal{T}_{\mathcal{U}}^\tau[u_0]$ is a contraction on the complete metric space $\overline{B}_r$ equipped with the topology induced by Z_τ. By the Banach contraction principle, there exists then a unique fixed point to $\mathcal{T}_{\mathcal{U}}^\tau[u_0]$. Moreover τ can be chosen as a continuous function of $\|u_0\|_{\mathcal{L}^\infty(\mathcal{U})}$.

Finally, the continuous dependency of (w,p) with respect to u_0 is a direct application of the continuous dependency of the fixed point with respect to a parameter [413, Proposition 1.2]. □

In order to show the semigroup property satisfied by (w,p) and to make the link with the integrated solutions to (3.2.1), we need the following technical Lemma.

Lemma 3.2.11 (The derivatives of p and h)**.** *Let $\mathcal{U} \subset \mathbb{R}$ be conull and $\tau > 0$ be given. Let $(w, p) \in \tilde{Z}^\tau_{\mathcal{U}}$ be a fixed point of $\mathcal{T}^\tau_{\mathcal{U}}[u_0]$. Then there exists a conull set $\mathcal{U}'$ such that*

(i) for any $t, s \in [0, \tau]$, the solution $h(t, s; x)$ to (3.2.12) is differentiable for each $x \in h(s, 0; \mathcal{U}')$ (therefore for almost every $x \in \mathbb{R}$) and we have

$$h_x(t, s; x) = \exp\left(\hat{\chi} \int_s^t w(l, x) - p(l, h(l, s; x))\mathrm{d}l\right) \text{ for a.e. } x \in \mathcal{U}. \tag{3.2.36}$$

(ii) for every $t \in [0, \tau]$ and $x \in \mathbb{R}$ we have

$$p(t, x) = \int_{\mathbb{R}} \rho(x - y) w(t, h(0, t; y))\mathrm{d}y \text{ and } p_x(t, x) = \int_{\mathbb{R}} \rho_x(x - y) w(t, h(0, t; y))\mathrm{d}y.$$

(iii) for every $x \in \mathcal{U}'$, the function $p_x(t, \cdot)$ is differentiable at $h(t, 0; x)$ and we have

$$\sigma^2 p_{xx}(t, h(t, 0; x)) = p(t, h(t, 0; x)) - w(t, x).$$

Proof. We divide the proof in three steps.

Step 1. We prove item (i).
Let $x \le y$ and $t, s \in [0, \tau]$ be given, we first remark that

$$\begin{aligned}
&p_x(t, h(t, 0; y)) - p_x(t, h(t, 0; x)) \\
&\quad= \int_{\mathbb{R}} \big(\rho_x(h(t, 0; y) - h(t, 0; z)) - \rho_x(h(t, 0; x) - h(t, 0; z))\big) u_0(z) e^{\int_0^t 1 - w(l,z)\mathrm{d}l} \mathrm{d}z \\
&\quad= \int_{-\infty}^{x} \big(\rho_x(h(t, 0; y) - h(t, 0; z)) - \rho_x(h(t, 0; x) - h(t, 0; z))\big) u_0(z) e^{\int_0^t 1 - w(l,z)\mathrm{d}l} \mathrm{d}z \\
&\qquad+ \int_{y}^{+\infty} \big(\rho_x(h(t, 0; y) - h(t, 0; z)) - \rho_x(h(t, 0; x) - h(t, 0; z))\big) u_0(z) e^{\int_0^t 1 - w(l,z)\mathrm{d}l} \mathrm{d}z \\
&\qquad- \frac{1}{2\sigma^2} \int_x^y \big(e^{\frac{h(t,0;y) - h(t,0;z)}{\sigma}} + e^{\frac{-h(t,0;x) + h(t,0;z)}{\sigma}}\big) u_0(z) e^{\int_0^t 1 - w(l,z)\mathrm{d}l} \mathrm{d}z \\
&\quad= \int_{-\infty}^{x} \big(\rho_x(h(t, 0; y) - h(t, 0; z)) - \rho_x(h(t, 0; x) - h(t, 0; z))\big) u_0(z) e^{\int_0^t 1 - w(l,z)\mathrm{d}l} \mathrm{d}z \\
&\qquad+ \int_{y}^{+\infty} \big(\rho_x(h(t, 0; y) - h(t, 0; z)) - \rho_x(h(t, 0; x) - h(t, 0; z))\big) u_0(z) e^{\int_0^t 1 - w(l,z)\mathrm{d}l} \mathrm{d}z \\
&\qquad- \frac{1}{2\sigma^2} \int_x^y \big(e^{\frac{h(t,0;y) - h(t,0;z)}{\sigma}} + e^{\frac{-h(t,0;x) + h(t,0;z)}{\sigma}}\big) u_0(z) e^{\int_0^t w(l,z)\mathrm{d}l} \\
&\qquad- 2u_0(x) e^{\int_0^t 1 - w(l,x)\mathrm{d}l} \mathrm{d}z - \frac{(y - x)}{\sigma^2} u_0(x) e^{\int_0^t 1 - w(l,x)\mathrm{d}l} \\
&\quad=: f(t; x, y)(h(t, 0; y) - h(t, 0; x)) - g(t; x, y)
\end{aligned}$$

where

$$f(t; x, y) := \left(\int_{-\infty}^{x} + \int_{y}^{+\infty}\right) \frac{\big(\rho_x(h(t, 0; y) - h(t, 0; z)) - \rho_x(h(t, 0; x) - h(t, 0; z))\big)}{h(t, 0; y) - h(t, 0; x)} \times u_0(z) e^{\int_0^t 1 - w(l,z)\mathrm{d}l} \mathrm{d}z$$

and

$$g(t; x, y) := \frac{1}{2\sigma^2} \int_x^y \big(e^{\frac{h(t,0;y) - h(t,0;z)}{\sigma}} + e^{\frac{-h(t,0;x) + h(t,0;z)}{\sigma}}\big) u_0(z) e^{\int_0^t 1 - w(l,z)\mathrm{d}l} - 2u_0(x) e^{\int_0^t 1 - w(l,x)\mathrm{d}l} \mathrm{d}z + \frac{(y - x)}{\sigma^2} u_0(x) e^{\int_0^t 1 - w(l,x)\mathrm{d}l}.$$

Next we remark that, with those functions f and g, we have

$$\begin{aligned} h(t,0;y)-h(t,0;x) &= y-x-\chi\int_0^t p_x(l,h(l,0;y))-p_x(l,h(l,0;x))\mathrm{d}l \\ &= y-x-\chi\int_s^t f(l;x,y)(h(l,0;y)-h(l,0;x))-g(l;x,y)\mathrm{d}l \\ &= (y-x)e^{-\chi\int_0^t f(l;x,y)\mathrm{d}l}+\chi\int_0^t g(\sigma;x,y)e^{-\chi\int_\sigma^t f(l;x,y)\mathrm{d}l}\mathrm{d}\sigma \end{aligned}$$

For a given $x\in\mathbb{R}$, we have

$$f(t;x,y)\xrightarrow[y\to x]{}\frac{1}{\sigma^2}p(t,h(t,0;x))$$

uniformly in t, because of Lebesgue's dominated convergence theorem.

Next we remark that, given $t\in[0,\tau]$, if x is a Lebesgue point of the function $z\mapsto u_0(z)e^{\int_0^t 1-w(l,z)\mathrm{d}l}\in C^0([0,\tau],\mathcal{L}^\infty(\mathcal{U}))$, then $\frac{g(t;x,y)}{y-x}$ has a limit as $y\to x$ and

$$\lim_{y\to x}\frac{g(t;x,y)}{y-x}=\frac{1}{\sigma^2}u_0(x)e^{\int_0^t 1-w(l,x)\mathrm{d}x}.$$

Applying Lemma 3.2.18, we conclude that there exists a conull set $\mathcal{U}'\subset\mathcal{U}$ on which $h(t,0;\cdot)$ is differentiable at every point $x\in\mathcal{U}'$ for all $t>0$ and we have

$$\begin{aligned} h_x(t,0;x) &= e^{-\hat{\chi}\int_0^t p(l,h(l,0;x))\mathrm{d}l}+\chi\sigma^{-2}\int_0^t u_0(x)e^{\int_0^\sigma 1-w(l,x)\mathrm{d}l}e^{-\hat{\chi}\int_\sigma^t p(l,h(l,0;x))\mathrm{d}l}\mathrm{d}\sigma \\ &= e^{-\hat{\chi}\int_0^t p(l,h(l,0;x))\mathrm{d}l}\left(1+\hat{\chi}\int_0^t u_0(x)e^{\int_0^\sigma 1+\hat{\chi}p(l,h(l,0;x))-w(l,x)\mathrm{d}l}\mathrm{d}\sigma\right) \\ &= e^{-\hat{\chi}\int_0^t p(l,h(l,0;x))\mathrm{d}l}\left(1+\int_0^t \hat{\chi}w(\sigma,x)e^{\hat{\chi}\int_0^\sigma w(l,x)\mathrm{d}x}\mathrm{d}\sigma\right) \\ &= e^{-\int_0^t p(l,h(l,0;x))\mathrm{d}l}\left(1+\int_0^t\left(e^{\int_0^\sigma \hat{\chi}w(l,x)\mathrm{d}x}\right)'\mathrm{d}\sigma\right) \\ &= \exp\left(\hat{\chi}\int_0^t w(l,x)-p(l,h(l,0;x))\mathrm{d}l\right). \end{aligned}$$

Since $h(0,t;x)=[h(t,0;\cdot)]^{-1}(x)$, the function $h(0,t;\cdot)$ is differentiable at each point $x\in h(t,0;\mathcal{U}')$ and

$$h_x(0,t;x)=\frac{1}{h_x(t,0;h(0,t;x))}=\exp\left(-\hat{\chi}\int_0^t w(l,h(0,t;x))-p(l,h(l,t;x))\mathrm{d}l\right).$$

The formula (3.2.36) can be deduced from the remark $h(t,s;x)=h(t,0;h(0,s;x))$, where the right-hand side is differentiable for all $x\in h(s,0;\mathcal{U}')$.

Step 2. We show item (ii).

We have, by definition,

$$p(t,x)=\int_{\mathbb{R}}\rho(x-h(t,0;z))u_0(z)e^{\int_0^t 1-w(l,z)\mathrm{d}l}\mathrm{d}z$$

and item (i) allows a change of variables which yields

$$\begin{aligned} p(t,x) &= \int_{\mathbb{R}}\rho(x-y)u_0(h(0,t;y))e^{\int_0^t 1-w(l,h(0,t;z))\mathrm{d}l}h_x(0,t;z)\mathrm{d}z \\ &= \int_{\mathbb{R}}\rho(x-y)u_0(h(0,t;y))e^{\int_0^t 1-w(l,h(0,t;z))\mathrm{d}l}e^{-\hat{\chi}\int_0^t w(l,h(0,t;y))-p(l,h(l,t;y))\mathrm{d}l}\mathrm{d}z \\ &= \int_{\mathbb{R}}\rho(x-y)u_0(h(0,t;y))e^{\int_0^t 1+\hat{\chi}p(l,h(l,t;x))-(1+\hat{\chi})w(l,h(0,t;z))\mathrm{d}l}\mathrm{d}z \\ &= \int_{\mathbb{R}}\rho(x-y)w(t,h(0,t;y))\mathrm{d}y. \end{aligned}$$

The formula for p_x is proven similarly. Item (ii) is proved.

Step 3. We show item (iii).

Using the formula for p_x established in item (ii), we have

$$\begin{aligned} p_x(t,y) - p_x(t,x) &= \int_{\mathbb{R}} (\rho_x(y-z) - \rho_x(x-z)) w(t, h(0,t;z)) \mathrm{d}z \\ &= \left(\int_{-\infty}^{x} + \int_{y}^{+\infty} \right) (\rho_x(y-z) - \rho_x(x-z)) w(t, h(0,t;z)) \mathrm{d}z \\ &\quad - \frac{1}{2\sigma^2} \int_x^y (e^{\frac{y-z}{\sigma}} + w^{\frac{-x+z}{\sigma}}) w(t, h(0,t;z)) \mathrm{d}z, \end{aligned}$$

therefore $p_x(t,\cdot)$ is differentiable each time x is a Lebesgue point of $z \mapsto w(t, h(0,t;z))$ and we have

$$p_{xx}(t,x) = p(t,x) - w(t, h(0,t;x)).$$

To finish our statement, we show that there exists $\mathcal{U}'' \subset \mathcal{U}'$ (see the definition of $\mathcal{U}'$ given in item (i)) such that every $x = h(t,0;x_0)$ with $x_0 \in \mathcal{U}''$ is a Lebesgue point of $z \mapsto w(t, h(0,t;z))$. Indeed, let $\mathcal{U}''$ be the set given by Lemma 3.2.18 applied to the function $w \in C^0([0,\tau], \mathcal{L}^\infty(\mathcal{U}'))$. If $x = h(t,0;x_0)$ we have:

$$\begin{aligned} &\frac{1}{y-x} \int_x^y |w(t, h(0,t;z)) - w(t, h(0,t;x))| \mathrm{d}z \\ &\qquad = \frac{1}{y-x} \int_{h(0,t;x)}^{h(0,t;y)} |w(t,z) - w(t,x_0)| h_x(t,0;z) \mathrm{d}z \\ &\qquad \le \frac{h(0,t;y) - h(0,t;x)}{y-x} \frac{1}{h(0,t;y) - h(0,t;x)} \\ &\qquad\qquad \times \int_{h(0,t;x)}^{h(0,t;y)} |w(t,z) - w(t,x_0)| \mathrm{d}z \| h_x(t,0;\cdot) \|_{L^\infty(\mathbb{R})}. \end{aligned}$$

Since $h(0,t;x)$ is differentiable for each $x \in h(t,0;\mathcal{U}') \supset h(t,0;\mathcal{U}'')$, the right-hand side converges to 0 as $y \to x$ when $x_0 \in \mathcal{U}''$ is a Lebesgue point of $w(t,\cdot)$. Lemma 3.2.11 is proved. □

Unfortunately, the solution (w,p) constructed in Theorem 3.2.10 does not satisfy a semigroup property. The reason is that, for a semigroup property to hold, the property $p(t,x) = \int_{\mathbb{R}} \rho(x-y) w(t,y) \mathrm{d}y$ would have to hold so that the vector $(w(t,\cdot), p(t,\cdot))$ can be taken as an initial condition; however, this is very unlikely in view of Lemma 3.2.11. In order to continue our construction of the integrated solutions, we first show that the solution can be defined in L^∞ with little modification.

Given $u_0 \in L^\infty(\mathbb{R})$, we define the operator induced by the family $\mathcal{T}^\tau_{\mathcal{U}}[u_0] : \tilde{Z}^\tau \to Z^\tau$ (for $\mathcal{U} \subset \mathbb{R}$ conull) as

$$\mathcal{T}^\tau[u_0](w,p) = \mathcal{T}^\tau_{\mathbb{R}}[u_0](w,p) \tag{3.2.37}$$

where $\mathcal{T}^\tau_{\mathbb{R}}[u_0]$ is obtained by (3.2.13) with an initial condition equal to u_0 a.e. and $Z^\tau := C^0([0,\tau], L^\infty(\mathbb{R})) \times Y^\tau$, $\tilde{Z}^\tau := C^0([0,\tau], L^\infty_+(\mathbb{R})) \times \tilde{Y}^\tau$. The fact that $\mathcal{T}^\tau[u_0]$ is well-defined is shown in the following Corollary.

Corollary 3.2.12 (Well-posedness in $L^\infty(\mathbb{R})$)**.** *Let $u_0 \in L^\infty(\mathbb{R})$ be given. Let $\mathcal{U}$ and $\mathcal{U}'$ be two conull set and $u_0^{\mathcal{U}} \in \mathcal{L}^\infty(\mathcal{U})$ and $u_0^{\mathcal{U}'} \in \mathcal{L}^\infty(\mathcal{U}')$ be such that $u_0 = u_0^{\mathcal{U}} = u_0^{\mathcal{U}'}$ almost everywhere. There exists $\tau = \tau(\|u_0\|_{L^\infty(\mathbb{R})}) > 0$ and a conull set $\mathcal{U}'' \subset \mathcal{U} \cap \mathcal{U}'$ such that the solutions $w^{\mathcal{U}} \in C^0([0,\tau^{\mathcal{U}}], \mathcal{L}^\infty(\mathcal{U}))$ and $w^{\mathcal{U}'} \in C^0([0,\tau^{\mathcal{U}'}], \mathcal{L}^\infty(\mathcal{U}'))$ given by Theorem 3.2.10 coincide for all $t \in [0,\tau^{\mathcal{U}}] \cap [0,\tau^{\mathcal{U}'}]$ and $x \in \mathcal{U}''$. Moreover we have $\tau \ge \max(\tau^{\mathcal{U}}, \tau^{\mathcal{U}'})$.*

In particular, let $\tilde{u}_0 \in \mathcal{L}^\infty(\mathbb{R})$ be such that $u_0 = \tilde{u}_0$ almost everywhere and $\|\tilde{u}_0\|_{\mathcal{L}^\infty(\mathbb{R})} = \|u_0\|_{L^\infty(\mathbb{R})}$ and define $w(t,\cdot)$ as the L^∞ class of the solution $\tilde{w} \in C^0([0,\tau], \mathcal{L}^\infty(\mathbb{R}))$ given by Theorem 3.2.10. Then $w \in C^0([0,\tau], L^\infty(\mathbb{R}))$ and w is the unique fixed point on the operator $\mathcal{T}^\tau[u_0]$ induced by the operator $\mathcal{T}^\tau_{\mathbb{R}}[\tilde{u}_0]$ defined in (3.2.13)*.*

Proof. Most of the arguments involved in the proof of Corollary 3.2.12 are very classical therefore we concentrate on the most important point which is the well-definition of w in L^∞. The set $\mathcal{U}'' \subset \mathcal{U} \cap \mathcal{U}'$ mentioned in the corollary can be defined as

$$\mathcal{U}'' = \mathcal{U} \cap \mathcal{U}' \cap \{u_0^{\mathcal{U}}(x) \le \|u_0\|_{L^\infty}\}.$$

Since the existence time given by Theorem 3.2.10 depends only on $\|u_0^{\mathcal{U}}\|_{\mathcal{L}^\infty(\mathcal{U}'')}$, we have $\tau^{\mathcal{U}''} \geq \max(\tau^{\mathcal{U}}, \tau^{\mathcal{U}'})$. Moreover since $\mathcal{U}'' \subset \mathcal{U}$ it follows from the uniqueness of the fixed point of $\mathcal{T}_{\mathcal{U}}^{\tau}[u_0]$ that $w^{\mathcal{U}}$ and $w^{\mathcal{U}''}$ coincide on $\mathcal{U}''$, and similarly $w^{\mathcal{U}'} = w^{\mathcal{U}''}$ on $\mathcal{U}''$. The remaining statements are classical. □

We are now equipped with a family of operators T_t defined for $u \in L^\infty(\mathbb{R})$ and $t \in [0, \tau(\|u_0\|_{L^\infty})]$ as

$$T_t u_0(x) := w(t, h(0, t; x)) \in L^\infty(\mathbb{R}), \tag{3.2.38}$$

where w and $\tau(\|u_0\|_{L^\infty})$ are given by Corollary 3.2.12. Next we show that the family T_t satisfies a semigroup property. We deduce the existence of a maximal solution for each $u_0 \in L^\infty(\mathbb{R})$.

Theorem 3.2.13 (Maximal solutions)**.** *Let $u_0 \in L^\infty(\mathbb{R})$ be given. The number*

$$\tau^*(u_0) := \sup\{\tau > 0 \,|\, \mathcal{T}^\tau[u_0] \text{ has a unique fixed point}\}$$

is well-defined and belongs to $(0, +\infty]$, where $\mathcal{T}^\tau[u_0]$ is the operator defined in (3.2.37)*. Moreover, there exists a conull set $\mathcal{U} \subset \mathbb{R}$ and $\tilde{u}_0 \in \mathcal{L}^\infty(\mathcal{U})$ such that the operator $\mathcal{T}_{\mathcal{U}}^\tau[u_0]$ has a unique fixed point $\tilde{w} \in C^0([0,\tau], \mathcal{L}^\infty(\mathcal{U}))$ for each $\tau \in (0, \tau^*(u_0))$ and*

$$\tilde{w}(t, x) = w(t, x) \text{ for a.e. } x \in \mathbb{R}.$$

The map $u_0 \in L^\infty(\mathbb{R}) \mapsto (\tilde{w}, p) \in Z_{\mathcal{U}}^\tau$ (and therefore $u_0 \in L^\infty(\mathbb{R}) \mapsto (w, p) \in Z^\tau$) is continuous for each $\tau \in (0, \tau^*(u_0))$.

Finally, the map $t \in [0, \tau^*(u_0)) \mapsto T_t u_0 \in L^\infty(\mathbb{R})$ is a semigroup which is continuous for the $L^1_\eta(\mathbb{R})$ topology for any $\eta \in (0,1)$, where T_t is defined by (3.2.38)*, and if $\tau^*(u_0) < +\infty$ then we have*

$$\limsup_{t \to \tau^*(u_0)^-} \|T_t u_0\|_{L^\infty(\mathbb{R})} = +\infty.$$

The map $u_0 \in L^\infty(\mathbb{R}) \mapsto T_t u_0 \in L^1_\eta(\mathbb{R})$ is continuous for each $t \in (0, \tau^*(u_0))$.

Proof. The positiveness of $\tau^*(u_0)$ is a consequence of Corollary 3.2.12. We show the existence of $\mathcal{U}$ as defined in the Theorem. Let $\mathcal{U}^0 := \mathbb{R}$ and let $\tilde{u}_0 \in \mathcal{L}^\infty(\mathbb{R})$ be a bounded measurable function on $\mathbb{R}$ such that $\|\tilde{u}_0\|_{\mathcal{L}^\infty(\mathbb{R})} = \|u_0\|_{L^\infty(\mathbb{R})}$. In the rest of the proof we identify u_0 and $\tilde{u}_0$ and consequently drop the tilde. We recursively construct a sequence of conull sets $\mathcal{U}^n$, $n \in \mathbb{R}$, such that $\mathcal{U}^{n+1} \subset \mathcal{U}^n$, and a sequence of functions $u_0^n \in L^\infty(\mathcal{U}^n)$, such that:

(i) $u_0^{n+1}(x) := w^n(\tau_n, h^n(0, \tau_n; x))$ where $\tau_n := \tau(\|u_0^n\|_{L^\infty})$, (w^n, p^n) is the unique fixed point of the operator $\mathcal{T}_{\mathcal{U}^n}^{\tau_n}$ (given by Theorem 3.2.10) with initial condition u_0^n and h^n is the solution of (3.2.12) corresponding to p^n.

(ii) $\mathcal{U}^{n+1} = \mathcal{U}^n \cap h^n(0, \tau_n; \mathcal{U}^n) \cap \{x \,|\, u_0^{n+1}(x) \leq \|u_0^{n+1}\|_{L^\infty}\}$.

We let $\mathcal{U} := \bigcap_{n \in \mathbb{N}} \mathcal{U}^n$. Remark that, since each $\mathcal{U}^n$ is conull, the set $\mathcal{U}$ is still conull. Next we show that $\mathcal{T}^\tau[u_0]$ has a unique fixed point for each $\tau \in [0, \sum_{n \in \mathbb{N}} \tau_n)$.

Let $T_0 = 0$ and $T_n := \sum_{k=0}^{n-1} \tau_{n+1}$, for all $t \in [T_n, T_n + 1)$ we define

$$w(t, x) := w^n(t - T_n, h_{n-1}(\tau_n, 0; x)) \text{ for all } x \in \mathcal{U},$$
$$p(t, x) := p^n(t - T_n, h_{n-1}(\tau_n, 0; x)) \text{ for all } x \in \mathbb{R}.$$

We show that (w, p) is the unique fixed point of $\mathcal{T}_{\mathcal{U}}^\tau[u_0]$ for all $\tau \in [0, T_\infty)$ by induction. Indeed, the property is a consequence of Theorem 3.2.10 for all $\tau \leq T_1$. Suppose that (w, p) is the unique fixed point of $\mathcal{T}_{\mathcal{U}}^\tau[u_0]$ for all $\tau \leq T_n$, $n \geq 1$. The formula

$$w(t, x) = u_0(x) \exp\left(\int_0^t 1 + \hat{\chi} p(l, h(l, 0; x)) - (1 + \hat{\chi}) w(l, x) \mathrm{d}l\right)$$

is valid for all $t \leq T_n$. For $t \in [T_n, T_{n+1}]$ we have

$$\begin{aligned} w^n(t-T_n,x) &= u_0^n(x)\exp\left(\int_0^{t-T_n} 1+\hat{\chi}p^n(l,h^n(l,0;x)) - (1+\hat{\chi})w^n(l,x)\mathrm{d}l\right) \\ &= w(T_n,h(T_n,0;x))\exp\left(\int_0^{t-T_n} 1+\hat{\chi}p^n(l,h^n(l,0;x)) - (1+\hat{\chi})w^n(l,x)\mathrm{d}l\right) \\ &= u_0(h(0,T_n;x)) \\ &\quad\times\exp\left(\int_0^{T_n} 1+\hat{\chi}p(l,h(l,0;h(0,T_n;x))) - (1+\hat{\chi})w(l,h(0,T_n;x))\mathrm{d}l\right) \\ &\quad\times\exp\left(\int_0^{t-T_n} 1+\hat{\chi}p^n(l,h^n(l,0;x)) - (1+\hat{\chi})w^n(l,x)\mathrm{d}l\right), \end{aligned}$$

so that

$$\begin{aligned} w^n(t-T_n,h(T_n,0;x)) &= u_0(x)\exp\left(\int_0^{T_n} 1+\hat{\chi}p(l,h(l,0;x)) - (1+\hat{\chi})w(l,x)\mathrm{d}l\right) \\ &\quad\times\exp\left(\int_{T_n}^{t} 1+\hat{\chi}p^n(l-T_n,h^n(l-T_n,0;h(T_n,0;x))) \right. \\ &\qquad\left. - (1+\hat{\chi})w^n(l-T_n,h(T_n,0;x))\mathrm{d}l\right). \quad (3.2.39) \end{aligned}$$

Next we remark that, by Lemma 3.2.11, the formula

$$\begin{aligned} p(T_n,x) &= \int_{\mathbb{R}} \rho(x-y)w(T_n,h(0,T_n;y))\mathrm{d}y = \int_{\mathbb{R}} \rho(x-y)u_0^n(y)\mathrm{d}y = p^n(0,x) \\ p_x(T_n,x) &= \int_{\mathbb{R}} \rho_x(x-y)w(T_n,h(0,T_n;y))\mathrm{d}y = \int_{\mathbb{R}} \rho_x(x-y)u_0^n(y)\mathrm{d}y = p^n(0,x) \end{aligned}$$

hold, therefore $p(t,x)$ can be extended to a function $p \in C^0([0,T_{n+1}],W^{1,\infty}(\mathbb{R}))$ by defining $p(t,x) = p^n(t-T_n,x)$ when $t \geq T_n$, and moreover the extended function $h(t,s;x)$ defined on $[0,T_{n+1}]\times[0,T_{n+1}]\times\mathbb{R}$ by

$$h(t,s;x) = \begin{cases} h(t,s;x) & \text{if } t,s \leq T_n \\ h^n(t-T_n,0;h(T_n,s;x)) & \text{if } s \leq T_n \leq t \\ h(t,T_n;h^n(0,s-T_n;x)) & \text{if } t \leq T_n \leq s \\ h^n(t,s;x) & \text{if } T_n \leq t,s \end{cases}$$

solves (3.2.12). Therefore (3.2.39) can be rewritten as:

$$\begin{aligned} w^n(t-T_n,h(0,T_n;x)) &= u_0(x)\exp\left(\int_0^{T_n} 1+\hat{\chi}p(l,h(l,0;x)) - (1+\hat{\chi})w(l,x)\mathrm{d}l \right. \\ &\qquad\left. + \int_{T_n}^{t} 1+\hat{\chi}p(l,h^n(l-T_n,0;h(T_n,0;x)) - (1+\hat{\chi})w^n(l-T_n,h(T_n,0;x))\mathrm{d}l\right) \\ &= u_0(x)\exp\left(\int_0^{t} 1+\hat{\chi}p(l,h(l,0;x)) - (1+\hat{\chi})w(l,x)\mathrm{d}l\right), \end{aligned}$$

where we have used the function $w \in C^0([0,T_{n+1}],\mathcal{L}^\infty(\mathcal{U}))$ defined by the equality $w(t,x) := w^n(t-T_n,h(0,T_n;x))$ when $t \geq T_n$. Finally

$$\begin{aligned} p(t,x) &= \int_{\mathbb{R}} \rho(x-y)w(t,h(0,t;y))\mathrm{d}y = \int_{\mathbb{R}} \rho(x-h(t,0;x)w(t,z)h_x(t,0;z)\mathrm{d}z \\ &= \int_{\mathbb{R}} \rho(x-h(t,0;z))u_0(z)e^{\int_0^t 1-w(l,z)\mathrm{d}l}\mathrm{d}z. \end{aligned}$$

We have shown that (w,p) is a fixed point of $\mathcal{T}_{\mathcal{U}}^{t}[u_0]$, for all $t \leq T_{n+1}$. Uniqueness follows from the remark: let $w, \tilde{w}$ of $\mathcal{T}_{\mathcal{U}}^{T_{n+1}}[u_0]$ be two fixed points of $\mathcal{T}_{\mathcal{U}}^{T_{n+1}}$. Then w and $\tilde{w}$ coincide in $[0,T_n]$ (by uniqueness of the fixed point) therefore $w(T_n,x) = \tilde{w}(T_n,x)$, $w(T_n,h(0,T_n;x)) = \tilde{w}(T_n,h(0,T_n;x))$ and by the uniqueness of the fixed point in the interval $[T_n,T_{n+1}]$ we conclude $w(t,\cdot) = \tilde{w}(t,\cdot)$. The uniqueness is proved. We have shown by induction that $\mathcal{T}_{\mathcal{U}}^{\tau}[u_0]$ has a unique fixed point for all $\tau \in [0,T_\infty]$. As a by-product, this is also true for $\mathcal{T}^{\tau}[u_0]$ and therefore $T_\infty \leq \tau^*(u_0)$.

Next we remark that $\tau_n = \tau(\|u_0^n\|_{L^\infty})$ is a positive continuous function of $\|u_0^n\|_{L^\infty}$ and therefore $T_\infty = \sum \tau_n < +\infty$ implies $\|w(T_n,\cdot)\|_{L^\infty} = \|u_0^n\|_{L^\infty} \to +\infty$. This shows that $\tau^*(u_0) \leq T_\infty$ and therefore

$$\tau^*(u_0) = T_\infty.$$

Obviously if $T_\infty = +\infty$ then we have $\tau^*(u_0) \geq T_\infty = +\infty$. We have shown the equality between the quantities.

Finally, the continuity of $u_0 \in \mathcal{L}^\infty(\mathcal{U}) \mapsto (w,p) \in Z_{\mathcal{U}}^{\tau}$ is a consequence of the continuity of the continuity of the map $u_0^n \mapsto (w^n,p^n) \in Z_{\mathcal{U}}^{\tau}$ given by Theorem 3.2.10.

Next we prove the semigroup property of $t \mapsto T_t u_0$. This follows from a direct computation: let $0 \leq t \leq s < \tau^*(u_0)$, then for almost all $x \in \mathbb{R}$ we have

$$\begin{aligned}
T_{t+s}u_0(x) &= u_0(h(0,t+s;x)) \exp\bigg(\int_0^{t+s} 1 + \hat{\chi} p(l,h(l,t+s;x)) \\
&\quad - (1+\hat{\chi}) w(l,h(0,t+s;x)) \mathrm{d}l \bigg) \\
&= \bigg[u_0(h(0,t;h(t,t+s))) \exp\bigg(\int_0^{t} 1 + \hat{\chi} p(l,h(l,t;h(t,t+s;x))) \\
&\quad - (1+\hat{\chi}) w(l,h(0,t;h(t,t+s;x)) \mathrm{d}l \bigg) \bigg] \\
&\quad \times e^{\int_t^{t+s} 1+\hat{\chi}p(l,h(l,t+s;x)) - (1+\hat{\chi})w(l,h(0,t+s;x))\mathrm{d}l} \\
&= T_t u_0(h(t,t+s;x)) \exp\bigg(\int_0^{s} 1 + \hat{\chi} p(t+l,h(t+l,t+s;x)) \\
&\quad - (1+\hat{\chi}) w(t+l,h(0,t;h(t,t+s;x))) \mathrm{d}l \bigg).
\end{aligned}$$

Let $\tilde{p}(t,x)$, $\tilde{h}(t,s;x)$, $\tilde{w}(t,x)$ be the quantities corresponding to the initial condition $\tilde{u}_0 = T_t u_0(x)$. By Lemma 3.2.11 we have

$$p(t,x) = \int_{\mathbb{R}} \rho(x-y) w(t,h(0,t;y)) \mathrm{d}y = \int_{\mathbb{R}} \rho(x-y) T_t(u_0)(y) \mathrm{d}y,$$

therefore by the uniqueness of the fixed point we have

$$\tilde{p}(l,y) = p(t+l,y), \qquad \tilde{h}(l,\sigma;x) = h(t+l,t+\sigma;x), \qquad \tilde{w}(l,x) = w(t+l,h(0,t;x)).$$

We conclude that

$$\begin{aligned}
T_{t+s}u_0(x) &= T_t u_0(\tilde{h}(0,s;x)) \exp\left(\int_0^s 1 + \hat{\chi}\tilde{p}(l,\tilde{h}(l,s;x)) - (1+\hat{\chi})\tilde{w}(l,\tilde{h}(0,s;x)) \mathrm{d}l \right). \\
&= T_s T_t u_0(x).
\end{aligned}$$

The continuity of $t \mapsto T_t u_0$ in the L^1_η topology follows directly from Lemma 3.2.11 and 3.2.9.

What remains to show is the continuity of $u_0 \in L^\infty(\mathbb{R}) \mapsto T_t u_0 \in L^1_\eta(\mathbb{R})$. We use the sequential characterization of continuity. Let $u_0, u_0^n \in L^\infty(\mathbb{R})$ be such that

$$\|u_0^n - u_0\|_{L^\infty(\mathbb{R})} \xrightarrow[n\to\infty]{} 0,$$

and let $0 < t < \tau^*(u_0)$. Let us recall that the map $u_0 \in L^\infty \mapsto (w,p) \in Z^\tau$ is continuous, therefore we have $\tau^*(u_n) > t$ for n sufficiently large and

$$\|w^n(t,\cdot) - w(t,\cdot)\|_{L^\infty(\mathbb{R})} \xrightarrow[n\to\infty]{} 0,$$

where (w^n, p_n) is the fixed point of $\mathcal{T}^t[u_0^n]$. Define h^n as the solution to (3.2.12) associated with u^n, then we have

$$\begin{aligned}
\|u(t,\cdot) - u^n(t,\cdot)\|_{L^1_\eta(\mathbb{R})} &= \frac{\eta}{2}\int_{\mathbb{R}} e^{-\eta|x|}|u(t,x) - u^n(t,x)|\mathrm{d}x \\
&= \frac{\eta}{2}\int_{\mathbb{R}} e^{-\eta|x|}|w(t,h(t,0;x)) - w^n(t,h^n(t,0;x))|\mathrm{d}x \\
&\le \frac{\eta}{2}\int_{\mathbb{R}} e^{-\eta|x|}|w(t,h(t,0;x)) - w(t,h^n(t,0;x))|\mathrm{d}x \\
&\quad + \frac{\eta}{2}\int_{\mathbb{R}} e^{-\eta|x|}|w(t,h^n(t,0;x)) - w(t,h^n(t,0;x))|\mathrm{d}x \\
&\le \frac{\eta}{2}\int_{\mathbb{R}} e^{-\eta|x|}|w(t,h(t,0;x)) - w(t,h^n(t,0;x))|\mathrm{d}x \\
&\quad + \|w(t,\cdot) - w^n(t,\cdot)\|_{L^\infty(\mathbb{R})}.
\end{aligned}$$

Next we remark that the function $w(t,h^n(t,0;x))$ converges to $w(t,h(t,0;x))$ for a.e. $x \in \mathbb{R}$. Indeed, let $x \in \mathbb{R}$ be a Lebesgue point of $w(t,h(t,0;\cdot))$, then we have

$$\begin{aligned}
&\frac{1}{2\varepsilon}\int_{x-\varepsilon}^{x+\varepsilon} |w(t,h(t,0;z)) - w(t,h^n(t,0;z))|\mathrm{d}z \\
&\qquad \le \frac{1}{2\varepsilon}\int_{x-\varepsilon}^{x+\varepsilon} |w(t,h(t,0;z)) - w(t,h(t,0;x))|\mathrm{d}z \\
&\qquad\quad + \frac{1}{2\varepsilon}\int_{x-\varepsilon}^{x+\varepsilon} |w(t,h(t,0;x)) - w(t,h^n(t,0;z))|\mathrm{d}z \\
&\qquad = \frac{1}{2\varepsilon}\int_{x-\varepsilon}^{x+\varepsilon} |w(t,h(t,0;z)) - w(t,h(t,0;x))|\mathrm{d}z \\
&\qquad\quad + \frac{1}{2\varepsilon}\int_{h(0,t;h^n(t,0;x-\varepsilon))}^{h(0,t;h^n(t,0;x+\varepsilon))} |w(t,h(t,0;x)) - w(t,h(t,0;y))| \\
&\qquad\quad \times h_x^n(t,0;h(t,0;y))h_x(t,0;y)\mathrm{d}y \\
&\qquad \le \frac{1}{2\varepsilon}\int_{x-\varepsilon}^{x+\varepsilon} |w(t,h(t,0;z)) - w(t,h(t,0;x))|\mathrm{d}z \\
&\qquad\quad + \frac{C}{2\varepsilon}\int_{h(0,t;h^n(t,0;x-\varepsilon))}^{h(0,t;h^n(t,0;x+\varepsilon))} |w(t,h(t,0;x)) - w(t,h(t,0;y))|\mathrm{d}y,
\end{aligned}$$

where $C := \|h_x^n(t,0;\cdot)\|_{L^\infty}\|h_x(t,0;\cdot)\|_{L^\infty}$, so that

$$\limsup_{n\to+\infty}\int_{x-\varepsilon}^{x+\varepsilon} |w(t,h(t,0;z)) - w(t,h^n(t,0;z))|\mathrm{d}z = o(\varepsilon).$$

Define

$$E_\delta := \{x \in \mathbb{R} \mid \limsup_{n\to\infty} |w(t,h(t,0;x)) - w(t,h^n(t,0;x))| \ge \delta\},$$

and take a compact set $\mathcal{K} \subset E_\delta$ which is contained in a open set $\mathcal{O}$ with finite Lebesgue measure. Then $\mathcal{K}$ can be covered by a finite union of the interval in the family Ω_μ of intervals $I_{x,\varepsilon,\mu} := (x-\varepsilon, x+\varepsilon)$ such that x is a Lebesgue point of $w(t,h(t,0;\cdot))$, $I \subset \mathcal{O}$ and

$$\limsup_{n\to+\infty}\int_{I_{x,\varepsilon,\mu}} |w(t,h(t,0;z)) - w(t,h^n(t,0;z))|\mathrm{d}z \le 2\mu\varepsilon.$$

Applying the Vitali covering lemma [342, Theorem 8.5 p. 154], there is a finite disjoint subcollection

$I_{x_k,\varepsilon_k,\mu} = (x_k, \varepsilon_k)$ $(1 \le k \le n < +\infty)$ such that $|\mathcal{K} \backslash \bigcup I_{x_n,\varepsilon_n,\mu}| = 0$ and therefore

$$\begin{aligned}
\delta|\mathcal{K}| &\le \int_{\mathcal{K}} \limsup_{n\to+\infty} |w(t,h(t,0;x)) - w(t,h^n(t,0;x))| \mathrm{d}x \\
&\le \sum_{k=1}^{n} \int_{I_{x_k,\varepsilon_k,\mu}} \limsup_{n\to+\infty} |w(t,h(t,0;x)) - w(t,h^n(t,0;x))| \mathrm{d}x \\
&\le \sum_{k=1}^{n} \limsup_{n\to+\infty} \int_{I_{x_k,\varepsilon_k,\mu}} |w(t,h(t,0;x)) - w(t,h^n(t,0;x))| \mathrm{d}x \\
&\le \sum_{k=1}^{n} 2\mu\varepsilon_k = \mu \sum_{k=1}^{n} |I_{x_k,\varepsilon_k,\mu}| \le \mu|\mathcal{O}|.
\end{aligned}$$

Since $\mathcal{O}$ is independent of μ we take the limit $\mu \to 0$ to find $|\mathcal{K}| = 0$ and therefore

$$|E_\delta| = \sup_{\mathcal{K} \text{ compact},\ \mathcal{K} \subset E_\delta} |\mathcal{K}| = 0.$$

Since $\delta > 0$ arbitrary we have shown that the set of where $w(t,h^n(t,0;x))$ does not converge to $w(t,h(t,0;x))$ is included in $\bigcup_{n\ge 0} E_{1/n}$, which is still negligible for the Lebesgue measure. We have shown the convergence of $w(t,h^n(t,0;\cdot))$ to $w(t,h(t,0;\cdot))$ almost everywhere in $\mathbb{R}$. The convergence of $u^n(t,\cdot)$ to $u(t,\cdot)$ in $L^1_\eta(\mathbb{R})$ is then a consequence of Lebesgue's dominated convergence Theorem. □

We are now in the position to link the constructed maximal solution with the integrated solutions to (3.2.1).

Proposition 3.2.14 (Integrated solutions)**.** *Let $\tau > 0$ and $u_0 \in L^\infty(\mathbb{R})$.*

(i) If $u \in C^0([0,\tau], L^1_{loc}(\mathbb{R}))$ is an integrated solution to (3.2.1)*, then $\tau^*(u_0) \ge \tau$ and $u(t,\cdot) = T_t u_0$ for all $t \in [0,\tau]$.*

(ii) Conversely, if $u(t,x) := T_t u_0(x)$ for all $t \in [0,\tau]$, then $u(t,x)$ is an integrated solution to (3.2.1)*.*

Proof. We first prove Item (i). Assume $u(t,x) \in C^0([0,\tau], L^1_{loc}(\mathbb{R})$ is an integrated solution. Define $p(t,x) := \int_{\mathbb{R}} \rho(x-y)u(t,y)\mathrm{d}y$. We first show that $p \in C^0([0,\tau], W^{1,\infty}(\mathbb{R}))$. We have:

$$\begin{aligned}
|p(t,x) - p(s,x)| &\le \int_{\mathbb{R}} \rho(x-y)|u(t,y) - u(s,y)|\mathrm{d}y, \\
|p_x(t,x) - p_x(s,x)| &\le \int_{\mathbb{R}} |\rho_x(x-y)||u(t,y) - u(s,y)|\mathrm{d}y,
\end{aligned}$$

and since $t \mapsto u(t,\cdot)$ is bounded in L^∞ and continuous in L^1_{loc} both right-hand sides can be made arbitrarily small (recall ρ and ρ_x are in L^1). This shows $p \in C^0([0,\tau], W^{1,\infty}(\mathbb{R}))$.

Next we show that $p(t,\cdot) \in W^{2,\infty}(\mathbb{R})$ for all $t \in [0,\tau]$ and that the inequality $\sup_{t\in[0,\tau]} \|p_{xx}(t,\cdot)\|_{L^\infty} < +\infty$ holds. Indeed, take $x \le y$, we have

$$\begin{aligned}
p_x(t,x) - p_x(t,y) &= \int_{\mathbb{R}} \left(\rho_x(x-z) - \rho_x(y-z)\right) u(t,z)\mathrm{d}z \\
&= \left(\int_{-\infty}^{x} + \int_{y}^{+\infty}\right) \big(\rho_x(x-z) - \rho_x(y-z)\big)u(t,z)\mathrm{d}z \\
&\quad - \frac{1}{2\sigma^2}\int_x^y (e^{\frac{y-z}{\sigma}} + e^{\frac{-x+z}{\sigma}})u(t,z) - 2u(t,x)\mathrm{d}z + \sigma^{-2}u(t,x),
\end{aligned}$$

therefore p_x is differentiable at each Lebesgue point of u and we have

$$\sigma^2 p_{xx}(t,x) = p(t,x) - u(t,x) \text{ for a.e. } x \in \mathbb{R}.$$

Next, define the solution h to (3.2.12). According to Definition 3.2.1, there exists a conull set $\mathcal{U}$ on which $t \mapsto u(t,h(t,0;x))$ is a classical solution to (3.2.9). Therefore, by a direct integration, we have

$$w(t,x) = u_0(x) \exp\left(\int_0^t 1 + \hat{\chi}p(l,h(l,0;x)) - (1+\hat{\chi})w(l,x)\mathrm{d}l\right),$$

where $w(t,x) := u(t,h(t,0;x))$. In particular, $w(t,x) \in C^0([0,\tau],\mathcal{L}^\infty(\mathcal{U}))$. By Lemma 3.2.18, there exists a subset $\mathcal{U}' \subset \mathcal{U}$ such that for each $x \in \mathcal{U}'$ and all $t \in [0,\tau]$, x is a Lebesgue point of $w(t,x)$. Since $h(t,s;\cdot)$ is Lipschitz continuous for all $t,s \in [0,\tau]$, we have

$$\begin{aligned}\int_{-1}^{1} |u(t,x+\varepsilon y)-u(t,x)|\mathrm{d}y &= \int_{h(0,t;x-\varepsilon)}^{h(0,t;x+\varepsilon)} |u(t,h(t,0;z))-u(t,x)|h_x(t,0;z)\mathrm{d}z \\ &\le \int_{h(0,t;x-\varepsilon)}^{h(0,t;x+\varepsilon)} |w(t,z)-w(t,h(0,t;x))|h_x(t,0;z)\mathrm{d}z \\ &\le K\int_{h(0,t;x)-K\varepsilon}^{h(0,t;x)+K\varepsilon} |w(t,z)-w(t,h(0,t;x))|\mathrm{d}z,\end{aligned}$$

where K is the Lipschitz constant of $h(t,0;\cdot)$. Therefore x is a Lebesgue point of u whenever $h(0,t;x)$ is a Lebesgue point of w. In particular, for $x \in \mathcal{U}'$, $p_{xx}(t,h(t,0;x))$ is the derivative of p_x and we have

$$\sigma^2 p_{xx}(t,h(t,0;x)) = p(t,h(t,0;x)) - w(t,x).$$

In particular, writing

$$\begin{aligned}h(t,0;,x)-h(t,0;y) &= x-y-\chi\int_0^t p_x(l,h(l,x))-p_x(l,h(l,y))\mathrm{d}l \\ &= x-y-\chi\int_0^t \frac{p_x(l,h(l,0;x))-p_x(l,0;h(l,y))}{h(l,0;x)-h(l,0;y)}(h(l,0;x)-h(l,0;y))\mathrm{d}l \\ &= (x-y)\exp\left(-\chi\int_0^t \frac{p_x(l,h(l,0;x))-p_x(l,0;h(l,y))}{h(l,0;x)-h(l,0;y)}\mathrm{d}l\right),\end{aligned}$$

we find that the formula

$$h_x(t,0;x) = e^{\hat{\chi}\int_0^t w(l,x)-p(l,h(l,0;x))\mathrm{d}l}$$

holds for all $x \in \mathcal{U}'$. Therefore

$$\begin{aligned}p(t,x) &= \int_{\mathbb{R}} \rho(x-y)u(t,y)\mathrm{d}y = \int_{\mathbb{R}} \rho(x-h(t,0;z))u(t,h(t,0;z))h_x(t,0;z)\mathrm{d}z \\ &= \int_{\mathbb{R}} \rho(x-h(t,0;z))w(t,z)e^{\hat{\chi}\int_0^t w(l,z)-p(l,h(l,0;z))\mathrm{d}l}\mathrm{d}z \\ &= \int_{\mathbb{R}} \rho(x-h(t,0;z))u_0(z)e^{\int_0^t 1-w(l,z)\mathrm{d}l}\mathrm{d}z.\end{aligned}$$

Therefore (w,p) is a fixed point of $\mathcal{T}^\tau_{\mathcal{U}}[u_0]$.

Conversely if $u(t,x) = T_t u_0(x)$ for all $t \in [0,\tau]$ then by definition u is a fixed point of $\mathcal{T}^\tau[u_0]$ and we have see in Theorem 3.2.13 that there exists $\mathcal{U} \subset \mathbb{R}$ conull such that $\mathcal{T}^\tau_{\mathcal{U}}[u_0](w,p) = (w,p)$ for a $p \in \tilde{Y}^\tau$, with $w(t,x) = u(t,h(t,0;x))$. It then follows from Lemma 3.2.11 that $p = \rho \star u$ and elementary computation then show that u is indeed a classical solution to (3.2.9) for all $x \in \mathcal{U}$. This proves Item (ii).

This finishes the proof of Proposition 3.2.14. □

Now we prove Lemma 3.2.8 which is used in the proof of Lemma 3.2.10. Next we prove that the solutions remain bounded by 0 and 1.

Lemma 3.2.15 (Boundedness of the solutions)**.** *Let $\tau > 0$ be given and let $u_0 \in L^\infty(\mathbb{R})$ satisfy $0 \le u_0(x) \le 1$. Let $u(t,x)$ be the corresponding integrated solution to* (3.2.1)*. Then*

$$0 \le u(t,x) \le 1.$$

Proof. Let $w(t,x) := u(t,h(t,0;x)) \in C^0\big([0,T];\mathcal{L}^\infty(\mathcal{U})\big)$ for some $T > 0$ and a conull set $\mathcal{U} \subset \mathbb{R}$ (the continuity of $t \mapsto w(t,\cdot)$ follows from Theorem 3.2.13) be such that $t \mapsto w(t,x)$ is a classical solution to (3.2.9) for each $x \in \mathcal{U}$. We prove the uniform bound:

$$\|w(t,\cdot)\|_{\mathcal{L}^\infty(\mathcal{U})} \le 1. \tag{3.2.40}$$

Let $\varepsilon > 0$ and assume by contradiction that there exists $t \in [0, T)$ with

$$\|w(t,.)\|_{\mathcal{L}^\infty(\mathcal{U})} > 1 + \varepsilon.$$

Define

$$t^* := \inf\left\{t > 0 \,|\, \|w(t,.)\|_{L^\infty} > 1 + \varepsilon\right\} < T.$$

Then by the continuity of $t \mapsto \|w(t,\cdot)\|_{\mathcal{L}^\infty(\mathcal{U})}$ we have $\|w(t^*,\cdot)\|_{\mathcal{L}^\infty(\mathcal{U})} = 1 + \varepsilon$. In particular there exists a sequence (t_n, x_n) with $t_n > t^*$, $t_n \to t^*$ as $n \to +\infty$ and $x \in \mathcal{U}$ which satisfies

$$\begin{aligned} &w(t_n, x_n) \to \|w(t^*,\cdot)\|_{\mathcal{L}^\infty(\mathcal{U})}, && \text{as } n \to \infty, \\ &w(t_n, x_n) > 1 + \varepsilon && \forall n \in \mathbb{N}. \end{aligned} \tag{3.2.41}$$

We claim that there exists a N such that for any $n \geq N$ and $t \in [t^*, t_n]$, we have

$$w(t, x_n) > \|w(t,\cdot)\|_{\mathcal{L}^\infty(\mathcal{U})} - \frac{\varepsilon}{2(1+\hat{\chi})} \text{ and } \|w(t,\cdot)\|_{\mathcal{L}^\infty(\mathcal{U})} \geq \|w(t^*,\cdot)\|_{\mathcal{L}^\infty(\mathcal{U})} - \frac{\varepsilon}{2\hat{\chi}}. \tag{3.2.42}$$

Indeed, for $t \in [t^*, t_n]$ we have

$$\begin{aligned} &\big|w(t,x_n) - \|w(t,\cdot)\|_{\mathcal{L}^\infty(\mathcal{U})}\big| \\ &\qquad \leq |w(t,x_n) - w(t^*,x_n)| + |w(t^*,x_n) - w(t_n,x_n)| \\ &\qquad\quad + |w(t_n,x_n) - \|w(t^*,\cdot)\|_{\mathcal{L}^\infty(\mathcal{U})}| + |\|w(t^*,\cdot)\|_{\mathcal{L}^\infty(\mathcal{U})} - \|w(t,\cdot)\|_{\mathcal{L}^\infty(\mathcal{U})}| \\ &\qquad \leq \|w(t,\cdot) - w(t^*,\cdot)\|_{\mathcal{L}^\infty(\mathcal{U})} + \|w(t^*,\cdot) - w(t_n,\cdot)\|_{\mathcal{L}^\infty(\mathcal{U})} \\ &\qquad\quad + |w(t_n,x_n) - \|w(t^*,\cdot)\|_{\mathcal{L}^\infty(\mathcal{U})}| + |\|w(t^*,\cdot)\|_{\mathcal{L}^\infty(\mathcal{U})} - \|w(t,\cdot)\|_{\mathcal{L}^\infty(\mathcal{U})}|. \end{aligned}$$

Due to the continuity of w in $\mathcal{L}^\infty(\mathcal{U})$ there exists $\delta_0 > 0$ such that $\|w(t,\cdot) - w(t^*,\cdot)\|_{\mathcal{L}^\infty(\mathcal{U})} \leq \frac{\varepsilon}{8(1+\hat{\chi})}$ if $|t - t^*| \leq \delta_0$ and by the continuity of $t \mapsto \|w(t,\cdot)\|_{\mathcal{L}^\infty(\mathcal{U})}$ there exists $\delta_1 > 0$ such that $|\|w(t^*,\cdot)\|_{\mathcal{L}^\infty(\mathcal{U})} - \|w(t,\cdot)\|_{\mathcal{L}^\infty(\mathcal{U})}| \leq \frac{\varepsilon}{8(1+\hat{\chi})}$ if $|t - t^*| \leq \delta_1$. Since $t_n \to t^*$ as $n \to +\infty$ and $w(t_n, x_n) \to \|w(t^*,\cdot)\|_{\mathcal{L}^\infty(\mathcal{U})}$ we can choose $N > 0$ such that for all $n \geq N$, we have $|t_n - t^*| \leq \min(\delta_0, \delta_1)$ and $|w(t_n,x_n) - \|w(t^*,\cdot)\|_{\mathcal{L}^\infty(\mathcal{U})}| \leq \frac{\varepsilon}{8(1+\hat{\chi})}$, in which case we have the inequality $\big|\|w(t,\cdot)\|_{\mathcal{L}^\infty(\mathcal{U})} - \|w(t^*,\cdot)\|_{\mathcal{L}^\infty(\mathcal{U})}\big| \leq \frac{\varepsilon}{8(1+\hat{\chi})} \leq \frac{\varepsilon}{1+\hat{\chi}}$ and

$$\big|w(t,x_n) - \|w(t,\cdot)\|_{\mathcal{L}^\infty(\mathcal{U})}\big| \leq \frac{\varepsilon}{2(1+\hat{\chi})}, \qquad \text{for all } t \in [t^*, t_n].$$

Finally, using (3.2.42) we have for all $t \in [t^*, t_n]$:

$$\begin{aligned} \frac{\mathrm{d}}{\mathrm{d}t} w(t,x_n) &= w(t,x_n)\big(1 + \hat{\chi}(\rho \star u)(t, h(t,0;x_n)) - (1+\hat{\chi})w(t,x_n)\big) \\ &\leq w(t,x_n)\left(1 + \hat{\chi}\|w(t,\cdot)\|_{\mathcal{L}^\infty(\mathcal{U})} - (1+\hat{\chi})\|w(t,\cdot)\|_{\mathcal{L}^\infty(\mathcal{U})} + \frac{\varepsilon}{2}\right) \\ &\leq w(t,x_n)\left(1 + \frac{\varepsilon}{2} - \|w(t,\cdot)\|_{\mathcal{L}^\infty(\mathcal{U})}\right) \\ &\leq w(t,x_n)\left(1 + \frac{\varepsilon}{2} - \|w(t^*,\cdot)\|_{\mathcal{L}^\infty(\mathcal{U})} + \frac{\varepsilon}{2}\right) \leq 0. \end{aligned}$$

This implies

$$w(t,x_n) \leq w(t^*,x_n) \leq 1 + \varepsilon, \quad \forall t \in [t^*, t_n].$$

On the other hand, due to (3.2.41) we have

$$w(t_n,x_n) > 1 + \varepsilon.$$

This is a contradiction. Thus for any $t > 0$, $\|w(t,\cdot)\|_{\mathcal{L}^\infty(\mathcal{U})} \leq 1 + \varepsilon$. Since ε is arbitrary, (3.2.40) holds. □

In particular, the solution constructed in Step 1 and 2 can be extended up to $T = +\infty$. We are now in the position to prove Theorem 3.2.2.

Proof of Theorem 3.2.2. Let $u_0 \in L^\infty(\mathbb{R})$.

Existence and uniqueness. The existence and uniqueness of the integrated solution follows directly from Theorem 3.2.13 (existence and uniqueness of a fixed-point problem) and Proposition 3.2.14 (consistency between the fixed-point problem and the integrated solutions).

Continuity. The continuity in the space $L^1_\eta(\mathbb{R})$ and the continuity of $u_0 \in L^\infty(\mathbb{R}) \mapsto T_t u_0 \in L^1_\eta(\mathbb{R})$ have been shown in Theorem 3.2.13.

Other properties. The semigroup property follows directly from the form of the operator has been shown in Theorem 3.2.13. The uniform bound when $0 \le u_0(x) \le 1$ has been shown in Lemma 3.2.15 and the fact that $\tau^*(u_0) = +\infty$ from the fact that the L^∞ norm of $u(t,\cdot)$ cannot blow-up in finite time.

This ends the proof of Theorem 3.2.2. □

Next we show that our model preserves certain properties of the initial condition.

Proposition 3.2.16 (Properties of the solutions)**.** *Let $u(t,x)$ be an integrated solution to* (3.2.1) *and suppose $u_0 \in L^\infty(\mathbb{R})$ with $0 \le u_0 \le 1$. Then*

(i) if $u_0(x)$ is continuous, then $u \in C^0([0,T]\times\mathbb{R})$.

(ii) if $u_0(x) \in C^1(\mathbb{R})$, then $u \in C^1([0,T]\times\mathbb{R})$ and u is then a classical solution to (3.2.1)*.*

(iii) if $u_0(x)$ is monotone, then $u(t,x)$ has the same monotony for each $t > 0$.

Proof. From (3.2.9) we can directly solve the solution $w(t,x) = u(t, h(t,0;x))$ as

$$w(t,x) = \frac{u_0(x)\exp\big(\int_0^t 1+\hat\chi(\rho\star u)(l,h(l,0;x))\mathrm{d}l\big)}{1+(1+\hat\chi)u_0(x)\int_0^t \exp\big(\int_0^l 1+\hat\chi(\rho\star u)(\sigma,h(\sigma,0;x))\mathrm{d}\sigma\big)\mathrm{d}l},$$

for all $t > 0$ and almost all $x \in \mathbb{R}$, which is equivalent to

$$u(t,x) = \frac{u_0(h(0,t;x))\exp\big(\int_0^t 1+\hat\chi(\rho\star u)(l,h(l,t;x))\mathrm{d}l\big)}{1+(1+\hat\chi)u_0(h(0,t;x))\int_0^t \exp\big(\int_0^l 1+\hat\chi(\rho\star u)(\sigma,h(\sigma,t;x))\mathrm{d}\sigma\big)\mathrm{d}l}.$$

Since $(t,x) \to h(t,s;x)$ is continuous, the right-hand side is a continuous function. This shows *(i)*.

Let us show *(ii)*. By *(i)* we have $u \in C^0([0,T]\times\mathbb{R})$. Thus, the spatial derivative of the vector field of (3.2.8) satisfies

$$-\sigma^2(\rho_x \star u)_x(t,x) = u(t,x) - (\rho\star u)(t,x) \in C^0([0,T]\times\mathbb{R}).$$

Therefore, the characteristic flow $(t,s,x) \mapsto h(t,s;x) \in C^1([0,T]\times[0,T]\times\mathbb{R})$. If we denote

$$\phi(t,x) := e^{\int_0^t 1+\hat\chi(\rho\star u)(l,h(l,0,x))dl}, \tag{3.2.43}$$

then $(t,x) \mapsto \phi(t,x)$ is C^1, which implies $w \in C^1([0,T]\times\mathbb{R})$. Since $u(t,x) = w(t,h(0,t;x))$ we have $u \in C^1([0,T]\times\mathbb{R})$.

Finally we show *(iii)*. We will assume that $u_0(x)$ is decreasing (the increasing case can be treated with a similar argument). We let $w(t,x) := u(t,h(t,x))$ where u is the solution to (3.2.1) starting from $u(t=0,x) \equiv u_0(x)$, and $h(t,s;x)$ be the corresponding characteristic flow, i.e. the solution to (3.2.12) with $p(t,x) := \int_{\mathbb{R}} \rho(x-z)w(t,h(0,t;z))\mathrm{d}z$. Our aim is to show that w is a fixed point of the map

$$\begin{aligned}\tilde{\mathcal{T}}_\tau :\quad & C^0\big([0,\tau],L^\infty(\mathbb{R})\big) \longrightarrow C^0\big([0,\tau],L^\infty(\mathbb{R})\big)\\ & \tilde w \longmapsto \frac{u_0(x)\exp\left(\int_0^t 1+\hat\chi\tilde p(s,h(s,0;x))\mathrm{d}s\right)}{1+(1+\hat\chi)u_0(x)\int_0^t \exp\left(\int_0^l 1+\tilde p(s,h(s,0;x))\mathrm{d}s\right)\mathrm{d}l},\end{aligned}$$

where $\tilde p(t,x)$ is defined in the above formula by

$$\tilde p(t,x) := \int_{\mathbb{R}} \rho(x-z)\tilde w(t,h(0,t;z))\mathrm{d}z$$

we stress that h is the characteristic flow corresponding to the "real" solution to (3.2.1) and is independent of $\tilde{w}$.

As the proof is more involved, we subdivide it in four steps.

Step one: Let $r > 0$, we show that there exists τ_0 such that the ball

$$B_r := \left\{ w \in C^0\big([0,\tau], L^\infty(\mathbb{R})\big) \,|\, \|w(t,x) - u_0(x)\|_{C^0\left([0,\tau],L^\infty(\mathbb{R})\right)} \le r \right\}$$

is left stable by $\tilde{\mathcal{T}}_\tau$ for $0 < \tau \le \tau_0$.

Let $w_0 \in B_r$. We compute:

$$\begin{aligned}
|\tilde{\mathcal{T}}_\tau(\tilde{w}) - u_0(x)| &= \left| \frac{u_0(x) e^{\int_0^t 1+\hat{\chi}\tilde{p}(s,h(s,0;x))\mathrm{d}s}}{1 + (1+\hat{\chi})u_0(x)\int_0^t e^{\int_0^l 1+\hat{\chi}\tilde{p}(s,h(s,0;x))\mathrm{d}s}\mathrm{d}l} - u_0(x) \right| \\
&\le |u_0(x)| \left| \frac{e^{\int_0^t 1+\hat{\chi}\tilde{p}(s,h(s,0;x))\mathrm{d}s} - 1 - (1+\hat{\chi})u_0(x)\int_0^t e^{\int_0^l 1+\hat{\chi}\tilde{p}(s,h(s,0;x))\mathrm{d}s}\mathrm{d}l}{1 + (1+\hat{\chi})u_0(x)\int_0^t e^{\int_0^l 1+\hat{\chi}\tilde{p}(s,h(s,0;x))\mathrm{d}s}\mathrm{d}l} \right| \\
&\le \|u_0\|_{L^\infty(\mathbb{R})} \Bigg(e^{1+\hat{\chi}\|u_0\|_{L^\infty(\mathbb{R})}+\hat{\chi}r} \left| \int_0^t 1 + \hat{\chi}\tilde{p}(s,h(s,0;x))\mathrm{d}s \right| \\
&\quad + (1+\hat{\chi})\|u_0\|_{L^\infty(\mathbb{R})} t e^{t(1+\hat{\chi}\|u_0\|_{L^\infty(\mathbb{R})}+\hat{\chi}r)} \Bigg) \\
&\le C\tau,
\end{aligned}$$

where C depends on $\|u_0\|_{L^\infty(\mathbb{R})}$, r, and $\hat{\chi}$. The existence of τ_0 is proved.

Step two: Let $r > 0$, we show that there exists $\tau_1 > 0$ such that $\tilde{\mathcal{T}}_\tau$ is contracting on B_r for $0 < \tau < \tau_1$.

Let $\tilde{w}_1, \tilde{w}_2 \in B_r$, and let $\kappa := 1 + r$ so that $\|w_1\|_{L^\infty(\mathbb{R})} \le \kappa$ and $\|w_2\|_{L^\infty(\mathbb{R})} \le \kappa$. For notational compactness we define in advance

$$\begin{aligned}
\tilde{p}_i(t,x) &:= \int_{\mathbb{R}} \rho(x-z)\tilde{w}_i(t,h(0,t;z))\mathrm{d}z, && i \in \{1,2\}, \\
D_i(t,x) &:= 1 + (1+\hat{\chi})u_0(x)\int_0^t \exp\left(\int_0^l 1 + \tilde{p}_i(s,h(s,0;x))\mathrm{d}s\right)\mathrm{d}l, && i \in \{1,2\}.
\end{aligned}$$

We compute:

$$\begin{aligned}
&\left|\tilde{\mathcal{T}}_\tau(w_1)(t,x) - \tilde{\mathcal{T}}_\tau(w_2)(t,x)\right| \\
&\quad = \left| \frac{u_0(x)e^{\int_0^t 1+\hat{\chi}\tilde{p}_1(s,h(s,0;x))\mathrm{d}s} D_2(t,x) - u_0(x)e^{\int_0^t 1+\hat{\chi}\tilde{p}_2(s,h(s,0;x))\mathrm{d}s} D_1(t,x)}{D_1(t,x)D_2(t,x)} \right| \\
&\quad \le u_0(x) \left| e^{\int_0^t 1+\hat{\chi}\tilde{p}_1(s,h(s,0;x))\mathrm{d}s} - e^{\int_0^t 1+\hat{\chi}\tilde{p}_2(s,h(s,0;x))\mathrm{d}s} \right| \\
&\qquad + (1+\hat{\chi})u_0(x)e^{(\kappa\chi+1)t} \int_0^t \Big| e^{\int_0^l 1+\hat{\chi}\tilde{p}_1(s,h(s,0;x))\mathrm{d}s + \int_0^t 1+\hat{\chi}\tilde{p}_2(s,h(s,0;x))\mathrm{d}s} \\
&\qquad - e^{\int_0^l 1+\hat{\chi}\tilde{p}_2(s,h(s,0;x))\mathrm{d}s + \int_0^t 1+\hat{\chi}\tilde{p}_1(s,h(s,0;x))\mathrm{d}s} \Big| \mathrm{d}l \\
&\quad \le \left(te^{(1+\kappa\chi)} + 2(1+\hat{\chi})t^2 e^{(1+\kappa\chi)(t+1)} \right) \|\chi\tilde{p}_1 - \chi\tilde{p}_2\|_{C^0([0,\tau],L^\infty(\mathbb{R}))} \\
&\quad \le \chi\tau \left(e^{1+\kappa\chi} + 2(1+\hat{\chi})\tau e^{(1+\kappa\chi)(\tau+1)} \right) \|\tilde{w}_1 - \tilde{w}_2\|_{C^0([0,\tau],L^\infty(\mathbb{R}))},
\end{aligned}$$

where we have used the inequalities $\|u_0\|_{L^\infty(\mathbb{R})} \le 1$ and $\|\tilde{p}_1 - \tilde{p}_2\|_{C^0([0,\tau],L^\infty(\mathbb{R}))} \le \|\tilde{w}_1 - \tilde{w}_2\|_{C^0([0,\tau],L^\infty(\mathbb{R}))}$.

The existence of τ_1 is proved.

Step three: We show that the map $\tilde{\mathcal{T}}_\tau$ preserves the monotony of u_0, i.e. the set

$$\mathcal{D} := \{ w \in C^0\big([0,\tau], L^\infty(\mathbb{R})\big) \,|\, w(t,\cdot) \text{ is nonincreasing} \}$$

is left stable by $\tilde{\mathcal{T}}_\tau$.

Indeed, let $\tilde{w}$ be nonincreasing with respect to x. Let $\tilde{w}^1(t,x) := \tilde{\mathcal{T}}_\tau(w)(t,x)$. We first show that $\tilde{P}$ is nonincreasing:

$$\tilde{p}(t,x) - \tilde{p}(t,y) = \int_{\mathbb{R}} \rho(z)\big(\tilde{w}(t,h(0,t;x-z)) - \tilde{w}(t,h(0,t;y-z))\big)\mathrm{d}z \le 0,$$

since the characteristic flow $h(t,s;\cdot)$ is increasing. Next we let

$$D(t,x) := 1 + (1+\hat{\chi}u_0(x)\int_0^t \exp\left(\int_0^l 1 + \hat{\chi}\tilde{p}(s,h(s,0;x))\mathrm{d}s\right)\mathrm{d}l.$$

We compute:

$$\begin{aligned}
&\tilde{w}^1(t,x) - \tilde{w}^1(t,y)\\
&\qquad = \frac{u_0(x)e^{\int_0^t 1+\hat{\chi}\tilde{p}(s,h(s,0;x))\mathrm{d}s}D(t,y) - u_0(y)e^{\int_0^t 1+\hat{\chi}\tilde{p}(s,h(s,0;y))\mathrm{d}s}D(t,x)}{D(t,x)D(t,y)}\\
&\qquad = \frac{u_0(x)e^{\int_0^t 1+\hat{\chi}\tilde{p}(s,h(s,0;x))\mathrm{d}s} - u_0(y)e^{\int_0^t 1+\hat{\chi}\tilde{p}(s,h(s,0;y))\mathrm{d}s}}{D(t,x)D(t,y)}\\
&\qquad\quad + \frac{u_0(x)u_0(y)}{D(t,x)D(t,y)}\int_0^t e^{\int_0^l 1+\hat{\chi}\tilde{p}(t,h(s,0;y))\mathrm{d}y + \int_0^t 1+\hat{\chi}\tilde{p}(s,h(s,0;x))\mathrm{d}s}\\
&\qquad\quad - e^{\int_0^l 1+\hat{\chi}\tilde{p}(t,h(s,0;x))\mathrm{d}y + \int_0^t 1+\hat{\chi}\tilde{p}(s,h(s,0;y))\mathrm{d}s}\mathrm{d}l\\
&\qquad \le \frac{u_0(x)u_0(y)}{D(t,x)D(t,y)}\int_0^t e^{\int_0^l 1+\hat{\chi}\tilde{p}(t,h(s,0;x))\mathrm{d}y + \int_0^t 1+\hat{\chi}\tilde{p}(s,h(s,0;y))\mathrm{d}s}\\
&\qquad\quad \times\left(e^{\hat{\chi}\int_l^t \tilde{p}(s,h(s,0;x))-\tilde{p}(s,h(s,0;y))\mathrm{d}s} - 1\right)\mathrm{d}l \le 0,
\end{aligned}$$

since $\tilde{P}$ is nonincreasing. This shows the stability of $\mathcal{D}$.

Step four: We conclude.

Let $\tau := \min(\tau_0,\tau_1)$ where τ_0,τ_1 are as in Step 1 and 2. By a direct application of the Banach contraction principle, $\tilde{\mathcal{T}}_\tau$ has a unique fixed point in B_r, which is w (since w happens to be a fixed point). Moreover w can be obtained as the limit of the iteration scheme:

$$w^0(t,x) := u_0(x), \qquad\qquad w^{n+1}(t,x) := \tilde{\mathcal{T}}_\tau(w^n)(t,x).$$

Since u_0 is nonincreasing and $\tilde{\mathcal{T}}_\tau$ preserves the monotony, it follows that w is nonincreasing ($\mathcal{D}$ is closed for the considered topology).

Since τ does not depend on u_0, the monotony of $u(t,\cdot)$ for all $t>0$ follows from an induction argument. □

Theorem 3.2.17 (Long-time behavior)**.** *Let $\delta \in (0,1)$ and $u_0(x)$ be such that $\delta \le u_0(x) \le 1$. Let $u(t,x)$ be the corresponding integrated solution to* (3.2.1)*. Then*

$$\lim_{t\to\infty} \|1 - u(t,\cdot)\|_{L^\infty(\mathbb{R})} = 0.$$

Proof. Let θ be defined as

$$\theta := \liminf_{t\to+\infty}\inf_{x\in\mathbb{R}} u(t,x),$$

and assume by contradiction that $\theta < 1$. We first remark that for any $x\in\mathbb{R}$ we have

$$\begin{cases} \partial_t w(t,x) = w(t,x)\left(1+\hat{\chi}(\rho\star u)(t,h(t,0;x)) - (1+\hat{\chi})w(t,x)\right)\\ \qquad\qquad \ge w(t,x)\big(1-(1+\hat{\chi})w(t,x)\big)\\ w(0,x) \quad \ge \delta. \end{cases} \qquad t>0,$$

Thus, for each $x\in\mathbb{R}$,

$$w(t,x) \ge \delta, \quad x\in\mathbb{R}, t>0.$$

In particular $(\rho\star u)(t,h(t,0;x))=\int_{\mathbb{R}}\rho(h(t,0;x)-y)u(t,y)\mathrm{d}y\geq\delta\int_{\mathbb{R}}\rho(h(t,0;x)-y)\mathrm{d}y=\delta$. We deduce that

$$\begin{cases}\partial_t w(t,x)=w(t,x)\left(1+\hat{\chi}(\rho\star u)(t,h(t,0;x))-(1+\hat{\chi})w(t,x)\right)\\ \qquad\qquad\geq w(t,x)\big(1+\hat{\chi}\delta-(1+\hat{\chi})w(t,x)\big)\\ w(0,x)\quad\geq\delta.\end{cases}\quad t>0,$$

This implies for any $t>0, x\in\mathbb{R}$

$$w(t,x)\geq\frac{\delta e^{t(1+\hat{\chi}\delta)}}{1+\frac{(1+\hat{\chi})\delta}{1+\hat{\chi}\delta}\left(e^{t(1+\hat{\chi}\delta)}-1\right)}\xrightarrow{t\to\infty}\frac{1+\hat{\chi}\delta}{1+\hat{\chi}}.$$

In particular

$$\theta\geq\frac{1+\hat{\chi}\delta}{1+\delta}>\frac{1}{1+\hat{\chi}}.\tag{3.2.44}$$

It is not difficult to see that for each $\alpha\in(0,1)$ there exists T_α such that, for all $t\geq T_\alpha$, we have

$$\inf_{x\in\mathbb{R}}w(t,x)\geq\alpha\theta.$$

Therefore for all $t\geq T_\alpha$,

$$(\rho\star u)(t,h(t,0;x))\geq\alpha\theta\int_{\mathbb{R}}\rho(h(t,0;x)-y)\mathrm{d}y=\alpha\theta,$$

which yields

$$\begin{cases}\partial_t w(t,x)=w(t,x)\left(1+(\rho\star u)(t,h(t,0;x))-(1+\hat{\chi})w(t,x)\right)\\ \qquad\qquad\geq w(t,x)\left(1+\alpha\theta-(1+\hat{\chi})w(t,x)\right)\\ w(T_1,x)\ \geq\frac{1+\hat{\chi}\frac{\delta}{2}}{1+\hat{\chi}}\end{cases}\quad t>T_1, x\in\mathbb{R}$$

and finally

$$\theta=\liminf_{t\to+\infty}\inf_{x\in\mathbb{R}}w(t,x)\geq\frac{1+\hat{\chi}\alpha\theta}{1+\hat{\chi}}.$$

This is a contradiction if α is chosen as

$$\alpha=1-\frac{1}{\hat{\chi}}\left(\frac{1}{\theta}-1\right),$$

and this choice is admissible because

$$\frac{1}{\hat{\chi}}\left(\frac{1}{\theta}-1\right)<\frac{1}{\hat{\chi}}\left(1+\hat{\chi}-1\right)=1$$

by (3.2.44). This concludes the proof of Theorem 3.2.17. □

Acknowledgements

Xiaoming Fu was supported by China Scholarship Council during research. His current affiliation is

- Key Laboratory of Advanced Control and Optimization for Chemical Processes, Ministry of Education, East China University of Science and Technology, Shanghai 200237, China.
- School of Biological Sciences, the University of Edinburgh, Max Born Crescent, Edinburgh, EH9 3JH, Scotland, United Kingdom.

Appendix

3.2.4 Lebesgue points along continuous trajectories

Here we show that the space $\mathcal{L}^\infty(\mathcal{U})$ is well-behaved with respect to Lebesgue points when $\mathcal{U}$ is a subset of $\mathbb{R}$.

Lemma 3.2.18 (Lebesgue points along continuous trajectories)**.** *Let $\mathcal{U} \subset \mathbb{R}$ be conull. Let $w \in \mathcal{C}^0([0,\tau], \mathcal{L}^\infty(\mathcal{U}))$ be given, then there exists a conull set $\mathcal{U}' \subset \mathcal{U}$ such that each $x \in \mathcal{U}'$ is a Lebesgue points of $w(t,\cdot)$ for all $t \in [0,\tau]$.*

Proof. Recall that a Lebesgue point of a measurable function $f : \mathcal{U} \to \mathbb{R}$ is characterized by the property

$$\lim_{\varepsilon \to 0} \frac{1}{2\varepsilon} \int_{x-\varepsilon}^{x+\varepsilon} |f(z) - f(x)| \mathrm{d}z = 0$$

or, equivalently,

$$\lim_{\varepsilon \to 0} \frac{1}{2} \int_{-1}^{1} |f(x+\varepsilon y) - f(x)| \mathrm{d}z = 0.$$

Let $w \in C^0([0,\tau], \mathcal{L}^\infty(\mathcal{U}))$ be given. Given $q \in \mathbb{Q} \cap [0,\tau]$ we define the failure set

$$\mathcal{F}_q := \{x \in \mathcal{U} \,|\, x \text{ is a not a Lebesgue point of } w\,(q,\cdot)\}\,.$$

It is classical that for each q the set $\mathcal{F}_q$ is negligible for the Lebesgue measure λ, *i.e.* $\lambda(\mathcal{F}_q) = 0$. Since the family $(\mathcal{F}_q)_{q \in \mathbb{Q} \cap [0,\tau]}$ is countable, we have

$$\lambda \left(\bigcup_{q \in \mathbb{Q} \cap [0,\tau]} \mathcal{F}_q \right) = 0$$

therefore the set $\mathcal{U}' := \mathcal{U} \setminus \bigcup_{q \in \mathbb{Q} \cap [0,\tau]} \mathcal{F}_q$ is conull.

Let us show that $\mathcal{U}'$ is composed of Lebesgue points of $w(t,\cdot)$. Let $x \in \mathcal{U}'$ and $t \in [0,\tau]$, then there exists a sequence of rational numbers $t_n \in \mathbb{Q}$ such that $t_n \to t$. By definition of $\mathcal{U}'$, x is not in any $\mathcal{F}_{t_n}$ and therefore x is a Lebesgue point of the functions $w(t_n,\cdot)$ for all $n \in \mathbb{N}$. We have:

$$\begin{aligned}
&\int_{-1}^{1} |w(t, x+\varepsilon y) - w(t,x)| \mathrm{d}y \\
&\qquad \leq \int_{-1}^{1} |w(t, x+\varepsilon y) - w(t_n, x+\varepsilon y)| \mathrm{d}y + \int_{-1}^{1} |w(t_n, x+\varepsilon y) - w(t_n, x)| \mathrm{d}y \\
&\qquad\quad + \int_{-1}^{1} |w(t_n, x) - w(t, x)| \mathrm{d}y \\
&\qquad \leq \int_{-1}^{1} |w(t_n, x+\varepsilon y) - w(t_n, x)| \mathrm{d}y + 2\|w(t,\cdot) - w(t_n,\cdot)\|_{\mathcal{L}^\infty(\mathcal{U})},
\end{aligned}$$

therefore the right-hand side is arbitrarily small when $\varepsilon \to 0$. We conclude that x is a Lebesgue point of $w(t,\cdot)$. Lemma 3.2.18 is proved. □

3.3 Sharp discontinuous traveling waves in a hyperbolic Keller–Segel equation

3.3.1 Introduction

In this section 3.3 we are concerned with the following diffusion equation with logistic source:

$$\begin{cases} \partial_t u(t,x) - \chi \partial_x \big(u(t,x)\partial_x p(t,x)\big) = u(t,x)(1-u(t,x)), \quad t>0,\ x\in\mathbb{R}, \\ u(t=0,x) = u_0(x), \end{cases} \tag{3.3.1}$$

where $\chi > 0$ is a *sensing coefficient* and $p(t,x)$ is an external pressure. Model (3.3.1) describes the behavior of a population of cells $u(t,x)$ living in a one-dimensional habitat $x \in \mathbb{R}$, which undergo a logistic birth and death population dynamics, and in which individual cells follow the gradient of a field p. The constant χ characterizes the response of the cells to the effective gradient p_x. In this work we will consider the case where p is itself determined by the state of the population $u(t,x)$ as

$$-\sigma^2 \partial_{xx} p(t,x) + p(t,x) = u(t,x), \quad t>0, x\in\mathbb{R}. \tag{3.3.2}$$

The above equation (3.3.2) corresponds to the limit of fast diffusion $\varepsilon \to 0$ of the parabolic equation (3.3.8). It corresponds to a scenario in which the field $p(t,x)$ is produced by the cells, diffuses to the whole space with diffusivity σ^2 (for $\sigma > 0$), and vanishes at rate one. As a result cells are pushed away from crowded area to emptier region.

A similar model has been successfully used in our recent work [P8] to describe the motion of cancer cells in a Petri dish in the context of cell co-culture experiments of Pasquier et al. [318]. Pasquier et al. [318] cultivated two types of breast cancer cells to study the transfer of proteins between them in a study of multi-drug resistance. It was observed that the two types of cancer cells form segregated clusters of cells of each kind after a 7-day co-culture experiment (Figure 3.3.1 **(a)**). In section 3.2, we studied the segregation property of a model similar to (3.3.1)–(3.3.2), set in a circular domain in two spatial dimensions $x \in \mathbb{R}^2$ representing a Petri dish. Starting from islet-like initial conditions representing cell clusters, it was numerically observed that the distribution of cells converges to a segregated state in the long run.

One may observe that in such an experiment the cells are well fed. So there is no limitation for food. As explained in Ducrot et al.[155], the limitations are due to space and the contact inhibition of growth is involved. Therefore the right hand side of (3.3.1), which is a logistic term (for simplicity), could possibly have the following form

$$f(x) = \frac{\beta x}{1+\alpha x} - \mu x$$

where β is the division rate and μ is the mortality rate. We believe that our results hold for such a non-linearity and this is left for future work.

Strikingly, even before the two species come in contact, a sharp transition is formed between the space occupied by one species and the empty space being invaded (Figure 3.3.1 **(b)**) and the distribution of cells looks like a very sharp traveling front. In an attempt to better understand the spatial behavior of cell populations growing in a Petri dish, in the present paper we investigate the mathematical properties of a simplified model for a single species on the real line. We are particularly interested in showing the existence of a sharp traveling front moving at a constant speed.

Our model can be included in the family of non-local advection models for cell-cell adhesion and repulsion. As pointed out by many biologists, cell-cell interactions do not only exist in a local scope, but a long-range interaction should be taken into account to guide the mathematical modeling. Armstrong, Painter and Sherratt [16] in their early work proposed a model (APS model) in which a local diffusion is added to the non-local attraction driven by the adhesion forces to describe the phenomenon of cell mixing, full/partial engulfment and complete sorting in the cell sorting problem. Based on the APS model, Murakawa and Togashi [296] thought that the population pressure should come from the cell volume size instead of the linear diffusion. Therefore, the linear diffusion was changed into a nonlinear diffusion in order to capture the sharp fronts and the segregation in cell co-culture. Carrillo et al. [105] recently proposed a new assumption on the adhesion velocity field and their model showed a good agreement in the experiments in the work of Katsunuma et al. [229]. The idea of the long-range attraction and short-range repulsion can also be seen in the work of Leverentz, Topaz and Bernoff [250]. They considered a non-local advection model to study the asymptotic behavior of the solution. By choosing a Morse-type kernel which follows the attractive-repulsive interactions, they found that the solution can asymptotically spread, contract (blow-up), or reach a steady-state. Burger, Fetecau and Huang [83] considered a similar non-local adhesion model with nonlinear

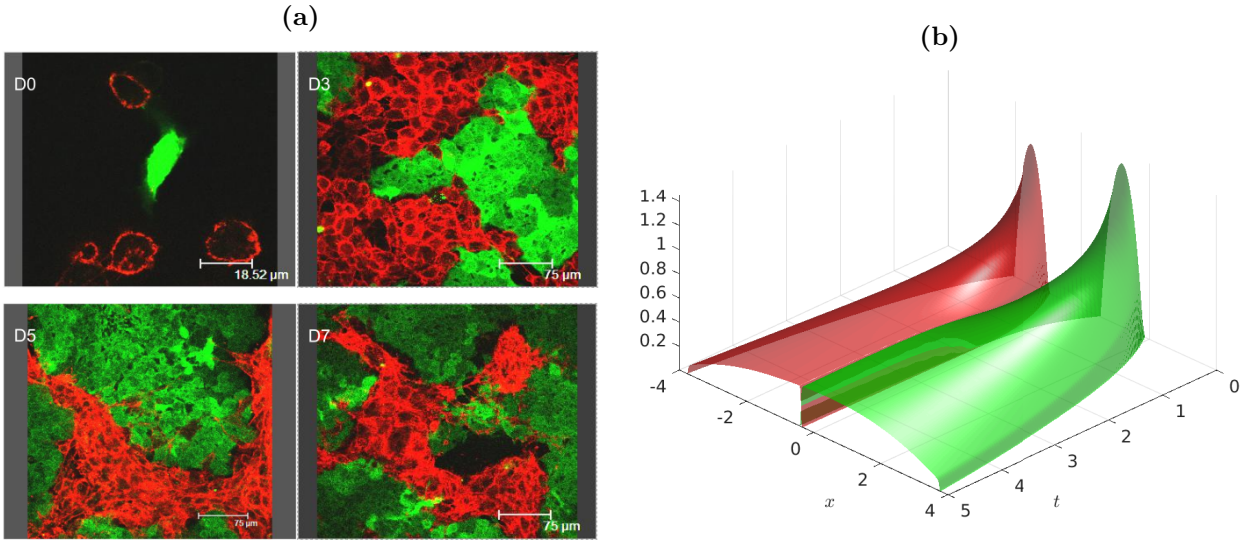

Figure 3.3.1: *[P8, Figure 1 and Figure 5 (b)].* ***(a)*** *Direct immunodetection of P-gp transfers in co-cultures of sensitive (MCF-7) and resistant (MCF-7/Doxo) variants of the human breast cancer cell line.* ***(b)*** *The temporal-spatial evolution of the two species in the 1D model. One can check that a discontinuity is forming near the front face of the green surface.*

diffusion, for which they investigated the well-posedness and proved the existence of a compactly supported, non-constant steady state. Dyson et al. [156] established the local existence of a classical solution for a non-local cell-cell adhesion model in spaces of uniformly continuous functions. For Turing and Turing-Hopf bifurcation due to the non-local effect, we refer to Ducrot et al. [151] and Song et al. [365]. We also refer to Mogliner et al. [288], Eftimie et al. [158], Ducrot and Magal [152], Ducrot and Manceau [153] for more topics on non-local advection equations. For the derivation of such models, we refer to the work of Bellomo et al. [44] and Morale, Capasso and Oelschläger [290].

Since the pressure $p(t,x)$ is a non-local function of the density $u(t,x)$ in (3.3.2), the spatial derivative appears as a *non-local advection* term in (3.3.1). In fact, our problem (3.3.1)–(3.3.2) can be rewritten as a transport equation in which the speed of particles is non-local in the density,

$$\begin{cases} l\partial_t u(t,x) - \chi\partial_x(u(t,x)\partial_x(\rho\star u)(t,x)) = u(t,x)(1-u(t,x)), \\ u(t=0,x) = u_0(x), \end{cases} \tag{3.3.3}$$

where

$$(\rho\star u)(x) = \int_{\mathbb{R}} \rho(x-y)u(t,y)dy, \quad \rho(x) = \frac{1}{2\sigma}e^{-\frac{|x|}{\sigma}}. \tag{3.3.4}$$

Traveling waves for a similar diffusive equation with logistic reaction have been investigated for quite general non-local kernels by Hamel and Henderson [198], who considered the model

$$u_t + (u\,(K\star u))_x = u_{xx} + u(1-u), \tag{3.3.5}$$

where $K \in L^p(\mathbb{R})$ is odd and $p \in [1,\infty]$. Notice that the attractive parabolic-elliptic Keller-Segel model (3.3.9) is included in this framework by the particular choice

$$K(x) = -\chi\ \operatorname{sign}(x)e^{-|x|/\sqrt{d}}/\left(2\sqrt{d}\right).$$

They proved a spreading result for this equation (initially compactly supported solutions to the Cauchy problem propagate to the whole space with constant speed) and explicit bounds on the speed of propagation. Diffusive non-local advection also appears in the context of swarm formation [289]. Pattern formation for a model similar to (3.3.5) by Ducrot, Fu and Magal [151]. Let us mention that the inviscid equation (3.3.3) has been studied in a periodic cell by Ducrot and Magal [152]. Other methods have been established for conservative systems of interacting particles and their kinetic limit (Balagué et al. [30], Carrillo et al. [104]) based on gradient flows set on measure spaces; those are difficult to adapt here because of the logistic term.

There is also related literature regarding traveling waves in nonlocal reaction-diffusion equations[121, P4, 393, 165, 154].

Recall that a traveling wave is a special solution having the specific form

$$u(t,x) = U(x - ct), \text{ for a.e. } (t,x) \in \mathbb{R}^2,$$

where the profile U has the following behavior at $\pm\infty$:

$$\lim_{z\to-\infty} U(z) = 1, \quad \lim_{z\to\infty} U(z) = 0.$$

The goal of this section 3.3 is to investigate sharp traveling waves namely

$$U(x) = 0, \text{ for all } x > 0.$$

Moreover as it is represented in Figure 3.3.2-(a) we will obtain the existence of such a wave with a discontinuity at $x = 0$ for the profile U. Discontinuous traveling waves in hyperbolic partial differential equations

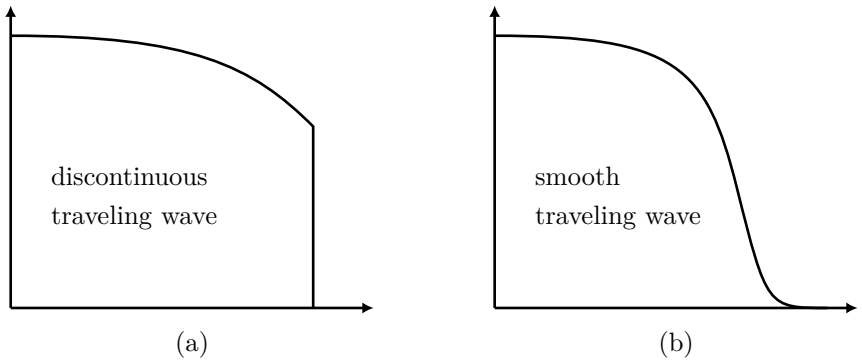

Figure 3.3.2: *An illustration of two types of traveling wave solutions.*

have appeared in the literature of the recent few years. Travelling wave solutions with a shock or jump discontinuity have been found *e.g.* in models of malignant tumor cells (Marchant, Norbury and Perumpanani [277], Harley *et al.* [202] where the existence of discontinuous waves is proved by means of geometric singular perturbation theory for ODEs) or chemotaxis (Landman, Pettet and Newgreen [247] where both smooth and discontinuous traveling waves are found using phase plane analysis).

It can be noticed that, in the limit of slow diffusivity $\sigma \to 0$ (and under the simplifying assumption that $\chi = 1$), we get $u(t,x) \equiv p(t,x)$ and (3.3.1) is equivalent to an equation with *porous medium-type diffusion* and logistic reaction

$$u_t - \frac{1}{2}(u^2)_{xx} = u(1-u). \tag{3.3.6}$$

We refer to the monograph of Vázquez [380] for more result about porous medium equation. The propagation dynamics for this kind of equation was first studied, to the extent of our knowledge, by Aronson [21], Atkinson, Reuter and Ridler-Rowe [23], and later by de Pablo and Vázquez [313], in the more general context of nonlinear diffusion

$$u_t = (u^m)_{xx} + u(1-u), \text{ with } m > 1. \tag{3.3.7}$$

In Section 3.3.3.3, we observe that the discontinuous sharp traveling obtained in the present section 3.3 converge (numerically) to the continuous profile described by Pablo and Vázquez [313].

The particular relation between the pressure $p(t,x)$ and the density $u(t,x)$ in (3.3.2) strongly reminds the celebrated model of chemotaxis studied by Patlak (1953) and Keller and Segel (1970) [320, 233, 232] (parabolic-parabolic Keller-Segel model) and, more specifically, the parabolic-elliptic Keller-Segel model which is derived from the former by a quasi-stationary assumption on the diffusion of the chemical [226]. Indeed Equation (3.3.2) can be formally obtained as the quasistatic approximation of the following parabolic equation

$$\varepsilon\partial_t p(t,x) = \chi p_{xx}(t,x) + u(t,x) - p(t,x), \tag{3.3.8}$$

when $\varepsilon \to 0$. A rigorous derivation of the limit has been achieved in the case of the Keller-Segel model by Carrapatoso and Mischler [103]. We also refer to de Mottoni and Rothe [293] for such a result in the context

of linear parabolic equations. We refer to Calvez and Corrias[94], Hillen and Painter[209], Perthame and Dalibard[323] and the references therein for a mathematical introduction and biological applications. In these models, the field $p(t,x)$ is interpreted as the concentration of a chemical produced by the cells rather than a physical pressure. One of the difficulties in attractive chemotaxis models is that two opposite forces compete to drive the behavior of the equations: the *diffusion* due to the random motion of cells, on the one hand, and on the other hand the *non-local advection* due to the attractive chemotaxis; the former tends to regularize and homogenize the solution, while the latter promotes cell aggregation and may lead to the blow-up of the solution in finite time [109, 226]. At this point let us mention that our study concerns *repulsive* cell-cell interaction with no diffusion, therefore no such blow-up phenomenon is expected in our study; however the absence of diffusion adds to the mathematical complexity of the study, because standard methods of reaction-diffusion equations cannot be employed here. Traveling waves for the (attractive) parabolic-elliptic Keller-Segel model were studied by Nadin, Perthame and Ryzhik [301], who constructed these traveling wave by a bounded interval approximation of the 1D system

$$\begin{cases} l u_t + \chi\,(u p_x)_x = u_{xx} + u(1-u), \\ \qquad\qquad -d\,p_{xx} + p = u, \end{cases} \tag{3.3.9}$$

set on the real line $x \in \mathbb{R}$, when the strength of the advection is not too strong $0 < \chi < \min(1,d)$, and gave estimates on the speed of such a traveling wave: $2 \le c_* \le 2 + \chi\sqrt{d}/(d-\chi)$. More recently, Salako and Shen [344, 345, 346] and Salako, Shen and Xue [347] published a series of articles concerning the asymptotic properties and spatial dynamics of chemotaxis models.

In this paper we focus on the particular case of (3.3.1)–(3.3.2) with $\sigma > 0$ and $\chi > 0$. The paper is organized as follows. In Section 2, we present our main results. In Section 3 we present numerical simulations to illustrate our theoretical results. In Section 4, we prove the propagation properties of the solution and describe the local behavior near the propagating boundary (see Proposition 3.3.6 for definition), including the formation of a discontinuity for time-dependent solutions. In Section 5 we prove the existence of sharp traveling waves. We also prove that smooth traveling waves are necessarily positive, which shows that sharp traveling waves are necessarily singular (in this case, discontinuous). In particular, a solution starting from a compactly supported initial condition with polynomial behavior at the boundary can never catch such a smooth traveling wave.

3.3.2 Main results and comments

We begin by defining our notion of solution to equation (3.3.1).

Definition 3.3.1 (Integrated solutions)**.** Let $u_0 \in L^\infty(\mathbb{R})$. A measurable function $u(t,x) \in L^\infty([0,T]\times\mathbb{R})$ is an *integrated solution* to (3.3.1) if the characteristic equation

$$\begin{cases} l\dfrac{\mathrm{d}}{\mathrm{d}t}h(t,x) = -\chi(\rho_x \star u)(t,h(t,x)) \\ \qquad\qquad h(t=0,x) = x. \end{cases} \tag{3.3.10}$$

has a classical solution $h(t,x)$ (*i.e.* for each $x \in \mathbb{R}$ fixed, the function $t \mapsto h(t,x)$ is in $C^1([0,T],\mathbb{R})$ and satisfies (3.3.10)), and for a.e. $x \in \mathbb{R}$, the function $t \mapsto u(t,h(t,x))$ is in $C^1([0,T],\mathbb{R})$ and satisfies

$$\begin{cases} l\dfrac{\mathrm{d}}{\mathrm{d}t}u(t,h(t,x)) = u(t,h(t,x))\big(1+\hat\chi(\rho\star u)(t,h(t,x)) - (1+\hat\chi)u(t,h(t,x))\big), \\ \qquad\qquad u(t=0,x) = u_0(x), \end{cases} \tag{3.3.11}$$

where $\hat\chi := \frac{\chi}{\sigma^2}$.

We define weighted space $L^1_\eta(\mathbb{R})$ as follows

$$L^1_\eta(\mathbb{R}) := \left\{ f : \mathbb{R} \to \mathbb{R} \text{ measurable} \,\middle|\, \int_{\mathbb{R}} |f(x)| e^{-\eta|x|}\mathrm{d}x < \infty \right\}.$$

$L^1_\eta(\mathbb{R})$ is a Banach space endowed with the norm

$$\|f\|_{L^1_\eta} := \frac{\eta}{2}\int_{\mathbb{R}} |f(y)| e^{-\eta|y|}\mathrm{d}y.$$

We first recall some results concerning the existence of integrated solutions for equation (3.3.1) in Theorem 3.3.2, Proposition 3.3.3 and Theorem 3.3.4. We prove those results in the companion paper [P11].

Theorem 3.3.2 (Well-posedness). *Let $u_0 \in L^\infty_+(\mathbb{R})$ and fix $\eta > 0$. There exists $\tau^*(u_0) \in (0, +\infty]$ such that for all $\tau \in (0, \tau^*(u_0))$, there exists a unique integrated solution $u \in C^0([0,\tau], L^1_\eta(\mathbb{R}))$ to (3.3.1) which satisfies $u(t=0,x) = u_0(x)$. Moreover $u(t,\cdot) \in L^\infty(\mathbb{R})$ for each $t \in [0, \tau^*(u_0))$ and the map $t \in [0, \tau^*(u_0)) \mapsto T_t u_0 := u(t,\cdot)$ is a semigroup which is continuous for the $L^1_\eta(\mathbb{R})$-topology. The map $u_0 \in L^\infty(\mathbb{R}) \mapsto T_t u_0 \in L^1_\eta(\mathbb{R})$ is continuous.*

Finally, if $0 \le u_0(x) \le 1$, then $\tau^*(u_0) = +\infty$ and $0 \le u(t,\cdot) \le 1$ for all $t > 0$.

The next result concerns the preservation properties satisfied by the solutions of (3.3.1) (see [P11, Proposition 2.2]).

Proposition 3.3.3 (Regularity of solutions). *Let $u(t,x)$ be an integrated solution to (3.3.1).*

1. *if $u_0(x)$ is continuous, then $u(t,x)$ is continuous for each $t > 0$.*
2. *if $u_0(x)$ is monotone, then $u(t,x)$ has the same monotony for each $t > 0$.*
3. *if $u_0(x) \in C^1(\mathbb{R})$, then $u \in C^1([0,T] \times \mathbb{R})$ and u is then a classical solution to (3.3.1).*

In this following theorem we consider the long-time behavior of some solutions to (3.3.1) (see [P11, Theorem 2.3]).

Theorem 3.3.4 (Long-time behavior). *Let $0 \le u_0(x) \le 1$ be a nontrivial non-negative initial condition and $u(t,x)$ be the corresponding integrated solution. Then $0 \le u(t,x) \le 1$ for all $t > 0$ and $x \in \mathbb{R}$. If moreover there exists $\delta > 0$ such that $\delta \le u_0(x) \le 1$ then*

$$u(t,x) \to 1, \ \text{as } t \to \infty$$

and the convergence holds uniformly in $x \in \mathbb{R}$.

We now arrive at the main interest of the paper, which is to describe the spatial dynamics of solutions to (3.3.1)–(3.3.2). To get insight about the asymptotic propagation properties of the solutions, we focus on initial conditions whose support is bounded towards $+\infty$. If the behavior of the initial condition in a neighbourhood of the boundary of the support is polynomial, we can establish a precise estimate of the location of the level sets relative to the position of the rightmost positive point. Our first assumption requires that the initial condition is supported in $(-\infty, 0]$.

Assumption 3.3.5 (Initial condition). We assume that $u_0(x)$ is a continuous function satisfying

$$\begin{aligned} 0 \le u_0(x) \le 1, &\qquad \text{for all } x \in \mathbb{R}, \\ u_0(x) = 0, &\qquad \text{for all } x \ge 0, \\ u_0(x) > 0, &\qquad \text{for all } x \in (-\delta_0, 0), \end{aligned}$$

for some $\delta_0 > 0$.

Under this assumption we show that u is propagating to the right.

Proposition 3.3.6 (The separatrix). *Let $u_0(x)$ satisfy Assumption 3.3.5, and $h^*(t) := h(t,0)$ be the separatrix. Then $h^*(t)$ stays at the rightmost boundary of the support of $u(t,\cdot)$, i.e.*

(i) we have

$$u(t,x) = 0 \text{ for all } x \ge h^*(t), \tag{3.3.12}$$

(ii) for each $t > 0$ there exists $\delta > 0$ such that

$$u(t,x) > 0 \text{ for all } x \in \big(h^*(t) - \delta, h^*(t)\big). \tag{3.3.13}$$

Moreover, u is propagating to the right i.e.

$$\frac{\mathrm{d}}{\mathrm{d}t} h^*(t) > 0 \text{ for all } t > 0.$$

We precise the behavior of the initial condition in a neighbourhood of 0 and estimate the steepness of u in positive time.

Assumption 3.3.7 (Polynomial behavior near 0)**.** In addition to Assumption 3.3.5, we require that there exists $\alpha \geq 1$ and $\gamma > 0$ such that

$$u_0(x) \geq \gamma |x|^\alpha, \qquad \text{for all } x \in (-\delta, 0).$$

Theorem 3.3.8 (Formation of a discontinuity)**.** *Let $u_0(x)$ satisfy Assumptions 3.3.5 and 3.3.7 and $u(t,x)$ solve* (3.3.1) *with $u(t=0,x) = u_0(x)$. For all $\delta > 0$ we have*

$$\limsup_{t \to +\infty} \sup_{x \in (h^*(t)-\delta, h^*(t))} u(t,x) \geq \frac{1}{1+\hat{\chi}+\alpha\chi} > 0. \tag{3.3.14}$$

More precisely, define the level set

$$\xi(t,\beta) := \sup\{x \in \mathbb{R} \,|\, u(t,x) = \beta\},$$

for all $t > 0$ and $0 < \beta < \frac{1}{1+\hat{\chi}+\alpha\chi}$. Then, for each $0 < \beta < \frac{1}{1+\hat{\chi}+\alpha\chi}$, the distance between $\xi(t,\beta)$ and the separatrix is decaying exponentially fast:

$$h^*(t) - \left(\frac{\beta}{\gamma}\right)^{\frac{1}{\alpha}} e^{-\frac{\eta}{2\alpha}t} \leq \xi(t,\beta) \leq h^*(t), \tag{3.3.15}$$

where $\eta \in (0,1)$ is given in Proposition 3.3.19 and $\hat{\chi} = \frac{\chi}{\sigma^2}$.

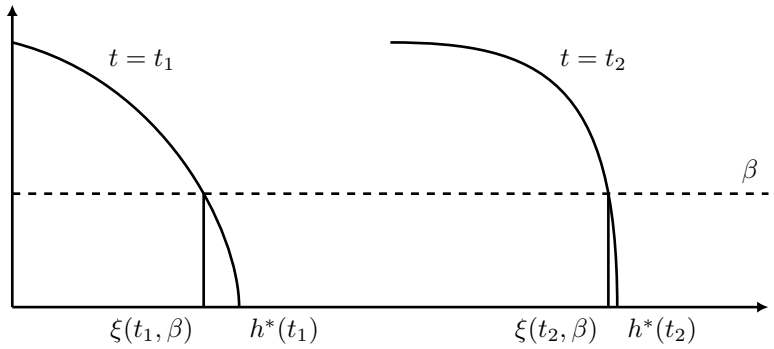

Figure 3.3.3: *A cartoon for the formation of the discontinuity. Here we choose $t_1 < t_2$ and $\xi(t,\beta), t = t_1, t_2$ are the level sets. Theorem 3.3.8 proves that when Assumptions 3.3.5 and 3.3.7 are satisfied, then the distance $|\xi(t,\beta) - h^*(t)|$ converges to 0 exponentially fast.*

In particular, the profile $u(t,x)$ forms a discontinuity near the boundary point $h^*(t)$ as $t \to +\infty$. By considering discontinuous integrated solutions, we are able to estimate the size of the jump for non increasing profiles, which leads to an estimate of the asymptotic speed.

Proposition 3.3.9 (Asymptotic jump near the separatrix)**.** *Let u_0 be a non increasing function satisfying $u_0(-\infty) \leq 1$, $u_0(0) > 0$ and $u_0(x) = 0$ for $x > 0$. Then*

$$\liminf_{t \to +\infty} u(t, h^*(t)) \geq \frac{2}{2+\hat{\chi}}, \tag{3.3.16}$$

$$\liminf_{t \to +\infty} \frac{\mathrm{d}}{\mathrm{d}t} h^*(t) \geq \frac{\sigma\hat{\chi}}{2+\hat{\chi}}, \tag{3.3.17}$$

where $\hat{\chi} = \frac{\chi}{\sigma^2}$.

We finally turn to traveling wave solutions $u(t,x) = U(x-ct)$, which are self-similar profiles traveling at a constant speed.

Definition 3.3.10 (Traveling wave solution)**.** A *traveling wave* is a nonnegative solution $u(t,x)$ to (3.3.1) such that there exists a function $U \in L^\infty(\mathbb{R})$ and a speed $c \in \mathbb{R}$ such that $u(t,x) = U(x-ct)$ for a.e. $(t,x) \in \mathbb{R}^2$. By convention, we also require that U has the following behavior at $\pm\infty$:

$$\lim_{z\to-\infty} U(z) = 1, \quad \lim_{z\to\infty} U(z) = 0.$$

The function U is the *profile* of the traveling wave.

Under a technical assumption on $\hat{\chi} = \frac{\chi}{\sigma^2}$, we can prove the existence of sharp traveling waves which present a jump at the vanishing point.

Assumption 3.3.11 (Bounds on $\hat{\chi}$)**.** Let $\chi > 0$ and $\sigma > 0$ be given and define $\hat{\chi} := \frac{\chi}{\sigma^2}$. We assume that $0 < \hat{\chi} < \bar{\chi}$, where $\bar{\chi}$ is the unique root of the function

$$\hat{\chi} \mapsto \ln\left(\frac{2-\hat{\chi}}{\hat{\chi}}\right) + \frac{2}{2+\hat{\chi}}\left(\frac{\hat{\chi}}{2}\ln\left(\frac{\hat{\chi}}{2}\right) + 1 - \frac{\hat{\chi}}{2}\right)$$

given in 3.3.27.

Remark 3.3.12. It follows from 3.3.27 that $\hat{\chi} = 1$ satisfies Assumption 3. Actually, numerical evidence suggest that $\bar{\chi} \approx 1.045$.

Theorem 3.3.13 (Existence of a sharp discontinuous traveling wave)**.** *Let Assumption 3.3.11 be satisfied. There exists a traveling wave $u(t,x) = U(x-ct)$ traveling at speed*

$$c \in \left(\frac{\sigma\hat{\chi}}{2+\hat{\chi}}, \frac{\sigma\hat{\chi}}{2}\right),$$

where $\hat{\chi} = \frac{\chi}{\sigma^2}$

Moreover, the profile U satisfies the following properties (up to a shift in space):

(i) U is sharp *in the sense that $U(x) = 0$ for all $x \geq 0$; moreover, U has a discontinuity at $x = 0$ with $U(0^-) \geq \frac{2}{2+\hat{\chi}}$.*

(ii) U is continuously differentiable and strictly decreasing on $(-\infty, 0]$, and satisfies

$$-cU' - \chi(UP')' = U(1-U)$$

pointwise on $(-\infty, 0)$, where $P(z) := (\rho \star U)(z)$.

Our proof is based on a fixed-point argument. Other methods could have been imagined, like a vanishing viscosity argument. This method consists in adding a small elliptic regularization $\varepsilon\partial_{xx}u$ in the right-hand side of equation (3.3.1), prove the existence of a traveling wave for the regularized problem (similar to (3.3.5)), then let the regularization vanish $\varepsilon \to 0$. With the appropriate estimates, it may then be possible to prove the existence of a traveling front for the original equation. However, the implementation of this method is not without difficulties. Firstly, the vanishing viscosity process $\varepsilon \to 0$ requires a kind of compactness, which cannot be provided by the Arzelà-Ascoli here because the limiting object is discontinuous. Secondly, the traveling wave problem (3.3.5) is itself non-trivial. The existing constructions [301, 344] are only valid for a parameter range which prevents the vanishing of the elliptic parameter. Overall the vanishing viscosity method may be as hard to implement as the present argument. Connecting the solutions to (3.3.5) to the ones of (3.3.1)–(3.3.2) is still an interesting problem and we plan to investigate it in a future work.

Finally, we show that continuous traveling waves cannot be sharp, *i.e.* are necessarily positive on $\mathbb{R}$.

Proposition 3.3.14 (Smooth traveling waves)**.** *Let $U(x)$ be the profile of a traveling wave solution to* (3.3.1) *and assume that U is continuous. Then $U \in C^1(\mathbb{R})$, U is strictly positive and we have the estimate:*

$$-\chi(\rho_x \star U)(x) < c, \text{ for all } x \in \mathbb{R}. \tag{3.3.18}$$

In particular, by Theorem 3.3.8, any solutions starting from an initial condition satisfying Assumption 3.3.7 may never catch such a traveling wave.

3.3.3 Numerical Simulations

We first describe the numerical framework of this study.

- The parameters σ and χ are fixed as $\sigma = 1$ and $\chi = 1$.
- We choose a bounded interval $[-L, L]$ and an initial distribution of $\phi \in C([-L, L])$;
- We solve numerically the following PDE using the upwind scheme (p being given)

$$\begin{cases} \partial_t u(t,x) - \partial_x\big(u(t,x)\partial_x p(t,x)\big) = u(t,x)(1-u(t,x)), \\ \nabla p(t,x)\cdot\nu = 0 \qquad\qquad\qquad\qquad\qquad\qquad t>0,\ x\in[-L,L]. \\ u(0,x) = \phi(x), \end{cases} \tag{3.3.19}$$

- The pressure p is defined as

$$p(t,x) = (I-\Delta)^{-1}_{\mathcal{N}} u(t,x), \quad t>0, x\in[-L,L], \tag{3.3.20}$$

  where $(I-\Delta)^{-1}_{\mathcal{N}}$ is the Laplacian operator with Neumann boundary condition. Due to the Neumann boundary condition of the pressure p, we do not need boundary condition on u (see section 3.2).

Our numerical scheme is detailed in 3.3.7.

3.3.3.1 Formation of a discontinuity

In this part, we use numerical simulations to verify the theoretical predictions in the previous section 3.3.2. Firstly, we choose the initial value $\phi \in C^1([-L, L])$ as follows

$$\phi(x) = \frac{(x-x_0)^2}{(L+x_0)^2}\mathbb{1}_{[-L,x_0]}(x), \quad L = 20,\ x_0 = -15. \tag{3.3.21}$$

Notice that this initial condition satisfies Assumptions 3.3.5 and 3.3.7. Due to Theorem 3.3.8, we should observe the formation of a discontinuity in space for large time.

We plot the evolution of the solution $u(t,x)$ starting from $u(0,x) = \phi(x)$ in Figure 3.3.4. We observe

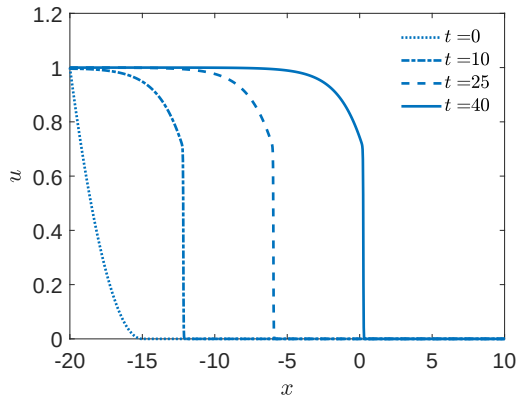

Figure 3.3.4: *We plot the propagation of the traveling waves under system* (3.3.19) *with the initial value* (3.3.21)*. We plot the propagation profile at* $t = 0, 10, 25, 40$ *(resp. dashed lines, dotted-dashed lines, dotted lines and solid lines).*

that the jump is formed for large time and the height of the jump is greater than 2/3 which is in accordance with Theorem 3.3.13.

Next, we study the propagation speed of different level sets, namely,

$$t \longmapsto \xi(t,\beta) + L,$$

where $\xi(t,\beta) := \sup\{x \in \mathbb{R} \,|\, u(t,x) = \beta\}$ and $\beta = 0, 0.2, 2/3, 0.8$. Note that the case $\beta = 0$ corresponds to the rightmost characteristic.

We compute the propagation speed in the following way: for different $\beta \in [0,1]$, we choose $t_1 = 15$ and $t_2 = 40$ where the propagation speed is almost stable after $t = t_1$. Thus we can compute the mean propagation speed as follows

$$\text{Propagation speed at level } \beta = \frac{\xi(t_2,\beta) - \xi(t_1,\beta)}{t_2 - t_1}. \tag{3.3.22}$$

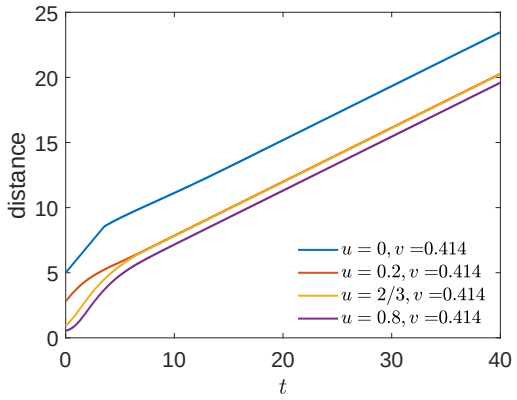

Figure 3.3.5: *We plot the evolution of different level sets* $t \longmapsto \xi(t,\beta) + L$ *under system* (3.3.19). *Our initial distribution is taken as* (3.3.21). *We plot the propagating speeds of the profile at* $\beta = 0, 0.2, 2/3, 0.8$. *The x-axis represents the time and the y-axis is the relative distance* $\xi(t,\beta) + L$. *The velocity is calculated by* (3.3.22) *for* $t_1 = 15$ *and* $t_2 = 40$.

Next we want to check whether the solutions of system (3.3.20) starting from two different initial values converge to the same discontinuous traveling wave solution. To that aim, given two different initial profiles ϕ_1 and ϕ_2 with $\phi_1 \le \phi_2$ on $[-L, L]$,

$$\phi_1(x) = -\frac{x+15}{5}\mathbb{1}_{[-20,-15]}(x), \quad \phi_2(x) = \mathbb{1}_{[-20,-17.5]}(x) - \frac{x+15}{10}\mathbb{1}_{[-17.5,-15]}(x) \tag{3.3.23}$$

We simulate the propagation of these two profiles in Figure 3.3.6.

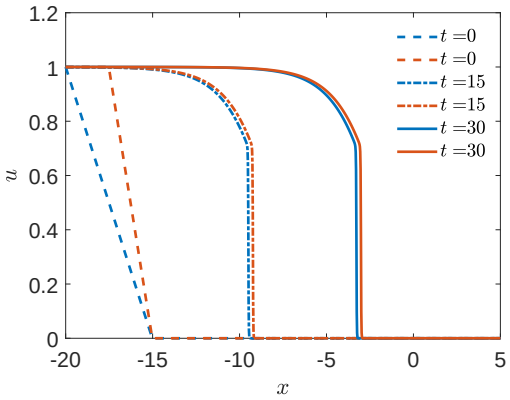

Figure 3.3.6: *We plot the propagation of two profiles under system* (3.3.19) *with initial distributions are taken as* (3.3.23). *The blue curves represent the profile with initial distribution* ϕ_1 *while the red curves represent the profile with initial distribution* ϕ_2. *We plot the propagation profiles at* $t = 0, 15$ *and* 30 *(resp. dashed lines, dotted-dashed lines and solid lines). The simulation shows that the two profiles converge to the same discontinuous traveling wave solution.*

3.3.3.2 Large speed traveling waves

As we know for porous medium equation, the existence of large speed $c > c_*$ traveling wave solutions is known [313] and it can be observed numerically by taking the exponentially decreasing function as initial value. In this part, instead of taking a compactly supported initial value, we set the initial value

$$\phi_\alpha(x) = \frac{1}{1 + e^{\alpha(x-x_0)}}, \quad x_0 = -15, \tag{3.3.24}$$

where $\alpha \geq 1$ is a parameter introduced to describe the decaying rate of the initial value.

We compare the following three different scenarios with different parameters $\alpha = 1, 2, 5$ in the initial value (3.3.24). We observe the large speed traveling waves in Figure 3.3.7 when $\alpha = 1, 2$. We note that as

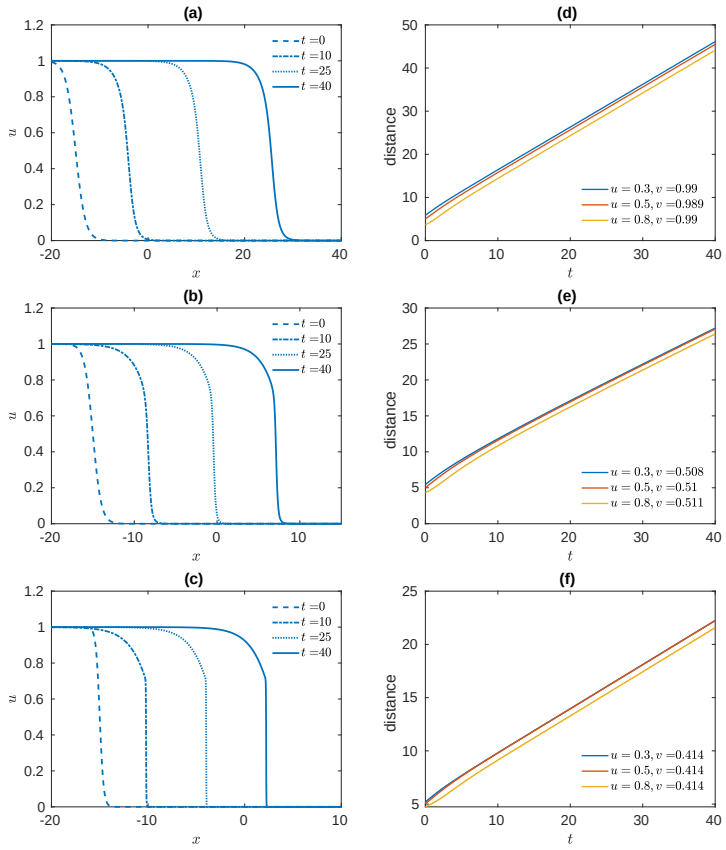

Figure 3.3.7: *We plot the propagation of the traveling waves under system* (3.3.19) *with the initial values* (3.3.24) *and the corresponding evolution of different level sets* $t \longmapsto \xi(t, \beta) + L$. *Figure (a) and (d) represent the evolution of the traveling wave and its level sets when* $\alpha = 1$. *Figure (b) and (e) correspond to the case when* $\alpha = 2$. *Figure (c) and (f) correspond to the case when* $\alpha = 5$.

the parameter α in (3.3.24) is increasing, the propagation speed is decreasing and $c \approx 1/\alpha$. When $\alpha = 5$, the propagation of the traveling waves is similar to the case in Figure 3.3.4 in which we started from the compactly supported initial value. In other word, we can observe the formation of discontinuity and the critical speed $c_* \approx 0.414$ is reached.

3.3.3.3 Comparison with porous medium equations: the vanishing jump

In this part, we compare the non-local advection model with the porous medium equation by varying the parameter σ

$$p(t, x) = (I - \sigma^2 \Delta)^{-1}_{\mathcal{N}} u(t, x) \tag{3.3.25}$$

Thus if $\sigma \to 0$ then formally we have $p(t,x) \to u(t,x)$. Thus, the first equation of (3.3.19) becomes

$$u_t - \frac{1}{2}(u^2)_{xx} = u(1-u),$$

which is the classical porous medium equation. It is well-known that this equation has the explicit traveling wave solution $U(z) = (1 - e^{z/\sqrt{2}})_+$ with critical speed $c_* = 1/\sqrt{2}$.

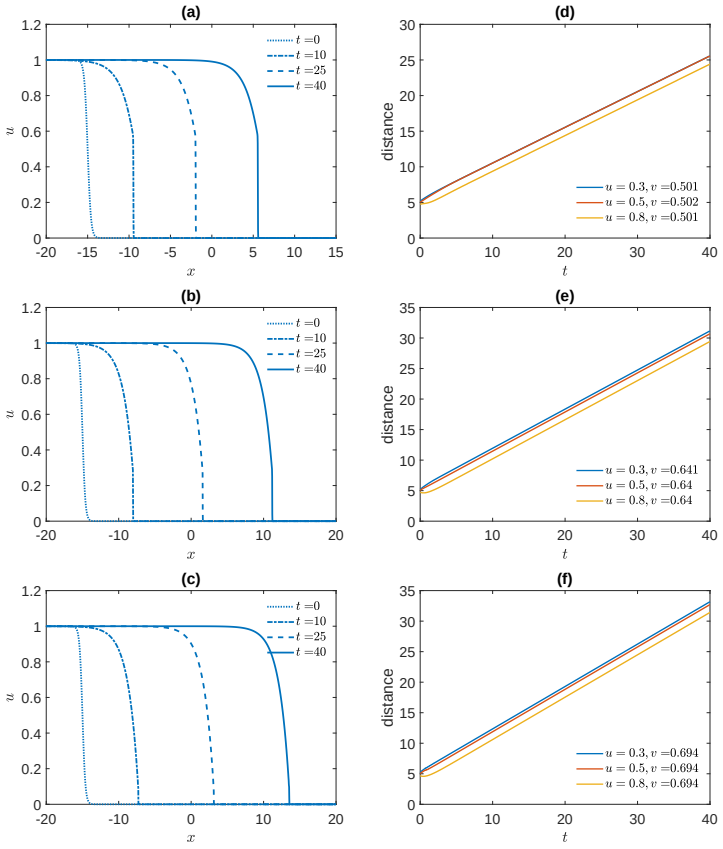

Figure 3.3.8: *We plot the propagation of the traveling waves for system* (3.3.19) *with the kernel* (3.3.25) *and the corresponding evolution of different level sets* $t \longmapsto \xi(t,\beta) + L$. *Figure (a) and (d) represent the evolution of the traveling wave and its level sets when* $\sigma^2 = 0.5$. *Figure (b) and (e) correspond to the case when* $\sigma^2 = 0.1$. *Figure (c) and (f) correspond to the case when* $\sigma^2 = 0.01$. *Our initial value is taken as in* (3.3.24) *with* $\alpha = 5$.

We consider the transition from the discontinuous traveling wave solution to the continuous sharp-type traveling wave solution by letting $\sigma \to 0$. Moreover, we want to see if the critical traveling speed of the discontinuous wavefront $c(\sigma)$ converges to $c_* = 1/\sqrt{2} \approx 0.707$ as $\sigma \to 0$. Our initial value is taken as $1/(1 + \exp(5 * (x + 15))), x \in [-20, 20]$ in (3.3.24). We compare the following three different scenarios with different parameters $\sigma^2 = 0.5, 0.1, 0.01$ in kernel (3.3.25).

In Figure 3.3.8 we can observe that as $\sigma \to 0$ in the kernel, the discontinuous jump is gradually vanishing from (a) to (c). Moreover, the critical speed $c(\sigma)$ is increasing as $\sigma \to 0$ and is approaching the critical speed $c_* = 1/\sqrt{2} \approx 0.707$ for the porous medium case.

To explore more about the relationship between parameter σ^2 and the critical speed $c(\sigma)$, we plot Figure 3.3.9.

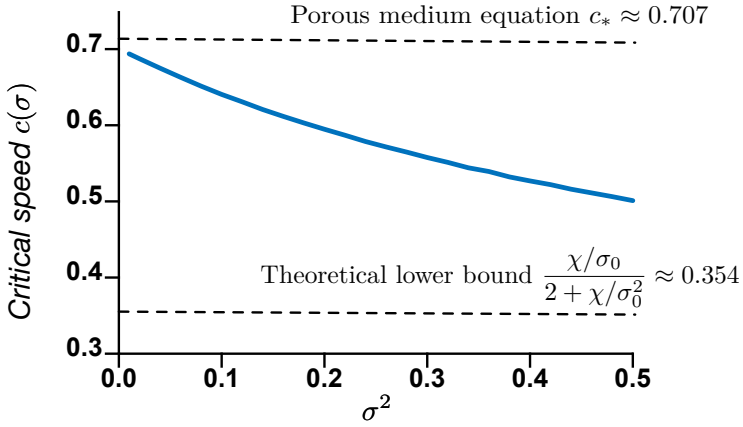

Figure 3.3.9: *The relationship between parameter σ^2 and the critical propagation speed $c(\sigma)$ by numerical simulations. Concerning the computation for the critical speed c, we take the speed on three level sets $t \to \xi(t,\beta)+L$ for $\beta = 0.3, 0.5, 0.8$ and we plot the mean value (the standard variation is negligible $\approx 10^{-3}$). As the critical speed $c(\sigma)$ is decreasing with respect to σ, the theoretical lower bound is obtained by setting $\chi = 1, \sigma_0 = 0.5$ in Theorem 3.3.13.*

3.3.4 Properties of the time-dependent solutions

3.3.4.1 The separatrix

In this section 3.3.4.1 we study the qualitative properties of solutions to (3.3.1) starting from an initial condition supported in $(-\infty, 0]$.

Proposition 3.3.15 (The separatrix)**.** *Let u be a solution integrated along the characteristics to* (3.3.1)*, starting from $u_0(x)$ satisfying Assumption 3.3.5. Let $h^*(t) := h(t,0)$ be the separatrix (as in Proposition 3.3.6). Then $h^*(t)$ stays at the rightmost boundary of the support of $u(t,\cdot)$, i.e.*

(i) we have

$$u(t,x) = 0 \text{ for all } x \geq h^*(t). \tag{3.3.26}$$

(ii) for each $t > 0$ there exists $\delta > 0$ such that

$$u(t,x) > 0 \text{ for all } x \in (h^*(t) - \delta, h^*(t)). \tag{3.3.27}$$

Proof. By definition the characteristics are well-defined by (3.3.10) as the flow of an ODE. In particular, if $x \geq h^*(t) = h(t,0)$ there exists $x_0 \geq 0$ such that $x = h(t,x_0)$. Since $u_0(x_0) = 0$ and in view of (3.3.11), we have indeed $u(t,x) = 0$. This proves Item (i)

By Assumption 3.3.5, there exists $\delta_0 > 0$ such that $u_0(x) > 0$ for $x \in (-\delta_0, 0)$. We remark that

$$\begin{aligned}\frac{\mathrm{d}}{\mathrm{d}t}u(t,h(t,x)) &= \hat{\chi}\, u(t,h(t,x))\big((\rho * u)(t,h(t,x)) - u(t,h(t,x))\big) \\ &\quad + u(t,h(t,x))\big(1 - u(t,h(t,x))\big) \\ &\geq u(t,h(t,x))\big(1 - (1+\hat{\chi})u(t,h(t,x))\big).\end{aligned}$$

By comparison with the solution to the ODE $v'(t) = v(t)(1-(1+\hat{\chi})v(t))$ starting from $v(t=0) = u_0(x) > 0$, we deduce that $u(t,x) \geq v(t) > 0$ for each $x \in (h(t,-\delta_0), h^*(t))$. Since $h(t,-\delta_0) < h(t,0) = h^*(t)$, this proves Item (ii). □

Next we investigate the propagation of u.

Proposition 3.3.16 (u is propagating)**.** *Let u_0 satisfy Assumption 3.3.5 and let u be the solution integrated along the characteristics to* (3.3.1) *starting from $u(t=0,x) = u_0(x)$. Then u is propagating to the right, i.e.*

$$\frac{\mathrm{d}}{\mathrm{d}t}h^*(t) > 0. \tag{3.3.28}$$

Moreover, we have the estimate:

$$\frac{\mathrm{d}}{\mathrm{d}t}h^*(t) \leq \frac{\chi}{2\sigma}. \tag{3.3.29}$$

Proof. We have the following estimates:

$$\begin{aligned}
\frac{\mathrm{d}}{\mathrm{d}t}h^*(t) &= -\chi(\rho_x * u)(t, h^*(t)) \\
&= -\chi \int_{-\infty}^{+\infty} \rho_x(y) u(t, h^*(t) - y)\mathrm{d}y \\
&= \chi \int_{-\infty}^{+\infty} \frac{\mathrm{sign}(y)}{2\sigma^2} e^{-\frac{|y|}{\sigma}} u(t, h^*(t) - y)\mathrm{d}y \\
&= \frac{\chi}{\sigma} \int_{0}^{+\infty} \rho(y) u(t, h^*(t) - y)\mathrm{d}y \\
&> 0,
\end{aligned}$$

since $u(t,x) = 0$ for all $x > h^*(t)$. (3.3.28) is proved.

Then, since $0 \leq u \leq 1$, we have

$$\begin{aligned}
\frac{\mathrm{d}}{\mathrm{d}t}h^*(t) &= \frac{\chi}{\sigma} \int_{0}^{+\infty} \rho(y) u(t, h^*(t) - y)\mathrm{d}y \\
&\leq \frac{\chi}{\sigma} \int_{0}^{+\infty} \rho(y)\mathrm{d}y = \frac{\chi}{2\sigma},
\end{aligned}$$

which proves (3.3.29). □

These first two propositions together yield a proof of Proposition 3.3.6.

Proof of Proposition 3.3.6. Items (i) and (ii) have been proved in Proposition 3.3.15, and the propagating property follows from Proposition 3.3.16. □

We continue with a technical lemma that will be used in the proof of Theorem 3.3.8.

Lemma 3.3.17 (Divergence speed near the separatrix)**.** *Let $u_0(x)$ satisfy Assumptions 3.3.5 and 3.3.7 and $u(t,x)$ be the corresponding solution to* (3.3.1)*. Let $h(t,x)$ be the characteristic flow of u and $h^*(t)$ be the separatrix of u, as defined in Proposition 3.3.6. For all $t \geq 0$ and $x < 0$ we have*

$$\frac{\mathrm{d}}{\mathrm{d}t}(h^*(t) - h(t,x)) \leq \chi\,(h^*(t) - h(t,x)) \sup_{y \in (h(t,x), h^*(t))} u(t,y). \tag{3.3.30}$$

Proof. Recall that, by Proposition 3.3.15, $u(t,x) = 0$ for each $x \geq h^*(t)$. For $x < 0$, we notice that:

$$\begin{aligned}
\frac{\mathrm{d}}{\mathrm{d}t}\big(h^*(t) - h(t,x)\big) &= -\chi(\rho_x \star u)(t, h^*(t)) + \chi(\rho_x \star u)(h(t,x)) \\
&= \chi \int_{\mathbb{R}} \big(\rho_x(h(t,x) - y) - \rho_x(h^*(t) - y)\big) u(t,y)\mathrm{d}y \\
&= \chi \int_{-\infty}^{h(t,x)} \big(\rho_x(h(t,x) - y) - \rho_x(h^*(t) - y)\big) u(t,y)\mathrm{d}y \\
&\quad + \chi \int_{h(t,x)}^{h^*(t)} \big(\rho_x(h(t,x) - y) - \rho_x(h^*(t) - y)\big) u(t,y)\mathrm{d}y.
\end{aligned}$$

Therefore,

$$\begin{aligned}
\frac{\mathrm{d}}{\mathrm{d}t}(h^*(t) - h(t,x)) \leq \chi \int_{-\infty}^{h(t,x)} &\big(\rho_x(h(t,x) - y) - \rho_x(h^*(t) - y)\big) u(t,y)\mathrm{d}y \\
&+ \chi(h^*(t) - h(t,x)) \times \sup_{y \in (h(t,x), h^*(t))} u(t,y).
\end{aligned}$$

Since $\rho_x(y) = -\frac{1}{2\sigma^2}\mathrm{sign}(y)e^{-\frac{|y|}{\sigma}}$ is increasing on $(0,+\infty)$, we have

$$\rho_x(h(t,x)-y) - \rho_x(h^*(t)-y) \le 0$$

for each $y \le h(t,x)$, which shows (3.3.30). Lemma 3.3.17 is proved. □

Proposition 3.3.18 (Formation of a discontinuity)**.** *Let $u_0(x)$ satisfy Assumptions 3.3.5 and 3.3.7 and $u(t,x)$ be the corresponding solution to* (3.3.1)*. For all $\delta > 0$ we have*

$$\limsup_{t\to+\infty} \sup_{x\in(h^*(t,x)-\delta,h^*(t))} u(t,x) \ge \frac{1}{1+\hat\chi+\alpha\chi} > 0. \tag{3.3.31}$$

Proof. We divide the proof in 2 steps.

Step 1: We show that for all $\delta > 0$,

$$\sup_{t>0} \sup_{x\in(h^*(t)-\delta,h^*(t))} u(t,x) \ge \frac{1}{1+\hat\chi+\alpha\chi}. \tag{3.3.32}$$

Assume by contradiction that there exists $\delta > 0$ such that

$$\text{for all } t>0, \sup_{x\in(h^*(t)-\delta,h^*(t))} u(t,x) \le \eta < \frac{1}{1+\hat\chi+\alpha\chi}, \tag{3.3.33}$$

where $\alpha \ge 1$ is the constant from Assumption 3.3.7.

We remark that the following inequality holds for $x \in (h^*(t)-\delta, h^*(t))$.

$$\begin{aligned}\frac{\mathrm{d}}{\mathrm{d}t}u(t,h(t,x)) &= \hat\chi\, u(t,h(t,x))(\rho\star u)(t,h(t,x)) + u(t,h(t,x))\big(1-(1+\hat\chi)u(t,h(t,x))\big)\\ &\ge u(t,h(t,x))\big(1-(1+\hat\chi)u(t,h(t,x))\big) \ge u(t,h(t,x))\,(1-(1+\hat\chi)\eta)\,,\end{aligned} \tag{3.3.34}$$

therefore

$$u(t,h(t,x)) \ge u(0,x)\exp\big(\big(1-(1+\hat\chi)\eta\big)t\big)\,,$$

provided the characteristic $h(t,x)$ does not leave the cylinder $(h^*(s)-\delta, h^*(s))$ for any $0 \le s \le t$.

Next by (3.3.30) and (3.3.33), we have

$$\frac{\mathrm{d}}{\mathrm{d}t}\big(h^*(t)-h(t,x)\big) \le \chi\big(h^*(t)-h(t,x)\big)\times\eta,$$

for each $x \in (h^*(t)-\delta, h^*(t))$. Hence by Grönwall's Lemma

$$\big(h^*(t)-h(t,x)\big) \le -xe^{\eta\chi t},$$

provided the characteristic $h(t,x)$ does not leave the cylinder $(h^*(s)-\delta, h^*(s))$ for any $0 \le s \le t$. In particular for $0 > -\frac{1}{2}\delta e^{-\eta\chi t} \ge x \ge -\delta e^{-\eta\chi t}$, we find

$$\begin{aligned}u(t,h(t,x)) &\ge u(0,x)\exp\left(\left(1-\frac{1+\hat\chi}{1+\hat\chi+\alpha\chi}\right)t\right) \ge \gamma(-x)^\alpha\exp\left(\left(1-\frac{1+\hat\chi}{1+\hat\chi+\alpha\chi}\right)t\right)\\ &\ge \frac{1}{2^\alpha}\gamma\delta^\alpha\exp\big(\big(1-(1+\hat\chi+\alpha\chi)\eta\big)t\big) \xrightarrow[t\to+\infty]{} +\infty,\end{aligned}$$

by our assumption that $\eta < \frac{1}{1+\hat\chi+\alpha\chi}$. This is a contradiction.

Step 2: We show (3.3.31).

Assume by contradiction that there exists $T > 0$ and $\delta > 0$ such that

$$\sup_{t\ge T} \sup_{x\in[h^*(t)-\delta,h^*(t)]} u(t,x) < \frac{1}{1+\hat\chi+\alpha\chi}.$$

Since the function $u(t,x+h^*(t))$ is continuous on the compact set $[0,T]\times[-\delta,0]$, it is uniformly continuous on this set and hence (recall that $u(t,h^*(t)) = 0$) there exists $0 < \delta_0 \le \delta$ such that

$$\sup_{t\in[0,T],x\in[-\delta_0,0]} u(t,x+h^*(t)) = \sup_{t\in[0,T],x\in[-\delta_0,0]} \big(u(t,x+h^*(t)) - u(t,h^*(t))\big) \le \frac{1}{1+\hat\chi+\alpha\chi}.$$

Hence we conclude

$$\sup_{t>0,x\in[-\delta_0,0]} u(t,x-h^*(t)) \le \frac{1}{1+\hat\chi+\alpha\chi}.$$

This is in contradiction with Step 1. Proposition 3.3.18 is proved. □

Proposition 3.3.19 (Refined estimate on the level sets)**.** *Let $u_0(x)$ satisfy Assumption 3.3.5 and 3.3.7. Define*

$$\xi(t,\beta) := \sup\{x\in\mathbb{R}\,|\,u(t,x)=\beta\}$$

for any $0<\beta<\frac{1}{1+\hat\chi+\alpha\chi}$. Then, the level set function $\xi(t,\beta)$ converges exponentially fast to $h^*(t)$

$$h^*(t) - \left(\frac{\beta}{\gamma}\right)^{\frac{1}{\alpha}} e^{-\frac{\eta}{2\alpha}t} \le \xi(t,\beta) \le h^*(t), \tag{3.3.35}$$

for each $0<\beta<\frac{1}{1+\hat\chi+\alpha\chi}$, where η is given by

$$\eta := 1 - \frac{1+\hat\chi+\alpha\chi}{\beta} \in (0,1).$$

Proof. Let $\eta\in(0,1)$ be given and set $\beta^* := \frac{1-\eta}{1+\hat\chi+\alpha\chi}$. Let us first remark that for any $\beta\in(0,\beta^*)$, $\xi(t,\beta)$ is well-defined by the continuity of $x\mapsto u(t,x)$ and Assumption 3.3.7, that $u(t,\xi(t,\beta))=\beta$ and that $\sup_{x\in(\xi(t,\beta),h^*(t))} u(t,x)\le\beta$. Moreover $\xi(0,\beta)<0$ and $u_0(\xi(0,\beta))=\beta\ge\gamma\big|\xi(0,\beta)\big|^\alpha$, therefore

$$\xi(0,\beta) \ge -\left(\frac{\beta}{\gamma}\right)^{\frac{1}{\alpha}} \tag{3.3.36}$$

for each $0<\beta\le\beta^*=\frac{1-\eta}{1+\hat\chi+\alpha\chi}$.

Step 1: We show that if u_0 satisfies Assumption 3.3.5 and (3.3.36), then

$$\xi(t,\beta) \ge h^*(t) - \left(\frac{\beta}{\gamma}\right)^{\frac{1}{\alpha}} e^{\frac{\eta}{2\alpha}t}, \tag{3.3.37}$$

for all $0\le t\le t^* := \frac{1}{1+\hat\chi}\ln\Big(1+\frac{\eta}{2(1-\eta)}\Big)$.

Let $0<\beta\le\beta^*$. We remark that, by Assumption 3.3.5, we have $0\le u(t,x)\le 1$ hence $0\le(\rho\star u)(t,x)\le 1$. It follows that, for all $t\ge 0$,

$$\frac{\mathrm{d}}{\mathrm{d}t}u(t,h(t,x)) = u(t,h(t,x))\big(1+\hat\chi\rho\star u-(1+\hat\chi)u(t,h(t,x))\big) \le (1+\hat\chi)u(t,h(t,x)).$$

In the remaining part of Step 1 we consider $t\in[0,t^*]$. Using (3.3.30) from Lemma 3.3.17 we establish the following estimates on u and h for $0\le t\le t^*$ and $\xi(0,\beta^*)\le x\le 0$:

• Since $\frac{\mathrm{d}}{\mathrm{d}t}u(t,h(t,x))\le(1+\hat\chi)u(t,h(t,x))$ we have $u(t,h(t,x))\le u_0(x)e^{(1+\hat\chi)t}$ for all $t\le t^*$ and hence if $x\ge\xi(0,\beta^*)$,

$$u(t,h(t,x)) \le \beta^* e^{\ln\left(1+\frac{\eta}{2(1-\eta)}\right)} = \frac{1-\eta}{1+\hat\chi+\alpha\chi}\left(1+\frac{\eta}{2(1-\eta)}\right) = \frac{1-\frac{\eta}{2}}{1+\hat\chi+\alpha\chi}. \tag{3.3.38}$$

• Using (3.3.38) in the equation along the characteristic (3.3.11):

$$\begin{aligned}\frac{\mathrm{d}}{\mathrm{d}t}u(t,h(t,x)) &= u(t,h(t,x))\big(1+\hat\chi(\rho\star u)(t,h(t,x))-(1+\hat\chi)u(t,h(t,x))\big)\\ &\ge \left(1-\frac{(1+\hat\chi)(1-\frac{\eta}{2})}{1+\hat\chi+\alpha\chi}\right)u(t,h(t,x)),\end{aligned}$$

we get

$$u(t,h(t,x)) \ge u_0(x)\exp\left[\left(1-\frac{(1+\hat\chi)(1-\frac{\eta}{2})}{1+\hat\chi+\alpha\chi}\right)t\right] \tag{3.3.39}$$

• For all $x \in (\xi(0,\beta^*),0)$, since

$$\sup_{y\in(h(t,x),h^*(t))} u(t,y) \le \sup_{y\in(h(t,\xi(0,\beta^*)),h^*(t)} u(t,y) \le \frac{1-\frac{\eta}{2}}{1+\hat{\chi}+\alpha\chi},$$

we have by (3.3.30):

$$h^*(t)-h(t,x) \le \exp\left(\frac{(1-\frac{\eta}{2})\chi}{1+\hat{\chi}+\alpha\chi}t\right)(h^*(0)-h(0,x)),$$

hence

$$h(t,x) \ge h^*(t) + x\exp\left(\frac{(1-\frac{\eta}{2})\chi}{1+\hat{\chi}+\alpha\chi}t\right). \tag{3.3.40}$$

Since $\beta \le \beta^*$, we have $\xi(0,\beta) \ge \xi(0,\beta^*)$. Using (3.3.39) with $x = \xi(0,\beta)$ we find that

$$u(t,h(t,\xi(0,\beta))) \ge \beta\exp\left[\left(1-\frac{(1+\hat{\chi})(1-\frac{\eta}{2})}{1+\hat{\chi}+\alpha\chi}\right)t\right],$$

which implies

$$\xi\left(t,\beta\exp\left[\left(1-\frac{(1+\hat{\chi})(1-\frac{\eta}{2})}{1+\hat{\chi}+\alpha\chi}\right)t\right]\right) \ge h(t,\xi(0,\beta)).$$

Now by using $x = \xi(0,\beta)$ in (3.3.40), we obtain

$$h(t,\xi(0,\beta)) \ge h^*(t) + \xi(0,\beta)\exp\left(\frac{(1-\frac{\eta}{2})\chi}{1+\hat{\chi}+\alpha\chi}t\right).$$

Using (3.3.36) we find that

$$\xi\left(0,\beta\exp\left[-\left(1-\frac{(1+\hat{\chi})(1-\frac{\eta}{2})}{1+\hat{\chi}+\alpha\chi}\right)t\right]\right) \ge -\left(\frac{\beta}{\gamma}\right)^{\frac{1}{\alpha}}\exp\left[-\frac{1}{\alpha}\left(1-\frac{(1+\hat{\chi})(1-\frac{\eta}{2})}{1+\hat{\chi}+\alpha\chi}\right)t\right]$$

which leads to

$$\begin{aligned}\xi(t,\beta) &\ge h^*(t) - \left(\frac{\beta}{\gamma}\right)^{\frac{1}{\alpha}}\exp\left[-\frac{1}{\alpha}\left(1-\frac{(1+\hat{\chi})(1-\frac{\eta}{2})}{1+\hat{\chi}+\alpha\chi}\right)t + \frac{(1-\frac{\eta}{2})\chi}{1+\hat{\chi}+\alpha\chi}t\right]\\ &= h^*(t) - \left(\frac{\beta}{\gamma}\right)^{\frac{1}{\alpha}}\exp\left[-\frac{\eta}{2\alpha}t\right]\end{aligned}$$

and this estimate holds for each $0 \le t \le t^*$ and $0 < \beta \le \beta^*$.

Step 2: We show that the estimate (3.3.37) can be extended by induction.

Define $\bar{u}_0(x) := u(t^*, x+h(t^*))$ and $\bar{\xi}(t,\beta) = \xi(t+t^*,\beta) - h^*(t^*)$. We have for each $0 < \beta \le \beta^*$

$$\bar{\xi}(0,\beta) \ge -\left(\frac{\beta}{\bar{\gamma}}\right)^{\frac{1}{\alpha}},$$

where $\bar{\gamma} = \gamma e^{\frac{\eta}{2}t^*}$. In particular the inequality (3.3.36) is satisfied by $\bar{u}_0(x)$, as well as Assumption 3.3.5. We can apply Step 1 and (3.3.37) gives

$$\begin{aligned}\bar{\xi}(t,\beta) &\ge \bar{h}^*(t) - \left(\frac{\beta}{\bar{\gamma}}\right)^{\frac{1}{\alpha}} e^{-\frac{\eta}{2\alpha}t} = h(t,h^*(t)) - h^*(t^*) - \left(\frac{\beta}{\gamma}\right)^{\frac{1}{\alpha}} e^{-\frac{\eta}{2\alpha}(t+t^*)}\\ &= h^*(t+t^*) - \left(\frac{\beta}{\gamma}\right)^{\frac{1}{\alpha}} e^{-\frac{\eta}{2\alpha}(t+t^*)},\end{aligned}$$

which yields

$$\xi(t+t^*,\beta) \ge h^*(t+t^*) - \left(\frac{\beta}{\gamma}\right)^{\frac{1}{\alpha}} e^{-\frac{\eta}{2\alpha}(t+t^*)}.$$

The proof is completed. □

We are now in the position to prove Theorem 3.3.8

Proof of Theorem 3.3.8. The first part, equation 3.3.14, has been shown in Proposition 3.3.18, while the second part (equation (3.3.15)) has been shown in Proposition 3.3.19. □

We conclude this section 3.3.4.1 by the proof of Proposition 3.3.9.

Proof of Proposition 3.3.9. Since $x \mapsto u(t,x)$ is nonincreasing, we have $u(t,x) \geq u(t,h^*(t))$ for each $x \leq h^*(t)$. Hence $(\rho \star u)(t,h^*(t)) \geq \frac{1}{2}u(t,h^*(t))$ and

$$\begin{aligned}\frac{\mathrm{d}}{\mathrm{d}t}u(t,h^*(t)) &= u(t,h^*(t))\big(1+\hat{\chi}\,\rho\star u-(1+\hat{\chi})u(t,h^*(t))\big)\\ &\geq u(t,h^*(t))\left(1-\left(1+\frac{\hat{\chi}}{2}\right)u(t,h^*(t))\right).\end{aligned}$$

This yields

$$u(t,h^*(t)) \geq \frac{u_0(0)}{\left(1+\frac{\hat{\chi}}{2}\right)u_0(0)+e^{-t}\left(1-\left(1+\frac{\hat{\chi}}{2}\right)u_0(0)\right)} \underset{t\to+\infty}{\longrightarrow} \frac{1}{1+\frac{\hat{\chi}}{2}} = \frac{2}{2+\hat{\chi}}.$$

(3.3.16) is shown. Next, we have $\frac{\mathrm{d}}{\mathrm{d}t}h^*(t) = -(\rho_x \star u)(t,h^*(t))$ which gives

$$\frac{\mathrm{d}}{\mathrm{d}t}h^*(t) = \frac{\chi}{\sigma}\int_0^\infty \rho(y)u\big(t,h^*(t)-y\big)\mathrm{d}y \geq u(t,h^*(t)) \times \frac{\chi}{2\sigma} \underset{t\to+\infty}{\longrightarrow} \frac{\sigma\hat{\chi}}{2+\hat{\chi}}.$$

This proves (3.3.17) and finishes the proof of Proposition 3.3.9. □

3.3.5 Traveling wave solutions

In this section 3.3.5 we investigate the existence of particular solutions which consist in a fixed profile traveling at a constant speed c (traveling waves). We are particularly interested in profiles which connect the stationary state 1 near $-\infty$ to the stationary solution 0 at a finite point of space, say, for any $x \geq 0$.

3.3.5.1 Existence of sharp traveling waves

We study the traveling wave solutions of equation (3.3.1):

$$\begin{cases}\partial_t u(t,x) - \chi\partial_x\big(u(t,x)\partial_x p(t,x)\big) = u(t,x)(1-u(t,x))\\ -\sigma^2\partial_x^2 p(t,x) + p(t,x) = u(t,x)\end{cases} \qquad t>0,\ x\in\mathbb{R}.$$

Let us formally derive an equation for the traveling wave solutions to (3.3.1). We consider the traveling wave solution $U(x-ct) = u(t,x)$. By using the resolvent formula of the second equation of (3.3.1) formula we deduce that

$$p(t,x) = \frac{1}{2\sigma}\int_{\mathbb{R}} e^{-\frac{|x-y|}{\sigma}}u(t,y)\mathrm{d}y = \frac{1}{2\sigma}\int_{\mathbb{R}} e^{-\frac{|x-ct-l|}{\sigma}}U(l)\mathrm{d}l = P(x-ct)$$

and the first equation in (3.3.1) becomes

$$-cU'(x-ct) - \chi\,\partial_x\Big(U(x-ct)\,\partial_x P(x-ct)\Big) = U(x-ct)(1-U(x-ct)), \quad t>0,\ x\in\mathbb{R}. \tag{3.3.41}$$

By developing the derivative in (3.3.41) we obtain

$$\big(-c-\chi P'(x-ct)\big)U'(x-ct) = U(x-ct)(1+\hat{\chi}P(x-ct)-(1+\hat{\chi})U(x-ct)),$$

for all $t>0$ and $x\in\mathbb{R}$, where $\hat{\chi} = \frac{\chi}{\sigma^2}$. Therefore, by letting $z = x-ct$, the traveling wave solutions of system (3.3.1) satisfy the following equation

$$\begin{cases}(-c-\chi P'(z))U'(z) = U(z)\big(1+\hat{\chi}P(z)-(1+\hat{\chi})U(z)\big),\\ -\sigma^2P''(z)+P(z) = U(z).\end{cases} \tag{3.3.42}$$

Let us finally remark that

$$P(z) = \frac{1}{2\sigma}\int_{\mathbb{R}} e^{-\frac{|y|}{\sigma}} U(z-y)\mathrm{d}y = \frac{1}{2\sigma}\int_{\mathbb{R}} e^{-\frac{|z-y|}{\sigma}} U(y)\mathrm{d}y. \tag{3.3.43}$$

In particular if U is non-constant and nonincreasing, then $z \mapsto P(z)$ is strictly decreasing.

The goal of this Section is to show that equation (3.3.42) can solved on the half-line $(-\infty, 0)$ which, as we will see later, will give a proof of Theorem 3.3.13. We begin by defining a set of admissible profiles, which is the set of function on which an appropriate fixed-point theorem will be used. The properties we impose are those who we suspect will be satisfied by the real profile of the traveling wave.

Definition 3.3.20. We say that the profile $U : \mathbb{R} \to [0, 1]$ is *admissible* if

(i) $U \in C((-\infty, 0), \mathbb{R})$ and $\lim_{z\to 0^-} U(z)$ exists and belongs to $\left[\frac{2}{2+\hat{\chi}}, 1\right]$;

(ii) $0 \leq U(z) \leq 1$ for any $z \in \mathbb{R}$;

(iii) the map $z \mapsto U(z)$ is non-increasing on $\mathbb{R}$;

(iv) $U(z) \equiv 0$ for any $z \geq 0$.

We denote $\mathcal{A}$ the set of all admissible functions.

Lemma 3.3.21. *Let Assumption 3.3.11 hold and suppose that U is admissible (as in Definition 3.3.20). Then the function P defined by $P = (\rho \star U)$ satisfies*

$$P'(0) < P'(z) \leq 0, \text{ for all } z \in \mathbb{R}\backslash\{0\}.$$

Moreover, this estimate is locally uniform in U on $(-\infty, 0)$ in the sense that for each $L > 1$ there is $\epsilon > 0$ independent of $U \in \mathcal{A}$ *such that*

$$P'(z) - P'(0) \geq \epsilon > 0, \text{ for all } z \in \left[-L, -\frac{1}{L}\right].$$

Proof. We divide the proof in five steps.

Step 1. We prove $P'(0) < P'(z)$ for any $z > 0$. Notice that, for $z > 0$, we have

$$P(z) = \frac{1}{2\sigma}\int_{-\infty}^{z} e^{-\frac{z-y}{\sigma}} U(y)\mathrm{d}y + \frac{1}{2\sigma}\int_{z}^{\infty} e^{\frac{z-y}{\sigma}} U(y)\mathrm{d}y = \frac{1}{2\sigma}e^{-\frac{z}{\sigma}}\int_{-\infty}^{0} e^{\frac{y}{\sigma}} U(y)\mathrm{d}y.$$

Thus, taking derivative gives

$$P'(z) = -\frac{1}{\sigma}e^{-\frac{z}{\sigma}}\frac{1}{2\sigma}\int_{-\infty}^{0} e^{y} U(y)\mathrm{d}y = e^{-\frac{z}{\sigma}} P'(0),$$

and since U is strictly positive for negative values of z, we deduce that $P'(0) < P'(z)$ for any $z > 0$.

Step 2. We prove that $P'(0) < P'(z)$ for any $-\sigma \ln(\frac{\hat{\chi}}{2}) < z < 0$. In fact, we prove the stronger result

$$P''(z) < 0 \text{ if } \sigma \ln\left(\frac{\hat{\chi}}{2}\right) < z < 0.$$

For any $z < 0$, we have

$$\begin{aligned} P''(z) &= \frac{1}{2\sigma^3}\int_{-\infty}^{z} e^{-\frac{z-y}{\sigma}} U(y)\mathrm{d}y + \frac{1}{2\sigma^3}\int_{z}^{\infty} e^{\frac{z-y}{\sigma}} U(y)\mathrm{d}y - \frac{1}{\sigma^2}U(z) \\ &= \frac{1}{2\sigma^3}\int_{-\infty}^{z} e^{-\frac{z-y}{\sigma}} U(y)\mathrm{d}y + \frac{1}{2\sigma^3}\int_{z}^{0} e^{\frac{z-y}{\sigma}} U(y)\mathrm{d}y - \frac{1}{\sigma^2}U(z). \end{aligned}$$

Due to the assumption $U \leq 1$ and the fact that U is decreasing we have

$$\begin{aligned}\sigma^2 P''(z) &\leq \frac{1}{2\sigma}\int_{-\infty}^{z} e^{-\frac{z-y}{\sigma}}\mathrm{d}y + \frac{1}{2\sigma}\int_{z}^{0} e^{\frac{z-y}{\sigma}}U(y)\mathrm{d}y - U(z)\\ &= \frac{1}{2} + \frac{1}{2\sigma}\int_{z}^{0} e^{\frac{z-y}{\sigma}}U(y)\mathrm{d}y - U(z) \leq \frac{1}{2} + \frac{1}{2\sigma}\int_{z}^{0} e^{\frac{z-y}{\sigma}}\mathrm{d}y U(z) - U(z)\\ &= \frac{1}{2} - \frac{1}{2}\left(1 + e^{\frac{z}{\sigma}}\right)U(z) \leq \frac{1}{2}\frac{2+\hat{\chi}-2(1+e^{\frac{z}{\sigma}})}{2+\hat{\chi}} = \frac{\hat{\chi}-2e^{\frac{z}{\sigma}}}{2(2+\hat{\chi})} < 0,\end{aligned}$$

provided $z \in (\sigma\ln(\hat{\chi}/2), 0)$. In particular

$$P'(z) - P'(0) = -\int_{z}^{0} P''(y)\mathrm{d}y \geq \frac{1}{\sigma(2+\hat{\chi})}\left(\frac{\hat{\chi}}{2\sigma}z + 1 - e^{\frac{z}{\sigma}}\right) > 0. \tag{3.3.44}$$

Step 3. We prove that $P'(0) < P'(z)$ for any $z < \sigma\ln\left(1-\frac{\hat{\chi}}{2}\right)$. For any $z < 0$, we have

$$\begin{aligned}\sigma P'(z) &= -\frac{1}{2\sigma}\int_{-\infty}^{z} e^{-\frac{z-y}{\sigma}}U(y)\mathrm{d}y + \frac{1}{2\sigma}\int_{z}^{0} e^{\frac{z-y}{\sigma}}U(y)\mathrm{d}y,\\ \sigma P'(0) &= -\frac{1}{2\sigma}\int_{-\infty}^{0} e^{\frac{y}{\sigma}}U(y)\mathrm{d}y,\end{aligned}$$

and

$$\sigma\big(P'(z) - P'(0)\big) = \frac{1}{2\sigma}\int_{-\infty}^{0} e^{\frac{y}{\sigma}}U(y)\mathrm{d}y - \frac{1}{2\sigma}\int_{-\infty}^{z} e^{-\frac{z-y}{\sigma}}U(y)\mathrm{d}y + \frac{1}{2\sigma}\int_{z}^{0} e^{\frac{z-y}{\sigma}}U(y)\mathrm{d}y.$$

Since for any $z \leq 0$, $\frac{2}{2+\hat{\chi}} \leq U(z) \leq 1$, we have the following estimate

$$\begin{aligned}\sigma\big(P'(z) - P'(0)\big) &\geq \frac{1}{2\sigma}\int_{-\infty}^{0} e^{\frac{y}{\sigma}} \times \frac{2}{2+\hat{\chi}}\mathrm{d}y - \frac{1}{2\sigma}\int_{-\infty}^{z} e^{-\frac{z-y}{\sigma}}\mathrm{d}y\\ &\quad + \frac{1}{2\sigma}\int_{z}^{0} e^{\frac{z-y}{\sigma}}\frac{2}{2+\hat{\chi}}\mathrm{d}y\\ &= \frac{1}{2+\hat{\chi}} - \frac{1}{2} + \frac{1}{2+\hat{\chi}}\left(1 - e^{\frac{z}{\sigma}}\right)\\ &= \frac{1}{2+\hat{\chi}}\left(2 - e^{\frac{z}{\sigma}} - \frac{1}{2}(2+\hat{\chi})\right) = \frac{1}{2+\hat{\chi}}\left(1 - \frac{\hat{\chi}}{2} - e^{\frac{z}{\sigma}}\right).\end{aligned} \tag{3.3.45}$$

By our assumption $z < \sigma\ln\left(1-\frac{\hat{\chi}}{2}\right)$, we deduce that $P'(z) - P'(0) > 0$.

Notice that, if $\hat{\chi} < 1$, we have $\sigma\ln\left(\frac{\hat{\chi}}{2}\right) < \sigma\ln\left(1-\frac{\hat{\chi}}{2}\right)$ and the estimate is done. If $1 \leq \hat{\chi} < 2$ we still need to fill a gap between the two bounds.

Step 4. We assume that $\hat{\chi} \geq 1$ and we prove that

$$\begin{aligned}P'(z) - P'(0) &\geq -\int_{z}^{0} P''(y)\mathrm{d}y\\ &\geq \frac{z}{2\sigma^2} - \frac{1}{2\sigma}\ln\left(\frac{\hat{\chi}}{2}\right) + \frac{1}{\sigma(2+\hat{\chi})}\left(\frac{\hat{\chi}}{2}\ln\left(\frac{\hat{\chi}}{2}\right) + 1 - \frac{\hat{\chi}}{2}\right) > 0\end{aligned} \tag{3.3.46}$$

for any $z \in \left[\sigma\ln\left(\frac{\hat{\chi}}{2}\right) - \frac{\sigma}{2+\hat{\chi}}\left(\frac{\hat{\chi}}{2}\ln\left(\frac{\hat{\chi}}{2}\right) + 1 - \frac{\hat{\chi}}{2}\right), \sigma\ln\left(\frac{\hat{\chi}}{2}\right)\right]$. Notice that

$$\frac{\hat{\chi}}{2}\ln\left(\frac{\hat{\chi}}{2}\right) + 1 - \frac{\hat{\chi}}{2} > 0,$$

because $x \mapsto x\ln(x)$ is strictly convex.

By Step 2 we have for all $z \leq 0$:

$$P''(z) \leq \frac{1}{2\sigma^2},$$

therefore if $z \in \left[\sigma \ln\left(\frac{\hat{\chi}}{2}\right) - \frac{\sigma}{2+\hat{\chi}}\left(\frac{\hat{\chi}}{2}\ln\left(\frac{\hat{\chi}}{2}\right) + 1 - \frac{\hat{\chi}}{2}\right), \sigma \ln\left(\frac{\hat{\chi}}{2}\right)\right]$ we have

$$\begin{aligned} P'(z) - P'(0) &= P'(z) - P'\left(\sigma \ln\left(\frac{\hat{\chi}}{2}\right)\right) + P'\left(\sigma \ln\left(\frac{\hat{\chi}}{2}\right)\right) - P'(0) \\ &\geq -\int_z^{\sigma \ln\left(\frac{\hat{\chi}}{2}\right)} P''(y)\mathrm{d}y + \frac{1}{\sigma(2+\hat{\chi})}\left(\frac{\hat{\chi}}{2\sigma}\sigma \ln\left(\frac{\hat{\chi}}{2}\right) + 1 - \frac{\hat{\chi}}{2}\right) \\ &\geq -\frac{1}{2\sigma^2}\left(\sigma \ln\left(\frac{\hat{\chi}}{2}\right) - z\right) + \frac{1}{\sigma(2+\hat{\chi})}\left(\frac{\hat{\chi}}{2}\ln\left(\frac{\hat{\chi}}{2}\right) + 1 - \frac{\hat{\chi}}{2}\right) \\ &\geq \frac{z}{2\sigma^2} - \frac{\ln\left(\frac{\hat{\chi}}{2}\right)}{2\sigma} + \frac{1}{\sigma(2+\hat{\chi})}\left(\frac{\hat{\chi}}{2}\ln\left(\frac{\hat{\chi}}{2}\right) + 1 - \frac{\hat{\chi}}{2}\right) > 0. \end{aligned}$$

We have proved the desired estimate.

Step 5. We show the local uniformity. If $\hat{\chi} < 1$ the local uniformity follows from Step 2 and Step 3 because $1 - \frac{\hat{\chi}}{2} < \frac{\hat{\chi}}{2}$. If $1 \leq \hat{\chi} < 2$, then

$$\ln\left(\frac{\hat{\chi}}{2}\right) - \frac{2}{2+\hat{\chi}}\left(\frac{\hat{\chi}}{2}\ln\left(\frac{\hat{\chi}}{2}\right) + 1 - \frac{\hat{\chi}}{2}\right) < \ln\left(1 - \frac{\hat{\chi}}{2}\right), \tag{3.3.47}$$

because of Assumption 3.3.11 and 3.3.27 (notice that (3.3.47) is equivalent to $f(\hat{\chi}) < 0$, where f is as defined in 3.3.27). By the estimates (3.3.44), (3.3.45) and (3.3.46) from Step 2, Step 3 and Step 4, we find that $P'(z) - P'(0) > 0$ on every compact subset of $(-\infty, 0)$ and is bounded from below by a constant independent of U. This finishes the proof of Lemma 3.3.21. □

Before resuming to the proof, let us define the mapping $\mathcal{T}$ to which we want to apply a fixed-point theorem. Fix $U \in \mathcal{A}$, we define $\mathcal{T}(U)$ as

$$\mathcal{T}(U)(z) := \mathcal{U}(\tau^{-1}(z)) \text{ for all } z < 0 \tag{3.3.48}$$

and $\mathcal{T}(U)(z) \equiv 0$ for all $z \geq 0$, where $\tau : \mathbb{R} \mapsto (-\infty, 0)$ is the solution of the following scalar ordinary differential equation

$$\begin{cases} \tau'(t) &= \chi\big(P'(0) - P'(\tau(t))\big), \\ \tau(0) &= -1, \end{cases} \tag{3.3.49}$$

and

$$\mathcal{U}(t) = \left[(1+\hat{\chi})\int_{-\infty}^{t} \exp\left(-\int_l^t 1 + \hat{\chi}P(\tau(s))\mathrm{d}s\right)\mathrm{d}l\right]^{-1}, \text{ for all } t \in \mathbb{R}.$$

Lemma 3.3.22 (Stability of $\mathcal{A}$)**.** *Let Assumption 3.3.11 be satisfied, let U be admissible in the sense of Definition 3.3.20 and $\mathcal{T}$ be the map defined by* (3.3.48)*. Then the image of U by $\mathcal{T}$ has the following properties:*

(i) $\dfrac{2}{2+\hat{\chi}} \leq \mathcal{T}(U)(z) \leq 1$ *for all* $z \leq 0$*;*

(ii) $\mathcal{T}(U)$ *is strictly decreasing on* $(-\infty, 0]$*;*

(iii) $\mathcal{T}(U) \in C^1((-\infty, 0), \mathbb{R})$ *and* $\mathcal{T}(U)(0^-) = \lim_{z\to 0^-} \mathcal{T}(U)(z) = \dfrac{1+\hat{\chi}P(0)}{1+\hat{\chi}}$.

In particular, $\mathcal{A}$ is left stable by $\mathcal{T}$

$$\mathcal{T}(\mathcal{A}) \subset \mathcal{A}.$$

Proof. We divide the proof in three steps.

Step 1. We prove that $\dfrac{2}{2+\hat{\chi}} \leq \mathcal{T}(U)(z) \leq 1$ for all $z < 0$. For any $z \in \mathbb{R}$ we have

$$\begin{aligned} P(z) &= \int_{-\infty}^{\infty} \rho(y)U(z-y)\mathrm{d}y \leq \int_{-\infty}^{+\infty} \rho(y)\mathrm{d}y = 1, \\ P(z) &= \int_{-\infty}^{\infty} \rho(y)U(z-y)\mathrm{d}y \geq 0. \end{aligned}$$

Since $\dfrac{2}{2+\hat{\chi}} \le U(z) \le 1$ for all $z<0$, we have for $z<0$

$$P(z) \ge \frac{1}{2\sigma}\int_z^{+\infty} \exp\left(-\frac{|y|}{\sigma}\right) \times \frac{2}{2+\hat{\chi}}\mathrm{d}y = \frac{2}{2+\hat{\chi}}\left(1-\frac{e^{\frac{z}{\sigma}}}{2}\right) \ge \frac{1}{2+\hat{\chi}}.$$

Thus, for any $z \le 0$, we have $\dfrac{1}{2+\hat{\chi}} \le P(z) \le 1$. Since $\tau(t)$ is the solution of

$$\begin{cases} \tau'(t) &= \chi\big(P'(0) - P'(\tau(t))\big) \\ \tau(0) &= -1, \end{cases}$$

and due to Lemma 3.3.21, $t \to \tau(t)$ is strictly decreasing, continuous and

$$\lim_{t\to-\infty}\tau(t) = 0, \quad \lim_{t\to+\infty}\tau(t) = -\infty.$$

Therefore,

$$\frac{1}{2+\hat{\chi}} \le P(\tau(t)) \le 1, \quad t \in \mathbb{R}.$$

Since by definition $\mathcal{U}(t) = \left[(1+\hat{\chi})\int_{-\infty}^t e^{-\int_l^t 1+\hat{\chi}P(\tau(s))\mathrm{d}s}\mathrm{d}l\right]^{-1}$, $\mathcal{U}$ is monotone with respect to P, and we compute on the one hand

$$\begin{aligned} \mathcal{U}(t) &\le \left[(1+\hat{\chi})\int_{-\infty}^t e^{-\int_l^t 1+\hat{\chi}\mathrm{d}s}\mathrm{d}l\right]^{-1} \\ &= \left[(1+\hat{\chi})\int_{-\infty}^t e^{-(1+\hat{\chi})(t-l)}\mathrm{d}l\right]^{-1} = 1. \end{aligned}$$

On the other hand, we can see that

$$\begin{aligned} \mathcal{U}(t) &\ge \left[(1+\hat{\chi})\int_{-\infty}^t \exp\left(-\int_l^t 1+\frac{\hat{\chi}}{2+\hat{\chi}}\mathrm{d}s\right)\mathrm{d}l\right]^{-1} \\ &= \left[(1+\hat{\chi})\int_{-\infty}^t \exp\left(-\left(1+\frac{\hat{\chi}}{2+\hat{\chi}}\right)(t-l)\right)\mathrm{d}l\right]^{-1} = \frac{2}{2+\hat{\chi}}. \end{aligned}$$

This implies $\frac{2}{2+\hat{\chi}} \le \mathcal{U}(t) \le 1$, for all $t \in \mathbb{R}$. Since τ^{-1} maps $(-\infty, 0)$ to $\mathbb{R}$, for any $z<0$ we have indeed

$$\frac{2}{2+\hat{\chi}} \le \mathcal{T}(U)(z) = \mathcal{U}(\tau^{-1}(z)) \le 1.$$

Item (i) is proved.

Step 2. We prove that $z \mapsto \mathcal{T}(U)(z)$ is strictly decreasing on $(-\infty, 0)$. First, we prove that $t \mapsto \mathcal{U}(t)$ is strictly increasing. Indeed $\mathcal{U}$ is differentiable and we have

$$\mathcal{U}'(t) = \frac{-1}{1+\hat{\chi}} \times \frac{1+\displaystyle\int_{-\infty}^t -\big(1+\hat{\chi}P(\tau(t))\big)e^{-\int_l^t 1+\hat{\chi}P(\tau(s))\mathrm{d}s}\mathrm{d}l}{\left[\displaystyle\int_{-\infty}^t \exp\left(-\int_l^t 1+P(\tau(s))\mathrm{d}s\right)\mathrm{d}l\right]^2} \tag{3.3.50}$$

Moreover, for any $l<t$, we have $\tau(t) < \tau(l)$. Since P is strictly decreasing, $P(\tau(l)) < P(\tau(t))$. We deduce

$$\begin{aligned} \int_{-\infty}^t e^{-\int_l^t 1+\hat{\chi}P(\tau(s))\mathrm{d}s}\big(1+\hat{\chi}P(\tau(t))\big)\mathrm{d}l &> \int_{-\infty}^t e^{-\int_l^t 1+\hat{\chi}P(\tau(s))\mathrm{d}s}\big(1+\hat{\chi}P(\tau(l))\big)\mathrm{d}l \\ &= \int_{-\infty}^t \frac{\mathrm{d}}{\mathrm{d}l}\Big(e^{-\int_l^t 1+\hat{\chi}P(\tau(s))\mathrm{d}s}\Big) = 1. \end{aligned}$$

This implies $\mathcal{U}'(t) > 0$ and $t \mapsto \mathcal{U}(t)$ is strictly increasing. Note that the inverse map $z \mapsto \tau^{-1}(z)$ is strictly decreasing, therefore the composition of two mappings

$$z \longmapsto \mathcal{T}(U)(z) = \mathcal{U}(\tau^{-1}(z))$$

is also strictly decreasing on $(-\infty, 0)$. Item (ii) is proved.

Step 3. We prove that $\mathcal{T}(U) \in C^1((-\infty,0),\mathbb{R})$ and compute the limit of $\mathcal{T}(U)$ as $z \to 0^-$.

Since for any $z < 0$

$$\sigma^2 P''(z) = -U(z) + P(z) \in C((-\infty,0),\mathbb{R}),$$

P belongs to $C^2((-\infty,0),\mathbb{R})$, which implies that $t \mapsto \tau(t)$ belongs to $C^1(\mathbb{R},(-\infty,0))$. By (3.3.50), the function $t \mapsto \mathcal{U}'(t)$ is continuous and the inverse map $z \to \tau^{-1}(z)$ is also of class C^1 from $(-\infty,0)$ to $\mathbb{R}$. Thus, the function

$$z \longmapsto \mathcal{T}(U)(z) = \mathcal{U}(\tau^{-1}(z))$$

is of class C^1 from $(-\infty,0)$ to $\mathbb{R}$. Moreover, the map $t \mapsto \mathcal{U}(t)$ is strictly decreasing and is bounded from below by $\frac{2}{2+\hat{\chi}} > 0$, thus $\lim_{t\to-\infty} \mathcal{U}(t)$ exists. In particular

$$\mathcal{T}(U)(0^-) := \lim_{z\to 0^-} \mathcal{U}(\tau^{-1}(z)) = \lim_{t\to-\infty} \mathcal{U}(t).$$

By the definition of $\mathcal{U}$

$$\begin{aligned}
\mathcal{T}(U)(0^-) &= \lim_{t\to-\infty} \mathcal{U}(t) \\
&= \lim_{t\to-\infty} \left[(1+\hat{\chi}) \int_{-\infty}^{t} e^{-\int_l^t 1+\hat{\chi}P(\tau(s))\mathrm{d}s} \mathrm{d}l\right]^{-1} \\
&= \lim_{t\to-\infty} \frac{e^{\int_0^t 1+\hat{\chi}P(\tau(s))\mathrm{d}s}}{(1+\hat{\chi})\int_{-\infty}^{t} e^{\int_0^l 1+\hat{\chi}P(\tau(s))\mathrm{d}s}\mathrm{d}l}.
\end{aligned}$$

By employing L'Hôpital rule

$$\begin{aligned}
\mathcal{T}(U)(0^-) &= \lim_{t\to-\infty} \frac{e^{\int_0^t 1+\hat{\chi}P(\tau(s))\mathrm{d}s}}{(1+\hat{\chi})\int_{-\infty}^{t} e^{\int_0^l 1+\hat{\chi}P(\tau(s))\mathrm{d}s}\mathrm{d}l} \\
&= \lim_{t\to-\infty} \frac{\big(1+\hat{\chi}P(\tau(t))\big)e^{\int_0^t 1+P(\tau(s))\mathrm{d}s}}{(1+\hat{\chi})\,e^{\int_0^t 1+P(\tau(s))\mathrm{d}s}} \\
&= \frac{1+\hat{\chi}P(0)}{1+\hat{\chi}}.
\end{aligned}$$

Therefore, $\mathcal{T}(U) \in C^1((-\infty,0),\mathbb{R}) \cap C((-\infty,0],\mathbb{R})$ and $\mathcal{T}(U)(0) = (1+\hat{\chi}P(0))/(1+\hat{\chi})$. This proves Item (iii) and concludes the proof of Lemma 3.3.22. □

Next we focus on the continuity of $\mathcal{T}$ for a particular topology.

Lemma 3.3.23 (Continuity of $\mathcal{T}$)**.** *Define the weighted norm*

$$\|U\|_\eta := \sup_{z\in(-\infty,0)} \alpha(z)|U(z)|, \tag{3.3.51}$$

where

$$\alpha(z) := \sqrt{-z}\, e^{\eta z} \le \frac{1}{\sqrt{2e\eta}}, \text{ for all } z \le 0,$$

with $0 < \eta < \sigma^{-1}$. If Assumption 3.3.11 is satisfied, then the map $\mathcal{T}$ is continuous on $\mathcal{A}$ for the distance induced by $\|\cdot\|_\eta$.

Proof. Let $U \in \mathcal{A}$ and $\varepsilon \in (0, 2\sqrt{2/\eta e})$ be given. Let $\tilde{U} \in \mathcal{A}$ be given and define the corresponding pressure and rescaled variable $\tilde{P} := \rho \star \tilde{U}$ and $\tilde{\tau}$ as the solution to (3.3.49) with U replaced by $\tilde{U}$. We remark that :

$$
\begin{aligned}
&|\mathcal{T}(U)(z) - \mathcal{T}(\tilde{U})(z)| = \\
&\qquad |\mathcal{T}(U)(z)\mathcal{T}(\tilde{U})(z)| \left| \int_{-\infty}^{\tilde{\tau}^{-1}(z)} e^{-\int_l^{\tilde{\tau}^{-1}(z)} 1+\hat{\chi}\tilde{P}(\tilde{\tau}(s)\mathrm{d}s} \mathrm{d}l - \int_{-\infty}^{\tau^{-1}(z)} e^{-\int_l^{\tau^{-1}(z)} 1+\hat{\chi}P(\tau(s)\mathrm{d}s} \mathrm{d}l \right| \\
&\qquad\qquad \leq \left| \int_{-\infty}^{\tilde{\tau}^{-1}(z)} e^{-\int_l^{\tilde{\tau}^{-1}(z)} 1+\hat{\chi}\tilde{P}(\tilde{\tau}(s))\mathrm{d}s} \mathrm{d}l - \int_{-\infty}^{\tau^{-1}(z)} e^{-\int_l^{\tau^{-1}(z)} 1+\hat{\chi}P(\tau(s))\mathrm{d}s} \mathrm{d}l \right|,
\end{aligned}
$$

by Lemma 3.3.22. Define $T_{-L}(U) := \int_{-L}^{\tau^{-1}(z)} e^{-\int_l^{\tau^{-1}(z)} 1+\hat{\chi}P(\tau(s))\mathrm{d}s} \mathrm{d}l$. We have $\mathcal{T}(U) = T_{-\infty}(U)$ and

$$
\begin{aligned}
&|T_{-\infty}(U) - T_{-\infty}(\tilde{U})| \\
&\qquad \leq \left| \int_{-\infty}^{\tilde{\tau}^{-1}(z)-L} e^{-\int_l^{\tilde{\tau}^{-1}(z)} 1+\hat{\chi}\tilde{P}(\tilde{\tau}(s))\mathrm{d}s} \mathrm{d}l - \int_{-\infty}^{\tau^{-1}(z)-L} e^{-\int_l^{\tau^{-1}(z)} 1+\hat{\chi}P(\tau(s))\mathrm{d}s} \mathrm{d}l \right| \\
&\qquad\quad + \left| \int_{\tilde{\tau}^{-1}(z)-L}^{\tilde{\tau}^{-1}(z)} e^{-\int_l^{\tilde{\tau}^{-1}(z)} 1+\hat{\chi}\tilde{P}(\tilde{\tau}(s))\mathrm{d}s} \mathrm{d}l - \int_{\tau^{-1}(z)-L}^{\tau^{-1}(z)} e^{-\int_l^{\tau^{-1}(z)} 1+\hat{\chi}P(\tau(s))\mathrm{d}s} \mathrm{d}l \right| \\
&\qquad \leq e^{-L} + e^{-L} \\
&\qquad\quad + \left| \int_{\tilde{\tau}^{-1}(z)-L}^{\tilde{\tau}^{-1}(z)} e^{-\int_l^{\tilde{\tau}^{-1}(z)} 1+\hat{\chi}P(\tilde{\tau}(s))\mathrm{d}s} \mathrm{d}l - \int_{\tau^{-1}(z)-L}^{\tau^{-1}(z)} e^{-\int_l^{\tau^{-1}(z)} 1+\hat{\chi}P(\tau(s))\mathrm{d}s} \mathrm{d}l \right| \\
&\qquad \leq \frac{\varepsilon}{2}\sqrt{2\eta e} \\
&\qquad\quad + \left| \int_{\tilde{\tau}^{-1}(z)-L}^{\tilde{\tau}^{-1}(z)} e^{-\int_l^{\tilde{\tau}^{-1}(z)} 1+\hat{\chi}\tilde{P}(\tilde{\tau}(s))\mathrm{d}s} \mathrm{d}l - \int_{\tau^{-1}(z)-L}^{\tau^{-1}(z)} e^{-\int_l^{\tau^{-1}(z)} 1+\hat{\chi}P(\tau(s))\mathrm{d}s} \mathrm{d}l \right| \\
&\qquad = \frac{\varepsilon}{2}\sqrt{2\eta e} + |T_{-L}(U)(z) - T_{-L}(\tilde{U})(z)|,
\end{aligned}
$$

for $L := -\ln\left(\frac{\varepsilon}{2}\sqrt{\frac{e\eta}{2}}\right) > 0$.

Let z_0 and z_1 be respectively the smallest and the biggest negative root of the equation

$$
\eta z + \frac{1}{2}\ln(-z) = \ln\left(\frac{\varepsilon}{4}\right).
$$

The choice of ε ensures that z_0 and z_1 exist. Then if $z \notin [z_0, z_1]$ we have $\sqrt{-z}e^{\eta z} \leq \frac{\varepsilon}{4}$ and, since $|T_{-L}(U)| \leq 1$ we have

$$
\begin{aligned}
\sqrt{-z}e^{\eta z}|T_{-L}(U)(z)| &= \sqrt{-z}e^{\eta z} \left| \int_{\tau^{-1}(z)-L}^{\tau^{-1}(z)} e^{-\int_l^{\tau^{-1}(z)} 1+\hat{\chi}P(\tau(s))\mathrm{d}s} \mathrm{d}l \right| \\
&\leq \frac{\varepsilon}{4} \int_{\tau^{-1}(z)-L}^{\tau^{-1}(z)} e^{-\int_l^{\tau^{-1}(z)} 1\mathrm{d}s} \mathrm{d}l = \frac{\varepsilon}{4}(1 - e^{-L}) \leq \frac{\varepsilon}{4}.
\end{aligned}
$$

Similarly, we have

$$
\sqrt{-z}e^{\eta z}|T_{-L}(\tilde{U})(z)| \leq \frac{\varepsilon}{4}.
$$

We have shown

$$
\sup_{z \notin [z_0, z_1]} \sqrt{-z}e^{\eta z}|\mathcal{T}(U)(z) - \mathcal{T}(\tilde{U})(z)| \leq \varepsilon.
$$

There remains to estimate $\sqrt{-z}e^{\eta z}|T_{-L}(U)(z) - T_{-L}(\tilde{U})(z)|$ when $z \in [z_0, z_1]$. We have

$$\begin{aligned}
&|T_{-L}(U)(z) - T_{-L}(\tilde{U})(z)| \\
&\qquad = \left| \int_{\tilde{\tau}^{-1}(z)-L}^{\tilde{\tau}^{-1}(z)} e^{-\int_l^{\tilde{\tau}^{-1}(z)} 1+\hat{\chi}\tilde{P}(\tilde{\tau}(s))\mathrm{d}s} \mathrm{d}l - \int_{\tau^{-1}(z)-L}^{\tau^{-1}(z)} e^{-\int_l^{\tau^{-1}(z)} 1+\hat{\chi}P(\tau(s))\mathrm{d}s} \mathrm{d}l \right| \\
&\qquad \leq 2|\tilde{\tau}^{-1}(z) - \tau^{-1}(z)| \\
&\qquad\quad + \left| \int_{\tau^{-1}(z)-L}^{\tau^{-1}(z)} e^{-\int_l^{\tilde{\tau}^{-1}(z)} 1+\hat{\chi}\tilde{P}(\tilde{\tau}(s))\mathrm{d}s} - e^{-\int_l^{\tau^{-1}(z)} 1+\hat{\chi}P(\tau(s))\mathrm{d}s} \mathrm{d}l \right| \\
&\qquad \leq 2|\tilde{\tau}^{-1}(z) - \tau^{-1}(z)| \\
&\qquad\quad + L \sup_{l \in (\tau^{-1}(z)-L, \tau^{-1}(z))} \left| e^{\int_l^{\tau^{-1}(z)} 1+\hat{\chi}P(\tau(s))\mathrm{d}s - \int_l^{\tilde{\tau}^{-1}(z)} 1+\hat{\chi}\tilde{P}(\tilde{\tau}(s))\mathrm{d}s} - 1 \right|,
\end{aligned}$$

and we remark that

$$\begin{aligned}
&\left| \int_l^{\tau^{-1}(z)} 1 + \hat{\chi}P(\tau(s))\mathrm{d}s - \int_l^{\tilde{\tau}^{-1}(z)} 1 + \hat{\chi}\tilde{P}(\tilde{\tau}(s))\mathrm{d}s \right| \\
&\qquad \leq 2|\tau^{-1}(z) - \tilde{\tau}^{-1}(z)| + \hat{\chi} \left| \int_l^{\tau^{-1}(z)} P(\tau(s)) - \tilde{P}(\tilde{\tau}(s))\mathrm{d}s \right| \\
&\qquad \leq 2|\tau^{-1}(z) - \tilde{\tau}^{-1}(z)| + \hat{\chi}L \sup_{s \in (\tau^{-1}(z)-L, \tau^{-1}(z))} |P(\tau(s)) - P(\tilde{\tau}(s))| \\
&\qquad\quad + \hat{\chi}L \sup_{s \in (\tau^{-1}(z)-L, \tau^{-1}(z))} |P(\tilde{\tau}(s)) - \tilde{P}(\tilde{\tau}(s))|.
\end{aligned}$$

To conclude the proof of the continuity of $\mathcal{T}$, we show that each of those three terms can be made arbitrarily small (uniformly on $[z_0, z_1]$) by choosing $\tilde{U}$ sufficiently close to U in the $\|\cdot\|_\eta$ norm. We start with the second one. We have for all $z \leq 0$:

$$\begin{aligned}
|P(z) - \tilde{P}(z)| &= \frac{1}{2\sigma} \left| \int_{-\infty}^0 e^{-\frac{|z-y|}{\sigma}} (U(y) - \tilde{U}(y))\mathrm{d}y \right| \\
&\leq \frac{1}{2\sigma} \int_{-\infty}^z e^{\frac{y-z}{\sigma}} |U(y) - \tilde{U}(y)|\mathrm{d}y + \frac{1}{2\sigma} \int_z^0 e^{\frac{z-y}{\sigma}} |U(y) - \tilde{U}(y)|\mathrm{d}y \\
&\leq \frac{1}{2\sigma} \sqrt{\frac{2\eta}{e}} e^{-\frac{z}{\sigma}} \int_{-\infty}^z \frac{e^{(1-\sigma\eta)\frac{y}{\sigma}}}{\sqrt{-y}} \|U - \tilde{U}\|_\eta \mathrm{d}y + \frac{1}{2} \sqrt{\frac{2\eta}{e}} e^{\frac{z}{\sigma}} \int_z^0 \frac{e^{-(1+\sigma\eta)\frac{y}{\sigma}}}{\sqrt{-y}} \|U - \tilde{U}\|_\eta \mathrm{d}y \\
&= \sigma^{-1} \sqrt{\frac{\eta}{2e}} \left[e^{-\frac{z}{\sigma}} \int_{-\infty}^z \frac{e^{(1-\sigma\eta)\frac{y}{\sigma}}}{\sqrt{-y}} \mathrm{d}y + e^{\frac{z}{\sigma}} \int_z^0 \frac{e^{-(1+\sigma\eta)\frac{y}{\sigma}}}{\sqrt{-y}} \mathrm{d}y \right] \|U - \tilde{U}\|_\eta \\
&=: C_P(z) \|U - \tilde{U}\|_\eta.
\end{aligned}$$

A similar computation shows that, for all $z \leq 0$,

$$\begin{aligned}
|P'(z) - \tilde{P}'(z)| &\leq \sigma^{-2} \sqrt{\frac{\eta}{2e}} \left[e^{-\frac{z}{\sigma}} \int_{-\infty}^z \frac{e^{(1-\sigma\eta)\frac{y}{\sigma}}}{\sqrt{-y}} \mathrm{d}y + e^{\frac{z}{\sigma}} \int_z^0 \frac{e^{-(1+\sigma\eta)\frac{y}{\sigma}}}{\sqrt{-y}} \mathrm{d}y \right] \|U - \tilde{U}\|_\eta \\
&= \frac{1}{\sigma} C_P(z) \|U - \tilde{U}\|_\eta.
\end{aligned}$$

In particular for $z = 0$ we have

$$|P'(0) - \tilde{P}'(0)| \leq \sigma^{-2} \sqrt{\frac{\eta}{2e}} \int_{-\infty}^0 \frac{e^{(1-\sigma\eta)\frac{y}{\sigma}}}{\sqrt{-y}} \mathrm{d}y \|U - \tilde{U}\|_\eta,$$

and therefore $P'(0)$ and $\tilde{P}'(0)$ can be chosen arbitrarily small. Next we show that $\tau(t)$ and $\tilde{\tau}(t)$ are uniformly close for $t \in [\tau^{-1}(z_0) - L, \tau^{-1}(z_1)]$. Indeed, we compute:

$$\begin{aligned}
|(\tau - \tilde{\tau})(t)| &= \chi \left| \int_0^t P'(0) - P'(\tau(s))\mathrm{d}s - \int_0^t \tilde{P}'(0) - \tilde{P}'(\tilde{\tau}(s))\mathrm{d}s \right| \\
&\leq \chi \left| t(P'(0) - \tilde{P}'(0)) + \int_0^t \tilde{P}'(\tau(s)) - P'(\tau(s))\mathrm{d}s \right| \\
&\quad + \chi \left| \int_0^t \tilde{P}'(\tilde{\tau}(s)) - \tilde{P}'(\tau(s))\mathrm{d}s \right| \\
&\leq \chi t[C_P(0) + \max_{0\leq s\leq t} C_P(\tau(s))]\|U - \tilde{U}\|_\eta + \hat{\chi} \int_0^t |\tilde{\tau}(s) - \tau(s)|\mathrm{d}s,
\end{aligned}$$

where we have used the fact that $\sigma^2|P''(z)| = |P(z) - U(z)| \leq 1$. By Grönwall's Lemma, we have therefore

$$|\tau(t) - \tilde{\tau}(t)| \leq \chi t\big[C_P(0) + \max_{0\leq s\leq t} C_P(\tau(s))\big]\|U - \tilde{U}\|_\eta e^{\hat{\chi}t},$$

and we have shown that τ and $\tilde{\tau}$ can be made arbitrarily close by choosing $\|U - \tilde{U}\|_\eta$ sufficiently small. This gives an arbitrary control on the term

$$\sup_{s\in(\tau^{-1}(z)-L,\tau^{-1}(z))} |P(\tau(s)) - P(\tilde{\tau}(s))| \leq |P'(0)||\tau(s) - \tilde{\tau}(s)|,$$

since $P'(0) < P'(z) \leq 0$ by Lemma 3.3.21, and on the term

$$\sup_{s\in(\tau^{-1}(z)-L,\tau^{-1}(z))} |P(\tilde{\tau}(s)) - \tilde{P}(\tilde{\tau}(s))| \leq \left[\sup_{s\in(\tau^{-1}(z)-L,\tau^{-1}(z))} C_P(\tilde{\tau}(s))\right] \|U - \tilde{U}\|_\eta.$$

Finally, we estimate $\tau^{-1}(z) - \tilde{\tau}^{-1}(z)$ by the remark:

$$\begin{aligned}
|\tau^{-1}(z) - \tilde{\tau}^{-1}(z)| &= \left| \int_{-1}^z \frac{1}{\tau'(\tau^{-1}(y))}\mathrm{d}y - \int_{-1}^z \frac{1}{\tilde{\tau}'(\tilde{\tau}^{-1}(y))}\mathrm{d}y \right| \\
&= \frac{1}{\chi} \left| \int_{-1}^z \frac{1}{P'(0) - P'(y)} - \frac{1}{\tilde{P}'(0) - \tilde{P}'(y)}\mathrm{d}y \right| \\
&\leq \frac{1}{\chi} \int_{-1}^z \frac{|P'(0) - \tilde{P}'(0)| + |P'(y) - \tilde{P}'(y)|}{|P'(0) - P'(y)||\tilde{P}'(0) - \tilde{P}'(y)|}\mathrm{d}y,
\end{aligned}$$

recalling that we have a uniform lower bound for $|P'(0) - P'(y)|$ and $|\tilde{P}'(0) - \tilde{P}'(y)|$ by Lemma 3.3.21.

This finishes the proof of Lemma 3.3.23. □

Lemma 3.3.24. *Suppose U is admissible in the sense of Definition 3.3.20 and that Assumption 3.3.11 holds. Then $\mathcal{T}(U) \in C^1((-\infty, 0], \mathbb{R})$ and*

$$\mathcal{T}(U)'(z) = \mathcal{T}(U)(z)\frac{1 + \hat{\chi}P(z) - (1 + \hat{\chi})\mathcal{T}(U)(z)}{\chi\big(P'(0) - P'(z)\big)}, \quad \text{for all } z < 0. \tag{3.3.52}$$

Moreover

$$\lim_{z\to 0^-} \mathcal{T}(U)'(z) = \frac{P'(0)}{1 + \hat{\chi}} \frac{1 + \hat{\chi}P(0)}{1 + \hat{\chi}U(0^-)}.$$

Proof. We divide the proof in two steps.

Step 1. We prove (3.3.52).

We observe that

$$\tau'(\tau^{-1}(z)) := \chi\big(P'(0) - P'(z)\big),$$

therefore $\mathcal{T}(U)$ is differentiable for each $z < 0$ and

$$\mathcal{T}(U)'(z) = \mathcal{U}'(\tau^{-1}(z))\frac{1}{\tau'(\tau^{-1}(z))} = \mathcal{U}'(\tau^{-1}(z))\frac{1}{\chi\big(P'(0) - P'(z)\big)}.$$

By Equation (3.3.50) in Lemma 3.3.22 we have

$$\begin{aligned}
\mathcal{U}'(t) &= \frac{1}{1+\hat{\chi}}\Big[\int_{-\infty}^{t} e^{-\int_l^t 1+\hat{\chi}P(\tau(s))\mathrm{d}s}\mathrm{d}l\Big]^{-2} \\
&\quad\times\Big(\int_{-\infty}^{t} e^{-\int_l^t 1+\hat{\chi}P(\tau(s))\mathrm{d}s}\big(1+\hat{\chi}P(\tau(t))\big)\mathrm{d}l - 1\Big) \\
&= \Big[(1+\hat{\chi})\int_{-\infty}^{t} e^{-\int_l^t 1+\hat{\chi}P(\tau(s))\mathrm{d}s}\mathrm{d}l\Big]^{-2} \\
&\quad\times\Big((1+\hat{\chi})\int_{-\infty}^{t} e^{-\int_l^t 1+\hat{\chi}P(\tau(s))\mathrm{d}s}\mathrm{d}l\big(1+\hat{\chi}P(\tau(t))\big) - (1+\hat{\chi})\Big) \\
&= \mathcal{U}^2(t)\Big(\mathcal{U}^{-1}(t)\big(1+\hat{\chi}P(\tau(t))\big) - (1+\hat{\chi})\Big) \\
&= \mathcal{U}(t)\Big(1+\hat{\chi}P(\tau(t)) - (1+\hat{\chi})\mathcal{U}(t)\Big).
\end{aligned}$$

Therefore, we can rewrite $\mathcal{T}(U)'(z)$ as

$$\begin{aligned}
\mathcal{T}(U)'(z) &= \frac{\mathcal{U}'(\tau^{-1}(z))}{\chi\big(P'(0)-P'(z)\big)} \\
&= \mathcal{U}(\tau^{-1}(z))\frac{1+\hat{\chi}P(z)-(1+\hat{\chi})\mathcal{U}(\tau^{-1}(z))}{\chi\big(P'(0)-P'(z)\big)} \\
&= \mathcal{T}(U)(z)\frac{1+\hat{\chi}P(z)-(1+\hat{\chi})\mathcal{T}(U)(z)}{\chi\big(P'(0)-P'(z)\big)}.
\end{aligned}$$

Equation (3.3.52) follows.

Step 2. Next we prove

$$\lim_{z\to 0^-}\mathcal{T}(U)'(z) = \frac{P'(0)}{1+\hat{\chi}}\frac{1+\hat{\chi}P(0)}{1+\hat{\chi}U(0)}.$$

Recall that

$$\begin{aligned}
\mathcal{T}(U)(z) = \mathcal{U}(\tau^{-1}(z)) &= \frac{1}{(1+\hat{\chi})\int_{-\infty}^{\tau^{-1}(z)} e^{-\int_l^{\tau^{-1}(z)} 1+\hat{\chi}P(\tau(s))\mathrm{d}s}\mathrm{d}l} \\
&= \frac{e^{\int_0^{\tau^{-1}(z)} 1+\hat{\chi}P(\tau(s))\mathrm{d}s}}{(1+\hat{\chi})\int_{-\infty}^{\tau^{-1}(z)} e^{\int_0^{l} 1+\hat{\chi}P(\tau(s))\mathrm{d}s}\mathrm{d}l}.
\end{aligned}$$

We have shown in Step 1 that for any $z<0$

$$\mathcal{T}(U)'(z) = \mathcal{T}(U)(z)\frac{1+\hat{\chi}P(z)-(1+\hat{\chi})\mathcal{T}(U)(z)}{\chi\big(P'(0)-P'(z)\big)}, \tag{3.3.53}$$

and by Lemma 3.3.22 we have

$$\lim_{z\to 0^-}\mathcal{T}(U)(z) = \frac{1+\hat{\chi}P(0)}{1+\hat{\chi}}.$$

Moreover,

$$\begin{aligned}
&\frac{1+\hat{\chi}P(z)-(1+\hat{\chi})\mathcal{T}(U)(z)}{\chi\big(P'(0)-P'(z)\big)} \\
&\qquad= \frac{(1+\hat{\chi}P(z))\int_{-\infty}^{\tau^{-1}(z)} e^{\int_0^{l} 1+\hat{\chi}P(\tau(s))\mathrm{d}s}\mathrm{d}l - e^{\int_0^{\tau^{-1}(z)} 1+\hat{\chi}P(\tau(s))\mathrm{d}s}}{\chi(P'(0)-P'(z))\int_{-\infty}^{\tau^{-1}(z)} e^{\int_0^{l} 1+\hat{\chi}P(\tau(s))\mathrm{d}s}} =: \frac{N(z)}{D(z)},
\end{aligned}$$

and

$$\frac{N'(z)}{D'(z)} = \frac{\hat{\chi}P'(z)\int_{-\infty}^{\tau^{-1}(z)} e^{\int_0^l 1+\hat{\chi}P(\tau(s))\mathrm{d}s}\mathrm{d}l}{-\chi P''(z)\int_{-\infty}^{\tau^{-1}(z)} e^{\int_0^l 1+\hat{\chi}P(\tau(s))\mathrm{d}s}\mathrm{d}s + \chi\big(P'(0)-P'(z)\big)(\tau^{-1})'(z)e^{\int_0^{\tau^{-1}(z)} 1+\hat{\chi}P(\tau(s))\mathrm{d}s}}$$
$$= \frac{P'(z)}{\hat{\chi}(U(z)-P(z))+(1+\hat{\chi})\mathcal{T}(U)(z)} \xrightarrow[z\to 0^-]{} \frac{P'(0)}{\hat{\chi}U(0^-)+1}.$$

Therefore, by using L'Hôpital's rule, $\mathcal{T}(U)'(z)$ admits a limit when $z \to 0^-$ and

$$\lim_{z\to 0^-} \mathcal{T}(U)'(z) = \frac{P'(0)}{1+\hat{\chi}}\frac{1+\hat{\chi}P(0)}{1+\hat{\chi}U(0^-)}.$$

□

Lemma 3.3.25 (Compactness of $\mathcal{T}$)**.** *Let Assumption 3.3.11 hold. The metric space $\mathcal{A}$ equipped with the distance induced by the $\|\cdot\|_\eta$ norm (defined in* (3.3.51)*) is a complete metric space on which the map $\mathcal{T}:\mathcal{A}\to\mathcal{A}$ is compact.*

Proof. Let us first briefly recall that the space $\mathcal{A}$ is complete. Let B_η be the set of all continuous functions defined on $(-\infty,0)$ with finite $\|\cdot\|_\eta$ norm:

$$B_\eta := \{u \in C^0\big((-\infty,0)\big) \,|\, \|u\|_\eta < +\infty\}.$$

It is classical that B_η equipped with the norm $\|\cdot\|_\eta$ is a Banach space. Therefore, in order to prove the completeness of $\mathcal{A}$, it suffices to show that $\mathcal{A}$ is closed in B_η. Let $U_n \in \mathcal{A}$, $U \in B_\eta$ be such that $\lim \|U_n - U\|_\eta = 0$. Then U_n converges to U locally uniformly on $(-\infty,0)$, and in particular we have

$$U(z) \in \left[\frac{2}{2+\hat{\chi}},1\right] \text{ for all } z \le 0,$$
$$U \text{ is non-increasing.}$$

Therefore $u \in \mathcal{A}$ and the completeness is proved.

Let us show that $\mathcal{T}$ is a compact map of the metric space $\mathcal{A}$. We have shown in Lemma 3.3.22 that $\mathcal{T}$ is continuous on $\mathcal{A}$ and leaves $\mathcal{A}$ stable. Let $U_n \in \mathcal{A}$, then combining Equation (3.3.52) and the local uniform lower bound of $P'(z)-P'(0)$ from Lemma 3.3.21, the family $\mathcal{T}(U_n)'|_{[-k,-1/k]}$ is uniformly Lipschitz continuous on $[-k,-1/k]$ for each $k \in \mathbb{N}$. Therefore the Ascoli-Arzelà applies and the set $\{\mathcal{T}(U_n)|_{[-k,-1/k]}\}_{n\ge 0}$ is relatively compact for the uniform topology on $[-k,-1/k]$ for each $k \in \mathbb{N}$. Using a diagonal extraction process, there exists a subsequence $\varphi(n)$ and a continuous function U such that $U_{\varphi(n)} \to U$ uniformly on every compact subset of $(-\infty,0)$. Let us show that $\|U_{\varphi(n)} - U\|_\eta \to 0$ as $n \to +\infty$. Let $\varepsilon > 0$ be given, and let z_0, z_1 be respectively the smallest and largest root of the equation:

$$\eta z + \frac{1}{2}\ln(-z) = \ln\left(\frac{\varepsilon}{2}\right).$$

Then, on the one hand, for any $z \notin [z_0,z_1]$, we have $\sqrt{-z}e^{\eta z} \le \frac{\varepsilon}{2}$ and therefore

$$\sqrt{-z}e^{\eta z}|\mathcal{T}(U_{\varphi(n)})(z) - \mathcal{T}(U)(z)| \le \sqrt{-z}e^{\eta z}(|U_{\varphi(n)}(z)| + |U(z)|) \le \varepsilon.$$

On the other hand, since $\mathcal{T}(U_{\varphi(n)})$ converges locally uniformly to $\mathcal{T}(U)$, there is $n_0 \ge 0$ such that

$$\sup_{z\in[z_0,z_1]} \sqrt{-z}e^{\eta z}|\mathcal{T}(U_{\varphi(n)})(z) - \mathcal{T}(U)(z)| \le \varepsilon, \text{ for all } n \ge n_0.$$

We conclude that

$$\|\mathcal{T}(U_{\varphi(n)}) - \mathcal{T}(U)\|_\eta \le \varepsilon,$$

for all $n \ge n_0$. The convergence is proved. This ends the proof of Lemma 3.3.25 □

We are now in the position to prove Theorem 3.3.13.

Proof of Theorem 3.3.13. We remark that the set of admissible functions $\mathcal{A}$ is a nonempty, closed, convex, bounded subset of the Banach space B_η, and $\mathcal{T}$ is a continuous compact operator on $\mathcal{A}$ (Lemma 3.3.25). Therefore, a direct application of the Schauder fixed-point Theorem (see e.g. [413, Theorem 2.A p. 57]) shows that $\mathcal{T}$ admits a fixed point U in $\mathcal{A}$:

$$\mathcal{T}(U) = U.$$

Applying Lemma 3.3.22 and 3.3.24, U is strictly decreasing on $(-\infty, 0)$, $U((-\infty, 0)) \subset [\frac{2}{2+\hat{\chi}}, 1]$, U is C^1 on $(-\infty, 0]$ and

$$\lim_{z\to 0^-} U(z) = \frac{1+\hat{\chi}P(0)}{1+\hat{\chi}} \text{ and } \lim_{z\to 0^-} U'(z) = \frac{P'(0)}{1+\hat{\chi}}\frac{1+\hat{\chi}P(0)}{1+\hat{\chi}U(0)}.$$

Finally

$$U'(z) = U(z)\frac{1+\hat{\chi}P(z) - (1+\hat{\chi})U(z)}{\chi\big(P'(0) - P'(z)\big)}, \text{ for all } z < 0, \tag{3.3.54}$$

therefore

$$\chi P'(0)U'(z) - \chi P'(z)U'(z) - \chi U(z)P''(z) = U(z)(1-U(z)), \text{ for all } z < 0,$$

and finally

$$\chi P'(0)U'(z) - \chi(P'(z)U(z))' = U(z)(1-U(z)), \text{ for all } z < 0.$$

We now prove that $U(-\infty) := \lim_{z\to\infty} U(z) = 1$. Since U is monotone decreasing on $(-\infty, 0)$ and is bounded by 1 from above, $U(-\infty)$ exists and, by a direct application of Lebesgue's dominated convergence theorem, P also converges to a limit near $-\infty$, $P(-\infty) = U(-\infty)$. Therefore $U'(z) \to 0$, $P'(z) \to 0$ and $P''(z) \to 0$ as $z \to -\infty$. We conclude that

$$\lim_{z\to-\infty} U(z)(1-U(z)) = 0,$$

which implies that $U(-\infty) = 1$.

Let us define $u(t,x) := U(x - ct)$, with $c := -\chi P'(0)$. The characteristics associated with $u(t,x)$ are

$$\frac{\mathrm{d}}{\mathrm{d}t}h(t,x) = -\chi(\rho_x \star u)(t, h(t,x)) = \chi(\rho \star U)(h(t,x) - ct) = -\chi P'(h(t,x) - ct),$$

and $u(t,x)$ satisfies for all x such that $h(t,x) - ct < 0$:

$$\begin{aligned}\partial_t u(t, h(t,x)) = \partial_t(U(h(t,x) - ct)) &= \left(\frac{\mathrm{d}}{\mathrm{d}t}(h(t,x) - ct)\right)U'(h(t,x) - ct)\\ &= \chi(-P'(h(t,x) - ct) + P'(0))U'(h(t,x) - ct)\\ &= u(t, h(t,x))(1 + \hat{\chi}(\rho \star u)(t, h(t,x)) - (1+\hat{\chi})u(t, h(t,x))).\end{aligned}$$

If $h(t,x) - ct > 0$ then $u(t, h(t,x)) = U(h(t,x) - ct) = 0$ (locally in t) and therefore

$$\partial_t u(t, h(t,x)) = 0 = u(t, h(t,x))(1 + \hat{\chi}(\rho \star u)(t, h(t,x)) - (1+\hat{\chi})u(t, h(t,x))).$$

Since $\{0\}$ is a negligible set for the Lebesgue measure, we conclude that $u(t,x)$ is a solution integrated along the characteristics to (3.3.1) and thus U is a traveling wave profile with speed $c = -P'(0) > 0$ as defined in Definition 3.3.10. Finally

$$c = -\chi P'(0) = \frac{\chi}{2\sigma}\int_{-\infty}^{0} e^y U(y)\mathrm{d}y \in \left(\frac{\chi}{\sigma(2+\hat{\chi})}, \frac{\chi}{2\sigma}\right) = \left(\frac{\sigma\hat{\chi}}{2+\hat{\chi}}, \frac{\sigma\hat{\chi}}{2}\right).$$

This finishes the proof of Theorem 3.3.13 □

3.3.5.2 Non-existence of continuous sharp traveling waves

Remark 3.3.26. This result tells us if U is a sharp traveling wave solution to (3.3.1), then it must be discontinuous. This situation is very different from the porous medium case. However, it does not exclude the existence of *positive* continuous traveling wave solutions which decay to zero near $+\infty$. In fact, as we shown in the numerical simulations in the section 3.3.3, we can observe numerically large speed traveling wave solutions that are smooth and strictly positive.

Proof of Proposition 3.3.14. We divide the proof in 3 steps.

Step 1: We show the estimate (3.3.18).

Assume by contradiction that there exists $x \in \mathbb{R}$ such that

$$-\chi \int_{\mathbb{R}} \rho_x(x-y)U(y)\mathrm{d}y = c. \tag{3.3.55}$$

We let $P(x) := (\rho \star U)(x) = \int_{\mathbb{R}} \rho(x-y)U(y)\mathrm{d}y$. Since $U \in C^0(\mathbb{R})$, we have that $P \in C^2(\mathbb{R})$. Differentiating, we find that

$$\begin{aligned} P'(x) &= \int_{\mathbb{R}} \rho_x(x-y)U(y)\mathrm{d}y = (\rho' \star U)(x), \\ \sigma^2 P''(x) &= \int_{\mathbb{R}} \rho(x-y)U(y)\mathrm{d}y - U(x) = P(x) - U(x). \end{aligned}$$

Letting $Y(x) := -\chi(\rho_x \star U)(x) - c = -\chi P'(x) - c$, then $Y \in C^1(\mathbb{R})$ and we have

$$Y'(x) = -\chi P''(x) = \hat{\chi}\big(U(x) - (\rho \star U)(x)\big). \tag{3.3.56}$$

Since $\lim_{x\to+\infty} U(x) = 0$, we have $\lim_{x\to+\infty} Y(x) = -c < 0$. Remark that by our assumption (3.3.55), Y has at least one zero and therefore the largest root of Y is well-defined:

$$x_* := \inf\{x \,|\, \text{ for all } y > x, Y(y) < 0\}.$$

We first remark that

$$\frac{\mathrm{d}}{\mathrm{d}t}\big(h(t,x) - ct\big) = \frac{\mathrm{d}}{\mathrm{d}t}h(t,x) - c = -\chi(\rho_x \star u)(t, h(t,x)) - c = Y(h(t,x) - ct), \tag{3.3.57}$$

where we recall that $u(t,x) := U(x-ct)$ is a solution to (3.3.1). In particular since $Y(x_*) = 0$ by the continuity of Y, we have $h(t,x_*) - ct = x_*$. Next by using (3.3.11) we have

$$\begin{aligned} \frac{\mathrm{d}}{\mathrm{d}t}u(t,h(t,x_*)) &= u(t,h(t,x_*))\big(1 + \hat{\chi}(\rho \star u)(t,h(t,x_*)) - (1+\hat{\chi})u(t,h(t,x_*))\big) \\ &= U(h(t,x_*) - ct)\big(1 + \hat{\chi}(\rho \star U)(h(t,x_*) - ct) \\ &\quad - (1+\hat{\chi})U(h(t,x_*) - ct)\big) \\ &= U(x_*)\big(1 + \hat{\chi}P(x_*) - (1+\hat{\chi})U(x_*)\big), \end{aligned}$$

and since $u(t,h(t,x_*)) = U(h(t,x_*) - ct) = U(x_*)$ does not depend on t, this yields

$$0 = U(x_*)\big(1 + \hat{\chi}P(x_*) - (1+\hat{\chi})U(x_*)\big).$$

We conclude that either $U(x_*) = 0$ or $U(x_*) = \frac{1+\hat{\chi}P(x_*)}{1+\hat{\chi}} > 0$. In the remaining part of this step we will show that these two cases lead to contradiction.

Case 1: $U(x_*) = \frac{1+\hat{\chi}P(x_*)}{1+\hat{\chi}} > 0$**.** By (3.3.56) we have:

$$Y'(x_*) = \hat{\chi}\big(U(x_*) - P(x_*)\big) = (1 - P(x_*))\frac{\hat{\chi}}{1+\hat{\chi}},$$

however $U(x) \in [0,1]$, $U(x) \not\equiv 1$ and thus $P(x_*) = (\rho \star U)(x_*) < 1$ which shows $Y'(x_*) > 0$. Yet by definition of x_* we have $Y(x_*) = 0$ and $Y(x) < 0$ for all $x > x_*$, hence $Y'(x_*) \le 0$, which is a contradiction.

Case 2: $U(x_*) = 0$**.** By (3.3.56) we have

$$Y'(x_*) = 0 - \hat{\chi}P(x_*) = -\hat{\chi}(\rho \star U)(x_*) < 0. \tag{3.3.58}$$

Hence by the continuity of Y, there exists a $x_0 < x_*$ such that

$$Y(x) > 0, \quad \text{for all } x \in [x_0, x_*).$$

Recall that, by (3.3.57), we have for all $t > 0$

$$\frac{\mathrm{d}}{\mathrm{d}t}(h(t,x_0) - ct) = Y(h(t,x_0) - ct) > 0$$

as well as $h(0,x_0) - c \times 0 = x_0$, therefore the function $t \mapsto h(t,x_0) - ct$ is increasing and converges to x_* as $t \to +\infty$. In particular as $t \to +\infty$ we have $u(t,h(t,x_0)) = U(h(t,x_0) - ct) \to U(x_*) = 0$. Let $T > 0$ be such that $0 < u(t,h(t,x_0)) \leq \frac{1}{2(1+\hat{\chi})}$ for all $t \geq T$. We have

$$\begin{aligned}\frac{\mathrm{d}}{\mathrm{d}t}u(t,h(t,x_0)) &= u(t,h(t,x_0))\big(1 + \hat{\chi}(\rho \star u)(t,h(t,x_0)) - (1+\hat{\chi})u(t,h(t,x_0))\big)\\ &\geq \frac{1}{2}u(t,h(t,x_0)),\end{aligned}$$

hence $u(t,h(t,x_0)) \geq u(T,h(T,x_0))e^{\frac{t-T}{2}}$. In particular letting

$$t^* := T - 2\ln\big(u(T,h(T,x_0))\big) > T,$$

we have

$$u\left(t^*,h(t^*,x_0)\right) \geq 1 > \frac{1}{2(1+\hat{\chi})},$$

which is a contradiction. Since both Case 1 and Case 2 lead to contradiction, we have shown (3.3.18).

Step 2: Regularity of u.

We have shown in Step 1 that for all $x \in \mathbb{R}$ the strict inequality:

$$Y(x) = -\chi P'(x) - c < 0$$

holds. Let $x \in \mathbb{R}$ and $t_0 > 0$. Then, there exists $y \in \mathbb{R}$ such that $h(t_0,y) = x$, where h is the characteristic semiflow defined by (3.3.10). Since

$$\frac{\mathrm{d}}{\mathrm{d}t}(h(t,y) - ct) = -\chi(\rho_x \star u)(t,h(t,y)) - c = Y(h(t,y)) \neq 0,$$

the mapping $t \mapsto h(t,y) - ct$ has a C^1 inverse which we denote $\varphi(z)$, i.e.

$$\text{for all } z \,|\, \exists t > 0, z = h(t,y) - ct, \qquad h(\varphi(z),y) - c\varphi(z) = z.$$

Then we have

$$U(h(t,y) - ct) = u(t,h(t,y)) \qquad \Leftrightarrow \qquad U(z) = u(\varphi(z),h(\varphi(z),y)),$$

with $z = h(t,y)$ in a neighbourhood of x. Since φ is C^1 and the function $t \mapsto u(t,h(t,y))$ is C^1, we conclude that U is C^1 in a neighbourhood of x. The regularity is proved.

Step 3: We show that u is positive.

Combining Step 1 and 2, we know that u is a classical solution to the equation:

$$\begin{aligned}-cU_x - \chi((\rho \star U)_x U)_x &= U(1-U)\\ (-c - \chi P')U_x &= U(1 + \hat{\chi}P - (1+\hat{\chi})U)\\ U_x &= \frac{U}{Y}(1 + \hat{\chi}P - (1+\hat{\chi})U),\end{aligned}$$

and since $Y < 0$, the right-hand side is a locally Lipschitz vector field in the variable U. In particular, the classical Cauchy-Lipschitz Theorem applies and the only solution with $U(x) = 0$ for some $x \in \mathbb{R}$ is $U \equiv 0$. Since U is non-trivial by assumption, U has to be positive. □

Appendix

3.3.6 An nonlinear function

We study a function used in the proof of Lemma 3.3.21 and Assumption 3.3.11.

Lemma 3.3.27. *The function*

$$f(x) := \ln\left(\frac{2-x}{x}\right) + \frac{2}{2+x}\left(\frac{x}{2}\ln\left(\frac{x}{2}\right) + 1 - \frac{x}{2}\right)$$

defined for $x \in (0,2)$ is strictly decreasing and satisfies

$$\lim_{x\to 0^+} f(x) = +\infty, \qquad \lim_{x\to 2^-} f(x) = -\infty.$$

In particular $f(x)$ has a unique root in $(0,2)$.

Finally, we have $f(1) > 0$.

Proof. The behavior of f at the boundary is standard. The strict monotony requires the computation of the derivative:

$$f'(x) = \left(\frac{-x-(2-x)}{x^2}\right) \times \frac{x}{2-x} + \frac{-2}{(2+x)^2}\left(\frac{x}{2}\ln\left(\frac{x}{2}\right) + 1 - \frac{x}{2}\right) + \frac{1}{2+x}\ln\left(\frac{x}{2}\right).$$

Recalling that

$$\frac{\hat{\chi}}{2}\ln\left(\frac{\hat{\chi}}{2}\right) + 1 - \frac{\hat{\chi}}{2} > 0, \tag{3.3.59}$$

for each $x \in (0,2)$ because $x \mapsto x\ln(x)$ is strictly convex, all three terms in the expression of $f'(x)$ are negative, therefore

$$f'(x) < 0$$

for all $x \in (0,2)$. The fact that $f(1) > 0$ can also be deduced from (3.3.59). Lemma 3.3.27 is proved. □

3.3.7 Numerical scheme

Our numerical scheme for the travalling waves in Section 3 reads

$$\begin{aligned}
&\frac{u_i^{n+1}-u_i^n}{\Delta t} + \frac{1}{\Delta x}\Big(G(u_{i+1}^n, u_i^n) - G(u_i^n, u_{i-1}^n)\Big) = u_i^n(1-u_i^n),\\
&i = 1, 2, \ldots, M,\ n = 0, 1, 2, \ldots\\
&u_0 = 1,\ u_{M+1} = 0,
\end{aligned}$$

with $G(u_{i+1}^n, u_i^n)$ defined as

$$G(u_{i+1}^n, u_i^n) = (v_{i+\frac{1}{2}}^n)^+ u_i^n - (v_{i+\frac{1}{2}}^n)^- u_{i+1}^n = \begin{cases} v_{i+\frac{1}{2}}^n u_i^n, & v_{i+\frac{1}{2}}^n \geq 0,\\ v_{i+\frac{1}{2}}^n u_{i+1}^n, & v_{i+\frac{1}{2}}^n < 0, \end{cases} \quad i = 1, \ldots, M.$$

Moreover, the velocity v is given by

$$v_{i+\frac{1}{2}}^n = -\frac{p_{i+1}^n - p_i^n}{\Delta x},\ i = 0, 1, 2, \cdots, M,$$

where from (3.3.20) we define

$$P^n := (I-A)^{-1}U^n, \quad P^n = \left(p_i^n\right)_{M\times 1} \quad U^n = \left(u_i^n\right)_{M\times 1}.$$

where $A = (a_{i,j})_{M\times M}$ is the usual linear diffusion matrix with Neumann boundary condition. Therefore, by Neumann boundary condition $p_0 = p_1$ and $p_{M+1} = p_M$, when $i = 1, M$ we have

$$\begin{aligned}
G(u_1^n, u_0^n) &= 0,\\
G(u_{M+1}^n, u_M^n) &= 0,
\end{aligned}$$

which gives

$$u_1^{n+1} = u_1^n - d\,\frac{\Delta t}{\Delta x} G(u_2^n, u_1^n) + \Delta t\, f(u_1^n),$$
$$u_M^{n+1} = u_M^n + d\,\frac{\Delta t}{\Delta x} G(u_M^n, u_{M-1}^n) + \Delta t\, f(u_M^n).$$

Owing to the boundary condition, we have the conservation of mass for Equation (3.3.19) when the reaction term equals zero.

Acknowledgements: Xiaoming Fu was supported by China Scholarship Council. The authors would like to thank the anonymous referees for their constructive comments which helped improve the quality of the paper.

Chapter 4

Long-time dynamics in epidemic models

4.1 Concentration estimates in a multi-host epidemiological model structured by phenotypic traits

4.1.1 Introduction

In this work we study the stationary states of the following system of equations

$$\begin{cases} \dfrac{\mathrm{d}S_k}{\mathrm{d}t}(t) = \xi_k \Lambda - \theta S_k(t) - S_k(t) \displaystyle\int_{\mathbb{R}^N} \beta_k(y) A(t,y) \mathrm{d}y, \quad k = 1,2, \\ \dfrac{\partial I_k}{\partial t}(t,x) = \beta_k(x) S_k(t) A(t,x) - (\theta + d_k(x)) I_k(t,x), \quad k = 1,2, \\ \dfrac{\partial A}{\partial t}(t,x) = -\delta A(t,x) + \displaystyle\int_{\mathbb{R}^N} m_\varepsilon(x-y) \left[r_1(y) I_1(t,y) + r_2(y) I_2(t,y) \right] \mathrm{d}y. \end{cases} \tag{4.1.1}$$

The above system describes the evolution of a pathogen producing spores in a heterogeneous plant population with two hosts. This model has been proposed in [263] to study the impact of resistant plants on the evolutionary adaptation of a fungal pathogen.

Here the state variables are nonnegative functions. The function $S_k(t)$ denotes the healthy tissue density of each host $k \in \{1,2\}$, $I_k(t,x)$ represents the density of tissue infected by pathogen with phenotypic trait value $x \in \mathbb{R}^N$, while $A(t,x)$ describes the density of airborne spores of pathogens with phenotypic trait value $x \in \mathbb{R}^N$. Here $N \in \mathbb{N} \setminus \{0\}$ is a given and fixed integer.

The positive parameters Λ, θ, δ respectively denote the influx of total new healthy tissue, the death rate of host tissue and the death rate of the spores. The parameters $\xi_k \in (0,1)$ correspond to the proportions of influx of new healthy tissue for each host population and therefore satisfy the relation $\xi_1 + \xi_2 = 1$. Note that in the absence of the disease, namely when $I_1 = I_2 = A = 0$, the density of tissue at equilibrium for each host k is equal to $\xi_k \Lambda / \theta$.

The phenotypic traits of the pathogen considered in the model are supposed to influence the functions r_k, β_k and d_k that respectively denote the spores production rates, the infection efficiencies and the infectious periods of the pathogen. Those parameters depend on the phenotypic value $x \in \mathbb{R}^N$ and the host $k = 1,2$.

The function m_ε is a probability kernel that characterises the mutations arising during the reproduction process. More precisely, given tissue infected by a mother spore with phenotypic value y, $m_\varepsilon(x-y)$ stands for the probability that a produced spore has a phenotypic value x. Therefore m_ε describes the dispersion in the phenotypic trait space $\mathbb{R}^N$ arising at each production of new spores.

Here we consider that produced spores cannot have a very different phenotypic value from the one of their mother. In other words, mutations are occurring within a small variance so that we assume that the mutation kernel is highly concentrated and depends on a small parameter $0 < \varepsilon \ll 1$ according to the following scaling form

$$m_\varepsilon(x) = \frac{1}{\varepsilon^N} m\left(\frac{x}{\varepsilon}\right), \quad \forall x \in \mathbb{R}^N,$$

where m is a fixed probability distribution (see Assumption 4.1.1 in Section 4.1.2 below).

In this work we aim at studying the existence and uniqueness of nontrivial steady states for the above system of equations. We also investigate the shape of these steady states for $\varepsilon \ll 1$ and we shall more

precisely study their concentrations around some specific phenotypic trait values when the mutation kernel is very narrow, *i.e.* for $\varepsilon \to 0$.

The above problem supplemented with an age of infection structure has been investigated by Djidjou *et al.* [146] using formal asymptotic expansions and numerical simulations. In the aforementioned work, the authors proved the convergence of the solution of the Cauchy problem toward highly concentrated steady states.

Moreover, the case of a single host population has already been studied thoroughly. A refined mathematical analysis of the stationary states has been carried out in [145] with a particular emphasis on the concentration property for $\varepsilon \ll 1$. We also refer to [85, 86] for the study of the dynamical behaviour and the transient regimes of a corresponding simplified Cauchy problem for a single host.

Model (4.1.1) is related to the selection-mutation models for a population structured by a continuous phenotypic trait introduced in [125, 237] to study the maintenance of genetic variance in quantitative characters. Since then, several studies have been devoted to this class of models in which mutation is frequently modelled by either a nonlocal or a Laplace operator. In many of these works the existence of steady state solutions is related to the existence of a positive eigenfunction of some linear operator and to the Krein-Rutman Theorem, see *e.g.* [64, 84, 92, 93]. In particular, in [92, 93] it is assumed that the rate of mutations is small; in this case the authors are able to prove that the steady state solutions tend to concentrate around some specific trait in the phenotypic space as the mutation rate tends to 0. In [9], the steady state solutions for a nonlocal reaction-diffusion model for adaptation are given in terms of the principal eigenfunction of a Schrödinger operator.

As far as dynamical properties are concerned and under the assumption of small mutations, another fruitful approach introduced in [140] consists in proving that the solutions of the mutation selection problem are asymptotically given by a Hamilton-Jacobi equation. This approach has led to many works, see *e.g.* [284, 285, 307].

Propagation properties have also been investigated in related models, see *e.g.* [1] and [P4] for spatially distributed systems of equations.

As already mentioned above, in this section 4.1 we are concerned with the steady states of (4.1.1). Using the symbol $\star$ to denote the convolution product in $\mathbb{R}^N$, steady state solutions of (4.1.1) solve the following system of equations

$$\begin{cases} S_k = \frac{\xi_k \Lambda}{\theta + \int_{\mathbb{R}^N} \beta_k(y) A(y) \mathrm{d}y}, \quad k = 1, 2, \\ I_k(x) = \frac{\beta_k(x)}{\theta + d_k(x)} S_k A(x), \quad k = 1, 2, \\ \delta A(x) = m_\varepsilon \star \left[r_1(\cdot) I_1(\cdot) + r_2(\cdot) I_2(\cdot) \right](x). \end{cases} \tag{4.1.2}$$

The above system can be rewritten in the form of a single equation for $A = A^\varepsilon \in L^1_+(\mathbb{R}^N)$

$$A^\varepsilon = T^\varepsilon \left(A^\varepsilon \right), \tag{4.1.3}$$

where the nonlinear operator T^ε is given by

$$T^\varepsilon(\varphi) = \sum_{k=1,2} \frac{L^\varepsilon_k(\varphi)}{1 + \theta^{-1} \int_{\mathbb{R}^N} \beta_k(z) \varphi(z) \mathrm{d}z}. \tag{4.1.4}$$

Here, for $k = 1, 2$, L^ε_k denotes the following linear operator

$$L^\varepsilon_k = \frac{\Lambda \xi_k}{\theta} m_\varepsilon \star \left(\Psi_k \cdot \right), \qquad k = 1, 2, \tag{4.1.5}$$

wherein Ψ_k corresponds to the fitness function of the pathogen in host k

$$\Psi_k(x) = \frac{\beta_k(x) r_k(x)}{\delta(\theta + d_k(x))}, \qquad x \in \mathbb{R}^N, \qquad k = 1, 2. \tag{4.1.6}$$

Conversely, if $A^\varepsilon \in L^1_+(\mathbb{R}^N)$ is a fixed point of T^ε, a stationary solution $(S^\varepsilon_1, S^\varepsilon_2, I^\varepsilon_1, I^\varepsilon_2, A^\varepsilon)$ to the original system (4.1.1) can be reconstructed by injecting A^ε into the first two equations of (4.1.2). The trivial solution $A^\varepsilon \equiv 0$ is always solution of (4.1.2) and corresponds to the disease-free equilibrium. When A^ε is nontrivial, the corresponding stationary state is said to be endemic.

This section 4.1 is organized as follows. In Section 4.1.2, we state the main results obtained in this work. In Section 4.1.3 we prove the existence of an endemic (nontrivial) equilibrium for model (4.1.1) by using dynamical system arguments and the theory of global attractors. In Section 4.1.4 we prove that any nontrivial fixed point of (4.1.4) roughly behaves as the superposition of the solution of two single host problems, corresponding to the fixed points of the non-linear operators

$$T_k^\varepsilon[\varphi] = \frac{\xi_k \Lambda}{\theta} \frac{m_\varepsilon \star (\Psi_k \varphi)}{1 + \theta^{-1} \int_{\mathbb{R}^N} \beta_k(z)\varphi(z)\mathrm{d}z}, \tag{4.1.7}$$

provided the fitness functions Ψ_k defined in (4.1.6) have disjoint supports. Finally, in Section 4.1.5, we investigate the uniqueness of the non-trivial fixed point of T^ε, for $\varepsilon \ll 1$. Our analysis relies on the precise description of the shape of A^ε coupled with topological degree theory.

4.1.2 Main results and comments

In this section 4.1.2 we state and discuss the main results that are proved in this section 4.1. Throughout this manuscript we make the following assumption on the model parameters.

Assumption 4.1.1. We assume that

a) the parameters ξ_1, ξ_2, Λ, θ and δ are positive constants with $\xi_1 + \xi_2 = 1$;

b) for each $k = 1, 2$, the functions β_k, d_k, r_k are continuous, nonnegative and bounded on $\mathbb{R}^N$ and the function Ψ_k defined in (4.1.6) is not identically 0 and satisfies

$$\lim_{\|x\| \to \infty} \Psi_k(x) = 0;$$

c) the function $m \in L^\infty_+(\mathbb{R}^N) \cap L^1_+(\mathbb{R}^N)$ is positive almost everywhere, symmetric and with unit mass, *i.e.*

$$m(x) > 0,\ m(-x) = m(x) \text{ a.e. in } \mathbb{R}^N, \text{ and } \int_{\mathbb{R}^N} m(x)\mathrm{d}x = 1.$$

Moreover for every $R > 0$, the function satisfies

$$x \longmapsto \sup_{\|y\| \le R} m(x + y) \in L^1(\mathbb{R}^N).$$

As already mentioned in the Introduction, in this work we discuss some properties of the nonnegative fixed points for the nonlinear operator T^ε in $L^1(\mathbb{R}^N)$. Recall that $A \equiv 0$ is always a solution of such an equation. Our first result provides a sharp condition for the existence of a nontrivial fixed point. This condition relies on the spectral radius $r_\sigma(L^\varepsilon)$ of the linear bounded operator $L^\varepsilon \in \mathcal{L}\left(L^1(\mathbb{R}^N)\right)$ defined by

$$L^\varepsilon(\varphi) := L_1^\varepsilon(\varphi) + L_2^\varepsilon(\varphi) = \frac{\Lambda}{\theta} m_\varepsilon \star \left[\left(\xi_1 \Psi_1 + \xi_2 \Psi_2\right)\varphi\right], \forall \varphi \in L^1(\mathbb{R}^N). \tag{4.1.8}$$

Our first result reads as follows.

Theorem 4.1.2 (Equilibrium points of System (4.1.1))**.** *Let Assumption 4.1.1 be satisfied and let $\varepsilon > 0$ be given.*

(i) If $r_\sigma(L^\varepsilon) \le 1$, then $A \equiv 0$ is the unique solution of (4.1.3) in $L^1_+(\mathbb{R}^N)$.

(ii) If $r_\sigma(L^\varepsilon) > 1$, then there exists at least a continuous function $A^\varepsilon > 0$ such that

$$A^\varepsilon \in L^1(\mathbb{R}^N) \cap L^\infty(\mathbb{R}^N) \text{ and } A^\varepsilon = T^\varepsilon\left(A^\varepsilon\right),$$

where the nonlinear operator T^ε is defined in (4.1.4). Furthermore, the solution A^ε belongs to $\mathcal{C}(\mathbb{R}^N)$, the space of bounded and continuous functions on $\mathbb{R}^N$, and the family $\{A^\varepsilon\}_{\varepsilon>0}$ is uniformly bounded in $L^1(\mathbb{R}^N)$.

The proof of the above Theorem involves the theory of global attractors applied to the discrete dynamical system generated by T^ε. Note that the operator L^ε is the Fréchet derivative of T^ε (see (4.1.4)) at $A \equiv 0$. The position of the spectral radius $r_\sigma(L^\varepsilon)$ with respect to 1 describes the stability and instability of the extinction state $A \equiv 0$ for the aforementioned dynamical system.

In our next result we consider the situation where $r_\sigma(L^\varepsilon) > 1$ and investigate the shape of the nontrivial and nonnegative solutions of the fixed point problem (4.1.3) for $\varepsilon \ll 1$. Observe that the threshold $r_\sigma(L^\varepsilon)$ converges to a limit when $\varepsilon \to 0$

$$\lim_{\varepsilon \to 0} r_\sigma(L^\varepsilon) = R_0 := \frac{\Lambda}{\theta} \|\xi_1 \Psi_1 + \xi_2 \Psi_2\|_{L^\infty}. \tag{4.1.9}$$

In addition to Assumption 4.1.1, we introduce further conditions on the functions β_k and on the decay rate of the mutation kernel m.

Assumption 4.1.3. We assume that the mutation kernel satisfies, for all $n \in \mathbb{N}$,

$$\lim_{\|x\| \to \infty} \|x\|^n m(x) = 0.$$

In other words, m satisfies $m(x) = o\left(\frac{1}{\|x\|^\infty}\right)$ as $\|x\| \to \infty$.

Furthermore, we assume that functions β_1 and β_2 have compact supports, separated in the sense

$$\text{dist } (\Sigma_1, \Sigma_2) > 0 \text{ with } \Sigma_k = \overline{\{x \in \mathbb{R}^N,\ \beta_k(x) > 0\}},\ k = 1, 2, \tag{4.1.10}$$

where dist is the usual distance between sets in $\mathbb{R}^N$

$$\text{dist}(\Sigma_1, \Sigma_2) := \inf_{x \in \Sigma_1} \inf_{y \in \Sigma_2} \|y - x\|.$$

This second assumption will allow us to reduce the study of the fixed points of T^ε to the two simpler fixed point problems associated with T_k^ε (defined in (4.1.7)) weakly coupled when $\varepsilon \ll 1$.

Our last assumption concerns the spectral gap of the bounded linear operators L_k^ε (see (4.1.5)). Let us recall that for each $\varepsilon > 0$ and $k = 1, 2$, the spectrum $\sigma\left(L_k^\varepsilon\right)$ of L_k^ε is composed of isolated eigenvalues (except 0) with finite algebraic multiplicities, among which $r_\sigma(L_k^\varepsilon)$ is a simple eigenvalue. Moreover,

$$\lim_{\varepsilon \to 0} r_\sigma(L_k^\varepsilon) = R_{0,k} := \frac{\xi_k \Lambda}{\theta} \|\Psi_k\|_{L^\infty},\ k = 1, 2. \tag{4.1.11}$$

We refer to Appendix 4.1.6 for a precise statement of those spectral properties. Recalling the definition of R_0 in (4.1.9), observe that, due to Assumption 4.1.3, we have

$$R_0 = \max\{R_{0,1}, R_{0,2}\}.$$

Next for $k = 1, 2$ we denote by $\lambda_k^{\varepsilon,1} > \lambda_k^{\varepsilon,2}$ the first and the second eigenvalues of the linear operator L_k^ε and we assume that the spectral gaps are not too small, namely

Assumption 4.1.4 (Spectral gap)**.** We assume that for each $k = 1, 2$ there exists $n_k \in \mathbb{N}$ such that

$$\liminf_{\varepsilon \to 0} \frac{\lambda_k^{\varepsilon,1} - \lambda_k^{\varepsilon,2}}{\varepsilon^{n_k}} > 0.$$

Note that the above assumption is satisfied for rather general functions Ψ_k. An asymptotic expansion of the first eigenvalues of the operators L_k^ε has been obtained in [145] when the mutation kernel has a fast decay at infinity and when Ψ_k are smooth functions. In that case, the asymptotic expansions for the first eigenvalues involve the derivative of the fitness functions Ψ_k at their maximum. Roughly speaking, for each $k = 1, 2$, Assumption 4.1.4 is satisfied when each – partial – fitness function Ψ_k achieves its global maximum at a finite number of optimal traits, and its behaviour around any two optimal traits differs by some derivative. Assumption 4.1.4 allows us to include the situation studied in [145] in a more general framework. A similar abstract assumption has been used in [85, 86] to derive refined information on the asymptotic and the transient behaviour of the solutions to (4.1.1) in the context of a single host population.

The single host problem

$$T_k^\varepsilon\left(A_k^\varepsilon\right) = A_k^\varepsilon \tag{4.1.12}$$

has been extensively studied in Djidjou *et al.* [145]. In particular it has been shown that, when $R_{0,k} > 1$, this equation admits a unique positive solution $A_k^{\varepsilon,*} \in L^1_+(\mathbb{R}^N)$ as soon as ε is sufficiently small. Our next result shows that any nontrivial solution of (4.1.3) is close to the superposition of the solutions to the two uncoupled problems (4.1.12) for $k = 1, 2$, when $\varepsilon \ll 1$.

Theorem 4.1.5 (Asymptotic shape of the solutions of (4.1.8))**.** *Let Assumptions 4.1.1, 4.1.3 and 4.1.4 be satisfied and assume further that $R_0 > 1$. Let $A^\varepsilon \in L^1_+(\mathbb{R}^N) \cap L^\infty(\mathbb{R}^N)$ be a nontrivial solution of* (4.1.3)*. Then the following estimate holds for $\varepsilon \ll 1$:*

$$\|A^\varepsilon - (A_1^{\varepsilon,*} + A_2^{\varepsilon,*})\|_{L^1(\mathbb{R}^N)} = o(\varepsilon^\infty),$$

where, for $k = 1, 2$, $A_k^{\varepsilon,*} \in L^1(\mathbb{R}^N)$ is the unique positive fixed-point of T_k^ε if $R_{0,k} > 1$ and $A_k^{\varepsilon,*} \equiv 0$ otherwise.

Remark 4.1.6. As will be shown in Lemma 4.1.11, it should be noted that $\|A_1^{\varepsilon,*}\|_{L^1(\Sigma_2)} = o(\varepsilon^\infty)$ and, similarly, $\|A_2^{\varepsilon,*}\|_{L^1(\Sigma_1)} = o(\varepsilon^\infty)$. Therefore, the following result holds as well

$$\|A^\varepsilon - A_1^{\varepsilon,*}\|_{L^1(\Sigma_1)} = o(\varepsilon^\infty), \quad \|A^\varepsilon - A_2^{\varepsilon,*}\|_{L^1(\Sigma_2)} = o(\varepsilon^\infty),$$
$$\|A^\varepsilon - (A_1^{\varepsilon,*} + A_2^{\varepsilon,*})\|_{L^1(\mathbb{R}^N \setminus (\Sigma_1 \cup \Sigma_2))} = o(\varepsilon^\infty).$$

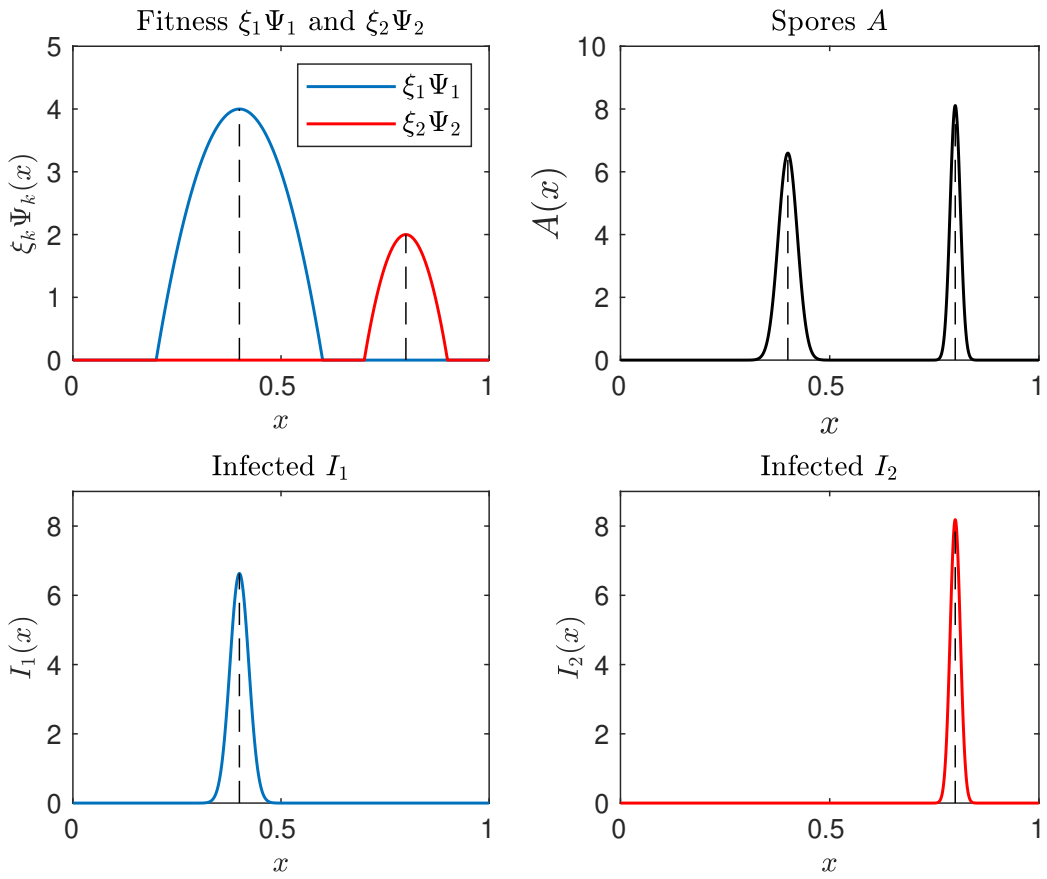

Figure 4.1.1: Fitness functions and endemic equilibrium in the case $R_{0,1} > 1$ and $R_{0,2} > 1$.

In particular, Theorem 4.1.5 ensures a concentration property for the nontrivial fixed point solutions of (4.1.3) and thus for the endemic solutions of (4.1.1) as $\varepsilon \to 0$ (see Figures 4.1.1 and 4.1.2). It shows that each infectious population I_k concentrates around phenotypic values maximising Ψ_k if $R_{0,k} > 1$ or goes to 0 a.e. if $R_{0,k} \leq 1$. As a special case, when each Ψ_k achieves its maximum at a single point $x_k \in \Sigma_k$, a slightly more precise result can be stated.

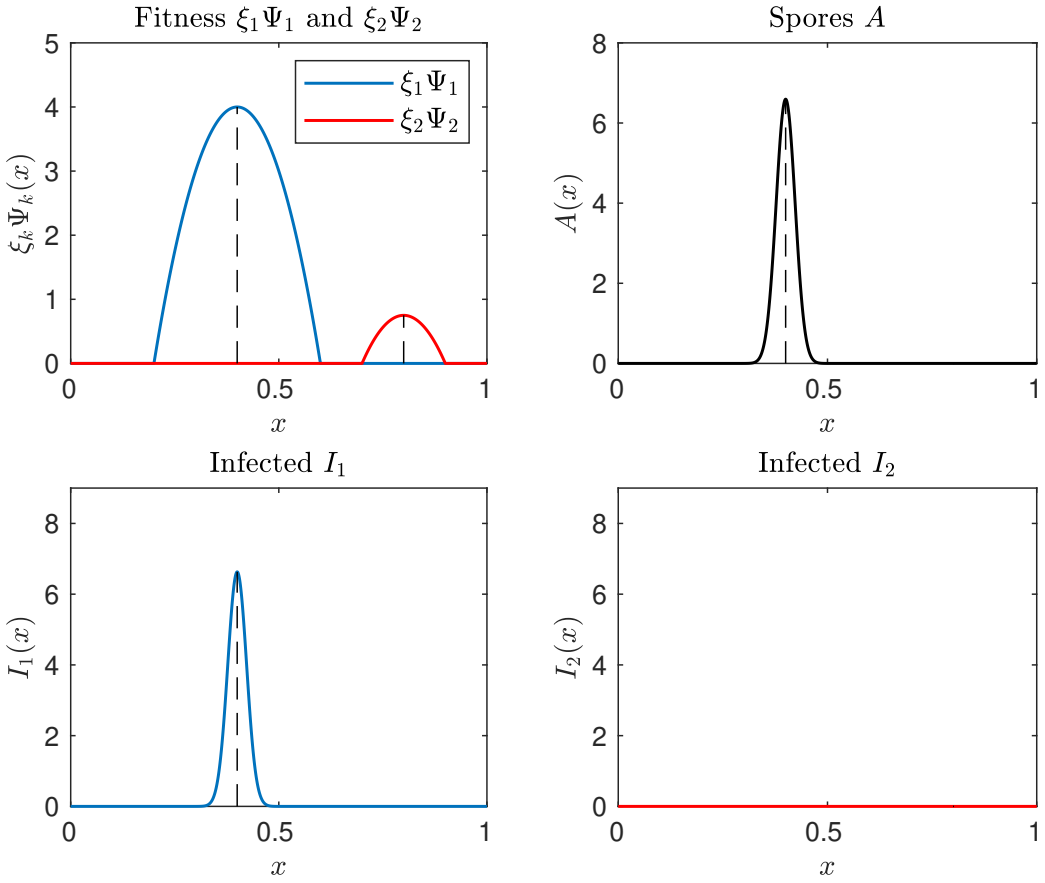

Figure 4.1.2: Fitness functions and endemic equilibrium in the case $R_{0,1} > 1$ and $R_{0,2} < 1$

Corollary 4.1.7 (Concentration property of the endemic equilibrium points)**.** *Assume that each fitness function Ψ_k admits a unique maximum at $x = x_k$ and that $R_{0,k} > 1$ for all $k = 1, 2$, that is*

$$R_{0,k} = \frac{\xi_k \Lambda}{\theta} \Psi_k(x_k) > 1, \ \forall k = 1, 2.$$

For $\varepsilon \ll 1$, denote by $(S_1^\varepsilon, S_2^\varepsilon, I_1^\varepsilon, I_2^\varepsilon, A^\varepsilon)$ any endemic equilibrium point of (4.1.1). Then, as $\varepsilon \to 0$, the following behaviour holds

$$\lim_{\varepsilon \to 0} S_k^\varepsilon = \frac{1}{\Psi_k(x_k)}$$

and for any function f continuous and bounded on $\mathbb{R}^N$, we have

$$\lim_{\varepsilon \to 0} \int_{\mathbb{R}^N} f(x) I_k^\varepsilon(x) \mathrm{d}x = \frac{R_{0,k} - 1}{\Psi_k(x_k) \left(1 + \frac{d_k(x_k)}{\theta}\right)} f(x_k)$$

and

$$\lim_{\varepsilon \to 0} \int_{\mathbb{R}^N} f(x) A^\varepsilon(x) \mathrm{d}x = \frac{\theta}{\beta_1(x_1)} (R_{0,1} - 1) f(x_1) + \frac{\theta}{\beta_2(x_2)} (R_{0,2} - 1) f(x_2).$$

Numerical explorations suggest that the latter concentration property may fail to hold when Assumption 4.1.3 does not hold. Indeed, we can find examples where $R_{0,1} > 1, R_{0,2} > 1$ and where the population of spores does not concentrate to either maximum of Ψ_1 or Ψ_2. Such an example is shown in Figure 4.1.3.

Finally, we are able to prove the uniqueness of the positive equilibrium of (4.1.1) given by Theorem 4.1.2, when ε is sufficiently small. The case where $\min(R_{0,1}, R_{0,2}) = 1$ requires an additional assumption on the

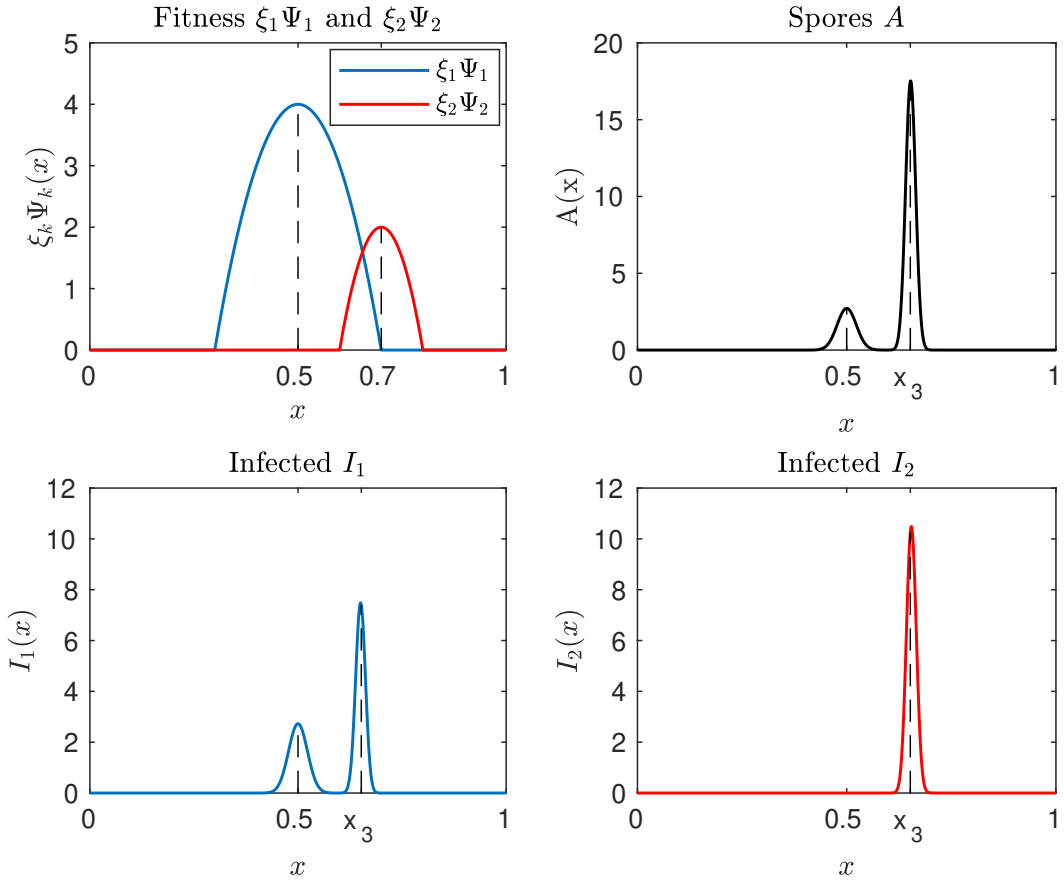

Figure 4.1.3: Fitness functions and endemic equilibrium when Assumption 4.1.3 does not hold. Though Ψ_2 takes its maximum value in $x = 0.7$, functions A, I_1 and I_2 concentrate around the trait value $x_3 \simeq 0.652$.

speed of convergence of the smallest spectral radius as $\varepsilon \to 0$, which is quite natural in our context (it holds for exponentially decaying mutation kernels [145]).

Theorem 4.1.8 (Uniqueness of the endemic equilibrium)**.** *Let Assumptions 4.1.1, 4.1.3 and 4.1.4 be satisfied. Assume moreover that $R_{0,1} > 1$ and that one of the following properties is satisfied:*

- *either $R_{0,2} \neq 1$,*
- *or $R_{0,2} = 1$ and the convergence of $r_\sigma(L_2^\varepsilon)$ towards $R_{0,2}$ is at most polynomial in ε, namely $r_\sigma(L_2^\varepsilon) \leq 1 - C\varepsilon^n$ for some $C > 0$, $n > 0$.*

Then, for $\varepsilon > 0$ sufficiently small, T^ε has exactly one nonnegative nontrivial fixed point.

Our proof is based on a computation of the Leray-Schauder degree in the positive cone of $\mathcal{C}(\Sigma_1) \times \mathcal{C}(\Sigma_2)$. The use of the Leray-Schauder degree is usually restricted to derive the existence of solutions to nonlinear problems, or to provide lower bounds on the number of solutions; here, we are able to derive the *uniqueness* of solution. Indeed, for $\varepsilon > 0$, we show that any equilibrium is *stable*, the topological degree provides a way to count the exact number of positive equilibria for the equation, and show uniqueness. Occurrences of such an argument in the literature are scarce but include [150] and more recently [253].

4.1.3 Proof of Theorem 4.1.2

This section 4.1.3 is devoted to the proof of Theorem 4.1.2. To do so, we investigate some dynamical properties of the nonlinear operator T^ε defined in (4.1.4). The existence of a nontrivial fixed point follows

from the theory of global attractors while the non-existence follows from comparison arguments. Throughout this section 4.1.3 we fix $\varepsilon > 0$. Set $\Psi = \xi_1\Psi_1 + \xi_2\Psi_2$, $\Omega \subset \mathbb{R}^N$ the open set given by

$$\Omega := \{x \in \mathbb{R}^N : \ \Psi(x) > 0\},$$

and let us denote by χ_A the characteristic function of a set A.

We split this section 4.1.3 into two parts. Section 4.1.3.1 is devoted to the proof of Theorem 4.1.2 (i), namely the non-existence of a nontrivial fixed point when $r_\sigma(L^\varepsilon) \leq 1$. In Section 4.1.3.2 we prove the existence of a nontrivial solution when $r_\sigma(L^\varepsilon) > 1$.

4.1.3.1 Proof of Theorem 4.1.2 (i)

Recall that $\varepsilon > 0$ is fixed. To prove the first part of the theorem, we suppose that $r_\sigma(L^\varepsilon) \leq 1$ and denote by $L^\varepsilon{}_{|L^1(\Omega)}$ the operator defined for every $\varphi \in L^1(\Omega)$ by:

$$L^\varepsilon_{|L^1(\Omega)}(\varphi)(x) = L^\varepsilon\tilde{\varphi}(x), \text{ a.e. } x \in \Omega;$$

where $\tilde{\varphi} \in L^1(\mathbb{R}^N)$ is defined by

$$\tilde{\varphi}(x) = \begin{cases} \varphi(x) & \text{if } x \in \Omega; \\ 0 & \text{if } x \in \mathbb{R}^N \setminus \Omega. \end{cases}$$

Lemma 4.1.21 then applies and ensures that the operator $L^\varepsilon{}_{|L^1(\Omega)} \in \text{Ł}(L^1(\Omega))$ is positivity improving, compact, has a positive spectral radius and satisfies

$$r_\sigma\left(L^\varepsilon{}_{|L^1(\Omega)}\right) = r_\sigma(L^\varepsilon).$$

Next using Lemma 4.1.22 (1), we have

$$\lim_{n\to\infty} \left\| \frac{(L^\varepsilon{}_{|L^1(\Omega)})^n(\varphi)}{\left(r_\sigma\left(L^\varepsilon{}_{|L^1(\Omega)}\right)\right)^n} - \Pi(\varphi) \right\|_{L^1(\Omega)} = 0, \ \forall \varphi \in L^1(\Omega), \tag{4.1.13}$$

where Π denotes the spectral projection associated to $L^\varepsilon{}_{|L^1(\Omega)}$ onto

$$\text{Ker}\left(I - \frac{(L^\varepsilon{}_{|L^1(\Omega)})}{\left(r_\sigma\left(L^\varepsilon{}_{|L^1(\Omega)}\right)\right)}\right).$$

Let $A \in L^1_+(\mathbb{R}^N)$ be a fixed point of T^ε. To prove Theorem 4.1.2 (i), let us show that $A \equiv 0$. To that aim note that we have

$$A_{|\Omega} = \chi_\Omega(T^\varepsilon)^n(A) \leq (L^\varepsilon{}_{|L^1(\Omega)})^n(A_{|\Omega}), \ \forall n \geq 0. \tag{4.1.14}$$

Now let us observe that, under the stronger assumption that $r_\sigma(L^\varepsilon) < 1$, then Lemma 4.1.22 applies and shows

$$\lim_{n\to\infty} \left\|\left(L^\varepsilon{}_{|L^1(\Omega)}\right)^n(A)\right\|_{L^1(\Omega)} = 0.$$

Hence $\|A\|_{L^1(\Omega)} = 0$ and therefore $A = T^\varepsilon(A) = 0$ a.e. in $\mathbb{R}^N$. This completes the proof of the result when $r_\sigma(L^\varepsilon) < 1$.

We now consider the limit case $r_\sigma(L^\varepsilon) = 1$. To handle this case let us recall that $\Pi\left(A_{|\Omega}\right) \in \text{Ker}\left(I - (L^\varepsilon{}_{|L^1(\Omega)})\right)$. This allows us to decompose and estimate (4.1.14) as follows:

$$\begin{aligned} \Pi(A_{|\Omega}) + (I-\Pi)(A_{|\Omega}) &= \chi_\Omega(T^\varepsilon)^n(A) \\ &\leq (L^\varepsilon{}_{|L^1(\Omega)})^n(\Pi(A_{|\Omega}) + (I-\Pi)(A_{|\Omega})) \\ &\leq \Pi(A_{|\Omega}) + (L^\varepsilon{}_{|L^1(\Omega)})^n(I-\Pi)(A_{|\Omega}), \end{aligned} \tag{4.1.15}$$

for every $n \geq 0$. This leads to

$$(I-\Pi)(A_{|\Omega}) \leq (L^\varepsilon{}_{|L^1(\Omega)})^n(I-\Pi)(A_{|\Omega}), \ \forall n \geq 1. \tag{4.1.16}$$

Next since $(I-\Pi)(A_{|\Omega}) \in \mathrm{Rg}(I-(L^\varepsilon{}_{|L^1(\Omega)}))$, the part of $L^\varepsilon{}_{|L^1(\Omega)}$ in $\mathrm{Rg}(I-(L^\varepsilon{}_{|L^1(\Omega)}))$ has a spectral radius strictly smaller than 1. Hence letting $n \to \infty$ in (4.1.16) leads to

$$(I-\Pi)(A_{|\Omega}) = 0.$$

Recalling (4.1.15) this yields

$$A_{|\Omega} = \chi_\Omega T^\varepsilon(A) = (L^\varepsilon{}_{|L^1(\Omega)})(A_{|\Omega}),$$

and this ensures that

$$\int_{\mathbb{R}^N} \beta_k(z) A_{|\Omega}(z)\mathrm{d}z = 0 \quad \forall k \in \{1,2\},$$

and therefore $A_{|\Omega} = 0$ a.e. in Ω (recall $\beta_1 + \beta_2 > 0$ on Ω by definition (4.1.6)). The equation $A = T^\varepsilon(A)$ ensures that $A = 0$ a.e. in $\mathbb{R}^N$, that completes the proof of Theorem 4.1.2 (i). □

4.1.3.2 Proof of Theorem 4.1.2 (ii)

We now turn to the proof of the existence of a nontrivial fixed point for the nonlinear operator T^ε. To that aim we shall make use of the theory of global attractors and uniform persistence theory for which we refer to [276]. To perform our analysis and prove the theorem we define the sets

$$\mathcal{M}_0 := \left\{ \varphi \in L^1_+(\mathbb{R}^N) : \int_\Omega \varphi(y)\mathrm{d}y > 0 \right\} \text{ and } \partial\mathcal{M}_0 = \{\varphi \in L^1_+(\mathbb{R}^N) : \chi_\Omega \varphi = 0 \ a.e.\}, \tag{4.1.17}$$

so that

$$L^1_+(\mathbb{R}^N) = \mathcal{M}_0 \cup \partial\mathcal{M}_0.$$

Note also that we have the following invariant properties

$$T^\varepsilon(\mathcal{M}_0) \subset M_0 \text{ and } T^\varepsilon(\partial\mathcal{M}_0) = \{0_{L^1}\} \subset \partial\mathcal{M}_0.$$

Next let us observe that T^ε is bounded on $L^1_+(\mathbb{R}^N)$. Indeed, recalling the definition of Ψ_k in (4.1.6) it is readily checked that

$$\|T^\varepsilon(\varphi)\|_{L^1(\mathbb{R}^N)} \le \frac{\Lambda}{\delta\theta}\left[\xi_1\|r_1\|_{L^\infty} + \xi_2\|r_2\|_{L^\infty}\right], \ \forall \varphi \in L^1_+(\mathbb{R}^N). \tag{4.1.18}$$

Our first lemma deals with the weak persistence of T^ε and T^ε_k as defined in (4.1.7). Our result reads as follows.

Lemma 4.1.9. *Let Assumption 4.1.1 be satisfied. If $r_\sigma(L^\varepsilon_k) > 1$ for some $k \in \{1,2\}$, then we have*

$$\limsup_{n\to\infty} \int_{\mathbb{R}^N} \beta_k(y)(T^\varepsilon_k)^n(\varphi)(y)\mathrm{d}y \ge \frac{\theta}{2}\left(r_\sigma(L^\varepsilon_k) - 1\right), \ \forall \varphi \in \mathcal{M}_0. \tag{4.1.19}$$

If now $r_\sigma(L^\varepsilon) > 1$, then there exists $k \in \{1,2\}$ such that

$$\limsup_{n\to\infty} \int_{\mathbb{R}^N} \beta_k(y)(T^\varepsilon)^n(\varphi)(y)\mathrm{d}y \ge \frac{\theta}{2}\left(r_\sigma(L^\varepsilon) - 1\right), \ \forall \varphi \in \mathcal{M}_0. \tag{4.1.20}$$

Proof. Let us first show (4.1.20). We argue by contradiction by assuming that there exists $\varphi \in \mathcal{M}_0$ such that

$$\limsup_{n\to\infty} \int_{\mathbb{R}^N} \beta_k(y)(T^\varepsilon)^n(\varphi)(y)\mathrm{d}y < \frac{\theta}{2}(r_\sigma(L^\varepsilon) - 1) =: \eta, \qquad k = 1,2.$$

Then, there exists an integer $n_0 \ge 1$ such that

$$\int_{\mathbb{R}^N} \beta_k(y)(T^\varepsilon)^n(\varphi)(y)\mathrm{d}y \le \eta, \qquad \text{for } k = 1,2 \text{ and } n \ge n_0$$

therefore

$$(T^\varepsilon)^{n_0+1}(\varphi)(x) \ge \left(\frac{\theta}{\theta+\eta}L^\varepsilon\right)((T^\varepsilon)^{n_0}(\varphi))(x), \qquad \text{for a.e. } x \in \mathbb{R}^N,$$

and by induction

$$(T^\varepsilon)^{n_0+n}(\varphi) \geq \left(\frac{\theta}{\theta+\eta}L^\varepsilon\right)^n ((T^\varepsilon)^{n_0}(\varphi))(x) \tag{4.1.21}$$

for a.e. $x \in \Omega$ and for every $n \geq 1$. Next set

$$\tilde{\varphi} = ((T^\varepsilon)^{n_0}(\varphi))_{|\Omega} \in L^1_+(\Omega)\backslash\{0\}.$$

By Lemma 4.1.21, the operator $\left(\frac{\theta}{\theta+\eta}L^\varepsilon\right)_{|L^1(\Omega)} \in Ł(L^1(\Omega))$ is positivity improving, compact and satisfies

$$r_\sigma\left(\left(\frac{\theta}{\theta+\eta}L^\varepsilon\right)_{|L^1(\Omega)}\right) = \frac{\theta}{\theta+\eta}r_\sigma(L^\varepsilon) = \frac{2r_\sigma(L^\varepsilon)}{1+r_\sigma(L^\varepsilon)} > 1$$

since $r_\sigma(L^\varepsilon) > 1$. Applying Lemma 4.1.22 yields

$$\lim_{n\to\infty}\left\|\left(\left(\frac{\theta}{\theta+\eta}L^\varepsilon\right)_{|L^1(\Omega)}\right)^n(\tilde{\varphi})\right\|_{L^1(\Omega)} = \infty,$$

so that (4.1.21) ensures that the sequence $\|(T^\varepsilon)^n(\varphi)\|_{L^1(\Omega)}$ is unbounded. This contradicts the point dissipativity of T^ε as stated in (4.1.18). The proofs of (4.1.19) for T_1^ε and T_2^ε are similar. □

We are now able to complete the proof of Theorem 4.1.2 (*ii*).

Proof of Theorem 4.1.2 (*ii*). Recall that throughout this section 4.1.3.2, $\varepsilon > 0$ is fixed. Assume that $r_\sigma(L^\varepsilon) > 1$. As $0 \leq T^\varepsilon \leq L^\varepsilon$ and as L^ε is compact (see Lemma 4.1.21), then T^ε is bounded and compact. Now Theorem 2.9 in [276] applies and ensures that there is a compact global attractor $\mathcal{A} \subset L^1_+(\mathbb{R}^N)$ for T^ε, *i.e.* $\mathcal{A}$ attracts every bounded subset of $L^1_+(\mathbb{R}^N)$ under the iteration of T^ε. Next by Lemma 4.1.9, T^ε is weakly uniformly persistent with respect to the decomposition pair $(\mathcal{M}_0, \partial\mathcal{M}_0)$ of the state space $L^1_+(\mathbb{R}^N)$. Next [276, Proposition 3.2]) applies and ensures that T^ε is also strongly uniformly persistent with respect to this decomposition, *i.e.* there exists $\kappa > 0$ such that

$$\liminf_{n\to+\infty}\|(T^\varepsilon)^n(\varphi)\|_{L^1(\Omega)} \geq \kappa,\ \forall\varphi \in \mathcal{M}_0.$$

As a consequence, according to [276], $T^\varepsilon_{|\mathcal{M}_0}$ admits a compact global attractor $\mathcal{A}_0 \subset \mathcal{M}_0$ and T^ε has at least one fixed point $A \in \mathcal{A}_0$. From the equation $A = T^\varepsilon(A)$, it is readily checked that $A > 0$ a.e. and belongs to $L^\infty(\mathbb{R}^N)$, while the uniform boundedness (with respect to ε) of such a fixed point follows from (4.1.18).

Finally, it remains to prove the continuity of the fixed point A. The facts that $\Psi_k A \in L^1(\mathbb{R}^N)$ for each $k = 1, 2$ and $m_\varepsilon \in L^\infty(\mathbb{R}^N)$, imply (see *e.g.* [63, Corollary 3.9.6, p. 207]) that $m_\varepsilon \star (\Psi_k A) \in \mathcal{C}(\mathbb{R}^N)$. From the expression (4.1.4) of T^ε, it follows that $A \in \mathcal{C}(\mathbb{R}^N)$. This completes the proof of Theorem 4.1.2 (*ii*). □

4.1.4 Proof of Theorem 4.1.5

In this section 4.1.4, we investigate the shape of the endemic equilibria and we prove Theorem 4.1.5. Hence we assume throughout this section 4.1.4 that Assumptions 4.1.1, 4.1.3 and 4.1.4 hold. We furthermore assume that

$$R_0 = \max\{R_{0,1}, R_{0,2}\} > 1.$$

Next recall that since $r_\sigma(L^\varepsilon) \to R_0$ as $\varepsilon \to 0$, Theorem 4.1.2 implies that Problem (4.1.3) has at least a nontrivial fixed point for all ε sufficiently small. We denote by $A^\varepsilon \in L^1_+(\mathbb{R}^N)$ such a nontrivial fixed point of T^ε, for all ε small enough. It is not difficult to check that $A^\varepsilon > 0$ a.e.

Recalling the definition of the open sets

$$\Omega_k = \{x \in \mathbb{R}^N :\ \Psi_k(x) > 0\},\ k = 1, 2, \qquad \Omega = \Omega_1 \sqcup \Omega_2 = \{x \in \mathbb{R}^N :\ \Psi(x) > 0\},$$

note that Assumption 4.1.3 ensures that there exists $\eta > 0$ such that $\|x - y\| \geq \eta$ for all $(x, y) \in \Omega_1 \times \Omega_2$. In what follows the functions χ_{Ω_k} denotes the characteristic functions for Ω_k.

Throughout this section 4.1.4, for all $\varepsilon > 0$ small enough, $A^\varepsilon \in L^1_+(\mathbb{R}^N) \setminus \{0\}$ denotes a positive solution to the equation:

$$A^\varepsilon = \frac{\Lambda\xi_1(m_\varepsilon \star \Psi_1 A^\varepsilon)}{\theta + \int_{\mathbb{R}^N}\beta_1(z)A^\varepsilon(z)\mathrm{d}z} + \frac{\Lambda\xi_2(m_\varepsilon \star \Psi_2 A^\varepsilon)}{\theta + \int_{\mathbb{R}^N}\beta_2(z)A^\varepsilon(z)\mathrm{d}z}. \tag{4.1.22}$$

4.1.4.1 Preliminary estimates

Recall the definition of L_k^ε in (4.1.5). Let $\phi_k^{\varepsilon,1} \in L^1_+(\mathbb{R}^N)$ with $\phi_k^{\varepsilon,1} > 0$ and $\|\phi_k^{\varepsilon,1}\|_{L^1(\mathbb{R}^N)} = 1$ be the principal eigenvector of L_k^ε associated to its principal eigenvalue, which is equal to the spectral radius $r_\sigma(L_k^\varepsilon)$. We now recall some results related to the one host model. We refer to [145] for more details (see also Lemma 4.1.21).

Lemma 4.1.10. *Let Assumption 4.1.1 be satisfied. Let $k \in \{1,2\}$ and $\varepsilon > 0$ be given and assume that $r_\sigma(L_k^\varepsilon) > 1$. Then the equation*

$$A_k = \frac{\Lambda \xi_k \chi_{\Omega_k}(m_\varepsilon * (\Psi_k A_k))}{\theta + \int_{\mathbb{R}^N} \beta_k(z) A_k(z) \mathrm{d}z}, \qquad A_k \in L^1_+(\mathbb{R}^N) \setminus \{0\},$$

has a unique solution, given by

$$A_k^{\varepsilon,*} = \nu_k^\varepsilon \phi_k^{\varepsilon,1} \text{ with } \nu_k^\varepsilon = \frac{\theta(r_\sigma(L_k^\varepsilon) - 1)}{\int_{\mathbb{R}^N} \beta_k(z) \phi_k^{\varepsilon,1}(z) \mathrm{d}z}. \tag{4.1.23}$$

Now, using the separation assumption on the sets $\Omega_k, k \in \{1,2\}$ and the decay at infinity of m, we derive the following preliminary lemma that will be used to prove Theorem 4.1.5 in the next section 4.1.4.2.

Lemma 4.1.11. *Suppose that Assumptions 4.1.1 and 4.1.3 are satisfied. Then, for each $(k,l) \in \{1,2\}^2$ with $k \neq l$, the following properties hold:*

(a) we have

$$\int_{\mathbb{R}^N} \chi_{\Sigma_l} \phi_k^{\varepsilon,1}(z) \mathrm{d}z = o(\varepsilon^\infty), \qquad \nu_k^\varepsilon \int_{\mathbb{R}^N} \chi_{\Sigma_l} \phi_k^{\varepsilon,1}(z) \mathrm{d}z = o(\varepsilon^\infty),$$

for all $\varepsilon \ll 1$, where Σ_l and ν_k^ε are respectively defined in (4.1.10) and (4.1.23).

(b) Let $p \in [1,\infty)$ be given. Then, for any $A \in L^1_+(\mathbb{R}^N)$, the following estimate holds

$$\|\chi_{\Sigma_k} m_\varepsilon * (\Psi_l A)\|_{L^p(\mathbb{R}^N)} = \|A\|_{L^1(\Omega_l)} \times o(\varepsilon^\infty), \tag{4.1.24}$$

where the term $o(\varepsilon^\infty)$ is independent of $A \in L^1_+(\mathbb{R}^N)$.

Proof. We first prove (a). To that aim let us first notice that, due to Assumption 4.1.3, there exists $\eta > 0$ such that $\|x - y\| \geq \eta$ for all $(x,y) \in \Sigma_1 \times \Sigma_2$. Thus, due to the decay assumption for m at infinity, one obtains

$$m_\varepsilon(x - y) = o(\varepsilon^\infty), \tag{4.1.25}$$

uniformly for (x,y) in the compact set $\Sigma_1 \times \Sigma_2$. Now let $(k,l) \in \{1,2\}^2, k \neq l$ be given. By the definition of $\phi_k^{\varepsilon,1}$ we have

$$\phi_k^{\varepsilon,1} = \frac{\Lambda \xi_k}{\theta r_\sigma\left(L_k^\varepsilon\right)} \left(m_\varepsilon \star (\Psi_k \phi_k^{\varepsilon,1}) \right). \tag{4.1.26}$$

Integrating (4.1.26) over Σ_l and recalling that $\|\phi_k^{\varepsilon,1}\|_{L^1(\mathbb{R}^N)} = 1$ we get

$$\int_{\mathbb{R}^N} \chi_{\Sigma_l} \phi_k^{\varepsilon,1}(z) \mathrm{d}z \leq \frac{\Lambda \xi_k |\Sigma_l|}{\theta r_\sigma\left(L_k^\varepsilon\right)} \|\Psi_k\|_{L^\infty(\mathbb{R}^N)} \sup_{(x,y) \in \Sigma_k \times \Sigma_l} m_\varepsilon(x - y).$$

Since $r_\sigma(L_k^\varepsilon) \to R_{0,k} > 0$ as $\varepsilon \to 0$ (recalling (4.1.11)), this yields

$$\int_{\mathbb{R}^N} \chi_{\Sigma_l} \phi_k^{\varepsilon,1}(z) \mathrm{d}z = o(\varepsilon^\infty) \text{ as } \varepsilon \to 0,$$

and completes the proof of the first estimate in (a). Next coming back to (4.1.26) and recalling the definition of Ψ_k in (4.1.6) we get for all $x \in \mathbb{R}^N$

$$\phi_k^{\varepsilon,1}(x) \leq \frac{\Lambda \xi_k}{\theta r_\sigma\left(L_k^\varepsilon\right)} \frac{\|m_\varepsilon\|_{L^\infty} \|r_k\|_{L^\infty}}{\delta \theta} \int_{\mathbb{R}^N} \beta_k(y) \phi_k^{\varepsilon,1}(y) \mathrm{d}y.$$

Hence since $\|\phi_k^{\varepsilon,1}\|_{L^1(\mathbb{R}^N)} = 1$ and $\|m_\varepsilon\|_{L^\infty} = \mathcal{O}(\varepsilon^{-N})$, integrating the above inequality over the bounded set Σ_k, there exists a constant $C > 0$ such that

$$\int_{\Sigma_k} \beta_k(y)\phi_k^{\varepsilon,1}(y)\mathrm{d}y \geq C\varepsilon^N,\ \forall \varepsilon \ll 1.$$

Hence we get

$$\nu_k^\varepsilon = \mathcal{O}(\varepsilon^{-N}) \text{ as } \varepsilon \to 0,$$

and the second estimate in (a) follows. We now turn to the proof of (b). Let $A \in L^1_+(\mathbb{R}^N)$ be given. Then we have, for all $\varepsilon > 0$,

$$|m_\varepsilon \star (\Psi_2 A)(x)| \leq \sup_{(y,z)\in\Sigma_1\times\Sigma_2} m_\varepsilon(y-z)\ \ \|\Psi_2\|_{L^\infty}\|A\|_{L^1(\Omega_2)},\ \forall x \in \Sigma_1.$$

Hence, integrating the above inequality on the compact set Σ_1, we obtain that, for all $p \in [1,\infty)$:

$$\|\chi_{\Sigma_1} m_\varepsilon \star (\Psi_2 A)(x)\|_{L^p(\mathbb{R}^N)} \leq |\Sigma_1|^{1/p} \sup_{(y,z)\in\Sigma_1\times\Sigma_2} m_\varepsilon(y-z)\ \ \|\Psi_2\|_{L^\infty}\|A\|_{L^1(\Omega_2)},$$

and the estimate with $k = 1$ and $l = 2$ follows recalling (4.1.25). The other estimate interchanging the index 1 and 2 is similar. This completes the proof of (b). □

4.1.4.2 Proof of Theorem 4.1.5

This section 4.1.4.2 is devoted to the proof of Theorem 4.1.5. Throughout this section 4.1.4.2 we assume that $R_0 > 1$ so that, since $r_\sigma(L^\varepsilon) \to R_0$ as $\varepsilon \to 0$, there exists $\varepsilon_0 > 0$ such that Problem (4.1.3) has a nontrivial fixed point A^ε for each $\varepsilon \in (0,\varepsilon_0]$ (see Theorem 4.1.2). Recall that since T^ε is bounded with respect to ε, there exists $M > 0$ such that

$$\|A^\varepsilon\|_{L^1(\mathbb{R}^N)} \leq M,\ \forall \varepsilon \in (0,\varepsilon_0].$$

As before, set

$$A_k^\varepsilon = \chi_{\Omega_k} A^\varepsilon,\ k = 1,2,\ \varepsilon \in (0,\varepsilon_0],$$

and observe that $\|A_1^\varepsilon\|_{L^1(\Omega_1)} + \|A_2^\varepsilon\|_{L^1(\Omega_2)} \leq M$ for all $\varepsilon \in (0,\varepsilon_0]$. Now let us define

$$\mu_k^\varepsilon = \theta + \int_{\mathbb{R}^N} \beta_k(z)A^\varepsilon(z)\mathrm{d}z, \quad \forall k \in \{1,2\}, \quad \forall \varepsilon \in (0,\varepsilon_0] \tag{4.1.27}$$

as well as

$$\Psi^\varepsilon := \frac{\Lambda\xi_1\Psi_1}{\mu_1^\varepsilon} + \frac{\Lambda\xi_2\Psi_2}{\mu_2^\varepsilon}.$$

With these notations, note that A^ε becomes a positive fixed point for the linear operator $K^\varepsilon \in Ł(L^1(\mathbb{R}^N))$ defined by

$$K^\varepsilon\varphi := m_\varepsilon \star (\Psi^\varepsilon\varphi), \qquad \varphi \in L^1(\mathbb{R}^N).$$

Our first step consists in proving the next lemma.

Lemma 4.1.12. *The following estimate holds*

$$r_\sigma(L_k^\varepsilon) \leq \frac{\mu_k^\varepsilon}{\theta},\ \forall \varepsilon \in (0,\varepsilon_0]. \tag{4.1.28}$$

Proof. Let us first note that

$$\theta \leq \mu_k^\varepsilon \leq \theta + M\|\beta_k\|_{L^\infty}, \quad \forall k \in \{1,2\}, \quad \forall \varepsilon \in (0,\varepsilon_0] \tag{4.1.29}$$

for some constant $M > 0$. Note that since $A^\varepsilon > 0$ and $K^\varepsilon A^\varepsilon = A^\varepsilon$, we obtain by a version of the Krein-Rutman theorem (see *e.g.* [281, Corollary 4.2.15 p.273]) that

$$r_\sigma(K^\varepsilon) = 1, \forall \varepsilon \in (0,\varepsilon_0].$$

On the other hand, we have $A^\varepsilon = K^\varepsilon A^\varepsilon = \frac{\theta}{\mu_1^\varepsilon}L_1^\varepsilon A^\varepsilon + \frac{\theta}{\mu_2^\varepsilon}L_2^\varepsilon A$, thus for $n \geq 1$ we have

$$0 \leq \left(\frac{\theta}{\mu_1^\varepsilon}L_1^\varepsilon\right)^n A^\varepsilon \leq \left(\frac{\theta}{\mu_1^\varepsilon}L_1^\varepsilon\right)^{n-1} A^\varepsilon \leq \ldots \leq \frac{\theta}{\mu_1^\varepsilon}L_1^\varepsilon A^\varepsilon \leq A^\varepsilon,$$

therefore the contrapositive of Lemma 4.1.22 item 2 shows that $\frac{\theta}{\mu_1^\varepsilon}r_\sigma(L_1^\varepsilon) \leq 1$. Similarly, we have $\frac{\theta}{\mu_2^\varepsilon}r_\sigma(L_2^\varepsilon) \leq 1$. □

We recall that throughout this section 4.1.4.2 the condition $R_0 = \max\{R_{0,1}, R_{0,2}\} > 1$ holds. We now set $\Theta_k = \sqrt{\Psi_k}$ and we define the self-adjoint operators $S_k^\varepsilon \in Ł(L^2(\Omega_k))$ (recall $\Omega_k = \{\Psi_k > 0\}$), for $k = 1, 2$, by

$$S_k^\varepsilon = \frac{\Lambda \xi_k}{\theta} \Theta_k (m_\varepsilon \star (\Theta_k \cdot)).$$

Here recall that $\sigma(S_k^\varepsilon) = \sigma(L_k^\varepsilon)$ since Ω_k is bounded (see Lemma 4.1.21). Our next lemma reads as follows.

Lemma 4.1.13. *Let $k \in \{1, 2\}$ be such that $R_{0,k} > 1$. Then we have*

$$\operatorname{dist}\left(\frac{\mu_k^\varepsilon}{\theta}, \sigma(S_k^\varepsilon)\right) = \operatorname{dist}\left(\frac{\mu_k^\varepsilon}{\theta}, \sigma(L_k^\varepsilon)\right) = o(\varepsilon^\infty),\ \forall \varepsilon \ll 1. \tag{4.1.30}$$

Proof. Let us assume that $R_{0,1} > 1$ (the case $R_{0,2} > 1$ is obtained by the symmetry of the problem with respect to the indices). We recall that

$$\Omega_k = \{x \in \mathbb{R}^N :\ \Psi_k > 0\},\ k = 1, 2,$$

and we denote by $\{\lambda_k^{\varepsilon,n}\}_{n\geq 1}$ the eigenvalues of S_k^ε (and of L_k^ε) ordered by decreasing modulus, so that $\lambda_k^{\varepsilon,1} = r_\sigma(S_k^\varepsilon) = r_\sigma(L_k^\varepsilon)$. Next multiplying (4.1.22) by Θ_1 and using Lemma 4.1.11 (b) yields

$$\frac{\mu_1^\varepsilon \Theta_1 A^\varepsilon}{\theta} - \frac{\Lambda \xi_1 \Theta_1 (m_\varepsilon \star (\Psi_1 A^\varepsilon))}{\theta} = \frac{\Lambda \xi_2 \mu_1^\varepsilon \Theta_1 (m_\varepsilon \star (\Psi_2 A^\varepsilon))}{\theta \mu_2^\varepsilon} = o(\varepsilon^\infty),$$

in $L^2(\Omega_1)$. Hence the following estimate holds

$$\left\| \left(\frac{\mu_1^\varepsilon}{\theta} I - S_1^\varepsilon \right) \Theta_1 A^\varepsilon \right\|_{L^2(\Omega_1)} = o(\varepsilon^\infty). \tag{4.1.31}$$

On the other hand, since S_1^ε is self-adjoint, then the following estimate holds (see *e.g.* [334])

$$\left\| \left(\frac{\mu_1^\varepsilon}{\theta} I - S_1^\varepsilon \right)^{-1} \right\|_{Ł(L^2(\Omega_1))} = \frac{1}{\operatorname{dist}\left(\frac{\mu_1^\varepsilon}{\theta}, \sigma(S_1^\varepsilon)\right)}.$$

By setting

$$y_1^\varepsilon := \left(\frac{\mu_1^\varepsilon}{\theta} I - S_1^\varepsilon \right) \Theta_1 A^\varepsilon,$$

we get

$$\Theta_1 A^\varepsilon = \left(\frac{\mu_1^\varepsilon}{\theta} I - S_1^\varepsilon \right)^{-1} y_1^\varepsilon, \qquad \|y_1^\varepsilon\|_{L^2(\Omega_1)} = o(\varepsilon^\infty),$$

so that

$$\|\Theta_1 A^\varepsilon\|_{L^2(\Omega_1)} \leq \frac{\|y_1^\varepsilon\|_{L^2(\Omega_1)}}{\operatorname{dist}\left(\frac{\mu_1^\varepsilon}{\theta}, \sigma(S_1^\varepsilon)\right)}$$

and

$$\operatorname{dist}\left(\frac{\mu_1^\varepsilon}{\theta}, \sigma(S_1^\varepsilon)\right) \leq \frac{\|y_1^\varepsilon\|_{L^2(\Omega_1)}}{\|\Theta_1 A^\varepsilon\|_{L^2(\Omega_1)}} \leq \frac{\sqrt{|\Omega_1|}\|y_1^\varepsilon\|_{L^2(\Omega_1)}}{\|\Theta_1 A^\varepsilon\|_{L^1(\Omega_1)}}, \tag{4.1.32}$$

where we have used the Cauchy-Schwarz inequality in $L^2(\Omega_1)$.

To complete the proof of the lemma, we show that the quantity $\|\Theta_1 A^\varepsilon\|_{L^1(\Omega_1)}$ does not become too small when $\varepsilon \to 0$. To do so, recall the definition of the nonlinear operator T_1^ε:

$$T_1^\varepsilon(\varphi) = \frac{L_1^\varepsilon(\varphi)}{1 + \theta^{-1} \int_{\Omega_1} \beta_1(x)\varphi(x)\mathrm{d}x},$$

for all $\varphi \in L^1_+(\Omega_1)$. Then, it follows from Lemma 4.1.9 that

$$\limsup_{n\to\infty} \int_{\mathbb{R}^N} \beta_1(y) \left(T_1^\varepsilon\right)^n (\varphi)(y)\mathrm{d}y \geq \frac{\theta}{2} \left(r_\sigma(L_1^\varepsilon) - 1\right) > 0,$$

for $\varepsilon > 0$ sufficiently small and every $\varphi \in L^1_+(\mathbb{R}^N) \setminus \{0\}$. Moreover, we also have

$$A^\varepsilon(x) = (T^\varepsilon)^n(A^\varepsilon)(x) \geq (T_1^\varepsilon)^n(A^\varepsilon)(x)$$

for a.e. $x \in \mathbb{R}^N$ and every $n \in \mathbb{N} \setminus \{0\}$. We get for ε sufficiently small:

$$\begin{aligned}\|\beta_1\|_{L^\infty}\|\chi_{\Sigma_1}A^\varepsilon\|_{L^1(\mathbb{R}^N)} &\geq \int_{\mathbb{R}^N}\beta_1(y)A^\varepsilon(y)\mathrm{d}y \\ &\geq \limsup_{n\to\infty}\int_{\mathbb{R}^N}\beta_1(y)\left(T_1^\varepsilon\right)^n(A^\varepsilon)(y)\mathrm{d}y \geq \frac{\theta}{2}\left(r_\sigma(L_1^\varepsilon)-1\right).\end{aligned}$$

Next multiplying (4.1.22) by χ_{Σ_1} and integrating leads us to

$$\frac{\Lambda\xi_1}{\theta}\|\Theta_1\|_{L^\infty}\|\Theta_1A^\varepsilon\|_{L^1(\Omega_1)} \geq \frac{\mu_1^\varepsilon\|\chi_{\Sigma_1}A^\varepsilon\|_{L^1(\mathbb{R}^N)}}{\theta} - \frac{\Lambda\xi_2\mu_1^\varepsilon}{\theta\mu_2^\varepsilon}\iint_{\Omega_1\times\Omega_2} m_\varepsilon(x-y)\Psi_2(y)A^\varepsilon(y)\mathrm{d}y\mathrm{d}x,$$

while Lemma 4.1.11 ensures that

$$\iint_{\Omega_1\times\Omega_2} m_\varepsilon(x-y)\Psi_2(y)A^\varepsilon(y)\mathrm{d}y\mathrm{d}x = o(\varepsilon^\infty).$$

As a consequence there exist $\overline{\varepsilon} > 0$ and $\eta > 0$ such that

$$\|\Theta_1A^\varepsilon\|_{L^1(\Omega_1)} \geq \eta,\ \forall\varepsilon \in (0,\overline{\varepsilon}].$$

The latter estimate combined with (4.1.32) completes the proof of the lemma. □

As a corollary of the above lemma, we also have the following result.

Corollary 4.1.14. *Let $k \in \{1,2\}$ be such that $R_{0,k} > 1$. Then the following holds true for $\varepsilon > 0$ sufficiently small*

$$\frac{\mu_k^\varepsilon}{\theta} = \lambda_k^{\varepsilon,1} + o(\varepsilon^\infty). \tag{4.1.33}$$

Proof. Here we consider the case where $R_{0,1} > 1$. The case where $R_{0.2} > 1$ is obtained similarly.

In view of Lemma 4.1.13, we argue by contradiction and assume that there exist a sequence $\{\varepsilon_k\} \subset (0,\infty)$ going to 0 as $k \to \infty$ and a sequence $n_k \in \mathbb{N} \setminus \{0,1\}$ such that for all k one has

$$\frac{\mu_1^{\varepsilon_k}}{\theta} = \lambda_1^{\varepsilon_k,n_k} + o(\varepsilon_k^\infty).$$

Firstly we have

$$\frac{\mu_1^{\varepsilon_k}}{\theta} = \lambda_1^{\varepsilon_k,n_k} + o(\varepsilon_k^\infty) \leq \lambda_1^{\varepsilon_k,2} + o(\varepsilon_k^\infty), \qquad \forall k \geq 0.$$

Next using Assumption 4.1.4 one has $\lambda_1^{\varepsilon_k,1} - \lambda_1^{\varepsilon_k,2} \geq c\varepsilon_k^{n_1}$ for all k large enough, where $c > 0$ and $n_1 \in \mathbb{N}$ are given constants independent of k. This yields

$$\frac{\mu_1^{\varepsilon_k}}{\theta} - r_\sigma(L_1^\varepsilon) = \frac{\mu_1^{\varepsilon_k}}{\theta} - \lambda_1^{\varepsilon_k,1} \leq -c\varepsilon_k^{n_1} + o(\varepsilon_k^\infty),\ \forall k \gg 1.$$

This contradicts the estimate provided by Lemma 4.1.12 and Corollary 4.1.14 is proved. □

Our next lemma describes the asymptotic shape as $\varepsilon \to 0$ of the fixed points in the domain Ω_k, when $R_{0,k} > 1$.

Lemma 4.1.15. *Let $k \in \{1,2\}$ such that $R_{0,k} > 1$ and A^ε be a positive solution to $T^\varepsilon A^\varepsilon = A^\varepsilon$. Then, the following estimate holds for $\varepsilon > 0$ sufficiently small:*

$$\left\|A^\varepsilon - \nu_k^\varepsilon\phi_k^{\varepsilon,1}\right\|_{L^2(\Omega_k)} = o(\varepsilon^\infty), \tag{4.1.34}$$

where ν_k^ε is defined in (4.1.23).

Proof. Here we only deal with the case $R_{0,1} > 1$, the case $R_{0,2} > 1$ being similar.

We first remark that, by definition of Ψ_1 (see (4.1.6)), $\Omega_1 \subset \Sigma_1$ and $\Psi_1 = \Theta_1 = 0$ on $\Sigma_1 \setminus \Omega_1$. Observe that Corollary 4.1.14 together with (4.1.31) yields

$$\|(\lambda_1^{\varepsilon,1} I - S_1^\varepsilon)\Theta_1 A^\varepsilon\|_{L^2(\Omega_1)} = o(\varepsilon^\infty),\ \varepsilon \ll 1. \tag{4.1.35}$$

Let us denote by Π_1 the positive one-dimensional rank projection on $\mathrm{Ker}(\lambda_1^{\varepsilon,1} I - S_1^\varepsilon)$. Consider $\mathcal{C} = \mathcal{C}^\varepsilon$ a closed circle with center $\lambda_1^{\varepsilon,1}$ and the radius $\eta_1(\varepsilon)$ given by

$$\eta_1(\varepsilon) = \frac{1}{2}\left|\lambda_1^{\varepsilon,1} - \lambda_1^{\varepsilon,2}\right|,$$

so that the resolvent $(\lambda I - S_1^\varepsilon)^{-1}$ exists for every $\lambda \in \mathcal{C}$. Recalling the formula for spectral projectors [129, Theorem 1.5.4], we obtain for ε sufficiently small:

$$\begin{aligned}\Theta_1 A^\varepsilon - \Pi_1(\Theta_1 A^\varepsilon) &= \frac{1}{2i\pi}\oint_{\mathcal{C}} (\lambda - \lambda_1^{\varepsilon,1})^{-1}\mathrm{d}\lambda \Theta_1 A^\varepsilon - \frac{1}{2i\pi}\oint_{\mathcal{C}} (\lambda - S_1^\varepsilon)^{-1}\mathrm{d}\lambda \Theta_1 A^\varepsilon \\ &= \frac{1}{2i\pi}\oint_{\mathcal{C}} (\lambda - S_1^\varepsilon)^{-1}(\lambda - \lambda_1^{\varepsilon,1})^{-1}(S_1^\varepsilon - \lambda_1^{\varepsilon,1})\Theta_1 A^\varepsilon \mathrm{d}\lambda.\end{aligned}$$

As a consequence, since S_1^ε is self-adjoint, we obtain the following estimate:

$$\begin{aligned}\|\Theta_1 A^\varepsilon - \Pi_1(\Theta_1 A^\varepsilon)\|_{L^2(\Omega_1)} &\le \left(\frac{1}{\eta_1(\varepsilon)}\right)^2 \|(\lambda_1^{\varepsilon,1} - S_1^\varepsilon)(\Theta_1 A^\varepsilon)\|_{L^2(\Omega_1)} \\ &\le \left(\frac{2}{\left|\lambda_1^{\varepsilon,1} - \lambda_1^{\varepsilon,2}\right|}\right)^2 \|(\lambda_1^{\varepsilon,1} - S_1^\varepsilon)\Theta_1 A^\varepsilon\|_{L^2(\Omega_1)}.\end{aligned}$$

Now recall that the spectral gap $\lambda_1^{\varepsilon,1} - \lambda_1^{\varepsilon,2}$ is at most polynomial (see Assumption 4.1.4), so that (4.1.35) leads us to the following estimate

$$\|\Theta_1 A^\varepsilon - \Pi_1(\Theta_1 A^\varepsilon)\|_{L^2(\Omega_1)} = o(\varepsilon^\infty),\ \varepsilon \ll 1. \tag{4.1.36}$$

We remind that $(\lambda_1^{\varepsilon,1}, \phi_1^{\varepsilon,1})$ is the principal eigenpair of L_1^ε. Hence $(\lambda_1^{\varepsilon,1}, \Theta_1\phi_1^{\varepsilon,1})$ becomes the principal eigenpair of S_1^ε and the spectral projector Π_1 is given by

$$\Pi_1(\varphi) = \|\Theta_1\phi_1^{\varepsilon,1}\|_{L^2(\Omega_1)}^{-2}\Theta_1\phi_1^{\varepsilon,1}\left(\int_{\Omega_1}\Theta_1(x)\phi_1^{\varepsilon,1}(x)\varphi(x)\mathrm{d}x\right).$$

Since $\Theta_1 = 0$ on $\Sigma_1 \setminus \Omega_1$, (4.1.36) becomes

$$\|\Theta_1 A^\varepsilon - \alpha_1^\varepsilon \nu_1^\varepsilon \Theta_1 \phi_1^{\varepsilon,1}\|_{L^2(\Omega_1)} = o(\varepsilon^\infty) \tag{4.1.37}$$

for some constant $\alpha_1^\varepsilon > 0$, that will be investigated below.

Note now that since A^ε is uniformly bounded in $L^1(\mathbb{R}^N)$, then (4.1.22) together with Lemma 4.1.11 (b) yield

$$\chi_{\Omega_1}\left(\theta + \int_{\mathbb{R}^N}\beta_1(z)A^\varepsilon(z)\mathrm{d}z\right)A^\varepsilon = \Lambda\xi_1\chi_{\Omega_1}(m_\varepsilon \star (\Psi_1 A^\varepsilon)) + o(\varepsilon^\infty),\ \forall\varepsilon \ll 1.$$

Next we deduce from the above equality that, for ε sufficiently small,

$$\begin{aligned}&\left\|\left(\theta + \int_{\mathbb{R}^N}\beta_1(z)A^\varepsilon(z)\mathrm{d}z\right)A^\varepsilon - \Lambda\xi_1\left(m_\varepsilon \star (\Psi_1\alpha_1^\varepsilon\nu_1^\varepsilon\phi_1^{\varepsilon,1})\right)\right\|_{L^2(\Omega_1)} \\ &\qquad \le \left\|\Lambda\xi_1\left(m_\varepsilon \star (\Psi_1 A^\varepsilon - \Psi_1\alpha_1^\varepsilon\nu_1^\varepsilon\phi_1^{\varepsilon,1})\right)\right\|_{L^2(\Omega_1)} + o(\varepsilon^\infty) \\ &\qquad \le \Lambda\xi_1\|m_\varepsilon\|_{L^1(\mathbb{R}^N)}\|\Theta_1\|_{L^\infty}\left\|\Theta_1 A^\varepsilon - \alpha_1^\varepsilon\nu_1^\varepsilon\Theta_1\phi_1^{\varepsilon,1}\right\|_{L^2(\Omega_1)}^2 + o(\varepsilon^\infty),\end{aligned}$$

so that (4.1.37) implies that

$$\left\| \left(\theta + \int_{\mathbb{R}^N} \beta_1(z) A^\varepsilon(z) \mathrm{d}z \right) A^\varepsilon - \Lambda \xi_1 \left(m_\varepsilon \star (\Psi_1 \alpha_1^\varepsilon \nu_1^\varepsilon \phi_1^{\varepsilon,1}) \right) \right\|_{L^2(\Omega_1)} = o(\varepsilon^\infty). \tag{4.1.38}$$

The above equality also rewrites as follows

$$\begin{aligned} &\left\| \left(\theta + \int_{\mathbb{R}^N} \beta_1(z) A^\varepsilon(z) \mathrm{d}z \right) A^\varepsilon - \alpha_1^\varepsilon \nu_1^\varepsilon \theta L_1^\varepsilon(\phi_1^{\varepsilon,1}) \right\|_{L^2(\Omega_1)} \\ &\qquad = \left\| \left(\theta + \int_{\mathbb{R}^N} \beta_1(z) A^\varepsilon(z) \mathrm{d}z \right) A^\varepsilon - \alpha_1^\varepsilon \nu_1^\varepsilon \theta \lambda_1^{\varepsilon,1} \phi_1^{\varepsilon,1} \right\|_{L^2(\Omega_1)} = o(\varepsilon^\infty). \end{aligned} \tag{4.1.39}$$

On the other hand we deduce from (4.1.27) and (4.1.33) that

$$\theta \lambda_1^{\varepsilon,1} = \theta + \int_{\mathbb{R}^N} \beta_1(z) A^\varepsilon(z) \mathrm{d}z + o(\varepsilon^\infty), \tag{4.1.40}$$

so that (4.1.39) becomes

$$\left\| \theta \lambda_1^{\varepsilon,1} A^\varepsilon - \theta \lambda_1^{\varepsilon,1} \alpha_1^\varepsilon \nu_1^\varepsilon \phi_1^\varepsilon \right\|_{L^2(\Omega_1)} = o(\varepsilon^\infty).$$

Since $\lambda_1^{\varepsilon,1} \to R_{0,1} > 1$ as $\varepsilon \to 0$, the above estimate rewrites as

$$\| A^\varepsilon - \alpha_1^\varepsilon \nu_1^\varepsilon \phi_1^{\varepsilon,1} \|_{L^2(\Omega_1)} = o(\varepsilon^\infty), \ \forall \varepsilon \ll 1. \tag{4.1.41}$$

To complete the proof of the lemma, it remains to show that α_1^ε is close to 1 when $\varepsilon \to 0$. In the following we check that $\alpha_1^\varepsilon = 1 + o(\varepsilon^\infty)$ as $\varepsilon \to 0$.

To do so, combining (4.1.40) with the definition of ν_1^ε in (4.1.23), that also rewrites as $\int_{\mathbb{R}^N} \beta_1(z) \nu_1^\varepsilon \phi_1^{\varepsilon,1}(z) \mathrm{d}z = \theta(\lambda_1^{\varepsilon,1} - 1)$, we obtain

$$\theta(1 - \alpha_1^\varepsilon)(\lambda_1^{\varepsilon,1} - 1) = \int_{\mathbb{R}^N} \beta_1(z) \left(A^\varepsilon(z) - \alpha_1^\varepsilon \nu_1^\varepsilon \phi_1^{\varepsilon,1}(z) \right) \mathrm{d}z + o(\varepsilon^\infty).$$

Since $\lambda_1^{\varepsilon,1} - 1 \to R_{0,1} - 1 > 0$ as $\varepsilon \to 0$, we obtain

$$1 - \alpha_1^\varepsilon = o(\varepsilon^\infty) \text{ as } \varepsilon \to 0$$

which completes the proof of the Lemma. □

Equipped with the above lemmas we are now in the position to complete the proof of Theorem 4.1.5.

Proof of Theorem 4.1.5. We split our argument into two parts. We first consider the case where $R_{0,1} > 1$ and $R_{0,2} > 1$ and show that the result directly follows from Lemma 4.1.15. In a second step we investigate the case where $R_{0,1} > 1$ and $R_{0,2} \leq 1$. Using the symmetry of the problem with respect to the indices, this covers all the possible cases.

First case: We suppose that $R_{0,1} > 1$ and $R_{0,2} > 1$. In this case, Lemma 4.1.15 applies and ensures that

$$\| A^\varepsilon{}_{|\Omega_k} - \nu_k^\varepsilon \phi_k^{\varepsilon,1}{}_{|\Omega_k} \|_{L^2(\Omega_k)} = o(\varepsilon^\infty), \ \forall \varepsilon \ll 1 \tag{4.1.42}$$

for each $k \in \{1, 2\}$. Moreover, since A^ε is a fixed point of T^ε, we have

$$A^\varepsilon(x) = \Lambda \int_{\mathbb{R}^N} m_\varepsilon(x - y) \left(\frac{\xi_1 \Psi_1(y)}{\theta + \int_{\mathbb{R}^N} \beta_1(s) A^\varepsilon(s) \mathrm{d}s} + \frac{\xi_2 \Psi_2(y)}{\theta + \int_{\mathbb{R}^N} \beta_2(s) A^\varepsilon(s) \mathrm{d}s} \right) A^\varepsilon(y) \mathrm{d}y \tag{4.1.43}$$

for every $x \in \mathbb{R}^N$. It follows from (4.1.26) that

$$\nu_k^\varepsilon \phi_k^{\varepsilon,1}(x) = \frac{\Lambda}{\theta \lambda_k^{\varepsilon,1}} \int_{\Omega_k} m_\varepsilon(x - y) \xi_k \Psi_k(y) \nu_k^\varepsilon \phi_k^{\varepsilon,1}(y) \mathrm{d}y$$

for each $k \in \{1,2\}$, where we recall that $\Omega_k = \{\Psi_k > 0\}$ and $\Omega = \Omega_1 \sqcup \Omega_2$. Injecting the latter equation into (4.1.43) leads to

$$\int_{\mathbb{R}^N\setminus\Omega} \left| A^\varepsilon - \nu_1^\varepsilon \phi_1^{\varepsilon,1} - \nu_2^\varepsilon \phi_2^{\varepsilon,1} \right| (x)\mathrm{d}x$$
$$\leq \sum_{k=1,2} \frac{\Lambda}{\theta\lambda_k^{\varepsilon,1}} \int_{\mathbb{R}^N\setminus\Omega} \int_{\mathbb{R}^N} m_\varepsilon(x-y)\xi_k\Psi_k(y) \left| \left(\frac{\theta\lambda_k^{\varepsilon,1} A^\varepsilon(y)}{\theta + \int_{\mathbb{R}^N} \beta_k(s)A^\varepsilon(s)\mathrm{d}s} \right) - \nu^\varepsilon \phi_k^{\varepsilon,1}(y) \right| \mathrm{d}y\mathrm{d}x.$$

We then infer from (4.1.40) that

$$\frac{\theta\lambda_k^{\varepsilon,1}}{\theta + \int_{\mathbb{R}^N} \beta_k(s)A^\varepsilon(s)\mathrm{d}s} = 1 + o(\varepsilon^\infty) \text{ for each } k \in \{1,2\}.$$

Recalling that $\lambda_k^{\varepsilon,1} \to R_{0,k} > 1$ as $\varepsilon \to 0$, and that the family $\{A^\varepsilon\}_{\varepsilon>0}$ is uniformly bounded in $L^1(\mathbb{R}^N)$ (see Theorem 4.1.2), one deduces that

$$\int_{\mathbb{R}^N\setminus\Omega} \left| A^\varepsilon - \nu_1^\varepsilon \phi_1^{\varepsilon,1} - \nu_2^\varepsilon \phi_2^{\varepsilon,1} \right| (x)\mathrm{d}x \leq \frac{\Lambda}{M\theta} \sum_{k=1,2} \|\Psi_k\|_{L^\infty} \|A^\varepsilon{}_{|\Omega_k} - \nu_k^\varepsilon \phi_k^{\varepsilon,1}{}_{|\Omega_k}\|_{L^1(\Omega_k)} + o(\varepsilon^\infty) = o(\varepsilon^\infty)$$

for some constant $M > 0$. Here we have used (4.1.42).

Finally, since $\|\chi_{\Omega_1}\phi_2^{\varepsilon,1}\|_{L^1(\mathbb{R}^N)} = o(\varepsilon^\infty)$ and $\|\chi_{\Omega_2}\phi_1^{\varepsilon,1}\|_{L^1(\mathbb{R}^N)} = o(\varepsilon^\infty)$, we obtain

$$\|A^\varepsilon - (\nu_1^\varepsilon \phi_1^{\varepsilon,1} + \nu_2^\varepsilon \phi_2^{\varepsilon,1})\|_{L^1(\mathbb{R}^N)} = o(\varepsilon^\infty),$$

that proves the result in the case where $R_{0,1} > 1$ and $R_{0,2} > 1$.

Second case: We assume now that $R_{0,1} > 1$ and $R_{0,2} \leq 1$. Note that Lemma 4.1.15 applies and ensures that (4.1.42) holds for A_1^ε. From Lemma 4.1.11 (b) and (4.1.43), we get

$$\int_{\Omega_2} A^\varepsilon(x)\mathrm{d}x = \frac{\Lambda\xi_2}{\theta + \int_{\mathbb{R}^N} \beta_2(s)A^\varepsilon(s)\mathrm{d}s} \int_{\Omega_2}\int_{\Omega_2} m_\varepsilon(x-y)\Psi_2(y)A^\varepsilon(y)\mathrm{d}y\mathrm{d}x + o(\varepsilon^\infty) \tag{4.1.44}$$
$$\leq \frac{\theta R_{0,2} \int_{\Omega_2} A^\varepsilon(y)\mathrm{d}y}{\theta + \int_{\mathbb{R}^N} \beta_2(s)A^\varepsilon(s)\mathrm{d}s} + o(\varepsilon^\infty).$$

It follows that

$$\left(1 - \frac{\theta R_{0,2}}{\theta + \|\beta_2 A^\varepsilon\|_{L^1(\mathbb{R}^N)}}\right) \int_{\Omega_2} A^\varepsilon(x)\mathrm{d}x = o(\varepsilon^\infty). \tag{4.1.45}$$

Now we prove that the following estimate holds

$$\int_{\Omega_2} A^\varepsilon(x)\mathrm{d}x = o(\varepsilon^\infty) \tag{4.1.46}$$

When $R_{0,2} < 1$, (4.1.45) implies:

$$(1 - R_{0,2}) \int_{\Omega_2} A^\varepsilon(x)\mathrm{d}x \leq \left(1 - \frac{R_{0,2}}{1 + \theta^{-1}\int_{\mathbb{R}^N} \beta_2(z)A_2^\varepsilon(z)\mathrm{d}z}\right) \int_{\Omega_2} A^\varepsilon(x)\mathrm{d}x = o(\varepsilon^\infty)$$

hence (4.1.46) holds.

Now suppose that $R_{0,2} = 1$. From (4.1.45), we see that

$$\frac{\left(\int_{\Omega_2} \beta_2(x)A^\varepsilon(x)\mathrm{d}x\right)^2}{\|\beta_2\|_{L^\infty}\left(\theta + M\|\beta_2\|_{L^\infty}\right)} \leq \frac{\int_{\mathbb{R}^N} \beta_2(x)A^\varepsilon(x)\mathrm{d}x \int_{\Omega_2} A^\varepsilon(x)\mathrm{d}x}{\theta + \|\beta_2 A^\varepsilon\|_{L^1(\mathbb{R}^N)}} = o(\varepsilon^\infty)$$

for some constant $M > 0$ such that $\|A^\varepsilon\|_{L^1(\mathbb{R}^N)} \leq M$ for all ε small. Therefore, we have

$$\int_{\Omega_2} \beta_2(x)A^\varepsilon(x)\mathrm{d}x = o(\varepsilon^\infty). \tag{4.1.47}$$

Next (4.1.44) allows us to control the quantity $\int_{\Omega_2} A^\varepsilon(z)\mathrm{d}z$ by $\int_{\Omega_2} \beta_2(z)A^\varepsilon(z)\mathrm{d}z$ as follows

$$\int_{\Omega_2} A^\varepsilon(x)\mathrm{d}x \leq \frac{\Lambda\xi_2\|r_2\|_{L^\infty}}{\delta\theta}\int_{\Omega_2}\beta_2(x)A^\varepsilon(x)\mathrm{d}x + o(\varepsilon^\infty)$$

and therefore (4.1.46) holds.

To complete the proof of the theorem, it remains to show that

$$\int_{\mathbb{R}^N\setminus\Omega}\left|A^\varepsilon(z) - \nu_1^\varepsilon\phi_1^{\varepsilon,1}(z)\right|\mathrm{d}z = o(\varepsilon^\infty).$$

To this end, we follow the proof of the first case to obtain

$$\begin{aligned}\int_{\mathbb{R}^N\setminus\Omega}\left|A^\varepsilon - \nu_1^\varepsilon\phi_1^{\varepsilon,1}\right|(x)\mathrm{d}x &\leq \frac{\Lambda\xi_2}{\theta+\int_{\mathbb{R}^N}\beta_2(x)A^\varepsilon(x)dx}\|\Psi_2\|_{L^\infty}\int_{\Omega_2}A^\varepsilon(x)dx\\ &+\frac{\Lambda}{\theta\lambda_1^{\varepsilon,1}}\int_{\mathbb{R}^N\setminus\Omega}\int_{\mathbb{R}^N} m_\varepsilon(x-y)\xi_1\Psi_1(y)\left|\left(\frac{\theta\lambda_1^{\varepsilon,1}A^\varepsilon(y)}{\theta+\int_{\mathbb{R}^N}\beta_1(s)A^\varepsilon(s)\mathrm{d}s}\right)-\nu^\varepsilon\phi_1^{\varepsilon,1}(y)\right|\mathrm{d}y\mathrm{d}x.\end{aligned}$$

From (4.1.46), we deduce that

$$\int_{\mathbb{R}^N\setminus\Omega}\left|A^\varepsilon - \nu_1^\varepsilon\phi_1^{\varepsilon,1}\right|(x)\mathrm{d}x \leq \frac{\Lambda}{\theta}\|\Psi_1\|_{L^\infty}\|A^\varepsilon - \nu_1^\varepsilon\phi_1^{\varepsilon,1}\|_{L^1(\Omega_1)} + o(\varepsilon^\infty) = o(\varepsilon^\infty),$$

by using the fact that (4.1.42) holds for A_1^ε, this concludes the proof of this second case and thus the proof of Theorem 4.1.5. □

4.1.5 Proof of Theorem 4.1.8

In this section 4.1.5 we handle the uniqueness of the endemic steady state for ε sufficiently small and we prove Theorem 4.1.8. To this end, we use degree theory (see *e.g.* [81, 413]).

Our strategy is as follows: we first derive estimates for the eigenvalues of the linearised equation around each stationary solution for all $\varepsilon > 0$ small enough. In particular we show that every positive stationary solution is locally stable for the discrete dynamical system generated by T^ε. Next, we compute the Leray-Schauder degree of the (nonlinear) operator in a subset of the positive cone which contains all the positive fixed point, and show that it is equal to one. Because of the additivity property of the Leray-Schauder degree, these two arguments combined together show that there cannot be more than one stationary solution.

Recall that $T^\varepsilon = T_1^\varepsilon + T_2^\varepsilon$ (see the definitions (4.1.4) and (4.1.7)). In this section 4.1.5, in order to work in a solid cone of a Banach space, we will be mainly interested in some properties of T^ε, T_1^ε and T_2^ε considered as operators acting on $\mathcal{C}(\Sigma)$, $\mathcal{C}(\Sigma_1)$ and $\mathcal{C}(\Sigma_2)$, where, according to Assumption 4.1.3, Σ_1 and Σ_2 are defined in (4.1.10) while Σ denote the compact set given by

$$\Sigma = \Sigma_1 \sqcup \Sigma_2.$$

Recall also that $\Omega_k = \{\Psi_k > 0\}$ and $\Omega = \Omega_1 \sqcup \Omega_2$. And note that due to the definition of Ψ_k in (4.1.6) one has $\Omega \subset \Sigma$ and $\Omega_k \subset \Sigma_k$ for each $k \in \{1,2\}$.

We will use the fact that the fixed-points of T^ε are close to the fixed-point of the uncoupled problem

$$A^{\varepsilon,*} := A_1^{\varepsilon,*} + A_2^{\varepsilon,*}, \tag{4.1.48}$$

where for each $k = 1,2$, $A_k^{\varepsilon,*} \in L^1(\mathbb{R}^N)\cap\mathcal{C}(\mathbb{R}^N)$ is the unique nontrivial solution of $T_k^\varepsilon A_k^{\varepsilon,*} = A_k^{\varepsilon,*}$ if $R_{0,k} > 1$ and $A_k^{\varepsilon,*} \equiv 0$ otherwise.

Recall finally that the spectra of L_1^ε and L_2^ε, considered as bounded operators on $L^p(\Omega_k)$, $L^p(\mathbb{R}^N)$ with $1 \leq p < \infty$, or $\mathcal{C}(\Sigma_k)$, consist in a real sequence of decreasing eigenvalues, independent of the space considered (see Lemma 4.1.21), which we denote

$$\sigma(L_k^\varepsilon) = \{\lambda_k^{\varepsilon,n}, n \geq 1\}, \quad k = 1,2.$$

Lemma 4.1.16 (Computation of the spectrum)**.** *Assume that $R_{0,1} > 1$ and that one of the following properties is satisfied:*

- *either* $R_{0,2} \neq 1$,
- *or* $R_{0,2} = 1$ *and the convergence of* $r_\sigma(L_2^\varepsilon)$ *is at most polynomial for small* ε, *namely* $r_\sigma(L_2^\varepsilon) \leq 1 - C\varepsilon^M$ *for some constants* $C > 0$ *and* $M > 0$.

Then, there exists $\varepsilon_0 > 0$ *such that for any* $0 < \varepsilon \leq \varepsilon_0$ *and for any nonnegative nontrivial fixed point* $A^\varepsilon \in \mathcal{C}(\Sigma)$ *of* T^ε, *we have*

$$\sigma(D_{A^\varepsilon} T^\varepsilon) \subset (-1, 1),$$

wherein $D_{A^\varepsilon} T^\varepsilon$ *denotes the Fréchet derivative of* T^ε *with respect to the* $\mathcal{C}(\Sigma)-$*topology.*

Proof. We divide the proof into three steps.

Step one: We show that

$$\sigma(D_{A_k^{\varepsilon,*}} T_k^\varepsilon) = \{0\} \cup \left\{ \frac{\lambda_k^{\varepsilon,n}}{\lambda_k^{\varepsilon,1}} \right\}_{n \geq 2} \cup \left\{ \frac{1}{\lambda_k^{\varepsilon,1}} \right\}, \qquad \forall k \in \{1, 2\},$$

if $R_{0,k} > 1$, and

$$\sigma(D_{A_k^{\varepsilon,*}} T_k^\varepsilon) = \sigma(L_k^\varepsilon) = \{0\} \cup \{\lambda_k^{\varepsilon,n}\}_{n \geq 1}$$

otherwise, where $A_k^{\varepsilon,*}$ is the solution to the uncoupled problem $T_k^\varepsilon A_k^{\varepsilon,*} = A_k^{\varepsilon,*}$ while $D_{A_k^{\varepsilon,*}} T_k^\varepsilon$ is the Fréchet differential of T_k^ε for the $\mathcal{C}(\Sigma_k)$ topology.

Let us consider the case $R_{0,k} > 1$. We first recall that T_k^ε is compact as $0 \leq T_k^\varepsilon \leq L_k^\varepsilon$ and as L_k^ε is compact by Lemma 4.1.21, then its Fréchet differential is also compact and its spectrum is consequently identical to its point spectrum. Let $k \in \{1, 2\}$ be given and let $L^2_{\Psi_k}(\Omega_k)$ be the weighted L^2 space defined by the inner product $\langle f, g \rangle_{\Psi_k} := \int_{\Omega_k} f(z) g(z) \Psi_k(z) \mathrm{d}z$. Since $L^\varepsilon_{k|L^2_{\Psi_k}(\Omega_k)}$ is self-adjoint in the space $L^2_{\Psi_k}(\Omega_k)$, there exists an Hilbert basis of $L^2_{\Psi_k}(\Omega_k)$ composed of eigenfunctions of the operator $L^\varepsilon_{k|L^2_{\Psi_k}(\Omega_k)}$, which we denote $\{\phi_k^{\varepsilon,n}\}_{n \geq 1}$, and related to the sequence of eigenvalues $\{\lambda_k^{\varepsilon,n}\}_{n \geq 1}$. Observe that

$$\forall f \in \mathcal{C}(\Sigma_k) : f_{|\Omega_k} \in L^2_{\Psi_k}(\Omega_k)$$

since $\Psi_k \in L^\infty(\mathbb{R}^N)$ and Σ_k is compact. Observe also that, contrary to the previous sections, here $\phi_k^{\varepsilon,1}$ is not normalized in $L^1(\mathbb{R}^N)$ but in $L^2_{\Psi_k}(\Omega_k)$, namely $\|\phi_k^{\varepsilon,1}\|_{L^2_{\Psi_k}(\Omega_k)} = 1$.

Moreover, every $\phi_k^{\varepsilon,n}$ can be extended to a function in $L^1(\mathbb{R}^N) \cap \mathcal{C}(\mathbb{R}^N)$ by the identity:

$$\phi_k^{\varepsilon,n}(x) := \frac{1}{\lambda_k^{\varepsilon,n}} \int_{\Omega_k} m_\varepsilon(x - y) \Psi_k(y) \phi_k^{\varepsilon,n}(y) \mathrm{d}y, \quad x \in \mathbb{R}^N \setminus \Omega_k.$$

Let $h \in \mathcal{C}(\Sigma_k)$ be given. Then we have

$$D_{A_k^{\varepsilon,*}} T_k^\varepsilon h = \frac{L_k^\varepsilon h}{1 + \theta^{-1} \int_{\mathbb{R}^N} \beta_k(y) A_k^{\varepsilon,*}(y) \mathrm{d}y} - \frac{L_k^\varepsilon A_k^{\varepsilon,*}}{\left(1 + \theta^{-1} \int_{\mathbb{R}^N} \beta_k(y) A_k^{\varepsilon,*}(y) \mathrm{d}y\right)^2} \frac{\int_{\mathbb{R}^N} \beta_k(y) h(y) \mathrm{d}y}{\theta}.$$

Let us write $h^n := \langle h, \phi_k^{\varepsilon,n} \rangle_{\Psi_k}$. Recalling that $1 + \theta^{-1} \int_{\mathbb{R}^N} \beta_k(z) A_k^{\varepsilon,*}(z) \mathrm{d}z = \lambda_k^{\varepsilon,1}$ and that $A_k^{\varepsilon,*} = \theta \frac{\lambda_k^{\varepsilon,1} - 1}{\int_{\mathbb{R}^N} \beta_k(z) \phi_k^{\varepsilon,1}(z) \mathrm{d}z} \phi_k^{\varepsilon,1}$, we compute

$$\begin{aligned}
\langle D_{A_k^{\varepsilon,*}} T_k^\varepsilon h, \phi_k^{\varepsilon,n} \rangle_{\Psi_k} &= \begin{cases} \dfrac{h^1 \lambda_k^{\varepsilon,1} - \dfrac{\lambda_k^{\varepsilon,1} \langle A_k^{\varepsilon,*}, \phi_k^{\varepsilon,1} \rangle_{\Psi_k}}{1 + \theta^{-1} \int_{\mathbb{R}^N} \beta_k(y) A_k^{\varepsilon,*}(y) \mathrm{d}y} \int_{\mathbb{R}^N} \dfrac{\beta_k(y)}{\theta} h(y) \mathrm{d}y}{1 + \theta^{-1} \int_{\mathbb{R}^N} \beta_k(y) A_k^{\varepsilon,*}(y) \mathrm{d}y}, & \text{if } n = 1, \\ \dfrac{h^n \lambda_k^{\varepsilon,n}}{1 + \theta^{-1} \int_{\mathbb{R}^N} \beta_k(y) A_k^{\varepsilon,*}(y) \mathrm{d}y}, & \text{otherwise,} \end{cases} \\
&= \begin{cases} h^1 - \dfrac{\lambda_k^{\varepsilon,1} - 1}{\lambda_k^{\varepsilon,1}} \dfrac{\int_{\mathbb{R}^N} \beta_k(y) h(y) \mathrm{d}y}{\int_{\mathbb{R}^N} \beta_k(z) \phi_k^{\varepsilon,1}(z) \mathrm{d}z}, & \text{if } n = 1, \\ \dfrac{\lambda_k^{\varepsilon,n}}{\lambda_k^{\varepsilon,1}} h^n, & \text{otherwise.} \end{cases}
\end{aligned} \tag{4.1.49}$$

We deduce that $\phi_k^{\varepsilon,1}$ is an eigenvector of $D_{A_k^{\varepsilon,*}}T_k^\varepsilon$ associated with the eigenvalue $\frac{1}{\lambda_k^{\varepsilon,1}}$, and that every function

$$\tilde{\phi}_k^{\varepsilon,n} := \phi_k^{\varepsilon,1} + \left(\frac{1-\lambda_k^{\varepsilon,n}}{\lambda_k^{\varepsilon,1}-1}\right)\frac{\int_{\mathbb{R}^N}\beta_k(z)\phi_k^{\varepsilon,1}(z)\mathrm{d}z}{\int_{\mathbb{R}^N}\beta_k(z)\phi_k^{\varepsilon,n}(z)\mathrm{d}z}\phi_k^{\varepsilon,n}$$

is an eigenvector of $D_{A_k^{\varepsilon,*}}T_k^\varepsilon$ associated with the eigenvalue $\frac{\lambda_k^{\varepsilon,n}}{\lambda_k^{\varepsilon,1}}$. Thus:

$$\sigma(D_{A_k^{\varepsilon,*}}T_k^\varepsilon) \supset \{0\} \cup \left\{\frac{\lambda_k^{\varepsilon,n}}{\lambda_k^{\varepsilon,1}}\right\}_{n\geq 2} \cup \left\{\frac{1}{\lambda_k^{\varepsilon,1}}\right\}$$

Conversely let $\lambda \in \sigma(D_{A_k^{\varepsilon,*}}T_k^\varepsilon)\setminus\{0\}$ be given and $h \in \mathcal{C}(\Sigma_k)\setminus\{0\}$ be an associated eigenfunction. If $\operatorname{supp} h \subset \Sigma_k \setminus \Omega_k$ then

$$\lambda h = -\frac{\lambda_k^{\varepsilon,1}-1}{\lambda_k^{\varepsilon,1}}\frac{\int_{\mathbb{R}^N}\beta_k(y)h(y)\mathrm{d}y}{\int_{\mathbb{R}^N}\beta_k(z)\phi_k^{\varepsilon,1}(z)\mathrm{d}z}\phi_k^{\varepsilon,1},$$

which implies $h = \phi_k^{\varepsilon,1}$ (up to the multiplication by a nonzero scalar), and this is a contradiction. Therefore $\operatorname{supp} h \cap \Omega_k \neq \varnothing$. Then, taking the scalar product with $\phi_k^{\varepsilon,n}$ one finds that (4.1.49) still holds. In particular, λ is either one of the $\frac{\lambda_k^{\varepsilon,n}}{\lambda_k^{\varepsilon,1}}$ or $\frac{1}{\lambda_k^{\varepsilon,1}}$. We have shown:

$$\sigma(D_{A_k^{\varepsilon,*}}T_k^\varepsilon) \subset \{0\} \cup \left\{\frac{\lambda_k^{\varepsilon,n}}{\lambda_k^{\varepsilon,1}}\right\}_{n\geq 2} \cup \left\{\frac{1}{\lambda_k^{\varepsilon,1}}\right\},$$

hence the equality holds.

If now $R_{0,1} \leq 1$, we have $A_k^{\varepsilon,*} \equiv 0$ and therefore $D_{A_k^{\varepsilon,*}}T_k^\varepsilon = L_k^\varepsilon$. Then

$$\sigma(D_{A_k^{\varepsilon,*}}T_k^\varepsilon) = \sigma(L_k^\varepsilon) = \{0\} \cup \{\lambda_k^{\varepsilon,n}\}_{n\geq 1}.$$

Since $\lambda_k^{\varepsilon,n} < \lambda_k^{\varepsilon,1}$ for any $k \in \{1,2\}$ and $n \geq 2$, we deduce that whenever $R_{0,k} \neq 1$, there exists $\varepsilon_0 > 0$ such that for every $\varepsilon \in (0,\varepsilon_0]$, we have:

$$\sigma\left(D_{A_k^{\varepsilon,*}}T_k^\varepsilon\right) \subset [0,1). \tag{4.1.50}$$

If $R_{0,k} = 1$, then (4.1.50) holds because of our assumption that $\lambda_k^{\varepsilon,1} \leq 1 - C\varepsilon^M$.

Step two: For each $\varepsilon > 0$, let $\lambda^\varepsilon \in \sigma(D_{A^\varepsilon}T^\varepsilon)\setminus\{0\}$ be given and consider a bounded family of associated eigenvectors $h^\varepsilon \in \mathcal{C}(\Sigma)$. We prove that

$$\sup_{\Sigma_k}\left|(D_{A_k^{\varepsilon,*}}T_k^\varepsilon - \lambda^\varepsilon I)h_k^\varepsilon\right| = o(\varepsilon^\infty), \quad k = 1,2, \tag{4.1.51}$$

for $\varepsilon > 0$ sufficiently small, wherein we have set $h_1^\varepsilon := \chi_{\Sigma_1}h^\varepsilon$ and $h_2^\varepsilon := \chi_{\Sigma_2}h^\varepsilon$.

Let us show the property for $k = 1$. The case $k = 2$ is similar. We rewrite the identity $\chi_{\Sigma_1}D_{A^\varepsilon}T^\varepsilon h^\varepsilon = \lambda^\varepsilon h_1^\varepsilon$ as follows

$$(D_{A_1^{\varepsilon,*}}T_1^\varepsilon - \lambda^\varepsilon I)h_1^\varepsilon = (D_{A_1^{\varepsilon,*}}T_1^\varepsilon h_1^\varepsilon - D_{A_1^\varepsilon}T_1^\varepsilon h_1^\varepsilon) - D_{A_2^\varepsilon}T_2^\varepsilon h_2^\varepsilon \quad \text{in } \Sigma_1. \tag{4.1.52}$$

Our next task is to show that the right-hand side of the previous equation has order $o(\varepsilon^\infty)$. We first remark that, by Lemma 4.1.11, we have

$$\sup_{x\in\Sigma_1}\left|D_{A_2^\varepsilon}T_2^\varepsilon h_2^\varepsilon(x)\right| = o(\varepsilon^\infty). \tag{4.1.53}$$

Next we claim that, for $k \in \{1,2\}$, one has

$$\sup_{\Sigma_k}\left|D_{A_1^\varepsilon}T_1^\varepsilon h_1^\varepsilon - D_{A_1^{\varepsilon,*}}T_1^\varepsilon h_1^\varepsilon\right| = o(\varepsilon^\infty). \tag{4.1.54}$$

Indeed, we have

$$\begin{aligned} D_{A_1^\varepsilon}T_1^\varepsilon h_1^\varepsilon - D_{A_1^{\varepsilon,*}}T_1^\varepsilon h_1^\varepsilon &= \left(\frac{1}{1+\theta^{-1}\int_{\mathbb{R}^N}\beta_1(y)A_1^\varepsilon(y)\mathrm{d}y} - \frac{1}{1+\theta^{-1}\int_{\mathbb{R}^N}\beta_1(y)A_1^{\varepsilon,*}(y)\mathrm{d}y}\right)L_1^\varepsilon h_1^\varepsilon \\ &\quad - \left(\frac{L_1^\varepsilon A_1^\varepsilon}{\left(1+\theta^{-1}\int_{\mathbb{R}^N}\beta_1(y)A_1^\varepsilon(y)\mathrm{d}y\right)^2} - \frac{L_1^\varepsilon A_1^{\varepsilon,*}}{\left(1+\theta^{-1}\int_{\mathbb{R}^N}\beta_1(y)A_1^{\varepsilon,*}(y)\mathrm{d}y\right)^2}\right)\int_{\mathbb{R}^N}\frac{\beta_1(y)}{\theta}h_1^\varepsilon(y)\mathrm{d}y. \end{aligned} \tag{4.1.55}$$

On the one hand, using Theorem 4.1.5, we have

$$\left|\frac{1}{1+\theta^{-1}\int_{\mathbb{R}^N}\beta_1(y)A_1^\varepsilon(y)\mathrm{d}y}-\frac{1}{1+\theta^{-1}\int_{\mathbb{R}^N}\beta_1(y)A_1^{\varepsilon,*}(y)\mathrm{d}y}\right|\leq\frac{\|\beta_1\|_{L^\infty}}{\theta^2}\|A_1^\varepsilon-A_1^{\varepsilon,*}\|_{L^1(\Sigma_1)}=o(\varepsilon^\infty),$$

which settles the first term on the right-hand side of (4.1.55). On the other hand, we also have

$$\begin{aligned}\frac{L_1^\varepsilon A_1^\varepsilon}{\left(1+\theta^{-1}\int_{\mathbb{R}^N}\beta_1(y)A_1^\varepsilon(y)\mathrm{d}y\right)^2}-\frac{L_1^\varepsilon A_1^{\varepsilon,*}}{\left(1+\theta^{-1}\int_{\mathbb{R}^N}\beta_1(y)A_1^{\varepsilon,*}(y)\mathrm{d}y\right)^2}&=\frac{L_1^\varepsilon(A_1^\varepsilon-A_1^{\varepsilon,*})}{\left(1+\theta^{-1}\int_{\mathbb{R}^N}\beta_1(y)A_1^\varepsilon(y)\mathrm{d}y\right)^2}\\&+\left(\frac{1}{\left(1+\theta^{-1}\int_{\mathbb{R}^N}\beta_1(y)A_1^\varepsilon(y)\mathrm{d}y\right)^2}-\frac{1}{\left(1+\theta^{-1}\int_{\mathbb{R}^N}\beta_1(y)A_1^{\varepsilon,*}(y)\mathrm{d}y\right)^2}\right)L_1^\varepsilon A_1^{\varepsilon,*},\end{aligned}$$

and, for all $x\in\Sigma_1$

$$\begin{aligned}\left|L_1^\varepsilon(A_1^\varepsilon-A_1^{\varepsilon,*})\right|(x)&=\frac{|\xi_1\int_{\Omega_1}m_\varepsilon(x-y)\Psi_1(y)(A_1^\varepsilon(y)-A_1^{\varepsilon,*}(y))\mathrm{d}y|}{(\theta+\int_{\mathbb{R}^N}\beta_1(y)A_1^{\varepsilon,*}(y)\mathrm{d}y)^2}\\&\leq\frac{\xi_1}{\theta^2}\|\Psi_1\|_{L^\infty}\int_{\Omega_1}m\left(\frac{x-y}{\varepsilon}\right)\frac{|A_1^\varepsilon(y)-A_1^{\varepsilon,*}(y)|}{\varepsilon^N}\mathrm{d}y\\&\leq\frac{\xi_1}{\theta^2}\|\Psi_1\|_{L^\infty}\|m\|_{L^\infty}\frac{\|A_1^\varepsilon-A_1^{\varepsilon,*}\|_{L^1(\Omega_1)}}{\varepsilon^N}=o(\varepsilon^\infty),\end{aligned}$$

thus (4.1.54) holds. Combining (4.1.52), (4.1.53) and (4.1.55), we have indeed shown (4.1.51).

Step three: Assume by contradiction that there exists a sequence $\lambda^\varepsilon\in\sigma(D_{A^\varepsilon}T^\varepsilon)$ with $\varepsilon\to0$ and such that

$$|\lambda^\varepsilon|\geq1.$$

Let $h^\varepsilon\in\mathcal{C}(\Sigma)$ be a sequence of associated normed (in $\mathcal{C}(\Sigma)$) eigenvectors. Then there is $k\in\{1,2\}$ such that $\sup_{\Sigma_k}|h_k^\varepsilon|=1$ for infinitely many $\varepsilon>0$. Using the symmetry with respect to the indices and the possible extraction of subsequences, we will assume in this step that $k=1$.

Let us first consider the case where $R_{0,1}>1$. Then, let us define $g^\varepsilon:=(D_{A_1^{\varepsilon,*}}T_1^\varepsilon-\lambda^\varepsilon I)h_1^\varepsilon$.

Due to (4.1.51) we have $\|g^\varepsilon\|_{\mathcal{C}(\Sigma_1)}=o(\varepsilon^\infty)$. Next taking the inner product with $\phi_1^{\varepsilon,n}$ yields, as in (4.1.49),

$$\langle h_1^\varepsilon,\phi_1^{\varepsilon,n}\rangle_{\Psi_1}=\frac{1}{\frac{\lambda_1^{\varepsilon,n}}{\lambda_1^{\varepsilon,1}}-\lambda^\varepsilon}g_n^\varepsilon,\quad\forall n\geq2,$$

where $g_n^\varepsilon:=\langle g^\varepsilon,\phi_1^{\varepsilon,n}\rangle_{\Psi_1}$. Then,

$$\left|\frac{\lambda_1^{\varepsilon,n}}{\lambda_1^{\varepsilon,1}}-\lambda^\varepsilon\right|\geq|\lambda^\varepsilon|-\left|\frac{\lambda_1^{\varepsilon,n}}{\lambda_1^{\varepsilon,1}}\right|\geq1-\frac{|\lambda_1^{\varepsilon,2}|}{|\lambda_1^{\varepsilon,1}|}\geq\frac{|\lambda_1^{\varepsilon,1}|-|\lambda_1^{\varepsilon,2}|}{|\lambda_1^{\varepsilon,1}|}\geq C\varepsilon^M,$$

for some $C>0$ and $M>0$ independent of ε and n. This shows

$$|\langle h_1^\varepsilon,\phi_1^{\varepsilon,n}\rangle_{\Psi_1}|=|g_n^\varepsilon|\times\mathcal{O}(\varepsilon^{-M}),\quad\forall n\geq2$$

therefore

$$\begin{aligned}\|h_1^\varepsilon-\langle h_1^\varepsilon,\phi_1^{\varepsilon,1}\rangle_{\Psi_1}\phi_1^{\varepsilon,1}\|_{L^2_{\Psi_1}}^2&=\sum_{n=2}^{+\infty}|\langle h_1^\varepsilon,\phi_1^{\varepsilon,n}\rangle_{\Psi_1}|^2=\sum_{n=2}^{+\infty}\left|\frac{1}{\frac{\lambda_1^{\varepsilon,n}}{\lambda_1^{\varepsilon,1}}-\lambda^\varepsilon}g_n^\varepsilon\right|^2\\&\leq C^{-2}\varepsilon^{-2M}\sum_{n=2}^{+\infty}|g_n^\varepsilon|^2\leq C^{-2}\varepsilon^{-2M}\|g^\varepsilon\|_{L^2_{\Psi_1}}^2=o(\varepsilon^\infty)\end{aligned}$$

by using (4.1.51).

Set $\mu^\varepsilon := h_1^\varepsilon - \langle h_1^\varepsilon, \phi_1^{\varepsilon,1}\rangle_{\Psi_1}\phi_1^{\varepsilon,1}$, then we have $\|L_1^\varepsilon \mu^\varepsilon\|_{\mathcal{C}(\Sigma_1)} = \mathcal{O}(\|\mu^\varepsilon\|_{L^2_{\Psi_1}}) = o(\varepsilon^\infty)$. By means of (4.1.51), we deduce that

$$\begin{aligned}\lambda^\varepsilon h_1^\varepsilon + o(\varepsilon^\infty) = D_{A_1^{\varepsilon,*}} T_1^\varepsilon h_1^\varepsilon &= \frac{L_1^\varepsilon(\mu^\varepsilon + \langle h_1^\varepsilon, \phi_1^{\varepsilon,1}\rangle_{\Psi_1}\phi_1^{\varepsilon,1})}{\lambda_1^{\varepsilon,1}} - \frac{\lambda_1^{\varepsilon,1}-1}{\lambda_1^{\varepsilon,1}}\frac{\int_{\mathbb{R}^N}\beta_1(y)h_1^\varepsilon(y)\mathrm{d}y}{\int_{\mathbb{R}^N}\beta_1(y)\phi_1^{\varepsilon,1}(y)\mathrm{d}y}\phi_1^{\varepsilon,1} \\ &= \left(\langle h_1^\varepsilon, \phi_1^{\varepsilon,1}\rangle_{\Psi_1} - \frac{\lambda_1^{\varepsilon,1}-1}{\lambda_1^{\varepsilon,1}}\frac{\int_{\mathbb{R}^N}\beta_1 h_1^\varepsilon}{\int_{\mathbb{R}^N}\beta_1\phi_1^{\varepsilon,1}}\right)\phi_1^{\varepsilon,1} + o(\varepsilon^\infty) := \alpha^\varepsilon\phi_1^{\varepsilon,1} + o(\varepsilon^\infty). \qquad (4.1.56)\end{aligned}$$

Next note that

$$1 \le |\lambda^\varepsilon| \sup_{x\in\Sigma_1}|h_1^\varepsilon(x)| = |\alpha^\varepsilon| \sup_{x\in\Sigma_1}\phi_1^{\varepsilon,1}(x) + o(\varepsilon^\infty),$$

where

$$\begin{aligned}\sup_{x\in\Sigma_1}\phi_1^{\varepsilon,1}(x) = \frac{1}{\lambda_1^{\varepsilon,1}}\sup_{x\in\Sigma_1}L_1^\varepsilon\phi_1^{\varepsilon,1}(x) &= \frac{1}{\lambda_1^{\varepsilon,1}}\sup_{x\in\Sigma_1}\frac{\Lambda\xi_1}{\theta}\int_{\mathbb{R}^N} m_\varepsilon(x-y)\Psi_1(y)\phi_1^{\varepsilon,1}(y)\mathrm{d}y \\ &\le \frac{\Lambda\xi_1}{\lambda_1^{\varepsilon,1}\theta}\frac{\|m\|_{L^\infty}}{\varepsilon^N}\|\Psi_1\|_{L^2(\mathbb{R})}\|\phi_1^{\varepsilon,1}\|_{L^2_{\Psi_k}} = \mathcal{O}(\varepsilon^{-N}),\end{aligned}$$

therefore $|\alpha^\varepsilon| \ge C\varepsilon^N$ for some constant $C > 0$. By definition of h^ε and using (4.1.53)-(4.1.56), it follows that

$$o(\varepsilon^\infty) = (D_{A_1^{\varepsilon,1}}T_1^\varepsilon - \lambda^\varepsilon I)h_1^\varepsilon = \frac{1}{\lambda^\varepsilon}(D_{A_1^{\varepsilon,1}}T_1^\varepsilon - \lambda^\varepsilon I)(\alpha^\varepsilon\phi_1^{\varepsilon,1} + o(\varepsilon^\infty)) = \frac{\alpha^\varepsilon}{\lambda^\varepsilon}\left(\frac{1}{\lambda_1^{\varepsilon,1}} - \lambda^\varepsilon\right)\phi_1^{\varepsilon,1} + o(\varepsilon^\infty),$$

then multiplying by $\phi_1^{\varepsilon,1}\Psi_1$ and integrating, we get

$$\left|\frac{1}{\lambda_1^{\varepsilon,1}} - \lambda^\varepsilon\right| = o(\varepsilon^\infty).$$

Since $\lambda^\varepsilon \ge 1$ and $\lambda_1^{\varepsilon,1} \to R_{0,1} > 1$ as $\varepsilon \to 0$, we obtain a contradiction.

Now we assume that $R_{0,1} \le 1$, then we have $A_1^{\varepsilon,*} \equiv 0$, hence

$$D_{A_1^{\varepsilon,*}}T_1^\varepsilon = L_1^\varepsilon,$$

which leads us to

$$r_\sigma(D_{A_1^{\varepsilon,*}}T_1^\varepsilon) = r_\sigma(L_1^\varepsilon) \xrightarrow[\varepsilon\to 0]{} R_{0,1} \le 1.$$

Moreover, by definition of λ^ε and using (4.1.51), we have $(L_1^\varepsilon - \lambda^\varepsilon I)h_1^\varepsilon =: g^\varepsilon = o(\varepsilon^\infty)$ hence

$$\|h_1^\varepsilon\|_{L^2_{\Psi_1}} \le \|(L_1^\varepsilon - \lambda^\varepsilon I)^{-1}g^\varepsilon\|_{L^2_{\Psi_1}} \le \|(L_1^\varepsilon - \lambda^\varepsilon I)^{-1}\|_{\mathcal{L}(L^2_{\Psi_1})}\|g^\varepsilon\|_{L^2_{\Psi_1}} = \frac{1}{\mathrm{dist}(\lambda^\varepsilon, \sigma(L_1^\varepsilon))}\|g^\varepsilon\|_{L^2_{\Psi_1}}.$$

Now let us observe that there exists some constant $C > 0$ such that $\|h_1^\varepsilon\|_{L^2_{\Psi_1}} \ge C\varepsilon^N$ for ε sufficiently small. To see this, note that one has, for all $x \in \Sigma_1$,

$$\begin{aligned}|h_1^\varepsilon|(x) = \frac{1}{|\lambda^\varepsilon|}|L_1^\varepsilon h_1^\varepsilon(x) - g^\varepsilon(x)| &\le \frac{1}{|\lambda^\varepsilon|}\left(\frac{\Lambda\xi_1}{\theta}\int_{\mathbb{R}^N} m_\varepsilon(x-y)|h_1^\varepsilon|(y)\Psi_1(y)\mathrm{d}y + |g^\varepsilon|(x)\right) \\ &\le \frac{c}{\varepsilon^N}\|h_1^\varepsilon\|_{L^2_{\Psi_1}} + o(\varepsilon^\infty),\end{aligned}$$

where $c > 0$ is some constant independent of ε. Finally recalling that $\|h_1^\varepsilon\|_{\mathcal{C}(\Sigma_1)} = 1$ this proves the expected lower bound for $\|h_1^\varepsilon\|_{L^2_{\Psi_1}}$. This estimate allows us to conclude that

$$\mathrm{dist}(\lambda^\varepsilon, \sigma(L_1^\varepsilon)) = o(\varepsilon^\infty),$$

which is a contradiction since $\lambda^\varepsilon \ge 1$ while

$$\sup\{|\lambda|, \lambda \in \sigma(L_1^\varepsilon)\} = r(L_1^\varepsilon) \le 1 - C\varepsilon^M,$$

by our assumptions and (4.1.50). This completes the proof of Lemma 4.1.16. □

Our next task is to compute the Leray-Schauder degree of the operator T^ε in a suitable subset of the positive cone, $\mathcal{C}_+(\Sigma)$, of $\mathcal{C}(\Sigma)$. For $\alpha > 0$ we define the open set

$$K_\alpha := \{A \in \mathcal{C}(\Sigma) : A(x) > \alpha \quad \forall x \in \Sigma\}.$$

Lemma 4.1.17 (Computation of the degree)**.** *Assume that $R_{0,1} > 1$. Then, for $\varepsilon > 0$ sufficiently small, there exists $\alpha = \alpha(\varepsilon) > 0$ such that for any nonnegative nontrivial fixed point $A \in \mathcal{C}(\Sigma)$ of T^ε, we have:*

$$A \in K_\alpha.$$

Moreover,

$$\deg(I - T^\varepsilon, K_\alpha) = 1, \tag{4.1.57}$$

where deg *denotes the Leray-Schauder degree.*

Proof. Our proof relies on the construction of a suitable homotopy which allows us to separate the variables and compute the Leray-Schauder degree. For technical reasons, we do not use the same homotopy in the case $R_{0,2} > 1$ and $R_{0,2} < 1$. Therefore, we split the proof into two parts.

Part 1: the case $R_{0,2} > 1$. Let us define, for $\tau \in [0,1]$, $A \in \mathcal{C}_+(\Sigma)$ and $(A_1, A_2) := (\chi_{\Sigma_1} A, \chi_{\Sigma_2} A)$, the operators

$$\begin{aligned}
T_1^{\varepsilon,\tau}(A) :&= \frac{\chi_{\Sigma_1} L_1^\varepsilon A_1}{1 + \theta^{-1}\int_{\mathbb{R}^N} \beta_1(y) A_1(y)\mathrm{d}y} + \tau \frac{\chi_{\Sigma_1} L_2^\varepsilon A_2}{1 + \theta^{-1}\int_{\mathbb{R}^N} \beta_2(y) A_2(y)\mathrm{d}y} = \chi_{\Sigma_1} T_1^\varepsilon A_1 + \tau \chi_{\Sigma_1} T_2^\varepsilon A_2,\\
T_2^{\varepsilon,\tau}(A) :&= \tau \frac{\chi_{\Sigma_2} L_1^\varepsilon A_1}{1 + \theta^{-1}\int_{\mathbb{R}^N} \beta_1(y) A_1(y)\mathrm{d}y} + \frac{\chi_{\Sigma_2} L_2^\varepsilon A_2}{1 + \theta^{-1}\int_{\mathbb{R}^N} \beta_2(y) A_2(y)\mathrm{d}y} = \tau \chi_{\Sigma_2} T_1^\varepsilon A_1 + \chi_{\Sigma_2} T_2^\varepsilon A_2,\\
T^{\varepsilon,\tau}(A) :&= T_1^{\varepsilon,\tau} A + T_2^{\varepsilon,\tau} A
\end{aligned} \tag{4.1.58}$$

where T_k^ε is defined in (4.1.7) for each $k \in \{1,2\}$. The map $(\tau, A) \mapsto T^{\varepsilon,\tau}(A)$ is continuous from $[0,1] \times \mathcal{C}_+(\Sigma)$ into $\mathcal{C}(\Sigma)$. Let us first observe that there exists $M > 0$ such that for all $\tau \in [0,1]$, if $A \in \mathcal{C}_+(\Sigma)$ satisfies $A = T^{\varepsilon,\tau}(A)$ then $\|A\|_{L^1(\Sigma)} \le M$. One may also notice that this upper bound can be chosen independently of $\varepsilon > 0$.

We first show that the fixed points of $T^{\varepsilon,\tau}$ can be estimated from below uniformly in $\tau \in (0,1)$. This will allow us to easily compute the Leray-Schauder degree, since $T^{\varepsilon,0}$ is completely uncoupled in its variables.

Step 1: We show that there exists $\alpha > 0$ (independent of $\tau \in [0,1]$) such that

$$\min_{x \in \Sigma}(A^\tau(x)) > \alpha, \tag{4.1.59}$$

for any nontrivial and nonnegative A^τ satisfying $T^{\varepsilon,\tau} A^\tau = A^\tau$ for some $\tau \in [0,1]$.

Let $\tau \in [0,1]$ and $(A_1^\tau, A_2^\tau) \in \mathcal{C}_+(\Sigma_1) \times \mathcal{C}_+(\Sigma_2) \subset L^1_+(\Sigma_1) \times L^1_+(\Sigma_2)$ be a nontrivial fixed point of $T^{\varepsilon,\tau}$, *i.e.* $T^{\varepsilon,\tau}(A_1^\tau + A_2^\tau) = (A_1^\tau + A_2^\tau)$. We remark that

$$T_1^{\varepsilon,\tau} A^\tau \ge T_1^{\varepsilon,\tau} A_1^\tau = \chi_{\Sigma_1} T_1^\varepsilon A_1^\tau \quad \text{and} \quad T_2^{\varepsilon,\tau} A^\tau \ge T_2^{\varepsilon,\tau} A_2^\tau = \chi_{\Sigma_2} T_2^\varepsilon A_2^\tau.$$

In particular, we have

$$A_k^\tau = (T_k^{\varepsilon,\tau})^n A^\tau \ge \chi_{\Sigma_k} (T_k^\varepsilon)^n A_k^\tau, \tag{4.1.60}$$

everywhere in Σ_k and for all $n \in \mathbb{N}$ and $k = 1,2$. Since $\lim_{\varepsilon \to 0} r_\sigma(L_k^\varepsilon) = R_{0,k} > 1$, we can find $\varepsilon_0 > 0$ such that $r_\sigma(L_1^\varepsilon) > 1$ and $r_\sigma(L_2^\varepsilon) > 1$ for any $\varepsilon \in (0, \varepsilon_0]$. Let $\varepsilon \in (0, \varepsilon_0]$ be given, then using (4.1.19) we get

$$\limsup_{n \to \infty} \int_{\mathbb{R}^N} \beta_k(y) (T_k^\varepsilon)^n(\varphi)(y)\mathrm{d}y \ge \frac{\theta}{2}(r_\sigma(L_k^\varepsilon) - 1) > 0,$$

for any $k \in \{1,2\}$ and any $\varphi \in L^1_+(\Sigma_k) \setminus \{0\}$. We deduce that there exists $\eta > 0$ (independent of ε small and τ) such that

$$\int_{\mathbb{R}^N} \beta_k(y) A_k^\tau(y)\mathrm{d}y \ge \limsup_{n \to \infty} \int_{\mathbb{R}^N} \beta_k(y) (T_k^\varepsilon)^n (A_k^\tau)(y)\mathrm{d}y \ge \eta \tag{4.1.61}$$

for any $k \in \{1,2\}$. Next, using (4.1.25) and since the fixed points of $T^{\varepsilon,\tau}$ are bounded by some constant M in $L^1(\Sigma)$, we obtain $A_k^\tau = T_k^{\varepsilon,\tau} A^\tau \leq L_k^\varepsilon A_k^\tau + o(\varepsilon^\infty)$ where $o(\varepsilon^\infty)$ is uniform with respect to $\tau \in [0,1]$ and $x \in \Sigma_k$. Hence we get

$$\begin{aligned}\eta &\leq \int_{\mathbb{R}^N} \beta_k(x) A_k^\tau(x) \mathrm{d}x \leq \frac{\Lambda \xi_k}{\theta} \iint_{\mathbb{R}^N \times \mathbb{R}^N} \beta_k(x) m_\varepsilon(x-y) A_k^\tau(y) \Psi_k(y) \mathrm{d}y \mathrm{d}x + o(\varepsilon^\infty) \\ &\leq \frac{\Lambda \xi_k \|\beta_k\|_{L^\infty}}{\theta} \int_{\mathbb{R}^N} \Psi_k(y) A_k^\tau(y) \mathrm{d}y + o(\varepsilon^\infty).\end{aligned}$$

Using (4.1.60), we get for any $k \in \{1,2\}$ and any $x \in \Sigma_k$:

$$\begin{aligned}A_k^\tau(x) &\geq \frac{\Lambda \xi_k}{\theta + M\|\beta_k\|_{L^\infty}} \int_{\Omega_k} m_\varepsilon(x-y) \Psi_k(y) A_k^\tau(y) \mathrm{d}y \\ &\geq \frac{\Lambda \xi_k}{\theta + M\|\beta_k\|_{L^\infty}} \min_{x \in \Sigma_k} \min_{\tau \in [0,1]} \int_{\Omega_k} m_\varepsilon(x-y) \Psi_k(y) A_k^{\varepsilon,\tau}(y) \mathrm{d}y \geq c(\varepsilon).\end{aligned}$$

for some constants $M > 0$ and $c(\varepsilon) > 0$ independent of A^τ and $\tau \in [0,1]$. This shows (4.1.59) and thus that, for $\varepsilon > 0$ sufficiently small, there exists $\alpha = \alpha(\varepsilon) > 0$ such that for any $\tau \in [0,1]$, any nontrivial and nonnegative fixed points A^τ of $T^{\varepsilon,\tau}$ satisfies $A^\tau \in K_\alpha$.

Step 2: We compute the Leray-Schauder degree of the operator T^ε in the open set K_α.

We have shown in the previous step that $A \in K_\alpha$ for any positive fixed point of the operator $T^{\varepsilon,\tau}$ with $\tau \in (0,1]$. In particular, there is no fixed point of $T^{\varepsilon,\tau}$ on the boundary of K_α for $\tau \in (0,1]$. For $\tau = 0$, the operator $T^{\varepsilon,0}$ is uncoupled and hence we can compute the set of nonnegative fixed points of $T^{\varepsilon,0}$, which is $\{(0,0), (A_1^{\varepsilon,*}, 0), (0, A_2^{\varepsilon,*}), (A_1^{\varepsilon,*}, A_2^{\varepsilon,*})\}$. None of those points lie in the boundary of K_α. In particular, [81, Theorem 11.8] applies and shows that the Leray-Schauder degree in K_α is independent of τ, *i.e.*

$$\deg(I - T^{\varepsilon,0}, K_\alpha) = \deg(I - T^{\varepsilon,1}, K_\alpha).$$

Since $T^{\varepsilon,0}$ is uncoupled with respect to $(A_1, A_2) \in \mathcal{C}(\Sigma_1) \times \mathcal{C}(\Sigma_2)$, the product property of the Leray-Schauder degree (see [81, Theorem 11.3]) implies that

$$\deg(I - T^{\varepsilon,0}, K_\alpha) = \deg(I - T_1^\varepsilon, K_\alpha^1) \times \deg(I - T_2^\varepsilon, K_\alpha^2),$$

where $K_\alpha^k := \{A_k \in \mathcal{C}(\Sigma_k) \,|\, A_k(x) > \alpha, \forall x \in \Sigma_k\}$ for $k \in \{1,2\}$. Finally, since T_k^ε has exactly one fixed point in K_α^k and $1 \notin \sigma\left(D_{A_k^{\varepsilon,*}} T_k^\varepsilon\right)$, the degree of the nonlinear operator T_k^ε can be linked to the degree of its Fréchet derivative near $A_k^{\varepsilon,*}$ (see [81, Theorem 22.3])

$$\deg(I - T_k^\varepsilon, K_\alpha^k) = \deg(I - D_{A_k^{\varepsilon,*}} T_k^\varepsilon, B(0,1)),$$

where $B(0,1)$ is the open ball of radius 1 in $\mathcal{C}(\Sigma_k)$. The explicit formula of the degree of linear operators (see [81, Theorem 21.10]) allows us to conclude that

$$\deg(I - D_{A_k^{\varepsilon,*}} T_k^\varepsilon, B(0,1)) = 1,$$

since $\sigma(D_{A_k^{\varepsilon,*}} T_k^\varepsilon) \subset (-1,1)$ for $k \in \{1,2\}$. This shows (4.1.57) and ends the proof of Lemma 4.1.17 in the case $R_{0,2} > 1$.

Part 2: the case $R_{0,2} \leq 1$. In this case we cannot use the same homotopy as in Part 1 to compute the Leray-Schauder degree, because T_2^ε has no nonnegative nontrivial fixed point. Instead, we define, for $\tau \in [0,1]$, $A \in \mathcal{C}_+(\Sigma)$ and $(A_1, A_2) := (\chi_{\Sigma_1} A, \chi_{\Sigma_2} A)$, the operators

$$\begin{aligned}T_1^{\varepsilon,\tau}(A) :&= \frac{\chi_{\Sigma_1} L_1^\varepsilon A_1}{1 + \theta^{-1} \int_{\mathbb{R}^N} \beta_1(y) A_1(y) \mathrm{d}y} + \frac{\chi_{\Sigma_1} L_2^{\varepsilon,\tau} A_2}{1 + \theta^{-1} \int_{\mathbb{R}^N} \beta_2^\tau(y) A_2(y) \mathrm{d}y}, \\ T_2^{\varepsilon,\tau}(A) :&= \frac{\chi_{\Sigma_2} L_1^\varepsilon A_1}{1 + \theta^{-1} \int_{\mathbb{R}^N} \beta_1(y) A_1(y) \mathrm{d}y} + \frac{\chi_{\Sigma_2} L_2^{\varepsilon,\tau} A_2}{1 + \theta^{-1} \int_{\mathbb{R}^N} \beta_2^\tau(y) A_2(y) \mathrm{d}y}, \\ T^{\varepsilon,\tau}(A) :&= T_1^{\varepsilon,\tau} A + T_2^{\varepsilon,\tau} A.\end{aligned} \tag{4.1.62}$$

where $\beta_2^\tau(y) := \left(1+\tau\left(\frac{2}{R_{0,2}}-1\right)\right)\beta_2(y)$, $\Psi_2^\tau(y) := \frac{\beta_2^\tau(y) r_2(y)}{\delta(\theta+d_2(y))}$ and

$$L_2^{\varepsilon,\tau}\varphi = \frac{\Lambda}{\theta}\int_{\Omega_2} m_\varepsilon(x-y)\xi_2\Psi_2^\tau(y)\varphi(y)\mathrm{d}y$$

which is well-defined since $R_{0,2}>0$ (recall that $\Psi_2 \not\equiv 0$ by Assumption 4.1.1). This corresponds to artificially increasing the basic reproductive number of the second equation until it becomes greater than 1. In particular, for $\tau = 1$ we are in the same situation as in Part 1 since

$$\frac{\Lambda}{\theta}\xi_2\|\Psi_2^1\|_{L^\infty} = 2.$$

Note that, as above, there exists $M>0$ such that for all $\tau\in[0,1]$, any fixed point $A^\tau \in \mathcal{C}_+(\Sigma)$ of $T^{\varepsilon,\tau}$ satisfies $\|A^\tau\|_{L^1(\Sigma)} \le M$. Here our only task consists in finding a uniform lower bound for the fixed point of $T^{\varepsilon,\tau}$.

Claim: There is $\alpha>0$ such that for any $\tau\in(0,1)$ and any nonnegative nontrivial A^τ solution to $T^{\varepsilon,\tau}A^\tau = A^\tau$, we have $A\in K_\alpha$.

Indeed, let A^τ be such a fixed point. We first remark that $A_1^\tau \ge \chi_{\Sigma_1}(T_1^\varepsilon)^n A_1^\tau$ for any $n\in\mathbb{N}$, hence:

$$\int_{\mathbb{R}^N}\beta_1(y)A_1^\tau(y)\mathrm{d}y \ge \limsup_{n\to\infty}\int_{\mathbb{R}^N}\beta_1(y)(T_1^\varepsilon)^n(A_1^\tau)(y)\mathrm{d}y \ge \frac{\theta}{2}(r_\sigma(L_1^\varepsilon)-1) > 0,$$

where we have used (4.1.19) as in the Step 1 of Part 1. Thus, we have

$$A_1^\tau(x) \ge \frac{\Lambda\xi_k c(\varepsilon)}{\theta + M\|\beta_1\|_{L^\infty}} \ge \eta > 0, \qquad \forall x\in\Sigma_1$$

for some constants $M>0$ and $\eta>0$. To estimate A_2^τ, we remark that

$$A_2^\tau \ge \chi_{\Sigma_2}T_1^\varepsilon A_1^\tau = \frac{\chi_{\Sigma_2}L_1^\varepsilon A_1^\tau}{1+\theta^{-1}\int_{\mathbb{R}^N}\beta_1(y)A_1^\tau(y)\mathrm{d}y} = \frac{\Lambda}{\theta}\frac{\chi_{\Sigma_2}\int_{\Omega_1} m_\varepsilon(\cdot-y)\xi_1\Psi_1(y)A_1^\tau(y)\mathrm{d}y}{1+\theta^{-1}\int_{\mathbb{R}^N}\beta_1(y)A_1^\tau(y)\mathrm{d}y}$$

and, as in Part one, we have $A_1^\tau = T_1^{\varepsilon,\tau}A^\tau \le L_1^\varepsilon A_1^\tau + o(\varepsilon^\infty)$, and thus

$$\begin{aligned}\eta &\le \int_{\mathbb{R}^N}\beta_1(x)A_1^\tau(x)\mathrm{d}x \le \frac{\Lambda\xi_1}{\theta}\iint_{\mathbb{R}^N\times\mathbb{R}^N}\beta_1(x)m_\varepsilon(x-y)A_1^\tau(y)\Psi_1(y)\mathrm{d}y\mathrm{d}x + o(\varepsilon^\infty)\\ &\le \frac{\Lambda\xi_1\|\beta_1\|_\infty}{\theta}\int_{\mathbb{R}^N}\Psi_1(y)A_1^\tau(y)\mathrm{d}y + o(\varepsilon^\infty).\end{aligned}$$

We conclude

$$A_2^\tau(x) \ge \frac{\Lambda\xi_1\eta}{\theta+M\|\beta_1\|_{L^\infty}}\min_{x\in\Sigma_2}\int_{\Omega_1} m_\varepsilon(x-y)\mathrm{d}y > 0$$

for every $x\in\Sigma_2$. This proves our Claim.

To finish the proof of the second part, we remark that the Leray-Schauder degree is independent of τ (see [81, Theorem 11.8]), *i.e.*

$$\deg(I-T^{\varepsilon,0},K_\alpha) = \deg(I-T^{\varepsilon,1},K_\alpha),$$

and we have proved in Part 1 that, for α sufficiently small, we have $\deg(I-T^{\varepsilon,1},K_\alpha)=1$. This finishes the proof of Lemma 4.1.17. □

Lemma 4.1.18. *There exists $\varepsilon_0>0$ such that for every $\varepsilon\in(0,\varepsilon_0]$, there is a finite number of nonnegative nontrivial fixed point of T^ε.*

Proof. Let $\varepsilon>0$ and assume by contradiction that there exist infinitely many fixed points of T^ε. Since T^ε is compact from $\mathcal{C}_+(\Sigma)$ into itself, there exist a sequence $A^n\in\overline{K_\alpha}$ of fixed points of T^ε and $\overline{A}$ such that

$$\|A^n-\overline{A}\|_{L^\infty} \xrightarrow[n\to\infty]{} 0.$$

By definition we have $T^\varepsilon(A^n) = A^n$ for every $n \in \mathbb{N}$. By the continuity of T^ε we get

$$T^\varepsilon(\overline{A}) = \overline{A}.$$

Since T^ε is Fréchet differentiable at the point $\overline{A}$, we have as $n \to \infty$

$$\frac{\overline{A} - A^n}{\|\overline{A} - A^n\|_{L^\infty}} = \frac{T^\varepsilon(\overline{A}) - T^\varepsilon(A^n)}{\|\overline{A} - A^n\|_{L^\infty}} = \frac{1}{\|\overline{A} - A^n\|_{L^\infty}} D_{\overline{A}} T^\varepsilon \left(A^n - \overline{A}\right) + o(1).$$

Let us define

$$U^n = \frac{\overline{A} - A^n}{\|\overline{A} - A^n\|_{L^\infty}},$$

then we have

$$U^n := D_{\overline{A}} T^\varepsilon U^n + o(1) \text{ as } n \to \infty.$$

By the compactness of T^ε, we can extract from U^n a subsequence $\bar{U}^n$ which converges to U^∞ with $\|U^\infty\|_{L^\infty} = 1$. We conclude

$$U^\infty = D_{\overline{A}} T^{\varepsilon,1} U^\infty$$

which is a contradiction since $1 \notin \sigma(D_{\overline{A}} T^{\varepsilon,1})$ by Lemma 4.1.16. This finishes the proof of Lemma 4.1.18. □

We can finally prove our uniqueness result for $\varepsilon > 0$ small.

Proof of Theorem 4.1.8. By Lemma 4.1.18, there exists a finite number N_ε of fixed points of T^ε_τ. Denote by $A^{\varepsilon,i}$, $i \in [\![1, N_\varepsilon]\!]$ an enumeration of the fixed points of T^ε_τ. By the additivity property of the Leray-Schauder degree (see [81, Theorem 11.4, p. 79] and [81, Theorem 11.5, p. 79]), we get

$$\begin{aligned} \deg\left(I - T^\varepsilon, K_\alpha\right) &= \deg\left(I - T^\varepsilon, \bigcup_{i=1}^{N_\varepsilon} B(A^{\varepsilon,i}, \eta)\right) \\ &= \sum_{i=1}^{N_\varepsilon} \deg\left(I - T^\varepsilon, B(A^{\varepsilon,i}, \eta)\right), \end{aligned} \tag{4.1.63}$$

for $\eta > 0$ sufficiently small, where $\alpha > 0$ is the constant from Lemma 4.1.17 and $B(A^{\varepsilon,i}, \eta)$ is the ball of center $A^{\varepsilon,i}$ and of radius η in $\mathcal{C}(\Sigma)$. Next, using [81, Theorem 22.3], we can link the degree of T^ε to the one of its Fréchet derivative close to a fixed point

$$\deg\left(I - T^{\varepsilon,1}, B(A^{\varepsilon,i}, \eta)\right) = \deg\left(I - D_{A^{\varepsilon,i}} T^{\varepsilon,1}, B(0,1)\right) = 1$$

for $\eta > 0$ sufficiently small and for every $i \in [\![1, N_\varepsilon]\!]$. This leads to

$$\deg\left(I - T^{\varepsilon,1}, K_\alpha\right) = N_\varepsilon,$$

where we have used (4.1.63). Since we have shown in Lemma 4.1.17 that $\deg(I - T^\varepsilon, K_\alpha) = 1$, we conclude that $N_\varepsilon = 1$. We have proven the uniqueness of the nonnegative nontrivial fixed point of T^ε for $\varepsilon > 0$ small, which completes the proof of Theorem 4.1.8. □

4.1.6 Spectral properties of a weighted convolution operator

In this appendix, we state and recall some basic spectral properties of a weighted convolution operator as in (4.1.8), *i.e.* of the form

$$L^\varepsilon = m_\varepsilon \star (\Psi\, \cdot), \tag{4.1.64}$$

where $m_\varepsilon = \varepsilon^{-N} m\left(\varepsilon^{-1}\cdot\right)$ with $\varepsilon > 0$. Throughout this appendix, we assume

Assumption 4.1.19. The function m satisfies Assumption 4.1.1 *c)* and $\Psi : \mathbb{R}^N \to [0, \infty)$ is a non-zero continuous function tending to 0 at $\|x\| = +\infty$.

The above assumption allows us to directly apply the results presented in this Appendix to operator L^ε as well as to L^ε_1 and L^ε_2 as defined in (4.1.5)

We start this section 4.1.6 by reminding the following definition about positive operators:

Definition 4.1.20. Let $p \in [1,\infty)$, $I \subset \mathbb{R}^N$ and $K \in Ł(L^p(I))$ be given. We denote by

$$L^p_+(I) := \{\varphi \in L^p(I) : \varphi(x) \geq 0 \text{ a.e.}\}$$

the positive cone of $L^p(I)$. Let $\langle \cdot, \cdot \rangle$ be the duality product between $L^p(I)$ and $L^{p'}(I)$ where $1/p + 1/p' = 1$. For $\varphi \in L^p(I)$, the notation $\varphi \gneqq 0$ will refer to $\varphi \in L^p_+(I)$ and $\varphi \not\equiv 0$ while the notation $\varphi > 0$ will refer to $\varphi \in L^p_+(I)$ and $\varphi(x) > 0$ a.e. We say that

1. K is positive if $K\left(L^p_+(I)\right) \subset L^p_+(I)$;
2. K is said to be positivity improving if K is positive and if, for every $\varphi \in L^p(I)$, $\varphi \gneqq 0$ and $\phi \in L^{p'}(I)$, $\phi \gneqq 0$, we have $\langle K\varphi, \phi \rangle > 0$.

Consider the non-empty open set $\Omega \subset \mathbb{R}^N$ given by

$$\Omega = \{x \in \mathbb{R}^N : \ \psi(x) \in (0,\infty)\}.$$

We will denote, in the following lemma only, by $L^\varepsilon_p, M^\varepsilon_p$, the operator L^ε defined in (4.1.8) and considered as endomorphisms on $L^p(\Omega), L^p(\mathbb{R}^N)$ respectively.

Lemma 4.1.21. *Let Assumption 4.1.19 be satisfied. Then the following properties are satisfied:*

1. *Let $p \geq 1$. The operators L^ε_p and M^ε_p are compact, their spectra $\sigma(L^\varepsilon_p)\backslash\{0\}$ and $\sigma(M^\varepsilon_p)\backslash\{0\}$ are composed of isolated eigenvalues with finite algebraic multiplicity. All these operators share the same spectral radius – independent of p – denoted by $r_\sigma(L^\varepsilon)$, which is a positive algebraically simple eigenvalue. There exists a function $\phi^{\varepsilon,1}_p \in L^p(\Omega)$ satisfying*

$$\phi^{\varepsilon,1}_p > 0, \qquad L^\varepsilon_p \phi^{\varepsilon,1}_p = r_\sigma(L^\varepsilon)\phi^{\varepsilon,1}_p.$$

   Moreover L^ε_p is positivity improving and, if $\phi \in L^p(\mathbb{R}^N)$, $\phi \gneqq 0$ satisfies the equality $L^\varepsilon_p \phi = \alpha\phi$ for some $\alpha \in \mathbb{R}$, then $\phi > 0$, $\phi \in span(\phi^{\varepsilon,1}_p)$ and $\alpha = r_\sigma(L^\varepsilon_p)$. Finally, we have $\sigma(M^\varepsilon_p) = \sigma(L^\varepsilon_p)$.

2. *Assume that Ω is bounded, let S^ε be the positive self-adjoint operator defined by*

$$S^\varepsilon : L^2(\Omega) \ni \varphi(x) \mapsto \sqrt{\Psi(x)} \int_{\mathbb{R}^N} m_\varepsilon(x-y)\sqrt{\Psi(y)}\varphi(y)\mathrm{d}y \in L^2(\Omega), \tag{4.1.65}$$

   then for every $p \geq 1$, we have $\sigma(S^\varepsilon) = \sigma(L^\varepsilon_p) \subset \mathbb{R}^+$, and the following Rayleigh formula holds

$$r_\sigma(L^\varepsilon) = r_\sigma(S^\varepsilon) = \sup_{\substack{\varphi \in L^2(\Omega) \\ \|\varphi\|_{L^2(\Omega)}=1}} \int_\Omega \int_\Omega \sqrt{\Psi(x)}\sqrt{\Psi(y)} m_\varepsilon(x-y)\varphi(x)\varphi(y)\mathrm{d}x\mathrm{d}y. \tag{4.1.66}$$

   Moreover, $r_\sigma(L^\varepsilon)$ satisfies

$$r_\sigma(L^\varepsilon) \xrightarrow[\varepsilon\to 0]{} \|\Psi\|_{L^\infty}.$$

3. *Suppose that Ω bounded and let $\Sigma \supset \Omega$ be a compact set. The operator L^ε_Σ, the realisation of L^ε in $\mathcal{C}(\Sigma)$, is compact and one has $\sigma(L^\varepsilon_\Sigma) = \sigma(L^\varepsilon_p)$ for any $p \geq 1$.*

Proof. Item 1 is rather classical and has been proved in [145, Theorem 4.1]. In short, the inclusion $\sigma(M^\varepsilon_p) \subset \sigma(L^\varepsilon_p)$ is straightforward, while the reverse inclusion comes from the fact that any eigenfunction ϕ^ε of L^ε_p related to the eigenvalue λ^ε can be extended from $L^p(\Omega)$ to $L^p(\mathbb{R}^N)$ by setting

$$\phi^\varepsilon(x) := \frac{1}{\lambda^\varepsilon} \int_\Omega m_\varepsilon(x-y)\Psi(y)\phi^\varepsilon(y)\mathrm{d}y, \quad \forall x \in \mathbb{R}^N \setminus \Omega. \tag{4.1.67}$$

Let us show Item 2. Recall that Ω is bounded. Let $p \geq 1$, $\lambda \in \sigma(L^\varepsilon_p)$ be an eigenvalue and $\varphi \in L^p(\Omega) \subset L^1(\Omega)$ be the associated eigenvector for L^ε_p, *i.e.*

$$L^\varepsilon_p \varphi(x) = \int_\Omega m_\varepsilon(x-y)\Psi(y)\varphi(y)\mathrm{d}y = \lambda\varphi(x)$$

so that $\varphi \in L^\infty(\Omega)$ by the Young inequality. Multiplying the above equation by $\sqrt{\Psi(x)}$, we get:

$$\sqrt{\Psi(x)}\int_\Omega m_\varepsilon(x-y)\sqrt{\Psi(y)}\sqrt{\Psi(y)}\varphi(y)\mathrm{d}y = \lambda\sqrt{\Psi(x)}\varphi(x) \iff S^\varepsilon\Phi(x) = \lambda\Phi(x),$$

with $\Phi := \sqrt{\Psi}\varphi \in L^\infty(\Omega) \subset L^2(\Omega)$. Therefore $\lambda \in \sigma(S^\varepsilon)$. We have shown:

$$\sigma(L_p^\varepsilon) \subset \sigma(S^\varepsilon), \quad \forall p \geq 1.$$

Let us show the reverse inclusion. Note that due to the first item, the operator S^ε is compact on $L^2(\Omega)$ and therefore $\sigma(S^\varepsilon)$ consists in isolated eigenvalues. Let $\lambda \in \sigma(S^\varepsilon)\backslash\{0\}$ be an eigenvalue and $\Phi \in L^2(\Omega)$ be an associated eigenvector, so that

$$\frac{\Phi(x)}{\sqrt{\Psi(x)}} = \frac{1}{\lambda}\cdot\int_\Omega m_\varepsilon(x-y)\sqrt{\Psi(y)}\Phi(y)\mathrm{d}y \in L^\infty(\Omega).$$

Hence there exists a non-zero function $\varphi \in L^\infty(\Omega) \subset L^p(\Omega), \forall p \geq 1$ such that $\Phi = \varphi\sqrt{\Psi}$ where the function φ satisfies

$$\lambda\varphi(x) = \int_\Omega m_\varepsilon(x-y)\sqrt{\Psi(y)}\sqrt{\Psi(y)}\varphi(y)\mathrm{d}y = L^\varepsilon\varphi(x).$$

Thus $\lambda \in \sigma(L_p^\varepsilon)$ for any $p \geq 1$ and we have shown

$$\sigma(S^\varepsilon) \subset \sigma(L_p^\varepsilon), \quad \forall p \geq 1.$$

Formula (4.1.66) is classical for positive and symmetric operators.

Now let $\phi^{\varepsilon,1}$ be the positive eigenfunction of L^ε associated with $r_\sigma(L^\varepsilon)$, normalised so that $\int_\Omega \phi^{\varepsilon,1}(y)\mathrm{d}y = 1$. We first notice that

$$\begin{aligned} r_\sigma(L^\varepsilon) = r_\sigma(L^\varepsilon)\int_\Omega \phi^{\varepsilon,1}(x)\mathrm{d}x &= \iint_{\Omega\times\Omega} m_\varepsilon(x-y)\Psi(y)\phi^{\varepsilon,1}(y)\mathrm{d}y\mathrm{d}x \\ &\leq \|\Psi\|_{L^\infty}\int_\Omega\int_\Omega m_\varepsilon(x-y)\mathrm{d}x\,\phi^{\varepsilon,1}(y)\mathrm{d}y \leq \|\Psi\|_{L^\infty}. \end{aligned}$$

Next let $x_0 \in \Omega$ be such that $\Psi(x_0) = \sup_{x\in\Omega}\Psi(x)$. Injecting the function $\frac{1}{\sqrt{|B(x_0,r)|}}\chi_{B(x_0,r)}(x)$ into (4.1.66) yields

$$\begin{aligned} r_\sigma(L^\varepsilon) = r_\sigma(S^\varepsilon) &\geq \frac{1}{|B(x_0,r)|}\iint_{\Omega\times\Omega}\sqrt{\Psi(x)}\sqrt{\Psi(y)}m_\varepsilon(x-y)\chi_{B(x_0,r)}(x)\chi_{B(x_0,r)}(y)\mathrm{d}y\mathrm{d}x \\ &\geq \left(\inf_{x\in B(x_0,r)}\sqrt{\Psi(x)}\right)^2\frac{1}{|B(x_0,r)|}\iint_{B(x_0,r)^2} m_\varepsilon(x-y)\mathrm{d}x\mathrm{d}y \\ &= \inf_{x\in B(x_0,r)}\Psi(x)\frac{1}{|B(x_0,r)|}\varepsilon^N\iint_{B(x_0,r/\varepsilon)^2} m\left(x-y\right)\mathrm{d}y\mathrm{d}x \\ &= \inf_{x\in B(x_0,r)}\Psi(x)\frac{\varepsilon^N\left|B\left(x_0,\frac{r}{\varepsilon}\right)\right|}{|B(x_0,r)|}\int_{B(0,r/\varepsilon)} m\left(y\right)\mathrm{d}y \\ &= \inf_{x\in B(x_0,r)}\Psi(x)\int_{B(0,r/\varepsilon)} m\left(y\right)\mathrm{d}y \underset{\varepsilon\to 0}{\longrightarrow} \inf_{x\in B(x_0,r)}\Psi(x), \end{aligned}$$

for all $r > 0$ sufficiently small so that $B(x_0,r) \subset \Omega$. This proves the following inequality

$$\inf_{x\in B(x_0,r)}\Psi(x) \leq \liminf_{\varepsilon\to 0} r_\sigma(L^\varepsilon) \leq \limsup_{\varepsilon\to 0} r_\sigma(L^\varepsilon) \leq \|\Psi\|_{L^\infty}.$$

Since $\lim_{r\to 0}\inf_{x\in B(x_0,r)}\Psi(x) = \|\Psi\|_{L^\infty}$, Item 2 is proved.

Finally we prove the last point, that is Item 3. As Σ is compact the fact that L_Σ^ε is compact follows from the Arzelà-Ascoli theorem. It remains to show that $\sigma(L_\Sigma^\varepsilon) = \sigma(L_p^\varepsilon)$ for any $p \geq 1$. The inclusion $\sigma(L_\Sigma^\varepsilon) \subset \sigma(L_p^\varepsilon)$ is immediate since $\mathcal{C}(\Sigma) \subset L^p(\Sigma)$ for every $p \geq 1$ and $\Omega \subset \Sigma$. Let $p \in [1,\infty)$ be given. The reverse inclusion follows from the identity (4.1.67) that allows to extend the eigenfunction from $L^p(\Omega)$ to $L^p(\Sigma)$. Let us notice that $m_\varepsilon \star (\Psi\phi) \in \mathcal{C}(\Sigma)$ as soon as $\phi \in L^p(\Sigma) \subset L^1(\Sigma)$ (see *e.g.* [63, Corollary 3.9.6, p. 207]).

This ends the proof of Lemma 4.1.21. □

We now give some asymptotic results for compact and positivity improving operators. The following result is classical but here we propose a proof for the sake of completeness.

Lemma 4.1.22. *Suppose that Assumption 4.1.19 holds and let L^ε be the operator defined in* (4.1.64)*, considered as an operator from $L^1(\Omega)$ into itself.*

1. *The operator L^ε satisfies $r_\sigma(L^\varepsilon) > 0$ and*

$$\lim_{n\to\infty} \left\| \frac{(L^\varepsilon)^n(\varphi)}{(r_\sigma(L^\varepsilon))^n} - \Pi(\varphi) \right\|_{L^1(\Omega)} = 0$$

   for every $\varphi \in L^1(\Omega)$, where Π is the finite-rank projection into $\mathrm{Ker}\left(I - \frac{L^\varepsilon}{r_\sigma(L^\varepsilon)}\right)$. Moreover Π is positivity improving.

2. *If $r_\sigma(L^\varepsilon) > 1$, then*

$$\lim_{n\to\infty} \|(L^\varepsilon)^n(\varphi)\|_{L^1(\Omega)} = \infty$$

   for every $\varphi \in L^1_+(\Omega) \setminus \{0\}$. If $r_\sigma(L^\varepsilon) < 1$, then

$$\lim_{n\to\infty} \|(L^\varepsilon)^n(\varphi)\|_{L^1(\Omega)} = 0$$

   for every $\varphi \in L^1_+(\Omega) \setminus \{0\}$.

Proof. **Step one:** since L^ε is compact and positivity improving, then $r_\sigma(L^\varepsilon) > 0$ by [314, Theorem 3] and $r_\sigma(L^\varepsilon)$ is a simple eigenvalue of L^ε (see Lemma 4.1.21). We recall that

$$L^1(\Omega) = \mathrm{Ker}\left(I - \frac{L^\varepsilon}{r_\sigma(L^\varepsilon)}\right) \oplus \mathrm{Rg}(I - \Pi).$$

Moreover the projection Π is given by the formula

$$\Pi(\varphi) = \frac{\langle \phi', \varphi \rangle}{\langle \phi', \phi \rangle} \phi$$

where ϕ and ϕ' denote respectively the eigenfunctions of L^ε and its dual $(L^\varepsilon)'$, associated to $r_\sigma(L^\varepsilon)$. Note that $r_\sigma(L^\varepsilon)$ is a pole of the resolvent of L^ε and an eigenvalue of $(L^\varepsilon)'$ by the Krein-Rutman theorem (see *e.g.* [281, Theorem 4.1.4, p. 250] and [281, Theorem 4.1.5, p. 251]). Moreover, $\phi' \gg 0$ (see *e.g.* [414, Proposition 4]). Consequently Π is positivity improving and for every $\varphi \in L^1(\Omega)$, we have

$$L^\varepsilon(\varphi) = L^\varepsilon(\Pi(\varphi)) + L^\varepsilon(I - \Pi)(\varphi) = r_\sigma(L^\varepsilon)\Pi(\varphi) + L^\varepsilon(I - \Pi)(\varphi).$$

By induction, for every $n \geq 0$, we get

$$(L^\varepsilon)^n(\varphi) = (r_\sigma(L^\varepsilon))^n \Pi(\varphi) + \left[L^\varepsilon(I - \Pi)\right]^n(\varphi).$$

Hence

$$\begin{aligned} \left\| \frac{(L^\varepsilon)^n(\varphi)}{(r_\sigma(L^\varepsilon))^n} - \Pi(\varphi) \right\|_{L^1(\Omega)} &= \frac{\|(L^\varepsilon(I - \Pi))^n(\varphi)\|_{L^1(\Omega)}}{(r_\sigma(L^\varepsilon))^n} \\ &\leq \frac{\|(L^\varepsilon(I - \Pi))^n\|_{\mathrm{Ł}(L^1(\Omega))}}{(r_\sigma(L^\varepsilon))^n} \|\varphi\|_{L^1(\Omega)}. \end{aligned}$$

On the one hand it is known (see *e.g.* [129, Theorem 1.5.4, p. 30]) that

$$\sigma(L^\varepsilon(I - \Pi)) = \sigma(L^\varepsilon) \setminus \{r_\sigma(L^\varepsilon)\},$$

and therefore

$$r_\sigma(L^\varepsilon(I - \Pi)) < r_\sigma(L^\varepsilon).$$

On the other hand, the Gelfand equality implies that

$$r_\sigma(L^\varepsilon(I - \Pi)) = \lim_{n\to\infty} \sqrt[n]{\|(L^\varepsilon(I - \Pi))^n\|_{\mathrm{Ł}(L^1(\Omega))}}$$

so that

$$\|(L^\varepsilon(I-\Pi))^n\|_{\mathrm{L}(L^1(\Omega))} \leq (r_\sigma(L^\varepsilon(I-\Pi))+\eta)^n$$

for any $\eta > 0$ and n large enough. Consequently we have

$$\lim_{n\to\infty} \left\| \frac{(L^\varepsilon)^n(\varphi)}{(r_\sigma(L^\varepsilon))^n} - \Pi(\varphi) \right\|_{L^1(\Omega)} \leq \lim_{n\to\infty} \left(\frac{r_\sigma(L^\varepsilon(I-\Pi))+\eta}{r_\sigma(L^\varepsilon)} \right)^n \|\varphi\|_{L^1(\Omega)} = 0$$

where $\eta > 0$ is chosen such that $r_\sigma(L^\varepsilon(I-\Pi))+\eta < r_\sigma(L^\varepsilon)$. This completes the proof of the first part of the lemma.

Step two: suppose first that $r_\sigma(L^\varepsilon) < 1$ and let $\varphi \in L^1_+(\Omega)$ be given. Due to the first item we have

$$0 = \limsup_{n\to\infty} \left\| \frac{(L^\varepsilon)^n(\varphi)}{(r_\sigma(L^\varepsilon))^n} - \Pi(\varphi) \right\|_{L^1(\Omega)} \geq \limsup_{n\to\infty} \left\| \frac{(L^\varepsilon)^n(\varphi)}{(r_\sigma(L^\varepsilon))^n} \right\|_{L^1(\Omega)} - \|\Pi(\varphi)\|_{L^1(\Omega)}.$$

Assume by contradiction that

$$\limsup_{n\to\infty} \|(L^\varepsilon)^n(\varphi)\|_{L^1(\Omega)} > 0.$$

Then, there exist $\eta > 0$ and a sequence $n_k \to \infty$ such that

$$\|(L^\varepsilon)^{n_k}\|_{L^1(\Omega)} \geq \eta > 0, \ \forall k \geq 0.$$

Therefore, we have

$$\frac{\eta}{(r_\sigma(L^\varepsilon))^{n_k}} \leq \left\| \frac{(L^\varepsilon)^{n_k}(\varphi)}{(r_\sigma(L^\varepsilon))^{n_k}} \right\|_{L^1(\Omega)} \leq \|\Pi(\varphi)\|_{L^1(\Omega)} + o(1) \text{ as } k \to \infty$$

which yields a contradiction.

Consider now the case where $r_\sigma(L^\varepsilon) > 1$ and let $\varphi \in L^1_+(\Omega)$ be such that $\int_\Omega \varphi(y)\mathrm{d}y > 0$. Using again the part part of the lemma, we have

$$0 = \limsup_{n\to\infty} \left\| \frac{(L^\varepsilon)^n(\varphi)}{(r_\sigma(L^\varepsilon))^n} - \Pi(\varphi) \right\|_{L^1(\Omega)} \geq \|\Pi(\varphi)\|_{L^1(\Omega)} - \limsup_{n\to\infty} \left\| \frac{(L^\varepsilon)^n(\varphi)}{(r_\sigma(L^\varepsilon))^n} \right\|_{L^1(\Omega)}.$$

Assume by contradiction that

$$\limsup_{n\to\infty} \|(L^\varepsilon)^n(\varphi)\|_{L^1(\Omega)} < \infty.$$

Then, there is $\eta > 0$ and a sequence $n_k \to \infty$ such that

$$\|(L^\varepsilon)^{n_k}\|_{L^1(\Omega)} \leq \eta < \infty, \ \forall k \geq 0.$$

Therefore, we have

$$\frac{\eta}{(r_\sigma(L^\varepsilon))^{n_k}} \geq \left\| \frac{(L^\varepsilon)^{n_k}(\varphi)}{(r_\sigma(L^\varepsilon))^{n_k}} \right\|_{L^1(\Omega)} \geq \|\Pi(\varphi)\|_{L^1(\Omega)} + o_{k\to\infty}(1),$$

which is a contradiction and item 2 is proved. This finishes the proof of Lemma 4.1.22. □

4.2 On the competitive exclusion principle for continuously distributed populations

In this section 4.2 we investigate the large time behavior of the system

$$\begin{cases} S_t(t) = \Lambda - \theta S(t) - S(t) \displaystyle\int_{\mathbb{R}^N} \alpha(x)\gamma(x) I(t, \mathrm{d}x), \ x \in \mathbb{R}^N, \\ I_t(t, \mathrm{d}x) = \big(\alpha(x)S(t) - 1\big)\gamma(x) I(t, \mathrm{d}x), \end{cases} \tag{4.2.1}$$

equipped with suitable non-negative initial data. This system of equations intervenes in theoretical ecology, in epidemiology and in genetics. In ecology, it describes the evolution of a population of individuals with density I that compete for a single limited resource with density $S = S(t)$. In epidemiology, this system describes the evolution of the number of susceptible S and of the density of infected individuals I who have been contaminated by different pathogen variants of some disease. In both cases, the density of individuals I is represented by a measure on the space $\mathbb{R}^N$, for some integer $N > 0$, of phenotypic traits. Representing the density I by a measure is natural in this context as one expects concentration properties of the density on one or several optimal traits as time goes to infinity. Note also that this model does not take into account mutations but only pure competition (or selection).

In the context of ecology, phenotypical traits are related to the competitors and how they interact with the resource via the continuous functions α and γ, while the last two parameters $\Lambda > 0$ and $\theta > 0$ are positive constants which encode the renewal and disappearance rates of the resource. The "Competitive exclusion principle" states that "Complete competitors cannot coexist", which in particular means that given a number of species competing for the same resource in the same place, only one can survive in the long run. This idea was already present to some extent in the book of Darwin, and is sometimes referred to as Gause's law [201]. The aim of the present section 4.2 is to investigate this principle in the case of a continuously distributed initial population. We will show in particular that, while it is true that the species have to maximize the fitness function in order to survive, the natural process of competition is not selecting a unique species but several species may coexist as long as they maximize the fitness function. In many cases it is possible to compute the eventual repartition of the surviving competitors. In some cases, species that maximize the fitness may still get extinct if the initial population is not sufficient, and we provide a way to characterize when this unexpected extinction happens. Considering a situation where $\mathcal{R}_0$ has more than one maximum at the same exact level may appear artificial but is not without biological interest. Indeed, the long-time behavior that we observe in these borderline cases can persist in transient time upon perturbing the function R_0. For example in the epidemiological context of [133], it has been observed that a strain 1 with a higher value of γ and a slightly lower $\mathcal{R}_0$ value than a strain 2 may nevertheless be dominant for some time, see Figure 4.2.8. These borderline cases shed light on our understanding of the transient dynamics, see also [85] where we explicit transient dynamics for a related evolutionary model depending on the local flatness of the fitness function.

This problem of survival of competitors has attracted the attention of mathematicians since the '70s and many studies have proved this property in many different contexts – let us mention the seminal works of Hsu, Hubbell and Waltman [218] and Hsu [217], followed by Armstrong and McGehee [17], Butler and Wolkowicz [89], Wolkowicz and Lu [401], Hsu, Smith and Waltman [216], Wolkowicz and Xia [402], Li [251], and more recently Rapaport and Veruete [333], to cite a few – and also disproved in other contexts, for instance in fluctuating environments, see Cushing [126] and Smith [360].

A common feature of the above-mentioned studies on the competitive exclusion principle is that they all focus on *finite* systems representing the different species competing for the resource. Yet quantitative traits such as the virulence or the transmission rate of a pathogen, the life expectancy of an individual and more generally any observable feature such as height, weight, muscular mass, speed, size of legs, etc. are naturally represented using continuous variables. Such a description of a population seems highly relevant and has been used mostly in modelling studies involving some kind of evolution [275, 272, 34, 33, 265, 266, 72, 331, P4]

A few studies actually focus on pure competition for a continuously structured population. Let us mention the work of Desvillettes, Mischler, Jabin and Raoul [139], and later Jabin and Raoul [225] and Raoul [332], who studied the logistic equation

$$\partial_t f(t,x) = \left(a(x) - \int b(x,y) f(y) \right) f(t,x),$$

and studied more precisely the asymptotic behavior of the solutions $f = f(t,x)$ when the initial condition is a Radon measure. Cañizo, Carrillo and Cuadrado [97] proved the well-posedness of several evolution equations in the sense of measures. Ackleh, Cleveland and Thieme devoted a part of their study [2] to purely competitive dynamics. Here the focus are equations of the type

$$\mu'(t)(E) = \int_E \big[B(\bar{\mu}(t),q) - D(\bar{\mu}(t),q)\big]\mu(t)(\mathrm{d}q),$$

where μ is a Radon measure on a space of strategies Q and $\bar{\mu}(t) = \mu(t)(Q)$. They show a persistence property for such a model and give more precise statements on the asymptotic behavior of the total mass; under the assumption that a unique strategy maximizing the carrying capacity, they show the convergence in the sense of measures to a Dirac mass concentrated on this strategy.

An important example of a biological system which allows the experimenter to observe the competitive exclusion principle is the so-called *chemostat*, a device in which living organisms (like cells, yeasts, bacteria...) are cultivated in a controlled environment where the in- and outflow of nutrients are monitored. Systems of the same type as (4.2.1) (as most systems in the literature cited above) are particularly well-adapted to the modeling of a population in a chemostat. We refer to the monograph of Smith and Waltman [363] for a detailed work on mathematical models for the chemostat. Recently, a lot of interest has been given to chemostat models as a mean to study the Darwinian evolution of a population, that is, the changes in frequency of common characteristics due to the processes of selection and mutation. An important difference of chemostat models is that they usually assume Michaelis-Menten functional response, contrary to our system where the functional response if linear.

The connections between chemostat and epidemic models has been remarked in [362], where an extensive review of the literature is conducted. A competitive exclusion principle for epidemic models has been established by Bremermann and Thieme [78]. The asymptotic behavior of epidemic models of SIR type has been investigated by Korobeinikov and Wake [243], Korobeinikov and Maini [242], Korobeinikov [239, 240, 241], McCluskey [279, 280], in the context of systems of ordinary differential equations. Our motivation for the study of System (4.2.1) comes from a model of Darwinian evolution of spore-producing plant pathogens [145, 85, P6]. The present work represents a first step (without mutation) towards a generalization of this previous model to cases where the mortality rate of the infected population, which is represented by function γ in (4.2.1), varies from one strain to another.

We add to the existing literature on systems related to (4.2.1) by considering the case when the initial condition $I_0(\mathrm{d}x)$ is a Radon measure. Considering measures as initial data is not a gratuitous generality. Indeed as we will show in Theorem 4.2.2, initial conditions in the usual space $L^1(\mathbb{R}^N)$ will converge, in many cases, towards a singular Radon measure. Therefore it is necessary to study the equation in a space of measures in order to investigate the long-time behavior of the solutions to (4.2.1). By doing so we were able to include the case of finite systems of ODE into our framework, see Section 4.2.1.2 below. Those results are extended to the case of countably many equations under the structural requirement that the coefficients converge to a limit. The system behaves as predicted and the density I converges towards a Dirac measure at some x^* when the basic reproduction number (fitness) associated to the phenotypic value x defined as $\mathcal{R}_0(x) := \frac{\Lambda}{\theta}\alpha(x)$ has a unique maximum on the support of I_0 and the initial data has a positive mass on the maximizing value x^*, see Section 4.2.1.3. The situation is more complex when this assumption is removed. In particular, the asymptotic behaviour of the solution strongly depends on the initial condition I_0, which may be related to the absence of mutations in the model. When the density of the initial condition vanished near the maximizing set of $\mathcal{R}_0(I_0)$, we uncovered a subtle dependency on the initial data and on the function γ of (4.2.1) (Section 4.2.1.3). It may happen, if the initial density decreases sufficiently fast near the maximizing set of the basic reproduction number, that the equilibrium reached by the system is different from the one predicted by heuristic arguments on the fitness function. This shows that the dynamics of the system with continuous phenotypic traits $x \in \mathbb{R}^N$ is far more rich than the one of discrete models.

4.2.1 Main results

In this section 4.2.1 we state and discuss the main results we shall prove in this note related to the large time behavior of (4.2.1). Before going to our results, we introduce some notations that will be used along this work. For a Borel set $K \subset \mathbb{R}^N$, we denote by $\mathcal{M}(K)$ the set of the signed Radon measures on K of finite mass. Recall that $\mathcal{M}(K)$ is a Banach space when endowed with the *absolute variation norm* given by:

$$\|\mu\|_{AV} = |\mu|(K),\ \forall \mu \in \mathcal{M}(K).$$

We also denote by $\mathcal{M}_+(K)$ the set of the finite nonnegative measures on K. Observe that one has $\mathcal{M}_+(K) \subset \mathcal{M}(K)$ and $\mathcal{M}_+(K)$ is a closed subset of $\mathcal{M}(K)$ for the norm topology of $\|\cdot\|_{AV}$. An alternate topology on $\mathcal{M}(K)$ can be defined by the so-called Kantorovitch-Rubinstein norm (see [63, Vol. II, Chap. 8.3 p. 191]),

$$\|\mu\|_0 := \sup\left\{\int f \mathrm{d}\mu \,:\, f \in \mathrm{Lip}_1(K), \sup_{x\in K} |f(x)| \le 1\right\},$$

wherein we have set

$$\mathrm{Lip}_1(K) := \left\{f \in BC(K) \,:\, |f(x) - f(y)| \le \|x-y\|,\ \forall (x,y) \in K^2\right\}.$$

Here (and below) $BC(K)$ denotes the set of the continuous and bounded functions from K into $\mathbb{R}$. Let us recall (see for instance [63, Theorem 8.3.2]) that the metric generated by $\|\cdot\|_0$ on $\mathcal{M}_+(K)$ is equivalent on this set to the weak topology obtained by identifying $\mathcal{M}(K)$ to the dual space of $BC(K)$. Note however that this equivalence is true only for $\mathcal{M}_+(K)$ and cannot be extended to $\mathcal{M}(K)$ since the latter space is not (in general) complete for the metric generated by $\|\cdot\|_0$. We denote by d_0 this metric on $\mathcal{M}_+(K)$, that is

$$d_0(\mu,\nu) := \|\mu - \nu\|_0 \text{ for all } \mu,\nu \in \mathcal{M}_+(K). \tag{4.2.2}$$

Now along this note we fix $I_0 = I_0(\mathrm{d}x) \in \mathcal{M}_+(\mathbb{R}^N)$.
About the parameters arising in (4.2.1) our main assumption reads as follows.

Assumption 4.2.1. The constants $\Lambda > 0$ and $\theta > 0$ are given. The functions $\alpha(x)$ and $\gamma(x)$ are continuous from $\mathbb{R}^N$ into $\mathbb{R}$ and there exist positive constants α^∞ and $\gamma_0 < \gamma^\infty$ such that

$$\alpha(x) \le \alpha^\infty, \qquad 0 < \gamma_0 \le \gamma(x) \le \gamma^\infty \qquad \text{for all } x \in \mathbb{R}^N.$$

Finally, define $\alpha^* := \sup_{x\in \mathrm{supp}\, I_0} \alpha(x)$. We assume that the set

$$L_\varepsilon(I_0) := \{\alpha \ge \alpha^* - \varepsilon\} \cap \mathrm{supp}\, I_0 = \{x \in \mathrm{supp}\, I_0 \,:\, \alpha(x) \ge \alpha^* - \varepsilon\}$$

is bounded when $\varepsilon > 0$ is sufficiently small.

Let us observe that if $S_0 \ge 0$ then (4.2.1) equipped with the initial data $S(0) = S_0$ and $I(0,\mathrm{d}x) = I_0(\mathrm{d}x)$ has a unique globally defined solution $S(t) \ge 0$ and $I(t,\mathrm{d}x) \in \mathcal{M}_+(\mathbb{R}^N)$ for all $t \ge 0$. In addition I is given by

$$I(t,\mathrm{d}x) = \exp\left(\gamma(x)\left(\alpha(x)\int_0^t S(s)\mathrm{d}s - t\right)\right) I_0(\mathrm{d}x).$$

The above formula ensures that $\mathrm{supp}\, I(t,\cdot) = \mathrm{supp}\, I_0$ for all $t \ge 0$. And to describe the large time behavior of I, we will use the values of α and γ on the support of I_0. Due to the above remark and since I_0 is given and fixed, along this section 4.2, for any $y \in \mathbb{R}$ we write

$$\alpha^{-1}(y) = \{x \in \mathrm{supp}\,(I_0) :\ \alpha(x) = y\} \subset \mathrm{supp}\,(I_0). \tag{4.2.3}$$

We also define the two quantities $\alpha^* \ge 0$ and $\mathcal{R}_0(I_0)$ by

$$\alpha^* =: \sup_{x\in \mathrm{supp}\, I_0} \alpha(x) \text{ and } \mathcal{R}_0(I_0) := \frac{\Lambda}{\theta}\alpha^*. \tag{4.2.4}$$

We now split our main results into several parts. We first derive very general results about the large time behavior of the solution (S,I) of (4.2.1) when I_0 is an arbitrary Radon measure. We roughly show that $I(t,\mathrm{d}x)$ concentrates on the points that maximize both α and γ. We then apply this result to consider the case where $I_0(\mathrm{d}x)$ is a finite or countable sum of Dirac masses. We continue our investigations with an absolutely continuous (with respect to Lebesgue measure) initial measure and a finite set $\alpha^{-1}(\alpha^*)$. In that setting we are able to fully characterize the points where the measure $I(t,\mathrm{d}x)$ concentrates as $t \to \infty$.

4.2.1.1 General results for measure-valued initial data

As mentioned above this section 4.2 is concerned with the large time behavior of the solution (S, I) of (4.2.1) where the initial measure $I_0(\mathrm{d}x)$ is an arbitrary Radon measure. Using the above notations our first result reads as follows.

Theorem 4.2.2 (Asymptotic behavior of measure-valued initial data)**.** *Let Assumption 4.2.1 be satisfied. Let $S_0 \geq 0$ be given and denote by $(S(t), I(t, \mathrm{d}x))$ the solution of (4.2.1) equipped with the initial data $S(0) = S_0$ and $I(0, \mathrm{d}x) = I_0(\mathrm{d}x)$. Recalling (4.2.4), suppose that $\mathcal{R}_0(I_0) > 1$. We distinguish two cases depending on the measure of this set w.r.t. I_0:*

i) If $I_0\big(\alpha^{-1}(\alpha^*)\big) > 0$, then one has

$$S(t) \xrightarrow[t\to+\infty]{} \frac{1}{\alpha^*} \text{ and } I(t, \mathrm{d}x) \xrightarrow[t\to+\infty]{} I^*_\infty(\mathrm{d}x) := \mathbb{1}_{\alpha^{-1}(\alpha^*)}(x) e^{\tau\gamma(x)} I_0(\mathrm{d}x),$$

where $\tau \in \mathbb{R}$ denotes the unique solution of the equation

$$\int_{\mathbb{R}^N} \gamma(x) \mathbb{1}_{\alpha^{-1}(\alpha^*)}(x) e^{\tau\gamma(x)} I_0(\mathrm{d}x) = \frac{\theta}{\alpha^*}\big(\mathcal{R}_0 - 1\big).$$

The convergence of $I(t, \mathrm{d}x)$ to $I^*_\infty(\mathrm{d}x)$ holds in the absolute variation norm $\|\cdot\|_{AV}$.

ii) If $I_0\big(\alpha^{-1}(\alpha^*)\big) = 0$, then one has $S(t) \to \frac{1}{\alpha^*}$ and $I(t, \mathrm{d}x)$ is uniformly persistent, namely

$$\liminf_{t\to+\infty} \int_{\mathbb{R}^N} I(t, \mathrm{d}x) > 0.$$

Moreover $I(t, \mathrm{d}x)$ is asymptotically concentrated as $t \to \infty$ on the set $\alpha^{-1}(\alpha^*)$, in the sense that

$$d_0\left(I(t, \mathrm{d}x), \mathcal{M}_+(\alpha^{-1}(\alpha^*))\right) \xrightarrow[t\to+\infty]{} 0,$$

where d_0 is the Kantorovitch-Rubinstein distance.

We continue our general result by showing that under additional properties for the initial measure I_0, the function $I(t, \mathrm{d}x)$ concentrates in the large times on the set of the points in $\alpha^{-1}(\alpha^*)$ that maximize the function $\gamma = \gamma(x)$.

The additional hypothesis for the initial measure $I_0(\mathrm{d}x)$ are expressed in term of some properties of its disintegration measure with respect to the function α. We refer to the book of Bourbaki [73, VI, §3, Theorem 1 p. 418] for a proof of the disintegration Theorem 4.2.35 which is recalled in Appendix 4.2.6.

Let $A(\mathrm{d}y)$ be the image of $I_0(\mathrm{d}x)$ under the continuous mapping $\alpha : \mathbb{R}^N \to \mathbb{R}$, then there exists a family of nonnegative measures $I_0(y, \mathrm{d}x)$ (the disintegration of I_0 with respect to α) such that for almost every $y \in \alpha(\operatorname{supp} I_0)$ with respect to A we have:

$$\operatorname{supp} I_0(y, \mathrm{d}x) \subset \alpha^{-1}(y), \quad \int_{\alpha^{-1}(y)} I_0(y, \mathrm{d}x) = 1 \text{ and } I_0(\mathrm{d}x) = \int I_0(y, \mathrm{d}x) A(\mathrm{d}y) \tag{4.2.5}$$

wherein the last equality means that

$$\int_{\mathbb{R}^N} f(x) I_0(\mathrm{d}x) = \int_{y\in\mathbb{R}} \int_{\alpha^{-1}(y)} f(x) I_0(y, \mathrm{d}x) A(\mathrm{d}y) \text{ for all } f \in BC(\mathbb{R}^N).$$

Note that, by definition, the measure A is supported on the set $\alpha(\operatorname{supp} I_0)$.

Remark 4.2.3 (Important example)**.** Suppose that $I_0 \in L^1(\mathbb{R}^n)$. Since we restrict to measures which are absolutely continuous with respect to the Lebesgue measure here, with a small abuse of notation we will omit the element $\mathrm{d}x$ when the context is clear. Assume that α is Lipschitz continuous on $\mathbb{R}^N$ and that

$$\frac{I_0(x)}{|\nabla\alpha(x)|} \in L^1(\mathbb{R}^N). \tag{4.2.6}$$

The coarea formula implies that, for all $g \in L^1(\mathbb{R}^N)$, we have

$$\int_{\mathbb{R}^N} g(x)|\nabla\alpha(x)|\mathrm{d}x = \int_{\mathbb{R}} \int_{\alpha^{-1}(y)} g(x)\mathcal{H}_{N-1}(\mathrm{d}x)\mathrm{d}y,$$

where $\mathcal{H}_{N-1}(\mathrm{d}x)$ is the $(N-1)$-dimensional Hausdorff measure (see Federer [166, §3.2]).

Therefore if $g(x) = f(x)\frac{I_0(x)}{|\nabla\alpha(x)|}$ we get

$$\int_{\mathbb{R}^N} f(x)I_0(x)\mathrm{d}x = \int_{\mathbb{R}} \int_{\alpha^{-1}(y)} f(x)\frac{I_0(x)}{|\nabla\alpha(x)|}\mathcal{H}_{N-1}(\mathrm{d}x)\mathrm{d}y, \tag{4.2.7}$$

and if moreover $f(x) = \varphi(\alpha(x))$ we get

$$\int_{\mathbb{R}} \varphi(y)A(\mathrm{d}y) = \int_{\mathbb{R}^N} \varphi(\alpha(x))I_0(x)\mathrm{d}x = \int_{\mathbb{R}} \varphi(y) \int_{\alpha^{-1}(y)} \frac{I_0(x)}{|\nabla\alpha(x)|}\mathcal{H}_{N-1}(\mathrm{d}x)\mathrm{d}y,$$

where we recall that $A(\mathrm{d}y)$ is the image measure of $I_0(\mathrm{d}x)$ through α. Therefore we have an explicit expression for $A(\mathrm{d}y)$:

$$A(\mathrm{d}y) = \int_{\alpha^{-1}(y)} \frac{I_0(x)}{|\nabla\alpha(x)|}\mathcal{H}_{N-1}(\mathrm{d}x)\mathrm{d}y \tag{4.2.8}$$

and (recalling (4.2.7)) we deduce the following explicit disintegration of I_0:

$$I_0(y, \mathrm{d}x) = \frac{\mathbb{1}_{x\in\alpha^{-1}(y)}\frac{I_0(x)}{|\nabla\alpha(x)|}\mathcal{H}_{N-1}(\mathrm{d}x)}{\int_{\alpha^{-1}(y)}\frac{I_0(z)}{|\nabla\alpha(z)|}\mathcal{H}_{N-1}(\mathrm{d}z)}. \tag{4.2.9}$$

Equations (4.2.8) and (4.2.9) give an explicit formula for the disintegration introduced in (4.2.5).

Remark 4.2.4. Suppose that α is a C^2 function with no critical point in $\operatorname{supp} I_0$ except for a finite number of regular maxima (in the sense that the bilinear form $D^2\alpha(x)$ is non-degenerate at each maximum). This is a typical situation. Then assumption (4.2.6) in Remark 4.2.3 is automatically satisfied if $N \geq 3$ and $I_0 \in L^\infty(\mathbb{R}^N)$. If $N = 2$ then a sufficient condition to satisfy (4.2.6) with $I_0 \in L^\infty(\mathbb{R}^N)$ should involve I_0 vanishing sufficiently fast in the neighborhood of each maximum of α.

We shall also make use, for all y $A-$almost everywhere, of the disintegration measure of $I_0(y, \mathrm{d}x)$ with respect to the function γ, as follows

$$I_0(y, \mathrm{d}x) = \int_{z\in\gamma(\alpha^{-1}(y))} I_0^{\alpha,\gamma}(y, z, \mathrm{d}x)I_0^\alpha(y, \mathrm{d}z),$$

that allows to the following reformulation of $I_0(\mathrm{d}x)$:

$$I_0(\mathrm{d}x) = \int_{y\in\mathbb{R}} \int_{z\in\gamma(\alpha^{-1}(y))} I_0^{\alpha,\gamma}(y, z, \mathrm{d}x)I_0^\alpha(y, \mathrm{d}z)A(\mathrm{d}y).$$

Now equipped with this disintegration of I_0 with respect to α we are now able to state our regularity assumption to derive more refine concentration information in the case where $I_0\left(\alpha^{-1}(\alpha^*)\right) = 0$.

Assumption 4.2.5 (Regularity with respect to α, γ)**.** Recalling (4.2.3), assume that $\alpha^{-1}(\alpha^*) \neq \emptyset$ and define $\gamma^* > 0$ by

$$\gamma^* := \sup_{x\in\alpha^{-1}(\alpha^*)} \gamma(x). \tag{4.2.10}$$

We assume that, for each value $\bar\gamma < \gamma^*$ there exist constants $\delta > 0$ and $m > 0$ such that

$$m \leq \int_{\gamma^{-1}([\bar\gamma,\gamma^*])\cap\alpha^{-1}(y)} I_0(y, \mathrm{d}x) \text{ for } A\text{-almost every } y \in (\alpha^* - \delta, \alpha^*].$$

Remark 4.2.6. The above assumption means that the initial measure $I_0(\mathrm{d}x)$ is uniformly positive in a small neighborhood of $\alpha^{-1}(\alpha^*)$. For instance, if the assumptions of Remark 4.2.3 are satisfied and if there exists an open set U containing $\alpha^{-1}(\alpha^*) \cap \gamma^{-1}(\gamma^*)$ on which $I_0(x)$ is almost everywhere uniformly positive, then Assumption 4.2.5 is automatically satisfied.

The next proposition ensures that, when the initial measure I_0 satisfies Assumption 4.2.5, then the function $I(t,\mathrm{d}x)$ concentrates on $\alpha^{-1}(\alpha^*)\cap\gamma^{-1}(\gamma^*)$.

Proposition 4.2.7. *Under the same assumptions as in Theorem 4.2.2, assume that* $I_0\left(\alpha^{-1}(\alpha^*)\right)=0$ *and let us furthermore assume that Assumption 4.2.5 holds, then recalling that* γ^* *is defined in* (4.2.10) *one has*

$$d_0\left(I(t,\mathrm{d}x),\mathcal{M}_+(\alpha^{-1}(\alpha^*)\cap\gamma^{-1}(\gamma^*))\right)\xrightarrow[t\to+\infty]{}0,$$

as well as the following asymptotic mass

$$\int_{\mathbb{R}^N} I(t,\mathrm{d}x)\xrightarrow[t\to+\infty]{}\frac{\theta}{\alpha^*\gamma^*}\big(\mathcal{R}_0(I_0)-1\big).$$

Let $U\subset\mathbb{R}^N$ *be a Borel set such that* $U\cap\alpha^{-1}(\alpha^*)\cap\gamma^{-1}(\gamma^*)\neq\varnothing$ *and*

$$\liminf_{\varepsilon\to 0}\ \operatorname*{ess\,inf}_{\alpha^*-\varepsilon\le y\le\alpha^*}^{A(\mathrm{d}y)}\ \operatorname*{ess\,inf}_{\gamma^*-\varepsilon\le z\le\gamma^*}^{I_0^\alpha(y,\mathrm{d}z)}\int_U I_0^{\alpha,\gamma}(y,z,\mathrm{d}x)>0,$$

then the following persistence occurs

$$\liminf_{t\to\infty}\int_U I(t,\mathrm{d}x)>0.$$

We now explore some numerical computations of (4.2.1) with various configurations.

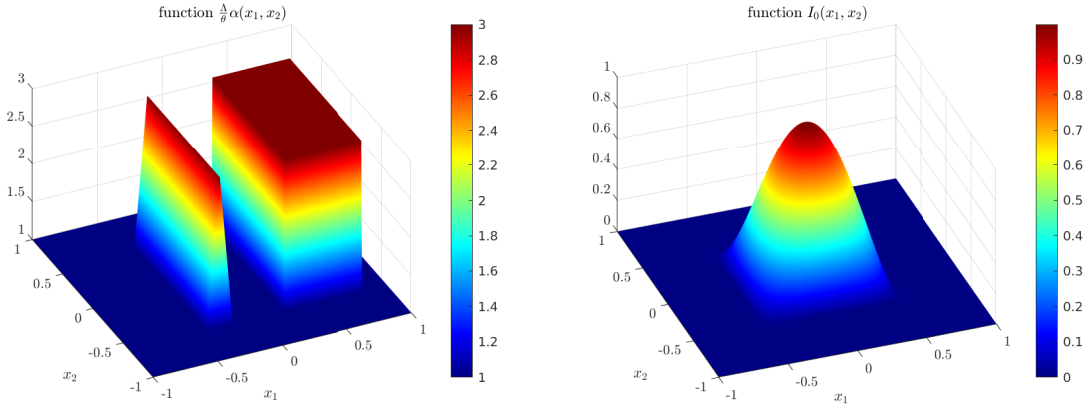

Figure 4.2.1: Illustration of Theorem 4.2.2 in the case i), *i.e.*, when $I_0\big(\alpha^{-1}(\alpha^*)\big)>0$. Parameters of this simulation are: $\Lambda=2$, $\theta=1$, $\alpha(x)=0.5+\big(\mathbb{T}_{[-0.4,-0.2]}(x_1)+\mathbb{1}_{[0.2,0.8]}(x_1)\big)\,\mathbb{1}_{[-0.6,0.6]}(x_2)$ where $x=(x_1,x_2)\in\mathbb{R}^2$ and $\mathbb{T}_{[-0.4,-0.2]}$ is the triangular function of height one and support $[-0.4,-0.2]$, and $\gamma=\frac{1}{2\alpha}$. Initial condition is given by $I_0(\mathrm{d}x)=I_0(x_1,x_2)\,\mathrm{d}x$ where $I_0(x_1,x_2)=\mathbb{1}_{[-0.5,0.5]}(x_1)\cos(\pi x_1)\mathbb{1}_{[-0.5,0.5]}(x_2)\cos(\pi x_2)$. In particular, we have $\alpha^*=3/2$ and $\alpha^{-1}(\alpha^*)=(\{-0.3\}\cup[0.2,0.8])\times[-0.6,0.6]$.

4.2.1.2 The case of discrete systems

In this section 4.2.1.2 we propose an application of the general result, namely Theorem 4.2.2, to the case of discrete systems. We start with the case of *finite* systems, *i.e.*, the case when system (4.2.1) can be written as follows:

$$\begin{cases}\dfrac{\mathrm{d}}{\mathrm{d}t}S(t)=\Lambda-\theta S(t)-S(t)\big(\alpha_1\gamma_1I^1(t)+\alpha_2\gamma_2I^2(t)+\ldots+\alpha_n\gamma_nI^n(t)\big)\\ \dfrac{\mathrm{d}}{\mathrm{d}t}I^1(t)=\big(\alpha_1S(t)-1\big)\gamma_1I^1(t)\\ \dfrac{\mathrm{d}}{\mathrm{d}t}I^2(t)=\big(\alpha_2S(t)-1\big)\gamma_2I^2(t)\\ \qquad\vdots\\ \dfrac{\mathrm{d}}{\mathrm{d}t}I^n(t)=\big(\alpha_nS(t)-1\big)\gamma_nI^n(t).\end{cases}\tag{4.2.11}$$

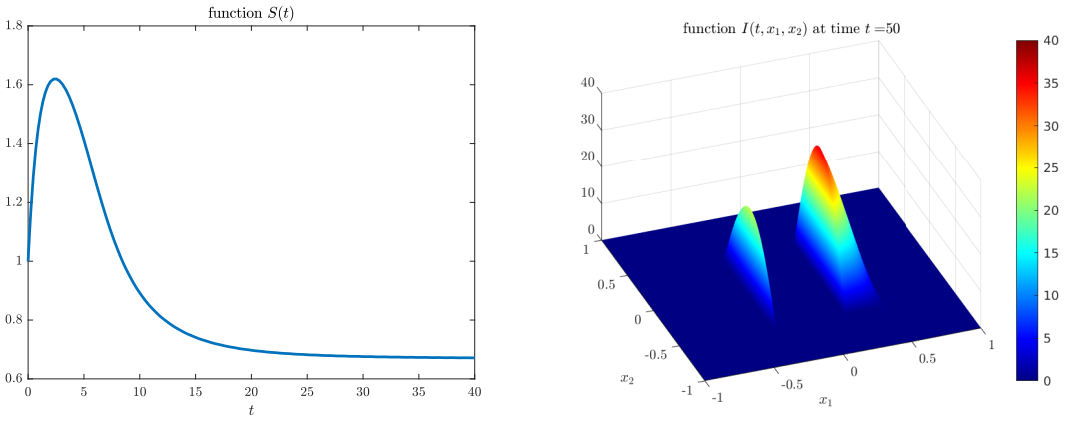

Figure 4.2.2: (continued from Fig. 4.2.1) Illustration of Theorem 4.2.2 in the case i), *i.e.*, when $I_0\big(\alpha^{-1}(\alpha^*)\big) > 0$. Function $t \to S(t)$ converges towards $1/\alpha^* = 2/3$ and function $x \to I(t,x)$ at time $t = 50$ is asymptotically concentrated on $\alpha^{-1}(\alpha^*) = (\{-0.3\} \cup [0.2, 0.8]) \times [-0.6, 0.6]$.

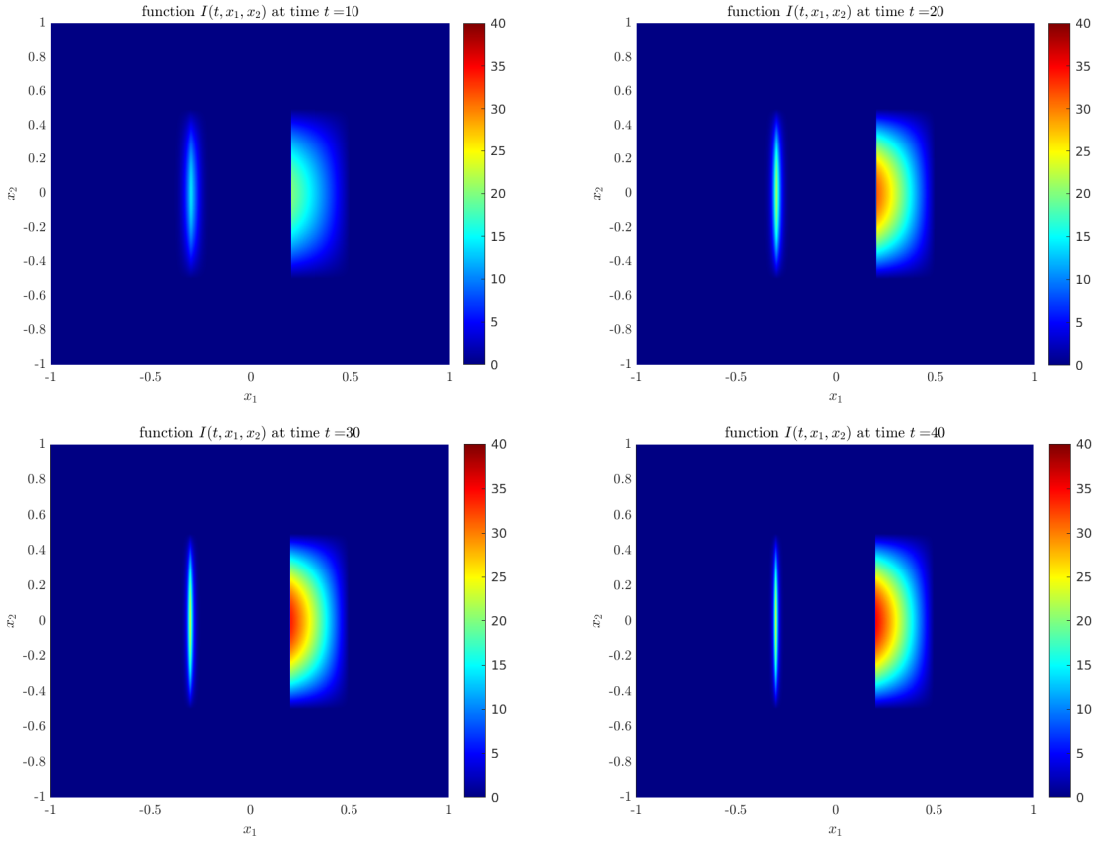

Figure 4.2.3: Illustration of Theorem 4.2.2 in the case i), *i.e.*, when $I_0\big(\alpha^{-1}(\alpha^*)\big) > 0$. Function $x \to I(t,x)$ at time $t = 10, 20, 30$ and 40. The function I remains bounded in this case.

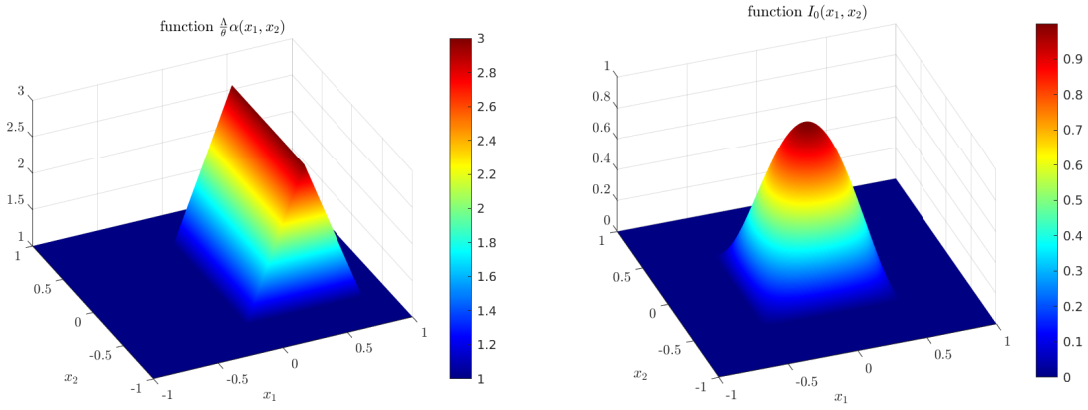

Figure 4.2.4: Illustration of Theorem 4.2.2 in the case ii), *i.e.*, when $I_0\big(\alpha^{-1}(\alpha^*)\big) = 0$. Parameters of this simulation are: $\Lambda = 2$, $\theta = 1$, $\alpha(x) = 0.5 + \mathbb{T}_{[-0.1,0.8]}(x_1)\mathbb{1}_{[-0.6,0.6]}(x_2)$ where $x = (x_1, x_2) \in \mathbb{R}^2$ and $\mathbb{T}_{[-0.1,0.8]}$ is the triangular function of height one and support $[-0.1, 0.8]$, $\gamma = \frac{1}{2\alpha}$. Initial condition is given by $I_0(\mathrm{d}x) = I_0(x_1, x_2)\,\mathrm{d}x$ where $I_0(x) = \mathbb{1}_{[-0.5,0.5]}(x_1)\cos(\pi x_1)\mathbb{1}_{[-0.5,0.5]}(x_2)\cos(\pi x_2)$. In particular, $\alpha^* = 3/2$ and $\alpha^{-1}(\alpha^*) = \{0.35\} \times [-0.6, 0.6]$.

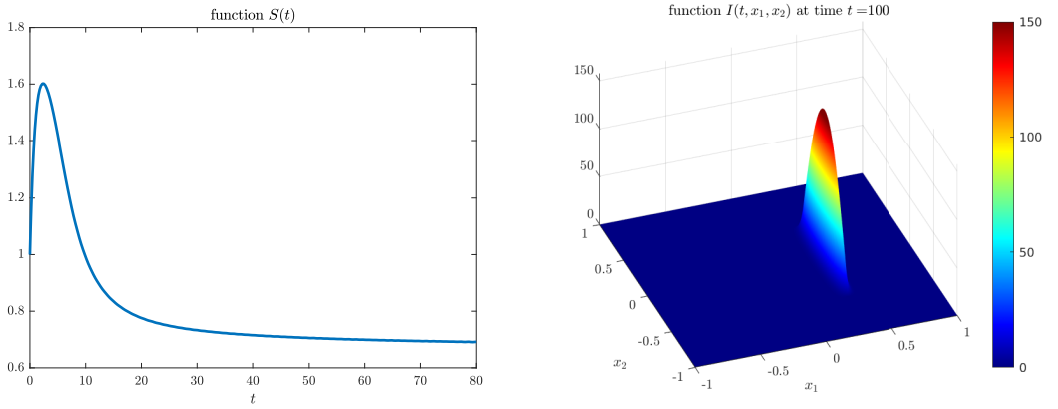

Figure 4.2.5: (continued from Fig. 4.2.4) Illustration of Theorem 4.2.2 in the case ii), *i.e.* when $I_0\big(\alpha^{-1}(\alpha^*)\big) = 0$. Function $t \to S(t)$ converges towards $1/\alpha^* = 2/3$. Function $x \to I(t, x)$ at time $t = 100$ is asymptotically concentrated on $\alpha^{-1}(\alpha^*) = \{0.35\} \times [-0.6, 0.6]$.

For the above system, we can completely characterize the asymptotic behavior of the population. To that aim we define the basic reproductive number (in the ecological or epidemiological sense) for species i as follows:

$$\mathcal{R}_0^i := \frac{\Lambda}{\theta}\alpha_i, \qquad i = 1, \ldots, n.$$

Then we can show that the only species that do not get extinct are the ones for which $\mathcal{R}_0^i$, $i = 1, \ldots, n$, is maximal and strictly greater than one.
In the case when several species have the same basic maximal reproductive number, then these species all survive and the asymptotic distribution can be computed explicitly as a function of the initial data I_0^i and of the values γ_i.

Theorem 4.2.8 (Asymptotic behavior of finite systems)**.** *Let $n \geq 1$ and $\alpha_1, \ldots, \alpha_n$ and $\gamma_1 > 0, \ldots, \gamma_n > 0$ be given. Set*

$$\alpha^* := \max\{\alpha_1, \cdots, \alpha_n\},$$

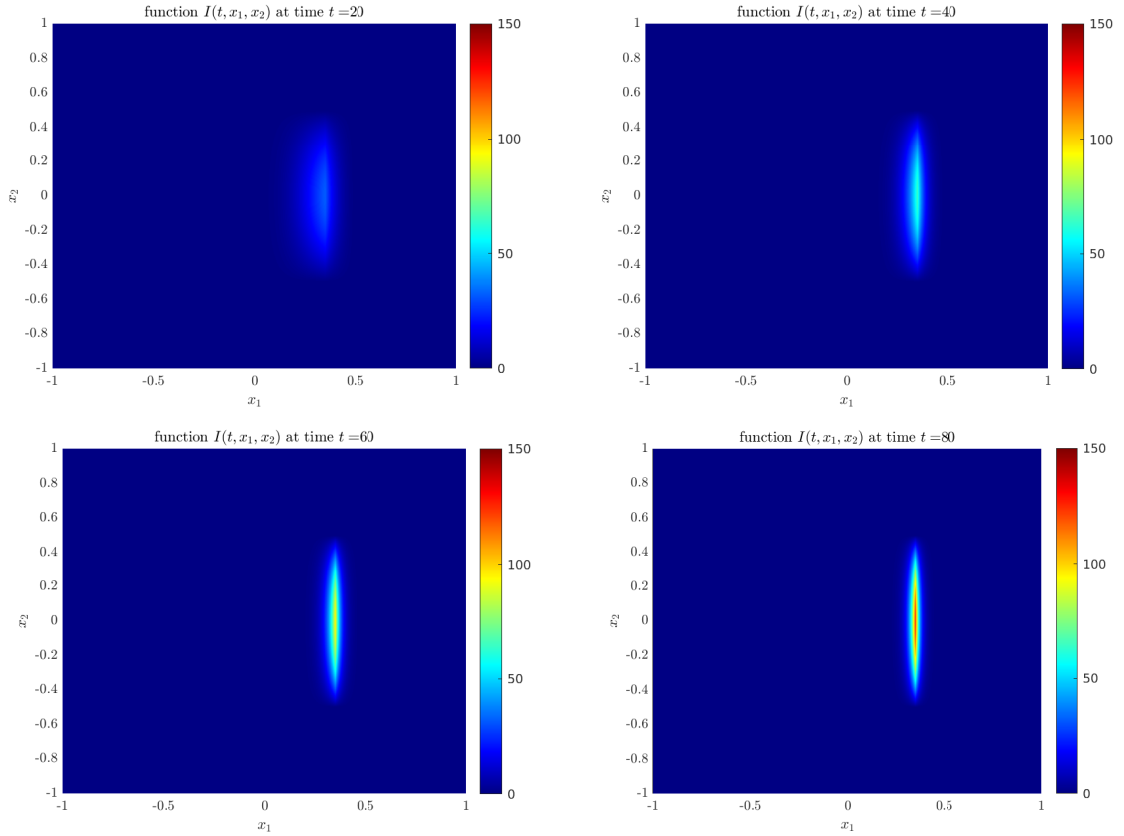

Figure 4.2.6: Illustration of Theorem 4.2.2 in the case ii), *i.e.*, when $I_0\big(\alpha^{-1}(\alpha^*)\big) = 0$. Function $x \to I(t,x)$ at time $t = 20, 40, 60$ and 80. The function I asymptotically converges towards a singular measure.

and assume that

$$\mathcal{R}_0^* := \frac{\Lambda}{\theta}\alpha^* = \max\left\{\mathcal{R}_0^1, \cdots, \mathcal{R}_0^n\right\} > 1.$$

Then, for any initial data $S_0 \geq 0$, $I_0^1 > 0, \cdots, I_0^n > 0$, *the corresponding solution to* (4.2.11) *converges in the large times to* $\big(S_\infty, \big(I_\infty^1, \cdots, I_\infty^n\big)\big)$ *given by*

$$S_\infty = \frac{1}{\alpha^*} \text{ and } I_\infty^i = \begin{cases} 0 & \text{if } \mathcal{R}_0^i < \mathcal{R}_0^*, \\ e^{\tau\gamma_i} I_0^i & \text{if } \mathcal{R}_0^i = \mathcal{R}_0^*, \end{cases} \text{ for all } i = 1, \ldots, n,$$

wherein the constant $\tau \in \mathbb{R}$ *is defined as the unique solution of the equation:*

$$\sum_{\{i\,:\,\mathcal{R}_0^i = \mathcal{R}_0^*\}} \gamma_i I_0^i \, e^{\tau\gamma_i} = \frac{\theta}{\alpha^*}(\mathcal{R}_0 - 1).$$

Note that in the case when the interaction of the species with the resource is described by the Michaelis-Menten kinetics instead of the mass action law, or when the growth of the resource obeys a logistic law (Hsu [217]), a similar result was already present in Hsu, Hubbell and Waltman [218] and Hsu [217], including the case when several species have the exact same reproduction number (or fitness) $\mathcal{R}_0^i$.

In the case of a *countable* system we can still provide a complete description when both α and γ converge to a limit near $+\infty$. We now investigate the following system

$$\begin{cases} \dfrac{\mathrm{d}}{\mathrm{d}t} S(t) = \Lambda - \theta S(t) - S(t) \displaystyle\sum_{i \in \mathbb{N}} \alpha_i \gamma_i I_i(t), \\ \dfrac{\mathrm{d}}{\mathrm{d}t} I^i(t) = \big(\alpha_i S(t) - 1\big)\gamma_i I^i(t), \qquad\qquad \text{for } i \in \mathbb{N}, \end{cases} \tag{4.2.12}$$

supplemented with some initial data

$$S(0) = S_0 > 0 \text{ and } I^i(0) = I_0^i > 0,\ \forall i \in \mathbb{N} \text{ with } \sum_{i\in\mathbb{N}} I_0^i < \infty. \tag{4.2.13}$$

Since components of (4.2.12) starting from a zero initial data will stay equal to zero in positive time, they can be removed from the system without impacting the dynamics and we may without loss of generality assume that $I_0^i > 0$ for all $i \in \mathbb{N}$ (as we did in (4.2.13)).

In the sequel we denote by $\big(S(t), I^i(t)\big)$ be the corresponding solution to (4.2.12) with initial data $S(0) = S_0$ and $I^i(0) = I_0^i$ for all $i \in \mathbb{N}$.

Theorem 4.2.9 (Asymptotic behavior of discrete systems)**.** *Let $(\alpha_i)_{i\in\mathbb{N}}$ and $(\gamma_i)_{i\in\mathbb{N}}$ be bounded sequences with $\gamma_i > 0$ for all $i \in \mathbb{N}$. Set*

$$\alpha^* := \sup\{\alpha_i,\ i \in \mathbb{N}\},$$

and assume that

$$\mathcal{R}_0^* := \frac{\Lambda}{\theta}\alpha^* > 1.$$

We distinguish two cases.

i) If the set $\{i \in \mathbb{N} : \alpha_i = \alpha^*\}$ is not empty, then $\big(S(t), I^i(t)\big)$ converges to the following asymptotic stationary state

$$S_\infty = \frac{1}{\alpha^*},\ \textit{and } I_\infty^i = \begin{cases} 0 & \textit{if } \mathcal{R}_0^i < \mathcal{R}_0^*, \\ e^{\tau\gamma_i} I_0^i & \textit{if } \mathcal{R}_0^i = \mathcal{R}_0^*, \end{cases} \textit{ for all } i \in \mathbb{N}\cup\{\infty\}.$$

where the constant $\tau \in \mathbb{R}$ is the unique solution of the equation:

$$\sum_{\{i\in\mathbb{N}\,:\,\mathcal{R}_0^i = \mathcal{R}_0^*\}} \gamma_i I_0^i\, e^{\tau\gamma_i} = \frac{\theta}{\alpha^*}(\mathcal{R}_0^* - 1).$$

ii) If the set $\{i \in \mathbb{N} : \alpha_i = \alpha^*\}$ is empty, then one has $S(t) \to \frac{1}{\alpha^*}$ and $I^i(t) \to 0$ for all $i \in \mathbb{N}$ as $t \to \infty$, while

$$\liminf_{t\to+\infty} \sum_{i\in\mathbb{N}} I^i(t) > 0.$$

If moreover one has $\alpha_n \to \alpha^*$ and $\gamma_n \to \gamma_\infty > 0$ as $n \to \infty$ with $n \in \mathbb{N}$ then the total mass converges to a positive limit

$$\lim_{t\to+\infty} \sum_{i\in\mathbb{N}} I^i(t) = \frac{\theta}{\alpha^*\gamma_\infty}(\mathcal{R}_0^* - 1). \tag{4.2.14}$$

Note that for more complex countable systems, such as if the ω-limit set of α_n or γ_n contains two or more distinct values, then it is no longer possible in general to state a result independent of the initial data. We will discuss a similar phenomenon for measures with a density with respect to the Lebesgue measure in Section 4.2.1.3

4.2.1.3 The case when $\alpha(x)$ has a finite number of regular maxima

We now go back to our analysis of (4.2.1) set on $\mathbb{R}^N$. If the function $\alpha(x)$ has a unique global maximum which is accessible to the initial data, then our analysis leads to a complete description of the asymptotic state of the population. This may be the unique case when the behvaior of the orbit is completely known, independently on the positivity of the initial mass of the fitness maximizing set $\{\alpha(x) = \alpha^*\}$.

Theorem 4.2.10 (The case of a unique global maximum)**.** *Let Assumption 4.2.1 be satisfied. Let $S_0 \geq 0$ and $I_0(\mathrm{d}x) \in \mathcal{M}_+(\mathbb{R}^N)$ be a given initial data. Suppose that the function $\alpha = \alpha(x)$ has a unique maximum α^* on the support of I_0 attained at $x^* \in \operatorname{supp} I_0$, and that*

$$\mathcal{R}_0(I_0) := \frac{\Lambda}{\theta}\alpha^* > 1.$$

Then it holds that

$$S(t) \xrightarrow[t\to+\infty]{} \frac{1}{\alpha^*}, \qquad d_0\left(I(t,\mathrm{d}x), I^\infty \delta_{x^*}(\mathrm{d}x)\right) \xrightarrow[t\to+\infty]{} 0,$$

where $\delta_{x^*}(\mathrm{d}x)$ denotes the Dirac measure at x^* and

$$I^\infty := \frac{\theta}{\alpha^*\gamma(x^*)}(\mathcal{R}_0(I_0)-1).$$

Next we describe the large time behavior of the solutions when the function α has a finite number of maxima on the support of $I_0(\mathrm{d}x)$. We consider an initial data $(S_0, I_0) \in [0,\infty)\times\mathcal{M}_+(\mathbb{R}^N)$ with I_0 absolutely continuous with respect to the Lebesgue measure $\mathrm{d}x$ in $\mathbb{R}^N$ (in other words and with a small abuse of notation, $I_0 \in L^1(\mathbb{R}^N)$) in a neighborhood of the maxima of the fitness function. Recalling the definition of α^* in (4.2.4), throughout this section 4.2.1.3, we shall make use of the following set of assumptions.

By a small abuse of notation, we will identify in this section 4.2.1.3 the function $I_0 \in L^1(\mathbb{R}^N)$ and the associated measure $I_0(x)\mathrm{d}x \in \mathcal{M}_+(\mathbb{R}^N)$ when the context is clear.

Assumption 4.2.11. We assume that:

(i) the set $\alpha^{-1}(\alpha^*)$ (given in (4.2.3)) is a finite set, namely there exist $x_1, ..., x_p$ in the interior of $\mathrm{supp}\,(I_0)$ such that $x_i \neq x_j$ for all $i \neq j$ and

$$\alpha^{-1}(\alpha^*) = \{x_1, \cdots, x_p\} \text{ and } \mathcal{R}_0 := \frac{\Lambda\alpha^*}{\theta} > 1.$$

(ii) There exist $\varepsilon_0 > 0$, $M > 1$ and $\kappa_1 \geq 0$,..,$\kappa_p \geq 0$ such that for all $i = 1, .., p$ and for almost all $x \in B(x_i, \varepsilon_0) \subset \mathrm{supp}\,(I_0)$ one has

$$M^{-1}|x - x_i|^{\kappa_i} \leq I_0(x) \leq M|x - x_i|^{\kappa_i}.$$

Here and along this note we use $|\cdot|$ to denote the Euclidean norm of $\mathbb{R}^N$.

(iii) The functions α and γ are of class C^2 and there exists $\ell > 0$ such that for each $i = 1, .., p$ one has

$$D^2\alpha(x_i)\xi^2 \leq -l|\xi|^2, \ \forall \xi \in \mathbb{R}^N.$$

Remark 4.2.12. Let us observe that since x_i belongs to the interior of $\mathrm{supp}\,(I_0)$ then $D\alpha(x_i) = 0$.

In order to state our next result, we introduce the following notation: we write $f(t) \asymp g(t)$ as $t \to \infty$ if there exists $C > 1$ and $T > 0$ such that

$$C^{-1}|g(t)| \leq |f(t)| \leq C|g(t)|, \ \forall t \geq T.$$

According to Theorem 4.2.2 (ii), one has $\alpha^* S(t) \to 1$ as $t \to \infty$, and as a special case we conclude that

$$\bar{S}(t) = \frac{1}{t}\int_0^t S(l)\mathrm{d}l \to \frac{1}{\alpha^*} \text{ as } t \to \infty.$$

As a consequence the function $\eta(t) := \alpha^*\bar{S}(t) - 1$ satisfies $\eta(t) = o(1)$ as $t \to \infty$. To describe the asymptotic behavior of the solution $(S(t), I(t,\mathrm{d}x))$ with initial data S_0 and I_0 as above, we shall derive a precise behavior of η for $t \gg 1$. This refined analysis will allow us to characterize the points of concentration of $I(t,\mathrm{d}x)$. Our result reads as follows.

Theorem 4.2.13. *Let Assumption 4.2.11 be satisfied. Then the function $\eta = \eta(t)$ satisfies the following asymptotic expansion*

$$\eta(t) = \varrho\frac{\ln t}{t} + O\left(\frac{1}{t}\right), \ \textit{as } t \to \infty. \tag{4.2.15}$$

wherein we have set

$$\varrho := \min_{i=1,\ldots,p} \frac{N+\kappa_i}{2\gamma(x_i)}. \tag{4.2.16}$$

Moreover there exists $\varepsilon_1 \in (0, \varepsilon_0)$ *such that for all* $0 < \varepsilon < \varepsilon_1$ *and all* $i = 1, .., p$ *one has*

$$\int_{|x-x_i|\leq\varepsilon} I(t, \mathrm{d}x) \asymp t^{\gamma(x_i)\varrho - \frac{N+\kappa_i}{2}} \text{ as } t \to \infty. \tag{4.2.17}$$

As a special case, for all $\varepsilon > 0$ *small enough and all* $i = 1, .., p$ *one has*

$$\int_{|x-x_i|\leq\varepsilon} I(t, \mathrm{d}x) \begin{cases} \asymp 1 \text{ if } i \in J \\ \to 0 \text{ if } i \notin J \end{cases} \quad \text{as } t \to \infty,$$

where J *is the set defined as*

$$J := \left\{ i = 1, .., p : \ \frac{N + \kappa_i}{2\gamma(x_i)} = \varrho \right\}. \tag{4.2.18}$$

The above theorem states that the function $I(t, \mathrm{d}x)$ concentrates on the set of points $\{x_i, \ i \in J\}$ (see Corollary 4.2.15 below). Here Assumption 4.2.5 on the uniform positiveness of the measure $I_0(\mathrm{d}x)$ around the points x_i is not satisfied in general, and the measure I concentrates on $\alpha^{-1}(\alpha^*)$ as predicted by Theorem 4.2.2, but not necessarily on $\alpha^{-1}(\alpha^*) \cap \gamma^{-1}(\gamma^*)$ as would have been given by Proposition 4.2.7.

In Figure 4.2.7 we provide a precise example of this non-standard behavior. The function $\alpha(x)$ is chosen to have two maxima $x_1 = -0.5$ and $x_2 = 0.5$; the precise definition of $\alpha(x)$ is

$$\alpha(x) = \mathbb{P}_{[x_1-\delta, x_1+\delta]}(x) + \mathbb{P}_{[x_2-\delta, x_2+\delta]}(x), \tag{4.2.19}$$

where

$$\mathbb{P}_{[a,b]}(x) := \max\left(1 - \frac{(a+b-2x)^2}{(a-b)^2}, 0\right)$$

is the downward parabolic function of height one and support $[a, b]$ and $\delta = 0.2$. The function $\alpha(x)$ has the exact same local behavior in the neighborhood of x_1 and x_2. The function $I_0(x)$ is chosen as

$$I_0(x) = \min\left(1, 1024\,(x - x_1)^8\right) \min\left(1, 4\,(x - x_2)^2\right) \mathbb{1}_{[-1,1]}(x), \tag{4.2.20}$$

so that $\kappa_1 = 8$ and $\kappa_2 = 2$. Finally we take

$$\gamma(x) = \frac{1}{1 + \mathbb{P}_{[x_1-\delta, x_1+\delta]}(x) + 3\mathbb{P}_{[x_2-\delta, x_2+\delta]}(x)} \tag{4.2.21}$$

so that $\gamma(x_1) = \frac{1}{2}$ and $\gamma(x_2) = \frac{1}{4}$. Summarizing, we have

$$\frac{N + \kappa_1}{2\gamma(x_1)} = 9 > 6 = \frac{N + \kappa_2}{2\gamma(x_2)},$$

so that Theorem 4.2.13 predicts that the mass $I(t, \mathrm{d}x)$ will vanish near $x_1 = \alpha^{-1}(\alpha^*) \cap \gamma^{-1}(\gamma^*)$ and concentrate on x_2.

In addition, the precise expansion of $\eta = \eta(t)$ provided in the above theorem allows us obtain the self-similar behavior of the solution $I(t, \mathrm{d}x)$ around the maxima of the fitness function. This asymptotic directly follows from (4.2.27).

Corollary 4.2.14. *For each* $i = 1, ..., p$ *and* $f \in C_c(\mathbb{R}^N)$*, the set of the continuous and compactly supported functions, one has as* $t \to \infty$*:*

$$t^{\frac{N}{2}} \int_{\mathbb{R}^N} f\left((x - x_i)\sqrt{t}\right) I(t, \mathrm{d}x) \asymp t^{\gamma(x_i)\varrho - \frac{N+\kappa_i}{2}} \int_{\mathbb{R}^N} f(x)|x|^{\kappa_i} \exp\left(\frac{\gamma(x_i)}{2\alpha^*} D^2\alpha(x_i)x^2\right) \mathrm{d}x. \tag{4.2.22}$$

Our next corollary relies on some properties of the $\omega-$limit set of the solution $I(t, \mathrm{d}x)$. Using the estimates of the mass around x_i given in (4.2.17), it readily follows that any limit measures of $I(t, \mathrm{d}x)$ belongs to a linear combination of δ_{x_i} with $i \in J$ and strictly positive coefficients of each of these Dirac masses. This reads as follows.

Corollary 4.2.15. *Under the same assumptions as in Theorem 4.2.13, the* $\omega-$*limit set* $\overline{\mathcal{O}}(I_0)$ *as defined in Lemma 4.2.19 satisfies that there exist* $0 < A < B$ *such that*

$$\overline{\mathcal{O}}(I_0) \subset \left\{ \sum_{i \in J} c_i \delta_{x_i} : \ (c_i)_{i \in J} \in [A, B]^J \right\}.$$

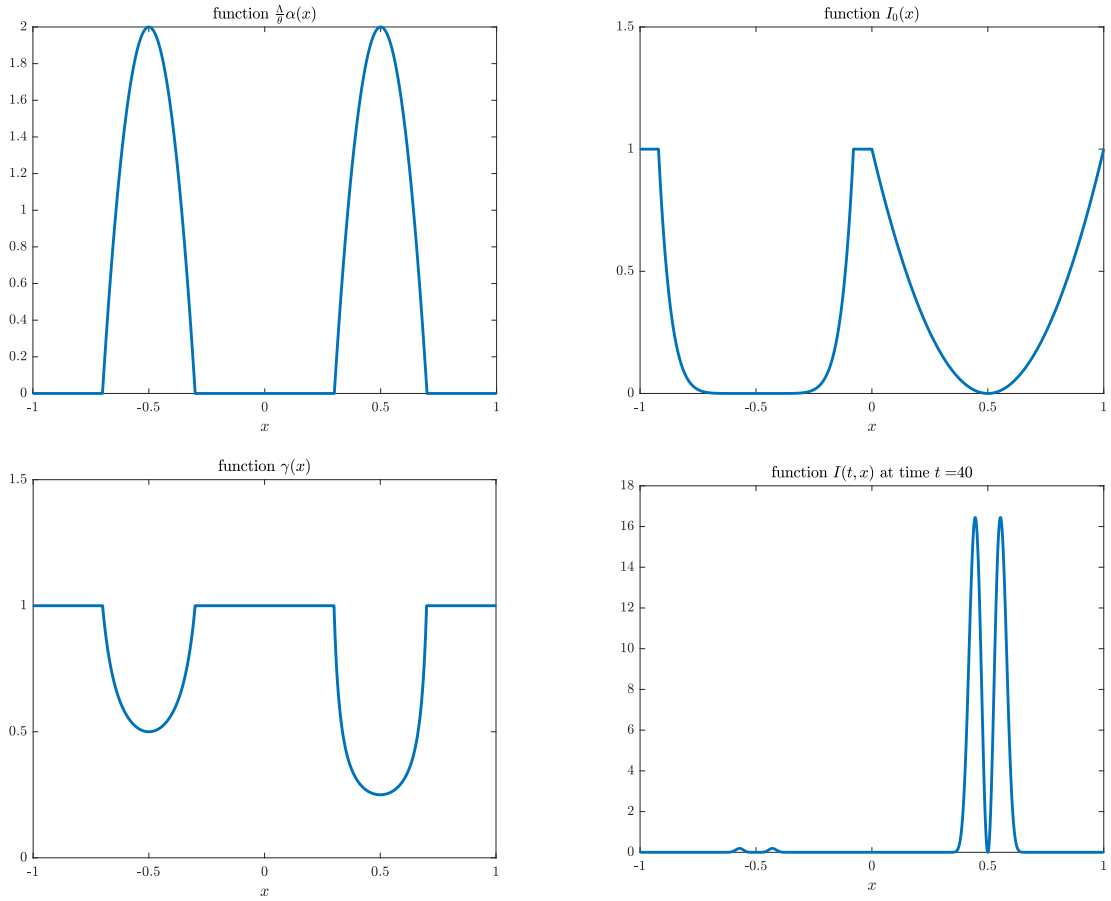

Figure 4.2.7: Illustration of Theorem 4.2.13 and Corollary 4.2.14. Parameters of this simulation are: $\Lambda = 2$, $\theta = 1$, $\alpha(x)$ is given by (4.2.19), $I_0(x)$ by (4.2.20) and $\gamma(x)$ by (4.2.21). In particular, $\alpha^* = 1$, $\alpha^{-1}(\alpha^*) = \{x_1, x_2\}$ with $x_1 = -0.5$, $x_2 = 0.5$, $\kappa_1 = 8$, $\kappa_2 = 2$, $\gamma(x_1) = 1/2$, $\gamma(x_2) = 1/4$, $\rho = 6$ and $J = \{2\}$. The initial condition I_0 vanishes more rapidly around x_1 than x_2 so that the solution $I(t,x)$ vanishes around x_1 as t goes to ∞, even though $\gamma(x_1) > \gamma(x_2)$, while around x_2 it takes the shape given by expression (4.2.14).

4.2.1.4 Transient dynamics on local maxima: a numerical example

In many biologically relevant situations it may be more usual to observe situations involving a fitness function with one global maximum and several (possibly many) local maxima, whose values are not exactly equal to the global maximum but very close. In such a situation, while the long-term distribution will be concentrated on the global maximum, one may observe a transient behavior in which the orbits stay close to the equilibrium of the several global maxima situation (corresponding to Theorem 4.2.13), before it concentrates on the eventual distribution. We leave the analytical treatment of such a situation open for future studies, however, we present a numerical experiment in Figure 4.2.8 which shows such a transient behavior.

In this simulation, we took a fitness function presenting one global maximum at $x_2 = +0.5$ and a local maximum at $x_1 = -0.5$, whose value is close to the global maximum. The precise definition of $\alpha(x)$ is

$$\alpha(x) = 0.95 \times \mathbb{P}_{[x_1-\delta, x_1+\delta]}(x) + \mathbb{P}_{[x_2-\delta, x_2+\delta]}(x) \text{ with } \delta = 0.2. \tag{4.2.23}$$

The function $I_0(x)$ is chosen as

$$I_0(x) = \min\left(1, 4\,(x-x_1)^2\right) \min\left(1, 4\,(x-x_2)^2\right) \mathbb{1}_{[-1,1]}(x), \tag{4.2.24}$$

so that $\kappa_1 = 2$ and $\kappa_2 = 2$. Finally,

$$\gamma(x) = \frac{1}{1 + \mathbb{P}_{[x_1-\delta, x_1+\delta]}(x) + 3\mathbb{P}_{[x_2-\delta, x_2+\delta]}(x)} \tag{4.2.25}$$

so that $\gamma(x_1) = \frac{1}{2}$ and $\gamma(x_2) = \frac{1}{4}$. Summarizing, we have

$$\frac{N+\kappa_1}{2\gamma(x_1)} = 3 < 6 = \frac{N+\kappa_2}{2\gamma(x_2)}.$$

If $\alpha(x)$ had two global maximum at the same level, Theorem 4.2.13 would predict that the mass $I(t, \mathrm{d}x)$ vanishes near x_2 and concentrates on x_1. Since the value of $\alpha(x_2)$ is slightly higher than the value of $\alpha(x_1)$, however, it is clear that the eventual distribution will be concentrated on x_2. We observe numerically (see Figure 4.2.8) that the distribution first concentrates on x_1 on a transient time scale, before the dynamics on x_2 takes precedence. We refer to [85] for a related model with mutations where these transient behaviors are analytically characterized.

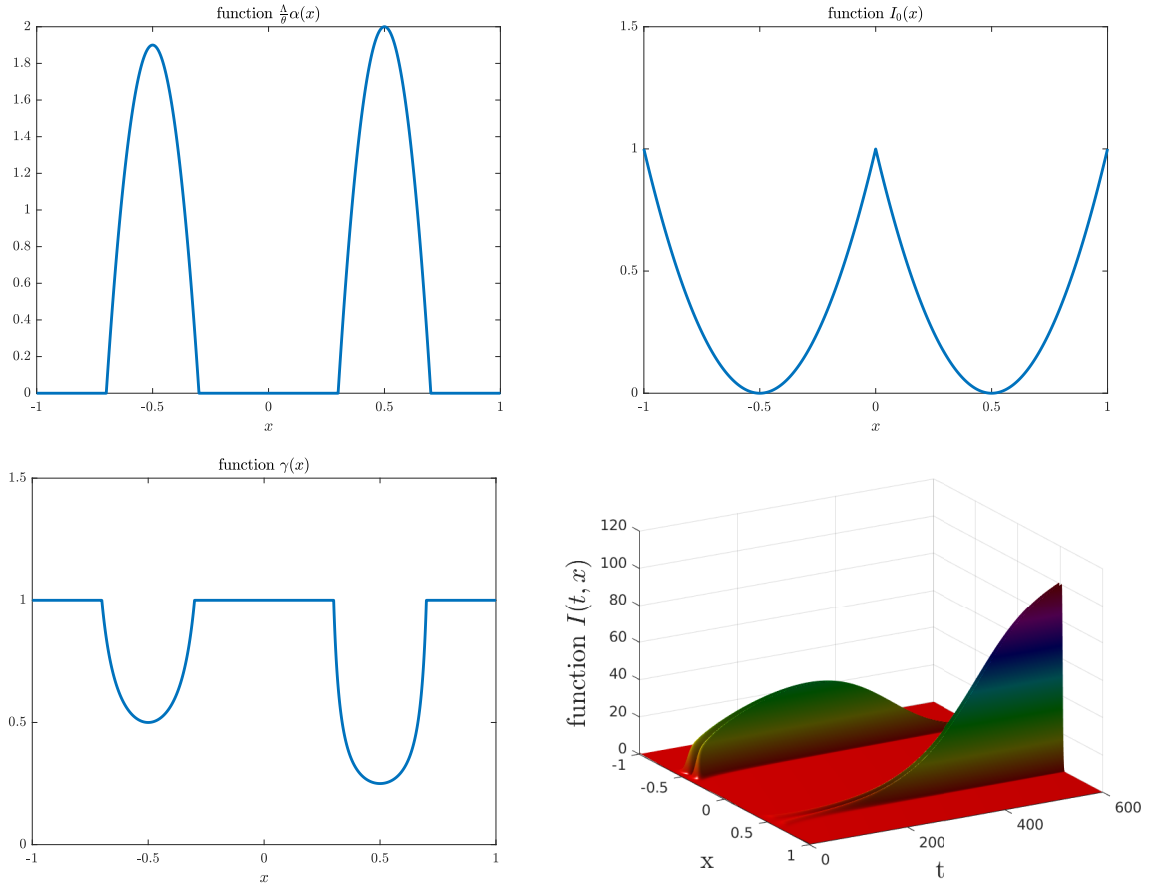

Figure 4.2.8: Illustration of a transient behavior for (4.2.1). Parameters of this simulation are: $\Lambda = 2$, $\theta = 1$, $\alpha(x)$ is given by (4.2.23), $I_0(x)$ by (4.2.24) and $\gamma(x)$ by (4.2.25). In particular, $\alpha^* = 1$, $\alpha^{-1}(\alpha^*) = \{x_2\}$ with $x_1 = -0.5$, $x_2 = 0.5$. Other parameters are $\kappa_1 = 2$, $\kappa_2 = 2$, $\gamma(x_1) = 1/2$, $\gamma(x_2) = 1/4$. The value of the local maximum at x_1, $\alpha(x_1) = 0.95$, being very close to α^*, observe that the distribution $I(t, x)$ first concentrates around x_1 before the global maximum x_2 becomes dominant (bottom right plot).

4.2.2 Measure-valued solutions and proof of Theorem 4.2.2

In this section 4.2.2 we derive general properties of the solution of (4.2.1) equipped with the given and fixed initial data $S(0) = S_0 \in [0, \infty)$ and $I_0(\mathrm{d}x) \in \mathcal{M}_+(\mathbb{R}^N)$. Recall that α^* and $\mathcal{R}_0(I_0)$ are both defined in (4.2.4). Next for $\varepsilon > 0$ let us denote by $L_\varepsilon(I_0)$ the following superlevel set:

$$L_\varepsilon(I_0) := \{x \in \operatorname{supp} I_0 \,:\, \alpha(x) \geq \alpha^* - \varepsilon\} = \bigcup_{\alpha^* - \varepsilon \leq y \leq \alpha^*} \alpha^{-1}(y). \tag{4.2.26}$$

Then the following lemma holds true.

Lemma 4.2.16. *Let Assumption 4.2.1 hold and let* $(S_0, I_0(\mathrm{d}x)) \in \mathbb{R}^+ \times \mathcal{M}_+(\mathbb{R}^N)$ *be a given initial condition. Denote* $\big(S(t), I(t,\mathrm{d}x)\big)$ *the corresponding solution of* (4.2.1). *Then* $\big(S(t), I(t,\mathrm{d}x)\big)$ *is defined for all* $t \geq 0$ *and*

$$0 < \frac{\min(\theta,\gamma_*)}{\theta\Lambda\min(\theta,\gamma_*) + \alpha^*\gamma^*} \leq \liminf_{t\to+\infty} S(t) \leq \limsup_{t\to+\infty} S(t) \leq \frac{\Lambda}{\theta} < +\infty,$$
$$\limsup_{t\to+\infty} \int_{\mathbb{R}^N} I(t,\mathrm{d}x) \leq \frac{\Lambda}{\min(\theta,\gamma_*)} < +\infty,$$

where $\gamma_* := \inf_{x\in\operatorname{supp} I_0} \gamma(x)$, $\gamma^* := \sup_{x\in\operatorname{supp} I_0} \gamma(x)$ *and* $\alpha^* := \sup_{x\in\operatorname{supp} I_0} \alpha(x)$.

Proof. We remark that

$$\frac{\mathrm{d}}{\mathrm{d}t}\left(S(t) + \int_{\mathbb{R}^N} I(t,\mathrm{d}x)\right) \leq \Lambda - \theta S(t) - \gamma_* \int_{\mathbb{R}^N} I(t,\mathrm{d}x),$$

therefore

$$S(t) + \int_{\mathbb{R}^N} I(t,\mathrm{d}x) \leq \frac{\Lambda}{\min(\theta,\gamma_*)} + \left(S_0 + \int_{\mathbb{R}^N} I_0(\mathrm{d}x) - \frac{\Lambda}{\min(\theta,\gamma_*)}\right) e^{-\min(\theta,\gamma_0)t}.$$

In particular $I(t,\mathrm{d}x)$ is uniformly bounded in $\mathcal{M}(\mathbb{R}^N)$ and therefore we have the global existence of the solution as well as

$$\limsup_{t\to+\infty} \int_{\mathbb{R}^N} I(t,\mathrm{d}x) \leq \frac{\Lambda}{\min(\theta,\gamma_*)} \text{ and } \limsup_{t\to+\infty} S(t) \leq \frac{\Lambda}{\min(\theta,\gamma_*)}.$$

Next we return to the S-component of equation (4.2.1) and let $\varepsilon > 0$ be given. We have, for t_0 sufficiently large and $t \geq t_0$,

$$S_t = \Lambda - \left(\theta + \int_{\mathbb{R}^N} \alpha(x)\gamma(x) I(t,\mathrm{d}x)\right) S(t) \geq \Lambda - \left(\theta + \alpha^*\gamma^* \frac{\Lambda}{\min(\theta,\gamma_*)} + \varepsilon\right) S(t),$$

therefore

$$S(t) \geq e^{-\left(\theta + \frac{\Lambda\alpha^*\gamma^*}{\min(\theta,\gamma_*)} + \varepsilon\right)(t-t_0)} S(t_0) + \frac{\Lambda\min(\theta,\gamma_*)}{(\theta+\varepsilon)\min(\theta,\gamma_*) + \Lambda\alpha^*\gamma^*} \left(1 - e^{-\left(\theta + \frac{\Lambda\alpha^*\gamma^*}{\min(\theta,\gamma_*)} + \varepsilon\right)(t-t_0)}\right),$$

so that finally by letting $t \to +\infty$ we get

$$\liminf_{t\to+\infty} S(t) \geq \frac{\min(\theta,\gamma_*)\Lambda}{(\theta+\varepsilon)\min(\theta,\gamma_*) + \Lambda\alpha^*\gamma^*}.$$

Since $\varepsilon > 0$ is arbitrary we have shown

$$\liminf_{t\to+\infty} S(t) \geq \frac{\min(\theta,\gamma_*)\Lambda}{\theta\min(\theta,\gamma_*) + \Lambda\alpha^*\gamma^*}.$$

The Lemma is proved. □

Lemma 4.2.17. *Let Assumption 4.2.1 hold and let* $(S_0, I_0(\mathrm{d}x)) \in \mathbb{R}^+ \times \mathcal{M}_+(\mathbb{R}^N)$ *be a given nonnegative initial condition. Let* $\big(S(t), I(t,\mathrm{d}x)\big)$ *be the corresponding solution of* (4.2.1). *Then*

$$\limsup_{T\to+\infty} \frac{1}{T} \int_0^T S(t)\mathrm{d}t \leq \frac{1}{\alpha^*},$$

where α^* *is given in* (4.2.4).

Proof. Let us remark that the second component of (4.2.1) can be written as

$$\begin{aligned} I(t,\mathrm{d}x) &= I_0(\mathrm{d}x) e^{\gamma(x)\left(\alpha(x)\int_0^t S(s)\mathrm{d}s - t\right)}, \\ &= I_0(\mathrm{d}x) \exp\left(\gamma(x)\int_0^t S(s)\mathrm{d}s \left[\alpha(x) - \frac{t}{\int_0^t S(s)\mathrm{d}s}\right]\right). \end{aligned} \tag{4.2.27}$$

Assume by contradiction that the conclusion of the Lemma does not hold, *i.e.* there exists $\varepsilon > 0$ and a sequence $T_n \to +\infty$ such that

$$\frac{1}{T_n}\int_0^{T_n} S(t)\mathrm{d}t \geq \frac{1}{\alpha^*} + \varepsilon.$$

Then

$$\frac{T_n}{\int_0^{T_n} S(t)\mathrm{d}t} \leq \frac{1}{\dfrac{1}{\alpha^*} + \varepsilon} \leq \alpha^* - \varepsilon',$$

where $\varepsilon' = (\alpha^*)^2\,\varepsilon + o(\varepsilon)$. Since the mapping $x \mapsto \alpha(x)$ is continuous, the set $L_\nu(I_0) = \{x \in \operatorname{supp} I_0 : \alpha(x) \geq \alpha^* - \nu\}$ has positive mass with respect to the measure $I_0(\mathrm{d}x)$ for all $\nu > 0$, *i.e.* $\int_{L_\nu(I_0)} I_0(\mathrm{d}x) > 0$. This is true, in particular, for $\nu = \frac{\varepsilon'}{2}$, therefore

$$\begin{aligned}
\int_{L_{\varepsilon'/2}(I_0)} I(T_n, \mathrm{d}x) &= \int_{L_{\varepsilon'/2}(I_0)} \exp\left(\gamma(x)\int_0^{T_n} S(s)\mathrm{d}s\left[\alpha(x) - \frac{T_n}{\int_0^{T_n} S(s)\mathrm{d}s}\right]\right) I_0(\mathrm{d}x)\\
&\geq \int_{L_{\varepsilon'/2}(I_0)} \exp\left(\gamma_*\int_0^{T_n} S(s)\mathrm{d}s\cdot\frac{\varepsilon'}{2}\right) I_0(\mathrm{d}x)\\
&= \int_{L_{\varepsilon'/2}(I_0)} I_0(\mathrm{d}x)\exp\left(\frac{\varepsilon'\gamma_*}{2}\int_0^{T_n} S(s)\mathrm{d}s\right),
\end{aligned}$$

where $\gamma_* = \inf_{x\in\operatorname{supp} I_0}\gamma(x)$. Since $\int_{L_{\varepsilon'/2}(I_0)} I_0(\mathrm{d}x) > 0$ and $\int_0^{T_n} S(t)\mathrm{d}t \to +\infty$ when $n \to +\infty$, we have therefore

$$\limsup_{t\to+\infty}\int_{\mathbb{R}^N} I(t,\mathrm{d}x) \geq \limsup_{n\to+\infty}\int_{L_{\varepsilon'/2}(I_0)} I(T_n,\mathrm{d}x) = +\infty,$$

which is a contradiction since $I(t,\mathrm{d}x)$ is bounded in $\mathcal{M}(\mathbb{R}^N)$ by Lemma 4.2.16. This completes the proof of the Lemma. □

The following kind of weak persistence property holds.

Lemma 4.2.18. *Let Assumption 4.2.1 hold and let $(S_0, I_0(\mathrm{d}x)) \in \mathbb{R}^+ \times \mathcal{M}_+(\mathbb{R}^N)$ be a given nonnegative initial condition. Let $\big(S(t), I(t,\mathrm{d}x)\big)$ be the corresponding solution of* (4.2.1)*. Recalling the definition of α^* in* (4.2.4)*, assume that*

$$\mathcal{R}_0(I_0) = \frac{\Lambda}{\theta}\alpha^* > 1.$$

Then

$$\limsup_{t\to+\infty}\int_{\mathbb{R}^N} I(t,\mathrm{d}x) \geq \frac{\theta}{\alpha^*\gamma^*}\big(\mathcal{R}_0(I_0) - 1\big) > 0,$$

where $\gamma^* := \sup_{x\in\operatorname{supp} I_0}\gamma(x)$.

Proof. Assume by contradiction that for t_0 sufficiently large we have

$$\int_{\mathbb{R}^N} I(t,\mathrm{d}x) \leq \eta' < \eta =: \frac{\theta}{\alpha^*\gamma^*}\big(\mathcal{R}_0(I_0) - 1\big) \text{ for all } t \geq t_0,$$

with $\eta' > 0$.

As a consequence of Lemma 4.2.17 we have

$$\liminf_{t\to+\infty} S(t) \leq \limsup_{T\to+\infty}\frac{1}{T}\int_0^T S(t)\mathrm{d}t \leq \frac{1}{\alpha^*}. \tag{4.2.28}$$

Let $\underline{S} := \liminf_{t\to+\infty} S(t)$. Let $(t_n)_{n\geq 0}$ be a sequence that tends to ∞ as $n \to \infty$ and such that $\lim_{n\to+\infty} S'(t_n) = 0$ and $\lim_{n\to+\infty} S(t_n) = \underline{S}$. As $\int_{\mathbb{R}^N} I(t_n,\mathrm{d}x) \leq \eta'$ for n large enough we deduce from the equality

$$S'(t_n) = \Lambda - \theta S(t_n) - S(t_n)\int_{\mathbb{R}^N}\alpha(x)\gamma(x)I(t_n,\mathrm{d}x),$$

that

$$0 \geq \Lambda - \theta \underline{S} - \underline{S}\alpha^*\gamma^*\eta'$$

so that

$$\underline{S} \geq \frac{\Lambda}{\theta + \alpha^*\gamma^*\eta'} > \frac{\Lambda}{\theta + \alpha^*\gamma^*\eta}$$

and by definition of η

$$\underline{S} > \frac{\Lambda}{\theta \mathcal{R}_0} = \frac{1}{\alpha^*},$$

which contradicts (4.2.28). □

Let us remind that $\mathcal{M}_+(\mathbb{R}^N)$, equipped with the Kantorovitch-Rubinstein metric d_0 defined in (4.2.2), is a complete metric space.

Lemma 4.2.19 (Compactness of the orbit and uniform persistence)**.** *Let Assumption 4.2.1 hold and let $(S_0, I_0(\mathrm{d}x)) \in \mathbb{R}^+ \times \mathcal{M}_+(\mathbb{R}^N)$ be a given nonnegative initial condition. Let $\big(S(t), I(t,\mathrm{d}x)\big)$ be the corresponding solution of* (4.2.1)*. Assume that there exists $\varepsilon > 0$ such that the superlevel set $L_\varepsilon(I_0)$ (defined in* (4.2.26)*) is bounded. Then, the closure of the orbit of I_0,*

$$\overline{\mathcal{O}}(I_0) := \left\{ \mu \in \mathcal{M}_+(\mathbb{R}^N) \,:\, \text{there exists a sequence } t_n \geq 0 \text{ such that } d_0(I(t_n,\mathrm{d}x),\mu) \xrightarrow[n\to+\infty]{} 0 \right\},$$

is compact for the topology induced by d_0 (i.e. the weak topology of measures).

If moreover $\mathcal{R}_0(I_0) > 1$, then it holds

$$\liminf_{t\to+\infty} \int I(t,\mathrm{d}x) > 0.$$

Proof. First of all let us remark that

$$I(t,\mathrm{d}x) = e^{\left(\int_0^t S(s)\mathrm{d}s\alpha(x) - t\right)\gamma(x)} I_0(\mathrm{d}x),$$

and therefore the orbit $t \mapsto I(t,\mathrm{d}x)$ is continuous for the metric d_0.

By Lemma 4.2.17 we have

$$\limsup_{T\to+\infty} \frac{1}{T}\int_0^T S(s)\mathrm{d}s \leq \frac{1}{\alpha^*},$$

where α^* defined in (4.2.4). Let $\varepsilon > 0$ be sufficiently small, so that the set $L_\varepsilon(I_0)$ is bounded and let $R := \sup_{x\in L_\varepsilon(I_0)} \|x\|$. Then there exists $T_0 = T_0(\varepsilon)$ such that

$$\frac{T}{\int_0^T S(t)\mathrm{d}t} \geq \alpha^* - \frac{\varepsilon}{2} \text{ for all } T \geq T_0.$$

Therefore if $T \geq T_0$, we have

$$\begin{aligned}
\int_{\|x\|\geq R} I(T,\mathrm{d}x) &= \int_{\|x\|\geq R} e^{\gamma(x)\int_0^T S(t)\mathrm{d}t\left(\alpha(x) - \frac{T}{\int_0^T S(t)\mathrm{d}t}\right)} I_0(\mathrm{d}x) \\
&\leq \int_{\|x\|\geq R} e^{\gamma(x)\int_0^T S(t)\mathrm{d}t\left(\alpha(x)-\alpha^*+\frac{\varepsilon}{2}\right)} I_0(\mathrm{d}x) \\
&\leq \int_{\|x\|\geq R} e^{-\frac{\varepsilon}{2}\gamma(x)\int_0^T S(t)\mathrm{d}t} I_0(\mathrm{d}x) \xrightarrow[T\to+\infty]{} 0.
\end{aligned}$$

In particular, the set $\{I(t,\mathrm{d}x) \,:\, t \geq 0\}$ is tight and bounded in the absolute variation norm (see Lemma 4.2.16), therefore precompact for the weak topology by Prokhorov's Theorem [63, Theorem 8.6.2, Vol. II p. 202].

Next we show the weak uniform persistence property if $\mathcal{R}_0(I_0) > 1$. Let $t_n \to +\infty$ be such that $I(t_n,\mathrm{d}x) \xrightarrow[n\to+\infty]{d_0} I^\infty(\mathrm{d}x)$. Then, for $\varepsilon > 0$ sufficiently small we will be fixed in the rest of the proof, we have

$$\inf_{x\in L_\varepsilon(I_0)} \frac{\Lambda}{\theta}\alpha(x) > 1. \tag{4.2.29}$$

By Lemma 4.2.17 we have

$$\frac{t_n}{\int_0^{t_n} S(t)\mathrm{d}t} \geq \alpha^* - \frac{\varepsilon}{2} \text{ for all } T \geq T_0,$$

for some $T_0 = T_0(\varepsilon)$. Therefore we get

$$\begin{aligned}\int_{\mathbb{R}^N\setminus L_\varepsilon(I_0)} I(t_n,\mathrm{d}x) &= \int_{\mathbb{R}^N\setminus L_\varepsilon(I_0)} e^{\gamma(x)\int_0^{t_n} S(t)\mathrm{d}t\left(\alpha(x)-\frac{t_n}{\int_0^{t_n} S(t)\mathrm{d}t}\right)} I_0(\mathrm{d}x)\\ &\leq \int_{\mathbb{R}^N\setminus L_\varepsilon(I_0)} e^{\gamma(x)\int_0^{t_n} S(t)\mathrm{d}t\left(\alpha(x)-\alpha^*+\frac{\varepsilon}{2}\right)} I_0(\mathrm{d}x)\\ &\leq \int_{\mathbb{R}^N\setminus L_\varepsilon(I_0)} e^{-\frac{\varepsilon}{2}\gamma(x)\int_0^{t_n} S(t)\mathrm{d}t} I_0(\mathrm{d}x) \xrightarrow[t_n\to+\infty]{} 0.\end{aligned}$$

In particular we have $\int_{\mathbb{R}^N\setminus L_\varepsilon(I_0)} I^\infty(\mathrm{d}x) = 0$. Recall that, as a consequence of (4.2.29), we have $\mathcal{R}_0(I^\infty) := \sup_{x\in\mathrm{supp}(I^\infty)} \frac{\Lambda}{\theta}\alpha(x) \geq \frac{\Lambda}{\theta}\inf_{x\in L_\varepsilon(I_0)}\alpha(x) > 1$. By Lemma 4.2.18 we have the alternative:

$$\text{either } I(\mathrm{d}x)\equiv 0 \text{ or } \int_{\mathbb{R}^N} I^\infty(\mathrm{d}x) \geq \frac{\theta}{\alpha^*\gamma^*}\left(\mathcal{R}_0(I^\infty)-1\right) \geq \frac{\theta}{\alpha^*\gamma^*}\left(\frac{\Lambda}{\theta}\inf_{x\in L_\varepsilon(I_0)}\alpha(x)-1\right) > 0.$$

This is precisely the weak uniform persistence in the metric space $\left(\overline{\mathcal{O}}(I_0), d_0\right)$, which is complete. As a consequence of [276, Proposition 3.2] in the complete (and compact) metric space $M = \overline{\mathcal{O}}(I_0)\cup\{0\}$ equipped with the metric d_0, with $M_0 = \overline{\mathcal{O}}(I_0)\setminus\{0\}$, $\partial M_0 = \{0\}$ and

$$\rho(\mathcal{I}) = \int_{\mathbb{R}^N} \mathcal{I}(\mathrm{d}x) = \langle \mathcal{I}, 1\rangle_{\mathcal{M}(\mathbb{R}^N),BC(\mathbb{R}^N)},$$

the Poincaré map is uniformly persistent, where the chevron $\langle\cdot,\cdot\rangle_{\mathcal{M}(\mathbb{R}^N),BC(\mathbb{R}^N)}$ denotes the canonical bilinear mapping on $\mathcal{M}(\mathbb{R}^N) = BC(\mathbb{R}^N)^*\times BC(\mathbb{R}^N)$. Hence this yields

$$\liminf_{t\to+\infty}\int_{\mathbb{R}^N} I(t,\mathrm{d}x) > 0,$$

and the Lemma is proved. □

Lemma 4.2.20. *Let Assumption 4.2.1 hold and let $(S_0, I_0(\mathrm{d}x)) \in \mathbb{R}^+\times\mathcal{M}_+(\mathbb{R}^N)$ be a given nonnegative initial condition. Let $\big(S(t), I(t,\mathrm{d}x)\big)$ be the corresponding solution of (4.2.1). Assume that $\mathcal{R}_0(I_0) > 1$ and that $L_\varepsilon(I_0)$ (defined in (4.2.26)) is bounded for $\varepsilon > 0$ sufficiently small. Then*

$$\liminf_{T\to+\infty}\frac{1}{T}\int_0^T S(t)\mathrm{d}t \geq \frac{1}{\alpha^*},$$

with α^* given in (4.2.4).

Proof. As in the proof of Lemma 4.2.20, we write

$$\begin{aligned}I(t,\mathrm{d}x) &= I_0(\mathrm{d}x)e^{\left(\alpha(x)\int_0^t S(s)\mathrm{d}s-t\right)\gamma(x)},\\ &= I_0(\mathrm{d}x)\exp\left(\gamma(x)\int_0^t S(s)\mathrm{d}s\left[\alpha(x)-\frac{t}{\int_0^t S(s)\mathrm{d}s}\right]\right).\end{aligned}$$

Assume by contradiction that the conclusion of the Lemma does not hold, *i.e.* there exists $\varepsilon > 0$ and a sequence $T_n\to+\infty$ such that

$$\frac{1}{T_n}\int_0^{T_n} S(t)\mathrm{d}t \leq \frac{1}{\alpha^*} - \varepsilon.$$

Then

$$\frac{T_n}{\int_0^{T_n} S(t)\mathrm{d}t} \geq \frac{1}{\frac{1}{\alpha^*}-\varepsilon} \geq \alpha^* + \varepsilon',$$

where $\varepsilon' = (\alpha^*)^2\,\varepsilon + o(\varepsilon)$, provided ε is sufficiently small. Therefore

$$\begin{aligned}\int_{\mathbb{R}^N} I(T_n, \mathrm{d}x)\mathrm{d}x &= \int_{\mathbb{R}^N} \exp\left(\gamma(x)\int_0^{T_n} S(s)\mathrm{d}s\left[\alpha(x) - \frac{T_n}{\int_0^{T_n} S(s)\mathrm{d}s}\right]\right) I_0(\mathrm{d}x)\\ &\leq \int_{\mathbb{R}^N} \exp\left(-\gamma_0\int_0^{T_n} S(s)\mathrm{d}s\cdot\varepsilon'\right) I_0(\mathrm{d}x)\\ &= \exp\left(-\varepsilon'\gamma_0\int_0^{T_n} S(s)\mathrm{d}s\right)\int_{\mathbb{R}^N} I_0(\mathrm{d}x),\end{aligned}$$

We have therefore

$$\liminf_{t\to+\infty}\int_{\mathbb{R}^N} I(t,\mathrm{d}x) \leq \liminf_{n\to+\infty}\int_{\mathbb{R}^N} I(T_n,\mathrm{d}x) = 0,$$

which is in contradiction with Lemma 4.2.19. This completes the proof of the Lemma. □

Remark 4.2.21. By combining Lemma 4.2.17 and Lemma 4.2.20 we obtain that $\frac{1}{T}\int_0^T S(t)\mathrm{d}t$ admits a limit when $T\to+\infty$ and

$$\lim_{T\to+\infty}\frac{1}{T}\int_0^T S(t)\mathrm{d}t = \frac{1}{\alpha^*}.$$

Lemma 4.2.22. *Let Assumption 4.2.1 hold and let $(S_0, I_0(\mathrm{d}x)) \in \mathbb{R}^+\times\mathcal{M}_+(\mathbb{R}^N)$ be a given nonnegative initial condition. Let $\big(S(t), I(t,\mathrm{d}x)\big)$ be the corresponding solution of* (4.2.1)*. Assume that $L_\varepsilon(I_0)$ (defined in* (4.2.26)*) is bounded for $\varepsilon > 0$ sufficiently small. Then one has*

$$d_0\left(I(t,\mathrm{d}x), \mathcal{M}_+(\alpha^{-1}(\alpha^*))\right) \xrightarrow[t\to+\infty]{} 0.$$

Proof. Let $\varepsilon > 0$ be as in the statement of Lemma 4.2.22. By Lemma 4.2.17, there exists $T \geq 0$ such that for all $t \geq T$ we have

$$\frac{t}{\int_0^t S(s)\mathrm{d}s} \geq \alpha^* - \frac{\varepsilon}{2},$$

where $\alpha^* := \sup_{x\in\operatorname{supp} I_0}\alpha(x)$. Hence for $t \geq T$ we have

$$\begin{aligned}\int_{\mathbb{R}^N\setminus L_\varepsilon(I_0)} I(t,\mathrm{d}x) &= \int_{\mathbb{R}^N\setminus L_\varepsilon(I_0)} \exp\left(\gamma(x)\int_0^t S(s)\mathrm{d}s\left(\alpha(x) - \frac{t}{\int_0^t S(s)\mathrm{d}s}\right)\right) I_0(\mathrm{d}x)\\ &\leq \int_{\mathbb{R}^N\setminus L_\varepsilon(I_0)} \exp\left(\gamma(x)\int_0^t S(s)\mathrm{d}s\left(\alpha^* - \varepsilon - \frac{t}{\int_0^t S(s)\mathrm{d}s}\right)\right) I_0(\mathrm{d}x)\\ &\leq \int_{\mathbb{R}^N\setminus L_\varepsilon(I_0)} e^{-\frac{\varepsilon}{2}\gamma(x)\int_0^t S(s)\mathrm{d}s} I_0(\mathrm{d}x) \xrightarrow[t\to+\infty]{} 0.\end{aligned}$$

In particular, if $I(t,\mathrm{d}x)|_{L_\varepsilon(I_0)}$ denotes the restriction of $I(t,\mathrm{d}x)$ to $L_\varepsilon(I_0)$, we have $\|I(t,\mathrm{d}x) - I(t,\mathrm{d}x)|_{L_\varepsilon(I_0)}\|_{AV} \xrightarrow[t\to+\infty]{} 0$ and hence

$$d_0\big(I(t,\mathrm{d}x), I(t,\mathrm{d}x)|_{L_\varepsilon(I_0)}\big) \leq d_{AV}\big(I(t,\mathrm{d}x), I(t,\mathrm{d}x)|_{L_\varepsilon(I_0)}\big) \xrightarrow[t\to+\infty]{} 0.$$

Here $\varepsilon > 0$ can be chosen arbitrarily small. By Lemma 4.2.16 we know moreover that

$$\limsup_{t\to+\infty}\int_{\mathbb{R}^N} I(t,\mathrm{d}x) \leq \frac{\Lambda}{\min(\theta,\gamma_*)},$$

so that for t sufficiently large, we have

$$\int_{\mathbb{R}^N} I(t,\mathrm{d}x) \leq 2\frac{\Lambda}{\min(\theta,\gamma_*)}.$$

Finally by using Proposition 4.2.31, we have

$$\begin{aligned}d_0\big(I(t,\mathrm{d}x), \mathcal{M}_+\left(\alpha^{-1}(\alpha^*)\right)\big) &\leq d_0\big(I(t,\mathrm{d}x), I(t,\mathrm{d}x)|_{L_\varepsilon(I_0)}\big) + d_0\big(I(t,\mathrm{d}x)|_{L_\varepsilon(I_0)}, \mathcal{M}_+\left(\alpha^{-1}(\alpha^*)\right)\big)\\ &\leq d_0\big(I(t,\mathrm{d}x), I(t,\mathrm{d}x)|_{L_\varepsilon(I_0)}\big) + 2\frac{\Lambda}{\min(\theta,\gamma_*)}\sup_{x\in L_\varepsilon(I_0)} d\big(x, \alpha^{-1}(\alpha^*)\big).\end{aligned}$$

Since

$$\sup_{x\in L_\varepsilon(I_0)} d\big(x,\alpha^{-1}(\alpha^*)\big) \xrightarrow[\varepsilon\to 0]{} 0,$$

the Kantorovitch-Rubinstein distance between $I(t,\mathrm{d}x)$ and $\mathcal{M}\big(\alpha^{-1}(\alpha^*)\big)$ can indeed be made arbitrarily small as $t\to+\infty$. This proves the Lemma. □

Lemma 4.2.23. *Let Assumption 4.2.1 hold and let $(S_0, I_0(\mathrm{d}x)) \in \mathbb{R}^+ \times \mathcal{M}_+(\mathbb{R}^N)$ be a given nonnegative initial condition. Let $\big(S(t), I(t,\mathrm{d}x)\big)$ be the corresponding solution of (4.2.1). Assume that $\alpha(x)\equiv\alpha^*$ is a constant function on $\operatorname{supp} I_0$ such that $\mathcal{R}_0(I_0)>1$. There exists a stationary solution $(S^*,i^*)\in\mathbb{R}^+\times L^1(I_0)$ such that*

$$S(t) \xrightarrow[t\to+\infty]{} S^* = \frac{1}{\alpha^*},$$
$$I(t,\mathrm{d}x) \xrightarrow[t\to+\infty]{AV} i^*(x)I_0(\mathrm{d}x).$$

i^* is a Borel-measurable function on $\mathbb{R}^N$, which is unique up to a negligible set with respect to $I_0(\mathrm{d}x)$. Moreover it satisfies $i^*(x)=e^{\tau\gamma(x)}$, where τ is the unique solution to the equation

$$\int_{\mathbb{R}^N}\gamma(x)e^{\tau\gamma(x)}I_0(\mathrm{d}x) = \frac{\theta}{\alpha^*}\left(\mathcal{R}_0-1\right). \tag{4.2.30}$$

Proof. First we check that the proposed stationary solution is indeed unique and a stationary solution. By Lemma 4.2.17–4.2.20, $S^*=\frac{1}{\alpha^*}$ is the only possible choice for S^*. Next, we remark that the map

$$\tau\mapsto\int_{\mathbb{R}^N}\gamma(x)e^{\tau\gamma(x)}I_0(\mathrm{d}x)$$

is strictly increasing and maps $\mathbb{R}$ onto $(0,+\infty)$, therefore (4.2.30) has a unique solution τ and the corresponding function $i^*(x)I_0(\mathrm{d}x) := e^{\tau\gamma(x)}I_0(\mathrm{d}x)$ satisfies

$$\int_{\mathbb{R}^N}\gamma(x)i^*(x)I_0(\mathrm{d}x) = \frac{\theta}{\alpha^*}\left(\mathcal{R}_0-1\right).$$

Therefore it is not difficult to check that $(S^*, i^*(x)I_0(\mathrm{d}x))$ is a stationary solution to the system of differential equations

$$\begin{cases} S'(t) = \Lambda - \theta S(t) - \displaystyle\int_{\mathbb{R}^N}\alpha^*\gamma(x)I(t,\mathrm{d}x) \\ I'(t,\mathrm{d}x) = \gamma(x)\left(\alpha^*S(t)-1\right)I(t,\mathrm{d}x), \end{cases}$$

which is equivalent to (4.2.1) on $\operatorname{supp} I_0$.

Next we show the convergence of an initial condition to (S^*,I^*) where $I^*(\mathrm{d}x)=i^*(x)I_0(\mathrm{d}x)$. To that aim we introduce the Lyapunov functional

$$V(S,I) := S^*g\left(\frac{S}{S^*}\right) + \int_{\mathbb{R}^N} i^*(x)g\left(\frac{I(x)}{i^*(x)}\right)I_0(\mathrm{d}x),$$

where $g(s)=s-\ln(s)$. $V(S,I)$ is well-defined when $\ln(I(x))\in L^1(I_0)$. Let us denote $I(t,\mathrm{d}x)=i(t,x)I_0(\mathrm{d}x)$ and remark that $V(S(t),i(t,x))$ is always well-defined since $i(t,x)=e^{\alpha(x)\overline{S}(t)-\gamma(x)t}$. We claim that $V'(S(t),i(t,\cdot))\le 0$. Indeed, writing $V_1(S)=S^*g\left(\frac{S(t)}{S^*}\right)$ and $V_2(t)=\int_{\mathbb{R}^N} i^*(x)g\left(\frac{i(t,x)}{i^*(x)}\right)I_0(\mathrm{d}x)$, we have

$$\begin{aligned}
V_1'(t) &= S^*\frac{S'(t)}{S^*}g'\left(\frac{S(t)}{S^*}\right) = \left(\Lambda-\theta S(t) - S(t)\int_{\mathbb{R}^N}\alpha^*\gamma(x)i(t,x)I_0(\mathrm{d}x)\right)\left(1-\frac{S^*}{S(t)}\right)\\
&= \left(\Lambda-\theta S(t) - S(t)\int_{\mathbb{R}^N}\alpha^*\gamma(x)i(t,x)I_0(\mathrm{d}x) - \Lambda + \theta S^* + S^*\int_{\mathbb{R}^N}\alpha^*\gamma(x)i^*(x)I_0(\mathrm{d}x)\right)\left(1-\frac{S^*}{S(t)}\right)\\
&= -\theta\frac{(S(t)-S^*)^2}{S(t)} + \left(S^*\int_{\mathbb{R}^N}\alpha^*\gamma(x)i^*(x)I_0(\mathrm{d}x) - S(t)\int_{\mathbb{R}^N}\alpha^*\gamma(x)i(t,x)I_0(\mathrm{d}x)\right)\left(1-\frac{S^*}{S(t)}\right),\\
&= -\theta\frac{(S(t)-S^*)^2}{S(t)} + S^*\int_{\mathbb{R}^N}\alpha^*\gamma(x)i^*(x)I_0(\mathrm{d}x) - \frac{(S^*)^2}{S(t)}\int_{\mathbb{R}^N}\alpha^*\gamma(x)i^*(x)I_0(\mathrm{d}x)\\
&\quad - S(t)\int_{\mathbb{R}^N}\alpha^*\gamma(x)i(t,x)I_0(\mathrm{d}x) + S^*\int_{\mathbb{R}^N}\alpha^*\gamma(x)i(t,x)I_0(\mathrm{d}x),
\end{aligned}$$

and

$$V_2'(t) = \int_{\mathbb{R}^N} i^*(x)\frac{i_t(t,x)}{i^*(x)}g'\left(\frac{i(t,x)}{i^*(x)}\right)I_0(\mathrm{d}x) = \int_{\mathbb{R}^N}\gamma(x)\left(\alpha^*S(t)-1\right)i(t,x)\left(1-\frac{i^*(x)}{i(t,x)}\right)I_0(\mathrm{d}x)$$
$$= \int_{\mathbb{R}^N}\gamma(x)\left(\alpha^*S(t)-1\right)\left(i(t,x)-i^*(x)\right)I_0(\mathrm{d}x)$$
$$= \int_{\mathbb{R}^N}\gamma(x)\alpha^*S(t)i(t,x)I_0(\mathrm{d}x) - \int_{\mathbb{R}^N}\gamma(x)i(t,x)I_0(\mathrm{d}x) - \int_{\mathbb{R}^N}\gamma(x)\alpha^*S(t)i^*(x)I_0(\mathrm{d}x)$$
$$+ \int_{\mathbb{R}^N}\gamma(x)i^*(x)I_0(\mathrm{d}x).$$

Recalling $S^* = \frac{1}{\alpha^*}$, we have therefore

$$\frac{\mathrm{d}}{\mathrm{d}t}V(S(t),i(t,\cdot)) = \frac{\mathrm{d}}{\mathrm{d}t}V_1(t) + \frac{\mathrm{d}}{\mathrm{d}t}V_2(t)$$
$$= -\theta\frac{(S(t)-S^*)^2}{S(t)} + 2\int_{\mathbb{R}^N}\gamma(x)i^*(x)\mathrm{d}x - \frac{(S^*)^2}{S(t)}\int_{\mathbb{R}^N}\alpha^*\gamma(x)i^*(x)I_0(\mathrm{d}x)$$
$$- \int_{\mathbb{R}^N}\alpha^*\gamma(x)S(t)i^*(t)I_0(\mathrm{d}x).$$

Since

$$\int_{\mathbb{R}^N}\alpha^*\gamma(x)i^*(x)\left(S(t)+\frac{(S^*)^2}{S(t)}\right)I_0(\mathrm{d}x) \geq \int_{\mathbb{R}^N}\alpha^*\gamma(x)i^*(x)\times 2S^*I_0(\mathrm{d}x),$$

which stems from the inequality $a+b\geq 2\sqrt{ab}$, we have proved that

$$\frac{\mathrm{d}}{\mathrm{d}t}V(S(t),i(t,\cdot)) \leq 0.$$

It then follows from classical arguments that $S(t)\to S^*$ and $i(t,\cdot)\to i^*(\cdot)$ as $t\to+\infty$ (where the last limit holds in $L^1(I_0)$). The Lemma is proved. □

Next we can determine the long-time behavior when the initial measure I_0 puts a positive mass on the set of maximal fitness. Recall that $\alpha^{-1}(\alpha^*)$ (see (4.2.3) and (4.2.4)) is the set of points in the support of I_0 that have maximal fitness, *i.e.*

$$\alpha^{-1}(\alpha^*) = \bigcap_{\varepsilon>0} L_\varepsilon(I_0) = \left\{x\in\operatorname{supp} I_0\ :\ \alpha(x)\geq\alpha(y) \text{ for all } y\in\operatorname{supp} I_0\right\}.$$

Lemma 4.2.24. *Assume that $L_\varepsilon(I_0)$ is bounded for $\varepsilon>0$ sufficiently small and that $\mathcal{R}_0(I_0)>1$. Suppose that $I_0(\alpha^{-1}(\alpha^*))>0$, or in other words,*

$$\int_{\alpha^{-1}(\alpha^*)} I_0(\mathrm{d}x) > 0.$$

Then the limit of $I(t,\mathrm{d}x)$ is completely determined by the part of I_0 in $\alpha^{-1}(\alpha^*)$, that is to say,

$$d_0\big(I(t,\mathrm{d}x), I^*_\infty(\mathrm{d}x)\big) \xrightarrow[t\to+\infty]{} 0,$$

where $I^*_\infty(\mathrm{d}x)$ is the stationary measure given by Lemma 4.2.23 associated with the initial condition $I^*_0(\mathrm{d}x) := I_0|_{\alpha^{-1}(\alpha^*)}(\mathrm{d}x)$, the restriction of $I_0(\mathrm{d}x)$ to the set $\alpha^{-1}(\alpha^*)$.

Proof. First, let us define $\alpha^* := \sup_{x\in\operatorname{supp} I_0}\alpha(x)$ (so that $\alpha(x)$ is a constant equal to α^* on $\alpha^{-1}(\alpha^*)$) and

$$\eta(t) := \alpha^*\overline{S}(t) - 1, \text{ with } \overline{S}(t) = \frac{1}{t}\int_0^t S(s)\mathrm{d}s.$$

Then $I(t,\mathrm{d}x)$ can be written as

$$I(t,\mathrm{d}x) = \exp\left(\gamma(x)t\left[\eta(t) + (\alpha(x)-\alpha^*)\frac{1}{t}\int_0^t S(s)\mathrm{d}s\right]\right)I_0(\mathrm{d}x).$$

We remark that the function $t \mapsto t\eta(t)$ is bounded. Indeed, by Jensen's inequality we have

$$\exp\left(\int_{\alpha^{-1}(\alpha^*)} \gamma(x) t\eta(t) \frac{I_0(\mathrm{d}x)}{\int_{\alpha^{-1}(\alpha^*)} I_0}\right) \leq \int_{\alpha^{-1}(\alpha^*)} e^{\gamma(x)t\eta(t)} \frac{I_0(\mathrm{d}x)}{\int_{\alpha^{-1}(\alpha^*)} I_0(\mathrm{d}z)},$$

so that

$$t\eta(t) \leq \frac{\int_{\alpha^{-1}(\alpha^*)} I_0}{\int_{\alpha^{-1}(\alpha^*)} \gamma(x) I_0(\mathrm{d}x)} \ln\left(\int_{\mathbb{R}^N} e^{\gamma(x)t\eta(t)} \frac{I_0(\mathrm{d}x)}{\int_{\mathbb{R}^N} I_0}\right) = \frac{\int_{\alpha^{-1}(\alpha^*)} I_0}{\int_{\alpha^{-1}(\alpha^*)} \gamma(x) I_0(\mathrm{d}x)} \ln\left(\frac{1}{\int_{\alpha^{-1}(\alpha^*)} I_0} \int_{\alpha^{-1}(\alpha^*)} I(t, \mathrm{d}x)\right).$$

Applying Lemma 4.2.16, $I(t, \mathrm{d}x)$ is bounded and we have indeed an upper bound for $t\eta(t)$. Next, writing

$$I(t, \mathrm{d}x) = \exp\left(\gamma(x)t\eta(t) + (\alpha(x) - \alpha^*) \int_0^t S(s)\mathrm{d}s\right) I_0(\mathrm{d}x)$$

and recalling that $\int_0^t S(s)\mathrm{d}s \to +\infty$ as $t \to +\infty$, the function $\exp\left(\gamma(x)t\eta(t) + (\alpha(x) - \alpha^*) \int_0^t S(s)\mathrm{d}s\right)$ converges almost everywhere (with respect to I_0) to 0 on $\mathbb{R}^N \backslash \alpha^{-1}(\alpha^*)$, so that by Lebesgue's dominated convergence theorem, we have

$$\lim_{t\to+\infty} \int_{\mathbb{R}^N \backslash \alpha^{-1}(\alpha^*)} I(t, \mathrm{d}x) = \int_{\mathbb{R}^N \backslash \alpha^{-1}(\alpha^*)} \lim_{t\to+\infty} \exp\left(\gamma(x)t\eta(t) + (\alpha(x) - \alpha^*) \int_0^t S(s)\mathrm{d}s\right) I_0(\mathrm{d}x) = 0.$$

Next it follows from Lemma 4.2.20 that $\liminf_{t\to+\infty} I(t, \mathrm{d}x) > 0$, so that

$$\liminf_{t\to+\infty} \int_{\alpha^{-1}(\alpha^*)} I(t, \mathrm{d}x) = \liminf_{t\to+\infty} \int_{\mathbb{R}^N} I(t, \mathrm{d}x) > 0.$$

Assume by contradiction that there is a sequence (t_n) such that $t_n\eta(t_n) \to -\infty$, then

$$\int_{\alpha^{-1}(\alpha^*)} I(t, \mathrm{d}x) = \int_{\alpha^{-1}(\alpha^*)} e^{\gamma(x)t_n\eta(t_n)} I_0(\mathrm{d}x) \leq \int_{\alpha^{-1}(\alpha^*)} e^{\gamma_* t_n \eta(t_n)} I_0(\mathrm{d}x) = e^{\gamma_* t_n \eta(t_n)} \int_{\alpha^{-1}(\alpha^*)} I_0(\mathrm{d}x) \xrightarrow[t\to+\infty]{} 0,$$

where $\gamma_* := \inf_{x \in \mathrm{supp}\, I_0} \gamma(x) > 0$. This is a contradiction. Therefore there is a constant $\underline{\eta} > 0$ such that

$$t\eta(t) \geq -\underline{\eta} > -\infty.$$

In particular, the function $t \mapsto t\eta(t)$ is bounded by two constants,

$$-\infty < -\underline{\eta} \leq t\eta(t) \leq \overline{\eta} < +\infty.$$

Suppose that there exists a sequence $t_n \to +\infty$ and $\eta^* \in [-\underline{\eta}, \overline{\eta}]$ such that

$$\lim_{n\to+\infty} t_n \eta(t_n) = \eta^*.$$

Upon replacing t_n by a subsequence, the function $S(t_n)$ converges to a limit S_0^* and therefore the shifted orbits satisfy

$$(S(t + t_n), I(t + t_n, \mathrm{d}x)) \xrightarrow[n\to+\infty]{} (S^*(t), I^*(t, \mathrm{d}x))$$

locally uniformly in time. The resulting orbit $(S^*(t), I^*(t, \mathrm{d}x))$ is a solution to (4.2.1), defined for all times $t \in \mathbb{R}$, and satisfying

$$S^*(0) = S_0,$$
$$I^*(0, \mathrm{d}x) = e^{\gamma(x)\eta^*} I_0^*(\mathrm{d}x),$$

where we recall that $I_0^*(\mathrm{d}x)$ is the restriction of $I_0(\mathrm{d}x)$ to $\alpha^{-1}(\alpha^*)$. By Lemma 4.2.23, this implies that $S_0^* = \frac{1}{\alpha^*}$ and $I^*(0, \mathrm{d}x) = e^{\tau\gamma(x)} I_0^*(\mathrm{d}x)$, where τ is uniquely defined by (4.2.30) (and independent of the sequence t_n). Therefore $\eta^* = \tau$. We conclude that

$$\lim_{t\to+\infty} t\eta(t) = \tau,$$

where τ is the constant uniquely defined by (4.2.30) with the initial measure $I_0^*(\mathrm{d}x)$. This ends the proof of the Lemma. □

When the set of maximal fitness $\alpha^{-1}(\alpha^*)$ is negligible for I_0, it is more difficult to obtain a general result for the long-time behavior of $I(t,\mathrm{d}x)$. We start with a short but useful estimate on the rate $\eta(t)$

Lemma 4.2.25. *Assume that $L_\varepsilon(I_0)$ is bounded for $\varepsilon > 0$ sufficiently small and that $\mathcal{R}_0(I_0) > 1$. Suppose that $I_0(\alpha^{-1}(\alpha^*)) = 0$ and set*

$$\eta(t) := \alpha^* \overline{S}(t) - 1, \text{ with } \overline{S}(t) = \frac{1}{t}\int_0^t S(s)\mathrm{d}s,$$

where $\alpha^* := \sup_{x\in \mathrm{supp}\, I_0} \alpha(x)$. Then it holds

$$t\eta(t) \xrightarrow[t\to\infty]{} +\infty.$$

Proof. Assume by contradiction that there exists a sequence $t_n \to +\infty$ such that $t_n\eta(t_n)$ has a uniform upper bound as $t_n \to +\infty$, then observe that the quantity

$$e^{\gamma(x)(\alpha(x)\overline{S}(t_n)-1)t_n} = e^{\gamma(x)(\alpha(x)-\alpha^*)\overline{S}(t_n)t_n+\gamma(x)\eta(t_n)t_n}$$

is uniformly bounded in t_n and vanishes as $t_n \to +\infty$ almost everywhere with respect to $I_0(\mathrm{d}x)$. By a direct application of Lebesgue's dominated convergence Theorem, we have therefore

$$\int_{\mathbb{R}^N} I(t_n,\mathrm{d}x) = \int_{\mathbb{R}^N} e^{\gamma(x)(\alpha(x)\overline{S}(t_n)-1)t_n} I_0(\mathrm{d}x) \xrightarrow[t_n\to+\infty]{} 0,$$

which is in contradiction with Lemma 4.2.19. We conclude that $t\eta(t) \to +\infty$ as $t \to +\infty$. □

We can now state our convergence result for measures which vanish on $\alpha^{-1}(\alpha^*)$, provided the behavior of I_0 at the boundary is not too pathological. Basically, it says that the selection filters the low values of $\gamma(x)$ near boundary points $x \in \alpha^{-1}(\alpha^*)$.

We are now in the position to prove Theorem 4.2.2.

Proof of Theorem 4.2.2. To show the convergence of $S(t)$ to $\frac{1}{\alpha^*}$ (which is present in both i) and ii)), we first remark that

$$\overline{S}(t) = \frac{1}{t}\int_0^t S(s)\mathrm{d}s \xrightarrow[t\to+\infty]{} \frac{1}{\alpha^*}, \tag{4.2.31}$$

as a consequence of Lemma 4.2.17 and 4.2.20. Next, let $t_n \to +\infty$ be an arbitrary sequence, then by the compactness of the orbit proved in Lemma 4.2.19 we can extract from $S(t_n)$ a subsequence which converges to a number S^*. It follows from (4.2.31) that $S^* = \frac{1}{\alpha^*}$.

The convergence of $I(t,\mathrm{d}x)$ in case i) was proved in Lemma 4.2.24.

The uniform persistence of $I(t,\mathrm{d}x)$ in case ii) is a consequence of 4.2.19. The concentration on the maximal fitness was proved in Lemma 4.2.22. The Theorem is proved. □

We now turn to the proof of Proposition 4.2.7 and we first prove that $I(t,\mathrm{d}x)$ concentrates on the set of points maximizing both α and γ. This property is summarized in the next lemma.

Lemma 4.2.26. *Assume that $L_\varepsilon(I_0)$ is bounded for $\varepsilon > 0$ sufficiently small and that $\mathcal{R}_0(I_0) > 1$. Suppose that $I_0(\alpha^{-1}(\alpha^*)) = 0$ and that Assumption 4.2.5 holds. Recalling the definition of α^* in (4.2.4) and γ^* in Assumption 4.2.5, set $\Gamma_0(I_0)$ be the set of maximal points of γ on $\alpha^{-1}(\alpha^*)$, defined by*

$$\Gamma_0(I_0) := \left\{x \in \alpha^{-1}(\alpha^*) \,:\, \gamma(x) \geq \gamma(y) \text{ for all } y \in \alpha^{-1}(\alpha^*)\right\} = \gamma^{-1}(\{\gamma^*\}) \cap \alpha^{-1}(\alpha^*).$$

Then one has

$$d_0\left(I(t,\mathrm{d}x), \mathcal{M}_+(\Gamma_0(I_0))\right) \xrightarrow[t\to+\infty]{} 0.$$

Proof. We decompose the proof in several steps.

Step 1: We show that $I(t,\mathrm{d}x)$ and $\mathbb{1}_{\alpha(x)\overline{S}(t)\geq 1} I(t,\mathrm{d}x)$ are asymptotically close in $\|\cdot\|_{AV}$. That is to say,

$$\|I(t,\mathrm{d}x) - \mathbb{1}_{\alpha(\cdot)\overline{S}(t)\geq 1} I(t,\mathrm{d}x)\|_{AV} \xrightarrow[t\to+\infty]{} 0.$$

Indeed we have

$$I(t,\mathrm{d}x) - \mathbb{1}_{\alpha(x)\overline{S}(t)\geq 1} I(t,\mathrm{d}x) = \mathbb{1}_{\alpha(x)\overline{S}(t)<1} I(t,\mathrm{d}x) = \mathbb{1}_{\alpha(x)\overline{S}(t)<1} e^{\gamma(x)(\alpha(x)\overline{S}(t)-1)t} I_0(\mathrm{d}x).$$

First note that the function $\mathbb{1}_{\alpha(x)\overline{S}(t)<1} I(t,\mathrm{d}x) = \mathbb{1}_{\alpha(x)\overline{S}(t)<1} e^{\gamma(x)(\alpha(x)\overline{S}(t)-1)t}$ is uniformly bounded. On the other hand, since $I_0(\alpha^{-1}(\alpha^*)) = 0$ recall that $\overline{S}(t) \to \frac{1}{\alpha^*}$ for $t \to \infty$, so that $\mathbb{1}_{\alpha(x)\overline{S}(t)<1} \to 0$ as $t \to \infty$ almost everywhere with respect to I_0. It follows from Lebesgue's dominated convergence Theorem that

$$\int_{\mathbb{R}^N} \mathbb{1}_{\alpha(x)\overline{S}(t)<1} e^{\gamma(x)(\alpha(x)\overline{S}(t)-1)t} I_0(\mathrm{d}x) \xrightarrow[t\to+\infty]{} 0.$$

Step 2: We show that the measure $\mathbb{1}_{\overline{S}(t)y\geq 1} e^{\bar{\gamma}(y\overline{S}(t)-1)t} A(\mathrm{d}y)$ is bounded when $t \to \infty$ for all $\bar{\gamma} < \gamma^*$.
Note that $I_0(\alpha^{-1}(\alpha^*)) = 0$ implies that $A(\{\alpha^*\}) = 0$ and remark that one has

$$\int_{\mathbb{R}^N} \mathbb{1}_{\alpha(x)\overline{S}(t)\geq 1} I(t,\mathrm{d}x) = \int_{\min\left(\alpha^*, 1/\overline{S}(t)\right)}^{\alpha^*} \int_{\{x\in\alpha^{-1}(y)\}} e^{\gamma(x)(y\overline{S}(t)-1)t} I_0(y,\mathrm{d}x) A(\mathrm{d}y),$$

so, according to Step 1, for t sufficiently large one has

$$\begin{aligned}
\int_{\gamma^{-1}([\bar{\gamma},\gamma^*])} I(t,\mathrm{d}x) &= \int_{\min(\alpha^*,1/\overline{S}(t))}^{\alpha^*} \int_{x\in\alpha^{-1}(y)\cap\gamma^{-1}([\bar{\gamma},\gamma^*])} e^{\gamma(x)(y\overline{S}(t)-1)t} I_0(y,\mathrm{d}x) A(\mathrm{d}y) + o(1) \\
&\geq \int_{\min(\alpha^*,1/\overline{S}(t))}^{\alpha^*} \int_{\{\alpha(x)=y\}\cap\gamma^{-1}([\bar{\gamma},\gamma^*])} e^{\bar{\gamma}(y\overline{S}(t)-1)t} I_0(y,\mathrm{d}x) A(\mathrm{d}y) + o(1) \\
&= \int_{\min(\alpha^*,1/\overline{S}(t))}^{\alpha^*} \int_{\{\alpha(x)=y\}\cap\gamma^{-1}([\bar{\gamma},\gamma^*])} I_0(y,\mathrm{d}x) e^{\bar{\gamma}(y\overline{S}(t)-1)t} A(\mathrm{d}y) + o(1) \\
&\geq m \int_{\min(\alpha^*,1/\overline{S}(t))}^{\alpha^*} e^{\bar{\gamma}(y\overline{S}(t)-1)t} A(\mathrm{d}y) + o(1),
\end{aligned}$$

wherein $m > 0$ is the constant associated with $\bar{\gamma}$ in Assumption 4.2.5. Recalling the upper bound for $I(t,\mathrm{d}x)$ from Lemma 4.2.16, we have

$$\limsup_{t\to+\infty} \int_{\min(\alpha^*,1/\overline{S}(t))}^{\alpha^*} e^{\bar{\gamma}(y\overline{S}(t)-1)t} A(\mathrm{d}y) \leq \limsup_{t\to+\infty} \frac{1}{m} \int_{\mathbb{R}^N} I(t,\mathrm{d}x) \leq \frac{\Lambda}{m\min(\theta,\gamma_0)} < +\infty.$$

This implies that

$$\limsup_{t\to+\infty} \int_{\alpha(\mathrm{supp}(I_0))} e^{\bar{\gamma}(y\overline{S}(t)-1)t} A(\mathrm{d}y) < \infty.$$

Note that, if the constant m is independent of $\bar{\gamma}$, then the above estimate does not depend on $\bar{\gamma}$ either.

Step 3: We show that $\int \mathbb{1}_{\gamma(x)<\bar{\gamma}} \mathbb{1}_{\overline{S}(t)\alpha(x)\geq 1} I(t,\mathrm{d}x)$ vanishes whenever $\bar{\gamma} < \gamma^*$.
Fix $\bar{\gamma} < \gamma^*$ and let $\varepsilon := \frac{\gamma^*-\bar{\gamma}}{2}$. Then we have

$$\begin{aligned}
\int_{\gamma^{-1}((-\infty,\bar{\gamma}])\cap\alpha^{-1}([1/\overline{S}(t),\infty))} I(t,\mathrm{d}x) &= \int_{\min(\alpha^*,1/\overline{S}(t))}^{\alpha^*} \int_{x\in\gamma^{-1}((-\infty,\bar{\gamma}])\cap\alpha^{-1}(y)} e^{\gamma(x)(y\overline{S}(t)-1)t} I_0(y,\mathrm{d}x) A(\mathrm{d}y) \\
&\leq \int_{\min(\alpha^*,1/\overline{S}(t))}^{\alpha^*} \int_{x\in\gamma^{-1}((-\infty,\bar{\gamma}])\cap\alpha^{-1}(y)} I_0(y,\mathrm{d}x) e^{(\gamma^*-2\varepsilon)(y\overline{S}(t)-1)t} A(\mathrm{d}y) \\
&\leq \int_{\min(\alpha^*,1/\overline{S}(t))}^{\alpha^*} \int_{x\in\alpha^{-1}(y)\}} I_0(y,\mathrm{d}x) e^{-\varepsilon(y\overline{S}(t)-1)t} e^{\bar{\gamma}(y\overline{S}(t)-1)t} A(\mathrm{d}y).
\end{aligned}$$

Reducing ε if necessary we may assume that $\frac{\bar\gamma}{\varepsilon} > 1$. Therefore it follows from Hölder's inequality that

$$\begin{aligned}\int_{\gamma^{-1}((-\infty,\bar\gamma])\cap\alpha^{-1}([1/\overline{S}(t),\infty))} I(t,\mathrm{d}x) &\le \left(\int_{\min(\alpha^*,1/\overline{S}(t))}^{\alpha^*} \left(e^{-\varepsilon(y\overline{S}(t)-1)t}\right)^{\frac{\bar\gamma}{\varepsilon}} e^{\bar\gamma(y\overline{S}(t)-1)t}A(\mathrm{d}y)\right)^{\frac{\varepsilon}{\bar\gamma}} \\ &\quad\times\left(\int_{\min(\alpha^*,1/\overline{S}(t))}^{\alpha^*}\left(\int_{\alpha(x)=y} I_0(y,\mathrm{d}x)\right)^{\frac{\bar\gamma}{\bar\gamma-\varepsilon}} e^{\bar\gamma(y\overline{S}(t)-1)t}A(\mathrm{d}y)\right)^{1-\frac{\varepsilon}{\bar\gamma}} \\ &\le \left(\int_{\min(\alpha^*,1/\overline{S}(t))}^{\alpha^*} A(\mathrm{d}y)\right)^{\frac{\varepsilon}{\bar\gamma}}\left(\int_{\min(\alpha^*,1/\overline{S}(t))}^{\alpha^*} e^{\bar\gamma(y\overline{S}(t)-1)t}A(\mathrm{d}y)\right)^{1-\frac{\varepsilon}{\bar\gamma}} \\ &= I_0(L_{\alpha^*-\min(\alpha^*,1/\overline{S}(t))}(I_0))^{\frac{\varepsilon}{\bar\gamma}}\left(\int_{\min(\alpha^*,1/\overline{S}(t))}^{\alpha^*} e^{\bar\gamma(y\overline{S}(t)-1)t}A(\mathrm{d}y)\right)^{1-\frac{\varepsilon}{\bar\gamma}}.\end{aligned} \tag{4.2.32}$$

Since $\overline{S}(t) \to 1/\alpha^*$ as $t\to\infty$, $I_0(L_\epsilon(I_0)) \xrightarrow[\epsilon\to 0]{} 0$ and by the boundedness of $\int_{\min(\alpha^*,1/\overline{S}(t))}^{\alpha^*} e^{\bar\gamma(y\overline{S}(t)-1)t}A(\mathrm{d}y)$ shown in Step 2, we have indeed

$$\int_{\gamma^{-1}((-\infty,\bar\gamma])\cap\alpha^{-1}([1/\overline{S}(t),\infty))} I(t,\mathrm{d}x) \xrightarrow[t\to+\infty]{} 0, \qquad \square$$

and this completes proof of Lemma 4.2.26.

Proof of Proposition 4.2.7. The concentration of the distribution to $\mathcal{M}_+(\alpha^{-1}(\alpha^*)\cap\gamma^{-1}(\gamma^*))$ was shown in Lemma 4.2.26.

Next we prove the asymptotic mass. Pick a sentence $t_n\to+\infty$. By the compactness of the orbit (proved in Lemma 4.2.19) we can extract from t_n a subsequence t_n' such that there exists a Radon measure $I^\infty(\mathrm{d}x)$ with

$$d_0(I(t,\mathrm{d}x), I^\infty(\mathrm{d}x)) \xrightarrow[t\to+\infty]{} 0,$$

and since $S(t)\to\frac{1}{\alpha^*}$ and upon further extraction, $S'(t_n')\to 0$. Therefore,

$$\int_{\mathbb{R}^N}\alpha(x)\gamma(x)I(t_n',\mathrm{d}x) = \frac{\Lambda - S_t(t_n')}{S(t_n')} - \theta \xrightarrow[n\to+\infty]{} \alpha^*\Lambda-\theta = \theta\left(\mathcal{R}_0(I_0)-1\right).$$

By the concentration result in Lemma 4.2.26, I^∞ is concentrated on $\alpha^{-1}(\alpha^*)\cap\gamma^{-1}(\gamma^*)$. Therefore

$$\alpha^*\gamma^*\int I^\infty(\mathrm{d}x) = \int\alpha(x)\gamma(x)I^\infty(\mathrm{d}x) = \lim_{n\to+\infty} I(t_n',\mathrm{d}x) = \theta\left(\mathcal{R}_0(I_0)-1\right),$$

so that

$$\lim_{n\to+\infty}\int I(t_n',\mathrm{d}x) = \int I^\infty(\mathrm{d}x) = \frac{\theta}{\alpha^*\gamma^*}\left(\mathcal{R}_0(I_0)-1\right).$$

Since the limit is independent of the sequence t_n, we have indeed shown that

$$\lim_{t\to+\infty}\int_{\mathbb{R}^N} I(t,\mathrm{d}x) = \frac{\theta}{\alpha^*\gamma^*}\left(\mathcal{R}_0(I_0)-1\right).$$

To prove the last statement, set

$$f(t) := \int_{\min(\alpha^*,1/\overline{S}(t))}^{\alpha^*}\int_{\bar\gamma}^{\gamma^*} e^{z(y\overline{S}(t)-1)t}I_0^\alpha(y,\mathrm{d}z)A(\mathrm{d}y),$$

where $\bar\gamma<\gamma^*$. It follows from (4.2.32) that

$$\int_{\gamma^{-1}((-\infty,\bar\gamma])\cap\alpha^{-1}([1/\overline{S}(t),\infty))} I(t,\mathrm{d}x) \xrightarrow[t\to+\infty]{} 0,$$

therefore

$$f(t)=\int_{\min(\alpha^*,1/\overline{S}(t))}^{\alpha^*}\int_{\bar\gamma}^{\gamma^*}\int_{\{\gamma(x)=z\}}e^{z(y\overline{S}(t)-1)t}I_0^{\alpha,\gamma}(y,z,\mathrm{d}x)I_0^{\alpha}(z,\mathrm{d}y)A(\mathrm{d}y)=\int_{\gamma^{-1}([\bar\gamma,\gamma^*])\cap\alpha^{-1}([1/\overline{S}(t),\infty))}I(t,\mathrm{d}x)$$

satisfies

$$0<\liminf_{t\to+\infty}\int I(t,\mathrm{d}x)=\liminf_{t\to+\infty}\int_{\gamma^{-1}((-\infty,\bar\gamma])\cap\alpha^{-1}([1/\overline{S}(t),\infty))}I(t,\mathrm{d}x)\le\liminf_{t\to+\infty}f(t)$$

Remark that

$$\begin{aligned}\int\mathbb{1}_U(x)\mathbb{1}_{\gamma\ge\bar\gamma}\mathbb{1}_{S(t)y\ge1}I(t,\mathrm{d}x)&=\int_{\min(\alpha^*,1/\overline{S}(t))}^{\alpha^*}\int_{\bar\gamma}^{\gamma^*}\int_{\{\gamma(x)=z\}}\mathbb{1}_U(x)e^{z(yS(t)-1)t}I_0^{\alpha,\gamma}(y,z,\mathrm{d}x)I_0^{\alpha}(y,\mathrm{d}z)A(\mathrm{d}y)\\&=\int_{\min(\alpha^*,1/\overline{S}(t))}^{\alpha^*}\int_{\bar\gamma}^{\gamma^*}\int_{\{\gamma(x)=z\}}\mathbb{1}_U(x)I_0^{\alpha,\gamma}(y,z,\mathrm{d}x)e^{z(yS(t)-1)t}I_0^{\alpha}(y,\mathrm{d}z)A(\mathrm{d}y)\\&\ge\int_{\min(\alpha^*,1/\overline{S}(t))}^{\alpha^*}\int_{\bar\gamma}^{\gamma^*}\frac{m}{2}e^{z(yS(t)-1)t}I_0^{\alpha}(y,\mathrm{d}z)A(\mathrm{d}y)\\&\ge f(t)\frac{m}{2},\end{aligned}$$

provided t is sufficiently large and $\bar\gamma$ is sufficiently close to γ^*, where

$$m:=\liminf_{\varepsilon\to0}\operatorname*{ess\,inf}_{\alpha^*-\varepsilon\le y\le\alpha^*}^{A(\mathrm{d}y)}\operatorname*{ess\,inf}_{\gamma^*-\varepsilon\le z\le\gamma^*}^{I_0^\alpha(y,\mathrm{d}z)}\int\mathbb{1}_{x\in U}I_0^{\alpha,\gamma}(y,z,\mathrm{d}x)>0.$$

Therefore

$$\liminf_{t\to+\infty}\int_U I(t,\mathrm{d}x)\ge\frac{m}{2}\liminf_{t\to+\infty}f(t)>0.$$

This completes proof of Proposition 4.2.7. □

4.2.3 The case of discrete systems. Proof of Theorem 4.2.8 and 4.2.9

In this section 4.2.3 we show how the theory for discrete systems can be included in the theory for measure-valued solutions to (4.2.1) in $\mathbb{R}^N$. Rather than doing a direct proof of the results, we show how the general results from Section 4.2.2 can be applied to prove Theorem 4.2.8 and 4.2.9. In particular, we rely heavily on Theorem 4.2.2, which has been proven in Section 4.2.2 (independently of Theorem 4.2.8 and 4.2.9).

Proof of Theorem 4.2.8. Let us choose n distinct real numbers $x_1,\dots,x_n$. Then there exist continuous functions $\alpha(x)$ and $\gamma(x)$ such that

$$\alpha(x_i)=\alpha_i \text{ and } \gamma(x_i)=\gamma_i \text{ for all } i=1,\dots,n.$$

There are many ways to construct $\alpha(x)$ and $\gamma(x)$; for instance one can work with Lagrange polynomials and interpolate with a constant value outside of a ball and when the values of $\gamma(x)$ become close to 0. In particular one can impose that $\alpha(x)$ and $\gamma(x)$ are bounded and that $\gamma(x)>0$ for all $x\in\mathbb{R}^N$, thus meeting Assumption 4.2.1. Now define the initial data

$$I_0(\mathrm{d}x):=\sum_{i=1}^n I_0^i\delta_{x_i}.$$

Clearly, the solution $\big(S(t),I(t,\mathrm{d}x)\big)$ to (4.2.1) can be identified with the solution $(S(t),I^i(t))$ to (4.2.11) by the formula

$$I(t,\mathrm{d}x)=\sum_{i=1}^n I^i(t)\delta_{x_i}.$$

Since the set $\{x:\alpha(x)=\alpha^*\}$ has non-zero measure for I_0, we are in the situation i) of Theorem 4.2.2 and Theorem 4.2.8 can therefore be deduced from Theorem 4.2.2. □

Proof of Theorem 4.2.9. As in the proof of Theorem 4.2.8, we identify the solutions to (4.2.12) with the solutions $I(t,\mathrm{d}x)$ to (4.2.1) through the formula

$$I_0(\mathrm{d}x) := \sum_{i=1}^{+\infty} I_0^i \delta_{x_i}, \qquad I(t,\mathrm{d}x) = \sum_{i=1}^{+\infty} I^i(t)\delta_{x_i},$$

only this time we choose $x_i = (\alpha_i, \gamma_i) \in \mathbb{R}^2$. Because of this particular choice, it is fairly easy to construct $\alpha(x)$ and $\gamma(x)$ by the formula

$$\alpha(x_1,x_2) := \alpha^\infty f\left(\frac{x_1}{\alpha^\infty}\right), \qquad \gamma(x_1,x_2) := \left|\gamma^\infty f\left(\frac{x_2-\gamma_0}{\gamma^\infty}\right)\right| + \gamma_0,$$

where $\alpha^\infty := \sup|\alpha_i|$, $\gamma^\infty := \sup|\gamma_i|$, $\gamma_0 = \inf\gamma_i$ and $f(x) := \min(\max(x,-1),1)$. Then the conclusions of Theorem 4.2.9 in case i) are given by a direct application of Theorem 4.2.2. Suppose that the set $\{i : \alpha_i = \alpha^*\}$ is empty, then we are in case ii) of Theorem 4.2.2, and we can readily conclude that

$$S(t) \xrightarrow[t\to+\infty]{} \frac{1}{\alpha^*} \text{ and } \liminf_{t\to+\infty} \sum_{i=1}^{+\infty} I^i(t) = \liminf_{t\to+\infty} \int_{\mathbb{R}^2} I(t,\mathrm{d}x) > 0.$$

If we assume moreover that $\alpha_n \to \alpha^*$ and $\gamma_n \to \gamma^*$, then the maximum of $\alpha(x)$ on $\operatorname{supp} I_0$ is attained at a single point (α^*,γ^*) and we can apply Theorem 4.2.10 to find that

$$I(t,\mathrm{d}x) \xrightarrow[t\to+\infty]{*} I^\infty \delta_{(\alpha^*,\gamma^*)},$$

where $I^\infty = \frac{\theta}{\gamma^*}(\mathcal{R}_0^* - 1)$. This finishes the proof of Theorem 4.2.9. □

4.2.4 The case of a finite number of regular maxima

In this section 4.2.4 we prove Theorem 4.2.13. To that aim, we shall make use of the following formula

$$I(t,\mathrm{d}x) = \exp\left(\gamma(x)\left(\alpha(x)\int_0^t S(s)\mathrm{d}s - t\right)\right) I_0(\mathrm{d}x). \tag{4.2.33}$$

Recall also the definition of $\eta(t)$:

$$\eta(t) = \alpha^* \frac{1}{t}\int_0^t S(s)\mathrm{d}s - 1 = \alpha^* \overline{S}(t) - 1.$$

Proof of Theorem 4.2.13. We split the proof of this result into three parts. We first derive a suitable upper bound. We then derive a lower bound in a second step and we conclude the proof of the theorem by estimating the large time asymptotic of the mass of I around each point of $\alpha^{-1}(\alpha^*)$.

Upper bound:

Let $i = 1,..,p$ be given. Recall that $\nabla\alpha(x_i) = 0$. Now due to (iii) in Assumption 4.2.11 there exist $m > 0$ and $T > \varepsilon_0^{-2}$ large enough such that for all $t \geq T$ and for all $y \in B\left(0, t^{-\frac{1}{2}}\right)$ we have

$$\alpha(x_i + y) - \alpha^* \leq -\alpha^* m\|y\|^2.$$

As a consequence, setting

$$\Gamma(x) = \gamma(x)\frac{\alpha(x)}{\alpha^*},$$

we infer from (4.2.33) and the lower estimate of I_0 around x_i given in Assumption 4.2.11 (ii), that for all $t > T$

$$\int_{\|x_i - x\| \leq t^{-\frac{1}{2}}} I(t,\mathrm{d}x) \geq M^{-1} \int_{|y|\leq t^{-\frac{1}{2}}} |y|^{\kappa_i} \exp\left[t\eta(t)\Gamma(x_i+y) - t\gamma(x_i+y)m|y|^2\right] \mathrm{d}y.$$

Next since the function $I = I(t, \mathrm{d}x)$ has a bounded mass, there exists some constant $C > 0$ such that

$$\int_{\mathbb{R}^N} I(t, \mathrm{d}x) \leq C, \ \forall t \geq 0.$$

Coupling the two above estimates yields for all $t > T$

$$\int_{|y| \leq t^{-\frac{1}{2}}} |y|^{\kappa_i} \exp\left[t\eta(t)\Gamma(x_i + y) - t\gamma(x_i + y)m|y|^2\right] \mathrm{d}y \leq MC.$$

Hence setting $z = y\sqrt{t}$ into the above integral rewrites as

$$\int_{|z| \leq 1} t^{-\frac{\kappa_i}{2}} |z|^{\kappa_i} \exp\left[t\eta(t)\Gamma(x_i + t^{-\frac{1}{2}}z) - \gamma(x_i + t^{-\frac{1}{2}}z)m|z|^2\right] \frac{\mathrm{d}z}{t^{N/2}} \leq MC, \ \forall t > T.$$

Now, since γ and α are both smooth functions, we have uniformly for $|z| \leq 1$ and $t \gg 1$:

$$\Gamma(x_i + t^{-\frac{1}{2}}z) = \gamma(x_i) + O\left(t^{-\frac{1}{2}}\right),$$
$$\gamma(x_i + t^{-\frac{1}{2}}z) = \gamma(x_i) + O\left(t^{-\frac{1}{2}}\right).$$

This yields for all $t \gg 1$

$$\int_{|z| \leq 1} t^{-\frac{\kappa_i}{2}} |z|^{\kappa_i} \exp\left[t\eta(t)\left(\gamma(x_i) + O\left(t^{-\frac{1}{2}}\right)\right) - \gamma(x_i)m|z|^2\right] \frac{\mathrm{d}z}{t^{N/2}} \leq CM,$$
$$t^{-\frac{\kappa_i}{2} - \frac{N}{2}} e^{t\eta(t)\left(\gamma(x_i) + O\left(t^{-\frac{1}{2}}\right)\right)} \int_{|z| \leq 1} |z|^{\kappa_i} e^{-\gamma(x_i)m|z|^2} \mathrm{d}z \leq CM,$$

that also ensures the existence of some constant $c_1 \in \mathbb{R}$ such that

$$t\eta(t)\left(\gamma(x_i) + O\left(t^{-\frac{1}{2}}\right)\right) - \frac{N + \kappa_i}{2} \ln t \leq c_1, \ \forall t \gg 1,$$

or equivalently

$$\eta(t) \leq \frac{N + \kappa_i}{2\gamma(x_i)} \frac{\ln t}{t} + O\left(\frac{1}{t}\right) \text{ as } t \to \infty.$$

Since the above upper-bound holds for all $i = 1, .., p$, we obtain the following upper-bound

$$\eta(t) \leq \varrho \frac{\ln t}{t} + O\left(\frac{1}{t}\right) \text{ as } t \to \infty, \tag{4.2.34}$$

where ϱ is defined in (4.2.16).

Lower bound:

Let $\varepsilon_1 \in (0, \varepsilon_0)$ small enough be given such that for all $i = 1, .., p$ and $|y| \leq \varepsilon_1$ one has

$$\alpha(x_i + y) \leq \alpha^* - \frac{\ell}{2}|y|^2.$$

Herein $\ell > 0$ is defined in Assumption 4.2.11 (iii). Next define $m > 0$ by

$$m = \frac{\ell}{2} \min_{i=1,..,p} \min_{|y| \leq \varepsilon_1} \gamma(x_i + y) > 0.$$

Recall that $\Gamma(x) = \frac{\alpha(x)\gamma(x)}{\alpha^*}$ and $\nabla\Gamma(x) = \frac{1}{\alpha^*}\left(\alpha(x)\nabla\gamma(x) + \gamma(x)\nabla\alpha(x)\right)$. Consider $M > 0$ such that for all $k = 1, .., p$ and all $|x - x_k| \leq \varepsilon_1$ one has

$$|\Gamma(x) - \gamma(x_k) - \nabla\gamma(x_k) \cdot (x - x_k)| \leq M|x - x_k|^2. \tag{4.2.35}$$

Next fix $i = 1, .., p$ and $\varepsilon \in (0, \varepsilon_1)$. Then one has for all $t > 0$

$$\int_{|x - x_i| \leq \varepsilon} I(t, \mathrm{d}x) \leq \int_{|x - x_i| \leq \varepsilon} \exp\left[t\eta(t)\Gamma(x) - tm|x - x_i|^2\right] I_0(\mathrm{d}x)$$
$$\leq e^{t\eta(t)\gamma(x_i)} \int_{|x - x_i| \leq \varepsilon} \exp\left[t\left(\eta(t)\nabla\gamma(x_i) \cdot (x - x_i) - (m + O(\eta(t))|x - x_i|^2\right)\right] I_0(\mathrm{d}x).$$

Now observe that for all $t \gg 1$ one has

$$\eta(t)\nabla\gamma(x_k)\cdot(x-x_i)-(m+O(\eta(t)))|x-x_i|^2 = -(m+O(\eta(t)))\left|x-x_i-\frac{\eta(t)\nabla\gamma(x_i)}{2(m+O(\eta(t)))}\right|^2+\frac{\eta(t)^2\|\nabla\gamma(x_i)\|^2}{4(m+O(\eta(t)))},$$

so that we get, using Assumption 4.2.11 (ii), that

$$\begin{aligned}\int_{|x-x_i|\leq\varepsilon} I(t,\mathrm{d}x) &\leq e^{t\eta(t)\gamma(x_i)+\frac{t\eta(t)^2\|\nabla\gamma(x_i)\|^2}{4(m+O(\eta(t))}}\int_{|x-x_i|\leq\varepsilon}\exp\left[-(m+O(\eta(t))t\left|x-x_i-\frac{\eta(t)\nabla\gamma(x_i)}{2(m+O(\eta(t))}\right|^2\right]I_0(\mathrm{d}x)\\ &\leq Me^{t\eta(t)\gamma(x_i)+\frac{t\eta(t)^2\|\nabla\gamma(x_i)\|^2}{4(m+O(\eta(t))}}\\ &\quad\times\int_{|x-x_i|\leq\varepsilon}|x-x_i|^{\kappa_i}\exp\left[-(m+O(\eta(t))t\left|x-x_i-\frac{\eta(t)\nabla\gamma(x_i)}{2(m+O(\eta(t))}\right|^2\right]\mathrm{d}x.\end{aligned}$$

We now make use of the following change of variables in the above integral

$$z=\sqrt{t}\left(x-x_i-\frac{\eta(t)\nabla\gamma(x_i)}{2(m+O(\eta(t))}\right),$$

so that we end up with

$$\int_{|x-x_i|\leq\varepsilon} I(t,\mathrm{d}x)\leq t^{-\frac{N+\kappa_i}{2}}e^{t\eta(t)\gamma(x_i)+\frac{t\eta(t)^2\|\nabla\gamma(x_i)\|^2}{4(m+O(\eta(t))}}C(t),$$

with $C(t)$ given by

$$C(t):=M\int_{|z|\leq\sqrt{t}(\varepsilon+O(\eta(t)))}|z+\sqrt{t}O(\eta(t))|^{\kappa_i}e^{-\frac{m+O(\eta(t))}{2}|z|^2}\mathrm{d}z.$$

Now let us recall that Lemma 4.2.25 ensures that

$$\lim_{t\to\infty} t\eta(t)=\infty.$$

Hence one already knows that $\eta(t)\geq 0$ for all $t\gg 1$. Moreover (4.2.34) ensures that

$$\lim_{t\to\infty}\sqrt{t}\eta(t)=0,$$

so that Lebesgue convergence theorem ensures that

$$C(t)\to C_\infty:=M\int_{\mathbb{R}^N}|z|^{\kappa_i}e^{-\frac{m}{2}|z|^2}\mathrm{d}z\in(0,\infty)\text{ as }t\to\infty.$$

As a conclusion of the above analysis, we have obtained that there exists some constant C' such that for all $\varepsilon\in(0,\varepsilon_1)$ and all $i=1,..,p$ one has

$$\int_{|x-x_i|\leq\varepsilon} I(t,\mathrm{d}x)\leq C't^{-\frac{N+\kappa_i}{2}}e^{t\eta(t)\gamma(x_i)},\ \forall t\gg 1. \tag{4.2.36}$$

Since $I(t,\mathrm{d}x)$ concentrates on $\alpha^{-1}(\alpha^*)$, then for all $\varepsilon\in(0,\varepsilon_1)$ one has

$$\int_{\mathbb{R}^N} I(t,\mathrm{d}x)=\sum_{i=1}^p\int_{|x-x_i|\leq\varepsilon} I(t,\mathrm{d}x)dx+o(1)\text{ as }t\to\infty.$$

Using the persistence of I stated in Theorem 4.2.2 (see Lemma 4.2.16), we end-up with

$$0<\liminf_{t\to\infty}\int_{\mathbb{R}^N} I(t,\mathrm{d}x)\leq\liminf_{t\to\infty}\sum_{i=1}^p\int_{|x-x_i|\leq\varepsilon} I(t,\mathrm{d}x),$$

so that (4.2.36) ensures that there exists $c > 0$ and $T > 0$ such that

$$0 < c \leq \sum_{i=1}^{p} e^{\gamma(x_i)\left(t\eta(t) - \frac{N+\kappa_i}{2\gamma(x_i)} \ln t\right)}, \ \forall t \geq T. \tag{4.2.37}$$

Now recalling the definition of ϱ and J in (4.2.16) and (4.2.18), the upper bound for $\eta(t)$ provided in (4.2.34) implies

$$\sum_{i \notin J} e^{\gamma(x_i)\left(t\eta(t) - \frac{N+\kappa_i}{2\gamma(x_i)} \ln t\right)} \to 0 \text{ as } t \to \infty,$$

and (4.2.37) rewrites as

$$0 < \frac{c}{2} \leq \sum_{i \in J} e^{\gamma(x_i)(t\eta(t) - \varrho \ln t)}, \ \forall t \gg 1.$$

This yields

$$\liminf_{t \to \infty} (t\eta(t) - \varrho \ln t) > -\infty,$$

that is

$$\eta(t) \geq \varrho \frac{\ln t}{t} + O\left(\frac{1}{t}\right) \text{ as } t \to \infty. \tag{4.2.38}$$

Then (4.2.15) follows coupling (4.2.34) and (4.2.38).

Estimate of the masses: In this last step we turn to the proof of (4.2.17). Observe first that the upper estimate directly follows from the asymptotic expansion of $\eta(t)$ in (4.2.15) together with (4.2.36). Next, the proof for the lower estimate follows from similar inequalities as the one derived in the second step above. □

Appendix

4.2.5 Measure theory on metric spaces

In this Section we let (M, d) be a complete metric space. Let $\mathcal{K}(M)$ be the set of compact subsets in M and let $K \in \mathcal{K}(M)$. We first recall that we can define a kind of frame of reference, internal to K, which allows to identify each point in K.

Let us denote $\mathcal{K}(M)$ the set formed by all compact subsets of M. Recall that $(\mathcal{K}(M), d_H)$ is a complete metric space, where d_H is the Hausdorff distance

$$d_H(K_1, K_2) = \max\left(\sup_{x \in K_1} d(x, K_2), \sup_{x \in K_2} d(x, K_1)\right).$$

Proposition 4.2.27 (Metric coordinates)**.** *There exists a finite number of points $x_1, \ldots, x_n \in K$ with the property that each $y \in K$ can be identified uniquely by the distance between y and $x_1, \ldots, x_n$. In other words the map*

$$y \overset{c_K}{\longmapsto} \begin{pmatrix} d(y, x_1) \\ \vdots \\ d(y, x_n) \end{pmatrix} \in \mathbb{R}^n_+,$$

is one-to-one. Moreover c_K is continuous and its reciprocal function $c_K^{-1} : c_K(K) \to K$ is also continuous.

Proof. Let us choose $x_1 \in K$ and $x_2 \in K$ such that $x_1 \neq x_2$. We recursively construct a sequence x_n and a compact set K_n such that

$$\begin{aligned} K_n &= \{y \in K \, : \, d(y, x_i) = d(y, x_1) \text{ for all } 1 \leq i \leq n\}, \\ x_{n+1} &\in K_n, \end{aligned}$$

the choice of x_{n+1} being arbitrary. Clearly K_n is a compact set and $K_{n+1} \subsetneq K_n$. Suppose by contradiction that $K_n \neq \varnothing$ for all $n \in \mathbb{N}$, then (because K is compact) one can construct a sequence $x_{\varphi(n)}$, extracted from x_n, and which converges to a point

$$x = \lim_{n \to +\infty} x_{\varphi(n)} \in \bigcap_{n \in \mathbb{N}} K_n =: K_\infty.$$

In particular K_∞ is not empty. However we see that, by definition of K_∞, we have $d(x, x_n) = d(x, x_1) > 0$ for all $n \in \mathbb{N}$, which contradicts the fact that

$$\lim_{n \to +\infty} d(x, x_{\varphi(n)}) = 0.$$

Hence we have shown by contradiction that there exists $n_0 \in \mathbb{N}$ such that $K_{n_0} = \varnothing$ and $K_{n_0 - 1} \neq \varnothing$. This is precisely the injectivity of the map $c_K : K \to \mathbb{R}^{n_0}$.

To show the continuity, we remark that c_K is continuous, and therefore for each closed set $F \subset K$, F is compact so that $c_K(F)$ is compact and therefore closed. Therefore $(c_K^{-1})^{-1}(F) = c_K(F)$ is closed in $c_K(K)$. The proposition is proved. □

Recall that the Borel σ-algebra $\mathcal{B}(M)$ is the closure of the set of all open sets in $\mathfrak{P}(M) = 2^M$ under the operations of complement and countable union. A function $\varphi : M \to N$ is Borel measurable if the reciprocal image of any Borel set is Borel, *i.e.* $\varphi^{-1}(B) \in \mathcal{B}(M)$ for all $B \in \mathcal{B}(N)$.

Proposition 4.2.28 (Borel function of choice)**.** *There exists a Borel measurable map $c : \big(\mathcal{K}(K), d_H\big) \to (K, d)$ such that*

$$c(K') \in K' \text{ for all } K' \in \mathcal{K}(K).$$

Proof. Let $c_K : K \to \mathbb{R}^{n_0}$ be the map constructed in Proposition 4.2.27. For a compact $K' \subset K$ we define

$$c(K') := c_K^{-1}\left(\min_{y \in c_K(K')} y\right),$$

where the minimum is taken with respect to the lexicographical order in $\mathbb{R}^{n_0}$ (which is a total order and therefore identifies a unique minimum for each $K' \in \mathcal{K}(K)$). Since the map $\widetilde{K} \subset \mathbb{R}^{n_0} \to \min_{y \in K} y$ is Borel for the topology on $\mathcal{K}(\mathbb{R}^{n_0})$ induced by the Hausdorff metric, so is c. The proposition is proved. □

Proposition 4.2.29 (Borel measurability of the metric projection)**.** *Let $K \subset M$ be compact. The map $P_K : M \to \mathcal{K}(K)$ defined by*

$$P_K(x) = \{y \in K \,:\, d(x, y) = d(x, K)\},$$

is Borel measurable.

Proof. First we remark that the map

$$P_K(x) := \{y \in K \,:\, d(x, y) = d(x, K)\} \in \mathcal{K}(M),$$

is well-defined for each $x \in M$, and therefore forms a mapping from M into $\mathcal{K}(K) \subset \mathcal{K}(M)$. Indeed $P_K(x)$ is clearly closed in the compact space K, therefore is compact.

To show the Borel measurability of P_K, we first remark that, given a compact space $K' \subset K$, the set

$$\widetilde{P_K^{-1}}(K') := \{x \in M \,:\, P_K(x) \cap K' \neq \varnothing\}$$

is closed. Indeed let $x_n \to x$ be a sequence in $\widetilde{P_K^{-1}}(K')$, then by definition there exists $y_n \in K'$ such that $d(x_n, y_n) = d(x_n, K)$. By the compactness of K', there exists $y \in K'$ and a subsequence $y_{\varphi(n)}$ extracted from y_n such that $y_{\varphi(n)} \to y$. Because of the continuity of $z \mapsto d(z, K)$, we have

$$d(x, y) = \lim_{n \to +\infty} d(x_{\varphi(n)}, y_{\varphi(n)}) = \lim_{n \to +\infty} d(x_{\varphi(n)}, K) = d(x, K),$$

therefore $y \in P_K(x) \cap K'$, which shows that $x \in \widetilde{P_K^{-1}}(K')$. Hence $\widetilde{P_K^{-1}}(K')$ is closed.

We are now in a position to show the Borel regularity of P_K. Let $C \in \mathcal{K}(K)$ and $R > 0$ be given. We defined $B_H(C, R)$ the ball of center C and radius R in the Hausdorff metric:

$$B_H(C, R) = \{C' \in \mathcal{K}(K) \,:\, d_H(C, C') \leq R\}.$$

Then

$$P_K^{-1}(B_H(C, R)) = \{x \in M \,:\, d_H(P_K(x), C) \leq R\} = B_1 \cap B_2,$$

where

$$B_1 := \{x \in M \,:\, d(y,C) \le R \text{ for all } y \in P_K(x)\}, \text{ and}$$
$$B_2 := \{x \in M \,:\, d(z,P_K(x)) \le R \text{ for all } z \in C\}.$$

It can be readily seen that B_1 is a Borel set by writing

$$B_1 = \widetilde{P_K^{-1}}(V_R(C)) \bigcap_{n\ge 1} \left(M \backslash \left(\widetilde{P_K^{-1}}(K \backslash V_{R+\frac{1}{n}}(C))\right)\right),$$

where $V_R(C) := \{y \in K \,:\, d(y,C) \le R\}$. To see that B_2 is a Borel set, we choose a sequence z_n which is dense in C and write

$$B_2 = \bigcap_{k\ge 1} \bigcap_{n\ge 1} \widetilde{P_K^{-1}}\big(B(z_n, R+1/k)\big).$$

Indeed if $x \in B_2$ then $P_K(x)$ intersects every ball of radius R and center $z \in C$; in particular $P_K(x)$ intersects every ball of radius $R+1/k$ and center z_n. Conversely suppose that $P_K(x)$ intersects every ball $B(z_n, R+1/k)$ for $n \ge 1$ and $k \ge 1$. If $z \in C$ then there is a sequence $z_{\varphi(k)}$ such that $z = \lim z_{\varphi(k)}$, and (by assumption) we have $P_K(x) \cap B(z_{\varphi(k)}, R+1/k) \neq \varnothing$. Therefore

$$d\big(z, P_K(x)\big) = \lim_{k\to+\infty} d\big(z_{\varphi(k)}, P_K(x)\big) \le \lim_{k\to+\infty} R + \frac{1}{k} = R.$$

Thus $x \in B_2$. The equality is proved.

We conclude that $P_K^{-1}(B_H(C,R))$ is a Borel set for all $C \in \mathcal{K}(K)$ and $R > 0$, and since those sets form a basis of the Borel σ-algebra, P_K is indeed Borel measurable. The Lemma is proved. □

Theorem 4.2.30 (Existence of a regular metric projection)**.** *Let $K \subset M$ be compact. There exists a Borel measurable map $P_K : M \to K$ such that*

$$d\big(x, P_K(x)\big) = d(x,K).$$

Proof. The proof is immediate by combining Proposition 4.2.29 Proposition 4.2.28. □

Proposition 4.2.31 (Metric projection on measure spaces)**.** *Let $K \in \mathcal{K}(\mathbb{R}^N)$ be a given compact set. Let $\mu \in \mathcal{M}_+(K)$ be a given nonnegative measure on K. Then the Kantorovitch-Rubinstein distance between μ and $\mathcal{M}_+(K)$ can be bounded by the distance between K and the furthest point in* $\operatorname{supp}\mu$*:*

$$d_0(\mu, \mathcal{M}_+(K)) \le \|\mu\|_{AV} \sup_{x\in\operatorname{supp}\mu} d(x,K).$$

Proof. Indeed, let us choose a Borel measurable metric projection P_K on K as in Theorem 4.2.30. Let μ^K be the image measure defined on $\mathcal{B}(K)$ by

$$\mu^K(B) := \mu\big(P_K^{-1}(B)\big), \text{ for all } B \in \mathcal{B}(K).$$

Then in particular for all $f \in BC(\mathbb{R}^N)$ we have

$$\int_{\mathbb{R}^N} f(P_K(x))\mathrm{d}\mu(x) = \int_K f(x)\mathrm{d}\mu^K(x).$$

Let $f \in \operatorname{Lip}_1(\mathbb{R}^N)$, then we have

$$\begin{aligned}
\int_{\mathbb{R}^N} f(x)\mathrm{d}(\mu-\mu^K)(x) &= \int_{\mathbb{R}^N} f(x)\mathrm{d}\mu(x) - \int_{\mathbb{R}^N} f(x)\mathrm{d}\mu^K(x) \\
&= \int_{\mathbb{R}^N} f(x)\mathrm{d}\mu(x) - \int_{\mathbb{R}^N} f(P_K(x))\mathrm{d}\mu(x) \\
&= \int_{\mathbb{R}^N} f(x) - f(P_K(x))\mathrm{d}\mu(x) \\
&\le \int_{\operatorname{supp}\mu} |x - P_K(x)|\mathrm{d}\mu(x) \\
&\le \sup_{y\in\operatorname{supp}\mu} d(y,K) \int_{\operatorname{supp}\mu} 1\mathrm{d}\mu = \|\mu\|_{AV} \sup_{x\in\operatorname{supp}K} d(x,K).
\end{aligned}$$

Therefore $d_0(\mu,\mu^K) \le \|\mu\|_{AV} \sup_{x\in\operatorname{supp} K} d(x,K)$ and, since $\mu^K \in \mathcal{M}_+(K)$,

$$d_0\big(\mu,\mathcal{M}_+(K)\big) \le d_0(\mu,\mu^K) \le \|\mu\|_{AV} \sup_{x\in\operatorname{supp}\mu} d(x,K).$$

The Proposition is proved. □

4.2.6 Disintegration of measures

We recall the disintegration theorem as stated in [73, VI, §3, Theorem 1 p. 418]. We use Bourbaki's version, which is proved by functional analytic arguments, for convenience, although other approaches exist which are based on measure-theoretic arguments and may be deemed more intuitive. We refer to Ionescu Tulcea and Ionescu Tulcea for a disintegration theorem resulting from the theory of (strong) liftings [223, 224].

Let us first we recall some background on adequate families. This is adapted from [73, V.16 §3] to the context of finite measures of $\mathbb{R}^N$. We let T and X be locally compact topological spaces and $\mu \in \mathcal{M}_+(T)$ be a fixed Borel measure.

Definition 4.2.32 (Scalarly essentially integrable family)**.** Let $\Lambda : t \mapsto \lambda_t$ be a mapping from T into $\mathcal{M}_+(X)$. Λ is *scalarly essentially integrable* for the measure μ if for every compactly supported continuous function $f \in C_c(X)$, the function $t \mapsto \int_X f(x)\lambda_t(\mathrm{d}x)$ is in $L^1(\mu)$. Setting $\nu(f) = \int_T \int_X f(x)\lambda_t(\mathrm{d}x)\mu(\mathrm{d}t)$ defines a linear form on $C_c(X)$, hence a measure ν, which is the *integral* of the family Λ, and we denote

$$\int_T \lambda_t\,\mu(\mathrm{d}t) := \nu.$$

Recall that every positive Borel measure μ on a locally compact space X defines a positive bounded linear functional on $C_c(X)$ equipped with the inductive limit of the topologies on $C_c(K)$ when K runs over the compact subsets of X. Conversely if μ is a positive bounded linear functional on $C_c(X)$, there are two canonical ways to define a measure on the Borel σ-algebra.

1. Outer-regular construction. Let $U \subset X$ be a open, then one can define

   $$\mu^*(U) := \sup\left\{\mu(f) \,:\, f \in C_c(X), 0 \le f(x) \le \mathbb{1}_U(x)\right\},$$

   then for an arbitrary Borel set B,

   $$\mu^*(B) := \inf\left\{\mu^*(U) \,:\, U \text{ open}, B \subset U\right\}.$$

   This notion corresponds to that of the *upper integral* discussed in [73, IV.1 §1].

2. Inner-regular construction. If $U \subset X$ is open, we define $\mu^\bullet(U) := \mu^*(U)$ and similarly if $K \subset X$ is compact, then $\mu^\bullet(K) := \mu^*(K)$. Then for an arbitrary Borel set B which is contained in an open set of finite measure: $B \subset U$ with $\mu^\bullet(U) < +\infty$, we define

   $$\mu^\bullet(B) := \sup\{\mu^\bullet(K) \,:\, K \text{ compact}, K \subset B\}.$$

   Else $\mu^\bullet(B) = +\infty$. This corresponds to the *essential upper integral* discussed in [73, V.1, §1].

It is always true that $\mu^\bullet \le \mu^*$, however it may happen that $\mu^* \ne \mu^\bullet$ when μ^* is not finite, see e.g. [63, II§7.11 p.113] or [73, V.1, §1]. If μ is a Borel measure, then we define the corresponding notions of $\mu^\bullet$ and μ^* associated with the linear functional $f \mapsto \int_X f(x)\mu(\mathrm{d}x)$. Note that if μ is Radon, then $\mu^* = \mu = \mu^\bullet$.

Definition 4.2.33 (Pre-adequate and adequate families)**.** We follow [73, Definition 1, V.17§3]. Let $\Lambda : t \mapsto \lambda_t$ be a scalarly essentially μ-integrable mapping from T into $\mathcal{M}_+(X)$, ν the integral of Λ.

We say that Λ is μ-pre-adequate if, for every lower semi-continuous function $f \ge 0$ defined on X, the function $t \mapsto \int f(x)\lambda_t^\bullet(\mathrm{d}x)$ is μ-measurable on T and

$$\int_X f(x)\nu^\bullet(\mathrm{d}x) = \int_T \int_X f(x)\lambda_t^\bullet(\mathrm{d}x)\mu^\bullet(\mathrm{d}t).$$

We say that Λ is μ-adequate if Λ is μ'-pre-adequate for every positive Borel measure $\mu' \le \mu$.

The last notion we need to define is the one of *μ-proper function*.

Definition 4.2.34 (μ-proper function)**.** We say that a function $p : T \to X$ is *μ-proper* if it is μ-measurable and, for every compact set $K \subset X$, the set $p^{-1}(K)$ is $\mu^\bullet$-measurable and $\mu^\bullet(p^{-1}(K)) < +\infty$.

If μ is Radon, in particular, then every μ-measurable mapping $p : T \to X$ (X being equipped with the Borel σ-algebra) is μ-proper. The following Theorem is taken from [73, Theorem 1, VI.41 No.1, §3].

Theorem 4.2.35 (Disintegration of measures)**.** *Let T and X be two locally compact spaces having countable bases, μ be a positive measure on T, p be a μ-proper mapping of T into X, and $\nu = p(\mu)$ the image of μ under p. There exists a ν-adequate family $x \mapsto \lambda_x$ ($x \in X$) of positive measures on T, having the following properties:*

a) $\|\lambda_x\| = 1$ *for all* $x \in p(T)$*;*

b) λ_x *is concentrated on the set* $p^{-1}(\{x\})$ *for all* $x \in p(T)$*, and* $\lambda_x = 0$ *for* $x \notin p(T)$*;*

c) $\mu = \int \lambda_x \, \nu(\mathrm{d}x)$.

Moreover, if $x \mapsto \lambda'_x$ ($x \in X$) is a second ν-adequate family of positive measures on T having the properties b) and c), then $\lambda'_x = \lambda_x$ almost everywhere in B with respect to the measure ν.

Chapter 5

Parameter identification in epidemiological models and application to the COVID-19 epidemic

5.1 Real-time prediction of the end of an epidemic wave: COVID-19 in China as a case-study

5.1.1 Introduction

The COVID-19 pandemic has now spread worldwide, causing over one million deaths and 40 million reported cases so far (as of 25 October, 2020[1]). SARS-CoV-2, the virus that causes COVID-19, emerged in China at the end of 2019. In early 2020, the Chinese government imposed strong public health measures, including enhanced epidemiological surveys and surveillance, travel restrictions, quarantine, contact tracing and isolation [316]. These intense interventions were sufficient to bring the epidemic wave under control, and since mid-March case numbers have remained low.

A key challenge in infectious disease epidemiology is forecasting the progression of an epidemic. Significant attention has been directed towards developing methods for estimating future numbers of cases and deaths, as well as forecasting the timing of the epidemic peak [117, 131, P7, 419, 261, 260, 258, 259, 262, 326, 372]. Predicting the ends of epidemic waves, on the other hand, has received considerably less attention [303], despite the fact that the end of an epidemic wave signals an opportunity to relax costly public health measures. Some previous studies have estimated the probability that an epidemic is over as a function of the time since the last observed case using renewal equation models [304, 248] or stochastic compartmental models [374]. However, predicting the end of the first COVID-19 epidemic wave in China was particularly challenging for two key reasons. First, evidence emerged early in the COVID-19 pandemic that infected individuals could transmit the virus prior to displaying symptoms ("presymptomatic infection"). Second, some infected individuals never display symptoms or display only mild symptoms, and therefore do not report disease ("asymptomatic infection"). It is now widely accepted that these presymptomatic and asymptomatic hosts play a significant role in SARS-CoV-2 transmission [168, 327, 341, 194, 373].

Early evidence for asymptomatic transmission included a study by Nishiura et al. [305], which reported early in the pandemic that 13 evacuees on charter flights from Wuhan (China) were infected and four of these individuals never developed symptoms. Chowell et al. [287] estimated the proportion of asymptomatic infections to be 17.9%. Research by Li et al. [252] generated an estimate that 86% of all infections were undocumented (95% CI: [82%-90%]) prior to the introduction of travel restrictions in China on January 23, 2020, and a team in China [316] suggested that there were 37,400 cases in Wuhan that authorities were unaware of by February 18, 2020. More recently, Ferretti et al. [168] split the reproduction number into components corresponding to transmission from symptomatic, presymptomatic and asymptomatic infectious individuals, as well as environmental transmission. Unreported cases, largely due to presymptomatic and asymptomatic infections, were a key driver of the rapid geographic spread of SARS-CoV-2 and explain why early containment of the virus was impossible (compared to, e.g. SARS [175]). In [P7], we consider the symptomatic reported and unreported patients and we prove that it is hopeless to estimate the fraction of reported (or unreported) patients by using SI models. In other words, several values of the fraction of

[1]Source: worldometers website, see `www.worldometers.info/coronavirus/` (Accessed November 27, 2021)

reported symptomatic patients give the exact same fit to the data. Finally, a study based on several cohorts of patients was conducted in Oran et al. [312].

Here, we consider a compartmental model characterising SARS-CoV-2 transmission, and parameterise it using data from the first (yet unique) epidemic wave in China. Our model incorporates key features of this epidemic wave, including explicit inclusion of public health measures designed to mitigate the severity of the epidemic, as well as presymptomatic and asymptomatic infections. When we conducted our analysis in real-time, the proportion of infected individuals that were symptomatic and reported disease was unknown (and, in fact, the precise value remains uncertain even now), so we consider a range of values of that parameter (f). We derive an analytic expression for predicting when an epidemic wave is likely to end, under the assumption that public health measures that are in place remain fixed until the epidemic wave is over. We use this expression to show how the predicted end of epidemic wave date changed as the epidemic wave continued, and compare these results to equivalent results obtained using model simulations. Not only do we provide a framework for predicting the ends of epidemic waves, but we also show that the times at which epidemic waves end depend on the proportion of detected cases. This emphasises the importance of intense surveillance to find infectious cases, including those who do not display clear symptoms.

5.1.2 Methods

5.1.2.1 Data

We use cumulative data describing daily numbers of cases in mainland China from January 20, 2020 to March 18, 2020, obtained from the National Health Commission of the People's Republic of China and Chinese Center for Disease Control and Prevention[2]. Up until February 10 2020, cases in the dataset were only those that were confirmed by laboratory testing. From February 11 to February 15, data were available not only for cases confirmed by laboratory testing, but also for cases that were clinically diagnosed based on medical imaging. From February 16 onwards, these two data types were combined in the dataset, so that it was impossible to distinguish between laboratory confirmed and clinically diagnosed cases. Changing case definitions in response to changes in case numbers is necessary and commonplace [377], however such changes make inferring epidemic trends based on case numbers challenging. To account for this and remove the substantial jump in cases on February 16 due to changes in testing practices, we calculated the cumulative number of clinically diagnosed cases between February 11 and February 15, and subtracted this from the cumulative numbers of cases from February 16 onwards. We therefore obtained approximate numbers of confirmed cases throughout the period from January 20 to March 18, 2020. The dataset, accounting for this adjustment, is shown in the Supplementary Information (Table 5.1.4).

We note that, on January 23, mainland China began implementing lockdowns, beginning with a lockdown in the city of Wuhan.

5.1.2.2 Mathematical model

To characterise changes in observed case numbers from January 20 to March 18 in mainland China, we considered a compartmental model in which we track the number of individuals that are either susceptible to the virus ($S(t)$), in early infection and infectious ($I(t)$) and in later infection and reporting disease ($R(t)$) or in later infection and not reporting disease ($U(t)$) [P10, 260]. Individuals that are in later infection and not reporting disease include those that are asymptomatic and those who develop only mild symptoms and so do not adhere to interventions targeting symptomatic individuals. The model is therefore given by:

$$\begin{cases} S'(t) = -\tau(t)S(t)[I(t) + U(t)], \\ I'(t) = \tau(t)S(t)[I(t) + U(t)] - \nu I(t), \\ R'(t) = \nu f I(t) - \eta R(t), \\ U'(t) = \nu(1-f)I(t) - \eta U(t), \end{cases} \tag{5.1.1}$$

with initial data

$$S(t_0) = S_0 > 0,\ I(t_0) = I_0 > 0,\ R(t_0) = R_0 \geq 0 \text{ and } U(t_0) = U_0 \geq 0. \tag{5.1.2}$$

[2]The National Health Commission of the People's Republic of China `http://www.nhc.gov.cn/xcs/yqtb/list_gzbd.shtml`(accessed on 10 April 2020).
Chinese Center for Disease Control and Prevention. `http://www.chinacdc.cn/jkzt/crb/zl/szkb_11803/jszl_11809/` (accessed on 10 April 2020).

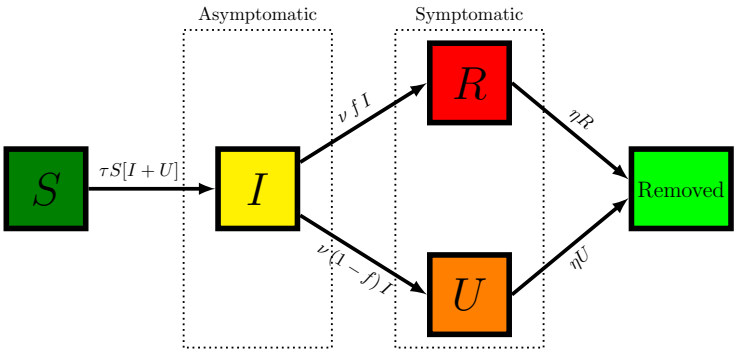

Figure 5.1.1: *Schematic showing the different compartments and transition rates in the model given by system of equations* (5.1.1).

In this model, $t \geq t_0$ is time in days and t_0 is the start date of the epidemic wave. A schematic illustrating the different model compartments is shown in Figure 5.1.1 and the model parameters - including whether the parameter values were assumed or obtained via model fitting - are listed in Table 5.1.1. It has previously been demonstrated that the latent period for COVID-19 is short [258], and COVID-19 patients have been found to have high viral loads early in infection [400, 205], so we do not include individuals who are presymptomatic and not yet infectious in the model. However, explicit inclusion of individuals who are infected but not yet infectious would be a straightforward extension of our model [259].

Symbol	**Interpretation**	**Method**
t_0	Epidemic start time	fitted
S_0	Number susceptible at time t_0	fixed
I_0	Number in early infection and infectious at time t_0	fitted
U_0	Number in later infection and not reporting disease at time t_0	fitted
$\tau(t)$	Transmission rate at time t, accounting for public health measures	fitted
$1/\nu$	Average duration of early infection	fixed
f	Fraction of infected individuals that go on to report disease	fixed
$1/\eta$	Average duration of later infection	fixed

Table 5.1.1: *Parameters and initial conditions of the model.*

Early infection (which corresponds to the incubation period, for individuals who develop clear symptoms) is assumed to last for an average period of $1/\nu$ days. The infectious period is assumed to be $1/\nu + 1/\eta$ days, although we assume that individuals that report disease do not transmit the virus during their symptomatic infectious period (i.e. they adhere to public health measures that are effective at reducing transmission). A fraction, f, of infected hosts report disease, whereas a fraction $1 - f$ do not report disease at any stage of their infection.

In the model, the transmission rate at time t, accounting for public health measures in place at that time, is denoted by $\tau(t)$. During the exponential growth phase, we assume that $\tau(t) \equiv \tau_0$ is constant. We then use a time-dependent decreasing transmission rate $\tau(t)$ to incorporate the effects of the strong measures taken by Chinese authorities to control the epidemic wave (see Introduction for a description of the different measures that were introduced):

$$\begin{cases} \tau(t) = \tau_0, \, 0 \leq t \leq N, \\ \tau(t) = \tau_0 \, \exp\left(-\mu \left(t - N\right)\right), \, t > N. \end{cases} \tag{5.1.3}$$

The date N and the value of μ are chosen so that daily numbers of cumulative reported cases in the numerical simulation of the epidemic align with the analogous values in the dataset.

The cumulative number of reported cases at time t is given by

$$CR(t) = \nu f \int_{t_0}^{t} I(\sigma) d\sigma, \text{ for } t \geq t_0, \tag{5.1.4}$$

and the cumulative number of unreported cases at time t is given by

$$CU(t) = \nu(1-f) \int_{t_0}^{t} I(\sigma) d\sigma, \text{ for } t \geq t_0. \tag{5.1.5}$$

The daily number of reported cases can be obtained by computing the solution of the following equation:

$$DR'(t) = \nu\, f\, I(t) - DR(t), \text{ for } t \geq t_0 \text{ and } DR(t_0) = 0. \tag{5.1.6}$$

5.1.2.3 Parameter values

Since there is substantial uncertainty surrounding the proportion of cases that are symptomatic and report disease for COVID-19, the value of f is unknown. Since intense interventions were introduced in China during the first epidemic wave, and the full extent of asymptomatic transmission was unknown, we assume in the baseline version of our analysis that $f = 0.8$. However, we checked the robustness of our results to this assumption by also considering different values ($f = 0.2, 0.4$ and 0.6).

We assume that the durations of early and late infection are $\nu = 1/7$ days and $\eta = 1/7$ days, respectively. By assuming that the mean duration of early infection (i.e. duration of infection prior to symptoms, for individuals that go on to develop symptoms) is 7 days, the expected generation time for individuals that develop symptoms might be expected to be around 3.5 days. This lies within the range of estimated generation times for COVID-19 (see e.g. [179]). COVID-19 patients have been found to shed virus up to around one week after hospitalisation, thereby motivating our assumed value of η [400].

To determine the initial conditions (equations (5.1.2)), we assumed that in the initial exponential growth phase of the epidemic wave (the earliest stages of the epidemic, which is assumed to be between January 19 and January 26, 2020), $CR(t)$ took the form:

$$CR(t) = \chi_1 \exp(\chi_2\, t) - \chi_3,\ t \geq t_0. \tag{5.1.7}$$

Following [261], expressions for I_0, U_0, R_0 can be obtained:

$$I_0 = \frac{\chi_2}{f(\nu f + \nu_2)},\ U_0 = \left(\frac{(1-f)(\nu f + \nu_2)}{\eta + \chi_2}\right) I_0,\ R_0 = 0. \tag{5.1.8}$$

Furthermore, the transmission rate during this exponential growth phase of the epidemic wave is given by the constant value

$$\tau(t) = \tau_0 = \left(\frac{\chi_2 + \nu f + \nu_2}{S_0}\right)\left(\frac{\eta + \chi_2}{\nu(1-f) + \eta + \chi_2}\right), \tag{5.1.9}$$

the epidemic start time is

$$t_0 = \frac{1}{\chi_2}\Big(\log(\chi_3) - \log(\chi_1)\Big), \tag{5.1.10}$$

and the value of the basic reproductive number is

$$\mathcal{R}_0 = \left(\frac{\tau_0 S_0}{\nu f + \nu_2}\right)\left(1 + \frac{\nu_2}{\eta}\right). \tag{5.1.11}$$

In the above, the value of $\chi_3 = 30$ is assumed and the values of χ_1 and χ_2 are obtained by fitting equation (5.1.7) to data on the cumulative numbers of cases per day using least squares estimation. Specifically, we use the "polyfit" Matlab function to estimate χ_1 and χ_2. The population size is assumed to be large, so that the initial number of susceptible individuals, S_0, corresponds to the total population size.

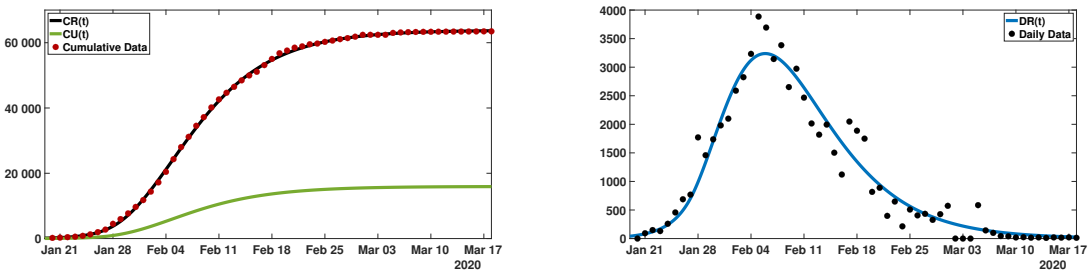

Figure 5.1.2: *Comparison of the model output with the data for mainland China. The parameter values and initial conditions are listed in Table 5.1.2, and* $f = 0.8$. *On the left hand side we plot the cumulative data (red dots), the simulated cumulative reported cases* $CR(t)$ *(black line) and unreported cases* $CU(t)$ *(green line). On the right hand side, we plot data on the daily numbers of cases (black dots) and the inferred daily number of cases using the model,* $DR(t)$ *(blue line).*

5.1.3 Results

5.1.3.1 Fitting the model to data

We first estimated the values of χ_1 and χ_2 using data on the cumulative number of confirmed cases in the earliest stages of the epidemic wave (January 19 to January 26, 2020). The values of τ_0 and the initial conditions (I_0, U_0 and t_0) are then obtained using formulae (5.1.8)-(5.1.10). The fitted parameter values are shown in Table 5.1.2. Analogous results for different values of the reporting fraction, f, are also shown.

χ_1	χ_2	χ_3	t_0	f	μ	N	I_0	U_0	S_0	τ_0
0.2601	0.3553	30	13.3617	0.8	0.1480	Jan. 26	93.2785	5.3494	1.40005×10^9	3.3655×10^{-10}
0.2601	0.3553	30	13.3617	0.6	0.1531	Jan. 26	124.3550	14.2646	1.40005×10^9	3.1920×10^{-10}
0.2601	0.3553	30	13.3617	0.4	0.1574	Jan. 26	186.5325	32.0953	1.40005×10^9	3.0358×10^{-10}
0.2601	0.3553	30	13.3617	0.2	0.1612	Jan. 26	373.0650	85.5875	1.40005×10^9	2.8942×10^{-10}

Table 5.1.2: *Values of parameters obtained by fitting to cumulative data from the initial exponential phase of the mainland China epidemic wave. The values of* I_0 U_0, τ_0, *and* t_0 *are obtained using formulae* (5.1.8)-(5.1.10). *Here we take* $\chi_3 = 30$ *in order to obtain non-zero integer values of* I_0 *and* U_0.

We then used the mathematical model (5.1.1) with these parameter values and initial conditions to project the cumulative number of reported cases forwards (black line in Figure 5.1.2 (left)), choosing μ so that $CR(t)$ matched the observed data (red dots in Figure 5.1.2 (left)). The inferred cumulative numbers of unreported cases are also shown in Figure 5.1.2 (left), assuming that $f = 0.8$. Daily numbers of reported cases corresponding to this forward projection are shown in Figure 5.1.2 (right).

5.1.3.2 Predicting the end of the epidemic wave

To predict the end of the epidemic wave, we are particularly interested in the time period in which cases are fading out and very few new infections are occurring. We consider a scenario in which the current time is day t_1, and we are attempting to predict when the epidemic will end. As long as t_1 is sufficiently long after the peak of the epidemic wave that the quantity $\tau(t)S(t) \leq \tau(t)S_0$ is small, the approximation

$$I'(t) \simeq -\nu I(t),$$

can be used instead of the second equation in system (5.1.1) when $t > t_1$. For the parameter values used in our model, temporal changes in $S_0\tau(t)$ are shown in the Supplementary Information (Figure 5.1.6), highlighting that $\tau(t)S(t)$ is small from the second half of March, 2020, onwards).

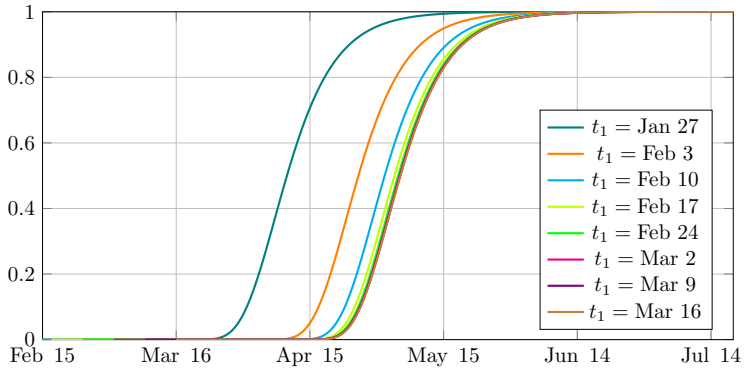

Figure 5.1.3: *Estimated extinction probabilities (using equation* (5.1.15)*). The numerical values for* I_1 *and* U_1 *were computed from the ODE model, considering* t_1 *values at 7 day intervals. In this figure, we assume that* $f = 0.8$ *(other parameter values are listed in Table 5.1.2).*

Hence, to obtain an analytic expression describing the predicted end of the epidemic wave, we considered the following approximate system of equations whenever $t \geq t_1$:

$$\begin{cases} I'(t) = -\nu I(t), \\ R'(t) = \nu f\, I(t) - \eta R(t), \\ U'(t) = \nu(1-f)\, I(t) - \eta U(t). \end{cases} \tag{5.1.12}$$

This system is supplemented by the initial data

$$I(t_1) = I_1, U(t_1) = U_1 \text{ and } R(t_1) = R_1. \tag{5.1.13}$$

where I_1, U_1 and R_1 are the values of the solutions of the original system (5.1.1)-(5.1.2) on day t_1. A schematic for the approximate model (5.1.12) is shown in the Supplementary Information (Figure 5.1.7).

The error between the original model and the approximate model is shown in the Supplementary Information (Figure 5.1.8), where the error is given by

$$\text{err}(t_1) = \sup_{t \geq t_1} \max\big(|I(t) - I_1(t)|, |U(t) - U_1(t)|\big). \tag{5.1.14}$$

In this expression, $I(t)$ and $U(t)$ are the solutions of the original system (5.1.1), and $I_1(t)$ and $U_1(t)$ are solutions of the approximate model. In both cases, the models are fitted to observed data on cumulative numbers of reported cases (hence, this error formula does not involve $R(t)$ which is very similar for the two models). When applied in the later stages of the epidemic wave, the approximate model is more accurate than earlier in the epidemic wave.

By considering the analogous continuous-time Markov chain to the approximate model (5.1.12), the probability that the epidemic is over on different future dates can be estimated analytically (see Supplementary Information section 5.1.5 for additional details). Specifically, the probability that no individuals remain in the I or U compartments can be calculated at different times in future:

$$\begin{aligned} &\mathbb{P}(I(s) + U(s) = 0 \text{ for } s \geq t \,|\, I(t_1) = I_1, U(t_1) = U_1) \\ &\qquad = \left(1 - e^{-\eta(t-t_1)}\right)^{U_1} \times \left(1 - e^{-\nu(t-t_1)} - (1-f)\nu(t-t_1)e^{-\eta(t-t_1)}\right)^{I_1}. \end{aligned} \tag{5.1.15}$$

The predictions generated by equation (5.1.15) for different values of t_1 are shown in Figure 5.1.3. We note that, as t_1 increases, the probability distribution of the date of extinction converges to a limit profile.

Furthermore, we also computed the earliest dates that corresponded to at least 90%, 95% and 99% probabilities that the epidemic was over, for different values of t_1, using equation (5.1.15). The results of this analysis are shown in Figure 5.1.4.

5.1.3.3 Comparing the analytic predictions with stochastic simulations

To investigate the accuracy of our analytic predictions, we also estimated the end of epidemic time using simulations of the analogous stochastic model to the system of equations (5.1.1). Specifically, as before,

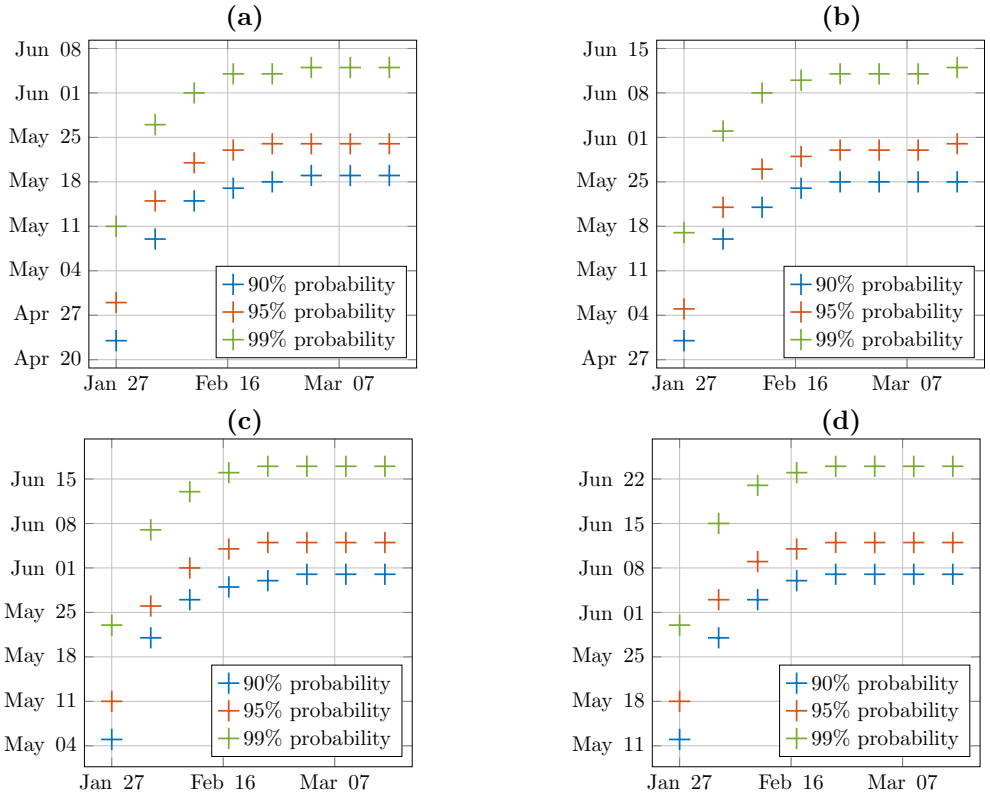

Figure 5.1.4: *For each panel, the x-axis corresponds to the day t_1 and the y-axis corresponds to the dates of epidemic wave extinction at different probability levels (90%, 95% and 99%) computed by using* (5.1.15). *Different panels correspond to different values of the parameter f ((a) $f = 0.8$; (a) $f = 0.6$; (a) $f = 0.4$; (a) $f = 0.2$). The values of I_1 and U_1 are computed by solving system of equations* (5.1.1) *numerically up to the time $t = t_1$. Parameter values are listed in Table 5.1.2.*

the deterministic model was fitted to the data on cumulative numbers of confirmed cases and used up until time t_1. Then from time t_1 onwards, stochastic simulations were run using the direct method version of the Gillespie stochastic simulation algorithm [188].

In Figure 5.1.5, we plot the cumulative distribution for the epidemic wave extinction probability obtained using the stochastic simulations. As can be seen in that figure, since the stochastic simulations involve using the exact model (equations (5.1.1)) rather than the approximate model, the predicted end dates of the epidemic wave are independent of t_1. The graph in Figure 5.1.5 corresponds to the limit profile discussed at the end of the previous section 5.1.3.2 (i.e. the analytic prediction when t_1 is sufficiently late in the epidemic that the analytic prediction is accurate). From Figure 5.1.3, it can be seen that that this approximation is accurate when t_1 is February 17, 2020, or later.

We also computed the error between the analytic end of epidemic time prediction and the analogous quantity using the stochastic simulations. More precisely, we computed the quantity

$$\mathrm{diff}(t_1) = \sup_{t \geq t_1} |f_{IBM}(t) - f_{\mathrm{analytic}}(t)| \tag{5.1.16}$$

for each value of t_1 presented in Figures 5.1.3 and 5.1.5, where f_{IBM} is the cumulative distribution computed by stochastic simulations (Figure 5.1.5) and f_{analytic} is the cumulative distribution given by equation (5.1.15) (Figure 5.1.3). The results are shown in the Supplementary Information (Table 5.1.6).

Finally, we compared the mean outputs from the stochastic simulations to the numerical solutions of the original model (system of equations (5.1.1)). Unsurprisingly, these quantities match closely (Figure 5.1.9). In Figure 5.1.10, we show the variability between different stochastic simulations obtained when the stochastic simulations are run throughout the epidemic (i.e. starting on day t_0). This high variability observed between different simulations is largely due to the small number of individuals infected initially; when instead stochastic simulations were run from day t_1 onwards, the variability between different stochastic simulations reduced (see Supplementary Information, Table 5.1.7).

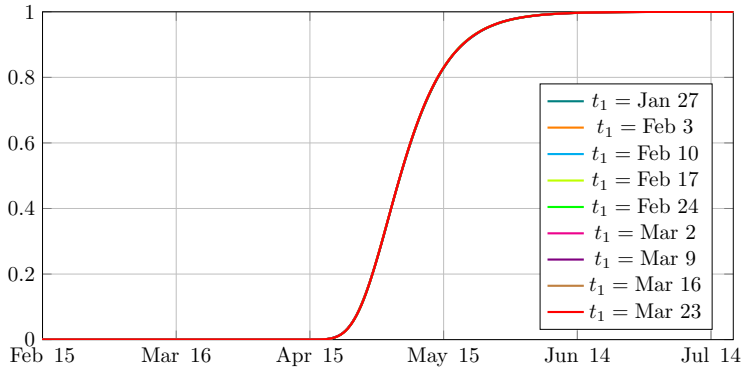

Figure 5.1.5: *Estimated cumulative probability distribution for the end of epidemic wave date obtained using stochastic simulations. Results are shown for different values of t_1, although as expected the different lines in this graph lie on top of each other. Initial conditions for the stochastic simulations were computed by rounding the solutions of equations* (5.1.1) *at $t = t_1$ to the nearest integers. 150,000 simulations were run for each value of t_1. In this figure, $f = 0.8$. Other parameter values are shown in Table 5.1.2.*

5.1.4 Discussion

Despite receiving surprisingly little attention from epidemiological modellers, predicting the ends of epidemic waves is important for estimating how long intense interventions are likely to be required [304, 248, 374, 303]. In this study, we developed a framework for predicting the ends of epidemic waves using compartmental epidemiological models. This involving fitting a compartmental model to case notification data and using an analytic expression to estimate when the epidemic wave is likely to end. We also compared our analytic prediction to analogous results obtained via model simulations, thereby demonstrating that our results are accurate whenever the underlying epidemiological model provides a realistic reflection of pathogen transmission.

In Table 5.1.3, we show the results that we obtained using this framework in real-time to predict the end of the first COVID-19 epidemic wave in China. Specifically, the results in this table correspond to those shown in Figure 3, after the end of epidemic wave probability converged to the limit profile (i.e. using values of t_1 from approximately mid-February onwards). Importantly, the predicted epidemic wave end date depended on the assumed proportion of infectious cases that report disease (f). Since this quantity was unknown, and remains uncertain even now, we conclude that accurate estimation of the reporting fraction is essential to forecast the ends of epidemic waves accurately.

Level of risk	10%	5%	1%
Extinction date ($f = 0.8$)	May 19	May 24	June 5
Extinction date ($f = 0.6$)	May 25	May 31	June 12
Extinction date ($f = 0.4$)	May 31	June 5	June 17
Extinction date ($f = 0.2$)	June 7	June 12	June 24

Table 5.1.3: *The predicted end of epidemic wave date inferred when t_1 was March 16, 2020, for different levels of risk aversion. For example, assuming $f = 0.8$, our model predicted a 10% chance that the epidemic wave would persist beyond May 19, 2020.*

Our intention here was to develop a basic modelling approach for predicting when an epidemic wave is likely to end. To improve the accuracy of predictions, this approach would require adjustments to account for important features of real-world epidemic waves. As well as uncertainty in the reporting fraction, another key assumption was that public health measures remained in place until the end of the epidemic wave. Of course, if measures such as isolation of infectious cases are relaxed before an epidemic wave has ended, then the epidemic end date is likely to be different to the one predicted using our modelling framework. In

that scenario, relaxation of interventions could in theory be integrated explicitly into the underlying model, and model simulations used to predict the end of epidemic waves. Since interventions are often included in compartmental models [131, 419, 372, 326], this is a straightforward extension of the research presented here. We also note that, if interventions are relaxed following the end of an epidemic wave, then additional cases could begin a second wave - a phenomenon that is now arguably being observed in a range of countries worldwide for COVID-19.

We note that there were very few cases in mainland China after mid-March, 2020. As a result, our modelling framework tended to estimate later end of epidemic wave dates than turned out to be the case. The most likely explanation for this is that, by characterising the impacts of control interventions using equation (5.1.3), public health measures did not have a sufficiently strong effect in the model. Testing the effects of different possible characterisations of the effects of public health measures is left as future work.

Since the precise method of parameter inference was not central to our framework, we used a basic approach to estimate the values of pathogen transmission parameters here, namely least squares estimation. Many different methods are used to estimate transmission parameters in real-time during epidemics [308, 80], and our modelling framework could be extended to use these more sophisticated methods.

Despite the many simplifications in our modelling approach as presented here, we have provided an initial framework for predicting the ends of epidemic waves, and demonstrated the key principle that the end date of an epidemic wave depends sensitively on the proportion of infectious cases that report disease. Extending this framework to include additional epidemiological realism, so that ends of epidemic waves can be forecasted as accurately as possible, is an important target for future research. This will allow public health decision makers to plan control interventions effectively during infectious disease epidemics.

5.1.5 Supplementary Information

5.1.5.1 Formula to compute the probability distribution of the extinction date

We use continuous-time Markov processes to compute the exact distribution of the date of end of the epidemic after the transmission rate is effectively taken as zero. We start on t_1 with initial values I_1, U_1, and R_1 for I-individuals, U-individuals and R-individuals, respectively. The evolution of each individual is guided by independent exponential processes, and we have the following:

(i) Each individual I will change state following an exponential clock of rate ν. When I changes its state, it will be transferred to the class of R-individuals with probability f and to the class of U-individuals with probability $(1-f)$;

(ii) Each individual in the state U will change state following an exponential clock with rate η and become removed individual;

(iii) Each individual in the state R will change state following an exponential clock with rate η and become removed individual

Since the class I has only outgoing fluxes, the law of extinction for the I-individuals is

$$\mathbb{P}(I(t)=0\,|\,I(t_1)=I_1)=\left(\int_{t_1}^{t}\nu e^{-\nu(s-t_1)}\mathrm{d}s\right)^{I_1}=\left(1-e^{-\nu(t-t_1)}\right)^{I_1},$$

and the probability to have some I-individual left at time t is

$$\mathbb{P}(I(t)=I\,|\,I(t_1)=I_1)=(1-e^{-\nu(t-t_1)})^{I_1-I}e^{-\nu I(t-t_1)}.$$

For the U-individuals and the R-individuals, the situation is more intricate. Indeed, the U-individuals and the R-individuals vanish at a constant rate η but new individuals appear from the I class at rate $(1-f)\nu$ and $f\nu$, respectively, depending on the remaining stock of I. Therefore the probability that U gets extinct before t also depends on the number of remaining I. It is actually easier to compute directly the extinction property for the sum $I+U$, which is our aim anyways.

When $\nu \neq \eta$, we obtain

$$\begin{aligned}
&\mathbb{P}(I(s)+U(s)=0\,\forall s \geq t \,|\, I(t_1)=I_1, U(t_1)=U_1)\\
&\quad=\left(1-e^{-\eta(t-t_1)}\right)^{U_1} \times \left(\int_{t_1}^{t} \mathbb{P}(U \to RR \text{ before } t \,|\, I \to U \text{ at } s)\mathbb{P}(I \to U \text{ at } s) + \mathbb{P}(I \to R \text{ at } s)\mathrm{d}s\right)^{I_1}\\
&\quad=\left(1-e^{-\eta(t-t_1)}\right)^{U_1} \times \left(\int_{t_1}^{t} \left(1-e^{-\eta(t-s)}\right) \times (1-f)\nu e^{-\nu(s-t_1)} + f\nu e^{-\nu(s-t_1)}\mathrm{d}s\right)^{I_1}\\
&\quad=\left(1-e^{-\eta(t-t_1)}\right)^{U_1} \times \left((1-f)\left(1-e^{-\nu(t-t_1)} - \nu\frac{e^{-\nu(t-t_1)}-e^{-\eta(t-t_1)}}{\eta-\nu}\right) + f(1-e^{-\nu(t-t_1)})\right)^{I_1}\\
&\quad=\left(1-e^{-\eta(t-t_1)}\right)^{U_1} \times \left(1-e^{-\nu(t-t_1)} - (1-f)\nu\frac{e^{-\nu(t-t_1)}-e^{-\eta(t-t_1)}}{\eta-\nu}\right)^{I_1},
\end{aligned}$$

where the RR-individuals are the removed individuals.

Similarly when $\eta = \nu$, we obtain

$$\begin{aligned}
&\mathbb{P}(I(s)+U(s)=0\,\forall s \geq t \,|\, I(t_1)=I_1, U(t_1)=U_1)\\
&\qquad\qquad=\left(1-e^{-\eta(t-t_1)}\right)^{U_1} \times \left(1-e^{-\nu(t-t_1)} - (1-f)\nu(t-t_1)e^{-\eta(t-t_1)}\right)^{I_1}. \qquad (5.1.17)
\end{aligned}$$

5.1.5.2 Cumulative distribution of the date of end of the epidemic

The stochastic simulations introduced in section 5.1.3.3 can be used, in particular, to precisely estimate the cumulative probability distribution of the date of end of the epidemic, defined as the last time at which the quantity $I+U$ is positive.

In order to get a measure of the precision we remark that the values taken by the cumulative probability distribution $f(t)$ can be estimated by the average of independent measures of the random variable

$$X = \mathbb{1}_{t_{ext} \leq t},$$

which follows an Bernouilli distribution of parameter $f(t)$. Consecutive runs of the individual-based simulations yield independent observations X_n of this distribution. By Hoeffding's inequality we have for all $\varepsilon > 0$ and $n \in \mathbb{N}$

$$\mathbb{P}\left(\left|\frac{1}{n}\sum_{i=1}^{n} X_n - f(t)\right| \geq \varepsilon\right) \leq 2\exp\left(-2\varepsilon^2 n\right) =: \alpha,$$

and we achieved an error of at most $\varepsilon = 10^{-3}$ at risk $\alpha \leq 10^{-3}$ by running $n = -\frac{2}{\varepsilon^2}\ln\left(\frac{\alpha}{2}\right) \approx 15201805$ independent individual-based simulations to estimate the probability distribution of the extinction time (Figure 5.1.5, $t_1 = 82$ *i.e.* March 23). Other curves are esimated on the basis of 152019 independent simulations, which amouts to an error of at most 10^{-2} at risk 10^{-3}.

Since the curves presented in Figure 5.1.3 are so similar that it is difficult to see any difference between them, we computed the absolute error between each curve and the "reference" of $t_1 = 82$. We present the numerical values in Table 5.1.5. Notice that the error is actually below the estimated precision of the approximation.

5.1.5.3 Supplementary figures

5.1.5.4 Supplementary tables

We use cumulative reported data from the National Health Commission of the People's Republic of China and the Chinese CDC for mainland China. Before February 11, the data was based on laboratory confirmations. From February 11 to February 15, the data included cases that were not tested for the virus, but were clinically diagnosed based on medical imaging (patients that showed signs of pneumonia). There were 17,409 such cases from February 11 to February 15. The data from February 11 to February 15 specified both types of reported cases. From February 16, the data did not separate the two types of reporting, but reported the sum of both types. We therefore subtracted 17,409 cases from the cumulative reported cases

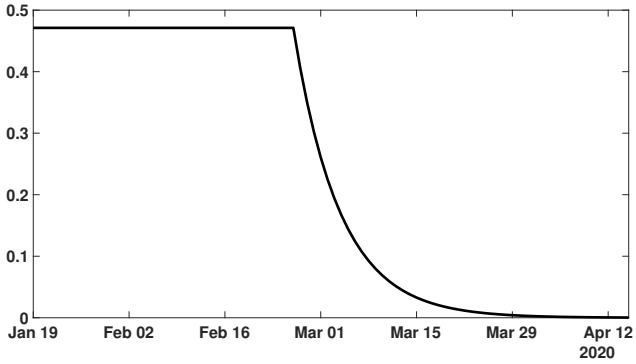

Figure 5.1.6: *Graph of* $\tau(t)S_0 = \tau_0 S_0 \exp\left(-\mu \max\left(t-N,0\right)\right)$ *with* $S_0 = 1.40005 \times 10^9$, $\tau_0 = 3.3655 \times 10^{-10}$, $N =$ *Jan.* 26, *and* $\mu = 0.148$. *The transmission rate is very small in the second half of March onwards. The parameter values correspond to the baseline case that we considered* ($f = 0.8$) *see Table 5.1.2.*

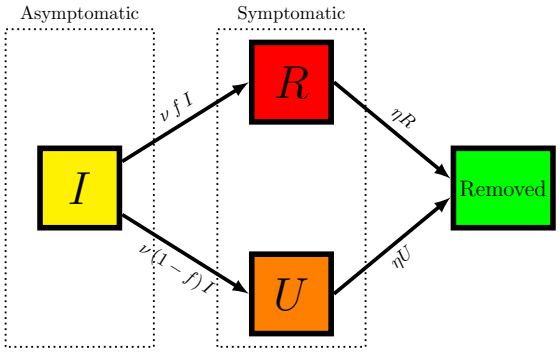

Figure 5.1.7: *Schematic of the model* (5.1.12).

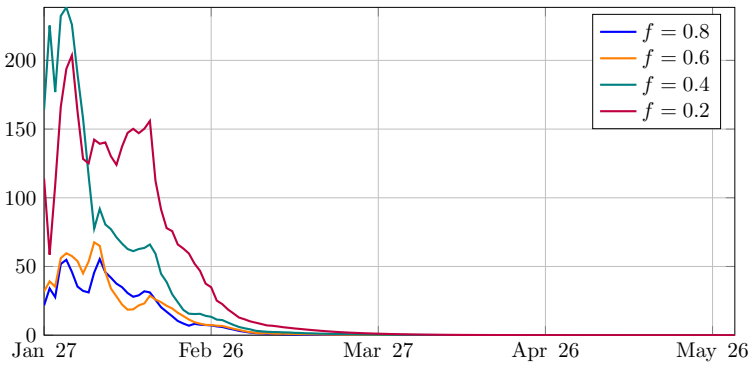

Figure 5.1.8: *In this figure the x-axis corresponds to* t_1 *and the y-axis correponds to the error* $err(t_1)$ *defined in* (5.1.14). *We observe that the smaller* f, *the larger the error. Parameter values are listed in Table 5.1.2.*

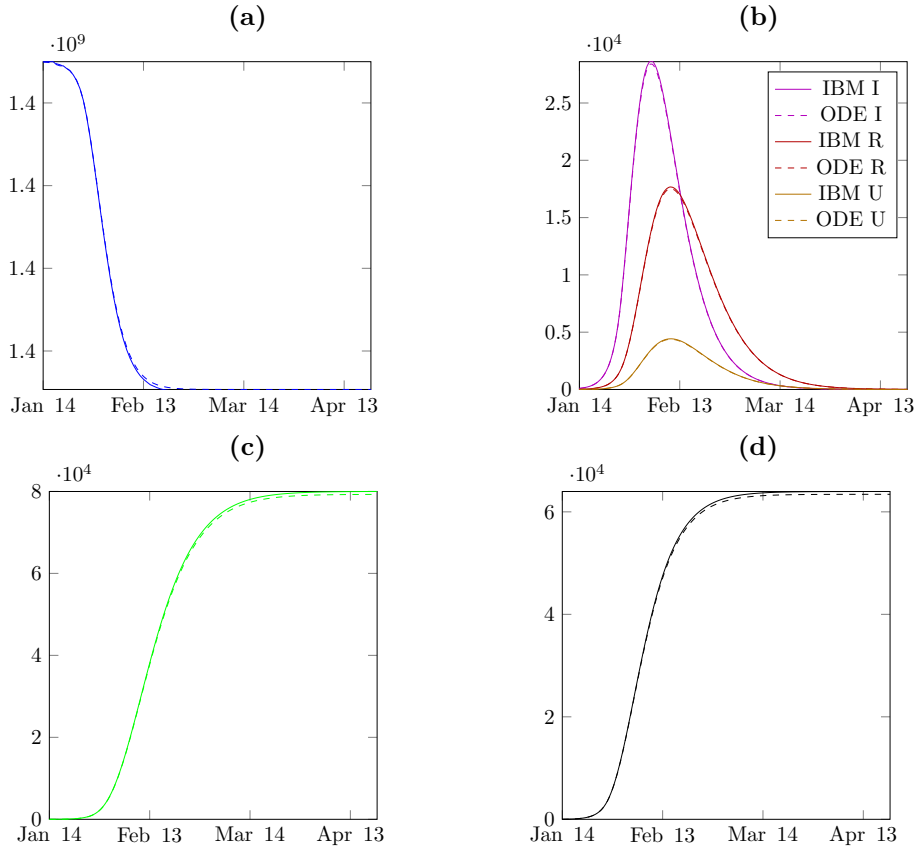

Figure 5.1.9: *In figure (a) we plot a comparison between the average S (susceptible) computed from the IBM and the S component of the solution of* (5.1.1). *In figure (b) we plot a comparison between the average I (asymptomatic), R (reported) and U (unreported) computed from the IBM and the components I, R and U of the solution of* (5.1.1). *In figure (c) we plot a comparison between the average RR (removed) computed from the IBM and the components RR of the solution of* (5.1.1). *In figure (d) we plot a comparison between the average CR (cumulative reported cases) computed from the IBM and the curve CR computed by* (5.1.1)-(5.1.4). *In this figure* 500 *independent runs of the IBM simulations are used and the corresponding components of the ODE model start from the same initial condition (at $t = t_0$). The parameters we used for both computations are the following: $I_0 = 93$, $U_0 = 5$, $S_0 = 1.40005 \times 10^9 - (I_0 + U_0)$, $R_0 = RR_0 = CR_0 = 0$ and $f = 0.8$, $\tau_0 = 3.3655 \times 10^{-10}$, $N = 26$, $\mu = 0.148$, $\nu = \frac{1}{7}$, $\eta = \frac{1}{7}$, $t_0 = 13.3617$.*

after February 15 to obtain approximate data for the cumulative numbers of reported cases based only on laboratory confirmations after February 15.The data is given in Table 5.1.4 with this adjustment.

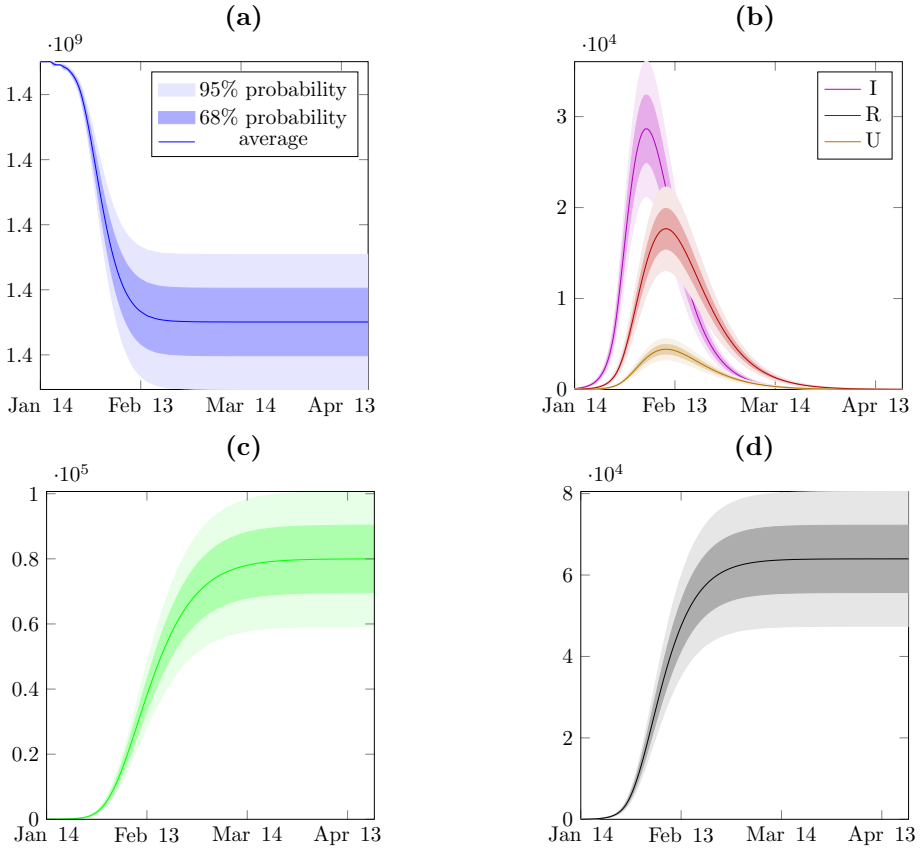

Figure 5.1.10: *In figure (a) we plot the mean value and variance of S (susceptible) computed from the IBM. The dark blue area contains 68% of the trajectories, and the light blue area 95%. In figure (b) we plot the mean value and variance of I (infected), R (reported) and U (unreported) computed from the IBM. The dark areas contains 68% of the trajectories, and the light areas 95%. In figure (c) we plot the mean value and variance of RR (removed) computed from the IBM. The dark green area contains 68% of the trajectories, and the light green area 95%. In figure (d) we plot the mean value and variance of CR (cumulated reported) computed from the IBM. The dark gray area contains 68% of the trajectories, and the light gray area 95%. We use* 500 *independent runs of the IBM simulations. The parameters we used for both computations are the following:* $I_0 = 93$, $U_0 = 5$, $S_0 = 1.40005 \times 10^9 - (I_0 + U_0)$, $R_0 = RR_0 = CR_0 = 0$ *and* $f = 0.8$, $\tau_0 = 3.3655 \times 10^{-10}$, $N = 26$, $\mu = 0.148$, $\nu = \frac{1}{7}$, $\eta = \frac{1}{7}$, $t_0 = 13.3617$.

January						
19	20	21	22	23	24	25
198	291	440	571	830	1287	1975
26	27	28	29	30	31	
2744	4515	5974	7711	9692	11791	
February						
1	2	3	4	5	6	7
14380	17205	20438	24324	28018	31161	34546
8	9	10	11	12	13	14
37198	40171	42638	44653	46472	48467	49970
15	16	17	18	19	20	21
51091	70548 − 17409	72436 − 17409	74185 − 17409	75002 − 17409	75891 − 17409	76288 − 17409
22	23	24	25	26	27	28
76936 − 17409	77150 − 17409	77658 − 17409	78064 − 17409	78497 − 17409	78824 − 17409	79251 − 17409
29						
79824 − 17409						
March						
1	2	3	4	5	6	7

t_1	26	33	40	47	54	61
date	Jan. 27	Feb. 3	Feb. 10	Feb. 17	Feb. 24	Mar. 2
$\mathrm{diff}(t_1)$	2.9×10^{-3}	2.1×10^{-3}	2.9×10^{-3}	1.8×10^{-3}	2.5×10^{-3}	1.4×10^{-3}
t_1	68	75	82			
date	Mar. 9	Mar. 16	Mar. 23			
$\mathrm{diff}(t_1)$	1.6×10^{-3}	1.2×10^{-3}	0.00			

Table 5.1.5: *Absolute difference between the cumulative distribution given by the stochastic simulations and the reference simulation* $t_1 = 82$. *For each* t_1 *we computed the error as* $\mathrm{diff}(t_1) = \sup_{t \geq t_1} |f_{t_1}(t) - f_{81}(t)|$, *where* f_{t_1} *is the estimated distribution computed simulations, for which the initial condition correspond to the components of* (5.1.1) *at* $t = t_1$ *rounded to the closest integer.*

t_1	26	33	40	47	54	61
date	Jan. 27	Feb. 3	Feb. 10	Feb. 17	Feb. 24	Mar. 2
$\mathrm{diff}(t_1)$	8.6×10^{-1}	4.4×10^{-1}	1.7×10^{-1}	6.4×10^{-2}	2.5×10^{-2}	8.1×10^{-3}
t_1	68	75	82			
date	Mar. 9	Mar. 16	Mar. 23			
$\mathrm{diff}(t_1)$	3.5×10^{-3}	8.5×10^{-4}	5.7×10^{-4}			

Table 5.1.6: *Absolute difference between the cumulative distribution given by the stochastic simulations and the analytic approximation using the approximate model* (5.1.12), *computed using equation* (5.1.16).

t_1	t_0	18	22	26	33	40
date	Jan. 14	Jan. 19	Jan. 23	Jan. 27	Feb. 3	Feb.10
$\max_{t \geq t_1} \sigma(t)$	3717	1685	787	401	186	106

Table 5.1.7: *Maximal standard deviation for the components* I, R *and* U *computed by stochastic simulations started at date* t_1 *with initial condition given by the solution to* (5.1.1) *with the parameters from Table 5.1.2. The ODE model* (5.1.1) *is solved up to* $t = t_1$, *and we take the solution to* (5.1.1) *at* $t = t_1$ *as initial condition for the stochastic simulations.* $\sigma(t)$ *is the maximum, at time* t, *of the standard deviations of the quantities* $I(t)$, $R(t)$ *and* $U(t)$ *in a sample of* $n = 1000$ *independent simulations started at* $t = t_1$, *and is expressed in number of individuals. We took* $f = 0.8$ *and other parameters are taken from Table 5.1.2.*

5.2 Unreported Cases for Age Dependent COVID-19 Outbreak in Japan

5.2.1 Introduction

COVID-19 disease caused by the severe acute respiratory syndrome coronavirus (SARS-CoV-2) first appeared in Wuhan, China, and the first cases were notified to WHO on 31 December 2019 [430, 422]. Beginning in Wuhan as an epidemic, it then spread very quickly and was characterized a pandemic on 11 March 2020 [430]. Symptoms of this disease include fever, shortness of breath, cough, and a non-negligible proportion of infected individuals may develop severe forms of the symptoms leading to their transfer to intensive care units and, in some cases, death, see e.g., Guan et al. [194] and Wei et al. [396]. Both symptomatic and asymptomatic individuals can be infectious [341, 396, 417], which makes the control of the disease particularly challenging.

The virus is characterized by its rapid progression among individuals, most often exponential in the first phase, but also a marked heterogeneity in populations and geographic areas [423, 415, 382]. The number of reported cases worldwide exceeded 3 millions as of 3 May 2020 [420]. The heterogeneity of the number of cases and the severity according to the age groups, especially for children and elderly people, aroused the interest of several researchers [102, 326, 268, 356, 375]. Indeed, several studies have shown that the severity of the disease increases with the age and co-morbidity of hospitalized patients (see e.g., To et al. [375] and Zhou et al. [415]). Wu et al. [404] have shown that the risk of developing symptoms increases by 4% per year in adults aged between 30 and 60 years old while Davies et al. [130] found that there is a strong correlation between chronological age and the likelihood of developing symptoms. Since completely asymptomatic individuals can also be contagious, a higher probability of developing symptoms does not necessarily imply greater infectiousness: Zou et al. [417] found that, in some cases, the viral load in asymptomatic patients was similar to that in symptomatic patients. Moreover while adults are more likely to develop symptoms, Jones et al. [227] found that the viral loads in infected children do not differ significantly from those of adults.

These findings suggest that a study of the dynamics of inter-generational spread is fundamental to better understand the spread of the coronavirus and most importantly to efficiently fight the COVID-19 pandemic. To this end the distribution of contacts between age groups in society (work, school, home, and other locations) is an important factor to take into account when modeling the spread of the epidemic. To account for these facts, some mathematical models have been developed [25, 108, 130, 326, 356]. In Ayoub et al. [25] the authors studied the dependence of the COVID-19 epidemic on the demographic structures in several countries but did not focus on the contacts distribution of the populations. In [108, 130, 326, 356] a focus on the social contact patterns with respect to the chronological age has been made by using the contact matrices provided in Prem et al. [325]. While Ayoub et al. [25], Chikina and Pegden [108] and Davies et al. [130] included the example of Japan in their study, their approach is significantly different from ours. Indeed, Ayoub et al. [25] use a complex mathematical model to discuss the influence of the age structure on the infection in a variety of countries, mostly through the basic reproduction number $\mathcal{R}_0$. They use parameter values from the literature and from another study of the same group of authors [26], where the parameter identification is done by a nonlinear least-square minimization. Chikina and Pegden [108] use an age-structured model to investigate age-targeted mitigation strategies. They rely on parameter values from the literature and do discuss using age-structured temporal series to fit their model. Finally, Davies et al. [130] also discuss age-related effects in the control of the COVID epidemic, and use statistical inference to fit an age-structured SIR variant to data; the model is then used to discuss the efficiency of different control strategies. We provide a new, explicit computational solution for the parameter identification of an age-structured model. The model is based on the SIUR model developed in Liu et al. [261], which accounts for a differentiated infectiousness for reported and unreported cases (contrary to, for instance, other SIR-type models). In particular, our method is significantly different from nonlinear least-squares minimization and does not involve statistical inference.

In this section 5.2 we focus on an epidemic model with unreported infectious symptomatic patients (i.e., with mild or no symptoms). Our goal is to investigate the age structured data of the COVID-19 outbreak in Japan. In section 5.2.2 we present the age structured data and in section 5.2.3 the mathematical models (with and without age structure). One of the difficulties in fitting the model to the data is that the growth rate of the epidemic is different in each age class, which lead us to adapt our early method presented in Liu et al. [261]. The new method is presented in the Appendix 5.2.6. In section 5.2.4 we present the comparison of the model with the data. In the last section 5.2.5 we discuss our results.

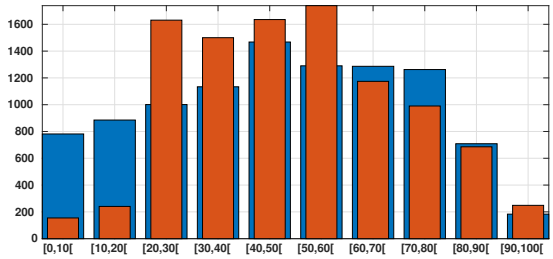

Figure 5.2.1: In this figure we plot in blue bars the age distribution of the Japanese population for 10,000 people and we plot in orange bars the age distribution of the number of reported cases of SARS-CoV-2 for 10,000 patient on 29 April (based on the total of 13,660 reported cases). We observe that 77% of the confirmed patients belong to the 20–60 years age class.

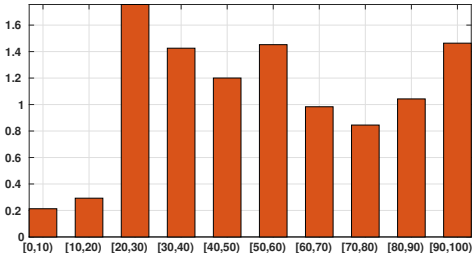

Figure 5.2.2: In this figure we plot the number of infected patients for each age class per 10,000 individuals of the same age class (i.e., the number of infected individuals divided by the population of the age class times 10,000). The figure shows that the individuals are more or less likely to becomes infected depending on their age class. The bars describe the susceptibility of people to the SARS-CoV-2 depending on their age class.

5.2.2 Data

Patient data in Japan have been made public since the early stages of the epidemic with the quarantine of the *Diamond Princess* in the Haven of Yokohama. We used data from the website covid19japan.com (`https://covid19japan.com`. Accessed 6 May 2020) which is based on reports from national and regional authorities. Patients are labeled "confirmed" when tested positive to COVID-19 by PCR. Interestingly, the age class of the patient is provided for 13,660 out of 13,970 confirmed patients (97.8% of the confirmed population) as of 29 April. The age distribution of the infected population is represented in Figure 5.2.1 compared to the total population per age class (data from the Statistics Bureau of Japan estimate for 1 October 2019). In Figure 5.2.2 we plot the number of reported cases per 10,000 people of the same age class (i.e., the number of infected patients divided by the population of the age class times 10,000). Both datasets are given in Table 5.2.1 and a statistical summary is provided by Table 5.2.2. Note that the high proportion of 20–60 years old confirmed patients may indicate that the severity of the disease is lower for those age classes than for older patients, and therefore the disease transmits more easily in those age classes because of a higher number of asymptomatic individuals. Elderly infected individuals might transmit less because they are identified more easily. The cumulative number of death (Figure 5.2.3) is another argument in favor of this explanation. We also reconstructed the time evolution of the reported cases in Figures 5.2.4 and 5.2.5. Note that the steepest curves precisely concern the 20–60-year old, probably because they are economically active and therefore have a high contact rate with the population.

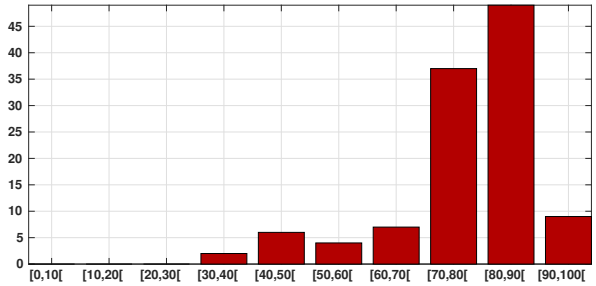

Figure 5.2.3: Cumulative number of SARS-CoV-2-induced deaths per age class (red bars). We observe that 83% of death occur in between 70 and 100 years old.

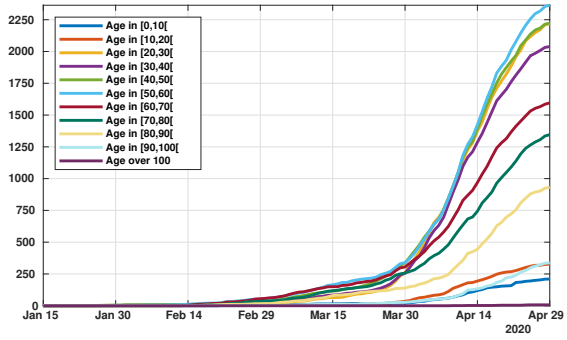

Figure 5.2.4: Time evolution of the cumulative number of reported cases of SARS-CoV-2 per age class. The vertical axis represents the total number of cumulative reported cases in each age class.

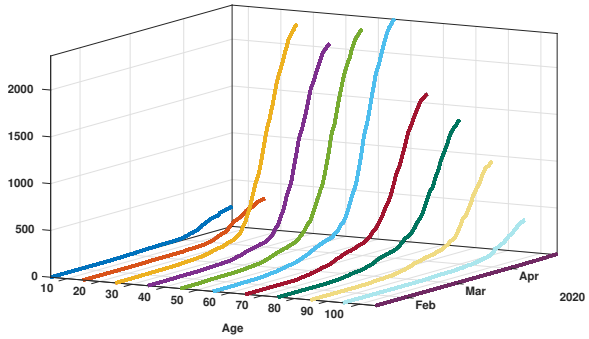

Figure 5.2.5: Time evolution of the cumulative number of reported cases of SARS-CoV-2 per age class. The vertical axis represents the total number of cumulative reported cases in each age class

Table 5.2.1: The age distribution of Japan is taken from the Statistics Bureau of Japan [427]. The number of cases and the number of death the data come from Prefectural Governments and Japan Ministry of Health, Labour and Welfare.

Age group	$[0, 10[$	$[10, 20[$	$[20, 30[$	$[30, 40[$	$[40, 50[$	$[50, 60[$	$[60, 70[$
Age class for 2019	9,859,515	11,171,044	12,627,964	14,303,042	18,519,755	16,277,853	16,231,582
Age class per 10,000 people	781	885	1000	1133	1467	1290	1286
Confirmed Cases	211	327	2216	2034	2220	2355	1566
Death	0	0	0	2	6	4	7

Table 5.2.2: Statistical summary of the data from Table 5.2.1.

Dataset	**Japanese Population**	**Infected**	**Deceased**
First Quartile	28	28	68
Median	48	44	75
Third Quartile	67	59	81

5.2.3 Methods

5.2.3.1 SIUR Model

The model consists of the following system of ordinary differential equations:

$$\begin{cases} S'(t) = -\tau(t)S(t)\dfrac{I(t)+U(t)}{N}, \\ I'(t) = \tau(t)S(t)\dfrac{I(t)+U(t)}{N} - \nu I(t), \\ R'(t) = \nu_1 I(t) - \eta R(t), \\ U'(t) = \nu_2 I(t) - \eta U(t). \end{cases} \tag{5.2.1}$$

This system is supplemented by initial data

$$S(t_0) = S_0 \geq 0,\ I(t_0) = I_0 \geq 0,\ R(t_0) \geq 0 \text{ and } U(t_0) = U_0 \geq 0. \tag{5.2.2}$$

Here $t \geq t_0$ is time in days, t_0 is the starting date of the epidemic in the model, $S(t)$ is the number of individuals susceptible to infection at time t, $I(t)$ is the number of asymptomatic infectious individuals at time t, $R(t)$ is the number of reported symptomatic infectious individuals at time t, and $U(t)$ is the number of unreported symptomatic infectious individuals at time t. A flow chart of the model is presented in Figure 5.2.6.

Asymptomatic infectious individuals $I(t)$ are infectious for an average period of $1/\nu$ days. Reported symptomatic individuals $R(t)$ are infectious for an average period of $1/\eta$ days, as are unreported symptomatic individuals $U(t)$. We assume that reported symptomatic infectious individuals $R(t)$ are reported and isolated immediately, and cause no further infections. The asymptomatic individuals $I(t)$ can also be viewed as having a low-level symptomatic state. All infections are acquired from either $I(t)$ or $U(t)$ individuals. A summary of the parameters involved in the model is presented in Table 5.2.3.

Our study begins in the second phase of the epidemics, i.e., after the pathogen has succeeded in surviving in the population. During this second phase $\tau(t) \equiv \tau_0$ is constant. When strong government measures such as isolation, quarantine, and public closings are implemented, the third phase begins. The actual effects of these measures are complex, and we use a time-dependent decreasing transmission rate $\tau(t)$ to incorporate these effects. The formula for $\tau(t)$ is

$$\begin{cases} \tau(t) = \tau_0,\ 0 \leq t \leq D, \\ \tau(t) = \tau_0 \exp\left(-\mu\left(t - D\right)\right),\ D < t. \end{cases} \tag{5.2.3}$$

The date D is the first day of public intervention and μ characterises the intensity of the public intervention.

A similar model has been used to describe the epidemics in mainland China, South Korea, Italy, and other countries, and give reasonable trajectories for the evolution of the epidemic based on actual data [P16, 261, 260, 258, 259, 262]. Compared with these models, we added a scaling with respect to the total population size N, for consistency with the age-structured model (5.2.12). This only changes the value of the parameter τ and does not impact the qualitative or quantitative behavior of the model.

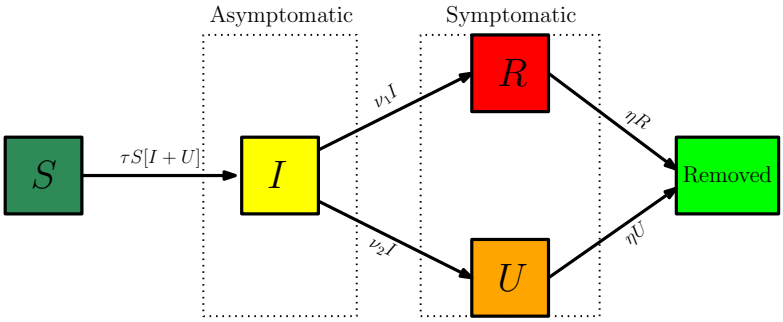

Figure 5.2.6: Compartments and flow chart of the model.

Table 5.2.3: Parameters of the model.

Symbol	Interpretation	Method
t_0	Time at which the epidemic started	fitted
S_0	Number of susceptible at time t_0	fixed
I_0	Number of asymptomatic infectious at time t_0	fitted
U_0	Number of unreported symptomatic infectious at time t_0	fitted
$\tau(t)$	Transmission rate at time t	fitted
D	First day of public intervention	fitted
μ	Intensity of the public intervention	fitted
$1/\nu$	Average time during which asymptomatic infectious are asymptomatic	fixed
f	Fraction of asymptomatic infectious that become reported symptomatic infectious	fixed
$\nu_1 = f\,\nu$	Rate at which asymptomatic infectious become reported symptomatic	fixed
$\nu_2 = (1-f)\,\nu$	Rate at which asymptomatic infectious become unreported symptomatic	fixed
$1/\eta$	Average time symptomatic infectious have symptoms	fixed

5.2.3.2 Comparison of the Model (5.2.1) with the Data

At the early stages of the epidemic, the infectious components of the model $I(t)$, $U(t)$ and $R(t)$ must be exponentially growing. Therefore, we can assume that

$$I(t) = I_0 \exp\left(\chi_2\,(t - t_0)\right).$$

The cumulative number of reported symptomatic infectious cases at time t, denoted by $CR(t)$, is

$$CR(t) = \nu_1 \int_{t_0}^{t} I(s)ds. \tag{5.2.4}$$

Since $I(t)$ is an exponential function and $CR(t_0) = 0$ it is natural to assume that $CR(t)$ has the following special form:

$$CR(t) = \chi_1 \exp\left(\chi_2 t\right) - \chi_3. \tag{5.2.5}$$

As in their early articles [261, 260, 258, 259, 262], the authors fix $\chi_3 = 1$ and we evaluate the parameters χ_1 and χ_2 by using an exponential fit to

$$\chi_1 \exp\left(\chi_2 t\right) \simeq CR_{data}(t).$$

We use only early data for this part, from day $t = d_1$ until day $t = d_2$, because we want to catch the exponential growth of the early epidemic and avoid the influence of saturation arising at later stages.

Remark 5.2.1. The estimated parameters χ_1 and χ_2 will vary if we change the interval $[d_1, d_2]$.

Once χ_1, χ_2, χ_3 are known, we can compute the starting time of the epidemic t_0 from (5.2.5) as :

$$CR(t_0) = 0 \Leftrightarrow \chi_1 \exp(\chi_2 t_0) - \chi_3 = 0 \;\Rightarrow\; t_0 = \frac{1}{\chi_2}\left(\ln(\chi_3) - \ln(\chi_1)\right).$$

We fix $S_0 = 126.8 \times 10^6$, which corresponds to the total population of Japan. The quantities I_0, R_0, and U_0 correspond to the values taken by $I(t)$, $R(t)$ and $U(t)$ at $t = t_0$ (and in particular R_0 should not be confused with the basic reproduction number $\mathcal{R}_0$). We fix the fraction f of symptomatic infectious cases that are reported. We assume that between 80% and 100% of infectious cases are reported. Thus, f varies between 0.8 and 1. We assume that the average time during which the patients are asymptomatic infectious $1/\nu$ varies between 1 day and 7 days. We assume that the average time during which a patient is symptomatic infectious $1/\eta$ varies between 1 day and 7 days. In other words we fix the parameters f, ν, η. Since f and ν are known, we can compute

$$\nu_1 = f\nu \text{ and } \nu_2 = (1-f)\,\nu. \tag{5.2.6}$$

Computing further (see below for more details), we should have

$$I_0 = \frac{\chi_1\chi_2 \exp(\chi_2 t_0)}{f\,\nu} = \frac{\chi_3\chi_2}{f\,\nu}, \tag{5.2.7}$$

$$\tau = N\frac{\chi_2 + \nu}{S_0}\frac{\eta + \chi_2}{\nu_2 + \eta + \chi_2}, \tag{5.2.8}$$

$$R_0 = \frac{\nu_1}{\eta + \chi_2} I_0 = \frac{f\nu}{\eta + \chi_2} I_0. \tag{5.2.9}$$

and

$$U_0 = \frac{\nu_2}{\eta + \chi_2} I_0 = \frac{(1-f)\nu}{\eta + \chi_2} I_0. \tag{5.2.10}$$

By using the approach described in Diekmann et al. [141], van den Driessche and Watmough [149], the basic reproductive number for model (5.2.1) is given by

$$\mathcal{R}_0 = \frac{\tau S_0}{\nu N}\left(1 + \frac{\nu_2}{\eta}\right).$$

By using (5.2.8) we obtain

$$\mathcal{R}_0 = \frac{\chi_2 + \nu}{\nu}\frac{(\eta + \chi_2)}{\nu_2 + \eta + \chi_2}\left(1 + \frac{\nu_2}{\eta}\right). \tag{5.2.11}$$

5.2.3.3 Model SIUR with Age Structure

In what follows we will denote $N_1, \ldots, N_{10}$ the number of individuals respectively for the age classes $[0, 10[, \ldots, [90, 100[$. The model for the number of susceptible individuals $S_1(t), \ldots, S_{10}(t)$, respectively for the age classes $[0, 10[, \ldots, [90, 100[$, is the following

$$\begin{cases} S_1'(t) = -\tau_1 S_1(t)\left[\phi_{1,1}\dfrac{(I_1(t) + U_1(t))}{N_1} + \ldots + \phi_{1,10}\dfrac{(I_{10}(t) + U_{10}(t))}{N_{10}}\right], \\ \vdots \\ S_{10}'(t) = -\tau_{10} S_{10}(t)\left[\phi_{10,1}\dfrac{(I_1(t) + U_1(t))}{N_1} + \ldots + \phi_{10,10}\dfrac{(I_{10}(t) + U_{10}(t))}{N_{10}}\right]. \end{cases} \tag{5.2.12}$$

The model for the number of asymptomatic infectious individuals $I_1(t), \ldots, I_{10}(t)$, respectively for the age classes $[0, 10[, \ldots, [90, 100[$, is the following

$$\begin{cases} I_1'(t) = \tau_1 S_1(t)\left[\phi_{1,1}\dfrac{(I_1(t) + U_1(t))}{N_1} + \ldots + \phi_{1,10}\dfrac{(I_{10}(t) + U_{10}(t))}{N_{10}}\right] - \nu I_1(t), \\ \vdots \\ I_{10}'(t) = \tau_{10} S_{10}(t)\left[\phi_{10,1}\dfrac{(I_1(t) + U_1(t))}{N_1} + \ldots + \phi_{10,10}\dfrac{(I_{10}(t) + U_{10}(t))}{N_{10}}\right] - \nu I_{10}(t). \end{cases} \tag{5.2.13}$$

The model for the number of reported symptomatic infectious individuals $R_1(t), \dots, R_{10}(t)$, respectively for the age classes $[0, 10[, \dots, [90, 100[$, is

$$\begin{cases} R_1'(t) = \nu_1^1 \, I_1(t) - \eta R_1(t), \\ \vdots \\ R_{10}'(t) = \nu_1^{10} \, I_{10}(t) - \eta R_{10}(t). \end{cases} \tag{5.2.14}$$

Finally the model for the number of unreported symptomatic infectious individuals $U_1(t), \dots, U_{10}(t)$, respectively in the age classes $[0, 10[, \dots, [90, 100[$, is the following

$$\begin{cases} U_1'(t) = \nu_2^1 \, I_1(t) - \eta U_1(t), \\ \vdots \\ U_{10}'(t) = \nu_2^{10} \, I_{10}(t) - \eta U_{10}(t). \end{cases} \tag{5.2.15}$$

In each age class $[0, 10[, \dots, [90, 100[$ we assume that there is a fraction $f_1, \dots, f_{10}$ of asymptomatic infectious individual who become reported symptomatic infectious (i.e., with severe symptoms) and a fraction $(1 - f_1), \dots, (1 - f_{10})$ who become unreported symptomatic infectious (i.e., with mild symptoms). Therefore we define

$$\begin{gathered} \nu_1^1 = \nu f_1 \text{ and } \nu_2^1 = \nu(1 - f_1), \\ \vdots \\ \nu_1^{10} = \nu f_{10} \text{ and } \nu_2^{10} = \nu(1 - f_{10}). \end{gathered} \tag{5.2.16}$$

In this model $\tau_1, \dots, \tau_{10}$ are the respective transmission rates for the age classes $[0, 10[, \dots, [90, 100[$.

The matrix ϕ_{ij} represents the probability for an individual in the class i to meet an individual in the class j. In their survey, Prem and co-authors [325] present a way to reconstruct contact matrices from existing data and provide such contact matrices for a number of countries including Japan. Based on the data provided by Prem et al. [325] for Japan we construct the contact probability matrix ϕ. More precisely, we inferred contact data for the missing age classes $[80, 90[$ and $[90, 100[$. The precise method used to construct the contact matrix γ is detailed in Appendix 5.2.7. An analogous contact matrix for Japan has been proposed by Munasinghe, Asai and Nishiura [295]. The contact matrix γ we used is the following

$$[\gamma_{ij}] = \begin{bmatrix} 4.03 & 0.92 & 0.47 & 1.69 & 0.83 & 0.92 & 0.78 & 0.56 & 0.57 & 0.57 \\ 0.71 & 8.06 & 1.38 & 1.36 & 1.96 & 1.74 & 0.75 & 0.86 & 0.74 & 0.57 \\ 0.55 & 1.05 & 4.63 & 2.25 & 1.84 & 1.92 & 0.94 & 0.46 & 0.74 & 0.73 \\ 1.52 & 1.20 & 2.54 & 4.97 & 2.98 & 2.40 & 1.76 & 0.99 & 0.53 & 0.73 \\ 0.69 & 1.42 & 1.93 & 2.87 & 3.91 & 2.76 & 1.35 & 1.33 & 0.95 & 0.53 \\ 0.34 & 0.48 & 1.20 & 1.46 & 1.61 & 2.97 & 1.40 & 0.98 & 1.23 & 0.95 \\ 0.28 & 0.18 & 0.20 & 0.52 & 0.38 & 0.77 & 2.67 & 1.72 & 0.92 & 1.23 \\ 0.12 & 0.10 & 0.09 & 0.18 & 0.19 & 0.25 & 0.76 & 1.99 & 1.18 & 0.93 \\ 0.09 & 0.10 & 0.08 & 0.09 & 0.13 & 0.17 & 0.27 & 0.64 & 1.61 & 1.19 \\ 0.09 & 0.09 & 0.10 & 0.08 & 0.09 & 0.13 & 0.17 & 0.27 & 0.64 & 1.61 \end{bmatrix}, \tag{5.2.17}$$

where the i^{th} line of the matrix γ_{ij} is the average number of contact made by an individuals in the age class i with an individual in the age class j during one day. Notice that the higher number of contacts are achieved within the same age class. The matrix of conditional probability ϕ of contact between age classes

is given by (5.2.18) and we plot a visual representation of this matrix in Figure 5.2.7.

$$[\phi_{ij}] = \begin{bmatrix} 0.35 & 0.08 & 0.04 & 0.14 & 0.07 & 0.08 & 0.06 & 0.04 & 0.05 & 0.05 \\ 0.03 & 0.44 & 0.07 & 0.07 & 0.10 & 0.09 & 0.04 & 0.04 & 0.04 & 0.03 \\ 0.03 & 0.06 & 0.30 & 0.14 & 0.12 & 0.12 & 0.06 & 0.03 & 0.04 & 0.04 \\ 0.07 & 0.06 & 0.12 & 0.25 & 0.15 & 0.12 & 0.08 & 0.05 & 0.02 & 0.03 \\ 0.03 & 0.07 & 0.10 & 0.16 & 0.22 & 0.15 & 0.07 & 0.07 & 0.05 & 0.03 \\ 0.02 & 0.03 & 0.09 & 0.11 & 0.12 & 0.23 & 0.11 & 0.07 & 0.09 & 0.07 \\ 0.03 & 0.02 & 0.02 & 0.05 & 0.04 & 0.08 & 0.30 & 0.19 & 0.10 & 0.13 \\ 0.02 & 0.01 & 0.01 & 0.03 & 0.03 & 0.04 & 0.13 & 0.34 & 0.20 & 0.16 \\ 0.02 & 0.02 & 0.01 & 0.02 & 0.02 & 0.03 & 0.06 & 0.14 & 0.36 & 0.27 \\ 0.02 & 0.02 & 0.03 & 0.02 & 0.02 & 0.03 & 0.05 & 0.08 & 0.19 & 0.48 \end{bmatrix}. \tag{5.2.18}$$

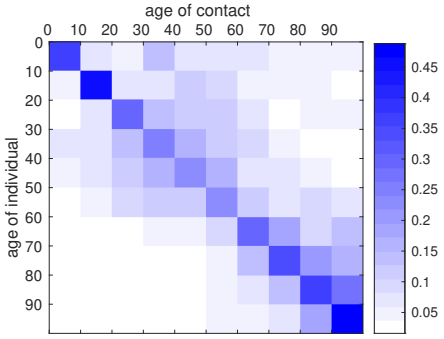

Figure 5.2.7: Graphical representation of the contact matrix ϕ. The intensity of blue in the cell (i, j) indicates the conditional probability that, given a contact between an individual of age group i and another individual, the latter belongs to the age class j. The matrix was reconstructed from the data of Prem et al. [325], with the method described in Appendix 5.2.7.

5.2.4 Results

5.2.4.1 Model without Age Structure

The daily number of reported cases from the model can be obtained by computing the solution of the following equation:

$$DR'(t) = \nu_1 I(t) - DR(t), \text{ for } t \geq t_0 \text{ and } DR(t_0) = DR_0. \tag{5.2.19}$$

In Figures 5.2.8 and 5.2.9 we employ the method presented previously in Liu et al. [262] to fit the data for Japan without age structure.

The model to compute the cumulative number of death from the reported individuals is the following

$$D'(t) = \eta_D \, p \, R(t), \text{ for } t \geq t_0 \text{ and } D(t_0) = 0, \tag{5.2.20}$$

where η_D is the death rate of reported infectious symptomatic individuals and p is the case fatality rate (namely the fraction of death per reported infectious individuals).

In the simulation we chose $1/\eta_D = 6$ days and the case fatality rate $p = 0.286$ is computed by using the cumulative number of confirmed cases and the cumulative number of deaths (as of 29 April) as follows

$$p = \frac{\text{cumulative number of deaths}}{\text{cumulative number of reported cases}} = \frac{393}{13744}. \tag{5.2.21}$$

In Figure 5.2.10 we plot the cumulative number of $D(t)$ by using the same simulations than in Figures 5.2.8 and 5.2.9.

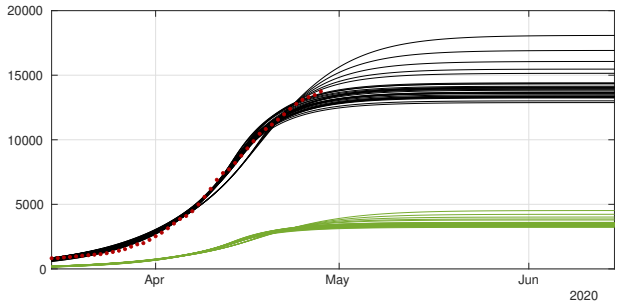

Figure 5.2.8: Cumulative number of cases. We plot the cumulative data (reds dots) and the best fits of the model $CR(t)$ (black curve) and $CU(t)$ (green curve). We fix $f = 0.8$, $1/\eta = 7$ days and $1/\nu = 7$ and we apply the method described in Liu et al. [262]. The best fit is $d_1 = 2$ April, $d_2 = 5$ April, $D = 27$ April, $\mu = 0.6$, $\chi_1 = 179$, $\chi_2 = 0.085$, $\chi_3 = 1$ and $t_0 = 13$ January.

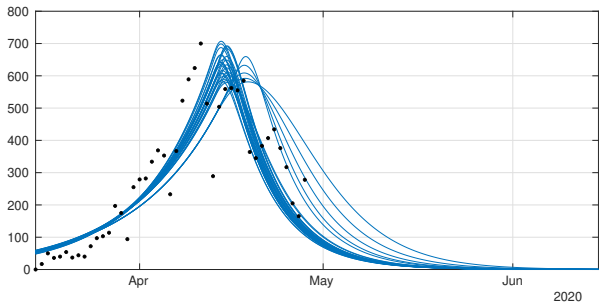

Figure 5.2.9: Daily number of cases. We plot the daily data (black dots) with $DR(t)$ (blue curve). We fix $f = 0.8$, $1/\eta = 7$ days and $1/\nu = 7$ and we apply the method described in Liu et al. [262]. The best fit is $d_1 = 2$ April, $d_2 = 5$ April, $N = 27$ April, $\mu = 0.6$, $\chi_1 = 179$, $\chi_2 = 0.085$, $\chi_3 = 1$ and $t_0 = 13$ January.

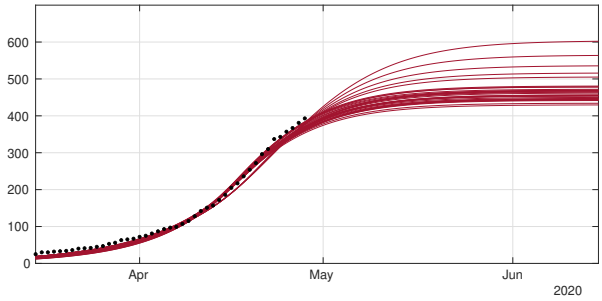

Figure 5.2.10: In this figure we plot the data for the cumulative number of death (black dots), and our best fits for $D(t)$ (red curves).

5.2.4.2 Model with Age Structure

In order to describe the confinement for the age structured model (5.2.12)–(5.2.15) we will use for each age class $i = 1, \ldots, 10$ a different transmission rate having the following form

$$\begin{cases} \tau_i(t) = \tau_i, \, 0 \leq t \leq D_i, \\ \tau_i(t) = \tau_i \, \exp\left(-\mu_i \left(t - D_i\right)\right), \, D_i < t. \end{cases} \tag{5.2.22}$$

The date D_i is the first day of public intervention for the age class i and μ_i is the intensity of the public intervention for each age class.

In Figure 5.2.11 we plot the cumulative number of reported cases as given by our model (5.2.12)–(5.2.15) (solid lines), compared with reported cases data (black dots). We used the method described in the Appendix 5.2.6 to estimate the parameters τ_i from the data. In Figure 5.2.12 we plot the cumulative

number of *unreported* cases (solid lines) as given by our model with the same parameter values, compared to the existing data of *reported* cases (black dots).

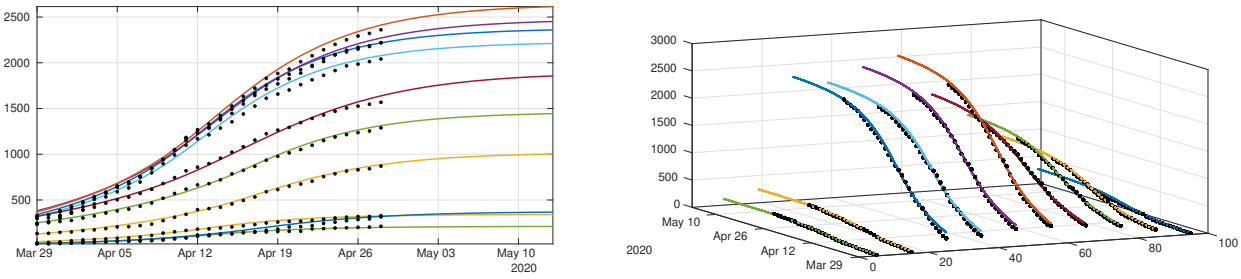

Figure 5.2.11: We plot a comparison between the model (5.2.12)–(5.2.15) and the age structured data from Japan by age class. We took $1/\nu = 1/\eta = 7$ days for each age class. Our best fit is obtained for f_i which depends linearly on the age class until it reaches 90%, with $f_1 = 0.1$, $f_2 = 0.2$, $f_3 = 0.3$, $f_4 = 0.4$, $f_5 = 0.5$, $f_6 = 0.6$, $f_7 = 0.7$, $f_8 = 0.8$, $f_9 = 0.9$, and $f_{10} = 0.9$. The values we used for the first day of public intervention are $D_i = 13$ April for the 0–20 years age class $i = 1, 2$, $D_i = 11$ April for the age class going from $[20, 30[$ to $[60, 70[$ $i = 3, 4, 5, 6, 7$, and $D_i = 16$ April for the remaining age classes. We fit the data from 30 March to 20 April to derive the value of χ_1^i and χ_2^i for each age class. For the intensity of confinement we use the values $\mu_1 = \mu_2 = 0.4829$, $\mu_3 = \mu_4 = 0.2046$, $\mu_5 = \mu_6 = 0.1474$, $\mu_7 = 0.0744$, $\mu_8 = 0.1736$, $\mu_9 = \mu_{10} = 0.1358$. By applying the method described in Appendix A, we obtain $\tau_1 = 0.1630$, $\tau_2 = 0.1224$, $\tau_3 = 0.3028$, $\tau_4 = 0.2250$, $\tau_5 = 0.1520$, $\tau_6 = 0.1754$, $\tau_7 = 0.1289$, $\tau_8 = 0.1091$, $\tau_9 = 0.1211$ and $\tau_{10} = 0.1642$. The matrix ϕ is the one defined in (5.2.18).

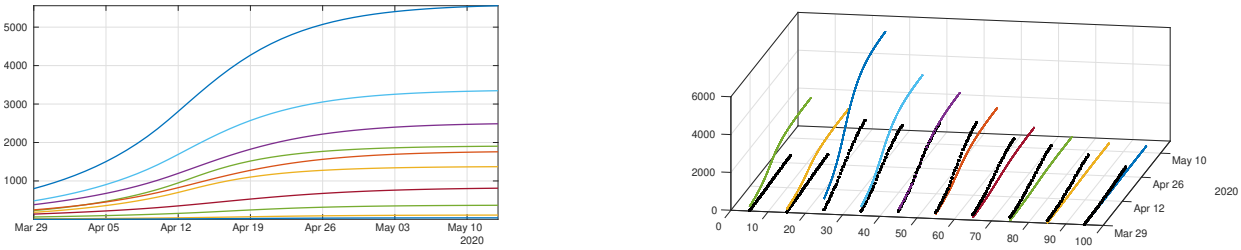

Figure 5.2.12: Cumulative number of unreported cases as given by the fit of the model (5.2.12)–(5.2.15) to Japanese data. The solid curves represent the solution of the model and the black dots correspond to the reported cases data. Parameter are the same as in Figure 5.2.11.

In order to understand the role of transmission network between age groups in this epidemic, we plot in Figure 5.2.13 the transmission matrices computed at different times. The transmission matrix is the following

$$C(t) = \text{diag}\,(\tau_1(t), \tau_2(t), \ldots, \tau_{10}(t)) \times \phi \tag{5.2.23}$$

where the matrix ϕ describes contacts and is given in (5.2.18), and the transmission rates are the ones fitted to the data as in Figure 5.2.11

$$\tau_i(t) = \tau_i^0(t) \exp(-\mu_i(t - D_i)_+).$$

During the early stages of the epidemic, the transmission seems to be evenly distributed among age classes, with a little bias towards younger age classes (Figure 5.2.13a). Younger age classes seem to react more quickly to social distancing policies than older classes, therefore their transmission rate drops rapidly (Figure 5.2.13b,c); one month after the start of social distancing measures, the transmission mostly occurs within elderly classes (60–100 years, Figure 5.2.13d).

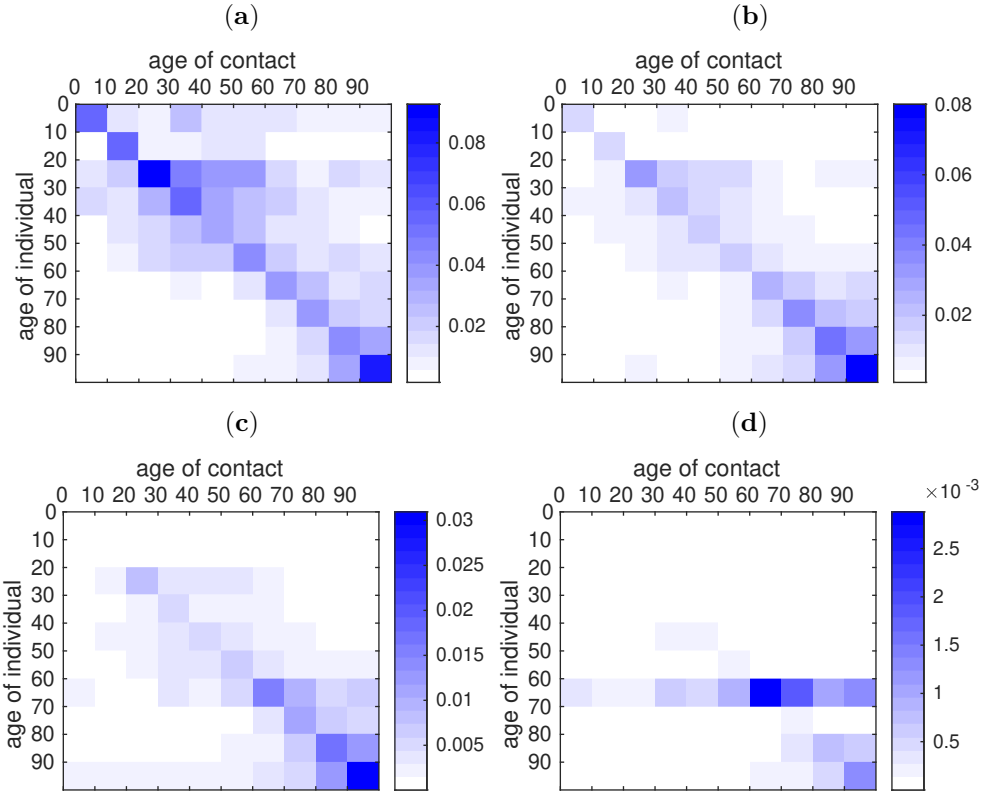

Figure 5.2.13: Rate of contact between age classes according to the fitted data. For each age class in the y-axis we plot the rate of contacts between one individual of this age class and another individual of the age class indicated on the x-axis. (**a**) is the rate of contacts before the start of public measures (11 April). (**b**) is the rate of contacts at the date of effect of the public measures for the last age class (16 April). (**c**) is the rate of contacts one week later (23 April). (**d**) is the rate of contacts one month later (16 May). In this figure we use $\tau_1 = 0.1630$, $\tau_2 = 0.1224$, $\tau_3 = 0.3028$, $\tau_4 = 0.2250$, $\tau_5 = 0.1520$, $\tau_6 = 0.1754$, $\tau_7 = 0.1289$, $\tau_8 = 0.1091$, $\tau_9 = 0.1211$ and $\tau_{10} = 0.1642$, $\mu_1 = \mu_2 = 0.4829$, $\mu_3 = \mu_4 = 0.2046$, $\mu_5 = \mu_6 = 0.1474$, $\mu_7 = 0.0744$, $\mu_8 = 0.1736$, $\mu_9 = \mu_{10} = 0.1358$, and $D_1 = D_2 = 13$ April, $D_3 = D_4 = D_5 = D_6 = D_7 = 11$ April, $D_8 = D_9 = D_{10} = 16$ April.

5.2.5 Discussion

The recent COVID-19 pandemic has lead many local governments to enforce drastic control measures in an effort to stop its progression. Those control measures were often taken in a state of emergency and without any real visibility concerning the later development of the epidemics, to prevent the collapse of the health systems under the pressure of severe cases. Mathematical models can precisely help see more clearly what could be the future of the pandemic provided that the particularities of the pathogen under consideration are correctly identified. In the case of COVID-19, one of the features of the pathogen which makes it particularly dangerous is the existence of a high contingent of unidentified infectious individuals who spread the disease without notice. This makes non-intensive containment strategies such as quarantine and contact-tracing relatively inefficient but also renders predictions by mathematical models particularly challenging.

Early attempts to reconstruct the epidemics by using SIUR models were performed in Liu et al. [261, 260, 258, 259], who used them to fit the behavior of the epidemics in many countries, by including undetected cases into the mathematical model. Here we extend our modeling effort by adding the time series of deaths into the equation. In section 5.2.4 we present an additional fit of the number of disease-induced deaths coming from symptomatic (reported) individuals (see Figure 5.2.10). In order to fit properly the data, we were forced to reduce the length of stay in the R-compartment to 6 days (on average), meaning that death induced by the disease should occur on average faster than recovery. A shorter period between infection and death (compared to remission) has also been observed, for instance, by Verity et al. [382].

The major improvement in this section 5.2 is to combine our early SIUR model with chronological age. Early results using age structured SIR models were obtained by Kucharski et al. [245] but no unreported

individuals were considered and no comparison with age-structured data were performed. Indeed in this section 5.2 we provide a new method to fit the data and the model. The method extends our previous method for the SIUR model without age (see Appendix 5.2.6).

The data presented in section 5.2.2 suggests that the chronological age plays a very important role in the expression of the symptoms. The largest part of the reported patients are between 20 and 60 years old (see Figure 5.2.1), while the largest part of the deceased are between 60 and 90 years old (see Figure 5.2.3). This suggests that the symptoms associated with COVID-19 infection are more severe in elderly patients, which has been reported in the literature several times (see e.g., Lu et al. [268], Zhou et al. [415]). In particular, the probability of being asymptomatic (our parameter f) should in fact depend on the age class.

Indeed, the best match for our model (see Figure 5.2.11) was obtained under the assumption that the proportion of symptomatic individual among the infected increases with the age of the patient. This linear dependency of f as a function of age is consistent with the observations of Wu et al. [404] that the severity of the symptoms increase linearly with age. As a consequence, unreported cases are a majority for young age classes (for age classes less than 50 years) and become a minority for older age classes (more than 50 years), see Figure 5.2.12. Moreover, our model reveals the fact that the policies used by the government to reduce contacts between individuals have strongly heterogeneous effects depending on the age classes. Plotting the transmission matrix at different times (see Figure 5.2.13) shows that younger age classes react more quickly and more efficiently than older classes. This may be due to the fact that the number of contacts in a typical day is higher among younger individuals. As a consequence, we predict that one month after the effective start of public measures, the new transmissions will almost exclusively occur in elderly classes. The observation that younger ages classes play a major roles in the transmission of the disease has been highlighted several times in the literature, see e.g., Davies et al. [130], Cao et al. [102], Kucharski et al. [245] for the COVID-19 epidemic, but also Mossong et al. [292] in a more general context.

We develop a new model for age-structured epidemic and provided a new and efficient method to identify the parameters of this model based on observed data. Our method differs significantly from the existing nonlinear least-squares and statistical inference methods and we believe that it produces high-quality results. Moreover, we only use the initial phase of the epidemic for the identification of the epidemiological parameters, which shows that the model itself is consistent with the observed phenomenon and argues against overfitting. Yet our study could be improved in several direction. We only use reported cases which were confirmed by PCR tests, and therefore the number of tests performed could introduce a bias in the observed data – and therefore our results. We are currently working on an integration of this number of tests in our model. We use a phenomenological model to describe the response of the population in terms of number of contacts to the mitigation measures imposed by the government. This could probably be described more precisely by investigating the mitigation strategies in terms of social network. Nevertheless we believe that our study offers a precise and robust mathematical method which adds to the existing literature.

5.2.6 Method to Fit of the Age Structured Model to the Data

We first choose two days d_1 and d_2 between which each cumulative age group grows like an exponential. By fitting the cumulative age classes $[0, 10[, [10, 20[, \dots$ and $[90, 100[$ between d_1 and d_2, for each age class $j = 1, \dots 10$ we can find χ_1^j and χ_2^j

$$CR_j^{data}(t) \simeq \chi_1^j \, e^{\chi_2^j t}.$$

We choose a starting time $t_0 \leq d_1$ and we fix

$$\chi_3^j = \chi_1^j \, e^{\chi_2^j t_0}, \forall j = 1, \dots, n,$$

and we obtain

$$\begin{cases} CR_1(t) = \chi_1^1 \, e^{\chi_2^1 t} - \chi_3^1, \\ \vdots \\ CR_n(t) = \chi_1^n \, e^{\chi_2^n t} - \chi_3^n i \end{cases} \tag{5.2.24}$$

where

$$\chi_j^i \geq 0, \forall i = 1, \dots, n, \; \forall j = 1, 2, 3.$$

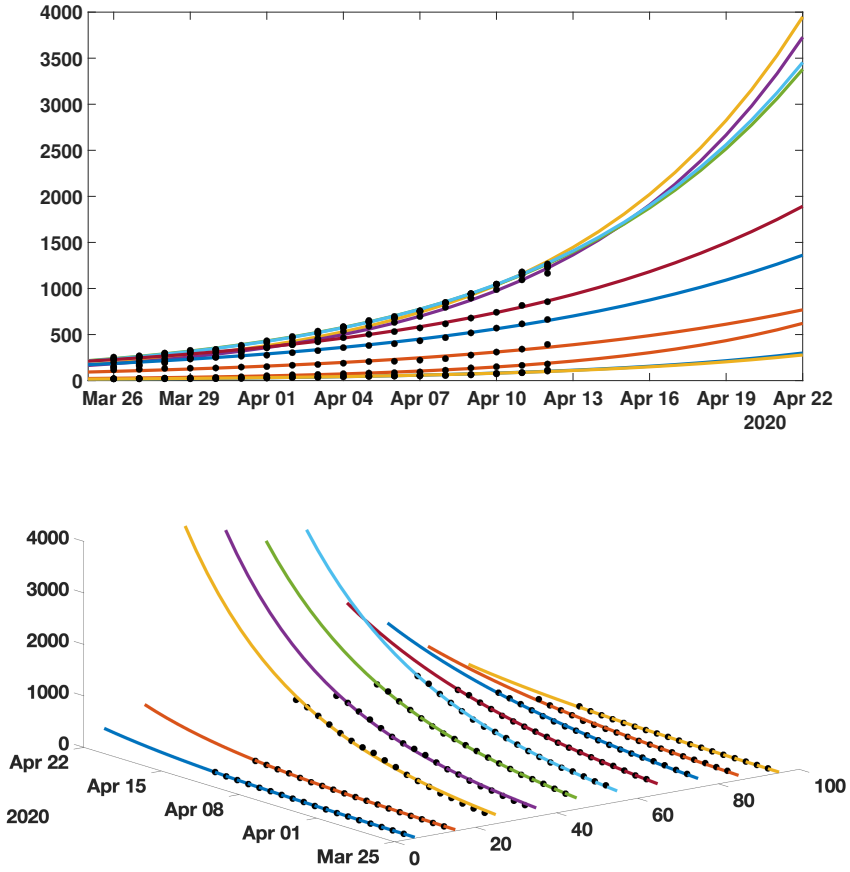

Figure 5.2.14: We plot an exponential fit for each age classes using the data from Japan.

We assume that

$$\begin{aligned} CR_1(t)' &= \nu_1^1 I_1(t), \\ &\vdots \\ CR_n(t)' &= \nu_1^n I_n(t), \end{aligned} \tag{5.2.25}$$

where

$$\nu_1^i = \nu\, f_i, \text{ and } \nu_2^i = \nu\,(1-f_i), \forall i = 1, \dots, n.$$

Therefore we obtain

$$I_j(t) = I_j^\star e^{\chi_2^j t} \tag{5.2.26}$$

where

$$I_j^\star := \frac{\chi_1^j \chi_2^j}{\nu_1^j}.$$

By assuming that the number of susceptible individuals remains constant we have

$$\begin{cases} I_1'(t) = \tau_1 S_1 \left[\phi_{11} \dfrac{I_1(t)+U_1(t)}{N_1} + \ldots + \phi_{1n} \dfrac{I_n(t)+U_n(t)}{N_n} \right] - \nu I_1(t), \\ \qquad\qquad \vdots \\ I_n'(t) = \tau_n S_n \left[\phi_{n1} \dfrac{I_1(t)+U_1(t)}{N_1} + \ldots + \phi_{nn} \dfrac{I_n(t)+U_n(t)}{N_n} \right] - \nu I_n(t), \end{cases} \tag{5.2.27}$$

and

$$\begin{cases} U_1'(t) = \nu_2^1\, I_1(t) - \eta U_1(t), \\ \qquad\vdots \\ U_n'(t) = \nu_2^n\, I_n(t) - \eta U_n(t). \end{cases} \tag{5.2.28}$$

If we assume that the $U_j(t)$ have the following form

$$U_j(t) = U_j^\star e^{\chi_2^j t}, \tag{5.2.29}$$

then by substituting in (5.2.28) we obtain

$$U_j^\star = \frac{\nu_2^j I_j^\star}{\eta + \chi_2^j}. \tag{5.2.30}$$

The cumulative number of unreported cases $CU_j(t)$ is computed as

$$CU_j(t)' = \nu_2^j I_j(t),$$

and we used the following initial condition:

$$CU_j(0) = CU_j^* = \int_{-\infty}^{0} \nu_2^j I_j^* e^{\chi_2^j s} ds = \frac{\nu_2^j I_j^*}{\chi_2^j}.$$

We define the error between the data and the model as follows

$$\begin{cases} \varepsilon_1(t) = I_1'(t) - \tau_1 S_1 \left[\phi_{11} \dfrac{I_1(t) + U_1(t)}{N_1} + \ldots + \phi_{1n} \dfrac{I_n(t) + U_n(t)}{N_n}\right] + \nu I_1(t), \\ \qquad\vdots \\ \varepsilon_n(t) = I_n'(t) - \tau_n S_n \left[\phi_{n1} \dfrac{I_1(t) + U_1(t)}{N_1} + \ldots + \phi_{nn} \dfrac{I_n(t) + U_n(t)}{N_n}\right] + \nu I_n(t), \end{cases} \tag{5.2.31}$$

or equivalently

$$\begin{cases} \varepsilon_1(t) = \left(\chi_2^1 + \nu\right) I_1^\star e^{\chi_2^1 t} - \tau_1 S_1 \left[\phi_{11} \dfrac{I_1^\star + U_1^\star}{N_1} e^{\chi_2^1 t} + \ldots + \phi_{1n} \dfrac{I_n^\star + U_n^\star}{N_n} e^{\chi_2^n t}\right], \\ \qquad\vdots \\ \varepsilon_n(t) = \left(\chi_2^n + \nu\right) I_n^\star e^{\chi_2^n t} - \tau_n S_n \left[\phi_{n1} \dfrac{I_1^\star + U_1^\star}{N_1} e^{\chi_2^1 t} + \ldots + \phi_{nn} \dfrac{I_n^\star + U_n^\star}{N_n} e^{\chi_2^n t}\right]. \end{cases} \tag{5.2.32}$$

Let the matrix ϕ be fixed. We look for the vector $\tau = (\tau_1, \ldots, \tau_n)$ which minimizes of

$$\min_{\tau \in \mathbb{R}^n} \sum_{j=1,\ldots,n} \int_{d_1}^{d_2} \varepsilon_j(t)^2 dt.$$

Define for each $j = 1, \ldots, n$

$$K_j(t) := \left(\chi_2^j + \nu\right) I_j^\star e^{\chi_2^j t}$$

and

$$H_j(t) := S_j \left[\phi_{j1} \frac{I_1^\star + U_1^\star}{N_1} e^{\chi_2^1 t} + \ldots + \phi_{jn} \frac{I_n^\star + U_n^\star}{N_n} e^{\chi_2^n t}\right],$$

so that

$$\varepsilon_j(t) = K_j(t) - \tau_j H_j(t).$$

Hence for each $j = 1, \ldots, n$

$$\int_{d_1}^{d_2} \varepsilon_j(t)^2 dt = \int_{d_1}^{d_2} K_j(t)^2 dt - 2\tau_j \int_{d_1}^{d_2} K_j(t) H_j(t) dt + \tau_j^2 \int_{d_1}^{d_2} H_j(t)^2 dt,$$

and by setting

$$0 = \frac{\partial}{\partial \tau_j} \int_{d_1}^{d_2} \varepsilon_j(t)^2 dt = -2 \int_{d_1}^{d_2} K_j(t) H_j(t) dt + 2\tau_j \int_{d_1}^{d_2} H_j(t)^2 dt$$

we deduce that

$$\tau_j = \frac{\int_{d_1}^{d_2} K_j(t) H_j(t) dt}{\int_{d_1}^{d_2} H_j(t)^2 dt}. \tag{5.2.33}$$

Remark 5.2.2. It does not seem possible to estimate the matrix of contact ϕ by using similar optimization method. Indeed, if we look for a matrix $\phi = (\phi_{ij})$ which minimizes

$$\min_{\phi \in M_n(\mathbb{R})} \sum_{j=1,\dots,n} \int_{d_1}^{d_2} \varepsilon_j(t)^2 dt,$$

it turn out that

$$\sum_{j=1,\dots,n} \int_{d_1}^{d_2} \varepsilon_j(t)^2 dt = 0$$

whenever ϕ is diagonal. Therefore the optimum is reached for any diagonal matrix. Moreover by using similar considerations, if several χ_j^2 are equal, we can find a multiplicity of optima (possibly with ϕ not diagonal). This means that trying to optimize by using the matrix ϕ does not yield significant and reliable information.

In the Figure 5.2.15 below, we present an example of application of our method to fit the Japanese data. We use the period going from 20 March to 15 April.

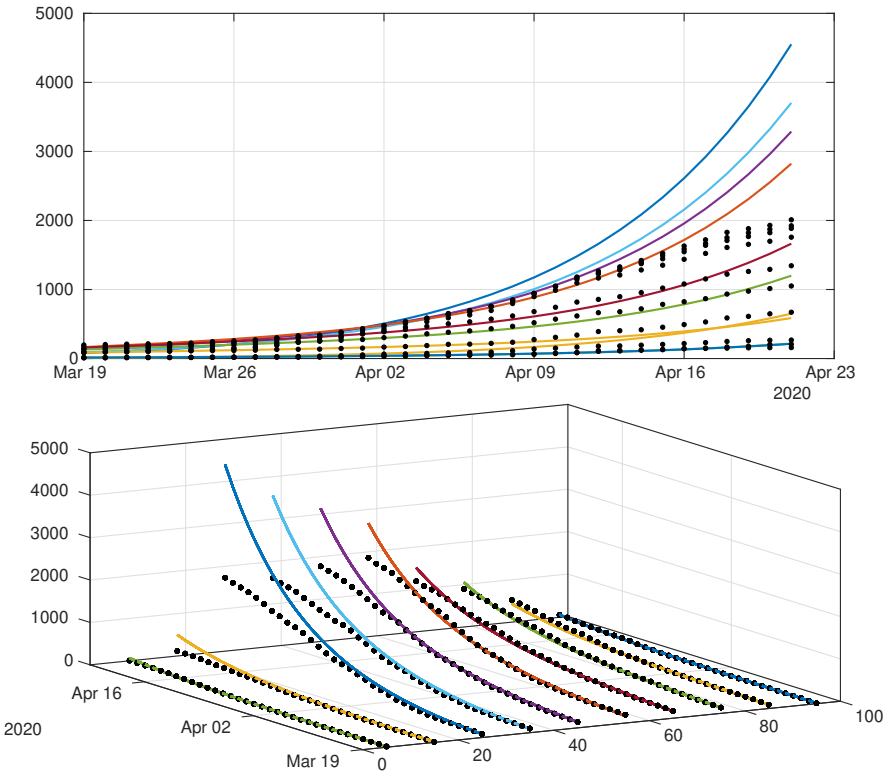

Figure 5.2.15: We plot a comparison between the model (5.2.12)–(5.2.15) (without public intervention) and the age structured data from Japan. We set $1/\nu = 1/\eta = 7$ days, f_i which actually depends on the age class, with $f_1 = 0.1$, $f_2 = 0.2$, $f_3 = 0.4$, $f_4 = 0.4$, $f_5 = 0.6$, $f_6 = 0.6$, $f_7 = 0.8$, $f_8 = 0.8$, $f_9 = 0.8$, and $f_{10} = 0.9$. and we obtain $\tau_1 = 0.1264$, $\tau_2 = 0.1655$, $\tau_3 = 0.3538$, $\tau_4 = 0.2966$, $\tau_5 = 0.1513$, $\tau_6 = 0.1684$, $\tau_7 = 0.1251$, $\tau_8 = 0.1168$, $\tau_9 = 0.1015$, $\tau_{10} = 0.1258$. The matrix ϕ is the one defined in (5.2.18).

5.2.7 Construction of the Contact Matrix

The survey [325] presents reconstructed contact matrices for a number of countries including Japan for the 5-year age classes $[0, 5)$, $[5, 10)$, ..., $[75, 80)$ at various locations (work, school, home, and other locations) and a compilation of those contact matrices to account for all locations. The precise description of the compilation is presented in the section 5.2. Note that this section 5.2 is a follow-up of Mossong et al. [292] where the survey procedure is described (including the data collection protocol) for several European countries participating in the POLYMOD study.

The data is publicly available online (Prem et al. [325], Supporting dataset, DOI: `https://doi.org/10.1371/journal.pcbi.1005697.s002`) and is presented in the form of a zipped collection of spreadsheets, containing the data for several countries in columns X1 X2 ... X16. The columns stand for the average number of contact of one individual of the corresponding age class (0–5 years for X1, 5–10 years for X2, etc...), with an individual of the age class indicated by the row (first row is 0–5 years, second is 5–10 years etc...). Since the age span covered by the study stops at 80, we had to infer the number of contacts for people over the age of 80. We postulated that most people aged 80 or more are retired and that their behaviour does not significantly differs from the behavior of people in the age class $[75, 80)$. Therefore we completed the missing columns by copying the last available information and shifting it to the bottom. We repeated the procedure for lines. We believe that the introduced bias is kept to a minimum since the numerical values are relatively low compared to the diagonal.

Because we use 10-year ages classes and the data is given in 5-year age classes, we had to combine adjacent columns to recover the average number of contacts. To combine columns together, we used the weighted average

$$C'_i = \frac{N_{2(i-1)+1}C_{2(i-1)+1} + N_{2(i-1)+2}C_{2(i-1)+2}}{N_{2(i-1)+1} + N_{2(i-1)+2}},$$

where the column C'_i corresponds to the average number of contacts of an individual taken at random in the $[10(i-1), 10i)$ and C_i is the average number of contacts of an individual taken at random in the age class $[5(i-1), 5i)$. To combine two lines, we simply use the sum of the data

$$L'_i = L_{2(i-1)+1} + L_{2(i-1)+2}.$$

The matrix γ in (5.2.17) is the transpose of the array obtained by the former procedure applied to the "all locations" dataset. Then ϕ is obtained by scaling the lines of γ to 1, i.e.,

$$\phi_{ij} = \frac{\gamma_{ij}}{\sum_{k=1}^{10} \gamma_{ik}}.$$

5.3 Clarifying predictions for COVID-19 from testing data: the example of New York State

5.3.1 Introduction

The epidemic of novel coronavirus (COVID-19) infections began in China in December 2019 and rapidly spread worldwide in 2020. Since the early beginning of the epidemic, mathematicians and epidemiologists have developed models to analyze the data and characterize the spread of the virus, and attempt to project the future evolution of the epidemic. Many of those models are based on the SIR or SEIR model which is classical in the context of epidemics. We refer to [403, 368] for the earliest articles devoted to such a question and to [12, 27, 77, 75, 76, 88, 142, 208, 231, 297, 371] for more models. In the course of the COVID-19 outbreak, it became clear for the scientific community that covert cases (asymptomatic or unreported infectious case) play an important role. An early description of an asymptomatic transmission in Germany was reported by Rothe et al. [341]. It was also observed on the Diamond Princess cruise ship in Yokohama in Japan by Mizumoto et al. [287] that many of the passengers were tested positive to the virus, but never presented any symptoms. We also refer to Qiu [327] for more information about this problem. At the early stage of the COVID-19 outbreak, a new class of epidemic models was proposed in Liu et al. [261] to take into account the contamination of susceptible individuals by contact with unreported infectious. Actually, this class of models was presented earlier in Arino et al. [15]. In [261] a new method to use the number of reported cases in SIR models was also proposed. This method and model was extended in several directions by the same group in [260, 258, 259] to include non-constant transmission rates and a period of exposure. More recently the method was extended and successfully applied to a Japanese age-structured dataset in [P10]. The method was also extended to investigate the predictability of the outbreak in several countries including China, South Korea, Italy, France, Germany and the United Kingdom in [262]. The application of the Bayesian method was also considered in [117].

In parallel with these modeling ideas, Bayesian methods have been widely used to identify the parameters in the models used for the COVID-19 pandemic (see e.g. Roques et al. [340, 339] where an estimate of the fatality ratio has been developed). A remarkable feature of those methods is to provide mechanisms to correct some of the known biases in the observation of cases, such as the daily number of tests. Here we embed the data for the daily number of tests into an epidemic model and compare the number of reported cases produced by the model and the data. Our goal is to understand the relationship between the data for the daily number of tests (which is an input of our model) and the data for the daily number of reported cases (which is an output of our model).

The plan of the section 5.3 is the following. In section 5.3.2, we present a model involving the daily number of tests. In section 5.3.3, we apply the method presented in [261] to our new model. In section 5.3.4, we present some numerical simulations and compare the model with the data. The last section 5.3.5 is devoted to the discussion.

5.3.2 Epidemic with testing data

Let $n(t)$ be the number of tests per unit of time. Throughout this section 5.3, we use one day as the unit of time. Therefore $n(t)$ can be regarded as the daily number of tests at time t. The function $n(t)$ is actually coming from a database for the New York State [428]. Let $N(t)$ be the cumulative number of tests from the beginning of the epidemic. Then

$$N'(t) = n(t), \text{ for } t \geq t_1 \text{ and } N(t_1) = N_1. \tag{5.3.1}$$

Remark 5.3.1. section 5.3.4 is devoted to numerical simulations. We use $n(t)$ as a piecewise constant function that varies day by day. Each day, $n(t)$ is equal to the number of tests that were performed that day. So $n(t)$ should be understood as the black curve in Figure 5.3.4.

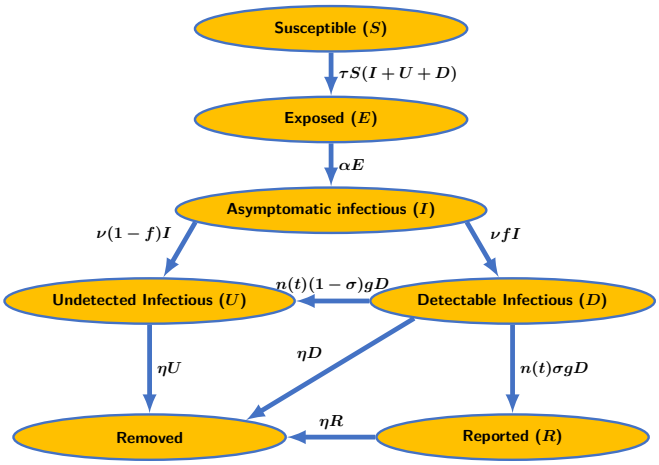

Figure 5.3.1: *Flow chart of the epidemic model with tests* (5.3.2). *In this diagram* $n(t)$ *is the daily number of tests at time* t. *We consider a fraction* $(1-\sigma)$ *of false negative tests and a fraction* σ *of true positive tests. The parameter* g *reflects the fact that the tests are devoted not only to the symptomatic patients but also to a large fraction of the population of New York state.*

The model consists of the following ordinary differential equation

$$\begin{cases} S'(t) = -\tau S(t)[I(t)+U(t)+D(t)], \\ E'(t) = \tau S(t)[I(t)+U(t)]+D(t)] - \alpha E(t), \\ I'(t) = \alpha E(t) - \nu I(t), \\ U'(t) = \nu\,(1-f)\,I(t) + n(t)\,(1-\sigma)\,g\,D(t) - \eta U(t), \\ D'(t) = \nu\,f\,I(t) - n(t)\,g\,D(t) - \eta D(t), \\ R'(t) = n(t)\,\sigma\,g\,D(t) - \eta R(t). \end{cases} \tag{5.3.2}$$

This system is supplemented by initial data (which are all non negative)

$$S(t_1) = S_1,\ E(t_1) = E_1,\ I(t_1) = I_1,\ U(t_1) = U_1,\ D(t_1) = D_1 \text{ and } R(t_1) = R_1. \tag{5.3.3}$$

The time t_1 corresponds to the time where the tests started to be used constantly. Therefore the epidemic started before t_1.

Here $t \geq t_1$ is the time in days. $S(t)$ is the number of individuals susceptible to infection. $E(t)$ is the number of exposed individuals (*i.e.* who are incubating the disease but not infectious). $I(t)$ is the number of individuals incubating the disease, but already infectious. $U(t)$ is the number of undetected infectious individuals (*i.e.* who are expressing mild or no symptoms), and the infectious that have been tested with a false negative result, are therefore not candidates for testing. $D(t)$ is the number of individuals who express severe symptoms and are candidates for testing. $R(t)$ is the number of individuals who have been tested positive to the disease. The flux diagram of our model is presented in Figure 5.3.1.

Susceptible individuals $S(t)$ become infected by contact with an infectious individual $I(t)$, $U(t)$ or $D(t)$. When they get infected, susceptibles are first classified as exposed individuals $E(t)$, that is to say that they are incubating the disease but not yet infectious. The average length of this exposed period (or noninfectious incubation period) is $1/\alpha$ days.

After the exposure period, individuals are becoming asymptomatic infectious $I(t)$. The average length of the asymptomatic infectious period is $1/\nu$ days. After this period, individuals are becoming either mildly symptomatic individuals $U(t)$ or individuals with severe symptoms $D(t)$. The average length of this infectious period is $1/\eta$ days. Some of the U-individuals may show no symptoms at all.

In our model, the transmission can occur between a S-individual and an I-, U- or R-individual. Transmissions of SARS-CoV-2 are described in the model by the term $\tau S(t)[I(t)+U(t)+D(t)]$ where τ is the transmission rate. Here, even though a transmission from R-individuals to a S-individuals is possible in

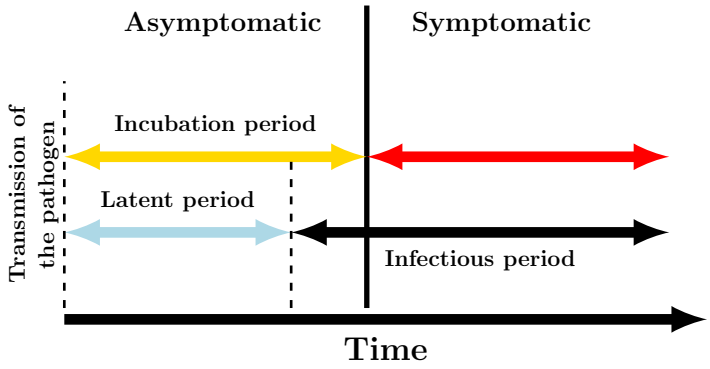

Figure 5.3.2: *Key time periods of COVID-19 infection: the latent or exposed period before the onset of symptoms and transmissibility, the incubation period before symptoms appear, the symptomatic period, and the transmissibility period, which may overlap the asymptomatic period.*

Symbol	Interpretation	Method
t_1	Date when the tests start to be used extensively	fixed
S_1	Number of susceptible at time t_1	fixed
E_1	Number of exposed at time t_1	fitted
I_1	Number of asymptomatic infectious at time t_1	fitted
U_1	Number of undetectable infectious at time t_1	fitted
D_1	Number of detectable infectious at time t_1	fitted
R_1	Number of reported (tested positive) cases at time t_1	fitted
τ	Transmission rate	fitted
$n(t)$	Number of tests per unit of time	fixed
$1/\alpha$	Average length of exposure	fixed
$1/\nu$	Average length of asymptomatic infectiousness	fixed
$1/\eta$	Average length of symptomatic infectiousness	fixed
f	Frequency of infectious with sever symptoms	fixed
σ	Fraction of true positive tests	fixed
g	Frequency of testable individuals	fixed

Table 5.3.1: *Parameters and initial conditions of the model.*

theory (e.g. if a tested patient infects its medical doctor), we consider that such a case is rare and we neglect it.

The last part of the model is devoted to the testing. The parameter σ is the fraction of true positive tests and $(1-\sigma)$ is the fraction of false negative tests. The quantity σ has been estimated at $\sigma = 0.7$ in the case of nasal or pharyngeal swabs for SARS-CoV-2 [316].

Among the detectable infectious, we assume that only a fraction g are tested per unit of time. This fraction corresponds to individuals with symptoms suggesting a potential infection to SARS-CoV-2. The fraction g is the frequency of testable individuals in the population of New York state. We can rewrite g as

$$g = \frac{1}{\kappa P} \tag{5.3.4}$$

where P is the total number of individuals in the population of the state of New York and $0 \leq \kappa \leq 1$ is the fraction total population with mild or sever symptoms that may induce a test.

Individuals who were tested positive $R(t)$ are infectious on average during a period of $1/\eta$ days. But we assume that they become immediately isolated and do not contribute to the epidemic anymore. In this model we focus on the testing of the D-individuals. The quantity $n(t)\,\sigma\,g\,D$ is a flux of successfully tested D-individuals which become R-individuals. The flux of tested D-individuals which are false negatives is

Symbol	Interpretation	Equation
t	Time (in days)	
$S(t)$	Number of susceptible at time t	(5.3.2)
$E(t)$	Number of exposed at time t	(5.3.2)
$I(t)$	Number of asymptomatic infectious at time t	(5.3.2)
$U(t)$	Number of undetectable infectious at time t	(5.3.2)
$D(t)$	Number of detectable infectious at time t	(5.3.2)
$R(t)$	Number of reported (tested infectious) cases at time t	(5.3.2)
$CR(t)$	Cumulative number of reported (tested infectious) cases at time t	(5.3.5)
$DR(t)$	Daily number of reported (tested infectious) cases at time t	(5.3.6)
$CD(t)$	Cumulative number of detectable infectious at time t	(5.3.7)
$CU(t)$	Cumulative number of undetectable infectious at time t	(5.3.8)

Table 5.3.2: *Variables used in the model.*

$n(t)\,(1-\sigma)\,g\,D$ which go from the class of D-individuals to the U-individuals. The parameters of the model and the initial conditions of the model are listed in Table 5.3.1.

Before describing our method we need to introduce a few useful identity. The cumulative number of reported cases is obtained by using the following equation

$$CR'(t) = n(t)\,\sigma\,g\,D(t). \tag{5.3.5}$$

The daily number of reported cases $DR'(t)$ is given by

$$DR(t)' = n(t)\,\sigma\,g\,D(t) - DR(t). \tag{5.3.6}$$

The cumulative number of detectable cases is given by

$$CD'(t) = \nu f I(t), \tag{5.3.7}$$

and the cumulative number of undetectable cases is given by

$$CU'(t) = \nu(1-f)I(t) + n(t)(1-\sigma)gD(t). \tag{5.3.8}$$

5.3.3 Method to fit the cumulative number of reported cases

In order to deal with data, we need to understand how to set the parameters as well as some components of the initial conditions. In order to do so, we extend the method presented first in [261]. The main novelty here concerns the cumulative number of tests which is assumed to grow linearly at the beginning. This property is satisfied for the New York State data as we can see in Figure 5.3.3. The black curve in this figure is close to a line from March 15 to April 15. Figure 5.3.4 shows day-by-day fluctuations of the number of tests while in Figure 5.3.3 the day-by-day fluctuations are not visible and the cumulative data allow to understand the growth tendency of the number of tests.

Phenomenological models for the tests : We fit a line to the cumulative number of tests in a suitable interval of days $[t_1, t_2]$. This means that we can find a pair of numbers a and b such that

$$N(t) = a \times (t - t_1) + N_1, \text{ for } t_1 \le t \le t_2. \tag{5.3.9}$$

where a the daily number of tests and N_1 is the cumulative number of tests on day t_1.

By using the fact that $N(t)' = n(t)$ we deduce that

$$n(t) = a, \text{ for } t_1 \le t \le t_2. \tag{5.3.10}$$

Remark 5.3.2. In the simulations we fit a line to the cumulative number of tests from mid-March to mid-April. Figure 5.3.3 shows that the linear growth assumption is reasonable for the New York State cumulative testing data.

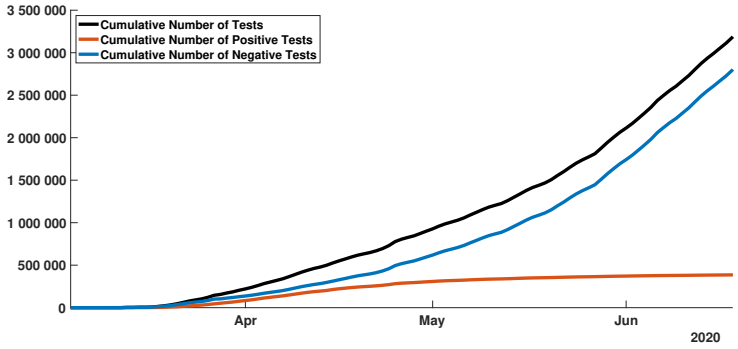

Figure 5.3.3: *In this figure, we plot the cumulative number of tests for the New York State. The black curve, orange curve, and blue curve correspond respectively to the number of tests, the number of positive tests, and the number of negative tests. We can see that at the early beginning of the epidemic, the cumulative number of tests (black curve) grows linearly from mid-March to mid-April.*

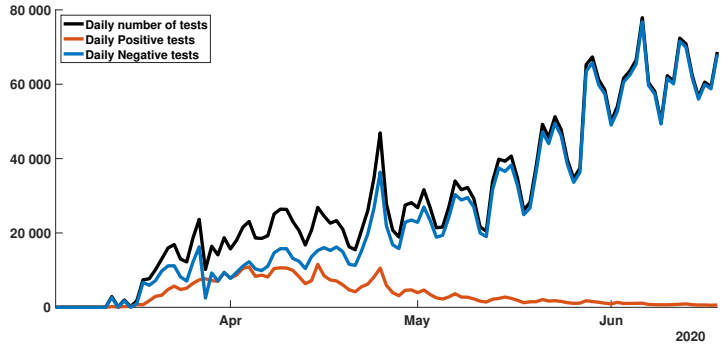

Figure 5.3.4: *In this figure, we plot the daily number of tests for the New York State. The black curve, orange curve, and blue curve correspond respectively to the number of tests, the number of positive tests, and the number of negative tests.*

Phenomenological models for the reported cases: At the early stage of the epidemic, we assume that all the infected components of the system grow exponentially while the number of susceptible remains unchanged during a relatively short period of time $t \in [t_1, t_2]$. Therefore, we assume that

$$E(t) = E_1 e^{\chi_2(t-t_1)}, I(t) = I_1 e^{\chi_2(t-t_1)}, D(t) = D_1 e^{\chi_2(t-t_1)} \text{ and } U(t) = U_1 e^{\chi_2(t-t_1)}. \tag{5.3.11}$$

We deduce that the cumulative number of reported cases satisfies

$$CR(t) = CR(t_1) + \int_{t_1}^{t} a\sigma g D(\theta) d\theta \tag{5.3.12}$$

hence by replacing $D(t)$ by the exponential formula (5.3.11)

$$CR(t) = CR(t_1) + \frac{a\sigma g}{\chi_2} D_1 \left(e^{\chi_2(t-t_1)} - 1 \right) \tag{5.3.13}$$

and it makes sense to assume that $CR(t) - CR(t_1)$ has the following form

$$CR(t) - CR(t_1) = \chi_1 e^{\chi_2(t-t_1)} - \chi_3. \tag{5.3.14}$$

By identifying (5.3.13) and (5.3.14) we deduce that

$$\chi_1 = \chi_3 = \frac{a\,\sigma\,g}{\chi_2} D_1. \tag{5.3.15}$$

Moreover by using (5.3.10) and the fact that the number of susceptible $S(t)$ remains constant equalling S_1 on the time interval $t \in [t_1, t_2]$, the E-equation, I-equation, U-equation and D-equation of the model (5.3.2) become

$$\begin{cases} E'(t) = \tau S_1[I(t) + U(t) + D(t)] - \alpha E(t), \\ I'(t) = \alpha E(t) - \nu I(t), \\ U'(t) = \nu\,(1-f)\,I(t) + a\,(1-\sigma)\,g\,D(t) - \eta U(t), \\ D'(t) = \nu\,f\,I(t) - a\,g\,D(t) - \eta D(t). \end{cases}$$

By using (5.3.11) we obtain

$$\begin{cases} \chi_2 E_1 = \tau S_1[I_1 + U_1 + D_1] - \alpha E_1, \\ \chi_2 I_1 = \alpha E_1 - \nu I_1, \\ \chi_2 U_1 = \nu\,(1-f)\,I_1 + a\,(1-\sigma)\,g\,D_1 - \eta U_1, \\ \chi_2 D_1 = \nu\,f\,I_1 - a\,g\,D_1 - \eta D_1. \end{cases}$$

Computing further, we get

$$\begin{cases} E_1 = \dfrac{\tau_1 S_1 (I_1 + U_1 + D_1)}{\chi_2 + \alpha} \\ I_1 = \dfrac{\alpha E_1}{\chi_2 + \nu} \\ U_1 = \dfrac{\nu I_1 + a\,(1-\sigma)\,g\,D_1}{\chi_2 + \eta} \\ D_1 = \dfrac{\nu\,f\,I_1}{\chi_2 + a\,g + \eta}. \end{cases} \tag{5.3.16}$$

Finally by using (5.3.15)

$$D_1 = \frac{\chi_2\,\chi_3}{\sigma\,a\,g}. \tag{5.3.17}$$

and by using (5.3.16) we obtain

$$\begin{cases} I_1 &= \dfrac{\chi_2 + a\,g + \eta}{\nu f} D_1 = \dfrac{\chi_2 + a\,g + \eta}{\nu} \times \dfrac{\chi_2\,\chi_3}{f\,\sigma\,a\,g} \\ U_1 &= \dfrac{\nu I_1 + (1-\sigma)\,a\,g\,D_1}{\chi_2 + \eta} = \dfrac{(\chi_2 + \eta + [1 + f(1-\sigma)]\;a\,g)}{\chi_2 + \eta} \times \dfrac{\chi_2\,\chi_3}{f\,\sigma\,a\,g} \\ E_1 &= \dfrac{(\chi_2 + \nu)}{\alpha} I_1 = \dfrac{(\chi_2 + \nu)}{\alpha} \times \dfrac{(\chi_2 + a\,g + \eta)}{\nu} \times \dfrac{\chi_2\,\chi_3}{f\,\sigma\,a\,g} \\ \tau_1 &= \dfrac{(\chi_2 + \alpha)}{S_1(I_1 + U_1 + D_1)} E_1 \\ &= \dfrac{(\chi_2 + \alpha)\,(\chi_2 + \nu)\,(\chi_2 + \eta)\,(\chi_2 + a\,g + \eta)}{\alpha S_1 \Big([\chi_2 + a\,g + \eta + \nu(f+1)]\,(\chi_2 + \eta) + \nu\,[1 + f(1-\sigma)]\;a\,g \Big)}, \end{cases} \tag{5.3.18}$$

where I_1 is the number of incubating infectious individuals at time t_1, U_1 is the number of unreported infectious individuals at time t_1, E_1 is the number of incubating non-infectious individuals at time t_1 (see (5.3.11)), and finally τ_1 is the transmission rate at time t_1.

5.3.4 Numerical simulations

We assume that the transmission coefficient takes the form

$$\tau(t) = \tau_0\big((1-\gamma)\exp(-\mu(t - T_m)_+) + \gamma\big), \tag{5.3.19}$$

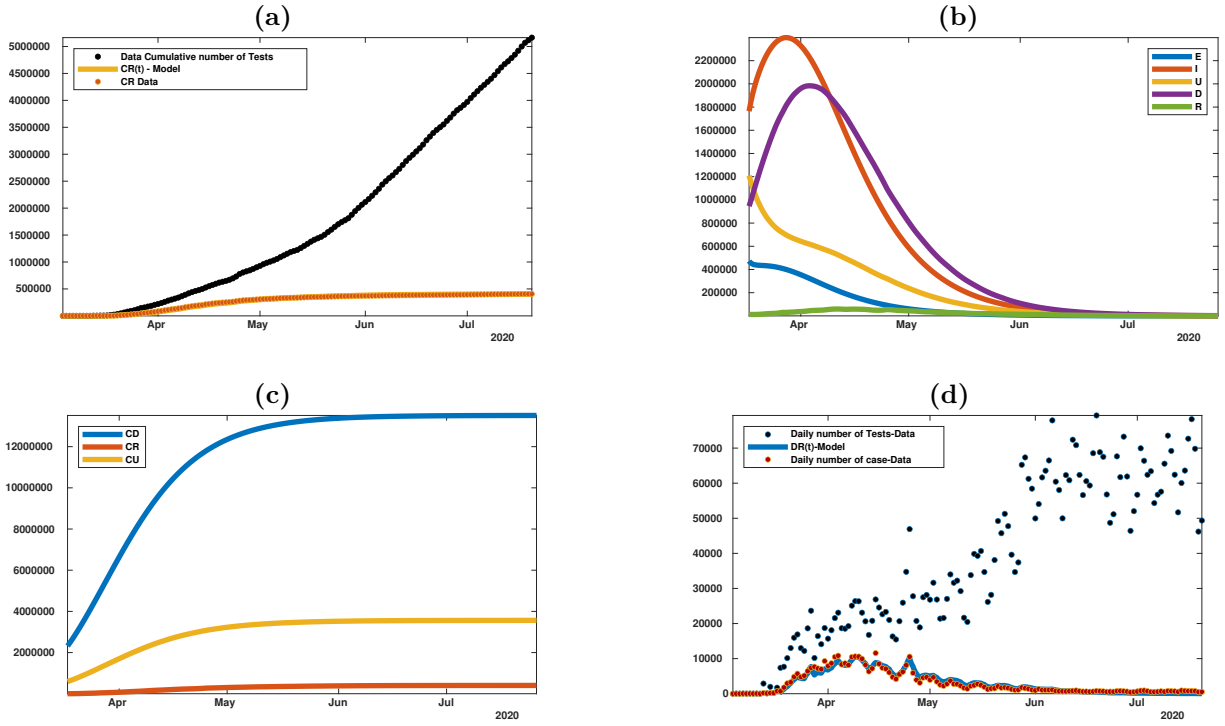

Figure 5.3.5: *Best fit of the model without confinement (or social distancing) measures (i.e. $\gamma = 1$).* ***Fitted parameters:*** *The transmission rate $\tau(t) \equiv \tau_0$ is constant according to the formula* (5.3.19) *with $\gamma = 1$ and τ_0 is fixed to the value τ_1 computed by using* (5.3.18). ***Parameter values:*** *$S_0 = 19453561$, $\alpha = 1$, $\nu = 1/6$, $\eta = 1/7$, $\sigma = 0.7$, $f = 0.8$ and $g = 6/S_0 = 3.08 \times 10^{-7}$. $t_1 = $ march 18, $t_2 = $ march 29, $a = 1.4874 \times 10^4$, $b = -2.1781 \times 10^5$, $\chi_1 = 2.8814 \times 10^4$, $\chi_2 = 0.1013$, $\chi_3 = 2.9969 \times 10^4$. In figure* ***(a)*** *we plot the cumulative number of tests (black dots), the cumulative number of positive cases (red dots) for the state of New York and the cumulative number of cases $CD(t)$ (yellow curve) obtained by fitting the model to the data. In figures* ***(b)–(c)*** *we plot the number of cases obtained from the model. We observe that most of the cases are unreported. In figure* ***(d)*** *we plot the daily number of tests (black dots), the daily number of positive cases (red dots) for the state of New York and the daily number of cases $DD(t)$ obtained from the data.*

where $\tau_0 > 0$ is the initial transmission coefficient, $T_m > 0$ is the time at which the social distancing starts in the population, and $\mu > 0$ controls the speed at which this social distancing is taking place.

To take into account the effect of social distancing and public measures, we assume that the transmission coefficient $\tau(t)$ can be modulated by γ. Indeed by closing schools and non-essential shops and by imposing social distancing in New York State, the number of contacts per day is reduced. This effect was visible on the news during the first wave of the COVID-19 epidemic in New York city since the streets were almost empty at some point. The parameter $\gamma > 0$ is the percentage of the number of transmissions that remain after a transition period (depending on μ), compared to a normal situation. A similar non-constant transmission rate was considered by Chowell et al. [111].

In Figure 5.3.5 we consider a constant transmission rate $\tau(t) \equiv \tau_0$ which corresponds to $\gamma = 1$ in (5.3.19). In order to evaluate the distance between the model and the data, we compare the distance between the cumulative number of cases CR produced by the model and the data (see the orange dots and orange curve in Figure 5.3.5-(a)). In Figure 5.3.5-(c) we observe that the cumulative number of cases increases up more than 14 millions of people, which indeed is not realistic. Nevertheless by choosing the parameter $g = 3.08 \times 10^{-7} = 1/\left(\frac{S_0}{6}\right)$ in Figure 5.3.5-(d) we can see that the orange dots and the blue curve match very well.

In the rest of this section 5.3.4, we focus on the model with confinement (or social distancing) measures. We assume that such social distancing measures have a strong impact on the transmission rate by assuming that $\gamma = 0.2 < 1$. It means that only 20% of the transmissions remain after a transition period.

In Figure 5.3.6-(c) we can observe that the cumulative number of cases increases up to 800 000 (blue curve) while the cumulative number reported cases goes up to 350 000. In Figure 5.3.6-(d) we can see that

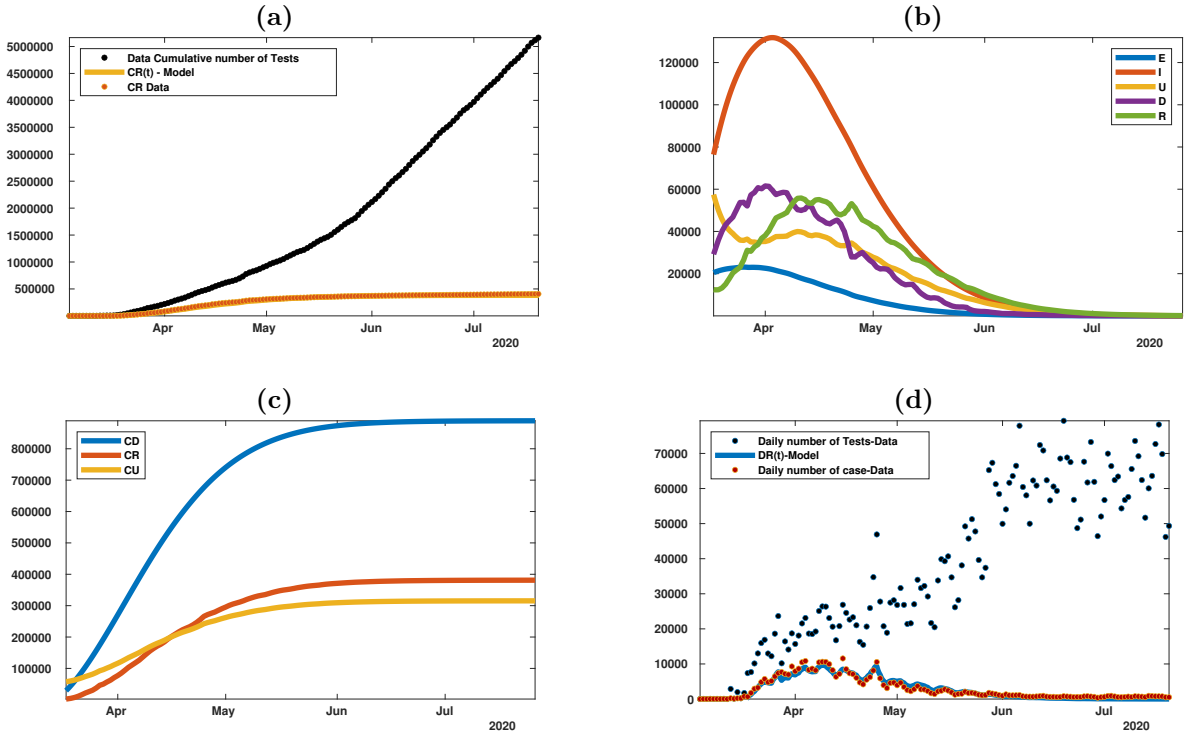

Figure 5.3.6: *Best fit of the model with confinement (or social distancing) measures.* ***Parameter values:*** *Same as in Figure 5.3.5, except the transmission coefficient which is not constant in time with* $\gamma = 0.2$, $T_m = 15$ *Mar (starting day of public measures),* $\mu = 0.0251$, $g = 10^{-5}$ *and* τ_0 *is fixed at the value* τ_1 *computed by using* (5.3.18). *In figure* ***(a)*** *we plot the cumulative number of tests (black dots), the cumulative number of positive cases (red dots) for the state of New York and the cumulative number of cases* $CD(t)$ *(yellow curve) obtained by fitting the model to the data. In figures* ***(b)–(c)*** *we plot the corresponding number of cases obtained from the model. With this set of parameters we observe that most of the cases are unreported. In figure* ***(d)*** *we plot the daily number of tests (black dots), the daily number of positive cases (red dots) for the state of New York and the daily number of cases* $DD(t)$ *obtained from the data.*

the orange dots and the blue curve match very well again. In order to get this fit we fix the parameter $g = 10^{-5}$.

Figure 5.3.7 (a) and (b), we aim at understanding the connection between the daily fluctuations of the number of reported cases (epidemic dynamic) and the daily number of tests (testing dynamics). The combination of the testing dynamics and the infection dynamics gives indeed a very complex curve parametrized by the time. It seems that the only reasonable comparison that we can make is between the cumulative number of reported cases and the cumulative number of tests. In Figure 5.3.7 (c) and (d), the comparison of the model and the data gives a very decent fit. In Figure 5.3.7, all the curves are time dependent parametrized curves. The abscissa is the number of tests (horizontal axis) and the ordinate is the number of reported cases (vertical axis). It corresponds (with our notations) to the parametric functions $t \to (n_{data}(t), DR(t))$ in figures (a) and (b) and their cumulative equivalent $t \to (N_{data}(t), CR(t))$ in figures (c) and (d). In figures (a) and (c) we use only the data, that is to say that we plot $t \to (n_{data}(t), DR_{data}(t))$ and $t \to (N_{data}(t), CR_{data}(t))$. In figures (b) and (d) we use only the model for the number of reported cases, that is to say that we plot $t \to (n_{data}(t), DR_{model}(t))$ and $t \to (N_{data}(t), CR_{model}(t))$.

In Figure 5.3.8, our goal is to investigate the effect of a change in the testing policy in the New York State. We are particularly interested in estimating the effect of an increase of the number of tests on the epidemic. Indeed increasing the number of tests may be thought as beneficial to reduce the number of cases. Here we challenge this idea by comparing an increase in the number of tests to the quantitative output of our model. In Figure 5.3.8, we replace the daily number of tests $n_{data}(t)$ (coming from the data for New York's state) in the model by either $2 \times n_{data}(t)$, $5 \times n_{data}(t)$, $10 \times n_{data}(t)$ or $100 \times n_{data}(t)$.

As expected, an increase of the number of tests is helping to reduce the number of cases at first. However, after increasing 10 times the number of tests, there is no significant difference (in the number of reported)

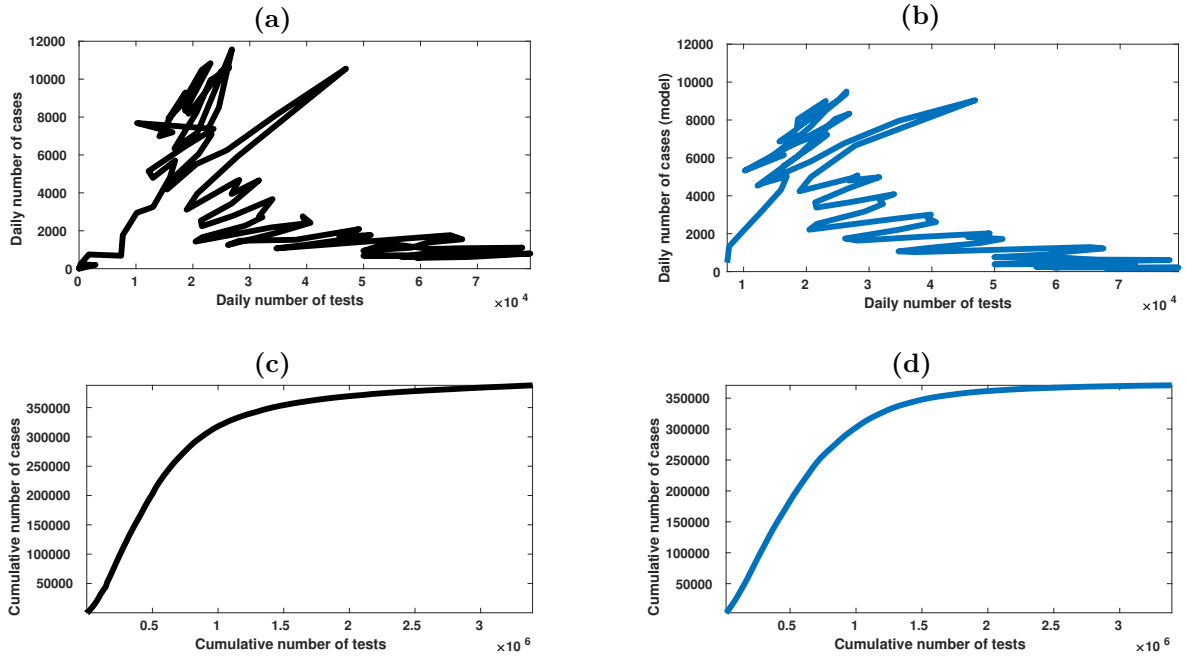

Figure 5.3.7: *In this figure we plot the curves of the number of reported cases as a function of the number of tests parametrized by the time. The top figures (a) and (b) correspond to the daily number of cases and the bottom figures (c) and (d) correspond to the cumulative number of cases. On the left-hand side we plot the data (a) and (c) while on the right-hand side we plot the model (b) and (d).* ***Parameter values:*** *Same as in Figure 5.3.6. In figure* ***(a)*** *we plot the daily number of cases coming from the data as a function of the daily number of tests. In figure* ***(b)*** *we plot the daily number of cases given by the model as a function of the daily number of tests coming from the data. In figure* ***(c)*** *we plot the cumulative number of cases coming from the data as a function of the cumulative number of tests. In figure* ***(d)*** *we plot the cumulative number of cases coming from the model as a function of the cumulative number of tests from the data.*

between 10 times and 100 times more tests. Therefore there must be an optimum between increasing the number of tests (which costs money and other limited resources) and being efficient to slow down the epidemic.

5.3.5 Discussion

In this section 5.3, we proposed a new epidemic model involving the daily number of tests as an input of the model. The model itself extends our previous models presented in [261, 260, 258, 259, P10, 262]. We proposed a new method to use the data in such a context based on the fact that the cumulative number of tests grows linearly at the early stage of the epidemic. Figure 5.3.3 shows that this is a reasonable assumption for the New York State data from mid-March to mid-April.

Our numerical simulations show a very good concordance between the number of reported cases produced by the model and the data in two very different situations. Indeed, Figures 5.3.5 and 5.3.6 correspond respectively to an epidemic without and with public intervention to limit the number of transmissions. This is an important observation since this shows that testing data and reported cases are not sufficient to evaluate the real amplitude of the epidemic. To solve this problem, the only solution seems to include a different kind of data to the models. This could be done by studying statistically representative samples in the population. Otherwise, biases can always be suspected. Such a question is of particular interest in order to evaluate the fraction of the population that has been infected by the virus and their possible immunity.

In Figure 5.3.7, we compared the testing dynamic (day to day variation in the number of tests) and the reported cases dynamic (day to day variation in the number of reported). Indeed, the dynamics of daily cases is extremely complex, but we also obtain a relatively robust curve for the cumulative numbers. Our model gives a good fit for this cumulative cases.

In Figure 5.3.8, we compared multiple testing strategies. By increasing 2, 5, 10 and 100 times the number of tests, we can project the efficiency of an increase in the daily number of tests. We observe that it is efficient

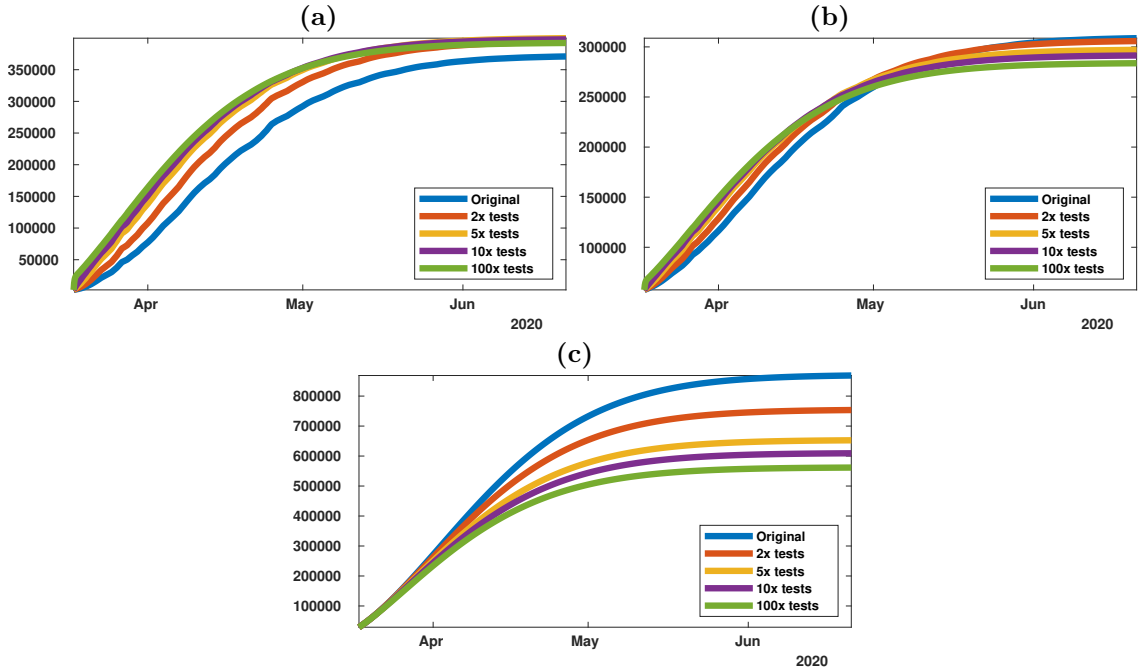

Figure 5.3.8: *Cumulative number of cases for different testing strategies: Original (blue curve), doubled (red curve), multiplied by 5 (yellow curve), multiplied by 10 (purple line) and multiplied by 100 (green curve). The transmission coefficient depends on the time, according to the formula* (5.3.19) *with* $\gamma = 0.2$, *and* τ_0 *is fitted by using* (5.3.18). ***Parameter values:*** *they are the same as in Figure 5.3.6. In figure* ***(a)*** *we plot the cumulated number of cases* $CR(t)$ *as a function of time. In figure* ***(b)*** *we plot the cumulative number of undetectable cases* $CU(t)$ *as a function of time. In figure* ***(c)*** *we plot the cumulative number of cases (including covert cases)* $CD(t)$ *as a function of time. Note that the total number of cases (including covert cases) is reduced by* 35% *when the number of tests is multiplied by* 100.

to increase this number up to 10 but the relative gain in absolute number of infected individuals rapidly drops after that. In particular, our projections do not show a big difference between a 10-times increase in the number of tests and a 100-times increase. Therefore there is a balance to find between the number of test and the efficiency in the evaluation of the number of cases, the optimal strategy being dependent on other factors like the monetary cost of the tests.

5.4 SI epidemic model applied to COVID-19 data in mainland China

5.4.1 Introduction

Estimating the average transmission rate is one of the most crucial challenges in the epidemiology of communicable diseases. This rate conditions the entry into the epidemic phase of the disease and its return to the extinction phase, if it has diminished sufficiently. It is the combination of three factors, one, the coefficient of virulence, linked to the infectious agent (in the case of infectious transmissible diseases), the other, the coefficient of susceptibility, linked to the host (all summarized into the probability of transmission), and also, the number of contact per unit of time between individuals (see Magal and Ruan [273]). The coefficient of virulence may change over time due to mutation over the course of the disease history. The second and third also, if mitigation measures have been taken. This was the case in China from the start of the pandemic (see Qiu, Chen and Shi [328])). Monitoring the decrease in the average transmission rate is an excellent way to monitor the effectiveness of these mitigation measures. Estimating the rate is therefore a central problem in the fight against epidemics.

The goal of this section 5.4 is to understand how to compare the SI model to the reported epidemic data and therefore the model can be used to predict the future evolution of epidemic spread and to test various possible scenarios of social mitigation measures. For $t \geq t_0$, the SI model is the following

$$\begin{cases} S'(t) = -\tau(t)S(t)I(t), \\ I'(t) = \tau(t)S(t)I(t) - \nu I(t), \end{cases} \tag{5.4.1}$$

where $S(t)$ is the number of susceptible and $I(t)$ the number of infectious at time t. This system is supplemented by initial data

$$S(t_0) = S_0 \geq 0,\ I(t_0) = I_0 \geq 0. \tag{5.4.2}$$

In this model, the rate of transmission $\tau(t)$ combines the number of contacts per unit of time and the probability of transmission. The transmission of the pathogen from the infectious to the susceptible individuals is described by a mass action law $\tau(t)\,S(t)\,I(t)$ (which is also the flux of new infectious).

The quantity $1/\nu$ is the average duration of the infectious period and $\nu I(t)$ is the flux of recovering or dying individuals. At the end of the infectious period, we assume that a fraction $f \in (0, 1]$ of the infectious individuals is reported. Let $\mathrm{CR}(t)$ be the cumulative number of reported cases. We assume that

$$\mathrm{CR}(t) = \mathrm{CR}_0 + \nu\, f\, \mathrm{CI}(t),\ \text{for } t \geq t_0, \tag{5.4.3}$$

where

$$\mathrm{CI}(t) = \int_{t_0}^{t} I(\sigma)\mathrm{d}\sigma. \tag{5.4.4}$$

Assumption 5.4.1. We assume that

- $S_0 > 0$ the number of susceptible individuals at time t_0 when we start to use the model;
- $\dfrac{1}{\nu} > 0$ the average duration of infectious period;
- $f > 0$ the fraction of reported individuals;

are known parameters.

Throughout this section 5.4, the parameter $S_0 = 1.4 \times 10^9$ will be the entire population of mainland China (since COVID-19 is a newly emerging disease). The actual number of susceptibles S_0 can be smaller since some individuals can be partially (or totally) immunized by previous infections or other factors. This is also true for Sars-CoV2, even if COVID-19 is a newly emerging disease. In fact, for COVID-19 the level of susceptibility may depend on blood group and genetic lineage. It is indeed suspected that the blood group O is associated with a lower susceptibility to SARS-CoV2 while a gene cluster inherited from Neanderthal has been identified as a risk factor for severe symptoms (see Zeberg et al. [411] and Guillon et al. [195]).

At the early beginning of the epidemic, the average duration of the infectious period $1/\nu$ is unknown, since the virus has never been investigated in the past. Therefore, at the early beginning of the COVID-19 epidemic, medical doctors and public health scientists used previously estimated average duration of the infectious period to make some public health recommendations. Here we show that the average infectious

period is impossible to estimate by using only the time series of reported cases, and must therefore be identified by other means. Actually, with the data of Sars-CoV2 in mainland China, we will fit the cumulative number of the reported case almost perfectly for any non-negative value $1/\nu < 3.3$ days. In the literature, several estimations were obtained: 11 days in [415], 9.5 days in [220], 8 days in [271], and 3.5 days in [252]. The recent survey by Byrne et al. [91] focuses on this subject.

Result

In Section 5.4.3, our analysis shows that

- It is hopeless to estimate the exact value of the duration of infectiousness by using SI models. Several values of the average duration of the infectious period give the exact same fit to the data.
- We can estimate an upper bound for the duration of infectiousness by using SI models. In the case of Sars-CoV2 in mainland China, this upper bound is 3.3 days.

In [341], it is reported that transmission of COVID-19 infection may occur from an infectious individual who is not yet symptomatic. In [423] it is reported that COVID-19 infected individuals generally develop symptoms, including mild respiratory symptoms and fever, on average $5-6$ days after the infection date (with a confience of 95%, range $1-14$ days). In [409] it is reported that the median time prior to symptom onset is 3 days, the shortest 1 day, and the longest 24 days. It is evident that these time periods play an important role in understanding COVID-19 transmission dynamics. Here the fraction of reported individuals f is unknown as well.

Result

In Section 5.4.3, our analysis shows that:

- It is hopeless to estimate the fraction of reported by using the SI models. Several values for the fraction of reported give the exact same fit to the data.
- We can estimate a lower bound for the fraction of unreported. We obtain $3.83 \times 10^{-5} < f \leq 1$. This lower bound is not significant. Therefore we can say anything about the fraction of unreported from this class of models.

As a consequence, the parameters $1/\nu$ and f have to be estimated by another method, for instance by a direct survey methodology that should be employed on an appropriated sample in the population in order to evaluate the two parameters.

The goal of this section 5.4 is to focus on the estimation of the two remaining parameters. Namely, knowing the above-mentioned parameters, we plan to identify

- I_0 the initial number of infectious at time t_0;
- $\tau(t)$ the rate of transmission at time t.

This problem has already been considered in several articles. In the early 70s, London and Yorke [264, 410] already discussed the time dependent rate of transmission in the context of measles, chickenpox and mumps. More recently, Wang and Ruan [390] the question of reconstructing the rate of transmission was considered for the 2002-2004 SARS outbreak in China. In Chowell et al. [111] a specific form was chosen for the rate of transmission and applied to the Ebola outbreak in Congo. Another approach was also proposed in Smirnova et al. [359].

In Section 5.4.2, we will explain how to apply the method introduce in Liu et al. [260] to fit the early cumulative data of Sars-CoV2 in China. This method provides a way to compute I_0 and $\tau_0 = \tau(t_0)$ at the early stage of the epidemic. In Section 5.4.3, we establish an identifiability result in the spirit of Hadeler [196].

In Section 5.4.4, we use the Bernoulli-Verhulst model as a phenomenological model to describe the data. As it was observed in several articles, the data from mainland China (and other countries as well) can be fitted very well by using this model. As a consequence, we will obtain an explicit formula for $\tau(t)$ and I_0 expressed as a function of the parameters of the Bernoulli-Verhulst model and the remaining parameters of

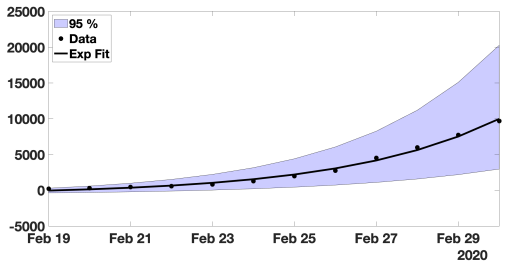

Figure 5.4.1: *In this figure, we plot the best fit of the exponential model to the cumulative number of reported cases of COVID-19 in mainland China between February 19 and March 1. We obtain* $\chi_1 = 3.7366$, $\chi_2 = 0.2650$ *and* $\chi_3 = 615.41$ *with* $t_0 = 19$ *Feb. The parameter* χ_3 *is obtained by minimizing the error between the best exponential fit and the data.*

the SI model. This approach gives a very good description of this set of data. The disadvantage of this approach is that it requires an evaluation of the final size CR_∞ from the early beginning (or at least it requires an estimation of this quantity).

Therefore, in order to be predictive, we will explore in the remaining subsections of the section 5.4 the possibility of constructing a day by day rate of transmission. Here we should refer to Bakhta et al. [29] where another novel forecasting method was proposed.

In Section 5.4.5, we will prove that the daily cumulative data can be approached perfectly by at most one sequence of day by day piecewise constant transmission rates. In Section 5.4.6, we propose a numerical methods to compute such a (piecewise constant) rate of transmission. Section 5.4.7 is devoted to the discussion, and we will present some figures showing the daily basic reproduction number for the COVID-19 outbreak in mainland China.

5.4.2 Estimating $\tau(t_0)$ and I_0 at the early stage of the epidemic

In this subsection 5.4.2, we apply the method presented in [261] to the SI model. At the early stage of the epidemic, we can assume that $S(t)$ is almost constant and equal to S_0. We can also assume that $\tau(t)$ remains constant equal to $\tau_0 = \tau(t_0)$. Therefore, by replacing these parameters into the I-equation of system (5.4.1) we obtain

$$I'(t) = (\tau_0 S_0 - \nu) I(t).$$

Therefore

$$I(t) = I_0 \exp\left(\chi_2 \left(t - t_0\right)\right),$$

where

$$\chi_2 = \tau_0 S_0 - \nu. \tag{5.4.5}$$

By using (5.4.3), we obtain

$$\mathrm{CR}(t) = \mathrm{CR}_0 + \nu\, f\, I_0\, \frac{e^{\chi_2 (t-t_0)} - 1}{\chi_2}. \tag{5.4.6}$$

We obtain a first phenomenological model for the cumulative number of reported cases (valid only at the early stage of the epidemic)

$$\mathrm{CR}(t) = \chi_1 e^{\chi_2\, t} - \chi_3. \tag{5.4.7}$$

In Figure 5.4.1, we compare the model to the COVID-19 data for mainland China. The data used in the section 5.4 are taken from [431, 429, 424] and reported in Section 5.4.8. In order to estimate the parameter χ_3, we minimize the distance between $\mathrm{CR}_{\mathrm{Data}}(t) + \chi_3$ and the best exponential fit $t \to \chi_1 e^{\chi_2\, t}$ (i.e. we use the MATLAB function fit(t, data, 'exp1')).

The estimated initial number of infected and transmission rate

By using (5.4.3) and (5.4.7) we obtain

$$I_0 = \frac{\mathrm{CR}'(t_0)}{\nu\, f} = \frac{\chi_1\, \chi_2 e^{\chi_2\, t_0}}{\nu\, f}, \tag{5.4.8}$$

and by using (5.4.5)

$$\tau_0 = \frac{\chi_2 + \nu}{S_0}. \tag{5.4.9}$$

Remark 5.4.2. Fixing $f = 0.5$ and $\nu = 0.2$, we obtain

$$I_0 = 3.7366 \times 0.2650 \times \exp(0.2650 \times 19)/(0.2 \times 0.5) = 1521,$$

and

$$\tau_0 = \frac{0.2650 + 0.2}{1.4 \times 10^9} = 3.3214 \times 10^{-10}.$$

The influence of the errors made in the estimations (at the early stage of the epidemic) has been considered in the recent article by Roda et al. [335]. To understand this problem, let us first consider the case of the rate of transmission $\tau(t) = \tau_0$ in the model (5.4.1). In that case (5.4.1) becomes

$$\begin{cases} S'(t) = -\tau_0 S(t) I(t), \\ I'(t) = \tau_0 S(t) I(t) - \nu I(t). \end{cases} \tag{5.4.10}$$

By using the S-equation of model (5.4.10) we obtain

$$S(t) = S_0 \exp\left(-\tau_0 \int_{t_0}^{t} I(\sigma)\mathrm{d}\sigma\right) = S_0 \exp\left(-\tau_0 \mathrm{CI}(t)\right)$$

where $\mathrm{CI}(t)$ is the cumulated number of infectious individuals. Substituting $S(t)$ by this formula in the I-equation of (5.4.10) we obtain

$$I'(t) = S_0 \exp\left(-\tau_0 \mathrm{CI}(t)\right) \tau_0 \mathrm{CI}'(t) - \nu I(t).$$

Therefore, by integrating the above equation between t and t_0 we obtain

$$\mathrm{CI}'(t) = I_0 + S_0 \left[1 - \exp\left(-\tau_0 \mathrm{CI}(t)\right)\right] - \nu \mathrm{CI}(t). \tag{5.4.11}$$

Remarkably, the equation (5.4.11) is monotone. We refer to Hal Smith [361] for a comprehensive presentation on monotone systems. By applying a comparison principle to (5.4.11), we are in a position to confirm the intuition about epidemics SI models. Notice that the monotone properties are only true for the cumulative number of infectious (this is false for the number of infectious).

Theorem 5.4.3. *Let $t > t_0$ be fixed. The cumulative number of infectious $\mathrm{CI}(t)$ is strictly increasing with respect to the following quantities*

(i) $I_0 > 0$ the initial number of infectious individuals;

(ii) $S_0 > 0$ the initial number of susceptible individuals;

(iii) $\tau > 0$ the transmission rate;

(iv) $1/\nu > 0$ the average duration of the infectiousness period.

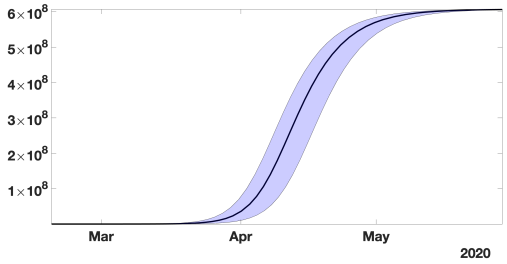

Figure 5.4.2: *In this figure, the black curve corresponds to the cumulative number of reported cases* $\mathrm{CR}(t)$ *obtained from the model* (5.4.10) *with* $\mathrm{CR}'(t) = \nu f I(t)$ *by using the values* $I_0 = 1521$ *and* $\tau_0 = 3.32 \times 10^{-10}$ *obtained from our method and the early data from February 19 to March 1. The blue region corresponds the* 95% *confidence interval when the rate of transmission* $\tau(t)$ *is constant and equal to the estimated value* $\tau_0 = 3.32 \times 10^{-10}$.

Error in the estimated initial number of infected and transmission rate

Assume that the parameters χ_1 and χ_2 are estimated with a 95% confidence interval

$$\chi^-_{1,95\%} \leq \chi_1 \leq \chi^+_{1,95\%},$$

and

$$\chi^-_{2,95\%} \leq \chi_2 \leq \chi^+_{2,95\%}.$$

We obtain

$$I^-_{0,95\%} := \frac{\chi^-_{1,95\%}\,\chi^-_{2,95\%} e^{\chi^-_{2,95\%}\,t_0}}{\nu\, f} \leq I_0 \leq I^+_{0,95\%} := \frac{\chi^+_{1,95\%}\,\chi^+_{2,95\%} e^{\chi^+_{2,95\%}\,t_0}}{\nu\, f}, \tag{5.4.12}$$

and

$$\tau^-_{0,95\%} := \frac{\chi^-_{2,95\%} + \nu}{S_0} \leq \tau_0 \leq \tau^+_{0,95\%} := \frac{\chi^+_{2,95\%} + \nu}{S_0}. \tag{5.4.13}$$

Remark 5.4.4. By using the data for mainland China we obtain

$$\chi^-_{1,95\%} = 1.57,\ \chi^+_{1,95\%} = 5.89,\ \chi^-_{2,95\%} = 0.24,\ \chi^+_{2,95\%} = 0.28. \tag{5.4.14}$$

In Figure 5.4.2, we plot the upper and lower solutions $\mathrm{CR}^+(t)$ (obtained by using $I_0 = I^+_{0,95\%}$ and $\tau_0 = \tau^+_{0,95\%}$) and $\mathrm{CR}^-(t)$ (obtained by using $I_0 = I^-_{0,95\%}$ and $\tau_0 = \tau^-_{0,95\%}$) corresponding to the blue region and the black curve corresponds to the best estimated value $I_0 = 1521$ and $\tau_0 = 3.3214 \times 10^{-10}$.

Recall that the final size of the epidemic corresponds to the positive equilibrium of (5.4.11)

$$0 = I_0 + S_0\left[1 - \exp\left(-\tau_0 \mathrm{CI}_\infty\right)\right] - \nu \mathrm{CI}_\infty. \tag{5.4.15}$$

In Figure 5.4.2 the changes in the parameters I_0 and τ_0 (in (5.4.12)-(5.4.13)) do not affect significantly the final size.

5.4.3 Theoretical formula for $\tau(t)$

By using the S-equation of model (5.4.1) we obtain

$$S(t) = S_0 \exp\left(-\int_{t_0}^{t} \tau(\sigma)\, I(\sigma) \mathrm{d}\sigma\right),$$

next by using the I-equation of model (5.4.1) we obtain

$$I'(t) = S_0 \exp\left(-\int_{t_0}^{t} \tau(\sigma)\, I(\sigma) \mathrm{d}\sigma\right) \tau(t)\, I(t) - \nu I(t),$$

and by taking the integral between t and t_0 we obtain a Volterra integral equation for the cumulative number of infectious

$$\mathrm{CI}'(t) = I_0 + S_0\left[1 - \exp\left(-\int_{t_0}^{t} \tau(\sigma)\, I(\sigma)\mathrm{d}\sigma\right)\right] - \nu \mathrm{CI}(t), \tag{5.4.16}$$

which is equivalent to (by using (5.4.3))

$$\mathrm{CR}'(t) = \nu\, f\left(I_0 + S_0\left[1 - \exp\left(-\frac{1}{\nu\, f}\int_{t_0}^{t} \tau(\sigma)\, \mathrm{CR}'(\sigma)\mathrm{d}\sigma\right)\right]\right) + \nu\, \mathrm{CR}_0 - \nu \mathrm{CR}(t). \tag{5.4.17}$$

The following result permits to obtain a perfect match between the SI model and the time-dependent rate of transmission $\tau(t)$.

Theorem 5.4.5. *Let S_0, ν, f, $I_0 > 0$ and $\mathrm{CR}_0 \geq 0$ be given. Let $t \to I(t)$ be the second component of system (5.4.1). Let $\widehat{\mathrm{CR}} : [t_0, \infty) \to \mathbb{R}$ be a two times continuously differentiable function satisfying*

$$\widehat{\mathrm{CR}}(t_0) = \mathrm{CR}_0, \tag{5.4.18}$$

$$\widehat{\mathrm{CR}}'(t_0) = \nu\, f\, I_0, \tag{5.4.19}$$

$$\widehat{\mathrm{CR}}'(t) > 0, \forall t \geq t_0, \tag{5.4.20}$$

and

$$\nu f\,(I_0 + S_0) - \widehat{\mathrm{CR}}'(t) - \nu\left(\widehat{\mathrm{CR}}(t) - \mathrm{CR}_0\right) > 0, \forall t \geq t_0. \tag{5.4.21}$$

Then

$$\widehat{\mathrm{CR}}(t) = \mathrm{CR}_0 + \nu f \int_{t_0}^{t} I\,(s)\, ds, \forall t \geq t_0, \tag{5.4.22}$$

if and only if

$$\tau(t) = \frac{\nu f\left(\dfrac{\widehat{\mathrm{CR}}''(t)}{\widehat{\mathrm{CR}}'(t)} + \nu\right)}{\nu f\,(I_0 + S_0) - \widehat{\mathrm{CR}}'(t) - \nu\left(\widehat{\mathrm{CR}}(t) - \mathrm{CR}_0\right)}. \tag{5.4.23}$$

Proof. Assume first (5.4.22) is satisfied. Then by using equation (5.4.16) we deduce that

$$S_0 \exp\left(-\int_{t_0}^{t} \tau(\sigma) I(\sigma) d\sigma\right) = I_0 + S_0 - I(t) - \nu \mathrm{CI}(t).$$

Therefore

$$\int_{t_0}^{t} \tau(\sigma) I(\sigma) d\sigma = \ln\left[\frac{S_0}{I_0 + S_0 - I(t) - \nu \mathrm{CI}(t)}\right] = \ln(S_0) - \ln\left[I_0 + S_0 - I(t) - \nu \mathrm{CI}(t)\right]$$

therefore by taking the derivative on both side

$$\tau(t) I(t) = \frac{I'(t) + \nu I(t)}{I_0 + S_0 - I(t) - \nu \mathrm{CI}(t)} \Leftrightarrow \tau(t) = \frac{\dfrac{I'(t)}{I(t)} + \nu}{I_0 + S_0 - I(t) - \nu \mathrm{CI}(t)} \tag{5.4.24}$$

and by using the fact that $\mathrm{CR}(t) - \mathrm{CR}_0 = \nu f \mathrm{CI}(t)$ we obtain (5.4.23).

Conversely, assume that $\tau(t)$ is given by (5.4.23). Then if we define $\widetilde{I}(t) = \widehat{\mathrm{CR}}'(t)/\nu f$ and $\widetilde{\mathrm{CI}}(t) = \left(\widehat{\mathrm{CR}}(t) - \mathrm{CR}_0\right)/\nu f$, by using (5.4.18) we deduce that

$$\widetilde{\mathrm{CI}}(t) = \int_{t_0}^{t} \widetilde{I}(\sigma) d\sigma,$$

and by using (5.4.19)

$$\widetilde{I}(t_0) = I_0. \tag{5.4.25}$$

Moreover from (5.4.23) we deduce that $\widetilde{I}(t)$ satisfies (5.4.24). By using (5.4.25) we deduce that $t \to \widetilde{\mathrm{CI}}(t)$ is a solution of (5.4.16). By uniqueness of the solution of (5.4.16), we deduce that $\widetilde{\mathrm{CI}}(t) = \mathrm{CI}(t), \forall t \geq t_0$ or equivalently $\mathrm{CR}(t) = \mathrm{CR}_0 + \nu f \int_{t_0}^{t} I\,(s)\, ds, \forall t \geq t_0$. The proof is completed. □

The formula (5.4.23) was already obtained by Hadeler [196, see Corollary 2].

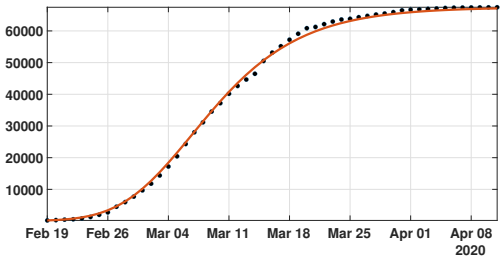

Figure 5.4.3: *In this figure, we plot the best fit of the Bernoulli-Verhulst model to the cumulative number of reported cases of COVID-19 in China. We obtain* $\chi_2 = 0.66$ *and* $\theta = 0.22$. *The black dots correspond to data for the cumulative number of reported cases and the blue curve corresponds to the model.*

5.4.4 Explicit formula for $\tau(t)$ and I_0

Many phenomenological models have been compared to the data during the first phase of the COVID-19 outbreak. We refer to the paper of Tsoularis and Wallace [378] for a nice survey on the generalized logistic equations. Let us consider here for example, the Bernoulli-Verhulst equation

$$\mathrm{CR}'(t) = \chi_2\,\mathrm{CR}(t)\left(1-\left(\frac{\mathrm{CR}(t)}{\mathrm{CR}_\infty}\right)^\theta\right), \forall t \geq t_0, \tag{5.4.26}$$

supplemented with the initial data

$$\mathrm{CR}(t_0) = \mathrm{CR}_0 \geq 0.$$

Let us recall the explicit formula for the solution of (5.4.26)

$$\mathrm{CR}(t) = \frac{e^{\chi_2(t-t_0)}\mathrm{CR}_0}{\left[1+\frac{\chi_2\theta}{\mathrm{CR}_\infty^\theta}\int_{t_0}^t \left(e^{\chi_2(\sigma-t_0)}\mathrm{CR}_0\right)^\theta d\sigma\right]^{1/\theta}} = \frac{e^{\chi_2(t-t_0)}\mathrm{CR}_0}{\left[1+\frac{\mathrm{CR}_0^\theta}{\mathrm{CR}_\infty^\theta}\left(e^{\chi_2\theta(t-t_0)}-1\right)\right]^{1/\theta}}. \tag{5.4.27}$$

Assumption 5.4.6. We assume that the cumulative numbers of reported cases $\mathrm{CR}_{\mathrm{Data}}(t_i)$ are known for a sequence of times $t_0 < t_1 < \cdots < t_{n+1}$.

Estimated initial number of infected

By combining (5.4.3) and the Bernoulli-Verhulst equation (5.4.26) for $t \to \mathrm{CR}(t)$, we deduce the initial number of infected

$$I_0 = \frac{\mathrm{CR}'(t_0)}{\nu\, f} = \frac{\chi_2\,\mathrm{CR}_0\left(1-\left(\frac{\mathrm{CR}_0}{\mathrm{CR}_\infty}\right)^\theta\right)}{\nu\, f}. \tag{5.4.28}$$

Remark 5.4.7. We fix $f = 0.5$, from the COVID-19 data in mainland China and formula (5.4.28) (with $\mathrm{CR}_0 = 198$), we obtain

$$I_0 = 1909 \text{ for } \nu = 0.1,$$

and

$$I_0 = 954 \text{ for } \nu = 0.2.$$

By using (5.4.26) we deduce that

$$\begin{aligned}\mathrm{CR}''(t) &= \chi_2\,\mathrm{CR}'(t)\left(1-\left(\frac{\mathrm{CR}(t)}{\mathrm{CR}_\infty}\right)^\theta\right) - \frac{\chi_2\theta}{\mathrm{CR}_\infty^\theta}\,\mathrm{CR}(t)\,(\mathrm{CR}(t))^{\theta-1}\,\mathrm{CR}'(t)\\ &= \chi_2\,\mathrm{CR}'(t)\left(1-\left(\frac{\mathrm{CR}(t)}{\mathrm{CR}_\infty}\right)^\theta\right) - \frac{\chi_2\theta}{\mathrm{CR}_\infty^\theta}\,(\mathrm{CR}(t))^{\theta}\,\mathrm{CR}'(t),\end{aligned}$$

therefore

$$\mathrm{CR}''(t) = \chi_2\,\mathrm{CR}'(t)\left(1-(1+\theta)\left(\frac{\mathrm{CR}(t)}{\mathrm{CR}_\infty}\right)^\theta\right). \tag{5.4.29}$$

Estimated rate of transmission

By using the Bernoulli-Verhulst equation (5.4.26) and substituting (5.4.29) in (5.4.23), we obtain

$$\tau(t) = \frac{\nu\, f\left(\chi_2\left(1-(1+\theta)\left(\frac{\mathrm{CR}(t)}{\mathrm{CR}_\infty}\right)^\theta\right)+\nu\right)}{\nu\, f\,(I_0+S_0)+\nu\mathrm{CR}_0-\mathrm{CR}(t)\left(\chi_2\left(1-\left(\frac{\mathrm{CR}(t)}{\mathrm{CR}_\infty}\right)^\theta\right)+\nu\right)}. \tag{5.4.30}$$

This formula (5.4.30) combined with (5.4.27) gives an explicit formula for the rate of transmission.

Since $\mathrm{CR}(t) < \mathrm{CR}_\infty$, by considering the sign of the numerator and the denominator of (5.4.30), we obtain the following proposition.

Proposition 5.4.8. *The rate of transmission $\tau(t)$ given by* (5.4.30) *is non negative for all $t \geq t_0$ if*

$$\nu \geq \chi_2\,\theta, \tag{5.4.31}$$

and

$$f\,(I_0+S_0)+\nu\mathrm{CR}_0 > \mathrm{CR}_\infty\,(\chi_2+\nu)\,. \tag{5.4.32}$$

Compatibility of the model SI with the COVID-19 data for mainland China

The model SI is compatible with the data only when $\tau(t)$ stays positive for all $t \geq t_0$. From our estimation of the Chinese's COVID-19 data we obtain $\chi_2\,\theta = 0.14$. Therefore from (5.4.31) we deduce that model is compatible with the data only when

$$1/\nu \leq 1/0.14 = 3.3 \text{ days}. \tag{5.4.33}$$

This means that the average duration of infectious period $1/\nu$ must be shorter than 3.3 days.

Similarly the condition (5.4.32) implies

$$f \geq \frac{\mathrm{CR}_\infty\chi_2+(\mathrm{CR}_\infty-\mathrm{CR}_0)\,\nu}{S_0+I_0} \geq \frac{\mathrm{CR}_\infty\chi_2+(\mathrm{CR}_\infty-\mathrm{CR}_0)\,\chi_2\,\theta}{S_0+I_0}$$

and since we have $CR_0 = 198$ and $\mathrm{CR}_\infty = 67102$, we obtain

$$f \geq \frac{67102\times 0.66+(67102-198)\times 0.14}{1.4\times 10^9} \geq 3.83\times 10^{-5}. \tag{5.4.34}$$

So according to this estimation the fraction of unreported $0 < f \leq 1$ can be almost as small as we want.

Figure 5.4.4 illustrates the Proposition 5.4.8. We observe that the formula for the rate of transmission (5.4.30) becomes negative whenever $\nu < \chi_2\theta$. In Figure 5.4.5 we plot the numerical simulation obtained from (5.4.1)-(5.4.3) when $t \to \tau(t)$ is replaced by the explicit formula (5.4.30). It is surprising that we can reproduce perfectly to the original Bernoulli-Verhulst even when $\tau(t)$ becomes negative. This was not guaranteed at first, since the I-class of individuals is losing some individuals which are recovering.

5.4.5 Computing numerically a day by day piecewise constant rate of transmission

Assumption 5.4.9. We assume that the rate of transmission $\tau(t)$ is piecewise constant and for each $i = 0,\ldots,n$,

$$\tau(t) = \tau_i, \text{ whenever } t_i \leq t < t_{i+1}. \tag{5.4.35}$$

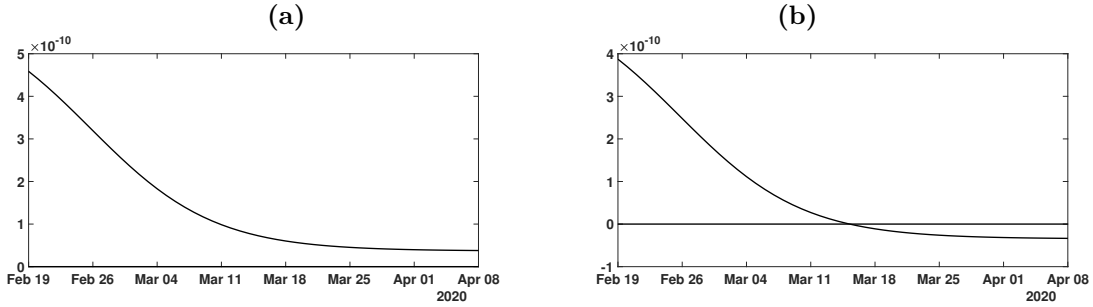

Figure 5.4.4: *In this figure, we plot the rate of transmission obtained from formula* (5.4.30) *with* $f = 0.5$, $\chi_2\,\theta = 0.14 < \nu = 0.2$ *(in Figure (a)) and* $\nu = 0.1 < \chi_2\,\theta = 0.14$ *(in Figure (b)),* $\chi_2 = 0.66$ *and* $\theta = 0.22$ *and* $\mathrm{CR}_\infty = 67102$ *which is the latest value obtained from the cumulative number of reported cases for China.*

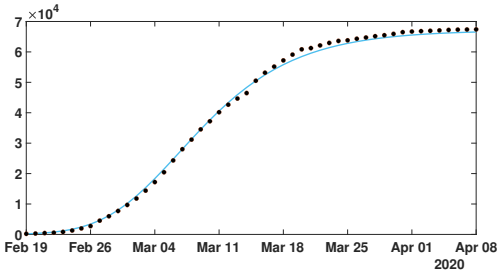

Figure 5.4.5: *In this figure, we plot the number of reported cases by using model* (5.4.1) *and* (5.4.3)*, and the rate of transmission is obtained in* (5.4.30)*. The parameters values are* $f = 0.5$, $\nu = 0.1$ *or* $\nu = 0.2$, $\chi_2 = 0.66$ *and* $\theta = 0.22$ *and* $\mathrm{CR}_\infty = 67102$ *is the latest value obtained from the cumulative number of reported cases for China. Furthermore, we use* $S_0 = 1.4 \times 10^9$ *for the total population of China and* $I_0 = 954$ *which is obtained from formula* (5.4.28)*. The black dots correspond to data for the cumulative number of reported cases observed and the blue curve corresponds to the model.*

For $t \in [t_{i-1}, t_i]$, we deduce by using Assumption 5.4.9 that

$$\int_{t_0}^{t} \tau(\sigma)\,\mathrm{CR}'(\sigma)\mathrm{d}\sigma = \sum_{j=0}^{i-2} \int_{t_j}^{t_{j+1}} \tau_j\,\mathrm{CR}'(\sigma)\mathrm{d}\sigma + \int_{t_{i-1}}^{t} \tau_{i-1}\,\mathrm{CR}'(\sigma)\mathrm{d}\sigma.$$

Therefore by using (5.4.17), for $t \in [t_{i-1}, t_i]$, we obtain

$$\mathrm{CR}'(t) = \nu\, f\left(I_0 + S_0\left[1 - \Pi_{i-1}\exp\left(-\frac{\tau_{i-1}}{\nu\, f}\left[\mathrm{CR}(t) - \mathrm{CR}(t_{i-1})\right]\right)\right]\right) + \nu\,\mathrm{CR}_0 - \nu\mathrm{CR}(t), \tag{5.4.36}$$

where

$$\Pi_{i-1} = \exp\left(-\sum_{j=0}^{i-2}\frac{\tau_j}{\nu\, f}\left[\mathrm{CR}(t_{j+1}) - \mathrm{CR}(t_j)\right]\right). \tag{5.4.37}$$

By fixing $\tau_{i-1} = 0$ on the right hand side of (5.4.36) we get

$$\mathrm{CR}'(t) \geq \nu\, f\,(I_0 + S_0\,[1 - \Pi_{i-1}]) + \nu\,\mathrm{CR}_0 - \nu\mathrm{CR}(t),$$

and when $\tau_{i-1} \to \infty$ we obtain

$$\mathrm{CR}'(t) \leq \nu\, f\,(I_0 + S_0) + \nu\,\mathrm{CR}_0 - \nu\mathrm{CR}(t).$$

By using the theory of monotone ordinary differential equations (see Smith [361]) we deduce that the map $\tau_i \to \mathrm{CR}(t_i)$ is monotone increasing, and we get the following result.

Theorem 5.4.10. *Let assumptions 5.4.1, 5.4.6 and 5.4.9 be satisfied. Let I_0 be fixed. Then we can find a unique sequence $\tau_0, \tau_1, \dots, \tau_n$ of non negative numbers such that $t \to \mathrm{CR}(t)$ the solution of (5.4.17) fits exactly the data at any time t_i, that is to say that*

$$\mathrm{CR}(t_i) = \mathrm{CR}_{\mathrm{Data}}(t_i), \forall i = 1, \dots, n+1,$$

if and only if the two following two conditions are satisfied for each $i = 0, 1, \dots, n+1$,

$$\mathrm{CR}_{\mathrm{Data}}(t_i) \geq e^{-\nu(t_i - t_{i_1})}\mathrm{CR}_{\mathrm{Data}}(t_{i-1}) + \int_{t_{i-1}}^{t_i} \nu e^{-\nu(t_i-\sigma)}\mathrm{d}\sigma \left(f\left(I_0 + S_0\left[1 - \Pi_{i-1}^{\mathrm{Data}}\right]\right) + \mathrm{CR}_0\right), \tag{5.4.38}$$

where

$$\Pi_{i-1}^{\mathrm{Data}} = \exp\left(-\sum_{j=0}^{i-2} \frac{\tau_j}{\nu f}\left[\mathrm{CR}_{\mathrm{Data}}(t_{j+1}) - \mathrm{CR}_{\mathrm{Data}}(t_j)\right]\right), \tag{5.4.39}$$

and

$$\mathrm{CR}_{\mathrm{Data}}(t_i) \leq e^{-\nu(t_i - t_{i_1})}\mathrm{CR}_{\mathrm{Data}}(t_{i-1}) + \int_{t_{i-1}}^{t_i} \nu e^{-\nu(t_i-\sigma)}\mathrm{d}\sigma \left(f\left(I_0 + S_0\right) + \mathrm{CR}_0\right). \tag{5.4.40}$$

Remark 5.4.11. The above theorem means that the data are identifiable for this model SI if and only if the conditions (5.4.38) and (5.4.40) are satisfied. Moreover, in that case, we can find a unique sequence of transmission rates $\tau_i \geq 0$ which gives a perfect fit to the data.

5.4.6 Numerical simulations

In this section 5.4.6, we propose a numerical method to fit the day by day rate of transmission. The goal is to take advantage of the monotone property of $\mathrm{CR}(t)$ with respect to τ_i on the time interval $[t_i, t_{i+1}]$. Recently more sophisticated methods were proposed by Bakha et al. [29] by using several types of approximation methods for the rate of transmission.

We start with the simplest Algorithm 1 in order to show the difficulties to identify the rate of transmission.

Algorithm 1

Step 1: *We* fix $S_0 = 1.4 \times 10^9$, $\nu = 0.1$ or $\nu = 0.2$ and $f = 0.5$. We consider the system

$$\begin{cases} S'(t) = -\tau S(t)I(t), \\ I'(t) = \tau S(t)I(t) - \nu I(t), \\ \mathrm{CR}'(t) = \nu f I(t), \end{cases} \tag{5.4.41}$$

on the interval of time $t \in [t_0, t_1]$. This system is supplemented by initial values $S(t_0) = S_0$ and $I(t_0) = I_0$ is given by formula (5.4.8) (if we consider the data only at the early stage) or formula (5.4.28) (if we consider all the data) and $\mathrm{CR}(t_0) = \mathrm{CR}_{\mathrm{Data}}(t_0)$ is obtained from the data.

The map $\tau \to \mathrm{CR}(t_1)$ being monotone increasing, we can apply a bisection method to find the unique value τ_0 solving

$$\mathrm{CR}(t_1) = \mathrm{CR}_{\mathrm{Data}}(t_1).$$

Then we proceed by induction.

Step i: *F*or each integer $i = 1, \dots, n$ we consider the system

$$\begin{cases} S'(t) = -\tau S(t)I(t), \\ I'(t) = \tau S(t)I(t) - \nu I(t), \\ \mathrm{CR}'(t) = \nu f I(t), \end{cases} \tag{5.4.42}$$

on the interval of time $t \in [t_i, t_{i+1}]$. This system is supplemented by initial values $S(t_i)$ and $I(t_i)$ obtained from the previous iteration and with $\mathrm{CR}(t_i) = \mathrm{CR}_{\mathrm{Data}}(t_i)$ obtained from the data.

The map $\tau \to \mathrm{CR}(t_i)$ being monotone increasing, we can apply a bisection method to find the unique value τ_i solving

$$\mathrm{CR}(t_i) = \mathrm{CR}_{\mathrm{Data}}(t_i).$$

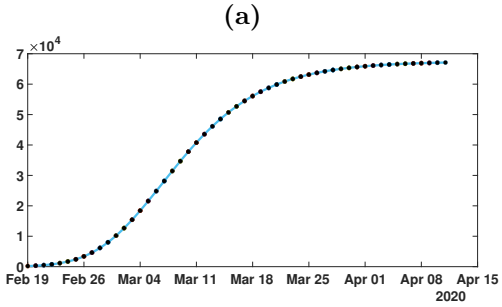

Figure 5.4.6: *In this figure, we plot the perfect fit of the cumulative number of reported cases of COVID-19 in China. We fix the parameters* $f = 0.5$ *and* $\nu = 0.2$ *or* $\nu = 0.1$ *and we apply our algorithm 1 to obtain the perfect fit. The black dots correspond to data for the cumulative number of reported cases and the blue curve corresponds to the model.*

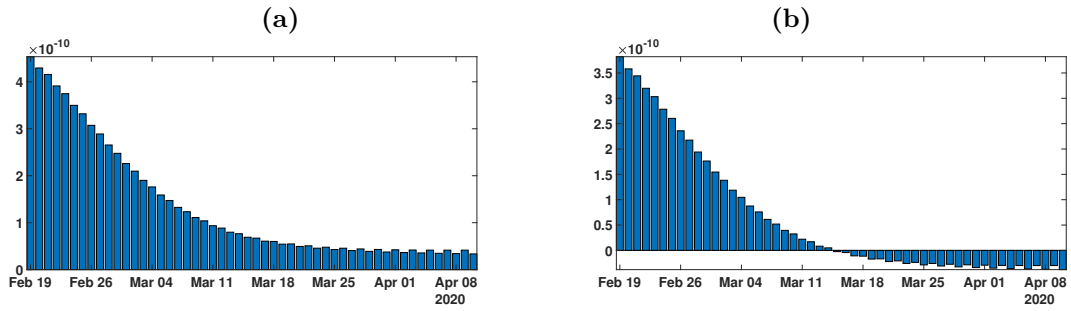

Figure 5.4.7: *In this figure, we plot the rate of transmission obtained for the reported cases of COVID-19 in China with the parameters* $f = 0.5$ *and* $\nu = 0.2$ *in figure (a) and* $\nu = 0.1$ *in figure (b). This rate of transmission corresponds to the perfect fit obtained in Figure 5.4.6.*

In Figure 5.4.6, we plot an example of such a perfect fit, which is the same for $\nu = 0.1$ and $\nu = 0.2$. In Figure 5.4.7 we plot the rate of transmission obtained numerically for $\nu = 0.2$ in (a) and $\nu = 0.1$ in (b). This is an example of a negative rate of transmission. Figure 5.4.7 should be compared to Figure 5.4.4 which gives similar result. In Figures 5.4.8-5.4.10 we use Algorithm 1 and we plot the rate of transmission obtained by using the reported cases of COVID-19 in China where the parameters are fixed as $f = 0.5$ and $\nu = 0.2$. In Figures 5.4.8-5.4.10, we observe an oscillating rate of transmission which is alternatively positive and negative back and forth. These oscillations are due to the amplification of the error in the numerical method itself. In Figure 5.4.8, we run the same simulation than in Figure 5.4.9 but during a shorter period. In Figure 5.4.8, we can see that the slope of $\mathrm{CR}(t)$ at the $t = t_i$ between two days (the black dots) is amplified one day to the next.

In Figure 5.4.10, we first smooth the original cumulative data by using the MATLAB function $\mathrm{CR}_{\mathrm{Data}} = \mathrm{smoothdata}(\mathrm{CR}_{\mathrm{Data}}, 'gaussian', 50)$ to regularize the data and we apply Algorithm 1. Unfortunately, smoothing the data does not help to solve the instability problem in Figure 5.4.10.

We need to introduce a correction when choosing the next initial value $I(t_i)$. In Algorithm 1 the errors are due to the following relationship which is not respected

$$\mathrm{CR}'(t) = \nu f I(t)$$

at the points $t = t_i$ which should be reflected by the algorithm.

In Figure 5.4.11, we smooth the data first by using the MATLAB function $\mathrm{CR}_{\mathrm{Data}} = \mathrm{smoothdata}(\mathrm{CR}_{\mathrm{Data}}, 'gaussian', 50)$, and we apply Algorithm 2 by approximating equation (5.4.46) by

$$I_i = [\mathrm{CR}_{\mathrm{Data}}(t_i) - \mathrm{CR}_{\mathrm{Data}}(t_{i-1})]/(\nu \times f). \tag{5.4.43}$$

In Figure 5.4.11 we no longer observe the oscillations of the rate of transmission.

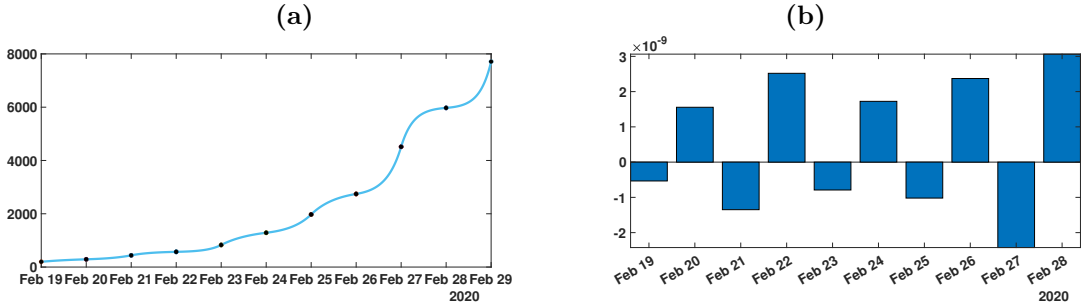

Figure 5.4.8: *In figure (a), we plot the cumulative number of reported cases obtained from the data (black dots) and the model (blue curve). In figure (b), we plot the daily rate of transmission obtained by using Algorithm 1. We see that we can fit the data perfectly. But the method is very unstable. We obtain a rate of transmission that oscillates from positive to negative values back and forth.*

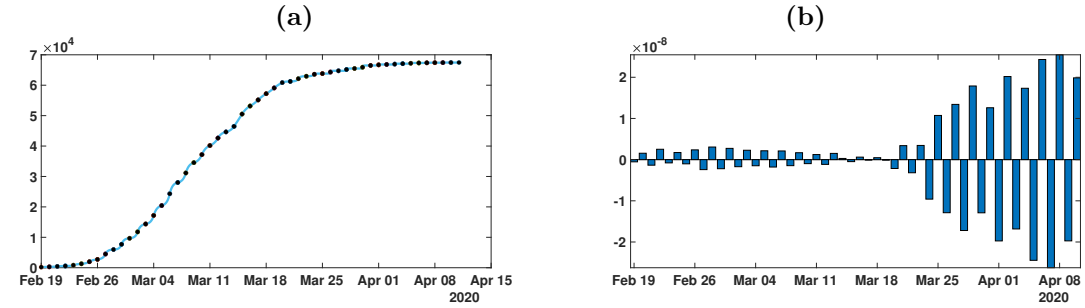

Figure 5.4.9: *In figure (a), we plot the cumulative number of reported cases obtained from the data (black dots) and the model (blue curve). In figure (b), we plot the daily rate of transmission obtained by using Algorithm 1. We see that we can fit the data perfectly. But the method is very unstable. We obtain a rate of transmission that oscillates from positive to negative values back and forth.*

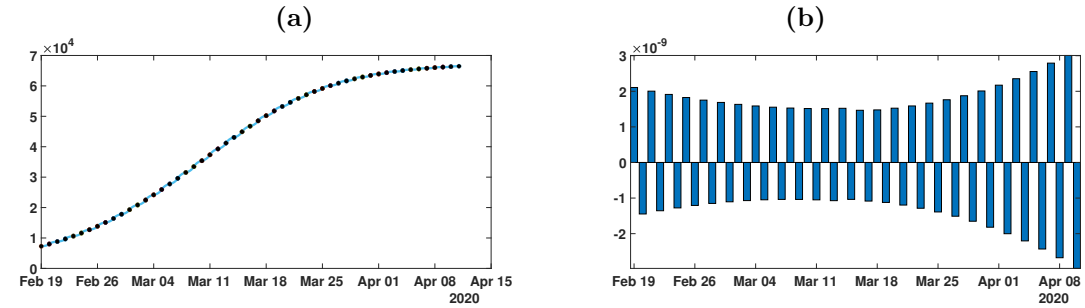

Figure 5.4.10: *We apply Algorithm 1 to the regularized data. In figure (a), we plot the regularized cumulative number of reported cases obtained from the data (black dots) and the model (blue curve). In figure (b), we plot the daily rate of transmission obtained by using Algorithm 1. We see that we can fit the data perfectly. But the method is very unstable. We obtain a rate of transmission that oscillates from positive to negative values back and forth.*

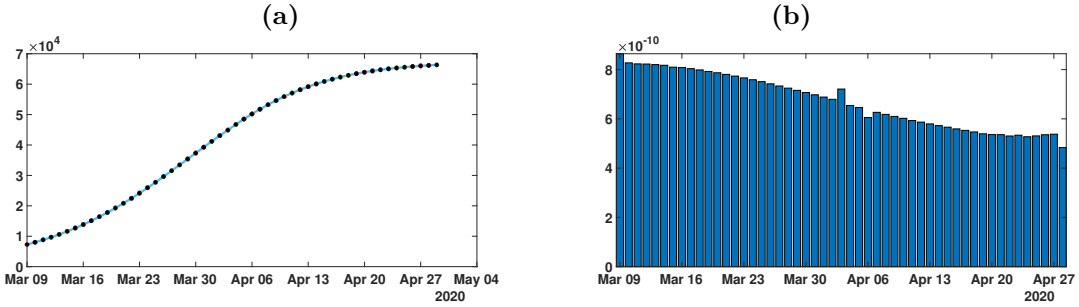

Figure 5.4.11: *In this figure, we plot the rate of transmission obtained by using the reported cases of COVID-19 in China with the parameters* $f = 0.5$ *and* $\nu = 0.2$. *We first regularize the data by applying the MATLAB function* $\mathrm{CR}_{\mathrm{Data}} = \mathrm{smoothdata}(\mathrm{CR}_{\mathrm{Data}}, 'gaussian', 50)$. *Then we apply Algorithm 2 to the regularized data. In figure (a), we plot the regularized cumulative number of reported cases obtained after smoothing (black dots) and the model (blue curve). In figure (b), we plot the daily rate of transmission obtained by using the Algorithm 2. We see that we can fit the data perfectly and this time the rate of transmission is becoming reasonable.*

Algorithm 2

We fix $S_0 = 1.4 \times 10^9$, $\nu = 0.1$ *or* $\nu = 0.2$ *and* $f = 0.5$. *Then we fit the data by using the method described in Section 5.4.2 to estimate the parameters* χ_1, χ_2 *and* χ_3 *from day* 1 *to* 10. *Then we use*

$$\begin{aligned} S_0 &= 1.40005 \times 10^9, \\ I_0 &= \chi_2\, \chi_1\, [\exp(\chi_2\, (t_0 - 1))]/(f\, \nu), \\ \mathrm{CR}_0 &= \chi_1\, exp(\chi_2\, t_0) - \chi_3. \end{aligned} \tag{5.4.44}$$

For each integer $i = 0, \ldots, n$, *we consider the system*

$$\begin{cases} S'(t) = -\tau S(t) I(t), \\ I'(t) = \tau S(t) I(t) - \nu I(t), \\ \mathrm{CR}'(t) = \nu f I(t), \end{cases} \tag{5.4.45}$$

for $t \in [t_i, t_{i+1}]$. *Then the map* $\tau \to \mathrm{CR}(t_{i+1})$ *being monotone increasing, we can apply a bisection method to find the unique* τ_i *solving*

$$\mathrm{CR}(t_{i+1}) = \mathrm{CR}_{\mathrm{Data}}(t_{i+1}).$$

The key idea of this new algorithm is the following correction on the I-component of the system. We start a new step by using the value $S(t_i)$ *obtained from the previous iteration and*

$$I_i = \mathrm{CR}'_{\mathrm{Data}}(t_i)/(\nu\, f), \tag{5.4.46}$$

and

$$\mathrm{CR}_i = \mathrm{CR}_{\mathrm{Data}}(t_i). \tag{5.4.47}$$

In Figure 5.4.12 we plot several types of regularized cumulative data in figure (a) and several types of regularized daily data in figure (b). Among the different regularization methods, an important one is the Bernoulli-Verhulst best fit approximation. In Figure 5.4.13 we plot the rate of transmission $t \to \tau(t)$ obtained by using Algorithm 2. We can see that the original data gives a negative transmission rate while at the other extreme the Bernoulli-Verhulst seems to give the most regularized transmission rate. In Figure 5.4.13-(a) we observe that we now recover almost perfectly the theoretical transmission rate obtained in Section 5.4.4. In Figure 5.4.13-(b) the rolling weekly average regularization and in Figure 5.4.13-(c) the Gaussian weekly average regularization still vary a lot and in both cases the transmission rate becomes negative after some time. In Figure 5.4.13-(c) the original data gives a transmission rate that is negative from the beginning. We conclude that it is crucial to find a "good" regularization of the daily number of case. So far the best regularization method is obtained by using the best fit of the Bernoulli-Verhulst model.

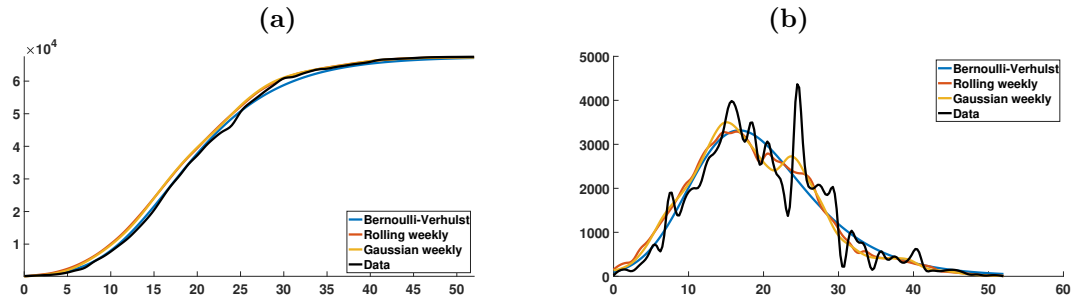

Figure 5.4.12: *In this figure, we plot the cumulative number of reported cases (left) and the daily number of reported cases (right). The black curves are obtained by applying the cubic spline matlab function "spline(Days,DATA)" to the cumulative data. The left-hand side is obtained by using the cubic spline function and right-hand side is obtained by using the derivative of the cubic spline interpolation. The blue curves are obtained by using cubic spline function to the day by day values of cumulative number of cases obtained from the best fit of the Bernoulli-Verhulst model. The orange curves are obtained by computing the rolling weekly daily number of cases (we use the matlab function "smoothdata(DAILY,'movmean',7)") and then by applying the cubic spline function the corresponding cumulative number of cases. The yellow curves are obtained by Gaussian the rolling weekly to the daily number of cases (we use the matlab function "smoothdata(DAILY,'gaussian',7)") and then by applying the cubic spline function to the corresponding cumulative number of cases.*

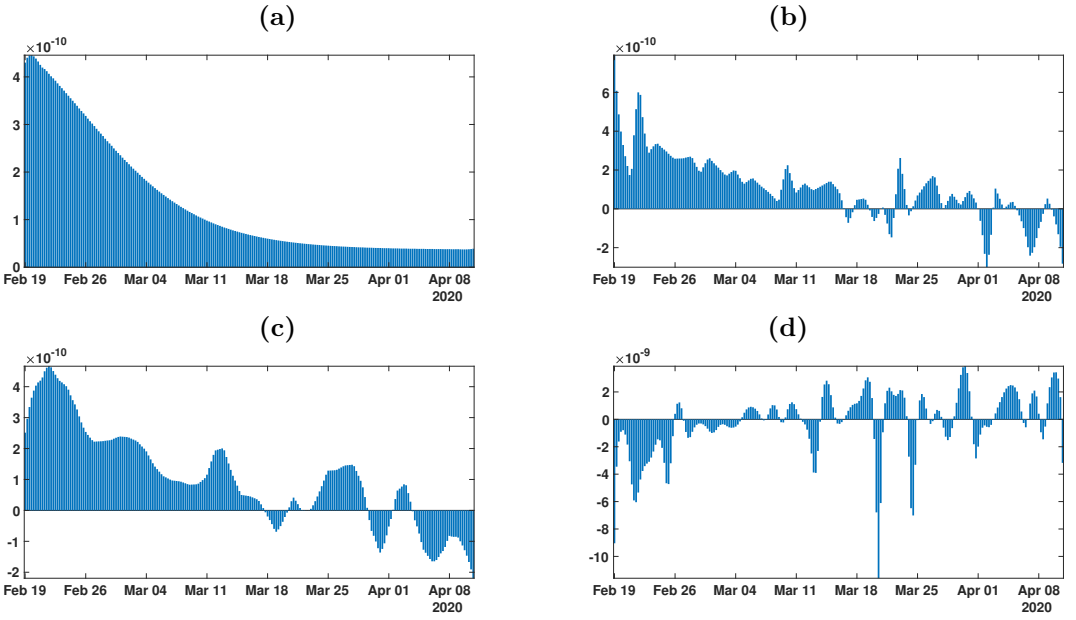

Figure 5.4.13: *In this figure we plot the transmission rates $t \to \tau(t)$ obtained by using Algorithm 2 with the parameters $f = 0.5$ and $\nu = 0.2$. In figure (a) we use the cumulative data obtained by using the Bernoulli-Verhulst regularization. In figure (b) we use the cumulative data obtained by using the rolling weekly average regularization. In figure (c) we use the cumulative data obtained by using the Gaussian weekly average regularization. In figure (d) we use the original cumulative data.*

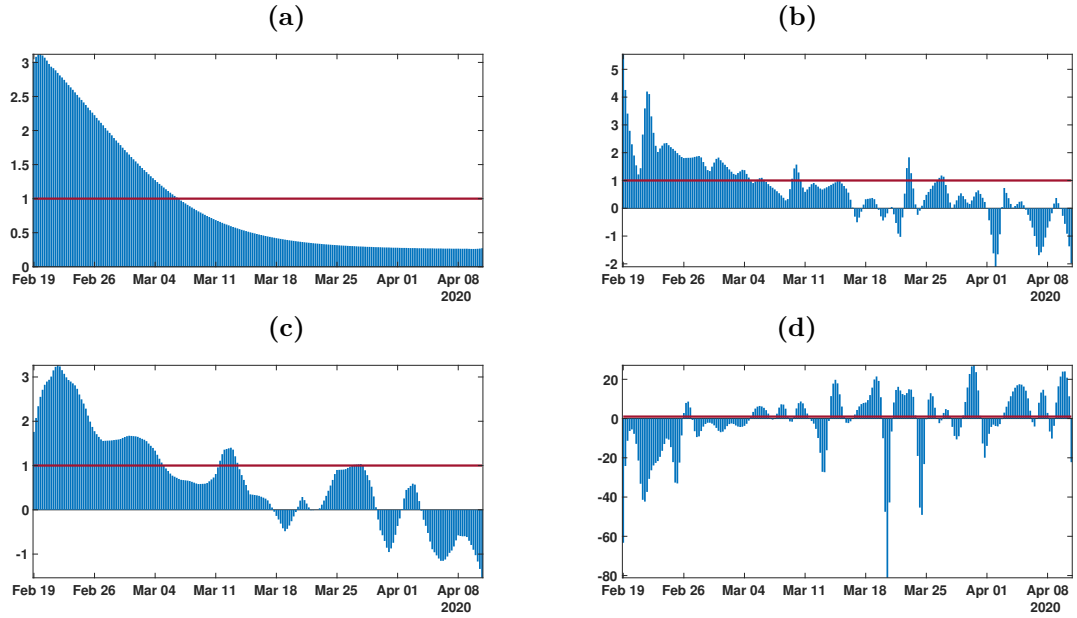

Figure 5.4.14: *In this figure we plot the daily basic reproduction number* $t \to R_0(t) = \tau(t)S(t)/\nu$ *obtained by using Algorithm 2 with the parameters* $f = 0.5$ *and* $\nu = 0.2$. *In figure (a) we use the cumulative data obtained by using the Bernoulli-Verhulst regularization. In figure (b) we use the cumulative data obtained by using the rolling weekly average regularization. In figure (c) we use the cumulative data obtained by using the Gaussian weekly average regularization. In figure (d) we use the original cumulative data.*

Remark 5.4.12. For each simulation Figure 5.4.13-(b) and Figure 5.4.13-(c), it is possible to obtain a transmission $t \to \tau(t)$ that is non negative for all time t by increasing sufficiently the parameter ν. Nevertheless, we do not present these simulations here because the corresponding values of ν to obtain a non negative $\tau(t)$ are unrealistic.

In Figure 5.4.14 (a) (b) (c) and (d) (respectively) we plot the daily basic reproduction number corresponding to the Figure 5.4.13 (a) (b) (c) and (d) (respectively). The red line corresponds to $R_0 = 1$. We see some complex behavior for the Figure 5.4.14 (b) (c) and the figure (d) is again unrealistic.

5.4.7 Discussion

Estimating the parameters of an epidemiological model is always difficult and generally requires strong assumptions about their value and their consistency and constancy over time. Despite this, it is often shown that many sets of parameter values are compatible with a good fit of the observed data. The new approach developed in this section 5.4 consists first of all in postulating a phenomenological model of growth of infectious, based on the very classic model of Verhulst, proposed in demography in 1838 [381]. Then, obtaining explicit formulas for important parameter values such as the transmission rate or the initial number of infected (or for lower and/or upper limits of these values), gives an estimate allowing an almost perfect reconstruction of the observed dynamics.

The uses of phenomenological models can also be regarded as a way a of smoothing the data. Indeed, the errors concerning the observations of new infected cases are numerous:

- the census is rarely regular and many countries report late cases that occurred during the weekend and at varying times over-add data from specific counts, such as those from homes for the elderly;
- the number of cases observed is still underestimated and the calculation of cases not reported new cases of infected is always a difficult problem [261];
- the raw data are sometimes reduced for medical reasons of poor diagnosis or lack of detection tools, or for reasons of domestic policy of states.

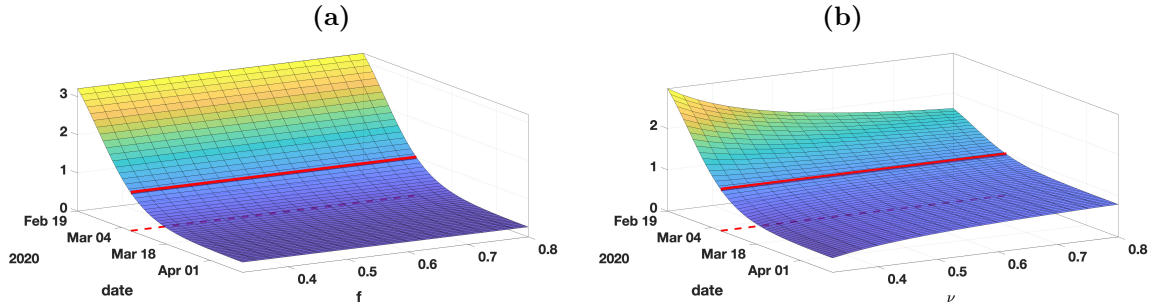

Figure 5.4.15: *In this figure plot* $R_0(t) = \dfrac{\tau(t)S(t)}{\nu}$ *the daily basic reproduction number and we vary the parameter* f *(left) and* ν *(right).*

For all these causes of error, it is important to choose the appropriate smoothing method (moving average, spline, Gaussian kernel, auto-regression, generalized linear model, etc.). In this section 5.4, several methods were used and the one which allowed the model to perfectly match the smoothed data was retained.

In this section 5.4, we developed several methods to understand how to reconstruct the rate of transmission from the data. In Section 5.4.2, we reconsidered the method presented in [261] based on an exponential fit of the early data. The approach gives a first estimation of I_0 and τ_0. In Section 5.4.3, we prove a result to connect the time dependent cumulative reported data and the transmission rate. In Section 5.4.4, we compare the data to the Bernoulli-Verhulst model and we use this model as a phenomenological model. The Bernoulli-Verhulst model fits the data for mainland China very well. Next by replacing the data by the solution of the Bernoulli-Verhulst model, we obtain an explicit formula for the transmission rate. So we derive some conditions on the parameters for the applicability of the SI model to the data for mainland China. In Section 5.4.5, we discretized the rate of transmission and we observed that given some daily cumulative data, we can get at most one perfect fit the data. Therefore, in Section 5.4.6, we provide two algorithms to compute numerically the daily rates of transmission. Such numerical questions turn out to be a delicate problem. This problem was previously considered by another French group Bakhta, Boiveau, Maday and Mula [29]. Here we use some simple ideas to approach the derivative of the cumulative reported cases combined with some smoothing method applied to the data.

To conclude this section 5.4 we plot the daily basic reproduction number

$$R_0(t) = \frac{\tau(t)S(t)}{\nu}$$

as a function of the time t and the parameters f or ν. The above simple formula for R_0 is not the real basic reproductive number in the sense of the number of newly infected produced by a single infectious. But this is a simple formula which gives a tendency about the growth or decay of the number of infectious. In Figure 5.4.14-(a), the daily basic reproduction number is almost independent of f, while in Figure 5.4.14-(b), $R_0(t)$ is depending on ν mostly for the small value of ν. The red curve on each surfaces in Figure 5.4.14 corresponds to the turning point (i.e. time $t \geq t_0$ for which $R_0(t) = 1$). We also see that turning point is not depending much on these parameters.

Concerning contagious diseases, public health physicians are constantly facing four challenges. The first concerns the estimation of the average transmission rate. Until now, no explicit formula had been obtained in the case of the SIR model, according to the observed data of the epidemic, that is to say the number of reported cases of infected patients. Here, from realistic simplifying assumptions, a formula is provided (formula (5.4.30)), making it possible to accurately reconstruct theoretically the curve of the observed cumulative cases. The second challenge concerns the estimation of the mean duration of the infectious period for infected patients. As for the transmission rate, the same realistic assumptions make it possible to obtain an upper limit to this duration (inequality (5.4.33)), which makes it possible to better guide the individual quarantine measures decided by the authorities in charge of public health. This upper bound also makes it possible to obtain a lower bound for the percentage of unreported infected patients (inequality (5.4.33)), which gives an idea of the quality of the census of cases of infected patients, which is the third challenge faced by epidemiologists, specialists of contagious diseases. The fourth challenge is the estimation of the average transmission rate for each day of the infectious period (dependent on the distribution of the transmission over the "ages" of infectivity), which will be the subject of further work and which poses

January						
19	20	21	22	23	24	25
198	291	440	571	830	1287	1975
26	27	28	29	30	31	
2744	4515	5974	7711	9692	11791	
February						
1	2	3	4	5	6	7
14380	17205	20438	24324	28018	31161	34546
8	9	10	11	12	13	14
37198	40171	42638	44653	46472	48467	49970
15	16	17	18	19	20	21
51091	70548 − 17409	72436 − 17409	74185 − 17409	75002 − 17409	75891 − 17409	76288 − 17409
22	23	24	25	26	27	28
76936 − 17409	77150 − 17409	77658 − 17409	78064 − 17409	78497 − 17409	78824 − 17409	79251 − 17409
29						
79824 − 17409						
March						
1	2	3	4	5	6	7
79824 − 17409	79824 − 17409	79824 − 17409	80409 − 17409	80552 − 17409	80651 − 17409	80695 − 17409
8	9	10	11	12	13	14
80735 − 17409	80754 − 17409	80778 − 17409	80793 − 17409	80813 − 17409	80824 − 17409	80844 − 17409
15	16	17	18			
80860 − 17409	80881 − 17409	80894 − 17409	80928 − 17409			

Table 5.4.1: *Cumulative data describing confirmed cases in mainland China from January 20, 2020 to March 18, 2020. The data are taken from [431, 429, 424].*

formidable problems, in particular those related to the age (biological age or civil age) class of the patients concerned. Another interesting prospect is the extension of methods developed in the present section 5.4 to the contagious non-infectious diseases (i.e., without causal infectious agent), such as social contagious diseases, the best example being that of the pandemic linked to obesity [138, 135, 137], for which many concepts and modeling methods remain available.

5.4.8 Supplementary tables

We use cumulative reported data from the National Health Commission of the People's Republic of China and the Chinese CDC for mainland China. Before February 11, the data was based on confirmed testing. From February 11 to February 15, the data included cases that were not tested for the virus, but were clinically diagnosed based on medical imaging showing signs of pneumonia. There were 17,409such cases from February 10 to February 15. The data from February 10 to February 15 specified both types of reported cases. From February 16, the data did not separate the two types of reporting, but reported the sum of both types. We subtracted 17,409 cases from the cumulative reported cases after February 15 to obtain the cumulative reported cases based only on confirmed testing after February 15.The data is given in Table 2 with this adjustment.

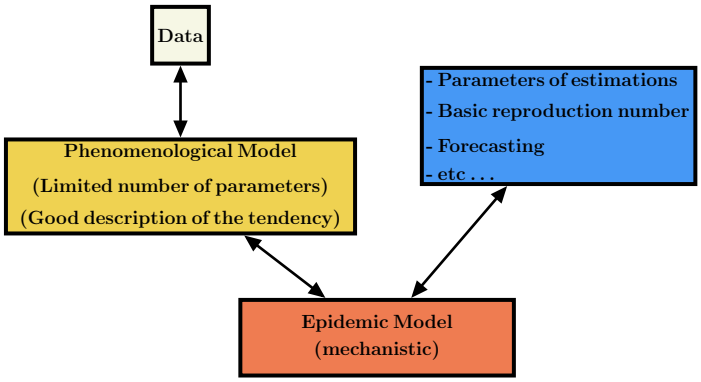

Figure 5.5.1: *We can apply statistical methods to estimate the parameters of the proposed phenomenological model and derive their average values with some confidence intervals. The phenomenological model is used at the first step of the modelling process, providing regularized data to the epidemic model and allowing the identification of its parameters.*

5.5 A robust phenomenological approach to investigate COVID-19 data for France

5.5.1 Introduction

Modeling endemic and epidemic phases of the infectious diseases such as smallpox which by the 16th century had become a predominant cause of mortality in Europe until the vaccination by E. Jenner in 1796, and present Covid-19 pandemic outbreak has always been a means of describing and predicting disease. D. Bernoulli proposed in 1760 a differential model [58] taking into account the virulence of the infectious agent and the mortality of the host, which showed a logistic formula [58, p.13] of the same type as the logistic equation by Verhulst [381]. The succession of an epidemic phase followed by an endemic phase had been introduced by Bernoulli and for example appears clearly in the Figures 9 and 10 in [143].

The aim of this section 5.5 is to propose a new approach to compare epidemic models with data from reported cumulative cases. Here we propose a phenomenological model to fit the observed data of cumulative infectious cases of COVID-19 that describe the successive epidemic phases and endemic intermediate phases. This type of problem dates back to the 1970s with the work of London and Yorke [264]. More recently, Chowell et al. [111] have proposed a specific function to model the temporal transmission speeds $\tau(t)$. In the context of COVID-19, a two-phase model has been proposed by Liu et al. [261] to describe the South Korean data with an epidemic phase followed by an endemic phase.

In this section 5.5, we use a phenomenological model to fit the data (see Figure 5.5.1). The phenomenological model is used in the modeling process between the data and the epidemic models. The difficulty here is to propose a simple phenomenological model (with a limited number of parameters) that would give a meaningful result for the time-dependent transmission rates $\tau(t)$. Many models could potentially be used as phenomenological models to represent the data (ex. cubic spline and others). The major difficulty here is to provide a model that gives a good description of the tendency for the data. It has been observed in our previous work that it is difficult to choose between the possible phenomenological models (see Figures 12-14 in [P7]). The phenomenological model can also be viewed as a regularization of data that should not fluctuate too much to keep the essential information. An advantage in our phenomenological model is the limited number of parameters (5 parameters during each epidemic phase and 2 parameters during each endemic phase). The last advantage of our approach is that once the phenomenological model has been chosen, we can compute some explicit formula for the transmission rate and derive some estimations for the other parameters.

5.5.2 Material and methods

5.5.2.1 Phenomenological model

In this section 5.5, the phenomenological model is compared with the cumulative reported case data taken from WHO [425]. The phenomenological model deals with data series of new infectious cases decomposed into two types of successive phases, 1) endemic phases, followed by 2) epidemic ones.

Endemic phase: During the endemic phase, the dynamics of new cases appear to fluctuate around an average value independently of the number of cases. Therefore the average cumulative number of cases is given by

$$\mathrm{CR}(t) = N_0 + (t - t_0) \times a, \text{ for } t \in [t_0, t_1], \tag{5.5.1}$$

where t_0 denotes the beginning of the endemic phase. a is the average value of $\mathrm{CR}(t_0)$ and N_0 the average value of the daily number of new cases.

In other words, we assume that the average daily number of new cases is constant. Therefore the daily number of new cases is given by

$$\mathrm{CR}'(t) = a. \tag{5.5.2}$$

Epidemic phase: In the epidemic phase, the new cases contribute to produce secondary cases. Therefore the daily number of new cases is no longer constant but varies with time as follows

$$\mathrm{CR}(t) = N_{\mathrm{base}} + N(t), \text{ for } t \in [t_0, t_1], \tag{5.5.3}$$

where

$$N(t) = \frac{e^{\chi(t-t_0)} N_0}{\left[1 + \frac{N_0^\theta}{N_\infty^\theta}\left(e^{\chi\theta(t-t_0)} - 1\right)\right]^{1/\theta}}. \tag{5.5.4}$$

In other words, the daily number of new cases follows the Bernoulli-Verhulst [58, 381] equation. Namely, by setting $N(t) = \mathrm{CR}(t) - N_{\mathrm{base}}$ we obtain

$$N'(t) = \chi\, N(t) \left[1 - \left(\frac{N(t)}{N_\infty}\right)^\theta\right] \tag{5.5.5}$$

with the initial value

$$N(t_0) = N_0. \tag{5.5.6}$$

In the model $N_{\mathrm{base}}+N_0$ corresponds to the value $\mathrm{CR}(t_0)$ of the cumulative number of cases at time $t = t_0$. The parameter $N_\infty + N_{\mathrm{base}}$ is the maximal increase of the cumulative reported case after the time $t = t_0$. $\chi > 0$ is a Malthusian growth parameter, and θ regulates the speed at which the $\mathrm{CR}(t)$ increases to $N_\infty + N_{\mathrm{base}}$.

Regularized model

Because the formula for $\tau(t)$ involves derivatives of the phenomenological model regularizing $\mathrm{CR}(t)$ (see equation (5.5.13)), we need to connect the phenomenological models of the different phases as smoothly as possible. We let $\widetilde{\mathrm{CR}}(t)$ be the model obtained by placing phenomenological models side by side for different phases. Outside of the time window where phenomenological models are used, we consider that the function $\widetilde{\mathrm{CR}}(t)$ is constant. We define the regularized model by using the convolution formula:

$$\mathrm{CR}(t) = \int_{-\infty}^{+\infty} \widetilde{\mathrm{CR}}(t-s) \times \frac{1}{\sigma\sqrt{2\pi}} e^{-\frac{s^2}{2\sigma^2}}\, \mathrm{d}s = (\widetilde{\mathrm{CR}} * \mathcal{G})(t), \tag{5.5.7}$$

where $\mathcal{G}(t) := \frac{1}{\sigma\sqrt{2\pi}} e^{-\frac{t^2}{2\sigma^2}}$ is the Gaussian function with variance σ^2. The parameter σ controls the trade-off between smoothness and precision: increasing σ reduces the variations in $\mathrm{CR}(t)$ and decreasing σ reduces the distance between $\mathrm{CR}(t)$ and $\widetilde{\mathrm{CR}}(t)$. In any case the resulting function $\mathrm{CR}(t)$ is very smooth (as well as its derivatives) and close to the original model $\widetilde{\mathrm{CR}}(t)$ when σ is not too large. In numerical applications, we take $\sigma = 2$ days.

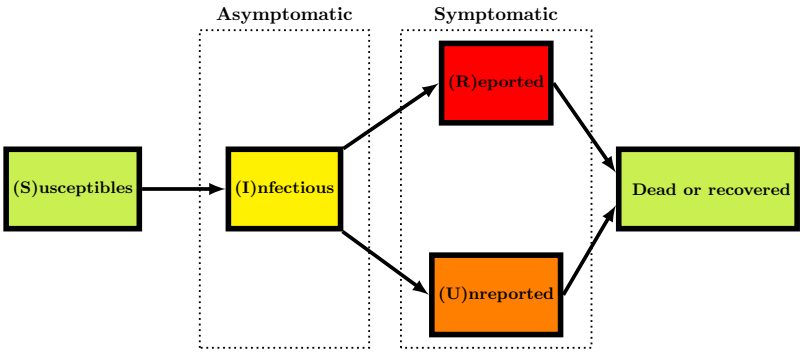

Figure 5.5.2: *Schematic view showing the different compartments and transition arrows in the epidemic model.*

Procedure to fit the phenomenological model to the data

To fit the model to the data, we used the regularized model (5.5.7) where the periods of the different phases are fixed as in Table 5.5.1. We use a standard curve-fitting algorithm to find the parameters of the regularized model. In numerical applications we used the Levenberg–Marquardt nonlinear least-squares algorithm provided by the MATLAB© function `fit`. Our 95% confidence intervals are the ones provided as an output of this algorithm. The best-fit parameters and the corresponding confidence intervals are provided in Table 5.5.1.

5.5.2.2 SI Epidemic model

The SI epidemic model used in this work is the same as in [P7]. It is summarized by the flux diagram in Figure 5.5.2.

The goal of this section 5.5 is to understand how to compare the SI model to the reported epidemic data and therefore the model can be used to predict the future evolution of epidemic spread and to test various possible scenarios of social mitigation measures. For $t \geq t_0$, the SI model is the following

$$\begin{cases} S'(t) = -\tau(t)S(t)I(t), \\ I'(t) = \tau(t)S(t)I(t) - \nu I(t), \end{cases} \tag{5.5.8}$$

where $S(t)$ is the number of susceptible and $I(t)$ the number of infectious at time t. This system is supplemented by initial data

$$S(t_0) = S_0 \geq 0,\ I(t_0) = I_0 \geq 0. \tag{5.5.9}$$

In this model, the rate of transmission $\tau(t)$ combines the number of contacts per unit of time and the probability of transmission. The transmission of the pathogen from the infectious to the susceptible individuals is described by a mass action law $\tau(t)\,S(t)\,I(t)$ (which is also the flux of new infectious).

The quantity $1/\nu$ is the average duration of the infectious period and $\nu I(t)$ is the flux of recovering or dying individuals. At the end of the infectious period, we assume that a fraction $f \in (0, 1]$ of the infectious individuals is reported. Let $\mathrm{CR}(t)$ be the cumulative number of reported cases. We assume that

$$\mathrm{CR}(t) = \mathrm{CR}_0 + \nu\, f\, \mathrm{CI}(t),\ \text{for } t \geq t_0, \tag{5.5.10}$$

where

$$\mathrm{CI}(t) = \int_{t_0}^{t} I(\sigma)\mathrm{d}\sigma. \tag{5.5.11}$$

Assumption 5.5.1 (Given parameters)**.** We assume that

- the number of susceptible individuals when we start to use the model $S_0 = 67$ millions;
- the average duration of infectious period $\dfrac{1}{\nu} = 3$ days;

- the fraction of reported individuals $f = 0.9$;

are known parameters.

Parameters estimated in the simulations: As described in [P7] the number of infectious at time t_0 is

$$I_0 = \frac{\mathrm{CR}'(t_0)}{\nu\, f} \tag{5.5.12}$$

The rate of transmission $\tau(t)$ at time t is given by

$$\tau(t) = \frac{\nu f \left(\dfrac{\mathrm{CR}''(t)}{\mathrm{CR}'(t)} + \nu\right)}{\nu f\,(I_0 + S_0) - \mathrm{CR}'(t) - \nu\,(\mathrm{CR}(t) - \mathrm{CR}_0)}. \tag{5.5.13}$$

Parameters estimated in the endemic phase: The initial number of infectious is given by

$$I_0 = \frac{a}{\nu\, f},$$

and the transmission rate is given by the explicit formula

$$\tau(t) = \frac{\nu^2 f}{\nu f\,(I_0 + S_0) - a - \nu(t - t_0) \times a}, \forall t \in [t_0, t_1].$$

Parameters estimated in the epidemic phase: The initial number of infectious is given by

$$I_0 = \frac{\chi\, N_0 \left[1 - \left(\dfrac{N_0}{N_\infty}\right)^\theta\right]}{\nu\, f},$$

and the transmission rate is given by the explicit formula

$$\tau(t) = \frac{\nu f \left(\dfrac{N''(t)}{N'(t)} + \nu\right)}{\nu f\,(I_0 + S_0) - N'(t) - \nu\,(N(t) - N_0)},$$

and since (recall (5.5.5))

$$N'(t) = \chi\, N(t) \left[1 - \left(\frac{N(t)}{N_\infty}\right)^\theta\right]$$

and

$$N''(t) = \chi\, N'(t) \left[1 - (1 + \theta)\left(\frac{N(t)}{N_\infty}\right)^\theta\right], \tag{5.5.14}$$

we obtain an explicit formula

$$\tau(t) = \frac{\nu f \left(\chi \left[1 - (1 + \theta)\left(\dfrac{N(t)}{N_\infty}\right)^\theta\right] + \nu\right)}{\nu f\,(I_0 + S_0) - \chi\, N(t) \left[1 - \left(\dfrac{N(t)}{N_\infty}\right)^\theta\right] - \nu\,(N(t) - N_0)}, \tag{5.5.15}$$

where $N(t)$ is given by (5.5.4):

$$N(t) = \frac{e^{\chi(t - t_0)} N_0}{\left[1 + \dfrac{N_0^\theta}{N_\infty^\theta}\left(e^{\chi\theta(t - t_0)} - 1\right)\right]^{1/\theta}}.$$

By using the Bernoulli-Verhulst model to represent the data, the daily number of new cases is nothing but the derivative $N'(t)$ (whenever the unit of time is one day). The daily number of new cases reaches its maximum at the turning point $t = t_p$, and by using (5.5.14), we obtain

$$N''(t_p) = 0 \Leftrightarrow N(t_p) = \left(\frac{1}{1+\theta}\right)^{1/\theta} N_\infty.$$

Therefore by using (5.5.5), the maximum of the daily number of cases equals

$$N'(t_p) = \chi\, N(t_p) \left[1 - \left(\frac{N(t_p)}{N_\infty}\right)^{\theta}\right].$$

By using the above formula, we obtain a new indicator for the amplitude of the epidemic.

Theorem 5.5.2. *The maximal daily number of cases in the course of the epidemic phase is given by*

$$\chi \times N_\infty \times \theta \times \left(\frac{1}{1+\theta}\right)^{\frac{1}{\theta}+1}. \tag{5.5.16}$$

5.5.2.3 Parameter bounds

The epidemic model (5.5.8) with time-dependent transmission rate is consistent only insofar as the transmission rate remains positive. This gives us a criterion to judge if a set of epidemic parameters has a chance of being consistent with the observed data: since we know the parameters N_0, N_∞, χ and θ from the phenomenological model, the formula (5.5.15) allows us to compute a criterion on ν and f which decides whether a given parameter values are compatible with the observed data or not. That is to say that, a set of parameter values is compatible if the transmission rate $\tau(t)$ in (5.5.15) remains positive for all $t \geq t_0$, and it is not compatible if the sign of $\tau(t)$ in (5.5.15) changes for some $t \geq t_0$. We refer to [P7, Proposition 4.3] for more results.

The value of the parameter ν is compatible with the model (5.5.15) if and only if

$$0 \leq \frac{1}{\nu} \leq \frac{1}{\chi\theta}, \tag{5.5.17}$$

and the value of the parameter f is compatible with the model (5.5.15) if and only if

$$f \geq \frac{N_\infty - N_0}{I_0 + S_0}. \tag{5.5.18}$$

Therefore, we obtain an information on the parameters ν and f, even though they are not directly identifiable (two different values of ν or f can produce exactly the same cumulative reported cases).

5.5.2.4 Computation of the basic reproduction number

In order to compute the reproduction number in Figure 5.5.5 we use the Algorithm 2 in [P7] and the day-by-day values of the phenomenological model.

5.5.3 Results

5.5.3.1 Phenomenological model compared to the French data

In Figure 5.5.3 we present the best fit of our phenomenological model for the cumulative reported case data of COVID-19 epidemic in France. The yellow regions correspond to the endemic phases and the blue regions correspond to the epidemic phases. Here we consider the two epidemic waves for France, and the chosen period, as well as the parameters values for each period, are listed in Table 5.5.1. In Table 5.5.1 we also give 95% confidence intervals for the fitted parameters values.

Figure 5.5.4 shows the corresponding daily number of new reported case data (black dots) and the first derivative of our phenomenological model (red curve).

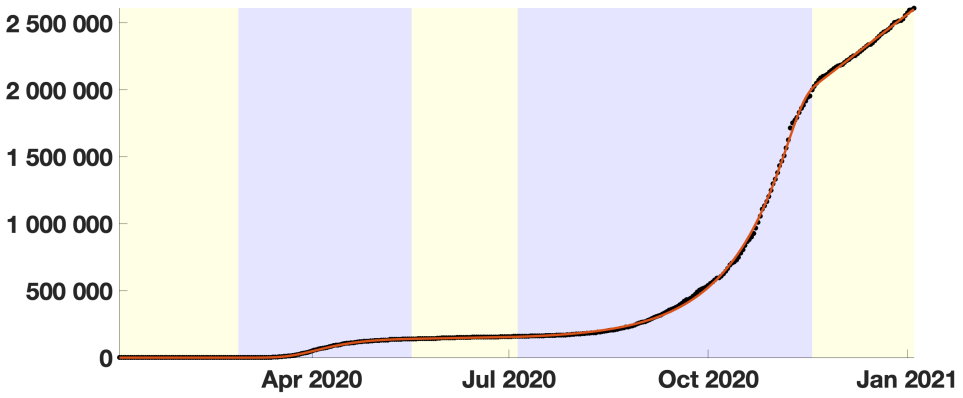

Figure 5.5.3: *The red curve corresponds to the phenomenological model and the black dots correspond to the cumulative number of reported cases in France.*

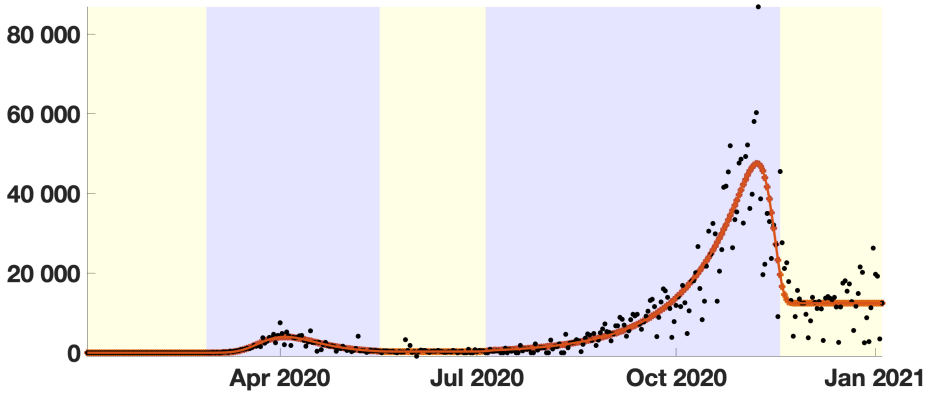

Figure 5.5.4: *The red curve corresponds to the first derivative of the phenomenological model and the black dots correspond to daily number of new reported cases in France.*

5.5.3.2 SI epidemic model compared to the French data

Some parameters of the model are known as $S_0 = 67$ millions for France (this is questionable). Some parameters of the epidemic model can not be precisely evaluated [P7].

Result

By using (5.5.17) we obtain the following conditions for the average duration of infectious period

- $0 < \dfrac{1}{\nu} \leq 1/(\chi\theta) = 12.5$ days during the first epidemic wave;
- $0 < \dfrac{1}{\nu} \leq 1/(\chi\theta) = 3.5$ days during the second epidemic wave.

We obtain no constraint for the fraction $f \in (0, 1]$ of reported new cases (between 0 and 1 for France).

Moreover by using the formula (5.5.16) we deduce that the maximal daily number of cases is

- 4110 during the first epidemic wave;
- 47875 during the second epidemic wave.

Period	Parameters value	Method	95% Confidence interval
Period 1: Endemic phase	$N_0 = -4.368$	computed	
Jan 03 - Feb 27	$a = 1.099 \times 10^{-1}$	fitted	$a \in [-8.582 \times 10^{1}, 8.604 \times 10^{1}]$
Period 2: Epidemic phase Feb 27 - May 17	$N_{base} = 0$	fixed	
	$N_0 = 1.675$	fitted	$N_0 \in [-3.807 \times 10^{1}, 4.142 \times 10^{1}]$
	$N_\infty = 1.445 \times 10^{5}$	fitted	$N_\infty \in [1.367 \times 10^{5}, 1.523 \times 10^{5}]$
	$\chi = 1.263$	fitted	$\chi \in [-1.171 \times 10^{1}, 1.424 \times 10^{1}]$
	$\theta = 6.315 \times 10^{-2}$	fitted	$\theta \in [-6.086 \times 10^{-1}, 7.349 \times 10^{-1}]$
Period 3: Endemic phase	$N_0 = 1.405 \times 10^{5}$	computed	
May 17 - Jul 05	$a = 3.11 \times 10^{2}$	computed	
Period 4: Epidemic phase Jul 05 - Nov 18	$N_{base} = 1.403 \times 10^{5}$	fitted	$N_{base} \in [1.367 \times 10^{5}, 1.439 \times 10^{5}]$
	$N_0 = 1.517 \times 10^{4}$	fitted	$N_0 \in [1.427 \times 10^{4}, 1.607 \times 10^{4}]$
	$N_\infty = 1.953 \times 10^{6}$	fitted	$N_\infty \in [1.92 \times 10^{6}, 1.986 \times 10^{6}]$
	$\chi = 3.671 \times 10^{-2}$	fitted	$\chi \in [3.62 \times 10^{-2}, 3.722 \times 10^{-2}]$
	$\theta = 7.679$	fitted	$\theta \in [6.256, 9.102]$
Period 5: Endemic phase	$N_0 = 4.45 \times 10^{-84}$	computed	
Nov 18 - Jan 04	$a = 1.099 \times 10^{-1}$	fitted	$a \in [1.222 \times 10^{4}, 1.265 \times 10^{4}]$

Table 5.5.1: *Fitted parameters and computed parameters for the whole epidemic going from January 03 2020 to January 04 2021.*

Importantly, by combining the phenomenological model from Section 5.5.3.1 and the epidemiological model from Section 5.5.2.2, we can reconstruct the time-dependent transmission rate given by (5.5.13) and the corresponding time-dependent basic reproduction number $\mathcal{R}_0(t) = \tau(t)S(t)/\nu$ (sometimes called "effective basic reproductive ratio"). The obtained basic reproduction number is presented in Figure 5.5.5. We observe that $\mathcal{R}_0(t)$ is decreasing during each epidemic wave, except at the very end where it becomes increasing. This is not necessarily surprising since the lockdown becomes less strictly respected towards the end. During the endemic phases, the $\mathcal{R}_0(t)$ becomes effectively equal to one, except again near the end. The variations observed close to the transition between two phases may be partially due to the smoothing method, which has an impact on the size of the "bumps". However, they remain very limited in number and size.

5.5.4 Discussion

In this section 5.4, we use a phenomenological model to reduce the number of parameters necessary for summarizing observed data without loss of pertinent information. The process of reduction consists of three stages: qualitative or quantitative detection of the boundaries between the different phases of the dynamics (here endemic and epidemic phases), choice of a reduction model (among different possible approaches: logistic, regression polynomials, splines, autoregressive time series, etc.) and smoothing of the derivatives at the boundary points corresponding to the breaks in the model.

In Figure 5.5.3, we have a very good agreement between the data and the phenomenological model, for both the original curve and its derivative. The relative error in Figure 5.5.3 is of order 10^{-2}, which means that the error is at most of the order of 100 000 individuals. In Figure 5.5.4 the red curve also gives a good tendency of the black dots corresponding to raw data.

In Figure 5.5.5, the phenomenological models are necessary to derive a significant basic reproduction number. Otherwise the resulting $\mathcal{R}_0(t)$ is not interpretable and even not computable after sometime. Similar results were obtained in Figures 12-14 in [P7]. The method to compute $\mathcal{R}_0$ can also be applied directly to the original data. We did not show the result here because the noise in the data is amplified by the method

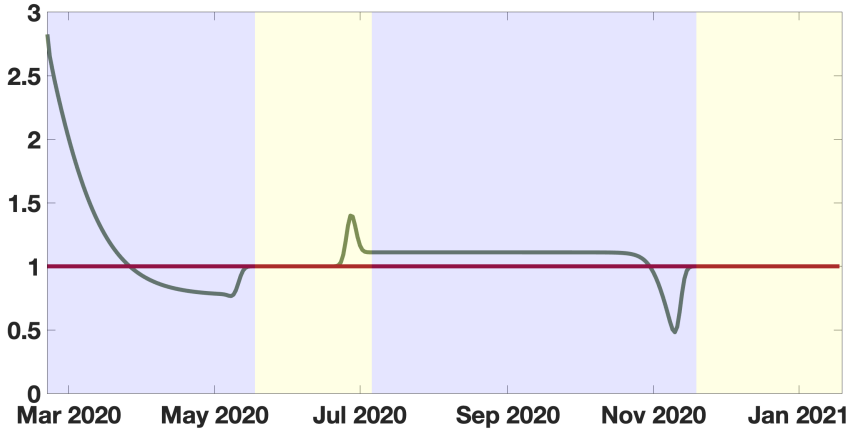

Figure 5.5.5: *In this figure we plot the time dependent basic reproduction number* $\mathcal{R}_0(t) := \tau(t)S(t)/\nu$. *We fix the average length of the asymptotic infectious period to* 3 *days. Notice that, contrary to Figure 5.5.3 and 5.5.4, we do not plot to first endemic phase because the basic reproduction number is meaningless before the first wave.*

and the results are not usable. This shows that it is important to use the phenomenological model to provide a good regularization of the data.

In Figure 5.5.5, the major difficulty is to know how to make the transition from an epidemic phase to an endemic phase and vice versa. This is a non-trivial problem that is solved by our regularization approach (using a convolution with a Gaussian). As we can see in Figure 5.5.5, the number of oscillations is very limited between two phases. Without regularization, there is a sharp corner at the transition between two phases which leads to infinite values in $\tau(t)$. The choice of the convolution with a Gaussian kernel for the regularization method is the result of an experimental process. We tried several different regularization methods, including a smooth explicit interpolation function and Hermite polynomials. Eventually, the convolution with a Gaussian kernel gives the best results.

To minimize the variations of the curve of $\mathcal{R}_0(t)$, the choice of the transition dates between two phases is critical. In Figure 5.5.5 we choose the transition dates so that the derivatives of the phenomenological model do not oscillate too much. Other choices lead to higher variations or increase the number of oscillations. Finally, the qualitative shape of the curve presented in Figure 5.5.5 is very robust to changes in the epidemic parameters, even though the quantitative values of $\mathcal{R}_0(t)$ are different for other values of the parameters ν and f.

In Figure 5.5.5, we observe that the quantitative value of the $\mathcal{R}_0(t)$ during the first part of the second epidemic wave (second blue region) is almost constant and equals 1.11. This value is significantly lower than the one observed at the beginning of the first epidemic wave (first blue region). Yet the number of cases produced during the second wave is much higher than the number of cases produced during the first wave.

We observe that the values of the parameters of the phenomenological model are quantitatively different between the first wave and the second wave. Several phenomena can explain this difference. The population was better prepared for the second wave. The huge difference in the number of daily reported cases during the second phase can be partially attributed to the huge increase in the number of tests in France during this period. But this is only a partial explanation for the explosion of cases during the second wave. We also observe that the average duration of the infectious period varies between the first epidemic wave (12.5 days) and the second epidemic wave (3.5 days). This may indicate a possible adaptation of the virus SARS CoV-2 circulating in France during the two periods, or the effect of the mitigation measures, with better respect of the social distancing and compulsory mask-wearing.

The huge difference between the initial values of $\mathcal{R}_0(t)$ in the first and the second waves is an apparent paradox which shows that $\mathcal{R}_0(t)$ has a limited explanatory value regarding the severity of the epidemic: even if the quantitative value of $\mathcal{R}_0(t)$ is higher at the start of the first wave, the number of cases produced during an equivalent period in the second wave is much higher. This paradox can be partially resolved by remarking that the $\mathcal{R}_0(t)$ behaves like an exponential rate and the number of secondary cases produced in the whole

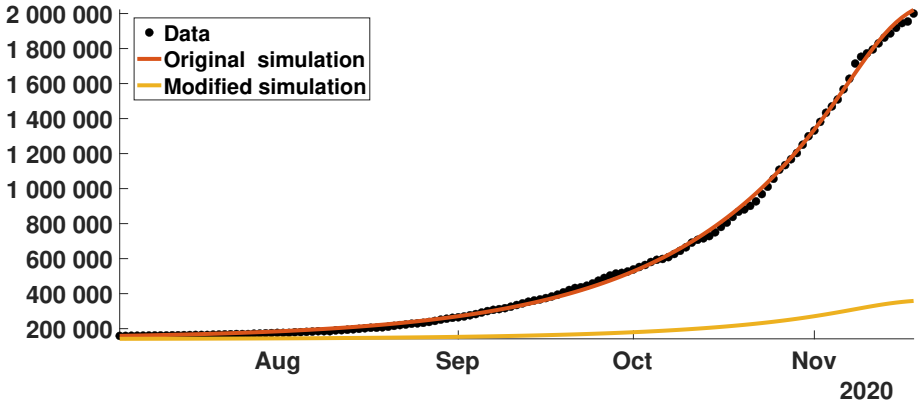

Figure 5.5.6: *Cumulative number of cases for the second epidemic wave obtained by using the SI model* (5.5.8) *with* $\tau(t)$ *given by* (5.5.13)*, the parameters from Table 5.5.1. We start the simulation at time* $t_0 =$ *July 05 with the initial value* $I_0 = \frac{\mathrm{CR}'(t_2)}{\nu f}$ *for the red curve and with* $I_0 = \frac{1}{10}\frac{\mathrm{CR}'(t_2)}{\nu f}$ *for yellow curve. The remaining parameters used are* $\nu = 1/3$*,* $f = 0.9$*,* $S_0 = 66841266$*. We observe the number is five times lower than then the original number of cases.*

population is therefore very sensitive to the number of active cases at time t. In other words, $\mathcal{R}_0(t)$ is blind to the epidemic state of the population and cannot be used as a reliable indicator of the severity of the epidemic. Other indicators have to be found for that purpose; we propose, for instance, the maximal value of the daily number of new cases, which can be forecasted by our method (see equation (5.5.16)), although other indicators can be imagined.

In Figure 5.5.6 we present an exploratory scenario assuming that during the endemic period preceding the second epidemic wave (May 17 - Jul 05) the daily number of cases is divided by 10. The resulting cumulative number of cases obtain is five lower the original one. We summarize this observation into the following statement.

Result

- The level of the daily number of cases during an endemic phase preceding an epidemic phase strongly influences the severity of this epidemic wave.
- In other words, maintaining social distancing between epidemic waves is essential.

In Figure 5.5.4, there is two order of magnitude in the daily number of cases in between $CR'(t_1) \approx 1$ (with $t_1 =$ Feb 27) at the early beginning of the first epidemic wave and $CR'(t_2) = 422$ (with $t_2 =$ July 05) at the early beginning of the second epidemic wave. That confirms our result. After the second wave, the average daily number of cases $CR'(t)$ in France is stationary and approximately equal to 12440. Therefore, if the above observation remains true and if a third epidemic wave occurs, the third epidemic wave is expected to be more severe than the first and second epidemic waves.

Our study can be extended in several directions. A statistical study of the parameters obtained by using our phenomenological model with data at the regional scale could be interesting. We could in particular investigate statistically the correlations existing between the parameters changes and the variations with demographic parameters as the median age and the population density, as well as geo-climatic factors as the elevation and temperature, etc. We also plan to extend our method to more realistic epidemic models, like the SEIUR model from [260], which includes the possibility of transmission from asymptomatic unreported patients.

5.6 What can we learn from COVID-19 data by using epidemic models with unidentified infectious cases?

5.6.1 Introduction

Since the first cases occurred in early December 2019, the COVID-19 crisis has been accompanied by unprecedented data release. The first cluster of cases was reported on December 31, 2019, by WHO (World Health Organization) [422]. Chinese authorities confirmed on January 7 that this cluster was caused by a novel coronavirus [421]. The disease then rapidly spread throughout the world; a case was identified in the U.S.A. as early as January 19, 2020, for instance [212]. According to the WHO database [425], the first cases in Japan date back to January 14, in Italy to January 29 (even though the cluster of cases was announced on January 21, 2020 [13]), in France to January 24, 2020, etc. The spread of the epidemic across countries was monitored, and the data was made publicly available at the international level by recognized scientific institutions such as WHO [425] and the Johns Hopkins University [148], who collected data provided by national health agencies. To the best of our knowledge, this is the first time in history that such detailed epidemiological data have been made publicly available on a global scale; this opens up new questions and new challenges for the scientific community.

Modeling efforts in order to analyze and predict the dynamics of the epidemics were initiated from the start [261, 245, 387]. Forecasting the propagation of the epidemic is, in particular, a key challenge in infectious disease epidemiology. It has quickly become clear to medical doctors and epidemiologists that covert cases (asymptomatic or unreported infectious cases) play an important role in the spread of the COVID-19. An early description of an asymptomatic transmission in Germany was reported by Rothe et al. [341]. It was also observed on the Diamond Princess cruise ship in Yokohama in Japan [287] that many of the passengers were tested positive for the virus but never presented any symptoms. On the French aircraft carrier Charles de Gaulle, clinical and biological data for all 1739 crew members were collected on arrival at the Toulon harbor and during quarantine: 1121 crew members (64%) were tested positive for COVID-19 using RT-PCR, and among these, 24% were asymptomatic [90]. The importance of covert cases in the silent propagation of the epidemic was highlighted by Qiu [327]. Models accounting for asymptomatic transmission, which agree with reported cases data, have been used from the start of the epidemic [261, 260, 258, 259]. The implementation of such models depends, however, on the *a priori* knowledge of some characteristic parameters of the host-pathogen interaction, among which is the ascertainment rate. Nishiura and collaborators [306] estimated this ascertainment rate as 9.2% on a 7.5-days detection window, based on testing data of repatriated Japanese nationals from Wuhan. This was corrected later to 44% for non-severe cases [311]. An early review of SARS-CoV-2 facts can be found in the work of Bar-On et al. [31].

To describe the spread of COVID-19 mathematically, Liu et al. [261] first took into account the infection of susceptible individuals by contacts with unreported infectious individuals. A new method using the number of reported cases in SIR models was also proposed in the same work. This method and the model were extended in several directions by the same group [260, 258, 259, 262] to include non-constant transmission rates and a period of exposure. More recently, the method was extended and successfully applied to a Japanese age-structured dataset by Griette, Magal, and Seydi [P10]. The method was also extended to investigate the predictability of the outbreak in several countries, including China, South Korea, Italy, France, Germany, and the United Kingdom by Liu, Magal, and Webb [262].

Phenomenological models were extensively used in the literature even before the SARS-CoV-2 pandemic to describe reported cases data, see e.g., [416, 214] for the 2003 SARS outbreak, and also [215, 391], to cite a few. In the case of the SARS-CoV-2 epidemic, articles related to phenomenological models are particularly numerous, see e.g., [106, 357, 418, 389, 337, 164, 24, 112, 278, 315]. More precisely, Castro et al. [106] investigate the possibility of predicting the turning point of an epidemic wave. Many studies use phenomenological models to issue short-term predictions on the epidemic [337, 278, 389, 357]. But these models can also be used to reconstruct the evolution of the epidemic a posteriori [24, 112, 418].

In previous works [261, 260, 258, 259], we have replaced the data with the phenomenological model, and we use this continuous description as the output of the epidemic model. This allows us to understand how to express part of the initial distribution and some parameters (e.g., the transmission rate) from the data and the given parameters of the model. By using this approach, we obtain an explicit formula for the time-dependent transmission rate expressed by using some given parameters of the model and some parameters of the phenomenological model. In [P7], we used a Bernoulli-Verhulst phenomenological model to describe a single epidemic wave and compute a time-dependent transmission rate.

There are many potential phenomenological models to represent a single epidemic wave [391, 24, 112].

However, except in the case of the logistic equation, there is usually no explicit formula for the solution. The explicit formula in the case considered here permits to develop a comprehensive statistical analysis. Phenomenological models also serve to regularize the data, which is a complex question. Indeed the idea is to get rid of the stochastic oscillations (due for example to the way the data are collected, or the stochastic nature of the contact between individuals). Some phenomenological models also redistribute the reported cases to dampen the fluctuations in the data. Let us stress here the fact that some oscillations in cases data may not be random and might correspond to complex transmission dynamics (delayed infection, peak in contact numbers during the day, etc.) This highlights one of the drawbacks of phenomenological models: while they allow a precise description of epidemic waves, they might also hide some valuable information on how the disease is transmitted in the population.

A key parameter in understanding the dynamics of the COVID-19 epidemic is the transmission rate, defined as the fraction of all possible contacts between susceptible and infected individuals that effectively result in a new infection per unit of time. Estimating the average transmission rate is one of the most crucial challenges in the epidemiology of communicable diseases. In practice, many factors can influence the actual transmission rate, (i) the coefficient of susceptibility; (ii) the coefficient of virulence; (iii) the number of contacts per unit of time [273]; (iv) the environmental conductivity [136]. Let us remark that the rate of contacts per units of time can also be investigated by agent models [392].

Epidemic models with time-dependent transmission rates have been considered in several articles in the literature. The classical approach is to fix a function of time that depends on some parameters and to fix these parameters by using the best fit to the data. In Chowell et al. [110] a specific form was chosen for the rate of transmission and applied to the Ebola outbreak in Congo. Huo et al [222] used a predefined transmission rate which is a Legendre polynomial depending on a tunable number of parameters. Let us also mention that kinetic model idea has been used to understand this problem in the paper by Dimarco et al. [144]. Here we are going the other way around. We reconstruct the transmission rate from the data by using the model without choosing a predefined function for the transmission rate. Such an approach was used in the early 70s by London and Yorke [264, 410] who used a discrete-time model and discussed the time-dependent rate of transmission in the context of measles, chickenpox, and mumps. More recently, several authors [29, P7, P13] used both an explicit formula and algorithms to reconstruct the transmission rate. These studies allow us to understand that the regularization of the data is a complex problem and is crucial in order to rebuild a meaningful time-dependent transmission rate.

In the present section 5.6, we apply a new method to compute the transmission rate from cumulative reported cases data. While the use of a predefined transmission rate $\tau(t)$ as a function of time can lead to very good fits of the data, here we are looking for a more intrinsic relationship between the data and the transmission rate. Therefore we propose a different approach and use a two-step procedure. Firstly, we use a phenomenological model to describe the data and extract the general trend of the epidemiological dynamics while removing the insignificant noise. Secondly, we derive an explicit relationship between the phenomenological model and the transmission rate. In other words, we compute the transmission rate directly from the data. As a result, we can reconstruct an estimation of the state of the population at each time, including covert cases. Our method also provides new indicators for the epidemiological dynamics that are related to the reproductive number.

5.6.2 Methods

5.6.2.1 COVID-19 data and phenomenological model

We regularized the time series of cumulative reported cases by fitting standard curves to the data to reconstruct the time-dependent transmission rate. We first identified the epidemic waves for each of the eight geographic areas. A Bernoulli–Verhulst curve was then fitted to each epidemic wave using the Levenberg–Marquardt algorithm [426]. We reported the detailed output of the algorithm in the supplementary material, including confidence bounds on the parameters. The model was completed by filling the time windows between two waves with straight lines. Finally, we applied a Gaussian filter with a standard deviation of 7 days to the curve to obtain a smooth model.

Data sources We used reported cases data for 8 different geographic areas, namely California, France, India, Israel, Japan, Peru, Spain, and the UK. Apart from California State, for which we used data from the COVID tracking project [428], the reported cases data were taken from the WHO database [425].

Phenomenological model used for multiple epidemic waves To represent the data, we used a phenomenological model to fit the curve of cumulative rate cases. Such an idea is not new since it was already proposed by Bernoulli [58] in 1760 in the context of the smallpox epidemic. Here we used the so-called Bernoulli–Verhulst [381] model to describe the epidemic phase. Bernoulli [58] investigated an epidemic phase followed by an endemic phase. This appears clearly in Figures 9 and 10 of the paper by Dietz, and Heesterbeek [143] who revisited the original article of Bernoulli. We also refer to Blower [59] for another article revisiting the original work of Bernoulli. Several works comparing cumulative reported cases data and the Bernoulli–Verhulst model appear in the literature (see [215, 391, 416]). The Bernoulli–Verhulst model is sometimes called Richard's model, although Richard's work came much later in 1959.

The phenomenological model deals with data series of new infectious cases decomposed into two successive phases: 1) endemic phases followed by 2) epidemic phases.

Endemic phase: During the endemic phase, the dynamics of new cases appears to fluctuate around an average value independently of the number of cases. Therefore the average cumulative number of cases is given by

$$\mathrm{CR}(t) = N_0 + (t - t_0) \times a, \text{ for } t \in [t_0, t_1], \tag{5.6.1}$$

where t_0 denotes the beginning of the endemic phase, and a is the average value of the daily number of new cases.

We assume that the average daily number of new cases is constant. Therefore the daily number of new cases is given by

$$\mathrm{CR}'(t) = a. \tag{5.6.2}$$

Epidemic phase: In the epidemic phase, the new cases are contributing to produce secondary cases. Therefore the daily number of new cases is no longer constant, but varies with time as follows

$$\mathrm{CR}(t) = N_{\mathrm{base}} + \frac{\mathrm{e}^{\chi(t-t_0)} N_0}{\left[1 + \frac{N_0^\theta}{N_\infty^\theta}\left(\mathrm{e}^{\chi\theta(t-t_0)} - 1\right)\right]^{1/\theta}}, \text{ for } t \in [t_0, t_1]. \tag{5.6.3}$$

In other words, the daily number of new cases follows the Bernoulli–Verhulst [58, 381] equation. Namely, by setting

$$N(t) = \mathrm{CR}(t) - N_{\mathrm{base}}, \tag{5.6.4}$$

we obtain

$$N'(t) = \chi\, N(t) \left[1 - \left(\frac{N(t)}{N_\infty}\right)^\theta\right], \tag{5.6.5}$$

completed with the initial value

$$N(t_0) = N_0.$$

In the model, $N_{\mathrm{base}} + N_0$ corresponds to the value $\mathrm{CR}(t_0)$ of the cumulative number of cases at time $t = t_0$. The parameter $N_\infty + N_{\mathrm{base}}$ is the maximal value of the cumulative reported cases after the time $t = t_0$. $\chi > 0$ is a Malthusian growth parameter, and θ regulates the speed at which $\mathrm{CR}(t)$ increases to $N_\infty + N_{\mathrm{base}}$.

Regularize the junction between the epidemic phases: Because the formula for $\tau(t)$ involves derivatives of the phenomenological model regularizing $\mathrm{CR}(t)$ (see Eqs (5.6.12)–(5.6.15)), we need to connect the phenomenological models of the different phases as smoothly as possible. Let $t_0, \ldots, t_n$ denote the $n + 1$ breaking points of the model, that is, the times at which there is a transition between one phase and the next one. We let $\widetilde{\mathrm{CR}}(t)$ be the global model obtained by placing the phenomenological models of the different phases side by side.

More precisely, $\widetilde{\mathrm{CR}}(t)$ is defined by Eq (5.6.3) during an epidemic phase $[t_i, t_{i+1}]$, or during the initial phase $(-\infty, t_0]$ or the last phase $[t_n, +\infty)$. During an endemic phase, $\widetilde{\mathrm{CR}}(t)$ is defined by Eq (5.6.1). The parameters are chosen so that the resulting global model $\widetilde{\mathrm{CR}}$ is continuous. We define the regularized model by using the convolution formula:

$$\mathrm{CR}(t) = \int_{-\infty}^{+\infty} \mathcal{G}(t - s) \times \widetilde{\mathrm{CR}}(s)\mathrm{d}s = (\mathcal{G} * \widetilde{\mathrm{CR}})(t), \tag{5.6.6}$$

where

$$\mathcal{G}(t) := \frac{1}{\sigma\sqrt{2\pi}} \mathrm{e}^{-\frac{t^2}{2\sigma^2}}$$

is the Gaussian function with mean 0 and variance σ^2. The parameter σ controls the trade-off between smoothness and precision: increasing σ reduces the variations in $\mathrm{CR}(t)$ and reducing σ reduces the distance between $\mathrm{CR}(t)$ and $\widetilde{\mathrm{CR}}(t)$. In any case the resulting function $\mathrm{CR}(t)$ is very smooth (as well as its derivatives) and close to the original model $\widetilde{\mathrm{CR}}(t)$ when σ is not too large. In the results section (Section 5.6.3), we fix $\sigma = 7$ days.

Numerically, we will need to compute some $t \to \mathrm{CR}(t)$ derivatives. Therefore it is convenient to take advantage of the convolution Eq (5.6.6) and deduce that

$$\frac{\mathrm{d}^n \mathrm{CR}(t)}{\mathrm{d}t^n} = \int_{-\infty}^{+\infty} \frac{\mathrm{d}^n \mathcal{G}(t-s)}{\mathrm{d}t^n} \times \widetilde{\mathrm{CR}}(s)\mathrm{d}s, \tag{5.6.7}$$

for $n = 1, 2, 3$.

5.6.2.2 Epidemic model

To reconstruct the transmission rate, we used the underlying mathematical model described by the flowchart presented in Figure 5.6.1.

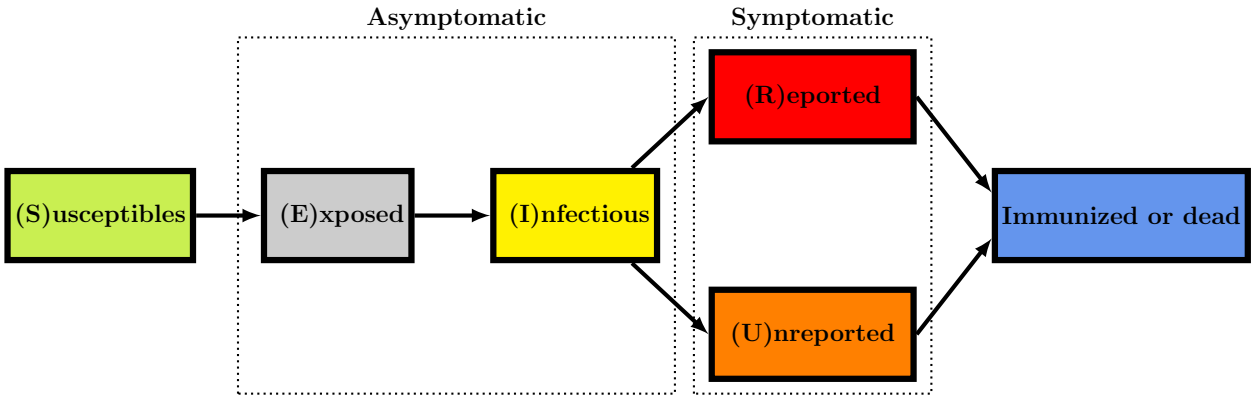

Figure 5.6.1: Flowchart for the model.

The model itself includes five parameters whose values were taken from the literature: the average length of the noninfectious incubation period (1 day, (E)xposed); the average length of the infectious incubation period (3 days, (I)nfectious); the average length of the symptomatic period (7 days, (R)eported or (U)nreported); the ascertainment rate (0.8). Additional parameters appear in the initial condition and could not be computed from the initial number of unreported individuals. The transmission rate was computed from the regularized data and the assumed parameters according to a methodology adapted from Demongeot et al. [P7].

Many epidemiological models are based on the SIR or SEIR model, which is classical in epidemic modelling. We refer to [404, 368] for the earliest articles devoted to such a question and to [12, 27, 77, 75, 76, 88, 142, 208, 231, 297, 371] for more models. In this chapter, we will compare the following SEIUR model to the cumulative reported cases data

$$\begin{cases} S'(t) = -\tau(t)\left[I(t) + \kappa\, U(t)\right] S(t), \\ E'(t) = \tau(t)\left[I(t) + \kappa\, U(t)\right] S(t) - \alpha\, E(t), \\ I'(t) = \alpha\, E(t) - \nu\, I(t), \\ U'(t) = \nu\,(1-f)\, I(t) - \eta\, U(t), \\ R'(t) = \nu\, f\, I(t) - \eta\, R(t), \end{cases} \tag{5.6.8}$$

where at time t, $S(t)$ is the number of susceptible, $E(t)$ the number of exposed (not yet capable of transmitting the pathogen), $I(t)$ the number of asymptomatic infectious, $R(t)$ the number of reported symptomatic infectious and $U(t)$ the number of unreported symptomatic infectious. This system is supplemented by initial data

$$S(t_0) = S_0,\ E(t_0) = E_0,\ I(t_0) = I_0,\ U(t_0) = U_0,\ \text{and}\ R(t_0) = R_0. \tag{5.6.9}$$

In this model, $\tau(t)$ is the rate of transmission, $1/\alpha$ is the average duration of the exposure period, $1/\nu$ is the average duration of the asymptomatic infectious period, and for simplicity, we subdivide the class of symptomatic patients into the fraction $0 \leq f \leq 1$ of patients showing some severe symptoms, and the fraction $1 - f$ of patients showing some mild symptoms assumed to be not detected. The quantity $1/\eta$ is the average duration of the symptomatic infectious period. In the model, we assume that the average time of infection is the same for Reported and Unreported infectious individuals. We refer to [230, 236] for more information about this topic. Finally, we assume that reported symptomatic individuals do not contribute significantly to the transmission of the virus.

The cumulative number of reported cases $\mathrm{CR}(t)$ is connected to the epidemic model by the following relationship

$$\mathrm{CR}(t) = \mathrm{CR}_0 + \nu\, f\, \mathrm{CI}(t),\ \text{for}\ t \geq t_0, \tag{5.6.10}$$

where

$$\mathrm{CI}(t) = \int_{t_0}^{t} I(\sigma)\mathrm{d}\sigma. \tag{5.6.11}$$

Given and estimated parameters

We assume that the following parameters of the model are known

$$S_0, U_0, R_0, f, \kappa, \alpha, \nu, \eta.$$

The goal of our method is to focus on the estimation of the three remaining parameters. Namely, knowing the parameters mentioned above, we plan to identify

$$E_0, I_0, \tau(t).$$

Computation of the rate of transmission

The transmission rate is fully determined by the parameters $\kappa, \alpha, \nu, \eta, f, S_0, E_0, I_0, U_0$, and the data that are represented by the function $t \to \mathrm{CR}(t)$, by using the three following equations

$$\tau(t) = \frac{1}{I(t) + \kappa U(t)} \times \frac{\mathrm{CE}''(t) + \alpha \mathrm{CE}'(t)}{E_0 + S_0 - \mathrm{CE}'(t) - \alpha \mathrm{CE}(t)}, \tag{5.6.12}$$

where

$$I(t) = \frac{\mathrm{CR}'(t)}{\nu\, f}, \tag{5.6.13}$$

$$\mathrm{CE}(t) = \frac{1}{\alpha\, \nu\, f}\left[\mathrm{CR}'(t) - \nu\, f\, I_0 + \nu\left(\mathrm{CR}(t) - \mathrm{CR}_0\right)\right], \tag{5.6.14}$$

$$U(t) = \mathrm{e}^{-\eta(t-t_0)} U_0 + \int_{t_0}^{t} \mathrm{e}^{-\eta(t-s)} \frac{(1-f)}{f} \mathrm{CR}'(s)\mathrm{d}s. \tag{5.6.15}$$

Instantaneous reproduction number computed for COVID-19 data We have only a single epidemic phase in the standard SI epidemic model because the epidemic exhausts the susceptible population. Here, the changes of regimes (epidemic phase versus endemic phase) are partly due to the decay in the number of susceptible. But these changes are also influenced by the changes in the transmission rate. These changes in the transmission rate are due to the limitation of contacts between individuals or to changes in climate (in summer) or other factors influencing transmissions.

In this section 5.6.2.2, we will observe that the main factors for the changes in the epidemic regimes are the changes in the transmission rate. To investigate this for the COVID-19 data, we use our method to compute the transmission rate, and we consider the *instantaneous reproduction number*

$$R_e(t) = \frac{\tau(t)S(t)}{\eta\nu}(\eta + \nu(1-f)), \tag{5.6.16}$$

and the *quasi-instantaneous reproduction number*

$$R_e^0(t) = \frac{\tau(t)S_0}{\eta\nu}(\eta + \nu(1-f)), \tag{5.6.17}$$

in which the transmission varies, but the size of the susceptible population remains constant equal to S_0. We refer to section 5.6.12 for detailed computations to obtain the Eq (5.6.16).

The comparison between $R_e(t)$ and $R_e^0(t)$ permits us to understand the contribution of the decay of the susceptible population in the variations of $R_e(t)$. Another interesting aspect is that $R_e^0(t)$ is proportional to the transmission rate $\tau(t)$. Therefore plotting $R_e^0(t)$ permits us to visualize the variation of $t \to \tau(t)$ only.

Computation of the initial value of the epidemic model Based on Eq (5.6.4), we can recover the initial number of asymptomatic infectious $I_0 = I(t_0)$ and the initial number of exposed $E_0 = E(t_0)$ for an epidemic phase starting at time t_0. Indeed by definition, we have $\mathrm{CR}'(t) = \nu f I(t)$ and therefore

$$I_0 = \frac{\mathrm{CR}'(t_0)}{\nu f} = \frac{\chi N_0 \left(1 - \left(\frac{N_0}{N_\infty}\right)^\theta\right)}{\nu f}.$$

Estimated initial number of infected

The initial number of asymptomatic infectious is given by

$$I_0 = \frac{\mathrm{CR}'(t_0)}{\nu\, f}. \tag{5.6.18}$$

In the special case of the Bernoulli–Verhulst model we obtain

$$I_0 = \frac{\chi}{\nu\, f}\, N_0 \left(1 - \left(\frac{N_0}{N_\infty}\right)^\theta\right). \tag{5.6.19}$$

By differentiating Eq (5.6.5) we deduce that

$$\begin{aligned} N''(t) &= \chi\, N'(t) \left(1 - \left(\frac{N(t)}{N_\infty}\right)^\theta\right) - \frac{\chi\theta}{N_\infty^\theta}\, N(t)\, (N(t))^{\theta-1}\, N'(t) \\ &= \chi\, N'(t) \left(1 - \left(\frac{N(t)}{N_\infty}\right)^\theta\right) - \frac{\chi\theta}{N_\infty^\theta}\, (N(t))^\theta\, N'(t), \end{aligned}$$

therefore

$$\mathrm{CR}''(t) = N''(t) = \chi^2\, N(t) \left(1 - \left(\frac{N(t)}{N_\infty}\right)^\theta\right) \left(1 - (1+\theta) \left(\frac{N(t)}{N_\infty}\right)^\theta\right).$$

By using the third equation in Eq (5.6.8) we obtain

$$E_0 = \frac{I'(t_0) + \nu I(t_0)}{\alpha} = \frac{\mathrm{CR}''(t_0) + \nu \mathrm{CR}'(t_0)}{\alpha} = \frac{N''(t_0) + \nu N'(t_0)}{\alpha}.$$

Estimated initial number of exposed

The initial number of exposed is given by

$$E_0 = \frac{\mathrm{CR}''(t_0) + \nu \mathrm{CR}'(t_0)}{\alpha}. \tag{5.6.20}$$

In the special case of the Bernoulli–Verhulst model, we obtain

$$E_0 = \frac{\chi}{\alpha\,\nu\,f} N_0 \left(1 - \left(\frac{N_0}{N_\infty}\right)^\theta\right)\left(\chi + \nu - \chi\,(1+\theta)\left(\frac{N_0}{N_\infty}\right)^\theta\right). \tag{5.6.21}$$

Theoretical formula for $\tau(t)$ We first remark that the S-equation of model (5.6.8) can be written as

$$\frac{\mathrm{d}}{\mathrm{d}t}\ln(S(t)) = \frac{S'(t)}{S(t)} = -\tau(t)\big[I(t) + \kappa U(t)\big],$$

therefore by integrating between t_0 and t we get

$$S(t) = S_0 \exp\left(-\int_{t_0}^{t} \tau(\sigma)\ [I(\sigma) + \kappa U(\sigma)]\,\mathrm{d}\sigma\right).$$

Next we plug the above formula for $S(t)$ into the E-equation of model (5.6.8) and obtain

$$\begin{aligned} E'(t) &= S_0 \exp\left(-\int_{t_0}^{t} \tau(\sigma)\ [I(\sigma) + \kappa U(\sigma)]\,\mathrm{d}\sigma\right)\tau(t)\ [I(t) + \kappa U(t)] - \alpha\,E(t) \\ &= -S_0 \frac{\mathrm{d}}{\mathrm{d}t}\left(-\int_{t_0}^{t} \tau(\sigma)\ [I(\sigma) + \kappa U(\sigma)]\,\mathrm{d}\sigma\right)\exp\left(-\int_{t_0}^{t} \tau(\sigma)\ [I(\sigma) + \kappa U(\sigma)]\,\mathrm{d}\sigma\right) \\ &\quad - \alpha\,E(t), \end{aligned}$$

and by integrating this equation between t_0 and t we obtain

$$E(t) = E_0 + S_0\left[1 - \exp\left(-\int_{t_0}^{t} \tau(\sigma)\ [I(\sigma) + \kappa U(\sigma)]\,\mathrm{d}\sigma\right)\right] - \alpha \int_{t_0}^{t} E(\sigma)\mathrm{d}\sigma. \tag{5.6.22}$$

Define the cumulative numbers of exposed, infectious and unreported individuals by

$$\mathrm{CE}(t) := \int_{t_0}^{t} E(\sigma)\mathrm{d}\sigma,\ \mathrm{CI}(t) := \int_{t_0}^{t} I(\sigma)\mathrm{d}\sigma,\ \text{and}\ \mathrm{CU}(t) := \int_{t_0}^{t} U(\sigma)\mathrm{d}\sigma,$$

and note that $\mathrm{CE}'(t) = E(t)$. We can rewrite the Eq (5.6.22) as

$$S_0 \exp\left(-\int_{t_0}^{t} \tau(\sigma)\ [I(\sigma) + \kappa U(\sigma)]\,\mathrm{d}\sigma\right) = E_0 + S_0 - \mathrm{CE}'(t) - \alpha\,\mathrm{CE}(t).$$

By taking the logarithm of both sides we obtain

$$\int_{t_0}^{t} \tau(\sigma)\ [I(\sigma) + \kappa U(\sigma)]\,\mathrm{d}\sigma = \ln(S_0) - \ln\left(E_0 + S_0 - \mathrm{CE}'(t) - \alpha\,\mathrm{CE}(t)\right),$$

and by differentiating with respect to t:

$$\tau(t)\ = \frac{1}{I(t) + \kappa U(t)} \times \frac{\mathrm{CE}''(t) + \alpha \mathrm{CE}'(t)}{E_0 + S_0 - \mathrm{CE}'(t) - \alpha\,\mathrm{CE}(t)}. \tag{5.6.23}$$

Therefore we have an explicit formula giving $\tau(t)$ as a function of $I(t)$, $U(t)$ and $\mathrm{CE}(t)$ and its derivatives. Next we explain how to identify those three remaining unknowns as a function of $\mathrm{CR}(t)$ and its derivatives. We first recall that, from Eq (5.6.10), we have

$$\mathrm{CR}(t) = \mathrm{CR}(t_0) + \nu\,f\,\mathrm{CI}(t).$$

The I-equation of model (5.6.8) can be rewritten as

$$\alpha E(t) = I'(t) + \nu I(t),$$

and by integrating this equation between t_0 and t we obtain

$$\alpha\,\mathrm{CE}(t) = \mathrm{CI}'(t) - I_0 + \nu\,\mathrm{CI}(t) = \frac{1}{\nu\, f}(\mathrm{CR}'(t) + \nu\mathrm{CR}(t) - \nu\mathrm{CR}(t_0)). \tag{5.6.24}$$

Finally, by applying the variation of constants formula to the U-equation of system (5.6.8) we obtain

$$\begin{aligned} U(t) &= \mathrm{e}^{-\eta(t-t_0)}U_0 + \int_{t_0}^{t} \mathrm{e}^{-\eta(t-s)}\nu\,(1-f)\,I(s)\mathrm{d}s \\ &= \mathrm{e}^{-\eta(t-t_0)}U_0 + \int_{t_0}^{t} \mathrm{e}^{-\eta(t-s)}\frac{1-f}{f}\mathrm{CR}'(s)\mathrm{d}s. \end{aligned} \tag{5.6.25}$$

From these computations we deduce that $\tau(t)$ can be computed thanks to Eq (5.6.23) from $\mathrm{CR}(t)$, α, ν, η, κ, f and U_0. The following theorem is a precise statement of this result.

Theorem 5.6.1. *Let $S_0 > 0$, $E_0 > 0$, $I_0 > 0$, $U_0 > 0$, $\mathrm{CR}_0 \geq 0$, α, ν, η and $f > 0$ be given. Let $t \mapsto \tau(t) \geq 0$ be a given continuous function and $t \to I(t)$ be the second component of system* (5.6.8)*. Let $\widehat{\mathrm{CR}} : [t_0, \infty) \to \mathbb{R}$ be a twice continuously differentiable function. Then*

$$\widehat{\mathrm{CR}}(t) = \mathrm{CR}_0 + \nu\, f \int_{t_0}^{t} I\,(s)\, ds, \forall t \geq t_0, \tag{5.6.26}$$

if and only if $\widehat{\mathrm{CR}}$ satisfies

$$\widehat{\mathrm{CR}}(t_0) = \mathrm{CR}_0, \tag{5.6.27}$$

$$\widehat{\mathrm{CR}}'(t_0) = \nu\, f\, I_0, \tag{5.6.28}$$

$$\widehat{\mathrm{CR}}''(t_0) + \nu\widehat{\mathrm{CR}}'(t_0) = \alpha\,\nu\, f\, E_0, \tag{5.6.29}$$

$$\widehat{\mathrm{CR}}'(t) > 0, \forall t \geq t_0, \tag{5.6.30}$$

$$\nu f\,(E_0 + S_0) - \left[\widehat{\mathrm{CR}}''(t) + \nu\widehat{\mathrm{CR}}'(t)\right] - \alpha\left[\widehat{\mathrm{CR}}'(t) - \nu\, f\, I_0 + \nu\widehat{\mathrm{CR}}(t)\right] > 0, \forall t \geq t_0, \tag{5.6.31}$$

and $\tau(t)$ is given by

$$\tau(t) = \frac{1}{\widehat{I}(t) + \kappa\widehat{U}(t)} \times \frac{\widehat{\mathrm{CE}}''(t) + \alpha\widehat{\mathrm{CE}}'(t)}{E_0 + S_0 - \widehat{\mathrm{CE}}'(t) - \alpha\widehat{\mathrm{CE}}(t)}, \tag{5.6.32}$$

where

$$\widehat{I}(t) := \frac{\widehat{\mathrm{CR}}'(t)}{\nu\, f}, \tag{5.6.33}$$

$$\widehat{\mathrm{CI}}(t) := \frac{1}{\nu\, f}\left[\widehat{\mathrm{CR}}(t) - \widehat{\mathrm{CR}}(t_0)\right], \tag{5.6.34}$$

$$\widehat{\mathrm{CE}}(t) := \frac{1}{\alpha}\left[\widehat{\mathrm{CI}}'(t) - I_0 + \nu\,\widehat{\mathrm{CI}}(t)\right] = \frac{1}{\alpha\,\nu\, f}\left[\widehat{\mathrm{CR}}'(t) - \nu\, f\, I_0 + \nu\left(\widehat{\mathrm{CR}}(t) - \mathrm{CR}_0\right)\right], \tag{5.6.35}$$

$$\widehat{U}(t) := \mathrm{e}^{-\eta(t-t_0)}U_0 + \int_{t_0}^{t} \mathrm{e}^{-\eta(t-s)}\frac{(1-f)}{f}\widehat{\mathrm{CR}}'(s)\mathrm{d}s. \tag{5.6.36}$$

Proof. Assume first that $\widehat{\mathrm{CR}}(t)$ satisfies Eq (5.6.26). Then by using the first equation of system (5.6.8) we deduce that

$$S_0 \exp\left(-\int_{t_0}^{t} \tau(\sigma)\,\left[I(\sigma) + \kappa U(\sigma)\right]\mathrm{d}\sigma\right) = E_0 + S_0 - E(t) - \alpha\mathrm{CE}(t). \tag{5.6.37}$$

Therefore

$$\begin{aligned}\int_{t_0}^{t} \tau(\sigma)\ [I(\sigma)+\kappa U(\sigma)]\,\mathrm{d}\sigma &= \ln\left[\frac{S_0}{E_0+S_0-E(t)-\alpha \mathrm{CE}(t)}\right]\\ &= \ln\left(S_0\right)-\ln\left[E_0+S_0-E(t)-\alpha \mathrm{CE}(t)\right],\end{aligned}$$

and by taking the derivative of both sides we obtain

$$\tau(t)\left[I(t)+\kappa U(t)\right]=\frac{E'(t)+\alpha E(t)}{E_0+S_0-E(t)-\alpha \mathrm{CE}(t)},$$

which is equivalent to

$$\tau(t)=\frac{E(t)}{I(t)+\kappa U(t)}\times\frac{\dfrac{E'(t)}{E(t)}+\alpha}{E_0+S_0-E(t)-\alpha \mathrm{CE}(t)}.$$

By using the fact that $E(t)=\mathrm{CE}'(t)$ and $I=\mathrm{CR}'(t)/(\nu f)$, we deduce Eq (5.6.32). By differentiating Eq (5.6.26), we get Eqs (5.6.28) and (5.6.30). Equation (5.6.29) is a consequence of the E-component of Eq (5.6.8). We get Eq (5.6.31) by combining Eqs (5.6.37) and (5.6.35) (since $\widehat{\mathrm{CE}}(t)=\mathrm{CE}(t)$).

Conversely, assume that $\tau(t)$ is given by Eq (5.6.31) and all the Eqs (5.6.27)–(5.6.36) hold. We define $\widehat{I}(t)=\widehat{\mathrm{CR}}'(t)/\nu f$ and $\widehat{\mathrm{CI}}(t)=\left(\widehat{\mathrm{CR}}(t)-\mathrm{CR}_0\right)/\nu f$. Then, by using Eq (5.6.27), we deduce that

$$\widehat{\mathrm{CI}}(t)=\int_{t_0}^{t}\widehat{I}(\sigma)\mathrm{d}\sigma, \tag{5.6.38}$$

and by using Eq (5.6.28), we deduce

$$\widehat{I}(t_0)=I_0. \tag{5.6.39}$$

Moreover, from Eq (5.6.31) and $\widehat{I}(t)=\widehat{\mathrm{CR}}'(t)/\nu f$ we deduce that

$$\tau(t)=\frac{1}{\widehat{I}(t)+\kappa\widehat{U}(t)}\times\frac{\widehat{\mathrm{CE}}''(t)+\alpha\widehat{\mathrm{CE}}'(t)}{E_0+S_0-\widehat{\mathrm{CE}}'(t)-\alpha\widehat{\mathrm{CE}}(t)}. \tag{5.6.40}$$

Multiplying Eq (5.6.40) by $\widehat{I}(t)+\kappa\widehat{U}(t)$ and integrating, we obtain

$$\begin{aligned}\int_{t_0}^{t}\tau(\sigma)\left[\widehat{I}(\sigma)+\kappa\widehat{U}(\sigma)\right]\mathrm{d}\sigma = \ &\ln\left(E_0+S_0-\widehat{\mathrm{CE}}'(t_0)-\alpha\widehat{\mathrm{CE}}(t_0)\right)\\ &-\ln\left(E_0+S_0-\widehat{\mathrm{CE}}'(t)-\alpha\widehat{\mathrm{CE}}(t)\right),\end{aligned} \tag{5.6.41}$$

where the right-hand side is well defined thanks to Eq (5.6.31). By combining Eqs (5.6.27), (5.6.28) and (5.6.35) we obtain

$$\widehat{\mathrm{CE}}(t_0)=0, \tag{5.6.42}$$

and by taking the derivative in Eq (5.6.35) we obtain

$$\widehat{\mathrm{CE}}'(t_0)=\frac{1}{\alpha\,\nu\,f}\left[\widehat{\mathrm{CR}}''(t)+\nu\widehat{\mathrm{CR}}'(t)\right]$$

therefore by using Eq (5.6.29) we deduce that

$$\widehat{\mathrm{CE}}'(t_0)=E_0. \tag{5.6.43}$$

In particular, $E_0+S_0-\widehat{\mathrm{CE}}'(t_0)-\alpha\widehat{\mathrm{CE}}(t_0)=S_0$ and, by taking the exponential of Eq (5.6.41), we obtain

$$S_0\mathrm{e}^{-\int_{t_0}^{t}\tau(\sigma)\left[\widehat{I}(\sigma)+\kappa\widehat{U}(\sigma)\right]\mathrm{d}\sigma}=E_0+S_0-\widehat{\mathrm{CE}}'(t)-\alpha\widehat{\mathrm{CE}}(t),$$

which, differentiating both sides, yields

$$\begin{aligned}-S_0\mathrm{e}^{-\int_{t_0}^{t}\tau(\sigma)\left[\widehat{I}(\sigma)+\kappa\widehat{U}(\sigma)\right]\mathrm{d}\sigma}\tau(t)\left[\widehat{I}(t)+\kappa\widehat{U}(t)\right] &= -\widehat{\mathrm{CE}}''(t)-\alpha\widehat{\mathrm{CE}}'(t)\\ &= -\widehat{E}'(t)-\alpha\widehat{E}(t),\end{aligned}$$

and therefore

$$\widehat{E}'(t) = \tau(t)\widehat{S}(t)\left[\widehat{I}(t) + \kappa\widehat{U}(t)\right] - \alpha\widehat{E}(t), \tag{5.6.44}$$

where $\widehat{E}(t) := \widehat{\mathrm{CE}}'(t)$ and $\widehat{S}(t) := S_0 \mathrm{e}^{-\int_{t_0}^{t} \tau(\sigma)\left[\widehat{I}(\sigma)+\kappa\widehat{U}(\sigma)\right]\mathrm{d}\sigma}$. Differentiating the definition of $\widehat{S}(t)$, we get

$$\widehat{S}'(t) = -\left[\widehat{I}(t) + \kappa\widehat{U}(t)\right]\widehat{S}(t). \tag{5.6.45}$$

Next the derivative of Eq (5.6.35) can be rewritten as

$$\widehat{I}'(t) = \frac{1}{\nu\, f}\widehat{\mathrm{CR}}''(t) = \alpha\widehat{\mathrm{CE}}'(t) - \nu\frac{1}{\nu\, f}\widehat{\mathrm{CR}}'(t) = \alpha\widehat{E}(t) - \nu\widehat{I}(t). \tag{5.6.46}$$

Finally, differentiating Eq (5.6.36) yields

$$\widehat{U}'(t) = \nu\,(1-f)\,\widehat{I}(t) - \eta\widehat{U}(t). \tag{5.6.47}$$

By combining Eqs (5.6.44)–(5.6.47) we see that $\big(\widehat{S}(t), \widehat{E}(t), \widehat{I}(t), \widehat{U}(t)\big)$ satisfies Eq (5.6.8) with the initial condition $\big(\widehat{S}(t_0), \widehat{E}(t_0), \widehat{I}(t_0), \widehat{U}(t_0)\big) = (S_0, E_0, I_0, U_0)$. By the uniqueness of the solutions of Eq (5.6.8) for a given initial condition, we conclude that $\big(\widehat{S}(t), \widehat{E}(t), \widehat{I}(t), \widehat{U}(t)\big) = \big(S(t), E(t), I(t), U(t)\big)$. In particular, $\mathrm{CR}(t)$ satisfies Eq (5.6.26). The proof is completed. □

Remark 5.6.2. The condition Eq (5.6.31) is equivalent to

$$E_0 + S_0 - \widehat{\mathrm{CE}}'(t) - \alpha\widehat{\mathrm{CE}}(t) > 0,\ \forall t \geq t_0.$$

Remark 5.6.3. The present computations have been previously done, in a different context, by Hadeler [196].

5.6.2.3 Computing the explicit formula for $\tau(t)$ during an epidemic phase

In this section 5.6.2.3, we assume that the curve of cumulative reported cases is given by the Bernoulli–Verhulst formula

$$N(t) := \mathrm{CR}(t) - N_{\mathrm{base}} = \frac{\mathrm{e}^{\chi(t-t_0)}N_0}{\left[1 + \frac{N_0^\theta}{N_\infty^\theta}\left(\mathrm{e}^{\chi\theta(t-t_0)} - 1\right)\right]^{1/\theta}},\ \text{for } t \in [t_0, t_1],$$

and we recall that

$$N'(t) = \chi N(t)\left(1 - \left(\frac{N(t)}{N_\infty}\right)^\theta\right).$$

Then we can compute an explicit formula for the components of the system (5.6.8). By definition we have

$$I(t) = \frac{\mathrm{CR}'(t)}{\nu f} = \frac{\chi}{\nu f}N(t)\left(1 - \left(\frac{N(t)}{N_\infty}\right)^\theta\right), \tag{5.6.48}$$

which gives

$$I'(t) = \frac{\mathrm{CR}''(t)}{\nu f} = \frac{\chi^2}{\nu f}N(t)\left(1 - \left(\frac{N(t)}{N_\infty}\right)^\theta\right)\left(1 - (1+\theta)\left(\frac{N(t)}{N_\infty}\right)^\theta\right),$$

so that by using the I-component in the system (5.6.8) we get

$$E(t) = \frac{1}{\alpha}\big(I'(t) + \nu I(t)\big) = \frac{1}{\alpha\nu f}\left(\mathrm{CR}''(t) + \nu\mathrm{CR}'(t)\right).$$

By integration, we get

$$\begin{aligned}
\mathrm{CE}(t) &= \frac{1}{\alpha\,\nu\,f}\left[\big(\mathrm{CR}'(t) - \mathrm{CR}_0'\big) + \nu\left[\mathrm{CR}(t) - \mathrm{CR}(t_0)\right]\right], \\
&= \frac{1}{\alpha\,\nu\,f}\left[\chi N(t)\left(1 - \left(\tfrac{N(t)}{N_\infty}\right)^\theta\right) - \nu\, f\, I_0 + \nu\left[N(t) - N_0\right]\right], \\
&= \frac{1}{\alpha\,\nu\,f}\left[N(t)\left(\chi + \nu - \chi\left(\frac{N(t)}{N_\infty}\right)^\theta\right) - \nu\, f\, I_0 - \nu N_0\right],
\end{aligned}$$

and since

$$\nu\, f\, I_0 = \mathrm{CR}'(t_0) = N'(t_0) = \chi\, N_0 \left(1 - \left(\frac{N_0}{N_\infty}\right)^\theta\right),$$

we obtain

$$\mathrm{CE}(t) = \frac{1}{\alpha\,\nu\, f}\left[N(t)\left(\chi+\nu-\chi\left(\frac{N(t)}{N_\infty}\right)^\theta\right) - N_0\left(\chi+\nu-\chi\left(\frac{N_0}{N_\infty}\right)^\theta\right)\right].$$

Note also that we have explicit formulas for $E(t) = \mathrm{CE}'(t)$ and $E'(t) = \mathrm{CE}''(t)$,

$$E(t) = \mathrm{CE}'(t) = \frac{\chi}{\alpha\nu f}\left[N(t)\left(1-\left(\frac{N(t)}{N_\infty}\right)^\theta\right)\left(\chi+\nu-\chi(1+\theta)\left(\frac{N(t)}{N_\infty}\right)^\theta\right)\right] \tag{5.6.49}$$

and

$$E'(t) = \mathrm{CE}''(t) = \frac{\chi^2}{\alpha\nu f}N(t)\left(1-\left(\frac{N(t)}{N_\infty}\right)^\theta\right) \times\left[\chi+\nu-(\chi(2+\theta)+\nu)(1+\theta)\left(\frac{N(t)}{N_\infty}\right)^\theta+\chi(1+\theta)(1+2\theta)\left(\frac{N(t)}{N_\infty}\right)^{2\theta}\right].$$

Next, recall the U-equation of Eq (5.6.8), that is,

$$U'(t) = \nu(1-f)I(t) - \eta U(t),$$

therefore by the variation of constant formula we have

$$\begin{aligned} U(t) &= \mathrm{e}^{-\eta(t-t_0)}U(t_0) + \int_{t_0}^t \mathrm{e}^{-\eta(t-s)}(1-f)\nu I(s)\mathrm{d}s \\ &= \mathrm{e}^{-\eta(t-t_0}U_0 + \int_{t_0}^t \mathrm{e}^{-\eta(t-s)}\frac{1-f}{f}CR'(s)\mathrm{d}s. \end{aligned} \tag{5.6.50}$$

Explicit formula for the transmission rate during an epidemic phase

The transmission rate $\tau(t)$ can be computed as

$$\tau(t) = \frac{\chi N(t)\left(1-\left(\frac{N(t)}{N_\infty}\right)^\theta\right)}{I(t)+\kappa U(t)} \times \frac{\left[A\left(\frac{N(t)}{N_\infty}\right)^{2\theta} - B\left(\frac{N(t)}{N_\infty}\right)^\theta + C\right]}{E_0+S_0-E(t)-\alpha\mathrm{CE}(t)}, \tag{5.6.51}$$

where

$$N(t) = \frac{\mathrm{e}^{\chi(t-t_0)}N_0}{\left[1+\frac{N_0^\theta}{N_\infty^\theta}\left(\mathrm{e}^{\chi\theta(t-t_0)}-1\right)\right]^{1/\theta}}, \text{ for } t \geq t_0, \tag{5.6.52}$$

and

$$A := \chi^2(1+\theta)(1+2\theta), \tag{5.6.53}$$
$$B := \chi(1+\theta)\big[\chi(2+\theta)+\nu+\alpha\big], \tag{5.6.54}$$
$$C := (\alpha+\chi)(\chi+\nu), \tag{5.6.55}$$

and $I(t)$ is given by Eq (5.6.48), $E(t)$ by Eq (5.6.49) and $U(t)$ by Eq (5.6.50).

Compatibility conditions for the positivity of the transmission rate Recall from Eq (5.6.51):

$$\tau(t) = \frac{\chi N(t)\left(1-\left(\frac{N(t)}{N_\infty}\right)^\theta\right)}{I(t)+\kappa U(t)} \times \frac{\left[A\left(\frac{N(t)}{N_\infty}\right)^{2\theta} - B\left(\frac{N(t)}{N_\infty}\right)^\theta + C\right]}{E_0+S_0-E(t)-\alpha \mathrm{CE}(t)}.$$

Here we require that the numerator and the denominator of the last fraction stay positive for all times.

Positivity of the numerator: The model is compatible with the data if the transmission rate $\tau(t)$ stays positive for all times $t \in \mathbb{R}$. The numerator

$$p(N) := AN^2 - BN + C$$

is a second-order polynomial with $N \in (0,1)$. Let $\Delta := B^2 - 4AC$ be the discriminant of $p(N)$. Since $p'(0) = -B < 0$ and

$$p'(N) = 0 \Leftrightarrow N = \frac{B}{2A}$$

we have two cases: 1) $\dfrac{B}{2A} \geq 1$; or 2) $0 < \dfrac{B}{2A} < 1$.

Case 1: If $\dfrac{B}{2A} \geq 1$, $p(N)$ is non-negative for all $N \in [0,1]$ if and only if

$$p(1) > 0 \Leftrightarrow A + C - B > 0. \tag{5.6.56}$$

Substituting A, B, C by their expression, we get

$$\begin{aligned} A+C-B &= \chi^2(1+\theta)(1+2\theta) + (\alpha+\chi)(\chi+\nu) - \chi(1+\theta)(\chi(2+\theta)+\alpha+\nu) \\ &= \chi^2 + 2\chi^2\theta + \chi^2\theta + 2\chi^2\theta^2 + \alpha\chi + \alpha\nu + \chi^2 + \chi\nu \\ &\quad - 2\chi^2 - \chi\theta - 2\chi^2\theta - \chi^2\theta^2 - \alpha\chi - \nu\chi - \alpha\chi\theta - \nu\chi\theta \\ &= \chi^2\theta^2 + \alpha\nu - \alpha\chi\theta - \nu\chi\theta \\ &= (\alpha - \chi\theta)(\nu - \chi\theta). \end{aligned}$$

Case 2: If $\dfrac{B}{2A} < 1$, $p(N)$ is non-negative for all $N \in [0,1]$ if and only if

$$p\left(\frac{B}{2A}\right)(1) > 0 \Leftrightarrow \Delta < 0 \Leftrightarrow B^2 - 4AC < 0. \tag{5.6.57}$$

Lemma 5.6.4. $\Delta < 0 \Rightarrow A + C - B > 0$.

Proof. We have

$$\Delta < 0 \Rightarrow B^2 - 4AC \leq (B-2A)^2 \Leftrightarrow B^2 - 4AC \leq B^2 - 4AB + 4A^2$$

and after simplifying the result follows. □

Positivity of the denominator: Next we turn to the denominator in the expression of τ, i.e., we want to ensure

$$E_0 + S_0 - E(t) - \alpha \mathrm{CE}(t) > 0 \text{ for all } t \in \mathbb{R}. \tag{5.6.58}$$

We let $Y := \dfrac{N(t)}{N_\infty}$ and observe that $E(t) + \alpha \mathrm{CE}(t)$ can be written as

$$\begin{aligned} E(t) + \alpha \mathrm{CE}(t) &= \frac{1}{\alpha\nu f}\big[\chi N_\infty Y(1-Y^\theta)(\chi+\nu-\chi(1+\theta)Y^\theta) \\ &\quad + \alpha N_\infty Y(\chi+\nu-\chi Y^\theta) - \alpha N_\infty Y_0(\chi+\nu-Y_0^\theta)\big] \\ &= \frac{N_\infty}{\alpha\nu f} Y\big[(\chi+\alpha)(\chi+\nu) - \chi(\alpha+\nu+\chi(2+\theta))Y^\theta + \chi^2(1+\theta)Y^{2\theta}\big] \\ &\quad - \frac{N_0}{\nu f}\left(\chi+\nu-Y_0^\theta\right), \end{aligned}$$

since we know that $A > 0$. Therefore Eq (5.6.58) becomes

$$Y\left[(\chi+\alpha)(\chi+\nu)-\chi(\chi+\nu+\chi(1+\theta)+\alpha)Y^{\theta}+\chi^2(1+\theta)Y^{2\theta}\right] \leq \frac{\alpha\nu f}{N_\infty}\left[E_0+S_0+\frac{N_0}{\nu f}\left(\chi+\nu-\left(\frac{N_0}{N_\infty}\right)^{\theta}\right)\right].$$

We let

$$g(Y) := Y\left[(\chi+\alpha)(\chi+\nu)-\chi(\alpha+\nu+\chi(2+\theta))Y^{\theta}+\chi^2(1+\theta)Y^{2\theta}\right]$$

and notice that

$$g'(Y) = (\chi+\alpha)(\chi+\nu)-\chi(1+\theta)(\alpha+\nu+\chi(2+\theta))Y^{\theta}+\chi^2(1+2\theta)(1+\theta)Y^{2\theta},$$

is exactly $p(N) := AN^2 - BN + C$.

Therefore, assuming that $A + C - B > 0$, the derivative $g'(Y)$ is positive and g is strictly increasing. So we only have to check the final value $g(1)$. We get

$$\begin{aligned}\frac{\alpha\nu f}{N_\infty}&\left(S_0+E_0+\frac{N_0}{\nu f}\left(\chi+\nu-\left(\frac{N_0}{N_\infty}\right)^{\theta}\right)\right)\\ &\geq (\chi+\alpha)(\chi+\nu)-\chi(\alpha+\nu-\chi(2+\theta))+\chi^2(1+\theta)\\ &= \chi^2+\alpha\nu+\alpha\chi+\nu\chi+\chi^2+\chi^2\theta-\alpha\chi-\nu\chi-2\chi^2-\chi^2\theta\\ &= \alpha\nu.\end{aligned}$$

Compatibility for the positivity

The SEIUR model is compatible with the data only when $\tau(t)$ stays positive for all $t \geq t_0$. Therefore the following two conditions should be met:

$$(\nu-\chi\theta)(\alpha-\chi\theta) \geq 0 \tag{5.6.59}$$

and

$$f+\frac{1}{\nu}\frac{N_0}{S_0+E_0}\left(\chi+\nu-\left(\frac{N_0}{N_\infty}\right)^{\theta}\right) \geq \frac{N_\infty}{S_0+E_0}. \tag{5.6.60}$$

Computing the explicit formula for $\tau(t)$ during an endemic phase Recall that during an endemic phase, the cumulative number of cases is assumed to be a line. Therefore,

$$\mathrm{CR}(t) = A\,(t-t_0)+B$$

and

$$\mathrm{CR}'(t) = A \text{ and } \mathrm{CR}''(t) = 0.$$

Therefore

$$I(t) = \frac{\mathrm{CR}'(t)}{\nu f} = \frac{A}{\nu f} \tag{5.6.61}$$

and

$$E(t) = \frac{I'(t)+\nu I(t)}{\alpha} = \frac{A}{\alpha f}. \tag{5.6.62}$$

Hence

$$\mathrm{CE}(t) = \frac{A}{\alpha f}\,(t-t_0)\,. \tag{5.6.63}$$

Moreover

$$U(t) = \mathrm{e}^{-\eta(t-t_0)}U_0 + \int_{t_0}^{t}\mathrm{e}^{-\eta(t-s)}\nu(1-f)I(s)ds,$$

and we obtain

$$U(t) = \mathrm{e}^{-\eta(t-t_0)}U_0 + \frac{(1-f)A}{\eta f}\left(1 - \mathrm{e}^{-\eta(t-t_0)}\right). \tag{5.6.64}$$

By combining Eqs (5.6.12) and (5.6.61)–(5.6.64) we obtain the following explicit formula.

Explicit formula for the transmission rate during an endemic phase

The transmission rate $\tau(t)$ can be computed as

$$\tau(t) = \frac{1}{\frac{A}{\nu f} + \kappa\left(\mathrm{e}^{-\eta(t-t_0)}U_0 + \frac{1-f}{\eta f}A\left(1 - \mathrm{e}^{-\eta(t-t_0)}\right)\right)} \times \frac{A}{fS_0 - A\,(t-t_0)}, \tag{5.6.65}$$

with the compatibility condition

$$t_0 \leq t < \frac{fS_0}{A} + t_0.$$

Remark 5.6.5. The above transmission rate corresponds to a constant number of daily infected A. Therefore it is impossible to maintain such a constant flux of new infected whenever the number of susceptible individuals is finite. The time $t = \frac{fS_0}{A} + t_0$ corresponds to the maximal time starting from t_0 during which we can maintain such a regime.

5.6.3 Results

5.6.3.1 Phenomenological model applied to COVID-19 data

Our method to regularize the data was applied to the eight geographic areas. The resulting curves are presented in Figure 5.6.2. The blue background color regions correspond to epidemic phases, and the yellow background color regions to endemic phases. We added a plot of the daily number of cases (black dots) and the derivative of the regularized model for comparison, even though the daily number of cases is not used in the fitting procedure. The figures show in general, an extremely good agreement between the time series of reported cases (top row, black dots) and the regularized model (top row, blue curve). The match between the daily number of cases (bottom row, black dots) and the derivative of the regularized model (bottom row, blue curve) is also excellent, even though it is not a part of the optimization process. Of course, we lose some of the information like the extremal values ("peaks") of the daily number of cases. This is because we focus on an averaged value of the number of cases. More information could be retrieved by studying statistically the variation around the phenomenological model. However, we leave such a study for future work. The relative error between the regularized curve and the data may be relatively high at the beginning of the epidemic because of the stochastic nature of the infection process and the small number of infected individuals but quickly drops below 1% (see the supplementary material for more details).

5.6.3.2 Bounds for the value of non-identifiable parameters

Even if some parameters of the mathematical model are not identifiable, we were able to gain some information on possible values for those parameters. Indeed, a mathematical model with a negative transmission rate $\tau(t)$ cannot be consistent with the real phenomenon. Therefore, parameter values which produce such negative transmission rates cannot be compatible with the data. Using this argument, we found that the average incubation period cannot exceed eight days. The actual value of the upper bound is highly variable across countries and epidemic waves. We report the values of the upper bound in section 5.6.11 of the supplementary material.

5.6.3.3 Instantaneous reproduction number computed for COVID-19 data

Our analysis allows us to compute the instantaneous transmission rate $\tau(t)$. We use this transmission rate to compute two different indicators of the epidemiological dynamics for each geographic area, the instantaneous reproduction number and the quasi-instantaneous reproduction number. Both coincide with the basic reproduction number R_0 on the first day of the epidemic. The instantaneous reproduction number

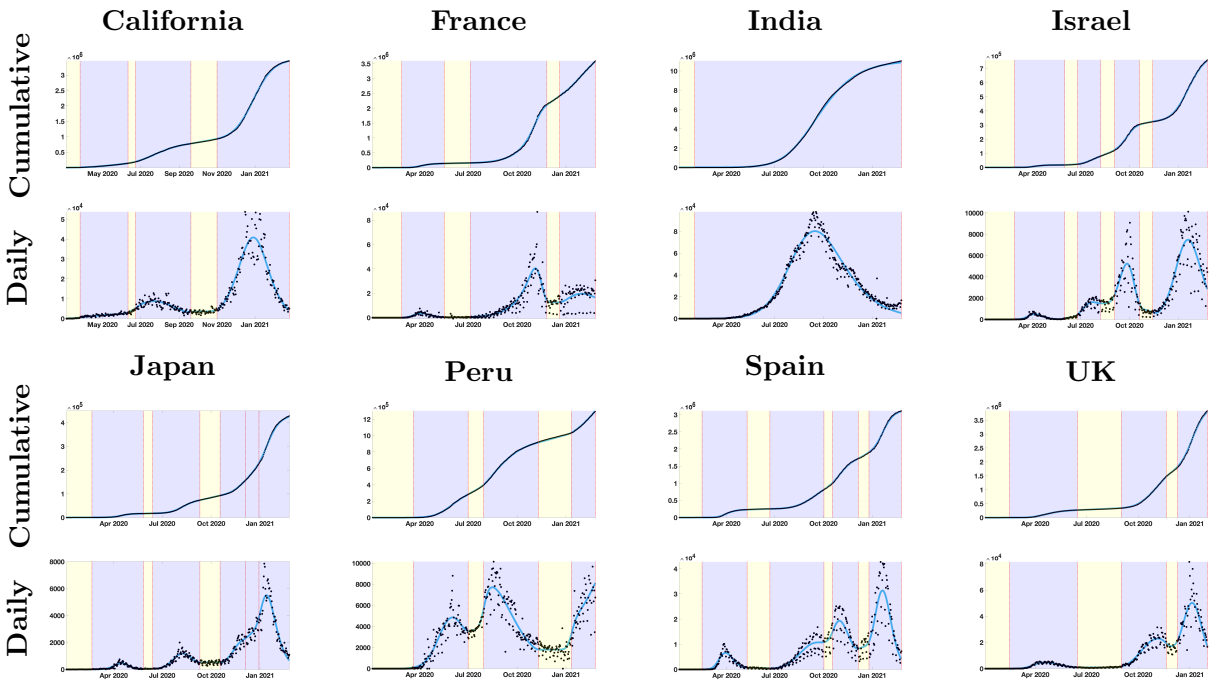

Figure 5.6.2: In the top rows, we plot the cumulative number of reported cases (black dots) and the best fit of the phenomenological model (blue curve). In the bottom rows, we plot the daily number of reported cases (black dots) and the first derivative of the phenomenological model (blue curve).

at time t, $R_e(t)$, is the basic reproduction number corresponding to an epidemic starting at time t with a constant transmission rate equal to $\tau(t)$ and with an initial population of susceptibles composed of $S(t)$ individuals (the number of susceptible individuals remaining in the population). The quasi-instantaneous reproduction number at time t, $R_e^0(t)$, is the basic reproduction number corresponding to an epidemic starting at time t with a constant transmission rate equal to $\tau(t)$ and with an initial population of susceptibles composed of S_0 individuals (the number of susceptible individuals at the start of the epidemic). The two indicators are represented for each geographic area in the top row of Figure 5.6.3 (black curve: instantaneous reproduction number; green curve: quasi-instantaneous reproduction number).

There is one interpretation for $R_e(t)$ and another for $R_e^0(t)$. The instantaneous reproduction number indicates if, given the current state of the population, the epidemic tends to persist or die out in the long term (note that our model assumes that recovered individuals are perfectly immunized). The quasi-instantaneous reproduction number indicates if the epidemic tends to persist or die out in the long term, provided the number of susceptible is the total population. In other words, we forget about the immunity already obtained by recovered individuals. Also, it is directly proportional to the transmission rate and therefore allows monitoring of its changes. Note that the value of $R_e^0(t)$ changed drastically between epidemic phases, revealing that $\tau(t)$ is far from constant. In any case, the difference between the two values starts to be visible in the figures one year after the start of the epidemic.

We also computed the reproduction number by using the method described in Cori et al [116], which we denote $R_e^c(t)$. The precise implementation is described in the supplementary material. It is plotted in the bottom row of Figure 5.6.3 (green curve), along with the instantaneous reproduction number $R_e(t)$ (green curve).

Remark 5.6.6. In the bottom of Figure 5.6.3, we compare the instantaneous reproduction numbers obtained by our method in black and the classical method of Cori et al. [116] in green. We observe that the two approaches are not the same at the beginning. This is because the method of Cori et al. [116] does not take into account the initial values I_0 and E_0 while we do. Indeed the method of Cori et al. [116] assumes that I_0 and E_0 are close to 0 at the beginning when it is viewed as a Volterra equation reformulation of the

Bernoulli–Kermack–McKendrick model with the age of infection. Our method, on the other hand, does not require such an assumption since it provides a way to compute the initial states I_0 and E_0.

Remark 5.6.7. It is essential to "regularize" the data to obtain a comprehensive outcome from SIR epidemic models. In general, the rate of transmission in the SIR model (applying identification methods) is not very noisy and meaningless. For example, at the beginning of the first epidemic wave, the transmission rate should be decreasing since peoples tend to have less and less contact while to epidemic growth. The standard regularization methods (like, for example, the rolling weekly average method) have been tested for COVID-19 data in Demongeot, Griette, and Magal [P7]. The outcome in terms of transmission rate is very noisy and even negative transmission (which is impossible). Regularizing the data is not an easy task, and the method used is very important in order to obtain a meaningful outcome for the models. Here, we tried several approaches to link an epidemic phase to the next endemic phase. So far, this regularization procedure is the best one.

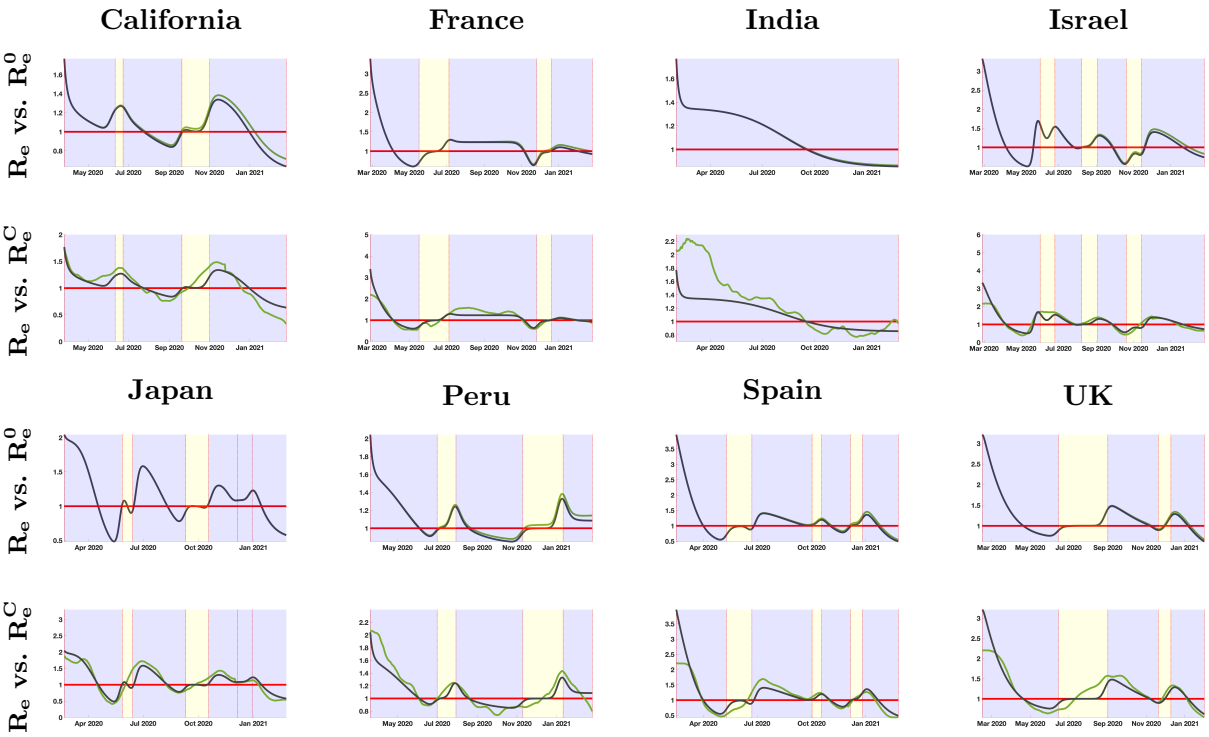

Figure 5.6.3: In the top rows, we plot the instantaneous reproduction number $R_e(t)$ (in black) and the quasi instantaneous reproduction number $R_e^0(t)$ (in green). In the bottom rows, we plot the instantaneous reproduction number $R_e(t)$ (in black) and the one obtained by the standard method [116, 350] $R_e^c(t)$ (in green).

5.6.3.4 Consequences for vaccination

It is essential to "regularize" the data to obtain a comprehensive outcome from SIR epidemic models. In general, the rate of transmission in the SIR model (applying identification methods) is not very noisy and meaningless. For example, at the beginning of the first epidemic wave, the transmission rate should be decreasing since peoples tend to have less and less contact while to epidemic growth. The standard regularization methods (like, for example, the rolling weekly average method) have been tested for COVID-19 data in Demongeot, Griette, and Magal [P7]. The outcome in terms of transmission rate is very noisy and even negative transmission (which is impossible). Regularizing the data is not an easy task, and the method used is critical in order to obtain a meaningful outcome for the models. Here, we tried several approaches

to link an epidemic phase to the next endemic phase. So far, this regularization procedure is the best one we tested.

5.6.4 Discussion

In this section 5.6, we presented a new phenomenological model to describe cumulative reported cases data. This model allows us to handle multiple epidemic waves and fits the data for the eight geographic areas considered very well. The use of Bernoulli-Verhulst curves to fit an epidemic wave is not necessary. We expect that a number of different phenomenological models could be employed for the same purpose; however, our method has the advantage of involving a limited number of parameters. Moreover, the Bernoulli-Verhulst model leads to an explicit algebraic formula for the compatibility conditions of non-identifiable parameters. It is far from obvious that the same computations can be carried out with other models. Our method also provides a very smooth curve with controlled upper bound for the first (four) derivatives, and we use the regularity obtained to compute the transmission rate. We refer to Demongeot, Griette, and Magal [P7] for several examples of problems that may occur when using other methods to regularize the data (rolling weekly average, etc.).

The first goal of the section 5.6 was to understand how to connect successive epidemic waves. As far as we know, this is new compared to the existing literature. A succession of epidemic waves separated by a short period of time with random transmissions is regularly observed in the COVID-19 epidemic data. But several consecutive epidemic phases may happen without endemic transition. An illustration of this situation is provided by the case of Japan, where the parameters of the Bernoulli-Verhulst model changed three times during the last epidemic phases (without endemic interruption). Therefore we subdivide this last epidemic wave into three epidemic phases.

Another advantage of our method is the connection with an epidemiological model. Our study provides a way to explain the data by using a single epidemic model with a time-dependent transmission rate. More precisely, we find that there exists precisely one model that matches the best fit to the data. The fact that the transmission rate corresponding to the data is not constant is, therefore, meaningful. This means that the depletion of susceptible hosts due to natural epidemiological dynamics is not sufficient to explain the reduction in the epidemic spread. Indeed, due to the social changes involving the distancing between individuals, the transmission rate should vary to take into account the changes in the number of contacts per unit of time. The variations in the observed dynamics of the number of cases mainly result from the modification of people's behavior. In other words, the social changes in the population have a stronger impact on the propagation of the disease than the pure epidemiological dynamics. By computing the transmission rate and the associated reproduction numbers, we propose a new method to quantify those social changes. Other factors may also influence the dynamics of the COVID-19 outbreak (temperature, humidity, etc.) and should be taken into account. However, the correlation between the dates of the waves and the mitigation measures imposed by local governments suggests that the former phenomenon takes a more significant role in the epidemiological dynamics.

Precisely because it involves an epidemiological model, our method provides an alternative, robust way to compute indicators for the future behavior of the epidemic: the instantaneous and quasi-instantaneous reproductive numbers $R_e(t)$ and $R_e^0(t)$. It is natural to compare them to an alternative in the literature, sometimes called "effective reproductive number". The method of Cori et al. [116] is a popular framework to estimate its value. Compared with this standard method, our indicators perform better near the beginning of the epidemic and close to the last data point and are less variable in time. That we require an *a priori* definition of epidemic waves can be considered as an advantage and a drawback. It is a drawback because the computed value of the indicator may slightly depend on the choice of the dates of the epidemic waves. On the other hand, this flexibility also allows testing different scenarios for the future evolution of the epidemic. Thanks to the explicit formula for $R_e(t)$ expressed in function of the parameters, we can also explore the dependency to the parameters (see supplementary material section 5.6.10).

It appears from our results that the instantaneous reproduction number in almost every geographic area considered is less than 3.5. Therefore, an efficient policy to eliminate the COVID-19 would be to vaccinate a fraction of $75 - 80\%$ of the population. Once this threshold is reached, the situation should go back to normal in all the geographic areas considered in this study. This proportion can even be reduced at the expense of partially maintaining the social distancing and the other anti-COVID measures for a sufficiently long period of time.

With a few modifications, our method could also include several other features. It is likely, for instance, that the vaccination of a large part of the population has an impact on the epidemiological dynamics, and

this impact is not taken into account for the time being. Different distributions of serial intervals could be taken into account by replacing the mathematical model of ordinary differential equations with integral equations. What we have shown is that the coupling of a phenomenological model to describe the data, with an epidemiological model to take into account the nature of the underlying phenomenon, should provide us with a new, untapped source of information on the epidemic.

Appendix

5.6.5 Table of estimated parameters for the phenomenological model

5.6.5.1 California

Table 5.6.1: In this table we list the parameters of the phenomenological model which gives the best fit to the cumulative number of cases data in California from January 03 2020 to February 25 2021.

Period	Parameters value	Method	95% Confidence interval
Period 1: Epidemic phase Mar 26, 2020 - Jun 11, 2020	$N_0 = 7.34 \times 10^3$	fitted	$N_0 \in [4.16 \times 10^3, 1.05 \times 10^4]$
	$N_{base} = 1.14 \times 10^{-5}$	fitted	$N_{base} \in [-4.33 \times 10^3, 4.33 \times 10^3]$
	$N_\infty = 3.24 \times 10^5$	fitted	$N_\infty \in [2.52 \times 10^5, 3.96 \times 10^5]$
	$\chi = 4.14 \times 10^4$	fitted	$\chi \in [7.74 \times 10^2, 8.20 \times 10^4]$
	$\theta = 4.62 \times 10^{-7}$	fitted	$\theta \in [2.39 \times 10^{-8}, 9.00 \times 10^{-7}]$
Period 2: Endemic phase Jun 11, 2020 - Jun 23, 2020	$a = 3.81 \times 10^3$	computed	
	$N_0 = 1.36 \times 10^5$	computed	
Period 3: Epidemic phase Jun 23, 2020 - Sep 20, 2020	$N_0 = 1.57 \times 10^5$	fitted	$N_0 \in [5.96 \times 10^4, 2.55 \times 10^5]$
	$N_{base} = 2.45 \times 10^4$	fitted	$N_{base} \in [-7.58 \times 10^4, 1.25 \times 10^5]$
	$N_\infty = 8.22 \times 10^5$	fitted	$N_\infty \in [7.36 \times 10^5, 9.08 \times 10^5]$
	$\chi = 5.54 \times 10^{-2}$	fitted	$\chi \in [5.32 \times 10^{-3}, 1.05 \times 10^{-1}]$
	$\theta = 7.18 \times 10^{-1}$	fitted	$\theta \in [-3.59 \times 10^{-2}, 1.47]$
Period 4: Endemic phase Sep 20, 2020 - Nov 01, 2020	$a = 3.66 \times 10^3$	computed	
	$N_0 = 7.76 \times 10^5$	computed	
Period 5: Epidemic phase Nov 01, 2020 - Feb 25, 2021	$N_0 = 6.27 \times 10^4$	fitted	$N_0 \in [4.95 \times 10^4, 7.59 \times 10^4]$
	$N_{base} = 8.67 \times 10^5$	fitted	$N_{base} \in [8.45 \times 10^5, 8.88 \times 10^5]$
	$N_\infty = 2.66 \times 10^6$	fitted	$N_\infty \in [2.64 \times 10^6, 2.67 \times 10^6]$
	$\chi = 6.36 \times 10^{-2}$	fitted	$\chi \in [5.73 \times 10^{-2}, 6.98 \times 10^{-2}]$
	$\theta = 1.02$	fitted	$\theta \in [8.79 \times 10^{-1}, 1.16]$

5.6.5.2 France

Table 5.6.2: In this table we list the parameters of the phenomenological model which gives the best fit to the cumulative number of cases data in France from January 03 2020 to February 25 2021.

Period	Parameters value	Method	95% Confidence interval
Period 1: Epidemic phase Feb 27, 2020 - May 17, 2020	$N_0 = 3.61 \times 10^{-4}$	fitted	$N_0 \in [-3.77, 3.77]$
	$N_{base} = 0.00$	fixed	
	$N_\infty = 1.43 \times 10^5$	fitted	$N_\infty \in [-1.58 \times 10^4, 3.01 \times 10^5]$
	$\chi = 1.17 \times 10^2$	fitted	$\chi \in [-1.09 \times 10^7, 1.09 \times 10^7]$
	$\theta = 7.29 \times 10^{-4}$	fitted	$\theta \in [-6.84 \times 10^1, 6.84 \times 10^1]$
Period 2: Endemic phase May 17, 2020 - Jul 05, 2020	$a = 3.14 \times 10^2$	computed	
	$N_0 = 1.39 \times 10^5$	computed	
Period 3: Epidemic phase Jul 05, 2020 - Nov 26, 2020	$N_0 = 1.50 \times 10^4$	fitted	$N_0 \in [1.36 \times 10^4, 1.65 \times 10^4]$
	$N_{base} = 1.40 \times 10^5$	fitted	$N_{base} \in [1.33 \times 10^5, 1.46 \times 10^5]$
	$N_\infty = 1.99 \times 10^6$	fitted	$N_\infty \in [1.97 \times 10^6, 2.01 \times 10^6]$
	$\chi = 3.68 \times 10^{-2}$	fitted	$\chi \in [3.60 \times 10^{-2}, 3.76 \times 10^{-2}]$
	$\theta = 6.55$	fitted	$\theta \in [5.52, 7.58]$
Period 4: Endemic phase Nov 26, 2020 - Dec 20, 2020	$a = 1.28 \times 10^4$	computed	
	$N_0 = 2.11 \times 10^6$	computed	
Period 5: Epidemic phase Dec 20, 2020 - Feb 25, 2021	$N_0 = 2.73 \times 10^5$	fitted	$N_0 \in [-2.43 \times 10^3, 5.48 \times 10^5]$
	$N_{base} = 2.15 \times 10^6$	fitted	$N_{base} \in [1.86 \times 10^6, 2.43 \times 10^6]$
	$N_\infty = 2.13 \times 10^6$	fitted	$N_\infty \in [1.88 \times 10^6, 2.39 \times 10^6]$
	$\chi = 5.88 \times 10^{-2}$	fitted	$\chi \in [-6.11 \times 10^{-2}, 1.79 \times 10^{-1}]$
	$\theta = 5.47 \times 10^{-1}$	fitted	$\theta \in [-9.19 \times 10^{-1}, 2.01]$

5.6.5.3 India

Period	Parameters value	Method	95% Confidence interval
Period 1: Epidemic phase Feb 01, 2020 - Feb 25, 2021	$N_0 = 5.83 \times 10^2$	fitted	$N_0 \in [3.45 \times 10^2, 8.20 \times 10^2]$
	$N_{base} = 1.97 \times 10^4$	fitted	$N_{base} \in [5.36 \times 10^3, 3.39 \times 10^4]$
	$N_\infty = 1.10 \times 10^7$	fitted	$N_\infty \in [1.10 \times 10^7, 1.11 \times 10^7]$
	$\chi = 4.89 \times 10^{-2}$	fitted	$\chi \in [4.59 \times 10^{-2}, 5.20 \times 10^{-2}]$
	$\theta = 5.12 \times 10^{-1}$	fitted	$\theta \in [4.71 \times 10^{-1}, 5.54 \times 10^{-1}]$

Table 5.6.3: In this table we list the parameters of the phenomenological model which gives the best fit to the cumulative number of cases data in India from January 03 2020 to February 25 2021.

5.6.5.4 Israel

Period	Parameters value	Method	95% Confidence interval
Period 1: Epidemic phase Feb 27, 2020 - Jun 01, 2020	$N_0 = 1.08 \times 10^{-2}$	fitted	$N_0 \in [-3.85 \times 10^{-2}, 6.02 \times 10^{-2}]$
	$N_{base} = 4.27 \times 10^{1}$	fitted	$N_{base} \in [-3.36 \times 10^{1}, 1.19 \times 10^{2}]$
	$N_\infty = 1.71 \times 10^{4}$	fitted	$N_\infty \in [1.70 \times 10^{4}, 1.72 \times 10^{4}]$
	$\chi = 9.18 \times 10^{-1}$	fitted	$\chi \in [1.71 \times 10^{-1}, 1.67]$
	$\theta = 1.05 \times 10^{-1}$	fitted	$\theta \in [1.55 \times 10^{-2}, 1.94 \times 10^{-1}]$
Period 2: Endemic phase Jun 01, 2020 - Jun 25, 2020	$a = 2.04 \times 10^{2}$	computed	
	$N_0 = 1.70 \times 10^{4}$	computed	
Period 3: Epidemic phase Jun 25, 2020 - Aug 08, 2020	$N_0 = 2.48 \times 10^{3}$	fitted	$N_0 \in [3.43 \times 10^{2}, 4.61 \times 10^{3}]$
	$N_{base} = 1.95 \times 10^{4}$	fitted	$N_{base} \in [1.70 \times 10^{4}, 2.20 \times 10^{4}]$
	$N_\infty = 8.66 \times 10^{4}$	fitted	$N_\infty \in [7.78 \times 10^{4}, 9.55 \times 10^{4}]$
	$\chi = 2.93 \times 10^{-1}$	fitted	$\chi \in [-2.61 \times 10^{-1}, 8.48 \times 10^{-1}]$
	$\theta = 2.04 \times 10^{-1}$	fitted	$\theta \in [-2.43 \times 10^{-1}, 6.50 \times 10^{-1}]$
Period 4: Endemic phase Aug 08, 2020 - Sep 03, 2020	$a = 1.54 \times 10^{3}$	computed	
	$N_0 = 7.97 \times 10^{4}$	computed	
Period 5: Epidemic phase Sep 03, 2020 - Oct 20, 2020	$N_0 = 4.59 \times 10^{4}$	fitted	$N_0 \in [2.88 \times 10^{4}, 6.31 \times 10^{4}]$
	$N_{base} = 7.38 \times 10^{4}$	fitted	$N_{base} \in [5.53 \times 10^{4}, 9.23 \times 10^{4}]$
	$N_\infty = 2.35 \times 10^{5}$	fitted	$N_\infty \in [2.19 \times 10^{5}, 2.52 \times 10^{5}]$
	$\chi = 5.05 \times 10^{-2}$	fitted	$\chi \in [3.77 \times 10^{-2}, 6.34 \times 10^{-2}]$
	$\theta = 3.45$	fitted	$\theta \in [1.96, 4.93]$
Period 6: Endemic phase Oct 20, 2020 - Nov 14, 2020	$a = 8.90 \times 10^{2}$	computed	
	$N_0 = 3.04 \times 10^{5}$	computed	
Period 7: Epidemic phase Nov 14, 2020 - Feb 25, 2021	$N_0 = 3.16 \times 10^{3}$	fitted	$N_0 \in [2.16 \times 10^{3}, 4.17 \times 10^{3}]$
	$N_{base} = 3.23 \times 10^{5}$	fitted	$N_{base} \in [3.21 \times 10^{5}, 3.25 \times 10^{5}]$
	$N_\infty = 4.87 \times 10^{5}$	fitted	$N_\infty \in [4.79 \times 10^{5}, 4.95 \times 10^{5}]$
	$\chi = 8.28 \times 10^{-2}$	fitted	$\chi \in [7.22 \times 10^{-2}, 9.34 \times 10^{-2}]$
	$\theta = 7.06 \times 10^{-1}$	fitted	$\theta \in [5.69 \times 10^{-1}, 8.43 \times 10^{-1}]$

Table 5.6.4: In this table we list the parameters of the phenomenological model which gives the best fit to the cumulative number of cases data in Israel from January 03 2020 to February 25 2021.

5.6.5.5 Japan

Period	Parameters value	Method	95% Confidence interval
Period 1: Epidemic phase Feb 20, 2020 - May 27, 2020	$N_0 = 5.83$	fitted	$N_0 \in [1.91, 9.74]$
	$N_{base} = 3.25 \times 10^2$	fitted	$N_{base} \in [2.55 \times 10^2, 3.95 \times 10^2]$
	$N_\infty = 1.63 \times 10^4$	fitted	$N_\infty \in [1.62 \times 10^4, 1.64 \times 10^4]$
	$\chi = 1.48 \times 10^{-1}$	fitted	$\chi \in [1.30 \times 10^{-1}, 1.65 \times 10^{-1}]$
	$\theta = 8.29 \times 10^{-1}$	fitted	$\theta \in [6.88 \times 10^{-1}, 9.70 \times 10^{-1}]$
Period 2: Endemic phase May 27, 2020 - Jun 13, 2020	$a = 7.07 \times 10^1$	computed	
	$N_0 = 1.65 \times 10^4$	computed	
Period 3: Epidemic phase Jun 13, 2020 - Sep 10, 2020	$N_0 = 1.49 \times 10^2$	fitted	$N_0 \in [8.52 \times 10^1, 2.13 \times 10^2]$
	$N_{base} = 1.75 \times 10^4$	fitted	$N_{base} \in [1.73 \times 10^4, 1.78 \times 10^4]$
	$N_\infty = 6.02 \times 10^4$	fitted	$N_\infty \in [5.93 \times 10^4, 6.10 \times 10^4]$
	$\chi = 1.19 \times 10^{-1}$	fitted	$\chi \in [1.03 \times 10^{-1}, 1.35 \times 10^{-1}]$
	$\theta = 6.28 \times 10^{-1}$	fitted	$\theta \in [5.04 \times 10^{-1}, 7.52 \times 10^{-1}]$
Period 4: Endemic phase Sep 10, 2020 - Oct 18, 2020	$a = 5.36 \times 10^2$	computed	
	$N_0 = 7.27 \times 10^4$	computed	
Period 5: Epidemic phase Oct 18, 2020 - Dec 05, 2020	$N_0 = 6.33 \times 10^3$	fitted	$N_0 \in [4.64 \times 10^3, 8.01 \times 10^3]$
	$N_{base} = 8.68 \times 10^4$	fitted	$N_{base} \in [8.48 \times 10^4, 8.88 \times 10^4]$
	$N_\infty = 9.10 \times 10^4$	fitted	$N_\infty \in [7.75 \times 10^4, 1.05 \times 10^5]$
	$\chi = 5.60 \times 10^{-2}$	fitted	$\chi \in [4.74 \times 10^{-2}, 6.46 \times 10^{-2}]$
	$\theta = 2.58$	fitted	$\theta \in [1.00, 4.16]$
Period 6: Epidemic phase Dec 05, 2020 - Dec 30, 2020	$N_0 = 1.23 \times 10^5$	fitted	$N_0 \in [-2.43 \times 10^5, 4.90 \times 10^5]$
	$N_{base} = 3.43 \times 10^4$	fitted	$N_{base} \in [-3.33 \times 10^5, 4.01 \times 10^5]$
	$N_\infty = 3.49 \times 10^5$	fitted	$N_\infty \in [-2.92 \times 10^7, 2.99 \times 10^7]$
	$\chi = 1.78 \times 10^{-2}$	fitted	$\chi \in [-3.59 \times 10^{-2}, 7.15 \times 10^{-2}]$
	$\theta = 7.84$	fitted	$\theta \in [-1.28 \times 10^3, 1.30 \times 10^3]$
Period 7: Epidemic phase Dec 30, 2020 - Feb 25, 2021	$N_0 = 2.00 \times 10^4$	fitted	$N_0 \in [1.59 \times 10^3, 3.84 \times 10^4]$
	$N_{base} = 2.05 \times 10^5$	fitted	$N_{base} \in [1.85 \times 10^5, 2.25 \times 10^5]$
	$N_\infty = 2.29 \times 10^5$	fitted	$N_\infty \in [2.11 \times 10^5, 2.47 \times 10^5]$
	$\chi = 7.98 \times 10^{-1}$	fitted	$\chi \in [-2.54, 4.13]$
	$\theta = 9.61 \times 10^{-2}$	fitted	$\theta \in [-3.15 \times 10^{-1}, 5.07 \times 10^{-1}]$

Table 5.6.5: In this table we list the parameters of the phenomenological model which gives the best fit to the cumulative number of cases data in Japan from January 03 2020 to February 25 2021.

5.6.5.6 Peru

Period	Parameters value	Method	95% Confidence interval
Period 1: Epidemic phase Mar 20, 2020 - Jul 01, 2020	$N_0 = 8.36 \times 10^2$	fitted	$N_0 \in [2.63 \times 10^2, 1.41 \times 10^3]$
	$N_{base} = 3.00 \times 10^{-5}$	fitted	$N_{base} \in [-1.74 \times 10^3, 1.74 \times 10^3]$
	$N_\infty = 3.61 \times 10^5$	fitted	$N_\infty \in [3.44 \times 10^5, 3.79 \times 10^5]$
	$\chi = 1.08 \times 10^{-1}$	fitted	$\chi \in [7.59 \times 10^{-2}, 1.41 \times 10^{-1}]$
	$\theta = 4.20 \times 10^{-1}$	fitted	$\theta \in [2.41 \times 10^{-1}, 5.98 \times 10^{-1}]$
Period 2: Endemic phase Jul 01, 2020 - Jul 30, 2020	$a = 3.67 \times 10^3$	computed	
	$N_0 = 2.83 \times 10^5$	computed	
Period 3: Epidemic phase Jul 30, 2020 - Nov 10, 2020	$N_0 = 1.86 \times 10^5$	fitted	$N_0 \in [-2.61 \times 10^4, 3.98 \times 10^5]$
	$N_{base} = 2.03 \times 10^5$	fitted	$N_{base} \in [-1.11 \times 10^4, 4.18 \times 10^5]$
	$N_\infty = 7.69 \times 10^5$	fitted	$N_\infty \in [5.65 \times 10^5, 9.72 \times 10^5]$
	$\chi = 4.84 \times 10^{-1}$	fitted	$\chi \in [-6.23, 7.20]$
	$\theta = 5.95 \times 10^{-2}$	fitted	$\theta \in [-7.74 \times 10^{-1}, 8.93 \times 10^{-1}]$
Period 4: Endemic phase Nov 10, 2020 - Jan 11, 2021	$a = 1.80 \times 10^3$	computed	
	$N_0 = 9.16 \times 10^5$	computed	
Period 5: Epidemic phase Jan 11, 2021 - Feb 25, 2021	$N_0 = 3.23 \times 10^5$	fitted	
	$N_{base} = 7.04 \times 10^5$	fitted	
	$N_\infty = 7.00 \times 10^6$	fitted	
	$\chi = 1.36 \times 10^{-2}$	fitted	
	$\theta = 3.67 \times 10^1$	fitted	

Table 5.6.6: In this table we list the parameters of the phenomenological model which gives the best fit to the cumulative number of cases data in Peru from January 03 2020 to February 25 2021.

5.6.5.7 Spain

Period	Parameters value	Method	95% Confidence interval
Period 1: Epidemic phase Feb 15, 2020 - May 10, 2020	$N_0 = 5.19 \times 10^{-4}$	fitted	$N_0 \in [-5.00 \times 10^{-3}, 6.04 \times 10^{-3}]$
	$N_{base} = 5.77 \times 10^{2}$	fitted	$N_{base} \in [-4.50 \times 10^{2}, 1.60 \times 10^{3}]$
	$N_\infty = 2.32 \times 10^{5}$	fitted	$N_\infty \in [2.30 \times 10^{5}, 2.34 \times 10^{5}]$
	$\chi = 9.80 \times 10^{-1}$	fitted	$\chi \in [-1.26 \times 10^{-1}, 2.09]$
	$\theta = 9.75 \times 10^{-2}$	fitted	$\theta \in [-1.83 \times 10^{-2}, 2.13 \times 10^{-1}]$
Period 2: Endemic phase May 10, 2020 - Jun 22, 2020	$a = 5.67 \times 10^{2}$	computed	
	$N_0 = 2.28 \times 10^{5}$	computed	
Period 3: Epidemic phase Jun 22, 2020 - Oct 02, 2020	$N_0 = 2.38 \times 10^{3}$	fitted	$N_0 \in [1.39 \times 10^{3}, 3.36 \times 10^{3}]$
	$N_{base} = 2.50 \times 10^{5}$	fitted	$N_{base} \in [2.48 \times 10^{5}, 2.53 \times 10^{5}]$
	$N_\infty = 9.89 \times 10^{5}$	fitted	$N_\infty \in [9.02 \times 10^{5}, 1.08 \times 10^{6}]$
	$\chi = 9.29 \times 10^{-2}$	fitted	$\chi \in [7.07 \times 10^{-2}, 1.15 \times 10^{-1}]$
	$\theta = 3.84 \times 10^{-1}$	fitted	$\theta \in [2.38 \times 10^{-1}, 5.29 \times 10^{-1}]$
Period 4: Endemic phase Oct 02, 2020 - Oct 18, 2020	$a = 1.09 \times 10^{4}$	computed	
	$N_0 = 8.14 \times 10^{5}$	computed	
Period 5: Epidemic phase Oct 18, 2020 - Dec 06, 2020	$N_0 = 1.68 \times 10^{5}$	fitted	$N_0 \in [-3.50 \times 10^{4}, 3.72 \times 10^{5}]$
	$N_{base} = 8.20 \times 10^{5}$	fitted	$N_{base} \in [6.12 \times 10^{5}, 1.03 \times 10^{6}]$
	$N_\infty = 9.85 \times 10^{5}$	fitted	$N_\infty \in [8.01 \times 10^{5}, 1.17 \times 10^{6}]$
	$\chi = 3.15 \times 10^{-1}$	fitted	$\chi \in [-1.05, 1.68]$
	$\theta = 2.02 \times 10^{-1}$	fitted	$\theta \in [-7.15 \times 10^{-1}, 1.12]$
Period 6: Endemic phase Dec 06, 2020 - Dec 26, 2020	$a = 9.15 \times 10^{3}$	computed	
	$N_0 = 1.72 \times 10^{6}$	computed	
Period 7: Epidemic phase Dec 26, 2020 - Feb 25, 2021	$N_0 = 5.94 \times 10^{4}$	fitted	$N_0 \in [3.86 \times 10^{4}, 8.02 \times 10^{4}]$
	$N_{base} = 1.84 \times 10^{6}$	fitted	$N_{base} \in [1.81 \times 10^{6}, 1.87 \times 10^{6}]$
	$N_\infty = 1.30 \times 10^{6}$	fitted	$N_\infty \in [1.28 \times 10^{6}, 1.32 \times 10^{6}]$
	$\chi = 1.30 \times 10^{-1}$	fitted	$\chi \in [9.90 \times 10^{-2}, 1.60 \times 10^{-1}]$
	$\theta = 7.84 \times 10^{-1}$	fitted	$\theta \in [5.50 \times 10^{-1}, 1.02]$

Table 5.6.7: In this table we list the parameters of the phenomenological model which gives the best fit to the cumulative number of cases data in Spain from January 03 2020 to February 01 2021.

5.6.5.8 United Kingdom

Period	Parameters value	Method	95% Confidence interval
Period 1: Epidemic phase Feb 15, 2020 - Jun 15, 2020	$N_0 = 2.65 \times 10^{-2}$	fitted	$N_0 \in [-8.82 \times 10^{-2}, 1.41 \times 10^{-1}]$
	$N_{base} = 1.12 \times 10^{2}$	fitted	$N_{base} \in [-4.82 \times 10^{2}, 7.06 \times 10^{2}]$
	$N_\infty = 2.86 \times 10^{5}$	fitted	$N_\infty \in [2.84 \times 10^{5}, 2.88 \times 10^{5}]$
	$\chi = 1.76$	fitted	$\chi \in [-1.46, 4.98]$
	$\theta = 2.76 \times 10^{-2}$	fitted	$\theta \in [-2.38 \times 10^{-2}, 7.90 \times 10^{-2}]$
Period 2: Endemic phase Jun 15, 2020 - Sep 01, 2020	$a = 9.43 \times 10^{2}$	computed	
	$N_0 = 2.70 \times 10^{5}$	computed	
Period 3: Epidemic phase Sep 01, 2020 - Nov 20, 2020	$N_0 = 7.85 \times 10^{3}$	fitted	$N_0 \in [3.63 \times 10^{3}, 1.21 \times 10^{4}]$
	$N_{base} = 3.36 \times 10^{5}$	fitted	$N_{base} \in [3.28 \times 10^{5}, 3.43 \times 10^{5}]$
	$N_\infty = 2.14 \times 10^{6}$	fitted	$N_\infty \in [1.93 \times 10^{6}, 2.36 \times 10^{6}]$
	$\chi = 2.41 \times 10^{-1}$	fitted	$\chi \in [2.16 \times 10^{-2}, 4.60 \times 10^{-1}]$
	$\theta = 1.32 \times 10^{-1}$	fitted	$\theta \in [-9.25 \times 10^{-3}, 2.74 \times 10^{-1}]$
Period 4: Endemic phase Nov 20, 2020 - Dec 10, 2020	$a = 1.61 \times 10^{4}$	computed	
	$N_0 = 1.48 \times 10^{6}$	computed	
Period 5: Epidemic phase Dec 10, 2020 - Feb 01, 2021	$N_0 = 2.26 \times 10^{5}$	fitted	$N_0 \in [1.16 \times 10^{5}, 3.35 \times 10^{5}]$
	$N_{base} = 1.58 \times 10^{6}$	fitted	$N_{base} \in [1.46 \times 10^{6}, 1.70 \times 10^{6}]$
	$N_\infty = 2.42 \times 10^{6}$	fitted	$N_\infty \in [2.34 \times 10^{6}, 2.51 \times 10^{6}]$
	$\chi = 8.57 \times 10^{-2}$	fitted	$\chi \in [5.14 \times 10^{-2}, 1.20 \times 10^{-1}]$
	$\theta = 1.08$	fitted	$\theta \in [4.85 \times 10^{-1}, 1.68]$

Table 5.6.8: In this table we list the parameters of the phenomenological model which gives the best fit to the cumulative number of cases data in United Kingdom from January 03 2020 to February 01 2021.

5.6.6 Plot of the multiple Bernoulli–Verhulst models fitted to each epidemic phase

In Figure 5.6.4, we present the details of the fit of the Bernoulli–Verhulst models to the successive epidemic waves in the 8 geographic areas considered. Each epidemic wave is associated with a different color.

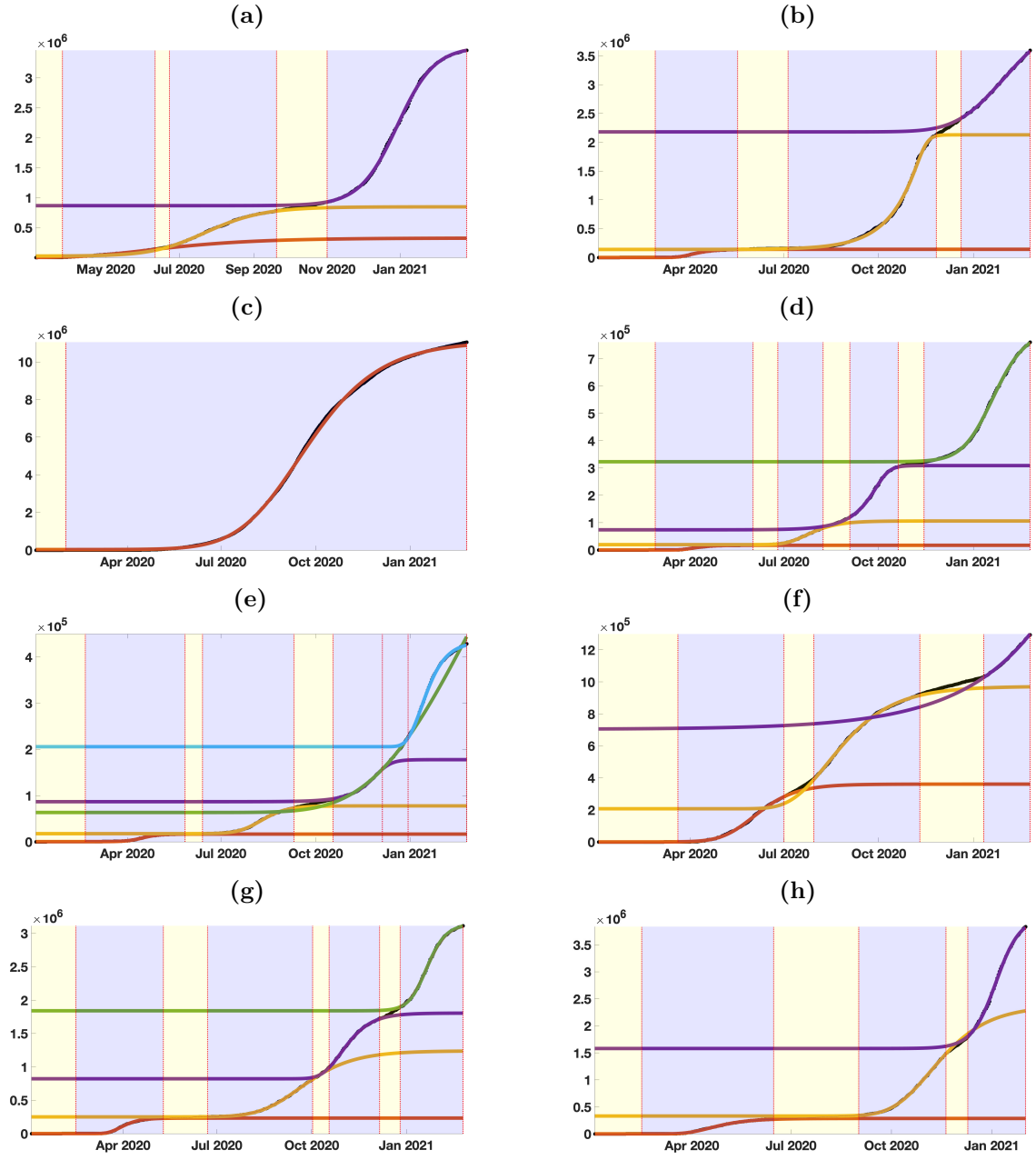

Figure 5.6.4: In this figure, we plot the cumulative number of cases (black dots) and the best fit of Bernoulli–Verhulst for each epidemic wave for (a) California; (b) France; (c) India; (d) Israel; (e) Japan; (f) Peru; (g) Spain; (h) United Kingdom.

5.6.7 Relative error of the fitted curve compared to the data in each geographic area

5.6.7.1 California

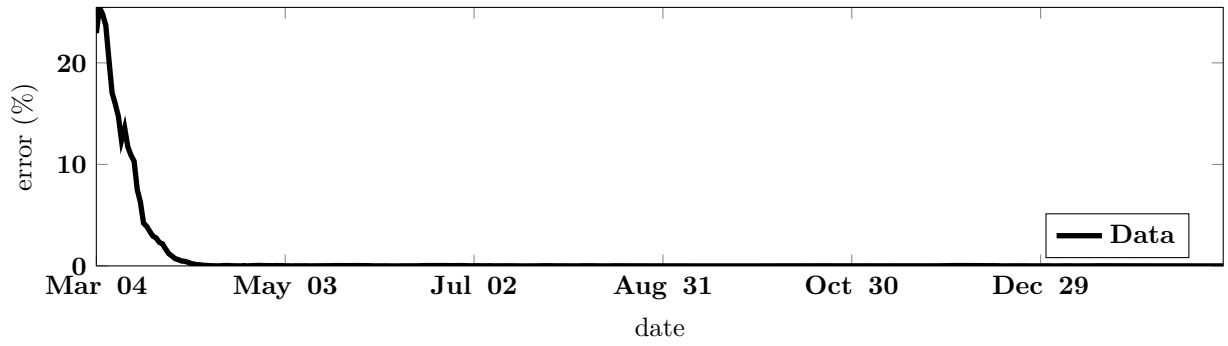

Figure 5.6.5: Relative error between the data and the model for California State, expressed in percent.

5.6.7.2 France

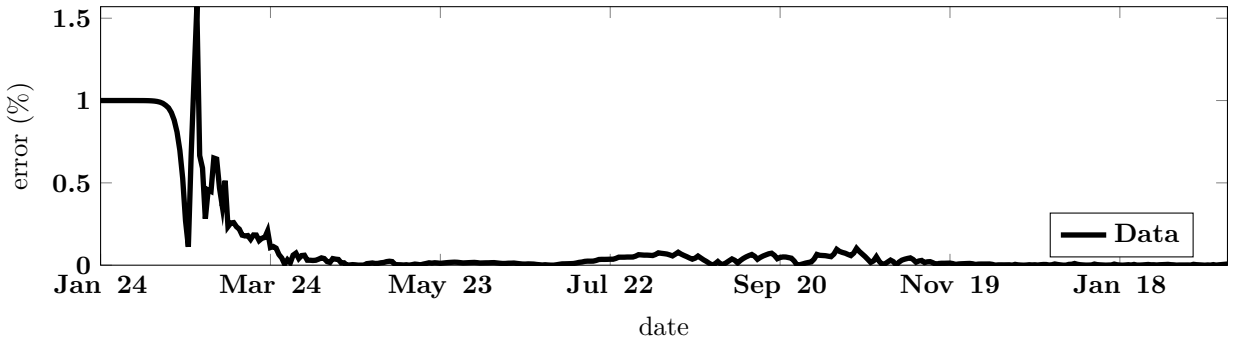

Figure 5.6.6: Relative error between the data and the model for France, expressed in percent.

5.6.7.3 India

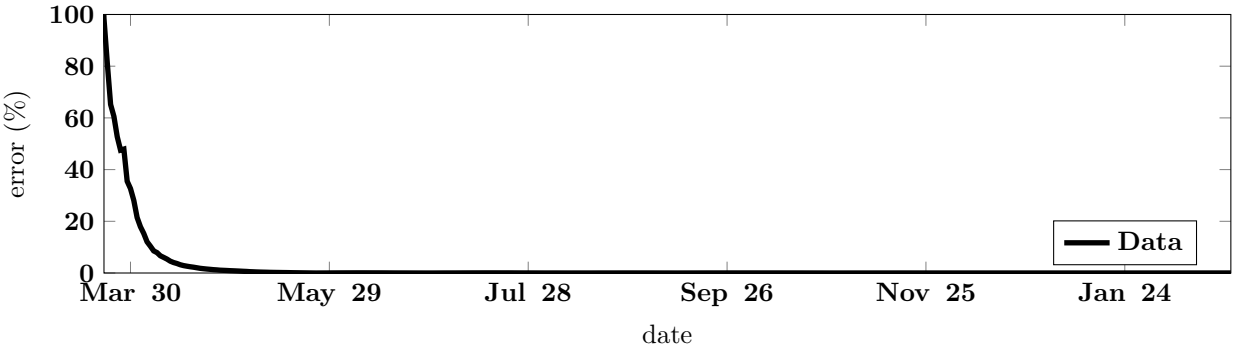

Figure 5.6.7: Relative error between the data and the model for India, expressed in percent.

5.6.7.4 Israel

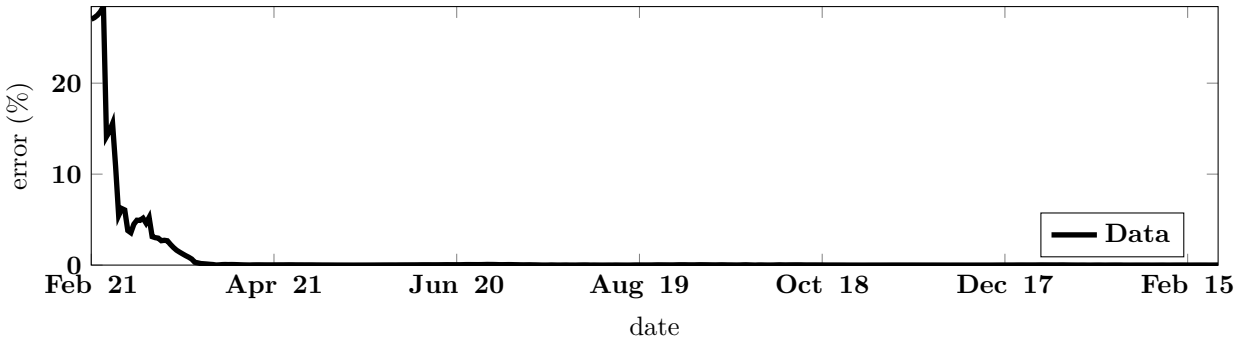

Figure 5.6.8: Relative error between the data and the model for Israel, expressed in percent.

5.6.7.5 Japan

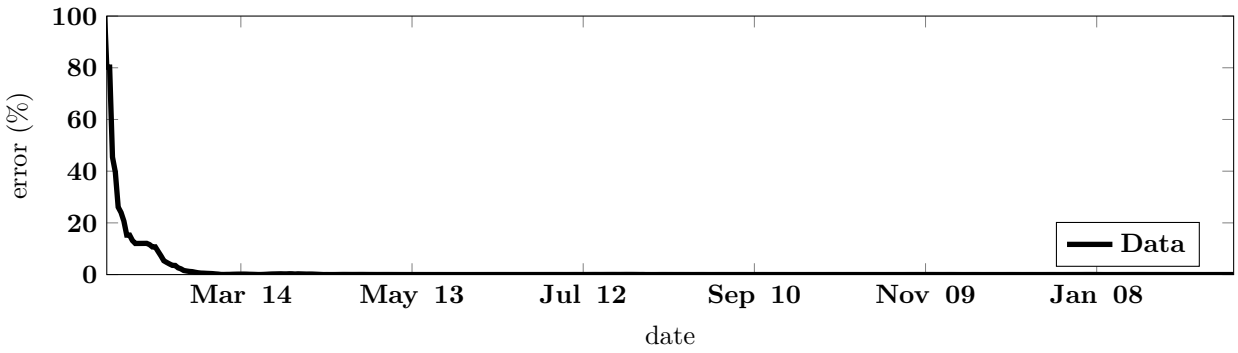

Figure 5.6.9: Relative error between the data and the model for Japan, expressed in percent.

5.6.7.6 Peru

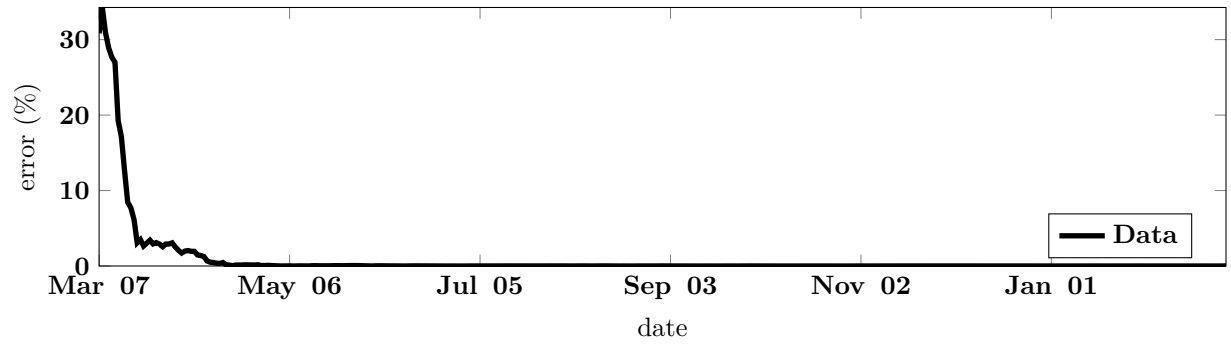

Figure 5.6.10: Relative error between the data and the model for Peru, expressed in percent.

5.6.7.7 Spain

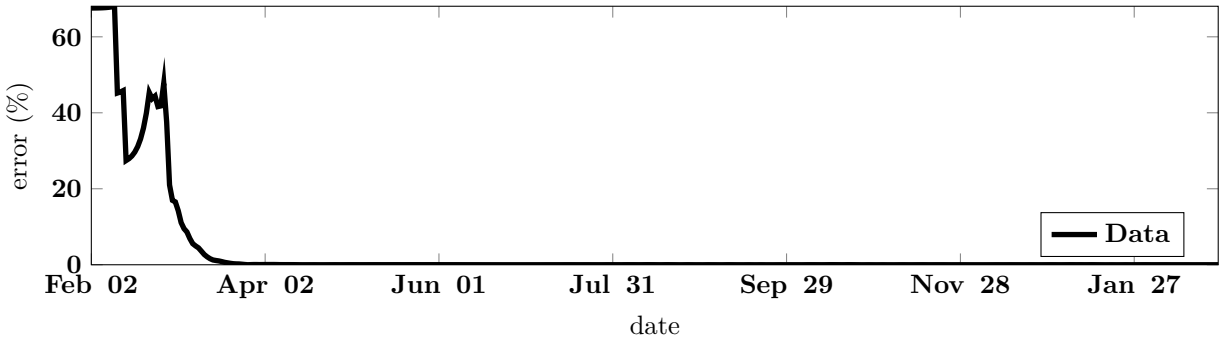

Figure 5.6.11: Relative error between the data and the model for Spain, expressed in percent.

5.6.7.8 United Kingdom

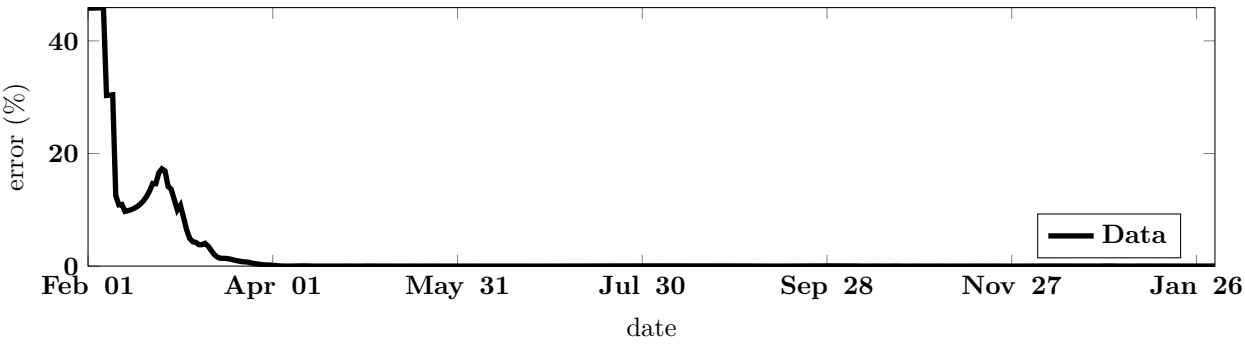

Figure 5.6.12: Relative error between the data and the model for UK, expressed in percent.

5.6.8 Table of estimated parameters for the phenomenological model

5.6.8.1 California

Period	Parameters value	Method	95% Confidence interval
Period 1: Epidemic phase Mar 26, 2020 - Jun 11, 2020	$N_0 = 7.34 \times 10^3$	fitted	$N_0 \in [4.16 \times 10^3, 1.05 \times 10^4]$
	$N_{base} = 1.14 \times 10^{-5}$	fitted	$N_{base} \in [-4.33 \times 10^3, 4.33 \times 10^3]$
	$N_\infty = 3.24 \times 10^5$	fitted	$N_\infty \in [2.52 \times 10^5, 3.96 \times 10^5]$
	$\chi = 4.14 \times 10^4$	fitted	$\chi \in [7.74 \times 10^2, 8.20 \times 10^4]$
	$\theta = 4.62 \times 10^{-7}$	fitted	$\theta \in [2.39 \times 10^{-8}, 9.00 \times 10^{-7}]$
Period 2: Endemic phase Jun 11, 2020 - Jun 23, 2020	$a = 3.81 \times 10^3$	computed	
	$N_0 = 1.36 \times 10^5$	computed	
Period 3: Epidemic phase Jun 23, 2020 - Sep 20, 2020	$N_0 = 1.57 \times 10^5$	fitted	$N_0 \in [5.96 \times 10^4, 2.55 \times 10^5]$
	$N_{base} = 2.45 \times 10^4$	fitted	$N_{base} \in [-7.58 \times 10^4, 1.25 \times 10^5]$
	$N_\infty = 8.22 \times 10^5$	fitted	$N_\infty \in [7.36 \times 10^5, 9.08 \times 10^5]$
	$\chi = 5.54 \times 10^{-2}$	fitted	$\chi \in [5.32 \times 10^{-3}, 1.05 \times 10^{-1}]$
	$\theta = 7.18 \times 10^{-1}$	fitted	$\theta \in [-3.59 \times 10^{-2}, 1.47]$
Period 4: Endemic phase Sep 20, 2020 - Nov 01, 2020	$a = 3.66 \times 10^3$	computed	
	$N_0 = 7.76 \times 10^5$	computed	
Period 5: Epidemic phase Nov 01, 2020 - Feb 25, 2021	$N_0 = 6.27 \times 10^4$	fitted	$N_0 \in [4.95 \times 10^4, 7.59 \times 10^4]$
	$N_{base} = 8.67 \times 10^5$	fitted	$N_{base} \in [8.45 \times 10^5, 8.88 \times 10^5]$
	$N_\infty = 2.66 \times 10^6$	fitted	$N_\infty \in [2.64 \times 10^6, 2.67 \times 10^6]$
	$\chi = 6.36 \times 10^{-2}$	fitted	$\chi \in [5.73 \times 10^{-2}, 6.98 \times 10^{-2}]$
	$\theta = 1.02$	fitted	$\theta \in [8.79 \times 10^{-1}, 1.16]$

Table 5.6.9: In this table we list the values of the parameters of the phenomenological model which give the best fit to the cumulative number of cases data in California from January 03 2020 to February 25 2021.

5.6.8.2 France

Period	Parameters value	Method	95% Confidence interval
Period 1: Epidemic phase Feb 27, 2020 - May 17, 2020	$N_0 = 3.61 \times 10^{-4}$	fitted	$N_0 \in [-3.77, 3.77]$
	$N_{base} = 0.00$	fixed	
	$N_\infty = 1.43 \times 10^5$	fitted	$N_\infty \in [-1.58 \times 10^4, 3.01 \times 10^5]$
	$\chi = 1.17 \times 10^2$	fitted	$\chi \in [-1.09 \times 10^7, 1.09 \times 10^7]$
	$\theta = 7.29 \times 10^{-4}$	fitted	$\theta \in [-6.84 \times 10^1, 6.84 \times 10^1]$
Period 2: Endemic phase May 17, 2020 - Jul 05, 2020	$a = 3.14 \times 10^2$	computed	
	$N_0 = 1.39 \times 10^5$	computed	
Period 3: Epidemic phase Jul 05, 2020 - Nov 26, 2020	$N_0 = 1.50 \times 10^4$	fitted	$N_0 \in [1.36 \times 10^4, 1.65 \times 10^4]$
	$N_{base} = 1.40 \times 10^5$	fitted	$N_{base} \in [1.33 \times 10^5, 1.46 \times 10^5]$
	$N_\infty = 1.99 \times 10^6$	fitted	$N_\infty \in [1.97 \times 10^6, 2.01 \times 10^6]$
	$\chi = 3.68 \times 10^{-2}$	fitted	$\chi \in [3.60 \times 10^{-2}, 3.76 \times 10^{-2}]$
	$\theta = 6.55$	fitted	$\theta \in [5.52, 7.58]$
Period 4: Endemic phase Nov 26, 2020 - Dec 20, 2020	$a = 1.28 \times 10^4$	computed	
	$N_0 = 2.11 \times 10^6$	computed	
Period 5: Epidemic phase Dec 20, 2020 - Feb 25, 2021	$N_0 = 2.73 \times 10^5$	fitted	$N_0 \in [-2.43 \times 10^3, 5.48 \times 10^5]$
	$N_{base} = 2.15 \times 10^6$	fitted	$N_{base} \in [1.86 \times 10^6, 2.43 \times 10^6]$
	$N_\infty = 2.13 \times 10^6$	fitted	$N_\infty \in [1.88 \times 10^6, 2.39 \times 10^6]$
	$\chi = 5.88 \times 10^{-2}$	fitted	$\chi \in [-6.11 \times 10^{-2}, 1.79 \times 10^{-1}]$
	$\theta = 5.47 \times 10^{-1}$	fitted	$\theta \in [-9.19 \times 10^{-1}, 2.01]$

Table 5.6.10: In this table we list the values of the parameters of the phenomenological model which give the best fit to the cumulative number of cases data in France from January 03 2020 to February 25 2021.

5.6.8.3 India

Period	Parameters value	Method	95% Confidence interval
Period 1: Epidemic phase Feb 01, 2020 - Feb 25, 2021	$N_0 = 5.83 \times 10^2$	fitted	$N_0 \in [3.45 \times 10^2, 8.20 \times 10^2]$
	$N_{base} = 1.97 \times 10^4$	fitted	$N_{base} \in [5.36 \times 10^3, 3.39 \times 10^4]$
	$N_\infty = 1.10 \times 10^7$	fitted	$N_\infty \in [1.10 \times 10^7, 1.11 \times 10^7]$
	$\chi = 4.89 \times 10^{-2}$	fitted	$\chi \in [4.59 \times 10^{-2}, 5.20 \times 10^{-2}]$
	$\theta = 5.12 \times 10^{-1}$	fitted	$\theta \in [4.71 \times 10^{-1}, 5.54 \times 10^{-1}]$

Table 5.6.11: In this table we list the values of the parameters of the phenomenological model which give the best fit to the cumulative number of cases data in India from January 03 2020 to February 25 2021.

5.6.8.4 Israel

Period	Parameters value	Method	95% Confidence interval
Period 1: Epidemic phase Feb 27, 2020 - Jun 01, 2020	$N_0 = 1.08 \times 10^{-2}$	fitted	$N_0 \in [-3.85 \times 10^{-2}, 6.02 \times 10^{-2}]$
	$N_{base} = 4.27 \times 10^{1}$	fitted	$N_{base} \in [-3.36 \times 10^{1}, 1.19 \times 10^{2}]$
	$N_\infty = 1.71 \times 10^{4}$	fitted	$N_\infty \in [1.70 \times 10^{4}, 1.72 \times 10^{4}]$
	$\chi = 9.18 \times 10^{-1}$	fitted	$\chi \in [1.71 \times 10^{-1}, 1.67]$
	$\theta = 1.05 \times 10^{-1}$	fitted	$\theta \in [1.55 \times 10^{-2}, 1.94 \times 10^{-1}]$
Period 2: Endemic phase Jun 01, 2020 - Jun 25, 2020	$a = 2.04 \times 10^{2}$	computed	
	$N_0 = 1.70 \times 10^{4}$	computed	
Period 3: Epidemic phase Jun 25, 2020 - Aug 08, 2020	$N_0 = 2.48 \times 10^{3}$	fitted	$N_0 \in [3.43 \times 10^{2}, 4.61 \times 10^{3}]$
	$N_{base} = 1.95 \times 10^{4}$	fitted	$N_{base} \in [1.70 \times 10^{4}, 2.20 \times 10^{4}]$
	$N_\infty = 8.66 \times 10^{4}$	fitted	$N_\infty \in [7.78 \times 10^{4}, 9.55 \times 10^{4}]$
	$\chi = 2.93 \times 10^{-1}$	fitted	$\chi \in [-2.61 \times 10^{-1}, 8.48 \times 10^{-1}]$
	$\theta = 2.04 \times 10^{-1}$	fitted	$\theta \in [-2.43 \times 10^{-1}, 6.50 \times 10^{-1}]$
Period 4: Endemic phase Aug 08, 2020 - Sep 03, 2020	$a = 1.54 \times 10^{3}$	computed	
	$N_0 = 7.97 \times 10^{4}$	computed	
Period 5: Epidemic phase Sep 03, 2020 - Oct 20, 2020	$N_0 = 4.59 \times 10^{4}$	fitted	$N_0 \in [2.88 \times 10^{4}, 6.31 \times 10^{4}]$
	$N_{base} = 7.38 \times 10^{4}$	fitted	$N_{base} \in [5.53 \times 10^{4}, 9.23 \times 10^{4}]$
	$N_\infty = 2.35 \times 10^{5}$	fitted	$N_\infty \in [2.19 \times 10^{5}, 2.52 \times 10^{5}]$
	$\chi = 5.05 \times 10^{-2}$	fitted	$\chi \in [3.77 \times 10^{-2}, 6.34 \times 10^{-2}]$
	$\theta = 3.45$	fitted	$\theta \in [1.96, 4.93]$
Period 6: Endemic phase Oct 20, 2020 - Nov 14, 2020	$a = 8.90 \times 10^{2}$	computed	
	$N_0 = 3.04 \times 10^{5}$	computed	
Period 7: Epidemic phase Nov 14, 2020 - Feb 25, 2021	$N_0 = 3.16 \times 10^{3}$	fitted	$N_0 \in [2.16 \times 10^{3}, 4.17 \times 10^{3}]$
	$N_{base} = 3.23 \times 10^{5}$	fitted	$N_{base} \in [3.21 \times 10^{5}, 3.25 \times 10^{5}]$
	$N_\infty = 4.87 \times 10^{5}$	fitted	$N_\infty \in [4.79 \times 10^{5}, 4.95 \times 10^{5}]$
	$\chi = 8.28 \times 10^{-2}$	fitted	$\chi \in [7.22 \times 10^{-2}, 9.34 \times 10^{-2}]$
	$\theta = 7.06 \times 10^{-1}$	fitted	$\theta \in [5.69 \times 10^{-1}, 8.43 \times 10^{-1}]$

Table 5.6.12: In this table we list the values of the parameters of the phenomenological model which give the best fit to the cumulative number of cases data in Israel from January 03 2020 to February 25 2021.

5.6.8.5 Japan

Period	Parameters value	Method	95% Confidence interval
Period 1: Epidemic phase Feb 20, 2020 - May 27, 2020	$N_0 = 5.83$	fitted	$N_0 \in [1.91, 9.74]$
	$N_{base} = 3.25 \times 10^2$	fitted	$N_{base} \in [2.55 \times 10^2, 3.95 \times 10^2]$
	$N_\infty = 1.63 \times 10^4$	fitted	$N_\infty \in [1.62 \times 10^4, 1.64 \times 10^4]$
	$\chi = 1.48 \times 10^{-1}$	fitted	$\chi \in [1.30 \times 10^{-1}, 1.65 \times 10^{-1}]$
	$\theta = 8.29 \times 10^{-1}$	fitted	$\theta \in [6.88 \times 10^{-1}, 9.70 \times 10^{-1}]$
Period 2: Endemic phase May 27, 2020 - Jun 13, 2020	$a = 7.07 \times 10^1$	computed	
	$N_0 = 1.65 \times 10^4$	computed	
Period 3: Epidemic phase Jun 13, 2020 - Sep 10, 2020	$N_0 = 1.49 \times 10^2$	fitted	$N_0 \in [8.52 \times 10^1, 2.13 \times 10^2]$
	$N_{base} = 1.75 \times 10^4$	fitted	$N_{base} \in [1.73 \times 10^4, 1.78 \times 10^4]$
	$N_\infty = 6.02 \times 10^4$	fitted	$N_\infty \in [5.93 \times 10^4, 6.10 \times 10^4]$
	$\chi = 1.19 \times 10^{-1}$	fitted	$\chi \in [1.03 \times 10^{-1}, 1.35 \times 10^{-1}]$
	$\theta = 6.28 \times 10^{-1}$	fitted	$\theta \in [5.04 \times 10^{-1}, 7.52 \times 10^{-1}]$
Period 4: Endemic phase Sep 10, 2020 - Oct 18, 2020	$a = 5.36 \times 10^2$	computed	
	$N_0 = 7.27 \times 10^4$	computed	
Period 5: Epidemic phase Oct 18, 2020 - Dec 05, 2020	$N_0 = 6.33 \times 10^3$	fitted	$N_0 \in [4.64 \times 10^3, 8.01 \times 10^3]$
	$N_{base} = 8.68 \times 10^4$	fitted	$N_{base} \in [8.48 \times 10^4, 8.88 \times 10^4]$
	$N_\infty = 9.10 \times 10^4$	fitted	$N_\infty \in [7.75 \times 10^4, 1.05 \times 10^5]$
	$\chi = 5.60 \times 10^{-2}$	fitted	$\chi \in [4.74 \times 10^{-2}, 6.46 \times 10^{-2}]$
	$\theta = 2.58$	fitted	$\theta \in [1.00, 4.16]$
Period 6: Epidemic phase Dec 05, 2020 - Dec 30, 2020	$N_0 = 1.23 \times 10^5$	fitted	$N_0 \in [-2.43 \times 10^5, 4.90 \times 10^5]$
	$N_{base} = 3.43 \times 10^4$	fitted	$N_{base} \in [-3.33 \times 10^5, 4.01 \times 10^5]$
	$N_\infty = 3.49 \times 10^5$	fitted	$N_\infty \in [-2.92 \times 10^7, 2.99 \times 10^7]$
	$\chi = 1.78 \times 10^{-2}$	fitted	$\chi \in [-3.59 \times 10^{-2}, 7.15 \times 10^{-2}]$
	$\theta = 7.84$	fitted	$\theta \in [-1.28 \times 10^3, 1.30 \times 10^3]$
Period 7: Epidemic phase Dec 30, 2020 - Feb 25, 2021	$N_0 = 2.00 \times 10^4$	fitted	$N_0 \in [1.59 \times 10^3, 3.84 \times 10^4]$
	$N_{base} = 2.05 \times 10^5$	fitted	$N_{base} \in [1.85 \times 10^5, 2.25 \times 10^5]$
	$N_\infty = 2.29 \times 10^5$	fitted	$N_\infty \in [2.11 \times 10^5, 2.47 \times 10^5]$
	$\chi = 7.98 \times 10^{-1}$	fitted	$\chi \in [-2.54, 4.13]$
	$\theta = 9.61 \times 10^{-2}$	fitted	$\theta \in [-3.15 \times 10^{-1}, 5.07 \times 10^{-1}]$

Table 5.6.13: In this table we list the values of the parameters of the phenomenological model which give the best fit to the cumulative number of cases data in Japan from January 03 2020 to February 25 2021.

5.6.8.6 Peru

Period	Parameters value	Method	95% Confidence interval
Period 1: Epidemic phase Mar 20, 2020 - Jul 01, 2020	$N_0 = 8.36 \times 10^2$	fitted	$N_0 \in [2.63 \times 10^2, 1.41 \times 10^3]$
	$N_{base} = 3.00 \times 10^{-5}$	fitted	$N_{base} \in [-1.74 \times 10^3, 1.74 \times 10^3]$
	$N_\infty = 3.61 \times 10^5$	fitted	$N_\infty \in [3.44 \times 10^5, 3.79 \times 10^5]$
	$\chi = 1.08 \times 10^{-1}$	fitted	$\chi \in [7.59 \times 10^{-2}, 1.41 \times 10^{-1}]$
	$\theta = 4.20 \times 10^{-1}$	fitted	$\theta \in [2.41 \times 10^{-1}, 5.98 \times 10^{-1}]$
Period 2: Endemic phase Jul 01, 2020 - Jul 30, 2020	$a = 3.67 \times 10^3$	computed	
	$N_0 = 2.83 \times 10^5$	computed	
Period 3: Epidemic phase Jul 30, 2020 - Nov 10, 2020	$N_0 = 1.86 \times 10^5$	fitted	$N_0 \in [-2.61 \times 10^4, 3.98 \times 10^5]$
	$N_{base} = 2.03 \times 10^5$	fitted	$N_{base} \in [-1.11 \times 10^4, 4.18 \times 10^5]$
	$N_\infty = 7.69 \times 10^5$	fitted	$N_\infty \in [5.65 \times 10^5, 9.72 \times 10^5]$
	$\chi = 4.84 \times 10^{-1}$	fitted	$\chi \in [-6.23, 7.20]$
	$\theta = 5.95 \times 10^{-2}$	fitted	$\theta \in [-7.74 \times 10^{-1}, 8.93 \times 10^{-1}]$
Period 4: Endemic phase Nov 10, 2020 - Jan 11, 2021	$a = 1.80 \times 10^3$	computed	
	$N_0 = 9.16 \times 10^5$	computed	
Period 5: Epidemic phase Jan 11, 2021 - Feb 25, 2021	$N_0 = 3.23 \times 10^5$	fitted	
	$N_{base} = 7.04 \times 10^5$	fitted	
	$N_\infty = 7.00 \times 10^6$	fitted	
	$\chi = 1.36 \times 10^{-2}$	fitted	
	$\theta = 3.67 \times 10^1$	fitted	

Table 5.6.14: In this table we list the values of the parameters of the phenomenological model which give the best fit to the cumulative number of cases data in Peru from January 03 2020 to February 25 2021.

5.6.8.7 Spain

Period	Parameters value	Method	95% Confidence interval
Period 1: Epidemic phase Feb 15, 2020 - May 10, 2020	$N_0 = 5.19 \times 10^{-4}$	fitted	$N_0 \in [-5.00 \times 10^{-3}, 6.04 \times 10^{-3}]$
	$N_{base} = 5.77 \times 10^{2}$	fitted	$N_{base} \in [-4.50 \times 10^{2}, 1.60 \times 10^{3}]$
	$N_\infty = 2.32 \times 10^{5}$	fitted	$N_\infty \in [2.30 \times 10^{5}, 2.34 \times 10^{5}]$
	$\chi = 9.80 \times 10^{-1}$	fitted	$\chi \in [-1.26 \times 10^{-1}, 2.09]$
	$\theta = 9.75 \times 10^{-2}$	fitted	$\theta \in [-1.83 \times 10^{-2}, 2.13 \times 10^{-1}]$
Period 2: Endemic phase May 10, 2020 - Jun 22, 2020	$a = 5.67 \times 10^{2}$	computed	
	$N_0 = 2.28 \times 10^{5}$	computed	
Period 3: Epidemic phase Jun 22, 2020 - Oct 02, 2020	$N_0 = 2.38 \times 10^{3}$	fitted	$N_0 \in [1.39 \times 10^{3}, 3.36 \times 10^{3}]$
	$N_{base} = 2.50 \times 10^{5}$	fitted	$N_{base} \in [2.48 \times 10^{5}, 2.53 \times 10^{5}]$
	$N_\infty = 9.89 \times 10^{5}$	fitted	$N_\infty \in [9.02 \times 10^{5}, 1.08 \times 10^{6}]$
	$\chi = 9.29 \times 10^{-2}$	fitted	$\chi \in [7.07 \times 10^{-2}, 1.15 \times 10^{-1}]$
	$\theta = 3.84 \times 10^{-1}$	fitted	$\theta \in [2.38 \times 10^{-1}, 5.29 \times 10^{-1}]$
Period 4: Endemic phase Oct 02, 2020 - Oct 18, 2020	$a = 1.09 \times 10^{4}$	computed	
	$N_0 = 8.14 \times 10^{5}$	computed	
Period 5: Epidemic phase Oct 18, 2020 - Dec 06, 2020	$N_0 = 1.68 \times 10^{5}$	fitted	$N_0 \in [-3.50 \times 10^{4}, 3.72 \times 10^{5}]$
	$N_{base} = 8.20 \times 10^{5}$	fitted	$N_{base} \in [6.12 \times 10^{5}, 1.03 \times 10^{6}]$
	$N_\infty = 9.85 \times 10^{5}$	fitted	$N_\infty \in [8.01 \times 10^{5}, 1.17 \times 10^{6}]$
	$\chi = 3.15 \times 10^{-1}$	fitted	$\chi \in [-1.05, 1.68]$
	$\theta = 2.02 \times 10^{-1}$	fitted	$\theta \in [-7.15 \times 10^{-1}, 1.12]$
Period 6: Endemic phase Dec 06, 2020 - Dec 26, 2020	$a = 9.15 \times 10^{3}$	computed	
	$N_0 = 1.72 \times 10^{6}$	computed	
Period 7: Epidemic phase Dec 26, 2020 - Feb 25, 2021	$N_0 = 5.94 \times 10^{4}$	fitted	$N_0 \in [3.86 \times 10^{4}, 8.02 \times 10^{4}]$
	$N_{base} = 1.84 \times 10^{6}$	fitted	$N_{base} \in [1.81 \times 10^{6}, 1.87 \times 10^{6}]$
	$N_\infty = 1.30 \times 10^{6}$	fitted	$N_\infty \in [1.28 \times 10^{6}, 1.32 \times 10^{6}]$
	$\chi = 1.30 \times 10^{-1}$	fitted	$\chi \in [9.90 \times 10^{-2}, 1.60 \times 10^{-1}]$
	$\theta = 7.84 \times 10^{-1}$	fitted	$\theta \in [5.50 \times 10^{-1}, 1.02]$

Table 5.6.15: In this table we list the values of the parameters of the phenomenological model which give the best fit to the cumulative number of cases data in Spain from January 03 2020 to February 01 2021.

5.6.8.8 United Kingdom

Period	Parameters value	Method	95% Confidence interval
Period 1: Epidemic phase Feb 15, 2020 - Jun 15, 2020	$N_0 = 2.65 \times 10^{-2}$	fitted	$N_0 \in [-8.82 \times 10^{-2}, 1.41 \times 10^{-1}]$
	$N_{base} = 1.12 \times 10^{2}$	fitted	$N_{base} \in [-4.82 \times 10^{2}, 7.06 \times 10^{2}]$
	$N_\infty = 2.86 \times 10^{5}$	fitted	$N_\infty \in [2.84 \times 10^{5}, 2.88 \times 10^{5}]$
	$\chi = 1.76$	fitted	$\chi \in [-1.46, 4.98]$
	$\theta = 2.76 \times 10^{-2}$	fitted	$\theta \in [-2.38 \times 10^{-2}, 7.90 \times 10^{-2}]$
Period 2: Endemic phase Jun 15, 2020 - Sep 01, 2020	$a = 9.43 \times 10^{2}$	computed	
	$N_0 = 2.70 \times 10^{5}$	computed	
Period 3: Epidemic phase Sep 01, 2020 - Nov 20, 2020	$N_0 = 7.85 \times 10^{3}$	fitted	$N_0 \in [3.63 \times 10^{3}, 1.21 \times 10^{4}]$
	$N_{base} = 3.36 \times 10^{5}$	fitted	$N_{base} \in [3.28 \times 10^{5}, 3.43 \times 10^{5}]$
	$N_\infty = 2.14 \times 10^{6}$	fitted	$N_\infty \in [1.93 \times 10^{6}, 2.36 \times 10^{6}]$
	$\chi = 2.41 \times 10^{-1}$	fitted	$\chi \in [2.16 \times 10^{-2}, 4.60 \times 10^{-1}]$
	$\theta = 1.32 \times 10^{-1}$	fitted	$\theta \in [-9.25 \times 10^{-3}, 2.74 \times 10^{-1}]$
Period 4: Endemic phase Nov 20, 2020 - Dec 10, 2020	$a = 1.61 \times 10^{4}$	computed	
	$N_0 = 1.48 \times 10^{6}$	computed	
Period 5: Epidemic phase Dec 10, 2020 - Feb 01, 2021	$N_0 = 2.26 \times 10^{5}$	fitted	$N_0 \in [1.16 \times 10^{5}, 3.35 \times 10^{5}]$
	$N_{base} = 1.58 \times 10^{6}$	fitted	$N_{base} \in [1.46 \times 10^{6}, 1.70 \times 10^{6}]$
	$N_\infty = 2.42 \times 10^{6}$	fitted	$N_\infty \in [2.34 \times 10^{6}, 2.51 \times 10^{6}]$
	$\chi = 8.57 \times 10^{-2}$	fitted	$\chi \in [5.14 \times 10^{-2}, 1.20 \times 10^{-1}]$
	$\theta = 1.08$	fitted	$\theta \in [4.85 \times 10^{-1}, 1.68]$

Table 5.6.16: In this table we list the values of the parameters of the phenomenological model which give the best fit to the cumulative number of cases data in United Kingdom from January 03 2020 to February 01 2021.

5.6.9 Additional information for the results section

Table 5.6.17: In this table we list the values of the parameters of the epidemic model used for the simulations.

Period	Interpretation	Parameters value	Method
U_0	Number of unreported symptomatic infectious at time t_0	1	Fixed
R_0	Number of reported symptomatic infectious at time t_0	0	Fixed
$\tau(t)$	Transmission rate	Eqs (5.6.27)–(5.6.32)	Computed
f	Fraction of reported symptomatic infectious	0.8	Fixed
κ	Fraction of unreported symptomatic infectious capable to transmit the pathogen	1	Fixed
$1/\alpha$	Average duration of the exposed period	1 days	Fixed
$1/\nu$	Average duration of the asymptomatic infectious period	3 days	Fixed
$1/\eta$	Average duration of the symptomatic infectious period	7 days	Fixed

5.6.9.1 California

Period	Interpretation	Parameters value	Method
t_0	Time at which we started the epidemic model	Mar 26, 2020	Fixed
S_0	Number of susceptibles at time t_0	3.95×10^7	Fixed
E_0	Number of exposed at time t_0	7.91×10^2	Computed
I_0	Number of asymptomatic infectious at time t_0	2.06×10^3	Computed

Table 5.6.18: In this table we list the values of the parameters of the epidemic model used for the simulations.

Compatibility condition between data and epidemic model

By using the Californian data for the first, the second and the third epidemic waves, we get from Eqs (5.6.59) and (5.6.60) the following estimates for the average duration of the exposed and asymptomatic infectious periods and the fraction of reported cases

First epidemic wave	$\frac{1}{\alpha}$ and $\frac{1}{\nu} \leq \frac{1}{\chi\theta} = 5.23 \times 10^1$ days	$f \geq \frac{N_\infty}{S_0} = 8.21 \times 10^{-3}$
Second epidemic wave	$\frac{1}{\alpha}$ and $\frac{1}{\nu} \leq \frac{1}{\chi\theta} = 2.52 \times 10^1$ days	$f \geq \frac{N_\infty}{S_0} = 2.08 \times 10^{-2}$
Third epidemic wave	$\frac{1}{\alpha}$ and $\frac{1}{\nu} \leq \frac{1}{\chi\theta} = 1.54 \times 10^1$ days	$f \geq \frac{N_\infty}{S_0} = 6.72 \times 10^{-2}$

5.6.9.2 France

Period	Interpretation	Parameters value	Method
t_0	Time at which we started the epidemic model	Feb 27, 2020	Fixed
S_0	Number of susceptibles at time t_0	6.50×10^7	Fixed
E_0	Number of exposed at time t_0	4.27×10^1	Computed
I_0	Number of asymptomatic infectious at time t_0	6.30×10^1	Computed

Table 5.6.19: In this table we list the values of the parameters of the epidemic model used for the simulations.

Compatibility condition between data and epidemic model

By using the French data for the first, the second and the third epidemic waves, we get from Eqs (5.6.59) and (5.6.60) the following estimates for the average duration of the exposed and asymptomatic infectious periods and the fraction of reported cases

First epidemic wave	$\frac{1}{\alpha}$ and $\frac{1}{\nu} \leq \frac{1}{\chi\theta} = 1.17 \times 10^1$ days	$f \geq \frac{N_\infty}{S_0} = 2.19 \times 10^{-3}$
Second epidemic wave	$\frac{1}{\alpha}$ and $\frac{1}{\nu} \leq \frac{1}{\chi\theta} = 4.15$ days	$f \geq \frac{N_\infty}{S_0} = 3.06 \times 10^{-2}$
Third epidemic wave	$\frac{1}{\alpha}$ and $\frac{1}{\nu} \leq \frac{1}{\chi\theta} = 3.11 \times 10^1$ days	$f \geq \frac{N_\infty}{S_0} = 3.28 \times 10^{-2}$

5.6.9.3 India

Figure 4 of the main text is devoted to the reproduction number of the model. The instantaneous reproduction number $t \to R_e(t)$ is decreasing from February 01, 2020 until February 25, 2021.

Period	Interpretation	Parameters value	Method
t_0	Time at which we started the epidemic model	Feb 01, 2020	Fixed
S_0	Number of susceptibles at time t_0	1.39×10^9	Fixed
E_0	Number of exposed at time t_0	4.29×10^1	Computed
I_0	Number of asymptomatic infectious at time t_0	1.12×10^2	Computed

Table 5.6.20: In this table we list the values of the parameters of the epidemic model used for the simulations.

Compatibility condition between data and epidemic model

By using the Indian data for the first single wave, we get from Eqs (5.6.59) and (5.6.60) the following estimates for the average duration of the exposed and asymptomatic infectious periods and the fraction of reported cases

First epidemic wave	$\frac{1}{\alpha}$ and $\frac{1}{\nu} \leq \frac{1}{\chi\theta} = 3.99 \times 10^1$ days	$f \geq \frac{N_\infty}{S_0} = 7.93 \times 10^{-3}$

5.6.9.4 Israel

Period	Interpretation	Parameters value	Method
t_0	Time at which we started the epidemic model	Feb 27, 2020	Fixed
S_0	Number of susceptibles at time t_0	8.74×10^6	Fixed
E_0	Number of exposed at time t_0	4.16	Computed
I_0	Number of asymptomatic infectious at time t_0	6.25	Computed

Table 5.6.21: In this table we list the values of the parameters of the epidemic model used for the simulations.

Compatibility condition between data and epidemic model

By using the Israeli data for the first, the second, the third and the fourth epidemic waves, we get from Eqs (5.6.59) and (5.6.60) the following estimates for the average duration of the exposed and asymptomatic infectious periods and the fraction of reported cases

First epidemic wave	$\frac{1}{\alpha}$ and $\frac{1}{\nu} \leq \frac{1}{\chi\theta} = 1.04 \times 10^1$ days	$f \geq \frac{N_\infty}{S_0} = 1.95 \times 10^{-3}$
Second epidemic wave	$\frac{1}{\alpha}$ and $\frac{1}{\nu} \leq \frac{1}{\chi\theta} = 1.67 \times 10^1$ days	$f \geq \frac{N_\infty}{S_0} = 9.91 \times 10^{-3}$
Third epidemic wave	$\frac{1}{\alpha}$ and $\frac{1}{\nu} \leq \frac{1}{\chi\theta} = 5.74$ days	$f \geq \frac{N_\infty}{S_0} = 2.69 \times 10^{-2}$
Fourth epidemic wave	$\frac{1}{\alpha}$ and $\frac{1}{\nu} \leq \frac{1}{\chi\theta} = 1.71 \times 10^1$ days	$f \geq \frac{N_\infty}{S_0} = 5.57 \times 10^{-2}$

5.6.9.5 Japan

Period	Interpretation	Parameters value	Method
t_0	Time at which we started the epidemic model	Feb 20, 2020	Fixed
S_0	Number of susceptibles at time t_0	1.26×10^8	Fixed
E_0	Number of exposed at time t_0	2.61	Computed
I_0	Number of asymptomatic infectious at time t_0	5.45	Computed

Table 5.6.22: In this table we list the values of the parameters of the epidemic model used for the simulations.

Compatibility condition between data and epidemic model

By using the Japanese data for the first, the second, the third, the fourth and the fifth epidemic waves, we get from Eqs (5.6.59) and (5.6.60) the following estimates for the average duration of the exposed and asymptomatic infectious periods and the fraction of reported cases

First epidemic wave	$\frac{1}{\alpha}$ and $\frac{1}{\nu} \leq \frac{1}{\chi\theta} = 8.18$ days	$f \geq \frac{N_\infty}{S_0} = 1.29 \times 10^{-4}$
Second epidemic wave	$\frac{1}{\alpha}$ and $\frac{1}{\nu} \leq \frac{1}{\chi\theta} = 1.34 \times 10^1$ days	$f \geq \frac{N_\infty}{S_0} = 4.77 \times 10^{-4}$
Third epidemic wave	$\frac{1}{\alpha}$ and $\frac{1}{\nu} \leq \frac{1}{\chi\theta} = 6.92$ days	$f \geq \frac{N_\infty}{S_0} = 7.22 \times 10^{-4}$
Fourth epidemic wave	$\frac{1}{\alpha}$ and $\frac{1}{\nu} \leq \frac{1}{\chi\theta} = 7.17$ days	$f \geq \frac{N_\infty}{S_0} = 2.77 \times 10^{-3}$
Fifth epidemic wave	$\frac{1}{\alpha}$ and $\frac{1}{\nu} \leq \frac{1}{\chi\theta} = 1.30 \times 10^1$ days	$f \geq \frac{N_\infty}{S_0} = 1.82 \times 10^{-3}$

5.6.9.6 Peru

Period	Interpretation	Parameters value	Method
t_0	Time at which we started the epidemic model	Mar 20, 2020	Fixed
S_0	Number of susceptibles at time t_0	3.32×10^7	Fixed
E_0	Number of exposed at time t_0	1.64×10^2	Computed
I_0	Number of asymptomatic infectious at time t_0	3.85×10^2	Computed

Table 5.6.23: In this table we list the values of the parameters of the epidemic model used for the simulations.

Compatibility condition between data and epidemic model

By using the Peruvian data for the first, the second and the third epidemic waves, we get from Eqs (5.6.59) and (5.6.60) the following estimates for the average duration of the exposed and asymptomatic infectious periods and the fraction of reported cases

First epidemic wave	$\frac{1}{\alpha}$ and $\frac{1}{\nu} \leq \frac{1}{\chi\theta} = 2.20 \times 10^1$ days	$f \geq \frac{N_\infty}{S_0} = 1.09 \times 10^{-2}$
Second epidemic wave	$\frac{1}{\alpha}$ and $\frac{1}{\nu} \leq \frac{1}{\chi\theta} = 3.47 \times 10^1$ days	$f \geq \frac{N_\infty}{S_0} = 2.32 \times 10^{-2}$
Third epidemic wave	$\frac{1}{\alpha}$ and $\frac{1}{\nu} \leq \frac{1}{\chi\theta} = 2.01$ days	$f \geq \frac{N_\infty}{S_0} = 2.11 \times 10^{-1}$

5.6.9.7 Spain

Period	Interpretation	Parameters value	Method
t_0	Time at which we started the epidemic model	Feb 15, 2020	Fixed
S_0	Number of susceptibles at time t_0	3.95×10^7	Fixed
E_0	Number of exposed at time t_0	5.10	Computed
I_0	Number of asymptomatic infectious at time t_0	6.87	Computed

Table 5.6.24: In this table we list the values of the parameters of the epidemic model used for the simulations.

Compatibility condition between data and epidemic model

By using the Spanish data for the first, the second, the third and the fourth epidemic waves, we get from Eqs (5.6.59) and (5.6.60) the following estimates for the average duration of the exposed and asymptomatic infectious periods and the fraction of reported cases

First epidemic wave	$\frac{1}{\alpha}$ and $\frac{1}{\nu} \leq \frac{1}{\chi\theta} = 1.05 \times 10^1$ days	$f \geq \frac{N_\infty}{S_0} = 5.87 \times 10^{-3}$
Second epidemic wave	$\frac{1}{\alpha}$ and $\frac{1}{\nu} \leq \frac{1}{\chi\theta} = 2.81 \times 10^1$ days	$f \geq \frac{N_\infty}{S_0} = 2.50 \times 10^{-2}$
Third epidemic wave	$\frac{1}{\alpha}$ and $\frac{1}{\nu} \leq \frac{1}{\chi\theta} = 1.58 \times 10^1$ days	$f \geq \frac{N_\infty}{S_0} = 2.49 \times 10^{-2}$
Fourth epidemic wave	$\frac{1}{\alpha}$ and $\frac{1}{\nu} \leq \frac{1}{\chi\theta} = 9.84$ days	$f \geq \frac{N_\infty}{S_0} = 3.29 \times 10^{-2}$

5.6.9.8 United Kingdom

Table 5.6.25: In this table we list the values of the parameters of the epidemic model used for the simulations.

Period	Interpretation	Parameters value	Method
t_0	Time at which we started the epidemic model	Feb 15, 2020	Fixed
S_0	Number of susceptibles at time t_0	6.81×10^7	Fixed
E_0	Number of exposed at time t_0	3.41	Computed
I_0	Number of asymptomatic infectious at time t_0	5.15	Computed

Compatibility condition between data and epidemic model

By using the data from Great Britain for the first, the second and the third epidemic waves, we get from Eqs (5.6.59) and (5.6.60) the following estimates for the average duration of the exposed and asymptomatic infectious periods and the fraction of reported cases

First epidemic wave	$\frac{1}{\alpha}$ and $\frac{1}{\nu} \leq \frac{1}{\chi\theta} = 2.06 \times 10^{1}$ days	$f \geq \frac{N_\infty}{S_0} = 4.20 \times 10^{-3}$
Second epidemic wave	$\frac{1}{\alpha}$ and $\frac{1}{\nu} \leq \frac{1}{\chi\theta} = 3.14 \times 10^{1}$ days	$f \geq \frac{N_\infty}{S_0} = 3.15 \times 10^{-2}$
Third epidemic wave	$\frac{1}{\alpha}$ and $\frac{1}{\nu} \leq \frac{1}{\chi\theta} = 1.08 \times 10^{1}$ days	$f \geq \frac{N_\infty}{S_0} = 3.56 \times 10^{-2}$

5.6.10 Dependency with respect to the parameters for the French data

Influence of f on basic reproduction number:

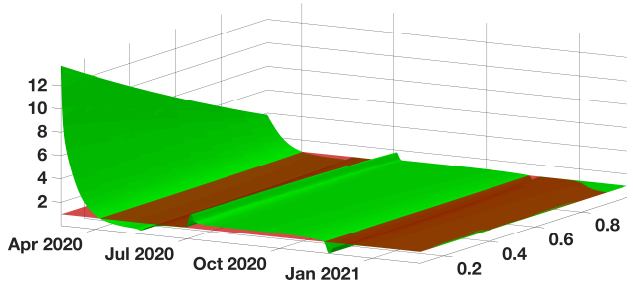

Figure 5.6.13: In this figure we plot $(t, f) \to R_e(t)$ when t varies from January 03 2020 to January 04 2021 and f varies from 0.1 to 1.

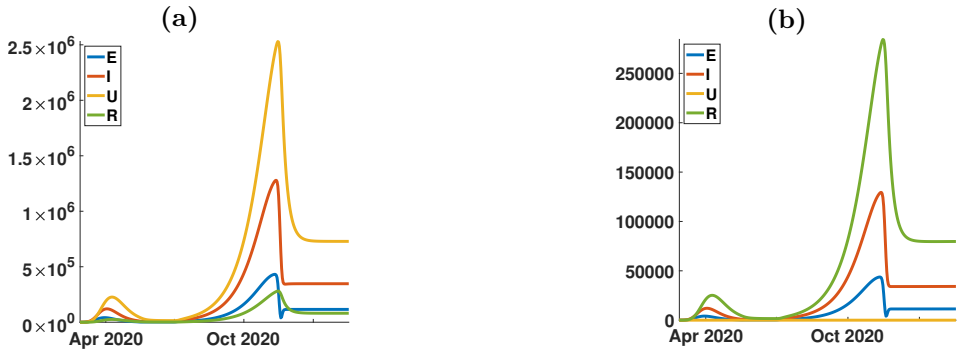

Figure 5.6.14: In this figure we explore the influence of the parameter f on the solution of model. The figure (a) corresponds to $f = 0.1$ and figure (b) corresponds to $f = 1$. The remaining parameters are unchanged.

Influence of κ on basic reproduction number:

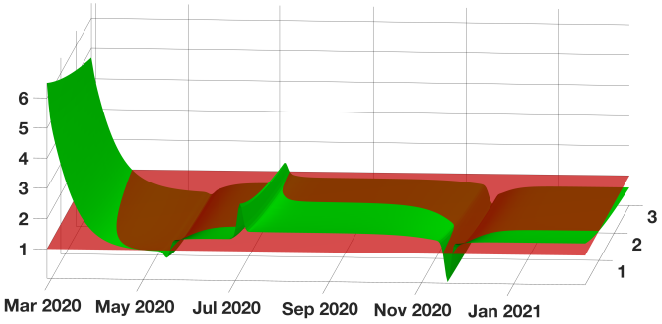

Figure 5.6.15: In this figure we plot $(t, \kappa) \to R_e(t)$ when t varies from January 03 2020 to January 04 2021 and κ varies from 0.1 to 3.

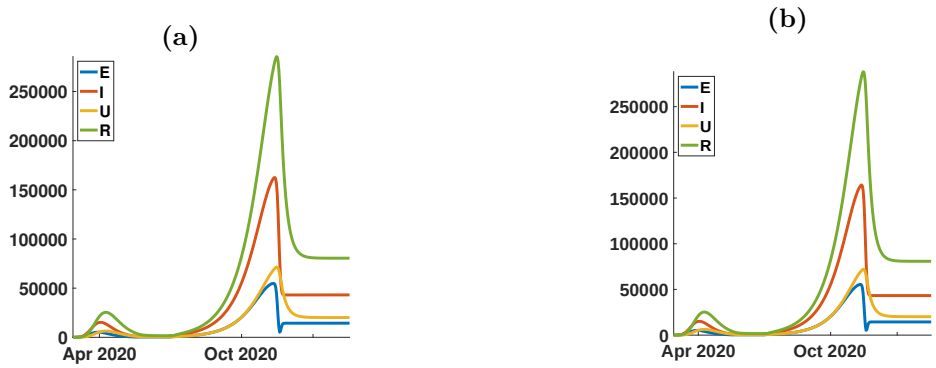

Figure 5.6.16: In this figure we explore the influence of the parameter f on the solution of model. The figure (a) corresponds to $\kappa = 0.1$ and figure (b) corresponds to $\kappa = 3$. The remaining parameters are unchanged.

Influence of ν on basic reproduction number:

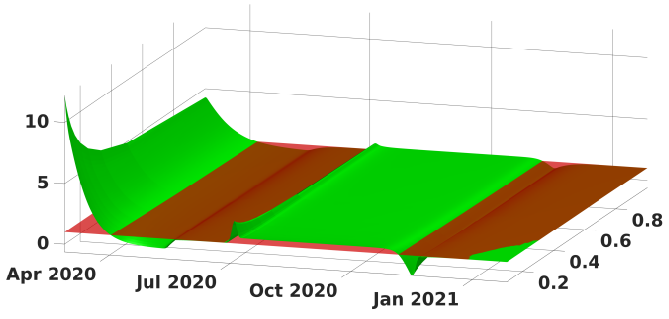

Figure 5.6.17: In this figure we plot $(t, \nu) \to R_e(t)$ when t varies from January 03 2020 to January 04 2021 and ν varies from 0.1 to 1 (or equivalently $1/\nu$ varies from 10 days to 1 day).

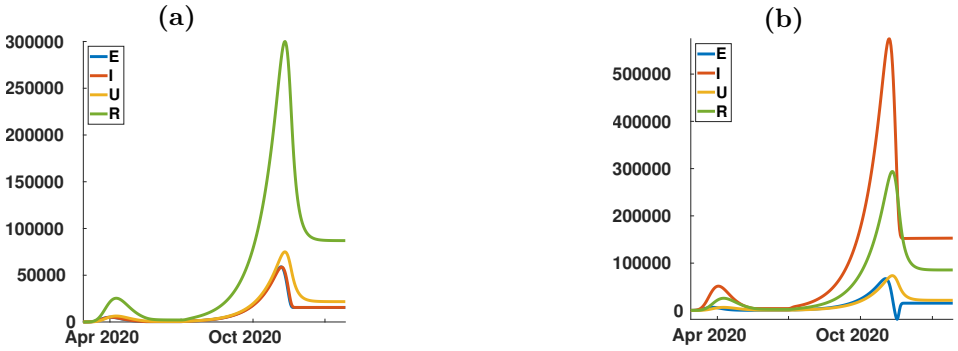

Figure 5.6.18: In this figure we explore the influence of the parameter $1/\nu$ on the solution of model. The figure (a) corresponds to $1/\nu = 1$ and figure (b) corresponds to $1/\nu = 10$. The remaining parameters are unchanged.

Influence of η on basic reproduction number:

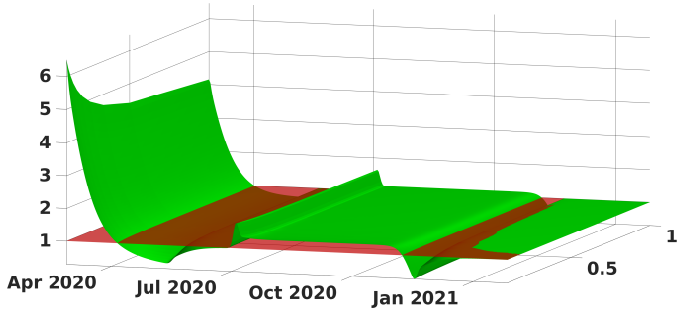

Figure 5.6.19: In this figure we plot $(t, \eta) \to R_e(t)$ when t varies from January 03 2020 to January 04 2021 and η varies from 0.1 to 1 (or equivalently $1/\eta$ varies from 10 days to 1 day).

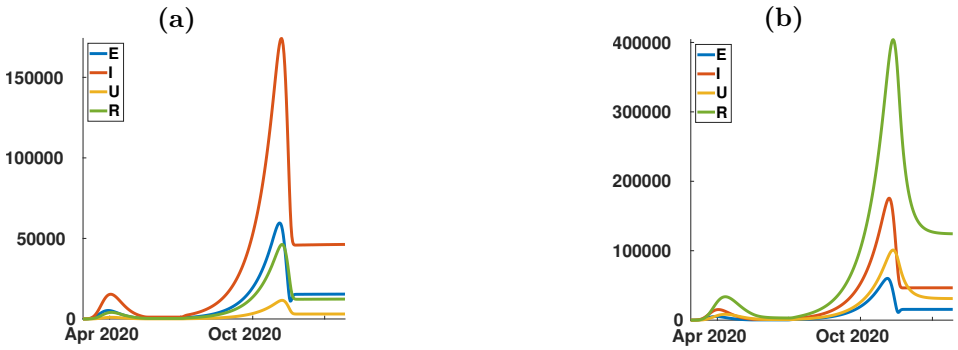

Figure 5.6.20: In this figure we explore the influence of the parameter f on the solution of model. The figure (a) corresponds to $1/\eta = 1$ days and figure (b) corresponds to $1/\eta = 10$ days. The remaining parameters are unchanged.

Influence of α on basic reproduction number:

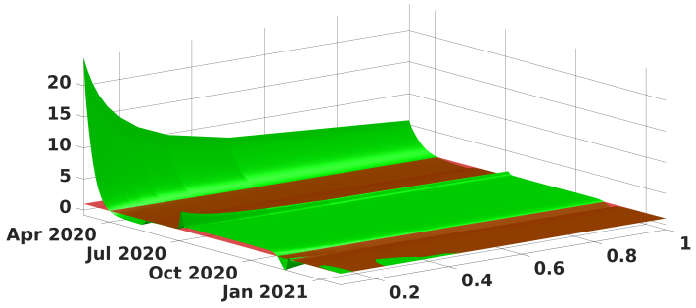

Figure 5.6.21: In this figure we plot $(t, \alpha) \to R_e(t)$ when t varies from January 03 2020 to January 04 2021 and α varies from 0.1 to 1 (or equivalently $1/\alpha$ varies from 10 days to 1 day).

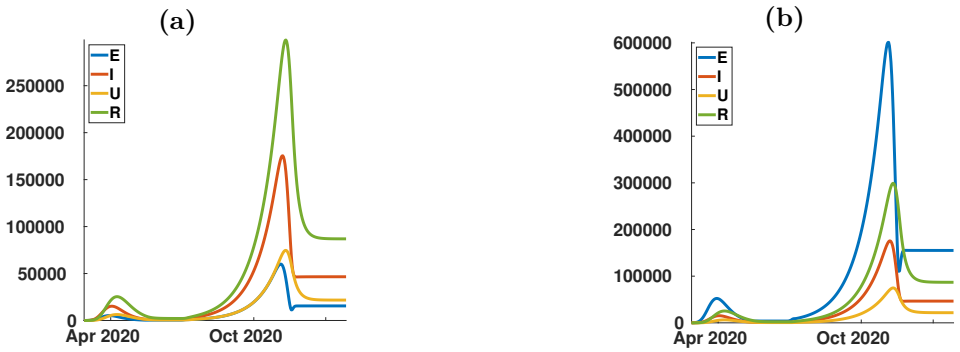

Figure 5.6.22: In this figure we explore the influence of the parameter f on the solution of model. The figure (a) corresponds to $1/\alpha = 1$ days and figure (b) corresponds to $1/\alpha = 10$ days. The remaining parameters are unchanged.

5.6.11 Upper bound of the duration for the exposed period and the asymptomatic infectious period

Let us finally mention that for each country and each epidemic wave we evaluated the parameter $1/(\chi\theta)$. In Figure 5.6.23 we plot the histogram of its estimated value and obtain a median value be 15.61 days. Therefore the length of exposure and the length asymptomatic infectious period should smaller than 15.61 days.

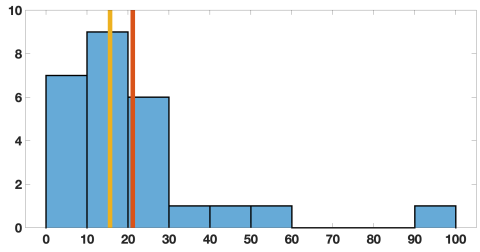

Figure 5.6.23: In this Figure we plot the histogram for the estimated values $1/(\chi\theta)$ (see Appendix E). The red vertical line is mean value which is equal to 21 days. The yellow vertical line is median value which is equal to 15.61 days.

In this section 5.6.11, we plot the estimated values of the parameter $1/(\chi\theta)$ for each epidemic period and each country consider in this study. The parameter corresponds to the upper bound of the length of the exposed period and asymptomatic infectious period. Indeed from the subsection devoted to the compatibility

condition we know that the average duration of the exposed period should satisfy

$$1/\nu \leq 1/(\chi\,\theta),$$

and the average duration of the asymptomatic infectious period should should satisfy

$$1/\alpha \leq 1/(\chi\,\theta).$$

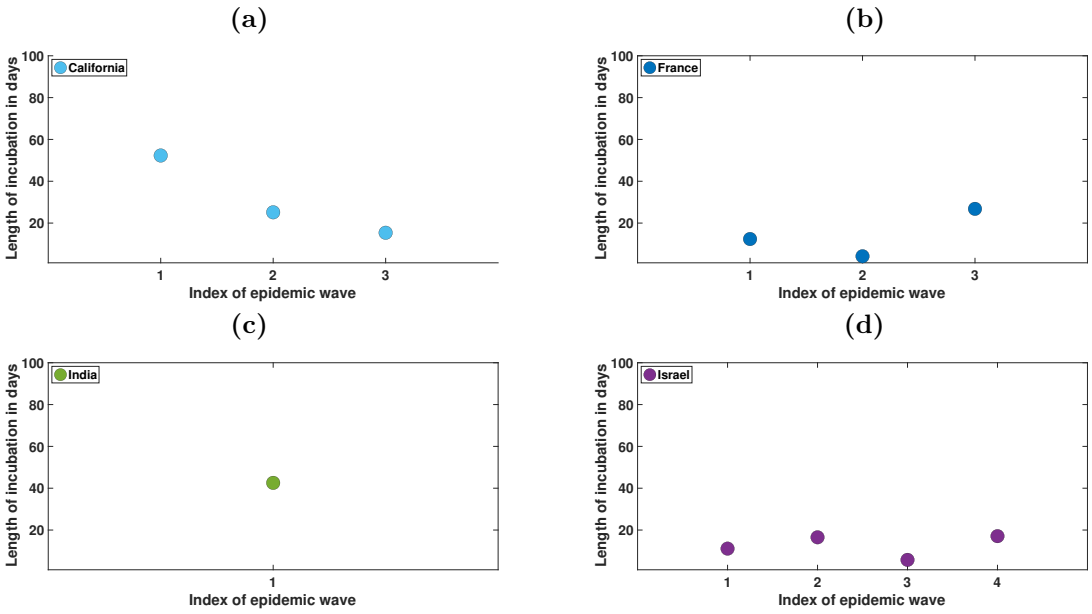

Figure 5.6.24: In this figure we plot the values of the parameter $1/(\chi\,\theta)$ estimated for each epidemic wave and for California (a), France (b), India (c), Israel (d). This parameter represents the maximal length of the incubation period. In each figure, we plot this parameter for each epidemic wave and for each country.

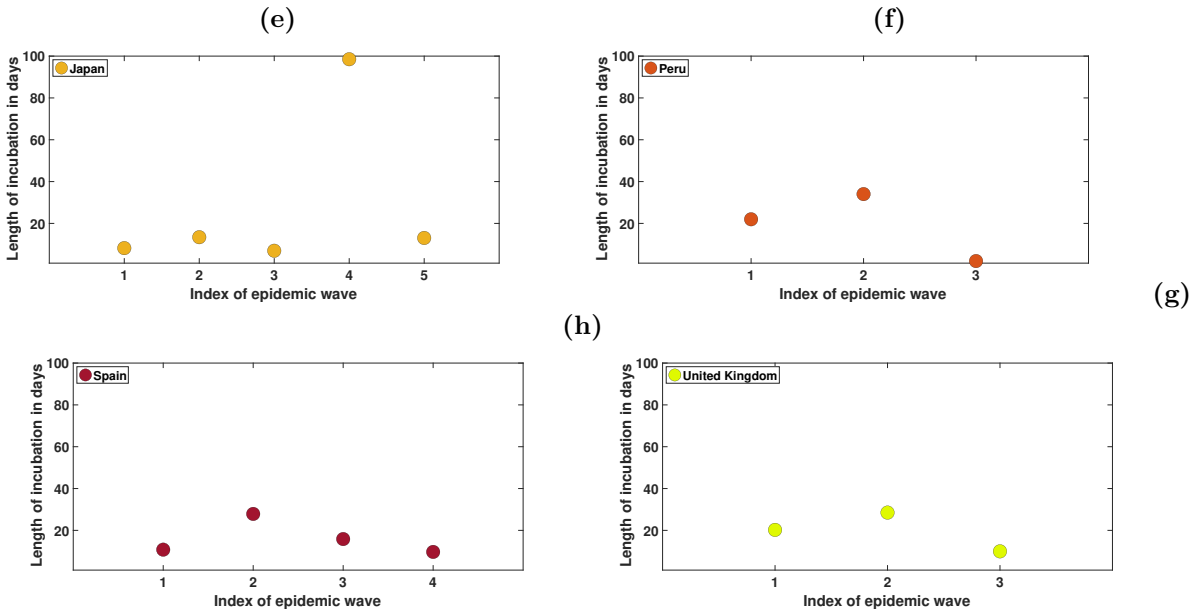

Figure 5.6.25: In this figure we plot the values of the parameter $1/(\chi\,\theta)$ estimated for each epidemic wave and for Japan (e), Peru (f), Spain (g) and United Kingdom (h). This parameter represents the maximal length of the incubation period. In each figure, we plot this parameter for each epidemic wave and for each country.

5.6.12 Computing R_0

The basic reproduction number R_0 can be computed for the SEIUR model by the formula (see [141, 149])

$$R_0 = \rho(FV^{-1}),$$

where F is the matrix containing new infections and V contains the rates of transfer between classes:

$$F := \begin{pmatrix} 0 & \tau S & \tau\kappa S & 0 \\ 0 & 0 & 0 & 0 \\ 0 & 0 & 0 & 0 \\ 0 & 0 & 0 & 0 \end{pmatrix}, \qquad V := \begin{pmatrix} \alpha & 0 & 0 & 0 \\ -\alpha & \nu & 0 & 0 \\ 0 & -\nu(1-f) & \eta & 0 \\ 0 & \nu(1-f) & 0 & \eta \end{pmatrix},$$

see [141] and [149] for details. Therefore

$$V^{-1} = \begin{pmatrix} 1/\alpha & 0 & 0 & 0 \\ 1/\nu & 1/\nu & 0 & 0 \\ (1-f)/\eta & (1-f)/\eta & 1/\eta & 0 \\ f/\eta & f/\eta & 0 & 1/\eta \end{pmatrix},$$

$$FV^{-1} = \frac{\tau S}{\eta\nu} \begin{pmatrix} \eta + \kappa\nu(1-f) & \eta + \kappa\nu(1-f) & \kappa\nu & 0 \\ 0 & 0 & 0 & 0 \\ 0 & 0 & 0 & 0 \\ 0 & 0 & 0 & 0 \end{pmatrix}.$$

It follows that

$$R_0 = \frac{\tau S}{\eta\nu}\big(\eta + \kappa\nu(1-f)\big).$$

5.6.13 Stochastic approach to effective reproductive ratio

In numerical applications, we also present the results obtained by applying the method described in the paper of Cori et al. [116]. Let us summarize the principle of the method. We consider that the incidence data (*i.e.,* the daily number of new reported cases) correspond to infection events that have occurred in the past. For each new reported case, we reconstruct the time the infectious period started by sampling a Gamma distribution (i.e. the time from the infection to the moment at which the individual is reported follows a Gamma distribution). The parameters of this Gamma distribution are computed to match the differential equation framework. In numerical application, $1/\mu = 10$ days, we took the average for the average of the Gamma distribution as well as its standard deviation. We denote I_t the resulting number of individuals that begin their infectious period on the day t. As described in [116], we use a smoothing window of τ days ($\tau = 14$ days in numerical applications). The resulting effective reproductive ratio R_t is then computed as

$$R_t = \frac{a + \displaystyle\sum_{s=t-\tau+1}^{t} I_s}{\frac{1}{b} + \sum_{s=t-\tau+1}^{t} \Lambda_s},$$

where a and b are a prior distribution on R_t (we took $a = 1$ and $b = 5$, as in [116]) and Λ_s is computed by the formula

$$\Lambda_s = \sum_{s=1}^{t} I_{t-s} w_s,$$

where w_s is the average infectiousness profile after time s. In numerical applications, and following [116, Web Appendix 11], we used the following formula for w_s

$$\begin{aligned} w_s = {} & sF_{\Gamma,\alpha,\beta}(s) + (s-2)F_{\Gamma,\alpha,\beta}(s-2) - 2(s-1)F_{\Gamma,\alpha,\beta}(s-1) \\ & + \alpha\beta(2F_{\Gamma,\alpha+1,\beta}(s-1) - F_{\Gamma,\alpha+1,\beta}(s-2) - F_{\Gamma,\alpha+1,\beta}(s)), \end{aligned}$$

where $F_{\Gamma,\alpha,\beta}(s)$ is the cumulative density of a Gamma distribution of parameters (α, β):

$$F_{\Gamma,\alpha,\beta}(t) = \int_0^t \frac{1}{\Gamma(\alpha)\beta^\alpha} s^{\alpha-1} e^{-\frac{s}{\beta}} \mathrm{d}s.$$

The parameters α and β are computed to match the Gamma distribution of the serial intervals which, in our case, have mean value $1/\mu = 10$ days and standard deviation as well of $1/\mu$, so that $\alpha = 1/\mu$ and $\beta = 1/\mu$.

Because of the sampling of random numbers involved in the computation of R_t, the procedure described above was repeated 100 times (each time drawing a new sequence of I_s from the daily number of new cases) and the final value of R_t presented in Figure 4 of the main text (green curves) is the average of the values obtained during these 100 simulations.

Bibliography

Articles published by the author

[P1] Q. Griette, G. Raoul, and S. Gandon. Virulence evolution at the front line of spreading epidemics. *Evolution* **69**.**11** (2015), pp. 2810–2819. DOI: 10.1111/evo.12781.

[P2] Q. Griette and G. Raoul. Existence and qualitative properties of travelling waves for an epidemiological model with mutations. *J. Differential Equations* **260**.**10** (2016), pp. 7115–7151. DOI: 10.1016/j.jde.2016.01.022.

[P3] M. Alfaro and Q. Griette. Pulsating fronts for Fisher-KPP systems with mutations as models in evolutionary epidemiology. *Nonlinear Anal. Real World Appl.* **42** (2018), pp. 255–289. DOI: 10.1016/j.nonrwa.2018.01.004.

[P4] Q. Griette. Singular measure traveling waves in an epidemiological model with continuous phenotypes. *Trans. Amer. Math. Soc.* **371**.**6** (2019), pp. 4411–4458. DOI: 10.1090/tran/7700.

[P5] Q. Griette and S. Motsch. Kinetic equations and self-organized band formations. In: *Active particles, Vol. 2*. Model. Simul. Sci. Eng. Technol. Birkhäuser/Springer, Cham, 2019, pp. 173–199.

[P6] J.-B. Burie, A. Ducrot, Q. Griette, and Q. Richard. Concentration estimates in a multi-host epidemiological model structured by phenotypic traits. *J. Differential Equations* **269**.**12** (2020), pp. 11492–11539. DOI: 10.1016/j.jde.2020.08.029.

[P7] J. Demongeot, Q. Griette, and P. Magal. SI epidemic model applied to COVID-19 data in mainland China. *R. Soc. Open Sci.* **7**.**12** (2020), p. 201878. DOI: 10.1098/rsos.201878.

[P8] X. Fu, Q. Griette, and P. Magal. A cell-cell repulsion model on a hyperbolic Keller-Segel equation. *J. Math. Biol.* **80**.**7** (2020), pp. 2257–2300. DOI: 10.1007/s00285-020-01495-w.

[P9] L. Girardin and Q. Griette. A Liouville-type result for non-cooperative Fisher-KPP systems and nonlocal equations in cylinders. *Acta Appl. Math.* **170** (2020), pp. 123–139. DOI: 10.1007/s10440-020-00327-9.

[P10] Q. Griette, P. Magal, and O. Seydi. Unreported Cases for Age Dependent COVID-19 Outbreak in Japan. *Biology* **9**.**6** (2020), p. 132. DOI: 10.3390/biology9060132.

[P11] X. Fu, Q. Griette, and P. Magal. Existence and uniqueness of solutions for a hyperbolic Keller-Segel equation. *Discrete Contin. Dyn. Syst. Ser. B* **26**.**4** (2021), pp. 1931–1966. DOI: 10.3934/dcdsb.2020326.

[P12] X. Fu, Q. Griette, and P. Magal. Sharp discontinuous traveling waves in a hyperbolic Keller-Segel equation. *Math. Models Methods Appl. Sci.* **31**.**5** (2021), pp. 861–905. DOI: 10.1142/S0218202521500214.

[P13] Q. Griette, J. Demongeot, and P. Magal. A robust phenomenological approach to investigate COVID-19 data for France. *Math. Appl. Sci. Eng.* **2**.**4** (2021), pp. 149–218. DOI: 10.5206/mase/14031.

[P14] Q. Griette and P. Magal. Clarifying predictions for COVID-19 from testing data: The example of New York State. *Infect. Dis. Model.* **6** (2021), pp. 273–283. DOI: https://doi.org/10.1016/j.idm.2020.12.011.

[P15] Q. Griette, J. Demongeot, and P. Magal. What can we learn from COVID-19 data by using epidemic models with unidentified infectious cases? *Math. Biosci. Eng.* **19**.**1** (2022), pp. 539–594. DOI: 10.3934/mbe.2022025.

Preprints submitted by the author

[P16] Q. Griette, Z. Liu, P. Magal, and R. Thompson. Real-time prediction of the end of an epidemic wave: COVID-19 in China as a case-study. *medRxiv* (2020). DOI: 10.1101/2020.04.14.20064824.

[P17] M. Alfaro, Q. Griette, D. Roze, and B. Sarels. The spatio-temporal dynamics of interacting genetic incompatibilities. Part I: The case of stacked underdominant clines. *arXiv preprint* (2021).

[P18] J.-B. Burie, A. Ducrot, and Q. Griette. *On the competitive exclusion principle for continuously distributed populations*. 2021.

[P19] Q. Griette and H. Matano. Propagation dynamics of solutions to spatially periodic reaction-diffusion systems with hybrid nonlinearity. *arXiv preprint* (2021).

General bibliography

[1] L. Abi Rizk, J.-B. Burie, and A. Ducrot. Travelling wave solutions for a non-local evolutionary-epidemic system. *J. Differential Equations* **267**.**2** (2019), pp. 1467–1509. DOI: 10.1016/j.jde.2019.02.012.

[2] A. S. Ackleh, J. Cleveland, and H. R. Thieme. Population dynamics under selection and mutation: long-time behavior for differential equations in measure spaces. *J. Differential Equations* **261**.**2** (2016), pp. 1472–1505. DOI: 10.1016/j.jde.2016.04.008.

[3] L. Addario-Berry, J. Berestycki, and S. Penington. Branching Brownian motion with decay of mass and the nonlocal Fisher-KPP equation. *Comm. Pure Appl. Math.* **72**.**12** (2019), pp. 2487–2577. DOI: 10.1002/cpa.21827.

[4] M. Alfaro, H. Berestycki, and G. Raoul. The effect of climate shift on a species submitted to dispersion, evolution, growth, and nonlocal competition. *SIAM J. Math. Anal.* **49**.**1** (2017), pp. 562–596. DOI: 10.1137/16M1075934.

[5] M. Alfaro and R. Carles. Replicator-mutator equations with quadratic fitness. *Proc. Amer. Math. Soc.* **145**.**12** (2017), pp. 5315–5327. DOI: 10.1090/proc/13669.

[6] M. Alfaro and J. Coville. Rapid traveling waves in the nonlocal Fisher equation connect two unstable states. *Appl. Math. Lett.* **25**.**12** (2012), pp. 2095–2099. DOI: 10.1016/j.aml.2012.05.006.

[7] M. Alfaro, J. Coville, and G. Raoul. Travelling waves in a nonlocal reaction-diffusion equation as a model for a population structured by a space variable and a phenotypic trait. *Comm. Partial Differential Equations* **38**.**12** (2013), pp. 2126–2154. DOI: 10.1080/03605302.2013.828069.

[8] M. Alfaro, J. Coville, and G. Raoul. Bistable travelling waves for nonlocal reaction diffusion equations. *Discrete Contin. Dyn. Syst.* **34**.**5** (2014), pp. 1775–1791. DOI: 10.3934/dcds.2014.34.1775.

[9] M. Alfaro and M. Veruete. Evolutionary branching via replicator-mutator equations. *J. Dynam. Differential Equations* **31**.**4** (2019), pp. 2029–2052. DOI: 10.1007/s10884-018-9692-9.

[10] S. Alizon, A. Hurford, N. Mideo, and M. Van Baalen. Virulence evolution and the trade-off hypothesis: history, current state of affairs and the future. *J. Evol. Biol.* **22**.**2** (2009), pp. 245–259. DOI: 10.1111/j.1420-9101.2008.01658.x.

[11] L. Ambrosio. Geometric evolution problems, distance function and viscosity solutions. In: *Calculus of variations and partial differential equations (Pisa, 1996)*. Springer, Berlin, 2000, pp. 5–93.

[12] R. M. Anderson and R. M. May. *Infectious diseases of humans: dynamics and control*. Oxford university press, 1992.

[13] E. Anzolin and A. Amante. First Italian dies of coronavirus as outbreak flares in north. *World News February* **21** (2020).

[14] N. Apreutesei, A. Ducrot, and V. Volpert. Travelling waves for integro-differential equations in population dynamics. *Discrete Contin. Dyn. Syst. Ser. B* **11**.**3** (2009), pp. 541–561. DOI: 10.3934/dcdsb.2009.11.541.

[15] J. Arino et al. Simple models for containment of a pandemic. *J. R. Soc. Interface* **3**.**8** (2006), pp. 453–457. DOI: 10.1098/rsif.2006.0112.

[16] N. J. Armstrong, K. J. Painter, and J. A. Sherratt. A continuum approach to modelling cell-cell adhesion. *J. Theoret. Biol.* **243.1** (2006), pp. 98–113. DOI: 10.1016/j.jtbi.2006.05.030.

[17] R. A. Armstrong and R. McGehee. Competitive exclusion. *Amer. Natur.* **115.2** (1980), pp. 151–170. DOI: 10.1086/283553.

[18] A. Arnold, L. Desvillettes, and C. Prévost. Existence of nontrivial steady states for populations structured with respect to space and a continuous trait. *Commun. Pure Appl. Anal.* **11.1** (2012), pp. 83–96. DOI: 10.3934/cpaa.2012.11.83.

[19] D. G. Aronson and H. F. Weinberger. Nonlinear diffusion in population genetics, combustion, and nerve pulse propagation. In: *Partial differential equations and related topics (Program, Tulane Univ., New Orleans, La., 1974)*. Springer, Berlin, 1975, 5–49. Lecture Notes in Math., Vol. 446.

[20] D. G. Aronson and H. F. Weinberger. Multidimensional nonlinear diffusion arising in population genetics. *Adv. in Math.* **30.1** (1978), pp. 33–76. DOI: 10.1016/0001-8708(78)90130-5.

[21] D. G. Aronson. Density-dependent interaction-diffusion systems. In: *Dynamics and modelling of reactive systems (Proc. Adv. Sem., Math. Res. Center, Univ. Wisconsin, Madison, Wis., 1979)*. Vol. 44. Publ. Math. Res. Center Univ. Wisconsin. Academic Press, New York-London, 1980, pp. 161–176.

[22] B. Ashby, S. Gupta, and A. Buckling. Spatial Structure Mitigates Fitness Costs in Host-Parasite Coevolution. *Am. Nat.* **183.3** (2014). PMID: 24561607, E64–E74. DOI: 10.1086/674826.

[23] C. Atkinson, G. E. H. Reuter, and C. J. Ridler-Rowe. Traveling wave solution for some nonlinear diffusion equations. *SIAM J. Math. Anal.* **12.6** (1981), pp. 880–892. DOI: 10.1137/0512074.

[24] A. Attanayake, S. Perera, and S. Jayasinghe. Phenomenological Modelling of COVID-19 Epidemics in Sri Lanka, Italy, the United States, and Hebei Province of China. *Comput. Math. Methods Med.* **2020** (2020). DOI: 10.1155/2020/6397063.

[25] H. H. Ayoub et al. Age could be driving variable SARS-CoV-2 epidemic trajectories worldwide. *PLoS One* **15.8** (2020), e0237959. DOI: 10.1371/journal.pone.0237959.

[26] H. H. Ayoub et al. Characterizing key attributes of COVID-19 transmission dynamics in China's original outbreak: Model-based estimations. *Glob. Epidemiol.* **2** (2020), p. 100042. DOI: 10.1016/j.gloepi.2020.100042.

[27] N. T. Bailey et al. *The mathematical theory of infectious diseases and its applications*. 2nd ediition. Charles Griffin & Company Ltd 5a Crendon Street, High Wycombe, Bucks HP13 6LE., 1975.

[28] P. C. Bailey et al. Single-cell tracking of breast cancer cells enables prediction of sphere formation from early cell divisions. *Iscience* **8** (2018), pp. 29–39. DOI: 10.1016/j.isci.2018.08.015.

[29] A. Bakhta, T. Boiveau, Y. Maday, and O. Mula. Epidemiological Forecasting with Model Reduction of Compartmental Models. Application to the COVID-19 Pandemic. *Biology* **10.1** (2021), p. 22. DOI: 10.3390/biology10010022.

[30] D. Balagué, J. A. Carrillo, T. Laurent, and G. Raoul. Nonlocal interactions by repulsive-attractive potentials: radial ins/stability. *Phys. D* **260** (2013), pp. 5–25. DOI: 10.1016/j.physd.2012.10.002.

[31] Y. M. Bar-On, A. Flamholz, R. Phillips, and R. Milo. Science Forum: SARS-CoV-2 (COVID-19) by the numbers. *eLife* **9** (2020), e57309. DOI: 10.7554/eLife.57309.

[32] G. Barles, L. C. Evans, and P. E. Souganidis. Wavefront propagation for reaction-diffusion systems of PDE. *Duke Math. J.* **61.3** (1990), pp. 835–858. DOI: 10.1215/S0012-7094-90-06132-0.

[33] G. Barles, S. Mirrahimi, and B. Perthame. Concentration in Lotka-Volterra parabolic or integral equations: a general convergence result. *Methods Appl. Anal.* **16.3** (2009), pp. 321–340. DOI: 10.4310/MAA.2009.v16.n3.a4.

[34] G. Barles and B. Perthame. Concentrations and constrained Hamilton-Jacobi equations arising in adaptive dynamics. In: *Recent developments in nonlinear partial differential equations*. Vol. 439. Contemp. Math. Amer. Math. Soc., Providence, RI, 2007, pp. 57–68. DOI: 10.1090/conm/439/08463.

[35] N. H. Barton. The dynamics of hybrid zones. *Heredity* **43** (1979), pp. 341–359. DOI: 10.1038/hdy.1979.87.

[36] N. H. Barton. Multilocus clines. *Evolution* **37** (1983), pp. 454–471. DOI: 10.1111/j.1558-5646.1983.tb05563.x.

[37] N. H. Barton and M. A. R. de Cara. The evolution of strong reproductive isolation. *Evolution* **63** (2009), pp. 1171–1190. DOI: 10.1111/j.1558-5646.2009.00622.x.

[38] N. H. Barton and K. S. Gale. Genetic analysis of hybrid zones. In: *Hybrid zones and the evolutionary process*. Ed. by R. G. Harrison. New York, USA: Oxford University Press, 1993, pp. 13–45.

[39] N. H. Barton and G. M. Hewitt. Analysis of hybrid zones. *Ann. Rev. Ecol. Sys.* **16** (1985), pp. 113–148. DOI: 10.1146/annurev.es.16.110185.000553.

[40] N. H. Barton and G. M. Hewitt. Adaptation, speciation and hybrid zones. *Nature* **341** (1989), pp. 497–503. DOI: 10.1038/341497a0.

[41] A. D. Bazykin. A hypothetical mechanism of speciation. *Evolution* **23** (1969), pp. 685–687. DOI: 10.2307/2406862.

[42] C. Beaumont, J.-B. Burie, A. Ducrot, and P. Zongo. Propagation of salmonella within an industrial hen house. *SIAM J. Appl. Math.* **72**.**4** (2012), pp. 1113–1148. DOI: 10.1137/110822967.

[43] G. Bell and A. Gonzalez. Adaptation and Evolutionary Rescue in Metapopulations Experiencing Environmental Deterioration. *Science* **332**.**6035** (2011), pp. 1327–1330. DOI: 10.1126/science.1203105.

[44] N. Bellomo, A. Bellouquid, J. Nieto, and J. Soler. On the asymptotic theory from microscopic to macroscopic growing tissue models: an overview with perspectives. *Math. Models Methods Appl. Sci.* **22**.**1** (2012), pp. 1130001, 37. DOI: 10.1142/S0218202512005885.

[45] A. Bensoussan, J.-L. Lions, and G. Papanicolaou. *Asymptotic analysis for periodic structures*. Corrected reprint of the 1978 original. AMS Chelsea Publishing, Providence, RI, 2011, pp. xii+398. DOI: 10.1090/chel/374.

[46] H. Berestycki, G. Nadin, B. Perthame, and L. Ryzhik. The non-local Fisher–KPP equation: travelling waves and steady states. *Nonlinearity* **22**.**12** (2009), p. 2813. DOI: 10.1088/0951-7715/22/12/002.

[47] H. Berestycki and L. Nirenberg. On the method of moving planes and the sliding method. *Bol. Soc. Brasil. Mat. (N.S.)* **22**.**1** (1991), pp. 1–37. DOI: 10.1007/BF01244896.

[48] H. Berestycki and F. Hamel. Front propagation in periodic excitable media. *Comm. Pure Appl. Math.* **55**.**8** (2002), pp. 949–1032. DOI: 10.1002/cpa.3022.

[49] H. Berestycki and F. Hamel. Gradient estimates for elliptic regularizations of semilinear parabolic and degenerate elliptic equations. *Comm. Partial Differential Equations* **30**.**1-3** (2005), pp. 139–156. DOI: 10.1081/PDE-200044478.

[50] H. Berestycki, F. Hamel, and L. Roques. Analysis of the periodically fragmented environment model. II. Biological invasions and pulsating travelling fronts. *J. Math. Pures Appl. (9)* **84**.**8** (2005), pp. 1101–1146. DOI: 10.1016/j.matpur.2004.10.006.

[51] H. Berestycki, F. Hamel, and L. Rossi. Liouville-type results for semilinear elliptic equations in unbounded domains. *Ann. Mat. Pura Appl. (4)* **186**.**3** (2007), pp. 469–507. DOI: 10.1007/s10231-006-0015-0.

[52] H. Berestycki, T. Jin, and L. Silvestre. Propagation in a non local reaction diffusion equation with spatial and genetic trait structure. *Nonlinearity* **29**.**4** (2016), pp. 1434–1466. DOI: 10.1088/0951-7715/29/4/1434.

[53] H. Berestycki, B. Nicolaenko, and B. Scheurer. Traveling wave solutions to combustion models and their singular limits. *SIAM J. Math. Anal.* **16**.**6** (1985), pp. 1207–1242. DOI: 10.1137/0516088.

[54] H. Berestycki and L. Rossi. On the principal eigenvalue of elliptic operators in $\mathbb{R}^N$ and applications. *J. Eur. Math. Soc. (JEMS)* **8**.**2** (2006), pp. 195–215. DOI: 10.4171/JEMS/47.

[55] H. Berestycki and L. Rossi. Generalizations and properties of the principal eigenvalue of elliptic operators in unbounded domains. *Comm. Pure Appl. Math.* **68**.**6** (2015), pp. 1014–1065. DOI: 10.1002/cpa.21536.

[56] T. W. Berngruber, R. Froissart, M. Choisy, and S. Gandon. Evolution of Virulence in Emerging Epidemics. *PLoS Pathog.* **9**.**3** (2013), e1003209. DOI: 10.1371/journal.ppat.1003209.

[57] A. J. Bernoff and C. M. Topaz. Nonlocal aggregation models: a primer of swarm equilibria [reprint of MR2788924]. *SIAM Rev.* **55**.**4** (2013), pp. 709–747. DOI: 10.1137/130925669.

[58] D. Bernoulli. Essai d'une nouvelle analyse de la petite Vérole, & des avantages de l'Inoculation pour la prévenir. *Histoire de l'Académie royale des sciences avec les mémoires de mathématique et de physique tirés de cette Académie* (1766), pp. 1–45.

[59] D. Bernoulli and S. Blower. An attempt at a new analysis of the mortality caused by smallpox and of the advantages of inoculation to prevent it. *Rev. Med. Virol.* **14.5** (2004), p. 275. DOI: 10.1002/rmv.443.

[60] A. L. Bertozzi, T. Laurent, and J. Rosado. L^p theory for the multidimensional aggregation equation. *Comm. Pure Appl. Math.* **64.1** (2011), pp. 45–83. DOI: 10.1002/cpa.20334.

[61] M. Bertsch, D. Hilhorst, H. Izuhara, and M. Mimura. A nonlinear parabolic-hyperbolic system for contact inhibition of cell-growth. *Differ. Equ. Appl.* **4.1** (2012), pp. 137–157. DOI: 10.7153/dea-04-09.

[62] A. Best, S. Webb, A. White, and M. Boots. Host resistance and coevolution in spatially structured populations. *Proc. R. Soc. Lond. B* **278.1715** (2011), pp. 2216–2222. DOI: 10.1098/rspb.2010.1978.

[63] V. I. Bogachev. *Measure theory. Vol. I, II*. Springer-Verlag, Berlin, 2007, Vol. I: xviii+500 pp., Vol. II: xiv+575. DOI: 10.1007/978-3-540-34514-5.

[64] O. Bonnefon, J. Coville, and G. Legendre. Concentration phenomenon in some non-local equation. *Discrete Contin. Dyn. Syst. Ser. B* **22.3** (2017), pp. 763–781. DOI: 10.3934/dcdsb.2017037.

[65] E. Bouin and V. Calvez. Travelling waves for the cane toads equation with bounded traits. *Nonlinearity* **27.9** (2014), pp. 2233–2253. DOI: 10.1088/0951-7715/27/9/2233.

[66] E. Bouin, V. Calvez, and G. Nadin. Propagation in a kinetic reaction-transport equation: travelling waves and accelerating fronts. *Arch. Ration. Mech. Anal.* **217.2** (2015), pp. 571–617. DOI: 10.1007/s00205-014-0837-7.

[67] E. Bouin, M. H. Chan, C. Henderson, and P. S. Kim. Influence of a mortality trade-off on the spreading rate of cane toads fronts. *Comm. Partial Differential Equations* **43.11** (2018), pp. 1627–1671. DOI: 10.1080/03605302.2018.1523190.

[68] E. Bouin, C. Henderson, and L. Ryzhik. Super-linear spreading in local and non-local cane toads equations. *J. Math. Pures Appl. (9)* **108.5** (2017), pp. 724–750. DOI: 10.1016/j.matpur.2017.05.015.

[69] E. Bouin, C. Henderson, and L. Ryzhik. The Bramson logarithmic delay in the cane toads equations. *Quart. Appl. Math.* **75.4** (2017), pp. 599–634. DOI: 10.1016/j.matpur.2017.05.015.

[70] E. Bouin, C. Henderson, and L. Ryzhik. The Bramson delay in the non-local Fisher-KPP equation. *Ann. Inst. H. Poincaré Anal. Non Linéaire* **37.1** (2020), pp. 51–77. DOI: 10.1016/j.anihpc.2019.07.001.

[71] E. Bouin and S. Mirrahimi. A Hamilton-Jacobi approach for a model of population structured by space and trait. *Commun. Math. Sci.* **13.6** (2015), pp. 1431–1452. DOI: 10.4310/CMS.2015.v13.n6.a4.

[72] E. Bouin et al. Invasion fronts with variable motility: phenotype selection, spatial sorting and wave acceleration. *C. R. Math. Acad. Sci. Paris* **350.15-16** (2012), pp. 761–766. DOI: 10.1016/j.crma.2012.09.010.

[73] N. Bourbaki. *Elements of Mathematics. Integration I*. Springer, Berlin, Heidelberg, 2004. DOI: 10.1007/978-3-642-59312-3.

[74] M. Bramson. Convergence of solutions of the Kolmogorov equation to travelling waves. *Mem. Amer. Math. Soc.* **44.285** (1983), pp. iv+190. DOI: 10.1090/memo/0285.

[75] F. Brauer and C. Castillo-Chavez. *Mathematical models in population biology and epidemiology*. Second. Vol. 40. Texts in Applied Mathematics. Springer, New York, 2012, pp. xxiv+508. DOI: 10.1007/978-1-4614-1686-9.

[76] F. Brauer, C. Castillo-Chavez, and Z. Feng. *Mathematical models in epidemiology*. Vol. 69. Texts in Applied Mathematics. With a foreword by Simon Levin. Springer, New York, 2019, pp. xvii+619. DOI: 10.1007/978-1-4939-9828-9.

[77] F. Brauer, P. Van den Driessche, and J. Wu. *Mathematical epidemiology*. Vol. 1945. Springer, 2008.

[78] H.-J. Bremermann and H. R. Thieme. A competitive exclusion principle for pathogen virulence. *J. Math. Biol.* **27.2** (1989), pp. 179–190. DOI: 10.1007/BF00276102.

[79] H. Brezis. *Functional analysis, Sobolev spaces and partial differential equations*. Universitext. Springer, New York, 2011, pp. xiv+599.

[80] T. Britton and E. Pardoux. Inference based on the diffusion approximation of epidemic models. In: *Stochastic epidemic models with inference*. Vol. 2255. Lecture Notes in Math. Springer, Cham, 2019, pp. 363–416. DOI: 10.1007/978-3-030-30900-8_14.

[81] R. F. Brown. *A topological introduction to nonlinear analysis*. Third edition. Springer, Cham, 2014, pp. x+240. DOI: 10.1007/978-3-319-11794-2.

[82] R. F. Brown. *A topological introduction to nonlinear analysis*. Second. Birkhäuser Boston, Inc., Boston, MA, 2004, pp. xiv+184. DOI: 10.1007/978-0-8176-8124-1.

[83] M. Burger, R. Fetecau, and Y. Huang. Stationary states and asymptotic behavior of aggregation models with nonlinear local repulsion. *SIAM J. Appl. Dyn. Syst.* **13.1** (2014), pp. 397–424. DOI: 10.1137/130923786.

[84] R. Bürger and I. Bomze. Stationary distributions under mutation-selection balance: structure and properties. *Adv. in Appl. Probab.* **28.1** (1996), pp. 227–251. DOI: 10.2307/1427919.

[85] J.-B. Burie, R. Djidjou-Demasse, and A. Ducrot. Asymptotic and transient behaviour for a nonlocal problem arising in population genetics. *European J. Appl. Math.* **31.1** (2020), pp. 84–110. DOI: 10.1017/s0956792518000487.

[86] J.-B. Burie, R. Djidjou-Demasse, and A. Ducrot. Slow convergence to equilibrium for an evolutionary epidemiology integro-differential system. *Discrete Contin. Dyn. Syst. Ser. B* **25.6** (2020), pp. 2223–2243. DOI: 10.3934/dcdsb.2019225.

[87] J. Busca and B. Sirakov. Harnack type estimates for nonlinear elliptic systems and applications. *Ann. Inst. H. Poincaré Anal. Non Linéaire* **21.5** (2004), pp. 543–590. DOI: 10.1016/j.anihpc.2003.06.001.

[88] S. Busenberg and K. Cooke. *Vertically transmitted diseases*. Vol. 23. Biomathematics. Models and dynamics. Springer-Verlag, Berlin, 1993, pp. xii+248. DOI: 10.1007/978-3-642-75301-5.

[89] G. J. Butler and G. S. K. Wolkowicz. A mathematical model of the chemostat with a general class of functions describing nutrient uptake. *SIAM J. Appl. Math.* **45.1** (1985), pp. 138–151. DOI: 10.1137/0145006.

[90] O. Bylicki, N. Paleiron, and F. Janvier. An outbreak of covid-19 on an aircraft carrier. *N. Engl. J. Med.* **384.10** (2021), p. 976. DOI: 10.1056/NEJMc2034424.

[91] A. W. Byrne et al. Inferred duration of infectious period of SARS-CoV-2: rapid scoping review and analysis of available evidence for asymptomatic and symptomatic COVID-19 cases. *BMJ Open* **10.8** (2020), e039856.

[92] A. Calsina and S. Cuadrado. Stationary solutions of a selection mutation model: the pure mutation case. *Math. Models Methods Appl. Sci.* **15.7** (2005), pp. 1091–1117. DOI: 10.1142/S0218202505000637.

[93] A. Calsina, S. Cuadrado, L. Desvillettes, and G. Raoul. Asymptotics of steady states of a selection-mutation equation for small mutation rate. *Proc. Roy. Soc. Edinburgh Sect. A* **143.6** (2013), pp. 1123–1146. DOI: 10.1017/S0308210510001629.

[94] V. Calvez and L. Corrias. The parabolic-parabolic Keller-Segel model in $\mathbb{R}^2$. *Commun. Math. Sci.* **6.2** (2008), pp. 417–447.

[95] V. Calvez and Y. Dolak-Struß. Asymptotic behavior of a two-dimensional Keller–Segel model with and without density control. In: *Mathematical Modeling of Biological Systems, Volume II*. Springer, 2008, pp. 323–337. DOI: 10.1007/978-0-8176-4556-4_29.

[96] V. Calvez et al. *Non-local competition slows down front acceleration during dispersal evolution*. 2019.

[97] J. A. Cañizo, J. A. Carrillo, and S. Cuadrado. Measure solutions for some models in population dynamics. *Acta Appl. Math.* **123** (2013), pp. 141–156. DOI: 10.1007/s10440-012-9758-3.

[98] R. S. Cantrell, C. Cosner, and Y. Lou. Evolutionary stability of ideal free dispersal strategies in patchy environments. *J. Math. Biol.* **65.5** (2012), pp. 943–965. DOI: 10.1007/s00285-011-0486-5.

[99] R. S. Cantrell, C. Cosner, Y. Lou, and D. Ryan. Evolutionary stability of ideal free dispersal strategies: a nonlocal dispersal model. *Can. Appl. Math. Q.* **20.1** (2012), pp. 15–38.

[100] R. S. Cantrell, C. Cosner, and X. Yu. Dynamics of populations with individual variation in dispersal on bounded domains. *J. Biol. Dyn.* **12.1** (2018), pp. 288–317. DOI: 10.1080/17513758.2018.1445305.

[101] R. S. Cantrell, C. Cosner, and X. Yu. Populations with individual variation in dispersal in heterogeneous environments: dynamics and competition with simply diffusing populations. *Sci. China Math.* **63.3** (2020), pp. 441–464. DOI: 10.1007/s11425-019-1623-2.

[102] Q. Cao, Y.-C. Chen, C.-L. Chen, and C.-H. Chiu. SARS-CoV-2 infection in children: Transmission dynamics and clinical characteristics. *J. Formos. Med. Assoc.* **119.3** (2020), p. 670.

[103] K. Carrapatoso and S. Mischler. Uniqueness and long time asymptotics for the parabolic-parabolic Keller-Segel equation. *Comm. Partial Differential Equations* **42.2** (2017), pp. 291–345. DOI: 10.1080/03605302.2017.1280682.

[104] J. A. Carrillo et al. Confinement in nonlocal interaction equations. *Nonlinear Anal.* **75.2** (2012), pp. 550–558. DOI: 10.1016/j.na.2011.08.057.

[105] J. A. Carrillo et al. A population dynamics model of cell-cell adhesion incorporating population pressure and density saturation. *J. Theoret. Biol.* **474** (2019), pp. 14–24. DOI: 10.1016/j.jtbi.2019.04.023.

[106] M. Castro, S. Ares, J. A. Cuesta, and S. Manrubia. The turning point and end of an expanding epidemic cannot be precisely forecast. *Proc. Natl. Acad. Sci. U.S.A.* **117.42** (2020), pp. 26190–26196. DOI: 10.1073/pnas.2007868117.

[107] T. Cazenave and A. Haraux. *An introduction to semilinear evolution equations*. Vol. 13. Oxford Lecture Series in Mathematics and its Applications. Translated from the 1990 French original by Yvan Martel and revised by the authors. The Clarendon Press, Oxford University Press, New York, 1998, pp. xiv+186.

[108] M. Chikina and W. Pegden. Modeling strict age-targeted mitigation strategies for COVID-19. *PloS one* **15.7** (2020), e0236237. DOI: 10.1371/journal.pone.0236237.

[109] S. Childress. Chemotactic collapse in two dimensions. In: *Modelling of patterns in space and time (Heidelberg, 1983)*. Vol. 55. Lecture Notes in Biomath. Springer, Berlin, 1984, pp. 61–66. DOI: 10.1007/978-3-642-45589-6_6.

[110] G. Chowell et al. Estimation of the reproduction number of dengue fever from spatial epidemic data. *Math. Biosci.* **208.2** (2007), pp. 571–589. DOI: 10.1016/j.mbs.2006.11.011.

[111] G. Chowell et al. The basic reproductive number of Ebola and the effects of public health measures: the cases of Congo and Uganda. *J. Theoret. Biol.* **229.1** (2004), pp. 119–126. DOI: 10.1016/j.jtbi.2004.03.006.

[112] A. M. Ćmiel and B. Ćmiel. A simple method to describe the COVID-19 trajectory and dynamics in any country based on Johnson cumulative density function fitting. *Sci. Rep.* **11.1** (2021), pp. 1–10. DOI: 10.1038/s41598-021-97285-5.

[113] P. Constantin, K. Domelevo, J.-M. Roquejoffre, and L. Ryzhik. Existence of pulsating waves in a model of flames in sprays. *J. Eur. Math. Soc. (JEMS)* **8.4** (2006), pp. 555–584. DOI: 10.4171/JEMS/67.

[114] M. Conti, S. Terracini, and G. Verzini. A variational problem for the spatial segregation of reaction-diffusion systems. *Indiana Univ. Math. J.* **54.3** (2005), pp. 779–815. DOI: 10.1512/iumj.2005.54.2506.

[115] R. B. Corbett-Detig et al. Genetic incompatibilities are widespread within species. *Nature* **504** (2013), pp. 135–139. DOI: 10.1038/nature12678.

[116] A. Cori, N. M. Ferguson, C. Fraser, and S. Cauchemez. A new framework and software to estimate time-varying reproduction numbers during epidemics. *Am. J. Epidemiol.* **178.9** (2013), pp. 1505–1512. DOI: 10.1093/aje/kwt133.

[117] R. M. Cotta, C. P. Naveira-Cotta, and P. Magal. Mathematical Parameters of the COVID-19 Epidemic in Brazil and Evaluation of the Impact of Different Public Health Measures. *Biology* **9.8** (2020). DOI: 10.3390/biology9080220.

[118] J. Coville. On a simple criterion for the existence of a principal eigenfunction of some nonlocal operators. *J. Differential Equations* **249.11** (2010), pp. 2921–2953. DOI: 10.1016/j.jde.2010.07.003.

[119] J. Coville. Singular measure as principal eigenfunctions of some nonlocal operators. *Appl. Math. Lett.* **26.8** (2013), pp. 831–835. DOI: 10.1016/j.aml.2013.03.005.

[120] J. Coville, J. Dávila, and S. Martínez. Pulsating fronts for nonlocal dispersion and KPP nonlinearity. *Ann. Inst. H. Poincaré Anal. Non Linéaire* **30.2** (2013), pp. 179–223. DOI: 10.1016/j.anihpc.2012.07.005.

[121] J. Coville and L. Dupaigne. Propagation speed of travelling fronts in non local reaction-diffusion equations. *Nonlinear Anal.* **60.5** (2005), pp. 797–819. DOI: 10.1016/j.na.2003.10.030.

[122] J. A. Coyne and H. A. Orr. *Speciation*. Sinauer Associates, Inc., Sunderland MA, 2004.

[123] M. G. Crandall and P. H. Rabinowitz. Bifurcation from simple eigenvalues. *J. Functional Analysis* **8** (1971), pp. 321–340. DOI: 10.1016/0022-1236(71)90015-2.

[124] E. C. M. Crooks et al. Spatial segregation limit of a competition-diffusion system with Dirichlet boundary conditions. *Nonlinear Anal. Real World Appl.* **5.4** (2004), pp. 645–665. DOI: 10.1016/j.nonrwa.2004.01.004.

[125] J. F. Crow and M. Kimura. *An introduction to population genetics theory*. Harper & Row, Publishers, New York-London, 1970, pp. xiv+591.

[126] J. M. Cushing. Two species competition in a periodic environment. *J. Math. Biol.* **10.4** (1980), pp. 385–400. DOI: 10.1007/BF00276097.

[127] L. Damascelli and F. Pacella. Symmetry results for cooperative elliptic systems via linearization. *SIAM J. Math. Anal.* **45.3** (2013), pp. 1003–1026. DOI: 10.1137/110853534.

[128] E. N. Dancer, D. Hilhorst, M. Mimura, and L. A. Peletier. Spatial segregation limit of a competition-diffusion system. *European J. Appl. Math.* **10.2** (1999), pp. 97–115. DOI: 10.1017/S0956792598003660.

[129] E. B. Davies. *Linear operators and their spectra*. Vol. 106. Cambridge Studies in Advanced Mathematics. Cambridge University Press, Cambridge, 2007, pp. xii+451. DOI: 10.1017/CBO9780511618864.

[130] N. G. Davies et al. Age-dependent effects in the transmission and control of COVID-19 epidemics. *Nat. Med.* **26.8** (2020), pp. 1205–1211. DOI: 10.1038/s41591-020-0962-9.

[131] N. G. Davies et al. Effects of non-pharmaceutical interventions on COVID-19 cases, deaths, and demand for hospital services in the UK: a modelling study. *Lancet Public Health* **5.7** (2020), e375–e385. DOI: 10.1016/S2468-2667(20)30133-X.

[132] M. Davis, R. Shaw, and J. Etterson. Evolutionary responses to changing climate. *Ecology* **86** (2005), pp. 1704–1714. DOI: 10.1890/03-0788.

[133] T. Day and S. Gandon. Applying population-genetic models in theoretical evolutionary epidemiology. *Ecology Letters* **10.10** (2007), pp. 876–888. DOI: 10.1111/j.1461-0248.2007.01091.x.

[134] F. Débarre, T. Lenormand, and S. Gandon. Evolutionary Epidemiology of Drug-Resistance in Space. *PLoS Comput. Biol.* **5.4** (Apr. 2009), pp. 1–8. DOI: 10.1371/journal.pcbi.1000337.

[135] J. Demongeot, O. Hansen, and C. Taramasco. Complex systems and contagious social diseases: example of obesity. *Virulence* **7** (2015), pp. 129–140.

[136] J. Demongeot, Y. Flet-Berliac, and H. Seligmann. Temperature decreases spread parameters of the new Covid-19 case dynamics. *Biology* **9.5** (2020), p. 94.

[137] J. Demongeot, M. Jelassi, and C. Taramasco. From susceptibility to frailty in social networks: The case of obesity. *Math. Popul. Stud.* **24.4** (2017), pp. 219–245. DOI: 10.1080/08898480.2017.1348718.

[138] J. Demongeot and C. Taramasco. Evolution of social networks: the example of obesity. *Biogerontology* **15.6** (2014), pp. 611–626. DOI: 10.1007/s10522-014-9542-z.

[139] L. Desvillettes, P.-E. Jabin, S. Mischler, and G. Raoul. On selection dynamics for continuous structured populations. *Commun. Math. Sci.* **6.3** (2008), pp. 729–747.

[140] O. Diekmann, P.-E. Jabin, S. Mischler, and B. Perthame. The dynamics of adaptation: An illuminating example and a Hamilton–Jacobi approach. *Theor. Popul. Biol.* **67.4** (2005), pp. 257–271. DOI: 10.1016/j.tpb.2004.12.003.

[141] O. Diekmann, J. A. P. Heesterbeek, and J. A. J. Metz. On the definition and the computation of the basic reproduction ratio R_0 in models for infectious diseases in heterogeneous populations. *J. Math. Biol.* **28**.**4** (1990), pp. 365–382. DOI: 10.1007/BF00178324.

[142] O. Diekmann, H. Heesterbeek, and T. Britton. *Mathematical tools for understanding infectious disease dynamics*. Princeton Series in Theoretical and Computational Biology. Princeton University Press, Princeton, NJ, 2013, pp. xiv+502.

[143] K. Dietz and J. A. P. Heesterbeek. Daniel Bernoulli's epidemiological model revisited. In: vol. 180. John A. Jacquez memorial volume. 2002, pp. 1–21. DOI: 10.1016/S0025-5564(02)00122-0.

[144] G. Dimarco, B. Perthame, G. Toscani, and M. Zanella. Kinetic models for epidemic dynamics with social heterogeneity. *J. Math. Biol.* **83**.**1** (2021), Paper No. 4, 32. DOI: 10.1007/s00285-021-01630-1.

[145] R. Djidjou-Demasse, A. Ducrot, and F. Fabre. Steady state concentration for a phenotypic structured problem modeling the evolutionary epidemiology of spore producing pathogens. *Math. Models Methods Appl. Sci.* **27**.**2** (2017), pp. 385–426. DOI: 10.1142/S0218202517500051.

[146] R. Djidjou-Demasse et al. Evolution of pathogen traits in response to quantitative host resistance in heterogeneous environments. *bioRxiv* (2020). DOI: 10.1101/423467.

[147] J. Dockery, V. Hutson, K. Mischaikow, and M. Pernarowski. The evolution of slow dispersal rates: a reaction diffusion model. *J. Math. Biol.* **37**.**1** (1998), pp. 61–83. DOI: 10.1007/s002850050120.

[148] E. Dong, H. Du, and L. Gardner. An interactive web-based dashboard to track COVID-19 in real time. *Lancet Infect. Dis.* **20**.**5** (2020), pp. 533–534. DOI: 10.1016/S1473-3099(20)30120-1.

[149] P. van den Driessche and J. Watmough. Reproduction numbers and sub-threshold endemic equilibria for compartmental models of disease transmission. In: vol. 180. John A. Jacquez memorial volume. 2002, pp. 29–48. DOI: 10.1016/S0025-5564(02)00108-6.

[150] A. Ducrot and S. Madec. Singularly perturbed elliptic system modeling the competitive interactions for a single resource. *Math. Models Methods Appl. Sci.* **23**.**11** (2013), pp. 1939–1977. DOI: 10.1142/S021820251350022X.

[151] A. Ducrot, X. Fu, and P. Magal. Turing and Turing-Hopf bifurcations for a reaction diffusion equation with nonlocal advection. *J. Nonlinear Sci.* **28**.**5** (2018), pp. 1959–1997. DOI: 10.1007/s00332-018-9472-z.

[152] A. Ducrot and P. Magal. Asymptotic behavior of a nonlocal diffusive logistic equation. *SIAM J. Math. Anal.* **46**.**3** (2014), pp. 1731–1753. DOI: 10.1137/130922100.

[153] A. Ducrot and D. Manceau. A one-dimensional logistic like equation with nonlinear and nonlocal diffusion: strong convergence to equilibrium. *Proc. Amer. Math. Soc.* **148**.**8** (2020), pp. 3381–3392. DOI: 10.1090/proc/14971.

[154] A. Ducrot and G. Nadin. Asymptotic behaviour of travelling waves for the delayed Fisher-KPP equation. *J. Differential Equations* **256**.**9** (2014), pp. 3115–3140. DOI: 10.1016/j.jde.2014.01.033.

[155] A. Ducrot et al. An *in vitro* cell population dynamics model incorporating cell size, quiescence, and contact inhibition. *Math. Models Methods Appl. Sci.* **21**.**suppl. 1** (2011), pp. 871–892. DOI: 10.1142/S0218202511005404.

[156] J. Dyson, S. A. Gourley, R. Villella-Bressan, and G. F. Webb. Existence and asymptotic properties of solutions of a nonlocal evolution equation modeling cell-cell adhesion. *SIAM J. Math. Anal.* **42**.**4** (2010), pp. 1784–1804. DOI: 10.1137/090765663.

[157] B. C. Eaves, A. J. Hoffman, U. G. Rothblum, and H. Schneider. Line-sum-symmetric scalings of square nonnegative matrices. In: 25. Mathematical programming, II. 1985, pp. 124–141. DOI: 10.1007/bfb0121080.

[158] R. Eftimie, G. de Vries, M. A. Lewis, and F. Lutscher. Modeling group formation and activity patterns in self-organizing collectives of individuals. *Bull. Math. Biol.* **69**.**5** (2007), pp. 1537–1565. DOI: 10.1007/s11538-006-9175-8.

[159] M. El Smaily. Pulsating travelling fronts: asymptotics and homogenization regimes. *European J. Appl. Math.* **19**.**4** (2008), pp. 393–434. DOI: 10.1017/S0956792508007511.

[160] M. El Smaily. Min-max formulae for the speeds of pulsating travelling fronts in periodic excitable media. *Ann. Mat. Pura Appl. (4)* **189.1** (2010), pp. 47–66. DOI: 10.1007/s10231-009-0100-2.

[161] M. El Smaily, F. Hamel, and L. Roques. Homogenization and influence of fragmentation in a biological invasion model. *Discrete Contin. Dyn. Syst.* **25.1** (2009), pp. 321–342. DOI: 10.3934/dcds.2009.25.321.

[162] L. C. Evans. *Partial differential equations*. Vol. 19. Graduate Studies in Mathematics. American Mathematical Society, Providence, RI, 1998, pp. xviii+662.

[163] J. Fang and X.-Q. Zhao. Monotone wavefronts of the nonlocal Fisher-KPP equation. *Nonlinearity* **24.11** (2011), pp. 3043–3054. DOI: 10.1088/0951-7715/24/11/002.

[164] D. Faranda et al. Asymptotic estimates of SARS-CoV-2 infection counts and their sensitivity to stochastic perturbation. *Chaos* **30.5** (2020), p. 051107. DOI: 10.1063/5.0008834.

[165] G. Faye and M. Holzer. Modulated traveling fronts for a nonlocal Fisher-KPP equation: a dynamical systems approach. *J. Differential Equations* **258.7** (2015), pp. 2257–2289. DOI: 10.1016/j.jde.2014.12.006.

[166] H. Federer. *Geometric measure theory*. Die Grundlehren der mathematischen Wissenschaften, Band 153. Springer-Verlag New York Inc., New York, 1969, pp. xiv+676. DOI: 10.1007/978-3-642-62010-2.

[167] N. Fei and J. Carr. Existence of travelling waves with their minimal speed for a diffusing Lotka-Volterra system. *Nonlinear Anal. Real World Appl.* **4.3** (2003), pp. 503–524. DOI: 10.1016/S1468-1218(02)00077-9.

[168] L. Ferretti et al. Quantifying SARS-CoV-2 transmission suggests epidemic control with digital contact tracing. *Science* **368.6491** (2020). DOI: 10.1126/science.abb6936.

[169] P. C. Fife and J. B. McLeod. The approach of solutions of nonlinear diffusion equations to travelling front solutions. *Arch. Ration. Mech. Anal.* **65.4** (1977), pp. 335–361.

[170] R. A. Fisher. THE WAVE OF ADVANCE OF ADVANTAGEOUS GENES. *Ann. Eugenic.* **7.4** (1937), pp. 355–369. DOI: 10.1111/j.1469-1809.1937.tb02153.x.

[171] J. Földes and P. Poláčik. On cooperative parabolic systems: Harnack inequalities and asymptotic symmetry. *Discrete Contin. Dyn. Syst.* **25.1** (2009), pp. 133–157. DOI: 10.3934/dcds.2009.25.133.

[172] R. L. Foote. Regularity of the distance function. *Proc. Amer. Math. Soc.* **92.1** (1984), pp. 153–155. DOI: 10.2307/2045171.

[173] C. Fraïsse, J. A. D. Elderfield, and J. J. Welch. The genetics of speciation: are complex incompatibilities easier to evolve? *J. Evol. Biol.* **27** (2014), pp. 688–699. DOI: 10.1111/jeb.12339.

[174] S. A. Frank. Host-symbiont conflict over the mixing of symbiotic lineage. *Proc. R. Soc. B* **263** (1996), pp. 339–344. DOI: 10.1098/rspb.1996.0052.

[175] C. Fraser, S. Riley, R. M. Anderson, and N. M. Ferguson. Factors that make an infectious disease outbreak controllable. *Proc. Natl. Acad. Sci. U.S.A* **101.16** (2004), pp. 6146–6151. DOI: 10.1073/pnas.0307506101.

[176] S. Frost et al. Neutralizing antibody responses drive the evolution of human immunodeficiency virus type 1 envelope during recent HIV infection. *Proc. Natl. Acad. Sci. U.S.A* **102** (51 2005), pp. 18514–18519. DOI: 10.1073/pnas.0504658102.

[177] X. Fu. Reaction-diffusion Equations with Nonlinear and Nonlocal Advection Applied to Cell Coculture. Theses. Université de Bordeaux, Nov. 2019.

[178] X. Fu and P. Magal. Asymptotic behavior of a nonlocal advection system with two populations. *J. Dynam. Differential Equations* (2021), pp. 1–43. DOI: 10.1007/s10884-021-09956-6.

[179] T. Ganyani et al. Estimating the generation interval for coronavirus disease (COVID-19) based on symptom onset data, March 2020. *Euro Surveill.* **25.17** (2020), p. 2000257. DOI: 10.2807/1560-7917.ES.2020.25.17.2000257.

[180] R. Gardner and J. Smoller. The existence of periodic travelling waves for singularly perturbed predator-prey equations via the Conley index. *J. Differential Equations* **47.1** (1983), pp. 133–161. DOI: 10.1016/0022-0396(83)90031-1.

[181] R. A. Gardner. Existence and stability of travelling wave solutions of competition models: a degree theoretic approach. *J. Differential Equations* **44.3** (1982), pp. 343–364. DOI: 10.1016/0022-0396(82)90001-8.

[182] J. Garnier, T. Giletti, F. Hamel, and L. Roques. Inside dynamics of pulled and pushed fronts. *J. Math. Pures Appl. (9)* **98.4** (2012), pp. 428–449. DOI: 10.1016/j.matpur.2012.02.005.

[183] S. Gavrilets. *Fitness landscapes and the origin of species*. Princeton University Press, Oxford, 2004.

[184] S. Genieys, V. Volpert, and P. Auger. Pattern and waves for a model in population dynamics with nonlocal consumption of resources. *Math. Model. Nat. Phenom.* **1.1** (2006), pp. 65–82. DOI: 10.1051/mmnp:2006004.

[185] M. Gerlinger et al. Intratumor heterogeneity and branched evolution revealed by multiregion sequencing. *N. Engl. J. Med.* **366** (2012), pp. 883–892. DOI: 10.1056/NEJMoa1113205.

[186] M.-È. Gil, F. Hamel, G. Martin, and L. Roques. Mathematical properties of a class of integro-differential models from population genetics. *SIAM J. Appl. Math.* **77.4** (2017), pp. 1536–1561.

[187] D. Gilbarg and N. S. Trudinger. *Elliptic partial differential equations of second order*. Classics in Mathematics. Reprint of the 1998 edition. Springer-Verlag, Berlin, 2001, pp. xiv+517.

[188] D. T. Gillespie. Exact stochastic simulation of coupled chemical reactions. *J. Phys. Chem.* **81.25** (1977), pp. 2340–2361. DOI: 10.1021/j100540a008.

[189] L. Girardin. Non-cooperative Fisher-KPP systems: asymptotic behavior of traveling waves. *Math. Models Methods Appl. Sci.* **28.6** (2018), pp. 1067–1104. DOI: 10.1142/S0218202518500288.

[190] L. Girardin. Non-cooperative Fisher-KPP systems: traveling waves and long-time behavior. *Nonlinearity* **31.1** (2018), pp. 108–164. DOI: 10.1088/1361-6544/aa8ca7.

[191] L. Girardin. Addendum to 'Non-cooperative Fisher-KPP systems: traveling waves and long-time behavior' [MR3746634]. *Nonlinearity* **32.1** (2019), pp. 168–171. DOI: 10.1088/1361-6544/aae93d.

[192] L. Girardin. Two components is too simple: an example of oscillatory Fisher-KPP system with three components. *Proc. Roy. Soc. Edinburgh Sect. A* **150.6** (2020), pp. 3097–3120. DOI: 10.1017/prm.2019.46.

[193] S. A. Gourley. Travelling front solutions of a nonlocal Fisher equation. *J. Math. Biol.* **41.3** (2000), pp. 272–284. DOI: 10.1007/s002850000047.

[194] W.-j. Guan et al. Clinical Characteristics of Coronavirus Disease 2019 in China. *N. Engl. J. Med.* **382.18** (2020), pp. 1708–1720. DOI: 10.1056/NEJMoa2002032.

[195] P. Guillon et al. Inhibition of the interaction between the SARS-CoV spike protein and its cellular receptor by anti-histo-blood group antibodies. *Glycobiology* **18.12** (2008), pp. 1085–1093.

[196] K. P. Hadeler. Parameter identification in epidemic models. *Math. Biosci.* **229.2** (2011), pp. 185–189. DOI: 10.1016/j.mbs.2010.12.004.

[197] F. Hamel. Qualitative properties of monostable pulsating fronts: exponential decay and monotonicity. *J. Math. Pures Appl. (9)* **89.4** (2008), pp. 355–399. DOI: 10.1016/j.matpur.2007.12.005.

[198] F. Hamel and C. Henderson. Propagation in a Fisher-KPP equation with non-local advection. *J. Funct. Anal.* **278.7** (2020), pp. 108426, 53. DOI: 10.1016/j.jfa.2019.108426.

[199] F. Hamel and L. Roques. Uniqueness and stability properties of monostable pulsating fronts. *J. Eur. Math. Soc. (JEMS)* **13.2** (2011), pp. 345–390. DOI: 10.4171/JEMS/256.

[200] F. Hamel and L. Ryzhik. On the nonlocal Fisher-KPP equation: steady states, spreading speed and global bounds. *Nonlinearity* **27.11** (2014), pp. 2735–2753. DOI: 10.1088/0951-7715/27/11/2735.

[201] G. Hardin. The competitive exclusion principle. *Science* **131.3409** (1960), pp. 1292–1297. DOI: 10.1126/science.131.3409.1292.

[202] K. Harley et al. Existence of traveling wave solutions for a model of tumor invasion. *SIAM J. Appl. Dyn. Syst.* **13.1** (2014), pp. 366–396. DOI: 10.1137/130923129.

[203] K. Hasik, J. Kopfová, P. Nábělková, and S. Trofimchuk. Traveling waves in the nonlocal KPP-Fisher equation: different roles of the right and the left interactions. *J. Differential Equations* **260.7** (2016), pp. 6130–6175. DOI: 10.1016/j.jde.2015.12.035.

[204] D. M. Hawley et al. Parallel Patterns of Increased Virulence in a Recently Emerged Wildlife Pathogen. *PLoS Biol.* **11.5** (2013), e1001570. DOI: 10.1371/journal.pbio.1001570.

[205] X. He et al. Temporal dynamics in viral shedding and transmissibility of COVID-19. *Nat. Med* **26.5** (2020), pp. 672–675. DOI: 10.1038/s41591-020-0869-5.

[206] S. Heilmann, K. Sneppen, and S. Krishna. Sustainability of Virulence in a Phage-Bacterial Ecosystem. *J. Virol.* **84.6** (2010), pp. 3016–3022. DOI: 10.1128/JVI.02326-09.

[207] C. Henderson. Pulsating fronts in a 2D reactive Boussinesq system. *Comm. Partial Differential Equations* **39.8** (2014), pp. 1555–1595. DOI: 10.1080/03605302.2013.850726.

[208] H. W. Hethcote. The mathematics of infectious diseases. *SIAM Rev.* **42.4** (2000), pp. 599–653. DOI: 10.1137/S0036144500371907.

[209] T. Hillen and K. J. Painter. A user's guide to PDE models for chemotaxis. *J. Math. Biol.* **58.1-2** (2009), pp. 183–217. DOI: 10.1007/s00285-008-0201-3.

[210] M. W. Hirsch, S. Smale, and R. L. Devaney. *Differential equations, dynamical systems, and an introduction to chaos*. Second. Vol. 60. Pure and Applied Mathematics (Amsterdam). Elsevier/Academic Press, Amsterdam, 2004, pp. xiv+417.

[211] E. Holmes. *The evolution and emergence of RNA viruses*. Oxford University Press, 2009.

[212] M. L. Holshue et al. First case of 2019 novel coronavirus in the United States. *N. Engl. J. Med.* (2020). DOI: 10.1056/NEJMoa2001191.

[213] D. Horstmann. From 1970 until present: the Keller-Segel model in chemotaxis and its consequences. I. *Jahresber. Deutsch. Math.-Verein.* **105.3** (2003), pp. 103–165.

[214] Y. Hsieh, H. Chang, and J. Lee. SARS epidemiology modeling. *Emerg. Infect. Dis.* **10.6** (). DOI: 10.3201/eid1006.031023.

[215] Y.-H. Hsieh. Richards model: a simple procedure for real-time prediction of outbreak severity. In: *Modeling and dynamics of infectious diseases*. Vol. 11. Ser. Contemp. Appl. Math. CAM. Higher Ed. Press, Beijing, 2009, pp. 216–236.

[216] S. B. Hsu, H. L. Smith, and P. Waltman. Competitive exclusion and coexistence for competitive systems on ordered Banach spaces. *Trans. Amer. Math. Soc.* **348.10** (1996), pp. 4083–4094. DOI: 10.1090/S0002-9947-96-01724-2.

[217] S.-B. Hsu. Limiting behavior for competing species. *SIAM J. Appl. Math.* **34.4** (1978), pp. 760–763. DOI: 10.1137/0134064.

[218] S.-B. Hsu, S. Hubbell, and P. Waltman. A mathematical theory for single-nutrient competition in continuous cultures of micro-organisms. *SIAM J. Appl. Math.* **32.2** (1977), pp. 366–383. DOI: 10.1137/0132030.

[219] S.-B. Hsu and X.-Q. Zhao. Spreading speeds and traveling waves for nonmonotone integrodifference equations. *SIAM J. Math. Anal.* **40.2** (2008), pp. 776–789. DOI: 10.1137/070703016.

[220] Z. Hu et al. Clinical characteristics of 24 asymptomatic infections with COVID-19 screened among close contacts in Nanjing, China. *Sci. China Life Sci.* **63.5** (2020), pp. 706–711. DOI: 10.1007/s11427-020-1661-4.

[221] W. Hudson and B. Zinner. Existence of traveling waves for reaction diffusion equations of Fisher type in periodic media. In: *Boundary value problems for functional-differential equations*. World Sci. Publ., River Edge, NJ, 1995, pp. 187–199.

[222] X. Huo, J. Chen, and S. Ruan. Estimating asymptomatic, undetected and total cases for the COVID-19 outbreak in Wuhan: a mathematical modeling study. **21.1** (2021), pp. 1–18. DOI: 10.1186/s12879-021-06078-8.

[223] A. Ionescu Tulcea and C. Ionescu Tulcea. On the lifting property. IV. Disintegration of measures. *Ann. Inst. Fourier (Grenoble)* **14.fasc. 2** (1964), pp. 445–472. DOI: 10.5802/aif.182.

[224] A. Ionescu Tulcea and C. Ionescu Tulcea. *Topics in the theory of lifting*. Ergebnisse der Mathematik und ihrer Grenzgebiete, Band 48. Springer-Verlag New York Inc., New York, 1969, pp. x+190. DOI: 10.1007/978-3-642-88507-5.

[225] P.-E. Jabin and G. Raoul. On selection dynamics for competitive interactions. *J. Math. Biol.* **63.3** (2011), pp. 493–517. DOI: 10.1007/s00285-010-0370-8.

[226] W. Jäger and S. Luckhaus. On explosions of solutions to a system of partial differential equations modelling chemotaxis. *Trans. Amer. Math. Soc.* **329.2** (1992), pp. 819–824. DOI: 10.2307/2153966.

[227] T. C. Jones et al. Estimating infectiousness throughout SARS-CoV-2 infection course. *Science* (2021). DOI: 10.1126/science.abi5273.

[228] T. Kato. *Perturbation theory for linear operators*. Classics in Mathematics. Reprint of the 1980 edition. Springer-Verlag, Berlin, 1995, pp. xxii+619.

[229] S. Katsunuma et al. Synergistic action of nectins and cadherins generates the mosaic cellular pattern of the olfactory epithelium. *J. Cell Biol.* **212.5** (2016), pp. 561–575. DOI: 10.1083/jcb.201509020.

[230] H. Kawasuji et al. Transmissibility of COVID-19 depends on the viral load around onset in adult and symptomatic patients. *PloS one* **15.12** (2020), e0243597.

[231] M. J. Keeling and P. Rohani. *Modeling infectious diseases in humans and animals*. Princeton University Press, Princeton, NJ, 2008, pp. xvi+368.

[232] E. F. Keller and L. A. Segel. Model for chemotaxis. *J. Theor. Biol.* **30.2** (1971), pp. 225–234. DOI: 10.1016/0022-5193(71)90050-6.

[233] E. F. Keller and L. A. Segel. Initiation of slime mold aggregation viewed as an instability. *J. Theoret. Biol.* **26.3** (1970), pp. 399–415. DOI: 10.1016/0022-5193(70)90092-5.

[234] S. Keller and D. Taylor. History, chance and adaptation during biological invasion: separating stochastic phenotypic evolution from response to selection. *Ecol. lett.* **11** (2008), pp. 852–866. DOI: 10.1111/j.1461-0248.2008.01188.x.

[235] J. E. Keymer et al. Bacterial metapopulations in nanofabricated landscapes. *Proc. Natl. Acad. Sci. U.S.A.* **103.46** (2006), pp. 17290–17295. DOI: 10.1073/pnas.0607971103.

[236] S. E. Kim et al. Viral kinetics of SARS-CoV-2 in asymptomatic carriers and presymptomatic patients. *Int. J. Infect. Dis.* **95** (2020), pp. 441–443.

[237] M. Kimura. A stochastic model concerning the maintenance of genetic variability in quantitative characters. *Proc. Natl. Acad. Sci. USA* **54.3** (1965), pp. 731–736. DOI: 10.1073/pnas.54.3.731.

[238] A. N. Kolmogorov, I. G. Petrovsky, and N. S. Piskunov. Étude de l'équation de la diffusion avec croissance de la quantité de matière et son application à un problème biologique. *Bull. Univ. Etat Moscou* **Sér. Inter. A 1** (1937), pp. 1–26.

[239] A. Korobeinikov. Lyapunov functions and global stability for SIR and SIRS epidemiological models with non-linear transmission. *Bull. Math. Biol.* **68.3** (2006), pp. 615–626. DOI: 10.1007/s11538-005-9037-9.

[240] A. Korobeinikov. Global properties of infectious disease models with nonlinear incidence. *Bull. Math. Biol.* **69.6** (2007), pp. 1871–1886. DOI: 10.1007/s11538-007-9196-y.

[241] A. Korobeinikov. Global properties of SIR and SEIR epidemic models with multiple parallel infectious stages. *Bull. Math. Biol.* **71.1** (2009), pp. 75–83. DOI: 10.1007/s11538-008-9352-z.

[242] A. Korobeinikov and P. K. Maini. A Lyapunov function and global properties for SIR and SEIR epidemiological models with nonlinear incidence. *Math. Biosci. Eng.* **1.1** (2004), pp. 57–60. DOI: 10.3934/mbe.2004.1.57.

[243] A. Korobeinikov and G. C. Wake. Lyapunov functions and global stability for SIR, SIRS, and SIS epidemiological models. *Appl. Math. Lett.* **15.8** (2002), pp. 955–960. DOI: 10.1016/S0893-9659(02)00069-1.

[244] M. A. Krasnosel'skii. *Topological methods in the theory of nonlinear integral equations*. A Pergamon Press Book. Translated by A. H. Armstrong; translation edited by J. Burlak. The Macmillan Company, New York, 1964, pp. xi + 395.

[245] A. J. Kucharski et al. Early dynamics of transmission and control of COVID-19: a mathematical modelling study. *Lancet Infect. Dis.* **20.5** (2020), pp. 553–558.

[246] O. A. Ladyženskaja, V. A. Solonnikov, and N. N. Ural'ceva. *Linear and quasilinear equations of parabolic type*. Translated from the Russian by S. Smith. Translations of Mathematical Monographs, Vol. 23. American Mathematical Society, Providence, R.I., 1968, pp. xi+648.

[247] K. A. Landman, G. J. Pettet, and D. F. Newgreen. Chemotactic cellular migration: smooth and discontinuous travelling wave solutions. *SIAM J. Appl. Math.* **63.5** (2003), pp. 1666–1681. DOI: 10.1137/S0036139902404694.

[248] H. Lee and H. Nishiura. Sexual transmission and the probability of an end of the Ebola virus disease epidemic. *J. Theor. Biol.* **471** (2019), pp. 1–12. DOI: 10.1016/j.jtbi.2019.03.022.

[249] R. J. LeVeque. *Finite volume methods for hyperbolic problems*. Cambridge Texts in Applied Mathematics. Cambridge University Press, Cambridge, 2002, pp. xx+558. DOI: 10.1017/CBO9780511791253.

[250] A. J. Leverentz, C. M. Topaz, and A. J. Bernoff. Asymptotic dynamics of attractive-repulsive swarms. *SIAM J. Appl. Dyn. Syst.* **8.3** (2009), pp. 880–908. DOI: 10.1137/090749037.

[251] B. Li. Global asymptotic behavior of the chemostat: general response functions and different removal rates. *SIAM J. Appl. Math.* **59.2** (1999), pp. 411–422. DOI: 10.1137/S003613999631100X.

[252] R. Li et al. Substantial undocumented infection facilitates the rapid dissemination of novel coronavirus (SARS-CoV-2). *Science* **368.6490** (2020), pp. 489–493. DOI: 10.1126/science.abb3221.

[253] S. Li, J. Wu, and Y. Dong. Uniqueness and stability of positive solutions for a diffusive predator-prey model in heterogeneous environment. *Calc. Var. Partial Differential Equations* **58.3** (2019), Art. 110, 42. DOI: 10.1007/s00526-019-1558-4.

[254] X. Liang and X.-Q. Zhao. Spreading speeds and traveling waves for abstract monostable evolution systems. *J. Funct. Anal.* **259.4** (2010), pp. 857–903. DOI: 10.1016/j.jfa.2010.04.018.

[255] G. Lin. Spreading speeds of a Lotka-Volterra predator-prey system: the role of the predator. *Nonlinear Anal.* **74.7** (2011), pp. 2448–2461. DOI: 10.1016/j.na.2010.11.046.

[256] S. Lion and M. Boots. Are parasites "prudent" in space ? *Ecol. Lett.* **13.5** (2010), pp. 1245–1255.

[257] S. Lion and S. Gandon. Evolution of spatially structured host-parasite interactions. *J. Evol. Biol.* **28.1** (2015), pp. 10–28. DOI: 10.1111/jeb.12551.

[258] Z. Liu, P. Magal, O. Seydi, and G. Webb. A COVID-19 epidemic model with latency period. *Infect. Dis. Model.* **5** (2020), pp. 323–337. DOI: 10.1016/j.idm.2020.03.003.

[259] Z. Liu, P. Magal, O. Seydi, and G. Webb. A Model to Predict COVID-19 Epidemics with Applications to South Korea, Italy, and Spain. *SIAM News* **53.4** (May 2020).

[260] Z. Liu, P. Magal, O. Seydi, and G. Webb. Predicting the cumulative number of cases for the COVID-19 epidemic in China from early data. *Math. Biosci. Eng.* **17.4** (2020), pp. 3040–3051. DOI: 10.3934/mbe.2020172.

[261] Z. Liu, P. Magal, O. Seydi, and G. Webb. Understanding unreported cases in the COVID-19 epidemic outbreak in Wuhan, China, and the importance of major public health interventions. *Biology* **9.3** (2020), p. 50. DOI: 10.3390/biology9030050.

[262] Z. Liu, P. Magal, and G. Webb. Predicting the number of reported and unreported cases for the COVID-19 epidemics in China, South Korea, Italy, France, Germany and United Kingdom. *J. Theor. Biol.* **509** (2021), p. 110501. DOI: 10.1016/j.jtbi.2020.110501.

[263] G. Lo Iacono, F. van den Bosch, and N. Paveley. The evolution of plant pathogens in response to host resistance: factors affecting the gain from deployment of qualitative and quantitative resistance. *J. Theoret. Biol.* **304** (2012), pp. 152–163. DOI: 10.1016/j.jtbi.2012.03.033.

[264] W. P. London and J. A. Yorke. Recurrent outbreaks of measles, chickenpox and mumps: I. Seasonal variation in contact rates. *Am. J. Epidemiol.* **98.6** (1973), pp. 453–468. DOI: 10.1093/oxfordjournals.aje.a121575.

[265] A. Lorz and B. Perthame. Long-term behaviour of phenotypically structured models. *Proc. R. Soc. Lond. Ser. A Math. Phys. Eng. Sci.* **470.2167** (2014), pp. 20140089, 10. DOI: 10.1098/rspa.2014.0089.

[266] A. Lorz, B. Perthame, and C. Taing. Dirac concentrations in a chemostat model of adaptive evolution. *Chin. Ann. Math. Ser. B* **38.2** (2017), pp. 513–538. DOI: 10.1007/s11401-017-1081-x.

[267] Y. Lou and W.-M. Ni. Diffusion, self-diffusion and cross-diffusion. *J. Differential Equations* **131.1** (1996), pp. 79–131. DOI: 10.1006/jdeq.1996.0157.

[268] X. Lu et al. SARS-CoV-2 Infection in Children. *N. Engl. J. Med.* **382**.**17** (2020). PMID: 32187458, pp. 1663–1665. DOI: 10.1056/NEJMc2005073.

[269] R. Lui. Biological growth and spread modeled by systems of recursions. I. Mathematical theory. *Math. Biosci.* **93**.**2** (1989), pp. 269–295. DOI: 10.1016/0025-5564(89)90026-6.

[270] A. Lunardi. *Analytic semigroups and optimal regularity in parabolic problems*. Modern Birkhäuser Classics. [2013 reprint of the 1995 original] [MR1329547]. Birkhäuser/Springer Basel AG, Basel, 1995, pp. xviii+424.

[271] S. Ma et al. Epidemiological parameters of coronavirus disease 2019: a pooled analysis of publicly reported individual data of 1155 cases from seven countries. *medRxiv* (2020). DOI: 10.1101/2020.03.21.20040329.

[272] P. Magal. Mutation and recombination in a model of phenotype evolution. *J. Evol. Equ.* **2**.**1** (2002), pp. 21–39. DOI: 10.1007/s00028-002-8078-x.

[273] P. Magal and S. Ruan. Susceptible-infectious-recovered models revisited: from the individual level to the population level. *Math. Biosci.* **250** (2014), pp. 26–40. DOI: 10.1016/j.mbs.2014.02.001.

[274] P. Magal and S. Ruan. *Theory and applications of abstract semilinear Cauchy problems*. Vol. 201. Applied Mathematical Sciences. With a foreword by Glenn Webb. Springer, Cham, 2018, pp. xxii+543. DOI: 10.1007/978-3-030-01506-0.

[275] P. Magal and G. F. Webb. Mutation, selection, and recombination in a model of phenotype evolution. *Discrete Contin. Dynam. Systems* **6**.**1** (2000), pp. 221–236. DOI: 10.3934/dcds.2000.6.221.

[276] P. Magal and X.-Q. Zhao. Global attractors and steady states for uniformly persistent dynamical systems. *SIAM J. Math. Anal.* **37**.**1** (2005), pp. 251–275. DOI: 10.1137/S0036141003439173.

[277] B. P. Marchant, J. Norbury, and A. J. Perumpanani. Travelling shock waves arising in a model of malignant invasion. *SIAM J. Appl. Math.* **60**.**2** (2000), pp. 463–476. DOI: 10.1137/S0036139998328034.

[278] J. Mazurek. The evaluation of COVID-19 prediction precision with a Lyapunov-like exponent. *PLOS one* **16**.**5** (2021), e0252394. DOI: 10.1371/journal.pone.0243597.

[279] C. C. McCluskey. Lyapunov functions for tuberculosis models with fast and slow progression. *Math. Biosci. Eng.* **3**.**4** (2006), pp. 603–614. DOI: 10.3934/mbe.2006.3.603.

[280] C. C. McCluskey. Global stability for a class of mass action systems allowing for latency in tuberculosis. *J. Math. Anal. Appl.* **338**.**1** (2008), pp. 518–535. DOI: 10.1016/j.jmaa.2007.05.012.

[281] P. Meyer-Nieberg. *Banach lattices*. Universitext. Springer-Verlag, Berlin, 1991, pp. xvi+395. DOI: 10.1007/978-3-642-76724-1.

[282] M. Mimura and K. Kawasaki. Spatial segregation in competitive interaction-diffusion equations. *J. Math. Biol.* **9**.**1** (1980), pp. 49–64. DOI: 10.1007/BF00276035.

[283] M. Mimura, Y. Nishiura, A. Tesei, and T. Tsujikawa. Coexistence problem for two competing species models with density-dependent diffusion. *Hiroshima Math. J.* **14**.**2** (1984), pp. 425–449.

[284] S. Mirrahimi, B. Perthame, E. Bouin, and P. Millien. Population formulation of adaptative meso-evolution: theory and numerics. In: *The mathematics of Darwin's legacy*. Math. Biosci. Interact. Birkhäuser/Springer Basel AG, Basel, 2011, pp. 159–174. DOI: 10.1007/978-3-0348-0122-5_9.

[285] S. Mirrahimi, B. Perthame, and J. Y. Wakano. Evolution of species trait through resource competition. *J. Math. Biol.* **64**.**7** (2012), pp. 1189–1223. DOI: 10.1007/s00285-011-0447-z.

[286] S. Mirrahimi. Adaptation and migration of a population between patches. *Discrete Contin. Dyn. Syst. Ser. B* **18**.**3** (2013), pp. 753–768. DOI: 10.3934/dcdsb.2013.18.753.

[287] K. Mizumoto, K. Kagaya, A. Zarebski, and G. Chowell. Estimating the asymptomatic proportion of coronavirus disease 2019 (COVID-19) cases on board the Diamond Princess cruise ship, Yokohama, Japan, 2020. *Euro Surveill.* **25**.**10** (2020), p. 2000180. DOI: 10.2807/1560-7917.ES.2020.25.10.2000180.

[288] A. Mogilner, L. Edelstein-Keshet, L. Bent, and A. Spiros. Mutual interactions, potentials, and individual distance in a social aggregation. *J. Math. Biol.* **47**.**4** (2003), pp. 353–389. DOI: 10.1007/s00285-003-0209-7.

[289] A. Mogilner and L. Edelstein-Keshet. A non-local model for a swarm. *J. Math. Biol.* **38.6** (1999), pp. 534–570. DOI: 10.1007/s002850050158.

[290] D. Morale, V. Capasso, and K. Oelschläger. An interacting particle system modelling aggregation behavior: from individuals to populations. *J. Math. Biol.* **50.1** (2005), pp. 49–66. DOI: 10.1007/s00285-004-0279-1.

[291] A. Morris, L. Börger, and E. Crooks. Individual Variability in Dispersal and Invasion Speed. *Mathematics* **7.9** (2019). DOI: 10.3390/math7090795.

[292] J. Mossong et al. Social Contacts and Mixing Patterns Relevant to the Spread of Infectious Diseases. *PLOS Med.* **5.3** (Mar. 2008), pp. 1–1. DOI: 10.1371/journal.pmed.0050074.

[293] P. de Mottoni and F. Rothe. A singular perturbation analysis for a reaction-diffusion system describing pattern formation. *Stud. Appl. Math.* **63.3** (1980), pp. 227–247. DOI: 10.1002/sapm1980633227.

[294] C. Mueller, L. Mytnik, and J. Quastel. Effect of noise on front propagation in reaction-diffusion equations of KPP type. *Invent. Math.* **184.2** (2011), pp. 405–453. DOI: 10.1007/s00222-010-0292-5.

[295] L. Munasinghe, Y. Asai, and H. Nishiura. Quantifying heterogeneous contact patterns in Japan: a social contact survey. *Theor. Biol. Med. Model.* **16.1** (2019), pp. 1–10. DOI: 10.1186/s12976-019-0102-8.

[296] H. Murakawa and H. Togashi. Continuous models for cell–cell adhesion. *J. Theor. Biol.* **374** (2015), pp. 1–12. DOI: 10.1016/j.jtbi.2015.03.002.

[297] J. D. Murray. *Mathematical biology. I.* Third. Vol. 17. Interdisciplinary Applied Mathematics. An introduction. Springer-Verlag, New York, 2002, pp. xxiv+551.

[298] G. Nadin. The principal eigenvalue of a space-time periodic parabolic operator. *Ann. Mat. Pura Appl. (4)* **188.2** (2009), pp. 269–295. DOI: 10.1007/s10231-008-0075-4.

[299] G. Nadin. The effect of the Schwarz rearrangement on the periodic principal eigenvalue of a nonsymmetric operator. *SIAM J. Math. Anal.* **41.6** (2010), pp. 2388–2406. DOI: 10.1137/080743597.

[300] G. Nadin. Some dependence results between the spreading speed and the coefficients of the space-time periodic Fisher-KPP equation. *European J. Appl. Math.* **22.2** (2011), pp. 169–185. DOI: 10.1017/S0956792511000027.

[301] G. Nadin, B. Perthame, and L. Ryzhik. Traveling waves for the Keller-Segel system with Fisher birth terms. *Interfaces Free Bound.* **10.4** (2008), pp. 517–538. DOI: 10.4171/IFB/200.

[302] W. Ni, J. Shi, and M. Wang. Global stability and pattern formation in a nonlocal diffusive Lotka-Volterra competition model. *J. Differential Equations* **264.11** (2018), pp. 6891–6932. DOI: 10.1016/j.jde.2018.02.002.

[303] H. Nishiura. Methods to determine the end of an infectious disease epidemic: a short review. In: *Mathematical and statistical modeling for emerging and re-emerging infectious diseases*. Springer, 2016, pp. 291–301.

[304] H. Nishiura, Y. Miyamatsu, and K. Mizumoto. Objective determination of end of MERS outbreak, South Korea, 2015. *Emerg. Infect. Dis.* **22.1** (2016), p. 146. DOI: 10.3201/eid2201.151383.

[305] H. Nishiura et al. Estimation of the asymptomatic ratio of novel coronavirus infections (COVID-19). *Int. J. Infect. Dis.* **94** (2020), p. 154. DOI: 10.1016/j.ijid.2020.03.020.

[306] H. Nishiura et al. The Rate of Underascertainment of Novel Coronavirus (2019-nCoV) Infection: Estimation Using Japanese Passengers Data on Evacuation Flights. *Journal of Clinical Medicine* **9.2** (2020). DOI: 10.3390/jcm9020419.

[307] S. Nordmann, B. Perthame, and C. Taing. Dynamics of concentration in a population model structured by age and a phenotypical trait. *Acta Appl. Math.* **155** (2018), pp. 197–225. DOI: 10.1007/s10440-017-0151-0.

[308] P. D. O'Neill. Introduction and snapshot review: relating infectious disease transmission models to data. *Stat. Med.* **29.20** (2010), pp. 2069–2077.

[309] T. Ogiwara and H. Matano. Monotonicity and convergence results in order-preserving systems in the presence of symmetry. *Discrete Contin. Dynam. Systems* **5.1** (1999), pp. 1–34. DOI: 10.3934/dcds.1999.5.1.

[310] T. Ogiwara and H. Matano. Stability analysis in order-preserving systems in the presence of symmetry. *Proc. Roy. Soc. Edinburgh Sect. A* **129.2** (1999), pp. 395–438. DOI: 10.1017/S0308210500021429.

[311] R. Omori, K. Mizumoto, and H. Nishiura. Ascertainment rate of novel coronavirus disease (COVID-19) in Japan. *Int. J. Infect. Dis.* **96** (2020), pp. 673–675. DOI: 10.1016/j.ijid.2020.04.080.

[312] D. P. Oran and E. J. Topol. Prevalence of asymptomatic SARS-CoV-2 infection: a narrative review. *Ann. Intern. Med.* **173.5** (2020), pp. 362–367.

[313] A. de Pablo and J. L. Vázquez. Travelling waves and finite propagation in a reaction-diffusion equation. *J. Differential Equations* **93.1** (1991), pp. 19–61. DOI: 10.1016/0022-0396(91)90021-Z.

[314] B. de Pagter. Irreducible compact operators. *Math. Z.* **192.1** (1986), pp. 149–153. DOI: 10.1007/BF01162028.

[315] L. Palatella, F. Vanni, and D. Lambert. A phenomenological estimate of the true scale of CoViD-19 from primary data. *Chaos Solitons Fractals* **146** (2021), p. 110854. DOI: 10.1016/j.chaos.2021.110854.

[316] A. Pan et al. Association of public health interventions with the epidemiology of the COVID-19 outbreak in Wuhan, China. *JAMA* **323.19** (2020), pp. 1915–1923. DOI: 10.7326/M20-3012.

[317] C. Parmesan and G. Yohe. A globally coherent fingerprint of climate change impacts across natural systems. *Nature* **421** (2003), pp. 37–42. DOI: 10.1038/nature01286.

[318] J. Pasquier et al. Consequences of cell-to-cell P-glycoprotein transfer on acquired multidrug resistance in breast cancer: a cell population dynamics model. *Biol. Direct* **6.1** (2011), pp. 1–18. DOI: 10.1186/1745-6150-6-5.

[319] J. Pasquier et al. Different modalities of intercellular membrane exchanges mediate cell-to-cell p-glycoprotein transfers in MCF-7 breast cancer cells. *J. Biol. Chem.* **287.10** (2012), pp. 7374–7387. DOI: 10.1074/jbc.M111.312157.

[320] C. S. Patlak. Random walk with persistence and external bias. *Bull. Math. Biophys.* **15** (1953), pp. 311–338. DOI: 10.1007/bf02476407.

[321] S. Penington. The spreading speed of solutions of the non-local Fisher-KPP equation. *J. Funct. Anal.* **275.12** (2018), pp. 3259–3302. DOI: 10.1016/j.jfa.2018.10.002.

[322] T. A. Perkins, B. L. Phillips, M. L. Baskett, and A. Hastings. Evolution of dispersal and life history interact to drive accelerating spread of an invasive species. *Ecol. Lett.* **16.8** (2013), pp. 1079–1087. DOI: 10.1111/ele.12136.

[323] B. Perthame and A.-L. Dalibard. Existence of solutions of the hyperbolic Keller-Segel model. *Trans. Amer. Math. Soc.* **361.5** (2009), pp. 2319–2335. DOI: 10.1090/S0002-9947-08-04656-4.

[324] B. L. Phillips and R. Puschendorf. Do pathogens become more virulent as they spread ? Evidence from the amphibian declines in Central America. *Proc. R. Soc. B* **280.1766** (2013). DOI: 10.1098/rspb.2013.1290.

[325] K. Prem, A. R. Cook, and M. Jit. Projecting social contact matrices in 152 countries using contact surveys and demographic data. *PLOS Comput. Biol.* **13.9** (Sept. 2017), pp. 1–21. DOI: 10.1371/journal.pcbi.1005697.

[326] K. Prem et al. The effect of control strategies to reduce social mixing on outcomes of the COVID-19 epidemic in Wuhan, China: a modelling study. *Lancet Public Health* **5.5** (2020), e261–e270. DOI: 10.1016/S2468-2667(20)30073-6.

[327] J. Qiu. Covert coronavirus infections could be seeding new outbreaks. *Nature* (2020). DOI: 10.1038/d41586-020-00822-x.

[328] Y. Qiu, X. Chen, and W. Shi. Impacts of social and economic factors on the transmission of coronavirus disease 2019 (COVID-19) in China. *J. Popul. Econ.* **33.4** (2020), pp. 1127–1172. DOI: 10.1007/s00148-020-00778-2.

[329] P. H. Rabinowitz. A note on a nonlinear eigenvalue problem for a class of differential equations. *J. Differential Equations* **9** (1971), pp. 536–548. DOI: 10.1016/0022-0396(71)90022-2.

[330] P. H. Rabinowitz. Some global results for nonlinear eigenvalue problems. *J. Functional Analysis* **7** (1971), pp. 487–513. DOI: 10.1016/0022-1236(71)90030-9.

[331] G. Raoul. Long time evolution of populations under selection and vanishing mutations. *Acta Appl. Math.* **114.1-2** (2011), pp. 1–14. DOI: 10.1007/s10440-011-9603-0.

[332] G. Raoul. Local stability of evolutionary attractors for continuous structured populations. *Monatsh. Math.* **165.1** (2012), pp. 117–144. DOI: 10.1007/s00605-011-0354-9.

[333] A. Rapaport and M. Veruete. A new proof of the competitive exclusion principle in the chemostat. *Discrete Contin. Dyn. Syst. Ser. B* **24.8** (2019), pp. 3755–3764. DOI: 10.3934/dcdsb.2018314.

[334] M. Reed and B. Simon. *Methods of modern mathematical physics. I. Functional analysis*. Academic Press, New York-London, 1972, pp. xvii+325.

[335] W. C. Roda, M. B. Varughese, D. Han, and M. Y. Li. Why is it difficult to accurately predict the COVID-19 epidemic? *Infect. Dis. Model.* **5** (2020), pp. 271–281. DOI: 10.1016/j.idm.2020.03.001.

[336] D. Roff. *Evolution Of Life Histories: Theory and Analysis*. The Evolution of Life Histories: Theory and Analysis. Springer, 1992.

[337] K. Roosa et al. Real-time forecasts of the COVID-19 epidemic in China from February 5th to February 24th, 2020. *Infect. Dis. Model.* **5** (2020), pp. 256–263. DOI: 10.1016/j.idm.2020.02.002.

[338] J.-M. Roquejoffre, D. Terman, and V. A. Volpert. Global stability of traveling fronts and convergence towards stacked families of waves in monotone parabolic systems. *SIAM J. Math. Anal.* **27.5** (1996), pp. 1261–1269. DOI: 10.1137/S0036141094267522.

[339] L. Roques et al. Impact of Lockdown on the Epidemic Dynamics of COVID-19 in France. *Frontiers in Medicine* **7** (2020), p. 274. DOI: 10.3389/fmed.2020.00274.

[340] L. Roques et al. Using early data to estimate the actual infection fatality ratio from COVID-19 in France. *Biology* **9.5** (2020), p. 97. DOI: 10.3390/biology9050097.

[341] C. Rothe et al. Transmission of 2019-nCoV Infection from an Asymptomatic Contact in Germany. *N. Engl. J. Med.* **382.10** (2020), pp. 970–971. DOI: 10.1056/NEJMc2001468.

[342] W. Rudin. *Real and complex analysis*. McGraw-Hill Book Co., New York-Toronto, Ont.-London, 1966, pp. xi+412.

[343] W. Rudin. *Real and complex analysis*. Second. McGraw-Hill Series in Higher Mathematics. McGraw-Hill Book Co., New York-Düsseldorf-Johannesburg, 1974, pp. xii+452.

[344] R. B. Salako and W. Shen. Spreading speeds and traveling waves of a parabolic-elliptic chemotaxis system with logistic source on $\mathbb{R}^N$. *Discrete Contin. Dyn. Syst.* **37.12** (2017), pp. 6189–6225. DOI: 10.3934/dcds.2017268.

[345] R. B. Salako and W. Shen. Existence of traveling wave solutions of parabolic-parabolic chemotaxis systems. *Nonlinear Anal. Real World Appl.* **42** (2018), pp. 93–119. DOI: 10.1016/j.nonrwa.2017.12.004.

[346] R. B. Salako and W. Shen. Parabolic-elliptic chemotaxis model with space-time-dependent logistic sources on $\mathbb{R}^N$. I. Persistence and asymptotic spreading. *Math. Models Methods Appl. Sci.* **28.11** (2018), pp. 2237–2273. DOI: 10.1142/S0218202518400146.

[347] R. B. Salako, W. Shen, and S. Xue. Can chemotaxis speed up or slow down the spatial spreading in parabolic-elliptic Keller-Segel systems with logistic source? *J. Math. Biol.* **79.4** (2019), pp. 1455–1490. DOI: 10.1007/s00285-019-01400-0.

[348] K. Sato, H. Matsuda, and A. Sasaki. Pathogen invasion and host extinction in lattice structured populations. *J. Math. Biol.* **32** (1994), pp. 251–268. DOI: 10.1007/BF00163881.

[349] D. H. Sattinger. On the stability of waves of nonlinear parabolic systems. *Advances in Math.* **22.3** (1976), pp. 312–355. DOI: 10.1016/0001-8708(76)90098-0.

[350] J. Scire et al. Reproductive number of the COVID-19 epidemic in Switzerland with a focus on the Cantons of Basel-Stadt and Basel-Landschaft. *Swiss Med. Wkly.* **150.19-20** (2020), w20271. DOI: 10.4414/smw.2020.20271.

[351] J. Shi, C. Wang, and H. Wang. Diffusive spatial movement with memory and maturation delays. *Nonlinearity* **32.9** (2019), pp. 3188–3208. DOI: 10.1088/1361-6544/ab1f2f.

[352] J. Shi, C. Wang, H. Wang, and X. Yan. Diffusive spatial movement with memory. *J. Dynam. Differential Equations* **32.2** (2020), pp. 979–1002. DOI: 10.1007/s10884-019-09757-y.

[353] N. Shigesada, K. Kawasaki, and E. Teramoto. Spatial segregation of interacting species. *J. Theor. Biol.* **79.1** (1979), pp. 83–99. DOI: 10.1016/0022-5193(79)90258-3.

[354] N. Shigesada, K. Kawasaki, and E. Teramoto. Traveling periodic waves in heterogeneous environments. *Theoret. Population Biol.* **30.1** (1986), pp. 143–160. DOI: 10.1016/0040-5809(86)90029-8.

[355] R. Shine, G. Brown, and B. Phillips. An evolutionary process that assembles phenotypes through space rather than through time. *Proc. Natl. Acad. Sci. USA* **108** (14 2011), pp. 5708–11. DOI: 10.1073/pnas.1018989108.

[356] R. Singh and R. Adhikari. Age-structured impact of social distancing on the COVID-19 epidemic in India. *arXiv preprint arXiv:2003.12055* (2020).

[357] R. K. Singh et al. Prediction of the COVID-19 pandemic for the top 15 affected countries: advanced autoregressive integrated moving average (ARIMA) model. *JMIR Public Health Surveill.* **6.2** (2020), e19115. DOI: 10.2196/19115.

[358] M. Slatkin. Gene flow and selection in a two-locus system. *Genetics* **81** (1975), pp. 787–802. DOI: 10.1093/genetics/81.4.787.

[359] A. Smirnova, L. deCamp, and G. Chowell. Forecasting epidemics through nonparametric estimation of time-dependent transmission rates using the SEIR model. *Bull. Math. Biol.* **81.11** (2019), pp. 4343–4365. DOI: 10.1007/s11538-017-0284-3.

[360] H. L. Smith. Competitive coexistence in an oscillating chemostat. *SIAM J. Appl. Math.* **40.3** (1981), pp. 498–522. DOI: 10.1137/0140042.

[361] H. L. Smith. *Monotone dynamical systems*. Vol. 41. Mathematical Surveys and Monographs. An introduction to the theory of competitive and cooperative systems. American Mathematical Society, Providence, RI, 1995, pp. x+174.

[362] H. L. Smith and H. R. Thieme. Chemostats and epidemics: competition for nutrients/hosts. *Math. Biosci. Eng.* **10.5-6** (2013), pp. 1635–1650. DOI: 10.3934/mbe.2013.10.1635.

[363] H. L. Smith and P. Waltman. *The theory of the chemostat*. Vol. 13. Cambridge Studies in Mathematical Biology. Dynamics of microbial competition. Cambridge University Press, Cambridge, 1995, pp. xvi+313. DOI: 10.1017/CBO9780511530043.

[364] J. Smoller. *Shock waves and reaction-diffusion equations*. Second. Vol. 258. Grundlehren der mathematischen Wissenschaften [Fundamental Principles of Mathematical Sciences]. Springer-Verlag, New York, 1994, pp. xxiv+632. DOI: 10.1007/978-1-4612-0873-0.

[365] Y. Song, S. Wu, and H. Wang. Spatiotemporal dynamics in the single population model with memory-based diffusion and nonlocal effect. *J. Differential Equations* **267.11** (2019), pp. 6316–6351. DOI: 10.1016/j.jde.2019.06.025.

[366] A. N. Stokes. On two types of moving front in quasilinear diffusion. *Math. Biosci.* **31.3-4** (1976), pp. 307–315. DOI: 10.1016/0025-5564(76)90087-0.

[367] R. L. Sutherland, R. E. Hall, and I. W. Taylor. Cell proliferation kinetics of MCF-7 human mammary carcinoma cells in culture and effects of tamoxifen on exponentially growing and plateau-phase cells. *Cancer Res.* **43.9** (1983), pp. 3998–4006.

[368] B. Tang et al. Estimation of the transmission risk of the 2019-nCoV and its implication for public health interventions. *J. Clin. Med.* **9.2** (2020), p. 462. DOI: 10.3390/jcm9020462.

[369] M. M. Tang and P. C. Fife. Propagating fronts for competing species equations with diffusion. *Arch. Rational Mech. Anal.* **73.1** (1980), pp. 69–77. DOI: 10.1007/BF00283257.

[370] H. B. Taylor et al. Cell segregation and border sharpening by Eph receptor–ephrin-mediated heterotypic repulsion. *J. R. Soc. Interface* **14.132** (2017), p. 20170338. DOI: 10.1098/rsif.2017.0338.

[371] H. R. Thieme. *Mathematics in population biology*. Princeton Series in Theoretical and Computational Biology. Princeton University Press, Princeton, NJ, 2003, pp. xx+543.

[372] R. N. Thompson. Epidemiological models are important tools for guiding COVID-19 interventions. *BMC Med.* **18** (2020), pp. 1–4. DOI: 10.1186/s12916-020-01628-4.

[373] R. N. Thompson, F. A. Lovell-Read, and U. Obolski. Time from symptom onset to hospitalisation of coronavirus disease 2019 (COVID-19) cases: implications for the proportion of transmissions from infectors with few symptoms. *J. Clin. Med.* **9.5** (2020), p. 1297. DOI: 10.3390/jcm9051297.

[374] R. N. Thompson, O. W. Morgan, and K. Jalava. Rigorous surveillance is necessary for high confidence in end-of-outbreak declarations for Ebola and other infectious diseases. *Philos. Trans. R. Soc. B* **374.1776** (2019), p. 20180431. DOI: 10.1098/rstb.2018.0431.

[375] K. K.-W. To et al. Temporal profiles of viral load in posterior oropharyngeal saliva samples and serum antibody responses during infection by SARS-CoV-2: an observational cohort study. *Lancet Infect. Dis.* **20.5** (2020), pp. 565–574.

[376] E. F. Toro. *Riemann solvers and numerical methods for fluid dynamics*. Third. A practical introduction. Springer-Verlag, Berlin, 2009, pp. xxiv+724. DOI: 10.1007/b79761.

[377] T. K. Tsang et al. Effect of changing case definitions for COVID-19 on the epidemic curve and transmission parameters in mainland China: a modelling study. *Lancet Public Health* **5.5** (2020), e289–e296. DOI: 10.1016/S2468-2667(20)30089-X.

[378] A. Tsoularis and J. Wallace. Analysis of logistic growth models. *Math. Biosci.* **179.1** (2002), pp. 21–55. DOI: 10.1016/S0025-5564(02)00096-2.

[379] O. Turanova. On a model of a population with variable motility. *Math. Models Methods Appl. Sci.* **25.10** (2015), pp. 1961–2014. DOI: 10.1142/S0218202515500505.

[380] J. L. Vázquez. *The porous medium equation*. Oxford Mathematical Monographs. Mathematical theory. The Clarendon Press, Oxford University Press, Oxford, 2007, pp. xxii+624.

[381] P. Verhulst. Notice sur la loi que la population poursuit dans son accroissement. *Correspondance mathématique et physique* **10** (1838), pp. 113–121.

[382] R. Verity et al. Estimates of the severity of coronavirus disease 2019: a model-based analysis. *Lancet Infect. Dis.* **20.6** (2020), pp. 669–677. DOI: 10.1016/S1473-3099(20)30243-7.

[383] A. I. Volpert, V. A. Volpert, and V. A. Volpert. *Traveling wave solutions of parabolic systems*. Vol. 140. Translations of Mathematical Monographs. Translated from the Russian manuscript by James F. Heyda. American Mathematical Society, Providence, RI, 1994, pp. xii+448. DOI: 10.1090/mmono/140.

[384] V. Volpert. *Elliptic partial differential equations. Volume 1: Fredholm theory of elliptic problems in unbounded domains*. Vol. 101. Monographs in Mathematics. Birkhäuser/Springer Basel AG, Basel, 2011, pp. xviii+639. DOI: 10.1007/978-3-0346-0537-3.

[385] V. Volpert and S. Petrovskii. Reaction–diffusion waves in biology. *Phys. Life Rev.* **6.4** (2009), pp. 267–310. DOI: 10.1016/j.plrev.2009.10.002.

[386] V. A. Volpert, A. I. Volpert, and J. F. Collet. Topological degree for elliptic operators in unbounded cylinders. *Adv. Differential Equations* **4.6** (1999), pp. 777–812. DOI: ade/1366030747.

[387] P. G. T. Walker et al. The impact of COVID-19 and strategies for mitigation and suppression in low- and middle-income countries. *Science* **369.6502** (2020), pp. 413–422. DOI: 10.1126/science.abc0035.

[388] H. Wang. Spreading speeds and traveling waves for non-cooperative reaction-diffusion systems. *J. Nonlinear Sci.* **21.5** (2011), pp. 747–783. DOI: 10.1007/s00332-011-9099-9.

[389] P. Wang, X. Zheng, J. Li, and B. Zhu. Prediction of epidemic trends in COVID-19 with logistic model and machine learning technics. *Chaos Solitons Fractals* **139** (2020), p. 110058. DOI: 10.1016/j.chaos.2020.110058.

[390] W. Wang and S. Ruan. Simulating the SARS outbreak in Beijing with limited data. *J. Theoret. Biol.* **227.3** (2004), pp. 369–379. DOI: 10.1016/j.jtbi.2003.11.014.

[391] X.-S. Wang, J. Wu, and Y. Yang. Richards model revisited: validation by and application to infection dynamics. *J. Theoret. Biol.* **313** (2012), pp. 12–19. DOI: 10.1016/j.jtbi.2012.07.024.

[392] Y. Wang, B. Li, R. Gouripeddi, and J. C. Facelli. Human activity pattern implications for modeling SARS-CoV-2 transmission. *Comput. Methods Programs Biomed.* **199** (2021), p. 105896. DOI: 10.1016/j.cmpb.2020.105896.

[393] Z.-C. Wang, W.-T. Li, and S. Ruan. Existence and stability of traveling wave fronts in reaction advection diffusion equations with nonlocal delay. *J. Differential Equations* **238.1** (2007), pp. 153–200. DOI: 10.1016/j.jde.2007.03.025.

[394] D. Waxman and J. R. Peck. Pleiotropy and the preservation of perfection. English. *Science* **279.5354** (1998), 1210–1213. DOI: {10.1126/science.279.5354.1210}.

[395] D. Waxman and J. R. Peck. The frequency of the perfect genotype in a population subject to pleiotropic mutation. English. *Theoretical Population Biology* **69.4** (2006), 409–418. DOI: 10.1016/j.tpb.2006.01.004.

[396] W. E. Wei et al. Presymptomatic transmission of SARS-CoV-2—Singapore, january 23–march 16, 2020. *Morb. Mortal. Wkly. Rep.* **69.14** (2020), p. 411. DOI: 10.15585/mmwr.mm6914e1.

[397] H. F. Weinberger. Long-time behavior of a class of biological models. *SIAM J. Math. Anal.* **13.3** (1982), pp. 353–396. DOI: 10.1137/0513028.

[398] H. F. Weinberger. On spreading speeds and traveling waves for growth and migration models in a periodic habitat. *J. Math. Biol.* **45.6** (2002), pp. 511–548. DOI: 10.1007/s00285-002-0169-3.

[399] H. F. Weinberger, M. A. Lewis, and B. Li. Analysis of linear determinacy for spread in cooperative models. *J. Math. Biol.* **45.3** (2002), pp. 183–218. DOI: 10.1007/s002850200145.

[400] R. Wölfel et al. Virological assessment of hospitalized patients with COVID-2019. *Nature* **581.7809** (2020), pp. 465–469. DOI: 10.1038/s41586-020-2196-x.

[401] G. S. K. Wolkowicz and Z. Q. Lu. Global dynamics of a mathematical model of competition in the chemostat: general response functions and differential death rates. *SIAM J. Appl. Math.* **52.1** (1992), pp. 222–233. DOI: 10.1137/0152012.

[402] G. S. K. Wolkowicz and H. Xia. Global asymptotic behavior of a chemostat model with discrete delays. *SIAM J. Appl. Math.* **57.4** (1997), pp. 1019–1043. DOI: 10.1137/S0036139995287314.

[403] J. T. Wu, K. Leung, and G. M. Leung. Nowcasting and forecasting the potential domestic and international spread of the 2019-nCoV outbreak originating in Wuhan, China: a modelling study. *Lancet* **395.10225** (2020), pp. 689–697. DOI: 10.1016/S0140-6736(20)30260-9.

[404] J. T. Wu et al. Estimating clinical severity of COVID-19 from the transmission dynamics in Wuhan, China. *Nat. Med.* **26.4** (2020), pp. 506–510. DOI: 10.1038/s41591-020-0822-7.

[405] J. Xin. Front propagation in heterogeneous media. *SIAM Rev.* **42.2** (2000), pp. 161–230. DOI: 10.1137/S0036144599364296.

[406] J. X. Xin. Existence of planar flame fronts in convective-diffusive periodic media. *Arch. Rational Mech. Anal.* **121.3** (1992), pp. 205–233. DOI: 10.1007/BF00410613.

[407] J. X. Xin. Existence and nonexistence of traveling waves and reaction-diffusion front propagation in periodic media. *J. Statist. Phys.* **73.5-6** (1993), pp. 893–926. DOI: 10.1007/BF01052815.

[408] X. Xin. Existence and stability of traveling waves in periodic media governed by a bistable nonlinearity. *J. Dynam. Differential Equations* **3.4** (1991), pp. 541–573. DOI: 10.1007/BF01049099.

[409] Z. Yang et al. Modified SEIR and AI prediction of the epidemics trend of COVID-19 in China under public health interventions. *J Thorac. Dis.* **12.3** (2020), p. 165. DOI: 10.21037/jtd.2020.02.64.

[410] J. A. Yorke and W. P. London. Recurrent outbreaks of measles, chickenpox and mumps: II. Systematic differences in contact rates and stochastic effects. *Am. J. Epidemiol.* **98.6** (1973), pp. 469–482. DOI: 10.1093/oxfordjournals.aje.a121576.

[411] H. Zeberg and S. Pääbo. The major genetic risk factor for severe COVID-19 is inherited from Neanderthals. *Nature* **587.7835** (2020), pp. 610–612. DOI: 10.1038/s41586-020-2818-3.

[412] M. L. Zeeman. Extinction in competitive Lotka-Volterra systems. *Proc. Amer. Math. Soc.* **123.1** (1995), pp. 87–96. DOI: 10.2307/2160613.

[413] E. Zeidler. *Nonlinear functional analysis and its applications. I.* Fixed-point theorems, Translated from the German by Peter R. Wadsack. Springer-Verlag, New York, 1986, pp. xxi+897. DOI: 10.1007/978-1-4612-4838-5.

[414] M. Zerner. Quelques propriétés spectrales des opérateurs positifs. *J. Funct. Anal.* **72.2** (1987), pp. 381–417. DOI: 10.1016/0022-1236(87)90094-2.

[415] F. Zhou et al. Clinical course and risk factors for mortality of adult inpatients with COVID-19 in Wuhan, China: a retrospective cohort study. *Lancet* **395.10229** (2020), pp. 1054–1062. DOI: 10.1016/S0140-6736(20)30566-3.

[416] G. Zhou and G. Yan. Severe acute respiratory syndrome epidemic in Asia. *Emerg. Infect. Dis.* **9.12** (2003), pp. 1608–1610. DOI: 10.3201/eid0912.030382.

[417] L. Zou et al. SARS-CoV-2 Viral Load in Upper Respiratory Specimens of Infected Patients. *N. Engl. J. Med.* **382**.**12** (2020). PMID: 32074444, pp. 1177–1179. DOI: 10.1056/NEJMc2001737.

[418] Y. Zou et al. Outbreak analysis with a logistic growth model shows COVID-19 suppression dynamics in China. *PloS one* **15**.**6** (2020), e0235247. DOI: 10.1371/journal.pone.0235247.

Technical reports

[419] N. Ferguson et al. *Report 9: Impact of non-pharmaceutical interventions (NPIs) to reduce COVID19 mortality and healthcare demand*. 77482. Imperial College London, 2020, pp. 491–497.

[420] World Health Organization. *Coronavirus disease 2019 (COVID-19): situation report, 104*. Technical documents. WHO, May 3, 2020, 15 p.

[421] World Health Organization. *Novel coronavirus – China.* Disease Outbreak News. Available at: https://www.who.int/emergencies/disease-outbreak-news/item/2020-DON233. Accessed June 30, 2021. WHO, Jan. 12, 2020.

[422] World Health Organization. *Pneumonia of unknown cause–China.* Disease Outbreak News. Available at: https://www.who.int/emergencies/disease-outbreak-news/item/2020-DON229. Accessed June 30, 2021. WHO, Jan. 5, 2020.

[423] World Health Organization. *Report of the WHO-China Joint Mission on Coronavirus Disease 2019 (COVID-19)*. WHO, Feb. 2020.

Links and URLs cited

[424] *Chinese Center for Disease Control and Prevention*. URL: http://www.chinacdc.cn/jkzt/crb/zl/szkb_11803/jszl_11809/ (visited on 11/28/2021).

[425] *Data from the World Health Organization*. URL: https://covid19.who.int/WHO-COVID-19-global-data.csv (visited on 11/28/2021).

[426] H. P. Gavin. *The Levenberg-Marquardt algorithm for nonlinear least squares curve-fitting problems*. 2020. URL: https://people.duke.edu/~hpgavin/ce281/lm.pdf (visited on 11/28/2021).

[427] *Portal Site of Official Statistics of Japan Website. Reference Table for the Year 2019: Computation of Population by Age (Single Years) and Sex—Total Population, Japanese Population. Published 2020-04-14*. URL: http://www.stat.go.jp/english/data/jinsui/index.htm (visited on 05/06/2020).

[428] *The COVID Tracking Project at The Atlantic*. URL: https://covidtracking.com/ (visited on 06/09/2021).

[429] *The National Health Commission of the People's Republic of China*. URL: http://www.nhc.gov.cn/yjb/pzhgli/new_list.shtml (visited on 11/28/2021).

[430] *WHO Timeline—COVID-19. (accessed May 21, 2020)*. URL: https://www.who.int/news-room/detail/27-04-2020-who-timeline---covid-19 (visited on 05/21/2020).

[431] Wikipedia contributors. *COVID-19 pandemic in mainland China — Wikipedia, The Free Encyclopedia*. URL: https://en.wikipedia.org/w/index.php?title=COVID-19_pandemic_in_mainland_China&oldid=987886059 (visited on 11/28/2021).